nutrients

Volume 1

Antioxidants in Health and Disease

Edited by
Maurizio Battino and Francesca Giampieri

Printed Edition of the Special Issue Published in *Nutrients*

MDPI

Antioxidants in Health and Disease

Volume 1

Special Issue Editors

Maurizio Battino
Francesca Giampieri

MDPI • Basel • Beijing • Wuhan • Barcelona • Belgrade

Special Issue Editors
Maurizio Battino
Università Politecnica delle Marche
Italy

Francesca Giampieri
Università Politecnica delle Marche
Italy

Editorial Office
MDPI
St. Alban-Anlage 66
Basel, Switzerland

This edition is a reprint of the Special Issue published online in the open access journal *Nutrients* (ISSN 2072-6643) from 2016–2018 (available at: http://www.mdpi.com/journal/nutrients/special_issues/antioxidants_health_disease).

For citation purposes, cite each article independently as indicated on the article page online and as indicated below:

Lastname, F.M.; Lastname, F.M. Article title. *Journal Name* **Year**, *Article number*, page range.

First Edition 2018

Volume 1
ISBN 978-3-03842-885-5 (Pbk)
ISBN 978-3-03842-886-2 (PDF)

Volume 1–2
ISBN 978-3-03842-941-8 (Pbk)
ISBN 978-3-03842-942-5 (PDF)

Table of Contents

About the Special Issue Editors

Maurizio Battino, PhD, Associate Professor of Biochemistry in the Department of Clinical Sciences, Faculty of Medicine, UNIVPM (Italy), has been the Director of the Centre for Health and Nutrition, Universidad Europea del Atlantico, Santander (Spain), since December 2014. He obtained a BSc in Bologna (1984) and a PhD in Catania (1990) and completed a post-doctoral training in Granada (1994); he also obtained a MSc in International Communication Technology in Medicine (2011) and was awarded a Doctor Honoris Causa degree by the University of Medicine and Pharmacy of Bucharest (2008). He currently reviews scientific articles for over 30 peer-reviewed journals, serves as the Editor-in-Chief for the Journal of Berry Research, the Mediterranean Journal of Nutrition & Metabolism, and Diseases, and as an Associate Editor for Molecules; he is also an editorial board member of Food Chemistry, Plant Food for Human Nutrition, Nutrition and Aging, and the International Journal of Molecular Sciences. In 2015, 2016, and 2017, he has been recognized as a Thomson Reuters Highly Cited Researcher.

Francesca Giampieri, PhD, works as a Post-Doctoral Research Fellow at the Department of Clinical Science, at the Polytechnic University of Marche (Ancona, Italy). She graduated in Biological Sciences and pursued a Specialization in Food Science at the Polytechnic University of Marche. She currently reviews scientific articles for over 20 peer-reviewed journals, serves as an Associate Editor for the Journal of Berry Research, and is an editorial board member of Molecules, Nutrients, the Annals of Translational Medicine, and the International Journal of Molecular Sciences (Bioactives and Nutraceuticals). She has extensive experience in the field of chemistry, in the assessment of the nutritional and phytochemical composition of different foodstuffs, in the field of biochemistry, in the evaluation of the role of dietary bioactive compounds in human health and, in particular, in the analysis of the biological mechanisms related to oxidative stress.

Preface to "Antioxidants in Health and Disease"

Oxidative stress is defined as an imbalance between the production of free radicals and the necessary antioxidant defenses. Free radicals are chemical species with one or more mismatched electrons that generally damage multiple cellular components, whereas antioxidants are reducing molecules that neutralize free radicals by donating an electron. Oxidative stress can lead to a wide range of biological effects: adaptation, by upregulating the natural defense system, which may protect, completely or in part, against cellular damage; tissue injury, by damaging all molecular targets (DNA, proteins, lipids, cell membranes, and several enzymes); cell death, by activating the processes of necrosis and apoptosis. However, accumulating evidence implicates that free radicals, under physiological and pathological conditions, are able to regulate several signaling pathways, affecting a variety of cellular processes, such as proliferation, metabolism, differentiation, survival, antioxidant and anti-inflammatory response, iron homeostasis, and DNA damage response. In few words, the generation of ROS, within certain boundaries, is essential to maintain cellular homeostasis. This new and more complex view of the role of oxidative stress in biological processes confirms once again the importance of a stable equilibrium between oxidant production and antioxidant defenses to preserve health and longevity.

Because of the cellular damage induced by oxidative stress, there is much interest in the so-called functional foods, encompassing dietary antioxidants, for preventing human disease. The consumption of dietary antioxidants, such as vitamin C, Vitamin E, β-carotene, and polyphenols, has been indeed associated with an improvement of inflammation, a reduction of atherosclerosis progression, a decrease in cellular proliferation and metastatization, and an amelioration of lipid metabolism. In other words, antioxidants modulate several pathways involved in cellular metabolism, survival, and proliferation, maintain well-being, and protect the human body against the development of the most common chronic pathologies, such as metabolic syndrome, diabetes, cancer, and cardiovascular diseases.

The goal of this book is to demonstrate that the consumption of food rich in antioxidants provide health benefits and should be widely recommended as part of a healthy diet.

Maurizio Battino and Francesca Giampieri

Special Issue Editors

nutrients

MDPI

Article

Proanthocyanidins Attenuation of Chronic Lead-Induced Liver Oxidative Damage in Kunming Mice via the Nrf2/ARE Pathway

Miao Long [1,2,†], Yi Liu [3,†], Yu Cao [1,2], Nan Wang [1,2], Meng Dang [1,2] and Jianbin He [1,*]

1 Key Laboratory of Zoonosis of Liaoning Province, College of Animal Science & Veterinary Medicine, Shenyang Agricultural University, Shenyang 110866, China; longjlau@126.com (M.L.); m15648566678@163.com (Y.C.); wn168168wn@163.com (N.W.); joydivisiondang@sina.com (M.D.)

2 College of Life Engineering, Shenyang Institute of Technology, Fushun 113122, China

3 School of Chemical Engineering, Sichuan University of Science and Engineering, Zigong 643000, China; liuyi0961@sina.com

* Correspondence: hejianbin69@163.com; Tel./Fax: +86-24-8848-7156

† These authors contributed equally to this study.

Received: 29 August 2016; Accepted: 14 October 2016; Published: 21 October 2016

Abstract: Lead is harmful for human health and animals. Proanthocyanidins (PCs), a natural antioxidant, possess a broad spectrum of pharmacological and medicinal properties. However, its protective effects against lead-induced liver damage have not been clarified. This study was aimed to evaluate the protective effect of PCs on the hepatotoxicity of male Kunming mice induced by chronic lead exposure. A total of 70 healthy male Kunming mice were averagely divided into four groups: control group, i.e., the group exposed to lead, the group treated with PCs, and the group co-treated with lead and PCs. The mice exposed to lead were given water containing 0.2% lead acetate. Mice treated in the PCs and PCs lead co-treated groups were given PC (100 mg/kg) in 0.9% saline by oral gavage. Lead exposure caused a significant elevation in the liver function parameters, lead level, lipid peroxidation, and inhibition of antioxidant enzyme activities. The induction of oxidative stress and histological alterations in the liver were minimized by co-treatment with PCs. Meanwhile, the number of Transferase-Mediated Deoxyuridine Triphosphate-Biotin Nick End Labeling (TUNEL)-positive cells was significantly reduced in the PCs/lead co-treated group compared to the lead group. In addition, the lead group showed an increase in the expression level of Bax, while the expression of Bcl-2 was decreased. Furthermore, the lead group showed an increase in the expression level of endoplasmic reticulum (ER) stress-related genes and protein (GRP78 and CHOP). Co-treated with PCs significantly reversed these expressions in the liver. PCs were, therefore, demonstrated to have protective, antioxidant, and anti-ER stress and anti-apoptotic activities in liver damage caused by chronic lead exposure in the Kunming mouse. This may be due to the ability of PCs to enhance the ability of liver tissue to protect against oxidative stress via the Nrf2/ARE signaling pathway, resulting in decreasing ER stress and apoptosis of liver tissue.

Keywords: proanthocyanidin; lead; oxidative damage; Nrf2/ARE pathway; liver; mice; apoptosis; ER stress

1. Introduction

Lead is a non-essential toxic heavy metal which has been a persistent public health problem in many countries around the world. Lead is an environmental toxicant which causes a broad range of adverse effects in both humans and animals [1]. In the human body, lead mainly accumulates in the nervous system, blood, digestive and cardiovascular systems, and also in the kidney and bone [2–4]. Lead has also been shown to inhibit growth [5,6]. Lead can cause oxidative damage in many tissues,

including the brain, heart, liver, kidney, and reproductive organs [7,8]. Recent studies have shown that oxidative stress caused by lead may damage the molecular mechanism at the cellular level [9] by inducing reactive oxygen species (ROS), depleting antioxidant capacity and increasing levels of lipid peroxidation [10,11]. Since lead poisoning principally arises from lead-contaminated air, dust, and soils, and by the lead-based paints, fertilizers, automobiles, cosmetics, batteries, etc., people are easily exposed to lead. Therefore, it is difficult to determine whether lead poisoning in people is caused by excessive intake of lead unless clinical symptoms appear. Since it is known that lead has a non-physiological role in the body, so after a long period of exposure to lead, the best way reduce its damage to the cell is to exclude lead.

As lead is a multi-target toxicant, it exerts a toxic manifestation by oxidative free radicals that mediate the disruption of the delicate pro- and anti-oxidant balance existing in mammalian cells, and a therapeutic strategy to elevate the antioxidant defenses of the body may be of assistance in protecting from lead toxicity. Recently, several anti-oxidative approaches have been proposed to alleviate the symptoms of lead damage [12–14]. Herbal and natural products possess antioxidant properties, and antioxidant molecules of plant origin have been widely investigated as scavengers of free radicals and suppressors of lipid peroxide (LPO). In this regard, numerous studies have exhibited the antioxidant activities of several natural products against many toxic metals [15].

Proanthocyanidins (PCs), also named condensed tannins, are oligomers and polymers of flavan-3-ols, contain various amounts of catechin and epicatechin [16], widely distributed in the plant kingdom, appearing in fruits, vegetables, seeds, nuts, flowers, and bark [17], and especially extracted from grape seeds [18]. They are highly water soluble, easy to extract, rich in various plants, and can be absorbed naturally [19]. PCs are powerful natural antioxidants and are efficient free radical scavengers, whose anti-oxidative ability exceeds that of vitamins C and E [20]. PCs have been reported to possess a broad spectrum of pharmacological and medicinal properties against oxidative stress. Some studies have revealed that PCs exhibit a wide range of biological effects, including anti-inflammatory, anti-arthritic, and anti-allergic properties [21]. Moreover, some studies demonstrated that they also have the ability to alleviate oxidative stress and degenerative diseases caused by some toxicants and medicines [22,23]. Some studies demonstrated that PCs could relieve oxidative stress in the small intestinal mucosa and reduce the injury induced by indomethacin [24], reverse pentylenetetrazole-induced impaired performance in the Morris water maze, oxidative stress, mitochondrial ROS generation [25], and significantly attenuate the doxorubicin-induced mutagencity via suppression of oxidative stress [26]. Many studies also showed that PCs could protect the reproductive toxicity induced by arsenic [27], cadmium [28], and formaldehyde [29], and the liver damage induced by carbon tetrachloride [30], gibberellic acid [31], and zearalenone [22].

However, to our knowledge, there are no similar studies available on the protective effects of PC on lead-induced hepatotoxicity in mice. If PCs have the ability to protect the liver, a diet comprising PCs would serve as useful clinical medicine against lead toxicity. Therefore, this study was aimed to elucidate whether PCs can prevent oxidative stress-induced hepatotoxicity and its possible mechanism.

2. Experimental Section

2.1. Animals

Male Kunming mice (15 $\pm$ 0.5 g and three weeks old) were purchased from the China Medical University (Shenyang, China). Mice received food and water randomly. All stress factors were reduced to a minimum. The experiments have been allowed by the ethics committee for laboratory animal care (Animal Ethics Procedures and Guidelines of the People's Republic of China) for the use of Shenyang Agricultural University, China (Permit No. SYXK<Liao>2011-0001).

2.2. Chemicals

Standard lead was purchased from the National Standard Material Research Center (Beijing, China). Lead acetate was purchased from Shanghai Biochemical Technology Co., Ltd. (Shanghai, China). PCs extracted from grape seeds (purity > 95%) were obtained from Zelang Medical Technology Company (Nanjing, China). The extract contained oligomeric proanthocyanidins (88.36%), catechin (6.68%), L-epicatechin (4.54%), and were diluted in distilled water before use. The mice anti-Nrf2 and anti-γ-GCS antibodies were acquired from Santa Cruz biotechnology (Dallas, TX, USA). The citatory number of the anti-Nrf2 antibody was sc-722, the anti-γ-GCS antibody was sc-22755, and the anti-GRP78 antibody was sc-1050. Anti-HO-1 and β-actin antibodies were obtained from Sangon Biotech (Shanghai, China); anti-CHOP antibody was purchased from Beyotime Biotech (Shanghai, China); these antibodies were all polyclonal antibodies. We also purchased the antibodies conjugated with the secondary goat anti-mouse and goat anti-rabbit horseradish peroxides (HRP) from Beijing Solarbio Science and Technology Co., Ltd. (Beijing, China). SYBR green RT-PCR kit from Takara (Otsu, Japan) and 4′,6-diamidino-2-phenylindole (DAPI) from Sigma Aldrich (St. Louis, MO, USA) were also employed. The primers for Nrf2, HO-1, γ-GCS, GRP78, CHOP, and β-actin were synthesized and purified by Sangon Biotech (Shanghai, China). Moreover, the preservation solution of RNA samples and the kits for total animal RNA extraction were obtained from Sangon Biotech Co., Ltd. (Shanghai, China). The kits for Revert Aid First Strand cDNA synthesis were purchased from MBI Fermentas (Burlington, ON, Canada); kits for the testing of glutathione peroxidase (GSH-Px), reduced glutathione (GSH), malondialdehyde (MDA), superoxide dismutase (SOD), alkaline phosphatase (ALP), alanine aminotransferase (ALT) and aspartate aminotransferase (AST) activities were obtained from Nanjing Jiancheng Bioengineering Institute (Nanjing, China).

2.3. Experimental Design and Treatment

Mice were allowed to acclimatize for one week prior to commencing experiments. Mice were given standard granulated food and drinking water and were divided randomly into four groups, as follows: control group (n = 7), mice were given 0.9% physiological saline at 1 mL/kg b.w.; lead acetate group (n = 21), mice were given 0.2% lead acetate in their drinking water for six weeks along with 0.9% saline at 1 mL/kg b.w; PC group (n = 21), mice were given PC in 0.9% physiological saline at 100 mg/kg b.w. for six weeks by oral gavage for six days every week and stopped for one day; lead co-treatment with PC group (n = 21), mice were given 0.2% lead acetate in drinking water with PC at a dose of 100 mg/kg b.w. every day for six weeks.

2.4. Determination of Lead in Serum and Liver Tissue of Mice

Whole blood (0.5 mL) and liver tissue (30 mg) samples were taken from mice and then mixed with 0.5 mol/L HNO_3 to dissolve the residue. Lead content was determined by a graphite furnace atomic absorption spectrophotometer.

2.5. Determination of Serum Enzymes

From the serum samples, commercially available enzyme linked immunosorbent assay (ELISA) kits were used to test the activities of ALP, ALT, and AST. Experimental procedures were carried out according to the manufacturer's instructions (Nanjing Jiancheng Institute of Biotechnology, Nanjing, China). In brief, the samples were transferred into a new 96-well plate containing substrates or buffer solution. After incubation at 37 °C, the plate was incubated for an additional time after adding a color developing agent and the absorbance at 510 or 520 nm was measured.

2.6. Determination of Oxidative Stress in Mice

The liver tissue was weighed and diluted to 10% liver homogenate and centrifuged for 15 min at 3000 rpm. The supernatant was removed and used for analysis. The contents of MDA and reduced

GSH, and the activities of GSH-Px and SOD were determined according to the instructions of the manufacturer for the specific kit (Nanjing Jiancheng Institute of Biotechnology). The concentration of MDA was assayed by monitoring thiobarbituric acid reactive substance formation. According to the instructions of the reduced glutathione assay kit (Nanjing Jiancheng Institute of Biotechnology), the concentration of reduced GSH was detected by the Dinitrothiocyano benzene (DNTB) rate colorimetric method.

2.7. TUNEL Analysis of Apoptosis

Mice liver paraffin slices were prepared for TUNEL assay, which was performed by using a commercial kit in accordance with the manufacturer's instructions. Briefly, the paraffin slices were fixed with dimethylbenzene for 15 min at the room temperature and washed with absolute ethyl alcohol twice, for three minutes each time, then washed with phosphate-buffered saline (PBS) for the third time, for five minutes. The fixed sections were incubated with 100 μL of 20 μg/mL proteinase K solution for 10 min. Subsequently, the 10 μL 5× reaction buffer, 38 μL ddH_2O, 1 μL fluorescein isothiocyanate (FITC)-labelled dUTP, and 1 μL terminal deoxynucleotidyl transferase (TdT) enzyme solution was mixed and added to the surface of one slide and incubated at 37 °C, for 1 h, in the dark. The sample was then strained by DAPI for 8 min. The labelled slices were washed and photographed under a fluorescence microscope. The nucleus of any apoptotic cells were brown, and the other nuclei were blue.

2.8. Western Blot Assay

The total protein and nuclear protein in 100 mg of the liver tissue of mice were extracted using Radio-Immunoprecipitation Assay (RIPA) lysis solution and a nuclear/cytoplasm protein extraction kit (Beyotime Biotech, Shanghai, China). The Bicinchoninic acid (BCA) protein assay kit (Beyotime, Shanghai, China) was used to determine the protein concentrations, and equivalent amounts of proteins (30 μg/lane) were loaded onto 12% sodium dodecyl sulfate-polyacrylamide gel electrophoresis gels (SDS-PAGE). After the proteins were separated by SDS-PAGE, they were transferred to a Modified as polyvinylidene fluoride (PVDF) membrane. Antibodies then were added for rabbit anti-Nrf2 (1:1000), anti-HO-1 (1:1000), anti-γ-GCS (1:500), anti-Bcl-2 (1:1000), anti-Bax (1:1000), and β-actin (1:2000) polyclonal antibodies, and incubated overnight at 4 °C. On the second day, HRP-labeled goat anti rabbit IgG was added and incubated at room temperature for 2 h. An Electrochemical luminescence (ECL) chemical luminescence method was then used to detect the color reaction. Images were acquired and the results of the gray scale image were analyzed using a Bio-Rad gel imaging system. The relative expression levels of proteins in each group were represented by the ratio of the gray value of the target protein and the β-actin.

2.9. Gene Expression

The total RNA of the 100 mg of the liver tissue in each group was extracted using TRIzol reagent. Then, the purity and the quantity of the total RNA were measured via the quotient for optical density (OD) at 260/280 nm (1.8–2.0). The 4 μg of total RNA from each sample was treated with DNAse. After DNAse treatment, 3 μg of DNA-free RNA in a total volume of 20 mL was then reverse transcribed into cDNA using MBI Ferments Prime Script RT reagent kit (Burlington, ON, Canada) according to the manufacturer's instructions. The cDNA was used as the template for further quantitative RT-PCR analysis. An ABI 7500 real-time PCR system and the SYBR Green PCR Kit were used to conduct real-time PCR. Each sample had been measured in triplicate. For qRT-PCR reactions, 2 μL product of cDNA, 0.4 μL reverse primers, 0.4 μL forward, 10 μL 2× SYBR® Premix Ex TaqTM, 6.8 μL of RNase-free water, and 0.4 μL ROX Reference Dye II (50×). The conditions of conducting the PCR reaction included: at the initial stage, denaturing at 95 °C for 5 min, and then denaturing at 95 °C for 15 s, annealing at 56 °C for 30 s, and extension at 72 °C for 30 s. The amount of the template was measured based on the standard curve of quantitative analysis. The primers of Nrf2, γ-GCS, Bcl-2, Bax,

GRP78, and CHOP were designed by using Primer 5 software (PREMIER Biosoft company, Palo Alto, CA, USA) (Table 1), and β-actin was employed as a house-keeping gene. The results were analyzed by using the $2^{-\Delta\Delta CT}$ assay.

Table 1. Primers for real-time PCR analyses.

Gene	Accession No.	Primer Sequences (5′-3′)	Product Size/bp
Nrf2	NM_010902.3	F: TCCTATGCGTGAATCCCAAT R: GCGGCTTGAATGTTTGTCTT	103 bp
Bcl-2	NM_009741.3	F: GTGGATGACTGAGTACCTGAACC R: AGCCAGGAGAAATCAAACAGAG	120 bp
Bax	NM_007527.3	F: CGACCCGTCCTTTGAATTTCT R: GCAAAGTAGAAGAGGGCAACCAC	197 bp
HO-1	NM_010442.2	F: GGGCTGTGAACTCTGTCCAAT R: GGTGAGGGAACTGTGTCAGG	162 bp
γ-GCS	U85414.1	F: TGGATGATGCCAACGAGTC R: CCTAGTGAGCAGTACCACGAATA	185 bp
GRP78	NC_000068.7	R: CACGTCCAACCCGAACGA F: ATTCCAAGTGCGTCCGATG	182 bp
CHOP	NM007837.3	F: CAGCGACAGAGCCAGAATAA R: TCAGGTGTGGTGGTGTATGAA	84 bp
β-actin	NM_007393.5	F: GTGCTATGTTGCTCTAGACTTCG R: ATGCCACAGGATTCCATACC	174 bp

2.10. Statistical Analyses

All data were processed using SPSS 17 statistical software (IBM, Almon, NY, USA). The significance level of statistic differences between mean values was determined using one-way ANOVA, and a p-value < 0.05 was considered as significant.

3. Results

3.1. The Effect of PC on the Lead Content of Whole Blood and Liver Tissue in Mice

As shown in Table 2, the lead levels detected in the blood and liver tissue of the lead-treated animals were significantly higher compared with the control group ($p < 0.05$). The experimental model was successful as a system to determine the effects of lead in the presence and absence of PCs in mice. However, lead levels in the blood and liver tissue of mice co-treated with lead and PCs showed no significant difference compared with the animals treated only with lead ($p > 0.05$), indicating that PCs did not significantly improve the status of the lead in the blood and liver tissue of mice.

Table 2. Lead contents in serum and liver of mice in each group ($n = 7$, $\overline{X} \pm s$).

Group	Blood Lead Level/(μg/L)	Liver Lead Level/(μg/L)
Control	36.42 ± 17.48	0.88 ± 0.21
PCs	35.26 ± 13.36	0.82 ± 0.18
Lead	214.64 ± 36.24 *	13.44 ± 2.84 *
Lead with PCs	206.49 ± 34.92 *	11.21 ± 2.30 *

Note: PCs: Proanthocyanidins. * $p < 0.05$ vs. control group.

3.2. The Effect of PCs on the Serum Enzymes of Mice Exposed to Lead

As shown in Table 3, the activities of ALP, ALT, and AST in the serum of the lead-treated group were significantly increased compared to the control group ($p < 0.05$). However, the activity of three enzymes in the group co-treated with PCs was significantly lower compared with those of the lead-treated group. These activities of these enzymes were not significantly altered in the PCs-only

treated group compared with the control group. Co-treatment with PCs significantly reduced the activities of ALP, ALT, and AST ($p < 0.05$). The ALP, ALT, and AST levels in the lead group were higher than the control group.

Table 3. The effect of PCs on serum enzyme levels in mice ($n = 7$, $\overline{X} \pm s$).

Group	ALP/(U/L)	ALT/(U/L)	AST/(U/L)
Control	129.47 ± 4.18	25.47 ± 7.16	57.92 ± 10.46
PC	124.42 ± 5.17 [b,c]	23.42 ± 6.45 [b,c]	50.21 ± 18.65 [b,c]
Lead	246.48 ± 6.15 [a,c]	59.23 ± 9.84 [a,c]	86.29 ± 14.53 [a,c]
Lead with PC	180.21 ± 7.96 [a,b]	35.21 ± 6.80 [a,b]	63.43 ± 11.24 [a,b]

Note: With each row, means superscripted with different letters are significantly different ($p < 0.05$), [a] significantly different from the control $p < 0.05$; [b] significantly different from the lead group $p < 0.05$; [c] significantly different from the lead co-treated with PCs group $p < 0.05$.

3.3. The Effect of PCs on Oxidative Stress-Related Factors in the Liver of Mice Exposed to Lead

As shown in Table 4, the activities of GSH-Px and SOD significantly increased in the co-treated lead and PC group compared with the group only treated with lead. The MDA levels in the group treated only with lead were also shown to be significantly increased ($p < 0.05$) and in comparison to PCs-co-treated animals. GSH was significantly increased ($p < 0.05$) in the group co-treated with lead and PCs compared with the animals only treated with lead. The levels of MDA were also significantly decreased ($p < 0.05$) in the co-treated group compared with the group treated only with lead. These results indicated that administration of PCs significantly improved the lipid peroxidation damage in the liver tissue in mice exposed to lead.

Table 4. The effect of PC on MDA, GSH content, and the activities of GSH-Px and SOD in the liver tissue of mice exposed to lead ($n = 7$, $\overline{X} \pm s$).

Group	MDA/(μmol/g Prot)	GSH/(mg/g Prot)	GSH-Px/(U/mg Prot)	SOD/(U/mg Prot)
Control	29.56 ± 4.78	18.47 ± 3.96	30.32 ± 3.69	132.63 ± 8.23
PC	23.44 ± 5.40	20.76 ± 3.45	36.42 ± 5.97	138.56 ± 6.24
Lead	64.32 ± 8.45 *	8.23 ± 2.14 *	11.73 ± 2.95 *	90.46 ± 4.23 *
Lead with PC	34.12 ± 5.36 [#]	16.27 ± 4.10 [#]	22.41 ± 2.74 *,[#]	116.45 ± 5.96 *,[#]

Note: Prot: protein. * $p < 0.05$ vs. the control group; [#] $p < 0.05$ vs. the lead group.

3.4. The Effect of PCs on the Liver Tissue Histopathological Variation of Mice Exposed to Lead

The results of the liver histopathological aspect are shown in Figure 1. Normal histological architecture was observed in the liver sections in the control group (Figure 1A) and PCs group (Figure 1B). However, in the lead group, it showed that the hepatic lobule structure was not integrated; the cells were arranged in a discontinuous and loose manner, the central vein tube wall was not integrated; the liver cells around the central vein were disordered; the liver cell size was not uniform, different sizes of vacuoles ere in the sytoplasmic; some nuclei of the hepatocytes were dissolved or pyknotic, and some hepatocytes were swollen and necrotic (Figure 1C). Animals co-treated with PCs largely improved the lead-induced histopathological changes in the liver tissue, showing clear borders of the hepatic tissue, a decrease of dissolved nuclei, and nuclei pyknosis (Figure 1D).

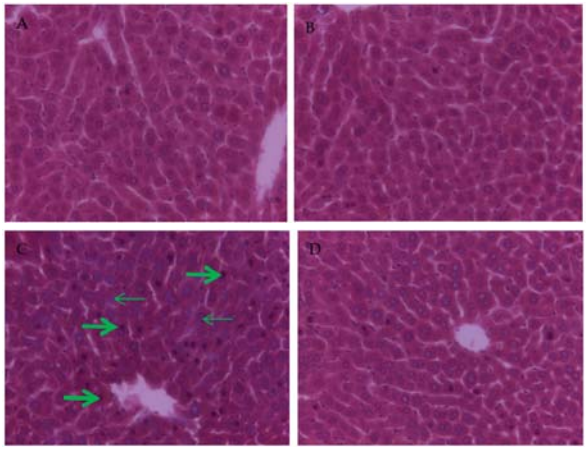

Figure 1. The effects of PCs on lead-induced liver histopathological changes in mice (original magnification of 400×). (**A**) Control group; (**B**) PCs group; (**C**) group administrated with lead; and (**D**) group co-treated with lead and PCs at a dose of 100 mg/kg. Thick arrow: nuclei pyknosis; Thin arrow: dissolved nuclei.

3.5. PCs Decreases Lead-Induced Apoptosis of Liver Cells

Compared with the control group (Figure 2A), the TUNEL-positive cells were significantly increased in the lead group ($p < 0.05$) (Figure 2C), which was obviously attenuated by the co-administration of PCs (Figure 2D). However, the TUNEL-positive cells in the PCs group were lower than that in the lead group ($p < 0.05$).

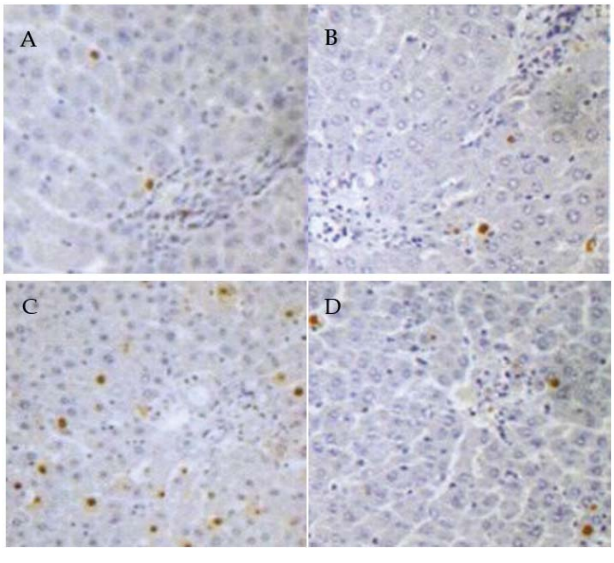

Figure 2. The effects of proanthocyanidins (PCs) on lead-induced liver apotosis. TUNEL-stained liver section (magnification, 200×), with brown granules indicating the positive cells. Mice were divided into the following groups: (**A**) control group; (**B**) PCs group; (**C**) group administrated with lead; (**D**) lead co-treated with PCs at a dose of 100 mg/kg.

3.6. The Effect of PC on the Expression of Bcl-2 and Bax in the Liver of Mice Exposed to Lead

As we know, Bcl-2 has a role in cells that inhibits the signal which induces apoptosis, Bax has a role in promoting cell apoptosis, and in order to analyze whether PC protects against the toxicity caused by lead related to inhibiting cell apoptosis in the liver of mice, the expression of Bcl-2 and Bax associated with apoptosis was examined, As shown in Figures 3 and 4, compared with the control group, the expression of Bcl-2 mRNA was down-regulated (Figure 3A) ($p < 0.05$), whereas the expression of Bax mRNA was up-regulated in the lead group (Figure 3B) ($p < 0.05$). However, compared with the lead group, the significant up-regulation of Bcl-2 mRNA (Figure 3A) ($p < 0.05$) and down-regulation of Bax (Figure 3B) ($p < 0.05$) were shown in the group co-treated with lead and PCs. Consistent with real-time PCR, the Western blot findings also showed low expression of Bcl-2 protein in lead-treated mice (Figure 4A) ($p < 0.05$), while moderate to strong expression was observed for Bax (Figure 4B) ($p < 0.05$). Compared with the lead-treated mice, those co-treated with PCs exhibited improvement, represented by increased expression of anti-apoptotic Bcl-2 protein and moderate expression of the pro-apoptotic protein Bax in the liver of mice (Figure 4A,B) ($p < 0.05$).

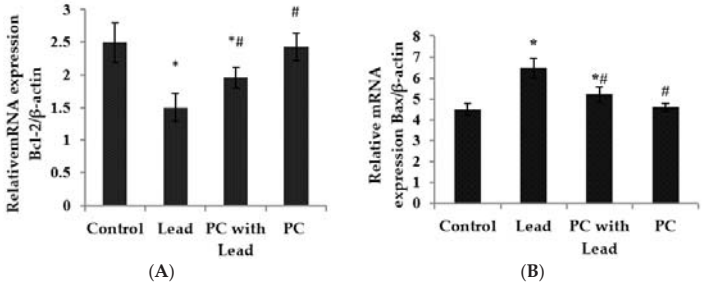

Figure 3. The effect of proanthocyanidin (PCs) on the mRNA levels of *Bcl-2* and *Bax* in the liver of mice exposed to lead. (**A**) *Bcl-2*; (**B**) *Bax*. All results are expressed as the mean ± SE ($n = 7$). * $p < 0.05$, significant change with respect to the control; # $p < 0.05$, significant change with respect to lead-treated mice.

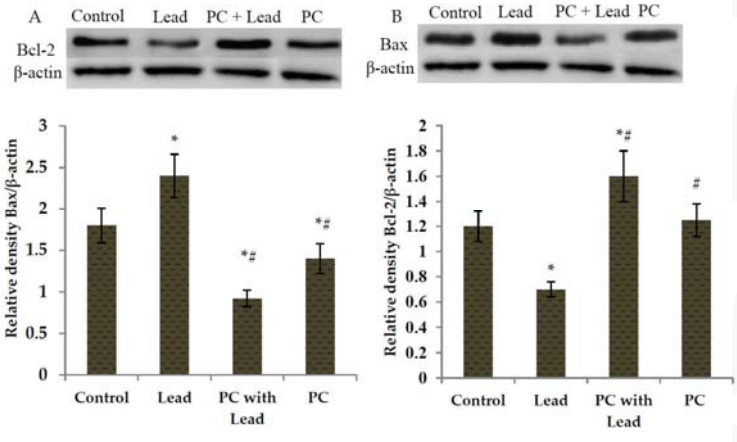

Figure 4. The effect of proanthocyanidins (PCs) on the protein expression levels of Bcl-2 and Bax in the liver of mice exposed to lead. (**A**) Bcl-2; (**B**) Bax. All results are expressed as the mean ± SE ($n = 7$). * $p < 0.05$, significant change with respect to the control; # $p < 0.05$, significant change with respect to lead-treated mice.

3.7. The Effect of PC on the Expression of Nuclear Nrf2, HO-1, and γ-GCS in the Liver of Mice Exposed to Lead

To analyze whether Nrf2 activation plays a role in PC protection against the toxicity caused by lead, the expression of Nrf2 and Nrf2-target proteins, HO-1 and γ-GCS, in the liver of mice were measured. As shown in Figure 5, compared with the control group, the Western blot results showed that the nuclear Nrf2, HO-1, and γ-GCS protein expression levels in the lead-treated group were increased without significant difference ($p > 0.05$), while these protein expressions were increased with significant difference in the PCs group ($p < 0.05$). Compared with the lead group, all of their expressions in the lead/PCs co-treated group were increased with significant difference ($p < 0.05$) (Figure 5A–C). Meanwhile, as shown in Figure 6, the RT-PCR results showed that, compared with the control group, the nuclear *Nrf2*, *Ho-1*, and γ-GCS mRNA expression levels in the lead-treated group were increased without significant difference ($p > 0.05$), while these mRNA expressions were increased with significant difference in the PCs group. Compared with the lead group, the mRNA expressions of these genes in the lead/PCs co-treated group and in PCs group were increased with significant difference ($p < 0.05$).

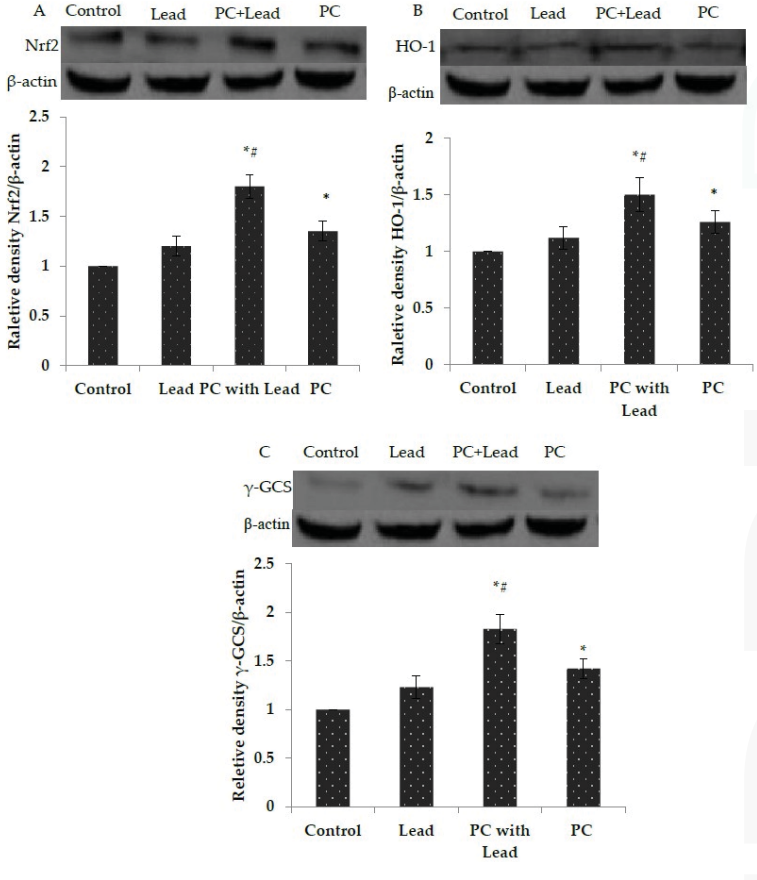

Figure 5. The effect of proanthocyanidins (PCs) on the protein expression levels of the nuclear Nrf2, HO-1, and γ-GCS protein in liver tissues of mice exposed to lead. (**A**) Nuclear erythroid 2-related factor 2 (Nrf2); (**B**) hemeoxygenase-1 (HO-1); and (**C**) γ-glutamyl cysteine synthetase (γ-GCS). All results are expressed as the mean ± SE ($n = 7$). * $p < 0.05$, significant change with respect to the control; # $p < 0.05$, significant change with respect to lead-treated mice.

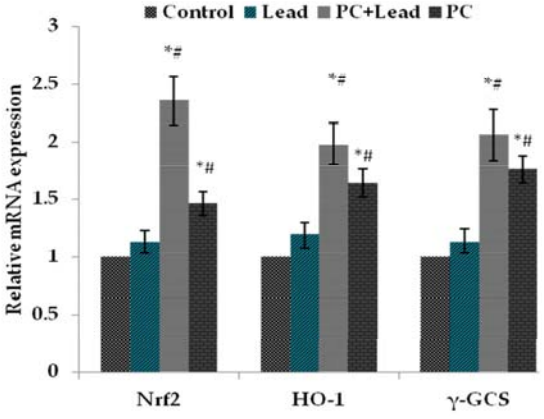

Figure 6. The effect of proanthocyanidins (PCs) on the mRNA expression levels of the nuclear *Nrf2*, *HO-1*, and *γ-GCS* in liver tissues of mice exposed to lead. All results are expressed as the mean ± SE ($n = 7$). * $p < 0.05$, significant change with respect to the control; # $p < 0.05$, significant change with respect to lead-treated mice.

3.8. The Effect of PC on the Expression of GRP78 and CHOP in the Liver of Mice Exposed to Lead

To analyze whether the protective effect of PCs on liver damage was related to inhibiting cell ER stress caused by lead, we measured the expression of GRP78 and CHOP, which were the ER stress-typical related proteins. As shown in Figure 7, compared with the control group, the Western blot results showed that the GRP78 and CHOP protein expression levels in the lead-treated group were increased with significant difference ($p > 0.05$), while these protein expressions were not significantly different in the PCs group. Compared with the lead group, all of the protein expressions in the lead/PCs co-treated group and PCs group were decreased with significant difference ($p < 0.05$) (Figure 7A,B). Meanwhile, as shown in Figure 8, the RT-PCR results showed that, compared with the control group, the *Grp78* and *Chop* mRNA expression levels in the lead-treated group were increased with significant difference ($p < 0.05$), while these mRNA expressions were not significantly different in the PCs group. Compared with the lead group, the mRNA expression of these genes in lead/PCs co-treated group and in PCs group were decreased with significant difference ($p < 0.05$).

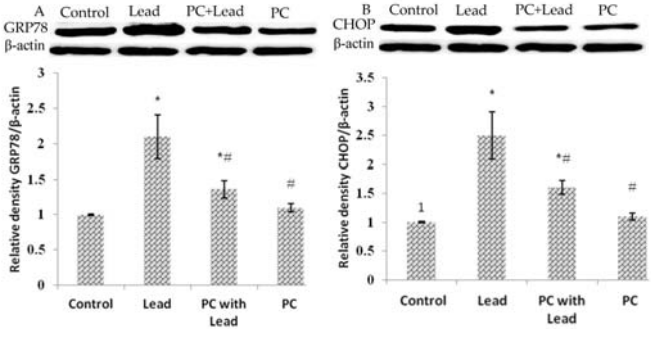

Figure 7. The effect of proanthocyanidins (PCs) on the protein expression levels of GRP78 and CHOP protein in liver tissues of mice exposed to lead. (**A**) GRP78; and (**B**) CHOP. All results are expressed as the mean ± SE ($n = 7$). * $p < 0.05$, significant change with respect to the control; # $p < 0.05$, significant change with respect to lead-treated mice.

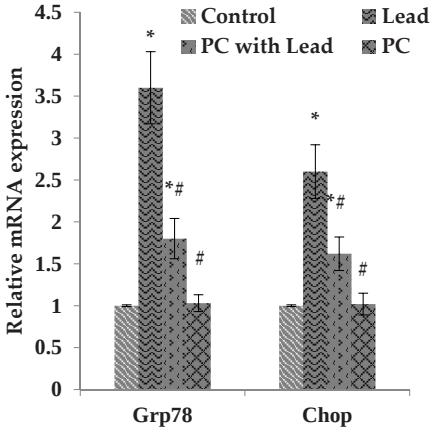

Figure 8. The effect of proanthocyanidins (PCs) on the mRNA expression levels of *Grp78* and *Chop* in liver tissues of mice exposed to lead. All results are expressed as the mean ± SE (n = 7). * $p < 0.05$, significant change with respect to the control; # $p < 0.05$, significant change with respect to lead-treated mice.

4. Discussion

In the present study, the choice of the doses of lead and lead exposure time was based on preliminary experiments by Wang et al. [32,33], which had successfully established the model of chronic lead poisoning in mice. PCs were given to mice at a dose of 100 mg/kg body weight since this was reported to be the most effective dose in previous studies [22,34,35].

The toxicity of the lead has been relatively well studied, particularly in the context of neuro- and nephrotoxicity. As the liver is the central organ in the processing and removal of harmful substances from the body, it is also highly susceptible to damage. In addition, because the liver, via the portal vein, is the first organ exposed to internally-absorbed Pb and is one of the major organs implicated in the storage, biotransformation, and elimination of Pb, the liver must be the target organ of lead and liver will be damaged by lead when lead is taken into the body. Moreover, the liver is the body's largest detoxification organ, a lot of detoxification enzymes, such as cysteine proteases, will be affected by lead. Previous studies have shown that lead exposure can cause oxidative damage in the liver by inhibiting the activities of antioxidant enzymes, decreasing the concentration of non-enzymatic antioxidants and increasing the concentration of reactive oxygen species [36–38]. Our results showed that lead acetate added to the drinking water for six weeks for mice resulted in severe histopathological changes in the liver tissue. In addition, the observed hepatotoxicity caused by lead acetate was accompanied with elevated activities of key liver enzymes, including AST, ALT, and ALP found in serum [39]. Our results of detection of serum biochemical parameters and pathology indicated that lead could accumulate in the liver and cause liver damage, and the reason for damage might be because lead mainly induces reactive oxygen species to attack the target organ and reduces a series of antioxidant enzymes, such as SOD, catalase, and the levels of some antioxidants (GSH) [40,41]. GSH is one of the main antioxidants found in liver tissue and it is central to the detoxification of the heavy metals in the liver. In the current study, it was observed that in the lead-treated group, the activity of GSH-Px was inhibited. As GSH-Px regulated the synthesis of GSH, the level of GSH was also shown to consequently decrease and the content of MDA, which was a product of lipid peroxidation, was shown to increase significantly. These results indicate that exposure to lead induced oxidative stress in the liver tissue of mice, which is in close agreement to previous observations reported by Senapati et al. [3] and Newairy et al. [42].

PCs are highly efficient natural antioxidants, their antioxidant activity is 50 times higher than that of vitamin E and 20 times that of vitamin C, and their effects have been reported in a wide range

of studies [12,27,43–47]. The results of the meta-analysis by Li et al. [47] indicated that PCs could effectively improve the activity of anti-oxidative enzymes and reduce lipid peroxidation products. Previous studies showed that antioxidant can be useful in preventing hepatocellular damage by inhibiting lipid peroxidation by free radicals generated by heavy metals. From our data, it was shown that the mice co-treated with PCs saw increased levels of reduced GSH and higher activity of GSH-Px, and decreased the level of MDA, a result that might indicate that PCs could directly reduce phospholipid hydroperoxides within the membrane and lipoproteins by removing the ROS' ability to inhibit lipid peroxidation of liver cells induced by lead. It may also be that PCs could improve the activity of GSH-Px by activating the intracellular antioxidant signaling pathway. In addition, the reduced GSH was at, or near, control levels; the reason might be that PCs may function by increasing the steady state levels of reduced GSH and/or its rate of synthesis, thereby conferring enhanced protection against oxidative stress. Combined with our result that PCs alleviated the liver tissue histopathological variation of mice exposed to lead, we concluded that PCs, via their anti-oxidant ability, protected the liver damage caused by lead.

Currently, Nrf2 is the key molecule which mediates the response of the endogenous antioxidant system. Activation of Nrf2 can promote the expression of antioxidant genes and induce synthesis of phase II detoxifying enzymes [48]. Studies have shown that Nrf2 plays a crucial role in cellular resistance to oxidation and exogenous damage [49,50]. Recent studies have indicated that activating the Nrf2/ARE pathway has a hepato-protective effect [51,52].

In our study, we found that the gene transcription level of Nrf2 and the expression protein level of Nrf2 were both increased in the lead group. This result indicated that the expression of Nrf2 could be induced by lead under chronic lead poisoning conditions. At the same time, the results indicated that under the chronic lead poisoning, in order to cope with the oxidative stress induced by lead, the cells opened the Nrf2/ARE signal pathway to compensate for the oxidation; however, the cells were still in a state of oxidative stress. When the mice were co-treated with PCs, the nuclear Nrf2 mRNA and protein expression were also increased with a significant difference compared with that in the control group and lead group. This result indicated that PCs could activate the expression of nuclear Nrf2 protein, indicating that the effect of PCs in antagonizing lead-induced oxidative stress in liver tissue was related to the Nrf2/ARE signaling pathway.

Previous studies have suggested that a variety of cytokines and antioxidants could counteract the action of such chemicals causing up-regulation of HO-1 and γ-GCS expression [53–57]. γ-GCS regulated by the Nrf2/ARE signaling pathway is the rate-limiting enzyme for synthesis of GSH [54]. Heme oxygenase 1 (HO-1), a known target of Nrf2-regulated transcription and an antioxidative, cytoprotective protein in different types of cells, plays an important role in cytoprotection when oxidative stress and cellular injury occurs, and Nrf2 directly regulates its expression [55,56]. Our results showed that PCs could up-regulate the Nrf2 downstream gene HO-1 and γ-GCS expression. This indicated that PCs could improve the expression of γ-GCS, resulting in accelerating GSH synthesis in the liver, then enhancing the ability to resist the oxidative stress in liver tissue caused by lead. Combined with our results that the reduced GSH was at, or near, control levels in mice co-treated with PCs, we demonstrated that PCs could increase the amount of reduced GSH through the Nrf2/ARE signaling pathway. Our results showed that PCs could improve the expression of HO1, resulting in increasing the ability of cells to fight against oxidative stress and then maintaining the redox balance. The present results demonstrated that promotion of HO-1 expression is required for PCs' anti-oxidative effects. These results further illustrated that PCs played important roles as antioxidants and in detoxification by improving the expression of the antioxidant enzymes via the Nrf2/ARE signaling pathway. However, the molecular signaling pathway responsible for the expression of Nrf2 was not determined and is worthy of further investigation.

Apoptosis plays a key role in some metal-induced toxicity. Lead exposure can induce apoptosis of nerve cells [57], liver cells [58], and kidney cells [15] through inducing the depolarization and swelling of mitochondria, which leads to the release of cytochrome C, resulting in selective apoptosis [59].

As we know, Bcl-2 and Bax in apoptosis behave opposite to each other: Bax is a pro-apoptotic gene, while Bcl-2 is anti-apoptotic gene. Our results showed that the levels of Bcl-2 mRNA and protein were significantly down-regulated, while the expression levels of Bax were significantly up-regulated in the liver caused by lead. Our results demonstrated lead-induced liver cell apoptosis. Our results were consistent with previous investigations that hepatic apoptosis induced by low-dose exposure was associated with mitochondrial injury and changes in levels of apoptogenic proteins, such as Bcl-2, Bax, and caspase-3 [60,61]. However, PCs reversed these gene expressions, as our results showed that PCs up-regulated the anti-apoptotic gene Bcl-2 expression and down-regulated the pro-apoptotic gene Bax expression. Combined with the TUNEL assay results, we confirmed that PCs could effectively inhibit cell apoptosis in the liver.

Previous studies showed that lead could induce endoplasmic reticulum (ER) stress responses in the nervous system [62,63]. Our results demonstrated that lead induced the ER stress in the liver by increasing the expression of ER stress-related protein GRP78 and CHOP, results which were consistent with the previous study by Liu et al. [64]. Meanwhile, our results showed that mice co-treated with PCs decreased the expression of the two proteins, indicating that ER stress may be relieved by PCs treatment, which meant that PCs might protect the liver from damage by inhibiting ER stress in the liver.

Recent studies have provided evidence that PCs can be used in the treatment and prevention of diseases, such as atherosclerosis, gastric ulcers, cataracts, and diabetes. For the first time, our results suggested that the protective effect of PCs on lead-induced liver damage by inhibiting the ER stress and apoptosis is due, at least in part, to their anti-oxidant stress activity and their ability to modulate the Nrf2/ARE signaling pathway. These findings may be attributed to the manifold effects of PCs as functional foods in future applications.

5. Conclusions

In conclusion, PCs could protect against damage resulting from ER stress and apoptosis induced by chronic lead exposure in the liver tissue of mice. The hepatoprotective effect of PCs might be that PCs activated the expression of HO-1and γ-GCS via the Nrf2/ARE pathway, resulting in decreasing ER stress and apoptosis of the liver tissue cells.

Acknowledgments: This work was financially supported by the National Natural Science Foundation of China (grants No. 31201961; grants No. 31302152; No. 31640084); China Postdoctoral Science Foundation project grants (2014M551125); and the General Program of Liaoning Provincial Department of Education Science Research (L2014561).

Author Contributions: Jianbin He, Miao Long conceived and designed the experiments; Yi Liu, Chang Xu, Yuan Wang, Yu Cao, Nan Wang, Meng Dang Zenggui Gao performed the experiments; Miao Long wrote the paper.

Conflicts of Interest: The authors declare no conflict of interest.

References

1. Tian, F.; Zhai, Q.; Zhao, J.; Liu, X.; Wang, G.; Zhang, H.; Zhang, H.; Chen, W. *Lactobacillus plantarum* CCFM8661 alleviates lead toxicity in mice. *Biol. Trace Elem. Res.* **2012**, *150*, 264–271. [CrossRef] [PubMed]
2. Solon, O.; Riddell, T.J.; Quimbo, S.A.; Butrick, E.; Aylward, G.P.; Lou Bacate, M.; Peabody, J.W. Associations between cognitive function, blood lead concentration, and nutrition among children in the central Philippines. *J. Pediatr.* **2008**, *152*, 237–243. [CrossRef] [PubMed]
3. Senapati, S.K.; Dey, S.; Dwivedi, S.K.; Swarup, D. Effect of garlic (*Allium sativum* L.) extract on tissue lead level in rats. *J. Ethnopharmacol.* **2001**, *76*, 229–232. [CrossRef]
4. Chang, W.; Chen, J.; Wei, Q.Y.; Chen, X.M. Effects of Brn-3a protein and RNA expression in rat brain following low level lead exposure during development on spatial learning and memory. *Toxicol. Lett.* **2006**, *164*, 63–70. [CrossRef] [PubMed]

5. Hamilton, J.D.; O'Flaherty, J.E. Influence of lead on mineralization during bone growth. *Fundam. Appl. Toxicol.* **1995**, *26*, 265–271. [CrossRef] [PubMed]
6. Maboeta, M.S.; Reinecke, A.J.; Reinecke, S.A. Effects of low levels of lead on growth and reproduction of the Asian earthworm *Perionyx excavatus* (Oligochaeta). *Ecotoxicol. Environ. Saf.* **1999**, *44*, 236–240. [CrossRef] [PubMed]
7. Ding, Y.; Gonick, H.C.; Vaziri, N.D.; Liang, K.; Wei, L. Lead-induced hypertension III: Increased hydroxyl radical production. *Am. J. Hypertens.* **2001**, *14*, 169–173. [CrossRef]
8. Patra, R.C.; Swarup, D.; Dwidedi, S.K. Antioxidant effects of α-tocopherol, ascorbic acid and L-methionine on lead-induced oxidative stress of the liver, kidney and brain in rats. *Toxicology* **2001**, *162*, 81–88. [CrossRef]
9. Adonaylo, V.N.; Oteiza, P.I. Pb^{2+} promotes lipid peroxidation and alteration in membrane physical properties. *Toxicology* **1999**, *132*, 19–32. [CrossRef]
10. Farmand, F.; Ehdaie, A.; Roberts, C.K.; Sindhu, R.K. Lead induced dysregulation of superoxide dismutases, catalase, glutathione peroxidase, and guanylate cyclase. *Environ. Res.* **2005**, *98*, 33–39. [CrossRef] [PubMed]
11. Gurer, H.; Ercal, N. Can antioxidants be beneficial in the treatment of lead poisoning? *Free Radic. Biol. Med.* **2000**, *29*, 927–945. [CrossRef]
12. Haleagrahara, N.; Jackie, T.; Chakravarthi, S.; Rao, M.; Kulur, A. Protective effect of *Etlingera elatior* (torch ginger) extract on lead acetate—Induced hepatotoxicity in rats. *J. Toxicol. Sci.* **2010**, *35*, 663–671. [CrossRef] [PubMed]
13. Khalaf, A.A.; Moselhy, W.A.; Abdel-Hamed, M.I. The protective effect of green tea extract on lead induced oxidative and DNA damage on rat brain. *Neurotoxicology* **2012**, *33*, 280–289. [CrossRef] [PubMed]
14. Mabrouk, A.; Bel Hadj Salah, I.; Chaieb, W.; Ben Cheikh, H. Protective effect of thymoquinone against lead-induced hepatic toxicity in rats. *Environ. Sci. Pollut. Res. Int.* **2016**, *23*, 12206–12215. [CrossRef] [PubMed]
15. Dkhil, M.A.; Al-Khalifa, M.S.; Al-Quraishy, S.; Zrieq, R.; Abdel Moneim, A.E. *Indigofera oblongifolia* mitigates lead-acetate-induced kidney damage and apoptosis in a rat model. *Drug Des. Dev. Ther.* **2016**, *10*, 1847–1856.
16. Malisch, C.S.; Lüscher, A.; Baert, N.; Engström, M.T.; Studer, B.; Fryganas, C.; Suter, D.; Mueller-Harvey, I.; Salminen, J.P. Large variability of proanthocyanidin content and composition in Sainfoin (*Onobrychis viciifolia*). *J. Agric. Food Chem.* **2015**, *63*, 10234–10242. [CrossRef] [PubMed]
17. Mouradov, A.; Spangenberg, G. Flavonoids: A metabolic network mediating plants adaptation to their real estate. *Front. Plant Sci.* **2014**, *5*, 620. [CrossRef] [PubMed]
18. Asl, M.N.; Hosseinzadeh, H. Review of the pharmacological effects of *Vitis vinifera* (grape) and its bioactive compounds. *Phytother. Res.* **2009**, *10*, 1002–1006.
19. Aruoma, O.I.; Sun, B.; Fujii, H.; Neergheen, V.S.; Bahorun, T.; Kang, K.S.; Sung, M.K. Low molecular proanthocyanidin dietary biofactor Oligonol: Its modulation of oxidative stress, bioefficacy, neuroprotection, food application and chemoprevention potentials. *Biofactors* **2006**, *27*, 245–265. [CrossRef] [PubMed]
20. Bagchi, D.; Garg, A.; Krohn, R.L.; Bagchi, M.; Tran, M.X.; Stohs, S.J. Oxygen free radical scavenging abilities of vitamins C and E, and a grape seed proanthocyanidin extract in vitro. *Res. Commun. Mol. Pathol. Pharmacol.* **1997**, *95*, 179–189. [PubMed]
21. Ariga, T. The antioxidative function, preventive action on disease and utilization of proanthocyanidins. *Biofactors* **2004**, *21*, 197–201. [CrossRef] [PubMed]
22. Long, M.; Yang, S.H.; Han, J.X.; Li, P.; Zhang, Y.; Dong, S.; Chen, X.; Guo, J.Y.; Wang, J.; He, J.B. The protective effect of grape-seed proanthocyanidin extract on oxidative damage induced by zearalenone in Kunming mice liver. *Int. J. Mol. Sci.* **2016**, *17*, 6. [CrossRef] [PubMed]
23. Mansouri, E.; Panahi, M.; Ghaffari, M.A.; Ghorbani, A. Effects of grape seed proanthocyanidin extract on oxidative stress induced by diabetes in rat kidney. *Iran. Biomed. J.* **2011**, *15*, 100–106. [PubMed]
24. Cheung, D.Y.; Kim, J.I.; Park, S.H.; Kim, J.K. Proanthocyanidin from grape seed extracts protects indomethacin-induced small intestinal mucosal injury. *Gastroenterol. Res. Pract.* **2014**, *2014*. [CrossRef] [PubMed]
25. Zhen, J.; Qu, Z.; Fang, H.; Fu, L.; Wu, Y.; Wang, H.; Zang, H.; Wang, W. Effects of grape seed proanthocyanidin extract on pentylenetetrazole-induced kindling and associated cognitive impairment in rats. *Int. J. Mol. Med.* **2014**, *34*, 391–398. [CrossRef] [PubMed]

26. Attia, S.M.; Al-Bakheet, S.A.; Al-Rasheed, N.M. Proanthocyanidins produce significant attenuation of doxorubicin-induced mutagenicity via suppression of oxidative stress. *Oxid. Med. Cell. Longev.* **2010**, *3*, 404–413. [CrossRef] [PubMed]
27. Li, S.G.; Ding, Y.S.; Niu, Q.; Xu, S.Z.; Pang, L.J.; Ma, R.L.; Jing, M.X.; Feng, G.L.; Liu, J.M.; Guo, S.X. Grape seed proanthocyanidin extract alleviates arsenic-induced oxidative reproductive toxicity in male mice. *Biomed. Environ. Sci.* **2015**, *28*, 272–280. [PubMed]
28. Hou, F.; Xiao, M.; Li, J.; Cook, D.W.; Zeng, W.; Zhang, C.; Mi, Y. Ameliorative effect of grape seed proanthocyanidin extract on cadmium-induced meiosis inhibition during oogenesis in chicken embryos. *Anat. Rec.* **2016**, *299*, 450–460. [CrossRef] [PubMed]
29. Uluçam, E.; Bakar, E. The effect of proanthocyanidin on formaldehyde-induced toxicity in rat testes. *Turk. J. Med. Sci.* **2016**, *46*, 185–193. [CrossRef] [PubMed]
30. Dai, N.; Zou, Y.; Zhu, L.; Wang, H.F.; Dai, M.G. Antioxidant properties of proanthocyanidins attenuate carbon tetrachloride (CCl_4)-induced steatosis/statuses and liver injury in rats via CYP2E1 regulation. *J. Med. Food* **2014**, *17*, 663–669. [CrossRef] [PubMed]
31. Hassan, H.A.; Al-Rawi, M.M. Grape seeds proanthocyanidin extract as a hepatic-reno-protective agent against gibberellic acid induced oxidative stress and cellular alterations. *Cytotechnology* **2013**, *65*, 567–576. [CrossRef] [PubMed]
32. Wang, C.; Liang, J.; Zhang, C.; Bi, Y.; Shi, X.; Shi, Q. Effect of ascorbic acid and thiamine supplementation at different concentrations on lead toxicity in liver. *Ann. Occup. Hyg.* **2007**, *51*, 563–569. [CrossRef] [PubMed]
33. Wang, C.; Zhang, Y.; Liang, J.; Shan, G.; Wang, Y.; Shi, Q. Impacts of ascorbic acid and thiamine supplementation at different concentrations on lead toxicity in testis. *Clin. Chim. Acta* **2006**, *370*, 82–88. [CrossRef] [PubMed]
34. Bagchi, D.; Garg, A.; Krohn, R.; Bagchi, M.; Bagchi, D.J.; Balmoori, J.; Stohs, S.J. Protective effects of grape seed proanthocyanidins and selected antioxidants against TPA-induced hepatic and brain lipid peroxidation and DNA fragmentation, and peritoneal macrophage activation in mice. *Gen. Pharmacol.* **1998**, *30*, 771–776. [CrossRef]
35. Sato, M.; Maulik, G.; Ray, P.S.; Bagchi, D.; Das, D.K. Cardio-protective effects of grape seed proanthocyanidin against ischemic reperfusion injury. *J. Mol. Cell. Cardiol.* **1999**, *31*, 1289–1297. [CrossRef] [PubMed]
36. Sandhir, R.; Gill, K.D. Effect of lead on lipid peroxidation in liver of rats. *Biol. Trace Elem. Res.* **1995**, *48*, 91–97. [CrossRef] [PubMed]
37. Sharma, S.; Raghuvanshi, S.; Jaswal, A.; Shrivastava, S.; Shukla, S. Lead acetate-induced hepatoxicity in Wistar rats: Possible protective role of combination therapy. *J. Environ. Pathol. Toxicol. Oncol.* **2015**, *34*, 23–34. [CrossRef] [PubMed]
38. Hasanein, P.; Kazemian-Mahtaj, A.; Khodadadi, I. Bioactive peptide carnosin protects against lead acetate-induced hepatotoxicity by abrogation of oxidative stress in rats. *Pharm. Biol.* **2016**, *25*, 1–7. [CrossRef] [PubMed]
39. Sharma, A.; Sharma, V.; Kansal, L. Amelioration of lead-induced hepatotoxicity by *Allium sativum* extracts in Swiss albino mice. *Libyan J. Med.* **2010**, *5*. [CrossRef]
40. Chiba, M.; Shinohara, A.; Matsushita, K.; Watanabe, H.; Inaba, Y. Indices of lead-exposure in blood and urine of lead-exposed workers and concentrations of major and trace elements and activities of SOD, GSH-Px and catalase/in their blood. *Tohoku J. Exp. Med.* **1996**, *178*, 49–62. [CrossRef] [PubMed]
41. Dafre, A.L.; Medeiros, I.D.; Müller, I.C.; Ventura, E.C.; Bainy, A.C. Antioxidant enzymes and thiol/disulfide status in the digestive gland of the brown mussel *Perna perna* exposed to lead and paraquat. *Chem. Biol. Interact.* **2004**, *149*, 97–105. [CrossRef] [PubMed]
42. Newairy, A.S.; Abdou, H.M. Protective role of flax lignans against lead acetate induced oxidative damage and hyperlipidemia in rats. *Food Chem. Toxicol.* **2009**, *47*, 813–818. [CrossRef] [PubMed]
43. Mansouri, E.; Khorsandi, L.; Abedi, H.A. Antioxidant effects of proanthocyanidin from grape seed on hepatic tissue injury in diabetic rats. *Iran. J. Basic Med. Sci.* **2014**, *17*, 460–464. [PubMed]
44. Bártíková, H.; Boušová, I.; Jedličková, P.; Lněničková, K.; Skálová, L.; Szotáková, B. Effect of standardized cranberry extract on the activity and expression of selected biotransformation enzymes in rat liver and intestine. *Molecules* **2014**, *19*, 14948–14960. [CrossRef] [PubMed]
45. Fu, C.; Wang, H.; Ng, W.L.; Song, L.; Huang, D. Antioxidant activity and proanthocyanidin profile of *Selliguea feei* rhizomes. *Molecules* **2013**, *18*, 4282–4292. [CrossRef] [PubMed]

46. Kresty, L.A.; Howell, A.B.; Baird, M. Cranberry proanthocyanidins mediate growth arrest of lung cancer cells through modulation of gene expression and rapid induction of apoptosis. *Molecules* **2011**, *16*, 2375–2390. [CrossRef] [PubMed]
47. Li, S.; Xu, M.; Niu, Q.; Xu, S.; Ding, Y.; Yan, Y.; Guo, S.; Li, F. Efficacy of procyanidins against in vivo cellular oxidative damage: A systematic review and meta-analysis. *PLoS ONE* **2015**, *10*, e0139455. [CrossRef] [PubMed]
48. Zhang, X.S.; Ha, S.; Wang, X.L.; Shi, Y.L.; Duan, S.S.; Li, Z.A. Tanshinone IIA protects dopaminergic neurons against 6-hydroxydopamine-induced neurotoxicity through miR-153/NF-E2-related factor 2/antioxidant response element signaling pathway. *Neuroscience* **2015**, *303*, 489–502. [CrossRef] [PubMed]
49. Niu, Q.; Mu, L.; Li, S.; Xu, S.; Ma, R.; Guo, S. Proanthocyanidin Protects Human Embryo Hepatocytes from Fluoride-induced oxidative stress by regulating iron metabolism. *Biol. Trace Elem. Res.* **2016**, *169*, 174–179. [CrossRef] [PubMed]
50. Ye, F.; Li, X.; Li, L.; Lyu, L.; Yuan, J.; Chen, J. The role of Nrf2 in protection against Pb-induced oxidative stress and apoptosis in SH-SY5Y cells. *Food Chem. Toxicol.* **2015**, *86*, 191–201. [CrossRef] [PubMed]
51. Jeong, G.S.; Lee, D.S.; Li, B.; Byun, E.; Kwon, D.Y.; Park, H.; Kim, Y.C. Protective effect of sauchinone by up-regulating heme-oxygenase-1 via the P38 MAPK and Nrf2/ARE pathways in HepG2 cells. *Planta Med.* **2010**, *76*, 41–47. [CrossRef] [PubMed]
52. Krajka-Kuźniak, V.; Paluszczak, J.; Oszmiański, J.; Baer-Dubowska, W. Hawthorn (*Crataegus oxyacantha* L.) bark extract regulates antioxidant response element (ARE)-mediated enzyme expression via Nrf2 pathway activation in normal hepatocyte cell line. *Phytother. Res.* **2014**, *28*, 593–602. [CrossRef] [PubMed]
53. Borroz, K.I.; Buetler, T.M.; Eaton, D.L. Modulation of gamma-glutamylcysteine synthetase large subunit mRNA expression by butylated hydroxyanisole. *Toxicol. Appl. Pharmacol.* **1994**, *126*, 150–155. [CrossRef] [PubMed]
54. Jin, X.; Liu, Q.; Jia, L.; Li, M.; Wang, X. Pinocembrin attenuates 6-OHDA-induced neuronal cell death through Nrf2/ARE pathway in SH-SY5Y cells. *Cell. Mol. Neurobiol.* **2015**, *35*, 323–333. [CrossRef] [PubMed]
55. Shi, M.M.; Kugelman, A.; Iwamoto, T.; Tian, L.; Forman, H.J. Quinine-induced oxidative stress elevates glutathione and induces gamma-glutamylcysteine synthetase activity in rat lung epithelial L2 cells. *J. Biol. Chem.* **1994**, *269*, 26512–26517. [PubMed]
56. Wang, Y.; Fang, J.; Huang, S.; Chen, L.; Fan, G.; Wang, C. The chronic effects of low lead level on the expressions of Nrf2 and Mrp1 of the testes in the rats. *Environ. Toxicol. Pharmacol.* **2013**, *35*, 109–116. [CrossRef] [PubMed]
57. Ye, F.; Li, X.; Li, L.; Yuan, J.; Chen, J. t-BHQ provides protection against lead neurotoxicity via Nrf2/HO-1 pathway. *Oxid. Med. Cell. Longev.* **2016**, *2016*. [CrossRef] [PubMed]
58. Dewanjee, S.; Dua, T.K.; Khanra, R.; Das, S.; Barma, S.; Joardar, S.; Bhattacharjee, N.; Zia-Ul-Haq, M.; Jaafar, H.Z. Water Spinach, *Ipomoea aquatic* (Convolvulaceae), Ameliorates lead toxicity by inhibiting oxidative stress and apoptosis. *PLoS ONE* **2015**, *10*, e0139831. [CrossRef] [PubMed]
59. He, L.; Poblenz, A.T.; Medrano, C.J.; Fox, D.A. Lead and calcium produce rod photoreceptor cell apoptosis by opening the mitochondrial permeability transition pore. *J. Biol. Chem.* **2000**, *275*, 12175–12184. [CrossRef] [PubMed]
60. Yuan, G.; Dai, S.; Yin, Z.; Lu, H.; Jia, R.; Xu, J. Sub-chronic lead and cadmium co-induce apoptosis protein expression in liver and kidney of rats. *Int. J. Clin. Exp. Pathol.* **2014**, *7*, 2905–2914. [PubMed]
61. Abdel Moneim, A.E. *Indigofera oblongifolia* prevents lead acetate-induced hepatotoxicity, oxidative stress, fibrosis and apoptosis in rats. *PLoS ONE* **2016**, *11*, e0158965. [CrossRef] [PubMed]
62. Qian, Y.; Tiffany-Castiglioni, E. Lead-induced endoplasmic reticulum (ER) stress responses in the nervous system. *Neurochem. Res.* **2003**, *28*, 153–162. [CrossRef] [PubMed]

63. Zhang, Y.; Sun, L.G.; Ye, L.P.; Wang, B.; Li, Y. Lead-induced stress response in endoplasmic reticulum of astrocytes in CNS. *Toxicol. Mech. Methods* **2008**, *18*, 751–757. [CrossRef] [PubMed]
64. Liu, C.M.; Zheng, G.H.; Ming, Q.L.; Sun, J.M.; Cheng, C. Protective effect of quercetin on lead-induced oxidative stress and endoplasmic reticulum stress in rat liver via the IRE1/JNK and PI3K/Akt pathway. *Free Radic. Res.* **2013**, *47*, 192–201. [CrossRef] [PubMed]

nutrients

MDPI

Article

Black Tea Increases Circulating Endothelial Progenitor Cells and Improves Flow Mediated Dilatation Counteracting Deleterious Effects from a Fat Load in Hypertensive Patients: A Randomized Controlled Study

Davide Grassi [1,*], Richard Draijer [2], Casper Schalkwijk [3], Giovambattista Desideri [1], Anatolia D'Angeli [1], Sandro Francavilla [1], Theo Mulder [2] and Claudio Ferri [1]

1 Department of Life, Health, and Environmental Sciences, University of L'Aquila, Viale S Salvatore, Delta 6 Medicina, 67100 L'Aquila, Italy; giovambattista.desideri@cc.univaq.it (G.D.); anatolia79@katamail.com (A.D.); sandro.francavilla@univaq.it (S.F.); claudio.ferri@cc.univaq.it (C.F.)

2 Unilever Research and Development, 3133 AT Vlaardingen, The Netherlands; richard.draijer@unilever.com (R.D.); Theo.Mulder@unilever.com (T.M.)

3 Department of Internal Medicine, CARIM School for Cardiovascular Diseases, Maastricht University Medical Center, 6229 HX Maastricht, The Netherlands; c.schalkwijk@maastrichtuniversity.nl

* Correspondence: davide.grassi@cc.univaq.it; Tel.: +39-0862-434-747; Fax: +39-0862-434-749

Received: 13 September 2016; Accepted: 7 November 2016; Published: 16 November 2016

Abstract: (1) Background: Endothelial dysfunction predicts cardiovascular events. Circulating angiogenic cells (CACs) maintain and repair the endothelium regulating its function. Tea flavonoids reduce cardiovascular risk. We investigated the effects of black tea on the number of CACs and on flow-mediated dilation (FMD) before and after an oral fat in hypertensives; (2) Methods: In a randomized, double-blind, controlled, cross-over study, 19 patients were assigned to black tea (150 mg polyphenols) or a placebo twice a day for eight days. Measurements were obtained in a fasted state and after consuming whipping cream, and FMD was measured at baseline and after consumption of the products; (3) Results: Compared with the placebo, black tea ingestion increased functionally active CACs (36 $\pm$ 22 vs. 56 $\pm$ 21 cells per high-power field; $p = 0.006$) and FMD (5.0% $\pm$ 0.3% vs. 6.6% $\pm$ 0.3%, $p < 0.0001$). Tea further increased FMD 1, 2, 3, and 4 h after consumption, with maximal response 2 h after intake ($p < 0.0001$). Fat challenge decreased FMD, while tea consumption counteracted FMD impairment ($p < 0.0001$); (4) Conclusions: We demonstrated the vascular protective properties of black tea by increasing the number of CACs and preventing endothelial dysfunction induced by acute oral fat load in hypertensive patients. Considering that tea is the most consumed beverage after water, our findings are of clinical relevance and interest.

Keywords: black tea; flavonoids; endothelial function; circulating endothelial cells; hypertension

1. Introduction

Hypertension is the leading risk factor for cardiovascular morbidity and mortality [1]. Several key mechanisms, including inflammation oxidative stress and endothelial dysfunction, play an important role in cardiovascular risk in late-life hypertension [1,2]. Over the past 25 years, a large body of clinical evidence has indicated a close relationship between the degree of endothelial dysfunction and clinical cardiovascular events in patients with cardiovascular risk factors, coronary heart disease, or both [3–9]. As a consequence, it has also been hypothesized that the reversal of endothelial dysfunction might slow down atherogenesis and improve individual cardiovascular prognosis [6–9].

Moreover, recent studies have shown that risk factors for vascular diseases are associated with a blunted capacity for repair of the endothelial damage evidenced by a dysfunction of bone marrow-derived circulating endothelial progenitor cells (EPCs) [10]. Indeed, a reduced ability of EPCs to proliferate ex vivo and to express an endothelial phenotype is associated with risk factors for coronary artery disease as well as endothelial dysfunction [10,11]. Cells grown under these conditions were formerly termed "early EPCs", but are currently referred to as "circulating angiogenic cells" (CACs) [12,13]. CAC quantity and function are robust biomarkers of vascular risk for a multitude of diseases, particularly cardiovascular disease. Importantly, infused ex vivo-expanded CACs have shown a potential for improved endothelial function, either reducing the risk of events or enhancing recovery from ischemia [10–14].

Among various risk factors, hypertension is shown to be the strongest predictor of CAC migratory impairment [14]. Indeed, CACs serve as a cellular reservoir to replace dysfunctional endothelium and to form a cellular patch at the site of denuding injury [10–14].

Epidemiological studies have shown an inverse correlation between flavonoid-rich diets and cardiovascular disease [15,16]. Tea accounts for a major proportion of total flavonoid intake in a number of Western countries [15–17]. Increasing attention is currently being paid to the link between tea ingestion and a suggested lower incidence of cardiovascular events [16,17].

Some dietary intervention studies reported that both acute and chronic [18–20] black tea consumption increases NO-mediated flow-mediated dilation (FMD) in healthy volunteers as well as in patients with cardiovascular disease. In response to this, we performed a dose-finding study with black tea, showing that the daily consumption of even a single cup of tea (100 mg tea flavonoids) per day increased the FMD of healthy volunteers, and improving further with escalating dose [20].

In contrast, previous studies have shown that a meal rich in fat decreases FMD and negatively modifies vascular function [21,22]. However, the effects of tea on endothelial function under these challenging conditions has not been completely clarified. Indeed, Hodgson et al. [23], aiming to evaluate only the acute effects of tea compared with hot water in pharmacologically treated patients with coronary artery disease aged between 45 and 70 years, suggested that a mixed meal with tea was able to improve endothelium-dependent dilatation, but tea alone was not able to positively affect this parameter. We recently reported that black tea consumption lowered wave reflections and blood pressure in the fasting state and, during the challenging hemodynamic conditions after a fat load, in hypertensives [24]. The effects of high doses of green tea (1 L per day) on CACs have been reported for chronic heavy smokers [25], but could not be confirmed in patients with chronic renal failure [26]. However, the effects of black tea when consumed at a moderate dose on the number of CACs have not been examined. Therefore, the aim of the present study was to investigate the effects of black tea on endothelial function before and after an oral fat load and the number of functionally active CACs in a group of never-treated grade I essential hypertensives without additional cardiovascular risk factors.

2. Methods

2.1. Subjects

Nineteen never-treated hypertensive patients (7 males and 12 females; mean age $\pm$ standard deviation 51.5 $\pm$ 8.4 years) referring to our outpatient unit were recruited. Entry criteria were $\geq$18 and $\leq$75 years of age; systolic BP (SBP) between 140 and 159 mmHg or diastolic BP (DBP) between 90 to 99 mmHg; body mass index between 18 and 30 kg/m^2. Individuals were excluded if they had an acute or chronic disease, including any type of metabolic abnormality, a major cardiovascular risk factor, or both. Patients on prescribed medication or dietary supplements within two weeks of entering the study as well as habitual smokers were excluded. Female participants not in a post-menopausal phase were also excluded. To further limit potential confounding factors, individuals were excluded if they reported daily intense sports activities (10 h/week), changes of 10% body weight within 6 months of entering the study, a current dietary treatment regimen, or participation in another clinical study

within 3 months of entering this trial. The local Ethics Committee of L'Aquila approved the study on 20 December 2007 (ref: 53/2007), all clinical investigation have been conducted according to the principles expressed in the Declaration of Helsinki, and all participants gave written informed consent. Some of the study results have been previously reported [24].

2.2. Diagnosis of Arterial Hypertension

Grade I essential hypertension was diagnosed according to the European Societies of Hypertension and Cardiology criteria [27]. For this purpose, before enrollment into the study, BP and heart rate were measured after 10 min in a seated position in a comfortable room. SBP/DBP for inclusion in the protocol were 140/90 and 160/100 mmHg on 4 visits performed at 1-week intervals. During each visit, BP was measured in quadruplicate with an oscillometric device (Omron 705 CP, Omron) at 2 min intervals. The first BP reading was discarded, and the average of the last 3 measurements recorded. On each occasion, BP was recorded by the same physician who was unaware of the study design, objectives, and results (i.e., was not a member of the research team). Secondary hypertension was excluded by clinical examination and appropriate tests.

2.3. Study Design

Participants were randomly assigned to consume a hot beverage containing 150 mg tea flavonoids or a placebo twice a day for eight days in a double-blind, cross-over design. During the two 8-day periods when the volunteers consumed the test products, they were asked to refrain from consuming tea, red wine, chocolate-based products, dietary supplements, and non-steroidal anti-inflammatory drugs (prostaglandin synthetase inhibitors). The wash-out period between the two treatments was 13 days. Vascular function was assessed on Day 7 of the intervention and was repeated on Day 8 with an oral fat load. Pre-weighted portions of the test products were supplied to the volunteers in coded sachets made from laminated aluminum foil. Compliance was checked by a questionnaire. Volunteers consumed two doses per day: approximately one hour before lunch and one hour before dinner. They were carefully instructed to add the contents of a sachet to 100–200 mL of boiling hot water and to stir the solution until the powder was completely dissolved. An addition of sugar, milk, lemon, etc. was not allowed. The product was consumed while it was still hot. On test days, the volunteers consumed the test product at the facility at the beginning of the test sequence ($t = 0$).

The composition of the products is given in Table 1. Before the start of the study and after the first visit to the test facility, volunteers received the intervention products. The number of returned empty sachets was used to check compliance. On the morning of Day 7 and Day 8 of the two test periods, volunteers came to the facility early in the morning in a fasted state. On both days, baseline FMD measurements were performed. Volunteers were subsequently asked to consume their morning dose of the test product. On Day 7, all measurements were performed in a fasted state; on Day 8, volunteers consumed ultra-heat-treated whipping cream (1 g fat per kg bodyweight; for 100 mL of product: 27 g of fats, 12.6 g of carbohydrates, 2.1 g of proteins; energy value 302 kcal) approximately 30 min after consuming the test product. The range of energy intakes was between 649 and 951 kcal. On Day 7, FMD was performed before ($t = 0$) and 1, 2, 3, and 4 h after consumption of the test product in a supine position in a quiet, temperature-controlled (22 °C–24 °C) room by trained, certified staff who were blind to the study protocol. This procedure was repeated on Day 8, but with a fat load. The study (participant recruitment and follow-up) was conducted between 1 March 2008 and 1 March 2011. The study was stopped from April 2009 to May 2010 due to the earthquake that occurred in L'Aquila. The trial has been registered under number ISRCTN27687092 (http://www.isrctn.com/ISRCTN27687092).

Table 1. Composition of the test products (mg per dose).

	Placebo	Tea
Tea solids	0	497.5
Polyphenols	0	150
Catechins	0	12.1
Theaflavins	0	5.0
Gallic acid	0	4.5
Caffeine	37.3	37.3
Theanine	0	9.1
Caramel colour	90	0
Tea flavor	10	0
Sucrose	1363	1403
Total weight of sachet	1500	1900

2.4. Endothelial Function

FMD of the brachial artery was measured before (baseline, t = 0) and 1, 2, 3, and 4 h after the tea intake during each scheduled visit. FMD of the brachial artery was assessed after 15 min at rest. FMD was always determined by the same physician, who was blinded to the study design and objectives. FMD of the brachial artery of the dominant arm was measured by ultrasonography (General Electric). The transducer was held at the same point throughout the scan by a stereotactic clamp. The arterial diameter was measured at approximately 5–10 cm above the elbow. After a 1 min baseline measurement, a cuff placed at the forearm below the elbow was inflated at 300 mmHg for 5 min and then released, resulting in a brief period of reactive hyperemia. The maximal dilation of the brachial artery was measured. The brachial artery diameter changes in response to increased blood flow were assessed for a further 3 min after cuff deflation. Using the FMDStudio system (QUIPU, Pisa, Italy) [28–31], the approximate position of the edges of the vessel was manually located before starting the examination. After this procedure, an automatic mathematical contour tracking operator locates and tracks the edges, supplying information about quality and the time course of measurements in real time [28–31]. Upon completion of the analysis, the device automatically generated a report with all recorded measurements. FMD is expressed as a percentage change from the baseline diameter. Endothelium-dependent vasodilation was considered the maximal dilation of the brachial artery induced by the increased flow [28–31].

2.5. Ex Vivo Expansion Assay and Characterization of CACs

Mononuclear cells (MNCs) were isolated using Ficoll density-gradient centrifugation from 20 mL of peripheral blood. MNCs washed three times in PBS and resuspended in an EBM-2 bullet kit (Cambrex Bio Science, Milano, Italy), supplemented with 20% fetal bovine serum (FBS) (Celbio, Milano, Italy), were seeded at 106 cells/cm^2 on fibronectin-coated culture plates 24 wells (Becton Dickinson, Milano, Italy). After 4 days of culture at 37 °C and 5% CO_2, the non-adherent cells were discarded by washing with phosphate buffer saline (PBS) (Celbio, Milano, Italy), while the adherent cells were maintained in culture for another three days and then underwent cytochemical analysis. Adherent cells were incubated with 1,1′-dioctadecyl-3,3,3′,3′-tetramethyl indocarbocyanine-labeled acetylated low-density lipoprotein (DiLDL) (Invitrogen, Milano, Italy) at a concentration of 2.4 μg/mL for 1 h at 37 °C. Cells were then fixed in 1% paraformaldehyde for 10 min and incubated with fluorescein isothiocyanate (FITC)-labeled Ulex europaeus agglutinin I (Sigma-Aldrich, Milano, Italy) at a concentration of 10 μg/mL for 1 h. Dual-staining cells positive for both DiLDL- and FITC-labelled UEA-1 were judged as functional CACs and were counted [13,32]. CACs were counted manually in 10 randomly selected microscopic fields by two independent investigators with an inverted fluorescence microscope (magnification ×20 times) (Zeiss, Oberkoken, Germany).

2.6. Haematochemistry and Blood Lipids

In all individuals, a routine hematochemical check was performed by standard methods after each active treatment phase. Fasting plasma glucose and insulin, serum total cholesterol, high-density lipoprotein (HDL) cholesterol, low-density lipoprotein (LDL) cholesterol, and triglyceride levels were assessed in the clinical chemistry laboratory using routine procedures. Plasma glucose and insulin values were used to calculate the index of insulin resistance, the homeostasis model assessment of insulin resistance (HOMA-IR) [24].

2.7. Biomarkers of Endothelial Dysfunction and Low-Grade Inflammation

Biomarkers of endothelial dysfunction (soluble vascular cell adhesion molecule 1 (sVCAM-1), soluble endothelial selectin (sE-selectin), and soluble intercellular adhesion molecule 1 (ICAM-1)) and of low-grade inflammation (C-reactive protein (CRP), serum amyloid A (SAA), interleukin (IL)-6, IL-8, IL1-β, tumor necrosis factor α (TNF-α), and sICAM-1) were measured via a multiarray detection system based on electrochemiluminescence technology (Meso Scale Discovery) in fasting EDTA plasma samples as previously described [33]. Endothelin-1 was measured by Elisa (R & D, R & D systems, Abingdon, UK).

2.8. Statistical Evaluation

Size of the Study Population

The power calculation was based on the change in FMD between the placebo and the active in the fasted state. Calculations were based on FMD data from a cross-over study in 60 slightly hypertensive subjects. FMD was measured at the end of each of the three interventions that each lasted for 4 weeks. The power calculation was based on an average FMD = 8.10%, within subject variance = 1.79% found in this study [20]. In the dose-finding study, a mean effect of 1.80% was detected at 400 mg/day of tea flavonoids, and the same effect was expected in the current study [20]. Based on these data, a group of 18 volunteers was required to detect a 1.8% difference between the placebo and the intervention (2-sided, alpha 0.05, and power 0.80). In order to account for a 10% drop-out, we included 20 volunteers. A randomization scheme was prepared by a statistician using computer generated random numbers. Randomization was done before the start of the study by assigning treatment orders to subject numbers with a block size of two and an allocation ratio of 1:1. Sachets with the test products were labeled with subject number and treatment period. Treatments were supplied in sealed in envelopes labeled with the subject number. These were opened in consecutive order by each participant. Participants, statisticians, care providers, and those assessing the outcome of the study were all blinded. The black tea and the placebo were as similar as possible in taste and appearance.

Data analysis was performed using the SAS software (SAS Institute, Cary, NC, USA, version 9.1). Descriptive analysis consisting of distribution statistics (number of available observations, mean and standard deviations) were presented for continuous data. Differences between the experimental groups and the placebo of the acute effect after one week intervention were evaluated by means of an analysis of covariance, integrating the data of 1, 2, 3, and 4 h after test product ingestion. The statistical model included the covariables baseline (t = 0), gender, age, and BMI. Fixed factors included in the model include treatment, period, day, time, and all their interactions. Other interactions in the model include baseline–treatment, baseline–period, and baseline–time. The chronic effects, after one week intervention, were calculated from the baseline data using a similar model, without the baseline covariable.

The influence of the interventions was assessed within each individual. Therefore, the variation due to the differences between individuals was separated from the relevant error variance in the analysis. A Dunnett test was performed in order to correct for multiple testing between the active treatment and the placebo with and without a fat load. The statistical analysis results are presented as LSmeans ± standard error (SE) or median (interquartile range) for data with a skewed distribution (plasma biomarkers). Statistical tests are two-sided for all analyses with a significance level of 0.05.

3. Results

Baseline characteristics of the study participants are given in Table 2.

Of the 20 individuals enrolled, 19 completed the study. One individual dropped out due to personal circumstances and was excluded from the statistical analysis. Compliance was 100% in all the volunteers for all the study phases.

Table 2. General characteristics of the study population (mean ± SD).

Characteristic	Value
Number of subjects (total/males)	19/5
Age (years)	51.3 ± 8.2
BMI (kg/m^2)	27.1 ± 1.2
Body weight (kg)	73.7 ± 7.2
LDL-cholesterol (mg/dL)	141.1 ± 27.3
HDL-cholesterol (mg/dL)	45.7 ± 8.2
Triglycerides (mg/dL)	116.8 ± 38.1
Plasma glucose (mg/dL)	86.8 ± 7.3
Plasma insulin (μU/mL)	11.3 ± 5.4

3.1. Endothelial Function

Compared with the placebo, one week of black tea ingestion increased baseline FMD (Day 7: 5.0% ± 0.25% vs. 6.8% ± 0.25%; Day 8: 5.2% ± 0.24% vs. 7.0% ± 0.24%; $p < 0.0001$ for both (Figure 1A,B). On Day 7, acute black tea administration additionally increased FMD (from 6.8% to 7.5%, 7.8% and 7.2% $p < 0.0001$) at 1, 2, and 3 h after intake, respectively. No significant changes were observed after acute placebo administration. On Day 8, in the placebo group, FMD fell from 5.2% at baseline to 4.4%, 4.1%, 4.4%, and 4.8% at 1, 2, 3, and 4 h ($p < 0.0001$), respectively, after the fat load (Figure 1B). This drop in FMD was almost completely prevented by concomitant intake of tea (Figure 1B).

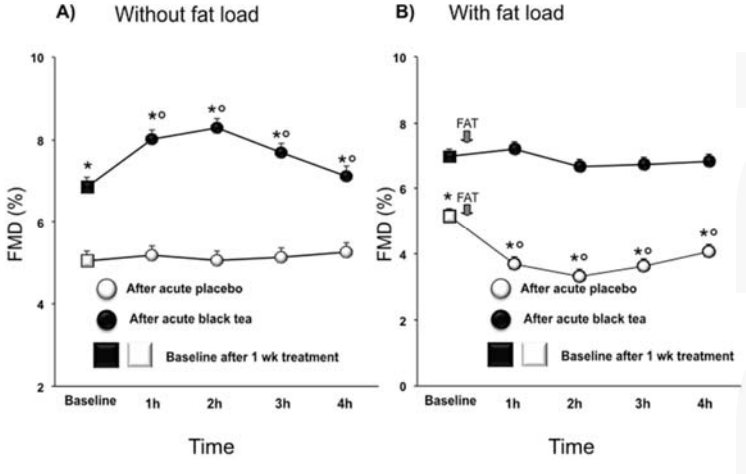

Figure 1. Effect of a 1 week placebo (**white**) and black tea (**black**) administration on baseline (square) values (**A**,**B**) of flow-mediated dilation (FMD) and acute effects without and with fat load (**A**,**B**). Data are presented as LSmeans ± SE. In all panels, vertical lines indicate SE, and asterisks (*) indicate significant differences with respect to the placebo phase (**A**,**B**), while circles (°) indicate significant differences from the baseline values (**A**,**B**). Differences are considered significant when $p < 0.05$.

3.2. Functional CACs

Compared with the placebo, the number of functionally active CACs indicated as double positive cells per high-power field was significantly higher after black tea intake (black tea mean: 56.0 ± 21; placebo mean: 36 ± 22 number of cells per field; $p = 0.006$) (Figure 2).

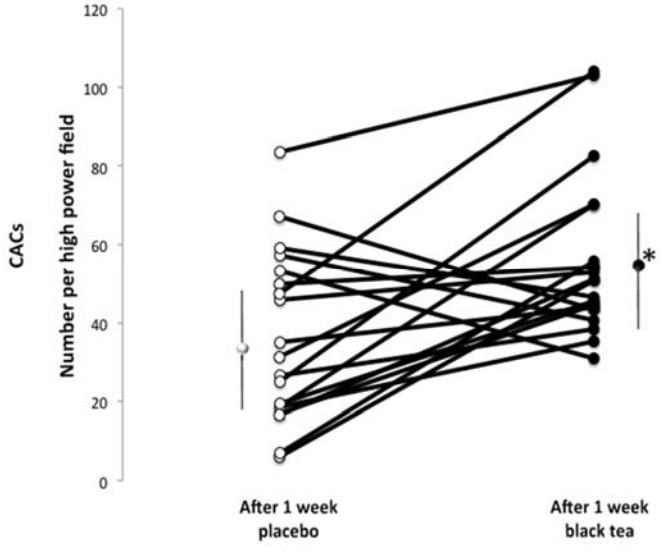

Figure 2. Absolute numbers of functional circulating angiogenic cells (CACs) per high-power field fluorescence microscopy (×20) before and after 1 week of treatment with placebo (**white**) and black tea (**black**) administration. Data are presented as LSmeans ± SE. Vertical lines indicate SD, and asterisks (*) indicate significant differences with respect to the placebo phase. Differences are considered significant when $p < 0.05$.

3.3. Plasma Lipoproteins, Glucose, Insulin, and Biomarkers

No significant differences were observed between the two treatments for plasma concentrations of biomarkers of endothelial dysfunction and low-grade inflammation (Table 3) and lipoproteins, glucose, and insulin (Table 4).

Table 3. Plasma concentrations of biomarkers of endothelial dysfunction and low-grade inflammation.

	CRP (mg/L)	**SAA (mg/L)**	**sICAM (ng/mL)**	**IL-1ß (ng/L)**	**IL-6 (ng/L)**	**IL-8 (ng/L)**	**TNF-α (ng/L)**	**sVCAM (ng/mL)**	**E-sel (ng/mL)**	**ET-1 (ng/L)**
Placebo	1.6 0.1–12.2	1.6 0.4–8.9	211 132–311	1.5 0.2–19.6	2.3 0.3–19.4	12.5 0.3–2788	9.8 4.7–25.5	320 163–598	158 35–480	1.4 0.8–2.3
Tea	0.9 0.1–16.1	1.6 0.3–11.4	201 150–253	1.7 0.2–17.0	2.5 0.7–7.8	8.9 0.5–696	10.8 6.0–18.4	337 180–576	125 55–347	1.5 1.0–2.1

Values are presented as median with 1st and 3rd quartile due to skewed nature of the data (not normal distributed). EDTA-plasma samples were derived from fasted blood samples. Values are not significantly different ($p > 0.1$) between interventions. CRP: C-reactive protein; SAA: serum amyloid A; sICAM: soluble intercellular adhesion molecule 1; IL-1β: Interleukin-1β; IL-6: interleukin-6; IL-8: interleukin-8; TNF-α: tumor necrosis factor α; sVCAM: soluble vascular adhesion molecule 1; E-sel: E-selectin; ET-1: endothelin-1.

Table 4. Plasma concentrations of lipoproteins, glucose, insulin, and biomarkers.

	TC (mg/dL)	LDL (mg/dL)	HDL (mg/dL)	TG (mg/dL)	Glucose (mg/dL)	Insulin (mU/L)
Placebo	211.1 ± 4.3	144.9 ± 4.1	46.1 ± 2.0	112.7 ± 7.8	86.8 ± 1.4	11.9 ± 0.9
Tea	208.9 ± 4.3	138.5 ± 4.1	45.3 ± 2.0	119.5 ± 7.8	86.8 ± 1.4	10.5 ± 0.9

Values are in LSmeans ± SE. EDTA-plasma samples were derived from fasted blood samples. Values are not significantly different ($p > 0.1$) between interventions. TC: total cholesterol; LDL: low-density lipoprotein; HDL: high-density lipoprotein; TG: triglycerides.

4. Discussion

Our study showed that, in grade I hypertensive patients, one-week consumption of black tea resulted in a significant improvement in endothelium-dependent FMD, with maximal response two hours after acute intake. This effect was observed with a moderate dose, the equivalent of two cups of tea per day. Moreover, the consumption of tea counteracted a fat challenge-induced impairment of FMD. The protective properties of tea were also reflected by a significantly increased number of CACs, circulating cells capable of repairing the vessel wall. These results suggest that the consumption of tea may improve or even protect endothelial function under challenge conditions.

Vascular endothelial dysfunction is determined by both genetic and environmental factors that cause decreased bioavailability of the vasodilator nitric oxide (NO). Under physiologic conditions, the endothelium regulates vascular tone via the balanced production of vasodilating substances such as NO. Impaired endothelium-dependent vasodilation has been reported after a fat load, probably by an increased production of oxygen-derived free radicals and a quenching of NO [22,34]. In particular, it has been observed [34] that acute fat load administered orally or intravenously significantly increased BP, impaired endothelial function, and activated the sympathetic nervous system via mechanisms not likely depending on changes in leptin, glucose, and insulin levels in obese healthy subjects. Thus, fat load has deleterious hemodynamic effects on obese subjects as well as on other conditions of cardiovascular risk, which may be involved in endothelial function [34,35]. Nevertheless, the effect of a high fat meal on endothelial function is not completely clear cut; indeed, Hodgson et al. [23] showed that a mixed meal with tea was able to improve endothelium-dependent dilatation, but tea alone was not able to positively affect this parameter. However, that study only evaluated the acute effects of tea compared with hot water, with a mixed meal (not specifically a fat load) in pharmacologically treated patients (with a number of putative confounding treatments: the use of aspirin, statins, or specific antihypertensive medications including angiotensin-converting enzyme inhibitors, angiotensin II receptor blockers, beta-blockers, calcium channel entry blockers, and diuretics) at very high cardiovascular risk (with coronary artery disease) aged between 45 and 70 years.

The increased FMD in fasted conditions and preserved postprandial FMD after tea intake may explain our observed findings on BP and arterial hemodynamics as described previously [23]. Taken together, our findings imply that the oral fat load may lead to a transient loss of NO bioavailability and transient vascular damage reflected in endothelial dysfunction and increased peripheral vascular tone and arterial stiffness.

The severity of endothelial dysfunction correlates with the development of coronary artery disease and predicts future cardiovascular events [3–8]. Thus, endothelial dysfunction may be considered a strategic target in the treatment of hypertension. The flavonoids in tea may increase or preserve the bioavailability of NO by decreasing the formation or scavenging of reactive oxygen and nitrogen species, increasing NO synthase activity, or both [16]. Besides the functionality of the endothelium, the morphologic integrity of the monolayer constituted by resident vascular endothelial cells plays a pivotal role in the maintenance of a number of vascular functions [36]. Anatomical or functional interruption continuity of the endothelial barrier is considered a fundamental step during the atherogenetic process [36]. The integrity of the vascular endothelial barrier is continuously maintained by the rapid migration of resident endothelial cells toward wounded areas of the

endothelium [35]. In addition to the migratory capability of resident vascular endothelial cells neighboring a damaged area, a growing body of evidence suggests that CACs also play a critical role in restoring the integrity of the endothelial monolayer [36]. Cardiovascular risk factors are associated with a reduced number of CACs [36], whereas, in turn, statins, angiotensin-converting enzyme inhibitors, and angiotensin II type 1 receptor blockers have been reported to increase the number of CACs [36]. Low levels of CACs in patients with increasing cardiovascular risk, such as hypertension, could have several mechanistic causes [10,11,14]. The most likely mechanism affected by tea flavonoids is the counteraction of oxidative stress, increasing NO bioavailability and FMD and decreasing BP levels in grade I hypertensive patients [24]. This hypothesis is supported by a study of Hill et al. [10] reporting a strong correlation between the number of CACs and the subjects' combined Framingham risk factor score ($r = -0.47$). Further, measurement of FMD also revealed a significant relationship between endothelial function and the number of EPCs ($r = 0.59$, $p < 0.001$), where the level of CACs was a better predictor of vascular reactivity than the presence or absence of conventional cardiovascular risk factors [10]. In addition, CACs from subjects at high risk for cardiovascular events had higher rates of in vitro senescence than cells from subjects at low risk. A study by Bocchio et al. [30] showed that the number of CACs was significantly reduced in patients with cardiovascular risk compared with controls ($p < 0.0001$). The percentage variation of CACs and of FMD after treatment was significantly associated with the presence of endothelial dysfunction at baseline. The close relationship between FMD and the number of CACs may be explained by the important role of eNOS in the mobilization of progenitor cells from bone marrow [37].

A number of biomarkers were analyzed in this study in an attempt to provide more mechanistic insight; however, as blood lipids and markers of endothelial dysfunction and low-grade inflammation were not modified by the intervention, these results do not provide links to potential underlying mechanisms.

The finding that tea improves FMD and increases the number of CACs has previously been reported by Kim et al. [25]. They observed in smokers that circulating and cultured angiogenic cells increased rapidly two weeks after green tea consumption. FMD correlated with CAC counts ($r = 0.67$) before and after treatment ($r = 0.60$). Of note, the flavonoid dose used by Kim et al. [24] was about three times higher than in the present study, and their study did not have a placebo group. Our hypothesis is that flavonoids in black tea increase the functionally active CACs numbers by the activation of eNOS, increasing NO bioavailability and concomitantly increasing FMD.

5. Conclusions

Therefore, the consumption of black tea in moderation improved FMD under fasted conditions and preserved FMD under postprandial conditions in hypertensive patients. The number of CACs doubled after the consumption of tea. Increased eNOS activity and NO bioavailability may be a common factor affected by tea flavonoids that explain both phenomena. Considering that tea is the most consumed beverage after water, our findings are of clinical relevance and interest, and our observations may have an impact on human health with important clinical consequences.

Acknowledgments: The study was supported by funding received from Unilever R & D Vlaardingen, The Netherlands.

Author Contributions: All authors conceived and designed the experiments; D.G. and G.D. performed the experiments; D.G., R.D., C.S., S.F., A.D., C.F., and T.M. analyzed the data; D.G., C.S., S.F., A.D., C.F., and T.M. contributed reagents/materials/analysis tools; D.G., R.D., C.S., and T.M. wrote the paper.

Conflicts of Interest: Authors did not receive grants. R.D. and T.M. are employed by the Unilever R & D Vlaardingen, The Netherlands. D.G., C.S., G.D., A.D., S.F., and C.F. had no personal or financial conflict of interest.

References

1. Ezzati, M.; Oza, S.; Danaei, G.; Murray, C.J. Trends and cardiovascular mortality effects of state-level blood pressure and uncontrolled hypertension in the United States. *Circulation* **2008**, *117*, 905–914. [CrossRef] [PubMed]

2. Struijker Boudier, H.A.; Cohuet, G.M.; Baumann, M.; Safar, M.E. The heart, macrocirculation and microcirculation in hypertension: A unifying hypothesis. *J. Hypertens. Suppl.* **2003**, *21*, S19–S23. [CrossRef] [PubMed]
3. Deanfield, J.E.; Halcox, J.P.; Rabelink, T.J. Endothelial function and dysfunction: Testing and clinical relevance. *Circulation* **2007**, *115*, 1285–1295. [PubMed]
4. Grassi, D.; Desideri, G.; Ferri, C. Cardiovascular risk and endothelial dysfunction: The preferential route for atherosclerosis. *Curr. Pharm. Biotechnol.* **2011**, *12*, 1343–1353. [CrossRef] [PubMed]
5. Anderson, T.J.; Uehata, A.; Gerhard, M.D.; Meredith, I.T.; Knab, S.; Delagrange, D.; Lieberman, E.H.; Ganz, P.; Creager, M.A.; Yeung, A.C.; et al. Close relation of endothelial function in the human coronary and peripheral circulations. *J. Am. Coll. Cardiol.* **1995**, *26*, 1235–1241. [CrossRef]
6. Yeboah, J.; Crouse, J.R.; Hsu, F.C.; Burke, G.L.; Herrington, D.M. Brachial flow-mediated dilation predicts incident cardiovascular events in older adults: The Cardiovascular Health Study. *Circulation* **2007**, *115*, 2390–2397. [CrossRef] [PubMed]
7. Halcox, J.P.; Donald, A.E.; Ellins, E.; Witte, D.R.; Shipley, M.J.; Brunner, E.J.; Marmot, M.G.; Deanfield, J.E. Endothelial function predicts progression of carotid intima-media thickness. *Circulation* **2009**, *119*, 1005–1012. [CrossRef] [PubMed]
8. Modena, M.G.; Bonetti, L.; Coppi, F.; Bursi, F.; Rossi, R. Prognostic role of reversible endothelial dysfunction in hypertensive postmenopausal women. *J. Am. Coll. Cardiol.* **2002**, *40*, 505–510. [CrossRef]
9. Charakida, M.; Masi, S.; Loukogeorgakis, S.P.; Deanfield, J.E. The role of flow-mediated dilatation in the evaluation and development of antiatherosclerotic drugs. *Curr. Opin. Lipidol.* **2009**, *20*, 460–466. [CrossRef] [PubMed]
10. Hill, J.M.; Zalos, G.; Halcox, J.P.; Schenke, W.H.; Waclawiw, M.A.; Quyyumi, A.A.; Finkel, T. Circulating endothelial progenitor cells vascular function, and cardiovascular risk. *N. Engl. J. Med.* **2003**, *348*, 593–600. [CrossRef] [PubMed]
11. Werner, N.; Kosiol, S.; Schiegl, T.; Ahlers, P.; Walenta, K.; Link, A.; Böhm, M.; Nickenig, G. Circulating endothelial progenitor cells and cardiovascular outcomes. *N. Engl. J. Med.* **2005**, *353*, 999–1007. [CrossRef] [PubMed]
12. Urbich, C.; Dimmeler, S. Endothelial progenitor cells. Characterization and role in vascular biology. *Circ. Res.* **2004**, *95*, 343–353. [CrossRef] [PubMed]
13. Rehman, J.; Li, J.; Orschell, C.M.; March, K.L. Peripheral blood "endothelial progenitor cells" are derived from monocyte/macrophages and secrete angiogenic growth factors. *Circulation* **2003**, *107*, 1164–1169. [CrossRef] [PubMed]
14. Vasa, M.; Fichtlscherer, S.; Aicher, A.; Adler, K.; Urbich, C.; Martin, H.; Zeiher, A.M.; Dimmeler, S. Number and migratory activity of circulating endothelial progenitor cells inversely correlate with risk factors for coronary artery disease. *Circ. Res.* **2001**, *89*, E1–E7. [CrossRef] [PubMed]
15. Geleijnse, J.M.; Launer, L.J.; Van der Kuip, D.A.; Hofman, A.; Witteman, J.C. Inverse association of tea and flavonoid intakes with incident myocardial infarction: The Rotterdam Study. *Am. J. Clin. Nutr.* **2002**, *75*, 880–886. [PubMed]
16. Grassi, D.; Aggio, A.; Onori, L.; Croce, G.; Tiberti, S.; Ferri, C.; Ferri, L.; Desideri, G. Tea, flavonoids, and nitric oxide-mediated vascular reactivity. *J. Nutr.* **2008**, *138*, 1554S–1560S. [PubMed]
17. Bravo, L. Polyphenols: Chemistry, dietary sources, metabolism, and nutritional significance. *Nutr. Rev.* **1998**, *56*, 317–333. [CrossRef] [PubMed]
18. Duffy, S.J.; Keaney, J.F.; Holbrook, M.; Gokce, N.; Swerdloff, P.L.; Frei, B.; Vita, J.A. Short- and long-term black tea consumption reverses endothelial dysfunction in patients with coronary artery disease. *Circulation* **2001**, *104*, 151–156. [CrossRef] [PubMed]
19. Hodgson, J.M.; Puddey, I.B.; Burke, V.; Watts, G.F.; Beilin, L.J. Regular ingestion of black tea improves brachial artery vasodilator function. *Clin. Sci.* **2002**, *102*, 195–201. [CrossRef] [PubMed]
20. Grassi, D.; Mulder, T.P.; Draijer, R.; Desideri, G.; Molhuizen, H.O.; Ferri, C. Black tea consumption dose-dependently improves flow-mediated dilation in healthy males. *J. Hypertens.* **2009**, *27*, 774–781. [CrossRef] [PubMed]
21. Rudolph, T.K.; Ruempler, K.; Schwedhelm, E.; Tan-Andresen, J.; Riederer, U.; Böger, R.H.; Maas, R. Acute effects of various fast-food meals on vascular function and cardiovascular disease risk markers: The Hamburg Burger Trial. *Am. J. Clin. Nutr.* **2007**, *86*, 334–340. [PubMed]

22. Gosmanov, A.R.; Smiley, D.D.; Robalino, G.; Siquiera, J.; Khan, B.; Le, N.A.; Patel, R.S.; Quyyumi, A.A.; Peng, L.; Kitabchi, A.E.; et al. Effects of oral and intravenous fat load on blood pressure, endothelial function, sympathetic activity, and oxidative stress in obese healthy subjects. *Am. J. Physiol. Endocrinol. Metab.* **2010**, *299*, E953–E958. [CrossRef] [PubMed]
23. Hodgson, J.M.; Burke, V.; Puddey, I.B. Acute effects of tea on fasting and postprandial vascular function and blood pressure in humans. *J. Hypertens.* **2005**, *23*, 47–54. [CrossRef] [PubMed]
24. Grassi, D.; Draijer, R.; Desideri, G.; Mulder, T.; Ferri, C. Black tea lowers blood pressure and wave reflections in fasted and postprandial conditions in hypertensive patients: A randomised study. *Nutrients* **2015**, *7*, 1037–1051. [CrossRef] [PubMed]
25. Kim, W.; Jeong, M.H.; Cho, S.H.; Yun, J.H.; Chae, H.J.; Ahn, Y.K.; Lee, M.C.; Cheng, X.; Kondo, T.; Murohara, T.; et al. Effect of green tea consumption on endothelial function and circulating endothelial progenitor cells in chronic smokers. *Circ. J.* **2006**, *70*, 1052–1057. [CrossRef] [PubMed]
26. Park, C.S.; Kim, W.; Woo, J.S.; Ha, S.J.; Kang, W.Y.; Hwang, S.H.; Park, Y.W.; Kim, Y.S.; Ahn, Y.K.; Jeong, M.H.; et al. Green tea consumption improves endothelial function but not circulating endothelial progenitor cells in patients with chronic renal failure. *Int. J. Cardiol.* **2010**, *145*, 261–262. [CrossRef] [PubMed]
27. Mancia, G.; De Backer, G.; Dominiczak, A.; Cifkova, R.; Fagard, R.; Germano, G.; Grassi, G.; Heagerty, A.M.; Kjeldsen, S.E.; Laurent, S.; et al. 2007 Guidelines for the Management of Arterial Hypertension: The Task Force for the Management of Arterial Hypertension of the European Society of Hypertension (ESH) and of the European Society of Cardiology (ESC). *J. Hypertens.* **2007**, *25*, 1105–1187. [CrossRef] [PubMed]
28. Corretti, M.C.; Anderson, T.J.; Benjamin, E.J.; Celermajer, D.; Charbonneau, F.; Creager, M.A.; Deanfield, J.; Drexler, H.; Gerhard-Herman, M.; Herrington, D.; et al. Guidelines for the ultrasound assessment of endothelial-dependent flow-mediated vasodilation of the brachial artery: A report of the International Brachial Artery Reactivity Task Force. *J. Am. Coll. Cardiol.* **2002**, *39*, 257–265. [CrossRef]
29. Grassi, D.; Desideri, G.; Necozione, S.; Ruggieri, F.; Blumberg, J.B.; Stornello, M.; Ferri, C. Protective effects of flavanol-rich dark chocolate on endothelial function and wave reflection during acute hyperglycemia. *Hypertension* **2012**, *60*, 827–832. [CrossRef] [PubMed]
30. Gemignani, V.; Faita, F.; Ghiadoni, L.; Poggianti, E.; Demi, M. A system for real-time measurement of the brachial artery diameter in B-mode ultrasound images. *IEEE Trans. Med. Imaging* **2007**, *26*, 393–404. [CrossRef] [PubMed]
31. Ghiadoni, L.; Faita, F.; Salvetti, M.; Cordiano, C.; Biggi, A.; Puato, M.; Di Monaco, A.; De Siati, L.; Volpe, M.; Ambrosio, G.; et al. Assessment of flow-mediated dilation reproducibility: A nationwide multicenter study. *J. Hypertens.* **2012**, *30*, 1399–1405. [CrossRef] [PubMed]
32. Bocchio, M.; Pelliccione, F.; Passaquale, G.; Mihalca, R.; Necozione, S.; Desideri, G.; Francavilla, F.; Ferri, C.; Francavilla, S. Inhibition of phosphodiesterase type 5 with tadalafil is associated to an improved activity of circulating angiogenic cells in men with cardiovascular risk factors and erectile dysfunction. *Atherosclerosis* **2008**, *196*, 313–319. [CrossRef] [PubMed]
33. Van Bussel, B.C.; Henry, R.M.; Ferreira, I.; van Greevenbroek, M.M.; van der Kallen, C.J.; Twisk, J.W.; Feskens, E.J.; Schalkwijk, C.G.; Stehouwer, C.D. A healthy diet is associated with less endothelial dysfunction and less low-grade inflammation over a 7-year period in adults at risk of cardiovascular disease. *J. Nutr.* **2015**, *145*, 532–540. [CrossRef] [PubMed]
34. Westphal, S.; Taneva, E.; Kästner, S.; Martens-Lobenhoffer, J.; Bode-Böger, S.; Kropf, S.; Dierkes, J.; Luley, C. Endothelial dysfunction induced by postprandial lipemia is neutralized by addition of proteins to the fatty meal. *Atherosclerosis* **2006**, *185*, 313–319. [CrossRef] [PubMed]
35. Coomber, B.L.; Gotlieb, A.I. In vitro endothelial wound repair. Interaction of cell migration and proliferation. *Arteriosclerosis* **1990**, *10*, 215–222. [CrossRef] [PubMed]
36. Werner, N.; Nickenig, G. Influence of cardiovascular risk factors on endothelial progenitor cells limitations for therapy? *Arterioscler. Thromb. Vasc. Biol.* **2006**, *26*, 257–261. [CrossRef] [PubMed]
37. Aicher, A.; Heeschen, C.; Mildner-Rihm, C.; Urbich, C.; Ihling, C.; Technau-Ihling, K.; Zeiher, A.M.; Dimmeler, S. Essential role of endothelial nitric oxide synthase for mobilization of stem and progenitor cells. *Nat. Med.* **2003**, *9*, 1370–1376. [CrossRef] [PubMed]

nutrients

MDPI

Article

Curcumin and *Boswellia serrata* Modulate the Glyco-Oxidative Status and Lipo-Oxidation in Master Athletes

Nino Cristiano Chilelli [1,*], Eugenio Ragazzi [2], Romina Valentini [1], Chiara Cosma [3], Stefania Ferraresso [1], Annunziata Lapolla [1] and Giovanni Sartore [1]

1 Department of Medicine-DIMED, University of Padova, Diabetology and Dietetics, ULSS 16, via dei Colli, 4, 35100 Padova, Italy; romina.valentini@unipd.it (R.V.); stefania.ferraresso@alice.it (S.F.); annunziata.lapolla@unipd.it (A.L.); g.sartore@unipd.it (G.S.)

2 Department of Pharmaceutical and Pharmacological Sciences, University of Padova, 35100 Padova, Italy; eugenio.ragazzi@unipd.it

3 Department of Laboratory Medicine, University of Padova, 35100 Padova, Italy; chiara.cosma@sanita.padova.it

* Correspondence: ninocristiano.chilelli@phd.unipd.it; Tel.: +39-49-821-6848; Fax: +39-49-821-6838

Received: 21 October 2016; Accepted: 15 November 2016; Published: 21 November 2016

Abstract: Background: Chronic intensive exercise is associated with a greater induction of oxidative stress and with an excess of endogenous advanced glycation end-products (AGEs). Curcumin can reduce the accumulation of AGEs in vitro and in animal models. We examined whether supplementation with curcumin and *Boswellia serrata* (BSE) gum resin for 3 months could affect plasma levels of markers of oxidative stress, inflammation, and glycation in healthy master cyclists. Methods. Forty-seven healthy male athletes were randomly assigned to Group 1, consisting of 22 subjects given a Mediterranean diet (MD) alone (MD group), and Group 2 consisted of 25 subjects given a MD plus curcumin and BSE (curcumin/BSE group). Interleukin-6 (IL-6), tumor necrosis factor-α (TNFα), high-sensitivity c-reactive protein (hs-CRP), total AGE, soluble receptor for AGE (sRAGE), malondialdehyde (MDA), plasma phospholipid fatty acid (PPFA) composition, and non-esterified fatty acids (NEFA) were tested at baseline and after 12 weeks. Results: sRAGE, NEFA, and MDA decreased significantly in both groups, while only the curcumin/BSE group showed a significant decline in total AGE. Only the changes in total AGE and MDA differed significantly between the curcumin/BSE and MD groups. Conclusions. Our data suggest a positive effect of supplementation with curcumin and BSE on glycoxidation and lipid peroxidation in chronically exercising master athletes.

Keywords: advanced glycation end-products; curcumin; inflammation; exercise; oxidative stress

1. Introduction

Reactive oxygen species (ROS) have an important role in maintaining homeostasis through immune functions and cellular signals [1], but an excess of ROS has the potential to damage deoxyribonucleic acid (DNA), proteins, and lipids. It has been shown that chronic intensive exercise may be associated with an increased induction of oxidative stress, which in turn has a negative impact on exercise performance and causes muscle damage [2]. Advanced glycation end-products (AGEs) are a heterogeneous group of macromolecules formed by the non-enzymatic glycation of proteins, lipids, and nucleic acids. Excessive glycation in humans can derive from exogenous AGEs ingested with foods, and from endogenous AGEs formed in the body—especially in conditions of chronic hyperglycemia or increased oxidative stress [3]. The harmful effect of AGEs is particularly associated with stiffening

of tissues rich in extracellular matrices and long-lived proteins, such as skeletal muscle, tendons, joints, bone, heart, arteries, lung, skin, and lens [4]. Very little is known about how effective dietary intervention and oral antioxidant supplementation may be in reducing oxidative stress in athletes who exercise intensively, but there is some evidence to suggest that the administration of antioxidants and anti-inflammatory nutrients within physiological ranges may reverse exercise-induced oxidative stress and muscle damage [5]. Curcumin, an important constituent of the turmeric (*Curcuma longa*) rhizome, possesses antioxidant and anti-inflammatory activities, and has been used to treat a variety of inflammatory conditions and chronic diseases [6]. It has also been demonstrated that curcumin can reduce the accumulation of AGEs in vitro and in animal models, suggesting that this anti-glycation mechanism may relate to the antioxidant effect of the compound [7]. Extracts of *Boswellia serrata* (BSE) gum resin have also demonstrated anti-inflammatory properties, suppressing local tissue tumor necrosis factor-α (TNFα) and interleukin-1β (IL-1β) in animal models [8].

No studies have ascertained whether oral curcumin supplementation has antioxidant and anti-glycation effects in the medium-term in master athletes chronically exercising intensively, who are particularly exposed to increased glycoxidative processes. Hence, our study aimed to establish whether curcumin and BSE supplementation for 3 months, combined with a Mediterranean diet (MD), could affect plasma levels of markers of oxidative stress, inflammation, and glycation in a cohort of well-trained healthy master cyclists.

2. Patients and Methods

2.1. Participants and Study Design

Forty-seven healthy male athletes aged 46 ± 8 years took part in this study after giving their written informed consent. The study complied with the Helsinki Declaration, and the local institutional Ethics Committee approved the study protocol. The trial was designed as a controlled, randomized, parallel group study.

Inclusion criteria were no history of cardiovascular disease or allergies, and no prior use of drugs or food supplements. Exclusion criteria were use of tobacco products, alcohol consumption, recent surgery, diabetes mellitus, hypertension, and chronic inflammatory diseases.

Table 1 shows the anthropometric features of the subjects enrolled in the study, including body composition, assessed using bioelectrical impedance analysis at baseline in all subjects. The participants volunteering for the study were cyclists with an average experience of 8 ± 2 years of competing in the nonprofessional category. They had usually been cycling about 200 km a week and 10,000/12,000 km a year. They were instructed not to change their lifestyle during the trial as regards exercise, diet, and other routine activities, and they were asked not to take any other medicinal herbs or drugs. The athletes were not involved in any special exercise sessions, because the aim of the study was to assess the effect of medium-term curcumin and BSE supplementation in conditions of real-life physical activity.

Table 1. Basal characteristics of the patients enrolled.

	Group "MD + Curcumin/BSE" (*n* = 25)		**Group "MD" (*n* = 22)**	
	Pre	***Post***	***Pre***	***Post***
Age (year)	45 ± 9	-	46 ± 8	-
Weight (kg)	72.4 ± 8.0	72.4 ± 7.9	71.8 ± 9.6	70.7 ± 21.7
BMI (kg/m^2)	23.7 ± 2.1	23.5 ± 2.0	23.7 ± 2.8	23.0 ± 6.4
FFM (%)	81 ± 4	80 ± 4	81 ± 6	79 ± 8
FM (%)	19 ± 4	19 ± 4	19 ± 6	21 ± 6

MD: Mediterranean diet; BSE: *Boswellia serrata* extract; BMI: body mass index; FFM: free fat mass; FM: fat mass.

At the baseline visit, we used 24-h recall—a self-reporting method for collecting data on eating behavior and for measuring energy intake by means of structured interviews—as described elsewhere [9]. An isocaloric Mediterranean-style dietary pattern was recommended to all subjects, with particular recommendation to avoid foods naturally containing curcumin. The athletes were assigned to two groups by means of a simple randomization procedure using a computer-generated random binary list. Group 1 consisted of 22 subjects given a MD alone (MD group); and Group 2 consisted of 25 subjects given a MD plus Fitomuscle® (ForFarma, Rome, Italy), a nutraceutical-combined pill (NCP) containing curcumin and BSE (curcumin/BSE group). One tablet of Fitomuscle® contains 50 mg of turmeric Phytosome®—corresponding to 10 mg of curcumin—and 140 mg of *Boswellia* extract, corresponding to 105 mg of boswellic acids. Phytosome® (registered by Indena, Milan, Italy) relies on an advanced formulation technology for delivering substances of herbal origin: this involves the dispersion of the drug in natural phospholipids to improve its absorption after oral administration [10]. The new formulation enables higher systemic levels of curcumin to be obtained than with other formulations [10].

Adherence to the treatment was ascertained by means of pill counts on the product returned at the follow-up visit.

2.2. Dietary Intake

Nutrients and food intake were measured using the Willett Food Frequency Questionnaire, which has been validated for a wide range of ages [11]. Full instructions were given on how to complete the questionnaire, together with a list of 120 foods, for each of which there was a full description of the usual serving size. Food preparation was also considered in order to include all the ingredients used. Participants were asked to keep a detailed record of their weekly food consumption, and they completed the questionnaire three times during the study, at the beginning, after the first month, and at the end. They were asked to record the amount of food they consumed and their food preparation methods. Participants were provided with pictures of standard meals and portion sizes to enable them to estimate the size of their portions. All completed questionnaires were checked by a dietitian for accuracy and completeness. The data in the questionnaires were assessed with the aid of a database for us in nutritional analysis (Medimatica S.r.l. 2004, Colonnella, Italy). A trained dietician taught participants how to complete the questionnaires and quantify their food servings. The dietary records were analyzed using the computerized nutritional analysis system Science Fit Diet 200A (Sciencefit, Athens, Greece).

2.3. Blood Sampling

The following markers were tested in blood and urine samples obtained at the baseline and after 12 weeks: interleukin-6 (IL-6), tumor necrosis factor-α (TNFα), high-sensitivity c-reactive protein (hs-CRP), total AGE, soluble receptor for AGE (sRAGE), malondialdehyde (MDA), non-esterified fatty acids (NEFA), total cholesterol, low density lipoprotein (LDL) cholesterol, high density lipoprotein (HDL) cholesterol, and triglycerides. Plasma phospholipid fatty acid (PPFA) composition was also ascertained. A competitive enzyme-linked immunosorbent assay (ELISA) was used to assess glycoxidation and inflammatory markers, as described elsewhere [12]. NEFA were assayed using a colorimetric method (Randox®, County Antrim, Northern Ireland) with a precision assuring a less than 5% coefficient of variation. PPFA composition was determined after lipid extraction by the method of Folch et al. [13]. All analyses were performed at the laboratory of Padua University Hospital.

2.4. Statistical Analysis

Values are expressed in terms of mean ± standard deviation (SD). Findings were considered in terms of the difference at follow-up (12 weeks after starting the study) vis-à-vis each subject's baseline situation. Negative values thus indicate an actual reduction in a given parameter after the treatment.

The statistical significance of any differences induced by the treatment was tested using Student's *t*-test for paired data. Differences were considered statistically significant when $p < 0.05$ (two-tailed test).

3. Results

Data were available for statistical analysis for all 47 subjects randomized. Participants did not differ in age, BMI, or body composition (Table 1). Body composition measurements obtained using bioelectrical impedance did not differ between the baseline and the follow-up 3 months later (Table 1), during which time the two groups of athletes continued to exercise as usual. To assess the effect of curcumin and BSE supplementation, we examined inflammatory markers (IL-6, TNFα, hs-CRP), glycoxidation (AGEs, sRAGE), and lipoxidation (MDA, NEFA). Plasma levels of NEFA and PPFA composition were obtained simultaneously to rule out the possibility of any changes in the two groups' markers of oxidation and glycation depending on the recommended diet.

As summarized in Table 2, neither group showed any significant changes in inflammatory markers at the follow-up, apart from a slight increase in TNFα in the MD group. sRAGE and NEFA decreased significantly in both groups, while total AGE levels decreased significantly after supplementation with curcumin and BSE, but not in the group given a MD alone. After 3 months, both groups showed a significant decrease in their levels of MDA (chosen as a marker of lipoxidation). Randomization resulted in a significant difference of AGE values at baseline between the two groups; therefore the comparison between the groups was performed by considering differences after minus before treatment (Table 3), obviating the observed differences in AGE: at this analysis, changes in total AGE and MDA differed significantly between the two groups. AGE remained significantly different between the two groups after normalizing for the differences at baseline ($-42.41\% \pm 18.66\%$ in MD + curcumin/BSE group vs. $4.18\% \pm 22.71\%$ in MD group, $p < 0.001$). No differences emerged between the curcumin/BSE group and MD groups as regards their PPFA composition (Supplementary Materials Table S1).

Table 2. Parameters of inflammation and glyco-/lipo-oxidative stress evaluated in the two groups, before and after therapeutic intervention.

	MD + Curcumin/BSE		MD	
	Before	*After*	*Before*	*After*
hs-CRP (mg/L)	2.90 ± 0.2	2.80 ± 0.2	2.60 ± 0.5	2.36 ± 1.0
NEFA (mmol/L)	1.05 ± 0.67	0.68 ± 0.52 **	1.24 ± 0.92	0.45 ± 0.18 ***
sRAGE (pg/mL)	475.73 ± 141.66	328.50 ± 164.49 ***	430.47 ± 123.59	312.34 ± 156.27 ***
AGE (μg/mL)	22.42 ± 18.08	10.83 ± 6.38 ***	9.07 ± 4.22	9.22 ± 4.07
MDA (μmol/L)	0.16 ± 0.09	0.05 ± 0.05 ***	0.10 ± 0.03	0.03 ± 0.01 ***
IL-6 (pg/mL)	17.62 ± 29.76	17.55 ± 29.58	23.76 ± 53.00	41.88 ± 50.69
TNFα (pg/mL)	7.29 ± 5.11	8.28 ± 5.42	7.05 ± 4.61	12.67 ± 11.07 *

NEFA: non-esterified fatty acids; sRAGE: soluble receptor for advanced glycation end products; AGE: advanced glycation end products; MDA: malondialdehyde; IL-6: interleukine-6; TNFα: tumor necrosis factor α; hs-CRP: high-sensitivity c-reactive protein. *** $p < 0.001$; ** $p < 0.01$; * $p < 0.05$. Student's *t*-test for paired data.

Table 3. Pre–post changes in biomarkers of inflammation and glyco-lipo-oxidation compared between the two groups.

	MD + Curcumin/BSE	MD	p †
hs-CRP (mg/L)	0.10 ± 0.2	0.24 ± 0.54	ns
NEFA (mmol/L)	−0.36 ± 0.61	−0.79 ± 0.89	ns
sRAGE (pg/mL)	−147.23 ± 109.02	−118.13 ± 117.01	ns
AGE (μg/mL)	−11.59 ± 12.49	0.15 ± 2.30	<0.001
MDA (μmol/L)	−0.10 ± 0.06	−0.07 ± 0.03	<0.02
IL−6 (pg/mL)	−0.07 ± 35.18	18.13 ± 59.73	ns
TNFα (pg/mL)	0.99 ± 6.88	5.62 ± 11.14	ns

NEFA: non-esterified fatty acids; sRAGE: soluble receptor for advanced glycation end products; AGE: advanced glycation end products; MDA: malondialdehyde; IL-6: interleukine-6; TNFα: tumor necrosis factor α; hsCRP: c-reactive protein. Variables are presented as the mean (±SD) change from baseline. † Data were compared using Student's *t*-test for unpaired data. ns: not statistically significant.

4. Discussion

In our pilot study, medium-term dietary supplementation with curcumin and BSE was effective in reducing markers of glycoxidation and lipoxidation in a group of master athletes chronically exercising intensively. Oral supplementation with curcumin and BSE for 3 months was associated with a significant reduction in total plasma AGEs and MDA.

Studies investigating whether exercise produces clinically significant oxidative stress have reached no definitive conclusions, partly because different types and intensities of exercise were considered, different markers of oxidative stress were measured, and participants had different levels of training [5]. Generally speaking, acute physical activity—be it aerobic or anaerobic—predisposes to an increased ROS production via multiple pathophysiological pathways. It has been suggested that the high ROS levels produced by acute bouts of exercise may be detrimental to the immune system, but recent studies have indicated that chronic exercise—high intensity endurance training in particular—could have a positive impact on redox status, especially because slightly higher levels of ROS may improve anti-oxidant defenses [14].

Few studies conducted to date have compared the effects of anaerobic exercise and aerobic exercise on oxidative stress [15,16], however, and only one study compared intermittent endurance and resistance exercise protocols in terms of oxidative stress in middle-aged women [2]. The chronic physical activity of nonprofessional cyclists combines endurance and resistance training sessions, in proportions that it is virtually impossible to quantify precisely in real life, as demonstrated by the lack of literature in this area.

Curcumin exhibits an antioxidant activity in several in vitro and in vivo models [17]. Curcumin is able to scavenge superoxide anion ($\cdot O_2^- \cdot$), hydroxyl radicals ($\cdot OH$), H_2O_2, singlet oxygen, nitric oxide, peroxynitrite, and peroxyl radicals (ROO·) [18–21]. It has also been shown to downregulate the expression of numerous proinflammatory cytokines, including TNFα, Vascular Endothelial Growth Factor (VEGF), and interleukins 1, 2, and 6 [22]. Gum resin extracts of BSE have also revealed anti-inflammatory properties, suppressing local tissue TNFα and IL-1β in animal models [8]. Moreover, an inhibitory activity on AGE has been demonstrated for BSE in vitro and in animal models [23].

Few studies have examined the effect of curcumin supplementation on exercise-induced oxidative stress and exercise performance in animal models [24,25]. One study found curcumin supplementation to be effective in attenuating exercise-induced oxidative stress in young athletes, also improving their antioxidant capacity [26].

AGEs are generated under conditions of hyperglycemia and oxidative stress, or a combination of the two [3]. The engagement of AGEs with their receptor (RAGE) has been implicated in the development of various disorders, including vascular disease [12], and it is related to an amplification of oxidative stress. A number of studies on animals and humans have confirmed an in vivo accumulation of advanced glycation products (AGE) with aging, and this AGE accumulation can occur at the

periphery of skeletal muscle fibers, intracellularly, or both [27]. While high levels of circulating AGE seem to predict cardiovascular-related mortality among older communities [28], the precise nature of AGE-induced protein modifications and their clinical significance in the aging process of skeletal muscle remain to be seen.

No studies published to date have considered the effect of curcumin and BSE on plasma levels of AGEs and sRAGE in humans, and in athletes in particular.

In the present study, master athletes with an average age of 46 years were engaging in non-professional cycling, an activity characterized mainly by high-intensity endurance training associated with short sessions of anaerobic resistance training (i.e., during climbs and shots). We chose these master athletes for our study because they reflect a significant proportion of the physically active population, they were older than competitive athletes, and received less medical and nutritional counseling. Moreover, numerous experimental animal and human data support an AGE accumulation and a depletion of anti-oxidant reserves with aging [29]. To our knowledge, no previous clinical studies have investigated the degree of glycoxidation in this particular population, or the effects of specific nutritional regimens associated with antioxidant supplementation.

The baseline AGEs and sRAGE levels observed in our sample were higher than in a population of healthy individuals of comparable age and ethnicity who were not chronically exercising intensively [30]. In this report of Kerkeni et al., 30 healthy subjects showed average serum AGE of 508.83 $\pm$ 119.68 pg/mL and average serum sRAGE of 148.72 $\pm$ 32.73 pg/mL. It is particularly difficult to establish standard reference values for serum AGE in healthy subjects, for many reasons: first, the great variability of the plasma concentration ranges between different populations; secondly, the differences between methods used for their blood assay; finally, the influence of the AGE content in foods [31,32]. However, in comparison to population studied by Kerkeni et al., our athletes have about three times higher values of RAGE, and serum AGE values (though determined with a different method) are much higher. This suggests that the type of exercise performed by our athletes can exacerbate chronic levels of oxidative stress, leading to a significant accumulation of AGEs over time.

In our study, a significant reduction in plasma AGEs was only found in the group of athletes given curcumin/BSE supplementation, while there was a decline in sRAGE in both groups.

The effect of exercise on sRAGE has been studied a little in healthy subjects and patients with and without diabetes, with contradictory results [33,34]. The physiological function of endogenous sRAGE remains to be seen, since many soluble variants derive from the splicing of the receptor. It is also not clear which of these variants exerts a protective effect by acting as a RAGE scavenger, and which of them amplify the oxidative intracellular signaling of RAGE themselves [35]. In diabetic patients, for example, sRAGE are believed to change dynamically, gradually switching from higher levels in the early stages of inflammation and atherosclerosis to a mild decline in the intermediate stage, before rising again in the acute phase of tissue damage and consequent inflammation [35]. Other authors have hypothesized an increase in the clearance of sRAGE from the circulation as a result of hemodynamic changes induced by a greater physical activity [34], and this latter effect could explain the results of our study.

By comparison with sRAGE, plasma levels of AGEs are certainly more stable and less affected by acute changes in oxidative stress due to exercise. They therefore better reflect chronic oxidative stress and are more reliable for the purpose of assessing the effects of long-term curcumin supplementation.

The indirect assessment of oxidative stress involves measuring the more stable molecular products formed by the reaction of ROS with certain biomolecules. Some of the common molecular products are the concentrations of oxidation target products, including lipid peroxidation end-products like malondialdehyde (MDA) [36]. A previous study found that intermittent anaerobic exercise, when performed intensively, resulted in acute lipid peroxidation and immune suppression in well-trained women aged 45 to 55 years [2].

The Mediterranean diet (MD) has been shown to exert a positive effect on the lipid profile and to have antioxidant properties, especially as regards the dietary intake of high-protein polyunsaturated

fatty acids (PUFAs). Malaguti et al. [37] reported that PUFA supplementation might increase susceptibility to lipid peroxidation in volleyball athletes followed up for 2 months: they concluded that the balance between the positive and negative effects of PUFA intake might depend on dosage, and that simply adhering to a MD seems to be a better option. A MD favors a higher intake of PUFAs—particularly of the *n*-3 series—and a lower ratio of *n*-6 to *n*-3 fatty acids than in other diets, thus affecting tissue lipids.

The participants enrolled in this study were all taught to adopt a MD during the 3 months of observation. PPFA composition and serum NEFA adapt dynamically to changes in the dietary fatty acid profile, and we tested these parameters to assess the effect of MD in our athletes.

As concerns lipid peroxidation, MDA levels dropped in both groups of athletes, but those taking the curcumin/BSE supplement showed a significantly sharper decline than the athletes enrolled in the group only given a MD. After 3 months, serum NEFA levels were similarly reduced in both groups, and we found no significant differences in the qualitative composition of their PUFAs. Therefore, we surmise that MD, although with a positive effect on the drop in NEFA, did not seem to induce any significant increase in PUFAs, which can exclude an eventual contribution to the drop in MDA levels.

Judging from the above observations, it is reasonable to infer that curcumin and BSE supplementation could have a direct and significant effect on plasma lipid peroxidation. Other than that, we found no changes in inflammatory status related to the MD or curcumin/BSE supplementation in either group of athletes, probably because of their already low grade of inflammation.

The main strength of this study lies in its originality. To the best of our knowledge, this is the first study to examine the effect of a food supplement containing curcumin and BSE on plasma levels of sRAGE and AGE in humans. It is also the first study to confirm the positive effect of the supplement in reducing markers of lipid peroxidation in a population of athletes chronically exercising intensively. This has an important implication in nutritional counseling for such athletes, who reflect a considerable proportion of the physically active individuals in the general population and are more prone to higher levels of oxidative stress. The effects of curcumin/BSE supplementation were also assessed over a considerable period of time, while the few studies in the literature considered only a single session of exercise.

Weaknesses of this study include the small number of participants enrolled and our failure to precisely quantify how much the athletes exercised. Having said that, the study was designed to examine people exercising in real life, and to assess the effectiveness of supplementation with curcumin in the medium term.

5. Conclusions

Our data suggest a positive effect of curcumin and BSE supplementation for 3 months on glycoxidation and lipid peroxidation in athletes chronically exercising intensively.

Further studies will test whether treatment with curcumin can result in a reduction of the accumulation of AGEs in muscle tissue, possibly improving muscle performance in the long term.

Supplementary Materials: The following are available online at http://www.mdpi.com/2072-6643/8/11/745/s1. Table S1: Percent differences (after treatment minus before treatment, normalized to before treatment value) in serum fatty acid profile of the two groups of subjects, before and after treatment. Negative values indicate a decrease of the parameter in comparison to before treatment.

Author Contributions: N.C.C. designed the study, analyzed the data and wrote the manuscript; E.R. analyzed the data and performed the statistical analysis; R.V. designed the study, conducted the study and collected data; C.C. collected and analyzed data; S.F. conducted the study and collected data; A.L. analyzed data and revised the manuscript; G.S. designed the study, analyzed data and revised the manuscript.

Conflicts of Interest: The authors declare no conflict of interest.

Abbreviations

The following abbreviations are used in this manuscript:

ROS	Reactive oxygen species
AGEs	Advanced glycation end-products
BSE	Boswellia serrate
MD	Mediterranean diet
IL-6	interleukin-6
TNFα	tumor necrosis factor-α
hs-CRP	high-sensitivity c-reactive protein
sRAGE	soluble receptor for AGE
MDA	malondialdehyde
NEFA	non-esterified fatty acids
PPFA	plasma phospholipid fatty acid
NCP	nutraceutical-combined pill
PUFA	polyunsaturated fatty acid
FFM	fat-free mass
FM	fat mass
BMI	body mass index

References

1. Strobel, N.A.; Peake, J.M.; Matsumoto, A.; Marsh, S.A.; Coombes, J.S.; Wadley, G.D. Antioxidant supplementation reduces skeletal muscle mitochondrial biogenesis. *Med. Sci. Sports Exerc.* **2011**, *43*, 1017–1024. [CrossRef] [PubMed]
2. Cardoso, A.M.; Bagatini, M.D.; Roth, M.A.; Martins, C.C.; Rezer, J.F.; Mello, F.F.; Lopes, L.F.; Morsch, V.M.; Schetinger, M.R. Acute effects of resistance exercise and intermittent intense aerobic exercise on blood cell count and oxidative stress in trained middle-aged women. *Braz. J. Med. Biol. Res.* **2012**, *45*, 1172–1182. [CrossRef] [PubMed]
3. Chilelli, N.C.; Burlina, S.; Lapolla, A. AGEs, rather than hyperglycemia, are responsible for microvascular complications in diabetes: A "glycoxidation-centric" point of view. *Nutr. Metab. Cardiovasc. Dis.* **2013**, *23*, 913–919. [CrossRef] [PubMed]
4. Monnier, V.M.; Mustata, G.T.; Biemel, K.L.; Reihl, O.; Lederer, M.O.; Zhenyu, D.; Sell, D.R. Cross-linking of the extracellular matrix by the Maillard reaction in aging and diabetes: an update on "a puzzle nearing resolution". *Ann. N. Y. Acad. Sci.* **2005**, *1043*, 533–544. [CrossRef] [PubMed]
5. Urso, M.L.; Clarkson, P.M. Oxidative stress, exercise, and antioxidant supplementation. *Toxicology* **2003**, *189*, 41–54. [CrossRef]
6. Elosta, A.; Ghous, T.; Ahmed, N. Natural products as anti-glycation agents: Possible therapeutic potential for diabetic complications. *Curr. Diabetes Rev.* **2012**, *8*, 92–108. [CrossRef] [PubMed]
7. Yu, W.; Wu, J.; Cai, F. Curcumin alleviates diabetic cardiomyopathy in experimental diabetic rats. *PLoS ONE* **2012**, *7*, e52013. [CrossRef] [PubMed]
8. Umar, S.; Umar, K.; Sarwar, A.H.; Khan, A.; Ahmad, N.; Ahmad, S.; Katiyar, C.K.; Husain, S.A.; Khan, H.A. *Boswellia serrata* extract attenuates inflammatory mediators and oxidative stress in collagen induced arthritis. *Phytomedicine* **2014**, *21*, 847–856. [CrossRef] [PubMed]
9. Thompson, F.E.; Subar, A.F. Dietary Assessment Methodology. In *Nutrition in the Prevention and Treatment of Disease*, 2nd ed.; Coulston, A.M., Broushey, C.J., Eds.; Academic Press: Bethesda, MA, USA, 2008; pp. 33–39.
10. Marczylo, T.H.; Verschoyle, R.D.; Cooke, D.N.; Morazzoni, P.; Steward, W.P.; Gescher, A.J. Comparison of systemic availability of curcumin with that of curcumin formulated with phosphatidylcholine. *Cancer Chemother. Pharmacol.* **2007**, *60*, 171–177. [CrossRef] [PubMed]
11. Martin-Moreno, J.M.; Boyle, P.; Gorgojo, L.; Maisonneuve, P.; Fernandez-Rodriguez, J.C.; Salvini, S.; Willett, W.C. Development and validation of a food frequency questionnaire in Spain. *Int. J. Epidemiol.* **1993**, *22*, 512–519. [CrossRef] [PubMed]

12. Piarulli, F.; Lapolla, A.; Ragazzi, E.; Susana, A.; Sechi, A.; Nollino, L.; Cosma, C.; Fedele, D.; Sartore, G. Role of endogenous secretory RAGE (esRAGE) in defending against plaque formation induced by oxidative stress in type 2 diabetic patients. *Atherosclerosis* **2013**, *226*, 252–257. [CrossRef] [PubMed]
13. Folch, J.; Lees, M.; Stanley, G.H.S. A single method for the isolation and purification of total lipids from animal tissue. *J. Biol. Chem.* **1957**, *226*, 497–507. [PubMed]
14. Gomes, E.C.; Silva, A.N.; de Oliveira, M.R. Oxidants, antioxidants, and the beneficial roles of exercise-induced production of reactive species. *Oxid. Med. Cell. Longev.* **2012**, *2012*, 756132. [CrossRef] [PubMed]
15. Bloomer, R.J.; Goldfarb, A.H.; Wideman, L.; McKenzie, M.J.; Consitt, L.A. Effects of acute aerobic and anaerobic exercise on blood markers of oxidative stress. *J. Strength Cond. Res.* **2005**, *9*, 276–285. [CrossRef]
16. Shi, M.; Wang, X.; Yamanaka, T.; Ogita, F.; Nakatani, K.; Takeuchi, T. Effects of anaerobic exercise and aerobic exercise on biomarkers of oxidative stress. *Environ. Health Prev. Med.* **2007**, *12*, 202–208. [CrossRef] [PubMed]
17. Trujillo, J.; Chirino, Y.I.; Molina-Jijón, E.; Andérica-Romero, A.C.; Tapia, E.; Pedraza-Chaverrí, J. Renoprotective effect of the antioxidant curcumin: recent findings. *Redox Biol.* **2013**, *17*, 448–456. [CrossRef] [PubMed]
18. Barzegar, A.; Moosavi-Movahedi, A.A. Intracellular ROS protection efficiency and free radical-scavenging activity of curcumin. *PLoS ONE* **2011**, *6*, e26012. [CrossRef] [PubMed]
19. Sreejayan, N.; Rao, M.N. Free radical scavenging activity of curcuminoids. *Arzneimittelforschung* **1996**, *46*, 169–171. [PubMed]
20. Sreejayan, R.M. Nitric oxide scavenging by curcuminoids. *J. Pharm. Pharmacol.* **1997**, *49*, 105–107. [CrossRef] [PubMed]
21. Sumanont, Y.; Murakami, Y.; Tohda, M.; Vajragupta, O.; Matsumoto, K.; Watanabe, H. Evaluation of the nitric oxide radical scavenging activity of manganese complexes of curcumin and its derivative. *Biol. Pharm. Bull.* **2004**, *27*, 170–173. [CrossRef] [PubMed]
22. Shehzad, A.; Ha, T.; Subhan, F.; Lee, Y.S. New mechanisms and the anti-inflammatory role of curcumin in obesity and obesity-related metabolic diseases. *Eur. J. Nutr.* **2011**, *50*, 151–161. [CrossRef] [PubMed]
23. Rao, A.R.; Veeresham, C.; Asres, K. In vitro and in vivo inhibitory activities of four Indian medicinal plant extracts and their major components on rat aldose reductase and generation of advanced glycation endproducts. *Phytother. Res.* **2013**, *27*, 753–760. [CrossRef] [PubMed]
24. Avci, G.; Kadioglu, H.; Sehirli, A.O.; Bozkurt, S.; Guclu, O.; Arslan, E.; Muratli, S.K. Curcumin protects against ischemia/reperfusion injury in rat skeletal muscle. *J. Surg. Res.* **2012**, *172*, e39–e46. [CrossRef] [PubMed]
25. Davis, J.M.; Murphy, E.A.; Carmichael, M.D.; Zielinski, M.R.; Groschwitz, C.M.; Brown, A.S.; Gangemi, J.D.; Ghaffar, A.; Mayer, E.P. Curcumin effects on inflammation and performance recovery following eccentric exercise-induced muscle damage. *Am. J. Physiol. Regul. Integr. Comp. Physiol.* **2007**, *292*, R2168–R2173. [CrossRef] [PubMed]
26. Takahashi, M.; Suzuki, K.; Kim, H.K.; Otsuka, Y.; Imaizumi, A.; Miyashita, M.; Sakamoto, S. Effects of curcumin supplementation on exercise-induced oxidative stress in humans. *Int. J. Sports Med.* **2014**, *35*, 469–475. [CrossRef] [PubMed]
27. Haus, J.M.; Carrithers, J.A.; Trappe, S.W.; Trappe, T.A. Collagen, cross-linking, and advanced glycation end products in aging human skeletal muscle. *J. Appl. Physiol.* **2007**, *103*, 2068–2076. [CrossRef] [PubMed]
28. Semba, R.D.; Ferrucci, L.; Sun, K.; Beck, J.; Dalal, M.; Varadhan, R.; Walston, J.; Guralnik, J.M.; Fried, L.P. Advanced glycation end products and their circulating receptors predict cardiovascular disease mortality in older community-dwelling women. *Aging Clin. Exp. Res.* **2009**, *21*, 182–190. [CrossRef] [PubMed]
29. Peppa, M.; Uribarri, J.; Vlassara, H. Aging and glycoxidant stress. *Hormones* **2008**, *7*, 123–132. [PubMed]
30. Kerkeni, M.; Saïdi, A.; Bouzidi, H.; Ben Yahya, S.; Hammami, M. Elevated serum levels of AGEs, sRAGE, and pentosidine in Tunisian patients with severity of diabetic retinopathy. *Microvasc. Res.* **2012**, *84*, 378–383. [CrossRef] [PubMed]
31. Uribarri, J.; Cai, W.; Sandu, O.; Peppa, M.; Goldberg, T.; Vlassara, H. Diet-derived advanced glycation end products are major contributors to the body's AGE pool and induce inflammation in healthy subjects. *Ann. N. Y. Acad. Sci.* **2005**, *1043*, 461–466. [CrossRef] [PubMed]
32. Chilelli, N.C.; Cremasco, D.; Cosma, C.; Ragazzi, E.; Francini Pesenti, F.; Bonfante, L.; Lapolla, A. Effectiveness of a diet with low advanced glycation end products, in improving glycoxidation and lipid peroxidation:

A long-term investigation in patients with chronic renal failure. *Endocrine* **2016**, *54*, 552–555. [CrossRef] [PubMed]
33. Choi, K.M.; Han, K.A.; Ahn, H.J.; Hwang, S.Y.; Hong, H.C.; Choi, H.Y.; Yang, S.J.; Yoo, H.J.; Baik, S.H.; Choi, D.S.; et al. Effects of exercise on sRAGE levels and cardiometabolic risk factors in patients with type 2 diabetes: A randomized controlled trial. *J. Clin. Endocrinol. Metab.* **2012**, *97*, 3751–3758. [CrossRef] [PubMed]
34. Santilli, F.; Vazzana, N.; Iodice, P.; Lattanzio, S.; Liani, R.; Bellomo, R.G.; Lessiani, G.; Perego, F.; Saggini, R.; Davì, G. Effects of high-amount-high-intensity exercise on in vivo platelet activation: modulation by lipid peroxidation and AGE/RAGE axis. *Thromb. Haemost.* **2013**, *110*, 1232–1240. [CrossRef] [PubMed]
35. Piarulli, F.; Sartore, G.; Lapolla, A. Glyco-oxidation and cardiovascular complications in type 2 diabetes: A clinical update. *Acta Diabetol.* **2013**, *50*, 101–110. [CrossRef] [PubMed]
36. Finaud, J.; Lac, G.; Filaire, E. Oxidative stress: relationship with exercise and training. *Sports Med.* **2006**, *36*, 327–358. [CrossRef] [PubMed]
37. Malaguti, M.; Baldini, M.; Angeloni, C.; Biagi, P.; Hrelia, S. High-protein PUFA supplementation, red blood cell membranes, and plasma antioxidant activity in volleyball athletes. *Int. J. Sport Nutr. Exerc. Metab.* **2008**, *18*, 301–312. [CrossRef] [PubMed]

nutrients

MDPI

Review

Fish Consumption and Age-Related Macular Degeneration Incidence: A Meta-Analysis and Systematic Review of Prospective Cohort Studies

Wei Zhu [1,†], Yan Wu [2,†], Yi-Fang Meng [1], Qian Xing [1], Jian-Jun Tao [1] and Jiong Lu [1,*]

[1] Department of Ophthalmology, Changshu No. 2 People's Hospital, Changshu 215500, China; shzhuwei0722@163.com (W.Z.); meng_yi_fang@163.com (Y.-F.M.); drzheng_gu@163.com (Q.X.); prxuming@163.com (J.-J.T.)

[2] Department of Ophthalmology, First Hospital Affiliated to Soochow University, Suzhou 215000, China; txwuyan@suda.edu.cn

* Correspondence: cslujiong@163.com

† Contributed equally on this work.

Received: 22 August 2016; Accepted: 11 November 2016; Published: 22 November 2016

Abstract: The association between fish consumption and risk of age-related macular degeneration (AMD) is still unclear. The aim of the current meta-analysis and systematic review was to quantitatively evaluate findings from observational studies on fish consumption and the risk of AMD. Relevant studies were identified by searching electronic databases (Medline and EMBASE) and reviewing the reference lists of relevant articles up to August, 2016. Prospective cohort studies that reported relative risks (RRs) and 95% confidence intervals (CIs) for the link between fish consumption and risk of AMD were included. A total of 4202 cases with 128,988 individuals from eight cohort studies were identified in the current meta-analysis. The meta-analyzed RR was 0.76 (95% CI, 0.65–0.90) when any AMD was considered. Subgroup analyses by AMD stages showed that fish consumption would reduce the risk of both early (RR, 0.83; 95% CI, 0.72–0.96) and late (RR; 0.76; 95% CI, 0.60–0.97) AMD. When stratified by the follow-up duration, fish consumption was a protective factor of AMD in both over 10 years (n = 5; RR, 0.81; 95% CI, 0.67–0.97) and less than 10 years (n = 3; RR, 0.70; 95% CI, 0.51 to 0.97) follow-up duration. Stratified analyses by fish type demonstrated that dark meat fish (RR, 0.68, 95% CI, 0.46–0.99), especially tuna fish (RR, 0.58; 95% CI, 95% CI, 0.47–0.71) intake was associated with reduced AMD risk. Evidence of a linear association between dose of fish consumption and risk of AMD was demonstrated. The results of this meta-analysis demonstrated that fish consumption can reduce AMD risk. Advanced, well-designed, randomized clinical trials are required in order to validate the conclusions in this study.

Keywords: age-related macular degeneration; fish; nutrients; meta-analysis

1. Introduction

Age-related macular degeneration (AMD) is now the leading cause of blindness in developed countries. AMD-related choroidal neovascularization (CNV) or geographic atrophy (GA), in the United States, is expected to increase by 50% by 2020 [1]. Effective treatments, for both early and late AMD, are presently lacking. Major efforts have been made in order to detect the pathogenetic mechanisms of AMD, but the exact etiology of AMD is still unclear [2]. Previous epidemiological studies showed that tobacco smoking was the only consistent causative factor and that other risk factors, such as alcohol consumption and cardiovascular diseases, are inconsistent for AMD incidence or progression [3]. The detections of the potential modifiable factors for AMD incidence would provide better strategies for primary prevention in the future.

As oxidative stress is one of the key pathogenetic factors in the development of AMD, use of antioxidant supplements has been regarded as an effective management strategy of AMD. Antioxidant supplement consumption, including polyunsaturated fatty acids (PUFAs) intake, has been postulated to be a protective factor of AMD [4]. Evidence from cross-sectional [5] and cohort studies [6] demonstrated a significant association between *n*-3 fatty acid consumption and reduced risk of late AMD. In a study of an elderly French population, high concentrations of plasma *n*-3 fatty acids were associated with a decreased risk of late AMD [7]. As we know, the main dietary source of PUFAs is oily fish (e.g., mackerel, tuna, salmon, sardines, and herring) [8], and fish consumption has been reported to be associated with a reduced risk of different types of cancers, diabetes, and several other diseases [9,10]. Based on cross-sectional [11,12], case-controlled [13], and cohort studies [14], fish intake was reported to be associated with a lower risk of AMD. However, there were also a few studies that demonstrated no effect of fish intake on AMD risk. The Eye Disease Case Control Study (EDCC) found no effect of fish intake on incidence for neovascular AMD [15]. In addition, a retrospective analysis of 1968 participants found that fish intake was not associated with AMD incidence compared to less frequent fish consumption [16].

Meta-analyses, which are a useful statistical tool, could pool the relevant, but independent, studies together and, thus, come to a more powerful conclusion. Meta-analysis was also used in the detection of potential risk factors for AMD. For instance, based on a combination of five prospective cohort studies, Chong et al. found that heavy alcohol consumption was associated with an increased risk of early AMD [17]. For these reasons, a meta-analysis and systematic review of the association between fish intake and risk of AMD may help to clarify this issue. The aim of the current meta-analysis was to quantitatively evaluate findings from observational studies on the association between fish consumption and AMD incidence.

2. Methods

2.1. Search Strategy and Inclusion Criteria

This current study was based on eligible observational studies, and the meta-analysis was conducted according to the Preferred Reporting Items for Systematic Reviews and Meta-Analyses (PRISMA) and Meta-analysis Of Observational Studies in Epidemiology (MOOSE) guidelines [18,19]. A comprehensive search of Pubmed, Embase, and Web of Science was conducted for relevant literature, published up to 15 August 2016, with the combination of "fish", "seafood", "life style", "dietary factor" with "age-related macular degeneration", "macular degeneration", "age-related maculopathy", "maculopathy", "retinal degeneration", "drusen", "choroidal neovascularisation", and "geographic atrophy". To acquire all the potential publications, no restrictions were set in the literature search. In addition, the reference lists of relevant articles were also reviewed in order to detect potential eligible studies. If duplicate reports from the same dataset were obtained, only the publications that provided the most comprehensive results were included. If more data from one publication was required, the corresponding author was contacted by e-mail.

The studies that met the following criteria were considered for inclusion in this meta-analysis: (1) the effect of fish consumption on the risk of AMD was reported; (2) results from prospective cohort studies; (3) the values of relative risk (RR) or odds ratio (OR) with 95% confidence intervals (CI) were provided.

2.2. Data Extraction and Assessment of Study Quality

Data were independently extracted by two authors (Wei Zhu and Yan Wu) and any disagreements were resolved through discussion with a third author (Yi-Fang Meng). The following data were extracted from each included publication: First author, year of publication, name of cohort, country, age and gender of participants, amount of cases and cohort participants, subtypes or processing methods of fish, adjusting status of the confounding factors, and OR/RR values with 95% CI.

Methodological quality assessment of each included study was assessed by two authors (Wei Zhu and Yan Wu). The assessment scores were checked, and any discord was discussed and a unanimous result was obtained. Considering that all the included studies were cohort studies, the Newcastle-Ottawa Scale (NOS), which was designed for the assessments of observational studies, was used in the assessment of the methodological quality of the included studies [20]. The maximum for NOS was 9 stars and $\geq$6 stars is considered high quality.

2.3. Statistical Methods for the Meta-Analysis

Both OR and RR were extracted from the included studies and used in the final quantitative synthesis. Considering the relative low incidence of AMD, OR values could be used to approximate RR. The adjusted OR/RR values were adopted in the meta-analysis if possible. Both χ^2 and I^2 methods were used in the assessment of heterogeneity in this study. The inter-study heterogeneity was considered statistically significant if $p < 0.1$ or $I^2 > 50\%$. A random-effects model was used in the estimation of the pooled effects when the inter-study heterogeneity was statistically significant. The effects of fish consumption on AMD risk were delineated with RR and a 95% CI. To conduct sensitivity analyses, we dropped included studies, one-by-one, and observed the modification to the conclusion.

A two-stage, random-effect, dose-response meta-analysis was conducted for the detection of a potential linear relationship between fish consumption and risk of AMD incidence. Restricted cubic splines with four knots, at percentiles of 5%, 35%, 65%, and 95% of the distribution, were used to examine the potential linear dose-response relationship. A p value for nonlinearity was detected by testing the null hypothesis that the coefficient of the second spline is equal to 0 [21,22].

Publication bias was assessed using two different methods: Visually evaluating a funnel plot and the quantitative Egger test. A p value < 0.05 was regarded as statistically significant. All analyses were conducted with STATA statistical software (version 12.0, Stata Corp LP, College Station, TX, USA).

3. Results

3.1. Identification and Selection of Studies

A total of 1420 records (697 from Pubmed, 401 from EMBASE, and 322 from Web of Science) were identified through searching the electronic databases. Additionally, 18 more studies were identified through reviewing the reference lists of relevant reviews. A total of 545 unrelated papers were excluded, and 165 publications were reviewed for potential inclusion. After excluding 134 reviews, reviews, case reports, and other articles that reported overlapped data, a total of 31 full texts were assessed for eligibility. Subsequently, a total of 23 studies (13 duplicated studies, eight studies without a usable format, and two studies without conclusive fish intake definitions) were excluded from inclusion, and a final total of eight cohort studies were included for quantitative synthesis [23–30]. The flow diagram is presented in Figure 1.

3.2. Study Characters and Quality Scores

A total of 4202 cases with 128,988 individuals from eight cohort studies were identified in this meta-analysis. The detailed characteristics of each included study are presented in Table 1. The included studies were published between 1993 and 2014. In the included studies, drusen, retinal pigment epithelial changes, geographic atrophy, subretinal neovascular membrane, and visual acuity are used in the definition of AMD. Among all the included studies, four studies were in the USA, two in Australia, one in Iceland, and one in the Netherlands. The age, gender distribution, number of cases and cohorts, categories of fish consumption, and adjustments of confounding factors are also demonstrated in Table 1.

Table 1. Characteristics of eligible studies.

Author, Year	Study; Follow-up	Duration	Study Design	Site	Age (Year)	Gender, Percent	No. of Case/Cohort	Adjustments of Confounding Factors	Question	Exposure Definition	Study Quality *
Tan et al., 2009 [23]	Melbourne Collaborative Cohort Study > 10 years	1992–2004	Population-based	Australia	≥49	F: 57%	232/2684	Age, sex, and smoking	145-item FFQ	<1/M (Q1) vs. ≥3/W (Q3)	8
Seddon et al., 2003 [24]	AREDS, 4.6 years	1989–1998	Hospital-based	USA	≥65	F: 61%	51/312	Age-sex group, education, body mass index, systolic blood pressure, cardiovascular disease, log energy, protein intake, energy-adjusted log beta carotene intake, alcohol intake, physical activity, and initial age-related macular degeneration grade, total intake of energy-adjusted log zinc, vitamin C, and vitamin E.	61-item FFQ	<1/W (Q1) vs. ≥2/W (Q3)	8
Christen et al., 2011 [25]	Women's Health Study, 10 years	1993–2004	Population-based	USA	≥45	F:100%	235/38257	Age, randomized treatment assignment, smoking, alcohol use, BMI, menopausal status and use of HT, history of hypertension, history of high cholesterol, history of diabetes multivitamin use, history of eye exam in the last 2 years	131-item FFQ	<1/M (Q1) vs. >1/M (Q3)	7
SanGiovanni et al., 2008 [26]	Massachusetts Eye and Ear Infirmary, 6.3 years	1992–1998	Population-based	USA	55–80	F: 56.1%	311/2623	Age, sex, AREDS therapy group, education, race, BMI, smoking, antacid use, iris colour, DHA intake, EPA intake, combined DHA-EPA intake	90-item FFQ	<1/M (Q1) vs. >2/M (Q5)	9
Chong et al., 2009 [27]	Nurses' Health Study, 13 years	1990–2006	Population-based	Australia	66–85	F: 61%	1099/7098	Age, sex, smoking (current, past, or never), energy, vitamin C, vitamin E, carotene, zinc, lutein, zeaxanthin, and supplements (vitamin C, vitamin E, cod liver oil and fish oil (yes/no))	121-item FFQ	0–0.5/W (Q1) vs. ≥2/W (Q3)	9
Cho et al., 2001 [28]	Blue Mountains Eye Study, 12 years	1984–1996	Population-based	USA	56	F: 59.0%	567/73056	2-year period, age , smoking, energy and lutein and zeaxanthin intakes, BMI, profession, physical activity (metabolic equivalent quintiles), and alcohol intake	130-item FFQ	≤1/M (Q1) vs. ≥4/W (Q5)	9
Arnarsson et al., 2006 [29]	Reykjavik Eye Study, 5 years	1996–2001	Population-based	Iceland	≥50	F: 55.8%	134/1379	Age, smoking, and sex	16-item FFQ	≤1/M (Q1) vs. ≥4/W(Q4)	7
Wang et al., 2014 [30]	Rotterdam Study, 15 years	1990–2001	Population-based	The Netherlands	≥55	F: 58.8%	1573/3579	Age- and sex-adjusted	170-item FFQ	<1/W (Q1) vs. ≥1/W(Q2)	8

F: Female; BMI: Body mass index; HT: Hormonal therapy; FFQ: Food frequency questionnaire; AREDS: Age-Related Eye Disease Study; DHA: Docosahexaenoic acid; EPA: Eicosapentaenoic acid. *: The study quality was assessed independently by two reviewers using the Newcastle-Ottawa scale (NOS). The maximum of NOS was 9 stars for a study, and a study with over 6 stars was regarded as being of relatively high quality.

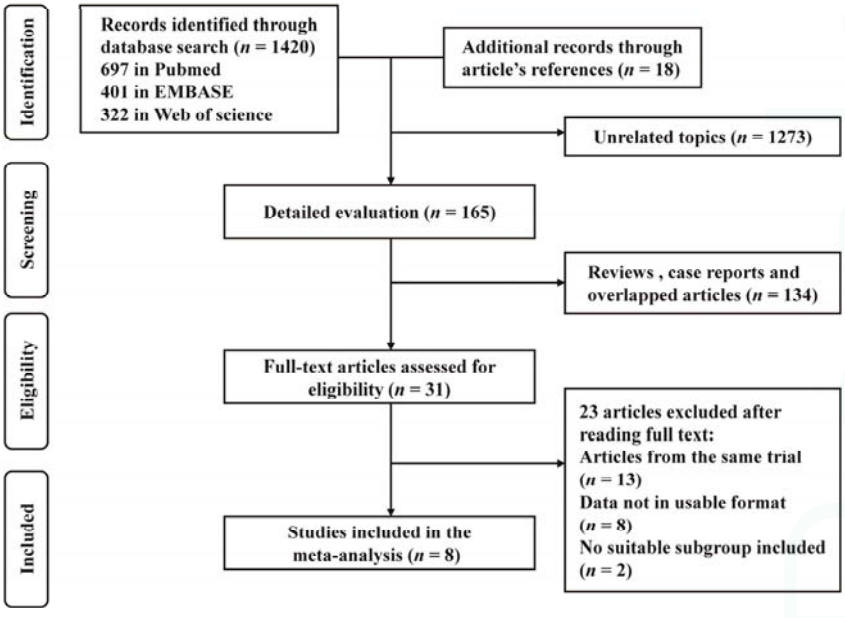

Figure 1. Flow diagram showing the identification of relevant studies in the meta-analysis. The initial 1438 articles were identified, and after 1273 unrelated papers and 134 reviews and case reports were excluded, 31 full texts were assessed for eligibility. Finally, after excluding 23 studies, a total of eight articles were included in this meta-analysis.

The methodological quality of each included study was detected using the NOS scale. NOS was obtained in order to assess the selection, comparability, and outcome of the cohort studies. The scores of each evaluation of all studies are shown in Table 1. All eight included studies were of relatively high quality (over 6 stars) and the mean NOS score was 8.125 stars (standard deviation: 0.295).

3.3. Fish Consumption and Risk of AMD

The pooled estimation on fish consumption and risk of AMD showed that fish consumption can reduce the incidence of AMD. In this meta-analysis, the meta-analyzed RR was 0.76 (95% CI, 0.65–0.90) when any AMD was considered (Figure 2A). Subgroup analysis by AMD stage showed that fish consumption could reduce the risk of both early (RR, 0.83; 95% CI, 0.72–0.96) and late (RR; 0.76; 95% CI, 0.60–0.97) AMD.

Stratified analysis was conducted by data source, study site, and follow-up duration. In the two data source subgroups, a significant association was detected in the population-based group (n = 7; RR, 0.75; 95% CI, 0.63–0.89), but not the hospital-based group (n = 1, RR, 0.88; 95% CI, 0.49–1.59). When the geographical distributions of the included studies were considered, the studies that were conducted in the USA (n = 4; RR, 0.84; 95% CI, 0.72–0.98) and Iceland (n = 1; RR, 0.61; 95% CI, 0.38–0.98) showed statistically significant results; however, no significant results were detected in Australia (n = 2; RR, 0.74; 95% CI, 0.48–1.14) or in the Netherlands (n = 1; RR, 0.98; 95% CI, 0.83–1.15). When stratified by the follow-up duration, fish consumption was a protective factor of AMD in both, over 10 years (n = 5; RR, 0.81; 95% CI, 0.67–0.97) and less than 10 years (n = 3; RR, 0.70; 95% CI, 0.51–0.97) follow-up durations. All the results of the subgroup analyses are presented in Table 2.

We also detected an association between different types of fish and risk of AMD. It was found dark meat fish (RR, 0.68, 95% CI, 0.46–0.99), especially tuna fish (RR, 0.58; 95% CI, 95% CI, 0.47–0.71)

was associated reduced AMD risk. However, no significant association between fish intake and AMD incidence was detected in neither other dark meat fish group (RR, 0.96; 95% CI, 0.75–1.24) nor non-dark meat fish group (RR, 0.82; 95% CI, 0.65–1.03). Subgroup analysis using the processing methods showed that no protective effects were detected in backed, fried or smoked fish group. The results of the detailed stratified analyses are presented in Table 3.

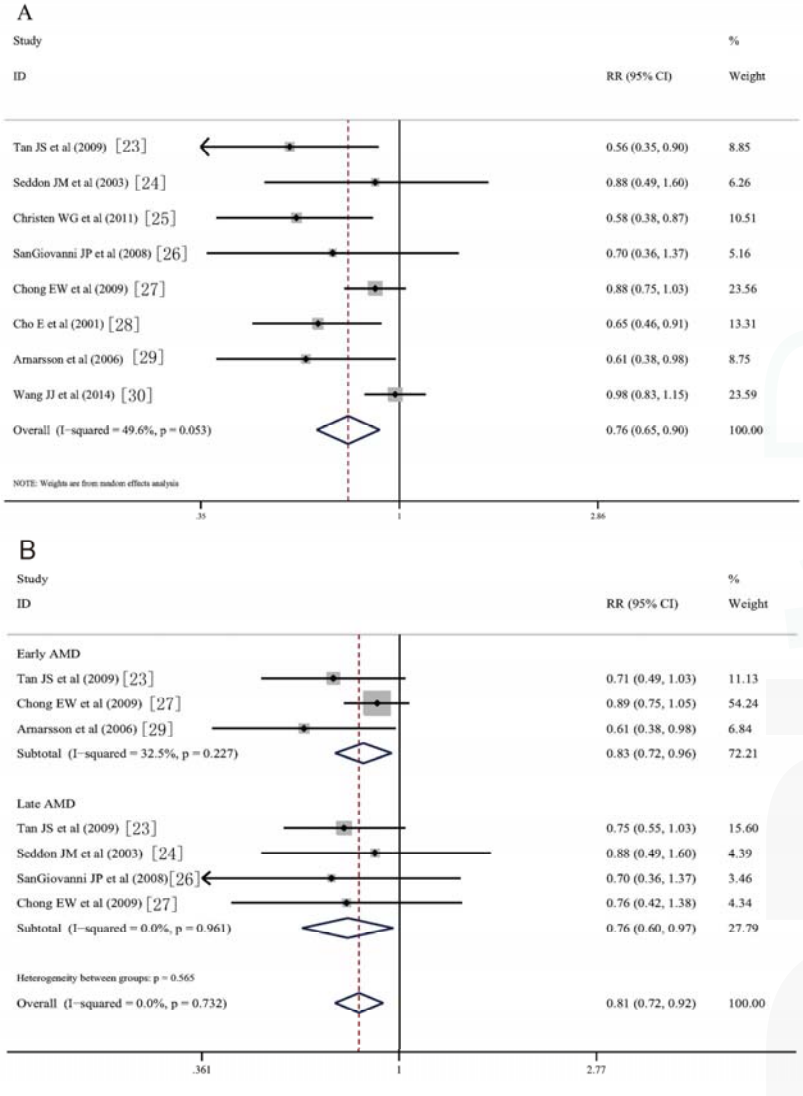

Figure 2. Forest plot of risk estimates of the association between fish intake and risk of age-related macular degeneration (AMD). (**A**) fish consumption and risk of any kind of AMD; (**B**) fish consumption and early and late AMD, through consulting the reference lists of relevant reviews and articles. The size of the shaded square is proportional to the percent weight of each study. Horizontal lines represent 95% confidence intervals (CIs). The diamond data markers indicate pooled odds ratios (ORs).

Table 2. Subgroup analysis of fish consumption and risk of AMD with combined relative risks (RR).

Subgroups	No. of Studies	Summary Effect		Study Heterogeneity	
		RR (95% CI)	*p* Value	I^2, %	*p* Value
Data source					
Population based	7	**0.75; (0.63–0.89)**	**0.001**	56.7	0.031
Hospital based	1	0.88 (0.49–1.59)	0.672	-	-
Country					
USA	4	**0.84 (0.72–0.98)**	**<0.001**	0	0.724
Australia	2	0.74 (0.48–1.14)	0.174	68.50	0.075
Iceland	1	**0.61 (0.38–0.98)**	**0.002**	-	-
Netherlands	1	0.98 (0.83–1.15)	0.787	-	-
Follow-up					
>10 years	5	**0.81 (0.67–0.97)**	**0.024**	53.6	0.072
< 10 years	3	**0.70 (0.51–0.97)**	**0.033**	0	0.638

AMD: age-related macular degeneration. RR: Relative risk; CI: Confidence interval. The result in bold demonstrate a significant outcome.

Table 3. Stratified analysis of fish subtypes and processing methods and risk of AMD with combined RR.

Subgroups	Summary Effect				Study Heterogeneity	
	RR	95% Lower Limiter	95% Upper Limiter	*p* Value	I^2, %	*p* Value
Fish types						
Dark meat fish	**0.68**	**0.46**	**0.99**	**0.047**	**53.70**	**0.091**
Tuna fish	**0.58**	**0.47**	**0.71**	**<0.001**	0	0.934
Other dark meat fish	0.96	0.75	1.24	0.34	-	-
Non-dark meat fish	0.82	0.65	1.03	0.088	0.80	0.315
Processing						
Baked or broiled	0.98	0.87	1.11	0.762	0	0.488
Fried fish	0.97	0.83	1.14	0.731	0	0.508
Smoked fish	0.88	0.54	1.43	0.600	0	0.974

RR: Relative risk. The results in bold demonstrate a significant outcome.

3.4. Heterogeneity and Sensitivity Analysis

Heterogeneity was not significant when all eight studies were pooled in the meta-analysis (I^2, 49.6%; $p = 0.053$). When subgroup analysis by AMD subtypes was conducted, no significant heterogeneity was detected in both groups. When the heterogeneity was significant in the subgroup analysis, a random-effects model was obtained to assess the pooled effect.

A one-way sensitivity analysis was conducted, and there was little change in the quantitative summary measures of RR or the 95% CI. There were no studies influencing results of fish consumption on AMD. The results of the one-way sensitivity analysis are presented in Figure 3.

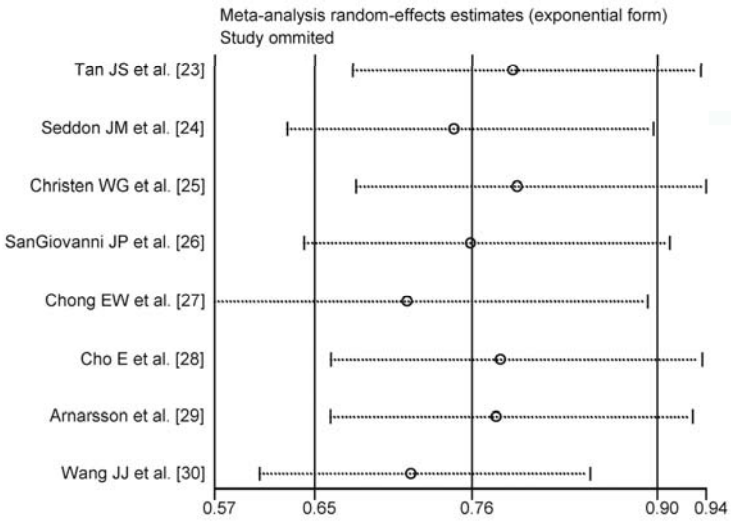

Figure 3. One-way sensitivity analysis for the association between fish intake and AMD risk. There were no studies influencing the result of fish consumption on AMD.

3.5. Dose-Response Meta-Analysis

Considering the significant relationship between fish consumption and the risk of AMD, the potential dose-response relationship was also assessed. It was found that there is a statistically significant association between dose of fish intake and risk of AMD incidence (p = 0.001). A one-time-per-week consumption of fish conferred a RR decrease of 0.11 (RR, 0.89, 95% CI, 0.83–0.96; Figure 4).

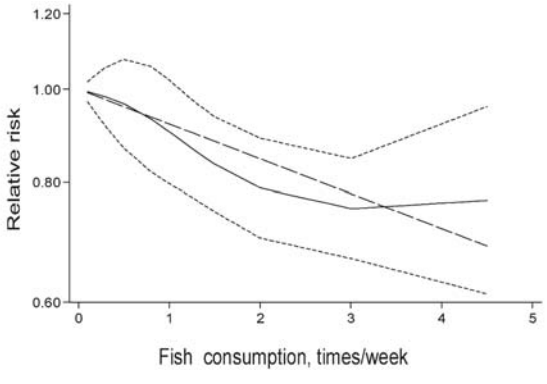

Figure 4. Dose-response relation between fish consumption and relative risks of AMD risk. Lines with short dashes represent the point wise 95% confidence intervals for the fitted nonlinear trend (solid line). Lines with long dashes represent the linear trend.

3.6. Publication Bias

No significant publication bias in the current meta-analysis was detected using either Begg's graph or Egger's test. The funnel plot was symmetrical on visual inspection (Figure 5). In the quantitative assessment, no significant publication bias was detected (Begg's test, p = 0.711; Egger's test, p = 0.068).

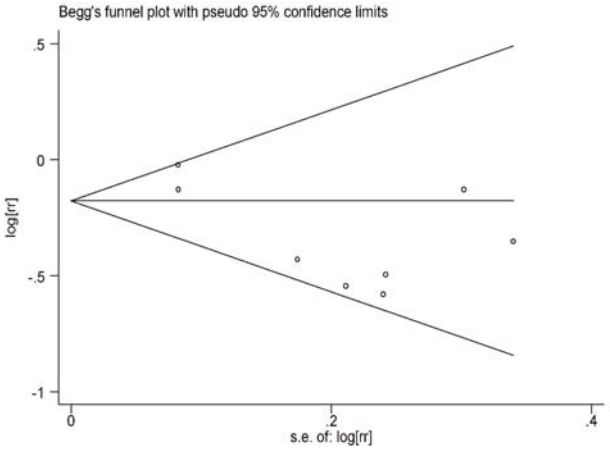

Figure 5. Funnel plot of fish consumption and risk of AMD in the evaluation of publication bias. No significant publication bias was detected through pooling the eight cohorts together.

4. Discussion

A total of 4202 cases with 128,988 individuals from eight cohort studies were identified in this meta-analysis. All the included studies demonstrated a relatively high methodological quality. The findings of this meta-analysis indicated that fish consumption was associated with a reduced risk of AMD. Meanwhile, subgroup analysis by AMD stages showed that fish consumption could reduce the risk of both early and late AMD. When stratified by the follow-up duration, fish consumption was a protective factor of AMD, in both over and less than a 10-year follow-up duration. We also detected an association between different types of fish and risk of AMD. Advanced subgroup analysis showed that dark meat fish and tuna fish showed a protective effect on AMD. In addition, obvious evidence of a statistically significant dose-response relationship between fish intake and AMD risk was detected.

It was reported that inflammation and oxidative stress were key pathologic processes in the development of AMD [31]. Those two examples have long been regarded as potential targets of pharma-projects and primary prevention. PUFAs, which are usually acquired from seafood intake, have been reported to modify the inflammatory reactions and oxidative stress in several diseases [32]. It is natural to presume that additional supplementation of PUFAs would lead to a prevention in the incidence and progression of AMD. Previous epidemiological studies and clinical trials have shown that PUFA supplementation could reduce the risk of AMD [33,34]. However, there were also two studies that reported an increased risk of AMD with higher *n*-3 PUFA consumption [5,35]. A meta-analysis on the association between *n*-3 PUFA intake and AMD risk showed that higher *n*-3 PUFA intake could reduce AMD risk [36]. Plasma *n*-3 PUFA, a nutritional biomarker of *n*-3 PUFA status, was reported to be associated with the incidence of AMD. In a population-based study on nutrition and age-related eye diseases, performed in 963 residents of Bordeaux (France) aged $\geq$73 years [7], it was found that high concentrations of plasma *n*-3 PUFAs are associated with a decreased risk for late AMD.

Fish, especially tuna fish, is the main source of PUFAs, and higher fish consumption can increase the concentrations of *n*-3 PUFA in blood [37]. In this study, we found that fish consumption could reduce the risk of AMD, and a dose-response effect of fish intake on the incidence of AMD was detected. This result was very consistent with the results from several previous studies. In this meta-analysis, only prospective cohort studies were included. Certainly, case-control studies and cross-sectional studies can provide clues of the related factors of diseases, however, the evidence from cohort studies avoid these types of potential selection biases. The meta-analysis of cohort studies can provide

evidence with a higher quality. In the US Twin Study, increased intake of fish reduced risk of AMD, particularly for two or more servings per week [38]. Another multicenter eye disease case-control study involving five US clinical ophthalmology centers showed interesting results; compared with age and sex matched controls, higher fish consumption tended to reduce risk of AMD when the diet was low in linoleic acid. In another case-control study, with 437 advanced AMD cases and 259 unrelated controls, risk of AMD incidence was found to be 51% lower in the highest quartile of fish intake compared to the lowest quartile (OR = 0.49, 95% CI, 0.26–0.90) [39]. Considering that most case-control showed a significant association between fish intake and reduced AMD incidence, it could be presumed that the exclusion of case-control studies in this current meta-analysis would not lead to a significant change in the main outcome.

In this meta-analysis, we found that it was tuna fish but not other types of fish that could reduce the risk of AMD. This was also found in the Nurses' Health Study (NHS) and the Health Professionals Follow-up Study, a significant inverse association was found only in tuna group. The pooled RR of participants who ate canned tuna more than once 4 times per week was significantly lower (RR, 0.61; 95% CI: 0.45, 0.83) [28]. Tuna fish is rich in PUFAs and it is usually consumed because of its low price. Tuna oil, which is from the muscles of deep sea tuna, contains high concentration of eicosapentaenoic acid (EPA) and docosahexaenoic acid (DHA). A previous cross-sectional study showed that both DHA and EPA consumption was associated with a reduced risk of neovascular AMD [40], while only DHA but not EPA was found to associated with AMD risk in NHS. High DHA content is detected in both brain and retina. Therefore a constant supply of DHA was required for normal regeneration of photoreceptor outer segments and thus produced protective effect in degenerative diseases such as AMD. Increasing evidence showed that the function of DHA on the photoreceptor and retinal degenerative diseases was quite important. DHA is very important on normal conduction in retinal light stimulation. Exogenous DHA helps to keep the fluidity retinal cell membrane. EPA can reduce blood viscosity, dissolve excess fat in the blood vessel wall and reduce blood fat, prevent and improve the effect of cardiovascular. Besides, EPA could help the normal function of DHA in the retina. Moreover, in the consumption of tuna salad, essential fatty acid in tuna salad was mixed vegetable fat and might thus produce more powerful protection in the AMD incidence. Additionally, some other components of tuna fish might affect the incidence or progression of AMD. As we know, different risks modified by fish intake were associated with processing methods. As we see, baked, broiled, fried, and smoked fish intake was not associated with a risk of AMD. We hypothesized that baking, broiling, frying, and smoking processing methods might be harmful to the beneficial materials in fish. In addition, the baked, broiled, fried, and smoked fish processing methods might produce harmful effects for AMD development. Besides, because more significant effect of DHA was detected in mechanism of action and epidemiological features, high DHA/EPA ratio in tuna might explain its particularly stronger inverse association with AMD. Considering few study focused the contribution of DHA/EPA ratio in the AMD progressing, advanced epidemiological studies and experimental studies were required. However, it should be noted that the amount of the publications included in the fish subtype meta-analysis was small and the results in this meta-analysis need to be further confirmed by advanced well-designed study.

Several previous trials were conducted in order to explore the effects of PUFA supplementation on the prevention of AMD. The Nutritional AMD Treatment 2 Study was conducted to evaluate the efficacy of DHA-enriched oral supplementation in preventing exudative AMD [41]. The study was a randomized, placebo-controlled, double-blind, parallel, comparative study, and a total of 263 patients with early AMD lesions and a visual acuity better than 0.4 logarithm of minimum angle of resolution units were included. In wet AMD cases, DHA-enriched supplementation for three years had no significant protective effect on choroidal neovascularization (CNV) incidence in the second eye, as did the placebo. The Age-Related Eye Disease Study 2 (AREDS2) was a multicenter, placebo-controlled RCT in 2006–2012. A total of 4203 participants who were at risk for AMD progression were included in the clinical trial and therapeutic effects of different treatment protocols were compared [42]. It was

reported that supplementation of lutein + zeaxanthin, DHA + EPA, or both, failed to further reduce the risk of progression to late AMD. The evidence from the RCTs showed the PUFA supplementation might be not associated with the incidence or progression of AMD. However, the conclusion that fish consumption could reduce the incidence of AMD may not be influenced. Fish is a kind of food with complex components and we cannot exclude the possibility that some other components in fish may also contribute to the association. It should be noted that tuna fish, especially tinned tuna, is an important source of meso-zeaxanthin. Meso-zeaxanthin supplementation has been shown to improve macular pigment optical density in both AMD patients and healthy subjects in a dose-response relationship [43]. In the Meso-zeaxanthin Ocular Supplementation Trial (MOST), it was found that a significant increase in macular pigment from baseline was observed in the meso-zeaxanthin treated group [44]. A previous meta-analysis regarding RCTs showed that *n*-3 PUFA supplementation in people with AMD does not increase the progression or development of AMD [45]. As reported in the SELECT Trial, it was found that men in the highest quartile *n*-3 PUFA level had an increased risk for prostate cancer [46]. It was observed that *n*-3 PUFA supplementation might produce certain harmful effects on chronic inflammation, and a possible explanation for this relates to the fact that polyunsaturated fatty acids act as a substrate for reactive oxygen damage. Dark meat fish, which was the richest source of (docosahexaenoic acid) DHA and (eicosapentaenoic acid) EPA, was associated with reduced AMD risk in this meta-analysis. Thus, additional well-designed studies are required for the detection of the protective effects of anti-oxidants in early AMD.

There are several strengths in this current meta-analysis: (1) A relative comprehensive literature search strategy was used in the search for related publications. We searched databases, including the key words "life style" OR "dietary factor" to detect all available studies; (2) Only prospective cohort studies were included in this meta-analysis, and all included studies demonstrate a relatively high quality. Thus, no significant selection bias influences the conclusion of this study. Robust conclusions were proven through detailed sensitivity analysis and, thus, it suggests that the conclusions of this study are quite credible; (3) A dose-response analysis was conducted and we detected a dose-response relationship between fish intake and AMD risk. The advanced analyses using available data could provide a better understanding of the effect of fish consumption on the risk of AMD.

As with any meta-analysis of observational studies, our study has several limitations. Firstly, the amount of included studies was small. Even through a comprehensive literature search was conducted, only eight studies were included in this meta-analysis. This limited the dependability of subgroup analysis, as only a few studies were included. Secondly, most studies did not provide data stratified by some important confounding factors, such as tobacco smoking and family history. Although all the RR values of the included studies were adjusted by key factors, the influence of these factors should not be ignored. These points all indicate the requirement of additional well-designed studies in the future.

5. Conclusions

In conclusion, the results from this meta-analysis of prospective cohort studies demonstrated that fish consumption, especially tuna fish, could reduce AMD incidence. There was a significant dose-response relationship between fish consumption and risk of AMD. However, additional longitudinal studies with more detailed data, such as fish subtypes or processing methods, are still required and would provide a better understanding on this issue.

Conflicts of Interest: The authors declare no conflict of interest.

References

1. Owen, C.G.; Jarrar, Z.; Wormald, R.; Cook, D.G.; Fletcher, A.E.; Rudnicka, A.R. The estimated prevalence and incidence of late stage age related macular degeneration in the UK. *Br. J. Ophthalmol.* **2012**, *96*, 752–756. [CrossRef] [PubMed]

2. Rodrigues, I.A.; Sprinkhuizen, S.M.; Barthelmes, D.; Blumenkranz, M.; Cheung, G.; Haller, J.; Johnston, R.; Kim, R.; Klaver, C.; McKibbin, M.; et al. Defining a Minimum Set of Standardized Patient-centered Outcome Measures for Macular Degeneration. *Am. J. Ophthalmol.* **2016**, *168*, 1–12. [CrossRef] [PubMed]
3. Saksens, N.T.; Lechanteur, Y.T.; Verbakel, S.K.; Groenewoud, J.M.; Daha, M.R.; Schick, T.; Fauser, S.; Boon, C.J.; Hoyng, C.B.; den Hollander, A.I. Analysis of Risk Alleles and Complement Activation Levels in Familial and Non-Familial Age-Related Macular Degeneration. *PLoS ONE* **2016**, *11*, e0144367. [CrossRef] [PubMed]
4. Akuffo, K.O.; Beatty, S.; Stack, J.; Dennison, J.; O'Regan, S.; Meagher, K.A.; Peto, T; Nolan, J. Central Retinal Enrichment Supplementation Trials (CREST): Design and methodology of the CREST randomized controlled trials. *Ophthalmic Epidemiol.* **2014**, *21*, 111–123. [CrossRef] [PubMed]
5. Parekh, N.; Voland, R.P.; Moeller, S.M.; Blodi, B.A.; Ritenbaugh, C.; Chappell, R.J.; Wallace, R.B.; Mares, J.A.; CAREDS Research Study Group. Association between dietary fat intake and age-related macular degeneration in the Carotenoids in Age-Related Eye Disease Study (CAREDS): An ancillary study of the Women's Health Initiative. *Arch. Ophthalmol.* **2009**, *127*, 1483–1493. [CrossRef] [PubMed]
6. Chua, B.; Flood, V.; Rochtchina, E.; Wang, J.J.; Smith, W.; Mitchell, P. Dietary fatty acids and the 5-year incidence of age-related maculopathy. *Arch. Ophthalmol.* **2006**, *124*, 981–986. [CrossRef] [PubMed]
7. Merle, B.M.; Delyfer, M.N.; Korobelnik, J.F.; Rougier, M.B.; Malet, F.; Feart, C.; Le Goff, M.; Peuchant, E.; Letenneur, L.; Dartigues, J.F.; et al. High concentrations of plasma *n*3 fatty acids are associated with decreased risk for late age-related macular degeneration. *J. Nutr.* **2013**, *143*, 505–511. [CrossRef] [PubMed]
8. Nettleton, J.A. Omega-3 fatty acids: Comparison of plant and seafood sources in human nutrition. *J. Am. Diet. Assoc.* **1991**, *91*, 331–337. [PubMed]
9. Mozaffarian, D.; Rimm, E.B. Fish intake, contaminants, and human health: Evaluating the risks and the benefits. *JAMA* **2006**, *296*, 1885–1899. [CrossRef] [PubMed]
10. Gong, Y.; Liu, Z.; Liao, Y.; Mai, C.; Chen, T.; Tang, H.; Tang, Y. Effectiveness of omega-3 Polyunsaturated Fatty Acids Based Lipid Emulsions for Treatment of Patients after Hepatectomy: A Prospective Clinical Trial. *Nutrients* **2016**, *8*, 357. [CrossRef] [PubMed]
11. Parekh, N.; Chappell, R.J.; Millen, A.E.; Albert, D.M.; Mares, J.A. Association between vitamin D and age-related macular degeneration in the Third National Health and Nutrition Examination Survey, 1988 through 1994. *Arch. Ophthalmol.* **2007**, *125*, 661–669. [CrossRef] [PubMed]
12. Smith, W.; Mitchell, P.; Leeder, S.R. Dietary fat and fish intake and age-related maculopathy. *Arch. Ophthalmol.* **2000**, *118*, 401–404. [CrossRef] [PubMed]
13. Seddon, J.M.; Rosner, B.; Sperduto, R.D.; Yannuzzi, L.; Haller, J.A.; Blair, N.P.; Willett, W. Dietary fat and risk for advanced age-related macular degeneration. *Arch. Ophthalmol.* **2001**, *119*, 1191–1199. [CrossRef] [PubMed]
14. Tan, J.S.; Mitchell, P.; Kifley, A.; Flood, V.; Smith, W.; Wang, J.J. Smoking and the long-term incidence of age-related macular degeneration: The Blue Mountains Eye Study. *Arch. Ophthalmol.* **2007**, *125*, 1089–1095. [CrossRef] [PubMed]
15. Seddon, J.M.; Ajani, U.A.; Sperduto, R.D.; Hiller, R.; Blair, N.; Burton, T.C.; Farber, M.D.; Gragoudas, E.S.; Haller, J.; Miller, D.T.; et al. Dietary carotenoids, vitamins A, C, and E, and advanced age-related macular degeneration. Eye Disease Case-Control Study Group. *JAMA* **1994**, *272*, 1413–1420. [CrossRef] [PubMed]
16. Mares-Perlman, J.A.; Brady, W.E.; Klein, R.; VandenLangenberg, G.M.; Klein, B.E.; Palta, M. Dietary fat and age-related maculopathy. *Arch. Ophthalmol.* **1995**, *113*, 743–748. [CrossRef] [PubMed]
17. Chong, E.W.; Kreis, A.J.; Wong, T.Y.; Simpson, J.A.; Guymer, R.H. Alcohol consumption and the risk of age-related macular degeneration: A systematic review and meta-analysis. *Am. J. Ophthalmol.* **2008**, *145*, 707–715. [CrossRef] [PubMed]
18. Moher, D.; Liberati, A.; Tetzlaff, J.; Altman, D.G. Preferred reporting items for systematic reviews and meta-analyses: The PRISMA statement. *BMJ* **2009**, *339*, b2535. [CrossRef] [PubMed]
19. Stroup, D.F.; Berlin, J.A.; Morton, S.C.; Olkin, I.; Williamson, G.D.; Rennie, D.; Moher, D.; Becker, B.J.; Sipe, T.A.; Thacker, S.B. Meta-analysis of observational studies in epidemiology: A proposal for reporting. Meta-analysis Of Observational Studies in Epidemiology (MOOSE) group. *JAMA* **2000**, *283*, 2008–2012. [CrossRef] [PubMed]
20. Stang, A. Critical evaluation of the Newcastle-Ottawa scale for the assessment of the quality of nonrandomized studies in meta-analyses. *Eur. J. Epidemiol.* **2010**, *25*, 603–605. [CrossRef] [PubMed]

21. Larsson, S.C.; Orsini, N.; Wolk, A. Vitamin B_6 and risk of colorectal cancer: A meta-analysis of prospective studies. *JAMA* **2010**, *303*, 1077–1083. [CrossRef] [PubMed]
22. Harrell, F.E., Jr.; Lee, K.L.; Pollock, B.G. Regression models in clinical studies: Determining relationships between predictors and response. *J. Natl. Cancer Inst.* **1988**, *80*, 1198–1202. [CrossRef] [PubMed]
23. Tan, J.S.; Wang, J.J.; Flood, V.; Mitchell, P. Dietary fatty acids and the 10-year incidence of age-related macular degeneration: The Blue Mountains Eye Study. *Arch. Ophthalmol.* **2009**, *127*, 656–665. [CrossRef] [PubMed]
24. Seddon, J.M.; Cote, J.; Rosner, B. Progression of age-related macular degeneration: Association with dietary fat, transunsaturated fat, nuts, and fish intake. *Arch. Ophthalmol.* **2003**, *121*, 1728–1737. [CrossRef] [PubMed]
25. Christen, W.G.; Schaumberg, D.A.; Glynn, R.J.; Buring, J.E. Dietary omega-3 fatty acid and fish intake and incident age-related macular degeneration in women. *Arch. Ophthalmol.* **2011**, *129*, 921–929. [CrossRef] [PubMed]
26. SanGiovanni, J.P.; Chew, E.Y.; Agron, E.; Clemons, T.E.; Ferris, F.L., III; Gensler, G.; Lindblad, A.S.; Milton, R.C.; Seddon, J.M.; Klein, R.; et al. The relationship of dietary omega-3 long-chain polyunsaturated fatty acid intake with incident age-related macular degeneration: AREDS report No. 23. *Arch. Ophthalmol.* **2008**, *126*, 1274–1279. [CrossRef] [PubMed]
27. Chong, E.W.; Robman, L.D.; Simpson, J.A.; Hodge, A.M.; Aung, K.Z.; Dolphin, T.K.; English, D.R.; Giles, G.G.; Guymer, R.H. Fat consumption and its association with age-related macular degeneration. *Arch. Ophthalmol.* **2009**, *127*, 674–680. [CrossRef] [PubMed]
28. Cho, E.; Hung, S.; Willett, W.C.; Spiegelman, D.; Rimm, E.B.; Seddon, J.M.; Colditz, G.A.; Hankinson, S.E. Prospective study of dietary fat and the risk of age-related macular degeneration. *Am. J. Clin. Nutr.* **2001**, *73*, 209–218. [PubMed]
29. Arnarsson, A.; Sverrisson, T.; Stefansson, E.; Sigurdsson, H.; Sasaki, H.; Sasaki, K.; Jonasson, F. Risk factors for five-year incident age-related macular degeneration: The Reykjavik Eye Study. *Am. J. Ophthalmol.* **2006**, *142*, 419–428. [CrossRef] [PubMed]
30. Wang, J.J.; Buitendijk, G.H.; Rochtchina, E.; Lee, K.E.; Klein, B.E.; van Duijn, C.M.; Flood, V.M.; Meuer, S.M.; Attia, J.; Myers, C.; et al. Genetic susceptibility, dietary antioxidants, and long-term incidence of age-related macular degeneration in two populations. *Ophthalmology* **2014**, *121*, 667–675. [CrossRef] [PubMed]
31. Iannaccone, A.; Giorgianni, F.; New, D.D.; Hollingsworth, T.J.; Umfress, A.; Alhatem, A.H.; Neeli, I.; Lenchik, N.I.; Jennings, B.J.; Calzada, J.I.; et al. Circulating Autoantibodies in Age-Related Macular Degeneration Recognize Human Macular Tissue Antigens Implicated in Autophagy, Immunomodulation, and Protection from Oxidative Stress and Apoptosis. *PLoS ONE* **2015**, *10*, e0145323. [CrossRef] [PubMed]
32. Cialdella-Kam, L.; Nieman, D.C.; Knab, A.M.; Shanely, R.A.; Meaney, M.P.; Jin, F.; Sha, W.; Ghosh, S. A Mixed Flavonoid-Fish Oil Supplement Induces Immune-Enhancing and Anti-Inflammatory Transcriptomic Changes in Adult Obese and Overweight Women—A Randomized Controlled Trial. *Nutrients* **2016**, *8*, 277. [CrossRef] [PubMed]
33. Querques, G.; Merle, B.M.; Pumariega, N.M.; Benlian, P.; Delcourt, C.; Zourdani, A.; Leisy, H.B.; Lee, M.D.; Smith, R.T.; Souied, E.H. Dynamic Drusen Remodelling in Participants of the Nutritional AMD Treatment-2 (NAT-2) Randomized Trial. *PLoS ONE* **2016**, *11*, e0149219. [CrossRef] [PubMed]
34. Dawczynski, J.; Jentsch, S.; Schweitzer, D.; Hammer, M.; Lang, G.E.; Strobel, J. Long term effects of lutein, zeaxanthin and omega-3-LCPUFAs supplementation on optical density of macular pigment in AMD patients: the LUTEGA study. *Graefe's Arch. Clin. Exp. Ophthalmol.* **2013**, *251*, 2711–2723. [CrossRef] [PubMed]
35. Robman, L.; Vu, H.; Hodge, A.; Tikellis, G.; Dimitrov, P.; McCarty, C.; Guymer, R. Dietary lutein, zeaxanthin, and fats and the progression of age-related macular degeneration. *Can. J. Ophthalmol.* **2007**, *42*, 720–726. [CrossRef] [PubMed]
36. Chong, E.W.; Kreis, A.J.; Wong, T.Y.; Simpson, J.A.; Guymer, R.H. Dietary omega-3 fatty acid and fish intake in the primary prevention of age-related macular degeneration: A systematic review and meta-analysis. *Arch. Ophthalmol.* **2008**, *126*, 826–833. [CrossRef] [PubMed]
37. Kabasawa, S.; Mori, K.; Horie-Inoue, K.; Gehlbach, P.L.; Inoue, S.; Awata, T.; Katayama, S.; Yoneya, S. Associations of cigarette smoking but not serum fatty acids with age-related macular degeneration in a Japanese population. *Ophthalmology* **2011**, *118*, 1082–1088. [CrossRef] [PubMed]
38. Seddon, J.M.; George, S.; Rosner, B. Cigarette smoking, fish consumption, omega-3 fatty acid intake, and associations with age-related macular degeneration: The US Twin Study of Age-Related Macular Degeneration. *Arch. Ophthalmol.* **2006**, *124*, 995–1001. [CrossRef] [PubMed]

39. Montgomery, M.P.; Kamel, F.; Pericak-Vance, M.A.; Haines, J.L.; Postel, E.A.; Agarwal, A.; Richards, M.; Scott, W.K.; Schmidt, S. Overall diet quality and age-related macular degeneration. *Ophthalmic Epidemiol* **2010**, *17*, 58–65. [CrossRef] [PubMed]
40. Augood, C.; Chakravarthy, U.; Young, I.; Vioque, J.; de Jong, P.T.; Bentham, G.; Rahu, M.; Seland, J.; Soubrane, G.; Tomazzoli, L.; et al. Oily fish consumption, dietary docosahexaenoic acid and eicosapentaenoic acid intakes, and associations with neovascular age-related macular degeneration. *Am. J. Clin. Nutr.* **2008**, *88*, 398–406. [PubMed]
41. Souied, E.H.; Delcourt, C.; Querques, G.; Bassols, A.; Merle, B.; Zourdani, A.; Smith, T.; Benlian, P.; Nutritional AMD Treatment 2 Study Group. Oral docosahexaenoic acid in the prevention of exudative age-related macular degeneration: the Nutritional AMD Treatment 2 study. *Ophthalmology* **2013**, *120*, 1619–1631. [CrossRef] [PubMed]
42. Age-Related Eye Disease Study 2 Research Group. Lutein + zeaxanthin and omega-3 fatty acids for age-related macular degeneration: The Age-Related Eye Disease Study 2 (AREDS2) randomized clinical trial. *JAMA* **2013**, *309*, 2005–2015.
43. Ma, L.; Liu, R.; Du, J.H.; Liu, T.; Wu, S.S.; Liu, X.H. Lutein, Zeaxanthin and Meso-zeaxanthin Supplementation Associated with Macular Pigment Optical Density. *Nutrients* **2016**, *8*, 426. [CrossRef] [PubMed]
44. Akuffo, K.O.; Nolan, J.M.; Howard, A.N.; Moran, R.; Stack, J.; Klein, R.; Klein, B.E.; Meuer, S.M.; Sabour-Pickett, S.; Thurnham, D.I.; et al. Sustained supplementation and monitored response with differing carotenoid formulations in early age-related macular degeneration. *Eye* **2015**, *29*, 902–912. [CrossRef] [PubMed]
45. Lawrenson, J.G.; Evans, J.R. Omega 3 fatty acids for preventing or slowing the progression of age-related macular degeneration. *Cochrane Database Syst. Rev.* **2015**, *11*, CD010015.
46. Brasky, T.M.; Darke, A.K.; Song, X.; Tangen, C.M.; Goodman, P.J.; Thompson, I.M.; Meyskens, F.L., Jr.; Goodman, G.E.; Minasian, L.M.; Parnes, H.L.; et al. Plasma phospholipid fatty acids and prostate cancer risk in the SELECT trial. *J. Natl. Cancer Inst.* **2013**, *105*, 1132–1141. [CrossRef] [PubMed]

nutrients

MDPI

Article

Regressive Effect of Myricetin on Hepatic Steatosis in Mice Fed a High-Fat Diet

Shu-Fang Xia [1,2,*], Guo-Wei Le [2], Peng Wang [3], Yu-Yu Qiu [1], Yu-Yu Jiang [1] and Xue Tang [2]

1 Wuxi School of Medicine, Jiangnan University, Wuxi 214122, China; yuyuqiu1102@aliyun.com (Y.-Y.Q.); doctoryuyu@126.com (Y.-Y.J.)

2 State Key Laboratory of Food Science and Technology, School of Food Science and Technology, Jiangnan University, Wuxi 214122, China; 1601050217@163.com (G.-W.L.); tangxue@jiangnan.edu.cn (X.T.)

3 COFCO Corporation Oilseeds Processing Division, Beijing 100020, China; wpeng@cofco.com

* Correspondence: sfxia2015@163.com; Tel.: +86-510-8532-8363

Received: 9 October 2016; Accepted: 5 December 2016; Published: 11 December 2016

Abstract: Myricetin is an effective antioxidant in the treatment of obesity and obesity-related metabolic disorders. The objective of this study was to explore the regressive effect of myricetin on pre-existing hepatic steatosis induced by high-fat diet (HFD). C57BL/6 mice were fed either a standard diet or a HFD for 12 weeks and then half of the mice were treated with myricetin (0.12% in the diet, *w/w*) while on their respective diets for further 12 weeks. Myricetin treatment significantly alleviated HFD-induced steatosis, decreased hepatic lipid accumulation and thiobarbituric acid reactive substance (TBARS) levels, and increased antioxidative enzyme activities, including catalase (CAT), superoxide dismutase (SOD), and glutathione peroxidase (GPx) activities. Microarray analysis of hepatic gene expression profiles showed that myricetin significantly altered the expression profiles of 177 genes which were involved in 12 biological pathways, including the peroxisome proliferator activated receptor (PPAR) signaling pathway and peroxisome. Further research indicated that myricetin elevated hepatic nuclear Nrf2 translocation, increased the protein expression of heme oxygenase-1 (HO-1) and NAD(P)H quinone dehydrogenase 1 (NQO1), reduced the protein expression of PPARγ, and normalized the expressions of genes that were involved in peroxisome and the PPAR signaling pathway. Our data indicated that myricetin might represent an effective therapeutic agent to treat HFD-induced hepatic steatosis via activating the Nrf2 pathway and the PPAR signaling pathway.

Keywords: myricetin; hepatic steatosis; Nrf2; PPARγ; oxidative stress

1. Introduction

Obesity is a condition of energy imbalance that is accompanied by excessive accumulation of lipids in non-adipose tissues [1]. Hepatic steatosis characterized by the accumulation of lipids in the liver is one such process and increasing in prevalence [2]. High-fat diets (HFD), especially those rich in saturated fat and monounsaturated fat could be responsible for the epidemic [3]. Hepatic steatosis and its related inflammatory state (non-alcoholic steatohepatitis, NASH) are the common hepatic complications of obesity and metabolic disorders. HFD-induced dyslipidemia and lipid accumulation initiate the development of hepatic steatosis, and may progress to NASH, fibrosis, cirrhosis and, ultimately, hepatocellular carcinoma [4], which comprises the non-alcoholic fatty liver disease (NAFLD). Excessive triglyceride accumulation in hepatocytes is the hallmark of NAFLD, which is significantly associated with insulin resistance in liver [5]. Based on the results of animal studies and epidemiological investigations, a two-hit hypothesis has been proposed for the pathogenesis of NAFLD: the first hit is excessive fat accumulation in the liver, and the second hit is oxidative stress (OS) that initiates hepatic steatosis to develop into NASH [6]. Although hepatic steatosis is often self-limited, it is necessary to treat it to avoid its progression to more serious diseases. Currently,

no treatments have been established for NAFLD beyond management of comorbidities and weight loss [4]. Lifestyle intervention and pharmacotherapy to treat hepatic steatosis are limited because of poor compliance and side effects. As a result, new approaches to improve hepatic steatosis are urgently necessary.

Rodent research and cell culture experiments demonstrated that antioxidant supplementation could effectively improve hepatic steatosis through attenuating oxidative stress and regulating signaling molecules [7]. Green tea extract attenuated hepatic stetosis by inhibiting adipose lipogenesis, restoring hepatic antioxidant defenses, as well as decreasing hepatic lipid peroxidation and inflammatory responses in *ob/ob* mice [8]. Niacin has also been demonstrated to effectively prevent and reverse experimental hepatic steatosis through decreasing hepatic triglyceride synthesis and lipid peroxidation [9]. When obese mice were treated with an NADPH oxidase inhibitor, reactive oxygen species (ROS) production in adipose tissue was decreased, and diabetes, hyperlipidemia, and hepatic steatosis were improved [10]. Thus, a need exists to verify approaches that alleviate the development and progression of hepatic steatosis and oxidative stress.

Myricetin, (3,5,7,3′,4′,5′-hexahydroxyflavone), a naturally occurring flavonoid, is widely distributed in fruits, vegetables, tea, and medicinal herbs and has been demonstrated to exert many bioactivities, including antioxidant, anti-inflammation, anti-tumor, neuroprotective and cardioprotective properties [11,12]. Myricetin reduced oxidative stress, inhibited hyperglycemia and glucose uptake, decreased hepatic triglyceride and cholesterol contents, and ameliorated liver injury [12–14]. Since initial lipid deposition in liver, and subsequent oxidative stress, is involved in NAFLD, myricetin may mitigate the "multiple hits" of NAFLD due to its hypolipidemic and antioxidant actions. The present study was designed to better define the regressive effect of myricetin on pre-existing hepatic steatosis induced by HFD.

2. Materials and Methods

2.1. Animals

C57BL/6 male mice (38, four-week old) were obtained from Model Animal Research Center of Nanjing University (Nanjing, Jiangsu, China) and housed in a controlled environment (a 12 h/12 h light/dark cycle, 08:00 h to 20:00 h, humidity: 60% ± 5%, temperature: 23 ± 2 °C). After acclimatization for one week on standard laboratory chow, the mice were randomly divided into a control group (Con, 16 mice fed a standard diet of 10% energy from fat) and a HFD group (22 mice fed a HFD diet of 45% energy from fat). The diets were based on a modification of the recommendations of American Institute of Nutrition Rodent Diets (AIN-93). After 12 weeks of feeding, six mice were randomly selected from the HFD group and sacrificed. The liver was harvested and Oil Red O staining was conducted to verify whether the hepatic steatosis was developed. The results showed that five mice, which were about 83% of the total mice, suffered from hepatic steatosis, indicating that the animal model of hepatic steatosis was successfully established. Then eight mice were randomly selected from each group and fed their respective diets with additional 0.12% myricetin (≥98% by high performance liquid chromatography, Aladdin Reagent Co., Shanghai, China) according to the previously published literature [13]. Thus, the present study included four groups: (i) Con; (ii) control diet with 0.12% myricetin (CM); (iii) HFD; and (iv) high-fat diet with 0.12% myricetin (HM). Feeding of all mice with their respective diets (two mice per cage) continued fora further 12 weeks. The animals had free access to the test diets and purified water. All mice were weighed weekly, and food intake was also recorded. All of the experimental procedures were approved by the Jiangnan University Institutional Animal Use and Care Committee (JN No. 5 2015) and according to the National Institutes of Health Guide for Care and Use of Laboratory Animals.

After the feeding period, all mice were fasted overnight and slightly anesthetized with pentobarbital. Blood from the orbital sinus was collected into anticoagulant tubes and plasma was separated after centrifugation (2500× *g* for 15 min at 4 °C) and stored at −20 °C until analyses. Livers

were harvested and weighed. Next, fat compartments that included perirenal, epididymal, and mesenteric fat were thoroughly removed and weighed. All the tissues were snap-frozen with liquid nitrogen and stored at −80 °C. Portions of liver were collected into RNALater (Ambion Inc., Austin, TX, USA) for real-time quantitative PCR analysis. The experiments were conducted between 8:00 and 10:00 to minimize possible circadian mRNA expression variation.

2.2. Indirect Calorimetric Analysis

The comprehensive laboratory animal monitoring system (CLAMS; Columbus Instruments, Inc., Columbus, OH, USA) was used to evaluate respiratory exchange ratio (RER), energy expenditure (EE = (3.815 + 1.232 × RER) × VO_2), and ambulatory activity. One week before the final sacrifice, each mouse was placed in the CLAMS for 24 h for measurement of all in vivo parameters, which include oxygen consumption, carbon dioxide production, and RER. Ambulatory activity was monitored in both horizontal and vertical directions using infrared beams to count the beam breaks during the experiment. Each time the mice were allowed to acclimatize in individual metabolic cages for one day and then the data of the second day were used for further analysis.

2.3. Plasma Biochemical Analysis

Fasting blood glucose (FBG) was assayed with a glucometer (One Touch; LifeScan Inc., Milpitas, CA, USA). Plasma insulin concentrations were analyzed by specific ELISA kits (Mercodia, Uppsala, Sweden). Homeostatic model assessment index of insulin resistance (HOMA-IR) was calculated as ((insulin, μUI/mL) plasma × (glucose, mmol/L) plasma)/22.5. Plasma total cholesterol (TC), low-density lipoprotein cholesterol (LDL-C), high-density lipoprotein cholesterol (HDL-C), and triglyceride (TG) concentrations, as well as aspartate and alanine aminotransferase (AST and ALT) activities were determined by the corresponding enzymatic colorimetric assay kits (Nanjing Jiancheng Bioengineering Institute, Nanjing, Jiangsu, China) according to the manufacturer's instructions. Plasma TG levels were determined by the glycerol phosphatase oxidase–phenol4-amino antipyrene peroxidase (GPO-PAP) method, and TC levels were determined by the cholesterol oxidase–phenol4-amino antipyrene peroxidase (CHOD-PAP) method. Plasma HDL-C and LDL-C levels were assayed by standardized selective precipitation methods, using phosphotungstic acid/$MgCl_2$ and polyvinyl sulfate as precipitating reagents, respectively.

2.4. Hepatic Oxidative Stress Biomarker Determination

Thiobarbituric acid reactive substances (TBARS) levels, catalase (CAT), glutathione peroxidase (GPx), superoxide dismutase (SOD) activities, and protein contents in liver were all determined by corresponding kits obtained from Nanjing Jiancheng Bioengineering Institute (Nanjing, Jiangsu, China) according to the instructions of the manufacturer. TBARS level was measured by monitoring the absorbance at 532 nm using 1,1,3,3-tetramethoxypropane as the standard. CAT was determined colorimetrically at 620 nm and expressed as 1 mol of H_2O_2 consumed/min. SOD activity was determined based on its ability to inhibit the reduction of nitrazobluetetrazolium (NBT). A unit of enzyme activity was expressed as 50% inhibition of NBT reduction/min. GPx activity was measured through the glutathione (GSH)/nicotinamide adenine dinucleotide phosphate (NADPH)/glutathione reductase (GR) system. H_2O_2 was used as the substrate. Hepatically reduced glutathione (GSH) levels were determined by a fluorometric method with the use of *o*-phthalaldehyde (OPT) as a fluorescent reagent [15]. Protein contents were determined by bicinchoninic acid (BCA) methods using a BCA commercial kit (Beyotime Institute of Biotechnology, Nantong, Jiangsu, China).

2.5. Liver Histology

Liver samples (n = 4) from the same position were randomly selected from each group and immersed in 4% paraformaldehyde and paraffin embedded sections were stained with hematoxylin and eosin (H & E, Baso, Taipei, Taiwan). Oil Red O (Baso, Taipei, Taiwan) staining for liver samples

(n = 4) was also conducted after embedded in OCT compound (Sakura Finetech, Tokyo, Japan). All of the pathological sections were observed under a light microscope (Leica DM4000B, Leica, Wetzlar, Germany).

2.6. Hepatic Lipid Content Determination

Hepatic lipids were measured using commercial kits (Wako Pure Chemical Industries, Osaka, Japan) according to the manufacturer's instructions. Briefly, the liver samples were extracted with mixed solvents of methanol-/chloroform (v/v = 1:2), followed by centrifugation, and the supernatants were used for further analysis. Protein contents in the supernatants were analyzed by BCA methods.

2.7. Nimblegen Gene Chip Microarray

In order to find the possible mechanism for ameliorative effects of myricetin on HFD-induced hepatic steatosis, microarray analysis was used to have a wide understanding of the altered genes and pathways that might be involved. Nimblegen gene chip microarray analysis was performed at CapitalBio Corporation (Beijing, China). Samples from HFD and HM groups were isolated from the frozen livers (n = 3 for each group) using Trizol reagent (Invitrogen, Carlsbad, CA, USA) and was further purified using NucleoSpin® RNA clean-up (Macherey-Nagel, Duren, Germany). Array hybridization, washing, and scanning were conducted according to the Nimblegen's Expression user's guide. In a comparison analysis, two-class unpaired method in the Significant Analysis of Microarrays (SAM, version 3.02, Stanford University, Stanford, CA, USA) was performed to identify significantly differentially expressed genes (DEGs) between HFD and HM groups. The DEGs were selected and put into Pathway-Express in Onto-Tools [16]. Pathway-Express searches the Kyoto Encyclopedia of Genes and Genomes (KEGG) pathway database for each input gene, and the impact analysis was performed in order to build a list of all associated pathways [17]. An impact factor (IF) is calculated for each pathway incorporating parameters, such as the normalized fold change of the DEGs, the statistical significance of the set of the pathway genes, and the topology of the signaling pathway. The corrected gamma p-value is the p-value provided by the impact analysis. The differences were considered to be significant when the corrected gamma p-value was less than 0.05.

2.8. Real-Time Quantitative RT-PCR Analyses

Total RNA was isolated from frozen livers using Trizol (Invitrogen, Carlsbad, CA, USA), and reverse transcribed to cDNA according to the manufacturer's instructions (Promega, Madison, WI, USA). Platinum Taq polymerase (Life Technologies, Gaithersburg, MD, USA) and SYBR Green I dye (SYBR Green Master Mix, Bioneer, Taejon, Korea) was used to measure in the exponential phase of amplification by an ABI prism 7500 Sequence Detection System (Applied Biosystems, Foster City, CA, USA). Samples were run in triplicate for both the genes of interest and β-actin. The primers for the genes were provided by Shenggong Biotechnology (Shanghai, China). The gene expression was normalized to β-actin. Melting curve analysis was applied to evaluate the specificity of the amplified PCR products.

2.9. Western Blotting

In order to determine the hepatic protein expression of PPARγ, NQO1, and HO-1, total protein was isolated from the liver in a cold radio-immunoprecipitation assay (RIPA) lysis buffer (Beyotime Institute of Biotechnology, Nantong, Jiangsu, China) with 1% phosphatase inhibitor cocktail and 1% phenylmethanesulfonyl fluoride (PMSF). To determine the nuclear translocation of Nrf2, the supernatants from the first step were gathered and re-centrifuged. The pellet was re-suspended in buffer to extract the hepatic nuclear protein. After the protein was extracted, equal protein contents were transferred to polyvinylidene fluoride (PVDF) membranes (Millipore, Billerica, MA, USA). The membranes were blocked in Tris-buffered saline (TBS) containing 5% (w/v) BSA and thereafter incubated with the primary antibodies, including Nrf2 (Santa Cruz Biotechnology, Santa Cruz, CA,

USA), NQO1 (Santa Cruz Biotechnology, Santa Cruz, CA, USA), HO-1 (Santa Cruz Biotechnology, Santa Cruz, CA, USA), PPARγ (Santa Cruz Biotechnology, Santa Cruz, CA, USA), GAPDH (Santa Cruz Biotechnology, Santa Cruz, CA, USA), and Lamin B1 (Serotec Ltd., Oxford, UK) at 4 °C overnight. Then, the blotted membrane was incubated with the secondary antibody (anti-rabbit peroxidase conjugate, 1:5000 dilutions in Tris-buffered saline containing 0.1% Triton X-100 (TBST); Cell Signaling Technology, Beverly, MA, USA) for 1 h at room temperature. Bands were visualized by enhanced chemiluminescence using an enhanced chemiluminescence (ECL) Western Blotting Detection kit (Amersham Biosciences, Piscataway, NJ, USA) using a Bio-Rad ChemiDocTM XRS system (Bio-Rad Laboratories, Inc., Hercules, CA, USA). The protein quantity was determined by densitometry analysis using ImageJ software (version 1.47, National Institutes of Health, Bethesda, MD, USA).

2.10. Statistical Analysis

Data were expressed as mean ± SEM. Between group differences of microarray data were performed by univariate analysis using Student's *t*-test. All other data were analyzed using one-way ANOVA with post-hoc Duncan's test. Statistical significance was determined as $p < 0.05$. Analysis was done with SPSS 17 (SPSS, Inc., Chicago, IL, USA).

3. Results

3.1. Effects of Myricetin on Body Weight, Food Intake, and Tissue Weight in HFD-Fed Mice

As illustrated in Figure 1, following dietary treatment for 12 weeks, mice in the HFD group exhibited significantly higher body weight than mice in control diet (Figure 1A, $F_{(3, 28)} = 18.22$, $p < 0.0001$). When half mice were administered with 0.12% myricetin, their body weight showed a sharp decrease in the 13th week and began to gradually increase in the later 11 weeks. Finally, HM mice had significantly lower body weight than HFD mice ($F_{(3, 28)} = 10.52$, $p < 0.0001$). The cumulative food intake after grouping demonstrated that HFD mice had significantly higher food intake than Con mice only in the 13th week. No significance was observed on the cumulative food intake among the four groups in the end of the experiment ($F_{(3, 12)} = 1.13$, $p = 0.377$). However, because of the different energy densities between control diet and high-fat diet, HFD mice showed significantly cumulative energy intake compared to Con mice in the later 12 weeks, and HM mice had decreased energy intake, but the difference was not significant (Figure 1B, $F_{(3, 12)} = 2.97$, $p = 0.075$).

Analysis of different fat compartments revealed that perirenal ($F_{(3, 28)} = 49.90$, $p < 0.0001$), epididymal ($F_{(3, 28)} = 105.73$, $p < 0.0001$) and mesenteric fat pad masses ($F_{(3, 28)} = 246.17$, $p < 0.0001$) of HFD mice were significantly higher than those of Con mice. Myricetin treatment significantly reduced the white adipose tissue accumulation compared to HFD mice, but failed to normalize these indexes relative to Con mice. HFD mice showed remarkably increased liver weight compared to Con mice ($F_{(3, 28)} = 93.13$, $p < 0.0001$), which could be normalized by myricetin treatment (Figure 1C). Myricetin, per se, did not affect body weight, energy intake, or tissue weight in mice.

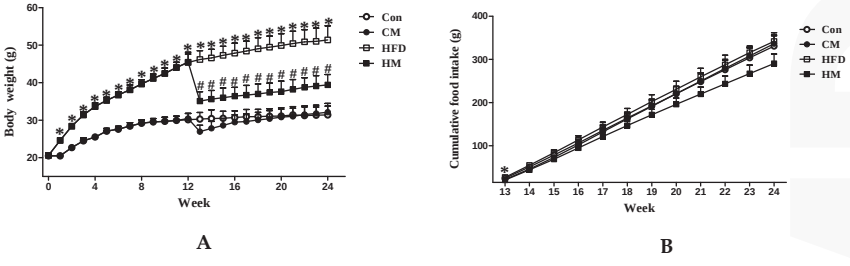

Figure 1. *Cont.*

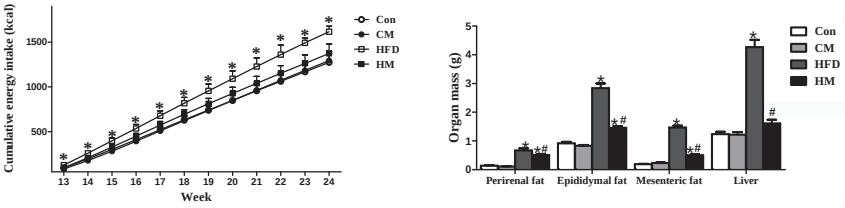

Figure 1. Effects of myricetin on body weight, cumulative food intake and energy intake, and organ mass of mice fed with a high-fat diet. (**A**) Body weight; (**B**) cumulative food intake; (**C**) cumulative energy intake; and (**D**) perirenal, epididymal, and mesenteric fat and liver weight. Values were presented as mean ± SEM (n = 8). Con, control diet; CM, control diet with additional 0.12% myricetin; HFD, high-fat diet; HM, high-fat diet with additional 0.12% myricetin. * $p < 0.05$ vs. the Con group; # $p < 0.05$ vs. the HFD group.

3.2. Effects of Myricetin on FBG and Plasma Parameters in HFD-Fed Mice

As illustrated in Table 1, after 24 weeks, HFD mice demonstrated significantly increased FBG ($F_{(3, 28)} = 3.43$, $p = 0.031$), insulin ($F_{(3, 28)} = 3.12$, $p = 0.042$), and HOMA-IR levels compared to Con mice, which could be alleviated by myricetin treatment. In addition, plasma TG ($F_{(3, 28)} = 6.26$, $p = 0.002$), TC ($F_{(3, 28)} = 14.40$, $p < 0.0001$), and LDL-C ($F_{(3, 28)} = 8.88$, $p < 0.0001$) levels were significantly increased and HDL-C levels were significantly decreased in HFD group compared to Con group. Myricetin treatment significantly improved TC, TG, LDL-C, and HDL-C levels. Myricetin, per se, did not affect FBG and plasma parameters in mice.

Table 1. Regressive effects of myricetin on blood glucose, plasma insulin and lipid profiles.

	Con	CM	HFD	HM
Fasting blood glucose (mg/dL)	113.96 ± 11.51	117.24 ± 12.23	166.19 ± 15.79 *	123.35 ± 12.55 #
Plasma insulin (μIU/mL)	14.47 ± 0.75	15.28 ± 1.93	20.63 ± 2.06 *	14.94 ± 1.46 #
HOMA-IR	4.05 ± 0.45	4.47 ± 0.87	8.67 ± 1.39 *	4.61 ± 0.60 #
Plasma TG (mmol/L)	2.53 ± 0.15	2.54 ± 0.16	3.36 ± 0.17 *	2.71 ± 0.15 #
Plasma TC (mmol/L)	4.09 ± 0.24	4.01 ± 0.27	6.57 ± 0.37 *	4.35 ± 0.38 #
Plasma HDL-C (mmol/L)	1.81 ± 0.08	1.92 ± 0.08	1.41 ± 0.05 *	1.69 ± 0.08 #
Plasma LDL-C (mmol/L)	2.08 ± 0.12	2.05 ± 0.09	2.81 ± 0.10 *	2.30 ± 0.07 #

Values were expressed as mean ± SEM (n = 8). Con, control diet; CM, control diet with 0.12% additional myricetin; HFD, high-fat diet; HM, high-fat diet with 0.12% additional myricetin; HOMA-IR, homeostatic model assessment index of insulin resistance; TG, triglyceride; TC, total cholesterol; HDL-C, high-density lipoprotein cholesterol; LDL-C, low-density lipoprotein cholesterol. * $p < 0.05$ vs. the Con group; # $p < 0.05$ vs. the HFD group.

3.3. Effects of Myricetin on RER, Energy Expenditure and Ambulatory Activities in HFD-Fed Mice

Myricetin successfully reduced body weight and fat pad masses compared to HFD mice. Apart from the difference in energy intake, we hypothesized that myricetin might exert these effects through increasing energy expenditure. Thus, we used indirect calorimetry to prove the hypothesis. Determinations of RER over a 24 h period demonstrated that HM mice showed decreased RER values than HFD mice in the daytime ($F_{(3, 44)} = 354.14$, $p < 0.0001$) and nighttime ($F_{(3, 44)} = 349.48$, $p < 0.0001$) (Figure 2A,B), indicating a shift in metabolism toward an increase in the utilization of lipids as substrate in mice that receiving myricetin treatment. Additionally, HM mice had significantly higher energy expenditure than HFD mice throughout the whole day (Figure 2C,D). Although no significance on ambulatory activity was observed between HFD and HM mice during the daytime ($F_{(3, 44)} = 1.71$, $p = 0.179$), the difference reached statistically significant levels during the dark period ($F_{(3, 44)} = 6.55$,

p = 0.001, Figure 2E,F). Myricetin, per se, had no effects on RER or energy expenditure, but remarkably increased ambulatory activities during the nighttime.

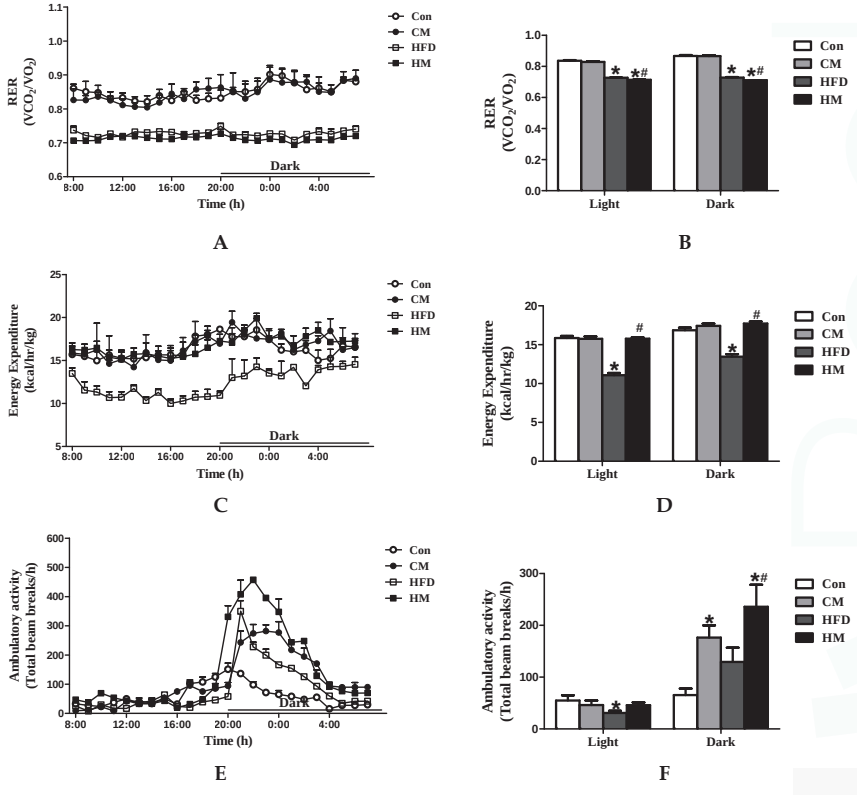

Figure 2. Myricetin increased energy expenditure and promoted the utilization of lipids as fuels. (**A**,**B**) RER; (**C**,**D**) energy expenditure; and (**E**,**F**) ambulatory activities of mice that were fed myricetin-enriched diets for additional 12 weeks after 12 weeks of Con or HFD feeding. Bar graphs represent mean values during the light and dark cycles. Values were presented as mean ± SEM (n = 8). Con, control diet; CM, control diet with additional 0.12% myricetin; HFD, high-fat diet; HM, high-fat diet with additional 0.12% myricetin. * $p < 0.05$ vs. the Con group; # $p < 0.05$ vs. the HFD group.

3.4. Effects of Myricetin on Hepatic Steatosis and Liver Function in HFD-Fed Mice

HFD mice demonstrated prominent and significant formation of lipid vacuoles in hepatocytes compared with Con mice, while such alterations were relieved by myricetin treatment (Figure 3A). Oil Red O staining of liver sections also confirmed that myricetin significantly reduced HFD-induced hepatic lipid accumulation (Figure 3B). Compared to Con mice, HFD mice had greater hepatic total lipids due to augmentation in TG ($F_{(3, 28)}$ = 3.95, p = 0.018), TC ($F_{(3, 28)}$ = 7.50, p = 0.001), and FFA ($F_{(3, 28)}$ = 4.51, p = 0.011) concentrations, which were fully normalized by myricetin (Figure 3C). Plasma ALT ($F_{(3, 28)}$ = 5.99, p = 0.003) and AST ($F_{(3, 28)}$ = 16.56, $p < 0.0001$) activities were also significantly decreased by myricetin administration (Figure 3D). Taken together, these results suggested that myricetin played a positive role in the alleviation of HFD-induced hepatic steatosis. Myricetin, per se, had no effects on liver function and histological appearance.

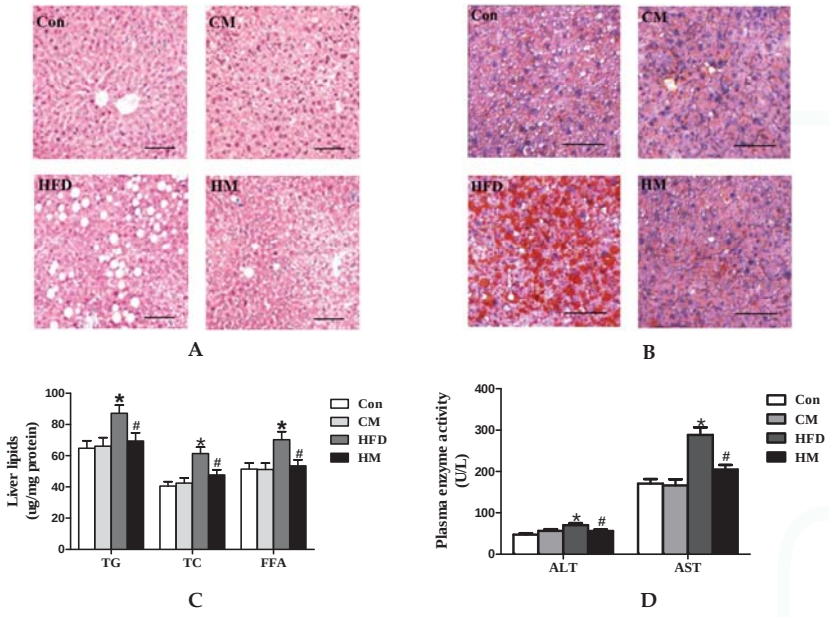

Figure 3. Myricetin reduced hepatic lipid accumulation and increased liver function of mice fed with a high-fat diet. (**A**) Representative images of liver H & E staining (n = 4); (**B**) representative images of liver Oil Red O staining (n = 4); (**C**) hepatic TG, TC, FFA levels (n = 8); (**D**) plasma ALT and AST activities (n = 8). Values were presented as mean ± SEM. Scale bars indicate 50 μm. Con, control diet; CM, control diet with additional 0.12% myricetin; HFD, high-fat diet; HM, high-fat diet with additional 0.12% myricetin. * $p < 0.05$ vs. the Con group; # $p < 0.05$ vs. the HFD group.

3.5. Effects of Myricetin on Hepatic Biological Pathways in HFD-Fed Mice

In microarray analysis 177 genes in the HM group showed more than two-fold higher or lower expression levels compared with those in the HFD group. These 177 genes were put into Pathway-Express, searched the KEGG pathways in the Onto-Tools database for each input gene, and built a list of pathways. Herein the biological pathways more than three DEGs were considered to be significantly changed. KEGG annotation showed that myricetin affected 12 biological pathways and the top 10 significantly affected pathways were shown in Table 2, in which the PPAR signaling pathway was one of the most significantly affected pathways since it had the highest impact factor and six DEGs (*Cd36*, *Scd1*, *Cyp7a1*, *Lpl*, *Pparγ*, and *Pck1*). Furthermore, peroxisome was also significantly changed by HM, in which antioxidative genes, such as *Sod2*, *Prdx1*, and *Prdx5* were all significantly down-regulated.

Pathway-Express was used for the pathway impact analysis in order to build a list of all associated pathways. An impact factor (IF) is calculated for each pathway incorporating parameters such as the normalized fold change of the differentially expressed genes, the statistical significance of the set of pathway genes and the topology of the signaling pathway. The corrected gamma p-value was provided by the impact analysis. The top 10 pathways that were significant at the 5% level on corrected p-values were presented. Altered genes were as follows: *Cd36* (–2.06), *Scd-1* (–2.49), *Cyp7a1* (2.70), *Lpl* (–2.45), *Pparg* (–2.10), *Pck1* (2.05), *Acot1* (2.43), *Acot3* (2.36), *Sod2* (2.32), *Prdx5* (2.28), *Prdx1* (2.08), *C4b* (–3.59), *Plg* (–6.35), *Serpina1a* (4.22), *Arnt* (–3.32), *Jun* (–2.15), *Raf1* (–4.16), *Araf* (2.09), *pla2g2d* (3.12), *Plcb1* (2.35), *Pla2g6* (–2.07), *Cxcl10* (–2.57), *Spp1* (3.00), *Srebf1* (–2.22), and *Ntrk2* (–2.11). Numbers in the parentheses indicated the ratio changes. Positive numbers indicated up-regulation of the HM group relative to the HFD group. Negative numbers indicated down-regulation of the HM group relative to the HFD group.

Table 2. Significantly altered biological pathways in livers of the HM mice compared to HFD mice.

Number	Pathway Name	Input Genes in Pathway	Impact Factor	Corrected Gamma *p*-Value	Significantly Altered Genes
1	PPAR signaling pathway	6	16.26	1.90×10^{-5}	*Cd36*, *Scd1*, *Cyp7a1*, *Lpl*, *Pparg*, *Pck1*
2	Biosynthesis of unsaturated fatty acids	3	10.26	0.00185	*Acot1*, *Acot3*, *Scd1*
3	Peroxisome	3	10.01	0.001974	*Sod2*, *Prdx5*, *Prdx1*
4	Complement and coagulation cascades	3	9.62	0.002971	*C4b*, *Plg*, *Serpina1a*
5	Renal cell carcinoma	3	8.26	0.008088	*Arnt*, *Jun*, *Raf1*
6	Long-term potentiation	4	7.02	0.01977	*Araf*, *pla2g2d*, *Plcb1*, *Raf1*
7	GnRH signaling pathway	3	6.44	0.029597	*Jun*, *Pla2g6*, *Raf1*
8	Toll-like receptor signaling pathway	3	5.92	0.032924	*Cxcl10*, *Jun*, *Spp1*
9	Insulin signaling pathway	3	5.64	0.041843	*Pck1*, *Raf1*, *Srebf1*
10	MAPK signaling pathway	3	5.60	0.043097	*Jun*, *Ntrk2*, *Pla2g6*

3.6. Effects of Myricetin on Expressions of PPAR Signaling Pathway-Related Genes and PPARγ Protein Expression

Previous research demonstrated that the PPAR signaling pathway was related to lipid metabolism [18]. According to the present microarray analysis results, the PPAR signaling pathway was the most significantly affected, indicating that the biological pathway might be a target for beneficial effects of myricetin on hepatic steatosis. The DEGs that were involved in the pathway and were important in lipid metabolism (including *Pparγ*, *Cd36*, *Scd1*, *Lpl*, and *Cyp7a1*) were further determined by qPCR. HFD induced significant down-regulation of *Cyp7a1* ($F_{(3, 28)} = 8.30$, $p < 0.0001$), along with remarkable up-regulation of *Pparγ* ($F_{(3, 28)} = 7.63$, $p = 0.001$), *Cd36* ($F_{(3, 28)} = 22.82$, $p < 0.0001$), *Scd1* ($F_{(3, 28)} = 40.96$, $p < 0.0001$), and *Lpl* ($F_{(3, 28)} = 21.26$, $p < 0.0001$), which could be totally normalized by myricetin treatment (Figure 4A). Considering the fact that PPARγ in the liver is related to the regulation of glucose and lipid metabolism by targeting on its responsive genes, such as *Lpl* and *Cd36*, Western blotting analysis was further used to determine the protein expression of PPARγ. As shown in Figure 4B, HFD consumption induced significantly increased protein expression of PPARγ in the liver ($F_{(3, 28)} = 9.65$, $p < 0.0001$), which could be attenuated by myricetin treatment. These data demonstrated that myricetin treatment ameliorated the HFD-induced hepatic steatosis, which might be associated with the PPAR signaling pathway. Myricetin, per se, had no effects on expressions of genes involved in lipid homeostasis and hepatic PPARγ protein expression.

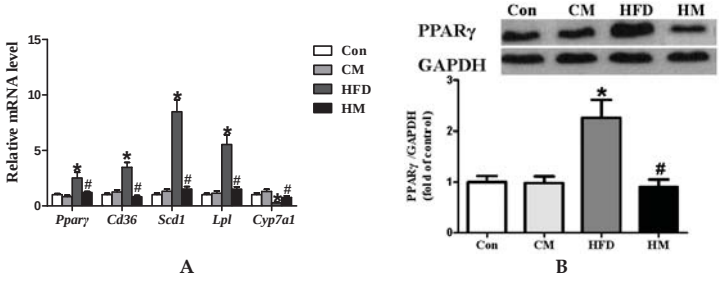

Figure 4. Myricetin normalized expressions of genes involved in lipid metabolism (**A**) and decreased protein expression of hepatic PPARγ (**B**). Values were presented as mean ± SEM ($n = 8$). Con, control diet; CM, control diet with additional 0.12% myricetin; HFD, high-fat diet; HM, high-fat diet with additional 0.12% myricetin. * $p < 0.05$ vs. the Con group; # $p < 0.05$ vs. the HFD group.

3.7. Effects of Myricetin on Hepatic Redox Status in HFD-Fed Mice

To evaluate the role of myricetin on oxidative stress, hepatic redox status of related biomarkers were determined. As illustrated in Figure 5, HFD consumption caused serious oxidative stress in the liver, as evidenced by significantly reduced GPx ($F_{(3, 28)} = 4.53$, $p = 0.01$), SOD ($F_{(3, 28)} = 4.05$, $p = 0.017$), CAT ($F_{(3, 28)} = 7.76$, $p = 0.001$) activities, and GSH ($F_{(3, 28)} = 4.23$, $p = 0.014$) levels, along with increased TBARS ($F_{(3, 28)} = 33.18$, $p < 0.0001$) levels in HFD group. Myricetin treatment fully normalized GPx, CAT, and SOD activities and lowered TBARS levels, but failed to significantly increase the GSH levels. These results demonstrated remarkable antioxidative characteristics of myricetin. Myricetin, per se, had no effects on hepatic redox status.

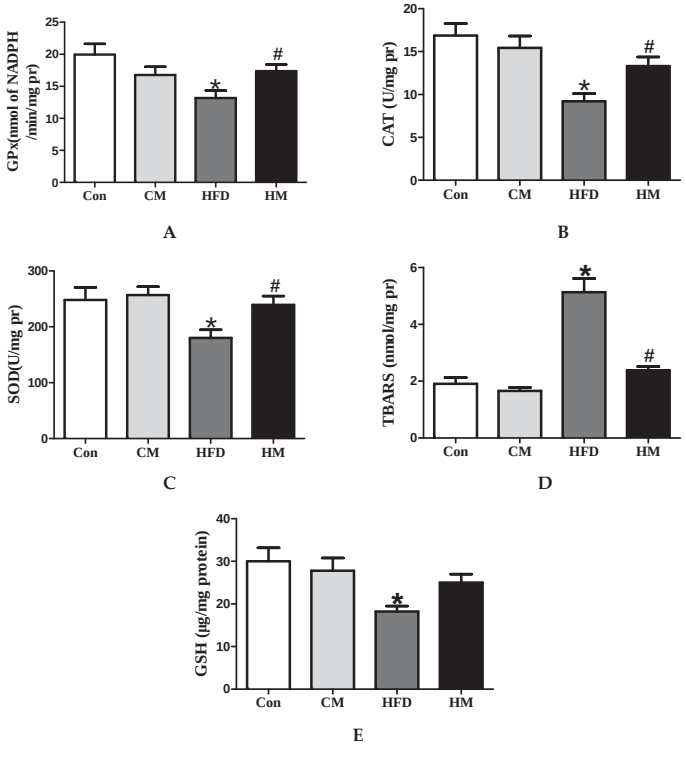

Figure 5. Myricetin alleviated hepatic oxidative stress induced by a high-fat diet. (**A**) GPx; (**B**) CAT; (**C**) SOD; (**D**) TBARS; and (**E**) GSH levels. Values were presented as mean ± SEM ($n = 8$). Con, control diet; CM, control diet with additional 0.12% myricetin; HFD, high-fat diet; HM, high-fat diet with additional 0.12% myricetin. * $p < 0.05$ vs. the Con group; # $p < 0.05$ vs. the HFD group.

3.8. Effects of Myricetin on Expressions of Oxidative Stress-Related Genes and Nrf2 Pathway

To explore whether the alleviation of myricetin on hepatic steatosis was related to the activation of Nrf2 pathway, we measured the protein expression of nuclear and cytosolic Nrf2, as well as NQO1 and HO-1. The results showed that protein expression of hepatic nuclear Nrf2 was significantly lower ($F_{(3, 28)} = 4.10$, $p = 0.016$) and cytosolic Nrf2 was evidently higher ($F_{(3, 28)} = 2.80$, $p = 0.058$) in HFD group than in control mice, which was mitigated by myricetin treatment (Figure 6A,B). Protein expression of NQO1 ($F_{(3, 28)} = 6.42$, $p = 0.002$) and HO-1 ($F_{(3, 28)} = 6.04$, $p = 0.003$), the targets of Nrf2, was also decreased by HFD and normalized by myrcetin treatment (Figure 6C). Real-time quantitative PCR data showed that the expressions of DEGs (*Sod2*, *Prdx1*, and *Prdx5*) selected from peroxisome

pathway, along with oxidative stress related *Cat*, *Gpx3*, and *Nrf2*, were noticeably down-regulated by HFD consumption and normalized by co-administration of myricetin, except for *Prdx5* (Figure 6D). These results indicated that myricetin could increase hepatic nuclear Nrf2 translocation to elevate antioxidative capacity possibly via activating Nrf2 pathway. Myricetin, per se, had no effects on the expressions of genes involved in oxidative stress and the Nrf2 pathway.

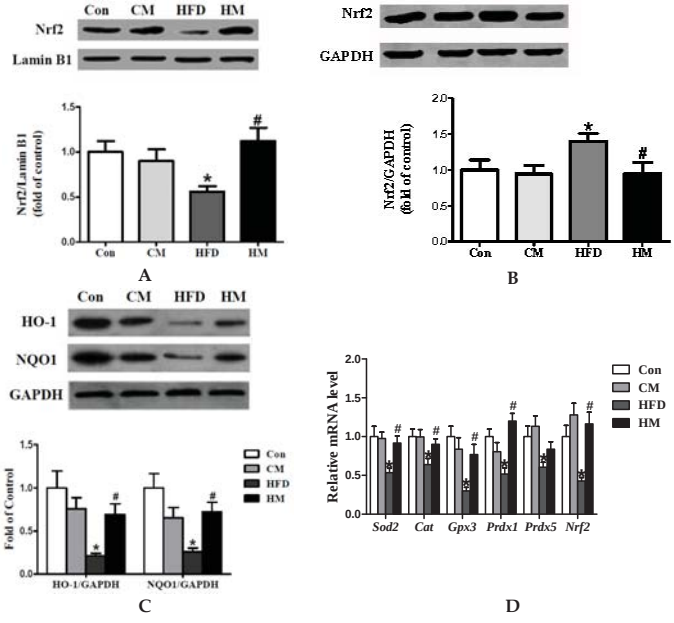

Figure 6. Myricetin activated the hepatic Nrf2 pathway and normalized expressions of genes involved in oxidative stress. (**A**) Protein expression of hepatic nuclear Nrf2; (**B**) protein expression of hepatic cytosolic Nrf2; (**C**) protein expression of hepatic NQO1 and HO-1; and (**D**) relative expression of genes involved in oxidative stress. Values were presented as mean ± SEM (n = 8). Con, control diet; CM, control diet with additional 0.12% myricetin; HFD, high-fat diet; HM, high-fat diet with additional 0.12% myricetin. * $p < 0.05$ vs. the Con group; # $p < 0.05$ vs. the HFD group.

4. Discussion

NAFLD, as an emerging health problem worldwide, has an estimated prevalence of 20%–40% in Western countries [19]. Epidemiological surveys have also revealed that community prevalence of NAFLD was about 15% in eastern and southern areas of China [20]. Although the pathogenesis of NAFLD is not entirely understood, the "two hits" hypothesis is widely accepted [6]. Hepatic steatosis, the "first hit" of NAFLD, is characterized by fat infiltration and excessive lipid accumulation in the liver, accompanied by an elevated liver/body ratio and higher plasma levels of enzyme markers of liver damage. Once the presence of hepatic steatosis is established, the "second hit", oxidative stress, will further amplify the degree of steatosis [21]. OS has been proved to play an important role in hepatic cell damage and dysfunction [22] and could be induced by a high-fat diet. Furthermore, OS has been demonstrated to enhance insulin resistance and fat accumulation in the liver [23]. Recently, lipid peroxidation has been considered as the trigger factor responsible for the transition from simple fat accumulation to more progressive steatohepatitis or NASH [24]. Since hepatic steatosis might progress to NASH without timely therapy, and the seriousness of NAFLD is highly related to the degree of OS [25], it is urgent to improve antioxidative capacity to avoid the development of more serious hepatic pathologies.

Antioxidants have been suggested to slow the progression and attenuate NAFLD [7]. Dietary antioxidant components, including polyphenols and green tea extracts, have been verified to improve biochemical indexes and histological appearance in NAFLD [26,27]. Myricetin is a type of typical polyphenol widely distributed in edible plants with several therapeutic potential, including anti-diabetic, hypolipidemic, and hepatoprotective effects [12,28]. The purpose of this study was to explore the effects of myricetin on pre-existing hepatic steatosis induced by HFD, which would be most relevant to the clinical situation in humans. Previous research confirmed that high-fat diet (40.8% of calories from fat) consumption for nine weeks resulted in liver steatosis in C57BL/6 mice [29]. Here, we fed the same strain mice with a high-fat diet (45% of calories from fat) for 12 weeks and hepatic histological appearance confirmed that HFD induced hepatic steatosis model successfully. Myricetin treatment for 12 weeks caused a significant regression of pre-existing hepatic steatosis, as assessed by hepatic lipid concentration determinations and histological analysis. For specific performance, myricetin could remarkably reduce high-fat diet-induced alterations of hepatic TG, TC, and FFA contents, as well as lipid accumulation demonstrated by H & E staining and Oil Red O staining. Furthermore, myricetin was effective in reducing body weight and white adipose fat accumulation by increasing energy expenditure and dietary fat utilization suggested by significant lower RER values in indirect calorimetry analysis.

In order to have a deeper understanding of the possible mechanisms that might be responsible for the regressive effect of myricetin on hepatic steatosis, a genome-wide expression profiling in the liver tissues was performed and pathway analysis revealed that the pathways involved in hepatic lipid homeostasis, such as the PPAR signaling pathway, biosynthesis of unsaturated fatty acids, and the insulin signaling pathway, were all evidently affected. The PPAR signaling pathway that was most significantly affected was chosen to verify the expression of related DEGs, in which *Scd1*, *Lpl*, *Cd36*, and *Pparγ* were all significantly down-regulated, along with noticeable up-regulation of *Cyp7a1* by myricetin treatment compared with the HFD group. Previous studies demonstrated that the PPAR signaling pathway was involved in glucose homeostasis and lipid metabolism, and might be a target for the development of novel efficient treatments for several metabolic disorders, including obesity and type 2 diabetes [17]. PPARγ, a ligand-activated transcription factor which belongs to the nuclear receptor family, plays a vital role in lipid metabolism by regulating the expression of its target genes, such as *Scd1*, *Lpl*, and *Fasn* [30]. The genetic deletion of *Pparγ* in livers of either *ob/ob* [31] or AZIP-F-1 [32] mice significantly alleviated the development of hepatic steatosis, which was independent of the existence of hyperglycemia or hyperinsulinemia. Hepatic lipoprotein lipase (LPL), a target of PPARγ, exerts a vital role in lipoprotein metabolism. It was found that hepatic *Lpl* mRNA expression was higher in obese patients than normal controls [33] and reducing hepatic LPL activity was effective in ameliorating diet-induced obesity and hepatic steatosis [34]. *Cd36* is another target gene of PPARγ that could promote steatosis [35]. Results in the present study showed that myricetin treatment could decrease hepatic PPARγ protein expression, as well as normalizing the relative expression of its target genes, which might be a cause for its role in regression of hepatic steatosis.

The peroxisome pathway, which plays a critical role in redox signaling and lipid homeostasis, contributes to many crucial metabolic processes, such as fatty acid oxidation, biosynthesis of ether lipids, and free radical detoxification [36], was also changed by myricetin treatment. The involved DEGs, including *Sod2*, *Prdx1*, and *Prdx5*, which strongly connected with oxidative stress, were also up-regulated. We further measured the hepatic antioxidant enzymes, including SOD, CAT, and GPx, which were of fundamental importance in designing the therapeutic approaches toward oxidative-based liver pathologies [37], and found that these antioxidative enzymes were all significantly normalized by myricetin treatment. The TBARS levels were also remarkably decreased, declaring that myricetin improved hepatic steatosis possibly via alleviating oxidative stress.

Considering the fact that the Nrf2 pathway played a critical role in cytoprotection against oxidative stress through up-regulating phase II detoxifying enzymes [38], and that oxidative stress could be served as the "second hit" that activate simple steatosis to progress to NASH, we further

explored whether myricetin alleviated hepatic steatosis via the Nrf2 pathway. Previous studies using mouse models have shown that activation of the Keap1/Nrf2 pathway, at least partially protected mice from diet-induced obesity and amelioration of hepatic steatosis [39,40]. As an effective antioxidant, myricetin has been reported to increase nuclear Nrf2 translocation [41] and ARE-binding activity to enhance Nrf2/ARE-mediated gene expressions [28]. Here we also showed that hepatic nuclear Nrf2 translocation was decreased by HFD and normalized by myricetin treatment. Moreover, hepatic NQO1 and HO-1 protein expression was also increased by myricetin, further indicating that myricetin reversed HFD-induced hepatic steatosis through the Nrf2 pathway, favoring enhancement of antioxidant capacity. However, studies have also indicated that the Nrf2 pathway activation attenuated inflammation-associated pathogenesis [42,43]. In the early phase of inflammation-mediated tissue damage, activation of Nrf2 signaling could inhibit the production or expression of pro-inflammatory mediators, including cytokines and chemokines [44]. Whether Nrf2 attenuated HFD-induced hepatic steatosis via inhibiting hepatic inflammation is unknown and still needs further research.

Nonetheless, there is evidence that PPARγ may directly regulate the expression of several antioxidant and prooxidant genes in response to OS, including *Cat*, *Sod2*, and *GPx* [45]. Emerging evidence also suggested that Nrf2 could crosstalk with metabolic pathways, increasing the repertoire of its target genes, such as *Pparγ* [46]. Meanwhile, PPARγ might act synergically with Nrf2 in the activation of antioxidant genes. Based on the present study, it is difficult to elucidate the underlying relationship between PPARγ and Nrf2 and further research is needed.

5. Conclusions

In conclusion, myricetin exhibited an excellent regressive effect against high-fat diet-induced hepatic steatosis, with such beneficial action accomplished via changing the PPAR signaling pathway and the Nrf2 pathway. These findings provide additional evidence in support of the use of myricetin as a promising functional food for the prevention or treatment of hepatic steatosis and other related metabolic disorders.

Acknowledgments: The study was supported by the Fundamental Research Funds for the Central Universities (JUSRP115A33) and Wuxi Science and Technology Development Fund (CSE31N1625).

Author Contributions: S.F.X., G.W.L. conceived and designed the experiments; P.W. performed the experiments; Y.Y.Q., Y.Y.J., and X.T. analyzed the data; S.F.X. drafted the article; G.W.L. contributed to the final approval.

Conflicts of Interest: The authors declare no conflict of interest.

References

1. Friedman, J. Diabetes: Fat in all the wrong places. *Nature* **2002**, *415*, 268–269. [CrossRef] [PubMed]
2. Seppala-Lindroos, A.; Vehkavaara, S.; Hakkinen, A.-M.; Goto, T.; Westerbacka, J.; Sovijarvi, A.; Halavaara, J.; Yki-Jarvinen, H. Fat accumulation in the liver is associated with defects in insulin suppression of glucose production and serum free fatty acids independent of obesity in normal men. *J. Clin. Endocr. Metab.* **2002**, *87*, 3023–3028. [CrossRef] [PubMed]
3. Westerbacka, J.; Lammi, K.; Hakkinen, A.-M.; Rissanen, A.; Salminen, I.; Aro, A.; Yki-Jarvinen, H. Dietary fat content modifies liver fat in overweight nondiabetic subjects. *J. Clin. Endocr. Metab.* **2005**, *90*, 2804–2809. [CrossRef] [PubMed]
4. Angulo, P. Nonalcoholic fatty liver disease. *N. Engl. J. Med.* **2002**, *346*, 1221–1231. [CrossRef] [PubMed]
5. Postic, C.; Girard, J. Contribution of de novo fatty acid synthesis to hepatic steatosis and insulin resistance: Lessons from genetically engineered mice. *J. Clin. Investig.* **2008**, *118*, 829–838. [CrossRef] [PubMed]
6. Day, C.P.; James, O.F. Steatohepatitis: A tale of two "hits"? *Gastroenterology* **1998**, *114*, 842–845. [CrossRef]
7. Mehta, K.; van Thiel, D.H.; Shah, N.; Mobarhan, S. Nonalcoholic fatty liver disease: Pathogenesis and the role of antioxidants. *Nutr. Rev.* **2002**, *60*, 289–293. [CrossRef] [PubMed]
8. Choi, K.M.; Lee, Y.S.; Shin, D.M.; Lee, S.; Yoo, K.S.; Lee, M.K.; Lee, J.H.; Kim, S.Y.; Lee, Y.M.; Hong, J.T.; et al. Green tomato extract attenuates high-fat-diet-induced obesity through activation of the AMPK pathway in C57BL/6 mice. *J. Nutr. Biochem.* **2013**, *24*, 335–342. [CrossRef] [PubMed]

9. Ganji, S.H.; Kukes, G.D.; Lambrecht, N.; Kashyap, M.L.; Kamanna, V.S. Therapeutic role of niacin in the prevention and regression of hepatic steatosis in rat model of nonalcoholic fatty liver disease. *Am. J. Physiol. Gastrointest. Liver Physiol.* **2014**, *306*, G320–G327. [CrossRef] [PubMed]
10. Furukawa, S.; Fujita, T.; Shimabukuro, M.; Iwaki, M.; Yamada, Y.; Nakajima, Y.; Nakayama, O.; Makishima, M.; Matsuda, M.; Shimomura, I. Increased oxidative stress in obesity and its impact on metabolic syndrome. *J. Clin. Investig.* **2004**, *114*, 1752–1761. [CrossRef] [PubMed]
11. Semwal, D.K.; Semwal, R.B.; Combrinck, S.; Viljoen, A. Myricetin: A dietary molecule with diverse biological activities. *Nutrients* **2016**, *8*, 90. [CrossRef] [PubMed]
12. Chang, C.J.; Tzeng, T.-F.; Liou, S.-S.; Chang, Y.-S.; Liu, I.-M. Myricetin increases hepatic peroxisome proliferator-activated receptor α protein expression and decreases plasma lipids and adiposity in rats. *Evid.-Based Complement. Altern. Med.* **2012**, *2012*, 787152. [CrossRef] [PubMed]
13. Choi, H.-N.; Kang, M.-J.; Lee, S.-J.; Kim, J.-I. Ameliorative effect of myricetin on insulin resistance in mice fed a high-fat, high-sucrose diet. *Nutr. Res. Pract.* **2014**, *8*, 544–549. [CrossRef] [PubMed]
14. Guo, J.; Meng, Y.; Zhao, Y.; Hu, Y.; Ren, D.; Yang, X. Myricetin derived from *Hovenia dulcis* Thunb. Ameliorates vascular endothelial dysfunction and liver injury in high choline-fed mice. *Food Funct.* **2015**, *6*, 1620–1634. [CrossRef] [PubMed]
15. Hissin, P.J.; Hilf, R. A fluorometric method for determination of oxidized and reduced glutathione in tissues. *Anal. Biochem.* **1976**, *74*, 214–226. [CrossRef]
16. Khatri, P.; Sellamuthu, S.; Malhotra, P.; Amin, K.; Done, A.; Draghici, S. Recent additions and improvements to the Onto-Tools. *Nucleic Acids Res.* **2005**, *33*, 762–765. [CrossRef] [PubMed]
17. Khatri, P.; Voichita, C.; Kattan, K.; Ansari, N.; Khatri, A.; Georgescu, C.; Tarca, A.L.; Draghici, S. Onto-Tools: New additions and improvements in 2006. *Nucleic Acids Res.* **2007**, *35*, W206–W211. [CrossRef] [PubMed]
18. Lemberger, T.; Desvergne, B.; Wahli, W. Peroxisome proliferator-activated receptors: A nuclear receptor signaling pathway in lipid physiology. *Annu. Rev. Cell. Dev. Biol.* **1996**, *12*, 335–363. [CrossRef] [PubMed]
19. Bedogni, G.; Miglioli, L.; Masutti, F.; Tiribelli, C.; Marchesini, G.; Bellentani, S. Prevalence of and risk factors for nonalcoholic fatty liver disease: The Dionysos nutrition and liver study. *Hepatology* **2005**, *42*, 44–52. [CrossRef] [PubMed]
20. Zhou, Y.J.; Li, Y.-Y.; Nie, Y.Q.; Ma, J.-X.; Lu, L.-G.; Shi, S.-L.; Chen, M.-H.; Hu, P.-J. Prevalence of fatty liver disease and its risk factors in the population of south China. *World. J. Gastroenterol.* **2007**, *13*, 6419–6424. [CrossRef] [PubMed]
21. Neuschwander-Tetri, B.A. Hepatic lipotoxicity and the pathogenesis of nonalcoholic steatohepatitis: The central role of nontriglyceride fatty acid metabolites. *Hepatology* **2010**, *52*, 774–788. [CrossRef] [PubMed]
22. Sheth, S.G.; Gordon, F.D.; Chopra, S. Nonalcoholic steatohepatitis. *Ann. Intern. Med.* **1997**, *126*, 137–145. [CrossRef] [PubMed]
23. Ouchi, N.; Parker, J.L.; Lugus, J.J.; Walsh, K. Adipokines in inflammation and metabolic disease. *Nat. Rev. Immunol.* **2011**, *11*, 85–97. [CrossRef] [PubMed]
24. Rolo, A.P.; Teodoro, J.S.; Palmeira, C.M. Role of oxidative stress in the pathogenesis of nonalcoholic steatohepatitis. *Free Radic. Biol. Med.* **2012**, *52*, 59–69. [CrossRef] [PubMed]
25. Chalasani, N.; Deeg, M.A.; Crabb, D.W. Systemic levels of lipid peroxidation and its metabolic and dietary correlates in patients with nonalcoholic steatohepatitis. *Am. J. Gastroenterol.* **2004**, *99*, 1497–1502. [CrossRef] [PubMed]
26. Ramirez-Tortosa, M.C.; Ramirez-Tortosa, C.L.; Mesa, M.D.; Granados, S.; Gil, A.; Quiles, J.L. Curcumin ameliorates rabbits's steatohepatitis via respiratory chain, oxidative stress, and TNF-α. *Free Radic. Biol. Med.* **2009**, *47*, 924–931. [CrossRef] [PubMed]
27. Nakamoto, K.; Takayama, F.; Mankura, M.; Hidaka, Y.; Egashira, T.; Ogino, T.; Kawasaki, H.; Mori, A. Beneficial effects of fermented green tea extract in a rat model of non-alcoholic steatohepatitis. *J. Clin. Biochem. Nutr.* **2009**, *44*, 239–246. [CrossRef] [PubMed]
28. Qin, S.; Chen, J.; Tanigawa, S.; Hou, D.X. Microarray and pathway analysis highlight Nrf2/ARE-mediated expression profiling by polyphenolic myricetin. *Mol. Nutr. Food Res.* **2013**, *57*, 435–446. [CrossRef] [PubMed]
29. DeAngelis, R.A.; Markiewski, M.M.; Taub, R.; Lambris, J.D. A high-fat diet impairs liver regeneration in C57BL/6 mice through overexpression of the NF-κB inhibitor, IKBα. *Hepatology* **2005**, *42*, 1148–1157. [CrossRef] [PubMed]

30. Inoue, M.; Ohtake, T.; Motomura, W.; Takahashi, N.; Hosoki, Y.; Miyoshi, S.; Suzuki, Y.; Saito, H.; Kohgo, Y.; Okumura, T. Increased expression of PPARγ in high fat diet-induced liver steatosis in mice. *Biochem. Biophys. Res. Commun.* **2005**, *336*, 215–222. [CrossRef] [PubMed]
31. Matsusue, K.; Haluzik, M.; Lambert, G.; Yim, S.-H.; Gavrilova, O.; Ward, J.M.; Brewer, B., Jr.; Reitman, M.L.; Gonzalez, F.J. Liver-specific disruption of PPARγ in leptin-deficient mice improves fatty liver but aggravates diabetic phenotypes. *J. Clin. Investig.* **2003**, *111*, 737–747. [CrossRef] [PubMed]
32. Gavrilova, O.; Haluzik, M.; Matsusue, K.; Cutson, J.J.; Johnson, L.; Dietz, K.R.; Nicol, C.J.; Vinson, C.; Gonzalez, F.J.; Reitman, M.L. Liver peroxisome proliferator-activated receptor γ contributes to hepatic steatosis, triglyceride clearance, and regulation of body fat mass. *J. Biol. Chem.* **2003**, *278*, 34268–34276. [CrossRef] [PubMed]
33. Pardina, E.; Baena-Fustegueras, J.A.; Llamas, R.; Catalan, R.; Galard, R.; Lecube, A.; Fort, J.M.; Llobera, M.; Allende, H.; Vargas, V. Lipoprotein lipase expression in livers of morbidly obese patients could be responsible for liver steatosis. *Obes. Surg.* **2009**, *19*, 608–616. [CrossRef] [PubMed]
34. Chiu, H.K.; Qian, K.; Ogimoto, K.; Morton, G.J.; Wisse, B.E.; Agrawal, N.; McDonald, T.O.; Schwartz, M.W.; Dichek, H.L. Mice lacking hepatic lipase are lean and protected against diet-induced obesity and hepatic steatosis. *Endocrinology* **2010**, *151*, 993–1001. [CrossRef] [PubMed]
35. Zhou, J.; Febbraio, M.; Wada, T.; Zhai, Y.; Kuruba, R.; He, J.; Lee, J.H.; Khadem, S.; Ren, S.; Li, S. Hepatic fatty acid transporter Cd36 is a common target of LXR, PXR, and PPARγ in promoting steatosis. *Gastroenterology* **2008**, *134*, 556–567. [CrossRef] [PubMed]
36. Fransen, M.; Nordgren, M.; Wang, B.; Apanasets, O. Role of peroxisomes in ROS/RNS-metabolism: Implications for human disease. *BBA-Mol. Basis Dis.* **2012**, *1822*, 1363–1373. [CrossRef] [PubMed]
37. Inoue, M. Protective mechanisms against reactive oxygen species. In *The Liver: Biology and Pathobiology*, 4th ed.; Arias, I.M., Boyer, J.L., Chisari, F.V., Fausto, N., Schachter, D., Shafritz, D.A., Eds.; Lippincott Williams & Wilkins: Philadelphia, PA, USA, 1994; pp. 443–459.
38. Tang, W.; Jiang, Y.F.; Ponnusamy, M.; Diallo, M. Role of Nrf2 in chronic liver disease. *World. J. Gastroenterol.* **2014**, *20*, 13079–13087. [CrossRef] [PubMed]
39. Yang, Y.; Li, W.; Liu, Y.; Sun, Y.; Li, Y.; Yao, Q.; Li, J.; Zhang, Q.; Gao, Y.; Gao, L. Alpha-lipoic acid improves high-fat diet-induced hepatic steatosis by modulating the transcription factors SREBP-1, FoxO1 and Nrf2 via the SIRT1/LKB1/AMPK pathway. *J. Nutr. Biochem.* **2014**, *25*, 1207–1217. [CrossRef] [PubMed]
40. Chartoumpekis, D.V.; Ziros, P.G.; Psyrogiannis, A.I.; Papavassiliou, A.G.; Kyriazopoulou, V.E.; Sykiotis, G.P.; Habeos, I.G. Nrf2 represses FGF21 during long-term high-fat diet-induced obesity in mice. *Diabetes* **2011**, *60*, 2465–2473. [CrossRef] [PubMed]
41. Zhang, Q.; Li, Z.; Wu, S.; Li, X.; Sang, Y.; Li, J.; Niu, Y.; Ding, H. Myricetin alleviates cuprizone-induced behavioral dysfunction and demyelination in mice by Nrf2 pathway. *Food Funct.* **2016**, *7*, 4332–4342. [CrossRef] [PubMed]
42. Braun, S.; Hanselmann, C.; Gassmann, M.G.; Keller, U.; Born-Berclaz, C.; Chan, K.; Kan, Y.W.; Werner, S. Nrf2 transcription factor, a novel target of keratinocyte growth factor action which regulates gene expression and inflammation in the healing skin wound. *Mol. Cell. Biol.* **2002**, *22*, 5492–5505. [CrossRef] [PubMed]
43. Chen, X.L.; Dodd, G.; Thomas, S.; Zhang, X.; Wasserman, M.A.; Rovin, B.H.; Kunsch, C. Activation of Nrf2/ARE pathway protects endothelial cells from oxidant injury and inhibits inflammatory gene expression. *Am. J. Physiol. Heart Circ. Physiol.* **2006**, *290*, 1862–1870. [CrossRef] [PubMed]
44. Thimmulappa, R.K.; Lee, H.; Rangasamy, T.; Reddy, S.P.; Yamamoto, M.; Kensler, T.W.; Biswal, S. Nrf2 is a critical regulator of the innate immune response and survival during experimental sepsis. *J. Clin. Investig.* **2006**, *116*, 984–995. [CrossRef] [PubMed]
45. Polvani, S.; Tarocchi, M.; Galli, A. PPARγ and Oxidative Stress: Con (β) Catenating NRF2 and FOXO. *PPAR Res.* **2012**, *2012*, 641087. [CrossRef] [PubMed]
46. Pi, J.; Leung, L.; Xue, P.; Wang, W.; Hou, Y.; Liu, D.; Yehuda-Shnaidman, E.; Lee, C.; Lau, J.; Kurtz, T.W. Deficiency in the nuclear factor E2-related factor-2 transcription factor results in impaired adipogenesis and protects against diet-induced obesity. *J. Biol. Chem.* **2010**, *285*, 9292–9300. [CrossRef] [PubMed]

nutrients

MDPI

Article

Impact of Proteins on the Uptake, Distribution, and Excretion of Phenolics in the Human Body

Richard Draijer [1,*], Ferdi A. van Dorsten [2], Yvonne E. Zebregs [3], Boudewijn Hollebrands [1], Sonja Peters [1], Guus S. Duchateau [1] and Christian H. Grün [1]

1 Unilever R&D Vlaardingen, Olivier van Noortlaan 120, Vlaardingen 3133 AT, The Netherlands; Boudewijn.hollebrands@unilever.com (B.H.); Sonja.kaal@unilever.com (S.P.); Guus.duchateau@unilever.com (G.S.D.); Christian.grun@unilever.com (C.H.G.)

2 Eurofins Spinnovation Analytical, Oss 5342 CC, The Netherlands; Ferdi.vandorsten@gmail.com

3 Eurofins Global Central Laboratory, Breda 4817 PA, The Netherlands; Yvonne.zebregs@gmail.com

* Correspondence: Richard.draijer@unilever.com; Tel.: +31-10-460-6789; Fax: +31-10-460-5993

Received: 4 November 2016; Accepted: 8 December 2016; Published: 15 December 2016

Abstract: Polyphenols, a complex group of secondary plant metabolites, including flavonoids and phenolic acids, have been studied in depth for their health-related benefits. The activity of polyphenols may, however, be hampered when consumed together with protein-rich food products, due to the interaction between polyphenols and proteins. To that end we have tested the bioavailability of representatives of a range of polyphenol classes when consumed for five days in different beverage matrices. In a placebo-controlled, randomized, cross-over study, 35 healthy males received either six placebo gelatine capsules consumed with 200 mL of water, six capsules with 800 mg polyphenols derived from red wine and grape extracts, or the same dose of polyphenols incorporated into 200 mL of either pasteurized dairy drink, soy drink (both containing 3.4% proteins) or fruit-flavoured protein-free drink . At the end of the intervention urine and blood was collected and analysed for a broad range of phenolic compounds using Gas Chromatography–Mass Spectrometry (GC-MS), Liquid Chromatography–Multiple Reaction Monitoring–Mass Spectrometry (LC-MRM-MS), and Nuclear Magnetic Resonance (NMR) spectroscopy techniques. The plasma and urine concentrations of the polyphenols identified increased with all formats, including the protein-rich beverages. Compared to capsule ingestion, consumption of polyphenol-rich beverages containing either dairy, soy or no proteins had minor to no effect on the bioavailability and excretion of phenolic compounds in plasma (118% $\pm$ 9%) and urine (98% $\pm$ 2%). We conclude that intake of polyphenols incorporated in protein-rich drinks does not have a major impact on the bioavailability of a range of different polyphenols and phenolic metabolites.

Keywords: bioavailability; flavonoids; catechins; protein; resveratrol; valerolactones

1. Introduction

Polyphenols are plant secondary metabolites characterized by the presence of more than one phenol group per molecule. These compounds are ubiquitous in fruits, vegetables, cereals, chocolate, and beverages, such as tea, coffee, or wine [1]. Epidemiological, clinical, and experimental studies support a role of polyphenols in the prevention of cardiovascular diseases, malignancies, neurodegenerative disorders, and metabolic syndrome, which sparked the discussion whether dietary reference intake values should be defined for these compounds [2–4]. Particularly, the polyphenols of red wine have been linked to the 'French paradox', referring to the French low mortality rate from ischaemic heart disease, whilst intake of saturated fat is high [5].

Affinity and binding of proteins from different sources to phenolic compounds is a well-known phenomenon [6]. Whether this interaction also impacts the bioavailability of polyphenols is still a

matter of debate, and the number of studies in humans is limited. Egert et al. [7] showed negative effects on the bioavailability of gallated catechins for caseinate, milk, and soy proteins, whilst the non-gallated forms were unaffected. Others have described a null-effect of milk on bioavailability for total plasma tea catechins or antioxidant capacity [8,9]. Accordingly, bioavailability of (epi)catechin in a milk chocolate drink was reported not to be substantially affected [10]. Bioavailability of the flavonols quercetin and kaempferol may not or weakly be affected by milk [11]. In contrast, protein-rich soybean flour has been suggested to protect anthocyanins from metabolism, thereby increasing their bioavailability [12].

However, one may question whether investigation of the impact of proteins on polyphenol parent compounds alone is of physiological relevance, considering the very low bioavailability of polyphenols as such [13]. The bulk of the dietary complex polyphenols ends up in the large bowel and the aromatic rings are metabolized by bacteria. The breakdown products consist of smaller and simpler phenolic acids that are absorbed into the human body in much higher quantities than the parent compounds [14–16]. Therefore, preferably alongside assessment of the bioavailability of polyphenol parent compounds, the excretion of phenolic metabolites should be taken into account.

Detection of (conjugated) intact polyphenols in plasma, as well as phenolic acids in urine, requires different analytical methods to be applied in a targeted, as well as untargeted, manner. Exposure of an organism to xenobiotics (e.g., polyphenols) results in subtle modifications in biochemical composition of plasma and urine, which can be profiled using ^{1}H Nuclear Magnetic Resonance (NMR) spectroscopic analysis [17–19]. The approach requires minimal sample preparation, and thus eliminates the necessity of making a priori assumptions as to the relative importance of various metabolite classes. Although ^{1}H NMR spectroscopy generates a comprehensive profile of exogenous and endogenous metabolites in biofluids, the sensitivity of this technique is limited to the detection of metabolites present at concentrations higher than approximately 10 μM. Thus, targeted analyses of simple phenolics need to be performed by the more sensitive, but labour-intensive technique Gas Chromatography–Mass Spectrometry (GC-MS). The (conjugated) intact polyphenols and their primary metabolites were analysed by using Liquid Chromatography–Multiple Reaction Monitoring–Mass Spectrometry (LC-MRM-MS).

The present study was set up to determine the impact of dairy and soy proteins, present in a relatively complex beverage format, on the absorption and appearance of polyphenols in the blood circulation as well as the urinary excretion of their phenolic metabolites. To that end, phenolic compounds were measured in blood and urine after consumption of red wine and grape polyphenols formulated in (1) a dairy drink (protein- and casein-rich); (2) a soy drink (protein-rich but casein-free); (3) a fruit-flavoured drink (protein-free) compared to polyphenols incorporated in gelatine capsules taken with water.

2. Experimental Section

2.1. Study Design

In the present placebo-controlled study, subjects were randomly assigned to one of the treatment sequence of a full crossover Williams design [20]. The following five treatments were allocated to the subjects:

- six cellulose-filled placebo hard-shell gelatine capsules taken with 200 mL of water (control)
- six hard-shell gelatine capsules containing a wine/grape extract mix taken with 200 mL of water (positive control)
- 200 g fruit-flavoured drink containing the wine/grape extract mix
- 200 g dairy drink containing the wine/grape extract mix
- 200 g soy drink containing the wine/grape extract mix

More information about the test products is provided in Section 2.3.

The total duration of the study was five weeks consisting of five consecutive five-day treatment periods with four two-day washout periods (WO) in-between. During each treatment period, subjects daily consumed one of the five test products one hour before breakfast. At the fourth day of each treatment period after intake of the test product subjects started collecting their urine for 24 h. On the fifth day of each period, subjects visited the study facility in a fasted state, handed in their 24 h-pooled urine collection container and received the last test product dose. On this day, blood was collected prior to (t = 0) and 1, 2, and 3 h after intake of the test product.

During the treatment periods subjects had to comply with a number of dietary restrictions. During each treatment period subjects were not allowed to consume milk products in the first three hours after intake of the test product. From day 2 in the evening (10.00 p.m.) until the last blood withdrawal on day 5, subjects were on a low polyphenol diet, avoiding consumption of wine, chocolate, coffee, and tea, and were not allowed to consume alcohol or fish (these food products may interfere with the spectral analysis of plasma and urine samples). The time periods were chosen in such a way that it would bring as little as possible inconvenience to the subjects, but still long enough to likely ensure reaching a steady state. On day 4 of each treatment period, subjects had to repeat the diet that they consumed on day 4 of the first treatment period. An overview of the treatment periods, restrictions, and measurement days is given in Figure 1.

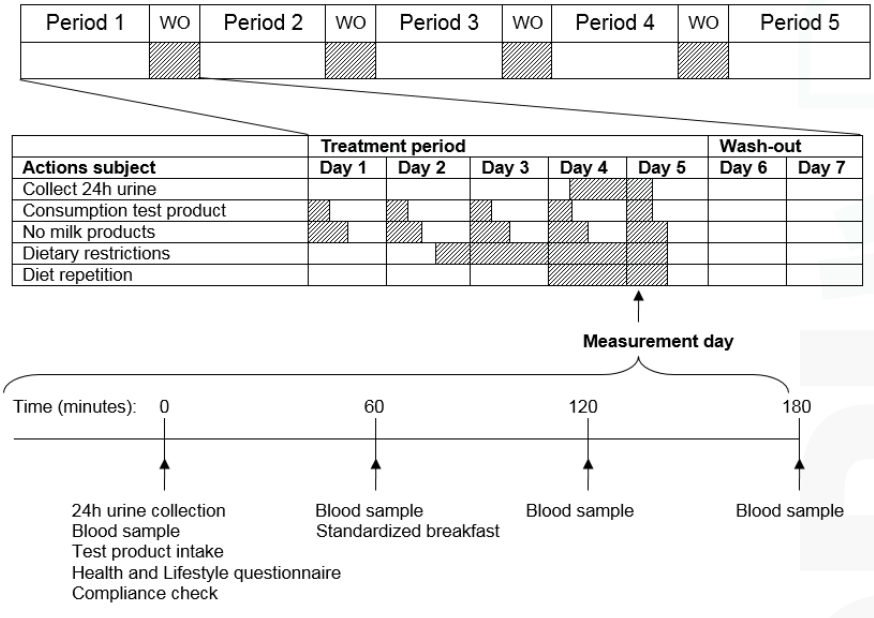

Figure 1. Study overview. In each period the subjects received one of the five treatments. Each period consisted of five days of treatment and two days of washout. On day 5, the measurement day, 24h urine was collected and venous blood was collected prior to (t = 0) and 1, 2 and 3 h after intake of the test product.

2.2. Recruitment of Subjects

2.2.1. Sample Size

The power calculation was based on urinary hippuric acid concentration as general indicator of uptake and excretion of phenolic metabolites. Based on a previous study [15], it was expected that urinary hippuric acid concentrations would increase with 0.35 g per 24 h urine collection with the selected dose of polyphenols in capsules as compared to placebo. A reduction of 25% (0.26 g increase in hippuric acid compared to placebo) due to interference of the food matrix was considered acceptable. In order to detect a significant increase of 0.26 g hippuric acid compared to placebo, with a within-subject variance of 0.11 g, a power of 80%, an alpha of 0.05, thirty subjects were required (Dunnett test correcting for multiple comparisons).

2.2.2. Recruitment and Screening

Apparently healthy males (18–70 years) were recruited among inhabitants of Vlaardingen and surroundings by sending a personal letter to volunteers in a Unilever subject database (1220 letters).

Sixty-eight persons were interested in joining one of the four information meetings. Sixty-one persons completed a questionnaire about general health and wellbeing, which covered a number of inclusion and exclusion criteria. Inclusion criteria were male gender, aged $\geq$18 and $\leq$70 years, body mass index (BMI) $\geq$19 and $\leq$30 kg/m^2, reported alcohol consumption <28 alcohol units/week, urinary and plasma clinical chemical parameters within the normal reference range. Exclusion criteria were the habit of smoking during the past year, a recorded history or current metabolic diseases, chronic gastrointestinal disorders, cardiovascular or renal disease, currently on a medically prescribed or slimming diet, reported intense sporting activities >10 h/week or taking prescribed medical treatment possibly interfering with the bioavailability of polyphenol metabolites (e.g., systemic antibiotics). Based on this questionnaire, 47 persons were invited for a second screening visit. Three persons cancelled their appointment for screening and three persons did not show up. On the morning of the screening appointment, all volunteers collected a urine sample and handed it in at the test facility. Forty-one volunteers signed an informed consent form before any measurement was performed. Subsequently, weight and height were measured, the accessibility of the veins was confirmed and 7 mL blood was taken to determine liver enzymes and to measure complete blood count. The morning urine samples were analysed by means of a dipstick. A total of eight subjects were excluded based on the results of the screening, considering the inclusion and exclusion criteria.

2.2.3. Participation

Thirty-three persons started the run-in period. A statistician randomised the personal codes to one of the 10 treatment sequences taking into account as much as possible order and period effects (Williams design). The personal code-test product combinations were kept concealed to investigators and subjects.

Subjects registered compliance to test product intake and background diet in a diary. For each treatment period, subjects received a separate diary. To make it easier for the subjects to repeat the diet on days 4 and 5 in all treatment periods, a copy of their own diary of treatment period 1 was given to each subject. Furthermore, to check compliance to test product intake subjects were requested to return the empty boxes and bottles on the measurement days. The present study has been approved by the independent ethics committee of the University of Wageningen (registration No. 07/07-ABR16833).

2.3. Study Test Products

The polyphenol-rich powder consisted of 870 mg red wine extract (Provinols, Seppic, Paris, France) and 540 mg grape juice extract (MegaNatural™ Rubired of Polyphenolics, Madera, CA, USA), containing in total 141 mg anthocyanins, 24 mg flavan-3-ols, 16 mg procyanidins, 10 mg phenolic acids,

9 mg flavonols, and 1 mg stilbenes. This mix was together with 900 mg of micro-crystalline cellulose formulated into six hard-shell gelatine capsules (size 00, Capsugel®, Bornem, Belgium). The active and placebo capsules (only containing cellulose) were formulated by Well Plus Trade (Hamburg, Germany). The wine/grape extract mix was also added at the same dose to each serving of the three drinks. The drinks (dairy drink, soy drink, and fruit-flavoured water) were produced in the pilot plant of Unilever Research and Development, (Vlaardingen, The Netherlands). Capsules were stored at room temperature and drinks at −20 °C until one week before distribution to the subjects. After microbiological clearance, subjects received the test products plus one spare product at the instruction meeting and at the measurement day of the previous treatment period. Each subject consumed one dose of six capsules or one bottle (200 mL) per day in a fasted state, one hour before breakfast. The first four days subjects consumed the test products at home. The fifth day they received their final dose at the test facility after the first blood collection. Nutrient composition and pH of the three drinks were determined before and after the intervention (Table 1).

Table 1. Nutrient composition of the three test drinks.

	Product		
	FF Drink	**Dairy Drink**	**Soy Drink**
Protein	0.04	3.4	3.4
Carbohydrates	3.9	6.0	4.5
Fat	1.73	1.40	2.10
Ash	0.04	0.56	0.42
Moisture	94.3	87.3	88.1
Glucose	0.2	0.7	0.1
Fructose	0.1	0.1	0.1
Lactose	<0.05	1.7	<0.05
Sucrose	3.0	2.9	3.4
Maltose	<0.05	<0.05	0.4
pH	4.3	4.0	4.2

Values expressed as g/100 g product. FF drink: fruit-flavoured drink. Ash: residue of inorganic material.

2.4. Collection Blood and Urine Samples

On day 4 after discarding their first morning urine, subjects started collecting their urine for a period of 24 h. Urine was collected in suitable containers with metaphosphoric acid as preservative. After measuring the volume of the 24 h pooled urine collection and homogenization, four 10 mL samples were stored at −20 °C as soon as possible. Blood samples were collected on day 5 of each treatment period just before (t = 0) and 1, 2, and 3 h after test product intake. On each time point 6 mL of blood was collected by venapuncture from the antecubital vein in tubes containing lithium heparin as anticoagulant. The blood samples were centrifuged directly after withdrawal at 1500× g, 10 min, 4 °C. Subsequently plasma samples were aliquoted in three samples of 0.8 mL and stored at −80 °C.

2.5. Laboratory Analyses

Polyphenol metabolites were determined in both urine and plasma samples, using different methods of analysis. For urine samples ^{1}H-NMR, GC-MS, and LC-MRM-MS data were obtained. Both GC-MS and LC-MRM-MS data were acquired from the plasma samples.

- ^{1}H-NMR profiling was used to generate a comprehensive profile of metabolites (both endogenous and exogenous)
- GC-MS was used to produce a fingerprint of phenolic acids in urine
- LC-MRM-MS was used to quantify selected intact and metabolized polyphenols in plasma

2.5.1. Quantitative Determination of Conjugated and Non-Conjugated Polyphenols in Plasma by LC-MRM-MS

All samples of a subject were analysed in one run with two quality control samples (QCs). The QCs were prepared by spiking blank human plasma (Pooled Normal Human Plasma, Innovative Research Inc., Novi, MI, USA) with polyphenol pure standards at a final concentration of 100 ng/mL. To 200 µL plasma, 20 µL of stabilizer solution (10% ascorbic acid containing 0.1% EDTA), 20 µL of 1.5 M NaOAc (pH 4.8), 40 µL of internal standard (±)-taxifolin (250 ng/mL in MeOH/H_2O 1:1), and 500 units of D-glucuronidase (*Helix pomatia* type H-1 containing sulphatase, Sigma-Aldrich, Zwijndrecht, The Netherlands) was added, mixed, and incubated at 37 °C for 45 min. The reaction was stopped by adding 300 µL of water and 10 µL of 2 mol/L HCl. Polyphenols were isolated by extracting twice with ethyl acetate. Ten microliters (10 µL) of 0.4% ascorbic acid was added to the combined organic layers and dried under N_2 at room temperature. Samples were dissolved in 100 µL methanol, vortexed, and sonicated for 10 min. One hundred microliters (100 µL) of water was added, vortexed, and sonicated for 10 min. Samples were centrifuged at 17,000× *g* for 10 min. Supernatants were transferred to a Greiner 96-well plate for analysis by LC-MRM-MS.

The LC-MRM-MS system consisted of an Agilent 1200SL binary pump (Agilent Technologies, Amstelveen, The Netherlands) equipped with a thermostated HTC PAL autosampler (CTC Analytics, Zwingen, Switzerland), an Agilent 1200 series degasser, and an Agilent 1200 series column oven connected to an Agilent 6410 triple quadrupole mass spectrometer. Samples were stored in the autosampler tray in the dark at 10 °C. Intact polyphenols and metabolites were separated on an XBridge Phenyl (2.1 × 150 mm, 3.5 µm) (Waters, Etten-Leur, The Netherlands) reversed-phase column protected by a guard column and eluted using a 45-min binary solvent gradient using solvents A (0.1% (*v*/*v*) acetic acid in MilliQ water) and B (0.1% (*v*/*v*) acetic acid in acetonitrile) as follows: 0–3 min 2% B, 3–4 min 2%–10% B, 4–14 min 10%–20% B, 14–29 min 14%–100% B, 29–34 min 100% B, 34–35 min, 100%–2% B, 35–45 min 2% B. The flow rate was 0.2 mL/min and the column was thermostated at 55 °C. Injection volumes were 5 µL. After every 20 plasma injections, the column was washed with methanol for 30 min. Blank injections preceded plasma injections. The mass spectrometer was operated in negative ion mode using an Agilent electrospray source. Compounds were analysed by multiple-reaction monitoring (MRM). Data were processed using Agilent's MassHunter Quantitative Analysis software (Agilent Technologies, Amstelveen, The Netherlands).

2.5.2. Semi-Quantitative Analysis of Colonic Metabolites Excreted in Urine by GC-MS

Urine samples were analysed by GC-MS for semi-quantitative determination of gut microbial breakdown products of dietary polyphenols. The protocol for urine sample preparation and subsequent GC-MS analysis has previously been described in detail [21]. Phenolic acids including 3-hydroxyphenylacetic acid, 3-hydroxyhippuric acid, and 4-hydroxyhippuric acid were identified on the basis of a specific retention-time-*m*/*z* pair, and by comparison with the GC-MS data of authentic reference standards. Semi-quantification of the phenolic acid concentrations was achieved by integration of the characteristic peaks in the total-ion-chromatogram. Peak areas were normalized to the peak area of the internal standard (*trans*-cinnamic acid-d_6), and the volume of the 24 h urine sample was used to arrive at an estimate of the 24-h cumulative excretion per phenolic acid.

2.5.3. Quantification of Hippuric Acid in Urine by NMR Spectroscopy

High-resolution 1D-^{1}H-NMR profiling of 24 h urine samples was performed basically as described previously [15]. In brief, NMR samples were prepared by (1:2) mixing of urine with a phosphate buffer solution (pH 6.5), containing 20% D_2O and 0.05 mg/mL 3-(trimethylsilyl)propionic acid-d_4 sodium salt (TSP) as a chemical shift reference. ^{1}H-NMR spectra were acquired at 600.13 MHz and at a temperature of 300 K on a Bruker Avance 600 NMR spectrometer equipped with a 5-mm TXI probe. A standard water-suppressed Noesypresat pulse sequence was used collecting 128 scans with 32 K data points over 8993 Hz. The spectra were manually phase and baseline corrected using Topspin 1.3 software

(Bruker Analytik, Rheinstetten, Germany). An exponential window function with a line-broadening factor of 0.3 Hz was applied to the free induction decay prior to Fourier transformation. Hippuric acid levels in urine were determined from the peak integral of its aromatic signal at 7.83 ppm and was expressed in grams excreted over a 24-h period and as molar ratio of hippuric acid/creatinine, adjusting for urine analyte concentrations in case of any incomplete urine collection over 24 h [22].

2.6. Statistical Analysis

The statistical analyses were performed using the SAS Software (SAS Institute, Cary, NC, USA, version 9.1) on the per protocol dataset. Descriptive analysis consisted of distribution statistics (number of available observations, mean, standard deviation, and 95% confidence intervals) for continuous data. Differences between the active groups and the placebo were evaluated by means of an analysis of variance. Overall mean effects of the plasma concentrations measured at t = 0, 1, 2, and 3 h after polyphenol consumption were statistically analysed. A Dunnett test was performed in order to correct for multiple testing between the active groups and the placebo.

3. Results

3.1. Baseline Characteristics of the Study Population

Thirty-three subjects started this study. One subject dropped out in treatment period 4 due to medical reasons. This person was not replaced. Data that was collected in treatment periods 1, 2, and 3 was included in the statistical analyses. Thirty-two subjects completed the study. The mean age of the study population was 50.6 $\pm$ 17.8 years (ranging from 18 to 69 years) with a BMI of 24.6 $\pm$ 2.8 kg·m^{-2}.

3.2. Adverse Events during the Study

A total of 29 reports of adverse events (AEs) were filed. Of these reports nine AE reports were reported by nine subjects receiving the placebo capsules, seven AE reports by six subjects receiving the active capsules, four AE reports by four subjects receiving the dairy drink, four reports by four subjects receiving the juice and five reports by five subjects receiving the soy drink. Most frequently reported AEs were headache and acute nasopharyngitis. There were no significant differences in frequencies of AEs between actives and placebo. No likely relation between any AE and the test products was found.

3.3. Compliance with the Test Product and Background Diet and Lifestyle Restrictions

Compliance with the test products was checked by means of a diary in which subjects daily reported the consumption of the test product and the time of consumption. A dietician evaluated compliance at each measurement day. The self-reported compliance of the intake of the test products was very high: 100% for the placebo capsules, the fruit-flavoured drink, and the soy drink. Two subjects consumed four out of five of the dairy drink and one person consumed four out of five of the positive control capsules. All other subjects consumed 100% of the dairy drink and active capsules. Deviations to background dietary guidelines were registered in the same diary and checked by a dietician. In total 21 urine samples and 28 blood samples were excluded from analysis mainly due to use of antibiotics during the study, medical reasons, coffee consumption, or consumption of proteins from other sources than the test products.

3.4. Polyphenols and Metabolites in Plasma and Urine

Upon consumption of the polyphenol-rich test products concentrations of phenolic compounds increased by 0.5 to 20-fold within the first three hours after consumption (Table 2; Figure 2). Urinary phenolic acid concentrations increased up to three-fold (Table 3). Urinary excretion of creatinine was not significantly different between interventions and periods (data not shown), indicating good compliance for 24 h urine collection. Compared to capsule ingestion, consumption of polyphenol-rich beverages containing either dairy, soy, or no proteins had minor to no effect on the

bioavailability and excretion of phenolic compounds in plasma (mean ± standard error: 118% ± 9%) and urine (98% ± 2%).

Table 2. Peak plasma concentration of sum of free and conjugated polyphenols and metabolites after consumption of different test products (n = 32).

	Control	Positive Control	Dairy Drink	Soy Drink	FF Drink
Resveratrol	0.17 (0.03–0.30)	0.56 *** (0.43–0.69)	0.61 *** (0.48–0.74)	0.58 *** (0.46–0.71)	0.70 *** (0.57–0.83)
Epicatechin	1.5 (−6.8–9.8)	15.7 * (8.4–23.0)	12.0 * (4.6–19.4)	22.6 ** (15.4–29.8)	20.5 ** (13.3–27.7)
Catechin	0.47 (−5.2–6.2)	4.4 (−0.5–9.3)	3.3 (−1.7–8.3)	12.1 * (7.3–17.0)	5.9 (1.0–10.7)
Valerolactone	0.61 (−3.3–4.5)	13.7 * (10.2–17.3)	12.5 * (9.0–16.0)	12.2 (8.8–15.6)	11.6 (8.1–15.1)
M-valerolactone	0.17 (−0.60–0.94)	2.4 * (1.7–3.2)	3.5 * (2.7–4.2)	3.3 * (2.5–4.0)	3.1 * (2.4–3.8)
M-gallic acid	3.6 (1.7–5.5)	23.5 *** (21.6–25.3)	21.7 *** (19.8–23.6)	25.2 *** (23.3–27.1)	34.1 ***,# (32.3–36.1)
Isorhamnetin	2.1 (1.6–2.5)	3.7 *** (3.2–4.1)	3.3 *** (2.9–3.8)	3.4 *** (2.9–3.8)	3.9 *** (3.5–4.4)

Mean (95% confidence interval) in ng/mL. Test products were cellulose-filled capsules (control), and wine and grape polyphenols incorporated into either capsules (positive control), a dairy drink, a soy drink, or a fruit-flavoured (FF) drink. Valerolactone: 5-(3′,4′-dihydroxyphenyl)-γ-valerolactone; M-valerolactone: 5-(3′-methoxy-4′-hydroxyphenyl)-γ-valerolactone; M-gallic acid: 3/4-*O*-methyl gallic acid. Statistically significant compared to control (placebo capsules): * $p < 0.05$, ** $p < 0.001$, *** $p < 0.0001$. Statistically significant compared to positive control (polyphenol-filled capsules): # $p < 0.0001$.

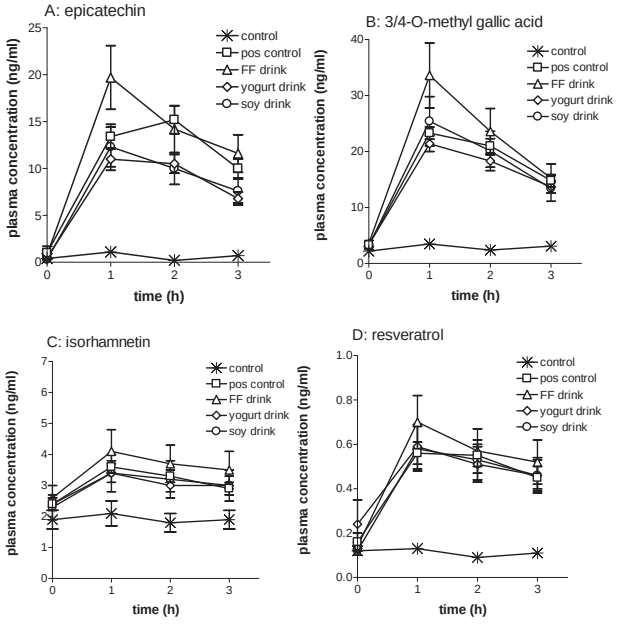

Figure 2. Plasma concentration (mean ± SEM, n = 32) versus time profiles for four individual polyphenols (including polyphenol-conjugates) for the five different formulation treatments. (**A**) Epicatechin; (**B**) 3/4-O-methyl gallic acid; (**C**) isorhamnetin; (**D**) resveratrol.

Table 3. Relative 24-h cumulative urinary excretion of phenolic metabolites after consumption of different test products with control as the reference (1.0).

	Control	Positive Control	Dairy Drink	Soy Drink	FF Drink
3-HHA	1.0 (0.6–1.4)	2.9 *** (2.2–3.7)	2.6 ** (1.8–3.4)	3.2 *** (2.0–4.5)	2.6 ** (1.8–3.3)
4-HHA	1.0 (0.7–1.3)	1.6 * (1.2–1.9)	1.5 * (0.9–2.0)	1.5 * (1.0–2.0)	1.6 * (1.2–2.0)
pyrogallol	1.0 (0.8–1.2)	1.3 * (1.1–1.5)	1.1 (1.0–1.3)	1.5 *** (1.2–1.8)	1.2 (1.0–1.4)
3-HPAA	1.0 (0.7–1.3)	2.5 *** (1.9–3.1)	2.4 *** (1.7–3.0)	2.5 *** (1.9–3.0)	2.6 *** (1.9–3.3)
3-HPPA	1.0 (0.8–1.2)	1.3 * (0.9–1.7)	1.3 (0.8–1.7)	1.4 * (0.9–1.9)	1.3 * (0.8–1.9)
Homovanillic acid	1.0 (0.9–1.1)	1.3 * (1.0–1.5)	1.2 (1.0–1.4)	1.2 * (1.0–1.3)	1.2 * (1.0–1.4)
Hydrocaffeic acid	1.0 (0.5–1.5)	1.4 * (1.1–1.7)	1.1 (0.8-1.5)	1.2 (0.9–1.5)	1.5 * (1.0–2.1)
Syringic acid	1.0 (0.8–1.2)	1.0 (0.8–1.2)	1.1 (0.8–1.3)	1.1 (0.9–1.3)	1.1 (0.8–1.3)
Vanilmandelic acid	1.0 (0.9–1.1)	1.1 * (1.0–1.3)	1.1 (0.9–1.2)	1.1 (0.9–1.2)	1.1 (0.9–1.2)
Hippuric acid	0.30 (0.24–0.35)	0.42 *** (0.37–0.47)	0.38 * (0.33–0.42)	0.42 ** (0.37–0.48)	0.39 * (0.32–0.46)
Hippuric acid/creatinine	0.083 (0.070–0.096)	0.114 *** (0.102–0.127)	0.108 ** (0.095–0.120)	0.116 *** (0.104–0.129)	0.108 ** (0.095–0.120)

Mean (95% confidence interval) data for 24-h cumulative excretion of urinary metabolites are shown as relative to control values, except for hippuric acid (in grams) and the hippuric acid/creatinine (in molar ratio). Test products were cellulose-filled capsules (control), and wine and grape polyphenols incorporated into either capsules (positive control), a dairy drink, a soy drink, or a fruit-flavoured (FF) drink. Statistically significant compared to control (placebo capsules): * $p < 0.05$, ** $p < 0.001$, *** $p < 0.0001$. 3-HHA: 3-hydroxy hippuric acid; 4-HHA: 4-hydroxy hippuric acid; pyrogallol: 1,2,3-trihydroxy-benzene; 3-HPAA: 3-hydroxy-phenyl acetic acid; 3-HPPA: 3-hydroxy-phenyl propionic acid.

4. Discussion

The present study demonstrates that the impact of proteins derived from animal and plant sources on the bioavailability of a range of polyphenols and their metabolites is minor to none for the first hours after consumption. Plasma concentrations of a number of identified phenolic compounds increased by approximately ten-fold or more, irrespective of the test product. Resveratrol (conjugates) plasma concentrations increased three to four times unaffected by the protein content, which is in accordance with bioavailability data described previously for resveratrol-containing wine consumed with different meals [23]. All test products increased the plasma concentration of the methylated metabolite of quercetin, isorhamnetin (phase II methyltransferase metabolite), by 50% or more. Previous research indicated that high fat meals may enhance the bioavailability of quercetin, resulting in higher plasma concentrations of isorhamnetin [24], but proteins do not seem to contribute to that effect. Red wine contains considerable amounts of gallic acid and its methylated form appears readily in plasma after wine consumption [25]. We confirmed the large rise in plasma concentration of methyl-gallic acid in the present study, and observed possibly minor effects of proteins present in the test products. The effects of proteins on the bioavailability of catechin and epicatechin seems mixed with a possible enhancement by soy proteins and inhibition by milk proteins. These data contrast to some extent with absence of effect found for proteins on the bioavailability of green tea non-gallated catechins published previously [7]. The valerolactones, microbial metabolites of flavan-3-ols, reach high plasma concentrations, typically five to eight hours after consumption of the polyphenols [14,26]. Nevertheless, these metabolites increased 20-fold within the first three hours after consumption of the test products.

Neither soy proteins nor dairy proteins seem to affect the valerolactone plasma concentrations within these first hours. Despite the relatively large portion of anthocyanins present in the test products, we were not able to detect these phenolic compounds. This may reflect the low bioavailability of anthocyanins, as shown by others, reaching at most nanomolar plasma concentrations with similar test dosages of grape-derived anthocyanins as we have included in the present study [27,28].

We assume that the study design has contributed significantly to these clear-cut results. Subjects were on a low polyphenol diet, and had to repeat as much as possible their intake pattern each intervention week. Baseline plasma concentrations of each phenolic compound was, repeatedly, low, enabling us to show increase in phenolic compound plasma concentrations due to the interventions. Moreover, we used a number of state-of-the art measurement tools for identification. What could, however, be considered a weakness in the current study design is the choice of the non-food reference format; gelatine capsules. As such, hard-shell capsules are an attractive format for this type of studies since they can be easily prepared to accommodate study design, extract type, and dose. Ideally, we would have used a non-protein capsule shell material such as hydroxy-propyl-methyl-cellulose (HPMC). This would have created a true non-protein reference and control situation. Unfortunately, HPMC material interacts with polyphenols, limiting severely the release in simulated gastrointestinal (GI) tract condition of the HPMC capsule content [29]. This effect is absent or less pronounced in the case of gelatine capsules, which are designed to disintegrate within minutes in the GI tract. In this study, however, we used six capsules, size 00, consisting in total of 0.75 g gelatine, and if compared to the 6.8 g of protein in the soy and dairy drinks may no longer be negligible. Similarly, the impact of 0.9 g cellulose (filler) in the capsules on the bioavailability of polyphenols is not known. It may explain why the plasma concentrations of the phenolic compounds seem to reach somewhat higher levels with the fruit-flavoured drinks compared to the capsule format (Figure 2).

One should realize that the data in the present study are relevant for consumer products such as milk chocolate drinks, tea, and coffee with milk and fruit drinks containing proteins, but is not conclusive towards complex meals. Different meal compositions may indeed impact the bioavailability of certain polyphenols, albeit may often be difficult to judge which macro- or micronutrients interfered [12,23,24,27,30]. Depending on the type of the polyphenols this impact of a meal on the bioavailability of polyphenols may vary to a large extent with many compound and physiological variables involved, all controlling absorption and bioavailability.

We also found no indication that urinary excretion of a range of phenolic acids combined with either milk or soy proteins was inhibited. This contrasts to the observations published by Urpi-Sarda et al. [31] who investigated phenolic excretion after consumption of cocoa with milk. Milk significantly reduced the urinary excretion of phenolic acids, including hippuric acid and 4-HHA that were unaffected in the present study. Mullen et al. [32] postulated an interesting hypothesis: the excretion of phenolic metabolites may be more affected by (milk) proteins of cocoa products relatively low in polyphenols (70 mg in their study) compared to highly concentrated ones. This may be a plausible explanation for the controversy among studies, although so far the phenolic bioavailability and metabolism of products with low vs. high levels of polyphenols have not been tested head-to-head. Our more precise conclusion may thus be that bioavailability and metabolism of wine and grape polyphenols is not importantly affected by milk or soy proteins when consumed in relatively high dose. The definition of a (sufficiently) high dose requires more research.

5. Conclusions

The bioavailability of polyphenols and the excretion of their phenolic metabolites is not significantly affected when polyphenols are consumed in protein-rich soy or dairy drinks compared to polyphenols formulated in capsules.

Acknowledgments: We would like to acknowledge Peter van Bruggen and Arne Jol for their expertise and conduct of the statistical analyses.

Author Contributions: R.D., F.A.D., Y.E.Z., G.S.D. and C.H.G. designed the study; F.A.D., Y.E.Z., B.H. and S.P. conducted the research; R.D. drafted the manuscript and F.A.D., Y.E.Z., G.S.D. and C.H.G. critically reviewed the manuscript.

Conflicts of Interest: At time of design, execution, and data interpretation of this study all authors were full time employees of Unilever. Unilever markets polyphenol-rich products, mainly tea.

References

1. Perez-Jimenez, J.; Neveu, V.; Vos, F.; Scalbert, A. Identification of the 100 richest dietary sources of polyphenols: An application of the phenol-explorer database. *Eur. J. Clin. Nutr.* **2010**, *64*, S112–S120. [CrossRef] [PubMed]
2. Jiang, W.; Wei, H.; He, B. Dietary flavonoids intake and the risk of coronary heart disease: A dose-response meta-analysis of 15 prospective studies. *Thromb. Res.* **2015**, *135*, 459–463. [CrossRef] [PubMed]
3. Williamson, G.; Holst, B. Dietary reference intake (DRI) value for dietary polyphenols: Are we heading in the right direction? *Br. J. Nutr.* **2008**, *99*, S55–S58. [CrossRef] [PubMed]
4. Cordova, A.C.; Sumpio, B.E. Polyphenols are medicine: Is it time to prescribe red wine for our patients? *Int. J. Angiol.* **2009**, *18*, 111–117. [CrossRef] [PubMed]
5. Biagi, M.; Bertelli, A.A. Wine, alcohol and pills: What future for the french paradox? *Life Sci.* **2015**, *131*, 19–22. [CrossRef] [PubMed]
6. Rashidinejad, A.; Birch, E.J.; Sun-Waterhouse, D.; Everett, D.W. Addition of milk to tea infusions: Helpful or harmful?; Evidence from in vitro and in vivo studies on antioxidant properties. *Crit. Rev. Food Sci. Nutr.* **2015**. [CrossRef] [PubMed]
7. Egert, S.; Tereszczuk, J.; Wein, S.; Muller, M.J.; Frank, J.; Rimbach, G.; Wolffram, S. Simultaneous ingestion of dietary proteins reduces the bioavailability of galloylated catechins from green tea in humans. *Eur. J. Nutr.* **2013**, *52*, 281–288. [CrossRef] [PubMed]
8. Reddy, V.C.; Vidya Sagar, G.V.; Sreeramulu, D.; Venu, L.; Raghunath, M. Addition of milk does not alter the antioxidant activity of black tea. *Ann. Nutr. Metab.* **2005**, *49*, 189–195. [CrossRef] [PubMed]
9. Van het Hof, K.H.; Kivits, G.A.; Weststrate, J.A.; Tijburg, L.B. Bioavailability of catechins from tea: The effect of milk. *Eur. J. Clin. Nutr.* **1998**, *52*, 356–359. [CrossRef] [PubMed]
10. Keogh, J.B.; McInerney, J.; Clifton, P.M. The effect of milk protein on the bioavailability of cocoa polyphenols. *J. Food Sci.* **2007**, *72*, S230–S233. [CrossRef] [PubMed]
11. Kyle, J.A.; Morrice, P.C.; McNeill, G.; Duthie, G.G. Effects of infusion time and addition of milk on content and absorption of polyphenols from black tea. *J. Agric. Food Chem.* **2007**, *55*, 4889–4894. [CrossRef] [PubMed]
12. Ribnicky, D.M.; Roopchand, D.E.; Oren, A.; Grace, M.; Poulev, A.; Lila, M.A.; Havenaar, R.; Raskin, I. Effects of a high fat meal matrix and protein complexation on the bioaccessibility of blueberry anthocyanins using the tno gastrointestinal model (TIM-1). *Food Chem.* **2014**, *142*, 349–357. [CrossRef] [PubMed]
13. Manach, C.; Williamson, G.; Morand, C.; Scalbert, A.; Remesy, C. Bioavailability and bioefficacy of polyphenols in humans. I. Review of 97 bioavailability studies. *Am. J. Clin. Nutr.* **2005**, *81*, 230S–242S. [PubMed]
14. Van Duynhoven, J.; van der Hooft, J.J.; van Dorsten, F.A.; Peters, S.; Foltz, M.; Gomez-Roldan, V.; Vervoort, J.; de Vos, R.C.; Jacobs, D.M. Rapid and sustained systemic circulation of conjugated gut microbial catabolites after single-dose black tea extract consumption. *J. Proteome Res.* **2014**, *13*, 2668–2678. [CrossRef] [PubMed]
15. Van Dorsten, F.A.; Grün, C.H.; van Velzen, E.J.; Jacobs, D.M.; Draijer, R.; van Duynhoven, J.P. The metabolic fate of red wine and grape juice polyphenols in humans assessed by metabolomics. *Mol. Nutr. Food Res.* **2010**, *54*, 897–908. [CrossRef] [PubMed]
16. Scalbert, A.; Williamson, G. Dietary intake and bioavailability of polyphenols. *J. Nutr.* **2000**, *130*, 2073S–2085S. [PubMed]
17. Whitfield, P.D.; German, A.J.; Noble, P.J. Metabolomics: An emerging post-genomic tool for nutrition. *Br. J. Nutr.* **2004**, *92*, 549–555. [CrossRef] [PubMed]
18. Daykin, C.A.; Van Duynhoven, J.P.; Groenewegen, A.; Dachtler, M.; Van Amelsvoort, J.M.; Mulder, T.P. Nuclear magnetic resonance spectroscopic based studies of the metabolism of black tea polyphenols in humans. *J. Agric. Food Chem.* **2005**, *53*, 1428–1434. [CrossRef] [PubMed]

19. Van Dorsten, F.A.; Daykin, C.A.; Mulder, T.P.; Van Duynhoven, J.P. Metabonomics approach to determine metabolic differences between green tea and black tea consumption. *J. Agric. Food Chem.* **2006**, *54*, 6929–6938. [CrossRef] [PubMed]
20. Williams, E.J. Experimental designs balanced for the estimation of residual effects of treatments. *Aust. J. Chem.* **1949**, *2*, 149–168. [CrossRef]
21. Grün, C.H.; van Dorsten, F.A.; Jacobs, D.M.; Le Belleguic, M.; van Velzen, E.J.; Bingham, M.O.; Janssen, H.G.; van Duynhoven, J.P. GC-MS methods for metabolic profiling of microbial fermentation products of dietary polyphenols in human and in vitro intervention studies. *J. Chromatogr. B Anal. Technol. Biomed. Life Sci.* **2008**, *871*, 212–219. [CrossRef] [PubMed]
22. Zamora-Ros, R.; Rabassa, M.; Cherubini, A.; Urpi-Sarda, M.; Llorach, R.; Bandinelli, S.; Ferrucci, L.; Andres-Lacueva, C. Comparison of 24-h volume and creatinine-corrected total urinary polyphenol as a biomarker of total dietary polyphenols in the invecchiare inchianti study. *Anal. Chim. Acta* **2011**, *704*, 110–115. [CrossRef] [PubMed]
23. Vitaglione, P.; Sforza, S.; Galaverna, G.; Ghidini, C.; Caporaso, N.; Vescovi, P.P.; Fogliano, V.; Marchelli, R. Bioavailability of trans-resveratrol from red wine in humans. *Mol. Nutr. Food Res.* **2005**, *49*, 495–504. [CrossRef] [PubMed]
24. Guo, Y.; Mah, E.; Davis, C.G.; Jalili, T.; Ferruzzi, M.G.; Chun, O.K.; Bruno, R.S. Dietary fat increases quercetin bioavailability in overweight adults. *Mol. Nutr. Food Res.* **2013**, *57*, 896–905. [CrossRef] [PubMed]
25. Caccetta, R.A.; Croft, K.D.; Beilin, L.J.; Puddey, I.B. Ingestion of red wine significantly increases plasma phenolic acid concentrations but does not acutely affect ex vivo lipoprotein oxidizability. *Am. J. Clin. Nutr.* **2000**, *71*, 67–74. [PubMed]
26. Wiese, S.; Esatbeyoglu, T.; Winterhalter, P.; Kruse, H.P.; Winkler, S.; Bub, A.; Kulling, S.E. Comparative biokinetics and metabolism of pure monomeric, dimeric, and polymeric flavan-3-ols: A randomized cross-over study in humans. *Mol. Nutr. Food Res.* **2015**, *59*, 610–621. [CrossRef] [PubMed]
27. Kuntz, S.; Rudloff, S.; Asseburg, H.; Borsch, C.; Frohling, B.; Unger, F.; Dold, S.; Spengler, B.; Rompp, A.; Kunz, C. Uptake and bioavailability of anthocyanins and phenolic acids from grape/blueberry juice and smoothie in vitro and in vivo. *Br. J. Nutr.* **2015**, *113*, 1044–1055. [CrossRef] [PubMed]
28. Stalmach, A.; Edwards, C.A.; Wightman, J.D.; Crozier, A. Gastrointestinal stability and bioavailability of (poly)phenolic compounds following ingestion of concord grape juice by humans. *Mol. Nutr. Food Res.* **2012**, *56*, 497–509. [CrossRef] [PubMed]
29. Glube, N.; Moos, L.; Duchateau, G. Capsule shell material impacts the in vitro disintegration and dissolution behaviour of a green tea extract. *Results Pharma Sci.* **2013**, *3*, 1–6. [CrossRef] [PubMed]
30. Chow, H.H.; Hakim, I.A.; Vining, D.R.; Crowell, J.A.; Ranger-Moore, J.; Chew, W.M.; Celaya, C.A.; Rodney, S.R.; Hara, Y.; Alberts, D.S. Effects of dosing condition on the oral bioavailability of green tea catechins after single-dose administration of polyphenon e in healthy individuals. *Clin. Cancer Res.* **2005**, *11*, 4627–4633. [CrossRef] [PubMed]
31. Urpi-Sarda, M.; Llorach, R.; Khan, N.; Monagas, M.; Rotches-Ribalta, M.; Lamuela-Raventos, R.; Estruch, R.; Tinahones, F.J.; Andres-Lacueva, C. Effect of milk on the urinary excretion of microbial phenolic acids after cocoa powder consumption in humans. *J. Agric. Food Chem.* **2010**, *58*, 4706–4711. [CrossRef] [PubMed]
32. Mullen, W.; Borges, G.; Donovan, J.L.; Edwards, C.A.; Serafini, M.; Lean, M.E.; Crozier, A. Milk decreases urinary excretion but not plasma pharmacokinetics of cocoa flavan-3-ol metabolites in humans. *Am. J. Clin. Nutr.* **2009**, *89*, 1784–1791. [CrossRef] [PubMed]

nutrients

MDPI

Review

Antioxidants and Dementia Risk: Consideration through a Cerebrovascular Perspective

Virginie Lam [1,2], Mark Hackett [1,3] and Ryusuke Takechi [1,2,*]

1 Curtin Health Innovation Research Institute, Curtin University, Perth WA 6845, Australia; Virginie.Lam@curtin.edu.au (V.L.); Mark.J.Hackett@curtin.edu.au (M.H.)
2 School of Public Health, Faculty of Health Sciences, Curtin University, Perth WA 6845, Australia
3 Department of Chemistry, Faculty of Science and Engineering, Curtin University, Perth WA 6845, Australia
* Correspondence: R.Takechi@curtin.edu.au; Tel.: +61-8-9266-2607

Received: 15 November 2016; Accepted: 16 December 2016; Published: 20 December 2016

Abstract: A number of natural and chemical compounds that exert anti-oxidative properties are demonstrated to be beneficial for brain and cognitive function, and some are reported to reduce the risk of dementia. However, the detailed mechanisms by which those anti-oxidative compounds show positive effects on cognition and dementia are still unclear. An emerging body of evidence suggests that the integrity of the cerebrovascular blood-brain barrier (BBB) is centrally involved in the onset and progression of cognitive impairment and dementia. While recent studies revealed that some anti-oxidative agents appear to be protective against the disruption of BBB integrity and structure, few studies considered the neuroprotective effects of antioxidants in the context of cerebrovascular integrity. Therefore, in this review, we examine the mechanistic insights of antioxidants as a pleiotropic agent for cognitive impairment and dementia through a cerebrovascular axis by primarily focusing on the current available data from physiological studies. Conclusively, there is a compelling body of evidence that suggest antioxidants may prevent cognitive decline and dementia by protecting the integrity and function of BBB and, indeed, further studies are needed to directly examine these effects in addition to underlying molecular mechanisms.

Keywords: antioxidants; blood-brain barrier; cognitive impairment; dementia

1. Introduction

As a consequence of rapidly aging populations, particularly in developed nations, dementia has become a major health and medical issue imposing an extraordinary economic burden. As reported by the World Health Organization and Alzheimer's disease International, the global cost of dementia-related healthcare was estimated to be $604 billion in 2010, which was equal to 1% of world gross domestic product, indicating a significant socioeconomic impact [1]. Studies also predict that this cost will greatly increase and is expected to double in the next 10–15 years. Indeed, the latest estimated global cost of dementia in 2015 based on a meta-analysis was $818 billion, an increase of 35% since 2010 [2]. Astoundingly, the estimated prevalence of dementia has increased from 35.6 million in 2010 to 46.8 million in 2015, an increase of 34% [2]. Clearly, there is an urgent necessity to establish effective therapeutic strategies to delay or prevent the onset and progression of this disorder.

Major subtypes of dementia are Alzheimer's disease (AD), vascular dementia, Lewy body dementia, and frontotemporal dementia, which accounts for approximately 43%, 15%, 5% and 1% of all dementia cases, respectively [3]. Although the pathology and pathogenesis of these disorders remain largely unclear, it is increasingly recognized that the integrity of cerebrovasculature is critical to the maintenance of healthy brain function and integrity [4]. The human brain ordinarily receives 20% of cardiac output despite its small volume (2% against total body mass), and the surface area of cerebrovascular network available for molecular exchange between the brain and blood is

approximately 20 m^2 [5]. Dysfunctional cerebrovascular integrity allows blood-to-brain extravasation of potentially neuroactive molecules, which thereafter trigger a neuroinflammatory cascade and subsequently, activation of neuronal apoptosis pathways, conditions which lead to neurodegeneration and if persisting, cognitive decline. Thus, it is highly plausible that subtle changes in cerebrovascular permeability can have substantial impacts on the brain and neurocognitive function.

In recent clinical and animal model studies, agents with anti-oxidative properties are reported to exert therapeutic effects on cognitive impairment and dementia [6–8]. However, whilst the majority of these studies demonstrated the beneficial effects of antioxidants on cognitive function via direct neuroprotective actions within the brain, no studies have implicated the efficacy of antioxidant therapy through the cerebrovascular axis. Therefore, this review summarizes the current available data from both animal and human studies to potentiate the role of antioxidants in the prevention of dementia and cognitive decline via mechanisms mediated through the cerebrovascular axis. Moreover, considerations for future studies examining the antioxidant effects on the cerebrovasculature are discussed.

2. Cerebrovascular Integrity in Neurodegeneration, Cognitive Decline and Dementia

The brain is a vital organ, yet extremely vulnerable to various endogenous and exogenous insults such as viral and bacterial pathogens, inflammatory cells, pro-inflammatory cytokines, reactive oxygen species (ROS), and macronutrients [5]. Therefore, in a healthy, non-pathological state, this organ is protected from the peripheral circulation by a structurally unique neurovascular unit, which constitutes the blood-brain barrier (BBB). The main feature of the BBB is a monolayer of endothelial cells that are tightly opposed to one another, forming a physical barrier between the brain and blood. The cells are fused each other by tight junctional and adheren junctional complexes, which consist of integral membrane tight junction proteins including occludin and claudin, anchored by cytoplasmic zonula occludens (ZO). This impermeable layer of endothelial cells is structurally supported by several layers of underlying basement membranes as well as pericytes and astrocytic endfeet. A healthy, functioning BBB strictly regulates molecular trafficking between the brain and blood, allowing only highly specific transcellular transport of particular molecules that are essential to the brain, such as glucose and oxygen. However, under certain pathological stress conditions, the integrity of this highly selective barrier system can be transiently or chronically compromised depending on the nature of the insults. The factors that can deteriorate BBB integrity and increase its permeability include inflammation, oxidative stress, hypertension, stroke, HIV, lipids, smoking, alcohol intake, mental stress, and lowered cerebral blood flow, although the underlying molecular mechanisms are not fully understood [4,9,10].

2.1. Dysfunction of the Cerebrovascular Blood-Brain Barrier

A dysfunctional BBB may occur via (i) impaired transcellular transport, mainly due to dysregulation of endothelial receptors and intracellular transporters; (ii) impaired paracellular unspecific extravasation of molecules due to a loss of tight junction complex; and/or (iii) loss of endothelial cells per se due to apoptosis or traumatic injury. Persistent disturbances of BBB allow substantial cerebral extravasation of blood-borne potentially neurotoxic molecules, which thereby promote the synthesis and release of pro-inflammatory cytokines resulting in the activation of microglial phagocytes and production of ROS [11]. Chronically heightened inflammatory and oxidative stress in the brain results in the production of toxic products that compromise cell function, alter cellular phenotypes, damage DNA, and eventually lead to neuroinflammation and neurodegeneration. The latter is increasingly suggested by a number of studies to be profoundly associated with the pathogenesis and pathology of cognitive decline and dementia including AD and vascular dementia [5]. Indeed, neuroinflammation, microgliosis and mitochondrial dysfunction are commonly observed in the brain of subjects with AD and vascular dementia [12–14].

2.2. Blood-Brain Barrier Dysfunction in Cognitive Deficits and Dementia

Despite decades of attempts in Alzheimer's research, anti-amyloid strategies have failed to consistently deliver positive results in the prevention and treatment of AD [7,15]. In fact, some neuropsychological and neuropathological characteristics of AD cannot be fully explained by the amyloid hypothesis alone. For example, some studies report that the severity of amyloidosis does not consistently correlate with the severity of AD, and the biosynthesis of β-amyloid in sporadic AD subjects is comparable to otherwise healthy individuals [9,16,17].

Emerging evidence substantiates the involvement of cerebrovascular dysfunction in the pathogenesis of AD and other dementias. In vivo and in vitro studies demonstrated that the transport of β-amyloid across the BBB is mediated by receptor for advanced glycation endproducts [18,19]. Thus, the dysregulation of such pathways is suggested to result in reduced β-amyloid clearance from the brain, which may consequently induce amyloid plaque formation. The vascular risk factors have been increasingly associated with heightened risk of dementia and AD, whereby a substantial body of work has reported exaggerated BBB permeability in the brains of individuals with cognitive impairment or dementia [4]. Post-mortem histological analyses revealed an accumulation of blood-borne proteins including albumin, immunoglobulins, and fibrinogen within the parenchyme of hippocampal formation and cortical regions of subjects with AD [20]. In addition, other post-mortem studies reported degeneration of BBB pericytes and reduced endothelial tight junction protein expression in human AD brain [21]. Further supportive evidence of BBB breakdown in individuals with AD and mild cognitive impairment is provided by studies showing increased concentration of albumin in cerebrospinal fluid relative to blood [22,23]. Moreover, signs of compromised BBB integrity are commonly reported in animal models of AD, leading to loss of endothelial tight junction complex and cerebral extravasation and accumulation of plasma derived macromolecules [9,24]. These data consistently implicate a strong association between dysfunctional BBB and cognitive decline and dementia.

There has been rigorous debate on whether the breakdown of BBB is a primary causative factor of neurodegeneration and dementia or whether it occurs as a downstream response [25]. An increasing number of studies to date report that BBB disruption precedes neurodegeneration and cognitive decline in clinical AD subjects, and in AD animal models, the appearance of hallmark pathophysiological features such as amyloid plaques, strongly suggesting a causal link rather than a consequential one [4]. Recent advances in neuroimaging and neurovascular imaging technologies using state-of-art dynamic contrast-enhanced MRI now allow non-invasive evaluation of regional BBB permeability in vivo with high sensitivity [26]. In 2016, an intriguing study from Maastricht University Medical Center elegantly demonstrated the substantially increased permeability of BBB at a very early stage of AD [27]. The study also revealed that the extent of BBB leakage positively associates with the severity of cognitive decline measured by Mini-Mental State Examination. In addition to this recent report, BBB breakdown was demonstrated to be evident in a murine model of AD Tg2576 mice as early as 4 months of age, which was 10 months before the distinct formation of amyloid plaques at 14 months [28]. Moreover, a recent study in our laboratory demonstrated that substantial disruption of BBB and neuroinflammation was observed prior to neurodegenerative changes and cognitive decline in a dietary-induced mouse model of cognitive decline (unpublished observations by Takechi et al.). Collectively, compelling evidence from experimental and clinical studies strongly indicate a causal association between compromised BBB integrity and the onset and progression of cognitive dysfunction and dementia.

3. Involvement of Oxidative Stress during Breakdown of the Blood-Brain Barrier

Oxidative stress is a state that arises from an inappropriate redox balance where the production of ROS exceeds the conversion/neutralization of ROS into less toxic derivatives by antioxidants such as glutathione and superoxide dismutase (SOD). ROS may be generated by several pathways, such as conversion of oxygen into superoxide by enzymatic activities of oxidase or altered metal homeostasis (Mn, Fe, Cu) and ensuing metal catalyzed free radical production through classic Fenton chemical

pathways. Superoxide is frequently converted into hydrogen peroxide, the most bioactive and stable form of ROS, however, superoxide may also react with nitric oxide generating additional free radicals. In addition, hydrogen peroxides can also be generated directly by some enzymes such as NADPH oxidase. Therefore, oxidative stress can occur by an overproduction of ROS by enzymes including NADPH oxidase, and/or from lowered antioxidant levels or activity including SOD. Studies report that elevated oxidative stress may have direct and indirect effects on the integrity of BBB [29].

An involvement of oxidative stress in the regulatory mechanisms of BBB integrity is supported by a number of studies [29–32] (Figure 1). A study using SOD deficient mice demonstrated a substantial breakdown of BBB allowing an extravasation of large blood-borne molecules into the brain [33]. Lochhead et al. demonstrated that oxidative stress induced through a process of hypoxia and reoxygenation in rats altered occludin structure and localization in cerebrovascular endothelial cells [30]. Increased oxidative stress disrupted BBB by attenuating the expression of tight junction proteins, ZO-1, occluding and claudin in diabetic mode rats [34]. In vitro studies confirmed ROS-mediated modulation of BBB permeability occurs in a time- and concentration-dependent manner [35,36]. Furthermore, Schreibelt et al. revealed in an in vitro model of BBB, ROS-induced BBB disruption occurred through a loss of tight junction claudin-5 and occludin was mediated by upregulated RhoA and PI3 kinase [37]. The study also for the first time reported the involvement of protein kinase B/Akt in ROS-induced alteration of BBB tight junction expression and localization. Moreover, a study using bovine brain microvascular endothelial cells indicated that increased superoxide induced F-actin stress fiber formation through a Rho-dependent pathway [37]. ROS is also documented to increase the expression of chemokine receptors, resulting in signaling flux and phosphorylation of myosin light chain, which thereafter modulates actin structure [38]. The latter findings are consistent with the cytoskeletal reorganization of BBB promoting the loss of BBB integrity.

Overall, the current literature implicates the substantial involvement of oxidative stress in BBB dysfunction (Figure 1), and hence implies the pleiotropic effects of antioxidants in the protection of BBB function and structure.

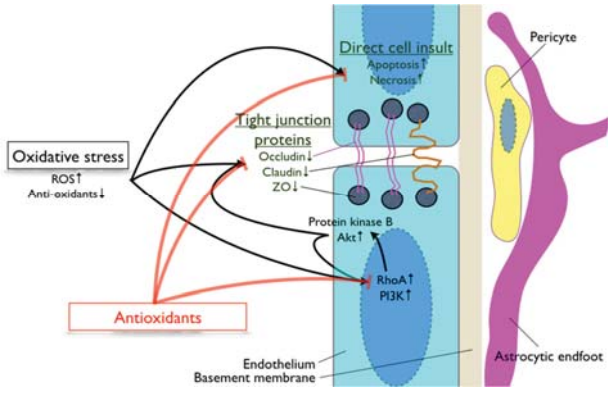

Figure 1. Involvement of oxidative stress in blood-brain barrier regulation. The diagram summarizes the oxidative stress pathways that are involved in the regulation of blood-brain barrier integrity. PI3K: phosphoinositide 3-kinase; RhoA: ras homolog gene family member A; ROS: reactive oxygen species; ZO: zonnula occluden.

4. Antioxidants, Cognitive Decline and Blood-Brain Barrier

Studies report that oxidative stress is positively associated with impaired cognitive function [39,40]. Consistently, multiple lines of evidence demonstrate beneficial effects of antioxidants on cognition and dementia [8]. As a wealth of recent evidence suggests that BBB dysfunction is associated with the pathogenesis and pathology of neurodegeneration and the associated-cognitive

deficits, the preservation of BBB structure and function may offer an innovative and robust therapeutic opportunity for cerebrovascular disorders. Whilst a number of studies have implicated antioxidant therapy as a therapeutic option against cognitive decline, few studies have considered the positive effects of antioxidants on cognition and dementia through a neurovascular axis. Therefore, in this chapter, we will summarize the available literature that report the effects of antioxidants on BBB integrity and cognition, and consider its use in dementia therapy through a cerebrovascular perspective (refer to Table 1 for summary).

4.1. Anti-Oxidative Vitamins

A number of studies report that diet and nutrients have a strong association to the risk of dementia including AD [41,42]. Vitamin A, C and E are known as potent anti-oxidants. In concert with the substantial involvement of oxidative stress pathways in the pathophysiology of AD, studies found that plasma and cerebrospinal fluid concentrations of Vitamins A and C were significantly lower in patients with AD despite comparable dietary intake to healthy control subjects [43,44]. In a Rotterdam study involving 5395 participants, high intake of dietary Vitamin C and Vitamin E was significantly associated with lowered risk of AD and dementia [45,46]. A prospective population study with 4740 participants revealed that the use of Vitamin C and E supplements for more than 3 years significantly reduced the risk of AD [47]. Furthermore, a randomized control trial by Li et al. showed co-supplementation of Vitamin E and C with β-carotene (another well-established dietary antioxidant) markedly improved cognitive function in otherwise healthy elderly individuals [48]. Consistent with these clinical findings, an animal study reported that acute treatment with Vitamin C attenuates the spatial learning and memory in APP/PSEN1 transgenic AD model mice and also in aged none-AD wild-type mice [49]. However, in the same study, supplementation of Vitamin C did not alter cerebral redox state, inflammation and amyloidosis, indicating that the anti-dementia effects of vitamins may not only be attributed to its anti-oxidative properties. Indeed, Vitamin C has been reported to prevent the oligomerization of Aβ [50]. An oral administration of Vitamin C is also reported to significantly suppress cerebral oxidative damage in cerebral ischemia-reperfusion [51]. In addition, in vivo and in vitro studies report that Vitamin A prevents neurodegeneration, and inhibits the formation of Aβ fibrils, decreasing its aggregation and oligomerization [44,52].

It has been suggested that anti-oxidative vitamins may prevent cognitive decline also by protecting BBB integrity. However, only a few studies have directly investigated the effects of anti-oxidative vitamins on dementia through cerebrovascular axis. A study by Kook et al. recently reported that high dose supplementation of Vitamin C reduced amyloidosis in the cortex and hippocampus of AD mice (5XFAD) via attenuation of BBB disruption and mitochondrial alteration [53]. Vitamin C is reported to prevent the disruption of BBB induced by compression of primary somatosensory cortex by upregulating the expression of tight junction proteins, occludin and claudin-5 [54]. In a model of stroke with substantial BBB disruption, a single injection of Vitamin C significantly reduced BBB permeability [55]. Similarly, in a mouse model of cerebral ischemia, Vitamin C prevented BBB dysfunction by protecting tight junction claudin-5 and attenuated edema and neuronal loss [56]. Moreover, an in vitro study provides supporting data that Vitamin C reversed hyperglycemia-mediated BBB disruption [57]. Similar to Vitamin C, Vitamin E is also reported to prevent BBB breakdown induced by oxidative stress by attenuation of endothelial oxidative stress and via increasing the expression of tight junction proteins in vivo [58]. In rats with convulsion under hyperthermic conditions, Vitamin E showed beneficial effects on modulation of BBB permeability [59]. Consistent with the latter, ingestion of Vitamin E deficient diet in wild-type rats resulted in increased BBB permeability and heightened oxidative stress [60].

Although the underlying mechanisms by which anti-oxidative vitamins protect BBB integrity are largely unknown, these studies collectively suggest that these vitamins may ameliorate neurodegenerative changes and cognitive decline by preserving the function and structure of BBB. More direct experimental and clinical evidence would provide further strength to such hypotheses.

Table 1. Literature summary.

Antioxidants	Condition	Study Type/Model	Neuronal Measure(s)	Blood-Brain Barrier Measure(s)	Others	Reference No.
Vitamin C&E	cerebral ischemia	mouse model	↓ neuronal loss	↑ claudin-5		[54]
	AD	mouse model (5XFAD)	↓ amyloid plaques	↓ BBB dysfunction		[51]
	BBB disruption	mouse model	N/A	↑ occludin, claudin-5		[52]
	stroke	rat model	N/A	↓ BBB dysfunction		[53]
	hyperglycemia	HBMEC	N/A	↓ BBB dysfunction		[55]
Vitamin E	Phospholipid transfer protein deficient	mouse model	N/A	↑ occludin, claudin-5, ZO-1		[56]
	healthy	rats under hyperthermic convulsion	N/A	↓ BBB dysfunction		[57]
	healthy	rats with Vitamin E deficient diet	N/A	↓ BBB dysfunction		[58]
Melatonin	hypobaric hypoxia	rats	↑ cognitive function; ↓ neuronal loss, neuroinflammation	↓ BBB dysfunction		[61]
	inflammation	rat brain microvascular endothelial cells	N/A	↑ ZO-1		[62]
	oxidative stress	bEnd.3 cells	N/A	↑ claudin-5; ↓ cell death		[63]
α-Lipoic acid	high-fat diet	mouse model	↓ neuroinflammation	↓ BBB dysfunction		[64]
	ischemic stroke	rat model	↓ neurological deficit, neuroinflammation	↓ BBB dysfunction		[65]
Aged garlic extract	high-fat diet	mouse model	↓ neuroinflammation	↓ BBB dysfunction		[64]
Apocynin	BBB disruption	rat perfusion model	N/A	↓ BBB dysfunction	improved vascular tone	[66]
	BBB disruption	HBMEC	N/A	↓ BBB dysfunction	↑ AMPK activation	[67]
	BBB disruption	HBMEC	N/A	↑ occludin, claudin-5	↑ AMPK activation	[68]
Baicalein	intracerebral hemorrhage	rat model	↓ neurological deficit	↑ ZO-1		[69]
Caffein	Parkinson's disease	mouse model	N/A	↑ occludin, ZO-1		[70]
	AD	rabbit model	↓ neuroinflammation	↑ occludin, ZO-1		[71]

Table 1. *Cont.*

Antioxidants	Condition	Study Type/Model	Neuronal Measure(s)	Blood-Brain Barrier Measure(s)	Others	Reference No.
Curcumin	subarachnoid hemorrhage	rat model	↓ neurological deficit, neuroinflammation	↓ BBB dysfunction		[72]
	cerebral ischemia	rat model	↓ neurological deficit	↓ BBB dysfunction	↓ infarct volume	[73]
	N/A	BMEC	N/A	↓ platelet recruitment		[74]
Pinocembrin	cerebral ischemia	rat model	↓ neurological deficit	↓ BBB dysfunction	↓ brain edema	[75]
	cerebral ischemia	rat model	↓ neuroinflammation	↑ occludin, ZO-1		[76]
Resveratrol	autoimmune encephalomyelitis	mouse model	↓ neuroinflammation, oxidative stress	↑ occludin, ZO-1, claudin-5; ↓ ICAM-1, VCAM-1		[77]
	BBB disruption	HBMEC	↓ oxidative stress	↓ BBB dysfunction		[78]
	AD	rat model	↓ neuroinflammation, β-amyloid	↑ claudin-5		[79]
	cerebral ischemia	rat model	↓ neuronal loss	↓ BBB dysfunction	↓ brain edema	[80]
	high-fat diet	mouse model	↓ neuronal loss	↑ occludin, ZO-1		[81]
Tanshinone IIA	autoimmune encephalomyelititis	mouse model	↓ neuroinflammation	↑ occludin, claudin-5, ZO-1		[82]
	hypoxia	HBMEC	N/A	↑ ZO-1		[83]
	cerebral ischemia	rat model	N/A	↑ occludin, ZO-1; ↓ ICAM-1	↓ brain edema	[84]
Statin	AD	in vitro BBB model	N/A	↓ BBB dysfunction		[85]
	high-fat diet	mouse model	N/A	↓ BBB dysfunction		[86]
Probucol	high-fat diet	mouse model	↓ neuroinflammation	↓ BBB dysfunction		[87,88]
Fenofibrate	BBB disruption	mouse model	↓ neurodegeneration, neuroinflammation	↓ BBB dysfunction		[89]
	BBB disruption	BMEC	N/A	↓ BBB dysfunction		[90]
Ibuprofen	high-fat diet	mouse model	N/A	↓ BBB dysfunction		[86]

4.2. Other Natural Antioxidants

Melatonin is a neurohormone found in animals, plants and bacteria, reported to exhibit strong anti-oxidative properties through protecting the mitochondrial membrane potential and thereby suppressing the production of superoxides [91,92]. Melatonin is approved by the FDA as a dietary supplement and readily available over the counter, commonly prescribed for treatment of insomnia. Studies report that plasma melatonin levels are significantly decreased in subjects with AD, showing a negative association with cognitive function, and a significant reduction is found even in healthy elderly [93–95]. In a rat model of sporadic AD, melatonin was demonstrated to prevent memory loss by attenuating amyloidosis and neurodegeneration [96]. Furthermore, in aged 22-month old wild-type mice with significantly impaired spatial cognition, melatonin improved cognitive performance by reducing cerebral amyloid burden through altered protein-cleaving secretase expression [97]. In addition, some studies showed that melatonin promotes hippocampal neuroplasticity and stimulates the proliferation and differentiation of neural stem cells in vitro and in vivo [98–100]. A number of studies have also demonstrated protective effects of melatonin on the BBB. A study by Vornicescu et al. demonstrated that melatonin administration prevents oxidative stress-induced breakdown of BBB and improves cognitive function [61]. In this study, a significant reduction in neuronal death and neuroinflammation was also observed in melatonin treated rats. In vitro studies further investigated mechanistic insights into the BBB protective effects of melatonin. A study using rat brain microvascular endothelial cells revealed that BBB disruption induced by inflammation was completely prevented by melatonin treatment via restoration of the expression of BBB tight junction ZO-1 and inhibiting matrix metalloproteinase-9 [62]. Similarly, in a bEnd.3 cell line model of oxidative stress-induced BBB dysfunction, treatment with melatonin prevented cell death and degradation of tight junction proteins by activating Akt and suppressing phosphorylation of JNK [63]. Overall, the data presented strongly suggests that melatonin may exert neuroprotective effects partially, if not entirely, through the protection of BBB from oxidative and inflammatory stressors.

α-Lipoic acid (ALA) is known to chelate transition metals and ROS, thus inhibiting hydroxyl radical formation. A clinical trial involving 43 AD patients over an observation period of 2 years demonstrated that subjects receiving ALA showed constant scores in two neuropsychological tests, while the untreated subjects showed significant decline in cognitive function [101]. Consistent with the latter, in a rat model of vascular dementia, ALA significantly restored cognitive functioning concomitant with markedly reduced ROS and malondialdehyde production and increased reduced glutathione levels in the hippocampal formation, the domain crucial to learning and memory [102]. Increased acetylcholine and choline acetyltransferase levels as well as decreased acetylcholinesterase activity were also observed in the hippocampus of ALA-treated rats. By using a murine model of accelerated ageing, senescence accelerated mouse prone-8, ALA was demonstrated to improve memory and supress oxidative stress during normal ageing [103]. However, few studies to date have directly considered BBB permeability in context of the neuroprotective properties of ALA. Takechi et al. reported in a dietary induced mouse model of BBB dysfunction, ALA preserved the integrity of BBB by inhibiting oxidative stress, which resulted in the prevention of blood-to-brain protein extravasation and significant attenuation of neuroinflammation [64]. Similarly, ALA was reported to ameliorate BBB disruption, neuroinflammation and neurological motor deficits in a rat model of ischemic stroke [65]. Although these studies strongly suggest that ALA may prevent cognitive decline through the protection of BBB, further studies are needed to directly investigate such association.

Another emerging potentially neuroprotective antioxidant is garlic. An extract of garlic contains a mixture of biologically active compounds such as S-allylcysteine (SAC) and S-allylmercaptocysteine, which are known to exert strong anti-oxidative effects. These compounds have repeatedly been shown to provide antioxidant action by scavenging ROS, enhancing SOD, catalase glutathione peroxidase, and increasing glutathione. A number of studies demonstrated the neuroprotective effects of garlic [104]. Although clinical evidence is limited, Chauhan et al. elegantly demonstrated the beneficial effects of garlic extracts in AD models [105]. In a study using Alzheimer's Tg2576 mice

supplemented with either aged garlic extract (AGE), SAC, or di-allyl-disulphide (DADS) for 4 months, mice treated with AGE as well as mice treated with SAC or DADS showed substantially lower cerebral amyloidosis compared to untreated mice [106]. Similarly, AGE, SAD and DADS significantly attenuated neuroinflammation and tau protein. The extent of the neuroprotective effects reported were ranked from AGE > SAC > DADS. Furthermore, a study using TgCRND8 AD model mice revealed that the provision of AGE improved hippocampal-dependent cognition and memory [107]. Additionally, in a study by Takechi et al., the cerebrovascular-protective effects of AGE via its anti-oxidative properties were demonstrated in a mouse model of BBB dysfunction, which coincided with significant attenuation of neuroinflammation [64]. In vitro and in vivo studies confirmed that the pleiotropic effects of garlic extracts may be attributed to its anti-oxidative action on neurons, including sympathetic neurons, preventing ROS-mediated oxidative insults [108]. The studies also revealed that SAC was the most potent neuroprotective compound in AGE [108]. The data collectively suggests that AGE, or its anti-oxidative components, may exert neuroprotective effects through various pathways including direct anti-oxidative protection of neuronal cells as well as the preservation of BBB integrity.

There are other natural antioxidants that are recently reported to exhibit potent BBB protective effects. These include apocynin [66–68], baicalein [69], caffeine [70,71,109], curcumin [72–74], niacin [64], nicotine [64], pinocembrin [75,76,110], resveratrol [77–81,111], polyphenols [112], and tanshinone IIA [82–84]. However, the number of studies investigating the effects of these agents on neurodegeneration and cognitive performance is limited. Further investigations to support the use of these agents for dementia prevention by focussing on the neurovascular integrity need to be conducted.

4.3. Lipid-Lowering Drugs with Anti-Oxidative Properties

Many clinical drugs for treatment of cardiovascular disease exert antioxidant effects. Statins, 3-hydroxy-3-methylglutaryl coenzyme A reductase inhibitors, are reported to show anti-oxidative properties by inhibiting the increase of 8-isoprostane and suppressing the activity of nitric oxide synthase [113,114]. While its effects on dementia are still controversial [115–117], case control and retrospective population studies indicate that statins significantly reduce the risk of dementia and cognitive impairment [118]. A 7-year follow-up study, the Rotterdam Study, revealed that statin users have a 43% lower incidence of AD [119]. A number of putative underlying mechanisms for statin's neuroprotective effects are suggested [120]. Studies in humans and animal models showed that statins attenuate cerebral amyloidosis in AD [121,122]. Other studies showed that cerebral oxidative stress and the production of pro-inflammatory cytokines were reduced by atorvastatin in animal models of AD [123,124]. An emerging body of recent studies also suggests statins' therapeutic potential for AD via protection of the neurovascular unit [125]. In a transgenic mouse model of AD, atorvastatin and pitavastatin improved memory and reduced amyloidosis and neuroinflammation by modulating the permeability of BBB. Similarly, simvastatin was shown to protect BBB integrity and attenuate neuropathophysiology and oxidative stress in APP transgenic AD mice [126]. In line with the latter, an in vitro study using human cerebral microvascular endothelial cells showed that simvastatin and lovastatin attenuated Aβ-induced BBB dysfunction [85]. Moreover, in a mouse model of dietary- induced BBB dysfunction, we demonstrated that atorvastatin and pravastatin reversed the disruption of BBB integrity [86]. Interestingly, all studies indicated here reported the BBB protective effects of statins independent of their lipid-lowering effects but rather occurred concomitant with attenuated oxidative stress, suggesting its cerebrovascular protective action through anti-oxidative pathways.

Probucol is a conventional cholesterol-lowering drug that possesses potent anti-oxidative properties, which attribute to attenuation of ROS by inhibiting the expression of Nox2 [127], and by increasing glutathione peroxidase activity [128]. A limited number of clinical trials report that probucol stabilizes cognitive function in AD [129]. Consistent with this notion, a study reported in a mouse model of cognitive and hippocampal synaptic impairment induced by an intracerebroventricular

injection of aggregated $A\beta_{1-40}$, probucol prevented hippocampal lipid peroxidation and attenuated loss of hippocampal-dependent learning and memory [130]. Similarly, in a mouse model of streptozotocin-induced cognitive impairment, probucol improved cognitive function by attenuating hippocampal oxidative stress [131]. Consistent with the hypothesis, studies in our laboratory reported that probucol prevented the disruption of BBB and neuroinflammation induced by an ingestion of a high-fat diet in mice [87,88]. These studies also revealed that the BBB protective effects of probucol was through its anti-oxidative effects by attenuating cerebral oxidative stress and neurovascular inflammation. A study by Russell et al. further supports this data by showing improved vascular endothelial function in a model of atherosclerosis by administration of probucol, independent of its cholesterol-lowering effects [132].

Fenofibrate is another lipid-lowering drug reported to lower cholesterol and triglycerides and increase HDL-cholesterol [133]. Besides its anti-atherosclerotic effects, fenofibrate is reported to exert anti-oxidative effects by reducing lipid peroxidation and increasing antioxidants including glutathione, in a rat model of Parkinson's disease [134]. Interestingly, in the same study by Uppalapati et al., fenofibrate attenuated neurodegeneration and improved cognitive function in a dose-dependent manner [134]. Consistently, in a brain irradiation-induced mouse model of cognitive impairment, fenofibrate significantly improved cognitive performance [135]. However, the clinical evidence of fenofibrate on cognitive function and dementia is limited [136]. In a murine model of BBB dysfunction induced by HIV Tat protein, Huang et al. demonstrated that fenofibrate attenuated BBB permeability, neuroinflammation and neurodegeneration [89]. Moreover, an in vitro study using mouse cerebral capillary endothelial cells showed that fenofibric acid (an active metabolite of fenofibrate) protected BBB integrity from oxygen-glucose deprivation-induced BBB hyper-permeability [90]. However, no studies to date have considered the neuroprotective effects of fenofibrate through modulation of BBB-specific pathways.

These studies suggest that the lipid-lowering pharmacological agents with anti-oxidative properties exert positive effects on neurodegeneration and cognitive deficits, at least in part, through protective mechanisms via the BBB. Further studies to identify more detailed molecular and cellular mechanisms to strengthen this evidence are required.

4.4. Other Pharmacological Agents with Anti-Oxidative Effects

There are several other pharmacological agents with anti-oxidative properties exerting vascular protective effects, and some are demonstrated to be beneficial for BBB. Ibuprofen is a widely utilized nonsteroidal anti-inflammatory drug (NSAID) reported to non-selectively attenuate the activity of cyclooxygenase and is reported to exert substantial oxidative effects [137]. A number of epidemiological and clinical studies reported that the use of ibuprofen and other NSAIDs delayed the onset and progression of AD [138,139]. Although the mechanisms by which NSAIDs reduce the risk of AD are yet to be elucidated, both in vivo and in vitro studies showed that NSAIDs including ibuprofen, flurbiprofen, indomethacin and sulindac, significantly attenuated the cerebral production and accumulation of Aβ [140] and suppressed neuroinflammation [141]. Combination therapy of ibuprofen with lipoic acid was also reported to show neuroprotective effects in a rat model of AD [142]. A recent study revealed significant alterations in protein and phosphoprotein expression including heat shock protein 8, dihydropyrimidinase-related protein 2 and γ-enolase, within the hippocampal formation [143]. In addition, a recent study reported that ibuprofen prevents the decrease of N-acetylaspartate and atrophy of hippocampal formation in a transgenic mouse model of AD via MRI neuroimaging and spectroscopy analysis [144]. However, none of these studies considered the effect of ibuprofen on cerebrovascular integrity. To our best knowledge, the only study demonstrating BBB modulating effects of ibuprofen is that by Pallebage-Gamarallage et al. [86]. The study reported novel findings in which ibuprofen treatment for 1 or 3 months can restore the compromised BBB integrity in a high fat-induced BBB dysfunction mouse model. Clearly, further investigation is necessary to elucidate the BBB protective role of ibuprofen in cognition and dementia.

5. Conclusions

Previous studies suggest that natural and chemical compounds with anti-oxidative properties have beneficial effects on neuroprotection and cognitive performance, although the underlying mechanisms are largely unknown. As summarized in the current review, clinical evidence suggests the therapeutic effects of antioxidants on dementia and cognitive impairment and findings from animal and in vitro studies support this evidence. Furthermore, a substantial body of evidence from animal and in vitro studies suggests that such neuroprotective effects of antioxidants may be entirely or partially attributed to the BBB protective effects of antioxidants. However, the number of studies directly considering the therapeutic effects of antioxidants on cognitive impairment through the axis of cerebrovascular BBB integrity remain limited. Further investigations should focus on simultaneously testing the neuroprotective effects as well as the BBB protective effects of antioxidants. Furthermore, the elucidation of such mechanisms may lead to the development and search for new agents to specifically target the protection of BBB, conferring neuroprotection.

Acknowledgments: The project was supported by National Heal and Medical Research Council of Australia and Alzheimer's Australia Dementia Research Foundation. R.T. is supported by Curtin Research Fellowship.

Author Contributions: The manuscript was designed and written by Virginie Lam, Mark Hackett and Ryusuke Takechi. All authors have read and approved the final manuscript.

Conflicts of Interest: The authors declare no conflicts of interest.

References

1. Organization, W.H. *Dementia a Public Health Priority*; World Health Organization: Geneva, Switzerland, 2012.
2. Wimo, A.; Guerchet, M.; Ali, G.C.; Wu, Y.T.; Prina, A.M.; Winblad, B.; Jonsson, L.; Liu, Z.; Prince, M. The worldwide costs of dementia 2015 and comparisons with 2010. *Alzheimers Dement.* **2016**. [CrossRef] [PubMed]
3. Goodman, R.A.; Lochner, K.A.; Thambisetty, M.; Wingo, T.S.; Posner, S.F.; Ling, S.M. Prevalence of dementia subtypes in US Medicare fee-for-service beneficiaries, 2011–2013. *Alzheimers Dement.* **2016**. [CrossRef] [PubMed]
4. Zlokovic, B.V. Neurovascular pathways to neurodegeneration in Alzheimer's disease and other disorders. *Nat. Rev. Neurosci.* **2011**, *12*, 723–738. [CrossRef] [PubMed]
5. Palmer, A.M. The blood-brain barrier. *Neurobiol. Dis.* **2010**, *37*, 1–2. [CrossRef] [PubMed]
6. Feng, Y.; Wang, X. Antioxidant therapies for Alzheimer's disease. *Oxid. Med. Cell. Longev.* **2012**, *2012*, 472932. [CrossRef] [PubMed]
7. Santos, M.A.; Chand, K.; Chaves, S. Recent progress in repositioning Alzheimer's disease drugs based on a multitarget strategy. *Future Med. Chem.* **2016**, *8*, 2113–2142. [CrossRef] [PubMed]
8. Farah, R.; Gilbey, P.; Asli, H.; Khamisy-Farah, R.; Assy, N. Antioxidant enzyme activity and cognition in obese individuals with or without metabolic risk factors. *Exp. Clin. Endocrinol. Diabetes* **2016**, *124*, 568–571. [PubMed]
9. Takechi, R.; Galloway, S.; Pallebage-Gamarallage, M.M.; Lam, V.; Mamo, J.C. Dietary fats, cerebrovasculature integrity and Alzheimer's disease risk. *Prog. Lipid Res.* **2010**, *49*, 159–170. [CrossRef] [PubMed]
10. Takechi, R.; Galloway, S.; Pallebage-Gamarallage, M.M.; Wellington, C.L.; Johnsen, R.D.; Dhaliwal, S.S.; Mamo, J.C. Differential effects of dietary fatty acids on the cerebral distribution of plasma-derived apo B lipoproteins with amyloid-β. *Br. J. Nutr.* **2010**, *103*, 652–662. [CrossRef] [PubMed]
11. Kalaria, R.N. Vascular basis for brain degeneration: Faltering controls and risk factors for dementia. *Nutr. Rev.* **2010**, *68* (Suppl. 2), S74–S87. [CrossRef] [PubMed]
12. Calabrese, V.; Giordano, J.; Signorile, A.; Laura Ontario, M.; Castorina, S.; De Pasquale, C.; Eckert, G.; Calabrese, E.J. Major pathogenic mechanisms in vascular dementia: Roles of cellular stress response and hormesis in neuroprotection. *J. Neurosci. Res.* **2016**, *94*, 1588–1603. [CrossRef] [PubMed]
13. Calsolaro, V.; Edison, P. Neuroinflammation in Alzheimer's disease: Current evidence and future directions. *Alzheimers Dement.* **2016**, *12*, 719–732. [CrossRef] [PubMed]

14. Cai, Z.; Hussain, M.D.; Yan, L.J. Microglia, neuroinflammation, and beta-amyloid protein in Alzheimer's disease. *Int. J. Neurosci.* **2014**, *124*, 307–321. [CrossRef] [PubMed]
15. Soejitno, A.; Tjan, A.; Purwata, T.E. Alzheimer's disease: Lessons learned from amyloidocentric clinical trials. *CNS Drugs* **2015**, *29*, 487–502. [CrossRef] [PubMed]
16. Takechi, R.; Galloway, S.; Pallebage-Gamarallage, M.M.; Mamo, J.C. Chylomicron amyloid-beta in the aetiology of Alzheimer's disease. *Atheroscler. Suppl.* **2008**, *9*, 19–25. [CrossRef] [PubMed]
17. Cummings, J.L.; Vinters, H.V.; Cole, G.M.; Khachaturian, Z.S. Alzheimer's disease: Etiologies, pathophysiology, cognitive reserve, and treatment opportunities. *Neurology* **1998**, *51*, S2–S17. [CrossRef] [PubMed]
18. Deane, R.; Du Yan, S.; Submamaryan, R.K.; LaRue, B.; Jovanovic, S.; Hogg, E.; Welch, D.; Manness, L.; Lin, C.; Yu, J.; et al. Rage mediates amyloid-β peptide transport across the blood-brain barrier and accumulation in brain. *Nat. Med.* **2003**, *9*, 907–913. [CrossRef] [PubMed]
19. Candela, P.; Gosselet, F.; Saint-Pol, J.; Sevin, E.; Boucau, M.C.; Boulanger, E.; Cecchelli, R.; Fenart, L. Apical-to-basolateral transport of amyloid-β peptides through blood-brain barrier cells is mediated by the receptor for advanced glycation end-products and is restricted by P-glycoprotein. *J. Alzheimers Dis.* **2010**, *22*, 849–859. [PubMed]
20. Hultman, K.; Strickland, S.; Norris, E.H. The apoe ε4/ε4 genotype potentiates vascular fibrin(ogen) deposition in amyloid-laden vessels in the brains of Alzheimer's disease patients. *J. Cereb. Blood Flow Metab.* **2013**, *33*, 1251–1258. [CrossRef] [PubMed]
21. Halliday, M.R.; Rege, S.V.; Ma, Q.; Zhao, Z.; Miller, C.A.; Winkler, E.A.; Zlokovic, B.V. Accelerated pericyte degeneration and blood-brain barrier breakdown in apolipoprotein E4 carriers with Alzheimer's disease. *J. Cereb. Blood Flow Metab.* **2016**, *36*, 216–227. [CrossRef] [PubMed]
22. Bowman, G.L.; Kaye, J.A.; Quinn, J.F. Dyslipidemia and blood-brain barrier integrity in Alzheimer's disease. *Curr. Gerontol. Geriatr. Res.* **2012**, *2012*, 184042. [CrossRef] [PubMed]
23. Montagne, A.; Barnes, S.R.; Sweeney, M.D.; Halliday, M.R.; Sagare, A.P.; Zhao, Z.; Toga, A.W.; Jacobs, R.E.; Liu, C.Y.; Amezcua, L.; et al. Blood-brain barrier breakdown in the aging human hippocampus. *Neuron* **2015**, *85*, 296–302. [CrossRef] [PubMed]
24. Takechi, R.; Galloway, S.; Pallebage-Gamarallage, M.; Wellington, C.; Johnsen, R.; Mamo, J.C. Three-dimensional colocalization analysis of plasma-derived apolipoprotein B with amyloid plaques in APP/PS_1 transgenic mice. *Histochem. Cell Biol.* **2009**, *131*, 661–666. [CrossRef] [PubMed]
25. Erickson, M.A.; Banks, W.A. Blood-brain barrier dysfunction as a cause and consequence of Alzheimer's disease. *J. Cereb. Blood Flow Metab.* **2013**, *33*, 1500–1513. [CrossRef] [PubMed]
26. Montagne, A.; Nation, D.A.; Pa, J.; Sweeney, M.D.; Toga, A.W.; Zlokovic, B.V. Brain imaging of neurovascular dysfunction in Alzheimer's disease. *Acta Neuropathol.* **2016**, *131*, 687–707. [CrossRef] [PubMed]
27. Van de Haar, H.J.; Burgmans, S.; Jansen, J.F.; van Osch, M.J.; van Buchem, M.A.; Muller, M.; Hofman, P.A.; Verhey, F.R.; Backes, W.H. Blood-brain barrier leakage in patients with early Alzheimer disease. *Radiology* **2016**, *281*, 521–535. [CrossRef] [PubMed]
28. Ujiie, M.; Dickstein, D.L.; Carlow, D.A.; Jefferies, W.A. Blood-brain barrier permeability precedes senile plaque formation in an Alzheimer disease model. *Microcirculation* **2003**, *10*, 463–470. [PubMed]
29. Pun, P.B.; Lu, J.; Moochhala, S. Involvement of ROS in BBB dysfunction. *Free Radic. Res.* **2009**, *43*, 348–364. [CrossRef] [PubMed]
30. Lochhead, J.J.; McCaffrey, G.; Quigley, C.E.; Finch, J.; DeMarco, K.M.; Nametz, N.; Davis, T.P. Oxidative stress increases blood-brain barrier permeability and induces alterations in occludin during hypoxia-reoxygenation. *J. Cereb. Blood Flow Metab.* **2010**, *30*, 1625–1636. [CrossRef] [PubMed]
31. Toklu, H.Z.; Tumer, N. Oxidative stress, brain edema, blood-brain barrier permeability, and autonomic dysfunction from traumatic brain injury. In *Brain Neurotrauma: Molecular, Neuropsychological, and Rehabilitation Aspects*; Kobeissy, F.H., Ed.; CRC Press: Boca Raton, FL, USA, 2015.
32. Ronaldson, P.T.; Davis, T.P. Targeting transporters: Promoting blood-brain barrier repair in response to oxidative stress injury. *Brain Res.* **2015**, *1623*, 39–52. [CrossRef] [PubMed]
33. Chrissobolis, S.; Faraci, F.M. The role of oxidative stress and nadph oxidase in cerebrovascular disease. *Trends Mol. Med.* **2008**, *14*, 495–502. [CrossRef] [PubMed]

34. VanGilder, R.L.; Kelly, K.A.; Chua, M.D.; Ptachcinski, R.L.; Huber, J.D. Administration of sesamol improved blood-brain barrier function in streptozotocin-induced diabetic rats. *Exp. Brain Res.* **2009**, *197*, 23–34. [CrossRef] [PubMed]
35. Schreibelt, G.; Musters, R.J.; Reijerkerk, A.; de Groot, L.R.; van der Pol, S.M.; Hendrikx, E.M.; Dopp, E.D.; Dijkstra, C.D.; Drukarch, B.; de Vries, H.E. Lipoic acid affects cellular migration into the central nervous system and stabilizes blood-brain barrier integrity. *J. Immunol.* **2006**, *177*, 2630–2637. [CrossRef] [PubMed]
36. Haorah, J.; Ramirez, S.H.; Schall, K.; Smith, D.; Pandya, R.; Persidsky, Y. Oxidative stress activates protein tyrosine kinase and matrix metalloproteinases leading to blood-brain barrier dysfunction. *J. Neurochem.* **2007**, *101*, 566–576. [CrossRef] [PubMed]
37. Schreibelt, G.; Kooij, G.; Reijerkerk, A.; van Doorn, R.; Gringhuis, S.I.; van der Pol, S.; Weksler, B.B.; Romero, I.A.; Couraud, P.O.; Piontek, J.; et al. Reactive oxygen species alter brain endothelial tight junction dynamics via RhoA, PI_3 kinase, and PKB signaling. *FASEB J.* **2007**, *21*, 3666–3676. [CrossRef] [PubMed]
38. Shiu, C.; Barbier, E.; Di Cello, F.; Choi, H.J.; Stins, M. HIV-1 gp120 as well as alcohol affect blood-brain barrier permeability and stress fiber formation: Involvement of reactive oxygen species. *Alcohol. Clin. Exp. Res.* **2007**, *31*, 130–137. [CrossRef] [PubMed]
39. Smith, M.A.; Perry, G.; Richey, P.L.; Sayre, L.M.; Anderson, V.E.; Beal, M.F.; Kowall, N. Oxidative damage in Alzheimer's. *Nature* **1996**, *382*, 120–121. [CrossRef] [PubMed]
40. Lovell, M.A.; Markesbery, W.R. Oxidative damage in mild cognitive impairment and early Alzheimer's disease. *J. Neurosci. Res.* **2007**, *85*, 3036–3040. [CrossRef] [PubMed]
41. Pistollato, F.; Sumalla Cano, S.; Elio, I.; Masias Vergara, M.; Giampieri, F.; Battino, M. Associations between sleep, cortisol regulation, and diet: Possible implications for the risk of Alzheimer disease. *Adv. Nutr.* **2016**, *7*, 679–689. [CrossRef] [PubMed]
42. Pistollato, F.; Sumalla Cano, S.; Elio, I.; Masias Vergara, M.; Giampieri, F.; Battino, M. Role of gut microbiota and nutrients in amyloid formation and pathogenesis of Alzheimer disease. *Nutr. Rev.* **2016**, *74*, 624–634. [CrossRef] [PubMed]
43. Riviere, S.; Birlouez-Aragon, I.; Nourhashemi, F.; Vellas, B. Low plasma Vitamin C in Alzheimer patients despite an adequate diet. *Int. J. Geriatr. Psychiatry* **1998**, *13*, 749–754. [CrossRef]
44. Bourdel-Marchasson, I.; Delmas-Beauvieux, M.C.; Peuchant, E.; Richard-Harston, S.; Decamps, A.; Reignier, B.; Emeriau, J.P.; Rainfray, M. Antioxidant defences and oxidative stress markers in erythrocytes and plasma from normally nourished elderly Alzheimer patients. *Age Ageing* **2001**, *30*, 235–241. [CrossRef] [PubMed]
45. Engelhart, M.J.; Geerlings, M.I.; Ruitenberg, A.; van Swieten, J.C.; Hofman, A.; Witteman, J.C.; Breteler, M.M. Dietary intake of antioxidants and risk of Alzheimer disease. *JAMA* **2002**, *287*, 3223–3229. [CrossRef] [PubMed]
46. Devore, E.E.; Grodstein, F.; van Rooij, F.J.; Hofman, A.; Stampfer, M.J.; Witteman, J.C.; Breteler, M.M. Dietary antioxidants and long-term risk of dementia. *Arch. Neurol.* **2010**, *67*, 819–825. [CrossRef] [PubMed]
47. Zandi, P.P.; Anthony, J.C.; Khachaturian, A.S.; Stone, S.V.; Gustafson, D.; Tschanz, J.T.; Norton, M.C.; Welsh-Bohmer, K.A.; Breitner, J.C.; Cache County Study, G. Reduced risk of Alzheimer disease in users of antioxidant vitamin supplements: The cache county study. *Arch. Neurol.* **2004**, *61*, 82–88. [CrossRef] [PubMed]
48. Li, Y.; Liu, S.; Man, Y.; Li, N.; Zhou, Y.U. Effects of vitamins E and C combined with β-carotene on cognitive function in the elderly. *Exp. Ther. Med.* **2015**, *9*, 1489–1493. [PubMed]
49. Harrison, F.E.; Hosseini, A.H.; McDonald, M.P.; May, J.M. Vitamin C reduces spatial learning deficits in middle-aged and very old APP/PSEN1 transgenic and wild-type mice. *Pharmacol. Biochem. Behav.* **2009**, *93*, 443–450. [CrossRef] [PubMed]
50. Montilla-Lopez, P.; Munoz-Agueda, M.C.; Feijoo Lopez, M.; Munoz-Castaneda, J.R.; Bujalance-Arenas, I.; Tunez-Finana, I. Comparison of melatonin versus Vitamin C on oxidative stress and antioxidant enzyme activity in Alzheimer's disease induced by okadaic acid in neuroblastoma cells. *Eur. J. Pharmacol.* **2002**, *451*, 237–243. [CrossRef]
51. Mukherjee, A.; Sarkar, S.; Swarnakar, S.; Das, N. Nanocapsulated ascorbic acid in combating cerebral ischemia reperfusion-induced oxidative injury in rat brain. *Curr. Alzheimer Res.* **2016**, *13*, 1363–1373.
52. Takasaki, J.; Ono, K.; Yoshiike, Y.; Hirohata, M.; Ikeda, T.; Morinaga, A.; Takashima, A.; Yamada, M. Vitamin A has anti-oligomerization effects on amyloid-β in vitro. *J. Alzheimers Dis.* **2011**, *27*, 271–280. [PubMed]

53. Kook, S.Y.; Lee, K.M.; Kim, Y.; Cha, M.Y.; Kang, S.; Baik, S.H.; Lee, H.; Park, R.; Mook-Jung, I. High-dose of Vitamin C supplementation reduces amyloid plaque burden and ameliorates pathological changes in the brain of 5XFAD mice. *Cell Death Dis.* **2014**, *5*, e1083. [CrossRef] [PubMed]
54. Lin, J.L.; Huang, Y.H.; Shen, Y.C.; Huang, H.C.; Liu, P.H. Ascorbic acid prevents blood-brain barrier disruption and sensory deficit caused by sustained compression of primary somatosensory cortex. *J. Cereb. Blood Flow Metab.* **2010**, *30*, 1121–1136. [CrossRef] [PubMed]
55. Allahtavakoli, M.; Amin, F.; Esmaeeli-Nadimi, A.; Shamsizadeh, A.; Kazemi-Arababadi, M.; Kennedy, D. Ascorbic acid reduces the adverse effects of delayed administration of tissue plasminogen activator in a rat stroke model. *Basic Clin. Pharmacol. Toxicol.* **2015**, *117*, 335–339. [CrossRef] [PubMed]
56. Song, J.; Park, J.; Kim, J.H.; Choi, J.Y.; Kim, J.Y.; Lee, K.M.; Lee, J.E. Dehydroascorbic acid attenuates ischemic brain edema and neurotoxicity in cerebral ischemia: An in vivo study. *Exp. Neurobiol.* **2015**, *24*, 41–54. [CrossRef] [PubMed]
57. Allen, C.L.; Bayraktutan, U. Antioxidants attenuate hyperglycaemia-mediated brain endothelial cell dysfunction and blood-brain barrier hyperpermeability. *Diabetes Obes. Metab.* **2009**, *11*, 480–490. [CrossRef] [PubMed]
58. Zhou, T.; He, Q.; Tong, Y.; Zhan, R.; Xu, F.; Fan, D.; Guo, X.; Han, H.; Qin, S.; Chui, D. Phospholipid transfer protein (PLTP) deficiency impaired blood-brain barrier integrity by increasing cerebrovascular oxidative stress. *Biochem. Biophys. Res. Commun.* **2014**, *445*, 352–356. [CrossRef] [PubMed]
59. Oztas, B.; Akgul, S.; Seker, F.B. Gender difference in the influence of antioxidants on the blood-brain barrier permeability during pentylenetetrazol-induced seizures in hyperthermic rat pups. *Biol. Trace Element Res.* **2007**, *118*, 77–83. [CrossRef] [PubMed]
60. Mohammed, H.O.; Starkey, S.R.; Stipetic, K.; Divers, T.J.; Summers, B.A.; de Lahunta, A. The role of dietary antioxidant insufficiency on the permeability of the blood-brain barrier. *J. Neuropathol. Exp. Neurol.* **2008**, *67*, 1187–1193. [CrossRef] [PubMed]
61. Vornicescu, C.; Bosca, B.; Crisan, D.; Yacoob, S.; Stan, N.; Filip, A.; Sovrea, A. Neuroprotective effect of melatonin in experimentally induced hypobaric hypoxia. *Rom. J. Morphol. Embryol.* **2013**, *54*, 1097–1106. [PubMed]
62. Alluri, H.; Wilson, R.L.; Anasooya Shaji, C.; Wiggins-Dohlvik, K.; Patel, S.; Liu, Y.; Peng, X.; Beeram, M.R.; Davis, M.L.; Huang, J.H.; et al. Melatonin preserves blood-brain barrier integrity and permeability via matrix metalloproteinase-9 inhibition. *PLoS ONE* **2016**, *11*, e0154427. [CrossRef] [PubMed]
63. Song, J.; Kang, S.M.; Lee, W.T.; Park, K.A.; Lee, K.M.; Lee, J.E. The beneficial effect of melatonin in brain endothelial cells against oxygen-glucose deprivation followed by reperfusion-induced injury. *Oxid. Med. Cell. Longev.* **2014**, *2014*, 639531. [CrossRef] [PubMed]
64. Takechi, R.; Pallebage-Gamarallage, M.M.; Lam, V.; Giles, C.; Mamo, J.C. Nutraceutical agents with anti-inflammatory properties prevent dietary saturated-fat induced disturbances in blood-brain barrier function in wild-type mice. *J. Neuroinflamm.* **2013**, *10*, 73. [CrossRef] [PubMed]
65. Wu, M.H.; Huang, C.C.; Chio, C.C.; Tsai, K.J.; Chang, C.P.; Lin, N.K.; Lin, M.T. Inhibition of peripheral TNF-α and downregulation of microglial activation by alpha-lipoic acid and etanercept protect rat brain against ischemic stroke. *Mol. Neurobiol.* **2016**, *53*, 4961–4971. [CrossRef] [PubMed]
66. Schreurs, M.P.; Cipolla, M.J. Cerebrovascular dysfunction and blood-brain barrier permeability induced by oxidized LDL are prevented by apocynin and magnesium sulfate in female rats. *J. Cardiovasc. Pharmacol.* **2014**, *63*, 33–39. [CrossRef] [PubMed]
67. Yu, H.Y.; Cai, Y.B.; Liu, Z. Activation of AMPK improves lipopolysaccharide-induced dysfunction of the blood-brain barrier in mice. *Brain Inj.* **2015**, *29*, 777–784. [CrossRef] [PubMed]
68. Zhao, Z.; Hu, J.; Gao, X.; Liang, H.; Liu, Z. Activation of AMPK attenuates lipopolysaccharide-impaired integrity and function of blood-brain barrier in human brain microvascular endothelial cells. *Exp. Mol. Pathol.* **2014**, *97*, 386–392. [CrossRef] [PubMed]
69. Chen, M.; Lai, L.; Li, X.; Zhang, X.; He, X.; Liu, W.; Li, R.; Ke, X.; Fu, C.; Huang, Z.; et al. Baicalein attenuates neurological deficits and preserves blood-brain barrier integrity in a rat model of intracerebral hemorrhage. *Neurochem. Res.* **2016**, *41*, 3095–3102. [CrossRef] [PubMed]
70. Chen, X.; Lan, X.; Roche, I.; Liu, R.; Geiger, J.D. Caffeine protects against MPTP-induced blood-brain barrier dysfunction in mouse striatum. *J. Neurochem.* **2008**, *107*, 1147–1157. [CrossRef] [PubMed]

71. Chen, X.; Gawryluk, J.W.; Wagener, J.F.; Ghribi, O.; Geiger, J.D. Caffeine blocks disruption of blood brain barrier in a rabbit model of Alzheimer's disease. *J. Neuroinflamm.* **2008**, *5*, 12. [CrossRef] [PubMed]
72. Zhang, Z.Y.; Jiang, M.; Fang, J.; Yang, M.F.; Zhang, S.; Yin, Y.X.; Li, D.W.; Mao, L.L.; Fu, X.Y.; Hou, Y.J.; et al. Enhanced therapeutic potential of nano-curcumin against subarachnoid hemorrhage-induced blood-brain barrier disruption through inhibition of inflammatory response and oxidative stress. *Mol. Neurobiol.* **2015**. [CrossRef] [PubMed]
73. Jiang, J.; Wang, W.; Sun, Y.J.; Hu, M.; Li, F.; Zhu, D.Y. Neuroprotective effect of curcumin on focal cerebral ischemic rats by preventing blood-brain barrier damage. *Eur. J. Pharmacol.* **2007**, *561*, 54–62. [CrossRef] [PubMed]
74. Zhang, L.; Gu, Z.L.; Qin, Z.H.; Liang, Z.Q. Effect of curcumin on the adhesion of platelets to brain microvascular endothelial cells in vitro. *Acta Pharmacol. Sin.* **2008**, *29*, 800–807. [CrossRef] [PubMed]
75. Meng, F.; Liu, R.; Gao, M.; Wang, Y.; Yu, X.; Xuan, Z.; Sun, J.; Yang, F.; Wu, C.; Du, G. Pinocembrin attenuates blood-brain barrier injury induced by global cerebral ischemia-reperfusion in rats. *Brain Res.* **2011**, *1391*, 93–101. [CrossRef] [PubMed]
76. Gao, M.; Zhu, S.Y.; Tan, C.B.; Xu, B.; Zhang, W.C.; Du, G.H. Pinocembrin protects the neurovascular unit by reducing inflammation and extracellular proteolysis in MCAO rats. *J. Asian Nat. Prod. Res.* **2010**, *12*, 407–418. [CrossRef] [PubMed]
77. Wang, D.; Li, S.P.; Fu, J.S.; Zhang, S.; Bai, L.; Guo, L. Resveratrol defends blood-brain barrier integrity in experimental autoimmune encephalomyelitis mice. *J. Neurophysiol.* **2016**, *116*, 2173–2179. [CrossRef] [PubMed]
78. Hu, M.; Liu, B. Resveratrol attenuates lipopolysaccharide-induced dysfunction of blood-brain barrier in endothelial cells via AMPK activation. *Korean J. Physiol. Pharmacol.* **2016**, *20*, 325–332. [CrossRef] [PubMed]
79. Zhao, H.F.; Li, N.; Wang, Q.; Cheng, X.J.; Li, X.M.; Liu, T.T. Resveratrol decreases the insoluble Aβ1–42 level in hippocampus and protects the integrity of the blood-brain barrier in AD rats. *Neuroscience* **2015**, *310*, 641–649. [CrossRef] [PubMed]
80. Wei, H.; Wang, S.; Zhen, L.; Yang, Q.; Wu, Z.; Lei, X.; Lv, J.; Xiong, L.; Xue, R. Resveratrol attenuates the blood-brain barrier dysfunction by regulation of the MMP-9/TIMP-1 balance after cerebral ischemia reperfusion in rats. *J. Mol. Neurosci.* **2015**, *55*, 872–879. [CrossRef] [PubMed]
81. Chang, H.C.; Tai, Y.T.; Cherng, Y.G.; Lin, J.W.; Liu, S.H.; Chen, T.L.; Chen, R.M. Resveratrol attenuates high-fat diet-induced disruption of the blood-brain barrier and protects brain neurons from apoptotic insults. *J. Agric. Food Chem.* **2014**, *62*, 3466–3475. [CrossRef] [PubMed]
82. Yang, X.; Yan, J.; Feng, J. Treatment with tanshinone IIA suppresses disruption of the blood-brain barrier and reduces expression of adhesion molecules and chemokines in experimental autoimmune encephalomyelitis. *Eur. J. Pharmacol.* **2016**, *771*, 18–28. [CrossRef] [PubMed]
83. Zhang, W.J.; Feng, J.; Zhou, R.; Ye, L.Y.; Liu, H.L.; Peng, L.; Lou, J.N.; Li, C.H. Tanshinone IIA protects the human blood-brain barrier model from leukocyte-associated hypoxia-reoxygenation injury. *Eur. J. Pharmacol.* **2010**, *648*, 146–152. [CrossRef] [PubMed]
84. Tang, C.; Xue, H.; Bai, C.; Fu, R.; Wu, A. The effects of tanshinone IIA on blood-brain barrier and brain edema after transient middle cerebral artery occlusion in rats. *Phytomed. Int. J. Phytother. Phytopharmacol.* **2010**, *17*, 1145–1149. [CrossRef] [PubMed]
85. Griffin, J.M.; Kho, D.; Graham, E.S.; Nicholson, L.F.; O'Carroll, S.J. Statins inhibit fibrillary β-amyloid induced inflammation in a model of the human blood brain barrier. *PLoS ONE* **2016**, *11*, e0157483. [CrossRef] [PubMed]
86. Pallebage-Gamarallage, M.; Lam, V.; Takechi, R.; Galloway, S.; Clark, K.; Mamo, J. Restoration of dietary-fat induced blood-brain barrier dysfunction by anti-inflammatory lipid-modulating agents. *Lipids Health Dis.* **2012**, *11*, 117. [CrossRef] [PubMed]
87. Takechi, R.; Galloway, S.; Pallebage-Gamarallage, M.M.; Lam, V.; Dhaliwal, S.S.; Mamo, J.C. Probucol prevents blood-brain barrier dysfunction in wild-type mice induced by saturated fat or cholesterol feeding. *Clin. Exp. Pharmacol. Physiol.* **2013**, *40*, 45–52. [CrossRef] [PubMed]
88. Takechi, R.; Pallebage-Gamarallage, M.M.; Lam, V.; Giles, C.; Mamo, J.C. Long-term probucol therapy continues to suppress markers of neurovascular inflammation in a dietary induced model of cerebral capillary dysfunction. *Lipids Health Dis.* **2014**, *13*, 91. [CrossRef] [PubMed]

89. Huang, W.; Chen, L.; Zhang, B.; Park, M.; Toborek, M. Ppar agonist-mediated protection against HIV Tat-induced cerebrovascular toxicity is enhanced in MMP-9-deficient mice. *J. Cereb. Blood Flow Metab.* **2014**, *34*, 646–653. [CrossRef] [PubMed]
90. Mysiorek, C.; Culot, M.; Dehouck, L.; Derudas, B.; Staels, B.; Bordet, R.; Cecchelli, R.; Fenart, L.; Berezowski, V. Peroxisome-proliferator-activated receptor-α activation protects brain capillary endothelial cells from oxygen-glucose deprivation-induced hyperpermeability in the blood-brain barrier. *Curr. Neurovasc. Res.* **2009**, *6*, 181–193. [CrossRef] [PubMed]
91. Hardeland, R. Antioxidative protection by melatonin: Multiplicity of mechanisms from radical detoxification to radical avoidance. *Endocrine* **2005**, *27*, 119–130. [CrossRef]
92. Reiter, R.J.; Acuna-Castroviejo, D.; Tan, D.X.; Burkhardt, S. Free radical-mediated molecular damage. Mechanisms for the protective actions of melatonin in the central nervous system. *Annu. N. Y. Acad. Sci.* **2001**, *939*, 200–215. [CrossRef]
93. Sirin, F.B.; Kumbul Doguc, D.; Vural, H.; Eren, I.; Inanli, I.; Sutcu, R.; Delibas, N. Plasma 8-isoPGF2α and serum melatonin levels in patients with minimal cognitive impairment and Alzheimer disease. *Turk. J. Med. Sci.* **2015**, *45*, 1073–1077. [CrossRef] [PubMed]
94. Scholtens, R.M.; van Munster, B.C.; van Kempen, M.F.; de Rooij, S.E. Physiological melatonin levels in healthy older people: A systematic review. *J. Psychosom. Res.* **2016**, *86*, 20–27. [CrossRef] [PubMed]
95. Obayashi, K.; Saeki, K.; Iwamoto, J.; Tone, N.; Tanaka, K.; Kataoka, H.; Morikawa, M.; Kurumatani, N. Physiological levels of melatonin relate to cognitive function and depressive symptoms: The HEIJO-KYO cohort. *J. Clin. Endocrinol. Metab.* **2015**, *100*, 3090–3096. [CrossRef] [PubMed]
96. Rudnitskaya, E.A.; Muraleva, N.A.; Maksimova, K.Y.; Kiseleva, E.; Kolosova, N.G.; Stefanova, N.A. Melatonin attenuates memory impairment, amyloid-β accumulation, and neurodegeneration in a rat model of sporadic Alzheimer's disease. *J. Alzheimers Dis.* **2015**, *47*, 103–116. [CrossRef] [PubMed]
97. Mukda, S.; Panmanee, J.; Boontem, P.; Govitrapong, P. Melatonin administration reverses the alteration of amyloid precursor protein-cleaving secretases expression in aged mouse hippocampus. *Neurosci. Lett.* **2016**, *621*, 39–46. [CrossRef] [PubMed]
98. Fu, J.; Zhao, S.D.; Liu, H.J.; Yuan, Q.H.; Liu, S.M.; Zhang, Y.M.; Ling, E.A.; Hao, A.J. Melatonin promotes proliferation and differentiation of neural stem cells subjected to hypoxia in vitro. *J. Pineal Res.* **2011**, *51*, 104–112. [CrossRef] [PubMed]
99. Sotthibundhu, A.; Phansuwan-Pujito, P.; Govitrapong, P. Melatonin increases proliferation of cultured neural stem cells obtained from adult mouse subventricular zone. *J. Pineal Res.* **2010**, *49*, 291–300. [CrossRef] [PubMed]
100. Stefanova, N.A.; Maksimova, K.Y.; Kiseleva, E.; Rudnitskaya, E.A.; Muraleva, N.A.; Kolosova, N.G. Melatonin attenuates impairments of structural hippocampal neuroplasticity in OXYS rats during active progression of Alzheimer's disease-like pathology. *J. Pineal Res.* **2015**, *59*, 163–177. [CrossRef] [PubMed]
101. Hager, K.; Kenklies, M.; McAfoose, J.; Engel, J.; Munch, G. α-lipoic acid as a new treatment option for Alzheimer's disease—A 48 months follow-up analysis. *J. Neural Transm. Suppl.* **2007**, 189–193.
102. Zhao, R.R.; Xu, F.; Xu, X.C.; Tan, G.J.; Liu, L.M.; Wu, N.; Zhang, W.Z.; Liu, J.X. Effects of alpha-lipoic acid on spatial learning and memory, oxidative stress, and central cholinergic system in a rat model of vascular dementia. *Neurosci. Lett.* **2015**, *587*, 113–119. [CrossRef] [PubMed]
103. Farr, S.A.; Price, T.O.; Banks, W.A.; Ercal, N.; Morley, J.E. Effect of alpha-lipoic acid on memory, oxidation, and lifespan in SAMP8 mice. *J. Alzheimers Dis.* **2012**, *32*, 447–455. [PubMed]
104. Mathew, B.; Biju, R. Neuroprotective effects of garlic: A review. *Libyan J. Med.* **2008**, *3*, 23–33. [CrossRef] [PubMed]
105. Ray, B.; Chauhan, N.B.; Lahiri, D.K. The "aged garlic extract" (AGE) and one of its active ingredients s-allyl-l-cysteine (SAC) as potential preventive and therapeutic agents for Alzheimer's disease (AD). *Curr. Med. Chem.* **2011**, *18*, 3306–3313. [CrossRef] [PubMed]
106. Chauhan, N.B. Effect of aged garlic extract on APP processing and tau phosphorylation in Alzheimer's transgenic model Tg2576. *J. Ethnopharmacol.* **2006**, *108*, 385–394. [CrossRef] [PubMed]
107. Chauhan, N.B.; Sandoval, J. Amelioration of early cognitive deficits by aged garlic extract in Alzheimer's transgenic mice. *Phytother. Res.* **2007**, *21*, 629–640. [CrossRef] [PubMed]
108. Ray, B.; Chauhan, N.B.; Lahiri, D.K. Oxidative insults to neurons and synapse are prevented by aged garlic extract and *S*-allyl-L-cysteine treatment in the neuronal culture and APP-Tg mouse model. *J. Neurochem.* **2011**, *117*, 388–402. [CrossRef] [PubMed]

109. Chen, X.; Ghribi, O.; Geiger, J.D. Caffeine protects against disruptions of the blood-brain barrier in animal models of Alzheimer's and Parkinson's diseases. *J. Alzheimers Dis.* **2010**, *20* (Suppl. 1), S127–S141. [PubMed]
110. Lan, X.; Wang, W.; Li, Q.; Wang, J. The natural flavonoid pinocembrin: Molecular targets and potential therapeutic applications. *Mol. Neurobiol.* **2016**, *53*, 1794–1801. [CrossRef] [PubMed]
111. Saha, A.; Sarkar, C.; Singh, S.P.; Zhang, Z.; Munasinghe, J.; Peng, S.; Chandra, G.; Kong, E.; Mukherjee, A.B. The blood-brain barrier is disrupted in a mouse model of infantile neuronal ceroid lipofuscinosis: Amelioration by resveratrol. *Hum. Mol. Genet.* **2012**, *21*, 2233–2244. [CrossRef] [PubMed]
112. Lian, Q.; Nie, Y.; Zhang, X.; Tan, B.; Cao, H.; Chen, W.; Gao, W.; Chen, J.; Liang, Z.; Lai, H.; et al. Effects of grape seed proanthocyanidin on Alzheimer's disease in vitro and in vivo. *Exp. Ther. Med.* **2016**, *12*, 1681–1692. [CrossRef] [PubMed]
113. Parihar, A.; Parihar, M.S.; Zenebe, W.J.; Ghafourifar, P. Statins lower calcium-induced oxidative stress in isolated mitochondria. *Hum. Exp. Toxicol.* **2012**, *31*, 355–363. [CrossRef] [PubMed]
114. Szczepanska-Szerej, A.; Kurzepa, J.; Wojczal, J.; Stelmasiak, Z. Simvastatin displays an antioxidative effect by inhibiting an increase in the serum 8-isoprostane level in patients with acute ischemic stroke: Brief report. *Clin. Neuropharmacol.* **2011**, *34*, 191–194. [CrossRef] [PubMed]
115. McGuinness, B.; Craig, D.; Bullock, R.; Passmore, P. Statins for the prevention of dementia. *Cochrane Database Syst. Rev.* **2016**. [CrossRef]
116. Mospan, C.M. Are statins protective or harmful to cognitive function? *JAAPA* **2016**, *29*, 11–12. [CrossRef] [PubMed]
117. Hendrie, H.C.; Hake, A.; Lane, K.; Purnell, C.; Unverzagt, F.; Smith-Gamble, V.; Murrell, J.; Ogunniyi, A.; Baiyewu, O.; Callahan, C.; et al. Statin use, incident dementia and Alzheimer disease in elderly African Americans. *Ethn. Dis.* **2015**, *25*, 345–354. [CrossRef] [PubMed]
118. Hajjar, I.; Schumpert, J.; Hirth, V.; Wieland, D.; Eleazer, G.P. The impact of the use of statins on the prevalence of dementia and the progression of cognitive impairment. *J. Gerontol. Ser. A Biol. Sci. Med. Sci.* **2002**, *57*, M414–M418. [CrossRef]
119. Haag, M.D.; Hofman, A.; Koudstaal, P.J.; Stricker, B.H.; Breteler, M.M. Statins are associated with a reduced risk of Alzheimer disease regardless of lipophilicity. The rotterdam study. *J. Neurol. Neurosurg. Psychiatry* **2009**, *80*, 13–17. [CrossRef] [PubMed]
120. Wanamaker, B.L.; Swiger, K.J.; Blumenthal, R.S.; Martin, S.S. Cholesterol, statins, and dementia: What the cardiologist should know. *Clin. Cardiol.* **2015**, *38*, 243–250. [CrossRef] [PubMed]
121. Shinohara, M.; Sato, N.; Kurinami, H.; Takeuchi, D.; Takeda, S.; Shimamura, M.; Yamashita, T.; Uchiyama, Y.; Rakugi, H.; Morishita, R. Reduction of brain β-amyloid (Aβ) by fluvastatin, a hydroxymethylglutaryl-CoA reductase inhibitor, through increase in degradation of amyloid precursor protein C-terminal fragments (APP-CTFS) and Aβ clearance. *J. Biol. Chem.* **2010**, *285*, 22091–22102. [CrossRef] [PubMed]
122. Li, G.; Larson, E.B.; Sonnen, J.A.; Shofer, J.B.; Petrie, E.C.; Schantz, A.; Peskind, E.R.; Raskind, M.A.; Breitner, J.C.; Montine, T.J. Statin therapy is associated with reduced neuropathologic changes of Alzheimer disease. *Neurology* **2007**, *69*, 878–885. [CrossRef] [PubMed]
123. Zhang, Y.Y.; Fan, Y.C.; Wang, M.; Wang, D.; Li, X.H. Atorvastatin attenuates the production of IL-1β, IL-6, and TNF-α in the hippocampus of an amyloid β1–42-induced rat model of Alzheimer's disease. *Clin. Interv. Aging* **2013**, *8*, 103–110. [PubMed]
124. Barone, E.; Cenini, G.; Di Domenico, F.; Martin, S.; Sultana, R.; Mancuso, C.; Murphy, M.P.; Head, E.; Butterfield, D.A. Long-term high-dose atorvastatin decreases brain oxidative and nitrosative stress in a preclinical model of Alzheimer disease: A novel mechanism of action. *Pharmacol. Res.* **2011**, *63*, 172–180. [CrossRef] [PubMed]
125. Kurata, T.; Kawai, H.; Miyazaki, K.; Kozuki, M.; Morimoto, N.; Ohta, Y.; Ikeda, Y.; Abe, K. Statins have therapeutic potential for the treatment of Alzheimer's disease, likely via protection of the neurovascular unit in the AD brain. *J. Neurol. Sci.* **2012**, *322*, 59–63. [CrossRef] [PubMed]
126. Tong, X.K.; Nicolakakis, N.; Fernandes, P.; Ongali, B.; Brouillette, J.; Quirion, R.; Hamel, E. Simvastatin improves cerebrovascular function and counters soluble amyloid-beta, inflammation and oxidative stress in aged APP mice. *Neurobiol. Dis.* **2009**, *35*, 406–414. [CrossRef] [PubMed]
127. Zhou, G.; Wang, Y.; He, P.; Li, D. Probucol inhibited Nox2 expression and attenuated podocyte injury in type 2 diabetic nephropathy of db/db mice. *Biol. Pharm. Bull.* **2013**, *36*, 1883–1890. [CrossRef] [PubMed]

128. Colle, D.; Santos, D.B.; Moreira, E.L.; Hartwig, J.M.; dos Santos, A.A.; Zimmermann, L.T.; Hort, M.A.; Farina, M. Probucol increases striatal glutathione peroxidase activity and protects against 3-nitropropionic acid-induced pro-oxidative damage in rats. *PLoS ONE* **2013**, *8*, e67658. [CrossRef] [PubMed]
129. Poirier, J.; Miron, J.; Picard, C.; Gormley, P.; Theroux, L.; Breitner, J.; Dea, D. Apolipoprotein E and lipid homeostasis in the etiology and treatment of sporadic Alzheimer's disease. *Neurobiol. Aging* **2014**, *35* (Suppl. 2), S3–S10. [CrossRef] [PubMed]
130. Santos, D.B.; Peres, K.C.; Ribeiro, R.P.; Colle, D.; dos Santos, A.A.; Moreira, E.L.; Souza, D.O.; Figueiredo, C.P.; Farina, M. Probucol, a lipid-lowering drug, prevents cognitive and hippocampal synaptic impairments induced by amyloid β peptide in mice. *Exp. Neurol.* **2012**, *233*, 767–775. [CrossRef] [PubMed]
131. Santos, D.B.; Colle, D.; Moreira, E.L.; Peres, K.C.; Ribeiro, R.P.; Dos Santos, A.A.; de Oliveira, J.; Hort, M.A.; de Bem, A.F.; Farina, M. Probucol mitigates streptozotocin-induced cognitive and biochemical changes in mice. *Neuroscience* **2015**, *284*, 590–600. [CrossRef] [PubMed]
132. Russell, J.C.; Graham, S.E.; Amy, R.M.; Dolphin, P.J. Cardioprotective effect of probucol in the atherosclerosis-prone JCR:LA-cp rat. *Eur. J. Pharmacol.* **1998**, *350*, 203–210. [CrossRef]
133. Tenenbaum, A.; Fisman, E.Z. Fibrates are an essential part of modern anti-dyslipidemic arsenal: Spotlight on atherogenic dyslipidemia and residual risk reduction. *Cardiovasc. Diabetol.* **2012**, *11*, 125. [CrossRef] [PubMed]
134. Uppalapati, D.; Das, N.R.; Gangwal, R.P.; Damre, M.V.; Sangamwar, A.T.; Sharma, S.S. Neuroprotective potential of peroxisome proliferator activated receptor-α agonist in cognitive impairment in Parkinson's disease: Behavioral, biochemical, and PBPK profile. *PPAR Res.* **2014**, *2014*, 753587. [CrossRef] [PubMed]
135. Greene-Schloesser, D.; Payne, V.; Peiffer, A.M.; Hsu, F.C.; Riddle, D.R.; Zhao, W.; Chan, M.D.; Metheny-Barlow, L.; Robbins, M.E. The peroxisomal proliferator-activated receptor (PPAR) α agonist, fenofibrate, prevents fractionated whole-brain irradiation-induced cognitive impairment. *Radiat. Res.* **2014**, *181*, 33–44. [CrossRef] [PubMed]
136. Ancelin, M.L.; Carriere, I.; Barberger-Gateau, P.; Auriacombe, S.; Rouaud, O.; Fourlanos, S.; Berr, C.; Dupuy, A.M.; Ritchie, K. Lipid lowering agents, cognitive decline, and dementia: The three-city study. *J. Alzheimers Dis.* **2012**, *30*, 629–637. [PubMed]
137. Zaminelli, T.; Gradowski, R.W.; Bassani, T.B.; Barbiero, J.K.; Santiago, R.M.; Maria-Ferreira, D.; Baggio, C.H.; Vital, M.A. Antidepressant and antioxidative effect of ibuprofen in the rotenone model of Parkinson's disease. *Neurotox. Res.* **2014**, *26*, 351–362. [CrossRef] [PubMed]
138. Int' Veld, B.A.; Ruitenberg, A.; Hofman, A.; Launer, L.J.; van Duijn, C.M.; Stijnen, T.; Breteler, M.M.; Stricker, B.H. Nonsteroidal antiinflammatory drugs and the risk of Alzheimer's disease. *N. Engl. J. Med.* **2001**, *345*, 1515–1521. [CrossRef] [PubMed]
139. Szekely, C.A.; Zandi, P.P. Non-steroidal anti-inflammatory drugs and Alzheimer's disease: The epidemiological evidence. *CNS Neurol. Disord. Drug Targets* **2010**, *9*, 132–139. [CrossRef] [PubMed]
140. Gasparini, L.; Ongini, E.; Wenk, G. Non-steroidal anti-inflammatory drugs (NSAIDS) in Alzheimer's disease: Old and new mechanisms of action. *J. Neurochem.* **2004**, *91*, 521–536. [CrossRef] [PubMed]
141. Lim, G.P.; Yang, F.; Chu, T.; Chen, P.; Beech, W.; Teter, B.; Tran, T.; Ubeda, O.; Ashe, K.H.; Frautschy, S.A.; et al. Ibuprofen suppresses plaque pathology and inflammation in a mouse model for Alzheimer's disease. *J. Neurosci.* **2000**, *20*, 5709–5714. [PubMed]
142. Zara, S.; De Colli, M.; Rapino, M.; Pacella, S.; Nasuti, C.; Sozio, P.; Di Stefano, A.; Cataldi, A. Ibuprofen and lipoic acid conjugate neuroprotective activity is mediated by Ngb/Akt intracellular signaling pathway in Alzheimer's disease rat model. *Gerontology* **2013**, *59*, 250–260. [CrossRef] [PubMed]
143. Matsuura, K.; Otani, M.; Takano, M.; Kadoyama, K.; Matsuyama, S. The influence of chronic ibuprofen treatment on proteins expressed in the mouse hippocampus. *Eur. J. Pharmacol.* **2015**, *752*, 61–68. [CrossRef] [PubMed]
144. Choi, J.K.; Carreras, I.; Aytan, N.; Jenkins-Sahlin, E.; Dedeoglu, A.; Jenkins, B.G. The effects of aging, housing and ibuprofen treatment on brain neurochemistry in a triple transgene Alzheimer's disease mouse model using magnetic resonance spectroscopy and imaging. *Brain Res.* **2014**, *1590*, 85–96. [CrossRef] [PubMed]

nutrients

MDPI

Article

Coenzyme Q10 and Oxidative Stress: Inflammation Status in Hepatocellular Carcinoma Patients after Surgery

Hsiao-Tien Liu [1,2], Shao-Bin Cheng [1,2,3], Yi-Chia Huang [2], Yin-Tzu Huang [2] and Ping-Ting Lin [2,4,*]

1 Division of General Surgery, Department of Surgery, Taichung Veterans General Hospital, Taichung 40705, Taiwan; langhsky@vghtc.gov.tw (H.-T.L.); sbc@vghtc.gov.tw (S.-B.C.)
2 Department of Nutrition, Chung Shan Medical University, Taichung 40201, Taiwan; ych@csmu.edu.tw (Y.-C.H.); scorpio5220@hotmail.com (Y.-T.H.)
3 School of Medicine, Chung Shan Medical University, Taichung 40201, Taiwan
4 Department of Nutrition, Chung Shan Medical University Hospital, Taichung 40201, Taiwan
* Correspondence: apt810@csmu.edu.tw; Tel.: +886-4-2473-0022 (ext. 12187); Fax: +886-4-2324-8175

Received: 25 November 2016; Accepted: 28 December 2016; Published: 4 January 2017

Abstract: (1) Background: Hepatocellular carcinoma (HCC) is the second leading cause of cancer deaths worldwide, and surgical resection is the main treatment for HCC. To date, no published study has examined the status of coenzyme Q10 in patients with HCC after surgery. Thus, the purpose of this study was to investigate the correlations between the level of coenzyme Q10, oxidative stress, and inflammation in patients with HCC after surgery; (2) Methods: 71 primary HCC patients were recruited. Levels of coenzyme Q10, vitamin E, oxidative stress (malondialdehyde), antioxidant enzymes activity (superoxidase dismutase, catalase, and glutathione peroxidase), and inflammatory markers (high sensitivity C-reactive protein; tumor necrosis factor-α; and interleukin-6) were measured; (3) Results: Patients with HCC had a significantly lower levels of coenzyme Q10 ($p = 0.01$) and oxidative stress ($p < 0.01$), and significantly higher levels of antioxidant enzymes activities and inflammation after surgery ($p < 0.05$). The level of coenzyme Q10 was significantly positively correlated with antioxidant capacity (vitamin E and glutathione peroxidase activity) and negatively correlated with inflammation markers after surgery; (4) Conclusion: Hepatocarcinogenesis is associated with oxidative stress, and coenzyme Q10 may be considered an antioxidant therapy for patients with HCC, particularly those with higher inflammation after surgery.

Keywords: coenzyme Q10; oxidative stress; inflammation; hepatocellular carcinoma; surgery

1. Introduction

The most recent reports from the World Health Organization (WHO, 2014) and the Ministry of Health and Welfare (2014) in Taiwan indicated that hepatocellular carcinoma (HCC) is the second leading cause of cancer deaths [1,2]. Surgical resection is the main treatment for primary HCC [3]. During or after surgical procedures, there is a physiological stress response that involves activation of inflammatory, endocrine, metabolic, and immunological mediators [4]. Oxidative stress, which is defined as a disturbance in the balance between the productions of reactive oxygen species (ROS) and antioxidant defenses [5]. The increase in the oxidative stress during or after surgery may be associated with increasing complications such as myocardial injury, sepsis, pulmonary edema, kidney and liver failure, and increased mortality [4,6,7]. As a result, oxidative stress and inflammation status is related to the prognosis of the disease after surgery in HCC patients.

Hepatocytic proteins, lipids, and DNA may affect ROS that are primarily produced in the mitochondria [8]. Coenzyme Q10 (also called ubiquinone) is a lipid-soluble benzoquinone that has 10 isoprenyl units in its side chain and is a key component of the mitochondrial respiratory chain for adenosine triphosphate synthesis [9,10]. Studies has been indicated that coenzyme Q10 is an intracellular antioxidant can protects membrane phospholipids, mitochondrial membrane protein, and low density lipoprotein-cholesterol (LDL-C) from free radical-induced oxidative damage [11,12]. In vitro or in vivo studies have demonstrated that coenzyme Q10 not only plays an antioxidant, but also has anti-inflammation effects [13,14] by modulating the expression of cyclooxygenase-2 and nuclear factor-κB (NF-κB) in the liver tissue of rats with HCC [15,16]. However, to date, no published study has examined the status of coenzyme Q10 in patients with HCC and the correlation between oxidative stress and inflammation with coenzyme Q10 after surgery. Thus, the purpose of this clinical study was to investigate the levels of coenzyme Q10, oxidative stress, and inflammation status in patients with HCC before and after surgery.

2. Materials and Methods

2.1. Participants

A total of 71 patients were diagnosed with primary HCC (International Classification of Diseases 9, code 155.0) were recruited from the Division of General Surgery of Taichung Veterans General Hospital, which is a teaching hospital in Taiwan. We excluded patients who were younger than 20 years of age or older than 80 years of age, as well as during pregnant or lactating women, patients undergoing chemotherapy or hormone therapy, and those with a history or current diagnosis of cardiovascular or renal disease. Informed consent was obtained from each subject. This study was approved by the Institutional Review Board of Taichung Veterans General Hospital, Taiwan (CF13197) and registered at Clinical Trials.gov Identifier: NCT01964001.

The following data were recorded for all subjects before surgery: age, body weight, height, waist and hip circumference, smoking and drinking habits, exercise frequency, body mass index (BMI), and the waist/hip ratio were calculated. Dietary intake was assessed by dietitians, and 24 h diet recall was used after one month of the surgery. The dietary records were analyzed using the Nutritionist Professional software package (E-Kitchen Business Corp., Taichung, Taiwan) and the nutrient database was based on the Taiwan food composition table (Food and Drug Administration, Ministry of Health and Welfare, Taipei, Taiwan).

2.2. Blood Collection and Biochemical Measurement

Fasting blood specimens were collected in vacutainer tubes without anticoagulant (Becton Dickinson, Rutherford, NJ, USA) before and month after surgery. Serum and plasma were prepared after centrifugation (3000 rpm, 4 °C, 15 min) and were then stored at −80 °C until analysis. Hematological entities, such as blood urea nitrogen, creatinine, glutamic oxaloacetic transaminase, glutamic pyruvate transaminase (GPT), and lipid profiles were measured using an automated biochemical analyzer (Hitachi-7180E, Tokyo, Japan). The level of high sensitivity C-reactive protein (hs-CRP) was quantified by particle-enhanced immunonephelometry with an image analyzer (Dade Behring, Chicago, IL, USA). Plasma tumor necrosis factor-α (TNF-α) (R & D Systems Inc., Minneapolis, MN, USA) and interleukin-6 (IL-6) (eBioscience, San Diego, CA, USA) levels were measured using an enzyme-linked immunosorbent assay (ELISA) with commercially available kits, according to the manufacturer's instructions.

Plasma coenzyme Q10 and vitamin E levels were measured using high-performance liquid chromatography (HPLC) and were detected with a UV detector at 275 nm and 292 nm, respectively [17,18]. Plasma malondialdehyde (MDA) was determined using the TBARs (thiobarbituric acid reactive substances) method, as described by Botsoglou [19]. The red blood cell (RBC) samples were washed with normal saline after removing the plasma. Then, the RBC samples were diluted

with a 25x sodium phosphate buffer for superoxide dismutase (SOD) and glutathione peroxidase (GPx) measurements, with a 250x sodium phosphate buffer for the catalase (CAT) measurement. The antioxidant enzymes activities (CAT, SOD, and GPx) were determined in the fresh samples, and the methods used to measure these activities have been previously described [20–22]. The protein content of the plasma and RBC was determined based on the biuret reaction of the bicinchoninic acid (BCA) kit (Thermo, Rockford, IL, USA). The values of the antioxidant enzymes activities were expressed as unit/mg of protein. All analyses were performed in duplicate.

2.3. Statistical Analysis

The data were expressed as means and standard deviations (SD), as well as medians. A Kolmogorov–Smirnov test was used to examine the normal distribution of variables. A paired *t*-test was used to compare mean values for continuous variables before and after surgery. Pearson product moment correlation was used to examine the correlations between the levels of antioxidant capacity, oxidative stress, and inflammatory markers in HCC patients and the change of coenzyme Q10, antioxidant capacity, oxidative stress, and inflammation in HCC patients after surgery. Simple linear regression was used to examine the correlations between the levels of coenzyme Q10 and vitamin E, and antioxidant enzyme activity (GPx) in HCC patients. Statistical significance was set at $p < 0.05$. All statistical analyses were performed using SigmaPlot software (version 12.0, Systat, San Jose, CA, USA).

3. Results

3.1. Participant Characteristics

The characteristics and dietary intake of the subjects are shown in Table 1. In total, 70% of the subjects were males, and the mean age of the subjects were 59 ± 11 years old. The frequencies of smoking, drinking, and exercise habits were 17%, 9%, and 44%, respectively. Additionally, 39% of the subjects had been infected with hepatitis B, 17% of the subjects had been infected with hepatitis C, and 14% of the subjects were cirrhosis. More than half of the subjects (56%) had HCC recurrence. With regard to the hematological data, the subjects had significantly higher levels of blood urea nitrogen (BUN), creatinine, and high density lipoprotein-cholesterol (HDL-C) and lower levels of glutamic oxalocetic transaminase (GOT) and total cholesterol to high density lipoprotein-cholesterol ratios (TC-to-HDL-C ratios) ($p < 0.01$) after surgery. With regard to dietary intake, subjects had a significantly higher protein intake of total calories ($p = 0.04$) and lower fat intake ($p = 0.07$) after surgery.

Table 1. Characteristics and dietary intake of subjects [1].

Subjects Characteristics	
males (*n*, %)	50 (70%)
age (years)	59.2 ± 11.3 (59.0)
SBP (mmHg)	125.3 ± 11.3 (123.0)
DBP (mmHg)	76.9 ± 12.3 (76.5)
waist circumference (cm)	88.9 ± 8.6 (90.0)
waist hip ratio	0.9 ± 0.1 (0.9)
BMI (kg/m^2)	24.4 ± 5.8 (24.0)
current smokers [2] (*n*, %)	12 (17%)
drink alcohol [3] (*n*, %)	6 (9%)
exercise [4] (*n*, %)	31 (44%)
Hepatitis B, *n* (%)	28 (39%)
Hepatitis C, *n* (%)	12 (17%)
Cirrhosis, *n* (%)	10 (14%)
Recurrence, *n* (%)	40 (56%)

Table 1. *Cont.*

Subjects Characteristics			
Hematology	**Before Surgery**	**After Surgery**	***p* Values**
BUN (mmol/L)	9.9 ± 3.6 (9.3)	11.6 ± 4.8 (10.7)	<0.01
creatinine (μmol/L)	70.7 ± 17.7 (70.7)	79.6± 26.5 (70.7)	<0.01
GOT (IU/L)	63.2 ± 61.4 (38.0)	40.1 ± 36.3 (40.0)	<0.01
GPT (IU/L)	60.4 ± 57.4 (38.5)	54.3 ± 47.8 (40.0)	0.79
TC (mmol/L)	4.3 ± 1.0 (4.2)	4.3 ± 0.8 (4.2)	0.20
TG (mmol/L)	1.1 ± 0.5 (1.0)	1.1 ± 0.4 (1.0)	0.64
LDL-C (mmol/L)	2.8 ± 0.9 (2.8)	2.7 ± 0.8 (2.6)	0.97
HDL-C (mmol/L)	1.2 ± 0.3 (1.1)	1.3 ± 0.3 (1.2)	<0.01
TC/HDL-C	3.8 ± 1.2 (3.5)	3.5 ± 1.0 (3.4)	<0.01
Dietary Intake			
energy (kcal/day)	1952.0 ± 546.8 (1819.9)	1796.2 ± 405.9 (1793.3)	0.21
protein (g/day)	67.6 ± 23.3 (64.9)	68.7 ± 20.6 (72.6)	0.28
% of total calories	13.7 ± 3.2 (13.0)	15.2 ± 3.7 (14.9)	0.04
fat (g/day)	66.7 ± 32.6 (54.8)	55.4 ± 22.0 (53.1)	0.07
% of total calories	30.3 ± 10.1 (29.0)	26.8 ± 7.7 (26.4)	0.10
carbohydrate (g/day)	274.0 ± 92.9 (253.0)	264.3 ± 66.9 (258.9)	0.52
% of total calories	55.9 ± 10.8 (57.0)	58.3 ± 7.8 (59.4)	0.26
dietary fiber (g/day)	14.5 ± 7.3 (13.0)	14.7 ± 7.4 (12.7)	0.47
cholesterol (mg/day)	244.1 ± 178.0 (186.6)	233.3 ± 147.3 (225.7)	0.63
vitamin E (mg α-TE/day)	271.8 ± 489.1 (13.0)	563.8 ± 888.1 (18.0)	0.28

[1] mean ± SD (medians); [2] current smokers: individuals who current smoke one or more cigarettes per day; [3] drink alcohol: individuals who regularly drink one or more drink per day; [4] exercise: individuals who exercise at least three times every week. BMI: body mass index; BUN: blood urea nitrogen; DBP: diastolic blood pressure; GOT: glutamic oxaloacetic transaminase; GPT: glutamic pyruvate transaminase; HDL-C: high-density lipoprotein-cholesterol; LDL-C: low density lipoprotein-cholesterol; SBP: systolic blood pressure; TC: total cholesterol; TG: triglyceride.

3.2. Levels of Coenzyme Q10, Oxidative Stress, and Inflammation

The levels of coenzyme Q10, vitamin E, oxidative stress and inflammatory markers after surgery are shown in Table 2. After surgery, the subjects had a significantly lower levels of coenzyme Q10 ($p = 0.01$) and MDA ($p < 0.01$), and significantly higher levels of vitamin E ($p < 0.01$) and antioxidant enzymes activities (SOD, $p < 0.01$; CAT, $p < 0.01$; GPx, $p = 0.04$). With regard to inflammatory markers, the subjects had significantly higher levels of hs-CRP ($p = 0.04$), TNF-α ($p < 0.01$) and IL-6 ($p < 0.01$) after surgery.

Table 2. Levels of coenzyme Q10, oxidative stress, and inflammation [1].

	Before Surgery	**After Surgery**	***p* Values**
Coenzyme Q10 (μM)	0.34 ± 0.11 (0.32)	0.33 ± 0.11 (0.28)	0.01
Vitamin E (μM)	10.4 ± 2.9 (11.8)	11.8 ± 2.6 (10.2)	<0.01
Oxidative Stress			
MDA (μM)	1.68 ± 0.40 (1.60)	1.43 ± 0.43 (1.36)	<0.01
Antioxidant Enzymes Activity			
SOD (U/mg protein)	13.2 ± 6.4 (12.4)	15.3 ± 6.8 (13.5)	<0.01
CAT (U/mg protein)	13.2 ± 5.7 (11.4)	15.3 ± 7.2 (12.5)	<0.01
GPx (U/mg protein)	15.7 ± 4.9 (16.3)	16.4 ± 4.6 (16.8)	0.04
Inflammatory Markers			
hs-CRP (mg/L)	4.6 ± 8.5 (1.3)	4.8 ± 5.0 (2.5)	0.04
TNF-α (pg/mL)	0.4 ± 0.7 (0.1)	0.9 ± 1.0 (0.8)	<0.01
IL-6 (pg/mL)	2.3 ± 1.9 (1.6)	3.6 ± 2.8 (2.5)	<0.01

[1] mean ± SD (medians). CAT: Catalase activity; MDA: Malondialdehyde; GPx: glutathione peroxidase; HCC: hepatocellular carcinoma; hs-CRP: high sensitivity C-reactive protein; IL-6: interleukin-6; SOD: superoxide dismutase; TNF-α: tumor necrosis factor-α.

3.3. Correlations between Coenzyme Q10, Oxidative Stress, and Inflammation

The correlations between coenzyme Q10, oxidative stress, and inflammation in HCC patients are shown in Table 3. There was a significantly negative correlation between oxidative stress (MDA) and antioxidant enzymes activities (SOD, $p = 0.05$; CAT, $p < 0.05$, and GPx, $p = 0.04$) (Table 3). With regard to the correlation between antioxidant capacity and inflammation, CAT activity shown to be significantly negatively correlated with the level of hs-CRP ($p = 0.02$), and GPx activity was significantly negatively correlated with the levels of TNF-α ($p = 0.02$) and IL-6 ($p < 0.01$).

Table 3. Correlations[1] between coenzyme Q10, oxidative stress, and inflammation in HCC patients.

	Oxidative Stress	Inflammatory Markers		
	MDA (μM)	**hs-CRP (mg/dL)**	**TNF-α (pg/mL)**	**IL-6 (pg/mL)**
Coenzyme Q10 (μM)	0.13	0.14	−0.06	0.02
vitamin E (μM)	0.07	0.09	−0.04	0.24
SOD (U/mg protein)	−0.10 †	0.00	0.18	0.13
CAT (U/mg protein)	−0.10 *	−0.15 *	0.51	0.14
GPx (U/mg protein)	−0.11 *	−0.08	−0.17 *	−0.19 *

[1] correlation coefficient (*r*). * $p < 0.05$; † $p = 0.05$. CAT: Catalase activity; MDA: Malondialdehyde; GPx: glutathione peroxidase; HCC: hepatocellular carcinoma; hs-CRP: high sensitivity C-reactive protein; IL-6: interleukin-6; SOD: superoxide dismutase; TNF-α: tumor necrosis factor-α.

Furthermore, we assessed the correlations between the changes in coenzyme Q10, oxidative stress, and inflammation in HCC patients, and these results are shown in Table 4. There was a significantly negative correlation between changes in the levels of coenzyme Q10 and inflammation markers (hs-CRP, $p = 0.02$; IL-6, $p = 0.05$) after surgery. In addition, changes in GPx activity were significantly negatively correlated with changes in oxidative stress (MDA, $p = 0.06$) and inflammation markers (hs-CRP, $p < 0.05$; IL-6, $p = 0.04$), and changes in SOD activity was significantly negatively correlated with changes in hs-CRP ($p = 0.04$) after surgery.

Table 4. Correlations[1] between changes in coenzyme Q10, oxidative stress, and inflammation.

	Changes of Oxidative Stress	Changes of Inflammatory Markers		
	MDA (μM)	**hs-CRP (mg/dL)**	**TNF-α (pg/mL)**	**IL-6 (pg/mL)**
Coenzyme Q10 (μM)	−0.11	−0.23 *	0.18	−0.16 *
vitamin E (μM)	0.01	0.09	−0.13	0.08
SOD (U/mg protein)	−0.04	−0.16 *	0.04	−0.07
CAT (U/mg protein)	−0.09	−0.03	0.24	0.01
GPx (U/mg protein)	−0.18 †	−0.26 *	−0.10	−0.20

[1] correlation coefficient (*r*). * $p < 0.05$; † $p = 0.06$. CAT: Catalase activity; MDA: Malondialdehyde; GPx: glutathione peroxidase; HCC: hepatocellular carcinoma; hs-CRP: high sensitivity C-reactive protein; IL-6: interleukin-6; SOD: superoxide dismutase; TNF-α: tumor necrosis factor-α.

3.4. Correlations between Coenzyme Q10 and Antioxidant Capacity

The correlations between coenzyme Q10 and antioxidant capacity is shown in Figure 1. The level of coenzyme Q10 was significantly positive correlated with vitamin E ($\beta = 9.85$, $p < 0.01$) and GPx activity ($\beta = 6.43$, $p = 0.04$) in HCC patients.

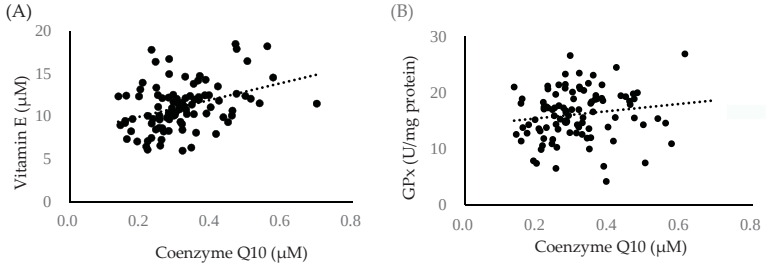

Figure 1. Correlations between the levels of coenzyme Q10 and vitamin E, and glutathione peroxidase activity (GPx) in HCC patients. (**A**) Correlation between the levels of coenzyme Q10 and vitamin E ($\beta = 9.85$, $p < 0.01$); (**B**) Correlation between the levels of coenzyme Q10 and glutathione peroxidase (GPx, $\beta = 6.43$, $p = 0.04$).

4. Discussion

This study is the first clinical study to investigate the coenzyme Q10 status in patients with HCC before and after surgery. The reference values of the level of coenzyme Q10 were suggested to be between 0.5 to 1.7 μM [23]. It is worth noting that the level of coenzyme Q10 was lower in patients with HCC before surgery (Table 2), and the level of coenzyme Q10 was further reduced significantly after surgery (Table 2, 0.34 ± 0.11 μM reduced to 0.30 ± 0.11 μM, $p < 0.01$). Coenzyme Q10 is a crucial cellular antioxidant [9,10], and our previous studies have demonstrated that coenzyme Q10 can significantly reduce oxidative stress and inflammation status via its antioxidant capacity [24–26]. In the present study, we found that the level of coenzyme Q10 was significantly correlated with vitamin E and antioxidant enzyme (GPx) activity in HCC patients (Figure 1). Patients with HCC suffer from a higher level of oxidative stress and inflammation [27], and a deficiency in coenzyme Q10 was found in HCC patients, we suggest that the administration of coenzyme Q10 supplements in patients with HCC during the surgery may be beneficial.

Surgical resection is the most efficient treatment of patients with HCC [3]. Over the past 10 years, surgical treatment has been considered safe, with an acceptable overall mortality rate (<5%), and resulted in good long-term survival (>50%) in HCC patients [28–30]. However, surgery may elicit the activation of systemic inflammatory, endocrine/metabolic, and immunological systems, which is referred to as the surgical stress response [4]. In the present study, it is interesting to note that, after one month of the surgery, patients with HCC exhibited significantly lower oxidative stress and higher antioxidant enzymes activities (Table 2). The level of oxidative stress (MDA) was significantly reduced by 15%, and the antioxidant activities of SOD, CAT, and GPx were significantly increased by 8.6%, 9.6%, and 3.1%, respectively. Although surgery improved the antioxidant capacity in HCC patients, compared with the administration of antioxidants, these increases were not high [24–26,31]. Our previous clinical intervention study have observed that the administration of coenzyme Q10 at a dose of 300 mg/day in patients with HCC could significantly increase the antioxidant enzymes activities of SOD by 67.3%, CAT by 42.6%, and GPx by 26.5% and reduce oxidative stress by 17.3% after 12 weeks of supplementation [31]. In the present study, we found a non-statistically negative correlation between the changes in coenzyme Q10 and the changes in oxidative stress (MDA) after surgery (Table 4) and the level of coenzyme Q10 was significantly positive correlated with vitamin E and antioxidant enzyme (GPx) activity in HCC patients (Figure 1). Additionally, the latest clinical study conducted by Cannistrà et al. [32] demonstrated that the rates for the morbidity, muscle weakness, and pleural effusion were significantly lower in elderly patients with HCC during surgical resection after coenzyme Q10 supplementation. Since hepatocarcinogenesis is associated with severe oxidative stress [33], antioxidants, such as coenzyme Q10, could be considered a complementary treatment strategy for patients with HCC after surgery.

With regard to inflammation status, surgery may elicit systemic immunological and inflammatory responses, including the activation of polymorphonuclear leucocytes, macrophages, monocytes, platelets, and mast cells, as well as the hyper-production of cytokines (e.g., IL-6 and TNF-α) [4]. Similar findings were observed in the present study, patients with HCC had a significantly higher inflammation status after surgery (Table 2). It is not surprising that a higher inflammation status in these patients due to the response to the surgery. However, in the present study, we found that changes in coenzyme Q10 were significantly negatively correlated with inflammation after surgery (Table 4). Most patients with HCC occur in cirrhotic livers and are associated with oxidative stress [30]. It is already known that inflammation is associated with NF-kB activation [34], and NF-κB can be activated by ROS, subsequently resulting in the upregulation of the expression of pro-inflammatory cytokines. Oxidative stress can also induce the production of a variety of cytokines in Kupffer cells, thus increasing inflammation and the apoptosis of hepatic cells [35]. As inflammation is correlated with oxidative stress, using antioxidants to inhibit the inflammatory-activating cascade could be considered. We suggest that administering antioxidants, such as coenzyme Q10, in HCC patients, particularly in those with a lower coenzyme Q10 status after surgery, is worth attempting.

5. Conclusions

In this clinical study, we clarified that patients with HCC exhibited lower levels of coenzyme Q10 and oxidative stress after surgery, and the level of coenzyme Q10 was associated with antioxidant capacity and inflammation. As hepatocarcinogenesis is chronic inflammation associated with severe oxidative stress, antioxidants, such as coenzyme Q10, could be considered a complementary treatment strategy for patients with HCC, particularly those with higher inflammation after surgery.

Acknowledgments: This study was supported by a grant from the Taichung Veterans General Hospital (TCVGH-1034601A and TCVGH-1044601A), Taiwan. We would like to express our sincere appreciation to the subjects for their participation. We thank the nurses at Taichung Veterans General Hospital and the technical advisor at the Taipei Institute of Pathology for providing expert assistance in blood sample collection and data analysis.

Author Contributions: H.T.L., S.B.J. and Y.C.H. performed the study and the data analyses. Y.T.H. helped to perform the study and analyze samples. P.T.L. conceived the study, participated in its design, and coordinated the study. H.T.L. and P.T.L. drafted the manuscript. All authors read and approved the final manuscript.

Conflicts of Interest: The authors declare no conflict of interest.

Abbreviations

The following abbreviations are used in this manuscript:

BMI	body mass index
BUN	blood urea nitrogen
CAT	catalase
DBP	diastolic blood pressure
GPx	glutathione peroxidase
GOT	glutamic oxaloacetic transaminase
GPT	glutamic pyruvate transaminase
HDL-C	high-density lipoprotein-cholesterol
hs-CRP	high sensitivity C-reactive protein
IL-6	interleukin-6
LDL-C	low density lipoprotein-cholesterol
MDA	malondialdehyde
SBP	systolic blood pressure
SOD	superoxide dismutase
TC	total cholesterol
TG	triglyceride

References

1. Stewart, B.W.; Wild, C.P. *World Cancer Report 2014*; IARC Nonserial Publication: Lyon, France, 2014. Available online: http://publications.iarc.fr/Non-Series-Publications/World-Cancer-Reports/World-Cancer-Report-2014 (accessed on 4 October 2016).
2. El-Serag, H.B. Hepatocellular carcinoma. *N. Engl. J. Med.* **2011**, *365*, 1118–1127. [CrossRef] [PubMed]
3. Helling, T.S. Liver failure following partial hepatectomy. *HPB* **2006**, *8*, 165–174. [CrossRef] [PubMed]
4. Kücükakin, B.; Gögenur, I.; Reiter, R.J.; Rosenberg, J. Oxidative stress in relation to surgery: Is there a role for the antioxidant melatonin? *J. Surg. Res.* **2009**, *152*, 338–347. [CrossRef] [PubMed]
5. Betteridge, D.J. What is oxidative stress? *Metab. Clin. Med.* **2000**, *49*, 3–8. [CrossRef]
6. Cornu-Labat, G.; Serra, M.; Smith, A.; McGregor, W.E.; Kasirajan, K.; Hirko, M.K.; Turner, J.J.; Rubin, J.R. Systemic consequences of oxidative stress following aortic surgery correlate with the degree of antioxidant defenses. *Ann. Vasc. Surg.* **2000**, *14*, 31–36. [CrossRef] [PubMed]
7. Hafez, H.M.; Berwanger, C.S.; McColl, A.; Richmond, W.; Wolfe, J.H.; Mansfield, A.O.; Stansby, G. Myocardial injury in major aortic surgery. *J. Vasc. Surg.* **2000**, *31*, 742–750. [CrossRef] [PubMed]
8. Cichoż-Lach, H.; Michalak, A. Oxidative stress as a crucial factor in liver diseases. *World J. Gastroenterol.* **2014**, *20*, 8082–8091. [CrossRef] [PubMed]
9. Ernster, L.; Dallner, G. Biochemical, physiological and medical aspects of ubiquinone function. *Biochim. Biophys. Acta Mol. Basic Dis.* **1995**, *1271*, 195–204. [CrossRef]
10. Bhagavan, H.N.; Chopra, R.K. Coenzyme Q10: Absorption, tissue uptake, metabolism and pharmacokinetics. *Free Radic. Res.* **2006**, *40*, 445–453. [CrossRef] [PubMed]
11. Alleva, R.; Tomasetti, M.; Battino, M.; Curatola, G.; Littarru, G.P.; Folkers, K. The roles of coenzyme Q10 and vitamin E on the peroxidation of human low density lipoprotein subfractions. *Proc. Natl. Acad. Sci. USA* **1995**, *92*, 9388–9391. [CrossRef] [PubMed]
12. Flowers, N.; Hartley, L.; Todkill, D.; Stranges, S.; Rees, K. Co-enzyme Q10 supplementation for the primary prevention of cardiovascular disease. *Cochrane Database Syst. Rev.* **2014**, *12*, CD010405.
13. Rauchová, H.; Battino, M.; Fato, R.; Lenaz, G.; Drahota, Z. Coenzyme Q-pool function in glycerol-3-phosphate oxidation in hamster brown adipose tissue mitochondria. *J. Bioenerg. Biomembr.* **1992**, *24*, 235–241. [CrossRef] [PubMed]
14. Yoneda, T.; Tomofuji, T.; Kawabata, Y.; Ekuni, D.; Azuma, T.; Kataoka, K.; Kunitomo, M.; Morita, M. Application of coenzyme Q10 for accelerating soft tissue wound healing after tooth extraction in rats. *Nutrients* **2014**, *6*, 5756–5769. [CrossRef] [PubMed]
15. Fouad, A.A.; Al-Mulhim, A.S.; Jresat, I. Therapeutic effect of coenzyme Q10 against experimentally-induced hepatocellular carcinoma in rats. *Environ. Toxicol. Pharmacol.* **2013**, *35*, 100–108. [CrossRef] [PubMed]
16. Kim, J.M.; Park, E. Coenzyme Q10 attenuated DMH-induced precancerous lesions in SD rats. *J. Nutr. Sci. Vitaminol.* **2010**, *56*, 139–144. [CrossRef] [PubMed]
17. Karpińska, J.; Mikołuć, B.; Motkowski, R.; Piotrowska-Jastrzebska, J. HPLC method for simultaneous determination of retinol, alpha-tocopherol and coenzyme Q10 in human plasma. *J. Pharm. Biomed. Anal.* **2006**, *42*, 232–236. [CrossRef] [PubMed]
18. Littarru, G.P.; Mosca, F.; Fattorini, D.; Bompadre, S. Method to Assay Coenzyme Q10 in Blood Plasma or Blood Serum. U.S. Patent 7303921, 4 December 2007.
19. Botsoglou, N.A. Rapid, sensitive, and specific thiobarbituric acid method for measuring lipid peroxidation in animal tissue, food and feedstuff samples. *J. Agric. Food Chem.* **1994**, *42*, 1931–1937. [CrossRef]
20. Paglia, D.; Valentine, W. Studies on the qualitative characterization of erythrocyte glutathione peroxidase. *J. Lab. Clin. Med.* **1967**, *70*, 159–169.
21. Marklund, S.; Marklund, G. Involvement of superoxide anion radical in autoxidation of pyrogallol and a convenient assay for superoxide dismutase. *Eur. J. Biochem.* **1974**, *47*, 469–474. [CrossRef] [PubMed]
22. Aebi, H. Catalase in vitro. *Methods Enzymol.* **1984**, *105*, 121–126. [PubMed]
23. Molyneux, S.L.; Young, J.M.; Florkowski, C.M.; Lever, M.; Georgr, P.M. Coenzyme Q10: Is there a clinical role and a case for measurement? *Clin. Biochem. Rev.* **2008**, *29*, 71–82. [PubMed]
24. Lee, B.J.; Huang, Y.C.; Chen, S.J.; Lin, P.T. Coenzyme Q10 supplements reduce oxidative stress and increase activities of antioxidant enzymes in patients with coronary artery disease. *Nutrition* **2012**, *28*, 250–255. [CrossRef] [PubMed]

25. Lee, B.J.; Huang, Y.C.; Chen, S.J.; Lin, P.T. Effects of coenzyme Q10 supplementation on inflammatory markers (high sensitivity C-reactive protein, interleukin-6 and homocysteine) in patients with coronary artery. *Nutrition* **2012**, *28*, 767–772. [CrossRef] [PubMed]
26. Lee, B.J.; Tseng, Y.F.; Yen, C.H.; Lin, P.T. Effects of coenzyme Q10 supplementation (300 mg/day) on antioxidation and anti-inflammation in coronary artery disease patients during statins therapy: A randomized, placebo-controlled trial. *Nutr. J.* **2013**, *12*, 142. [CrossRef] [PubMed]
27. Yahya, R.S.; Ghanem, O.H.; Foyouh, A.A.; Atwa, M.; Enany, S.A. Role of interleukin-8 and oxidative stress in patients with hepatocellular carcinoma. *Clin. Lab.* **2013**, *59*, 969–976. [PubMed]
28. Belghiti, J.; Kianmanesh, R. Surgical treatment of hepatocellular carcinoma. *HPB* **2005**, *7*, 42–49. [CrossRef] [PubMed]
29. Makuuchi, M.; Sano, K. The surgical approach to HCC: Our progress and results in Japan. *Liver Transpl.* **2004**, *10*, S46–S52. [CrossRef] [PubMed]
30. Poon, R.T.; Fan, S.T.; Lo, C.M.; Ng, I.O.; Liu, C.L.; Lam, C.M.; Wong, J. Improving survival results after resection of hepatocellular carcinoma: A prospective study of 377 patients over 10 years. *Ann. Surg.* **2001**, *234*, 63–70. [CrossRef] [PubMed]
31. Liu, H.T.; Huang, Y.C.; Cheng, S.B.; Huang, Y.T.; Lin, P.T. Effects of coenzyme Q10 supplementation on antioxidant capacity and inflammation in hepatocellular carcinoma patients after surgery: A randomized, placebo-controlled trial. *Nutr. J.* **2016**, *15*, 85. [CrossRef] [PubMed]
32. Cannistrà, M.; Grande, R.; Ruggiero, M.; Novello, M.; Zullo, A.; Bonaiuto, E.; Vaccarisi, S.; Cavallari, G.; Serra, R.; Nardo, B. Resection of hepatocellular carcinoma in elderly patients and the role of energy balance. *Int. J. Surg.* **2016**, *33*, S119–S125. [CrossRef] [PubMed]
33. Muriel, P. Role of free radicals in liver diseases. *Hepatol. Int.* **2009**, *3*, 526–536. [CrossRef] [PubMed]
34. Lawrence, T. The nuclear factor NF-κB pathway in inflammation. *Cold Spring Harb. Perspect. Biol.* **2009**, *1*, a001651. [CrossRef] [PubMed]
35. Li, S.; Tan, H.Y.; Wang, N.; Zhang, Z.J.; Lao, L.; Wong, C.W.; Feng, Y. The role of oxidative stress and antioxidants in liver diseases. *Int. J. Mol. Sci.* **2015**, *16*, 26087–26124. [CrossRef] [PubMed]

nutrients

MDPI

Article

Preventive Effects of Drinking Hydrogen-Rich Water on Gingival Oxidative Stress and Alveolar Bone Resorption in Rats Fed a High-Fat Diet

Toshiki Yoneda [1], Takaaki Tomofuji [1,2], Muneyoshi Kunitomo [1], Daisuke Ekuni [1,*], Koichiro Irie [1], Tetsuji Azuma [1], Tatsuya Machida [1], Hisataka Miyai [1], Kouhei Fujimori [1] and Manabu Morita [1]

[1] Department of Preventive Dentistry, Okayama University Graduate School of Medicine, Dentistry and Pharmaceutical Sciences, 2-5-1 Shikata-cho, Kita-ku, Okayama 700-8558, Japan; de17057@s.okadai.jp (T.Y.); tomofu@md.okayama-u.ac.jp (T.T.); de19013@s.okayama-u.ac.jp (M.K.); coichiro@md.okayama-u.ac.jp (K.I.); tetsuji@md.okayama-u.ac.jp (T.A.); de17046@s.okadai.jp (T.M.); plzs3rog@okayama-u.ac.jp (H.M.); pyyq1hgd@s.okayama-u.ac.jp (K.F.); mmorita@md.okayama-u.ac.jp (M.M.)

[2] Advanced Research Center for Oral and Craniofacial Sciences, Okayama University Dental School, 2-5-1 Shikata-cho, Kita-ku, Okayama 700-8558, Japan

* Correspondence: dekuni7@md.okayama-u.ac.jp; Tel.: +81-86-235-6712

Received: 29 November 2016; Accepted: 11 January 2017; Published: 13 January 2017

Abstract: Obesity induces gingival oxidative stress, which is involved in the progression of alveolar bone resorption. The antioxidant effect of hydrogen-rich water may attenuate gingival oxidative stress and prevent alveolar bone resorption in cases of obesity. We examined whether hydrogen-rich water could suppress gingival oxidative stress and alveolar bone resorption in obese rats fed a high-fat diet. Male Fischer 344 rats (n = 18) were divided into three groups of six rats each: a control group (fed a regular diet and drinking distilled water) and two experimental groups (fed a high-fat diet and drinking distilled water or hydrogen-rich water). The level of 8-hydroxydeoxyguanosine was determined to evaluate oxidative stress. The bone mineral density of the alveolar bone was analyzed by micro-computerized tomography. Obese rats, induced by a high-fat diet, showed a higher gingival level of 8-hydroxydeoxyguanosine and a lower level of alveolar bone density compared to the control group. Drinking hydrogen-rich water suppressed body weight gain, lowered gingival level of 8-hydroxydeoxyguanosine, and reduced alveolar bone resorption in rats on a high-fat diet. The results indicate that hydrogen-rich water could suppress gingival oxidative stress and alveolar bone resorption by limiting obesity.

Keywords: alveolar bone loss; obesity; oxidative stress; hydrogen-rich water; animal disease model

1. Introduction

Obesity, defined as abnormal or excessive fat accumulation that increases the risk of chronic disease, has been increasingly linked with periodontal disease. Reports show that individuals who become obese have a higher risk of developing periodontal disease (relative risk (RR) = 1.33, 95% confidence interval (CI) = 1.21–1.47) compared with counterparts of normal weight [1]. Obese individuals have also been shown to have a significantly higher risk of experiencing periodontal disease progression than individuals with normal weight after adjusting for important co-factors (RR = 1.36, 95% CI = 1.04–1.78) [2]. These observations indicate that obesity is a risk for periodontal disease.

Obesity is associated with a systemic increase in reactive oxygen species (ROS) production [3,4]. Although ROS are products of normal cellular metabolism, overproduction of ROS induces oxidative stress by damaging DNA, lipids, and protein [5]. Oxidative stress plays a crucial role in the pathogenesis

of a number of diseases, including periodontal disease [6]. In vitro studies have shown that oxidative stress stimulates osteoclast differentiation [7,8]. Animal studies have also suggested that oxidative stress is involved in the progression of alveolar bone resorption [9–12]. In a recent review, the basis for the relationship between obesity and periodontitis lies at a fundamental intracellular level, which includes oxidative stress [13]. Thus, gingival oxidative stress due to obesity may induce the progression of periodontal disease through increased alveolar bone resorption.

Molecular hydrogen is an antioxidant that can reduce oxidative stress [14], and drinking hydrogen-rich water (HW) can increase the concentration of molecular hydrogen in blood and tissues [15]. In dentistry, animal studies have demonstrated that HW can reduce gingival oxidative stress following aging [16] and periodontal disease [17]. A recent study also revealed that drinking HW activated the gene expression of antioxidant defense, contributing to an acceleration of oral mucosal wound healing in rats [18]. These studies used rats with normal weight. Therefore, the antioxidative effect of HW may offer clinical benefits even in obese rats by limiting obesity-induced oxidative stress. However, it is unclear how HW affects gingival oxidative stress and alveolar bone resorption resulting from obesity.

In the present study, we hypothesized that drinking HW might prevent gingival oxidative stress and alveolar bone resorption in obesity. 8-Hydroxydeoxyguanosine (8-OHdG), which is formed when the guanine in DNA undergoes oxidative damage, is generally accepted as a reliable indicator of oxidative stress [19]. In addition, feeding test subjects a high-fat diet is one of the useful experimental models to investigate periodontal disease progression in obesity [20,21]. The purpose of the present study was to investigate the effects of HW on gingival 8-OHdG levels and alveolar bone resorption in obese rats fed a high-fat diet.

2. Materials and Methods

2.1. Animals

Male Fischer 344 rats (8 weeks old) were used in this study. The rats were housed in an air-conditioned room (23–25 °C) with a 12 h light–dark cycle. The experiments were performed in accordance with the institutional guidelines of the Animal Research Control Committee of Okayama University (OKA-2014200).

2.2. Experimental Design

The rats were randomly divided into three groups of six rats each: For the control group, rats were given pure water (distilled water) and a regular diet (MF, Oriental Yeast Co. Ltd., Osaka, Japan); for the high-fat diet (HFD) group, rats were given pure water and a high-fat diet (F2HFD1, Oriental Yeast Co. Ltd., Osaka, Japan) [22]; for the HFD + HW group, rats were given HW and a high-fat diet. In this study, we did not induce experimental periodontitis in all groups. Pure water or HW was given to the rats every 12 h, morning and night, in a closed glass vessel until they reached 20 weeks old. HW was given immediately after it was prepared. The glass vessel with sipper tube was attached to the cage, and the rats drank water using the sipper tube [16,17]. HW was prepared by electrolysis of water using BLUE OCEAN H2mini (HWP-200WWD, Tech. Co. Ltd., Tokyo, Japan). Water was electrolyzed to afford the following chemical products: $2H_2O \rightarrow 2H_2 + O_2$. We measured the hydrogen concentration in HW (1 min and 24 h after electrolysis of water) using a dissolved hydrogen meter (KM2100DH, Kyoei Electronic Laboratory Co. Ltd., Saitama, Japan) three times at each stage. The hydrogen concentration (mean $\pm$ standard deviation, μg/L) after 1 min was 301.7 $\pm$ 65.1, and that after 24 h was 186.3 $\pm$ 55 μg/L.

After the experimental period, the animals were sacrificed under deep anesthesia with diethyl ether.

2.3. Measurements of Serum Parameters

Blood samples were collected from the heart. Serum was separated by centrifugation at 1500× *g* for 15 min and stored at −80 °C until analysis. Serum total cholesterol, very low-density lipoprotein

(VLDL) cholesterol, low-density lipoprotein (LDL) cholesterol, high-density lipoprotein (HDL) cholesterol, total triglycerides, VLDL triglycerides, LDL triglycerides, and HDL triglycerides were measured using a gel permeation high performance liquid chromatography system (Skylight Biotech, Akita, Japan) [23]. The level of serum 8-OHdG was also analyzed using an ELISA kit (Japan Institute for the Control of Aging, Shizuoka, Japan) [24].

2.4. Measurements of Gingival Level of 8-OHdG

Mitochondrial DNA was isolated from gingival tissue of maxillary molar regions using a DNA extractor kit (Wako Pure Chemical Industries, Osaka, Japan). The level of 8-OHdG in the isolated mitochondrial DNA was analyzed using an ELISA kit (Japan Institute for the Control of Aging, Shizuoka, Japan) [24].

2.5. Micro-Computed Tomography (CT) Assessment of Mandible

Mandibular bones were scanned with a micro-CT device (RmCT, Rigaku, Tokyo, Japan) with the following settings: (1) a slice thickness of 50 μm; (2) a voltage of 90 kV; and (3) an electrical current of 0.1 mA. Three-dimensional images were obtained using a bone analysis system (TRI/3D-BON, Ratoc, Tokyo, Japan). The furcation area of the first molar root was taken for analysis of the percentage of bone volume/total volume (BV/TV%), trabecular number (Tb. N), trabecular thickness (Tb. Th), and trabecular separation (Tb. Sp). The distance between the cemento-enamel junction (CEJ) and the alveolar bone crest (ABC) was measured at 5 points for each mandibular molar (first molar [M1] to third molar [M3]) as alveolar bone resorption [25]. The distances from these 5 points were summed as alveolar bone resorption (Figure 1) [25].

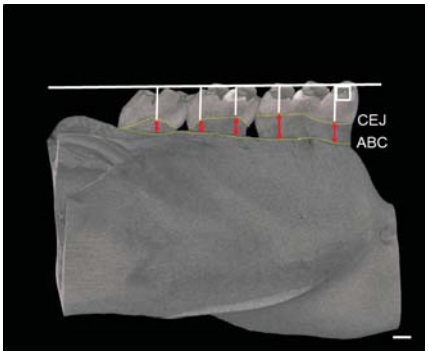

Figure 1. Measurement regions for alveolar bone resorption in rats. The μCT image shows how to measure the distance between CEJ and ABC. The red arrowheads indicate the degree of alveolar bone resorption. CEJ: cemento-enamel junction; ABC: alveolar bone crest. Bar = 500 μm.

2.6. RNA Isolation and PCR Array Analysis

Total RNA of the HFD group and the HFD + HW group was extracted from gingival tissue (100 mg per rat) of the mandibular molar regions using the mirVavaTM PARISTM Kit (Life Technologies, Carlsbad, CA, USA). RNA of the same group was pooled (two rats per one sample). RNA content was measured with a spectrophotometer (Beckman Du 640) (Beckman Coulter, Brea, CA, USA). Total RNA (1 μg RNA from each sample) was used for reverse-transcription with an RT2 First Strand Kit (Qiagen, Hilden, Germany). To profile gene expression, PCR array analysis was performed using an RT2 Profiler PCR Array (rat oxidative stress, PARN-065ZA) (Qiagen) and an RT2 SYBR Green qPCR Master Mix (Qiagen) on an Mx3000P Real-Time QPCR System (Agilent Technologies, Tokyo, Japan). The cycle threshold (*Ct*) values were obtained, and data of the gene expression were analyzed with an online analysis tool (RT2 Profiler

PCR array Data Analysis version 3.5, http://pcrdataanalysis.sabiosciences.com/pcr/arrayanalysis.php) (Qiagen). Data were screened for the expression of 84 genes related to oxidative stress. Fold change values up- or down regulation (HFD + HW group/HFD group) were calculated from gene expression ($2 - \Delta Ct$).

2.7. Statistical Analysis

Data were expressed as means ± standard deviations. A one-way ANOVA followed by Tukey's method was used for the three-group comparison using a statistical software package (SPSS version 22.0; IBM, Tokyo, Japan). A Student's *t*-test was used for PCR array analysis.

3. Results

3.1. Results of Body Weight and Gain of Body Weight

At baseline, there were no significant differences among the three groups with regard to body weight. At 20 weeks old, the HFD group, but not the HFD + HW group, showed greater body weight than did the control group ($p < 0.05$) (Table 1). The body weight gain during the experimental period was higher in the HFD group than that in the control group ($p < 0.05$) and that the HFD + HW group ($p < 0.05$). There was no significant difference in body weight gain between that of the control group and that of the HFD + HW group during the experimental period.

Table 1. Changes in body weight during the experimental period.

	Control	HFD	HFD + HW
body weight (baseline) (g)	269 ± 12	278 ± 14	276 ± 9
body weight (20 weeks old) (g)	338 ± 14	360 ± 16 *	342 ± 12
body weight gain (20 weeks old—base line) (g)	69 ± 8	82 ± 10 *	66 ± 7 †

Values are presented as the mean ± standard deviation of six rats. * $p < 0.05$ compared with control group, † $p < 0.05$ compared with the HFD group. The *p*-value was calculated by Tukey's methods.

3.2. Results of Serum Levels of Cholesterols and 8-OHdG

Serum levels of total cholesterol and VLDL cholesterol in the HFD group and serum levels of VLDL cholesterol in the HFD + HW group were significantly higher than those in the control group ($p < 0.05$) (Table 2). The serum level of total triglycerides in the HFD + HW group was significantly lower than that in the control group ($p < 0.05$). Serum levels of VLDL triglycerides were significantly lower in the HFD group in the HFD + HW group than those in the control group ($p < 0.05$). On the other hand, no significant differences in serum cholesterol and triglyceride between those in the HFD and the HFD + HW groups were found. In addition, serum levels of 8-OHdG in the HFD group were significantly higher than those in the control group ($p < 0.05$), and those in the HFD + HW group was significantly lower than those in the HFD group ($p < 0.05$).

Table 2. Serum parameters.

	Control	HFD	HFD + HW
total cholesterol (mg/dL)	43.2 ± 24.8	101.1 ± 53.7 *	94.3 ± 18.0
VLDL cholesterol (mg/dL)	5.2 ± 3.3	34.6 ± 20.3 *	34.1 ± 6.4 *
LDL cholesterol (mg/dL)	14.9 ± 9.6	15.6 ± 7.7	16.8 ± 4.2
HDL cholesterol (mg/dL)	21.7 ± 11.5	27.3 ± 11.9	27.9 ± 5.2
total triglycerides (mg/dL)	65.3 ± 46.8	27.6 ± 14.3	19.1 ± 5.3 *
VLDL triglycerides (mg/dL)	43.3 ± 29.5	14.2 ± 8.0 *	10.1 ± 3.4 *
LDL triglycerides (mg/dL)	4.88 ± 3.4	2.86 ± 1.3	1.98 ± 0.4
HDL triglycerides (mg/dL)	3.6 ± 2.1	3.0 ± 1.1	2.6 ± 0.5
8-OHdG (ng/mL)	0.12 ± 0.03	0.17 ± 0.05 *	0.12 ± 0.03 †

Values are presented as the mean ± standard deviation of six rats. * $p < 0.05$ compared with control group, † $p < 0.05$ compared with the HFD group. The *p*-value was calculated by Tukey's methods.

3.3. Results of Gingival Level of 8-OHdG

Gingival levels of 8-OHdG in the HFD group and the HFD + HW group were higher than those in the control group ($p < 0.05$) (Figure 2). The gingival level of 8-OHdG in the HFD + HW group was also lower than that in the HFD group ($p < 0.05$).

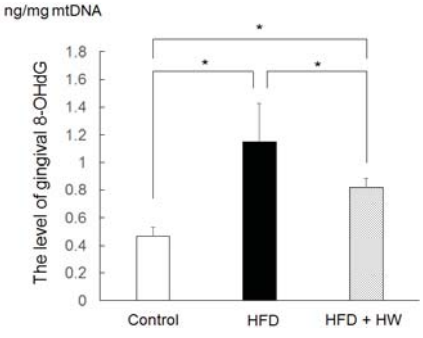

Figure 2. The level of gingival 8-OHdG in rats. Values are presented as the mean ± standard deviation of six rats. * $p < 0.05$, using Tukey's methods.

3.4. Results of Micro-CT Analyses of Mandibular Bone

The HFD group, compared with the control group, showed a greater distance between the CEJ-ABC ($p < 0.05$), a lower BT/TV ($p < 0.05$), and a higher Tb. Sp ($p < 0.05$) (Figure 3). The HFD + HW group, compared with the HFD group, also showed a lower distance between the CEJ-ABC ($p < 0.05$) and a greater BT/TV ($p < 0.05$), and these values did not differ from the control group. As for Tb. N and Tb. Th, there were no significant differences among the three groups.

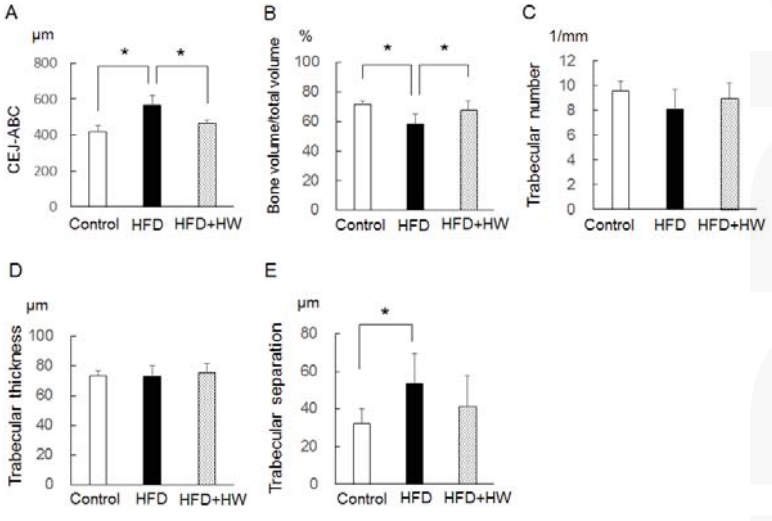

Figure 3. Bone morphogenetic analyses of rat mandible at 20 weeks old. (**A**) Distance between CEJ-ABC; (**B**) percentage of bone volume/total volume; (**C**) trabecular number; (**D**) trabecular thickness; (**E**) trabecular separation. Values are presented as the mean ± standard deviation of six rats. * $p < 0.05$, using Tukey's methods.

3.5. Results of Changes in Oxidative Stress-Related Gene Expression

In the PCR array analysis, four genes involved in oxidative stress showed significant differential gene expression between the HFD and HFD + HW groups, with the values of fold upregulation (>2) or downregulation (<−2) (Table 3). Of these, three genes (isocitrate dehydrogenase 1 (Idh1), superoxide dismutase (Sod) 2, and Sod3) were upregulated and one gene (Fanconi anemia group C (Fancc)) was downregulated in the HFD + HW group. This section may be divided by subheadings. It should provide a concise and precise description of the experimental results, their interpretation, and the experimental conclusions that can be drawn.

Table 3. Differentially expressed genes involved in oxidative stress of gingival tissue between the HFD group and the HFD + HW group.

Gene Symbol	Description	Fold Up- or Down Regulation (HFD+HW Group/HFD Group)	*p*-Value
Idh1	isocitrate dehydrogenase (NADP(+)) 1, cytosolic	4.04	0.014
Sod2	superoxide dismutase 2	2.25	0.032
Sod3	superoxide dismutase 3	3.35	0.034
Fancc	Fanconi anemia, complementation group C	−2.88	0.046

The *p*-value was calculated by Student's *t*-test.

4. Discussion

In the present study, the rats on a high-fat diet, compared with the control rats, showed increased body weight gain and higher levels of serum and gingival 8-OHdG at 20 weeks. 8-OHdG is an indicator of oxidative stress [18]. These findings indicate that, in the obese rats, a high-fat diet induced a systemic increase in oxidative stress. On the other hand, drinking HW suppressed the effects of a high-fat diet on body weight gain, and showed lower levels of serum and gingival 8-OHdG compared with the obese rats. It is feasible that HW suppresses obesity, which in turn might inhibit a systemic increase in oxidative stress, including gingival oxidative stress.

Some studies have investigated the anti-oxidative effects of HW in obesity. For instance, one animal study has revealed that drinking HW reduced obesity and reduced hepatic oxidative stress in a mice model [26]. A clinical study also showed that consumption of HW decreased the level of urinary lipid peroxidation significantly from baseline to Week 8 in obese subjects [27]. These are consistent with our findings, which exhibited that drinking HW prevented obesity and gingival oxidative stress.

In our findings, the obese rats on a high-fat diet showed a greater distance between the CEJ-ABC, a lower BT/TV, and a higher Tb. Sp than the control rats, suggesting that the progression of alveolar bone resorption follows obesity. The results also revealed that the rats fed a high-fat diet and HW, compared with the HFD rats showed a lower distance between the CEJ-ABC and a greater BT/TV. Gingival oxidative stress is involved in the progression of alveolar bone resorption [11,12]. Suppression of obesity by drinking HW may attenuate alveolar bone resorption by limiting gingival oxidative stress.

This study exhibited that drinking HW upregulated the gene expression of Sod2 and Sod3 in gingival tissues. Sod2 and Sod3 are antioxidant enzymes that catalyze the conversion of superoxide radicals into hydrogen peroxide and oxygen [28,29]. This suggests that the increased antioxidative properties of gingival tissues by HW might also protect periodontal tissues from a systemic increase in oxidative stress.

The present results also showed that HW downregulated the gene expression of Fancc. Since Fancc is considered an oxidative stress responsive gene [30], and it is suggested that the downregulation of Fancc reflected decreased gingival oxidative stress.

It is reported that drinking HW can improve cholesterol metabolism [27], which may have a direct influence on bone resorption [31]. However, in our findings, there were no significant differences in serum cholesterol and triglyceride between the rats with and without HW intake. These suggest

that gingival oxidative stress and alveolar bone resorption were not related to serum cholesterol and triglyceride in our animal model.

In this study, the rats on a high-fat diet tended to exhibit lower levels of total and VLDL triglycerides in serum compared to the control rats. These findings are similar to those of the previous study in birds on a high-fat diet [32]. The reduced serum triglyceride concentrations may reflect a possible metabolic overcompensation in response to the added dietary fat [33].

A clinical study showed that obesity may influence periodontal tissue destruction and disease severity by increasing the level of oxidative stress in the presence of periodontal disease [34]. Another study also suggested that periodontal oxidative stress generated by obesity seems to be associated with periodontal disease [35]. Such evidence supports the concept that obesity may lead to the progression of periodontal disease by increasing oxidative stress. On the other hand, the present report showed that drinking HW suppressed obesity, gingival oxidative stress, and alveolar bone resorption in rat models. Our previous study also found that exercise training prevented obesity and gingival oxidative stress in rats on a high-fat diet [22]. Anti-obesity therapy to reduce oxidative stress may be useful in preventing periodontal disease related to obesity.

In our previous study, broccoli supplementation inhibited the effects of a high-cholesterol diet on osteoclast differentiation in the periodontal tissue [36]. It is also reported that supplementation of coenzyme 10 counteracted the negative effects of n-6 polyunsaturated fatty acid on age-related alveolar bone loss [37]. Furthermore, the present study demonstrated that drinking HW attenuates alveolar bone resorption related to obesity. Action of adequate nutrient consumption would be important to maintain and/or improve periodontal health.

When taking medicine, it is necessary to be careful about side effects. However, HW has no known side effects in previous animal and human studies [16–18,27]. Therefore, HW may constitute useful preventive treatment against periodontal disease related to obesity without side effects.

Our study has some limitations. For instance, no data were collected with regard to the circulating inflammatory molecules, such as tumor necrosis factor-α. Obesity could indirectly result in an increase in the circulation of inflammatory molecules that could augment the inflammation induced by bacterial pathogens. In addition, while we showed preventive effects of HW on obesity and gingival oxidative stress, we could not fully elucidate the relationship between these pathological mechanisms and the effects of HW. Further studies are needed to clarify this point.

5. Conclusions

In conclusion, within the limits of the study, drinking HW can inhibit gingival oxidative stress induced by obesity, and thus prevent alveolar bone resorption in rat models. However, clinical trials will be necessary to clarify whether drinking HW can prevent obesity-related complications, including periodontal disease.

Acknowledgments: This work was supported by Grants-in-Aid for Scientific Research (No. 16K11855, No. 16K11856 and No. 16K20693) from the Ministry of Education, Culture, Sports, Science and Technology, Tokyo, Japan.

Author Contributions: Toshiki Yoneda, Takaaki Tomofuji, Daisuke Ekuni, Tetsuji Azuma, and Manabu Morita conceived and designed the experiments. Toshiki Yoneda, Takaaki Tomofuji, Koichiro Irie, Muneyoshi Kunitomo, Tetsuji Azuma, Tatsuya Machida, Hisataka Miyai, and Kouhei Fujimori performed the experiments and contributed reagents/materials/analysis tools. Toshiki Yoneda, Takaaki Tomofuji, Daisuke Ekuni, and Manabu Morita wrote the manuscript. All authors have read and approved the final manuscript.

Conflicts of Interest: The authors declare no conflict of interest.

References

1. Nascimento, G.G.; Leite, F.R.; Do, L.G.; Peres, K.G.; Correa, M.B.; Demarco, F.F.; Peres, M.A. Is weight gain associated with the incidence of periodontitis? A systematic review and meta-analysis. *J. Clin. Periodontol.* **2015**, *42*, 495–505. [CrossRef] [PubMed]

2. Gaio, E.J.; Haas, A.N.; Rosing, C.K.; Oppermann, R.V.; Albandar, J.M.; Susin, C. Effect of obesity on periodontal attachment loss progression: A 5-year population-based prospective study. *J. Clin. Periodontol.* **2016**, *43*, 557–565. [CrossRef] [PubMed]
3. Fernandez-Sanchez, A.; Madrigal-Santillan, E.; Bautista, M.; Esquivel-Soto, J.; Morales-Gonzalez, A.; Esquivel-Chirino, C.; Durante-Montiel, I.; Sanchez-Rivera, G.; Valadez-Vega, C.; Morales-Gonzalez, J.A. Inflammation, oxidative stress, and obesity. *Int. J. Mol. Sci.* **2011**, *12*, 3117–3132. [CrossRef] [PubMed]
4. Manna, P.; Jain, S.K. Obesity, oxidative stress, adipose tissue dysfunction, and the associated health risks: Causes and therapeutic strategies. *Metab. Syndr. Relat. Disord.* **2015**, *13*, 423–444. [CrossRef] [PubMed]
5. Halliwell, B. Free radicals, antioxidants, and human disease: Curiosity, cause, or consequence? *Lancet* **1994**, *344*, 721–724. [CrossRef]
6. Chapple, I.L. Reactive oxygen species and antioxidants in inflammatory diseases. *J. Clin. Periodontol.* **1997**, *24*, 287–296. [CrossRef] [PubMed]
7. Hyeon, S.; Lee, H.; Yang, Y.; Jeong, W. Nrf2 deficiency induces oxidative stress and promotes RANKL-induced osteoclast differentiation. *Free Radic. Biol. Med.* **2013**, *65*, 789–799. [CrossRef] [PubMed]
8. Bartell, S.M.; Kim, H.N.; Ambrogini, E.; Han, L.; Iyer, S.; Serra Ucer, S.; Rabinovitch, P.; Jilka, R.L.; Weinstein, R.S.; Zhao, H.; et al. FoxO proteins restrain osteoclastogenesis and bone resorption by attenuating H_2O_2 accumulation. *Nat. Commun.* **2014**, *5*, 3773. [CrossRef] [PubMed]
9. Sanbe, T.; Tomofuji, T.; Ekuni, D.; Azuma, T.; Tamaki, N.; Yamamoto, T. Oral administration of vitamin C prevents alveolar bone resorption induced by high dietary cholesterol in rats. *J. Periodontol.* **2007**, *78*, 2165–2170. [CrossRef] [PubMed]
10. Kanzaki, F.; Shinohara, F.; Kajiya, M.; Kodama, T. The Keap1/Nrf2 protein axis plays a role in osteoclast differentiation by regulating intracellular reactive oxygen species signaling. *J. Biol. Chem.* **2013**, *288*, 23009–23020. [CrossRef] [PubMed]
11. Ohnishi, T.; Bandow, K.; Kakimoto, K.; Machigashira, M.; Matsuyama, T.; Matsuguchi, T. Oxidative stress causes alveolar bone loss in metabolic syndrome model mice with type 2 diabetes. *J. Periodontal Res.* **2009**, *44*, 43–51. [CrossRef] [PubMed]
12. Bosca, A.B.; Miclaus, V.; Ilea, A.; Campian, R.S.; Rus, V.; Ruxanda, F.; Ratiu, C.; Uifalean, A.; Parvu, A.E. Role of nitro-oxidative stress in the pathogenesis of experimental rat periodontitis. *Clujul Med.* **2016**, *89*, 150–159. [CrossRef] [PubMed]
13. Bullon, P.; Newman, H.N.; Battino, M. Obesity, diabetes mellitus, atherosclerosis and chronic periodontitis: A shared pathology via oxidative stress and mitochondrial dysfunction? *Periodontology 2000* **2014**, *64*, 139–153. [CrossRef] [PubMed]
14. Ohsawa, I.; Ishikawa, M.; Takahashi, K.; Watanabe, M.; Nishimaki, K.; Yamagata, K.; Katsura, K.; Katayama, Y.; Asoh, S.; Ohta, S. Hydrogen acts as a therapeutic antioxidant by selectively reducing cytotoxic oxygen radicals. *Nat. Med.* **2007**, *13*, 688–694. [CrossRef] [PubMed]
15. Sobue, S.; Yamai, K.; Ito, M.; Ohno, K.; Ito, M.; Iwamoto, T.; Qiao, S.; Ohkuwa, T.; Ichihara, M. Simultaneous oral and inhalational intake of molecular hydrogen additively suppresses signaling pathways in rodents. *Mol. Cell Biochem.* **2015**, *403*, 231–241. [CrossRef] [PubMed]
16. Tomofuji, T.; Kawabata, Y.; Kasuyama, K.; Endo, Y.; Yoneda, T.; Yamane, M.; Azuma, T.; Ekuni, D.; Morita, M. Effects of hydrogen-rich water on aging periodontal tissues in rats. *Sci. Rep.* **2014**, *4*, 5534. [CrossRef] [PubMed]
17. Kasuyama, K.; Tomofuji, T.; Ekuni, D.; Tamaki, N.; Azuma, T.; Irie, K.; Endo, Y.; Morita, M. Hydrogen-rich water attenuates experimental periodontitis in a rat model. *J. Clin. Periodontol.* **2011**, *38*, 1085–1090. [CrossRef] [PubMed]
18. Tamaki, N.; Orihuela-Campos, R.C.; Fukui, M.; Ito, H.O. Hydrogen-rich water intake accelerates oral palatal wound healing via activation of the Nrf2/antioxidant defense pathways in a rat model. *Oxid. Med. Cell. Longev.* **2016**, *2016*, 5679040. [CrossRef] [PubMed]
19. Kasai, H. Chemistry-based studies on oxidative DNA damage: Formation, repair, and mutagenesis. *Free Radic. Biol. Med.* **2002**, *33*, 450–456. [CrossRef]
20. Fujita, Y.; Maki, K. High-fat diet-induced obesity triggers alveolar bone loss and spontaneous periodontal disease in growing mice. *BMC Obes.* **2016**, *3*. [CrossRef] [PubMed]

21. Muluke, M.; Gold, T.; Kiefhaber, K.; Al-Sahli, A.; Celenti, R.; Jiang, H.; Cremers, S.; van Dyke, T.; Schulze-Spate, U. Diet-induced obesity and its differential impact on periodontal bone loss. *J. Dent. Res.* **2016**, *95*, 223–229. [CrossRef] [PubMed]
22. Azuma, T.; Tomofuji, T.; Endo, Y.; Tamaki, N.; Ekuni, D.; Irie, K.; Kasuyama, K.; Kato, T.; Morita, M. Effects of exercise training on gingival oxidative stress in obese rats. *Arch. Oral Biol.* **2011**, *56*, 768–774. [CrossRef] [PubMed]
23. Usui, S.; Yasuda, H.; Koketsu, Y. Lipoprotein cholesterol and triglyceride concentrations associated with dog body condition score; effect of recommended fasting duration on sample concentrations in Japanese private clinics. *J. Vet. Med. Sci.* **2015**, *77*, 1063–1069. [CrossRef] [PubMed]
24. Ekuni, D.; Tomofuji, T.; Tamaki, N.; Sanbe, T.; Azuma, T.; Yamanaka, R.; Yamamoto, T.; Watanabe, T. Mechanical stimulation of gingiva reduces plasma 8-OHdG level in rat periodontitis. *Arch. Oral Biol.* **2008**, *53*, 324–329. [CrossRef] [PubMed]
25. Koide, M.; Kobayashi, Y.; Ninomiya, T.; Nakamura, M.; Yasuda, H.; Arai, Y.; Okahashi, N.; Yoshinari, N.; Takahashi, N.; Udagawa, N. Osteoprotegerin-deficient male mice as a model for severe alveolar bone loss: Comparison with RANKL-overexpressing transgenic male mice. *Endocrinology* **2013**, *154*, 773–782. [CrossRef] [PubMed]
26. Kamimura, N.; Nishimaki, K.; Ohsawa, I.; Ohta, S. Molecular hydrogen improves obesity and diabetes by inducing hepatic FGF21 and stimulating energy metabolism in db/db mice. *Obesity* **2011**, *19*, 1396–1403. [CrossRef] [PubMed]
27. Nakao, A.; Toyoda, Y.; Sharma, P.; Evans, M.; Guthrie, N. Effectiveness of hydrogen rich water on antioxidant status of subjects with potential metabolic syndrome-an open label pilot study. *J. Clin. Biochem. Nutr.* **2010**, *46*, 140–149. [CrossRef] [PubMed]
28. Zelko, I.N.; Mariani, T.J.; Folz, R.J. Superoxide dismutase multigene family: A comparison of the CuZn-SOD (SOD1), Mn-SOD (SOD2), and EC-SOD (SOD3) gene structures, evolution, and expression. *Free Radic. Biol. Med.* **2002**, *33*, 337–349. [CrossRef]
29. Landis, G.N.; Tower, J. Superoxide dismutase evolution and life span regulation. *Mech. Ageing Dev.* **2005**, *126*, 365–379. [CrossRef] [PubMed]
30. Pagano, G.; Youssoufian, H. Fanconi anaemia proteins: Major roles in cell protection against oxidative damage. *Bioessays* **2003**, *25*, 589–595. [CrossRef] [PubMed]
31. Tanko, L.B.; Bagger, Y.Z.; Nielsen, S.B.; Christiansen, C. Does serum cholesterol contribute to vertebral bone loss in postmenopausal women? *Bone* **2003**, *32*, 8–14. [CrossRef]
32. Donaldson, J.; Pillay, K.; Madziva, M.T.; Erlwanger, K.H. The effect of different high-fat diets on erythrocyte osmotic fragility, growth performance and serum lipid concentrations in male, Japanese quail (*Coturnix coturnix japonica*). *J. Anim. Physiol. Anim. Nutr.* **2014**, *99*, 281–289. [CrossRef] [PubMed]
33. Peebles, E.D.; Cheaney, J.D.; Brake, J.D.; Boyle, C.R.; Latour, M.A.; McDaniel, C.D. Effects of added lard fed to broiler chickens during the starter phase. 2. Serum lipids. *Poult. Sci.* **1997**, *76*, 1648–1654. [CrossRef] [PubMed]
34. Atabay, V.E.; Lutfioglu, M.; Avci, B.; Sakallioglu, E.E.; Aydogdu, A. Obesity and oxidative stress in patients with different periodontal status: A case-control study. *J. Periodontal Res.* **2016**. [CrossRef] [PubMed]
35. Dursun, E.; Akalin, F.A.; Genc, T.; Cinar, N.; Erel, O.; Yildiz, B.O. Oxidative stress and periodontal disease in obesity. *Medicine* **2016**, *95*, e3136. [CrossRef] [PubMed]
36. Tomofuji, T.; Ekuni, D.; Azuma, T.; Irie, K.; Endo, Y.; Yamamoto, T.; Ishikado, A.; Sato, T.; Harada, K.; Suido, H.; et al. Supplementation of broccoli or Bifidobacterium longum-fermented broccoli suppresses serum lipid peroxidation and osteoclast differentiation on alveolar bone surface in rats fed a high-cholesterol diet. *Nutr. Res.* **2012**, *31*, 301–307. [CrossRef] [PubMed]
37. Varela-Lopez, A.; Bullon, P.; Battino, M.; Ramirez-Tortosa, M.C.; Ochoa, J.J.; Cordero, M.D.; Ramirez-Tortosa, C.L.; Rubini, C.; Zizzi, A.; Quiles, J.L. Coenzyme Q protects against age-related alveolar bone loss associated to n-6 polyunsaturated fatty acid rich-diets by modulating mitochondrial mechanisms. *J. Gerontol. A Biol. Sci. Med. Sci.* **2016**, *71*, 593–600. [CrossRef] [PubMed]

nutrients

MDPI

Article

Effects of an Encapsulated Fruit and Vegetable Juice Concentrate on Obesity-Induced Systemic Inflammation: A Randomised Controlled Trial

Evan J. Williams, Katherine J. Baines, Bronwyn S. Berthon and Lisa G. Wood *

Priority Research Centre for Healthy Lungs, Hunter Medical Research Institute, University of Newcastle, Callaghan NSW 2308, Australia; evan.j.williams@uon.edu.au (E.J.W.); katherine.baines@newcastle.edu.au (K.J.B.); bronwyn.berthon@newcastle.edu.au (B.S.B.)

* Correspondence: Lisa.wood@newcastle.edu.au; Tel.: +61-240-420-147

Received: 20 December 2016; Accepted: 24 January 2017; Published: 8 February 2017

Abstract: Phytochemicals from fruit and vegetables reduce systemic inflammation. This study examined the effects of an encapsulated fruit and vegetable (F&V) juice concentrate on systemic inflammation and other risk factors for chronic disease in overweight and obese adults. A double-blinded, parallel, randomized placebo-controlled trial was conducted in 56 adults aged ≥40 years with a body mass index (BMI) ≥28 kg/m^2. Before and after eight weeks daily treatment with six capsules of F&V juice concentrate or placebo, peripheral blood gene expression (microarray, quantitative polymerase chain reaction (qPCR)), plasma tumour necrosis factor (TNF)α (enzyme-linked immunosorbent assay (ELISA)), body composition (Dual-energy X-ray absorptiometry (DEXA)) and lipid profiles were assessed. Following consumption of juice concentrate, total cholesterol, low-density lipoprotein (LDL) cholesterol and plasma TNFα decreased and total lean mass increased, while there was no change in the placebo group. In subjects with high systemic inflammation at baseline (serum C-reactive protein (CRP) ≥3.0 mg/mL) who were supplemented with the F&V juice concentrate (n = 16), these effects were greater, with decreased total cholesterol, LDL cholesterol and plasma TNFα and increased total lean mass; plasma CRP was unchanged by the F&V juice concentrate following both analyses. The expression of several genes involved in lipogenesis, the nuclear factor-κB (NF-κB) and 5′ adenosine monophosphate-activated protein kinase (AMPK) signalling pathways was altered, including phosphomevalonate kinase (PMVK), zinc finger AN1-type containing 5 (ZFAND5) and calcium binding protein 39 (CAB39), respectively. Therefore, F&V juice concentrate improves the metabolic profile, by reducing systemic inflammation and blood lipid profiles and, thus, may be useful in reducing the risk of obesity-induced chronic disease.

Keywords: obesity; systemic Inflammation; fruit and vegetable concentrate; blood lipids

1. Introduction

The global epidemic of obesity, "globesity", is rapidly becoming a major public health problem in many parts of the world [1]. In the U.S., 78.6 million adults (35% of the population) are obese [2]. Australia is not far behind, with 28% of adults being obese [3]. Obesity develops due to high caloric intake and/or inadequate energy expenditure over time, with genetic susceptibility also likely to have contributed to obesity rates [4]. Overweight and obesity are associated with an epidemic of many chronic diseases, including type 2 diabetes mellitus (T2DM), cardiovascular disease (CVD), stroke, hypertension and certain cancers [1].

Obesity is characterised by chronic, low-grade systemic inflammation, due to the release of pro-inflammatory mediators from adipose tissue [5,6]. Adipose tissue from lean individuals contains small, insulin-sensitive adipocytes, as well as tissue-resident macrophages of the alternatively-activated

phenotype (M2) [6,7]. With the development of obesity, adipose tissue becomes characterised by large insulin-resistant adipocytes accompanied by the presence of classically-activated macrophages (M1), which are pro-inflammatory [6,7]. Adipocyte hypertrophy and death, adipose tissue hypoxia and changes in immune cell populations alter adipokine secretory patterns [8]. This process leads to the development of insulin resistance [6].

In obese individuals, adipose tissue produces and secretes adipokines, such as leptin and adiponectin, and pro-inflammatory mediators, including tumour necrosis factor (TNF)α [9]. The production and release of TNFα is the first step in a cascade of pro-inflammatory mediator release [10,11]. TNFα is a mediator in energy metabolism, immune function and apoptosis [12] and increases the activation of neutrophils [13]. C-reactive protein (CRP) is another inflammatory mediator that is produced by both adipocytes and the liver, in response to cytokines, such as TNFα and interleukin (IL)-6 [14]. CRP is also positively associated with the degree of obesity [10,11] and is an independent predictor of myocardial infarction risk, stroke and T2DM [10].

Toll-like receptors (TLRs) and nuclear factor-κB (NF-κB)-associated mechanisms have been proposed as primary molecular pathways mediating adipose tissue inflammation [15]. TLRs activate NFκB [15], a transcription factor and potent inducer of gene transcription of pro-inflammatory cytokines. A plethora of inflammatory pathways is activated in obesity with mechanisms, such as, phosphorylation of mitogen-activated protein kinases (MAPKs) [16] and AMP-activated protein kinase (AMPK) activity modulating adipose tissue inflammation [17]. Peroxisome proliferator-activated receptor-α (PPARα), a nuclear receptor primarily expressed in the liver and potent inducer of fat oxidizing genes, has also been reported to reduce adipose tissue inflammation [8,18].

Systemic inflammation puts obese individuals at increased risk of chronic diseases that have an inflammatory pathology, including CVD, diabetes and cancer [19,20]. Weight loss, achieved via energy restriction, is one approach, which has been shown to correct or improve the overall metabolic profile. Weight loss significantly reduces circulating CRP [21,22], TNFα [21–25] and leptin [22]. Indeed, for every 1 kg of weight lost, there is a corresponding reduction in CRP of 0.13 mg/L [26], accompanied by improvements in systemic insulin resistance [27,28]. However, it is well accepted that achieving and maintaining weight loss is unattainable for some individuals. Hence, alternative approaches for improving the metabolic profile of obese individuals are needed.

Many studies, in both humans and animals, demonstrate that the consumption of dietary bioactive compounds found in fruit and vegetables, such as polyphenols and carotenoids, is able to improve the metabolic profile and reduce the risk of chronic diseases via signalling pathways involving NF-κB, MAPKs and AMPK [8]. A recent study in overweight individuals found that a two-fold increase in fruit and vegetable intake for 16 weeks significantly decreased body mass index (BMI) and supine systolic blood pressure and increased plasma concentrations of the antioxidants α-carotene, β-carotene and lutein [29]. Another study found that supplementing healthy individuals with 500 g of strawberries, rich in vitamin C and anthocyanins, daily for one month improved the lipid profile by decreasing total cholesterol, low-density lipoprotein (LDL) cholesterol and triglycerides, as well as decreasing markers of oxidative stress, including plasma malondialdehyde, urinary 8-OHdG and isoprostane levels [30]. There is also emerging evidence that supplements containing dietary bioactive compounds can provide similar benefits. A recent review, including 18 human trials with a total of 1363 adults, reported that fruit and vegetable concentrate supplements significantly increased serum levels of antioxidants (β-carotene, vitamins C and E), as well as folate. In addition, the supplements reduced homocysteine and markers of oxidative stress [31].

In this study, we hypothesised that obesity-associated inflammation could be suppressed using a fruit and vegetable concentrate supplement. The aim of this study was to examine the effects of an encapsulated fruit and vegetable juice concentrate on systemic inflammation and other risk factors for chronic disease in overweight and obese adults.

2. Materials and Methods

2.1. Study Design

This was a double-blinded, parallel, randomised, placebo-controlled trial in 56 subjects aged ≥40 years and with a BMI ≥28 kg/m^2, recruited from March 2014 to September 2014. Subjects were randomised to receive a fruit and vegetable (F&V) concentrate supplement (Juice Plus+® Orchard, Garden and Berry Blends) (n = 28) or placebo (n = 28) for 8 weeks. Subjects commenced a low fruit and vegetable diet (≤3 serves per day of fruit and vegetables combined) two weeks before randomisation as a washout period, and continued this diet for the duration of the study. Subjects were assessed at commencement of the study (Week 0) and again after supplementation (Week 8) at the Clinical Trials Facility at the Hunter Medical Research Institute. At both visits, anthropometric measures, blood pressure, pulse wave velocity and body composition were measured, and blood samples were collected. Subjects were non-smokers and had an absence of or irregular menses if they were female. Subjects were excluded if they were unwilling or unable to limit the intake of fruit and vegetables to no more than 3 servings/day, if they had used dietary or nutritional supplements within the previous 4 weeks, if they were current smokers, were currently participating in a weight management program or actively attempting to lose weight, were currently using any medication known to significantly influence inflammation, had an allergy to the supplement ingredients or chronic excessive alcohol consumption, which is associated with a high risk of chronic health problems, defined as ≥43 standard drinks per week for men and ≥29 drinks per week for women [32]. Unused capsules were collected at the end of the study to determine adherence with the intervention. Participants with adherence of >85% were included in the analysis, determined by the pill count back method.

2.2. Randomization

Subjects were randomly allocated to the treatment or placebo group. Subjects were screened to determine eligibility, and those eligible were assigned a unique study number according to the randomisation schedule. The randomisation schedule was computer generated with blocks of variable size and stratified by BMI and gender. Randomisation was managed by an independent statistician at the Hunter Medical Research Institute. During the treatment phase, both the subjects and the investigators were blinded to the allocation.

2.3. Study Supplement

The F&V concentrate capsules contained a blended fruit, vegetable and berry juice powder concentrate derived from the following: acerola, cherry, apple, bilberry, blackberry, black currant, blueberry, beetroot, broccoli, cabbage, carrot, concord grape, cranberry, elderberry, kale, orange, peach, papaya, parsley, pineapple, raspberry, red currant, spinach and tomato (Juice Plus+® Orchard, Garden and Berry Blends) as described previously [33]. Briefly, the F&V concentrate capsules provided; β-carotene 3.05 mg/day, α-tocopherol 4.8 mg/day, vitamin C 300 mg/day, folate 350 mg/day and polyphenols ~600 mg/day [34]. The placebo capsules were identical in appearance, opaque white capsules containing microcrystalline cellulose. All subjects were instructed to take three capsules twice daily with meals, in agreement with the label use instructions for the retail product, for a total of six capsules per day.

2.4. Ethics

The study was conducted according to the guidelines laid down in the Declaration of Helsinki, and all procedures involving human subjects were approved by the Hunter New England Health Human Research Ethics Committee (14/02/19/3.01) and registered with the University of Newcastle Human Research Ethics Committee. Written informed consent was obtained from all subjects. The trial was prospectively registered with the Australian New Zealand Clinical Trials Registry (ANZCTRN12614000079640).

2.5. Anthropometric Measures and Quality of Life

Anthropometric assessments (height and weight) were performed following an overnight fast. Body mass index (BMI) was calculated as body weight (kg)/(height (m))^2. Height (metres) was measured using the stretch stature method to 2 decimal places using a wall-mounted stadiometer (Seca 220, Seca, Hamburg, Germany). Body weight (kg) was measured to 1 decimal place with subjects wearing light clothing and without shoes, using calibrated electronic scales. Quality of life was assessed by the short form health survey (SF-36) questionnaire [35]. Waist circumference (WC) was measured to the nearest 0.1 cm at the midpoint between the lower costal edge and the iliac crest, using a non-extensible steel tape (Lufkin W606PM, Apex Tool Group, Sparks, MD, USA).

2.6. Blood Pressure

A blood pressure cuff was placed firmly around the upper arm of the participant, centred over the brachial artery. After resting quietly in a seated position for 10 min, four consecutive blood pressure and heart rate readings were taken at one-minute intervals by a single observer using an electronic vital signs monitor (6000 Series, Welch Allyn, Skaneateles Falls, NY, USA). The first reading was discarded and an average of the remaining measurements recorded for analysis.

2.7. Dual Energy X-ray Absorptiometry

Body composition was measured using a dual energy X-ray absorptiometry (DXA) machine and associated software (DXA Lunar Prodigy; Encore 2007 Version 11.40.004, GE Medical Systems, Madison, WI, USA). Total and regional absolute and percentage of fat and lean mass were calculated (kg).

2.8. Peripheral Blood Biomarkers

Fasting blood was collected into ethylenediaminetetraacetic acid (EDTA) tubes, then centrifuged at 3000× *g*, at 10 °C for 10 min. Plasma was separated and stored at −80 °C for batched analysis at the end of the study. TNFα, soluble (s)TNF receptor (R) 1 and sTNFR2 were measured by Human Quantikine ELISA Kits (R&D Systems, Minneapolis, Minnesota, USA). Oxidised (ox)-LDL was also analysed by ELISA (Mercodia, Uppsala, Sweden). Serum CRP, total cholesterol, LDL cholesterol, high-density lipoprotein (HDL) cholesterol, triglycerides and haemoglobin A1c (HbA1c) were measured in peripheral blood by an accredited pathology service (Hunter Area Pathology Service, Newcastle, NSW, Australia).

2.9. Plasma Antioxidant Levels

Plasma carotenoids (α-carotene, β-carotene, lutein, lycopene, β-cryptoxanthin) and plasma α-tocopherol were analysed by reverse phase high-performance liquid chromatography (HPLC) (Agilent LC 1200 System, Agilent Technologies, Santa Clara, CA, USA) using methods established in our laboratory [36–38]. Briefly, ethanol:ethyl acetate (1:1) containing internal standards (canthaxanthin and α-tocopherol acetate) and butylated hydroxytoluene were added to the sample. The solution was centrifuged (3000× *g*, 48 °C, 5 min), and the supernatant was collected; this was repeated 3 times adding ethyl acetate twice and then hexane to the pellet. Ultrapure water was then added to the pooled supernatant fluid, and the mixture was centrifuged. The supernatant was then decanted, and the solvents were evaporated with nitrogen. The sample was then reconstituted in dichloromethane:methanol (1:2). Chromatography was performed on a Hypersil ODS column with a flow rate of 0.3 mL/min, using the mobile phase of acetonitrile:dichloromethane:methanol 0.05% ammonium acetate (85:10:5). Carotenoids and tocopherols were detected at 450 nm and 290, respectively, using a photodiode array.

2.10. Dietary Analysis

Usual dietary intake over the previous 12 months was assessed at Week 0 by food frequency questionnaire using the Dietary Questionnaire for Epidemiological Studies v2 (DQES) (Victorian Cancer Council [39]). A 24-h food recall was also recorded at Week 0 and Week 8 by a dietitian and analysed using nutrient analysis software (FoodWorks Version 7, Xyris Software P/L, Kenmore Hills, QLD, Australia). Serving sizes were those as defined by the National Health and Medical Research Council Australian Dietary Guidelines [40]. Briefly, 75 grams of vegetables are equivalent to one serving and 150 grams of fruit counted as one serving.

2.11. Microarray Analysis

Microarray analysis was conducted in the F&V concentrate group only, to detect differences in gene expression before and after the intervention. Whole blood RNA was extracted from PAXgene tubes using the PAXgene Blood RNA Extraction Kit (Qiagen, Hilden, Germany), as per the manufacturer's instructions. RNA was quantitated and the quality assessed using Bioanalyser and Quant-iT Ribogreen RNA Reagent (Molecular Probes, Invitrogen, Carlsbad, CA, USA); the average RNA integrity number was 8.07. Whole genome gene expression was determined in 500 ng of blood RNA, which was amplified using the Illumina TotalPrep RNA Amplification Kit (Ambion, Waltham, MA, USA). Seven hundred fifty nanograms of amplified RNA were then hybridised to HumanHT-12 Version 4 Expression BeadChip (Illumina, San Diego, CA, USA). Microarrays were then scanned using the Illumina Bead Station. The microarray primary data used in this study are available at the national centre for biotechnology information (NCBI) Gene Expression Omnibus [41] under Accession Number GSE87454.

2.12. PCR Analysis

Real-time PCR testing was performed on 2 key genes, which demonstrated the greatest fold difference in expression and had biological relevance to the study hypothesis. Two hundred nanograms of extracted RNA (see above) were converted to cDNA using the High Capacity cDNA Reverse Transcription Hit (Applied Biosystems, Foster city, CA, USA). Standard Taqman methods were used. Taqman qPCR primer and probes of target genes were purchased in kit form (Applied Biosystems, Foster city, CA, USA). Target gene expression was measured relative to the housekeeping gene 18S, and the stability value of 18S was calculated as 0.045 using NormFinder [42]. All reactions were carried out using the ABI 7500 Real-Time PCR Machine (Applied Biosystems, Foster city, CA, USA). Taqman Assay IDs are as follows; phosphomevalonate kinase (PMVK) (Hs00559915_m1) and zinc finger AN1-type containing 5 (ZFAND5) (Hs04400278_g1).

2.13. Sample Size and Statistical Analysis

Sample size was determined using the Power and Sample Size calculation programme (PS Version 3.0.43, Vanderbilt University, Nashville, TN, USA) [43]. Based on our previous studies of the expression of multiple genes involved in inflammatory pathways, we required $n = 26$ subjects per group to have 80% power to detect a mean difference in expression of genes of 20%, with standard deviation (SD) = 25%. Our initial recruitment target of $n = 64$ allowed for 20% dropouts; however, recruitment was ceased at $n = 61$, as a very low dropout rate of 8% was achieved.

Per protocol analysis was conducted in 2 stages; Part 1: analysis of the full cohort; Part 2: analysis of the subset of individuals who are at increased risk of chronic disease due to high systemic inflammation levels at baseline, defined as serum CRP $\geq$3.0 mg/mL. The normality of all data was assessed using the D'Agostino–Pearson omnibus normality test.

Baseline data: demographics, biomarkers and dietary intake were compared using the unpaired Student's *t*-test (parametric data) or Mann–Whitney U-test (non-parametric data).

Intervention results: following the intervention, within-group differences were compared using paired *t*-tests for parametric data or the Wilcoxon rank sum test for non-parametric data. Between-group differences were analysed using analysis of covariance (ANCOVA) to test for differences between treatment groups after adjusting for baseline values. Associations between variables were assessed using Pearson's correlation for normally distributed variables and Spearman's rank correlation coefficient for non-parametric data.

Microarray whole genome gene expression analysis: data were exported to RStudio Version 3.2.2 (RStudio, Boston, MA, USA) using Illumina's Genome Studio 3.0 (Illumina, San Diego, CA, USA) and processed using the R packages lumi [44] and limma [45]. Data were normalised via log transformation and the baseline converted to the median of all samples. Data were filtered based on whether the gene was detected as present in 28 or more samples, as this was half the samples available from the intervention group. Gene profiles were analysed for differential expression by paired *t*-test for significance and fold change in RStudio Version 3.2.2.

3. Results

3.1. Part 1: Analysis of Full Cohort

3.1.1. Participant Flow

Sixty-one subjects were randomised, with five withdrawing after visit 1 (Figure 1). Of those who withdrew, one was suffering from constipation and fluid retention, one was suffering from diarrhoea and stomach pain, one had difficulty swallowing the study medication, one required anti-inflammatory treatment for a prior knee injury and one no longer wished to participate in the study. Of the 56 subjects who completed the study, 28 were in the F&V concentrate group and 28 were in the placebo group. The mean adherence rate was 97.7%.

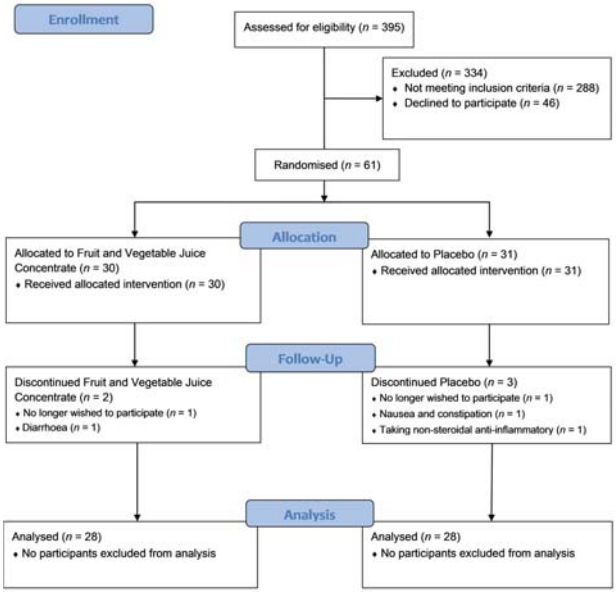

Figure 1. Patient flow consolidated standards of reporting trials (CONSORT) diagram. A total of 395 patients were screened for eligibility to participate; 61 of those who were eligible and wished to participate were randomised to either the fruit and vegetable juice concentrate intervention group or placebo, each taking three capsules twice daily.

3.1.2. Subject Demographics, Dietary Intake and Plasma Nutrient Levels

At baseline, there were no differences between groups in demographics or nutrient intakes (Table 1). Daily intake of fruit and vegetables was also not different at baseline between the groups and was well below the recommended levels (Table 2). Fruit and vegetable intake did not change during the intervention (Table 2). After eight weeks, plasma β-carotene and total carotenoids increased significantly within the F&V concentrate group and compared to the placebo group (Table 2). Plasma lycopene levels decreased in the placebo group compared to the F&V concentrate group.

Table 1. Baseline subject demographics and nutrient intake. F&V, fruit and vegetables.

	F&V Concentrate (n = 28)	Placebo (n = 28)	p-Value
Demographics			
Gender (male/female)	11/17	13/15	0.788
Age (years) [a]	61.4 ± 1.5	57.9 ± 1.4	0.091
BMI (kg/m^2) [a]	34.6 ± 0.7	37.0 ± 1.3	0.271
Smoking Status (never/ex)	14/14	16/12	0.592
Nutrient Intake			
Total Energy (KJ/day) [b]	7785 (6145, 10,371)	6986 (5573, 8448)	0.110
Total fat (g/day) [b]	78 (63, 107)	70 (59, 87)	0.229
SFA (g/day) [b]	32 (25, 45)	28 (24, 37)	0.205
PUFA (g/day) [a]	12 ± 1	12 ± 1	0.626
MUFA (g/day) [a]	31 ± 2	28 ± 2	0.286
Protein (g/day) [a]	101 ± 7	77 (73, 99)	0.103
Carbohydrates (g/day) [a]	202 ± 15	177 ± 11	0.169
Fibre (g/day) [a]	23 ± 2	21 ± 1	0.285
Calcium (mg/day) [a]	965 ± 50	857 ± 50	0.134
Folate (µg/day) [a]	342 ± 17	238 ± 14	0.046
Iron (mg/day) [b]	14 (10, 21)	11 (9, 14)	0.103
Magnesium (mg/day) [a]	319 ± 21	270 ± 14	0.060
Niacin (mg/day) [b]	22 (17, 29)	18 (14, 25)	0.126
Phosphorus (mg/day) [a]	1732 ± 118	1459 ± 77	0.058
Potassium (mg/day) [b]	3078 (2312, 3534)	2409 (2065, 3014)	0.051
Retinol (µg/day) [b]	351 (303, 443)	340 (277, 435)	0.651
Riboflavin (mg/day) [a]	3 ± 0	2 ± 0	0.055
Sodium (mg/day) [a]	2647 ± 197	2476 ± 158	0.500
Thiamine (mg/day) [a]	2 ± 0	1 ± 0	0.064
Vitamin C (mg/day) [a]	105 ± 11	95 ± 8	0.417
Vitamin E (mg/day) [a]	7 ± 1	6 ± 0	0.273
Zinc (mg/day) [b]	13 (9, 18)	10 (9, 12)	0.114
α-carotene (µg/day) [b]	811 (416, 1244)	643 (324, 830)	0.122
β-carotene (µg/day) [a]	4068 ± 387	3255 ± 273	0.092
β-cryptoxanthin (µg/day) [b]	125 (48, 284)	169 (85, 234)	0.675
Lutein/zeaxanthin (µg/day) [a]	862 ± 78	723 ± 65	0.177
Lycopene (µg/day) [b]	3967 (2602, 6338)	3807 (2324, 7564)	0.950

BMI: body mass index; SFA: saturated fatty acids; MUFA: monounsaturated fatty acids; PUFA: polyunsaturated fatty acids; [a] mean ± standard error of the mean (SEM); [b] median (Q1, Q3).

Table 2. Fruit and vegetable intake, plasma carotenoids and plasma α-tocopherol before and after the intervention.

	F&V Concentrate (n = 28)			Placebo (n = 28)			
	0	8 Weeks	p-Value *	0	8 Weeks	p-Value *	ANCOVA ‡ p-Value
Fruit and Vegetable Intake (Servings/Day)							
Fruit [b]	1.00 (0.00, 1.88)	0.75 (0.00, 1.00)	0.517	1.00 (0.00, 1.00)	0.50 (0.00, 1.00)	0.149	0.222
Vegetables [a]	1.45 ± 0.19	1.52 ± 0.18	0.784	1.34 ± 0.20	1.46 ±. 023	0.683	0.945
Total [a]	2.38 ± 0.21	2.30 ± 0.16	0.788	2.14 ± 0.23	2.00 ± 0.23	0.665	0.383
Plasma Carotenoids (mg/L)							
Lutein [b]	0.43 (0.36, 0.52)	0.45 (0.34, 0.59)	0.545	0.37 (0.30, 0.52)	0.37 (0.28, 0.49)	0.922	0.127
β-cryptoxanthin [b]	0.09 (0.05, 0.15)	0.07 (0.05, 0.12)	0.375	0.07 (0.04, 0.16)	0.06 (0.03, 0.13)	0.200	0.269
Lycopene [b]	0.10 (0.08, 0.14)	0.12 (0.08, 0.18)	0.213	0.11 (0.07, 0.17)	0.08 (0.04, 0.11)	0.007	0.005

Table 2. *Cont.*

	F&V Concentrate (n = 28)			Placebo (n = 28)			
	0	8 Weeks	p-Value *	0	8 Weeks	p-Value *	ANCOVA ‡ p-Value
Plasma Carotenoids (mg/L)							
α-carotene [b]	0.01 (0.00, 0.15)	0.01 (0.00, 0.01)	0.188	0.01 (0.00, 0.02)	0.01 (0.00, 0.01)	0.018	0.095
β-carotene [b]	0.11 (0.07, 0.15)	0.16 (0.11, 0.26)	<0.001	0.07 (0.00, 0.16)	0.06 (0.00, 0.11)	0.127	<0.001
Total Carotenoids [b]	0.73 (0.60, 1.05)	0.85 (0.76, 0.99)	0.017	0.72 (0.51, 1.01)	0.59 (0.49, 0.80)	0.019	<0.001
Plasma α-Tocopherol (mg/L) [b]	13.6 (11.3, 15.9)	14.2 (12.1, 15.4)	0.849	14.3 (11.3, 25.6)	14.4 (11.6, 17.7)	0.360	0.568

* The p-value refers to the change between baseline and eight weeks within each group; ‡ analysis of covariance (ANCOVA) was used to compare the change in the F&V concentrate group to the change in the placebo group; [a] mean ± standard error of the mean (SEM); [b] median (Q1, Q3).

3.1.3. Lipid Profile, Glycated Haemoglobin and Systemic Inflammatory Markers

Total cholesterol and LDL cholesterol decreased within the F&V concentrate group only, while triglycerides increased in the placebo group. Comparison of the two groups showed that only the change (Δ) in triglycerides was different between the F&V concentrate and placebo groups. Glycated haemoglobin (HbA1c) was unchanged after the intervention in both the F&V concentrate and placebo groups (Table 3). Plasma TNFα decreased following the F&V concentrate supplementation, and the difference in ΔTNFα between the F&V concentrate and placebo groups approached significance (p = 0.071). There was a negative correlation between Δβ-carotene and ΔTNFα (r = −0.352, p = 0.018). Plasma sTNFR2 concentration increased in the placebo group, while plasma sTNFR1, ox-LDL and CRP were unchanged in the F&V concentrate and placebo groups at Week 8 (Table 3).

Table 3. Lipid profiles, glycated haemoglobin and systemic inflammation before and after the intervention.

	F&V Concentrate (n = 28)			Placebo (n = 28)			
	0	8 Weeks	p-Value *	0	8 Weeks	p-Value *	ANCOVA ‡ p-Value
Total Cholesterol (mmol/L)	5.70 (5.00, 6.30)	5.50 (4.83, 6.15)	0.015	5.90 (4.50, 6.70)	5.60 (4.60, 6.20)	0.532	0.359
LDL Cholesterol (mmol/L)	3.63 (3.17, 4.36)	3.50 (2.95, 4.27)	0.032	4.15 (3.03, 4.63)	3.51 (2.89, 4.10)	0.089	0.904
HDL Cholesterol (mmol/L)	1.20 (1.10, 1.40)	1.20 (1.10, 1.30)	0.815	1.20 (1.00, 1.40)	1.20 (1.00, 1.40)	0.941	0.308
Total/HDL Cholesterol	4.50 (4.00, 5.10)	4.55 (4.05, 5.00)	0.221	4.60 (3.90, 5.60)	4.60 (3.90, 5.50)	0.587	0.634
Triglycerides (mmol/L)	1.24 (0.86, 1.81)	1.23 (1.01, 1.67)	0.344	1.36 (0.97, 1.83)	1.53 (1.06, 1.84)	0.012	0.022
HbA1c (%)	5.40 (5.20, 5.60)	5.30 (5.10, 5.50)	0.570	5.40 (5.20, 5.70)	5.30 (5.10, 5.50)	0.149	0.407
TNFα (pg/mL)	1.04 (0.87, 1.41)	1.02 (0.55, 1.41)	0.037	1.07 (0.79, 1.22)	0.94 (0.82, 1.26)	0.797	0.071
sTNFR1 (pg/mL)	1140 (1017, 1382)	1108 (992, 1335)	0.829	1120 (967, 1319)	1147 (953, 1383)	0.378	0.668
sTNFR2 (pg/mL)	2479 (2257, 3034)	2345 (2209, 3130)	0.467	2332 (1986, 2677)	2547 (2047, 2754)	0.006	0.299
Ox-LDL (mU/L)	48,620 (41,249, 62,976)	48,352 (41,937, 57,960)	0.990	50,053 (41,262, 64,661)	48,911 (43,400, 59,733)	0.551	0.781
CRP (mg/mL)	3.1 (1.7, 5.1)	3.9 (1.2, 5.9)	0.536	3.2 (1.7, 5.2)	2.5 (1.5, 5.4)	0.769	0.301

* The p-value refers to the change between baseline and eight weeks within each group; ‡ ANCOVA was used to compare the change in the F&V concentrate group to the change in the placebo group; all data are presented as the median (Q1, Q3). Low-density lipoprotein (LDL); high-density lipoprotein (HDL); haemoglobin A1c (HbA1c); tumour necrosis factor (TNF) α; soluble TNF receptor 1 (sTNFR1); soluble TNF receptor 2 (sTNFR2); oxidized-LDL (ox-LDL); C-reactive protein (CRP).

3.1.4. Body Composition, Blood Pressure and Quality of Life before and after the Intervention

Weight, BMI and waist circumference did not change in both the F&V concentrate and placebo groups (Table 4). Total lean mass increased within the F&V concentrate group, and the change compared to the placebo group approached significance ($p = 0.057$). Systolic blood pressure was significantly decreased after eight weeks in both the F&V concentrate and placebo groups; however, the difference between groups was not significant. Diastolic blood pressure, pulse and quality of life (SF36) were not changed after the F&V concentrate supplementation or the placebo (Table 4).

Table 4. Body composition, blood pressure and quality of life before and after the intervention.

	F&V Concentrate ($n = 28$)			Placebo ($n = 28$)			
	0	8 Weeks	p-Value *	0	8 Weeks	p-Value *	ANCOVA ‡ p-Value
BMI (kg/m^2) [a]	34.6 ± 0.7	34.6 ± 0.8	0.076	37.0 ± 1.3	36.1 ± 1.2	0.781	0.336
Waist circumference (cm) [a]	113.7 ± 2.2	112.5 ± 2.3	0.649	116.6 ± 2.8	116.0 ± 2.9	0.863	0.699
Body Composition							
Total Body Fat (kg) [a]	42.6 ± 1.7	42.7 ± 1.7	0.728	45.1 ± 2.4	44.8 ± 2.5	0.231	0.618
% Body Fat [a]	46.7 ± 1.5	46.4 ± 1.5	0.168	45.0 ± 1.5	44.4 ± 1.6	0.384	0.134
Total Lean Mass (kg) [a]	49.3 ± 2.4	50.0 ± 2.4	0.018	54.4 ± 2.0	55.0 ± 2.1	0.836	0.057
% Lean Mass [a]	51.4 ± 1.4	51.9 ± 1.4	0.078	53.5 ± 1.5	54.0 ± 1.5	0.560	0.096
Android: Gynoid Fat Ratio [a]	1.2 ± 0.0	1.2 ± 0.0	0.499	1.1 ± 0.0	1.1 ± 0.0	0.270	0.649
Systolic BP (mmHg) [a]	131.7 ± 2.3	125.9 ± 1.9	0.005	136.7 ± 2.8	132.4 ± 2.3	0.037	0.110
Diastolic BP (mmHg) [a]	80.6 ± 1.2	79.0 ± 1.0	0.097	82.6 ± 1.0	82.3 ± 1.0	0.665	0.055
Pulse (BPM) [a]	66.1 ± 1.7	68.6 ± 1.7	0.175	67.8 ± 1.7	66.4 ± 1.6	0.709	0.178
Quality of Life (SF-36)							
Physical [a]	47.2 ± 1.6	47.8 ± 1.5	0.788	46.6 ± 1.9	49.2 ± 1.6	0.678	0.682
Mental [b]	51.6 (43.6, 58.7)	54.1 (48.3, 59.1)	0.211	56.4 (40.1, 59.8)	54.0 (45.3, 58.1)	0.897	0.290

BMI: body mass index; BP: blood pressure; * the p-value refers to the change between baseline and eight weeks within each group; ‡ ANCOVA was used to compare the change in the F&V concentrate group to the change in the placebo group; [a] mean ± SEM; [b] median (Q1, Q3). 36 item short form health survey (SF-36).

3.2. Part 2: Analysis of a Subgroup with High Baseline CRP (≥3.0 mg/mL)

3.2.1. Subject Demographics, Dietary Intake and Plasma Nutrient Levels

To determine whether the effects of the F&V concentrate supplement were more evident in subjects with elevated systemic inflammation, a subgroup analysis was performed in subjects with baseline CRP ≥3.0 mg/mL. By using this criteria, the number of participants in the F&V concentrate and placebo groups was reduced to $n = 17$ and $n = 15$, respectively. The baseline demographics and dietary intakes of these groups were analysed (Table 5) and found to be similar, except for BMI, which was higher in the placebo group. Baseline daily intake of fruit and vegetables was not different between the groups and was well below recommended levels. Fruit and vegetable intake did not change during the intervention (Table 6). Plasma β-carotene and total carotenoids were both increased within the F&V concentrate group compared to the placebo group at Week 8. Lycopene was significantly decreased within the placebo group compared to the F&V concentrate group (Table 6).

Table 5. Baseline subject demographics and nutrient intake of subjects with high baseline CRP (≥3.0 mg/mL).

	F&V Concentrate ($n = 16$)	Placebo ($n = 15$)	p-Value
Demographics			
Gender (male/female)	3/13	6/9	0.252
BMI (kg/m^2) [a]	35.6 ± 1.1	40.2 ± 1.5	0.016
Age (years) [a]	60.8 ± 1.5	56.6 ± 2.0	0.097
Smoking Status (never/ex)	9/8	8/7	1.000

Table 5. *Cont.*

	F&V Concentrate (n = 16)	Placebo (n = 15)	p-Value
Nutrient Intake			
Total Energy (KJ/day) [a]	7884 ± 792	7569 ± 625	0.758
Total fat (g/day) [a]	83 ± 9	81 ± 7	0.857
SFA (g/day) [b]	30 (24, 45)	28 (24, 43)	0.688
PUFA (g/day) [a]	11 ± 1	12 ± 1	0.609
MUFA (g/day) [a]	30 ± 3	30 ± 3	>0.999
Protein (g/day) [b]	94 (67, 120)	77 (73, 110)	0.858
Carbohydrates (g/day) [a]	190 ± 20	181 ± 16	0.738
Fibre (g/day) [a]	22 ± 2	20 ± 2	0.429
Calcium (mg/day) [a]	926 ± 64	871 ± 67	0.559
Folate (µg/day) [b]	267 (194, 329)	213 (189, 294)	0.418
Iron (mg/day) [b]	12 (9, 20)	10 (9, 14)	0.509
Magnesium (mg/day) [a]	312 ± 31	271 ± 20	0.271
Niacin (mg/day) [b]	20 (14, 25)	18 (14, 26)	0.800
Phosphorus (mg/day) [b]	1500 (1250, 2002)	1357 (1140, 1859)	0.377
Potassium (mg/day) [b]	2847 (2090, 3609)	2501 (2081, 2896)	0.533
Retinol (µg/day) [b]	342 (254, 507)	376 (311, 473)	0.688
Riboflavin (mg/day) [b]	2 (2, 3)	2 (2, 3)	0.397
Sodium (mg/day) [b]	2177 (1797, 2738)	2286 (1845, 3623)	0.463
Thiamine (mg/day) [b]	2 (1, 2)	1 (1, 2)	0.558
Vitamin C (mg/day) [b]	88 (63, 111)	90 (57, 111)	0.883
Vitamin E (mg/day) [a]	7 ± 1	6 ± 1	0.702
Zinc (mg/day) [b]	13 (8, 16)	10 (9, 14)	0.716
α-Carotene (µg/day) [a]	916 ± 128	684 ± 121	0.198
β-Carotene (µg/day) [a]	351 ± 36	3350 ± 412	0.352
β-Cryptoxanthin (µg/day) [b]	105 (48, 193)	164 (89, 225)	0.222
Lutein/zeaxanthin (µg/day) [b]	803 (584, 903)	744 (332, 1134)	0.509
Lycopene (µg/day) [b]	3523 (2409, 4931)	2829 (2040, 9169)	0.887

BMI: body mass index; SFA: saturated fatty acids; MUFA: monounsaturated fatty acids; PUFA: polyunsaturated fatty acids; [a] mean ± SEM; [b] median (Q1, Q3).

Table 6. Fruit and vegetable intake, plasma carotenoids and plasma α-tocopherol before and after the intervention in subjects with high baseline CRP (≥3.0 mg/mL).

	F&V Concentrate (n = 16)			Placebo (n = 15)			
	0	8 Weeks	p-Value *	0	8 Weeks	p-Value *	ANCOVA ‡ p-Value
Fruit and Vegetable Intake (Servings/Day)							
Fruit [b]	1.00 (0.00, 1.00)	0.75 (0.00, 2.00)	0.899	0.75 (0.00, 1.38)	0.50 (0.00, 1.00)	0.475	0.283
Vegetables [b]	1.25 (0.63, 2.00)	1.75 (1.00, 2.00)	0.606	1.00 (0.13, 1.88)	1.00 (0.50, 2.00)	0.435	0.893
Total [a]	2.13 ± 0.26	2.38 ± 0.23	0.478	1.78 ± 0.25	2.00 ± 0.32	0.596	0.475
Plasma Carotenoids (mg/L)							
Lutein [b]	0.41 (0.37, 0.47)	0.45 (0.33, 0.55)	0.519	0.36 (0.29, 0.42)	0.35 (0.28, 0.40)	0.855	0.204
β-cryptoxanthin [b]	0.08 (0.05, 0.13)	0.07 (0.05, 0.12)	0.900	0.07 (0.02, 0.13)	0.06 (0.02, 0.13)	0.500	0.491
Lycopene [b]	0.10 (0.08, 0.15)	0.12 (0.08, 0.14)	0.850	0.11 (0.09, 0.19)	0.10 (0.03, 0.12)	0.003	0.026
α-carotene [b]	0.01 (0.00, 0.02)	0.01 (0.00, 0.01)	0.148	0.01 (0.00, 0.02)	0.00 (0.00, 0.02)	0.059	0.410
β-carotene [b]	0.11 (0.06, 0.14)	0.15 (0.10, 0.26)	0.003	0.09 (0.00, 0.17)	0.00 (0.00, 0.15)	0.393	0.002
Total Carotenoids [b]	0.72 (0.60, 0.88)	0.89 (0.61, 0.98)	0.035	0.72 (0.44, 0.94)	0.54 (0.48, 0.80)	0.066	<0.0001
Plasma α-Tocopherol (mg/L) [b]	14.1 (12.5, 16.3)	14.8 (13.6, 16.7)	0.677	14.5 (12.8, 17.2)	14.5 (11.8, 17.3)	0.761	0.826

* The p-value refers to the change between baseline and eight weeks within each group; ‡ ANCOVA was used to compare the change in the F&V concentrate group to the change in the placebo group; [a] mean ± SEM; [b] median (Q1, Q3).

3.2.2. Blood Lipids, Glycated Haemoglobin and Systemic Inflammatory Markers

Cholesterol and LDL cholesterol were significantly decreased within the F&V concentrate group, but were not different compared to the placebo group (Table 7). Triglycerides, HDL cholesterol, total

cholesterol/HDL ratio and HbA1c were unchanged within either the F&V concentrate or placebo groups. Plasma levels of TNFα were significantly decreased within the F&V concentrate group and also compared to the placebo group (Table 7). The soluble receptors, sTNFR1 and sTNFR2, were significantly different between groups following the intervention, due to an increase in concentration in the placebo group. Oxidised-LDL and CRP were unchanged in both groups (Table 7).

Table 7. Blood lipids, glycated haemoglobin and systemic inflammation before and after the intervention in subjects with high baseline CRP (≥3.0 mg/mL).

	F&V Concentrate (n = 16)			Placebo (n = 15)			
	0	8 Weeks	p-Value *	0	8 Weeks	p-Value *	ANCOVA ‡ p-Value
Total Cholesterol (mmol/L)	6.10 (5.30, 6.45)	5.65 (5.40, 6.20)	0.016	6.30 (4.70, 6.70)	5.95 (4.95, 6.43)	0.538	0.549
LDL Cholesterol (mmol/L)	3.98 (3.37, 4.48)	3.82 (3.34, 4.33)	0.016	4.21 (2.87, 4.67)	3.91 (3.22, 4.50)	0.279	0.854
HDL Cholesterol (mmol/L)	1.30 (1.10, 1.40)	1.20 (1.13, 1.38)	0.656	1.20 (1.00, 1.40)	1.20 (1.00, 1.40)	0.941	0.804
Total/HDL Cholesterol	4.90 (3.95, 5.40)	4.80 (4.40, 5.08)	0.324	5.20 (4.30, 5.90)	4.80 (3.95, 5.73)	0.398	0.944
Triglycerides (mmol/L)	1.30 (0.98, 2.24)	1.41 (1.17, 1.82)	0.520	1.58 (1.16, 1.85)	1.77 (1.09, 1.91)	0.268	0.205
HbA1c (mmol/mol)	36.0 (32.5, 38.0)	34.0 (33.0, 37.0)	0.197	36.5 (33.8, 40.3)	36.0 (33.0, 37.5)	0.783	0.662
HbA1c (%)	5.40 (5.15, 5.60)	5.30 (5.13, 5.48)	0.128	5.45 (5.28, 5.83)	5.40 (5.20, 5.55)	0.629	0.284
TNFα (pg/mL)	1.13 (0.95, 1.52)	0.95 (0.70, 1.40)	0.007	1.07 (0.79, 1.30)	0.96 (0.87, 1.26)	0.632	0.035
sTNFR1 (pg/mL)	1140 (980, 1491)	1143 (988, 1414)	0.324	1294 (1047, 1371)	1347 (1176, 1442)	0.212	0.031
sTNFR2 (pg/mL)	2698 (2371, 3152)	2389 (2205, 3005)	0.198	2554 (2313, 2881)	2711 (2532, 2998)	0.002	0.009
Ox-LDL (mU/L)	48,833 (43,191, 63,536)	50,719 (42,229, 61,437)	0.357	52,683 (39,688, 64,661)	45,559 (43,009, 62,543)	0.536	0.852
CRP (mg/mL)	4.8 (3.6, 9.4)	5.2 (3.8, 6.6)	0.930	5.0 (4.1, 7.4)	5.4 (3.8, 7.1)	0.820	0.861

* The p-value refers to the change between baseline and eight weeks within each group; ‡ ANCOVA was used to compare the change in the F&V concentrate group to the change in the placebo group; all data are presented as the median (Q1, Q3).

3.2.3. Body Composition, Blood Pressure and Quality of Life Before and after the Intervention

At the completion of the trial, weight, BMI, waist circumference, blood pressure and quality of life were unchanged in both groups (Table 8). Total lean mass and pulse rate significantly increased within the F&V concentrate group, but were not different compared to the placebo group.

Table 8. Body composition, blood pressure and quality of life before and after the intervention in subjects with high baseline CRP (≥3.0 mg/mL).

	F&V Concentrate (n = 16)			Placebo (n = 15)			
	0	8 Weeks	p-Value *	0	8 Weeks	p-Value *	ANCOVA ‡ p-Value
BMI (kg/m^2) [a]	35.6 ± 1.1	35.5 ± 1.2	0.263	40.2 ± 1.5	40.3 ± 1.5	0.721	0.531
Waist circumference (cm) [a]	113.8 ± 3.4	113.5 ± 3.7	0.480	123.4 ± 3.9	124.3 ± 3.6	0.806	0.939
Body Composition							
Total Body Fat (kg) [a]	45.5 ± 2.3	44.6 ± 2.4	0.362	52.9 ± 2.7	53.2 ± 2.8	0.345	0.421
% Body Fat [a]	49.9 ± 1.7	48.9 ± 1.8	0.062	47.7 ± 1.7	47.8 ± 1.7	0.615	0.069
Total Lean Mass (kg) [a]	46.1 ± 3.0	46.9 ± 3.2	0.049	58.1 ± 3.1	58.2 ± 3.2	0.919	0.221
% Lean Mass [a]	48.5 ± 1.6	49.5 ± 1.7	0.077	50.7 ± 1.6	50.7 ± 1.6	0.811	0.115
Android: Gynoid Fat Ratio [a]	1.1 ± 0.0	1.1 ± 0.0	0.892	1.1 ± 0.0	1.1 ± 0.0	0.951	0.996
Systolic BP (mmHg) [a]	131.8 ± 3.5	129.1 ± 2.8	0.243	140.1 ± 3.3	134.0 ± 3.4	0.052	0.953
Diastolic BP (mmHg) [a]	80.3 ± 1.8	80.0 ± 1.1	0.999	84.7 ± 1.6	83.5 ± 1.2	0.371	0.306

Table 8. *Cont.*

	F&V Concentrate (n = 16)			Placebo (n = 15)			
	0	8 Weeks	p-Value *	0	8 Weeks	p-Value *	ANCOVA ‡ p-Value
Pulse (BPM) [b]	67.0 (61.5, 71.8)	71.0 (67.0, 78.0)	0.021	68.0 (63.0, 71.0)	69.0 (62.0, 72.0)	0.988	0.138
Quality of Life (SF-36)							
Physical [a]	45.9 ± 2.4	46.4 ± 2.0	0.862	44.4 ± 2.4	44.4 ± 2.1	0.843	0.665
Mental [a]	48.8 ± 3.3	53.7 ± 2.3	0.076	48.6 ± 3.4	49.6 ± 2.9	0.596	0.259

BMI: body mass index; BP: blood pressure; * the p-value refers to the change between baseline and eight weeks within each group; ‡ ANCOVA was used to compare the change in the F&V concentrate group to the change in the placebo group; [a] mean ± SEM; [b] median (Q1, Q3).

3.2.4. Peripheral Blood Gene Expression

In the subgroup of participants with high baseline CRP (n = 16), microarray analysis revealed that 1632 genes were differentially expressed after supplementation with the F&V concentrate. One thousand one hundred forty six genes were upregulated, while 486 genes were downregulated, with the highest absolute fold change being 1.44 and the lowest fold change being 1.03.

From the genes that were significantly differentially expressed, several genes were identified that are involved in biologically-relevant signalling pathways, including: lipogenesis, NF-kB and AMPK pathways (Table 9). Pathways analysis was also performed on genes that were differentially expressed with a $p < 0.05$, using gene ontology tool to help explain relationships (GATHER) [46]. The upregulated genes were found to be involved in five different pathways, those being: the insulin signalling pathway, neuroactive ligand-receptor interaction, adherens junction, regulation of the actin cytoskeleton and the wnt signalling pathway. There were 18 upregulated genes involved in the insulin signalling pathway: calmodulin 1 (CALM1), casitas B-lineage lymphoma (CBL), crk-like protein (CRKL), hexokinase 2 (HK2), insulin receptor substrate 2 (IRS2), mitogen-activated protein kinase kinase 1 (MAP2K1), mitogen-activated protein kinase 6 (MAPK6), phosphodiesterase 3B (PDE3B), phosphorylase kinase regulatory subunit beta (PHKB), phosphatidylinositol-4, 5-biphosphate 3-kinase catalytic subunit beta isoform (PIK3CB), protein phosphatase 1 catalytic subunit gamma (PPP1CC), 5′-AMP-activated protein kinase subunit gamma-2 (PRKAG2), cAMP-dependent protein kinase type I-alpha regulatory subunit (PRKAR1A), tyrosine-protein phosphatase non-receptor type 1 (PTPN1), glycogen phosphorylase, liver form (PYGL), raf-1 proto-oncogene, serine/threonine kinase (RAF1), ras homolog enriched in brain (RHEB), ras-related protein R-Ras2 (RRAS2). Two gene targets for qPCR analysis were chosen to validate the microarray data; ZFAND5 and PMVK. Figure 2 shows that ZFAND5 and PMVK mRNA expression had similar fold changes following the intervention when assessed using both microarray and qPCR. As seen in the microarray analysis, gene expression of ZFAND5 as determined by PCR analysis was also significantly upregulated following supplementation with the F&V concentrate. While PMVK expression was downregulated in the microarray analysis, the downregulated expression in the PCR analysis was not statistically significant (Figure 3).

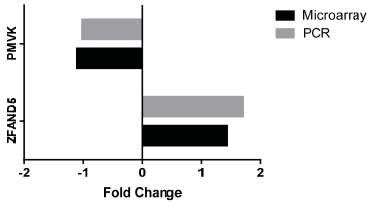

Figure 2. Validation of microarray analysis; fold changes in gene expression following the intervention as determined by microarray versus quantitative polymerase chain reaction (qPCR). Zinc finger, AN1-type domain 5 (ZFAND5); Phosphomevalonate kinase (PMVK).

Table 9. Microarray analysis: biologically-relevant genes that were differentially regulated following F&V concentrate supplementation in subjects with high baseline CRP (≥3.0 mg/mL).

Gene	Gene Name	Gene Function	Fold Change	*p*-Value
Lipogenesis				
PMVK	Phosphomevalonate kinase	Catalyses the conversion of mevalonate 5-phosphate into mevalonate 5-diphosphate, the fifth reaction of the cholesterol biosynthetic pathway	−1.102	0.005
FDFT1	Farnesyl-diphosphate farnesyltransferase 1	First specific enzyme in cholesterol biosynthesis, catalyses dimerization farnesyl diphosphate to form squalene	1.08	0.014
FDPS	Farnesyl diphosphate synthase	Catalyses the production of intermediates in cholesterol biosynthesis	−1.06	0.034
NF-κB				
ZFAND5	Zinc finger, AN1-type domain 5	Inhibits TNF, IL-1 and TLR-induced NF-κB activation	1.438	0.005
ATM	ATM serine/threonine kinase	Regulates tumour suppressor and DNA repair genes	1.242	0.006
PTGS2	Prostaglandin-endoperoxide synthase 2	Key enzyme in prostaglandin biosynthesis	1.199	0.042
PARP1	Poly (adenosine diphosphate (ADP)-ribose) polymerase 1	Differentiation, proliferation and tumour transformation	1.194	0.008
PLCG2	Phospholipase C, gamma 2 (phosphatidylinositol-specific)	Catalyses the conversion of 1-phosphatidyl-1D-myo-inositol 4,5-bisphosphate to 1D-myo-inositol 1,4,5-trisphosphate (IP3) and diacylglycerol (DAG), important second messenger molecules	1.161	0.019
BCL2	B-cell chronic lymphoid leukemia (CLL)/lymphoma 2	Important anti-apoptotic protein, classified as an oncogene	1.141	0.003
TLR4	Toll-like receptor 4	Pattern recognition receptor implicated in LPS signal transduction	1.118	0.017
MAP3K7	Mitogen-activated protein kinase kinase kinase 7	Forms complex with Transforming growth factor beta activated kinase (TAB)-1 or TAB2 which is required for NF-κB	1.112	0.042
PRKCQ	Protein kinase C, theta	Important for T-cell activation and NF-κB transcription factor activation	1.082	0.020
PRKCB	Protein kinase C, beta	Phosphorylates protein targets involved in B cell activation, apoptosis, endothelial cell proliferation, intestinal sugar absorption	1.072	0.048
MALT1	Mucosa-associated lymphoid tissue lymphoma translocation protein 1	Proteolytic activity, many targets involved in regulation of inflammation	1.067	0.028
TNFAIP3	Tumour necrosis factor-induced protein 3	Induced by TNF, inhibits NF-κB and TNF-mediated apoptosis	1.059	0.042
AMPK				
CAB39	Calcium binding protein 39	Stimulates STK11 activity, which is an upstream kinase of AMPK	1.418	0.004
RAB10	RAB10; RAS oncogene family	Regulates intracellular vesicle trafficking	1.279	0.020
SIRT1	Sirtuin 1	Involved in regulating AMPK expression	1.152	0.019
IRS2	Insulin receptor substrate 2	Mediates effects of insulin, insulin-like growth factor 1, and cytokines	1.137	0.009
RHEB	Ras homolog enriched in brain	involved in the mechanistic targeting of rapamycin (mTOR) pathway and the regulation of the cell cycle	1.119	0.048
MAP3K7	Mitogen-activated protein kinase kinase kinase 7	Forms complex with TAB1 or TAB2, which is required for NF-κB	1.112	0.042

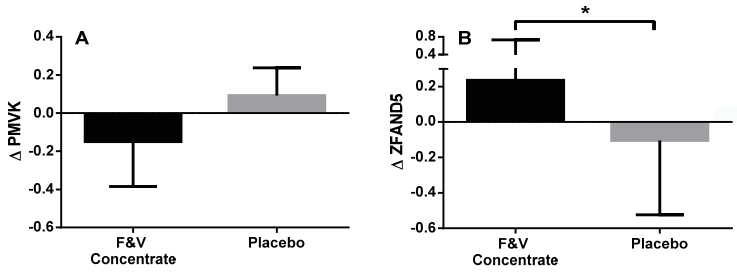

Figure 3. Change in peripheral blood mRNA expression of PMVK (**A**) and ZFAND5 (**B**) at baseline compared to Week 8 in the fruit and vegetable juice concentrate (F&V concentrate) and placebo groups; measured using qPCR; the data presented are the median (IQR); the statistical test used was the Mann–Whitney test; * $p < 0.05$ versus baseline.

4. Discussion

In this study, we found that in older subjects who are overweight or obese, F&V concentrate supplementation led to decreases in total cholesterol, LDL cholesterol, TNFα and systolic blood pressure. We conducted a secondary analysis of the subgroup of participants who had high systemic inflammation at baseline, as we hypothesised that these participants were more likely to obtain an improvement in metabolic health as a result of the supplement. Similar results were observed in the subgroup analysis, with F&V concentrate supplementation leading to a decrease in total cholesterol, LDL cholesterol and TNFα, and indeed, the size of the effects was greater. A number of genes associated with lipogenesis, AMPK and NF-κB signalling pathways were differentially expressed following the intervention. Pathways analysis also revealed that several genes involved in the insulin signalling pathway were upregulated in the subgroup of participants with high baseline CRP.

Total and LDL cholesterol were both found to be significantly decreased after the F&V concentrate intervention with greater changes seen in the subgroup with high baseline CRP. A recent Cochrane review used meta-analyses to demonstrate that increased fruit and vegetable consumption can reduce cholesterol levels [47]. Included studies achieved an average increase in fruit and vegetable intake of 1.88 (95% confidence interval (CI): 1.07 to 2.70) servings per day and total blood cholesterol levels reduced by 0.11 mmol/L (95% CI: −0.19 to −0.03). We observed a much greater decrease in total cholesterol in the high baseline CRP subgroup in this study. Importantly, the size of the decreases in total and LDL cholesterol that were observed in this study are substantial and clinically important. In the full cohort analysis, we observed a 0.2 mmol/L (3.5%) reduction in total cholesterol, which is estimated to be equivalent to a weight loss of 4 kg and an 8% to 9% reduction in CVD risk [48,49]. We also observed a 0.13 mmol/L (3.5%) decrease in LDL cholesterol, estimated to be equivalent to a 6.5 kg weight loss and 5% reduction in CVD risk [48,49]. In subjects who had elevated systemic inflammation at baseline, we observed a 0.45 mmol/L (7.4%) reduction in total cholesterol, which is estimated to be equivalent to a weight loss of 9 kg and an 18% to 19% reduction in CVD risk [48,49]. In this group, we also observed a 0.16 mmol/L (4.0%) decrease in LDL cholesterol, estimated to be equivalent to an 8 kg weight loss and a 4% reduction in CVD risk [48,49].

Serum triglycerides were found to be unchanged by the F&V concentrate in both the full cohort analysis and the high baseline CRP subgroup analysis. However, we did observe an inverse correlation between Δβ-carotene and Δtriglycerides. There is previous evidence that F&V concentrate supplementation and polyphenol-rich diets can lower triglyceride levels in overweight boys with elevated baseline triglycerides [50] and in overweight or obese adults [51]. It is likely that F&V concentrate supplementation would have the greatest effect in individuals with elevated triglycerides, which may explain the lack of change in this study, as the majority of subjects had normal triglyceride levels at baseline. Interestingly, in the placebo group, triglycerides significantly increased in the full

cohort analysis after the intervention. This may be related to the decrease in total carotenoids that was observed in the placebo group after eight weeks, which indicates that bioactive compounds continued to washout during the intervention period. This may have also masked the effect of the F&V concentrate, if dietary sources of carotenoids and other phytochemicals were continuing to washout during the intervention phase.

Microarray analysis revealed differential expression of several key genes involved in lipogenesis following the F&V concentrate supplementation. *PMVK* (or phosphomevalonate kinase) was found to be significantly downregulated. *PMVK* catalyses conversion of mevalonate 5-phosphate into mevalonate 5-diphosphate, which is the fifth reaction of the cholesterol biosynthetic pathway [52]. Similarly, gene expression of farnesyl diphosphate synthase (*FDPS*) was downregulated. This may also lead to reduced cholesterol production as the gene encodes an enzyme that catalyses the production of farnesyl diphosphate (*FPP*), a key biosynthetic intermediate used in the formation of cholesterol [53]. Interestingly, a recent study has shown that supplementation with the same F&V concentrate used in this study led to increased levels of circulating fatty acid binding protein 4 (FABP4), possibly via modulation of PPAR activity, resulting in altered lipid metabolism and accumulation [54]. Hence, there are several mechanisms by which the F&V concentrate may have led to the reduced blood lipid levels that were observed in this study.

Following intervention with the F&V concentrate, there was a small, but statistically-significant reduction in TNFα in the full cohort analysis, with a much greater reduction seen in the high baseline CRP subgroup analysis. TNFα is a cell signalling protein involved in systemic inflammation, with a primary role of regulating immune cells. Previous studies have shown that increasing fruit and vegetable intake reduces systemic inflammation, specifically CRP concentration [55,56], while a previous study of F&V concentrate supplementation showed that monocyte chemotactic protein 1 (MCP-1), macrophage inflammatory protein 1b (MIP-1b) and regulated on activation, normal T cell expressed and secreted (RANTES) were reduced [57]. The F&V concentrate used in this study is rich in β-carotene, which has been shown to reduce inflammatory mediator production, including TNFα [58,59]. For example, a study in mice found that β-carotene reduced the inflammatory response to LPS, including TNFα production [59]. Another study in a non-alcoholic fatty liver model in rats found that TNFα levels were markedly ameliorated with the administration of β-carotene [58]. Hence, the potential for carotenoids to reduce inflammation has previously been demonstrated.

TNFR1 and TNFR2 are the receptors to TNFα. Upon binding, inflammation is induced via various pathways, including activation of NF-kB and MAPK pathways. In this study, TNFR2 increased in the placebo group, in both the full cohort analysis and the subgroup analysis. Again, we speculate that this may have been a result of the decrease in total carotenoids that occurred in the placebo group during the intervention period, which suggests that the two-week washout period was not long enough to washout background levels of carotenoids prior to the intervention period.

A number of key genes involved in adenosine monophosphate-activated protein kinase (AMPK) and NF-κB signalling were found to be differentially expressed following intervention with F&V concentrate, and these may have contributed to the anti-inflammatory effect that we observed. AMPK is a key regulator of energy metabolism homeostasis, as AMPK inhibits energy consuming activities, such as protein, fatty acid and cholesterol synthesis, and stimulates energy production through glucose and lipid catabolism [60]. AMPK activation can also inhibit NF-κB signalling, thus reducing inflammation [60], and impaired AMPK activity has been shown to lead to insulin resistance [61,62]. AMPK signalling genes that were upregulated following the F&V concentrate intervention that have known anti-inflammatory effects include: *IRS2*, *CAB39* and *SIRT1*. Previously, a study found that knockdown of *IRS2* expression resulted in mice developing insulin resistance due to increased inflammation [63], while another study in mice found that AMPK signalling activated by *CAB39* inhibits NF-κB activation [64]. SIRT1, a downstream target of AMPK, inhibits NF-κB signalling, thus reducing inflammation [60,65–67]. Other genes that were upregulated in our analysis include *BCL2* and *TNF-AIP3*, which are known inhibitors of NF-κB signalling [68–77]. Another gene found

to be upregulated following intervention with the F&V concentrate was ZFAND5, also known as ZNF216 [78]. A previous study on ZFAND5 found that it was an inhibitor of NF-κB activation, by reducing TNFα, IL-1 and TLR4 in a dose-dependent manner [79]. Hence, our data show several pathways by which the F&V concentrate appears to be having an anti-inflammatory effect, with several AMPK and NF-κB signalling pathway genes contributing to this effect.

F&V concentrate supplementation has previously been shown to reduce homeostatic model assessment-insulin resistance (HOMA-IR) in a group of overweight boys [50]. While there was no change in HbA1C in the intervention group in our study, pathways analysis using GATHER found that a number of genes involved in the insulin signalling pathway were upregulated following intervention with the F&V concentrate. In the high baseline CRP subgroup analysis, the increased expression of the genes *HK2, IRS2, PDE3B, PHKB, PRKAG2, PTPN1* and *RHEB* suggests that the intervention with the F&V concentrate increases insulin sensitivity, as these genes are all involved in reducing blood glucose levels via the insulin signalling pathway [80–86]. This provides further evidence of the ability of the F&V concentrate to improve the metabolic profile of obese individuals.

Following the intervention with the F&V concentrate, systolic blood pressure (SBP) was found to be reduced in the full cohort analysis. A previous observational study found there was an inverse relationship between β-carotene levels and SBP [87]. In another intervention study, increasing fruit and vegetable consumption to at least five daily portions significantly reduced SBP [88]. This reduction in SBP indicates a decreased risk of cardiovascular diseases, such as myocardial infarction, stroke and congestive heart failure [15]. Interestingly, however, there was also a significant reduction in SBP in the placebo group. Hence, we cannot rule out the possibility that subjects in the trial experienced the 'white coat effect' prior to their baseline visit, with their blood pressure becoming elevated due to anxiety about attending the research centre for the first time [89].

F&V concentrate supplementation led to an increase in total lean mass in both the full cohort analysis and the high baseline CRP subgroup analysis, likely due, at least in part, to the decrease in TNFα that we observed. TNFα plays a central role in muscle wasting [90]. Circulating TNFα binds to peripheral muscle cell receptors, stimulating the production of reactive oxygen species (ROS) and cellular apoptosis. In addition, the receptor binding stimulates NF-κB activation, possibly enhanced by ROS. The result is protein loss, caused directly via increased ubiquitin activity and indirectly via decreased myogenic differentiation (MyoD) expression, which decreases myofibril synthesis [90]. This observation suggests that F&V concentrate supplementation may be beneficial in settings where muscle wasting is undesirable, e.g., during aging or cachexia.

Baseline intake of fruit and vegetables was well below recommended levels for both the F&V concentrate and placebo groups. Following the intervention with the F&V concentrate, β-carotene and total carotenoids were significantly increased in the full cohort analysis, as well as the high baseline CRP subgroup analysis. α-tocopherol was found to be unchanged by the F&V concentrate intervention. The F&V concentrate used in this study provides a daily dose of 3.5 mg β-carotene and 4.8 mg α-tocopherol. These daily doses correspond approximately to 100% of the usual daily intake of β-carotene, but only ~50% of the usual daily intake of α-tocopherol [3]. Hence, it is not surprising that we observed an increase in circulating levels of β-carotene, but not α-tocopherol. The supplement also contains polyphenols (at least 119 compounds), including ellagitannins, gallotannins, dihydrochalcones, flavan-3-ols including proanthocyanidins, flavanones, flavones, flavonols, anthocyanins, hydroxybenzoic acids, hydroxycinnamic acids, phenylethanoids and lignans [34]. Whilst we were unable to analyse the circulating levels of these compounds or their metabolites in the samples from this study, it is likely that they would have contributed to the effects that we observed, as the dose delivered (~600 mg/day) is approaching the usual daily dose for most populations [34]. As previously discussed, total carotenoids decreased in the placebo group following the eight-week intervention. This suggests that the two-week run-in period on the low fruit and vegetable washout diet was not long enough, and hence, carotenoids continued to decrease during the eight-week intervention period. Importantly, if the washout period was not adequate, this would

also have affected the results in the intervention group, as the potential benefits of the supplement may have been masked, as background levels of carotenoids continued to wash out throughout the intervention period. In future trials, a longer wash out period is recommended.

5. Summary and Conclusions

To summarise, this randomised controlled trial in obese, older individuals shows that F&V concentrate supplementation has the potential to improve the metabolic profile of overweight and obese individuals by reducing blood lipid levels and systemic inflammation, as well as improving body composition. The size of the improvements is clinically significant, as the reduction in total cholesterol that we observed in the full cohort is estimated to be equivalent to a weight loss of 4 kg and an 8% to 9% reduction in CVD risk [48,49]. In the subset of participants who had elevated systemic inflammation at baseline, the reduction in total cholesterol was equivalent to a 9 kg weight loss and an 18% to 19% reduction in CVD risk [48,49]. Interestingly, while significant changes were seen in the whole group of participants, the changes were more pronounced in subjects who had elevated CRP levels at baseline. Hence, while all obese individuals are likely to gain some benefit from supplementation with F&V concentrate, those with high baseline systemic inflammation or blood lipids appear likely to obtain the greatest improvements. We conclude that in obese individuals, who typically have a low fruit and vegetable intake, F&V concentrate supplementation may be beneficial for improving the metabolic profile, thus reducing the risk of developing chronic inflammatory disease.

Acknowledgments: The authors acknowledge the contribution of the Hunter Medical Research Institute Respiratory Research group sample processing team. Financial support for this project, including the supply of study supplements, was received from NSA LLC (Collierville, TN, USA). NSA LLC had no role in the design, analysis nor writing of this article.

Author Contributions: Evan Williams contributed to the data acquisition, analysis and interpretation, drafting of the manuscript and final approval of the version of the manuscript to be published. Katherine Baines contributed to the study design, data analysis and interpretation, manuscript review and final approval of the version to be published. Bronwyn Berthon contributed to the data acquisition, analysis and interpretation, manuscript review and final approval of the version to be published. Lisa Wood contributed to the study design, data analysis and interpretation, drafting of the manuscript and final approval of the version to be published.

Conflicts of Interest: The authors declare no conflict of interest.

References

1. WHO Global Database on Body Mass Index. Available online: http://apps.who.int/bmi/ (accessed on 11 July 2013).
2. Ogden, C.L.; Carroll, M.D.; Kit, B.K.; Flegal, K.M. PRevalence of childhood and adult obesity in the United States, 2011–2012. *JAMA* **2014**, *311*, 806–814. [CrossRef] [PubMed]
3. Australian Bureau of Statistics. *Australian Health Survey: Updated Results*; Australian Bureau of Statistics: Canberra, Australia, 2011–2012.
4. Damcott, C.M.; Sack, P.; Shuldiner, A.R. The genetics of obesity. *Endocrinol. Metab. Clin. N. Am.* **2003**, *32*, 761–786. [CrossRef]
5. Mraz, M.; Haluzik, M. The role of adipose tissue immune cells in obesity and low-grade inflammation. *J. Endocrinol.* **2014**, *222*, R113–R127. [CrossRef] [PubMed]
6. Kalupahana, N.S.; Moustaid-Moussa, N.; Claycombe, K.J. Immunity as a link between obesity and insulin resistance. *Mol. Aspects Med.* **2012**, *33*, 26–34. [CrossRef] [PubMed]
7. Lumeng, C.N.; Bodzin, J.L.; Saltiel, A.R. Obesity induces a phenotypic switch in adipose tissue macrophage polarization. *J. Clin. Investig.* **2007**, *117*, 175–184. [CrossRef] [PubMed]
8. Siriwardhanaa, N.; Kalupahanab, N.S.; Cekanovac, M.; LeMieuxa, M.; Greerd, B.; Moustaid-Moussaa, N. Modulation of adipose tissue inflammation by bioactive food compounds. *J. Nutr. Biochem.* **2013**, *24*, 613–623. [CrossRef] [PubMed]
9. Fantuzzi, G. Adipose tissue, adipokines, and inflammation. *J. Allergy Clin. Immunol.* **2005**, *115*, 911–919. [CrossRef] [PubMed]

10. Bulló, M.; Casas-Agustench, P.; Amigó-Correig, P.; Aranceta, J.; Salas-Salvadó, J. Inflammation, obesity and comorbidities: The role of diet. *Public Health Nutr.* **2007**, *10*, 1164–1172. [CrossRef] [PubMed]
11. Poulain, M.; Doucet, M.; Major, G.C.; Drapeau, V.; Sériès, F.; Boulet, L.-P.; Tremblay, A.; Maltais, F. The effect of obesity on chronic respiratory diseases: Pathophysiology and therapeutic strategies. *CMAJ* **2006**, *174*, 1293–1299. [CrossRef] [PubMed]
12. Cawthorn, W.P.; Sethi, J.K. TNF-α and adipocyte biology. *FEBS Lett.* **2008**, *582*, 117–131. [CrossRef] [PubMed]
13. Zarkesh-Esfahani, H.; Pockley, A.G.; Wu, Z.; Hellewell, P.G.; Weetman, A.P.; Ross, R.J. Leptin indirectly activates human neutrophils *via* induction of TNF-α. *J. Immunol.* **2004**, *172*, 1809–1814. [CrossRef] [PubMed]
14. Das, U.N. Is Obesity an Inflammatory Condition? *Nutrition* **2001**, *17*, 953–966. [CrossRef]
15. Vitseva, O.I.; Tanriverdi, K.; Tchkonia, T.T.; Kirkland, J.L.; McDonnell, M.E.; Apovian, C.M.; Freedman, J.; Gokce, N. Inducible Toll-like receptor and NF-kappaB regulatory pathway expression in human adipose tissue. *Obesity (Silver Spring)* **2008**, *16*, 932–937. [CrossRef] [PubMed]
16. Bost, F.; Aouadi, M.; Caron, L.; Binetruy, B. The role of MAPKs in adipocyte differentiation and obesity. *Biochimie* **2005**, *87*, 51–56. [CrossRef] [PubMed]
17. Gauthier, M.S.; O'Brien, E.L.; Bigornia, S.; Mott, M.; Cacicedo, J.M.; Xu, X.J.; Gokce, N.; Apovian, C.; Ruderman, N. Decreased AMP-activated protein kinase activity is associated with increased inflammation in visceral adipose tissue and with whole-body insulin resistance in morbidly obese humans. *Biochem. Biophys. Res. Commun.* **2011**, *404*, 382–387. [CrossRef] [PubMed]
18. Moller, D.E.; Berger, J.P. Role of PPARs in the regulation of obesity-related insulin sensitivity and inflammation. *Int. J. Obes. Relat. Metab. Disord.* **2003**, *27*, S17–S21. [CrossRef] [PubMed]
19. Dandona, P.; Aljada, A.; Bandyopadhyay, A. Inflammation: The link between insulin resistance, obesity and diabetes. *Trends. Immunol.* **2004**, *25*, 4–7. [CrossRef] [PubMed]
20. Franks, P.W. Obesity, inflammatory markers and cardiovascular disease: Distinguishing causality from confounding. *J. Hum. Hypertens* **2006**, *20*, 837–840. [CrossRef] [PubMed]
21. Nicklas, B.J.; Ambrosius, W.; Messier, S.P.; Miller, G.D.; Penninx, B.W.J.H.; Loeser, R.F.; Palla, S.; Bleecker, E.; Pahor, M. Diet-induced weight loss, exercise, and chronic inflammation in older, obese adults: A randomized controlled clinical trial. *Am. J. Clin. Nutr.* **2004**, *79*, 544–551. [PubMed]
22. Forsythe, L.K.; Wallace, J.M.; Livingstone, M.B.E. Obesity and inflammation: The effects of weight loss. *Nutr. Res. Rev.* **2008**, *21*, 117–133. [CrossRef] [PubMed]
23. Jung, S.H.; Park, H.S.; Kim, K.-S.; Choi, W.H.; Ahn, C.W.; Kim, B.T.; Kim, S.M.; Lee, S.Y.; Ahn, S.M.; Kim, Y.K.; et al. Effect of weight loss on some serum cytokines in human obesity: Increase in IL-10 after weight loss. *J. Nutr. Biochem.* **2008**, *19*, 371–375. [CrossRef] [PubMed]
24. Barinas-Mitchell, E.; Kuller, L.H.; Sutton-Tyrrell, K.; Hegazi, R.; Harper, P.; Mancino, J.; Kelley, D.E. Effect of Weight Loss and Nutritional Intervention on Arterial Stiffness in Type 2 Diabetes. *Diabetes Care* **2006**, *29*, 2218–2222. [CrossRef] [PubMed]
25. Marfella, R.; Esposito, K.; Siniscalchi, M.; Cacciapuoti, F.; Giugliano, F.; Labriloa, D.; Ciotola, M.; Di Palo, C.; Misso, L.; Giugliano, D. Effect of Weight Loss on Cardiac Synchronization and Proinflammatory Cytokines in Premenopausal Obese Women. *Diabetes Care* **2004**, *27*, 47–52. [CrossRef] [PubMed]
26. Selvin, E.; Paynter, N.P.; Erlinger, T.P. The Effect of Weight Loss on C-Reactive Protein: A Systematic Review. *Arch. Intern. Med.* **2007**, *167*, 31–39. [CrossRef] [PubMed]
27. Higami, Y.; Barger, J.L.; Page, G.P.; Allison, D.B.; Smith, S.R.; Prolla, T.A.; Weindruch, R. Energy restriction lowers the expression of genes linked to inflammation, the cytoskeleton, the extracellular matrix, and angiogenesis in mouse adipose tissue. *J. Nutr.* **2006**, *136*, 343–352. [PubMed]
28. Larson-Meyer, D.E.; Heilbronn, L.K.; Redman, L.M.; Newcomer, B.R.; Frisard, M.I.; Anton, S.; Smith, S.R.; Alfonso, A.; Ravussin, E. Effect of calorie restriction with or without exercise on insulin sensitivity, beta-cell function, fat cell size, and ectopic lipid in overweight subjects. *Diabetes Care* **2006**, *29*, 1337–1344. [CrossRef] [PubMed]
29. Jarvi, A.; Karlstrom, B.; Vessby, B.; Becker, W. Increased intake of fruits and vegetables in overweight subjects: Effects on body weight, body composition, metabolic risk factors and dietary intake. *Br. J. Nutr.* **2016**, *115*, 1760–1768. [CrossRef] [PubMed]

30. Alvarez-Suarez, J.M.; Giampieri, F.; Tulipani, S.; Casoli, T.; Di Stefano, G.; González-Paramás, A.M.; Santos-Buelga, C.; Busco, F.; Quiles, J.L.; Cordero, M.D.; et al. One-month strawberry-rich anthocyanin supplementation ameliorates cardiovascular risk, oxidative stress markers and platelet activation in humans. *J. Nutr. Biochem.* **2014**, *25*, 289–294. [CrossRef] [PubMed]
31. Esfahani, A.; Wong, J.M.; Truan, J.; Villa, C.R.; Mirrahimi, A.; Srichaikul, K.; Kendall, C.W. Health effects of mixed fruit and vegetable concentrates: A systematic review of the clinical interventions. *J. Am. Coll. Nutr.* **2011**, *30*, 285–294. [CrossRef] [PubMed]
32. Heale, P.; Stockwell, T.; Dietze, P.; Chikritzhs, T.; Catalano, P. *Patterns of Alcohol Consumption in Australia, 1998*; National Alcohol Indicators Project, Bulletin No. 3. National Drug Research Institute; Curtin University of Technology: Perth, Australia, 2000.
33. Lamprecht, M.; Obermayer, G.; Steinbauer, K.; Cvirn, G.; Hofmann, L.; Ledinski, G.; Greilberger, J.F.; Hallstroem, S. Supplementation with a juice powder concentrate and exercise decrease oxidation and inflammation, and improve the microcirculation in obese women: Randomised controlled trial data. *Br. J. Nutr.* **2013**, *110*, 1685–1695. [CrossRef] [PubMed]
34. Bresciani, L.; Calani, L.; Cossu, M.; Mena, P.; Sayegh, M.; Ray, S.; Del Rio, D. (Poly)phenolic characterization of three food supplements containing 36 different fruits, vegetables and berries. *PharmaNutrition* **2015**, *3*, 11–19. [CrossRef]
35. Ware, J.E., Jr.; Sherbourne, C.D. The MOS 36-item short-form health survey (SF-36). Conceptual framework and item selection. *Med. Care* **1992**, *30*, 473–483. [CrossRef] [PubMed]
36. Wood, L.G.; Gibson, P.G. Reduced circulating antioxidant defences are associated with airway hyper-responsiveness, poor control and severe disease pattern in asthma. *Br. J. Nutr.* **2010**, *103*, 735–741. [CrossRef] [PubMed]
37. Wood, L.G.; Garg, M.L.; Powell, H.; Gibson, P.G. Lycopene-rich treatments modify noneosinophilic airway inflammation in asthma: Proof of concept. *Free Radic. Res.* **2008**, *42*, 94–102. [CrossRef] [PubMed]
38. Wood, L.G.; Garg, M.L.; Blake, R.J.; Garcia-Caraballo, S.; Gibson, P.G. Airway and circulating levels of carotenoids in asthma and healthy controls. *J. Am. Coll. Nutr.* **2005**, *24*, 448–455. [CrossRef] [PubMed]
39. Giles, G.; Ireland, P. *Dietary Questionnaire for Epidemiological Studies*, version 2; The Cancer Council Victoria: Melbourne, Australia, 1996.
40. National Health and Medical Research Council. *Australian Dietary Guidelines*; National Health and Medical Research Council: Canberra, Australia, 2013.
41. National Center for Biotechnology Information. Gene Expression Omnibus (GEO). 2017. Available online: https://www.ncbi.nlm.nih.gov/geo/query/acc.cgi?acc=GSE87454 (accessed on 8 September 2016).
42. Andersen, C.L.; Jensen, J.L.; Orntoft, T.F. Normalization of real-time quantitative reverse transcription-PCR data: A model-based variance estimation approach to identify genes suited for normalization, applied to bladder and colon cancer data sets. *Cancer Res.* **2004**, *64*, 5245–5250. [CrossRef] [PubMed]
43. Dupont, W.D.; Plummer, W.D. Power and Sample Size Calculations for Studies Involving Linear Regression. *Controll. Clin. Trials* **1998**, *19*, 589–601. [CrossRef]
44. Du, P.; Kibbe, W.A.; Lin, S.M. Lumi: A pipeline for processing Illumina microarray. *Bioinformatics* **2008**, *24*, 1547–1548. [CrossRef] [PubMed]
45. Ritchie, M.E.; Phipson, B.; Wu, D.; Hu, Y.; Law, C.W.; Shi, W.; Smyth, G.K. Limma powers differential expression analyses for RNA-sequencing and microarray studies. *Nucl. Acids Res.* **2015**, *43*, e47. [CrossRef] [PubMed]
46. Chang, J.T.; Nevins, J.R. GATHER: A systems approach to interpreting genomic signatures. *Bioinformatics* **2006**, *22*, 2926–2933. [CrossRef] [PubMed]
47. Rees, K.; Dyakova, M.; Ward, K.; Thorogood, M.; Brunner, E. Dietary advice for reducing cardiovascular risk. *Cochrane Database Syst. Rev.* **2013**. [CrossRef]
48. Anderson, J.W.; Konz, E.C. Obesity and disease management: Effects of weight loss on comorbid conditions. *Obes. Res.* **2001**, *9*, 326S–334S. [CrossRef] [PubMed]
49. Dattilo, A.M.; Kris-Etherton, P.M. Effects of weight reduction on blood lipids and lipoproteins: A meta-analysis. *Am. J. Clin. Nutr.* **1992**, *56*, 320–328. [PubMed]
50. Canas, J.A.; Damaso, L.; Altomare, A.; Killen, K.; Hossain, J.; Balagopal, P. Insulin resistance and adiposity in relation to serum beta-carotene levels. *J. Pediatr.* **2012**, *161*, 58–64. [CrossRef] [PubMed]

51. Annuzzi, G.; Bozzetto, L.; Costabile, G.; Giacco, R.; Mangione, A.; Anniballi, G.; Vitale, M.; Vetrani, C.; Cipriano, P.; Della Corte, G.; et al. Diets naturally rich in polyphenols improve fasting and postprandial dyslipidemia and reduce oxidative stress: A randomized controlled trial. *Am. J. Clin. Nutr.* **2014**, *99*, 463–471. [CrossRef] [PubMed]
52. Olivier, L.M.; Chambliss, K.L.; Michael Gibson, K.; Krisans, S.K. Characterization of phosphomevalonate kinase: Chromosomal localization, regulation, and subcellular targeting. *J. Lipid Res.* **1999**, *40*, 672–679. [PubMed]
53. Aripirala, S.; Gonzalez-Pacanowska, D.; Oldfield, E.; Kaiser, M.; Amzel, L.M.; Gabelli, S.B. Structural and thermodynamic basis of the inhibition of Leishmania major farnesyl diphosphate synthase by nitrogen-containing bisphosphonates. *Acta Crystallogr. Sect. D Biol. Crystallogr.* **2014**, *70*, 802–810. [CrossRef] [PubMed]
54. Canas, J.A.; Damaso, L.; Hossain, J.; Balagopal, P.B. Fatty acid binding proteins 4 and 5 in overweight prepubertal boys: Effect of nutritional counselling and supplementation with an encapsulated fruit and vegetable juice concentrate. *J. Nutr. Sci.* **2015**, *4*, e39. [CrossRef] [PubMed]
55. Esposito, K.; Marfella, R.; Ciotola, M.; Di Palo, C.; Giugliano, F.; Giugliano, G.; D'Armiento, M.; D'Andrea, F.; Giugliano, D. Effect of Mediterranean-Style diet on endothelial dysfunction and markers of vascular inflammation in the metabolic syndrome. *JAMA* **2004**, *292*, 1440–1446. [CrossRef] [PubMed]
56. Watzl, B.; Kulling, S.E.; Moseneder, J.; Barth, S.W.; Bub, A. A 4-wk intervention with high intake of carotenoid-rich vegetables and fruit reduces plasma C-reactive protein in healthy, nonsmoking men. *Am. J. Clin. Nutr.* **2005**, *82*, 1052–1058. [PubMed]
57. Jin, Y.; Cui, X.; Singh, U.P.; Chumanevich, A.A.; Harmon, B.; Cavicchia, P.; Hofseth, A.B.; Kotakadi, V.; Stroud, B.; Volate, S.R.; et al. Systemic inflammatory load in humans is suppressed by consumption of two formulations of dried, encapsulated juice concentrate. *Mol. Nutr. Food Res.* **2010**, *54*, 1506–1514. [CrossRef] [PubMed]
58. Seif El-Din, S.H.; El-Lakkany, N.M.; El-Naggar, A.A.; Hammam, O.A.; Abd El-Latif, H.A.; Ain-Shoka, A.A.; Ebeid, F.A. Effects of rosuvastatin and/or beta-carotene on non-alcoholic fatty liver in rats. *Res. Pharm. Sci.* **2015**, *10*, 275–287. [PubMed]
59. Bai, S.K.; Lee, S.J.; Na, H.J.; Ha, K.S.; Han, J.A.; Lee, H.; Kwon, Y.G.; Chung, C.K.; Kim, Y.M. beta-Carotene inhibits inflammatory gene expression in lipopolysaccharide-stimulated macrophages by suppressing redox-based NF-kappaB activation. *Exp. Mol. Med.* **2005**, *37*, 323–334. [CrossRef] [PubMed]
60. Salminen, A.; Hyttinen, J.M.T.; Kaarniranta, K. AMP-activated protein kinase inhibits NF-κB signaling and inflammation: Impact on healthspan and lifespan. *J. Mol. Med.* **2011**, *89*, 667–676. [CrossRef] [PubMed]
61. Lage, R.; Dieguez, C.; Vidal-Puig, A.; Lopez, M. AMPK: A metabolic gauge regulating whole-body energy homeostasis. *Trends Mol. Med.* **2008**, *14*, 539–549. [CrossRef] [PubMed]
62. Ruderman, N.B.; Cacicedo, J.M.; Itani, S.; Yagihashi, N.; Saha, A.K.; Ye, J.M.; Chen, K.; Zou, M.; Carling, D.; Boden, G.; et al. Malonyl-CoA and AMP-activated protein kinase (AMPK): Possible links between insulin resistance in muscle and early endothelial cell damage in diabetes. *Biochem. Soc. Trans.* **2003**, *31*, 202–206. [CrossRef] [PubMed]
63. Vinué, Á.; Andrés-Blasco, I.; Herrero-Cervera, A.; Piqueras, L.; Andrés, V.; Burks, D.J.; Sanz, M.J.; González-Navarro, H. Ink4/Arf locus restores glucose tolerance and insulin sensitivity by reducing hepatic steatosis and inflammation in mice with impaired IRS2-dependent signalling. *Biochim. Biophys. Acta (BBA) Mol. Basis Dis.* **2015**, *1852*, 1729–1742. [CrossRef] [PubMed]
64. Hur, W.; Lee, J.H.; Kim, S.W.; Kim, J.H.; Bae, S.H.; Kim, M.; Hwang, D.; Kim, Y.S.; Park, T.; Um, S.J.; et al. Downregulation of microRNA-451 in non-alcoholic steatohepatitis inhibits fatty acid-induced proinflammatory cytokine production through the AMPK/AKT pathway. *Int. J. Biochem. Cell Biol.* **2015**, *64*, 265–276. [CrossRef] [PubMed]
65. Yoshizaki, T.; Schenk, S.; Imamura, T.; Babendure, J.L.; Sonoda, N.; Bae, E.J.; Oh, D.Y.; Lu, M.; Milne, J.C.; Westphal, C.; et al. SIRT1 inhibits inflammatory pathways in macrophages and modulates insulin sensitivity. *Am. J. Physiol. Endocrinol. Metab.* **2010**, *298*, E419–E428. [CrossRef] [PubMed]
66. Salminen, A.; Kauppinen, A.; Suuronen, T.; Kaarniranta, K. SIRT1 longevity factor suppresses NF-kappaB -driven immune responses: Regulation of aging via NF-kappaB acetylation? *Bioessays* **2008**, *30*, 939–942. [CrossRef] [PubMed]

67. Yang, H.; Zhang, W.; Pan, H.; Feldser, H.G.; Lainez, E.; Miller, C.; Leung, S.; Zhong, Z.; Zhao, H.; Sweitzer, S.; et al. SIRT1 activators suppress inflammatory responses through promotion of p65 deacetylation and inhibition of NF-kappaB activity. *PLoS ONE* **2012**, *7*, e46364.
68. Elton, L.; Carpentier, I.; Staal, J.; Driege, Y.; Haegman, M.; Beyaert, R. MALT1 cleaves the E3 ubiquitin ligase HOIL-1 in activated T cells, generating a dominant negative inhibitor of LUBAC-induced NF-kappaB signaling. *FEBS J.* **2016**, *283*, 403–412. [CrossRef] [PubMed]
69. Ba, X.; Garg, N.J. Signaling mechanism of poly(ADP-ribose) polymerase-1 (PARP-1) in inflammatory diseases. *Am. J. Pathol.* **2011**, *178*, 946–955. [CrossRef] [PubMed]
70. Piret, B.; Schoonbroodt, S.; Piette, J. The ATM protein is required for sustained activation of NF-kappaB following DNA damage. *Oncogene* **1999**, *18*, 2261–2271. [CrossRef] [PubMed]
71. Macrae, K.; Stretton, C.; Lipina, C.; Blachnio-Zabielska, A.; Baranowski, M.; Gorski, J.; Marley, A.; Hundal, H.S. Defining the role of DAG, mitochondrial function, and lipid deposition in palmitate-induced proinflammatory signaling and its counter-modulation by palmitoleate. *J. Lipid Res.* **2013**, *54*, 2366–2378. [CrossRef] [PubMed]
72. Kim, H.; Zamel, R.; Bai, X.-H.; Liu, M. PKC Activation Induces Inflammatory Response and Cell Death in Human Bronchial Epithelial Cells. *PLoS ONE* **2013**, *8*, e64182. [CrossRef] [PubMed]
73. Hellmann, J.; Tang, Y.; Zhang, M.J.; Hai, T.; Bhatnagar, A.; Srivastava, S.; Spite, M. Atf3 negatively regulates Ptgs2/Cox2 expression during acute inflammation. *Prostaglandins Other Lipid Mediat.* **2015**, *116–117*, 49–56. [CrossRef] [PubMed]
74. Badrichani, A.Z.; Stroka, D.M.; Bilbao, G.; Curiel, D.T.; Bach, F.H.; Ferran, C. Bcl-2 and Bcl-X(L) serve an anti-inflammatory function in endothelial cells through inhibition of NF-κB. *J. Clin. Investig.* **1999**, *103*, 543–553. [CrossRef] [PubMed]
75. Zehavi, L.; Schayek, H.; Jacob-Hirsch, J.; Sidi, Y.; Leibowitz-Amit, R.; Avni, D. MiR-377 targets E2F3 and alters the NF-kB signaling pathway through MAP3K7 in malignant melanoma. *Mol. Cancer* **2015**, *14*, 68. [CrossRef] [PubMed]
76. Guijarro-Munoz, I.; Compte, M.; Alvarez-Cienfuegos, A.; Alvarez-Vallina, L.; Sanz, L. Lipopolysaccharide activates Toll-like receptor 4 (TLR4)-mediated NF-kappaB signaling pathway and proinflammatory response in human pericytes. *J. Biol. Chem.* **2014**, *289*, 2457–2468. [CrossRef] [PubMed]
77. Liu, J.; Zhu, L.; Xie, G.L.; Bao, J.F.; Yu, Q. Let-7 miRNAs Modulate the Activation of NF-kappaB by Targeting TNFAIP3 and Are Involved in the Pathogenesis of Lupus Nephritis. *PLoS ONE* **2015**, *10*, e0121256.
78. Wullaert, A.; Heyninck, K.; Janssens, S.; Beyaert, R. Ubiquitin: Tool and target for intracellular NF-kappaB inhibitors. *Trends Immunol.* **2006**, *27*, 533–540. [CrossRef] [PubMed]
79. Huang, J.; Teng, L.; Li, L.; Liu, T.; Li, L.; Chen, D.; Xu, L.G.; Zhai, Z.; Shu, H.B. ZNF216 Is an A20-like and IkappaB kinase gamma-interacting inhibitor of NFkappaB activation. *J. Biol. Chem.* **2004**, *279*, 16847–16853. [CrossRef] [PubMed]
80. Sears, D.D.; Hsiao, G.; Hsiao, A.; Yu, J.G.; Courtney, C.H.; Ofrecio, J.M.; Chapman, J.; Subramaniam, S. Mechanisms of human insulin resistance and thiazolidinedione-mediated insulin sensitization. *Proc. Natl. Acad. Sci. USA* **2009**, *106*, 18745–18750. [CrossRef] [PubMed]
81. Valverde, A.M.; Burks, D.J.; Fabregat, I.; Fisher, T.L.; Carretero, J.; White, M.F.; Benito, M. Molecular mechanisms of insulin resistance in IRS-2-deficient hepatocytes. *Diabetes* **2003**, *52*, 2239–2248. [CrossRef] [PubMed]
82. Ahmad, F.; Lindh, R.; Tang, Y.; Ruishalme, I.; ÖSt, A.; Sahachartsiri, B.; StrÅLfors, P.; Degerman, E.; Manganiello, V.C. Differential regulation of adipocyte PDE3B in distinct membrane compartments by insulin and the β(3)-adrenergic receptor agonist CL316243: Effects of caveolin-1 knockdown on formation/maintenance of macromolecular signalling complexes. *Biochem. J.* **2009**, *424*, 399–410. [CrossRef] [PubMed]
83. Terashima, M.; Fujita, Y.; Togashi, Y.; Sakai, K.; De Velasco, M.A.; Tomida, S.; Nishio, K. KIAA1199 interacts with glycogen phosphorylase kinase beta-subunit (PHKB) to promote glycogen breakdown and cancer cell survival. *Oncotarget* **2014**, *5*, 7040–7050. [CrossRef] [PubMed]
84. Zhang, B.L.; Xu, R.L.; Zhang, J.; Zhao, X.X.; Wu, H.; Ma, L.P.; Hu, J.Q.; Zhang, J.L.; Ye, Z.; Zheng, X.; et al. Identification and functional analysis of a novel PRKAG2 mutation responsible for Chinese PRKAG2 cardiac syndrome reveal an important role of non-CBS domains in regulating the AMPK pathway. *J. Cardiol.* **2013**, *62*, 241–248. [CrossRef] [PubMed]

85. Galic, S.; Hauser, C.; Kahn, B.B.; Haj, F.G.; Neel, B.G.; Tonks, N.K.; Tiganis, T. Coordinated Regulation of Insulin Signaling by the Protein Tyrosine Phosphatases PTP1B and TCPTP. *Mol. Cell. Biol.* **2005**, *25*, 819–829. [CrossRef] [PubMed]
86. Saucedo, L.J.; Gao, X.; Chiarelli, D.A.; Li, L.; Pan, D.; Edgar, B.A. Rheb promotes cell growth as a component of the insulin/TOR signalling network. *Nat. Cell Biol.* **2003**, *5*, 566–571. [CrossRef] [PubMed]
87. Chen, J.; He, J.; Hamm, L.; Batuman, V.; Whelton, P.K. Serum antioxidant vitamins and blood pressure in the United States population. *Hypertension* **2002**, *40*, 810–816. [CrossRef] [PubMed]
88. John, J.H.; Ziebland, S.; Yudkin, P.; Roe, L.S.; Neil, H.A.W. Effects of fruit and vegetable consumption on plasma antioxidant concentrations and blood pressure: A randomised controlled trial. *Lancet* **2002**, *359*, 1969–1974. [CrossRef]
89. Pickering, T. Blood pressure measurement and detection of hypertension. *Lancet* **1994**, *344*, 31–35. [CrossRef]
90. Sevenoaks, M.J.; Stockley, R.A. Chronic obstructive pulmonary disease, inflammation and co-morbidity—A common inflammatory phenotype. *Respir. Res.* **2006**, *7*, 70. [CrossRef] [PubMed]

nutrients

MDPI

Article

Oxyresveratrol Supplementation to C57bl/6 Mice Fed with a High-Fat Diet Ameliorates Obesity-Associated Symptoms

Hui Yuan Tan, Iris Mei Ying Tse, Edmund Tsze Shing Li and Mingfu Wang *

School of Biological Sciences, The University of Hong Kong, Hong Kong, China; totanhy@gmail.com (H.Y.T.); mytsea@hku.hk (I.M.Y.T.); etsli@hku.hk (E.T.S.L.)
* Correspondence: mfwang@hku.hk; Tel.: +852-2299-0338

Received: 16 January 2017; Accepted: 13 February 2017; Published: 16 February 2017

Abstract: Oxyresveratrol has been proven effective in inhibiting adipogenesis in a 3T3-L1 cell model. We investigated the preventive effect of oxyresveratrol supplementation on obesity development in high-fat diet-fed mice. Male C57bl/6 mice were randomly subjected to control (5% fat by weight, LF), high-fat (30% fat by weight, HF), and high-fat supplemented with 0.25% and 0.5% oxyresveratrol (OXY1 and OXY2, respectively) diet groups for eight weeks. Oxyresveratrol supplementation effectively alleviated obesity-associated symptoms such as insulin resistance, hyperglycemia, and hepatic steatosis in high-fat diet-fed mice. Compared to the high-fat diet group, oxyresveratrol supplementation suppressed expression of glucose-6-phosphatase, sterol regulatory element-binding proteins 1, fatty acid synthase and CCAAT/Enhancer-binding proteins α, and elevated AMP-activated protein kinase (α2-catalytic subunit) level in liver, upregulated insulin-dependent glucose transporter type 4 level in adipose tissue, and increased expression of insulin receptor substrate 1, insulin-dependent glucose transporter type 4, AMP-activated protein kinase α, peroxisome proliferator-activated receptor γ coactivator-1α, and sirtuin 1 in muscle to regulate lipid and glucose homeostasis in these tissues. This study demonstrated that oxyresveratrol supplementation effectively ameliorated obesity-associated symptoms in high-fat diet-fed mice, presumably attributed to mediating critical regulators involved in lipid and glucose homeostasis in liver, visceral fat, and muscle.

Keywords: oxyresveratrol supplementation; amelioration; high-fat diet; obesity; glucose homeostasis; lipid homeostasis

1. Introduction

Over the years, the prevalence of obesity has been increasing worldwide with the obese population more than doubling since 1980. Around the world, more than 1.9 billion adults were overweight or obese in 2014. Additionally, in 2014, 41 million children under the age of 5 were reported to suffer from overweight or obesity [1]. More and more adults as well as children suffer from abnormal or excessive body fat with a variety of comorbidities, such as hypertension, dyslipidemia, type 2 diabetes, cardiovascular disease, stroke, sleep apnea, knee osteoarthritis, and certain cancers [2,3]. Obesity has been considered a global epidemic disease [1,4]. Soaring demands for effective anti-obesity strategies are driving industry and academia to conduct research in this field. To prevent or heal obesity with the supplementation of phenolic compounds have generated intense interest in recent years. Among the studied phenolics, resveratrol (Figure 1a) has been extensively studied with both in vitro and in vivo studies demonstrating that resveratrol has great potential in the management of obesity. Supplementation of resveratrol is capable of relieving the harmful effects induced by a high-calorie diet such as reducing the rodents body weight gain, adipose tissue depots, plasma triglycerides, and increasing their survival and motor function [5].

Being similar in structure with resveratrol, oxyresveratrol (OXY) (Figure 1b) possesses an additional hydroxyl group on its aromatic ring [6,7]. OXY is a natural polyphenol first isolated from the heartwood of *Artocarpus lakoocha* Roxb and also rich in mulberry (*Morus alba* L.) twigs and woods [8]. Studies on OXY have revealed that it possesses similar biological activities as resveratrol and the potential beneficial effects include anti-inflammatory, anti-oxidative, anti-viral, and neuroprotective activities [9–14]. It has also been considered a potent free radical scavenger, a tyrosinase inhibitor, and an anti-browning agent that could be used in food industry for cloudy apple juices and fresh-cut apples [7,15,16].

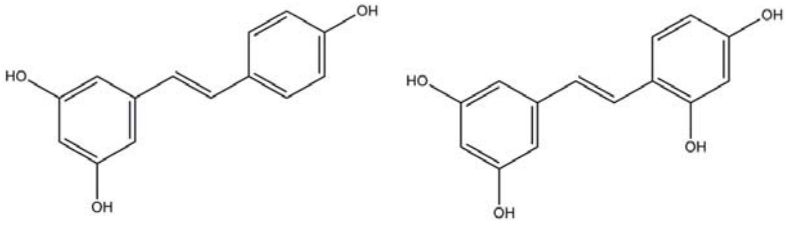

(**a**) (**b**)

Figure 1. Structures of resveratrol (**a**) and oxyresveratrol (**b**).

Our previous study demonstrated that OXY, at non-cytotoxic doses, possesses anti-adipogenic ability in 3T3-L1 cells by inhibition of differentiation through inducing cell cycle arrest [17]. However, little is known about OXY's impact on obesity in vivo. The present study thus aimed at investigating the preventive effects of OXY supplementation on the development of obesity in mice fed with a high-fat diet. C57bl/6 male mice were randomly assigned to control (5% fat by weight, LF), high-fat (30%, HF), and high-fat supplemented with 0.25% and 0.5% OXY (OXY1 and OXY2, respectively) diet groups for eight weeks. Growth parameters, organ and adipose tissue weights, serum biochemical parameters, and the expressions of relevant mRNA/protein in liver, adipose tissues, and muscles were examined to identify the putative anti-obesity effect of OXY and gain insight on the underlying mechanism.

2. Materials and Methods

2.1. Oxyresveratrol and Experimental Diets

OXY (≥98% pure, CAS registry No. 29700-22-9) was purchased from Great Forest Biomedical Ltd., Hangzhou, China. The purity was confirmed by High Performance Liquid Chromatography analysis.

The formulation for the experimental diets was modified based on the AIN-93G recommendation [18]. The control diet was the low-fat diet (LF, 5% fat *w*/*w*) that comprised corn oil (50 g/kg) as lipids. The high-fat diet (HF, 30% fat *w*/*w*) comprised corn oil (150 g/kg) and Crisco shortening (150 g/kg) as lipids. The two treatment groups were the high-fat diets supplemented with 0.25% OXY (OXY1) and 0.5% OXY (OXY2). OXY was added to the high-fat diet at the expense of cornstarch. OXY1 and OXY2 diets contained 2.5 g and 5 g OXY/kg, respectively. Diet compositions with energy density were stated in Table 1. All prepared diets were stored at −40 °C and fresh diets were provided every other day.

Table 1. Composition of the experimental diets [1].

Ingredient	LF [2]	HF [3]	OXY1 [4]	OXY2 [5]
			g/kg	
Casein [6], 87.5%	200	235	235	235
Corn starch [6]	549.5	255.5	253	250.5
Sucrose [6]	100	100	100	100
Cellulose (fiber) [6]	50	50	50	50
Crisco [7]	0	150	150	150
Corn oil [8]	50	150	145	145
Oxyresveratrol	0	0	2.5	5
Mineral [6], AIN-93G-MX	35	42	42	42
Vitamin [6], AIN-93-VM	10	12	12	12
Choline bitartrate	2.5	2.5	2.5	2.5
L-Cystine	3	3	3	3
Tert-butylhydroquinone	0.014	0.014	0.014	0.014
Energy [9], kJ/g	15.69	20.69	20.46	20.42

[1] Based on AIN-93G diet with modification. [2] LF: Low-fat diet. [3] HF: High-fat diet. [4] OXY1: High-fat diet supplemented with 0.25% oxyresveratrol. [5] OXY2: High-fat diet supplemented with 0.5% oxyresveratrol. [6] Harlan Teklad (Madison, WI, USA). [7] Crisco, partially hydrogenated vegetable shortening (Procter & Gamble, Orrville, OH, USA). [8] Mazola (CPC, Kuala Lumpur, Malaysia). [9] Based on energy densities: 16.74 kJ/g for protein and carbohydrates and 37.66 kJ/g for fat.

2.2. Experimental Design

39 male C57bl/6 mice, four weeks of age, were obtained from the animal unit of Faculty of Medicine, The University of Hong Kong, Hong Kong. The animals were housed individually under controlled temperature and 12 h light-dark cycle and had free access to water. The mice were randomly assigned to one of the four diet groups (n = 8–11) for eight weeks: low-fat diet (LF, 5% fat w/w); high-fat diet (HF, 30% fat w/w); high-fat diets supplemented with 0.25% OXY (OXY1) and 0.5% OXY (OXY2). Food intake and body weight were monitored every other day. At the end of eight weeks, blood was drawn from the abdominal vena cava from each mouse and then the mouse was killed by cervical dislocation. Tissues including liver, visceral fat, and gastrocnemius muscle were collected and stored at −80 °C for assays of biochemical parameters, and gene/protein expression. All the procedures were performed with the approval of the ethics committee on the Use of Live Animals in Teaching and Research at The University of Hong Kong (No. 3263-14).

2.3. Measurement of Biochemical Parameters

Serum was prepared by leaving the blood to clot undisturbed at room temperature for 30 min and then removing the clot by centrifuging at 2000 g for 10 min at 4 °C. Serum glucose was determined by Glucose Assay Kit (Abcam, Cambridge, UK). Serum high-density lipoprotein (HDL) cholesterol was assayed by Cholesterol, HDL Test, Precipitating Reagent (Stanbio Laboratory, Boerne, TX, USA). Cholesterol was determined with Cholesterol LiquiColor (Stanbio Laboratory, Boerne, TX, USA). Serum insulin was measured by Mercodia Mouse Insulin ELISA kit (Mercodia, Uppsala, Sweden). The HOMA-IR (homeostasis model assessment of insulin resistance) index was calculated as (fasting serum glucose (mmol/L) × fasting serum insulin (mIU/L)/22.5) to assess insulin resistance [19,20]. Serum and liver triglyceride (TG) were assayed using Triglycerides LiquiColor (Stanbio Laboratory, Boerne, TX, USA). Non-esterified fatty acid (NEFA) was measured by LabAssay NEFA kit (Wako Pure Chemical Industries, Osaka, Japan).

2.4. Total RNA Isolation and Real-Time Reverse Transcriptase Polymerase Chain Reaction (PT-PCR) Analysis

Total RNA from liver, visceral fat, and gastrocnemius muscle were extracted with Trizol reagent (Invitrogen, Waltham, MA, USA) following the manufacturer's instructions. cDNA was synthesized from 0.5 μg of total RNA using iScript Select cDNA Synthesis Kit (Bio-Rad Laboratories, Hercules, CA, USA). cDNA and TaqMan probes were subjected to quantitative Real-Time PCR amplification by TaqMan Universal Master Mix II (Applied Biosystems, Carlsbad, CA, USA) on the StepOnePlus Real-Time PCR System (Applied Biosystems, Carlsbad, CA, USA). The thermal profile settings were 50 °C for 2 min and 95 °C for 10 min and then 40 cycles at 95 °C for 15 s and 60 °C for 1 min. Relative expression levels of the mRNA of the target genes were normalized to GAPDH mRNA levels.

2.5. Protein Extraction and Western Blotting Analysis

Mice liver tissue fragments were homogenized in an ice cold lysis buffer (25 mM 4-(2-hydroxyethyl)-1-piperazineethanesulfonic acid (pH 7.5), 150 mM sodium chloride, 1 mM ethylenediaminetetraacetic acid disodium salt, 1 mM dithiothreitol, 1% Triton X-100) with added 4% protease inhibitor cocktail, 1% phosphatase inhibitor cocktail B, and 2% phosphatase inhibitor cocktail C for protein collection. Protein concentration in samples was determined using the Bradford Reagent (Bio-Rad Protein Assay Dye Reagent Concentrate). 30 μg of protein of each sample was applied for electrophoresis on 12% sodium dodecyl sulfate polyacrylamide gel electrophoresis gels and transferred to polyvinylidene diflouride membrane. Membranes were blocked with 5% nonfat dried milk powder in phosphate buffered saline (PBS) solution with tween-20 or tris buffered saline (TBS) solution with tween-20 (0.1% *v*/*v* tween-20 in PBS or TBS) overnight at 4 °C. The membranes were then incubated for 2 h with specific antibodies at room temperature. Equal sample loading was verified by anti-β-actin. Membranes were developed using SuperSignal West Pico Chemiluminescent Substrate (Pierce Biotechnology, Rockford, IL, USA). The bands were quantified densitometrically using the software ImageJ 1.47v (Wayne Rasband, Bethesda, MD, USA).

2.6. Statistical Analysis

The data were presented as means ± S.E.M. (the standard error of the mean). One-way ANOVA with Duncan corrections was used to determine significance for multiple comparisons. For all analyses, the accepted level of significance was $p < 0.05$. The calculations were performed using SPSS statistical package version 11.0 for Windows (International Business Machines Corporation, Armonk, NY, USA).

3. Results

3.1. Effects of Oxyresveratrol on Body Weight, Energy Intake, Energy Efficiency, and Tissue Weights

After feeding with designated diets for eight weeks, the HF mice had significantly higher body weight gain, energy intake and energy efficiency than that of the LF mice (Figure 2, Table 2, $p < 0.05$). While, OXY supplemented high-fat feeding mice (OXY1, OXY2) had significantly reduced body weight gain, energy intake and energy efficiency as compared to those of the HF mice (Figure 2, Table 2, $p < 0.05$). Comparing the two OXY supplemented groups, both body weight gain and energy efficiency were significantly lower in the OXY2 group, while energy intakes were not significantly different (Figure 2, Table 2, $p < 0.05$). Furthermore, as indicated in Table 2, there was no significant difference in gastrocnemius muscle weights among the four groups, while the weights of liver and visceral fat in OXY1 and OXY2 mice were significantly reduced as compared to those of the HF mice (Table 2, $p < 0.05$).

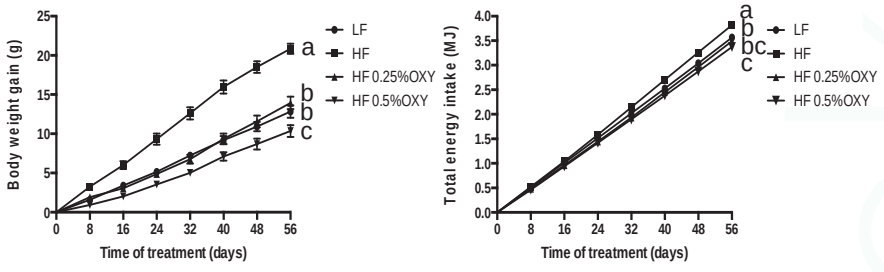

(**a**) (**b**)

Figure 2. Effects of oxyresveratrol supplementation on body weight gain (**a**) and total energy intake (**b**). C57bl/6 mice were fed low-fat or high-fat diet with or without oxyresveratrol (n = 8–11/group) for eight weeks. Values are presented as means ± S.E.M. Means by different letters are significantly different at $p < 0.05$.

Table 2. Effects of oxyresveratrol supplementation on body weight, energy intake, energy efficiency, and tissue weights of mice [1,2].

Parameters	LF [3]	HF [4]	OXY1 [5]	OXY2 [6]
Body weight				
Starting body weight, g	19.61 ± 0.21	19.71 ± 0.20	19.56 ± 0.25	19.56 ± 0.31
Final body weight, g	32.46 ± 0.84 [b]	40.54 ± 0.71 [a]	33.51 ± 0.82 [b]	29.92 ± 0.93 [c]
Body weight gain, g	12.85 ± 0.81 [b]	20.83 ± 0.67 [a]	13.95 ± 0.79 [b]	10.35 ± 0.77 [c]
Energy intake				
Fat intake, MJ	0.43 ± 0.01 [c]	2.09 ± 0.02 [a]	1.89 ± 0.02 [b]	1.84 ± 0.05 [b]
Energy intake, MJ	3.57 ± 0.05 [b]	3.82 ±0.04 [a]	3.49 ± 0.04 [bc]	3.37 ± 0.09 [c]
Energy efficiency [7], g/MJ	3.60 ± 0.00 [b]	5.45 ± 0.00 [a]	3.98 ± 0.00 [b]	3.04 ± 0.00 [c]
Tissue weights				
Liver, g	1.12 ± 0.04 [b]	1.34 ± 0.07 [a]	1.08 ± 0.04 [bc]	0.96 ± 0.04 [c]
Visceral fat, g	1.75 ± 0.13 [c]	3.31 ± 0.07 [a]	2.35 ± 0.15 [b]	1.60 ± 0.15 [c]
Gastrocnemius muscle, g	0.31 ± 0.03	0.29 ± 0.02	0.29 ± 0.01	0.30 ± 0.01

[1] Values are mean ± S.E.M. n = 8–11 per group at eight weeks. [2] Means in each row with superscripts without a common letter differ, $p < 0.05$. [3] LF: Low-fat diet. [4] HF: High-fat diet. [5] OXY1: High-fat diet supplemented with 0.25% oxyresveratrol. [6] OXY2: High-fat diet supplemented with 0.5% oxyresveratrol. [7] Energy efficiency: body weight gain (g)/energy intake (MJ). Energy efficiency is calculated as described by Li et al. [21].

3.2. Effects of Oxyresveratrol on Serum Concentration of Glucose and Insulin

As shown in Table 3, the serum concentrations of glucose and insulin in HF mice were significantly higher than those of the LF mice; the OXY supplementation significantly suppressed the levels of these two parameters in serum of high-fat fed mice, and the serum insulin level was decreased to the level of the LF mice (Table 3, $p < 0.05$). Compared to that of other three groups, the HOMA-IR index for the high fat group was significantly increased. Meanwhile, no difference in the HOMA-IR index was observed among the OXY supplemented mice and the LF mice (Table 3, $p < 0.05$).

3.3. Effects of Oxyresveratrol on Lipid Profiles in Serum and Liver

Compared to the HF group, 0.5% OXY supplementation to a high-fat diet for eight weeks significantly lowered serum levels of TG, cholesterol, and NEFA and also liver levels of TG and cholesterol (Table 3, $p < 0.05$).

Table 3. Effects of oxyresveratrol supplementation on serum and liver biological parameters of mice [1,2].

Biological Parameters	LF [3]	HF [4]	OXY1 [5]	OXY2 [6]
Serum				
Glucose, mM	4.8 ± 0.4^{c}	9.6 ± 0.8^{a}	6.7 ± 0.6^{b}	7.2 ± 0.3^{b}
Insulin, μg/L	0.5 ± 0.3^{b}	1.5 ± 0.3^{a}	0.4 ± 0.1^{b}	0.3 ± 0.2^{b}
HOMA-IR index [7]	4.4 ± 1.7^{b}	20.1 ± 4.6^{a}	4.7 ± 1.2^{b}	3.2 ± 1.4^{b}
Triglyceride, mg/dL	132.7 ± 5.8^{a}	110.4 ± 7.4^{b}	105.3 ± 5.3^{b}	84.6 ± 5.9^{c}
Cholesterol, mg/dL	139.7 ± 4.9^{ab}	153.4 ± 3.3^{a}	142.3 ± 4.9^{ab}	134.0 ± 4.7^{b}
HDL cholesterol, mg/dL	89.4 ± 2.7	92.7 ± 1.0	91.4 ± 2.0	86.8 ± 3.0
NEFA, mEq/L	1.7 ± 0.1^{a}	1.5 ± 0.1^{ab}	1.5 ± 0.1^{b}	1.1 ± 0.1^{c}
Hepatic lipids				
Triglyceride, mg/g liver	14.1 ± 0.4^{a}	14.1 ± 0.5^{a}	12.9 ± 0.3^{ab}	11.9 ± 0.5^{b}
Cholesterol, mg/g liver	2.5 ± 0.2^{a}	2.4 ± 0.1^{a}	1.8 ± 0.1^{b}	1.7 ± 0.1^{b}
NEFA, 10^{-3} mEq/g liver	3.6 ± 0.2^{b}	4.6 ± 0.3^{ab}	4.9 ± 0.4^{ab}	5.6 ± 0.7^{a}

[1] Values are mean ± S.E.M. n = 8–11 per group at eight weeks. [2] Means in each row with superscripts without a common letter differ, $p < 0.05$. [3] LF: Low-fat diet. [4] HF: High-fat diet. [5] OXY1: High-fat diet supplemented with 0.25% oxyresveratrol. [6] OXY2: High-fat diet supplemented with 0.5% oxyresveratrol. [7] HOMA-IR index: fasting serum glucose (mmol/L) × fasting serum insulin (mIU/L)/22.5.

3.4. Effects of Oxyresveratrol on mRNA Expression of Liver, Visceral Fat, and Gastrocnemius Muscle

In OXY supplemented HF groups (especially in OXY2 group), hepatic mRNA expression of AMP-activated protein kinase α2 (AMPKα2) was upregulated, whilst glucose-6-phosphatase (G6pase) level was downregulated compared to the HF group (Figure 3a,b). Hepatic mRNA expressions of carnitine palmitoyltransferase IA (CPT-1a), carnitine palmitoyltransferase IB (CPT-1b) in oxyresveratrol OXY groups were similar to those of the HF group (Figure 3c,d). Mice fed with a high-fat diet for eight weeks had decreased mRNA expressions of glucose transporter type 4 (GLUT4) in visceral fat, whereas GLUT4 level was upregulated in OXY supplemented HF groups (Figure 4). In gastrocnemius muscle, mRNA expressions of GLUT4, insulin receptor substrate 1 (IRS-1), SIRT1, peroxisome proliferator-activated receptor gamma coactivator 1-alpha (PGC-1α), AMPKα1 and AMPKα2 were all upregulated in OXY supplemented groups (especially in OXY2) compared to the HF group (Figure 5).

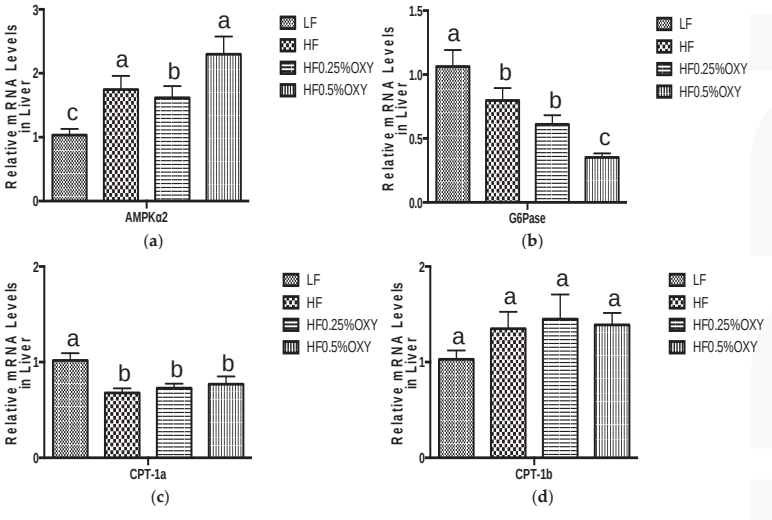

Figure 3. Relative mRNA expression levels of AMPKα2 (**a**), G6Pase (**b**), CPT-1a (**c**), and CPT-1b (**d**) in liver of C57bl/6 mice that were fed low-fat or high-fat diet with or without oxyresveratrol (n = 8–11/group) for eight weeks. Values are presented as means ± S.E.M. Within each treatment, bars topped by different letters are significantly different at $p < 0.05$.

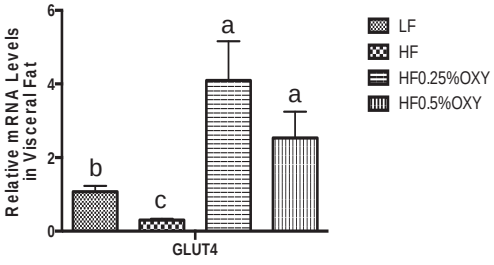

Figure 4. Relative mRNA expression level of GLUT4 in visceral fat of C57bl/6 mice that were fed low-fat or high-fat diet with or without oxyresveratrol (n = 8–11/group) for eight weeks. Values are presented as means ± S.E.M. Within each treatment, bars topped by different letters are significantly different at $p < 0.05$.

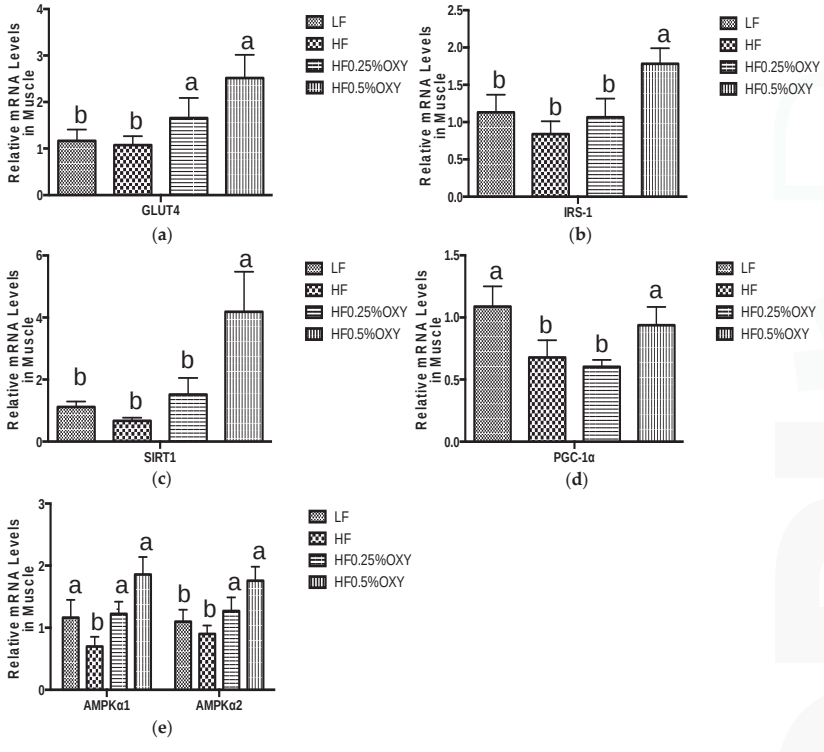

Figure 5. Relative mRNA expression levels of GLUT4 (**a**), IRS1 (**b**), SIRT1 (**c**), PGC-1α (**d**), AMPKα1 (**e**), and AMPKα2 (**e**) in gastrocnemius muscle of C57bl/6 mice that were fed low-fat or high-fat diet with or without oxyresveratrol (n = 8–11/group) for eight weeks. Values are presented as means ± S.E.M. Within each treatment, bars topped by different letters are significantly different at $p < 0.05$.

3.5. Effects of Oxyresveratrol on Hepatic Protein Expression

In liver, protein levels of sterol regulatory element-binding proteins 1 (SREBP-1), CCAAT/Enhancer-binding proteins α (C/EBPα), and fatty acid synthase (FAS) were significantly downregulated in OXY supplemented high-fat diets groups (Figure 6a–c,f). While no significant difference on

CCAAT/Enhancer-binding proteins β (C/EBPβ) and peroxisome proliferator-activated receptor γ (PPARγ) has been observed among the four mice groups (Figure 6d–f).

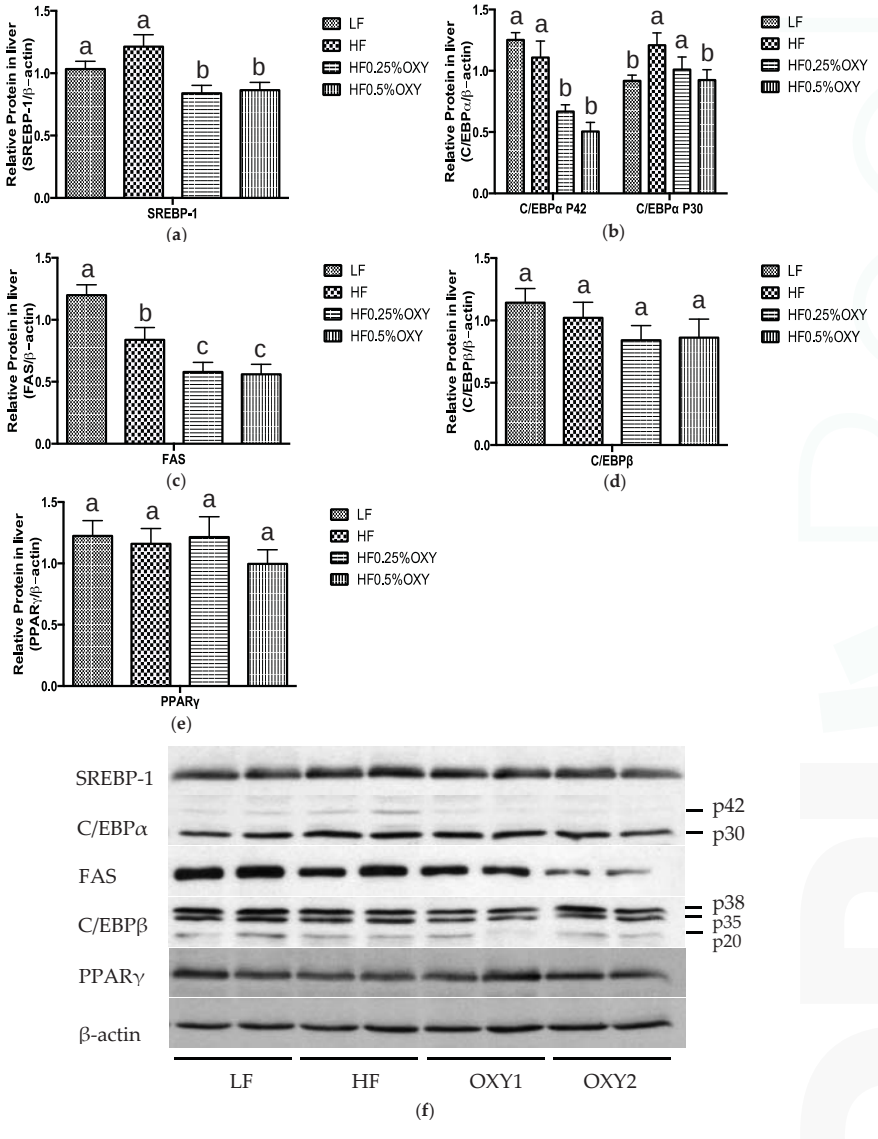

Figure 6. Protein expressions of SREBP-1 (**a**,**f**), C/EBPα (**b**,**f**), FAS (**c**,**f**), C/EBPβ (**d**,**f**), and PPARγ (**e**,**f**) in liver of C57bl/6 mice that were fed low-fat or high-fat diet with or without oxyresveratrol (n = 8–11/group) for eight weeks. Protein expressions were quantified densitometrically using the software ImageJ 1.47v (Wayne Rasband, Bethesda, MD, USA), and were arbitrary units after correction for loading differences by measuring the amount of β-actin. Values are presented as means ± S.E.M. Within each treatment, bars topped by different letters are significantly different at $p < 0.05$.

4. Discussion

In recent years, resveratrol has been demonstrated to effectively lower body weight and adiposity in rodents fed a high-calorie diet by inducing favorable changes in specific gene and protein expression [5]. Being similar in structure with resveratrol, OXY has been identified to hold various biological functions that are comparable to those of resveratrol. However, little is known about its anti-obesity property. Our previous in vitro study determined that OXY possesses anti-adipogenic property in 3T3-L1 cells by regulating some key transcriptional factors, as well as inducing cell cycle arrest through modulation of specific cell cycle regulatory molecules [17], which encouraged us to study the potential effect of OXY in regulating obesity in vivo. In the present study, OXY was evaluated of its impact on weight management, obesity-related biochemical parameters, and the regulation of adiposity related gene and protein expression in high-fat diet-fed mice. The results clearly manifested that, compared to the HF group, OXY supplementation remarkably induced suppression of body weight (up to 26%), and organ weight of liver (up to 28%), and visceral fat (up to 51%), restored serum level of glucose and insulin, and ameliorated the lipid profile of serum and liver in high-fat diet-fed mice.

Diet composition is closely related to energy efficiency. Mice with high-fat diet induced obese would have increased energy efficiency, partly resulting from the high energy content of triglycerides, which are stored in essentially anhydrous form other than the hydrated form for polysaccharides, reducing the energy stores' efficiency as fuel [21–23]. In this study, an increase in energy efficiency has been observed in the HF group, while OXY1 diet (2.5 g OXY/kg HF diet) decreased energy efficiency in mice and normalized it to that of the low-fat diet group. Moreover, comparing to the OXY1 group, mice fed with OXY2 diet (5 g OXY/kg HF diet) had significantly lower body weight gain, energy efficiency, and visceral fat weight without changing the energy intake, which suggested that there might be a dose dependent effect for OXY to regulate obesity.

Insulin, a peptide hormone secreted by the β cells in the pancreas, functions to suppress serum level of glucose by catalyzing glucose transfer into adipose tissue and muscle, and reducing hepatic glucose production [24]. Obesity development could lead to insulin resistance, characterized by the raised level of circulating insulin, as well as suppressed insulin sensitivity [25,26]. In this study, serum insulin level and insulin resistance index, HOMA-IR, in the HF group mice was significantly elevated compared to those of the LF group, while OXY supplementation alleviated them in high-fat diet-fed mice and reduced their levels to those of the LF mice.

Under the condition of insulin resistance, cells in insulin dependent tissues, principally adipose tissues and muscles, are resistant to insulin and fail to respond to it effectively, inducing a high level of serum glucose [27]. In this study, serum glucose level was significantly elevated in the HF group compared to that of the LF group, while OXY supplementation significantly reduced its level. For adipocytes and muscle cells, intracellular glucose uptake is insulin-dependent via GLUT4, a major glucose transporter protein. Adipose tissue is supposed to account for around 10% of insulin-regulated whole body glucose uptake [27]. Through GLUT4, excess blood glucose is diffused into adipocytes, stimulating the synthesis of fatty acid and glycerol, while suppressing lipolysis. Similar with what happens to adipocytes, the transportation of intracellular glucose into muscle cells is also via GLUT4 under the regulation of insulin. Muscle is the primary site of insulin-stimulated glucose disposal, and accounts for around 60%–70% of whole body glucose uptake [27,28]. Earlier researches suggested that GLUT4 gene expression is decreased in adipose tissue, while retained in muscle under various insulin resistant states [28]. With the increased GLUT4 expression in adipose tissue or muscle, or both, glucose tolerance and insulin sensitivity could be elevated in normal, obese, or diabetic mice [28]. In this study, the mRNA expression of GLUT4 was downregulated in visceral fat, but preserved in muscles of the HF group compared to that of the LF group, and the results are consistent with those previous studies. Nevertheless, the OXY supplementation significantly upregulated GLUT4 expression in both visceral fat tissue and muscle of high-fat fed mice, which might stimulate insulin sensitivity, increasing blood

glucose uptake into adipocytes and muscle cells, reducing serum glucose level in OXY supplemented mice groups.

Apart from GLUT4, IRS-1—a member of the insulin receptor substrate family of adaptor molecules—also plays vital role in intracellular glucose uptake. It is involved in insulin signaling through tyrosine phosphorylation in response to insulin, insulin growth factor-1, and cytokines [29]. The reduced insulin receptor and IRS-1 levels, their depressed tyrosine phosphorylation together with the diminished IRS1-associated phosphatidylinositol-3 kinase activity all devote to the defective insulin-stimulated glucose transport through impairing GLUT4 translocation in muscle in obese subjects [30,31]. In this study, mRNA levels of IRS-1 and GLUT4 were both significantly increased in muscle of OXY treated group (OXY2) compared to the HF group, suggesting that OXY supplementation might increase glucose uptake and disposal in muscle through ameliorating insulin resistance by stimulating IRS-1 and GLUT4 expression.

The decreased mRNA expression of hepatic G6Pase in the OXY supplemented groups might also due to the ameliorated hyperglycemia. G6Pase is a multifunctional enzyme capable of hydrolyzing glucose-6-phosphate, and producing free glucose, which is released from liver to blood [32]. The downregulation of G6Pase in OXY supplemented groups might result in the reduced production of hepatic glucose, thus lowering the release of glucose into the bloodstream. The above results demonstrated that hyperglycemia induced by high-fat diet in mice could be effectively alleviated by OXY supplementation, presumably attributed to OXY's ameliorative effect in insulin resistance by elevating glucose uptake into peripheral tissues and depressing hepatic glycogenolysis.

During obesity development, the defective hepatic metabolism as well as the excessive adiposity lead to an increase in plasma free fatty acids level [24]. In this study, serum triglyceride, cholesterol, and NEFA levels, as well as hepatic triglyceride and cholesterol levels were significantly lowered in OXY supplemented group (OXY2) compared to the HF group. In liver, the protein expressions of SREBP-1 and FAS were both diminished in OXY supplemented groups than those of the HF group. SREBP-1, a member of the basic helix-loop-helix leucine zipper family, regulates triglyceride synthesis through mediating the transcription and expression of lipogenic proteins, such as FAS, which is a multi-functional enzyme mainly involved in catalyzing the synthesis of long chain fatty acids [33,34]. OXY supplementation might reduce fat content in liver through the SREBP-1 pathway by suppressing SREBP-1 expression and, hence diminishing FAS activity to lower fatty acid and triglyceride synthesis and storage.

Meanwhile, the hepatic expression of C/EBPα protein was suppressed in OXY supplemented groups compared to the HF group. C/EBPs are members of the basic leucine zipper family of transcriptional factors and mainly function by directing the adipose-specific gene expression during adipocyte transition process [35,36]. C/EBPα is primarily expressed in hepatocytes and adipocytes and has been well documented to involve in energy homeostasis [37,38]. The deficiency of hepatic C/EBPα could decrease body lipid level by diminishing the induction of lipogenic genes to reduce hepatic TG and cholesterol concentration [38]. Therefore, apart from the SREBP-1 pathway, OXY may also restrict hepatic lipid synthesis through the downregulation of hepatic C/EBPα.

Also, hepatic AMPKα2 expression was elevated in OXY supplemented groups. AMPK is an energy sensing enzyme that plays a vital role in regulating metabolic homeostasis through mediating mitochondrial biogenesis in response to energy deprivation [39]. AMPKα is a subunit of AMPK with two isoforms—namely, AMPKα1 and AMPKα2 [31]. AMPKα1 is widely expressed, whereas AMPKα2 is the dominant catalytic form of AMPK in the liver, muscle, and hypothalamus and essential for the modulation of metabolic homeostasis and insulin sensitivity [40]. In liver, AMPK is capable of suppressing hepatic glucose, free fatty acid, TG, and cholesterol synthesis by inactivating specific gene and protein expressions in gluconeogenesis and lipogenesis [31]. In this study, the increased hepatic AMPKα2 expression thus may be a result of the reduced hepatic glucose and lipids synthesis. Therefore, OXY may ameliorate hepatic fat accumulation mainly through mediating the expression of adipogenic gene/proteins (SREBP-1, FAS, C/EBPα, and AMPKα2). The alleviated hepatic metabolism

together with the reduced adiposity in OXY supplemented groups may work collaboratively to regulate lipid profile in serum.

In the OXY supplemented group (OXY2), muscle mRNA expressions of AMPKα, PGC-1α, and SIRT1 were all upregulated compared to the HF group. PGC-1α, a metabolic co-activator, functions in stimulating mitochondrial biogenesis and respiration through interacting with transcription factors [41]. It controls fiber-type switching and the expression of various genes involved in lipid oxidation and mitochondrial metabolism [42]. AMPK can activate PGC-1α by direct phosphorylation, enhancing its transcriptional activity [39]. Meanwhile, AMPK needs PGC-1α to regulate the expression of several important genes involved in mitochondrial and glucose metabolism [42]. SIRT1, which is well documented for its beneficial effect in life span extension, can also interact with PGC-1α in muscle directly by deacetylation, promoting mitochondrial activity, thus improving exercise performance and thermogenic activity [42,43]. In muscle, AMPK and SIRT1 work cooperatively to mediate energy metabolism, and AMPK could enhance SIRT1 activity through upregulating cellular nicotinamide adenine dinucleotide level, leading to the deacetylation and regulation of the activity of downstream SIRT1 targets [39]. A recent in vivo study indicated that AMPK, PGC-1α, and SIRT1 act as an energy sensing network to promote metabolic fitness, suggesting that OXY supplementation might benefit metabolic homeostasis through stimulating the expression of AMPK, PGC-1α, and SIRT1 in muscle to advance their network [42]. However, further studies are needed to verify their connections and effects on obesity development.

5. Conclusions

OXY supplementation remarkably induced suppression on body weight (up to 26%), organ weight of liver (up to 28%), and visceral fat (up to 51%). It restored serum level of glucose and insulin, which was presumably through increasing intracellular glucose uptake in muscle and adipose tissue by upregulating expression of key glucose transportation genes (GLUT4/IRS1) in these tissues, as well as repressing free glucose production in liver by suppressing hepatic G6Pase expression. Meanwhile, lipid profile of serum and liver was significantly ameliorated in OXY supplemented high-fat diet-fed groups, which was presumably through mediating expression of major adipogenic genes/proteins (SREBP-1, FAS, C/EBPα, AMPKα2) in liver. Also, OXY might promote metabolic fitness in high-fat diet-fed mice by elevating the expressions of AMPKα, PGC-1α, and SIRT1 in muscle. To our knowledge, this is the first study providing in vivo evidence for OXY's anti-obesity property. Further research in other animal models or in humans should be considered to verify OXY's effect in counteracting obesity.

Acknowledgments: This research was supported by the University of Hong Kong. Wai Hung Sit is acknowledged for providing technical help. Ka Ho Ling, Yizhen Wu, and Juanying Ou are acknowledged for providing help in mice tissue collection.

Author Contributions: H.Y.T., I.M.Y.T., E.T.S.L. and M.W. have designed the study; H.Y.T. and I.M.Y.T. have conducted the study; H.Y.T. and E.T.S.L. have analyzed the data; H.Y.T. and M.W. have written the manuscript. E.T.S.L. and M.W. have reviewed the manuscript. All authors read and approved the final manuscript.

Conflicts of Interest: The authors declare no conflict of interest.

References

1. World Health Organization. Obesity and Overweight, Fact Sheet n°311. Available online: http://www.who.int/mediacentre/factsheets/fs311/en/ (accessed on 25 October 2016).
2. Heo, M.; Allison, D.B.; Faith, M.S.; Zhu, S.; Fontaine, K.R. Obesity and quality of life: Mediating effects of pain and comorbidities. *Obes. Res.* **2003**, *11*, 209–216. [CrossRef] [PubMed]
3. Must, A.; Spadano, J.; Coakley, E.H.; Field, A.E.; Colditz, G.; Dietz, W.H. The disease burden associated with overweight and obesity. *JAMA* **1999**, *282*, 1523–1529. [CrossRef] [PubMed]
4. World Health Organization. *Obesity: Preventing and Managing the Global Epidemic—Report of a WTO Consultation*; World Health Organization: Geneva, Switzerland, 2000.

5. Szkudelska, K.; Szkudelski, T. Resveratrol, obesity and diabetes. *Eur. J. Pharmacol.* **2010**, *635*, 1–8. [CrossRef] [PubMed]
6. Galindo, I.; Hernáez, B.; Berná, J.; Fenoll, J.; Cenis, J.L.; Escribano, J.M.; Alonso, C. Comparative inhibitory activity of the stilbenes resveratrol and oxyresveratrol on African swine fever virus replication. *Antivir. Res.* **2011**, *91*, 57–63. [CrossRef] [PubMed]
7. Lorenz, P.; Roychowdhury, S.; Engelmann, M.; Wolf, G.; Horn, T.F.W. Oxyresveratrol and resveratrol are potent antioxidants and free radical scavengers: Effect on nitrosative and oxidative stress derived from microglial cells. *Nitric Oxide* **2003**, *9*, 64–76. [CrossRef] [PubMed]
8. Deng, H.; He, X.; Xu, Y.; Hu, X. Oxyresveratrol from mulberry as a dihydrate. *Acta Crystallogr. Sect. E.-Struct Rep. Online* **2012**, *68*, o1318–o1319. [CrossRef] [PubMed]
9. Chung, K.O.; Kim, B.Y.; Lee, M.H.; Kim, Y.R.; Chung, H.Y.; Park, J.H.; Moon, J.O. In-vitro and in-vivo anti-inflammatory effect of oxyresveratrol from morus alba l. *J. Pharm. Pharmacol.* **2003**, *55*, 1695–1700. [CrossRef] [PubMed]
10. Aftab, N.; Likhitwitayawuid, K.; Vieira, A. Comparative antioxidant activities and synergism of resveratrol and oxyresveratrol. *Nat. Prod. Res.* **2010**, *24*, 1726–1733. [CrossRef] [PubMed]
11. Likhitwitayawuid, K.; Sritularak, B.; Benchanak, K.; Lipipun, V.; Mathew, J.; Schinazi, R.F. Phenolics with antiviral activity from millettia erythrocalyx and artocarpus lakoocha. *Nat. Prod. Res.* **2005**, *19*, 177–182. [CrossRef] [PubMed]
12. Chuanasa, T.; Phromjai, J.; Lipipun, V.; Likhitwitayawuid, K.; Suzuki, M.; Pramyothin, P.; Hattori, M.; Shiraki, K. Anti-herpes simplex virus (HSV-1) activity of oxyresveratrol derived from thai medicinal plant: Mechanism of action and therapeutic efficacy on cutaneous HSV-1 infection in mice. *Antivir. Res.* **2008**, *80*, 62–70. [CrossRef] [PubMed]
13. Chao, J.; Yu, M.S.; Ho, Y.S.; Wang, M.; Chang, R.C.C. Dietary oxyresveratrol prevents parkinsonian mimetic 6-hydroxydopamine neurotoxicity. *Free Radic. Biol. Med.* **2008**, *45*, 1019–1026. [CrossRef] [PubMed]
14. Andrabi, S.A.; Spina, M.G.; Lorenz, P.; Ebmeyer, U.; Wolf, G.; Horn, T.F.W. Oxyresveratrol (trans-2,3′, 4,5′-tetrahydroxystilbene) is neuroprotective and inhibits the apoptotic cell death in transient cerebral ischemia. *Brain Res.* **2004**, *1017*, 98–107. [CrossRef] [PubMed]
15. Shin, N.H.; Ryu, S.Y.; Choi, E.J.; Kang, S.H.; Chang, I.L.M.; Min, K.R.; Kim, Y. Oxyresveratrol as the potent inhibitor on dopa oxidase activity of mushroom tyrosinase. *Biochem. Biophys. Res. Commun.* **1998**, *243*, 801–803. [CrossRef] [PubMed]
16. Li, H.; Cheng, K.-W.; Cho, C.-H.; He, Z.; Wang, M. Oxyresveratrol as an antibrowning agent for cloudy apple juices and fresh-cut apples. *J. Agric. Food Chem.* **2007**, *55*, 2604–2610. [CrossRef] [PubMed]
17. Tan, H.-Y.; Iris, M.Y.; Li, E.T.S.; Wang, M. Inhibitory effects of oxyresveratrol and cyanomaclurin on adipogenesis of 3T3-L1 cells. *J. Funct. Foods* **2015**, *15*, 207–216. [CrossRef]
18. Reeves, P.G.; Nielsen, F.H.; Fahey, G.C, Jr. AIN-93 purified diets for laboratory rodents: Final report of the american institute of nutrition ad hoc writing committee on the reformulation of the AIN-76A rodent diet. *J. Nutr.* **1993**, *123*, 1939–1951. [PubMed]
19. Patarrão, R.S.; Lautt, W.W.; Macedo, M.P. Assessment of methods and indexes of insulin sensitivity. *Rev. Port. Endocrinol. Diabetes Metab.* **2014**, *9*, 65–73. [CrossRef]
20. Fraulob, J.C.; Ogg-Diamantino, R.; Fernandes-Santos, C.; Aguila, M.B.; Mandarim-de-Lacerda, C.A. A mouse model of metabolic syndrome: Insulin resistance, fatty liver and non-alcoholic fatty pancreas disease (NAFPD) in C57BL/6 mice fed a high fat diet. *J. Clin. Biochem. Nutr.* **2010**, *46*, 212. [CrossRef] [PubMed]
21. Li, S.; Iris, M.Y.; Li, E.T.S. Maternal green tea extract supplementation to rats fed a high-fat diet ameliorates insulin resistance in adult male offspring. *J. Nutr. Biochem.* **2012**, *23*, 1655–1660. [CrossRef] [PubMed]
22. Lin, P.-Y.; Romsos, D.R.; Vander Tuig, J.G.; Leveille, G.A. Maintenance energy requirements, energy retention and heat production of young obese (ob/ob) and lean mice fed a high-fat or a high-carbohydrate diet. *J. Nutr.* **1979**, *109*, 1143–1153. [PubMed]
23. Spiegelman, B.M.; Flier, J.S. Obesity and the regulation of energy balance. *Cell* **2001**, *104*, 531–543. [CrossRef]
24. Kahn, B.B.; Flier, J.S. Obesity and insulin resistance. *J. Clin. Investig.* **2000**, *106*, 473. [CrossRef] [PubMed]
25. Kahn, S.E.; Hull, R.L.; Utzschneider, K.M. Mechanisms linking obesity to insulin resistance and type 2 diabetes. *Nature* **2006**, *444*, 840–846. [CrossRef] [PubMed]
26. Pan, H.; Guo, J.; Su, Z. Advances in understanding the interrelations between leptin resistance and obesity. *Physiol. Behav.* **2014**, *130*, 157–169. [CrossRef] [PubMed]

27. Wilcox, G. Insulin and insulin resistance. *Clin. Biochem. Rev.* **2005**, *26*, 19. [PubMed]
28. Epstein, F.H.; Shepherd, P.R.; Kahn, B.B. Glucose transporters and insulin action—Implications for insulin resistance and diabetes mellitus. *N. Engl. J. Med.* **1999**, *341*, 248–257. [CrossRef] [PubMed]
29. Gual, P.; Le Marchand-Brustel, Y.; Tanti, J.-F. Positive and negative regulation of insulin signaling through IRS-1 phosphorylation. *Biochimie* **2005**, *87*, 99–109. [CrossRef] [PubMed]
30. Björnholm, M.; Kawano, Y.; Lehtihet, M.; Zierath, J.R. Insulin receptor substrate-1 phosphorylation and phosphatidylinositol 3-kinase activity in skeletal muscle from niddm subjects after in vivo insulin stimulation. *Diabetes* **1997**, *46*, 524–527. [CrossRef] [PubMed]
31. Misra, P.; Chakrabarti, R. The role of AMP kinase in diabetes. *Indian J. Med. Res.* **2007**, *125*, 389–398. [PubMed]
32. Nordlie, R.C.; Jorgenson, R.A. Glucose-6-phosphatase. In *The Enzymes of Bioligical Membranes*, 1st ed.; Martonosi, A.N., Ed.; Springer: New York, NY, USA, 1976; Volume 2, pp. 465–491.
33. Alberts, A.W.; Strauss, A.W.; Hennessy, S.; Vagelos, P.R. Regulation of synthesis of hepatic fatty acid synthetase: Binding of fatty acid synthetase antibodies to polysomes. *Proc. Natl. Acad. Sci. USA* **1975**, *72*, 3956–3960. [CrossRef] [PubMed]
34. Sekiya, M.; Yahagi, N.; Matsuzaka, T.; Najima, Y.; Nakakuki, M.; Nagai, R.; Ishibashi, S.; Osuga, J.I.; Yamada, N.; Shimano, H. Polyunsaturated fatty acids ameliorate hepatic steatosis in obese mice by SREBP-1 suppression. *Hepatology* **2003**, *38*, 1529–1539. [CrossRef] [PubMed]
35. Darlington, G.J.; Ross, S.E.; MacDougald, O.A. The role of C/EBP genes in adipocyte differentiation. *J. Biol. Chem.* **1998**, *273*, 30057–30060. [CrossRef] [PubMed]
36. Gregoire, F.M.; Smas, C.M.; Sul, H.S. Understanding adipocyte differentiation. *Physiol. Rev.* **1998**, *78*, 783–809. [PubMed]
37. Flodby, P.; Barlow, C.; Kylefjord, H.; Ahrlund-Richter, L.; Xanthopoulos, K.G. Increased hepatic cell proliferation and lung abnormalities in mice deficient in ccaat/enhancer binding protein α. *J. Biol. Chem.* **1996**, *271*, 24753–24760. [CrossRef] [PubMed]
38. Matsusue, K.; Gavrilova, O.; Lambert, G.; Brewer, H.B., Jr.; Ward, J.M.; Inoue, Y.; LeRoith, D.; Gonzalez, F.J. Hepatic CCAAT/enhancer binding protein α mediates induction of lipogenesis and regulation of glucose homeostasis in leptin-deficient mice. *Mol. Endocrinol.* **2004**, *18*, 2751–2764. [CrossRef] [PubMed]
39. Cantó, C.; Gerhart-Hines, Z.; Feige, J.N.; Lagouge, M.; Noriega, L.; Milne, J.C.; Elliott, P.J.; Puigserver, P.; Auwerx, J. AMPK regulates energy expenditure by modulating NAD+ metabolism and SIRT1 activity. *Nature* **2009**, *458*, 1056–1060. [CrossRef] [PubMed]
40. Zhang, W.; Zhang, X.; Wang, H.; Guo, X.; Li, H.; Wang, Y.; Xu, X.; Tan, L.; Mashek, M.T.; Zhang, C. AMP-activated protein kinase α1 protects against diet-induced insulin resistance and obesity. *Diabetes* **2012**, *61*, 3114–3125. [PubMed]
41. Gerhart-Hines, Z.; Rodgers, J.T.; Bare, O.; Lerin, C.; Kim, S.H.; Mostoslavsky, R.; Alt, F.W.; Wu, Z.; Puigserver, P. Metabolic control of muscle mitochondrial function and fatty acid oxidation through SIRT1/PGC-1α. *EMBO J.* **2007**, *26*, 1913–1923. [CrossRef] [PubMed]
42. Cantó, C.; Auwerx, J. PGC-1alpha, SIRT1 and AMPK, an energy sensing network that controls energy expenditure. *Curr. Opin. Lipidol.* **2009**, *20*, 98. [CrossRef] [PubMed]
43. Rodgers, J.T.; Lerin, C.; Haas, W.; Gygi, S.P.; Spiegelman, B.M.; Puigserver, P. Nutrient control of glucose homeostasis through a complex of PGC-1α and SIRT1. *Nature* **2005**, *434*, 113–118. [CrossRef] [PubMed]

nutrients

MDPI

Article

Age-Related Loss in Bone Mineral Density of Rats Fed Lifelong on a Fish Oil-Based Diet Is Avoided by Coenzyme Q_{10} Addition

Alfonso Varela-López [1], Julio J. Ochoa [1], José M. Llamas-Elvira [2], Magdalena López-Frías [1], Elena Planells [1], MCarmen Ramirez-Tortosa [3], Cesar L. Ramirez-Tortosa [4], Francesca Giampieri [5], Maurizio Battino [5] and José L. Quiles [1,*]

1 Institute of Nutrition and Food Technology "José Mataix Verdú", Department of Physiology, Biomedical Research Center, University of Granada, 18100 Granada, Spain; alvarela@ugr.es (A.V.-L.); jjochoa@ugr.es (J.J.O.); maglopez@ugr.es (M.L.-F.); elenamp@ugr.es (E.P.)
2 Nuclear Medicine Service, Hospital Virgen de las Nieves, 18014 Granada, Spain; josem.llamas.sspa@juntadeandalucia.es
3 Institute of Nutrition and Food Technology "José Mataix Verdú", Department of Biochemistry and Molecular Biology II, Biomedical Research Center, University of Granada, 18100 Granada, Spain; mramirez@ugr.es
4 Department of Pathology, Complejo Hospitalario de Jaén, 23007 Jaén, Spain; cesarl.ramirez.sspa@juntadeandalucia.es
5 Department of Scienze Cliniche Specialistiche ed Odontostomatologiche, Università Politecnica delle Marche, 60131 Ancona, Italy; fgiampie@mta01.univpm.it (F.G.); m.a.battino@univpm.it (M.B.)
* Correspondence: jlquiles@ugr.es; Tel.: +34-958-241-000 (ext. 20316)

Received: 11 November 2016; Accepted: 13 February 2017; Published: 22 February 2017

Abstract: During aging, bone mass declines increasing osteoporosis and fracture risks. Oxidative stress has been related to this bone loss, making dietary compounds with antioxidant properties a promising weapon. Male Wistar rats were maintained for 6 or 24 months on diets with fish oil as unique fat source, supplemented or not with coenzyme Q_{10} (CoQ_{10}), to evaluate the potential of adding this molecule to the *n*-3 polyunsaturated fatty acid (*n*-3 PUFA)-based diet for bone mineral density (BMD) preservation. BMD was evaluated in the femur. Serum osteocalcin, osteopontin, receptor activator of nuclear factor-κB ligand, ostroprotegerin, parathyroid hormone, urinary F_2-isoprostanes, and lymphocytes DNA strand breaks were also measured. BMD was lower in aged rats fed a diet without CoQ_{10} respect than their younger counterparts, whereas older animals receiving CoQ_{10} showed the highest BMD. F_2-isoprostanes and DNA strand breaks showed that oxidative stress was higher during aging. Supplementation with CoQ_{10} prevented oxidative damage to lipid and DNA, in young and old animals, respectively. Reduced oxidative stress associated to CoQ_{10} supplementation of this *n*-3 PUFA-rich diet might explain the higher BMD found in aged rats in this group of animals.

Keywords: antioxidants; dietary fat; *n*-3 PUFA; oxidative stress; ubiquinone

1. Introduction

Bone is continuously remodeled by two groups of cells with opposite activities, osteoblasts implicated in bone formation and osteoclasts implicated in bone resorption. Maturation processes and function of both kinds of cells can be altered during aging. When bone resorption rate exceeds osteoblasts rate of new bone formation by osteoclasts, calcium, collagen, and protein depletions will occur [1]. It is known that, regardless of sex, bone mass declines progressively with advancing age in humans [2]. Moreover, such decline is coupled with modifications of bone architecture

and bone components organization [3]. All these age-associated changes [2–4] would explain the increased prevalence of osteoporosis reported in the elderly [5]. Osteoporosis has been defined as "a skeletal disorder characterized by compromised bone strength and predisposing to an increased risk of fracture" [6]. The former fact is particularly important since fractures are responsible for a significant mortality and morbidity in older people [7,8]. Osteoporosis is a disease that mostly affects elderly women, but it is also a major health problem for aged men [9], in whom this pathology shows an important association with substantial morbidity, mortality, and health care costs [10]. Because osteoporotic fractures involve considerable economic and healthcare burdens [11], promotion of effective prevention and treatment strategies to counterbalance them is imperative [12].

Amongst others, different nutritional factors have an important role in skeletal health during aging. Traditionally, calcium, vitamin D, and proteins have received special attention since they contribute to skeletal health by supporting bone matrix production and mineralization [13–15]. However, other dietary factors might influence bone and mineral homeostasis and could be important for long-term bone health [12]. In that sense, there is a growing body of evidence emphasizing the importance of dietary fat in bone aging and osteoporosis. Overall, high-fat diets, particularly those rich in saturated fats have been negatively associated with bone health [16,17], whereas polyunsaturated fatty acids (PUFA) seem to have some positive effects [18–21]. Notwithstanding, PUFA may also have important implications due to a wide range of possible mechanisms [22–25]. In relation to *n*-3 PUFA intake, there is evidence of a positive role of this type of fatty acid on bone mineral density (BMD), bone mineral content (BMC), or bone calcium levels [26–35]. This role of *n*-3 PUFA has been particularly notable when their effects are compared with those from *n*-6 PUFA in both humans [27] and animals [29–33,36]. However, some experiments with rats have suggested that this effect is dose-dependent [36] andthe positive role of *n*-3 PUFA could be conditioned by a ceiling [32,37]. In that sense, there are studies indicating some detrimental effects of a diet with a very high proportion of *n*-3 PUFA on other tissues and organs [38]. This is not entirely surprising since detrimental effects of diets rich in *n*-3 PUFA have been previously shown in other tissues [38]. Moreover, results from some in vitro studies have suggested possible negative effects on bone formation for some particular *n*-3 PUFA [39,40].

Along with dietary conditions and changes in several hormones levels, oxidative stress has also been shown to be implicated in the pathogenesis of osteoporosis or has been related to high bone loss during aging [41–43]. It is known that PUFA is highly susceptible to reactive oxygen species (ROS) attack, subsequently increasing the oxidative damage in the organism, especially during aging [44]. PUFA susceptibility to lipid peroxidation would also involve *n*-3 PUFA. In fact, it has been suggested that dietary compounds with antioxidant and anti-inflammatory properties could have promising bone protective effects [45,46]. Supplementation with antioxidants would preserve the advantages of PUFA on bone while preventing their deleterious effects and, in addition, modulate the effects of free radicals on bone health. In relation to aging, several studies in preclinical models have reported positive effects of dietary coenzyme Q (CoQ) [47–49]. CoQ is a key electron carrier in mitochondrial respiratory chain [6,23,26–29], and constitutes an important lipid-soluble antioxidant present in all biological membranes [50]. It has been shown to efficiently prevent oxidation of proteins, lipids, and DNA [51–54]. Likewise, other interesting physiological roles in cells related to these activities have been suggested for this molecule [50,55,56]. Based on these properties, the use of CoQ supplements under certain nutritional conditions associated with high oxidative stress levels could prove to be particularly interesting. In that sense, the effect of dietary CoQ has been investigated in the aging of some tissues and organs from rats fed with "pro-oxidant" PUFA-rich diets offering promising results [40,44,57–61]. However, knowledge about the effect of dietary CoQ on bone health is limited, and there are no studies on the effect of the combination of this antioxidant and *n*-3 PUFA-rich diet on bone health. On the other hand, research on diet and bone health have been mainly performed on postmenopausal rodent models (i.e., ovarectomized) using very young animals or directly on postmenopausal women with osteoporosis. However, rats reach skeletal maturity at the age of approximately 12 months [11], so results from many studies are not based on a good senile osteoporosis model. In addition, little

research addressed male subjects. However, an age-dependent decline of bone mass and strength in sex steroid-sufficient female or male mice has been also reported [41]. In this context, the present study was designed to evaluate the potential of adding coenzyme Q_{10} (CoQ_{10}) to a normocaloric and normolipidic diet with fish oil as a unique dietary fat source (rich in *n*-3 PUFA) for whole-life on bone aging and health in a male rat model of aging.

2. Materials and Methods

2.1. Experimental Design

Twenty-four male Wistar rats (*Rattus norvegicus*) weighing 80–90 g were housed three per cage and maintained in a 12-h light/12-h darkness cycle, with free access to food and water. The rats were randomly assigned into two experimental groups and fed from weaning until 24 months of age on a semi-synthetic and isoenergetic diet according to the AIN93 criteria [62] with the exception of dietary fat consisting only in fish oil. Diet composition was the following (in % weight/weight): 14% casein, 46.57% starch, 10% sucrose, 4% fish oil, 15.5% dextrose, 5% cellulose, 0.25% choline, 0.185 L-cystine, 1% vitamin mixture, and 3.5% mineral mixture. In addition, a supplemented version of each diet was prepared to reach 2.5 mg/kg per day of CoQ_{10}. Two experimental groups were established: animals fed a fish oil-based diet without added CoQ_{10} (only the fish oil group) and those on the same diet but supplemented with CoQ_{10} (fish oil + CoQ). The rats were killed by cervical dislocation followed by decapitation, at the same time of the day, to avoid any circadian fluctuation. From each group, half of the rats were killed at 6 months of age and the other half at 24 months of age. Such ages were chosen because rats are respectively considered as young adults and elderly subjects, but not too old [63]. Blood was collected for plasma and serum isolation. Femur bones were isolated, physically cleaned from remaining soft tissues, weighted, and preserved in 70% ethanol until analysis. The animals were treated in accordance with the guidelines of the Spanish Society for Laboratory Animals, and the experiment was approved by the Ethical Committee of the University of Granada (permit number 20-CEA-2004).

2.2. Plasma Fatty Acid Profile and Total Coenzyme Q_{10} Levels Determination

Plasma fatty acid profile in rats was determined by following Lepage and Roy's method [64] with previously described modifications [65]. Plasma levels of CoQ_{10} were assayed by high-performance liquid chromatography (HPLC) with electrochemical detection according to MacCrehan [66] as previously described [67]. A Spherisorb S5 ODS1 (Merck, Darmnstadt, Germany) column was used and ethanol/purified water 97:3 (*v/v*) acted as mobile phase. Retention times of individual standards were predetermined to identify CoQ_{10}.

2.3. Determination of Bone Mineral Density

BMD and area were measured in the proximal half of the isolated femur bones by dual energy X-ray absorptiometry (DXA) using a Hologic QDR-4500 Elite densitometer (Hologic, Inc., Bedford, MA, USA). BMD was then calculated as bone mineral content (BMC)/area.

2.4. Determination of Bone Metabolism Markers, RANKL, Osteoprotegerin, and Hormones Circulating Levels

Serum levels of osteoprotegerin (OPG), receptor activator of nuclear factor kappa-B ligand (RANKL), osteocalcin, osteopontin, parathyroid hormone (PTH), and adenocorticotropin (ACTH) were measured simultaneously using a high sensitivity human cytokine multiplex immunoassay (Milliplex™ MAP, Merck Millipore, Billerica, MA, USA) according to the kit manufacturer's instructions. Kits contained biotinylated antibodies, phycoerythrin-conjugated streptavidin, and different types of antibody-coated microspheres (Mixed Beads) with a specific antibody for each analyzed molecule. First, serum samples (25 µL) were incubated overnight at 4 °C with 25 µL of Mixed Beads. Then, the microsphere–protein complexes formed were washed and incubated at room temperature for 1 h

with 50 µL of biotinylated antibodies, which specifically bind to proteins present on the microspheres. Finally, a final incubation with 50 µL of phycoerythrin-labeled streptavidin was carried out at room temperature for 30 min. After phycoerythrin-labeled streptavidin bind the biotinylated antibodies, the microspheres were loaded into a Luminex® X-MAP Bio-Plex 200 System Bioanalyzer (Luminex Corp., Austin, TX, USA) where the assays were run. The bioanalyzer quantifies the amount of phycoerythrin fluorescence present in each of the distinct microsphere groups. Assays were calibrated using duplicate 8-point standard curves and at least 50 individual microspheres were counted for each analyte using the median fluorescence intensity for subsequent calculations. Machine performance was verified using quality control samples at low, medium, and high levels for each analyte. All standard and quality control samples were analyzed in a complex matrix to match the sample background. Serum samples were analyzed at optimized dilutions. RANKL/OPG ratio was calculated for each subject using the values of RANKL and OPG levels obtained by this method.

2.5. Urinary F_2-Isoprostanes Determination

Urine was stored at −80 °C until analyzed for F_2-isoprostanes. Total F_2-isoprostanes were measured by a competitive enzyme immunoassay (R&D Systems, Minneapolis, MN, USA). Results were normalized to urinary creatinine.

2.6. Determination of DNA Strand Breaks

Single cell gel electrophoresis assay or comet assay was used to measure DNA strand breaks in peripheral blood lymphocytes [68]. For this, collected fresh blood was centrifuged. Then the "buffy coat" was isolated and diluted 1:1 with RPMI-1640 medium, layered onto an equivalent volume of Histopaque®-1077 (Sigma-Aldrich, St. Louis, MO, USA) to obtain peripheral blood lymphocytes. The assay was then carried out as previously described [57,69]. Briefly, isolated lymphocytes were suspended in a warmed 1% low melting point agarose in Phosphate-buffered saline (PBS) (pH 7.4) and pipetted onto microscope slides precoated with a (1% in PBS) high melting point agarose layer. Slides were maintained at 4 °C for 5 min and immersed in a lysis solution (2.5 M NaCl, 100 mM ethylenediaminetetraacetic acid (EDTA), 10 mM Tris at pH, 10, 1% Triton X-100 *v/v*) at 4 °C for 1 h. After lysis treatment, they were placed in an electrophoresis tank containing 0.3 M NaOH and 1 mM EDTA, pH 10 at 4 °C for 40 min to allow the separation of the two DNA strands. Finally, electrophoresis was performed at 1 V/cm and 300 mA for 30 min, and slides were washed three times for 5 min each with a neutralizing solution (0.4 M Tris, pH 7.5) at 4 °C before staining with 1 mg/mL of 4,6-diamidino-2-phenylindole (DAPI). Individual DAPI-stained nucleoids in each gel were examined under a UV-microscope Leica DM/LS (Leica Microsystems, Wetzlar, Germany) with an excitation filter of 435 nm and a magnification of 400 registered using a CCD camera (Hitachi, Tokyo, Japan) and analyzed with image analysis sofware Komet 5.0 (Kinetic Imaging Ltd., Liverpool, UK). A total of 100 comets per gel were count. The mean percent of DNA in the tail per gel was taken as a measure of DNA break frequency for each sample.

2.7. Statistical Analysis

Results were presented as mean and standard error of mean of six animals. Prior to any statistical analysis, all variables were checked for normal distribution and homogeneity of variances using the Shapiro–Wilk and the Levene tests, respectively. When a variable was found to follow a normal distribution, a Student's *t*-test was used to compare different dietary groups at the same age or different age groups fed a same diet. Otherwise, the non-parametric Mann–Whitney *U*-test was used for the variables that did not follow a normal distribution (Urinary F_2-Isoprostanes, DNA strand breaks and RANKL and ACTH levels). Data were analyzed using the IBM SPSS Statistics for Windows Version 22.0 (IBM Corp., Armonk, NY, USA). A *p*-value under 0.05 was considered significant in all cases.

3. Results

3.1. Animal Weights

During the 24-month follow-up, the fish oil group presented no significant weight differences (604.0 ± 23.3 g) compared to the fish oil + CoQ group (624 ± 20 g). From the observation of body weight evolution and food spillage, no differences concerning food intake were inferred between groups or in relation to age.

3.2. Plasma Fatty Acid Profile and Total Coenzyme Q_{10} Levels

The sum of plasma monounsaturated fatty acids (MUFA) in 6-month-old animals was 31.6 ± 2.4 g/100 g of total fatty acids. Concerning *n*-6 PUFA, a total value of 9.4 ± 0.4 g/100 g was found. For *n*-3 PUFA, 18.3 ± 1.2 g/100 g were noted. Such differences were maintained for old animals that showed values of 30.6 ± 2.1, 8.9 ± 1.1, and 19.5 ± 1.5 g/100 g for MUFA, *n*-6 PUFA, and *n*-3 PUFA, respectively; no differences with animals receiving CoQ_{10}-supplementation were observed (data not shown). Concerning plasma CoQ_{10} content, those animals supplemented with CoQ_{10} for 6 months showed significantly higher concentrations than their non-supplemented counterparts (Figure 1). At 24 months of age, these differences were maintained.

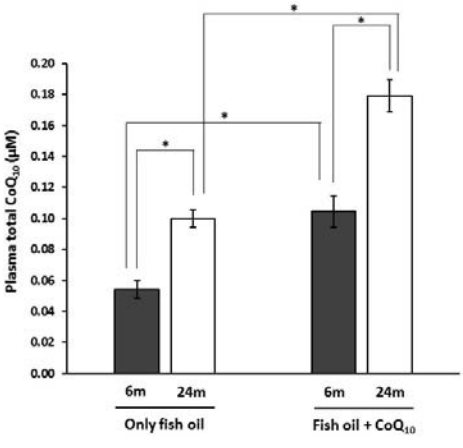

Figure 1. Effects of supplementation with coenzyme Q_{10} (CoQ_{10}) on plasma total CoQ_{10} levels in 6- and 24-month-old (m) rats fed fish oil as dietary fat. Results are expressed as mean ± standard error of mean of six animals. * Statistically significant differences ($p < 0.05$) determined by the Student's *t*-test.

3.3. Bone Mineral Density

Results from BMD measurement are represented in Figure 2. Concerning aging, BMD was lower in old animals fed non-supplemented fish oil compared to their younger counterparts. However, in animals receiving CoQ_{10}, older subjects displayed higher values. Regarding differences between dietary groups, BMD was lower in animals fed fish oil without CoQ_{10} but only at 24 months of age.

3.4. Urinary F_2-Isoprostanes and DNA Strand Breaks

Results from analysis of urinary F_2-isoprostanes levels and DNA strand breaks in lymphocytes are shown in Figure 3. Concerning the CoQ_{10} effect, a lower value was found in CoQ_{10}-supplemented animals at 6 months for F_2-isoprostanes, but there were no differences at 24 months. In contrast, no differences were observed for DNA strand break at 6 months but animals receiving CoQ showed

lower values at 24 months. Moreover, 24-month-old rats showed higher values than their younger counterparts for both in all cases.

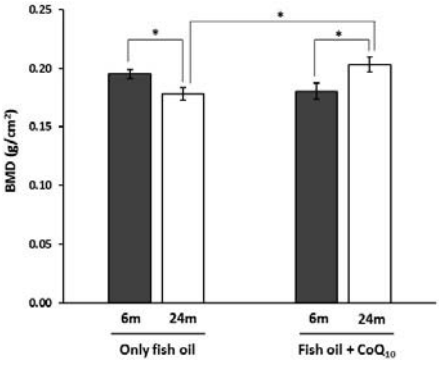

Figure 2. Effects of supplementation with coenzyme Q_{10} (CoQ_{10}) on bone mineral density (BMD) in 6- and 24-month-old (m) rats fed fish oil as dietary fat. Results are expressed as mean ± standard error of mean of six animals. * Statistically significant differences ($p < 0.05$) determined by the Student's *t*-test.

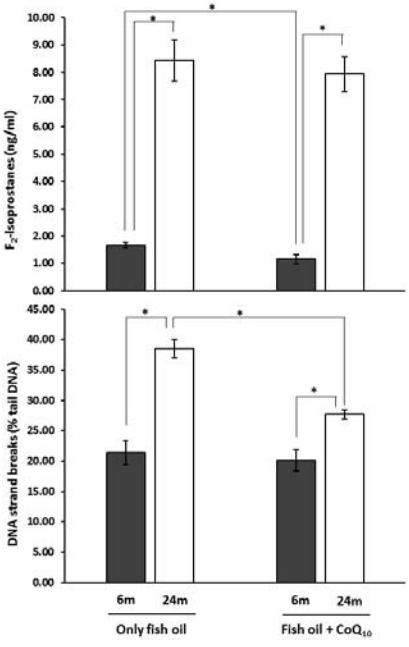

Figure 3. Effects of supplementation with coenzyme Q_{10} (CoQ_{10}) on urinary levels of F_2-isprostanes and DNA strand breaks in lymphocytes in 6- and 24-month-old (m) rats fed fish oil as dietary fat. Results are expressed as mean ± standard error of mean of six animals. * Statistically significant differences ($p < 0.05$) determined by the Mann–Whitney *U*-test.

3.5. Circulating Levels of Bone Metabolism Markers, OPG, RANKL, and Serum RANKL/OPG Ratio

Results from analysis of serum levels of osteocalcin and osteopontin are presented in Figure 4. No differences were found between dietary groups for osteocalcin levels in serum at any age, but in the case of osteopontin, a higher level was found in older rats on non-supplemented diets compared to those receiving CoQ_{10} supplements at the same age. Older animals showed lower levels of osteocalcin than their younger counterparts. However, concerning osteopontin, only supplemented animals showed significant differences between age groups with 24-month-old animals displaying the highest values.

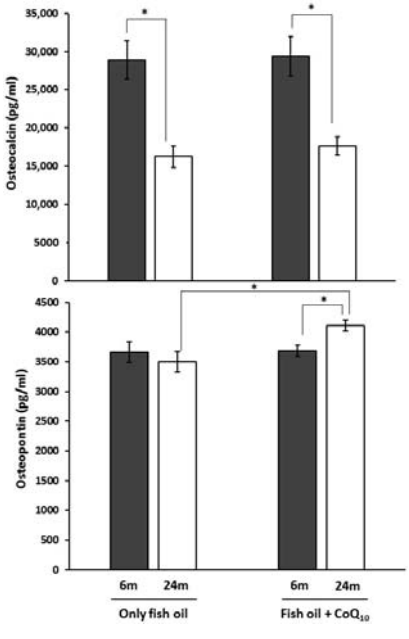

Figure 4. Effects of supplementation with coenzyme Q_{10} (CoQ_{10}) on serum levels of bone metabolism markers (osteocalcin and osteopontin) in 6- and 24-month-old (m) rats fed fish oil as dietary fat. Results are expressed as mean ± standard error of mean of six animals. * Statistically significant differences ($p < 0.05$) determined by the Student's *t*-test.

Results from RANKL, OPG serum levels, and serum RANKL/OPG ratio are presented in Table 1. No statistically differences were found between animals kept on different diets at the same age for any of the mentioned parameters. Regarding aging, lower values were found for older animals in both groups for all.

Table 1. Effects of supplementation with coenzyme Q_{10} (CoQ_{10}) on serum levels of osteoprotegerin (OPG), receptor activator of the nuclear factor κB ligand (RANKL), and RANKL/OPG ratio in 6- and 24-month-old (m) rats fed fish oil as dietary fat.

Diet	Only Fish Oil		Fish Oil + CoQ_{10}	
Age	**6 Months**	**24 Months**	**6 Months**	**24 Months**
RANKL (pg/mL)	46.97 ± 5.74 *	30.20 ± 3.99	50.76 ± 2.97 #	28.59 ± 5.18
OPG (pg/mL)	751.87 ± 76.64 *	1161.08 ± 108.56	708.89 ± 82.98 #	1177.95 ± 73.92
RANKL/OPG	0.067 ± 0.011 *	0.028 ± 0.005	0.075 ± 0.007 #	0.024 ± 0.005

Results are expressed as mean ± standard error of mean of six animals. * Statically significant differences ($p < 0.05$) between 6 and 24 months old animals fed non-supplemented fish oil; # Statically significant differences ($p < 0.05$) between 6 and 24 months old animals fed CoQ_{10}-supplemented fish oil.

3.6. Circulating Levels of PTH and ACTH

Figure 5 shows collected data about the circulating level of analyzed hormones, PTH, and ACTH. Statistical analysis revealed no significant differences between dietary groups. Regarding age, a higher level was found in older animals but only when they received CoQ_{10} supplements.

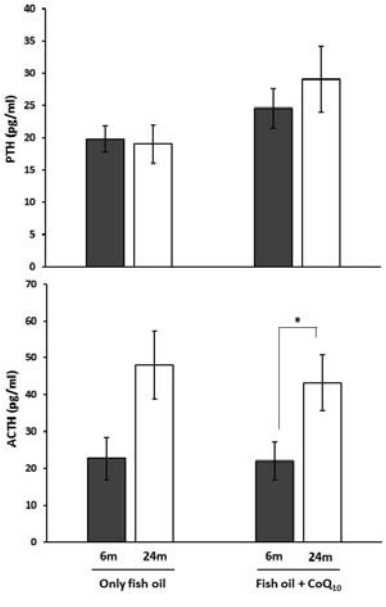

Figure 5. Effects of supplementation with coenzyme Q_{10} (CoQ_{10}) on circulating levels of parathyroid hormone and adrenocorticotropin (ACTH) in 6- and 24-month-old (m) rats fed fish oil as dietary fat. Results are expressed as mean ± standard error of mean of six animals. * Statistically significant differences ($p < 0.05$) determined by the Mann–Whitney *U*-test.

4. Discussion

Different reports have indicated a positive association between aging and bone loss or risk of osteoporosis with increased probabilities of sustaining fractures [3,4,6]. Amongst other nutritional factors, dietary fat type has been shown to have implications in bone health. In particular, studies on *n*-3 PUFA effects have shown contradictory results that could be explained by the high susceptibility to lipid peroxidation associated to the different PUFA. With this background, here, rats were life-long fed *n*-3 PUFA-rich diets (with fish oil as unique dietary fat source) with or without addition of CoQ_{10}, to

test if this antioxidant and electron carrier can impose benefits of *n*-3 PUFA on BMD at different ages. BMD is a major parameter determining bone strength that is used for the diagnosis of osteoporosis and is expected to decrease during aging. Firstly, to attribute any effect on health to the dietary treatments, it was necessary to test if the diets provided were able to modify the lipid composition of body fluids and cellular structures. Results on plasma fatty acid profiles and CoQ_{10} plasma content confirmed a proper adaptation to the diets consumed since these resembled to those of the diets. This was expected according to previous studies on similar aging models [70,71].

Areal BMD is a major determinant of bone strength usually used to diagnose osteoporosis [72]. Results from the evaluation of BMD in rat proximal femur by DXA suggested an age-associated decrease in animals fed non-supplemented-diets, but when CoQ_{10} was added, the inverse change was observed, leading to higher values of BMD in old animals compared with their non-supplemented counterparts. Generally, to diagnose osteoporosis in humans, individual BMD values are expressed in relation to a reference population in standard deviation units. This allows reducing the difficulties associated with calibration of the instruments. In particular, when these units are used in relation to the young healthy population, this measurement is referred to as the *T*-score. Here, if values of young animals belonging to the fish oil group are used as reference to determine *T*-score, old animals receiving only fish oil would be in the low bone mass (osteopenia) category according to the WHO proposal modified by the International Osteoporosis Foundation for men and women [73,74], whereas BMD in fish oil + CoQ group at 24 months was normal. However, the clinical significance of these categories lies in the fracture risks that arise. A strong gradient of risk has been reported for fracture prediction using DXA, particularly at the proximal femur and lumbar spine. Namely, it was indicated that the risk of hip fracture increased 2.6-fold for each SD decrease in BMD at the femoral neck [75]. In this sense, it has been estimated that women in the threshold for osteopenia have a 50% lifetime risk of fracture [76].

Therefore, life-long supplementation with CoQ_{10} has an interesting potential for the prevention of osteoporosis and the maintenance of bone strength. The positive effect of CoQ on BMD has also been suggested by a study in rats where short-term treatment with CoQ_{10} prevented bone and mineral content loss induced by spinal cord injury [77]. According to Jacob and Nair [78] and the U.S. Food and Drug Administration (FDA) proposal for the Human Equivalent Dose (HED), the dose administrated to rats from the present study would be 0.26 mg/kg per day if we assume a weight of 70 kg as male mean value. This implies that a 70 kg man would need to take at least 18.43 mg to note similar effects. In previous interventions with CoQ in humans, doses ranged from 100 to 2400 mg per day [55]. This difference is very important, because although most human studies gave higher doses for limited periods of time when people were older or had a health problem, we verified that maintaining CoQ throughout life at lower doses has an interesting preventive role. In the present study, CoQ_{10} in its oxidized form (ubiquinone) was used, instead of ubiquinol, given its easy commercial access together with its better stability, as well as lower costs. However, ubiquinol is also available on the market, but at a higher price, and it has been shown to be more efficiently absorbed [79–81]. Therefore, ubiquinol might be an interesting alternative to the use of ubiquinone, particularly for short-time periods or at lower doses.

Along with BMD, bone remodeling is also a major determinant of bone strength since it influences bone structure. In this sense, studies reporting the positive effects of *n*-3 PUFA or fish oil on bone mass or density have shown increases [82], but also decreases in markers of bone formation [83]. On the other hand, there are no data about the role of CoQ on this issue. In the present study, serum levels of osteocalcin and osteopontin were measured to assess changes in bone turnover and resorption. Osteocalcin was lower for the aged groups, irrespective of the treatment. On the other hand, only an age-associated increase in rats receiving CoQ was observed in relation to osteopontin. Osteopontin is a protein from bone extracellular matrix where it controls mineralization, coupling of bone formation, and attachment of osteogenic cells to the bone matrix and resorption [84,85]. However, this protein is also expressed in a variety of tissues different from bone where it is usually

expressed only in response to stimulus such as inflammation [86]. These include bone marrow derived gland cells, cartilage, dentine, cementum, kidney, brain, vascular tissues, specialized epithelia found in mammary, salivary, sweat glands, in bile and pancreatic ducts, in distal renal tubules, gut, and activated macrophages and lymphocytes [87]. Likewise, many physiological roles such as calcification, immune system modulation, inflammation, regulation of cell adhesion migration, and cell survival have been attributed to osteopontin [88]. Different evidence suggests that it participates in multiple physiological and pathological processes including pathological calcifications of soft tissues, wound healing, cardiovascular diseases and kidney diseases [87]. In fact, its plasma levels have been found to be associated with various inflammatory diseases, including cardiovascular diseases in clinical studies [86]. Consequently, changes in its blood levels observed here could reflect some physiological changes in other parts of the body and not necessarily the bone resorption rate. On the other hand, osteocalcin is an extracellular matrix protein that is released into blood during both new matrix formation and existing matrix breakdown [89]. Thus, its serum levels can be indicative of the rate of bone turnover. However, according to these results, the CoQ effect was not relevant to it.

As has been stated, bone health, in particular BMD, has been associated with oxidative stress levels in humans [90–94]. Moreover, in male and female mice, an association with age-dependent decline of bone mass and strength in sex steroid-sufficient animals has been also reported [41]. Thus, the effect of dietary CoQ_{10} on bone found here could be directly or indirectly related to its antioxidant activity. In that sense, it has been previously reported that the addition of this molecule to other PUFA-rich diets, namely *n*-6 PUFA, attenuated or reduced oxidative stress during aging [57–59,61]. To test the possible consequences on oxidative stress of supplementation with CoQ in animals from the present study (all of them fed an *n*-3 PUFA-rich diet), two markers of oxidative damage were used, each for a different type of macromolecules. These were urinary F_2-isoprostanes and DNA strand breaks in lymphocytes estimated by a single cell gel electrophoresis assay (comet assay). These markers could provide a good picture about oxidation in lipids and DNA, respectively. Differences found between age groups for both markers suggest that aged animals had higher oxidative stress. Supplementation with CoQ_{10} prevented accumulation of DNA damage with aging, in parallel to the prevention of BMD decrease. This could contribute to the lowest loss of BMD found in CoQ_{10}-supplemented animals. Supporting the positive effect of CoQ_{10} on DNA oxidative damage, it has been shown that CoQ_{10} addition to Mediterranean diet improved DNA repair systems in humans [95,96], which may also help by preventing DNA damage accumulation. Concerning lipids, oxidative damage was lower in young animals when these received supplementation but not in older subjects. This could indicate that, under conditions of the present study, dietary CoQ reduced oxidative stress from early in life, but this was not enough to lead to differences in lipid damage among older animals. However, it would prevent accumulation of damage to DNA, which would appear later in life.

As is well known, several hormones can influence bone metabolism [97,98]. Here, PTH and ACTH were evaluated. PTH is a hormone with a dual role in relation bone mass. It is known that this hormone induces bone resorption and mobilizes bone calcium into blood to balance low calcium levels in blood. Thus, high levels of PTH have been associated with a higher bone resorption rate. However, it has been reported that moderate levels of PTH maintained during short periods of time could even increase bone mass despite punctual increases in resorption rate [99]. Amongst other mechanisms, it has been previously suggested that *n*-3 PUFA's protective effect on aging-induced loss of BMD was due to a modulation of systemic calcitrophic hormones, including PTH, in a study in male rats [83]. In the present study, no relevant effects of dietary CoQ_{10} were observed on PTH. Concerning ACTH, it has been traditionally considered to produce a negative impact on bone mass as a consequence of its activity stimulating cortisol release [100,101]. However, it has been proposed that cortisol might not have a detrimental effect on bone proliferation or differentiation at physiological levels [102]. An ACTH receptor, MC2R, is expressed in osteoblast and inflammatory cells [101,103]. In vitro experiments have shown anabolic effects for ACTH in osteoblasts at high concentrations, whereas lower concentrations opposed osteoblast differentiation [97]. In addition, MC2R expression is strongest at sites of active bone

deposition, and thus ACTH response probably varies with osteoblastic activity or stage of osteoblast differentiation. In relation to CoQ_{10}, it has been shown that pituitary-dependent adrenal diseases with defective activity of pituitary-adrenal axis are associated with low levels of this molecule [104,105]. Here, ACTH serum levels were significantly higher in old animals fed CoQ_{10} compared with their younger counterparts, but this difference was not significant in animals not receiving CoQ_{10}. However, no significant effect was found for CoQ_{10}, so no clear conclusion can be inferred from the study of these markers. Notwithstanding, isolated osteoclasts synthesize and release ACTH into the culture medium [106], so maybe local concentrations are more important for stimulation of bone formation.

Furthermore, a possible implication of osteoclastogenesis regulation in CoQ_{10} effect on BMD was also evaluated in the present study by serum RANKL/OPG ratio. RANKL and OPG are two regulatory proteins with antagonist roles. RANKL is a membrane protein presented by osteoblasts and other bone cells, which binds to the RANK receptor on osteoclast precursor cells, activating NF-κβ and promoting osteoclast differentiation [106]. OPG is a soluble decoy receptor for RANKL that competitively antagonizes RANKL–RANK interaction, inhibiting osteoclastogenesis [107]. Therefore, the RANKL/OPG ratio would indicate bone resorption rate [108]. Results from the present study suggest that the serum RANKL/OPG ratio is lower with aging in all groups, which is in agreement with previous studies [109,110]. Nevertheless, in the present study, there is not any statistically significant effect of CoQ_{10} on the RANKL/OPG ratio for any of the dietary groups. Likewise, when RANKL and OPG levels are observed separately, a similar pattern was observed. This difference associated to age is consistent with results from other studies in similar models of aging [61,111]. Since these diets did not lead to age-associated increases in RANKL, oxidative stress level could influence osteoclasts response to RANKL stimulation. In fact, it has been suggested that intracellular ROS can act as "secondary messengers" in osteoclasts or osteoclast progenitor cells enhancing their differentiation [112,113]. In particular, the RANKL pathway downstream transcription factor NF-κB is also an oxidative stress-responsive and may be activated by free radicals. Therefore, the higher oxidative stress levels observed in aged rats particularly when they were on diets rich in polyunsaturated fat [44,60,68,70,114–116] could led to an increase in sensitivity to RANKL-stimulation, explaining, at least in part, the existence of an age-associated increase in osteoclastogenesis and bone resorption despite the decrease in RANKL levels. Thus, the in vivo antioxidant activity shown by CoQ_{10} in the present study during aging might help to prevent bone loss as a consequence of a reduction of ROS in osteoclasts and osteoclast progenitor cells. In vitro studies support this hypothesis. In fact, in RANKL-stimulated bone marrow-derived monocytes and RAW 264.7 cells, a model of osteoclast, CoQ_{10} inhibited osteoclastogenesis [112,113]. Evidence suggests that CoQ_{10} strongly suppressed H_2O_2-induced IκBα, p38 signaling pathways [110]. Therefore, and considering results from the present study, oxidative stress might help to explain age-associated changes in BMD, as well as the preservation of BMD found in old animals supplemented on CoQ_{10}. Still, oxidative stress can also damage other cells implicated in bone metabolism such as osteoblasts as well as suppress their differentiation [117].

5. Conclusions

Compared with young subjects, a lower BMD was found in old animals maintained on an *n*-3 PUFA-rich diet based on fish oil. This lower BMD associated to age was prevented by CoQ_{10} supplementation that even improved this parameter compared to young animals. In parallel, CoQ_{10} supplementation led to the prevention of oxidative damage to lipids and to DNA in young and old animals, respectively. However, CoQ_{10} had no clear effect in other factors affecting bone metabolism. Altogether, results from the present study suggest that, under our experimental conditions, oxidative stress might be among the causes of the lower BMD observed during aging. For this reason, it is feasible that CoQ_{10} could collaborate in the reduction of age-related loss of bone mass due to its antioxidant activity. According to other studies, this could be due, at least in part, to mitigation of osteoclastogenesis or osteoclast activity as consequence of intracellular ROS scavenging. Nevertheless,

although such studies suggest that the dietary CoQ_{10} effect on age-related changes in BMD is mediated by a decrease in resorption rate, this molecule could also influence bone formation but the effect of this molecule, or oxidative stress, on osteoblasts has not been widely studied. Therefore, to clarify this issue, markers for each cell type formation and activity such as collagen breakdown products, TRAP5b, should be performed in the future. In the same way, it is known that many osteogenic progenitor cells turn out to be adipocytes during aging [118]. Since this phenomenon also reduces bone acquisition capacity, it will be interesting also to evaluate the possible effect of dietary fat and antioxidants on it. Therefore, these and other possible mechanisms for explaining CoQ_{10} effects on age-related BMD preservation need to be further investigated in this type of aging model. Likewise, it is imperative to extend this research to female individuals, although a more complex experimental design which would fit better to what happens in humans would be required.

Acknowledgments: This work was supported by the Spanish Ministry of Education and Science (AGL2008-01057) and the Autonomous Government of Andalusia (AGR832). A.V.-L. is recipient of a grant for doctors from University of Granada's own plan.

Author Contributions: J.L.Q. and J.J.O.H. conceived and designed the experiments; J.M.L.E., M.L.F., E.P. and M.C.R.T. performed the experiments; C.L.R.T., F.G., M.B., A.V.L. and J.L.Q. analyzed the data; M.B. and J.L.Q. contributed reagents/materials/analysis tools; A.V.L., J.L.Q.M. and M.B. wrote de paper.

Conflicts of Interest: The authors declare no conflict of interest.

References

1. Alvioli, L.V.; Lindsay, R. The female osteoporotic syndrome(s). In *Metabolic Bone Disease and Clinically Related Disorder*; Alvioli, L.V., Krane, S.M., Eds.; WB Saunders Company: Philadelphia, PA, USA, 1990; pp. 397–451.
2. Sowers, M. Clinical epidemiology and osteoporosis. Measures and their interpretation. *Endocrinol. Metab. Clin. N. Am.* **1997**, *26*, 219–231. [CrossRef]
3. Szulc, P.; Seeman, E.; Duboeuf, F.; Sornay-Rendu, E.; Delmas, P.D. Bone fragility: Failure of periosteal apposition to compensate for increased endocortical resorption in postmenopausal women. *J. Bone Miner. Res. Off. J. Am. Soc. Bone Miner. Res.* **2006**, *21*, 1856–1863. [CrossRef] [PubMed]
4. Lauretani, F.; Bandinelli, S.; Griswold, M.E.; Maggio, M.; Semba, R.; Guralnik, J.M.; Ferrucci, L. Longitudinal changes in BMD and bone geometry in a population-based study. *J. Bone Miner. Res. Off. J. Am. Soc. Bone Miner. Res.* **2008**, *23*, 400–408. [CrossRef] [PubMed]
5. Edwards, M.H.; Dennison, E.M.; Aihie Sayer, A.; Fielding, R.; Cooper, C. Osteoporosis and sarcopenia in older age. *Bone* **2015**, *80*, 126–130. [CrossRef] [PubMed]
6. National Institute of Health. NIH Consensus Development Panel on Osteoporosis Prevention, Diagnosis, and Therapy Osteoporosis prevention, diagnosis, and therapy. *JAMA* **2001**, *285*, 785–795.
7. Bliuc, D.; Nguyen, N.D.; Milch, V.E.; Nguyen, T.V.; Eisman, J.A.; Center, J.R. Mortality risk associated with low-trauma osteoporotic fracture and subsequent fracture in men and women. *JAMA* **2009**, *301*, 513–521. [CrossRef] [PubMed]
8. Willson, T.; Nelson, S.D.; Newbold, J.; Nelson, R.E.; LaFleur, J. The clinical epidemiology of male osteoporosis: A review of the recent literature. *Clin. Epidemiol.* **2015**, *7*, 65–76. [PubMed]
9. Penrod, J.D.; Litke, A.; Hawkes, W.G.; Magaziner, J.; Doucette, J.T.; Koval, K.J.; Silberzweig, S.B.; Egol, K.A.; Siu, A.L. The association of race, gender, and comorbidity with mortality and function after hip fracture. *J. Gerontol. A. Biol. Sci. Med. Sci.* **2008**, *63*, 867–872. [CrossRef] [PubMed]
10. Endo, Y.; Aharonoff, G.B.; Zuckerman, J.D.; Egol, K.A.; Koval, K.J. Gender differences in patients with hip fracture: A greater risk of morbidity and mortality in men. *J. Orthop. Trauma* **2005**, *19*, 29–35. [CrossRef] [PubMed]
11. Chin, K.-Y.; Ima-Nirwana, S. Olives and Bone: A Green Osteoporosis Prevention Option. *Int. J. Environ. Res. Public. Health.* **2016**, *13*, 755. [CrossRef] [PubMed]
12. Sacco, S.M.; Horcajada, M.-N.; Offord, E. Phytonutrients for bone health during ageing. *Br. J. Clin. Pharmacol.* **2013**, *75*, 697–707. [CrossRef] [PubMed]
13. Bonjour, J.-P. Protein intake and bone health. *Int. J. Vitam. Nutr. Res.* **2011**, *81*, 134–142. [CrossRef] [PubMed]

14. Heaney, R.P. Calcium, dairy products and osteoporosis. *J. Am. Coll. Nutr.* **2000**, *19*, 83S–99S. [CrossRef] [PubMed]
15. Heaney, R.P. Skeletal development and maintenance: The role of calcium and vitamin D. *Adv. Endocrinol. Metab.* **1995**, *6*, 17–38. [PubMed]
16. Corwin, R.L.; Hartman, T.J.; Maczuga, S.A.; Graubard, B.I. Dietary saturated fat intake is inversely associated with bone density in humans: Analysis of NHANES III. *J. Nutr.* **2006**, *136*, 159–165. [PubMed]
17. Kato, I.; Toniolo, P.; Zeleniuch-Jacquotte, A.; Shore, R.E.; Koenig, K.L.; Akhmedkhanov, A.; Riboli, E. Diet, smoking and anthropometric indices and postmenopausal bone fractures: A prospective study. *Int. J. Epidemiol.* **2000**, *29*, 85–92. [CrossRef] [PubMed]
18. Järvinen, R.; Tuppurainen, M.; Erkkilä, A.T.; Penttinen, P.; Kärkkäinen, M.; Salovaara, K.; Jurvelin, J.S.; Kröger, H. Associations of dietary polyunsaturated fatty acids with bone mineral density in elderly women. *Eur. J. Clin. Nutr.* **2012**, *66*, 496–503. [CrossRef] [PubMed]
19. Kruger, M.C.; Claassen, N.; Smuts, C.M.; Potgieter, H.C. Correlation between essential fatty acids and parameters of bone formation and degradation. *Asia Pac. J. Clin. Nutr.* **1997**, *6*, 235–238. [PubMed]
20. Kruger, M.C.; Schollum, L.M. Is docosahexaenoic acid more effective than eicosapentaenoic acid for increasing calcium bioavailability? *Prostaglandins Leukot. Essent. Fatty Acids* **2005**, *73*, 327–334. [CrossRef] [PubMed]
21. Macdonald, H.M.; New, S.A.; Golden, M.H.N.; Campbell, M.K.; Reid, D.M. Nutritional associations with bone loss during the menopausal transition: Evidence of a beneficial effect of calcium, alcohol, and fruit and vegetable nutrients and of a detrimental effect of fatty acids. *Am. J. Clin. Nutr.* **2004**, *79*, 155–165. [PubMed]
22. Harris, M.; Farrell, V.; Houtkooper, L.; Going, S.; Lohman, T. Associations of polyunsaturated fatty acid intake with bone mineral density in postmenopausal women. *J. Osteoporos.* **2015**, *2015*, 737521. [CrossRef] [PubMed]
23. Muraki, S.; Yamamoto, S.; Ishibashi, H.; Oka, H.; Yoshimura, N.; Kawaguchi, H.; Nakamura, K. Diet and lifestyle associated with increased bone mineral density: Cross-sectional study of Japanese elderly women at an osteoporosis outpatient clinic. *J. Orthop. Sci. Off. J. Jpn. Orthop. Assoc.* **2007**, *12*, 317–320. [CrossRef] [PubMed]
24. Poulsen, R.C.; Kruger, M.C. Detrimental effect of eicosapentaenoic acid supplementation on bone following ovariectomy in rats. *Prostaglandins Leukot. Essent. Fatty Acids* **2006**, *75*, 419–427. [CrossRef] [PubMed]
25. Virtanen, J.K.; Mozaffarian, D.; Cauley, J.A.; Mukamal, K.J.; Robbins, J.; Siscovick, D.S. Fish consumption, bone mineral density, and risk of hip fracture among older adults: The cardiovascular health study. *J. Bone Miner. Res. Off. J. Am. Soc. Bone Miner. Res.* **2010**, *25*, 1972–1979. [CrossRef] [PubMed]
26. Mangano, K.M.; Kerstetter, J.E.; Kenny, A.M.; Insogna, K.L.; Walsh, S.J. An investigation of the association between omega 3 FA and bone mineral density among older adults: Results from the National Health and Nutrition Examination Survey years 2005–2008. *Osteoporos. Int. J. Establ. Result Coop. Eur. Found. Osteoporos. Natl. Osteoporos. Found. USA* **2014**, *25*, 1033–1041. [CrossRef] [PubMed]
27. Weiss, L.A.; Barrett-Connor, E.; von Mühlen, D. Ratio of *n*-6 to *n*-3 fatty acids and bone mineral density in older adults: The Rancho Bernardo Study. *Am. J. Clin. Nutr.* **2005**, *81*, 934–938. [PubMed]
28. Högström, M.; Nordström, P.; Nordström, A. *n*-3 Fatty acids are positively associated with peak bone mineral density and bone accrual in healthy men: The NO_2 Study. *Am. J. Clin. Nutr.* **2007**, *85*, 803–807. [PubMed]
29. Sun, D.; Krishnan, A.; Zaman, K.; Lawrence, R.; Bhattacharya, A.; Fernandes, G. Dietary *n*-3 fatty acids decrease osteoclastogenesis and loss of bone mass in ovariectomized mice. *J. Bone Miner. Res. Off. J. Am. Soc. Bone Miner. Res.* **2003**, *18*, 1206–1216. [CrossRef] [PubMed]
30. Sun, L.; Tamaki, H.; Ishimaru, T.; Teruya, T.; Ohta, Y.; Katsuyama, N.; Chinen, I. Inhibition of osteoporosis due to restricted food intake by the fish oils DHA and EPA and perilla oil in the rat. *Biosci. Biotechnol. Biochem.* **2004**, *68*, 2613–2615. [CrossRef] [PubMed]
31. Claassen, N.; Potgieter, H.C.; Seppa, M.; Vermaak, W.J.; Coetzer, H.; Van Papendorp, D.H.; Kruger, M.C. Supplemented gamma-linolenic acid and eicosapentaenoic acid influence bone status in young male rats: Effects on free urinary collagen crosslinks, total urinary hydroxyproline, and bone calcium content. *Bone* **1995**, *16*, 385S–392S. [CrossRef]
32. Mollard, R.C.; Kovacs, H.R.; Fitzpatrick-Wong, S.C.; Weiler, H.A. Low levels of dietary arachidonic and docosahexaenoic acids improve bone mass in neonatal piglets, but higher levels provide no benefit. *J. Nutr.* **2005**, *135*, 505–512. [PubMed]

33. Green, K.H.; Wong, S.C.F.; Weiler, H.A. The effect of dietary *n*-3 long-chain polyunsaturated fatty acids on femur mineral density and biomarkers of bone metabolism in healthy, diabetic and dietary-restricted growing rats. *Prostaglandins Leukot. Essent. Fatty Acids* **2004**, *71*, 121–130. [CrossRef] [PubMed]
34. Liu, D.; Veit, H.P.; Denbow, D.M. Effects of long-term dietary lipids on mature bone mineral content, collagen, crosslinks, and prostaglandin E2 production in Japanese quail. *Poult. Sci.* **2004**, *83*, 1876–1883. [CrossRef] [PubMed]
35. Musacchio, E.; Priante, G.; Budakovic, A.; Baggio, B. Effects of unsaturated free fatty acids on adhesion and on gene expression of extracellular matrix macromolecules in human osteoblast-like cell cultures. *Connect. Tissue Res.* **2007**, *48*, 34–38. [CrossRef] [PubMed]
36. Watkins, B.A.; Li, Y.; Seifert, M.F. Dietary ratio of *n*-6/*n*-3 PUFAs and docosahexaenoic acid: Actions on bone mineral and serum biomarkers in ovariectomized rats. *J. Nutr. Biochem.* **2006**, *17*, 282–289. [CrossRef] [PubMed]
37. Watkins, B.A.; Lippman, H.E.; Le Bouteiller, L.; Li, Y.; Seifert, M.F. Bioactive fatty acids: Role in bone biology and bone cell function. *Prog. Lipid Res.* **2001**, *40*, 125–148. [CrossRef]
38. González-Alonso, A.; Ramírez-Tortosa, C.L.; Varela-López, A.; Roche, E.; Arribas, M.I.; Ramírez-Tortosa, M.C.; Giampieri, F.; Ochoa, J.J.; Quiles, J.L. Sunflower Oil but Not Fish Oil Resembles Positive Effects of Virgin Olive Oil on Aged Pancreas after Life-Long Coenzyme Q Addition. *Int. J. Mol. Sci.* **2015**, *16*, 23425–23445. [CrossRef] [PubMed]
39. Coetzee, M.; Haag, M.; Joubert, A.M.; Kruger, M.C. Effects of arachidonic acid, docosahexaenoic acid and prostaglandin E(2) on cell proliferation and morphology of MG-63 and MC3T3-E1 osteoblast-like cells. *Prostaglandins Leukot. Essent. Fatty Acids* **2007**, *76*, 35–45. [CrossRef] [PubMed]
40. Maurin, A.C.; Chavassieux, P.M.; Vericel, E.; Meunier, P.J. Role of polyunsaturated fatty acids in the inhibitory effect of human adipocytes on osteoblastic proliferation. *Bone* **2002**, *31*, 260–266. [CrossRef]
41. Almeida, M.; Han, L.; Martin-Millan, M.; Plotkin, L.I.; Stewart, S.A.; Roberson, P.K.; Kousteni, S.; O'Brien, C.A.; Bellido, T.; Parfitt, A.M.; et al. Skeletal involution by age-associated oxidative stress and its acceleration by loss of sex steroids. *J. Biol. Chem.* **2007**, *282*, 27285–27297. [CrossRef] [PubMed]
42. Callaway, D.A.; Jiang, J.X. Reactive oxygen species and oxidative stress in osteoclastogenesis, skeletal aging and bone diseases. *J. Bone Miner. Metab.* **2015**, *33*, 359–370. [CrossRef] [PubMed]
43. Manolagas, S.C. From estrogen-centric to aging and oxidative stress: A revised perspective of the pathogenesis of osteoporosis. *Endocr. Rev.* **2010**, *31*, 266–300. [CrossRef] [PubMed]
44. Ochoa, J.J.; Quiles, J.L.; Huertas, J.R.; Mataix, J. Coenzyme Q_{10} protects from aging-related oxidative stress and improves mitochondrial function in heart of rats fed a polyunsaturated fatty acid (PUFA)-rich diet. *J. Gerontol. Biol. Sci. Med. Sci.* **2005**, *60*, 970–975. [CrossRef]
45. Pasco, J.A.; Henry, M.J.; Wilkinson, L.K.; Nicholson, G.C.; Schneider, H.G.; Kotowicz, M.A. Antioxidant vitamin supplements and markers of bone turnover in a community sample of nonsmoking women. *J. Womens Health* **2006**, *15*, 295–300. [CrossRef] [PubMed]
46. Sanders, K.M.; Kotowicz, M.A.; Nicholson, G.C. Potential role of the antioxidant *N*-acetylcysteine in slowing bone resorption in early post-menopausal women: A pilot study. *Transl. Res. J. Lab. Clin. Med.* **2007**, *150*, 215. [CrossRef] [PubMed]
47. Ayaz, M.; Tuncer, S.; Okudan, N.; Gokbel, H. Coenzyme Q(10) and alpha-lipoic acid supplementation in diabetic rats: Conduction velocity distributions. *Methods Find. Exp. Clin. Pharmacol.* **2008**, *30*, 367–374. [CrossRef] [PubMed]
48. Shetty, K. The role of salivary cytokines in the etiology and progression of periodontal disease. *Gen. Dent.* **2006**, *54*, 140–143. [PubMed]
49. Yan, J.; Fujii, K.; Yao, J.; Kishida, H.; Hosoe, K.; Sawashita, J.; Takeda, T.; Mori, M.; Higuchi, K. Reduced coenzyme Q_{10} supplementation decelerates senescence in SAMP1 mice. *Exp. Gerontol.* **2006**, *41*, 130–140. [CrossRef] [PubMed]
50. López-Lluch, G.; Rodríguez-Aguilera, J.C.; Santos-Ocaña, C.; Navas, P. Is coenzyme Q a key factor in aging? *Mech. Ageing Dev.* **2010**, *131*, 225–235. [CrossRef] [PubMed]
51. Ernster, L.; Dallner, G. Biochemical, physiological and medical aspects of Ubiquinone function. *Biochim. Biophys. Acta* **1995**, *1271*, 195–204. [CrossRef]
52. Frei, B.; Kim, M.C.; Ames, B.N. Ubiquinol-10 is an effective lipid-soluble antioxidant at physiological concentrations. *Proc. Natl. Acad. Sci. USA* **1990**, *87*, 4879–4883. [CrossRef] [PubMed]

53. Bentinger, M.; Tekle, M.; Dallner, G. Coenzyme Q–biosynthesis and functions. *Biochem. Biophys. Res. Commun.* **2010**, *396*, 74–79. [CrossRef] [PubMed]
54. Mitchell, P. Protonmotive redox mechanism of the cytochrome b-c_1 complex in the respiratory chain: Protonmotive ubiquinone cycle. *FEBS Lett.* **1975**, *56*, 1–6. [CrossRef]
55. Varela-López, A.; Giampieri, F.; Battino, M.; Quiles, J.L. Coenzyme Q and Its Role in the Dietary Therapy against Aging. *Molecules* **2016**, *21*, 373. [CrossRef] [PubMed]
56. Genova, M.L.; Lenaz, G. New developments on the functions of coenzyme Q in mitochondria. *Biofactors* **2011**, *37*, 330–354. [CrossRef] [PubMed]
57. Quiles, J.L.; Ochoa, J.J.; Huertas, J.R.; Mataix, J. Coenzyme Q supplementation protects from age-related DNA double-strand breaks and increases lifespan in rats fed on a PUFA-rich diet. *Exp. Gerontol.* **2004**, *39*, 189–194. [CrossRef] [PubMed]
58. Ochoa, J.J.; Quiles, J.L.; López-Frías, M.; Huertas, J.R.; Mataix, J. Effect of lifelong coenzyme Q_{10} supplementation on age-related oxidative stress and mitochondrial function in liver and skeletal muscle of rats fed on a polyunsaturated fatty acid (PUFA)-rich diet. *J. Gerontol. Biol. Sci. Med. Sci.* **2007**, *62*, 1211–1218. [CrossRef]
59. Quiles, J.L.; Pamplona, R.; Ramirez-Tortosa, M.C.; Naudí, A.; Portero-Otin, M.; Araujo-Nepomuceno, E.; López-Frías, M.; Battino, M.; Ochoa, J.J. Coenzyme Q addition to an *n*-6 PUFA-rich diet resembles benefits on age-related mitochondrial DNA deletion and oxidative stress of a MUFA-rich diet in rat heart. *Mech. Ageing Dev.* **2010**, *131*, 38–47. [CrossRef] [PubMed]
60. Ochoa, J.J.; Pamplona, R.; Ramirez-Tortosa, M.C.; Granados-Principal, S.; Perez-Lopez, P.; Naudí, A.; Portero-Otin, M.; López-Frías, M.; Battino, M.; Quiles, J.L. Age-related changes in brain mitochondrial DNA deletion and oxidative stress are differentially modulated by dietary fat type and coenzyme Q_{10}. *Free Radic. Biol. Med.* **2011**, *50*, 1053–1064. [CrossRef] [PubMed]
61. Varela-Lopez, A.; Bullon, P.; Battino, M.; Ramirez-Tortosa, M.C.; Ochoa, J.J.; Cordero, M.D.; Ramirez-Tortosa, C.L.; Rubini, C.; Zizzi, A.; Quiles, J.L. Coenzyme Q protects against age-related alveolar bone loss associated to *n*-6 PUFA rich-diets by modulating mitochondrial mechanisms. *J. Gerontol. A Biol. Sci. Med. Sci.* **2015**, *71*, 593–600. [CrossRef] [PubMed]
62. Reeves, P.G. Components of the AIN-93 diets as improvements in the AIN-76A diet. *J. Nutr.* **1997**, *127*, 838S–841S. [PubMed]
63. Sengupta, P. The Laboratory Rat: Relating Its Age with Human's. *Int. J. Prev. Med.* **2013**, *4*, 624–630. [PubMed]
64. Lepage, G.; Roy, C.C. Direct transesterification of all classes of lipids in a one-step reaction. *J. Lipid Res.* **1986**, *27*, 114–120. [PubMed]
65. Quiles, J.L.; Huertas, J.R.; Mañas, M.; Ochoa, J.J.; Battino, M.; Mataix, J. Oxidative stress induced by exercise and dietary fat modulates the coenzyme Q and vitamin A balance between plasma and mitochondria. *Int. J. Vitam. Nutr. Res.* **1999**, *69*, 243–249. [CrossRef] [PubMed]
66. MacCrehan, W.A. Determination of retinol, alpha-tocopherol, and beta-carotene in serum by liquid chromatography. *Methods Enzymol.* **1990**, *189*, 172–181. [PubMed]
67. Quiles, J.L.; Ochoa, J.J.; Ramirez-Tortosa, M.C.; Linde, J.; Bompadre, S.; Battino, M.; Narbona, E.; Maldonado, J.; Mataix, J. Coenzyme Q concentration and total antioxidant capacity of human milk at different stages of lactation in mothers of preterm and full-term infants. *Free Radic. Res.* **2006**, *40*, 199–206. [CrossRef] [PubMed]
68. Collins, A.R.; Dusinská, M.; Gedik, C.M.; Stětina, R. Oxidative damage to DNA: Do we have a reliable biomarker? *Environ. Health Perspect.* **1996**, *104*, 465–469. [CrossRef] [PubMed]
69. Quiles, J.L.; Ochoa, J.J.; Ramirez-Tortosa, C.; Battino, M.; Huertas, J.R.; Martín, Y.; Mataix, J. Dietary fat type (virgin olive vs. sunflower oils) affects age-related changes in DNA double-strand-breaks, antioxidant capacity and blood lipids in rats. *Exp. Gerontol.* **2004**, *39*, 1189–1198. [CrossRef] [PubMed]
70. Quiles, J.L.; Martínez, E.; Ibáñez, S.; Ochoa, J.J.; Martín, Y.; López-Frías, M.; Huertas, J.R.; Mataix, J. Ageing-related tissue-specific alterations in mitochondrial composition and function are modulated by dietary fat type in the rat. *J. Bioenerg. Biomembr.* **2002**, *34*, 517–524. [CrossRef] [PubMed]
71. Quiles, J.L.; Huertas, J.R.; Mañas, M.; Battino, M.; Mataix, J. Physical exercise affects the lipid profile of mitochondrial membranes in rats fed with virgin olive oil or sunflower oil. *Br. J. Nutr.* **1999**, *81*, 21–24. [PubMed]

72. Kanis, J.A.; Burlet, N.; Cooper, C.; Delmas, P.D.; Reginster, J.-Y.; Borgstrom, F.; Rizzoli, R.; and on behalf of the Scientific Advisory Board of the European Society for Clinical and Economic Aspects of Osteoporosis and Osteoarthritis (ESCEO) and the Committee of Scientific Advisors of the International Osteoporosis Foundation (IOF). European guidance for the diagnosis and management of osteoporosis in postmenopausal women. *Osteoporos. Int.* **2008**, *19*, 399–428. [CrossRef] [PubMed]
73. World Health Organization (WHO). *Assessment of osteoporosis at the primary health care level. Summary Report of a WHO Scientific Group 2007*; WHO: Geneva, Switzerland.
74. Kanis, J.A.; on behalf of the World Health Organization Scientific Group. *Assessment of Osteoporosis at the Primary Health-Care Level*; WHO Collaborating Centre, University of Sheffield: Sheffield, UK, 2007.
75. Marshall, D.; Johnell, O.; Wedel, H. Meta-analysis of how well measures of bone mineral density predict occurrence of osteoporotic fractures. *Br. Med. J.* **1996**, *312*, 1254–1259. [CrossRef]
76. Kanis, J.A. Diagnosis of osteoporosis and assessment of fracture risk. *Lancet* **2002**, *359*, 1929–1936. [CrossRef]
77. Zhang, X.-X.; Qian, K.-J.; Zhang, Y.; Wang, Z.-J.; Yu, Y.-B.; Liu, X.-J.; Cao, X.-T.; Liao, Y.-H.; Zhang, D.-Y. Efficacy of coenzyme Q_{10} in mitigating spinal cord injury-induced osteoporosis. *Mol. Med. Rep.* **2015**, *12*, 3909–3915. [CrossRef] [PubMed]
78. Nair, A.B.; Jacob, S. A simple practice guide for dose conversion between animals and human. *J. Basic Clin. Pharm.* **2016**, *7*, 27–31. [CrossRef] [PubMed]
79. Miles, M.V.; Horn, P.; Miles, L.; Tang, P.; Steele, P.; DeGrauw, T. Bioequivalence of coenzyme Q_{10} from over the counter supplements. *Nutr. Res.* **2002**, *22*, 919–929. [CrossRef]
80. Hosoe, K.; Kitano, M.; Kishida, H.; Kubo, H.; Fuji, K.; Kitahara, M. Study on safety and bioavailability of ubiquinol (Kaneka QH TM) after single and 4-week multiple oral administration to healthy volunteers. *Regul. Toxicol. Pharmacol.* **2007**, *47*, 19–28. [CrossRef] [PubMed]
81. Evans, M.; Baisley, J.; Barss, S.; Guthrie, N. A randomized, double-blind trial on the bioavailability of two CoQ_{10} formulations. *J. Funct. Food* **2009**, *1*, 65–73. [CrossRef]
82. Van Papendorp, D.H.; Coetzer, H.; Kruger, M.C. Biochemical profile of osteoporotic patients on essential fatty acid supplementation. *Nutr. Res.* **1995**, *15*, 325–334. [CrossRef]
83. Shen, C.-L.; Yeh, J.K.; Rasty, J.; Li, Y.; Watkins, B.A. Protective effect of dietary long-chain *n*-3 polyunsaturated fatty acids on bone loss in gonad-intact middle-aged male rats. *Br. J. Nutr.* **2006**, *95*, 462–468. [CrossRef] [PubMed]
84. Subraman, V.; Thiyagarajan, M.; Malathi, N.; Rajan, S.T. OPN–Revisited. *J. Clin. Diagn. Res. JCDR* **2015**, *9*, ZE10–ZE13. [CrossRef] [PubMed]
85. Wang, K.X.; Shi, Y.F.; Ron, Y.; Kazanecki, C.C.; Denhardt, D.T. Plasma osteopontin modulates chronic restraint stress-induced thymus atrophy by regulating stress hormones: Inhibition by an anti-osteopontin monoclonal antibody. *J. Immunol.* **2009**, *182*, 2485–2491. [CrossRef] [PubMed]
86. Scatena, M.; Liaw, L.; Giachelli, C.M. Osteopontin. *Arterioscler. Thromb. Vasc. Biol.* **2007**, *27*, 2302–2309. [CrossRef] [PubMed]
87. Standal, T.; Borset, M.; Sundan, A. Role of osteopontin in adhesion, migration, cell survival and bone remodeling. *Exp. Oncol.* **2004**, *26*, 179–184. [PubMed]
88. Anborgh, P.H.; Mutrie, J.C.; Tuck, A.B.; Chambers, A.F. Pre- and post-translational regulation of osteopontin in cancer. *J. Cell Commun. Signal.* **2011**, *5*, 111–122. [CrossRef] [PubMed]
89. Das, U.N. Essential fatty acids and osteoporosis. *Nutrition* **2000**, *16*, 386–390. [CrossRef]
90. Altindag, O.; Erel, O.; Soran, N.; Celik, H.; Selek, S. Total oxidative/anti-oxidative status and relation to bone mineral density in osteoporosis. *Rheumatol. Int.* **2008**, *28*, 317–321. [CrossRef] [PubMed]
91. Basu, S.; Michaëlsson, K.; Olofsson, H.; Johansson, S.; Melhus, H. Association between oxidative stress and bone mineral density. *Biochem. Biophys. Res. Commun.* **2001**, *288*, 275–279. [CrossRef] [PubMed]
92. Cervellati, C.; Bonaccorsi, G.; Cremonini, E.; Bergamini, C.M.; Patella, A.; Castaldini, C.; Ferrazzini, S.; Capatti, A.; Picarelli, V.; Pansini, F.S.; et al. Bone mass density selectively correlates with serum markers of oxidative damage in post-menopausal women. *Clin. Chem. Lab. Med.* **2013**, *51*, 333–338. [CrossRef] [PubMed]
93. Maggio, D.; Barabani, M.; Pierandrei, M.; Polidori, M.C.; Catani, M.; Mecocci, P.; Senin, U.; Pacifici, R.; Cherubini, A. Marked decrease in plasma antioxidants in aged osteoporotic women: Results of a cross-sectional study. *J. Clin. Endocrinol. Metab.* **2003**, *88*, 1523–1527. [CrossRef] [PubMed]

94. Sharma, T.; Islam, N.; Ahmad, J.; Akhtar, N.; Beg, M. Correlation between bone mineral density and oxidative stress in postmenopausal women. *Indian J. Endocrinol. Metab.* **2015**, *19*, 491–497. [PubMed]
95. Yubero-Serrano, E.M.; Gonzalez-Guardia, L.; Rangel-Zuñiga, O.; Delgado-Lista, J.; Gutierrez-Mariscal, F.M.; Perez-Martinez, P.; Delgado-Casado, N.; Cruz-Teno, C.; Tinahones, F.J.; Villalba, J.M.; et al. Mediterranean Diet Supplemented With Coenzyme Q_{10} Modifies the Expression of Proinflammatory and Endoplasmic Reticulum Stress–Related Genes in Elderly Men and Women. *J. Gerontol. Biol. Sci. Med. Sci.* **2012**, *67A*, 3–10. [CrossRef] [PubMed]
96. Gutierrez-Mariscal, F.M.; Perez-Martinez, P.; Delgado-Lista, J.; Yubero-Serrano, E.M.; Camargo, A.; Delgado-Casado, N.; Cruz-Teno, C.; Santos-Gonzalez, M.; Rodriguez-Cantalejo, F.; Castaño, J.P.; et al. Mediterranean diet supplemented with coenzyme Q_{10} induces postprandial changes in p53 in response to oxidative DNA damage in elderly subjects. *Age Drodr.* **2011**, *34*, 389–403. [CrossRef] [PubMed]
97. Isales, C.M.; Zaidi, M.; Blair, H.C. ACTH is a novel regulator of bone mass. *Ann. N. Y. Acad. Sci.* **2010**, *1192*, 110–116. [CrossRef] [PubMed]
98. Jilka, R.L.; Weinstein, R.S.; Bellido, T.; Roberson, P.; Parfitt, A.M.; Manolagas, S.C. Increased bone formation by prevention of osteoblast apoptosis with parathyroid hormone. *J. Clin. Investig.* **1999**, *104*, 439–446. [CrossRef] [PubMed]
99. Chen, A.B.; Minami, K.; Raposo, J.F.; Matsuura, N.; Koizumi, M.; Yokota, H.; Ferreira, H.G. Transient modulation of calcium and parathyroid hormone stimulates bone formation. *Endocrine* **2016**, *54*, 232–240. [CrossRef] [PubMed]
100. Mancini, T.; Doga, M.; Mazziotti, G.; Giustina, A. Cushing's syndrome and bone. *Pituitary* **2004**, *7*, 249–252. [CrossRef] [PubMed]
101. Silverman, S.L.; Lane, N.E. Glucocorticoid-induced osteoporosis. *Curr. Osteoporos. Rep.* **2009**, *7*, 23–26. [CrossRef] [PubMed]
102. Boden, S.D.; Hair, G.; Titus, L.; Racine, M.; McCuaig, K.; Wozney, J.M.; Nanes, M.S. Glucocorticoid-induced differentiation of fetal rat calvarial osteoblasts is mediated by bone morphogenetic protein-6. *Endocrinology* **1997**, *138*, 2820–2828. [CrossRef] [PubMed]
103. Zhong, Q.; Sridhar, S.; Ruan, L.; Ding, K.-H.; Xie, D.; Insogna, K.; Kang, B.; Xu, J.; Bollag, R.J.; Isales, C.M. Multiple melanocortin receptors are expressed in bone cells. *Bone* **2005**, *36*, 820–831. [CrossRef] [PubMed]
104. Mancini, A.; Leone, E.; Silvestrini, A.; Festa, R.; Di Donna, V.; De Marinis, L.; Pontecorvi, A.; Littarru, G.P.; Meucci, E. Evaluation of antioxidant systems in pituitary-adrenal axis diseases. *Pituitary* **2010**, *13*, 138–145. [CrossRef] [PubMed]
105. Mancini, A.; Bianchi, A.; Fusco, A.; Sacco, E.; Leone, E.; Tilaro, L.; Porcelli, T.; Giampietro, A.; Principi, F.; De Marinis, L.; et al. Coenzyme Q_{10} evaluation in pituitary-adrenal axis disease: Preliminary data. *BioFactors Oxf. Engl.* **2005**, *25*, 197–199. [CrossRef]
106. Nakagawa, N.; Kinosaki, M.; Yamaguchi, K.; Shima, N.; Yasuda, H.; Yano, K.; Morinaga, T.; Higashio, K. RANK is the essential signaling receptor for osteoclast differentiation factor in osteoclastogenesis. *Biochem. Biophys. Res. Commun.* **1998**, *253*, 395–400. [CrossRef] [PubMed]
107. Yasuda, H.; Shima, N.; Nakagawa, N.; Yamaguchi, K.; Kinosaki, M.; Goto, M.; Mochizuki, S.I.; Tsuda, E.; Morinaga, T.; Udagawa, N.; et al. A novel molecular mechanism modulating osteoclast differentiation and function. *Bone* **1999**, *25*, 109–113. [CrossRef]
108. Raggatt, L.J.; Partridge, N.C. Cellular and molecular mechanisms of bone remodeling. *J. Biol. Chem.* **2010**, *285*, 25103–25108. [CrossRef] [PubMed]
109. Kerschan-Schindl, K.; Wendlova, J.; Kudlacek, S.; Gleiss, A.; Woloszczuk, W.; Pietschmann, P. Serum levels of receptor activator of nuclear factor kappaB ligand (RANKL) in healthy women and men. *Exp. Clin. Endocrinol. Diabetes Off. J. Ger. Soc. Endocrinol. Ger. Diabetes Assoc.* **2008**, *116*, 491–495. [CrossRef] [PubMed]
110. Liu, J.M.; Zhao, H.Y.; Ning, G.; Zhao, Y.J.; Chen, Y.; Zhang, Z.; Sun, L.H.; Xu, M.-Y.; Chen, J.L. Relationships between the changes of serum levels of OPG and RANKL with age, menopause, bone biochemical markers and bone mineral density in Chinese women aged 20–75. *Calcif. Tissue Int.* **2005**, *76*, 1–6. [CrossRef] [PubMed]
111. Bullon, P.; Battino, M.; Varela-Lopez, A.; Perez-Lopez, P.; Granados-Principal, S.; Ramirez-Tortosa, M.C.; Ochoa, J.J.; Cordero, M.D.; Gonzalez-Alonso, A.; Ramirez-Tortosa, C.L.; et al. Diets based on virgin olive oil or fish oil but not on sunflower oil prevent age-related alveolar bone resorption by mitochondrial-related mechanisms. *PLoS ONE* **2013**, *8*, e74234. [CrossRef] [PubMed]

112. Moon, H.-J.; Ko, W.-K.; Han, S.W.; Kim, D.-S.; Hwang, Y.-S.; Park, H.-K.; Kwon, I.K. Antioxidants, like coenzyme Q_{10}, selenite, and curcumin, inhibited osteoclast differentiation by suppressing reactive oxygen species generation. *Biochem. Biophys. Res. Commun.* **2012**, *418*, 247–253. [CrossRef] [PubMed]
113. Moon, H.-J.; Ko, W.-K.; Jung, M.-S.; Kim, J.H.; Lee, W.-J.; Park, K.-S.; Heo, J.-K.; Bang, J.B.; Kwon, I.K. Coenzyme Q_{10} regulates osteoclast and osteoblast differentiation. *J. Food Sci.* **2013**, *78*, H785–H891. [CrossRef] [PubMed]
114. Huertas, J.R.; Martinez-Velasco, E.; Ibáñez, S.; López-Frias, M.; Ochoa, J.J.; Quiles, J.; Parenti Castelli, G.; Mataix, J.; Lenaz, G. Virgin olive oil and coenzyme Q_{10} protect heart mitochondria from peroxidative damage during aging. *Biofactors* **1999**, *9*, 337–343. [CrossRef] [PubMed]
115. Ochoa, J.J.; Quiles, J.L.; Ibáñez, S.; Martínez, E.; López-Frías, M.; Huertas, J.R.; Mataix, J. Aging-related oxidative stress depends on dietary lipid source in rat postmitotic tissues. *J. Bioenerg. Biomembr.* **2003**, *35*, 267–275. [CrossRef] [PubMed]
116. Roche, E.; Ramírez-Tortosa, C.L.; Arribas, M.I.; Ochoa, J.J.; Sirvent-Belando, J.E.; Battino, M.; Ramírez-Tortosa, M.C.; González-Alonso, A.; Pérez-López, M.P.; Quiles, J.L. Comparative analysis of pancreatic changes in aged rats fed life long with sunflower, fish, or olive oils. *J. Gerontol. A Biol. Sci. Med. Sci.* **2014**, *69*, 934–944. [CrossRef] [PubMed]
117. Fatokun, A.A.; Stone, T.W.; Smith, R.A. Responses of differentiated MC3T3-E1 osteoblast-like cells to reactive oxygen species. *Eur. J. Pharmacol.* **2008**, *587*, 35–41. [CrossRef] [PubMed]
118. Bethel, M.; Chitteti, B.R.; Srour, E.F.; Kacena, M.A. The changing balance between osteoblastogenesis and adipogenesis in aging and its impact on hematopoiesis. *Curr. Osteoporos. Rep.* **2013**, *11*, 99–106. [CrossRef] [PubMed]

nutrients

MDPI

Article

The Combination of Blueberry Juice and Probiotics Ameliorate Non-Alcoholic Steatohepatitis (NASH) by Affecting SREBP-1c/PNPLA-3 Pathway via PPAR-α

Tingting Ren [1,†], Juanjuan Zhu [2,3,†], Lili Zhu [3] and Mingliang Cheng [2,*]

1 Biochemistry Department, Affiliated Hospital of Guiyang Medical College, Guiyang 550004, China; tingting1@163.com
2 Department of Infectious Diseases, Affiliated Hospital of Guiyang Medical College, Guiyang 550004, China; juanjuan2@163.com
3 Baiyun Hospital, Affiliated Hospital of Guiyang Medical College, Guiyang 550004, China; zhulili1@163.com
* Correspondence: minglianggy@163.com; Tel./Fax: +86-851-565-7879
† These two authors contributed to the present work equally.

Received: 17 December 2016; Accepted: 21 February 2017; Published: 27 February 2017

Abstract: Nonalcoholic steatohepatitis (NASH) is liver inflammation and a major threat to public health. Several pharmaceutical agents have been used for NASH therapy but their high-rate side effects limit the use. Blueberry juice and probiotics (BP) have anti-inflammation and antibacterial properties, and may be potential candidates for NASH therapy. To understand the molecular mechanism, Sprague Dawley rats were used to create NASH models and received different treatments. Liver tissues were examined using HE (hematoxylin and eosin) and ORO (Oil Red O) stain, and serum biochemical indices were measured. The levels of peroxisome proliferators-activated receptor (PPAR)-α, sterol regulatory element binding protein-1c (SREBP-1c), Patatin-like phospholipase domain-containing protein 3 (PNPLA-3), inflammatory cytokines and apoptosis biomarkers in liver tissues were measured by qRT-PCR and Western blot. HE and ORO analysis indicated that the hepatocytes were seriously damaged with more and larger lipid droplets in NASH models while BP reduced the number and size of lipid droplets ($p < 0.05$). Meanwhile, BP increased the levels of SOD (superoxide dismutase), GSH (reduced glutathione) and HDL-C (high-density lipoprotein cholesterol), and reduced the levels of AST (aspartate aminotransferase), ALT (alanine aminotransferase), TG (triglycerides), LDL-C (low-density lipoprotein cholesterol) and MDA (malondialdehyde) in NASH models ($p < 0.05$). BP increased the level of PPAR-α (Peroxisome proliferator-activated receptor α), and reduced the levels of SREBP-1c (sterol regulatory element binding protein-1c) and PNPLA-3 (Patatin-like phospholipase domain-containing protein 3) ($p < 0.05$). BP reduced hepatic inflammation and apoptosis by affecting IL-6 (interleukin 6), TNF-α (Tumor necrosis factor α), caspase-3 and Bcl-2 in NASH models. Furthermore, PPAR-α inhibitor increased the level of SREBP-1c and PNPLA-3. Therefore, BP prevents NASH progression by affecting SREBP-1c/PNPLA-3 pathway via PPAR-α.

Keywords: non-alcoholic steatohepatitis; blueberry juices; probiotics; Peroxisome proliferator-activated receptor α; Sterol regulatory element-binding transcription factor 1c; Patatin-like phospholipase domain-containing protein 3; biochemical indices; apoptosis; anti-oxidant

1. Introduction

Non-alcoholic steatohepatitis (NASH) is a kind of liver diseases caused by oxidant and inflammation stress over a long time and results in liver damage. NASH can cause some serious complications, such as liver failure [1], cirrhosis [2,3] and hepatocellular carcinoma [4]. Furthermore, NASH risk is increasing worldwide [5–7]. Drug therapy is still the main option to control NASH

progression [8–10]. The common drugs for NASH treatment are vitamin E [11], pioglitazone [12], peroxisome proliferator-activated receptors (PPAR)-α and PPAR-γ agonist [13], etc. Vitamin E has antioxidant activities and is widely used for treating chronic liver disorders. Vitamin E lowers the levels of alanine aminotransferase (ALT) and aspartate aminotransferase (AST) in patients with NASH [14]. Pioglitazone shows inhibitory effects on the level of vascular endothelial growth factor (VEGF), which is related to many ischemic and inflammatory disorders, and the main factor contributing to the progression of liver fibrosis and hepatic carcinogenesis [15]. The activation of PPAR-α and PPAR-γ ameliorates NASH by regulating the gene expression in hepatic and adipose tissues [13]. However, all these medicines have obvious side effects. Long-term consumption of vitamin E will cause nausea, vomiting, diarrhea, headache, dizziness, and cerebrovascular disorders, as well as increase the risk of cancers [16]. Pioglitazone belongs to PPAR-γ agonist thiazolidinedione and has many side effects [17], including weight gain, pedal edema, bone loss and heart failure [18]. Thiazolidinedione, as an extracellular signal-regulated kinase (ERK) docking domain inhibitor, may cause angioneurosis edema. PPAR-γ, an important regulator of lipid metabolism and energy balance, is involved in the progression of insulin resistance and obesity [19]. Furthermore, thiazolidinedione may induce side effects via PPAR since thiazolidinedione-induced activation of PPAR-γ changes the transcription of many genes associated with glucose and lipid metabolism [20]. Generally, these side effects cannot be tolerated by most patients. Thus, it is critical to find non-pharmaceutical therapy and fruit-based food products for NASH treatment with few side effects.

Oxidative stress may be an important factor for causing NASH. Genetic SNPs (single nucleotide polymorphisms) have been reported to be associated with fatty acid oxidation and contribute to NASH [21]. An earlier report showed that increasing CYP2E1 (Catalase and cytochrome P450 2E1) will increase oxidative stress and plays an important role in the progression of NASH [22]. Some data suggested that NASH patients could receive antioxidant therapies according to the oxidative stresses in their serum [23]. Inflammation is another important factor causing NASH because NASH is mainly characterized by hepatic lipid accumulation and is associated with progressive inflammatory liver disease [24,25]. The liver kinetics of gadolinium-ethoxybenzyl-diethylenetriamine-pentaacetic acid and complications are associated with inflammation in animal NASH models [26]. The distribution of gut microbiota also plays an important role in the progression of NASH [27].

Blueberry juice has significant anti-oxidant and anti-inflammation functions. Blueberry has rich anthocyanins, which protect organs from oxidative destruction and it can be used as functional fruits to control liver disorders caused by oxidative stress [28]. The anthocyanins can decrease the levels of reactive oxygen species (ROS) and heme oxygenase-1 (HO-1) and increase the levels of superoxide dismutase (SOD) and HO-1. Anthocyanins show protecting effects for inflammatory disorders and protect cells from diabetes-induced oxidant and inflammatory injuries by affecting Nrf-2/HO-1 (Nuclear factor erythroid 2-related factor 2/heme oxygenase-1) signal pathway [29]. The rich glycosides in blueberries also enhance their antioxidant capacities [28]. Phenolic acid is also an important composition of blueberry and antioxidant protection for most cell and. The mixture of phenolic acid in blueberry also shows anti-inflammatory functions by reducing the levels of nuclear factor-kappa B and increasing the level of tumor necrosis factor (TNF)-α and interleukin-6 (IL-6) [30]. Blueberry has abundant polyphenols and some beneficial compounds, which can be used by gut probiotics and affect digestive system and the distribution of intestinal microflora. Bifidobacterium, a kind of probiotics, is considered beneficial for human health. Long-term consumption of blueberry juice has been proven to improve the distribution of the intestinal microflora [31]. On the other hand, blueberries provide health benefits for preventing the progression of various cancers. The anticancer functions of blueberries are attributed to their high-content phytochemicals and antioxidant properties. The main ingredients of blueberries show protective effects against cancer by suppressing inflammation, oxidative stress, proliferation and angiogenesis via many pathways including nuclear factor kappa-B, Wnt/beta-catenin, the phosphatidylinositol-3-kinase and the mammalian target of Rapamycin, and extracellular signal-regulated kinase/mitogen-activated protein kinase [32]. Blueberry-enriched diet

can control metabolic disorders including endothelial dysfunction and inflammation in the obese animal models [33]. Probiotics have also been approved for NASH treatment in an animal model [34]. Thus, the combination of blueberry juice and probiotics (BP) may have protective functions in NASH therapy since inflammation, oxidant stress and gut microbiota are associated with the development of NASH.

However, the molecular mechanism of the effects of blueberry juice on the development of NASH remains widely unclear. The mutual interaction between lipid metabolism and inflammation may exacerbate atherosclerosis progression [35], which will contribute to NASH [36]. Sterol regulatory element-binding protein-1c (SREBP-1c) and PPAR-α have been reported to affect the development of NASH. Low-level expression of PPAR-α will induce the risk of NASH, which can be treated well by chicory (*Cichoriumintybus* L.) seed extract by affecting the level of PPAR-α [37] while PPAR-α activation will inhibit SREBP-1c pathway [38]. On the other hand, SREBP-1c and patatin-like phospholipase domain-containing protein 3 (PNPLA-3) pathways may affect the progression of NASH [39,40]. The pathway may be associated with inflammation [41] and oxidative stress [42]. PNPLA-3 has been reported to be related to the increase in the level of total glycerol and risk of hepatic injuries [43]. The PNPLA-3 mutant is associated with the risks of hepatic steatosis [44], hepatic enzymes [45], hepatosteatosis [46], and alcohol-induced cirrhosis [47]. PNPLA-3 encodes a 481-aa protein with apatatin-like domain at the *N*-terminus. The over-expression of PNPLA-3 has been found in adipose tissue [48]. PNPLA-3 is similar with PNPLA2, which is a main kind of hormone-sensitive lipase in adipose tissue. Both PNPLA2 and PNPLA-3 can hydrolyze triglyceride [49]. Furthermore, PNPLA-3 level is higher in obese and insulin-resistant animal models [50].

Blueberry may affect NASH development by affecting SREBP-1c/PNPLA-3 pathway. Therefore, the molecular mechanism for the functional role of BP in NASH treatment was explored by investigating SREBP-1c/PNPLA-3 pathway. Meanwhile, the modulator PPAR-α of SREBP-1c/PNPLA-3 pathway, and oxidative and inflammatory factors were also measured.

2. Materials and Methods

2.1. Animals

All the protocols were approved by the animal care and ethical committee of Affiliated Hospital of Guiyang Medical College (Approval No. GY2015R29). A total of 56 male Sprague Dawley rats (6- to 8-week old and 250 ± 20 g) were purchased from the experimental animal center, Third Military Medical University (Chongqing, China). All animal-handling procedures were performed according to the guide for the care and use of laboratory animals of NIH, and followed the guidelines of the animal welfare act. All animals were housed in a 12 Light:12 Dark cycle with ad libitum access to food and water.

2.2. Materials

Blueberries were purchased from Majiang Blueberry Plant (Guiyang, China) and preserved at −20 °C immediately. Blueberry juice was prepared according to an earlier report [51]. Briefly, 1 kg blueberry blend was thawed at 4 °C for 8 h and milled using Braun Global Hand Blender MR300 (De'Longhi Kenwood A.P.A Ltd., Hong Kong, China). The crushed blueberries were pressed in a bag press mod with the maximum pressure at 0.9 MPa. The blueberry juice was used as food for rats immediately. The main composition of blueberry juice was measured according to an earlier report [52]. The probiotics mixture with *Bifidobacterium lactis*, *Lactobacillus bulgaricus* and *Streptococcus thermophilus* were from Inner Mongolia Double Odd Pharmaceutical Co. (Tongliao, China). Probiotics were prepared freshly at log stage and used immediately. RNA purification kit was from Thermo Fisher Scientific (Waltham, MA, USA), SYBR Premix Ex Taq and PrimeScript RT reagent Kit from TaKaRa Bio Inc. (Dalian, Liaoning, China). SREBP-1c rabbit anti-rat antibodies (ab28481) and Anti-PNPLA-3 antibody (ab69170) were from Abcam (Cambridge, MA, USA). Monoclonal rabbit anti-rat PPAR-α

antibody (sc-50252) was from Santa Cruz Biotechnology Inc. (Delaware Ave., Santa Cruz, CA, USA). Rabbit anti-rat IL-6 antibody (ab6672), rabbit anti-rat TNF (tumor necrosis factor) antibody (ab6671), rabbit anti-rat caspase-3 antibody (ab44976) and rabbit anti-rat BCL-2 antibody (ab59348) were also from Abcam. Caspase 3 GAPDH rabbit anti-rat antibody (ab37168) and Goat anti-rabbit IgG H&L (HRP, ab6721) were from Abcam.

2.3. The Effects of PPAR-α Antagonist and Blueberry Juice on the Growth of Liver Cells

According to previous reports [53–55], human liver cell line HL7702 and HepG2 were selected for NASH research and purchased from Shanghai Cell bank (Chinese Academy of Science, Shanghai, China), and cultured in DMEM with 25 mM glucose, 5 mM glutamine, 10% fetal bovine serum (FBS), 100 μg/mL penicillin and 100 μg/mL streptomycin at 37 °C under a 5% CO_2 environment. The cell concentrations were adjusted to 1×10^5/mL and 200 μL was added to each cell in a 96-cell plate. GW6471, a PPAR-α antagonist, was purchased from Santa Cruz Biotechnology, Inc. (Santa Cruz, CA, USA). Either 20 μg/mL GW6471 or 10 μg/mL blueberry juice, or both, was added to each cell in a 96-cell plate and further cultured for 3 days. Adherent cells were detached by using 0.1% trypsin and 0.04% EDTA and resuspended in CASYton solution (Roche Applied Science, cat. no. 05651808 001). The debris was removed using a 100-μm nylon filter (Falcon Business USA Inc., Fairfield, CT, USA). Cell concentrations were measured using a glass hemocytometer and coverslip daily.

2.4. The Establishment of NASH Rat Model and Animal Groups

Eight Sprague-Dawley rats were fed with a normal diet as a control group (Table 1). Forty-eight Sprague-Dawley rats were fed with high-fat diet (normal diet + two percent cholesterol and ten percent lard) for two months (Table 1). The NASH rat model was evaluated by a histological feature scoring system that addresses the full spectrum of lesions of NAFLD and NASH. A NAFLD activity score (NAS) $\geq$5 was associated with a diagnosis of NASH, and less than 3 would be diagnosed as "not NASH" [56]. Twenty-four NASH rats were intra-articularly intraperitoneally injected with PPAR-α antagonist, GW6471, in 20 mL/kg solution for a week.

Table 1. Ingredient and nutrient composition of the diets (g/kg).

Ingredients (g/kg)	Normal Diet	HFD Diet
Casein	200.0	200.0
Starch	615.0	435.0
Sucrose	-	150.0
Corn oil	80.0	-
lard oil	-	100.0
cholesterol	-	20
Cellulose	50.0	50.0
Vitamin-Mineral mixture	50.0	50.0
DL-Methionine	3.0	3.0
Choline chloride	2.0	2.0
Chromium, mg/kg	0.066	0.097

The doses of blueberry [57], probiotics [58], and PPAR α antagonist (GW6471) [59] were administrated according to previous reports. As shown in Figure 1, all rat NASH models were evenly and randomly assigned to 6 groups: model group (MG, the model rats were intraperitoneally injected with 50 μL/kg saline solution and orally received 20 mL/kg liquid placebo daily); blueberry juice group (BG, the model rats were intraperitoneally injected with 50 μL/kg saline solution and orally received 10 mL/kg blueberry juice and 10 mL/kg liquid placebo daily); Blueberry juice and probiotic bacteria group (BPG, the model rats were intraperitoneally injected with 50 μL/kg normal saline solution and orally received 10 mL/kg blueberry juice and 10 mL/kg probiotics daily); PPAR-α inhibitor group (PIG, the model rats were intraperitoneally injected with 50 μL/kg PPAR-α in saline

solution); blueberry juice and PPAR-α inhibitor group (BPIG, the model rats were intraperitoneally injected with 50 μL/kg PPAR-α in saline solution and orally received 10 mL/kg blueberry juice and 10 mL/kg liquid placebo daily); and blueberry juice, probiotics, and PPAR-α inhibitor group (BPPIG, the model rats were intraperitoneally injected with 50 μL/kg PPAR-α in saline solution and orally received 10 mL/kg blueberry juice and 10 mL/kg probiotics daily). Meanwhile, 8 healthy rats were used as a control group (CG, the healthy rats were intraperitoneally injected with 50 μL/kg normal saline solution and orally received 20 mL/kg liquid placebo daily). The whole treatment period was ten days.

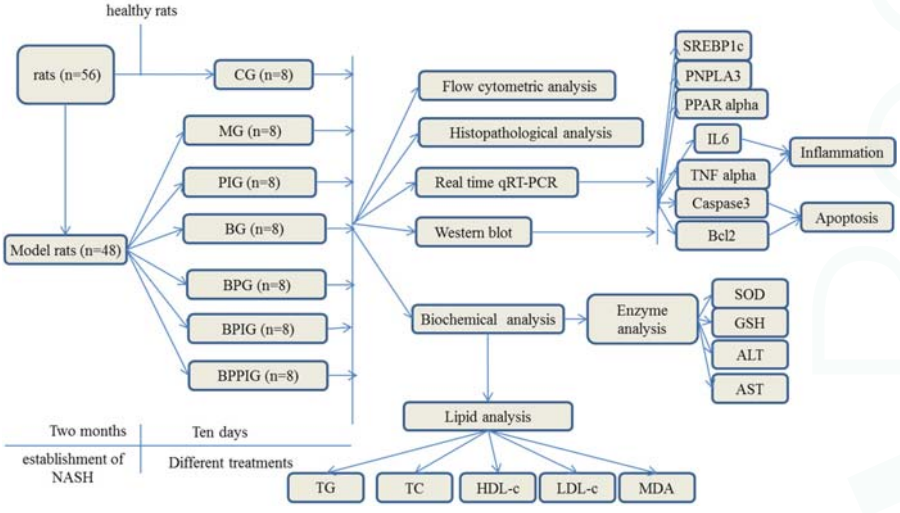

Figure 1. The flow chart of the study.

2.5. Measurement of PPAR-α

The activity of PPAR-α was measured using PPAR-α assay kit (Cat. No. ab133107, Abcam (Shanghai) branch, Shanghai, China) among different groups after ten-day blueberry and/or BP treatment.

2.6. Histological Analysis

After ten-day blueberry and probiotic and/or -PPAR-α treatment, all rats were sacrificed by decapitation. Blood samples were obtained and centrifuged at 5000× *g* for 10 min, and serum was purified and stored at −80 °C. Liver tissue was cut and fixed in ten percent formalin, and paraffin-embedded sections were prepared. All sections were stained by hematoxylin and eosin (HE) and Oil Red O (ORO). The sections were observed under an A12.1503 microscope (Opto-Edu (Beijing) Co., Ltd., Beijing, China). The diameters of droplets were calculated using a hemocytometer. After being stained with HE, the sections were washed with ddH_2O and 60% isopropanol for three times. Oil Red O was extracted with 100% isopropanol for five minutes. The solution was measured at 540 nm.

2.7. Flow Cytometry Analysis

The apoptotic rates of hepatic cells were measured by using an EC800 flow cytometer (Shinagawa-ku, Tokyo, Japan). All hepatic tissues were pulverized using a pestle and mortar and single cells were separated by a Nycodenz density gradient. A total of 100 μL of cells with the concentration of 1×10^5/mL were transferred into 5-mL flow tubes. Annexin V, conjugated to green-fluorescent

FITC dye, was added, and apoptotic rate was calculated according to the fluorescence intensity of Annexin V-FITC.

2.8. Biochemical Analysis

Some molecules involving in oxidative stress were analyzed because oxidative stress is an important element for the development of NASH [21,22]. The serum activity of superoxide dismutase (SOD) was measured by formazan-WST method [60]. WST1 produces water soluble formazan dye on reduction with superoxide anion. Reduction rate is linearly associated with the activities of anthine oxidase, which can be repressed by SOD. Serum sample was treated with WST for 20 min at 37 °C. The absorbing values were recorded at 450 nm and inhibiting rates were calculated. The term "0.5 O.D." is defined as having 1 unit of SOD activity. The serum concentration of reduced glutathione (GSH) was determined by the Dithiobis-2-nitrobenzoic acid (DTNB) method [61]. DTNB reacts with the sulfhydryl group of GSH and produces yellow TNB and GS-TNB, which is then reduced by GSH and β-nicotinamide adenine dinucleotide phosphate (β-NADPH). The TNB production is associated with the concentration of GSH in serum samples. TNB absorbing values were measured at 412 nm. One unit is defined as the amount of enzyme required to catalyze the reduction of one micromole of substrate per min. The serum concentrations of aspartate amino-transaminase (AST) and alanine aminotransferase (ALT) were evaluated by using Hitachi 7170A/7180 Biochemical Analyzer (Hitachi, Japan). Malondialdehyde (MDA) serum concentrations were determined by using an MDA kit (GENMED, Shanghai, China). The units for AST and ALT are defined as one absorbing unit per minute in the serum samples. NASH development is often associated with the disorder of lipid metabolism. Therefore, the serum levels of total triglycerides (TG), total cholesterol (TC), high-density lipoprotein-cholesterol (HDL-C), and low-density lipoprotein-cholesterol (LDL-C) were also determined by Hitachi 7170A/7180 Biochemical Analyzer. Serum levels of IL-6 and TNF-α were measured by using different ELISA kits (Cat. No. ab100772 and ab108913) from Abcam (Cambridge, MA, USA).

2.9. qRT-PCR

Total hepatic RNA was exacted and purified by using a RNA purification kit. cDNA was produced based on the instructions of RT-PCR kit. qRT-PCR was performed to assay the mRNA levels of PPAR-α SREBP-1c, PNPLA-3, caspase-3 and Bcl-2 genes. GAPDH was a control to normalize the copy number of each sample. All the primer sequences are listed in Table 2. qRT-PCR was performed on The CFX96 Touch Real-Time PCR Detection System (Bio-Rad, Hercules, CA, USA). The mean Ct value represented the mRNA levels of the individual gene.

Table 2. The primer sequences used in qRT-PCR.

		Sequences (5′-3′)	Size (bp)
PPAR-α	Forward Reverse	GTCAGCTGCCCTGCTGTCCC CGAAAGAAGCCCTTGCAGCC	130
SREBP-1c	Forward Reverse	CGCTTCTTACAGCACAGCAA TGCCCAAGGACAAGGGGCTA	220
PNPLA-3	Forward Reverse	CGCACTTTCTTCGGCTGCTC AATGTTGAAGAACGGGTGGA	150
IL-6	Forward Reverse	CACAACAGACCAGTATATAC GTATTTCTGGAAGTTTCAG	160
TNF-α	Forward Reverse	GTGGCGGGGGCCACCACGCTC CGAGTTTTGAGAAGATGATC	141
Caspase3	Forward Reverse	ATGTCAGCTCGCAATGGTAC CGTTCCAAAAATTACTCC	210
Bcl-2	Forward Reverse	GTGCACCGAGACACGGCTGC CGACGGTAGCGACGAGAGAA	140
GAPDH	Forward Reverse	TGTTCCAGTATGACTCTACC TCACCCCATTTGATGTTAGC	130

2.10. Western Blot Analysis

Protein was extracted and the concentration was determined by a Bradford protein assay kit (Beyotime Biotechnology, Beijing, China). Thirty micrograms of protein were taken from each group, separated by 12% sodium dodecyl sulfate polyacrylamide gel electrophoresis (SDS-PAGE), and then transferred to a Polyvinylidene difluoride (PVDF) membranes (Millipore Corporation, Bedford, MA, USA), which was blocked by 5% non-fat milk. The membrane was treated with primary antibodies at 4 °C for 10 h. Secondary antibodies were added and incubated for 1 h. Protein bands were shown after 1-h exposure with GE's Amersham ECL + Chemiluminescent CCD camera. The protein level was indicated as the value according to relative ratio to loading control GAPDH.

2.11. Statistical Analysis

All data are presented as mean values ± standard deviation (S.D.). The differences were compared using the analysis of variance (ANOVA) among different groups. SPSS Statistical Package 20.0 (SPSS Inc., Chicago, IL, USA) was used to analyze these data. There was statistical significance of difference if $p < 0.05$.

3. Results

3.1. Establishment of NASH Model

NASH models were determined according to an earlier report [56]. The scores of all rats were more than 8 (Table 3). A NAFLD activity score (NAS) ≥5 was associated with a diagnosis of NASH, and <3 would be diagnosed as "not NASH" [56]. Therefore, the model was established successfully and would be useful in NASH experiment.

Table 3. NASH model evaluated by NASH Research Network Scoring System Definitions and Scores in Study Set.

Items	Definition	Scores	*n* = 48
Steatosis Grade	Low- to medium-power evaluation of parenchymal involvement by steatosis		
	<5%	0	0%
	5%–33%	1	0%
	>33%–66%	2	29%
	>66%	3	70%
Location	Predominant distribution pattern		
	Zone 3	0	0%
	Zone 1	1	2%
	Azonal	2	56%
	Panacinar	3	42%
Microvesicular steatosis	Contiguous patches		
	Not present	0	83%
	Present	1	17%
Fibrosis stage			
	None	0	42%
	Perisinusoidal or periportal	1	2%
	Mild, zone 3, perisinusoidal	1	2%
	Moderate, zone 3, perisinusoidal	1	8%
	Portal/periportal	1	8%
	Perisinusoidal and portal/periportal	2	25%
	Bridging fibrosis	3	4%
	Cirrhosis	4	4%
Inflammation			
Lobular inflammation	Overall assessment of all inflammatory foci		
	No foci	0	0%
	<2 foci per 200× field	1	2%
	2–4 foci per 200× field	2	56%
	>4 foci per 200× field	3	42%

Table 3. *Cont.*

Items	Definition	Scores	*n* = 48
Microgranulomas	Small aggregates of macrophages		
	Absent	0	63%
	Present	1	37%
Large lipogranulomas	Usually in portal areas or adjacent to central veins		
	Absent	0	73%
	Present	1	27%
Portal inflammation	Assessed from low magnification		
	None to minimal	0	52%
	Greater than minimal	1	48%
Liver cell injury			
Ballooning			
	None	0	21%
	Few balloon cells	1	58%
	Many cells/prominent ballooning	2	21%
Acidophil bodies			
	None to rare	0	87%
	Many	1	13%
Pigmented macrophages			
	None to rare	0	83%
	Many	1	17%
Megamitochondria			
	None to rare	0	75%
	Many	1	24%
Other findings			
Mallory's hyaline	Visible on routine stains		
	None to rare	0	67%
	Many	1	33%
Glycogenated nuclei	Contiguous patches		
	None to rare	0	52%
	Many	1	48%
Diagnostic classification			
Not steatohepatitis		0	0%
Possible/borderline		1	0%
Definite steatohepatitis		2	100%

3.2. BP Increase Weight Loss of Rat NASH Model

There were statistical differences for body weight, liver index and epididymal fat weight between control and model groups after three months and ten days (Table 4, $p < 0.05$). Comparatively, *PPAR-α* silence increased the weight while blueberry juice and/or probiotics treatment reduced the weight compared to models (Table 4, $p < 0.05$).

Table 4. The comparison of liver and fat body weights among different groups.

	CG	MG	PIG	BG	BPG	BPIG	BPPIG
Body weight (g)	368.2 ± 32.7	397.4 ± 36.6	410.4 ± 47.5	390.3 ± 32.6	384.8 ± 28.9	394.7 ± 36.8	388.4 ± 33.2
Liver index (%)	2.6 ± 0.3	3.2 ± 0.4	3.4 ± 0.5	3.0 ± 0.3	2.8 ± 0.3	3.1 ± 0.3	2.9 ± 0.3
epididymal fat weight (g)	8.4 ± 1.3	9.8 ± 1.6	11.2 ± 1.8	9.1 ± 1.6	8.8 ± 1.3	9.3 ± 1.4	8.9 ± 1.5

Note: Liver index was presented as liver weight/body weight × 100%. All rat NASH models were evenly and randomly assigned to 6 groups: model group (MG, the model rats were intraperitoneally injected with 50 μL/kg saline solution and orally received 20 mL/kg liquid placebo daily); blueberry juice group (BG, the model rats were intraperitoneally injected with 50 μL/kg saline solution and orally received 10 mL/kg blueberry juice and 10 mL/kg liquid placebo daily); Blueberry juice and probiotic bacteria group (BPG, the model rats were intraperitoneally injected with 50 μL/kg normal saline solution and orally received 10 mL/kg blueberry juice and 10 mL/kg probiotics daily); PPAR-α inhibitor group (PIG, the model rats were intraperitoneally injected with 50 μL/kg PPAR-α in saline solution); blueberry juice and PPAR-α inhibitor group (BPIG, the model rats were intraperitoneally injected with 50 μL/kg PPAR-α in saline solution and orally received 10 mL/kg blueberry juice and 10 mL/kg liquid placebo daily); and blueberry juice, probiotics, and PPAR-α inhibitor group (BPPIG, the model rats were intraperitoneally injected with 50 μL/kg PPAR-α in saline solution and orally received 10 mL/kg blueberry juice and 10 mL/kg probiotics daily). Meanwhile, 8 healthy rats were used as a control group (CG, the healthy rats were intraperitoneally injected with 50 μL/kg normal saline solution and orally received 20 mL/kg liquid placebo daily).

3.3. BP Improve Antiinflammatory Activities of Rat NASH Model

There were statistical differences for the levels of inflammatory cytokines between control and model groups after three months and ten days (Table 5, $p < 0.05$). Comparatively, PPAR-α silence increased the levels while blueberry juice and/or probiotics treatment reduced the levels compared to models (Table 5, $p < 0.05$).

Table 5. The comparison of inflammatory cytokines among different groups.

	CG	MG	PIG	BG	BPG	BPIG	BPPIG
IL-6 (pg/mL)	12.34 ± 2.65	42.59 ± 6.18	46.81 ± 7.52	28.42 ± 5.17	22.32 ± 4.77	38.52 ± 5.34	29.33 ± 4.18
TNF α (pg/mL)	5.42 ± 2.41	14.59 ± 12.03	16.36 ± 2.87	12.35 ± 2.44	9.34 ± 1.38	13.55 ± 2.69	11.46 ± 2.79

3.4. BP Improve Antioxidant Activities of Rat NASH Model

Serum biochemical index analysis showed that serum levels of ALT and AST were the highest in PIG compared to all other groups (Table 6) ($p < 0.05$). In contrast, the serum levels of SOD and GSH were lowest compared to all other groups (Table 6) ($p < 0.05$). Blueberry juice and/or BP reduced the serum levels of ALT and AST, and increased the levels of SOD and GSH in NASH models and the models with the treatment of PPAR-α inhibitor (Table 6) ($p < 0.05$). Serum levels of ALT and AST were lowest, and the levels of SOD and GSH were highest in CG (Table 6) ($p < 0.05$). Biochemical analysis showed that there was statistical significance of differences for the serum levels of SOD, GSH, ALT and AST among different groups (Table 6) ($p < 0.05$). The results suggest that BP improve antioxidant activities of rat NASH model.

Table 6. Biochemical parameters of enzyme activities for NASH.

Group (n = 8)	SOD (U/mL)	GSH (ng/L)	ALT (U/mL)	AST (U/mL)
CG	27.24 ± 3.26 ^{b,c,d,f}	24.15 ± 2.14 ^{b,d,f}	45.12 ± 10.43 ^{b,c,d,e}	103.32 ± 25.17 ^{b,c,f}
MG	12.25 ± 4.16 ^{a,c,d,e,f}	13.23 ± 1.93 ^{a,c,e,f}	87.79 ± 8.40 ^{a,c,e,}	208.26 ± 19.64 ^{a,c,e}
PIG	9.34 ± 2.32 ^{a,b,c,d,e,f}	10.28 ± 1.74 ^{a,b,c,e,f}	123.79 ± 12.36 ^{a,b,c,e}	289.42 ± 24.48 ^{a,b,c,e}
BG	22.34 ± 3.48 ^{a,b,d,e}	22.38 ± 1.02 ^{b,a,d,f}	61.45 ± 12.18 ^{b,a,d,}	146.19 ± 25.28 ^{b,d,f}
BPIG	17.68 ± 2.43 ^{a,b,c,e}	14.28 ± 1.61 ^{a,c,e}	105.25 ± 15.82 ^{a,b,c,e}	253.24 ± 17.54 ^{a,b,c,e,f}
BPG	28.52 ± 4.53 ^{b,c,d,f}	25.64 ± 2.28 ^{b,c,d,f}	56.34 ± 12.16 ^{b,a,d}	128.63 ± 22.38 ^{b,d,f}
BPPIG	20.25 ± 4.47 ^{a,b,e}	17.331 ± 1.64 ^{a,b,c,d,e}	95.18 ± 7.28 ^{a,c,e}	186.61 ± 22.35 ^{a,c,d,e}

Note: Eight blood samples were analyzed in each group. All data are presented as mean value ± S.D. ^{a} $p < 0.05$ vs. the control group (CG); ^{b} $p < 0.05$ vs. the model group (MG); ^{c} $p < 0.01$ vs. the BG group; ^{d} $p < 0.05$ vs. BPIG (Blueberry juice and the treatment of PPAR-α inhibitor); ^{e} $p < 0.05$ vs. the BPG (BP treatment); ^{f} $p < 0.05$ vs. the BPPIG group (BP and the treatment of PPAR-α inhibitor).

3.5. Blueberry Juice and Probiotics Improve Lipid Patterns of Rat NASH Model

Lipid pattern analysis showed that serum MDA, TG, TC, and LDL-C reached the highest level in PIG compared to other groups (Table 7) ($p < 0.05$). In contrast, the serum HDL-C reached the lowest level. Blueberry juice and/or BP treatment reduced serum levels of MDA, TG, TC, and LDL-C, and increased the levels of HDL-C in NASH models and the models with the treatment of PPAR-α inhibitor. Comparatively, serum MDA, TG, TC, and LDL-C were at the lowest level and HDL-C was at the highest level in CG (Table 7) ($p < 0.05$). Lipid profile analysis also showed that there was statistical significance of differences for the serum levels of TG, TC, HDL-C, LDL-C and MDA among different groups (Table 7) ($p < 0.05$).

Table 7. Biochemical parameters of lipid metabolism for NASH (mmol/L).

Group (n = 8)	TG	TC	HDL-C	LDL-C	MDA
CG	$0.84 \pm 0.16^{b,c,d,f}$	$2.55 \pm 0.49^{b,f}$	$1.36 \pm 0.28^{b,c,d,f}$	$1.13 \pm 0.48^{b,c,d,e,f}$	$0.48 \pm 0.17^{b,d,f}$
MG	$1.76 \pm 0.42^{a,c,d,e,f}$	$3.34 \pm 1.50^{a,c,d,e,f}$	$0.67 \pm 0.48^{a,c,e,f}$	$1.84 \pm 0.66^{a,c,e,f}$	$1.45 \pm 0.44^{a,c,d,e,f}$
PIG	$2.38 \pm 0.32^{a,b,c,d,e,f}$	$3.64 \pm 1.29^{a,b,c,d,\ e,f}$	$0.56 \pm 0.29^{a,b,c,e,f}$	$2.09 \pm 0.43^{a,b,c,e,f}$	$1.64 \pm 0.37^{a,b,c,d,e,f}$
BG	$1.19 \pm 0.15^{a,b,d,e,f}$	$3.26 \pm 0.74^{b,d,f}$	$1.12 \pm 0.29^{a,b,d}$	$1.52 \pm 0.68^{a,b,d,e,}$	$0.56 \pm 0.39^{b,d,f}$
BPIG	$2.03 \pm 0.65^{a,b,c,e,f}$	$3.47 \pm 0.53^{a,c,e,f}$	$0.76 \pm 0.25^{a,c,e,f}$	$1.73 \pm 0.28^{a,c,e}$	$1.12 \pm 0.36^{a,b,c,e,f}$
BPG	$0.92 \pm 0.31^{a,b,c,d,f}$	$3.12 \pm 0.46^{b,d,f}$	$1.24 \pm 0.30^{b,d,f}$	$1.36 \pm 0.59^{a,b,c,d,f}$	$0.41 \pm 0.28^{b,a,d,f}$
BPPIG	$1.26 \pm 0.18^{a,b,c,d,e}$	$3.52 \pm 0.68^{a,b,c,d,e}$	$0.98 \pm 0.27^{a,b,c,d,e}$	$1.66 \pm 0.49^{a,b,e}$	$0.72 \pm 0.38^{a,b,c,d,e}$

Note: Eight blood samples were analyzed in each group. All data are presented as mean value ± S.D. [a] $p < 0.05$ vs. the control group (CG); [b] $p < 0.05$ vs. the model group (MG); [c] $p < 0.01$ vs. the BG group; [d] $p < 0.05$ vs. BPIG (Blueberry juice and the treatment of PPAR-α inhibitor); [e] $p < 0.05$ vs. the BPG (Blueberry juice and probiotics); [f] $p < 0.05$ vs. the BPPIG group (Blueberry juice and probiotics and the treatment of PPAR-α inhibitor).

The results suggested that the combination of BP is better than only blueberry consumption for improving serum biochemical indices (Table 6) and lipid pattern (Table 7) in NASH models. When PPAR-α inhibitor was used, there was statistical significance of the differences between PIG and MG groups in most cases ($p > 0.05$) (Tables 6 and 7), suggesting PPAR-α may play an important role in the progression of NASH. Blueberry juice and the combination of BP reduced the progression of NASH by improving its biochemical indices and lipid patterns in NASH models or the models with the treatment of PPAR-α inhibitor ($p < 0.05$) (Tables 6 and 7).

3.6. The Effects of PPAR-α Antagonist and/or Blueberry Juice on the Growth of Liver Cells

There was no statistical significance of differences for the cell concentrations among all groups in cell line HL7702 ($p > 0.05$) (Figure 2A) and cell line HepG2 ($p > 0.05$) (Figure 2B) before the treatment of PPAR α antagonist. After treatment, Figure 2A showed that GW6471 inhibited the growth rate of cell line HL7702 while blueberry juice increased the growth rates of HL7702 cells ($p < 0.05$). Meanwhile, blueberry reduced the inhibition of PPAR-α activity caused by GW6471 in HL7702 cells ($p < 0.05$). Similarly, Figure 2B shows that GW6471 inhibited the growth rate of cell line HepG2 while blueberry juice increased the growth rates of HepG2 cells ($p < 0.05$). Meanwhile, blueberry reduced the inhibition of PPAR-α activity caused by GW6471 in HepG2 cells ($p < 0.05$). All these results suggest that blueberry juice prevents the inhibition of PPAR-α activity caused by GW6471 in both kinds of liver cell lines.

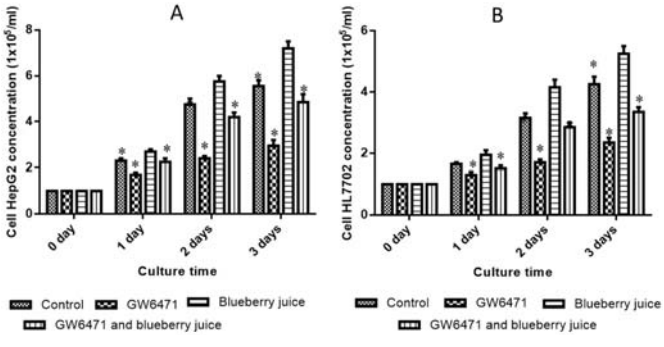

Figure 2. The effects of PPAR-α antagonist and blueberry juice on the growth of human liver cells: (**A**) the effects of PPAR-α antagonist and blueberry juice on the growth rate of cell line HL7702; and (**B**) the effects of PPAR-α antagonist and blueberry juice on the growth rate of liver cell line HepG2. All data are presented as mean value ± S.D. Five samples were analyzed in each group. * $p < 0.05$ via a blueberry juice group.

3.7. Measurement of PPAR-α Activity

There was no statistical significance of differences for the activity of PPAR-α among all groups in cell line HL7702 ($p > 0.05$) (Figure 3A) and cell line HepG2 ($p > 0.05$) (Figure 3B) before the treatment of PPAR-α antagonist. Compared with controls, the antagonist of PPAR-α reduced the activity of PPAR-α significantly in HL7702 (Figure 3A) and HepG2 (Figure 3B) liver cells ($p < 0.05$). There was statistical significance of differences in the PPAR-α activity between GW6471 and GW6471 + blueberry juice treatment in HL7702 (Figure 3A) and HepG2 (Figure 3B) cells ($p < 0.05$).

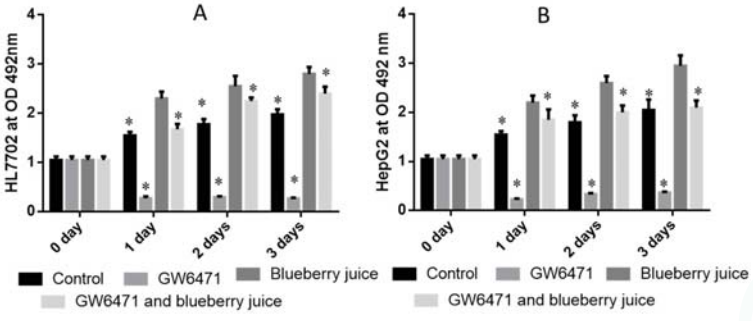

Figure 3. The activity of PPAR-α in different cells: (**A**) the effects of BP on the antagonist of PPAR-α in HL7702 cells; and (**B**) the effects of BP on the antagonist of PPAR-α in HepG2 cells. Five samples were analyzed in each group. All data are presented as mean value ± S.D. * $p < 0.05$ via a blueberry juice group BG.

Similarly, compared with controls, the antagonist reduced the activity of PPAR-α significantly in PIG (Figure 4, $p < 0.05$). There was statistical significance of differences in the PPAR-α activity between PIG and BPIG or BPPIG (Figure 4) ($p < 0.05$). All these results suggest that blueberry juice can prevent the inhibition of PPAR-α activity caused by GW6471.

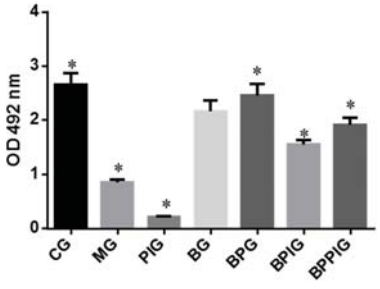

Figure 4. The activity of PPAR-α in different groups: The effects of BP on the antagonist of PPAR-α in different groups by using blood samples. Eight samples were analyzed in each group. All data are presented as mean value ± S.D. * $p < 0.05$ via a blueberry juice group BG.

3.8. Blueberry Juice and Probiotics Ameliorate NASH

Figure 5 showed the liver tissues stained by HE in different groups. For healthy rats, hepatic cells encircled a tubular section regularly, and all lipid droplets were small. In MG, the structures of hepatic cells were destructed and widely distributed with many lipid droplets. In PIG, the lobular structure was heavily destroyed and filled with many large lipid droplets compared to the liver tissues from the model group. Many large lipid droplets were produced when the activity of PPAR-α was

blocked by its antagonist GW6471, suggesting that PPAR-α plays an important role in maintaining the normal structure of liver cells. The size of lipid droplets was decreased in the BG and BPG groups compared to the tissues in MG, PIG, BPIG, and BPPIG groups. In BPG, the hepatic cords were radially arranged around a central vein and there were fewer lipid droplets. In the BPPIG, the hepatic structure was destroyed and the lipid droplets were small. Although the number of droplets in BPIG was greater than in PIG (Figure 5A), the average size of droplets was larger in PIG than in BPIG (Figure 5B). These findings suggested that the combination of blueberry juice and probiotics attenuates NASH better than the group only fed blueberry juice.

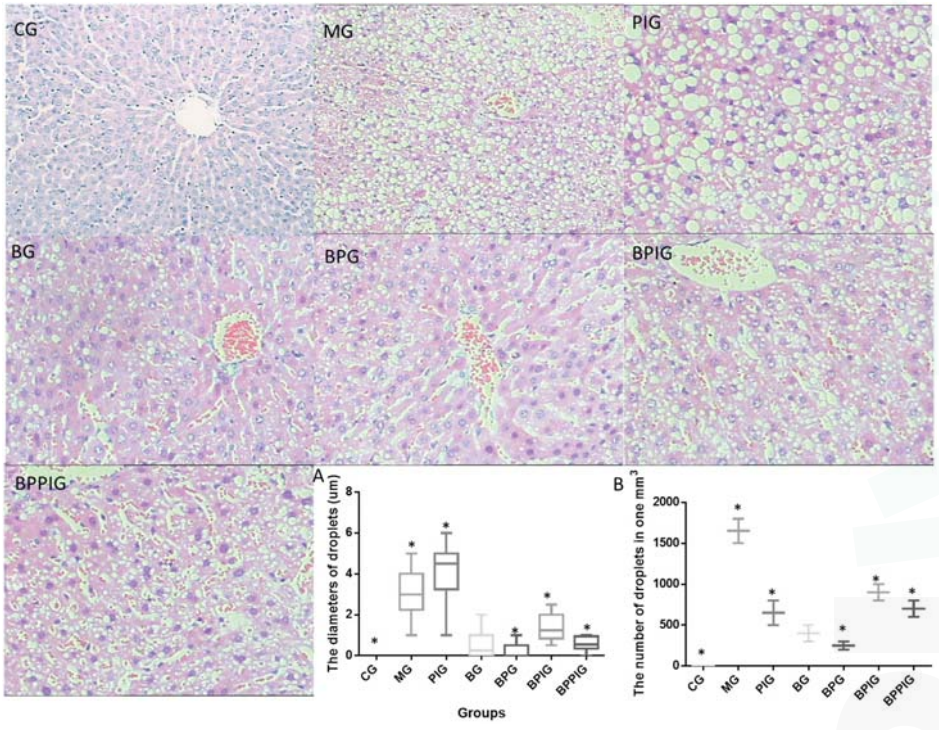

Figure 5. HE analysis for the effects of BP on NASH and liver damage: (**A**) the diameters of lipid droplets in different groups; and (**B**) the concentration of lipid droplets in different groups. Eight liver samples were analyzed in each group. All data are presented as mean value ± S.D. * $p < 0.05$ via a blueberry juice group BG.

Figure 6 shows the liver tissues stained using ORO from different groups. In CG, the liver tissues were little stained with ORO while the liver tissues were most stained with ORO in PIG. Blueberry juice reduced the staining in animal models and the model treated with GW6471. BP treatment reduced the staining better than only blueberry juice. The absorbing values for ORO showed a similar changing trend in different groups (Figure 6A). The value was highest in PIG and lowest in CG. BP reduced the values in BG, BPG, BPIG and BPPIG. Comparatively, the number and size of droplets were highest in PIG compared to other groups while the number and size of droplets were lowest in CG compared to other groups (Figure 6B). Blueberry juice and/or probiotics treatment reduced the number and size of droplets compared to PIG (Figure 6B, $p < 0.05$).

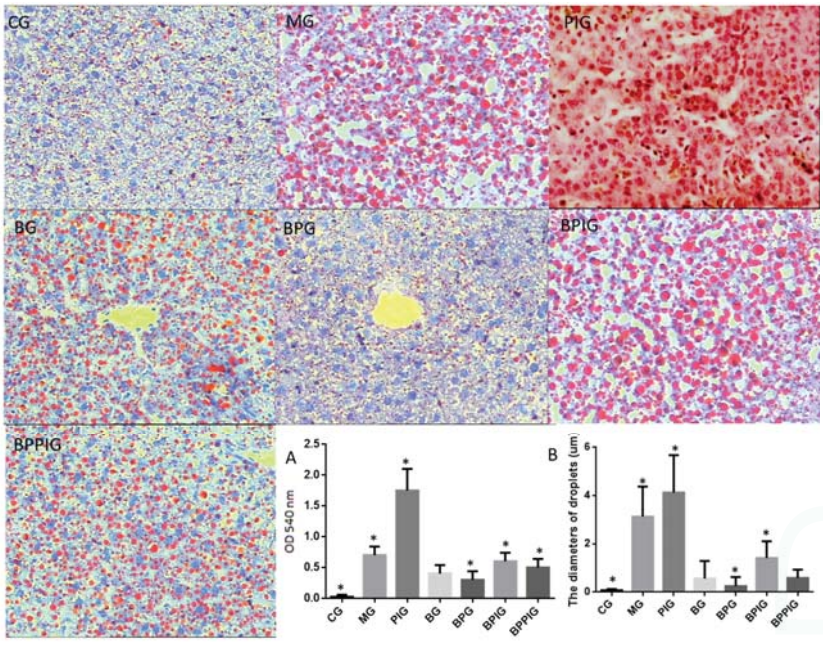

Figure 6. ORO analysis for the effects of BP on NASH and liver damage: (**A**) the absorbing value of the solvent of ORO extraction at 540 nm in different groups; and (**B**) the diameters of droplets in different groups. Eight liver samples were analyzed in each group. All data are presented as mean value ± S.D. * $p < 0.05$ via a blueberry juice group BG.

3.9. Liver Apoptosis

The degree of apoptosis for NASH liver tissues was analyzed by flow cytometer. The results showed that the apoptotic rate was lowest in CG and highest in PIG compared to other groups (Figure 7) ($p < 0.05$). Blueberry juice treatment and/or BP treatment reduced apoptotic rates in NASH models. Blueberry juice treatment and/or BP treatment also significantly reduced apoptotic rates in NASH models treated with GW6471. All these results showed that of BP treatment reduced apoptotic rates of NASH than only blueberry consumption (Figure 7A).

3.10. Relative mRNA Levels of PPAR-α, SREBP-1c and PNPLA-3

qRT-PCR analysis indicated that the mRNA levels of Srebp-1c and Pnpla-3 were higher in MG, PIG, BPIG and BPPIG than in CG, BG, and BPG (Figure 8) ($p < 0.05$). Comparatively, the mRNA level of *PPAR-α* was higher in CG, BG, BPG, BPIG, and BPPIG than in MG and PIG ($p < 0.05$) (Figure 8). The results suggest that BP increased the mRNA levels of PPAR-α, which reduced the level of SREBP-1c and PNPLA-3. After the treatment of PPAR-α inhibitor, the mRNA level of PPAR-αwas stable but the mRNA levels of SREBP-1c and PNPLA-3 were reduced, suggesting that PPAR-αantagonist reduced the activity of PPAR-α and resulted in the increase of the mRNA levels of SREBP-1c and PNPLA-3. Thus, the results confirmed that blueberry juice can inhibit the progression of NASH by down-regulating SREBP-1c/PNPLA-3 pathway via PPAR-α.

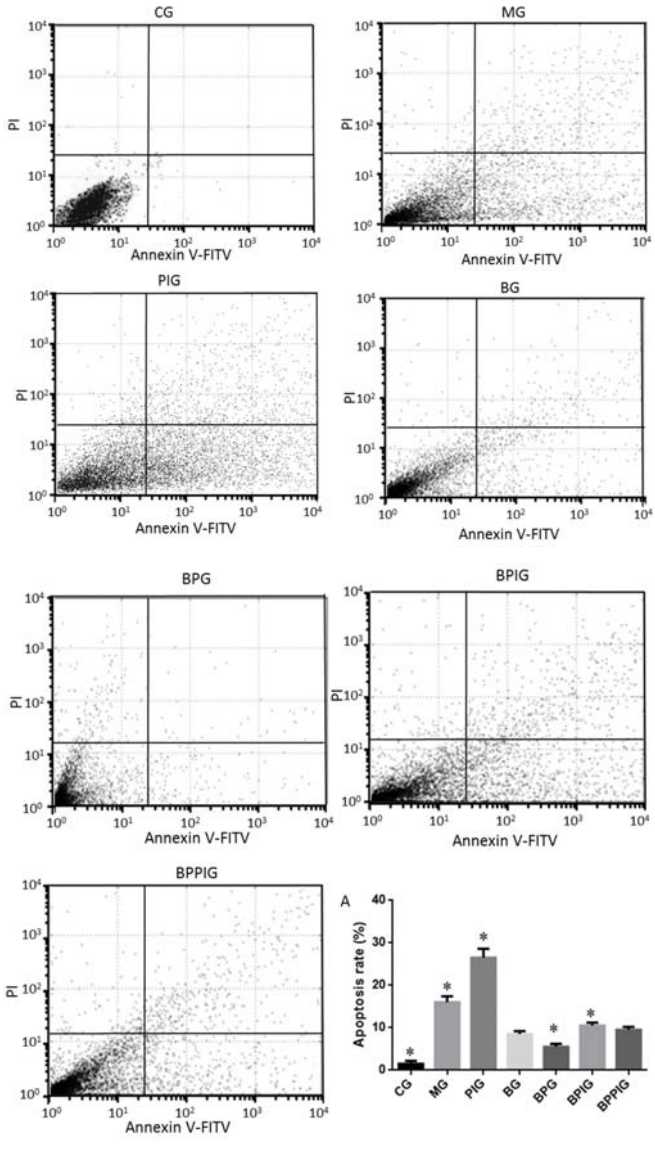

Figure 7. Flow cytometer analysis for the apoptosis of liver tissue: apoptotic rate of liver tissues in different groups (**A**). Eight liver samples were analyzed in each group. All data are presented as mean value ± S.D. * $p < 0.05$ via a blueberry juice group BG.

3.11. Relative mRNA Levels of Apoptosis-Inducing Factors (caspase-3 and Bcl-2)

qRT-PCR analysis indicated that the mRNA levels of caspase-3 and Bcl-2 were higher in MG, PIG, BPIG and BPPIG than in CG, BG, and BPG (Figure 9) ($p < 0.05$). The results suggest that BP treatment reduced the mRNA level of caspase-3 and Bcl-2. After the treatment of PPAR-α inhibitor, the mRNA level of PPAR-α was stable but the mRNA levels of caspase-3 and Bcl-2 were increased, suggesting that the inhibition of PPAR-α activity will increase the mRNA levels of caspase-3 and Bcl-2.

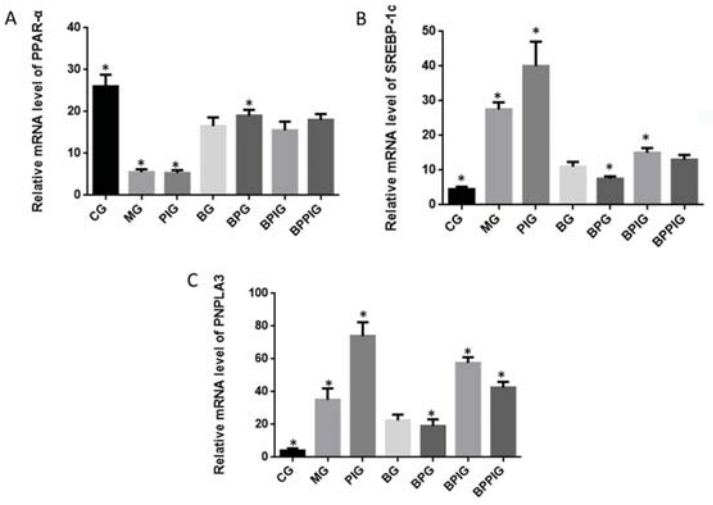

Figure 8. Real-time quantitative RT-PCR analysis of the mRNA levels of SREBP-1c/PNPLA-3 pathway and its interacting molecules. (**A**) Relative mRNA level of PPAR-α; (**B**) Relative mRNA level of SREBP-1C; (**C**) Relative mRNA level of PNPLA3. Eight liver samples were analyzed in each group. All data are presented as mean value ± S.D. * $p < 0.05$ via a blueberry juice group BG.

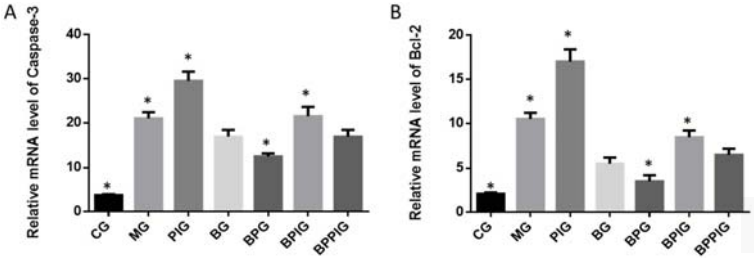

Figure 9. Real-time quantitative RT-PCR analysis of the mRNA levels of apoptotic factors: (**A**) relative mRNA levels of caspase-3; and (**B**) relative mRNA levels of Bcl-2. Five liver samples were analyzed in each group. All data are presented as mean value ± S.D. * $p < 0.05$ via a blueberry juice group BG.

3.12. Relative mRNA Levels of Inflammatory Cytokines (IL-6 and TNF-α)

Similar to caspase-3 and Bcl-2, qRT-PCR analysis indicated that the mRNA levels of IL-6 and TNF-α were higher in MG, PIG, BPIG and BPPIG than in CG, BG, and BPG (Figure 10) ($p < 0.05$). The results suggest that BP treatment will reduce the level of IL-6 and TNF-α. After the treatment of PPAR-α inhibitor, the mRNA level of PPAR-α was stable but the mRNA levels of IL-6 and TNF-α were increased, suggesting that the inhibition of PPAR-α activity will result in the increase of the mRNA levels of IL-6 and TNF-α.

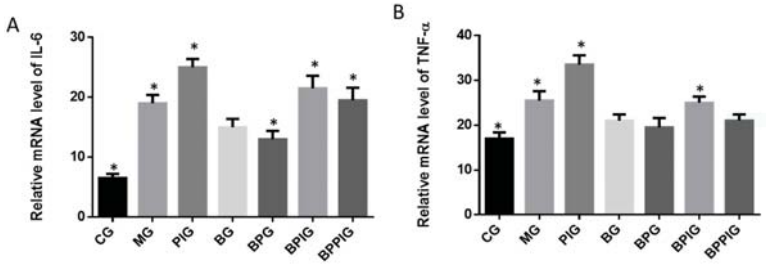

Figure 10. Real-time quantitative RT-PCR analysis of the mRNA levels of inflammatory cytokines: (**A**) relative mRNA levels of IL-6; and (**B**) relative mRNA levels of TNF-α. Five liver samples were analyzed in each group. All data are presented as mean value ± S.D. * $p < 0.05$ via a blueberry juice group BG.

3.13. Relative Protein Levels of PPAR-α, SREBP-1c and PNPLA-3

qRT-PCR analysis indicated that the protein levels of SREBP-1c and PNPLA-3 were higher in MG, PIG, BPIG and BPPIG than in CG, BG, and BPG (Figure 11) ($p < 0.05$). Comparatively, the protein level of PPAR-α was higher in the CG, BG, BPG, BPIG, and BPPIGs than in the MG and PIG groups ($p < 0.05$) (Figure 11). The results suggest that BP increased the protein levels of PPAR-α while the inhibition of PPAR-α activity will increase the level of SREBP-1c and PNPLA-3. Thus, the results confirmed that blueberry juice can inhibit the progression of NASH by affecting SREBP-1c-PNPLA-3 pathway via PPAR-α.

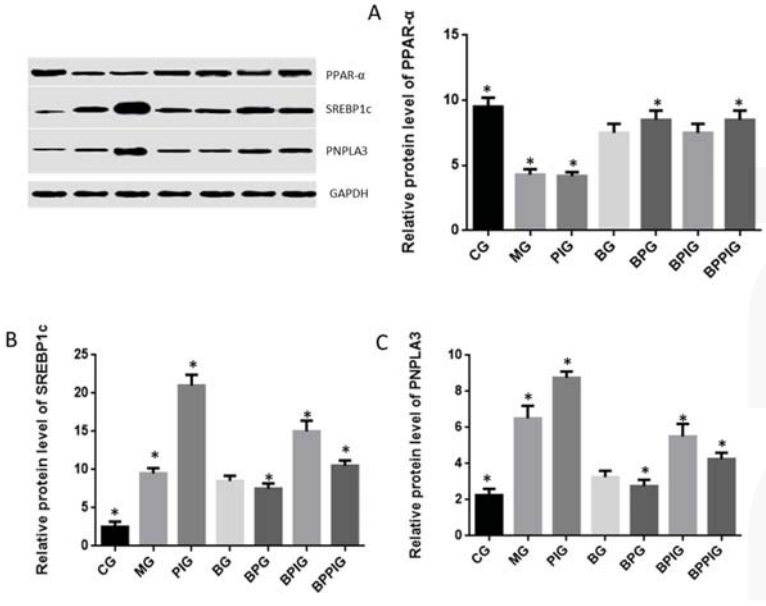

Figure 11. Western blot analysis of the protein levels of SREBP-1c/PNPLA-3 pathway and its interacting molecules. (**A**) relative protein level of PPAR-α; (**B**) relative protein level of SREBP-1c; (**C**) relative protein level of PNPLA3. Eight liver samples were analyzed in each group. All data are presented as mean value ± S.D. * $p < 0.05$ via a blueberry juice group BG.

3.14. Relative Protein Levels of Apoptosis-Inducing Factors (caspase-3 and Bcl-2)

qRT-PCR analysis indicated that the protein levels of caspase-3 and Bcl-2 were higher in MG, PIG, BPIG and BPPIG than in CG, BG, and BPG (Figure 12) ($p < 0.05$). The results suggest that BP reduces the protein level of caspase-3 and Bcl-2. After the treatment of PPAR-α inhibitor, the protein level of PPAR-α was stable but the protein levels of casepase-3 and Bcl-2 were increased, suggesting that PPAR-α antagonist increased the protein levels of caspase-3 and Bcl-2.

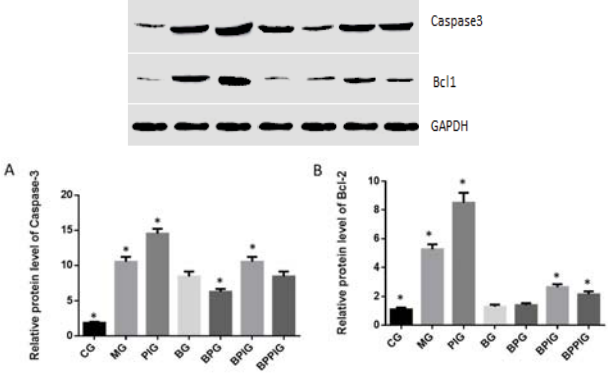

Figure 12. Western blot analysis of the protein levels of casepase-3 and Bcl-2. Eight liver samples were analyzed in each group. (**A**) relative protein level of caspase-3; (**B**) relative protein level of Bcl-2. All data are presented as mean value ± S.D. * $p < 0.05$ via a blueberry juice group BG.

3.15. Relative Protein Levels of Inflammatory Cytokines (IL-6 and TNF-α)

Just as caspase-3 and Bcl-2, Western Blot analysis indicated that the protein levels of IL-6 and TNF-α were higher in MG, PIG, BPIG and BPPIG than in CG, BG, and BPG (Figure 13) ($p < 0.05$). The results suggest that BP increased the protein levels of PPAR-α, which reduced the level of IL-6 and TNF-α. After the treatment of PPAR-α inhibitor, the protein level of PPAR-α was stable but the protein levels of IL-6 and TNF-α were increased, suggesting that PPAR-α antagonist increased the protein levels of IL-6 and TNF-α.

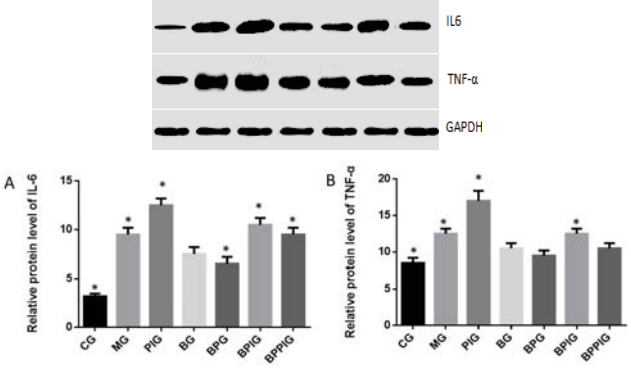

Figure 13. Western blot analysis of the protein levels of IL-6 and TNF-α. Eight liver samples were analyzed in each group. **A**, relative protein level of IL-6. **B**, relative protein level of TNF-α. All data are presented as mean value ± S.D. * $p < 0.05$ via a blueberry juice group BG.

4. Discussion

Inflammation is the main reason for the pathogenesis of NASH [24,25]. Quantitative real-time PCR and Western blot analysis showed that the combination of blueberry juice and probiotic bacteria had a significant inhibitory effect on inflammatory cytokines IL-6 and TNF-α. The levels of inflammatory cytokines in the BPG group was lower than that in the BG group ($p < 0.05$) (Figures 10 and 13), suggesting that there is a cumulative effect of the combination of BP for NASH treatment by reducing the levels of cytokines. On the other hand, the combination of BP also increased the level of PPAR-α. PPAR-α has been reported to play an important role in many physiological activities, such as lipid metabolism [62,63], glucose homeostasis [64] and anti-inflammatory action [65–67]. PPAR-α has been reported to play an important role in many physiological activities, such as lipid metabolism [62,63], glucose homeostasis [64] and anti-inflammatory action [65,66]. At cell levels, blueberry increased the growth rate of HL7702 (Figure 3A) and HepG2 (Figure 3B) cells compared to other groups without blueberry treatment ($p < 0.05$). Similarly, compared with controls, the antagonist reduced the activity of PPAR-α significantly in PIG (Figure 4, $p < 0.05$). All these results suggest that blueberry juice may reduce the inhibitory functions of the antagonist for PPAR-α and promote the growth of liver cells. However, the exact molecular mechanism remains unknown. Further work is needed to confirm the results and explore the related molecular mechanism.

The dysfunction of lipid metabolism is another main reason for the pathogenesis of NASH. The dysfunction of lipid metabolism often produces reactive oxygen species (ROS), which lead to hepatic apoptosis. On the other hand, caspase-3 and Bcl-2 are important apoptotic biomarkers. Blueberry and/or probiotics consumption increased the levels of SOD and GSH, and reduced the levels of ALT, AST, caspase-3 and Bcl-2. Thus, the results will prevent ROS production and apoptosis in hepatocytes and maintain the normal development and homeostasis of liver tissues. This study reports the pathogenesis of NASH and shows the destruction of hepatic tissues because of the changes in the activity of PPAR-α. According to an earlier report, the consumption of *n*-3 long-chain polyunsaturated fatty acids reduced the ratios of SREBP-1c to PPAR-α, which contributes to favored fatty acid oxidation and attenuate steatosis [68]. The combination of blueberry juice and probiotic bacteria increased the level of PPAR-α and reduced the level of SREBP-1c. According to an earlier report, oxidative stresses increase in NASH patients by increasing total oxidant status. Antioxidant treatment and increasing total antioxidant status are therapeutic options for NASH patients [69]. Elevated serum level of ALT is a marker of inflammation and oxidative stress [70]. AST is also related to oxidative stress and increasing all-cause mortality [71]. SOD is an important antioxidant biomarker by detoxifying normally generated reactive oxygen species. The increase of PPAR-α will enhance antioxidant functions of liver cells by affecting the level of SOD, ALT and AST [13,72]. In contrast, SREBP-1c will increase the level of ROS in hepatocytes and aggravate inflammatory injury of liver tissues [73]. Therefore, the results reduced lipid deposition, inflammation, necrosis, and fibrosis in hepatic tissues by enhancing the activity of the anti-oxidant enzyme SOD and decreasing the levels of biomarkers of oxidative stress ALT and AST. Comparatively, the antioxidant activities were measured by earlier reports. There was positive correlation between antioxidant activity and the polyphenols and vitamin C content in *Actinidia kolomikta*, *Actinidia arguta*, and *Actinidia chinensis* [74]. Another report showed that strawberry extract had no cytotoxic effects on HepG2 cell lines with high concentration of strawberry extracts, while 250 μg/mL had cytotoxic for HepG2 after 48- and 72-hour culture [75].

Hepatocyte apoptosis is greatly enhanced in NASH patients with NASH and the apoptosis is associated with NASH severity, suggesting that anti-apoptotic treatment will be useful for preventing the progression of NASH [76]. Flow cytometer analysis showed that the combined therapy of BP had a significant inhibitory effect on hepatic apoptosis. The apoptotic rate in the BPG group was lower than that in the BG group ($p < 0.05$) (Figure 7A), also suggesting that there was a synergistic effect of the combination of BP for NASH treatment. However, an exact molecular mechanism for the synergetic functions of BP still needs to be explored.

According to earlier reports, SREBP-1c plays a critical role in NASH progression and involves in tissue apoptosis [3,77], cell cycle control [78,79], transcription regulation [80], lipid metabolism [81,82], and many other life activities. All these are related to the development of NASH. Polyphenol is one of main component of blueberry juice [83,84] and observed to reduce the SREBP-1c level [85]. Present findings indicated that BP increase PPAR-α activity, which prevented the expression of SREBP-1c and resulted in the decrease of PNPLA-3 level.

Furthermore, BP can reduce the severity of NASH even antagonist of PPAR-α is used. The result suggests that other molecular mechanisms maybe existed for controlling NASH progression via BP. Probiotics and blueberry cooperatively increase the protecting functions for liver tissues of NASH models. The probiotics mixture with *Bifidobacterium lactis*, *Lactobacillus bulgaricus* and *Streptococcus thermophiles* had an additional effect to prevent NASH and/or its related events. The reason is complex. Systemic and local inflammation of NASH is often associated with the resident microbiota of the human gastro-intestinal tract. Thus, the administration of probiotics mixture may modulate systemic immune, and prevent the metabolic syndrome, liver injury, inflammatory bowel disorder, and enteritis [86]. All these activities may be beneficial for improving NASH.

Clearer molecular mechanism still needs to be explored in the future. On the other hand, PPAR-α activation prevents triglyceride synthesis in liver cells, which may be caused by inhibiting SREBP1 activity [87] while SREBP-1c expression has been widely reported to be associated with steatosis [68,88]. PNPLA-3 is associated with lipid accumulation in hepatic tissues, especially in steatosis progression. Steatosis progression will contribute to increasing the risk of NASH [89]. One important question should be considered here. SREBP-1c is not involved in cholesterol homeostasis. Why were the cholesterol levels changed by the NASH diet and PPARα antagonist? According to previous reports, PPAR-α and PPAR-γ activation induce cholesterol removal from human cells [90]. This result suggests that PPARα antagonist will cause the increase of cholesterol levels. On the other hand, cholesterol overloading will result in the increase in the expression of SREBP-1c [91]. BP can increase PPAR-α level, resulting in the decrease of cholesterol levels.

SIRT1 regulates lipid homeostasis by upregulating PPAR-α [92]. Present results showed the increased level of PPAR-α would reduce the levels of SREBP-1c and PNPLA-3. Thus, PPAR-α may inhibit the activity of SREBP-1c and PNPLA-3 ways. Thus, SIRT-1 signaling pathway may control SREBP-1c/PNPLA-3 pathway.

There were the following limitations in the present work: (1) The antagonist of PPAR-α was not used in healthy animals. The following reasons were considered: present work mainly focuses on animal NASH models, and, to reduce the number of animals and injury, fewer animals were used finally; (2) A clinical trial was not performed, although all the materials are safe for human consumption. Therefore, further work is needed to be done in NASH patients in the future; (3) Although probiotic has been regarded as a treatment option for NASH because of its effects on the gut flora, no randomized clinical trial was identified for such proposal [93]. We guess probiotic alone cannot prevent the progression of NASH. Therefore, the experiment was not performed here; (4) SREBP1c-PNPLA3 pathway has been regarded as a "disease module" that promotes hepatic fibrogenesis [94] while the latter is associated with the progression of NASH. Thus, we guess PPAR α may affect NASH development by affecting SREBP1c-PNPLA3 pathway. Further work is needed to confirm this proposal.

5. Conclusions

This study showed that BP has synergistic effects for preventing the development of NASH. BP can reduce the injuries and apoptosis of liver tissues in NASH models by improving the activity of PPAR-α, which inhibits the levels of SREBP-1c and PNPLA-3. The results increased the levels of anti-oxidant enzymes to remove oxygen free radicals, reduced lipid peroxidation and protected hepatocytes. Therefore, BP reduces the apoptosis and inflammation of hepatocytes in NASH by

affecting the SREBP-1c/PNPLA-3 pathway via PPAR-α. BP should be developed food additives for preventing the progression of NASH.

Acknowledgments: We are very grateful to three anonymous reviewers for their critical comments, which have significantly improved the quality of present paper. The work is supported by the National Natural Science Foundation of China (NSFC) (Project No. 81560100) and the project for Guizhou Provincial Science and Technology (No. ZLYJZFCG-2012-7).

Author Contributions: T.R. and J.Z. conceived and designed the experiments; L.Z. performed the experiments; L.Z. and M.C. analyzed the data; M.C. contributed reagents/materials/analysis tools; and L.Z. and M.C. wrote the paper.

Conflicts of Interest: The authors declare no conflict of interest.

References

1. Day, C.P. NASH-related liver failure: One hit too many? *Am. J. Gastroenterol.* **2002**, *97*, 1872–1874. [CrossRef] [PubMed]
2. Canbay, A.; Sowa, J.P.; Syn, W.K.; Treckmann, J. NASH Cirrhosis—The New Burden in Liver Transplantation: How Should It Be Managed? *Visc. Med.* **2016**, *32*, 234–238. [CrossRef] [PubMed]
3. Xu, H.; Zhou, Y.; Liu, Y.; Ping, J.; Shou, Q.; Chen, F.; Ruo, R. Metformin improves hepatic IRS2/PI3K/Akt signaling in insulin-resistant rats of NASH and cirrhosis. *J. Endocrinol.* **2016**, *229*, 133–144. [CrossRef] [PubMed]
4. Ambade, A.; Satishchandran, A.; Saha, B.; Gyongyosi, B.; Lowe, P.; Kodys, K.; Catalano, D.; Szabo, G. Hepatocellular carcinoma is accelerated by NASH involving M2 macrophage polarization mediated by HIF-1alphainduced IL-10. *Oncoimmunology* **2016**, *5*, e1221557. [CrossRef] [PubMed]
5. Michelotti, G.A.; Machado, M.V.; Diehl, A.M. NAFLD, NASH and liver cancer. *Nat. Rev. Gastroenterol. Hepatol.* **2013**, *10*, 656–665. [CrossRef] [PubMed]
6. Sanyal, A.J. NASH: A global health problem. *Hepatol. Res.* **2011**, *41*, 670–674. [CrossRef] [PubMed]
7. Ong, J.P.; Younossi, Z.M. Epidemiology and natural history of NAFLD and NASH. *Clin. Liver Dis.* **2007**, *11*, 1–16. [CrossRef] [PubMed]
8. Chi, K.R. The NASH drug dash. *Nat. Rev. Drug Discov.* **2015**, *14*, 447–448. [CrossRef] [PubMed]
9. Argo, C.K.; Iezzoni, J.C.; Al-Osaimi, A.M.; Caldwell, S.H. Thiazolidinediones for the treatment in NASH: sustained benefit after drug discontinuation? *J. Clin. Gastroenterol.* **2009**, *43*, 565–568. [CrossRef] [PubMed]
10. Feher, J.; Lengyel, G. A new approach to drug therapy in non-alcoholic steatohepatitis (NASH). *J. Int. Med. Res.* **2003**, *31*, 537–551. [CrossRef] [PubMed]
11. Ji, H.F. Vitamin E therapy on aminotransferase levels in NAFLD/NASH patients. *Nutrition* **2015**, *31*, 899. [CrossRef] [PubMed]
12. Tsuchiya, S.; Amano, Y.; Isono, O.; Imai, M.; Shimizu, F.; Asada, M.; Imai, S.; Harada, A.; Yasuhara, Y.; Tozawa, R.; et al. Pharmacological evaluation of pioglitazone and candesartan cilexetil in a novel mouse model of non-alcoholic steatohepatitis, modified choline-deficient, amino acid-defined diet fed low-density lipoprotein receptor knockout mice. *Hepatol. Res.* **2016**. [CrossRef] [PubMed]
13. Abd El-Haleim, E.A.; Bahgat, A.K.; Saleh, S. Effects of combined PPAR-gamma and PPAR-alpha agonist therapy on fructose induced NASH in rats: Modulation of gene expression. *Eur. J. Pharmacol.* **2016**, *773*, 59–70. [CrossRef] [PubMed]
14. Ji, H.F.; Sun, Y.; Shen, L. Effect of vitamin E supplementation on aminotransferase levels in patients with NAFLD, NASH, and CHC: Results from a meta-analysis. *Nutrition* **2014**, *30*, 986–991. [CrossRef] [PubMed]
15. Surapaneni, K.M.; Vishnu Priya, V.; Mallika, J. Effect of pioglitazone, quercetin, and hydroxy citric acid on vascular endothelial growth factor messenger RNA (VEGF mRNA) expression in experimentally induced nonalcoholic steatohepatitis (NASH). *Turk. J. Med. Sci.* **2015**, *45*, 542–546. [PubMed]
16. Yafi, F.A.; Pinsky, M.R.; Sangkum, P.; Hellstrom, W.J. Therapeutic advances in the treatment of Peyronie's disease. *Andrology* **2015**, *3*, 650–660. [CrossRef] [PubMed]
17. Shadid, S.; Jensen, M.D. Angioneurotic edema as a side effect of pioglitazone. *Diabetes Care* **2002**, *25*, 405. [CrossRef] [PubMed]
18. Shah, P.; Mudaliar, S. Pioglitazone: Side effect and safety profile. *Expert Opin. Drug Saf.* **2010**, *9*, 347–354. [CrossRef] [PubMed]

19. Zhang, F.; Lavan, B.E.; Gregoire, F.M. Selective Modulators of PPAR-gamma Activity: Molecular Aspects Related to Obesity and Side-Effects. *PPAR Res.* **2007**, *2007*, 32696. [CrossRef] [PubMed]
20. Hauner, H. The mode of action of thiazolidinediones. *Diabetes Metab. Res. Rev.* **2002**, *18*, S10–S15. [CrossRef] [PubMed]
21. Oliveira, C.P.; Stefano, J.T. Genetic polymorphisms and oxidative stress in non-alcoholic steatohepatitis (NASH): A mini review. *Clin. Res. Hepatol. Gastroenterol.* **2015**, *39*, S35–S40. [CrossRef] [PubMed]
22. Minato, T.; Tsutsumi, M.; Tsuchishima, M.; Hayashi, N.; Saito, T.; Matsue, Y.; Toshikuni, N.; Arisawa, T.; George, J. Binge alcohol consumption aggravates oxidative stress and promotes pathogenesis of NASH from obesity-induced simple steatosis. *Mol. Med.* **2014**, *20*, 490–502. [CrossRef] [PubMed]
23. Stiuso, P.; Scognamiglio, I.; Murolo, M.; Ferranti, P.; De Simone, C.; Rizzo, M.R.; Tuccillo, C.; Caraglia, M.; Loguercio, C.; Federico, A. Serum oxidative stress markers and lipidomic profile to detect NASH patients responsive to an antioxidant treatment: A pilot study. *Oxid. Med. Cell. Longev.* **2014**, *2014*, 169216. [CrossRef] [PubMed]
24. Li, J.; Chanda, D.; van Gorp, P.J.; Jeurissen, M.L.; Houben, T.; Walenbergh, S.M.; Debets, J.; Oligschlaeger, Y.; Gijbels, M.J.; Neumann, D.; et al. Macrophage Stimulating Protein Enhances Hepatic Inflammation in a NASH Model. *PLoS ONE* **2016**, *11*, e0163843. [CrossRef] [PubMed]
25. Reid, D.T.; Reyes, J.L.; McDonald, B.A.; Vo, T.; Reimer, R.A.; Eksteen, B. Kupffer Cells Undergo Fundamental Changes during the Development of Experimental NASH and Are Critical in Initiating Liver Damage and Inflammation. *PLoS ONE* **2016**, *11*, e0159524. [CrossRef] [PubMed]
26. Yamada, T.; Obata, A.; Kashiwagi, Y.; Rokugawa, T.; Matsushima, S.; Hamada, T.; Watabe, H.; Abe, K. Gd-EOB-DTPA-enhanced-MR imaging in the inflammation stage of nonalcoholic steatohepatitis (NASH) in mice. *Magn. Reson. Imaging* **2016**, *34*, 724–729. [CrossRef] [PubMed]
27. Smith, K. Microbiota: Gut microbiota produce alcohol in patients with NASH. *Nat. Rev. Gastroenterol. Hepatol.* **2012**, *9*, 687. [CrossRef] [PubMed]
28. Huang, W.; Zhu, Y.; Li, C.; Sui, Z.; Min, W. Effect of Blueberry Anthocyanins Malvidin and Glycosides on the Antioxidant Properties in Endothelial Cells. *Oxid. Med. Cell. Longev.* **2016**, *2016*, 1591803. [CrossRef] [PubMed]
29. Song, Y.; Huang, L.; Yu, J. Effects of blueberry anthocyanins on retinal oxidative stress and inflammation in diabetes through NRF2/HO-1 signaling. *J. Neuroimmunol.* **2016**, *301*, 1–6. [CrossRef] [PubMed]
30. Kang, J.; Thakali, K.M.; Jensen, G.S.; Wu, X. Phenolic acids of the two major blueberry species in the US Market and their antioxidant and anti-inflammatory activities. *Plant. Foods Hum. Nutr.* **2015**, *70*, 56–62. [CrossRef] [PubMed]
31. Vendrame, S.; Guglielmetti, S.; Riso, P.; Arioli, S.; Klimis-Zacas, D.; Porrini, M. Six-week consumption of a wild blueberry powder drink increases bifidobacteria in the human gut. *J. Agric. Food Chem.* **2011**, *59*, 12815–12820. [CrossRef] [PubMed]
32. Afrin, S.; Giampieri, F.; Gasparrini, M.; Forbes-Hernandez, T.Y.; Varela-Lopez, A.; Quiles, J.L.; Mezzetti, B.; Battino, M. Chemopreventive and Therapeutic Effects of Edible Berries: A Focus on Colon Cancer Prevention and Treatment. *Molecules* **2016**, *21*, 169. [CrossRef] [PubMed]
33. Dorothy, K.-Z.; Vendrame, S.; Kristo, A.S. Wild blueberries attenuate risk factors of the metabolic syndrome. *J. Berry Res.* **2016**, *6*, 225–236.
34. Mencarelli, A.; Cipriani, S.; Renga, B.; Bruno, A.; D'Amore, C.; Distrutti, E.; Fiorucci, S. VSL#3 resets insulin signaling and protects against NASH and atherosclerosis in a model of genetic dyslipidemia and intestinal inflammation. *PLoS ONE* **2012**, *7*, e45425.
35. Van Diepen, J.A.; Berbée, J.F.; Havekes, L.M.; Rensen, P.C. Interactions between inflammation and lipid metabolism: Relevance for efficacy of anti-inflammatory drugs in the treatment of atherosclerosis. *Atherosclerosis* **2013**, *228*, 306–315. [CrossRef] [PubMed]
36. Bieghs, V.; Rensen, P.C.; Hofker, M.H.; Shiri-Sverdlov, R. NASH and atherosclerosis are two aspects of a shared disease: Central role for macrophages. *Atherosclerosis* **2012**, *220*, 287–293. [CrossRef] [PubMed]
37. Ziamajidi, N.; Khaghani, S.; Hassanzadeh, G.; Vardasbi, S.; Ahmadian, S.; Nowrouzi, A.; Ghaffari, S.M.; Abdirad, A. Amelioration by chicory seed extract of diabetes- and oleic acid-induced non-alcoholic fatty liver disease (NAFLD)/non-alcoholic steatohepatitis (NASH) via modulation of PPARalpha and SREBP-1. *Food Chem. Toxicol.* **2013**, *58*, 198–209. [CrossRef] [PubMed]

38. Yoshikawa, T.; Ide, T.; Shimano, H.; Yahagi, N.; Amemiya-Kudo, M.; Matsuzaka, T.; Yatoh, S.; Kitamine, T.; Okazaki, H.; Tamura, Y. Cross-talk between peroxisome proliferator-activated receptor (PPAR) α and liver X receptor (LXR) in nutritional regulation of fatty acid metabolism. I. PPARs suppress sterol regulatory element binding protein-1c promoter through inhibition of LXR signaling. *Mol. Endocrinol.* **2003**, *17*, 1240–1254. [PubMed]
39. Grove, J.I.; Austin, M.; Tibble, J.; Aithal, G.P.; Verma, S. Monozygotic twins with NASH cirrhosis: Cumulative effect of multiple single nucleotide polymorphisms? *Ann. Hepatol.* **2016**, *15*, 277–282. [PubMed]
40. Wada, T.; Miyashita, Y.; Sasaki, M.; Aruga, Y.; Nakamura, Y.; Ishii, Y.; Sasahara, M.; Kanasaki, K.; Kitada, M.; Koya, D.; et al. Eplerenone ameliorates the phenotypes of metabolic syndrome with NASH in liver-specific SREBP-1c TG mice fed high-fat and high-fructose diet. *Am. J. Physiol. Endocrinol. Metab.* **2013**, *305*, E1415–E1425. [CrossRef] [PubMed]
41. Da Silva Morais, A.; Lebrun, V.; Abarca-Quinones, J.; Brichard, S.; Hue, L.; Guigas, B.; Viollet, B.; Leclercq, I.A. Prevention of steatohepatitis by pioglitazone: Implication of adiponectin-dependent inhibition of SREBP-1c and inflammation. *J. Hepatol.* **2009**, *50*, 489–500. [CrossRef] [PubMed]
42. Qin, S.; Yin, J.; Huang, K. Free Fatty Acids Increase Intracellular Lipid Accumulation and Oxidative Stress by Modulating PPARalpha and SREBP-1c in L-02 Cells. *Lipids* **2016**, *51*, 797–805. [CrossRef] [PubMed]
43. Romeo, S.; Kozlitina, J.; Xing, C.; Pertsemlidis, A.; Cox, D.; Pennacchio, L.A.; Boerwinkle, E.; Cohen, J.C.; Hobbs, H.H. Genetic variation in PNPLA3 confers susceptibility to nonalcoholic fatty liver disease. *Nat. Genet.* **2008**, *40*, 1461–1465. [CrossRef] [PubMed]
44. Browning, J.D.; Kumar, K.S.; Saboorian, M.H.; Thiele, D.L. Ethnic differences in the prevalence of cryptogenic cirrhosis. *Am. J. Gastroenterol.* **2004**, *99*, 292–298. [CrossRef]
45. Kollerits, B.; Coassin, S.; Kiechl, S.; Hunt, S.C.; Paulweber, B.; Willeit, J.; Brandstatter, A.; Lamina, C.; Adams, T.D.; Kronenberg, F. A common variant in the adiponutrin gene influences liver enzyme values. *J. Med. Genet.* **2010**, *47*, 116–119. [CrossRef]
46. Sookoian, S.; Castano, G.O.; Burgueno, A.L.; Gianotti, T.F.; Rosselli, M.S.; Pirola, C.J. A nonsynonymous gene variant in the adiponutrin gene is associated with nonalcoholic fatty liver disease severity. *J. Lipid Res.* **2009**, *50*, 2111–2116. [CrossRef] [PubMed]
47. Tian, C.; Stokowski, R.P.; Kershenobich, D.; Ballinger, D.G.; Hinds, D.A. Variant in PNPLA3 is associated with alcoholic liver disease. *Nat. Genet.* **2010**, *42*, 21–23. [CrossRef] [PubMed]
48. Graff, M.; North, K.E.; Franceschini, N.; Reiner, A.P.; Feitosa, M.; Carr, J.J.; Gordon-Larsen, P.; Wojczynski, M.K.; Borecki, I.B. PNPLA3 gene-by-visceral adipose tissue volume interaction and the pathogenesis of fatty liver disease: The NHLBI Family Heart Study. *Int. J. Obes.* **2013**, *37*, 432–438. [CrossRef] [PubMed]
49. He, S.; McPhaul, C.; Li, J.Z.; Garuti, R.; Kinch, L.; Grishin, N.V.; Cohen, J.C.; Hobbs, H.H. A sequence variation (I148M) in PNPLA3 associated with nonalcoholic fatty liver disease disrupts triglyceride hydrolysis. *J. Biol. Chem.* **2010**, *285*, 6706–6715. [CrossRef]
50. Lake, A.C.; Sun, Y.; Li, J.L.; Kim, J.E.; Johnson, J.W.; Li, D.; Revett, T.; Shih, H.H.; Liu, W.; Paulsen, J.E.; et al. Expression, regulation, and triglyceride hydrolase activity of Adiponutrin family members. *J. Lipid Res.* **2005**, *46*, 2477–2487. [CrossRef] [PubMed]
51. Rossi, M.; Giussani, E.; Morelli, R.; Lo Scalzo, R.; Nani, R.C.; Torreggiani, D. Effect of fruit blanching on phenolics and radical scavenging activity of highbush blueberry juice. *Food Res. Int.* **2003**, *36*, 999–1005. [CrossRef]
52. GuangQin, W.; Fei, N.; YouJiang, L. Comparative analysis of physicochemical component content in blueberry fruit and their function evaluation. *Acta Agric. Jiangxi* **2012**, *24*, 117–119.
53. Li, S.; Liao, X.; Meng, F.; Wang, Y.; Sun, Z.; Guo, F.; Li, X.; Meng, M.; Li, Y.; Sun, C. Therapeutic role of ursolic acid on ameliorating hepatic steatosis and improving metabolic disorders in high-fat diet-induced non-alcoholic fatty liver disease rats. *PLoS ONE* **2014**, *9*, e86724. [CrossRef] [PubMed]
54. Chanda, D.; Li, J.; Oligschlaeger, Y.; Jeurissen, M.L.; Houben, T.; Walenbergh, S.M.; Shiri-Sverdlov, R.; Neumann, D. MSP is a negative regulator of inflammation and lipogenesis in ex vivo models of non-alcoholic steatohepatitis. *Exp. Mol. Med.* **2016**, *48*, e258. [CrossRef] [PubMed]

55. Bashiri, A.; Nesan, D.; Tavallaee, G.; Sue-Chue-Lam, I.; Chien, K.; Maguire, G.F.; Naples, M.; Zhang, J.; Magomedova, L.; Adeli, K.; et al. Cellular cholesterol accumulation modulates high fat high sucrose (HFHS) diet-induced ER stress and hepatic inflammasome activation in the development of non-alcoholic steatohepatitis. *Biochim. Biophys. Acta* **2016**, *1861*, 594–605. [CrossRef] [PubMed]
56. Kleiner, D.E.; Brunt, E.M.; Van Natta, M.; Behling, C.; Contos, M.J.; Cummings, O.W.; Ferrell, L.D.; Liu, Y.C.; Torbenson, M.S.; Unalp-Arida, A.; et al. Design and validation of a histological scoring system for nonalcoholic fatty liver disease. *Hepatology* **2005**, *41*, 1313–1321. [CrossRef] [PubMed]
57. Kujawska, M.; Ignatowicz, E.; Ewertowska, M.; Oszmianski, J.; Jodynis-Liebert, J. Protective effect of chokeberry on chemical-induced oxidative stress in rat. *Hum. Exp. Toxicol.* **2011**, *30*, 199–208. [CrossRef] [PubMed]
58. Bisson, J.F.; Hidalgo, S.; Rozan, P.; Messaoudi, M. Preventive effects of different probiotic formulations on travelers' diarrhea model in wistar rats: Preventive effects of probiotics on TD. *Dig. Dis. Sci.* **2010**, *55*, 911–919. [CrossRef] [PubMed]
59. Cluny, N.L.; Keenan, C.M.; Lutz, B.; Piomelli, D.; Sharkey, K.A. The identification of peroxisome proliferator-activated receptor alpha-independent effects of oleoylethanolamide on intestinal transit in mice. *Neurogastroenterol. Motil.* **2009**, *21*, 420–429. [CrossRef] [PubMed]
60. Tan, A.S.; Berridge, M.V. Superoxide produced by activated neutrophils efficiently reduces the tetrazolium salt, WST-1 to produce a soluble formazan: A simple colorimetric assay for measuring respiratory burst activation and for screening anti-inflammatory agents. *J. Immunol. Methods* **2000**, *238*, 59–68. [CrossRef]
61. Smith, I.K.; Vierheller, T.L.; Thorne, C.A. Assay of glutathione reductase in crude tissue homogenates using 5,5′-dithiobis(2-nitrobenzoic acid). *Anal. Biochem.* **1988**, *175*, 408–413. [CrossRef]
62. Feng, L.; Luo, H.; Xu, Z.; Yang, Z.; Du, G.; Zhang, Y.; Yu, L.; Hu, K.; Zhu, W.; Tong, Q.; et al. Bavachinin, as a novel natural pan-PPAR agonist, exhibits unique synergistic effects with synthetic PPAR-gamma and PPAR-alpha agonists on carbohydrate and lipid metabolism in db/db and diet-induced obese mice. *Diabetologia* **2016**, *59*, 1276–1286. [CrossRef] [PubMed]
63. Van Diepen, J.A.; Jansen, P.A.; Ballak, D.B.; Hijmans, A.; Hooiveld, G.J.; Rommelaere, S.; Galland, F.; Naquet, P.; Rutjes, F.P.; Mensink, R.P.; et al. PPAR-alpha dependent regulation of vanin-1 mediates hepatic lipid metabolism. *J. Hepatol.* **2014**, *61*, 366–372. [CrossRef] [PubMed]
64. Cariou, B.; Zair, Y.; Staels, B.; Bruckert, E. Effects of the new dual PPAR alpha/delta agonist GFT505 on lipid and glucose homeostasis in abdominally obese patients with combined dyslipidemia or impaired glucose metabolism. *Diabetes Care* **2011**, *34*, 2008–2014. [CrossRef] [PubMed]
65. Paterniti, I.; Campolo, M.; Cordaro, M.; Impellizzeri, D.; Siracusa, R.; Crupi, R.; Esposito, E.; Cuzzocrea, S. PPAR-alpha Modulates the Anti-Inflammatory Effect of Melatonin in the Secondary Events of Spinal Cord Injury. *Mol. Neurobiol.* **2016**. [CrossRef] [PubMed]
66. Carniglia, L.; Durand, D.; Caruso, C.; Lasaga, M. Effect of NDP-alpha-MSH on PPAR-gamma and -beta expression and anti-inflammatory cytokine release in rat astrocytes and microglia. *PLoS ONE* **2013**, *8*, e57313. [CrossRef] [PubMed]
67. Duval, C.; Fruchart, J.C.; Staels, B. PPAR alpha, fibrates, lipid metabolism and inflammation. *Arch. Mal. Coeur Vaiss* **2004**, *97*, 665–672. [PubMed]
68. Dossi, C.G.; Tapia, G.S.; Espinosa, A.; Videla, L.A.; D'Espessailles, A. Reversal of high-fat diet-induced hepatic steatosis by *n*-3 LCPUFA: Role of PPAR-alpha and SREBP-1c. *J. Nutr. Biochem.* **2014**, *25*, 977–984. [CrossRef] [PubMed]
69. Baskol, M.; Dolbun Seckin, K.; Baskol, G. Advanced oxidation protein products, total thiol levels and total oxidant/antioxidant status in patients with nash. *Turk. J. Gastroenterol.* **2014**, *25*, 32–37. [CrossRef] [PubMed]
70. Yamada, J.; Tomiyama, H.; Yambe, M.; Koji, Y.; Motobe, K.; Shiina, K.; Yamamoto, Y.; Yamashina, A. Elevated serum levels of alanine aminotransferase and gamma glutamyltransferase are markers of inflammation and oxidative stress independent of the metabolic syndrome. *Atherosclerosis* **2006**, *189*, 198–205. [CrossRef] [PubMed]
71. Josekutty, J.; Iqbal, J.; Iwawaki, T.; Kohno, K.; Hussain, M.M. Microsomal triglyceride transfer protein inhibition induces endoplasmic reticulum stress and increases gene transcription via Ire1alpha/cJun to enhance plasma ALT/AST. *J. Biol. Chem.* **2013**, *288*, 14372–14383. [CrossRef] [PubMed]

72. Kaviarasan, K.; Pugalendi, K.V. Influence of flavonoid-rich fraction from Spermacoce hispida seed on PPAR-alpha gene expression, antioxidant redox status, protein metabolism and marker enzymes in high-fat-diet fed STZ diabetic rats. *J. Basic Clin. Physiol. Pharmacol.* **2009**, *20*, 141–158. [CrossRef] [PubMed]
73. Li, X.; Huang, W.; Gu, J.; Du, X.; Lei, L.; Yuan, X.; Sun, G.; Wang, Z.; Li, X.; Liu, G. SREBP-1c overactivates ROS-mediated hepatic NF-kappaB inflammatory pathway in dairy cows with fatty liver. *Cell Signal.* **2015**, *27*, 2099–2109. [CrossRef] [PubMed]
74. Zuo, L.L.; Wang, Z.Y.; Fan, Z.L.; Tian, S.Q.; Liu, J.R. Evaluation of antioxidant and antiproliferative properties of three Actinidia (Actinidia kolomikta, Actinidia arguta, Actinidia chinensis) extracts in vitro. *Int. J. Mol. Sci.* **2012**, *13*, 5506–5518. [CrossRef] [PubMed]
75. Forbes-Hernandez, T.Y.; Gasparrini, M.; Afrin, S.; Mazzoni, L.; Reboredo, P.; Giampieri, F. A comparative study on cytotoxic effects of strawberry extract on different cellular models. *J. Berry Res.* **2016**, *6*, 263–275. [CrossRef]
76. Feldstein, A.E.; Canbay, A.; Angulo, P.; Taniai, M.; Burgart, L.J.; Lindor, K.D.; Gores, G.J. Hepatocyte apoptosis and fas expression are prominent features of human nonalcoholic steatohepatitis. *Gastroenterology* **2003**, *125*, 437–443. [CrossRef]
77. Li, X.; Chen, Y.T.; Josson, S.; Mukhopadhyay, N.K.; Kim, J.; Freeman, M.R.; Huang, W.C. MicroRNA-185 and 342 inhibit tumorigenicity and induce apoptosis through blockade of the SREBP metabolic pathway in prostate cancer cells. *PLoS ONE* **2013**, *8*, e70987. [CrossRef] [PubMed]
78. Esquejo, R.M.; Jeon, T.I.; Osborne, T.F. Lipid-cell cycle nexus: SREBP regulates microRNAs targeting Fbxw7. *Cell Cycle* **2014**, *13*, 339–340. [CrossRef] [PubMed]
79. Nakakuki, M.; Shimano, H.; Inoue, N.; Tamura, M.; Matsuzaka, T.; Nakagawa, Y.; Yahagi, N.; Toyoshima, H.; Sato, R.; Yamada, N. A transcription factor of lipid synthesis, sterol regulatory element-binding protein (SREBP)-1α causes G(1) cell-cycle arrest after accumulation of cyclin-dependent kinase (CDK) inhibitors. *FEBS J.* **2007**, *274*, 4440–4452. [CrossRef] [PubMed]
80. Steen, V.M.; Skrede, S.; Polushina, T.; Lopez, M.; Andreassen, O.A.; Ferno, J.; Hellard, S.L. Genetic evidence for a role of the SREBP transcription system and lipid biosynthesis in schizophrenia and antipsychotic treatment. *Eur. Neuropsychopharmacol.* **2016**. [CrossRef] [PubMed]
81. Jiang, Z.; Huang, X.; Huang, S.; Guo, H.; Wang, L.; Li, X.; Huang, X.; Wang, T.; Zhang, L.; Sun, L. Sex-Related Differences of Lipid Metabolism Induced by Triptolide: The Possible Role of the LXRalpha/SREBP-1 Signaling Pathway. *Front. Pharmacol.* **2016**, *7*, 87. [CrossRef] [PubMed]
82. Zhao, Y.; Li, H.; Zhang, Y.; Li, L.; Fang, R.; Li, Y.; Liu, Q.; Zhang, W.; Qiu, L.; Liu, F.; Zhang, X.; Ye, L. Oncoprotein HBXIP Modulates Abnormal Lipid Metabolism and Growth of Breast Cancer Cells by Activating the LXRs/SREBP-1c/FAS Signaling Cascade. *Cancer Res.* **2016**, *76*, 4696–4707. [CrossRef] [PubMed]
83. Siddiq, M.; Dolan, K.D. Characterization of polyphenol oxidase from blueberry (*Vaccinium corymbosum* L.). *Food Chem.* **2017**, *218*, 216–220. [CrossRef] [PubMed]
84. Terefe, N.S.; Delon, A.; Buckow, R.; Versteeg, C. Blueberry polyphenol oxidase: Characterization and the kinetics of thermal and high pressure activation and inactivation. *Food Chem.* **2015**, *188*, 193–200. [CrossRef] [PubMed]
85. Ikarashi, N.; Toda, T.; Okaniwa, T.; Ito, K.; Ochiai, W.; Sugiyama, K. Anti-Obesity and Anti-Diabetic Effects of Acacia Polyphenol in Obese Diabetic KKAy Mice Fed High-Fat Diet. *Evid. Based Complement. Alternat. Med.* **2011**, *2011*, 952031. [CrossRef] [PubMed]
86. Hakansson, A.; Molin, G. Gut microbiota and inflammation. *Nutrients* **2011**, *3*, 637–682. [CrossRef] [PubMed]
87. Konig, B.; Koch, A.; Spielmann, J.; Hilgenfeld, C.; Hirche, F.; Stangl, G.I.; Eder, K. Activation of PPARalpha and PPARgamma reduces triacylglycerol synthesis in rat hepatoma cells by reduction of nuclear SREBP-1. *Eur. J. Pharmacol.* **2009**, *605*, 23–30. [CrossRef] [PubMed]
88. Yan, C.; Chen, J.; Chen, N. Long noncoding RNA MALAT1 promotes hepatic steatosis and insulin resistance by increasing nuclear SREBP-1c protein stability. *Sci. Rep.* **2016**, *6*, 22640. [CrossRef] [PubMed]
89. Greenhill, C. NASH: Understanding how steatosis progresses to NASH. *Nat. Rev. Endocrinol.* **2017**, *13*, 5. [CrossRef] [PubMed]
90. Chinetti, G.; Lestavel, S.; Bocher, V.; Remaley, A.T.; Neve, B.; Torra, I.P.; Teissier, E.; Minnich, A.; Jaye, M.; Duverger, N.; et al. PPAR-alpha and PPAR-gamma activators induce cholesterol removal from human macrophage foam cells through stimulation of the ABCA1 pathway. *Nat. Med.* **2001**, *7*, 53–58. [PubMed]

91. Field, F.J.; Born, E.; Murthy, S.; Mathur, S.N. Regulation of sterol regulatory element-binding proteins in hamster intestine by changes in cholesterol flux. *J. Biol. Chem.* **2001**, *276*, 17576–17583. [CrossRef] [PubMed]
92. Purushotham, A.; Schug, T.T.; Xu, Q.; Surapureddi, S.; Guo, X.; Li, X. Hepatocyte-specific deletion of SIRT1 alters fatty acid metabolism and results in hepatic steatosis and inflammation. *Cell Metab.* **2009**, *9*, 327–338. [CrossRef] [PubMed]
93. Lirussi, F.; Mastropasqua, E.; Orando, S.; Orlando, R. Probiotics for non-alcoholic fatty liver disease and/or steatohepatitis. *Cochrane Database Syst. Rev.* **2007**. [CrossRef]
94. Krawczyk, M.; Grunhage, F.; Lammert, F. Identification of combined genetic determinants of liver stiffness within the SREBP1c-PNPLA3 pathway. *Int. J. Mol. Sci.* **2013**, *14*, 21153–21166. [CrossRef] [PubMed]

nutrients

MDPI

Article

Enantioselective Modulatory Effects of Naringenin Enantiomers on the Expression Levels of *miR-17-3p* Involved in Endogenous Antioxidant Defenses

Valeria Curti [1,2], Arianna Di Lorenzo [1,2], Daniela Rossi [1], Emanuela Martino [3], Enrica Capelli [3], Simona Collina [1] and Maria Daglia [1,*]

1 Department of Drug Sciences, Medicinal Chemistry and Pharmaceutical Technology Section, Pavia University, Viale Taramelli 12, 27100 Pavia, Italy; valeria.curti86@hotmail.it or valeriacurti@kolinpharma.com (V.C.); arianna.dilorenzo01@universitadipavia.it or ariannadilorenzo@kolinpharma.com (A.D.L.); daniela.rossi@unipv.it (D.R.); simona.collina@unipv.it (S.C.)

2 KOLINPHARMA S.p.A., Lainate, Corso Europa 5, 20020 Lainate, Italy

3 Department of Earth and Environmental Sciences, University of Pavia, Via S. Epifanio 14, 27100 Pavia, Italy; emanuela.martino@unipv.it (E.M.); enrica.capelli@unipv.it (E.C.)

* Correspondence: maria.daglia@unipv.it; Tel.: +39-0382987388

Received: 28 November 2016; Accepted: 24 February 2017; Published: 28 February 2017

Abstract: Naringenin is a flavanone present in citrus fruit as a mixture of chiral isomers. The numerous biological properties attributed to this compound include antioxidant and anti-inflammatory activities, even though the molecular mechanisms of these remain unknown. This study aims to evaluate the effects of racemic and enantiomeric naringenin on the expression levels of *miR-17-3p*, *miR-25-5p* and relative mRNA targets, to elucidate the mechanisms underlying these antioxidant and anti-inflammatory properties. Caco-2 cells, a well characterized in vitro model which mimics the intestinal barrier, were treated with subtoxic concentrations of racemate and enantiomers. The expression levels of *miR-17-3p* and *miR-25-5p* were determined by Real-Time PCR and were found to be decreased for both miRNAs. *miR-17-3p* behavior was in agreement with the increased levels of target mRNAs coding for two antioxidant enzymes, manganese-dependent superoxide dismutase (MnSOD) and glutathione peroxidase 2 (GPx2), while expression levels of *miR-25-5p* were not in agreement with its target mRNAs, coding for two pro-inflammatory cytokines, Tumor necrosis factor-alpha (TNF-α) and Interleukin-6 (IL-6). These results lead to the conclusion that naringenin could exert its antioxidant activity through epigenetic regulation operated by miRNAs, while anti-inflammatory activity is regulated by other miRNAs and/or mechanisms.

Keywords: naringenin racemate; naringenin enantiomers; antioxidant enzymes; pro-inflammatory cytokines; caco-2 cells; microRNA; epigenetics

1. Introduction

Naringenin (5,7,4-thihydroxyflavanone) is a chiral flavonoid belonging to the class of flavanones. It is widely distributed in fruits of *Citrus* species, especially in grapefruit (*Citrus paradisi* Macfad.) and oranges (*Citrus* sinensis (L.) Osbeck), as well as tomatoes (*Solanum lycopersicum* L.) [1,2]. In *Citrus* fruits, naringenin is mainly found bound to glucose (naringenin-7-*O*-glucoside, also called prunin) [3], rutinose (naringenin-7-*O*-rutinoside, narirutin), and rhamnose (naringenin 7-rhamnoglucoside, naringin) [4]. In grapefruit, naringin content depends on the variety and ranges from 115 to 384 mg/L [5]. In tomatoes, naringenin is mainly found in its free form (ranging from 0.8 to 4.2 mg/100 g of whole red tomato) [2]. When naringenin is present as an aglycone, it occurs as a mixture of enantiomers whose ratio depends on the ripeness of the fruit and the purification methods used to isolate the isomers [6,7].

A number of in vitro studies have shown that naringenin possesses many physiological and pharmacological activities such as antioxidant and anti-inflammatory activities, which have been most studied, and hepatoprotective, anti-mutagenic and anticancer effects [1,6,8,9]. Thus, its bioavailability must be seen as a key aspect affecting its subsequent in vivobiological activity. Many studies have shown the presence of naringenin in both urine and in plasma following the intake of naringin, either alone or as part of *Citrus* fruit juices [10–12]. Despite the high rate of absorption that occurs especially at gut level, the naringenin bioavailability is poor, and this may be due to the first-pass effect and hepatic metabolism [13–15].

Despite its poor bioavailability, in vivo studies have shown that naringenin possesses anti-inflammatory and antioxidant capacities. Chtourou et al., in 2016, showed that administration of naringenin at a dose of 50 mg/body weight in rats previously exposed for 90 days to a high cholesterol diet, led to the restoration of both enzymatic and non-enzymatic antioxidant defenses (i.e., superoxide dismutase (SOD), catalase (CAT), glutathione peroxidase (GPx), nonprotein sulfhydryl groups (NPSH), glutathione (GSH), Vitamin C and Vitamin E) [16]. Ozkaya et al. showed that naringenin supplementation (50 mg/body weight) on the hepatic damage induced by lead (Pb) in rats increased CAT and GPx concentrations in groups of rats treated with naringenin and lead acetate, than in those treated with lead acetate alone [17]. Furthermore, Liu et al. have demonstrated that naringenin, administered at doses of both 25 and 50 mg/body weight/day, reduced oxidative stress in cardiorenal syndrome in a rat model. A similar increase was found in the mRNA levels coding for *Nrf*2 (a well known transcription factor regulating antioxidant response), and *GCLc* (regulating the glutathione synthesis), underling that naringenin acts on transcription activity [18].

Moreover, recently, Chtourou et al. [19] showed that naringenin is able to decrease pro-inflammatory mediators such as *TNF-α*, *IL-6* and *IL-1b* in rats, and suggested that its anti-inflammatory activity could be due to the inhibition of NF-kB, a signal transduction pathway that promotes the transcription of gene coding for pro-inflammatory proteins. Recent studies have demonstrated that naringenin also possesses anti-inflammatory properties in the gut [20,21]. (*R*) naringenin was found to be the most effective enantiomer in reducing *TNF-α* and *IL-6* levels in human peripheral blood mononuclear cells (hPMBC). These results demonstrate that the anti-inflammatory effect of naringenin is enantioselective and that (*R*) naringenin is the eutomer [7].

Many studies have shown that polyphenols also modify gene expression by acting on the regulation of epigenetic mechanisms. They are able to modulate DNA methylation, hystonic modifications and microRNA (miRNA) expression [22]. miRNAs are small non-coding RNAs with an average length of 22 nucleotides, which control various biological processes such as cell development, differentiation, proliferation and apoptosis [23–29]. Literature data show that *miR-17-3p* and *miR-25-5p* are involved in the oxidative stress and inflammatory response, respectively. *miR-17-3p* has three mRNA targets coding for mitochondrial antioxidant enzymes (manganese superoxide dismutase (MnSOD), glutathione peroxidase-2 (GPx2), and thioredoxin reductase-2 (TrxR2)) [30]. *miR-17-3p* has been found to be regulated by different polyphenols, such as resveratrol and quercetin [31,32]. Our previous studies, which involved treating ECV-304 (human vascular endothelial cells) and hPBMC cells with increasing subtoxic concentrations of methyl 3-*O*-methyl gallate, demonstrated that this polyphenol induces an underexpression of *miR-17-3p*, and relative upregulation of target mRNA expression levels [33], placing this molecular mechanism at the base of the antioxidant effects registered in both in vitro and in vivostudies [34]. As far as *miR-25-5p* is concerned, it is strictly involved in the inflammatory response and its over or down regulation is associated with changes in cytokine levels during the inflammation process [35,36]. Few articles have been published on the capacity of naringenin to modulate miRNA expression to date. In 2012, Milenkovic et al. [37] reported that nutritional doses of naringenin resulted in a modification of miRNA expression levels in mouse liver. Taken together, these results make naringenin and its enantiomers promising candidates in risk prevention against the occurrence of inflammatory-based diseases, such as inflammatory bowel diseases.

Thus, considering: (a) the bioavailability of naringenin, albeit modest; (b) its involvement in the modulation of oxidative stress and inflammatory response (especially at the intestinal level); (c) the different activities exerted by naringenin enantiomers; and (d) its capacity to modulate the expression of some miRNAs, the aim of this investigation was to study the molecular mechanisms underlying the effects of racemic and enantiomeric naringenin on oxidative stress and the anti-inflammatory response, in which *miR-17-3p* and *miR-25-5p* play a key role.

2. Materials and Methods

2.1. Reagents and Instruments

(*R*/*S*) Naringenin (5,7-dihydroxy-2-(4-hydroxyphenyl)chroman-4-one) was obtained from Sigma-Aldrich (Milan, Italy). The HPLC grade solvents used as eluents were obtained from Merck-VWR (Milan, Italy). Analytical chiral resolutions were performed with a Jasco system consisting of a AS-2055 plus autosampler, a PU-2089 plus pump and a MD-2010 plus multi-wavelength detector coupled with a CD-2095 plus circular dichroism detector (Jasco Europe S.r.l., Cremella, LC, Italy). The preparative separations were carried out on an HPLC apparatus produced by Varian Chromatographic Systems (Walnut Creek, CA, USA), which consists of two Rainin SD-1 pumps with 500 mL/min pump heads, a 410 Varian autosampler, a 320 Varian Prostar UV-detector and a 320 Varian fraction collection module. A DIP 1000 photoelectric polarimeter from Jasco (JASCO Europe, Cremella, LC, Italy) was used for [α] measurements that were recorded at room temperature using a 1 dm cell and a sodium lamp.

MiRNeasy Mini kit was purchased from Qiagen GmbH (Hilden, Germany). A Quant-it RNA HS was purchased from Invitrogen (Grand Island, NY, USA). A Brilliant III Ultra-Fast SYBR® Green RT-PCR Master Mix was purchased from Agilent Technologies (Santa Clara, CA, USA).

2.2. Naringenin Enantioresolution

The chiral resolution of naringenin was performed via preparative enantioselective chromatography employing a Chiralpak® AD column (500 mm × 50 mm I.D., d_p = 20 μm), Chiral Technologies Europe (Illkirch, France) according to Gaggeri et al. [8].Enantiomeric resolution in g-scale was achieved, eluting with methanol at room temperature with a flow rate of 40 mL/min. The partitioning of the eluate was effected according to the UV profile (detection at 290 nm) and the analytical in-process control of collected fractions performed using a Chiralpak AD-H column (250 mm × 4.6 mm ID; d_p = 5 μm) eluting with methanol (flow rate 1 mL/min, UV detector at 290 nm). Accordingly, the fractions containing the enantiomers were evaporated at 334 mbar and 40 °C and dried in a vacuum oven at 0.1 mbar and 25 °C, furnishing2.1 g of (−)-(*S*) naringenin, ($[\alpha]_D^{25} = -28.7°$, c = 0.36% in ethanol, ee = 96%) and 1.8 g of (+)-(*R*) naringenin ($[\alpha]_D^{25} = +22.8°$, c = 0.30% in ethanol, ee = 94%).

2.3. Cell Culture and Treatments

Human colon adenocarcinoma (CaCo-2) cells were purchased from the American Type Culture Collection (Rockville, MD, USA). The cells were cultured in D-MEM supplemented with 10% fetal bovine serum, L-glutamine (2 mM), 100 IU/mL penicillin and 100 μg/mL streptomycin (all from Invitrogen Co., Paisley, Scotland, UK). Cells were grown at 37°C in a humidified atmosphere containing 5% CO_2. The treatments were performed for 24 h with different concentrations of racemate and (*S*) and (*R*) enantiomers, with the concentration of DMSO never exceeding 0.4%.

2.4. MTT Assay

Cell viability was detected by MTT assay, testing a wide range of doses of racemate and (*S*) and (*R*) naringenin enantiomers (i.e., from 1 to 1000 μg/mL). In brief, cells were seeded into permeable polyester membrane filter supports (Transwell, 12-mm diameter, 0.4-mm pore size; Corning Costar) at

a density of 0.25×10^6 cells/cm^2. After a 24 h incubation period, the percentage of viable cells in each well was calculated relative to that of control cells.

2.5. RNA Extraction and Quantitative Real Time PCR (RT-PCR)

Total RNA was extracted from cells using the miRNeasy Mini kit (Qiagen, Hilden, Germany), according to the manufacturer's instructions. The quality of RNA was assessed by gel electrophoresis using denaturing agarose gel 1.2%. Quantitative RNA analysis was performed using a fluorimetric method by means of the Qubit^R 2.0 platform (Invitrogen, Grand Island, NY, USA) using the Quant-iT RNA HS Assay with the following conditions: 2 μL of RNA was added to 198 μL of working solution obtained by mixing 1 μL of Qubit™ RNA HS reagent to 199 μL of Qubit™ RNA HSbuffer. Quantitative real-time PCR (RT-PCR) was done using cDNA obtained by a reverse transcription reaction using the miRCURY LNA™ Universal RT micro RNA PCR kit: 4 μL of total RNA (5 ng/μL) was added to 4 μL of 5× reaction buffer, 2 μL of enzyme mix, 1 μL of synthetic spike-in and 9 μL of nuclease free water. The mixture was then incubated in a thermo cycler (SureCycler 8800-Agilent Technologies, Santa Clara, California) at 42 °C for 60 min, 95 °C for 5 min, and then immediately cooled to 4 °C. To evaluate the expression of *miR-17-3p* and *25-5p*, RT-PCR reactions were performed with the AriaMX Real Time PCR System (Agilent Technologies, Santa Clara, California) using the Universal cDNA Synthesis and SYBRGreen Master Mix kits (Exiqon (Qiagen), Hilden, Germany). PCR amplification was performed in a 10 μL reaction mixture containing 4 μL of 1:80 diluted cDNA, 5 μL of SYBR Green master mix, and 1 μL of specific LNA probes (Exiqon, (Qiagen), Hilden, Germany) using the following reaction conditions: a first step at 95 °C for 10 min, 45 amplification cycles of 95 °C for 10 s followed by a step at 60 °C for 1 min. U6 small nuclear RNA (snU6) was used to normalize the expression data of miRNAs and every assay was performed in triplicate. To evaluate the levels of mRNA coding for MnSOD, GPx2 and TrxR2, which are validated targets of *miR-17-3p*, and of *TNF-a* and *IL-6*, which are targets of *miR-25-5p*,RT-PCR reactions were performed with the AriaMX Real Time PCR System using Brilliant III Ultra-Fast SYBR® Green RT-PCR Master Mix (Agilent Santa Clara, California) according to the manufacturer's protocol. Primers were designed using Primer-BLAST software (available online on 27 February 2017: http://www.ncbi.nlm.nih.gov/tools/primer-blast). The sequences for the used primers were:

MnSOD forward: 5′-AAACCTCAGCCCTAACGGTG-3′
MnSOD reverse: 5′-CCAGGCTTGATGCACATCTTA-3′
GPx2 forward: 5′-GAGGTGAATGGGCAGAACGA-3′
GPx2 reverse: 5′-CTCTGCAGTGAAGGGGACTG-3′
TNF-α forward: 5′-CCTCTCTGCCATCAAGAGCC-3′
TNF-α reverse: 5′-TTGAGTAACTTCGCCTGCGT-3′
IL-6 forward: 5′-GTCCAGTTGCCTTCTCCCTG-3′
IL-6 reverse: 5′-AGGGAATGAGGACACACCCA-3′

To determine relative mRNA expression, glyceraldehyde 3-phosphate dehydrogenase (GAPDH) was used as an endogenous control. The sequences for the used primers were:

GAPDH forward: 5′-CACTAGGCGCTCACTGTTCTC-3′
GAPDH reverse: 5′-GACTCCACGACGTACTCAGC-3′

2.6. Statistical Analysis

Statistical analysis of Cq values was carried out using software R (ver. 3.0.3, R e2sCore Team, 2014) [38]. Differences between group means were estimated using one-way analysis of variance followed by Tukey's post hoc test, with measurements of $p < 0.05$ being taken as significant. In the figures, the mean ± standard deviation has been represented over repeats of inverse Delta Cq values (-Delta Cq) because these reflect the behavior of the expression levels of miRNA and mRNA directly.

3. Results

In order to dispose of both naringenin enantiomers, the resolution of commercially available (*R/S*) naringenin was accomplished via preparative enantioselective chromatography employing a Chiralpak AD-H column, as according to our previous protocol [7]. In brief, 5 g of (*R/S*) naringenin was processed, yielding (*S*) and (*R*) enantiomers of naringenin in quantities and purity suitable for an in depth biological investigation (chemical purity higher than 99%, ee > 94%).

Human Caco-2 cell cultures, a well characterized intestinal in vitro model which mimics the intestinal barrier and allows the evaluation of the effects of naringenin following oral consumption as a component of food, were treated with increasing concentrations (from 1 to 1000 μg/mL) of racemic and enantiomeric naringenin. At the highest concentration (1000 μg/mL), racemate and (*S*) and (*R*) naringenin enantiomers caused cell cytotoxicity rates of about 80%, while the lower concentrations (1, 10, and 100 μg/mL) were not cytotoxic (Figure 1). Thus, Caco-2 cell cultures were grown in the absence (control cell culture) and in the presence (treated cell cultures) of racemic and enantiomeric naringenin at concentrations of 1, 10, and 100 μg/mL.

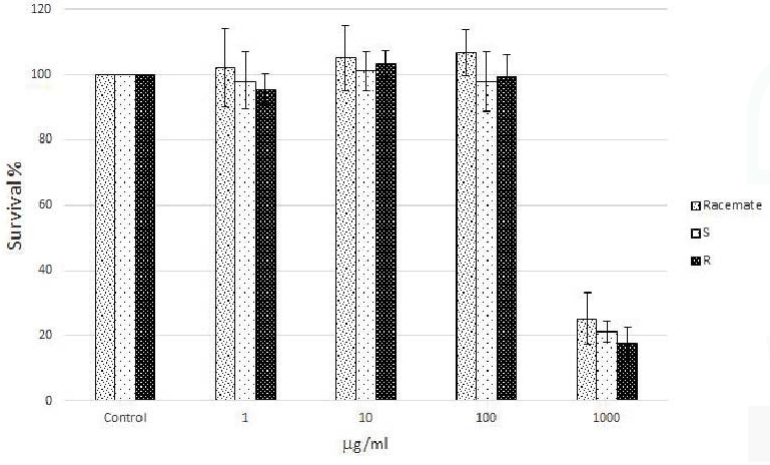

Figure 1. Survival percentage calculated against control (untreated cells) following the treatment of Caco-2 cells with increasing concentrations (1, 10, 100 and 1000 μg/mL) of racemic naringenin and, (*R*) and (*S*) enantiomers for 24 h. Boxes and error bars represent the mean ± standard deviation over repeat measurements.

To evaluate the mechanisms through which naringenin exerts its antioxidant and anti-inflammatory activities, we determined the expression levels of *miR-17-3p* and *miR-25-5p* in Caco-2 cell cultures treated with racemic naringenin, (*S)* and (*R*) enantiomers. Total RNA was extracted from treated and control cell cultures, as according to the Material and Methods Section, and RT-PCR assays were performed. The results show that cell treatment with racemic naringenin at the highest concentration tested (100 μg/mL) induced a significant change ($F = 9.459$, $p < 0.001$) in the expression levels of *miR-17-3p*, leading to it being underexpressed (Tukey, $p < 0.001$). (*S*) and (*R*) naringenin enantiomers induced significant changes in *miR-17-3p* expression levels [(*S*) enantiomer: $F = 28.173$, $p < 0.001$; (*R*) enantiomer: $F = 10.431$, $p < 0.001$], leading to it being underexpressed at the higher concentrations tested, in comparison with untreated cell cultures [(*S*)enantiomer: Tukey, $p < 0.001$; (*R*) naringenin: Tukey, $p < 0.01$] (Figure 2). No statistical differences were registered ($p > 0.05$) between (*S*) and (*R*) enantiomer treatments.

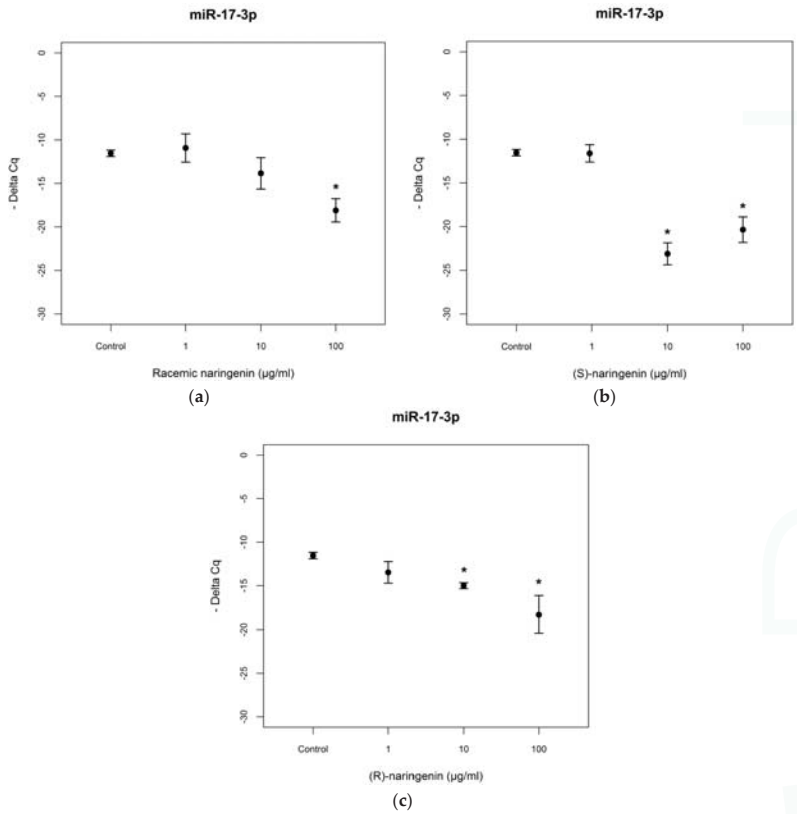

Figure 2. Expression levels, reported as Delta Cq, of miR-17-3p in Caco-2 cells treated with increasing concentrations of (**a**) racemic naringenin, (**b**) (*S*), and (**c**) (*R*) naringenin (1–100 μg/mL). * Indicates statistically significant differences between treated and untreated cell cultures, as reported in the text.

Then, we investigated the expression levels of mRNAs coding for the antioxidant enzymes, MnSOD and GPx2, reported to be tagets of *miR-17-3p*. RT-PCR assays revealed that the racemate induced an overexpression of mRNA coding for MnSOD at the concentration of 100 μg/mL, in agreement with data obtained for *miR-17-3p* expression levels. Both enantiomers also induced an overexpression of mRNA coding for MnSOD at the higher concentrations tested [(*S*) enantiomer: $F = 4.541$, $p < 0.05$, Tukey, $p < 0.05$; (*R*) enantiomer: $F = 105.65$, $p < 0.001$, Tukey, $p < 0.05$] (Figure 3).

As far as mRNA levels coding for GPx2 are concerned, the data obtained resulted to be similar to those obtained for mRNA coding for MnSOD (racemate: $F = 75.97$, $p < 0.001$, Tukey, $p < 0.05$; (*S*) naringenin: $F = 14.94$, $p < 0.05$, Tukey, $p < 0.05$; (*R*) naringenin: $F = 7.89$ $p < 0.001$, Tukey, $p < 0.05$) (Figure 4). No statistical differences ($p > 0.05$) were found between the effects of both enantiomers, on mRNA tagets of *mi-17-3p*.

As far as *miR-25-5p* is concerned, the racemate did not induce significant miRNA variation (data not reported). In the cases of enantiomeric naringenin treatments, *miR-25-5p* levels decreased in cell cultures treated with 10 and 100 μg/mL for both enantiomers tested [(*S*) enantiomer: $F = 3.544$, $p < 0.05$; Tukey, $p < 0.05$; (*R*) enantiomer: $F = 2.67$, $p < 0.05$, Tukey, $p < 0.05$] (Figure 5). In this case too, no statistical differences were registered in the comparison of the treatments with the two enantiomers ($p > 0.05$).

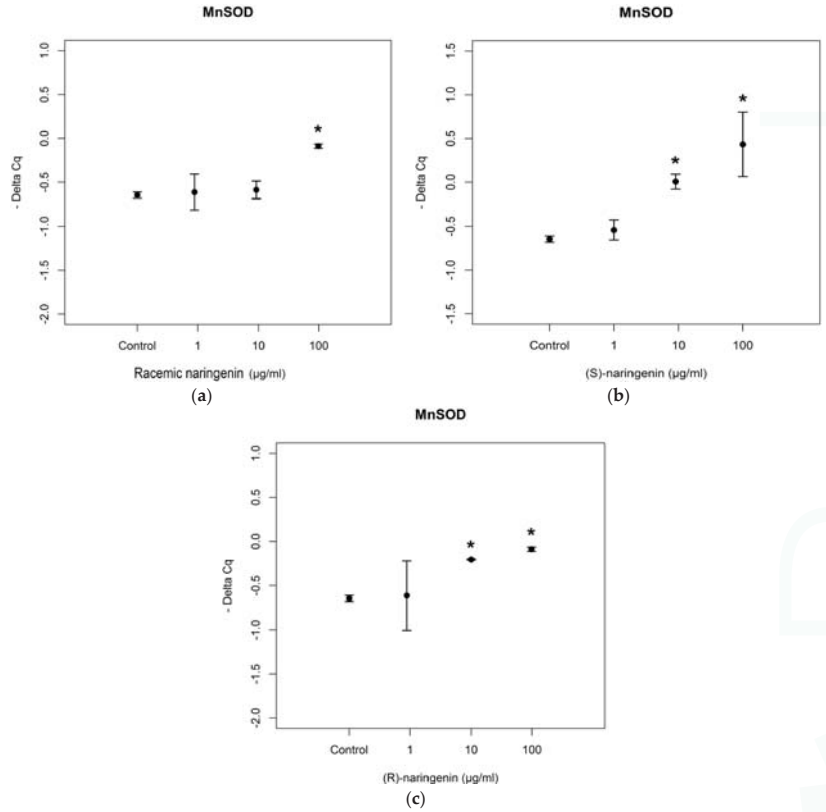

Figure 3. Expression levels, reported as Delta Cq, of mRNA coding for MnSOD in Caco-2 cells treated with increasing concentrations of (**a**) racemic naringenin, (**b**) (*S*), and (**c**) (*R*) naringenin (1–100 µg/mL). * Indicates statistically significant differences between treated and untreated cell cultures, as reported in the text.

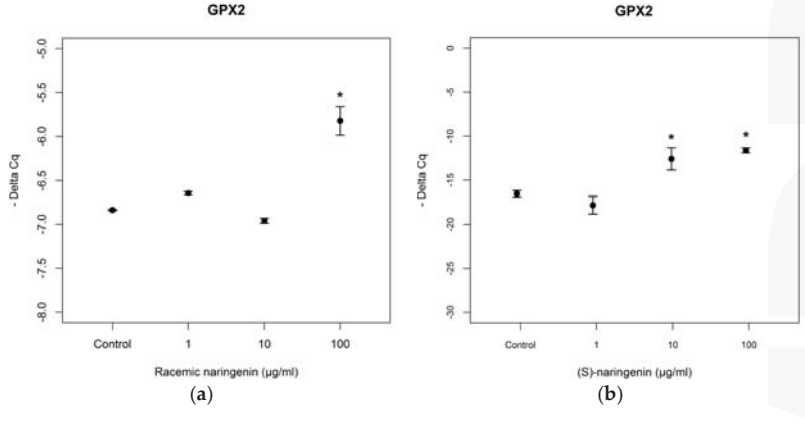

Figure 4. *Cont.*

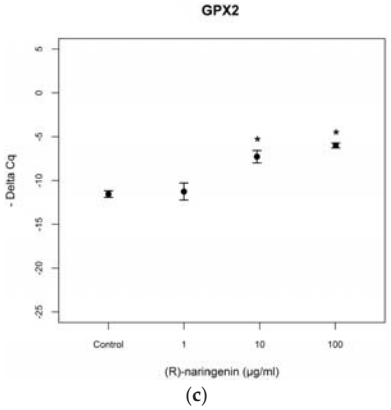

(**c**)

Figure 4. Expression levels, reported as Delta Cq, of mRNA coding for GPx2 in Caco-2 cells treated with increasing concentrations of (**a**) racemic naringin, (**b**) (*S*), and (**c**) (*R*) naringenin enantiomers (1–100 µg/mL). * Indicates statistically significant differences between treated and untreated cell cultures, as reported in the text.

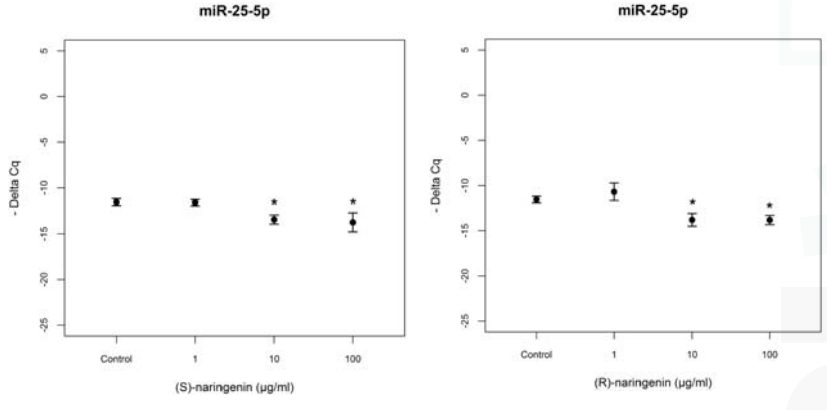

(**a**) (**b**)

Figure 5. Expression levels, reported as Delta Cq, of *miR-25-5p* in Caco-2 cells treated with increasing concentrations of (**a**) (*S*), and (**b**) (*R*) naringenin enantiomers (1–100 µg/mL). * Indicates statistically significant differences between treated and untreated cell cultures, as reported in the text.

As far as mRNA targets are concerned, the expression levels of mRNAs coding for TNF-α and *IL-6* were studied. According to the results obtained for *miR-25-5p*, its mRNA targets did not show any variation in expression levels after treatment with racemate (data not reported). TNF-α mRNA expression levels were significantly decreased after (*S*)- and (*R*)-enantiomer treatments ((*S*)-enantiomer: $F = 21.824$, $p < 0.05$; (*R*)-enantiomer: $F = 264.2$, $p < 0.001$). For the (*S*)-enantiomer treatment, TNF-α mRNA was underexpressed in cells treated with 10 µg/mL (Tukey, $p < 0.05$), compared to control cell cultures. Treatment with (*R*)-enantiomer gave rise to TNF-α mRNA underexpression at all concentrations tested (Tukey, $p < 0.05$) including the lowest concentration (1 µg/mL). With regards to the expression levels of mRNA coding for IL-6, we registered underexpression following treatment with 1 and 10 µg/mL of the (*S*)-enantiomer, and with 10 µg/mL of the (*R*)-enantiomer ((*S*)-enantiomer: $F = 44.591$, $p < 0.001$, Tukey, $p < 0.001$; (*R*)-enantiomer: $F = 27.945$, $p < 0.001$; Tukey, $p < 0.001$) (Figure 6).

No statistical differences ($p > 0.05$) were found between the effects of (*S*)- and (*R*)-enantiomer treatment on mRNA targets of *mi-25-5p*.

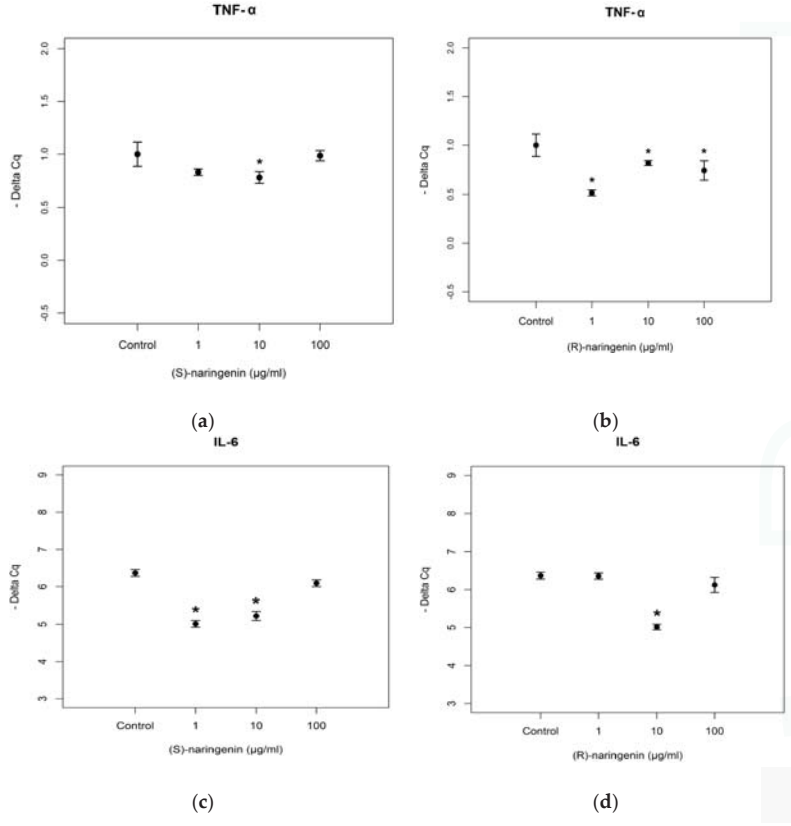

Figure 6. Expression levels, reported as Delta Cq, of mRNA coding for *TNF-α* in Caco-2 cells treated with increasing concentrations of (**a**) (*S*), and (**b**) (*R*) naringenin enantiomers (1–100 μg/mL) and and *IL-6* in Caco-2 cells treated with increasing concentrations of (**c**) (*S*) and (**d**)(*R*) naringenin enantiomers (1–100 μg/mL). * Indicates statistically significant differences between treated and untreated cell cultures, as reported in the text.

4. Discussion

Naringenin is a component of many plant foods commonly consumed within the diet. Therefore, this polyphenol can be considered a common constituent of our dietary pattern. Over the last decade, a large body of evidence suggests that naringenin exerts antioxidant and anti-inflammatory activities in in vitro and in vivostudies. Nevertheless, the mechanism of action of this flavanone is still largely unknown at a molecular level, as is the case for many other polyphenols. Thus, to unravel the potential mechanism of action of naringenin, we studied its effect on the expression levels of miRNAs involved in the endogenous antioxidant system (*miR-17-3p*) and inflammatory response (*miR-25-5p*) in human cells. In fact, these miRNAs are known to provide additional control to the complex regulation of gene expression at the post-transcriptional level, through the selective binding to complementary sequences of mRNAs coding for antioxidant enzymes and pro-inflammatory cytokines, besides other biochemical events ranging from extracellular stimuli, intracellular signaling

pathways, and transcription factors. As far as the changes induced on *miR-17-3p* expression levels are concerned, in our experimental conditions, we found that (*S*) and (*R*) naringenin possessed similar activity, downregulating *miR-17-3p* from a concentration of 10 µg/mL. Racemate showed less activity, maintaining the ability to down-regulate *miR-17-3p* expression at only the highest concentration. These results seem to suggest that the enantiomers alone are more active than their equimolar mixture.

The biological significance of the modulation exerted by racemic and enantiomeric naringenin on the expression levels of *miR-17-3p* has been proven by the upregulation of the expression levels of the mRNAs coding for MnSOD and GPx2, which are reported to be validated targets of *miR-17-3p* [30]. In fact, in agreement with the downregulation of *miR-17-3p* levels, we registered an overexpression of mRNAs coding for MnSOD and GPx2 at identical concentrations of racemic and enantiomeric naringenin, respectively. In this case too, results obtained on mRNAs seem to suggest that the enantiomers alone, which showed similar activity, are more active than their equimolar mixture.

The fact that the expression levels of mRNAs coding for MnSOD and GPx2 are upregulated in response to the downregulation of *miR-17-3p* suggests a possible direct interaction between miRNA and naringenin that prevents the binding of *miR-17-3p* to its targets, allowing to these latter to be overexpressed. This hypothesis is in agreement with the results reported by Baselga-Escudero et al. that demonstrated the direct binding of some polyphenols to miRNAs by means of ^{1}H NMR spectroscopy, suggesting a new posttranscriptional mechanism by which polyphenols could exert their modulation of protein synthesis. In addition, no statistical differences were evidenced for both(*S*) and (*R*) enantiomers, suggesting that the binding between miRNA and naringenin involves only the benzopyran moiety and not the chiral center [39].

As far as *miR-25-5p* is concerned, both enantiomers showed the capacity to modulate its expression, inducing the modification of the *miR-25-5p* expression levels only at the higher concentrations. Here too, a decrease of activity was registered in the presence of racemic naringenin, to the extent that no changes in the expression level of this miRNA are registered after this treatment. The expression levels of mRNAs coding for TNF-α and IL-6 are not in agreement with those obtained from *miR-25-5p*, as in both cases we have registered an under-expression. These results suggest that *miR-25-5p* is not the only miRNA involved in the modulation of TNF-α and IL-6 mRNA. In fact, literature data report that a single miRNA is able to bind hundreds of mRNAs, even if to date only a small fraction of miRNA–mRNA interactions has been validated experimentally [40]. These results show that naringenin enantiomers exert a beneficial effect regardless of their effect on the mRNA, inducing a reduction in the gene expression of mRNA coding for TNF-α and IL-6.

Overall, the results obtained for these two latter mRNAs are consistent with those obtained from earlier studies performed in in vivoconditions on racemic naringenin and in in vitro conditions on naringenin enantiomers. In fact, Al-Rejaie et al. [41] showed that pretreatment with naringenin (50 and 100 mg/kg per day), or with mesalazine (300 mg/kg per day) used as positive control, for seven days before the induction of ulcerative colitis (through the treatment of 4% acetic acid), decreased the levels of pro-inflammatory cytokines (i.e., TNF-α, IL-1β, and IL-6) and prostaglandin E2. In addition, naringenin pretreatment induced an increase in catalase and superoxide dismutase at doses of 50 and 100 mg/Kg and 100 mg/kg, respectively confirming our data regarding the antioxidant activity. Moreover, regarding the in vitro studies, we demonstrated that in hPBMC cultures naringenin enantiomers significantly decreased pro-inflammatory cytokine levels (i.e., TNF-α and IL-6) [7].

5. Conclusions

This study confirms the epigenetic activity of racemic naringenin and reveals the effects of racemic and enantiomeric naringenin on the expression levels of *miR-17-3p*, involved in the antioxidant defense system, and *miR-25-5p*, involved in the anti-inflammatory response. As far as *miR-17-3p* is concerned, the downregulation of its expression levels correspond to an upregulation of mRNA coding for MnSOD and GPx2, showing an increase in antioxidant enzyme transcriptions and therefore in the antioxidant defense system. These findings can at least partly explain the well-known antioxidant activity of

naringenin and, for the first time, show that this property is exerted through an epigenetic mechanism. As far as *miR-25-5p* is concerned, the underexpression of mRNA coding for the two cytokines, TNF-α and IL-6, is not supported by its behavior. This suggests that the modulation of these two mRNAs is not strictly under the control of *miR-25-5p*, and that this miRNA could act with other miRNAs, giving rise to synergistic and/or antagonistic effects.

Moreover, both naringeninenantiomers were found to be equally active on miRNAs at a higher level than the racemate, causing down-regulation in both cases, suggesting a negative synergism between enantiomers. (*S*) and (*R*) naringenin showed different activity on target mRNAs, suggesting that other epigenetic mechanisms (other miRNAs, DNA methylations, histone protein modifications) could be involved in the expression of the tested mRNAs. In addition, it seems to suggest that the mechanisms underlying these interactions, enantiomer–miRNA and enantiomer–mRNA, are different. Thus, further studies are needed to understand in what way naringenin and its enantiomers are able to modulate levels of miRNA, through both direct and indirect interaction.

In conclusion, our results show the role of naringenin (both racemic and enantiomeric) as antioxidant agent acting through an epigenetic mechanism of action and support the hypothesis that long-term consumption of foods rich in naringenin could counteract oxidative stress through the increase of enzymatic antioxidant defense. The growing body of evidence demonstrating the antioxidant activity of naringenin as well asthese results lead to expect that naringenin could actually exert antioxidant effects also in vivo. Accordingly, in vivoinvestigations are needed for future applications of naringenin as an antioxidant agent in functional foods or food supplements.

Acknowledgments: The authors would like to thank Michele Ghitti for his excellent statistical data analysis throughout this study.

Author Contributions: M.D., S.C. and E.C. conceived and designed the experiments; E.C. performed the cell cultures; V.C. and A.D.L. performed miRNA and mRNA expression assays; D.R. and E.M. performed naringenin enantioresolution; and M.D. and V.C. wrote the paper. All authors revised the paper and approved the final manuscript.

Conflicts of Interest: The authors have declared no conflict of interest.

References

1. Patel, K.; Singh, G.K.; Patel, D.K. Review on pharmacological and analytical aspects of naringenin. *Chin. J. Integr. Med.* **2014**, *14*, 1–13. [CrossRef] [PubMed]
2. Bugianesi, R.; Catasta, G.; Spigno, P.; D'Uva, A.; Maiani, G. Naringenin from cooked tomato paste is bioavailable in men. *J. Nutr.* **2002**, *132*, 3349–3352. [PubMed]
3. Vallverdu'-Queralt, A.; Jauregui, O.; Medina-Remon, A.; Andres-Lacueva, C; Lamuela-Raventos, R.M. Improved characterization of tomato polyphenols using liquid chromatography/electrospray ionization linear ion trap quadrupole Orbitrap mass spectrometry and liquid chromatography/electrospray ionization tandem mass spectrometry. *Rapid Commun. Mass Spectrom.* **2010**, *24*, 2986–2992. [CrossRef] [PubMed]
4. Ho, P.C.; Saville, D.J.; Coville, P.F.; Wanwimolruk, S. Content of *CYP3A4* inhibitors, naringin, naringenin and bergapten in grapefruit and grapefruit juice products. *Pharm. Acta Helv.* **2000**, *74*, 379–385. [CrossRef]
5. Tomas-Barberen, F.A.; Clifford, M.N. Flavanones, chalcones and dihydrochalcones—Nature, occurrence and dietary burden. *J. Sci. Food Agric.* **2000**, *80*, 1073–1080. [CrossRef]
6. Orhan, I.E.; Nabavi, S.F.; Daglia, M.; Tenore, G.C.; Mansouri, K.; Nabavi, S.M. Naringenin and atherosclerosis: A review of literature. *Curr. Pharm. Biotechnol.* **2015**, *16*, 245–251. [CrossRef] [PubMed]
7. Gaggeri, R.; Rossi, D.; Daglia, M.; Leoni, F.; Avanzini, M.A.; Mantelli, M.; Juza, M.; Collina, S. An eco-friendly enantioselective access to (*R*)-naringenin as inhibitor of proinflammatory cytokine release. *Chem. Biodivers.* **2013**, *10*, 1531–1538. [CrossRef] [PubMed]
8. Gaggeri, R.; Rossi, D.; Christodoulou, M.S.; Passarella, D.; Leoni, F.; Azzolina, O.; Collina, S. Chiral flavanones from AmygdaluslycioidesSpach: Structural elucidation and identification of TNFalpha inhibitors by bioactivity-guided fractionation. *Molecules* **2012**, *17*, 1665–1674. [CrossRef] [PubMed]

9. Song, H.M.; Park, G.H.; Eo, H.J.; Lee, J.W.; Kim, M.K.; Lee, J.R.; Lee, M.H.; Koo, J.S.; Jeong, J.B. Anti-Proliferative Effect of Naringenin through p38-Dependent Downregulation of Cyclin D1 in Human Colorectal Cancer Cells. *Biomol. Ther. (Seoul)* **2015**, *23*, 339–344. [CrossRef] [PubMed]
10. Wilcox, L.J.; Borradaile, N.M.; Huff, M.W. Antiatherogenic properties of naringenin, a citrus flavonoid. *Cardiovasc. Drug Rev.* **1999**, *17*, 160–178. [CrossRef]
11. Erlund, I.; Meririnne, E.; Alfthan, G.; Aro, A. Plasma kinetics and urinary excretion of the flavanones naringenin and hesperetin in humans after ingestion of orange juice and grapefruit juice. *J. Nutr.* **2001**, *131*, 235–241. [PubMed]
12. Manach, C.; Morand, C.; Gil-Izquierdo, A.; Bouteloup-Demange, C.; Re'mesy, C. Bioavailability in humans of the flavanones hesperidin and narirutin after the ingestion of two doses of orange juice. *Eur. J. Clin. Nutr.* **2003**, *57*, 235–242. [CrossRef] [PubMed]
13. Manach, C.; Scalbert, A.; Morand, C.; Rémésy, C.; Jiménez, L. Polyphenols: Food sources and bioavailability. *Am. J. Clin. Nutr.* **2004**, *79*, 727–747. [PubMed]
14. Felgines, C.; Texier, O.; Morand, C.; Manach, C.; Scalbert, A.; Régerat, F.; Rémésy, C. Bioavailability of the flavanone naringenin and its glycosides in rats. *Am. J. Physiol. Gastrointest. Liver Physiol.* **2000**, *279*, G1148–G1154. [PubMed]
15. Orrego-Lagarón, N.; Martínez-Huélamo, M.; Vallverdú-Queralt, A.; Lamuela-Raventos, R.M.; Escribano-Ferrer, E. High gastrointestinal permeability and local metabolism of naringenin: Influence of antibiotic treatment on absorption and metabolism. *Br. J. Nutr.* **2015**, *114*, 169–180. [CrossRef] [PubMed]
16. Chtourou, Y.; Kamoun, Z.; Zarrouk, W.; Kebieche, M.; Kallel, C.; Gdoura, R.; Fetoui, H. Naringenin ameliorates renal and platelet purinergic signalling alterations in high-cholesterol fed rats through the suppression of ROS and NF-κB signaling pathways. *Food Funct.* **2016**, *7*, 183–193. [CrossRef] [PubMed]
17. Ozkaya, A.; Sahin, Z.; Dag, U.; Ozkaraca, M. Effects of Naringenin on Oxidative Stress and Histopathological Changes in the Liver of Lead Acetate Administered Rats. *J. Biochem. Mol. Toxicol.* **2016**, *30*, 243–248. [CrossRef] [PubMed]
18. Liu, Y.; An, W.; Gao, A. Protective effects of naringenin in cardiorenal syndrome. *J. Surg. Res.* **2016**, *203*, 416–423. [CrossRef]
19. Chtourou, Y.; Fetoui, H.; Jemai, R.; Ben Slima, A.; Makni, M.; Gdoura, R. Naringenin reduces cholesterol-induced hepatic inflammation in rats by modulating matrix metalloproteinases-2, 9 via inhibition of nuclear factor κB pathway. *Eur. J. Pharmacol.* **2015**, *746*, 96–105. [CrossRef] [PubMed]
20. Azuma, T.; Shigeshiro, M.; Kodama, M.; Tanabe, S.; Suzuki, T. Supplemental naringenin prevents intestinal barrier defects and inflammation in colitic mice. *J. Nutr.* **2013**, *143*, 827–834. [CrossRef] [PubMed]
21. Dou, W.; Zhang, J.; Sun, A.; Zhang, E.; Ding, L.; Mukherjee, S.; Wei, X.; Chou, G.; Wang, Z.T.; Mani, S. Protective effect of naringenin against experimental colitis via suppression of Toll-like receptor 4/NF-κBsignalling. *Br. J. Nutr.* **2013**, *110*, 599–608. [CrossRef] [PubMed]
22. Blade, C.; Baselga-Escudero, L.; Arola-Arnal, A. microRNAs as new targets of dietary polyphenols. *Curr. Pharm. Biotechnol.* **2014**, *15*, 343–351. [CrossRef] [PubMed]
23. Bartel, D.P. MicroRNAs: Genomics, biogenesis, mechanism, and function. *Cell* **2004**, *116*, 281–297. [CrossRef]
24. Wu, X.; Tan, X.; Fu, S.W. May Circulating microRNAs be Gastric Cancer Diagnostic Biomarkers? *J. Cancer* **2015**, *6*, 1206–1213. [CrossRef] [PubMed]
25. Fu, X.M.; Zhou, Y.Z.; Cheng, Z.; Liao, X.B.; Zhou, X.M. MicroRNAs: Novel Players in Aortic Aneurysm. *BioMed Res. Int.* **2015**, *2015*, 831641. [CrossRef] [PubMed]
26. Femminella, G.D.; Ferrara, N.; Rengo, G. The emerging role of microRNAs in Alzheimer's disease. *Front. Physiol.* **2015**, *12*, 6–40. [CrossRef] [PubMed]
27. Yanaihara, N.; Caplen, N.; Bowman, E.; Seike, M.; Kumamoto, K.; Yi, M.; Stephens, R.M.; Okamoto, A.; Yokota, J.; Tanaka, T.; et al. Unique microRNA molecular profiles in lung cancer diagnosis and prognosis. *Cancer Cell* **2006**, *9*, 189–198. [CrossRef] [PubMed]
28. Iorio, M.V.; Ferracin, M.; Liu, C.G.; Veronese, A.; Spizzo, R.; Sabbioni, S.; Magri, E.; Pedriali, M.; Fabbri, M.; Campiglio, M.; et al. MicroRNA gene expression deregulation in human breastcancer. *Cancer Res.* **2005**, *65*, 7065–7070. [CrossRef] [PubMed]
29. Ozen, M.; Creighton, C.J.; Ozdemir, M.; Ittmann, M. Widespread deregulation of microRNA expression in human prostate cancer. *Oncogene* **2008**, *27*, 1788–1793. [CrossRef] [PubMed]

30. Xu, Y.; Fang, F.; Zhang, J.; Josson, S.; St Clair, W.H.; St Clair, D.K. miR-17* suppresses tumorigenicity of prostate cancer by inhibiting mitochondrial antioxidant enzymes. *PLoS ONE* **2010**, *5*, e14356. [CrossRef] [PubMed]
31. Tili, E.; Michaille, J.J.; Alder, H.; Volinia, S.; Delmas, D.; Latruffe, N.; Croce, C.M. Resveratrol modulates the levels of microRNAs targeting genes encoding tumor-suppressors and effectors of TGFβ signaling pathway in SW480 cells. *Biochem. Pharmacol.* **2010**, *80*, 2057–2065. [CrossRef] [PubMed]
32. Lesjak, M.; Hoque, R.; Balesaria, S.; Skinner, V.; Debnam, E.S.; Surjit, K.S.; Srai, S.K.; Sharp, P.A. Quercetin inhibits intestinal iron absorption and ferroportin transporter expression in vivo and in vitro. *PLoS ONE* **2014**, *9*, e102900. [CrossRef] [PubMed]
33. Curti, V.; Capelli, E.; Boschi, F.; Nabavi, S.F.; Bongiorno, A.I.; Habtemariam, S.; Nabavi, S.M.; Daglia, M. Modulation of human miR-17-3p expression by methyl 3-*O*-methyl gallate as explanation of its in vivo protective activities. *Mol. Nutr. Food Res.* **2014**, *58*, 1776–1784. [CrossRef] [PubMed]
34. Nabavi, S.M.; Habtemariam, S.; Nabavi, S.F.; Sureda, A.; Daglia, M.; Moghaddam, A.H.; Amani, M.A. Protective effect of gallic acid isolated from Peltiphyllumpeltatum against sodium fluoride-induced oxidative stress in rat's kidney. *Mol. Cell. Biochem.* **2013**, *372*, 233–239. [CrossRef] [PubMed]
35. Lee, T.W.; Tan, E.L.; Ng, C.C.; Gan, S.Y. The Effect of Cytokines on MicroRNA Expression in TW01 Nasopharyngeal Carcinoma Cells. *Br. J. Med. Med. Res.* **2013**, *3*, 543–554. [CrossRef]
36. Mei, Z.; Chen, S.; Chen, C.; Xiao, B.; Li, F.; Wang, Y.; Tao, Z. Interleukin-23 Facilitates Thyroid Cancer Cell Migration and Invasion by Inhibiting *SOCS4* Expression via MicroRNA-25. *PLoS ONE* **2015**, *10*, e0139456. [CrossRef]
37. Milenkovic, D.; Deval, C.; Gouranton, E.; Landrier, J.F.; Scalbert, A.; Morand, C.; Mazur, A. Modulation of miRNA expression by dietary polyphenols in apoE deficient mice: A new mechanism of the action of polyphenols. *PLoS ONE* **2012**, *7*, e29837. [CrossRef]
38. R Core Team. R: A language and Environment for Statistical Computing, R Foundation for Statistical Computing, Vienna, Austria. 2014. Available online: http://www.R-project.org/ (accessed on 30 July 2016).
39. Baselga-Escudero, L.; Blade, C.; Ribas-Latre, A.; Casanova, E.; Suárez, M.; Torres, J.L.; Salvadó, M.J.; Arola, L.; Arola-Arnal, A. Resveratrol and EGCG bind directly and distinctively to miR-33a and miR-122 and modulate divergently their levels in hepatic cells. *Nucleic Acids Res.* **2014**, *42*, 882–892. [CrossRef] [PubMed]
40. Helwak, A.; Kudla, G.; Dudnakova, T.; Tollervey, D. Mapping the Human miRNA Interactome by CLASH Reveals Frequent Noncanonical Binding. *Cell* **2013**, *153*, 654–665. [CrossRef] [PubMed]
41. Al-Rejaie, S.S.; Abuohashish, H.M.; Al-Enazi, M.M.; Al-Assaf, A.H.; Parmar, M.Y.; Ahmed, M.M. Protectiveeffect of naringenin on acetic acid-induced ulcerative colitis in rats. *World J. Gastroenterol.* **2013**, *19*, 5633–5644. [CrossRef] [PubMed]

nutrients

MDPI

Review

Antioxidants for Healthy Skin: The Emerging Role of Aryl Hydrocarbon Receptors and Nuclear Factor-Erythroid 2-Related Factor-2

Masutaka Furue [1,2,3,*], Hiroshi Uchi [1], Chikage Mitoma [1,2], Akiko Hashimoto-Hachiya [1], Takahito Chiba [1], Takamichi Ito [1], Takeshi Nakahara [1,3] and Gaku Tsuji [1,2]

1 Department of Dermatology, Kyushu University, Maidashi 3-1-1, Higashi-ku, Fukuoka 812-8582, Japan; uchihir@dermatol.med.kyushu-u.ac.jp (H.U.); mchikage@dermatol.med.kyushu-u.ac.jp (C.M.); ahachi@dermatol.med.kyushu-u.ac.jp (A.H.-H.); allheartakita@yahoo.co.jp (T.C.); takamiti@dermatol.med.kyushu-u.ac.jp (T.I.); nakahara@dermatol.med.kyushu-u.ac.jp (T.N.); gakku@dermatol.med.kyushu-u.ac.jp (G.T.)

2 Research and Clinical Center for Yusho and Dioxin, Kyushu University, Fukuoka 812-8582, Japan

3 Division of Skin Surface Sensing, Department of Dermatology, Kyushu University, Fukuoka 812-8582, Japan

* Correspondence: furue@dermatol.med.kyushu-u.ac.jp; Tel.: +81-92-642-5581; Fax: +81-92-642-5600

Received: 1 February 2017; Accepted: 28 February 2017; Published: 3 March 2017

Abstract: Skin is the outermost part of the body and is, thus, inevitably exposed to UV rays and environmental pollutants. Oxidative stress by these hazardous factors accelerates skin aging and induces skin inflammation and carcinogenesis. Aryl hydrocarbon receptors (AHRs) are chemical sensors that are abundantly expressed in epidermal keratinocytes and mediate the production of reactive oxygen species. To neutralize or minimize oxidative stress, the keratinocytes also express nuclear factor-erythroid 2-related factor-2 (NRF2), which is a master switch for antioxidant signaling. Notably, there is fine-tuned crosstalk between AHR and NRF2, which mutually increase or decrease their activation states. Many NRF2-mediated antioxidant phytochemicals are capable of up- and downmodulating AHR signaling. The precise mechanisms by which these phytochemicals differentially affect the AHR and NRF2 system remain largely unknown and warrant future investigation.

Keywords: antioxidants; reactive oxygen species; aryl hydrocarbon receptor; nuclear factor-erythroid 2-related factor-2; phytochemicals

1. Introduction

Oxidative stress is defined as an imbalance between the formation of oxidative free radicals and the antioxidant defense capacity of cells of the body [1]. Oxidative stress has been shown in many dermatological diseases, including vitiligo, atopic dermatitis, alopecia areata, photoaging, carcinogenesis, and chemotoxicity [2–12]. Most free radicals in the body exist in the form of reactive oxygen species (ROS). Excessive free radicals impair not only DNA, but also cellular proteins and lipids [9,10].

In living cells, ROS are continuously generated as a byproduct of oxidative energy metabolism to make adenosine triphosphate from glucose in mitochondria, by xanthine oxidase for the degradation of purine nucleotides, by nitric oxide synthase to make nitric oxide, and so on [10]. In addition, external stimuli, such as ionizing and ultraviolet (UV) radiation, environmental pollutants, contact allergens, and drugs, are potent inducers of ROS production [9,12–15]. Inflammatory cytokines are also responsible for ROS generation [9,10,16]. Since the skin is the outermost organ of the body, these oxidative stimulants adversely affect the proper differentiation and barrier function of the skin. One of

the major sensors recognizing these stimulants in the skin is aryl hydrocarbon receptor (AHR), which was originally called dioxin receptor [13].

The excessive production of ROS should be neutralized or minimized by antioxidants in order to maintain skin homeostasis. The antioxidant molecules, including glutathione, vitamin E, and vitamin C work together with enzymatic antioxidants, such as NAD(P)H:quinone oxidoreductase 1 (NQO1), heme oxygenase-1 (HO-1), and glutathione S-transferase [17]. The induction of these antioxidant enzymes is regulated by nuclear factor-erythroid 2-related factor-2 (NRF2), which is a master switch for antioxidant signaling [13,17].

Various phytochemicals and herbal extracts exert their antioxidant properties by activating the NRF2 system in an AHR-dependent or AHR-independent manner in human epidermal keratinocytes [18–22]. Certain antioxidant phytochemicals also upregulate the expression of filaggrin (FLG), which plays a pivotal role in maintaining epidermal barrier function [19–21,23].

2. Aryl Hydrocarbon Receptor Regulating both Oxidative and Antioxidant Pathways

AHR is a xenobiotic chemical sensor abundantly expressed in the epidermal keratinocytes [13,24]. Various external and internal ligands, such as dioxins, polycyclic aromatic pollutants, benzo[a]pyrene, phytochemicals, and food metabolites bind to, and activate, AHR [13,24]. Tryptophan photoproduct 6-formylindolo[3,2-b]carbazole (FICZ), generated by UV irradiation, is also known as a high-affinity endogenous ligand for AHR [25,26]. Historically, the signaling pathway of AHR has been elucidated in studies investigating the toxicity of dioxins and polycyclic aromatic pollutants [13,27,28]. Upon ligation by dioxins, the activated AHR translocates from the cytoplasm into the nucleus (Figure 1). This translocated AHR binds to its specific DNA recognition site, namely, xenobiotic-responsive element, and upregulates the transcription of responsive genes, such as cytochrome P450 1A1 (*CYP1A1*) [13,27,28]. CYP1A1 is a member of a multigene family of xenobiotic-metabolizing enzymes [13,27,28]. Besides its physiological role in the detoxification of dioxins, the activity of CYP1A1 can be deleterious because it generates mutagenic metabolites and ROS. FICZ binds to AHR and upregulates the expression of CYP1A1 in an efficient but transient manner; this is because FICZ is rapidly metabolized by CYP1A1 in a feedback mechanism [25,29]. Extensive studies on the function of AHR using AHR-deficient mice have demonstrated that AHR is responsible for most, if not all, of the toxic effects caused by dioxins [30].

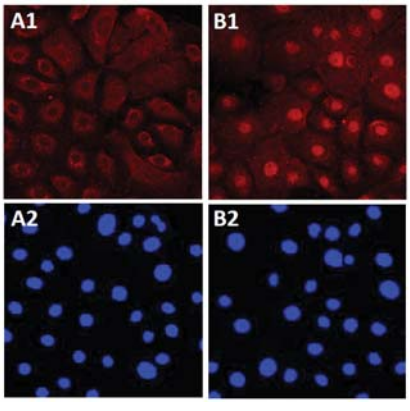

Figure 1. Activation of AHR. In untreated normal human keratinocytes, AHR (red) is mainly located in the cytoplasm (**A1**). Nuclei are stained with 4′,6-diamidino-2-phenylindole (blue, **A2**). In the presence of soybean tar glyteer, AHR is translocated from the cytoplasm to the nucleus (**B1**, red). Nuclei are stained with 4′,6-diamidino-2-phenylindole (blue, **B2**).

In addition to oxidative stress, recent studies have demonstrated that the AHR system mediates antioxidative and protective signaling in response to certain ligands, such as flavonoids, herbal medicines, and azoles [16,18,19,21,31–33]. For example, ligation of AHR by ketoconazole induces the nuclear translocation of AHR without producing ROS. Instead, it activates the NRF2-NQO1 pathway, which protects cells from ROS-induced oxidative damage [16]. There are several types of AHR ligands. Dioxins, benzo[a]pyrene, and other polycyclic aromatic pollutants bind to AHR with high affinity and induce tremendously high *CYP1A1* expression with damaging ROS production [14,30]. Although subsequent NRF2 activation does occur after AHR ligation by dioxins [34], the oxidative stress overwhelms the antioxidant protection in response to these hazardous compounds [14,31]. A plethora of beneficial and antioxidant phytochemicals, such as cynaropicrin, activate the AHR-NRF2 signaling pathway without any appreciable production of ROS [18]. On the other hand, the antioxidant cinnamaldehyde instead inhibits AHR activation. However, it potently activates the NRF2 pathway and exerts antioxidant activity in an AHR-independent manner [22]. The precise mechanisms by which these chemicals differentially affect the AHR-NRF2 system remain largely unknown. Since AHR forms a molecular complex with Hsp90, XAP2, and p23 in the cytoplasm and with AHR nuclear translocator (ARNT) in the nucleus, these partner molecules may potentially define the oxidative and antioxidant outcome [30].

Another intriguing paradigm for AHR signaling is its enhancing effects on epidermal barrier function. The barrier function is significantly disrupted in *Ahr*-null mice, indicating that AHR plays a pivotal role in skin barrier integrity [35]. FLG is one of the major components of barrier proteins [23,36]. Loss-of-function mutation of *FLG* causes dry skin and is critically involved in the pathogenesis of atopic dermatitis [37–39]. Antioxidant folk medicines such as *Houttuynia cordata* extract and *Opuntia ficus-indica* extract potently activate the AHR-NRF2 pathway and upregulate *FLG* expression [20,21]. The bifunctional (antioxidant and barrier-protection) properties of these folk remedies are particularly promising for maintaining the health of the skin.

3. Nuclear Factor-Erythroid 2-Related Factor-2, a Master Transcription Factor for Inducing Antioxidant Enzymes

The transcription factor NRF2 is a master switch for inducing antioxidant enzymes and is expressed in epidermal keratinocytes at high levels [16,17,31,32]. The antioxidant enzymes downstream of NRF2 include NQO1, HO-1, glutathione S-transferase, UDP-glucuronosyltransferases, epoxide hydrolase, glutathione reductase, thioredoxin reductase, catalase, and superoxide dismutase. NRF2 also activates the transcription of non-enzymatic antioxidant protein genes, such as thioredoxin and ferritin [17]. Under physiological conditions, the level of NRF2 in the cytoplasm is regulated by the formation of the NRF2-KEAP1-CUL3 complex [17]. KEAP1 binds to NRF2 and, therefore, directly inhibits its activity, resulting in simultaneous NRF2 ubiquitination catalyzed by CUL3. However, the oxidative condition in the cell leads to the oxidation of cysteine residues in the KEAP1 molecule, changing its conformation and causing dissociation of NRF2 from the complex. This free NRF2 is translocated to the nucleus and initiates the transcription of antioxidant genes (Figure 2) [17].

In *Nrf2*-null mice, UVB-induced sunburn reaction became significantly stronger and longer-lasting with a reduction of inducible HO-1 expression compared with that in wild-type mice [40,41]. In addition, mutation of the NRF2 gene has been suggested to be oncogenic in some squamous cell carcinoma cases [42]. The expression of NRF2 protein is downregulated in human malignant skin tumors [43]. On the other hand, excessive antioxidant activity does hamper the epidermal barrier function. K5-Cre-Nrf2 transgenic mice generated by Schäfer et al. were found to express high levels of constitutively-active Nrf2 in the epidermis together with the overexpression of Nqo1 and other antioxidative enzymes. Unexpectedly, their skin is dry with hair loss, scaling, epidermal acanthosis, and hyperkeratosis [44,45]. The Nrf2 transgenic mice gradually developed severe chloracne-like lesions, which are highly reminiscent to the patients with chloracene/metabolizing acquired dioxin-induced skin hamartomas [45]. Furthermore, the Nrf2 activation promotes the human papilloma virus-induced

or arsenite-induced carcinogenesis by upregulating the survival and proliferation of transformed keratinocytes [46,47]. These studies stress the importance of an appropriate balance between oxidative and antioxidative processes in maintaining epidermal homeostasis.

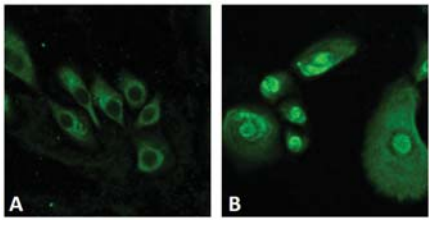

Figure 2. Activation of NRF2. In untreated normal human keratinocytes, NRF2 (green) is mainly located in the cytoplasm (**A**); *Opuntia ficus-indica* extract activates NRF2 and induces its cytoplasmic to nuclear translocation (**B**).

4. Phytogenic Antioxidants

Most phytogenic antioxidants are plant phenolic compounds. Approximately 8000 different structures of plant phenolics are known [48]. These phenolic compounds are classified into flavonols, flavones, flavonones, flavanols, isoflavones, anthocyanidins, hydroxycinnamic acids, hydroxybenzoic acids, tannins, stilbens, and lignans [48]. Some phytochemicals have been shown to bind to AHR with different affinities [49–51]. Below, we discuss in detail several phytogenic antioxidants, with special reference to AHR and NRF2 signaling in epidermal keratinocytes (Figure 3).

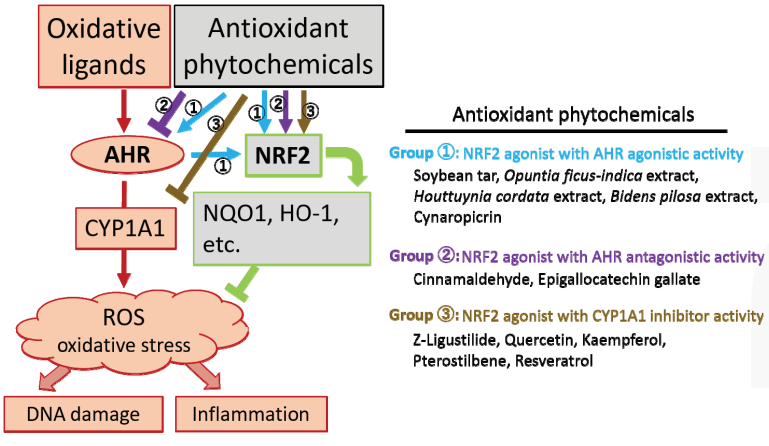

Figure 3. Antioxidant phytochemicals differentially modulate aryl hydrocarbon receptor (AHR), cytochrome P450 1A1 (CYP1A1) and nuclear factor-erythroid 2-related factor-2 (NRF2). Oxidative ligands, such as ultraviolet radiation, dioxins, and environmental polycyclic pollutants, activate the AHR and CYP1A1 system, which generates reactive oxygen species (ROS) and causes DNA damage and inflammation. Antioxidant phytochemicals exert their antioxidant capacity by activating NRF2, which is a master transcription factor for the induction of antioxidant enzymes such as NAD(P)H: quinone oxidoreductase 1 (NQO1) and heme oxygenase-1 (HO-1). These antioxidant enzymes neutralize or minimize ROS production. Antioxidant phytochemicals are categorized into at least three groups based on their capacity for up- and downmodulating AHR and CYP1A1. Group 1 contains NRF2 agonists with AHR agonistic activity (①). Group 2 contains NRF2 agonists with AHR antagonistic activity (②). Group 3 contains NRF2 agonists with CYP1A1 inhibitor activity (③).

4.1. NRF2 Agonist with AHR Agonistic Activity

4.1.1. Soybean Tar

Soybean tar glyteer has been widely used for the treatment of various inflammatory skin diseases in Japan since 1924, as an alternative to coal tar remedy [19]. As has been demonstrated for coal tar [52], glyteer inhibits the ROS production by benzo[a]pyrene and TNFα via NQO1 upregulation [19]. The antioxidant activity of soybean tar is mediated by the AHR-NRF2 pathway because it was shown to be attenuated by transfection with small interfering RNA against either AHR or NRF2 [19]. In addition, glyteer upregulates FLG expression in an AHR-dependent manner [19].

4.1.2. Opuntia Ficus-Indica Extract

Opuntia ficus-indica is a cactus species widely used as an anti-inflammatory, antilipidemic, and hypoglycemic agent [21]. Studies have suggested that its extract can downregulate oxidative stress via benzo[a]pyrene and TNFα (Figure 4). Its potent antioxidant activity is also mediated by the AHR-NRF2-NQO1 pathway [21]. *Opuntia ficus-indica* extract also stimulates AHR and upregulates FLG expression [21].

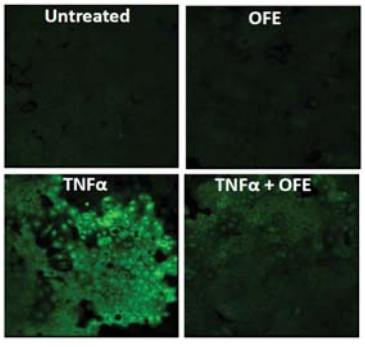

Figure 4. Antioxidant activity of *Opuntia ficus-indica* extract (OFE). Reactive oxygen species (ROS) are visualized with dichloro-dihydro-fluorescein diacetate staining (green). The production of ROS is not active in the untreated or OFE-treated human keratinocytes. Tumor necrosis factor α (TNFα) induces ROS production, which is significantly inhibited by OFE (TNFα + OFE).

4.1.3. *Houttuynia cordata* Extract

Houttuynia cordata, which is called "dokudami" in Japanese, is an aromatic medicinal herb that has been traditionally eaten as a folk medicine for various ailments, such as diabetes, obesity, cough, fever and skin diseases, in Asia [20]. Similar to glyteer and *Opuntia ficus-indica* extract, *Houttuynia cordata* extract inhibits the ROS production by benzo[a]pyrene and TNFα via the AHR-NRF2-NQO1 pathway [20].

4.1.4. *Bidens pilosa* Extract

Bidens pilosa is a tropical weed that grows widely in tropical and subtropical regions. This plant is used in various folk medicines and as a popular ingredient in herbal tea for its blood-pressure-lowering, liver-protective and hypoglycemic effects [53]. In the therapeutic guidelines for vasculitis and vascular disorders of the Japanese Dermatological Association, *B. pilosa* extract is recognized as an effective remedy for the treatment of livedo vasculopathy [53]. This extract potently inhibits the ROS production of endothelial cells by upregulating NRF2 and NQO1, which are abrogated by the knockdown of AhR or Nrf2 [53].

4.1.5. Cynaropicrin

Artichoke (*Cynara scolymus*) is one of the most ancient plants grown in the world and has been used as a folk medicine in the treatment of hepatitis, hyperlipidemia, obesity and dyspeptic disorders [18]. Cynaropicrin, a sesquiterpene lactone, is one of the major bioactive phytochemicals in artichoke extract [18]. The ROS production in UVB-irradiated keratinocytes is significantly downregulated by cynaropicrin [18]. The antioxidant activity of cynaropicrin is AHR-NRF2-dependent and inhibits the ROS production by benzo[a]pyrene and tumor necrosis factor α (TNFα) [18]. However, the AHR agonistic potency of cynaropicrin is very weak compared with those of soybean tar, *Opuntia ficus-indica* extract, *Houttuynia cordata* extract, and *Bidens pilosa* extract [19–21,53].

4.2. NRF2 Agonist with AHR Antagonistic Activity

4.2.1. Cinnamaldehyde

Cinnamaldehyde (3-phenyl-2-propenal) is the major constituent of the bark of *Cinnamomum cassia*, and it is known to have various biological activities including anti-inflammatory and anti-bacterial properties [22]. Cinnamaldehyde exerts its antioxidant activity via NRF2 and HO-1 expression and downregulates benzo[a]pyrene-induced oxidative stress [22]. However, cinnamaldehyde is unable to activate AHR, but instead significantly inhibits its action [22], which is in sharp contrast to cynaropicrin, soybean tar, *Opuntia ficus-indica* extract, *Houttuynia cordata* extract, and *Bidens pilosa* extract [19–21,53]. The dual functions of cinnamaldehyde, namely, inhibition of AHR and activation of NRF2, may be particularly beneficial for the treatment of intoxication of environmental pollutants such as dioxin [22].

4.2.2. Epigallocatechin Gallate

The green tea flavonoid epigallocatechin gallate upregulates Nrf2 and HO-1 expression [54] and inhibits AHR action [55,56]. It has been increasingly used for cosmetic purposes [57]. *Galactomyces* fermentation filtrate is also an AHR-stimulant generally used in cosmetics [58]. Interestingly, epigallocatechin gallate and *Galactomyces* fermentation filtrate exhibit synergistic antioxidant activity against TNFα-induced ROS production (Figure 5). The antagonistic or agonistic potency of epigallocatechin gallate for AHR may vary depending on the cell type [59].

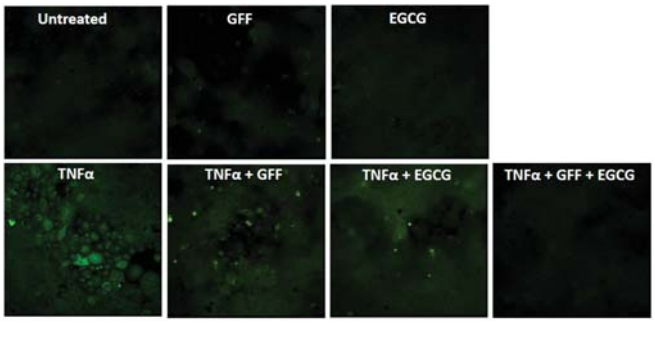

Figure 5. Synergistic antioxidant activity of *Galactomyces* ferment filtrate (GFF; 0.1%) and epigallocatechin gallate (EGCG; 10 μM). Reactive oxygen species (ROS) are visualized with dichloro-dihydro-fluorescein diacetate staining (green). The production of ROS is very slight in the human keratinocytes treated with medium control (untreated), a low concentration of GFF, or a low concentration of EGCG. Tumor necrosis factor α (TNFα) induces ROS production, which is weakly inhibited by a low concentration of either GFF (TNFα + GFF) or EGCG (TNFα + EGCG). The ROS production by TNFα is markedly downregulated by the simultaneous addition of GFF and EGCG (TNFα + GFF + EGCG).

4.3. NRF2 Agonist with CYP1A1 Inhibitor Activity

4.3.1. Z-Ligustilide

Z-Ligustilide is the major bioactive phthalide of *Cnidium officinale* and *Angelica acutiloba*, which are widely used in folk medicine in East Asia [60,61]. Z-Ligustilide ameliorates UVB-induced oxidative stress and inflammatory cytokine production through upregulation of the NRF2/HO-1 pathway and the suppression of NF-κB signaling [61]. Z-Ligustilide is not an AHR ligand, but it significantly inhibits benzo[a]pyrene-induced CYP1A1 expression via NRF2 activation [60].

4.3.2. Quercetin, Kaempferol, and Pterostilbene

Quercetin, kaempferol, and pterostilbene are abundant in berries and have potent antioxidant capacity, which is also mediated by the activation of NRF2 [62]. They also exhibit synergistic antioxidant activity when added in combination at appropriate concentrations [62]. Quercetin is not a direct ligand for AHR [26]. It sustains and enhances the ligand activity of AHR, such as FICZ, by inhibiting the CYP1A1-mediated degradation of ligand [26].

4.3.3. Resveratrol

Resveratrol is a widely-available polyphenol found in red wine and other sources that are thought to have health benefits [63]. It is also a potent NRF2 activator and shows antioxidant activity [63]. In addition, it activates sirtuin 1 and AMP-activated protein kinase, an enzyme that initiates autophagy [63]. Resveratrol inhibits the proliferation of human keratinocytes via sirtuin 1 activation [64]. Like quercetin, resveratrol enhances the activity of endogenous FICZ by inhibiting the CYP1A1-mediated degradation of AHR ligands [26].

5. Conclusions

Skin is inevitably exposed to UV rays and environmental pollutants. To a greater or lesser extent, these external stimulants induce oxidative stress and accelerate skin aging, leading to skin inflammation and carcinogenesis [13,24]. AHR is a capricious receptor that senses various chemical compounds and plays an essential role in photo-induced and chemically-induced oxidative stress [13,19,24,25]. Various antioxidant phytochemicals activate the NRF2 transcription factor and upregulate a series of antioxidant enzymes that neutralize the oxidative stress and protect the keratinocytes from oxidative damage [13,17]. Notably, there is finely-tuned crosstalk between AHR and NRF2, which mutually increase or decrease their activation states. Many NRF2-mediated antioxidant phytochemicals are capable of modulating AHR signaling. There are at least three groups of antioxidant phytochemicals when we categorize their capacity to modulate NRF2, AHR, and CYP1A1 (Figure 3). However, the modulatory capacity of phytochemicals on these three mutually related molecules may be cell-type-specific and concentration-dependent; therefore, the categorization may vary depending on the experimental protocol. The precise mechanisms by which these phytochemicals differentially affect the AHR and NRF2 system remain largely unknown and warrant future investigation.

Acknowledgments: This work was partly supported by grants from the Ministry of Health, Labour, and Welfare, and P&G Inovation Godo Kaisha.

Author Contributions: Masutaka Furue and Gaku Tsuji conceived and designed the experiments; Akiko Hashimoto-Hachiya and Takeshi Nakahara performed the experiments; Takahito Chiba and Takamichi Ito analyzed the data; Hiroshi Uchi and Chikage Mitoma contributed reagents/materials/analysis tools; Masutaka Furue wrote the paper.

Conflicts of Interest: The authors declare no conflict of interest.

References

1. Kruk, J.; Duchnik, E. Oxidative stress and skin diseases: Possible role of physical activity. *Asian Pac. J. Cancer Prev.* **2014**, *15*, 561–568. [CrossRef] [PubMed]
2. Furue, M.; Kadono, T. Nonsegmental vitiligo update. *Dermatol. Sin.* **2016**, *34*, 173–176. [CrossRef]
3. Ji, H.; Li, X.K. Oxidative stress in atopic dermatitis. *Oxid. Med. Cell. Longev.* **2016**, *2016*, 2721469. [CrossRef] [PubMed]
4. Prie, B.E.; Voiculescu, V.M.; Ionescu-Bozdog, O.B.; Petrutescu, B.; Iosif, L.; Gaman, L.E.; Clatici, V.G.; Stoian, I.; Giurcaneanu, C. Oxidative stress and alopecia areata. *J. Med. Life* **2015**, *8*, 43–46. [PubMed]
5. Katta, R.; Brown, D.N. Diet and skin cancer: The potential role of dietary antioxidants in nonmelanoma skin cancer prevention. *J. Skin Cancer* **2015**, *2015*, 893149. [CrossRef] [PubMed]
6. Saewan, N.; Jimtaisong, A. Natural products as photoprotection. *J. Cosmet. Dermatol.* **2015**, *14*, 47–63. [CrossRef] [PubMed]
7. Bosch, R.; Philips, N.; Suárez-Pérez, J.A.; Juarranz, A.; Devmurari, A.; Chalensouk-Khaosaat, J.; González, S. Mechanisms of photoaging and cutaneous photocarcinogenesis, and photoprotective strategies with phytochemicals. *Antioxidants (Basel)* **2015**, *4*, 248–268. [CrossRef] [PubMed]
8. Godic, A.; Poljšak, B.; Adamic, M.; Dahmane, R. The role of antioxidants in skin cancer prevention and treatment. *Oxid. Med. Cell. Longev.* **2014**, *2014*, 860479. [CrossRef] [PubMed]
9. Bickers, D.R.; Athar, M. Oxidative stress in the pathogenesis of skin disease. *J. Investig. Dermatol.* **2006**, *126*, 2565–2575. [CrossRef] [PubMed]
10. Chen, L.; Hu, J.Y.; Wang, S.Q. The role of antioxidants in photoprotection: A critical review. *J. Am. Acad. Dermatol.* **2012**, *67*, 1013–1024. [CrossRef] [PubMed]
11. Giampieri, F.; Alvarez-Suarez, J.M.; Gasparrini, M.; Forbes-Hernandez, T.Y.; Afrin, S.; Bompadre, S.; Rubini, C.; Zizzi, A.; Astolfi, P.; Santos-Buelga, C.; et al. Strawberry consumption alleviates doxorubicin-induced toxicity by suppressing oxidative stress. *Food Chem. Toxicol.* **2016**, *94*, 128–137. [CrossRef] [PubMed]
12. Eto, H.; Tsuji, G.; Chiba, T.; Furue, M.; Hyodo, F. Non-invasive evaluation of atopic dermatitis based on redox status using in vivo dynamic nuclear polarization magnetic resonance imaging. *Free Radic. Biol. Med.* **2016**, *103*, 209–215. [CrossRef] [PubMed]
13. Furue, M.; Takahara, M.; Nakahara, T.; Uchi, H. Role of AhR/ARNT system in skin homeostasis. *Arch. Dermatol. Res.* **2014**, *306*, 769–779. [CrossRef] [PubMed]
14. Tsuji, G.; Takahara, M.; Uchi, H.; Takeuchi, S.; Mitoma, C.; Moroi, Y.; Furue, M. An environmental contaminant, benzo(a)pyrene, induces oxidative stress-mediated interleukin-8 production in human keratinocytes via the aryl hydrocarbon receptor signaling pathway. *J. Dermatol. Sci.* **2011**, *62*, 42–49. [CrossRef] [PubMed]
15. Yasukawa, S.; Miyazaki, Y.; Yoshii, C.; Nakaya, M.; Ozaki, N.; Toda, S.; Kuroda, E.; Ishibashi, K.; Yasuda, T.; Natsuaki, Y.; et al. An ITAM-Syk-CARD9 signalling axis triggers contact hypersensitivity by stimulating IL-1 production in dendritic cells. *Nat. Commun.* **2014**, *5*, 3755. [CrossRef] [PubMed]
16. Tsuji, G.; Takahara, M.; Uchi, H.; Matsuda, T.; Chiba, T.; Takeuchi, S.; Yasukawa, F.; Moroi, Y.; Furue, M. Identification of ketoconazole as an AhR-Nrf2 activator in cultured human keratinocytes: The basis of its anti-inflammatory effect. *J. Investig. Dermatol.* **2012**, *132*, 59–68. [CrossRef] [PubMed]
17. Gęgotek, A.; Skrzydlewska, E. The role of transcription factor Nrf2 in skin cells metabolism. *Arch. Dermatol. Res.* **2015**, *307*, 385–396. [CrossRef] [PubMed]
18. Takei, K.; Hashimoto-Hachiya, A.; Takahara, M.; Tsuji, G.; Nakahara, T.; Furue, M. Cynaropicrin attenuates UVB-induced oxidative stress via the AhR-Nrf2-Nqo1 pathway. *Toxicol. Lett.* **2015**, *234*, 74–80. [CrossRef] [PubMed]
19. Takei, K.; Mitoma, C.; Hashimoto-Hachiya, A.; Uchi, H.; Takahara, M.; Tsuji, G.; Kido-Nakahara, M.; Nakahara, T.; Furue, M. Antioxidant soybean tar Glyteer rescues T-helper-mediated downregulation of filaggrin expression via aryl hydrocarbon receptor. *J. Dermatol.* **2015**, *42*, 171–180. [CrossRef] [PubMed]
20. Doi, K.; Mitoma, C.; Nakahara, T.; Uchi, H.; Hashimoto-Hachiya, A.; Takahara, M.; Tsuji, G.; Nakahara, M.; Furue, M. Antioxidant *Houttuynia. cordata* extract upregulates filaggrin expression in an aryl hydrocarbon-dependent manner. *Fukuoka Igaku Zasshi* **2014**, *105*, 205–213. [PubMed]

21. Nakahara, T.; Mitoma, C.; Hashimoto-Hachiya, A.; Takahara, M.; Tsuji, G.; Uchi, H.; Yan, X.; Hachisuka, J.; Chiba, T.; Esaki, H.; et al. Antioxidant *Opuntia. ficus-indica* extract activates AHR-NRF2 signaling and upregulates filaggrin and loricrin expression in human keratinocytes. *J. Med. Food* **2015**, *18*, 1143–1149. [CrossRef] [PubMed]
22. Uchi, H.; Yasumatsu, M.; Morino-Koga, S.; Mitoma, C.; Furue, M. Inhibition of aryl hydrocarbon receptor signaling and induction of NRF2-mediated antioxidant activity by cinnamaldehyde in human keratinocytes. *J. Dermatol. Sci.* **2016**. [CrossRef] [PubMed]
23. Furue, M.; Tsuji, G.; Mitoma, C.; Nakahara, T.; Chiba, T.; Morino-Koga, S.; Uchi, H. Gene regulation of filaggrin and other skin barrier proteins via aryl hydrocarbon receptor. *J. Dermatol. Sci.* **2015**, *80*, 83–88. [CrossRef] [PubMed]
24. Esser, C.; Bargen, I.; Weighardt, H.; Haarmann-Stemmann, T.; Krutmann, J. Functions of the aryl hydrocarbon receptor in the skin. *Semin. Immunopathol.* **2013**, *35*, 677–691. [CrossRef] [PubMed]
25. Fritsche, E.; Schäfer, C.; Calles, C.; Bernsmann, T.; Bernshausen, T.; Wurm, M.; Hübenthal, U.; Cline, J.E.; Hajimiragha, H.; Schroeder, P.; et al. Lightening up the UV response by identification of the arylhydrocarbon receptor as a cytoplasmatic target for ultraviolet B radiation. *Proc. Natl. Acad. Sci. USA* **2007**, *104*, 8851–8856. [CrossRef] [PubMed]
26. Mohammadi-Bardbori, A.; Bengtsson, J.; Rannug, U.; Rannug, A.; Wincent, E. Quercetin, resveratrol, and curcumin are indirect activators of the aryl hydrocarbon receptor (AHR). *Chem. Res. Toxicol.* **2012**, *25*, 1878–1884. [CrossRef] [PubMed]
27. Denison, M.S.; Soshilov, A.A.; He, G.; DeGroot, D.E.; Zhao, B. Exactly the same but different: Promiscuity and diversity in the molecular mechanisms of action of the aryl hydrocarbon (dioxin) receptor. *Toxicol. Sci.* **2011**, *124*, 1–22. [CrossRef] [PubMed]
28. Ikuta, T.; Namiki, T.; Fujii-Kuriyama, Y.; Kawajiri, K. AhR protein trafficking and function in the skin. *Biochem. Pharmacol.* **2009**, *77*, 588–596. [CrossRef] [PubMed]
29. Wincent, E.; Bengtsson, J.; Mohammadi Bardbori, A.; Alsberg, T.; Luecke, S.; Rannug, U.; Rannug, A. Inhibition of cytochrome P4501-dependent clearance of the endogenous agonist FICZ as a mechanism for activation of the aryl hydrocarbon receptor. *Proc. Natl. Acad. Sci. USA* **2012**, *109*, 4479–4484. [CrossRef] [PubMed]
30. Mimura, J.; Fujii-Kuriyama, Y. Functional role of AhR in the expression of toxic effects by TCDD. *Biochim. Biophys. Acta* **2003**, *1619*, 263–268. [CrossRef]
31. Haarmann-Stemmann, T.; Abel, J.; Fritsche, E.; Krutmann, J. The AhR-Nrf2 pathway in keratinocytes: On the road to chemoprevention? *J. Investig. Dermatol.* **2012**, *132*, 7–9. [CrossRef] [PubMed]
32. Jaiswal, A.K. Nrf2 signaling in coordinated activation of antioxidant gene expression. *Free Radic. Biol. Med.* **2004**, *36*, 1199–1207. [CrossRef] [PubMed]
33. Niestroy, J.; Barbara, A.; Herbst, K.; Rode, S.; van Liempt, M.; Roos, P.H. Single and concerted effects of benzo[a]pyrene and flavonoids on the AhR and Nrf2-pathway in the human colon carcinoma cell line Caco-2. *Toxicol. In Vitro* **2011**, *25*, 671–683. [CrossRef] [PubMed]
34. Yeager, R.L.; Reisman, S.A.; Aleksunes, L.M.; Klaassen, C.D. Introducing the "TCDD-inducible AhR-Nrf2 gene battery". *Toxicol. Sci.* **2009**, *111*, 238–246. [CrossRef] [PubMed]
35. Haas, K.; Weighardt, H.; Deenen, R.; Köhrer, K.; Clausen, B.; Zahner, S.; Boukamp, P.; Bloch, W.; Krutmann, J.; Esser, C. Aryl hydrocarbon receptor in keratinocytes is essential for murine skin barrier integrity. *J. Investig. Dermatol.* **2016**, *136*, 2260–2269. [CrossRef] [PubMed]
36. Kypriotou, M.; Huber, M.; Hohl, D. The human epidermal differentiation complex: Cornified envelope precursors, S100 proteins and the 'fused genes' family. *Exp. Dermatol.* **2012**, *21*, 643–649. [CrossRef]
37. Böhme, M.; Söderhäll, C.; Kull, I.; Bergström, A.; van Hage, M.; Wahlgren, C.F. Filaggrin mutations increase the risk for persistent dry skin and eczema independent of sensitization. *J. Allergy Clin. Immunol.* **2012**, *129*, 1153–1155. [CrossRef] [PubMed]
38. Kawasaki, H.; Nagao, K.; Kubo, A.; Hata, T.; Shimizu, A.; Mizuno, H.; Yamada, T.; Amagai, M. Altered stratum corneum barrier and enhanced percutaneous immune responses in filaggrin-null mice. *J. Allergy Clin. Immunol.* **2012**, *129*, 1538–1546. [CrossRef] [PubMed]
39. Palmer, C.N.; Irvine, A.D.; Terron-Kwiatkowski, A.; Zhao, Y.; Liao, H.; Lee, S.P.; Goudie, D.R.; Sandilands, A.; Campbell, L.E.; Smith, F.J.; et al. Common loss-of-function variants of the epidermal barrier protein filaggrin are a major predisposing factor for atopic dermatitis. *Nat. Genet.* **2006**, *38*, 441–446. [CrossRef] [PubMed]

40. Kawachi, Y.; Xu, X.; Taguchi, S.; Sakurai, H.; Nakamura, Y.; Ishii, Y.; Fujisawa, Y.; Furuta, J.; Takahashi, T.; Itoh, K.; et al. Attenuation of UVB-induced sunburn reaction and oxidative DNA damage with no alterations in UVB-induced skin carcinogenesis in Nrf2 gene-deficient mice. *J. Investig. Dermatol.* **2008**, *128*, 1773–1779. [CrossRef] [PubMed]
41. Saw, C.L.; Yang, A.Y.; Huang, M.T.; Liu, Y.; Lee, J.H.; Khor, T.O.; Su, Z.Y.; Shu, L.; Lu, Y.; Conney, A.H.; et al. Nrf2 null enhances UVB-induced skin inflammation and extracellular matrix damages. *Cell. Biosci.* **2014**, *4*, 39. [CrossRef] [PubMed]
42. Kim, Y.R.; Oh, J.E.; Kim, M.S.; Kang, M.R.; Park, S.W.; Han, J.Y.; Eom, H.S.; Yoo, N.J.; Lee, S.H. Oncogenic NRF2 mutations in squamous cell carcinomas of oesophagus and skin. *J. Pathol.* **2010**, *220*, 446–451. [CrossRef] [PubMed]
43. Choi, C.Y.; Kim, J.Y.; Wee, S.Y.; Lee, J.H.; Nam, D.H.; Kim, C.H.; Cho, M.K.; Lee, Y.J.; Nam, H.S.; Lee, S.H.; et al. Expression of nuclear factor erythroid 2 protein in malignant cutaneous tumors. *Arch. Plast. Surg.* **2014**, *41*, 654–660. [CrossRef] [PubMed]
44. Schäfer, M.; Farwanah, H.; Willrodt, A.H.; Huebner, A.J.; Sandhoff, K.; Roop, D.; Hohl, D.; Bloch, W.; Werner, S. Nrf2 links epidermal barrier function with antioxidant defense. *EMBO Mol. Med.* **2012**, *4*, 364–379. [CrossRef] [PubMed]
45. Schäfer, M.; Willrodt, A.H.; Kurinna, S.; Link, A.S.; Farwanah, H.; Geusau, A.; Gruber, F.; Sorg, O.; Huebner, A.J.; Roop, D.R.; et al. Activation of Nrf2 in keratinocytes causes chloracne (MADISH)-like skin disease in mice. *EMBO Mol. Med.* **2014**, *6*, 442–457. [CrossRef] [PubMed]
46. Rolfs, F.; Huber, M.; Kuehne, A.; Kramer, S.; Haertel, E.; Muzumdar, S.; Wagner, J.; Tanner, Y.; Böhm, F.; Smola, S.; et al. Nrf2 Activation Promotes Keratinocyte Survival during Early Skin Carcinogenesis via Metabolic Alterations. *Cancer Res.* **2015**, *75*, 4817–4829. [CrossRef] [PubMed]
47. Wang, D.; Ma, Y.; Yang, X.; Xu, X.; Zhao, Y.; Zhu, Z.; Wang, X.; Deng, H.; Li, C.; Gao, F.; et al. Hypermethylation of the Keap1 gene inactivates its function, promotes Nrf2 nuclear accumulation, and is involved in arsenite-induced human keratinocyte transformation. *Free Radic. Biol. Med.* **2015**, *89*, 209–219. [CrossRef] [PubMed]
48. Działo, M.; Mierziak, J.; Korzun, U.; Preisner, M.; Szopa, J.; Kulma, A. The potential of plant phenolics in prevention and therapy of skin disorders. *Int. J. Mol. Sci.* **2016**, *17*, 160. [CrossRef] [PubMed]
49. Amakura, Y.; Tsutsumi, T.; Nakamura, M.; Kitagawa, H.; Fujino, J.; Sasaki, K.; Yoshida, T.; Toyoda, M. Preliminary screening of the inhibitory effect of food extracts on activation of the aryl hydrocarbon receptor induced by 2,3,7,8-tetrachlorodibenzo-p-dioxin. *Biol. Pharm. Bull.* **2002**, *25*, 272–274. [CrossRef] [PubMed]
50. Amakura, Y.; Tsutsumi, T.; Sasaki, K.; Yoshida, T.; Maitani, T. Screening of the inhibitory effect of vegetable constituents on the aryl hydrocarbon receptor-mediated activity induced by 2,3,7,8-tetrachlorodibenzo-p-dioxin. *Biol. Pharm. Bull.* **2003**, *26*, 1754–1760. [CrossRef] [PubMed]
51. Amakura, Y.; Tsutsumi, T.; Sasaki, K.; Nakamura, M.; Yoshida, T.; Maitani, T. Influence of food polyphenols on aryl hydrocarbon receptor-signaling pathway estimated by in vitro bioassay. *Phytochemistry* **2008**, *69*, 3117–3130. [CrossRef] [PubMed]
52. Van den Bogaard, E.H.; Bergboer, J.G.; Vonk-Bergers, M.; van Vlijmen-Willems, I.M.; Hato, S.V.; van der Valk, P.G.; Schröder, J.M.; Joosten, I.; Zeeuwen, P.L.; Schalkwijk, J. Coal tar induces AHR-dependent skin barrier repair in atopic dermatitis. *J. Clin. Investig.* **2013**, *123*, 917–927. [CrossRef] [PubMed]
53. Kohda, F.; Takahara, M.; Hachiya, A.; Takei, K.; Tsuji, G.; Yamamura, K.; Furue, M. Decrease of reactive oxygen species and reciprocal increase of nitric oxide in human dermal endothelial cells by *Bidens. pilosa* extract: A possible explanation of its beneficial effect on livedo vasculopathy. *J. Dermatol. Sci.* **2013**, *72*, 75–77. [CrossRef] [PubMed]
54. Na, H.K.; Surh, Y.J. Modulation of Nrf2-mediated antioxidant and detoxifying enzyme induction by the green tea polyphenol EGCG. *Food Chem. Toxicol.* **2008**, *46*, 1271–1278. [CrossRef] [PubMed]
55. Han, S.G.; Han, S.S.; Toborek, M.; Hennig, B. EGCG protects endothelial cells against PCB 126-induced inflammation through inhibition of AhR and induction of Nrf2-regulated genes. *Toxicol. Appl. Pharmacol.* **2012**, *261*, 181–188. [CrossRef] [PubMed]
56. Mukai, R.; Shirai, Y.; Saito, N.; Fukuda, I.; Nishiumi, S.; Yoshida, K.; Ashida, H. Suppression mechanisms of flavonoids on aryl hydrocarbon receptor-mediated signal transduction. *Arch. Biochem. Biophys.* **2010**, *501*, 134–141. [CrossRef] [PubMed]

57. Zillich, O.V.; Schweiggert-Weisz, U.; Hasenkopf, K.; Eisner, P.; Kerscher, M. Release and in vitro skin permeation of polyphenols from cosmetic emulsions. *Int. J. Cosmet. Sci.* **2013**, *35*, 491–501. [CrossRef] [PubMed]
58. Takei, K.; Mitoma, C.; Hashimoto-Hachiya, A.; Takahara, M.; Tsuji, G.; Nakahara, T.; Furue, M. Galactomyces fermentation filtrate prevents T helper 2-mediated reduction of filaggrin in an aryl hydrocarbon receptor-dependent manner. *Clin. Exp. Dermatol.* **2015**, *40*, 786–793. [CrossRef] [PubMed]
59. Netsch, M.I.; Gutmann, H.; Schmidlin, C.B.; Aydogan, C.; Drewe, J. Induction of CYP1A by green tea extract in human intestinal cell lines. *Planta Med.* **2006**, *72*, 514–520. [CrossRef] [PubMed]
60. Wu, Z.; Uchi, H.; Morino-Koga, S.; Shi, W.; Furue, M. Z-ligustilide ameliorated ultraviolet B-induced oxidative stress and inflammatory cytokine production in human keratinocytes through upregulation of Nrf2/HO-1 and suppression of NF-κB pathway. *Exp. Dermatol.* **2015**, *24*, 703–708. [CrossRef] [PubMed]
61. Wu, Z.; Uchi, H.; Morino-Koga, S.; Nakamura-Satomura, A.; Kita, K.; Shi, W.; Furue, M. Z-Ligustilide inhibits benzo(a)pyrene-induced CYP1A1 upregulation in cultured human keratinocytes via ROS-dependent Nrf2 activation. *Exp. Dermatol.* **2014**, *23*, 260–265. [CrossRef] [PubMed]
62. Saw, C.L.; Guo, Y.; Yang, A.Y.; Paredes-Gonzalez, X.; Ramirez, C.; Pung, D.; Kong, A.N. The berry constituents quercetin, kaempferol, and pterostilbene synergistically attenuate reactive oxygen species: Involvement of the Nrf2-ARE signaling pathway. *Food Chem. Toxicol.* **2014**, *72*, 303–311. [CrossRef] [PubMed]
63. Tamaki, N.; Cristina Orihuela-Campos, R.; Inagaki, Y.; Fukui, M.; Nagata, T.; Ito, H.O. Resveratrol improves oxidative stress and prevents the progression of periodontitis via the activation of the Sirt1/AMPK and the Nrf2/antioxidant defense pathways in a rat periodontitis model. *Free Radic. Biol. Med.* **2014**, *75*, 222–229. [CrossRef] [PubMed]
64. Wu, Z.; Uchi, H.; Morino-Koga, S.; Shi, W.; Furue, M. Resveratrol inhibition of human keratinocyte proliferation via SIRT1/ARNT/ERK dependent downregulation of aquaporin 3. *J. Dermatol. Sci.* **2014**, *75*, 16–23. [CrossRef] [PubMed]

nutrients

MDPI

Article

Inhibition of Neoplastic Transformation and Chemically-Induced Skin Hyperplasia in Mice by Traditional Chinese Medicinal Formula Si-Wu-Tang

Mandy M. Liu [1], Kevin M. Huang [1], Steven Yeung [1], Andy Chang [1], Suhui Zhang [2,3], Nan Mei [3], Cyrus Parsa [4], Robert Orlando [4] and Ying Huang [1,*]

1 Department of Pharmaceutical Sciences, College of Pharmacy, Western University of Health Sciences, Pomona, CA 91766, USA; mmliu@westernu.edu (M.M.L.); huang.2834@buckeyemail.osu.edu (K.M.H.); skyeung@westernu.edu (S.Y.); chang.andy.y@gmail.com (A.C.)

2 Department of Pharmacology and Toxicology, Shanghai Institute for Food and Drug Control, Shanghai 201203, China; suhuizhangbc@gmail.com

3 Division of Genetic and Molecular Toxicology, National Center for Toxicological Research, Jefferson, AR 72079, USA; nan.mei@fda.hhs.gov

4 Department of Clinical Sciences, College of Osteopathic Medicine, Western University of Health Sciences, Pomona, CA 91766, USA; cparsa@westernu.edu (C.P.); rorlando@beverly.org (R.O.)

* Correspondence: yhuang@westernu.edu; Tel.: +1-909-469-5220

Received: 9 February 2017; Accepted: 12 March 2017; Published: 18 March 2017

Abstract: Exploring traditional medicines may lead to the development of low-cost and non-toxic cancer preventive agents. Si-Wu-Tang (SWT), comprising the combination of four herbs, Rehmanniae, Angelica, Chuanxiong, and Paeoniae, is one of the most popular traditional Chinese medicines for women's diseases. In our previous studies, the antioxidant Nrf2 pathways were strongly induced by SWT in vitro and in vivo. Since Nrf2 activation has been associated with anticarcinogenic effects, the purpose of this study is to evaluate SWT's activity of cancer prevention. In the Ames test, SWT demonstrated an antimutagenic activity against mutagenicity induced by the chemical carcinogen 7,12-dimethylbenz(a)anthracene (DMBA). In JB6 P+ cells, a non-cancerous murine epidermal model for studying tumor promotion, SWT inhibited epidermal growth factor (EGF)-induced neoplastic transformation. The luciferase reporter gene assays demonstrated that SWT suppressed EGF-induced AP-1 and TNF-α-induced NF-κB activation, which are essential factors involved in skin carcinogenesis. In a DMBA-induced skin hyperplasia assay in 'Sensitivity to Carcinogenesis' (SENCAR) mice, both topical and oral SWT inhibited DMBA-induced epidermal hyperplasia, expression of the proliferation marker Proliferating cell nuclear antigen (PCNA), and H-*ras* mutations. These findings demonstrate, for the first time, that SWT prevents tumor promoter and chemical-induced carcinogenesis in vitro and in vivo, partly by inhibiting DNA damage and blocking the activation of AP-1 and NF-κB.

Keywords: cancer prevention; DMBA; skin cancer; AP-1; NF-κB; SWT; SENCAR mice; EGF; JB6; Ames test

1. Introduction

Traditional Chinese herbal medicines provide a rich source for the development of alternative and complimentary medicines for cancer therapy and prevention. Si-Wu-Tang [SWT, Si-Wu decoction (Chinese name), Samultang (Korean name), or Shimotsu-to (Japanese name)], comprising the combination of four herbs: Paeoniae (*Radix paeonia alba*), Angelicae (*Radix angelica Sinensis*), Chuanxiong (*Rhizoma chuanxiong*), and Rehmanniae (*Radix rehmanniae preparata*), is one of the most popular traditional medicines for women's health [1]. It has been used in Eastern Asia for more than one

thousand years and ranks first as the most frequently used Chinese medicines [2]. It is an inexpensive over-the-counter preparation used for the relief of menstrual discomfort, climacteric syndrome, peri- or post-menopausal syndromes and other estrogen-related diseases [1–5]. In previous animal studies, SWT has shown sedative, anti-coagulant, and anti-bacterial activities, as well as a protective effect on radiation-induced bone marrow damage [6,7]. Several in vitro and in vivo studies show a preventive activity of SWT on endometrial carcinogenesis induced by chemical carcinogen sand estrogen [8,9]. However, the mechanisms and bioactive constituents mediating these effects are unknown.

The nuclear factor erythroid 2-related factor 2 (Nrf2), a basic zip (bZIP) transcription factor, is a key molecule that regulates detoxifying and antioxidant genes [10]. The Nrf2 pathway has become a promising molecular target for the chemoprevention of cancer (for review, see [11]). Using DNA microarray and connectivity map-based analysis of the gene expression profiles in the MCF-7 breast cancer cells, our previous studies revealed the potential mechanism of SWT, which involves the activation of Nrf2-regulated antioxidant genes, such as *HMOX1*, *GCLC*, *GCLM*, *SLC7A11*, and *NQO1* [12]. We further provide experimental evidence to show that SWT protected cells against oxidative stress, and enhanced the translocation of Nrf2 into the nucleus in non-cancerous mammary epithelial cells [13]. In a study using healthy Sprague−Dawley rats to evaluate the in vivo pharmacodynamic effect of SWT, short-term oral administration of SWT (1000 mg/kg per day for six consecutive days) caused an increased expression of Nrf2-regulated genes *Hmox1* and *Slc7A11* in the liver [13]. In addition, SWT has been previously reported to have a suppressive effect on estrogen-induced inflammatory enzyme COX-2 [14].

Since carcinogenesis involves multiple abnormal genes/pathways, using an herbal formula, such as SWT, may be superior to agents that target a single molecular event. While there are other natural products known as Nrf2 activators, SWT provides a good option due to multiple mechanisms and its clinical safety record. Therefore, in the present study, we investigated SWT's effect on mutagenicity and carcinogenesis in several in vitro and in vivo model systems, mainly of skin cancer. We further explored possible mechanisms that may underlie the chemopreventive effects. Based on these experimental data, we predict that the chemopreventive activity of SWT is not limited to skin cancer, but with a broad application for other types of cancer associated with oxidative stress.

2. Materials and Methods

2.1. Compounds

7,12-dimethylbenz[a]anthracene (DMBA) and 2-nitrofluorene were purchased from Sigma-Aldrich (St. Louis, MO, USA). EGF was purchased from Peprotech (Rocky Hill, NJ, USA) and dissolved in sterile deionized water as 100 μg/mL stock and stored at −20 °C in a freezer.

2.2. Preparation of Herbal Extracts

The SWT extract and its component single herb extracts were kindly provided by Dr. Z. Zuo at the School of Pharmacy, Chinese University of Hong Kong. These products were manufactured under Good Manufacturing Practice (GMP) conditions at the Hong Kong Institute of Biotechnology (Hong Kong, China) according to the protocol described in Chinese Pharmacopoeia 2005 [15] with slight modification. Therefore, these products are named as 'Chinese University-SWT' ('CU-SWT'), and the single herb extracts named as CU-Angelicae, CU-Chuanxiong, CU-Paeoniae, and CU-Rehmanniae. The formulae were made in solid dosages (powder form). The sources and ratio of the herbal components, as well as chemical fingerprints of the SWT product used in this study, have been described before [1]. In brief, Angelicae and Chuanxiong (2.5 kg each) were soaked in water for 0.5 h followed by steam distillation, after which the volatile oil phase, aqueous phase, and the solid residues were collected. To 2.5 L volatile oil, 125 g hydroxypropyl-beta-cyclodextrin was added, and the vessel was covered to protect from light during mixing by magnetic stirring at room temperature for one hour. To the residue of the herbs, Paeoniae and Rehmanniae (2.5 kg each) were added and decocted

with boiling water three times, successively. All of the aqueous phase solutions from each decoction were combined. The aqueous and oil phase extracts were spray dried and freeze dried, respectively, to produce the corresponding powders before combining to obtain the final product. Previous study has developed methods to identify markers in SWT products [1]. Five compounds are detectable in all batches of SWT extracts, including 'CU-SWT' used in this study. For the compounds paeoniflorin, ferulic acid, gallic acid, z-Liguistilide, and senkyunolide A, the CU-SWT extract contains 0.82%, 0.076%, 0.084%, 0.14% and 0.0082%, respectively. The preparation of single herb products was also carried out according to the aforementioned procedure. The herbal solutions were prepared fresh from powder right before the experiment in medium and sonicated for 30 min. The powders were only partially dissolved. Without centrifugation, the whole solutions were added to the cell culture experiments described below (Sections 2.7–2.9).

2.3. Bacterial Strains and Growth Conditions

The *Salmonella typhimurium* strain TA100 is a histidine-requiring mutant, as previously described by Maron and Ames [16], and was purchased from MOLTOX (Boone, NC, USA) and stored at −80 °C. Tests of histidine requirements, as well as the genotypes of *rfa*, *uvr*B mutation, and R factor, were carried out to confirm the genotypes of TA100 (data not shown). TA100 contains the base-pair substitution mutation hisG46. It was grown for 10 h with gentle shaking in nutrient broth No. 2 (Oxoid, Hampshire, UK) at 37 °C.

2.4. Mutagenicity Testing

The test was conducted based on the plates incorporation method [16], using TA100 with or without exogenous metabolic activation system S9, purchased from MOLTOX (Boone, NC, USA). The Ames test without S9 can only detect direct mutagens, while with S9 metabolic activation allows the detection of indirect mutagens, often caused by conjugation reactions of metabolic oxidation systems [16]. Various concentrations of SWT were added to the top agar (2.5 mL), supplemented with 0.5 mM L-histidine and 0.5 mM D-biotine, mixed with 100 μL of bacterial culture (approximately 1.4–1.6 × 10^8 cells), and then poured onto a minimal glucose agar plate and incubated at 37 °C for 48 h before counting the his+ revertant colonies. Five hundred microliters of S9 mixture were added into top agar (2.0 mL) to test the influence of metabolic activation. Dimethyl sulfoxide (DMSO) was added into the top agar as a negative control group. The number of revertants per plate in the negative control and positive control groups were within the normal limits found in our laboratory. The data were collected in mean ± SD in three plates (n = 3).

2.5. Antimutagenicity Testing

Using a procedure the same as the mutagenicity testing was employed to determine the effect of SWT on mutagenicity induced by 2-nitrofluorene or DMBA. The test agents, together with S9 mix (500 μL), mutagens (100 μL), SWT (100 μL), and 100 μL of bacteria culture, were added into 2 mL or 2.5 mL of top agar. The plates were incubated at 37 °C for 48 h and then the his+ revertant colonies were counted. The inhibition rate of mutagenicity (%) was calculated using the following equation:

$$\text{Inhibition rate (\%)} = 1 - (A/B) \times 100\% \quad (1)$$

where A is the number of revertants per plate in the presence of direct or indirect mutagen and SWT, and B is the number of revertants per plate in positive control group.

2.6. Cell Culture

JB6 CI 41-5a (JB6 P+), sensitive to the promotion of transformation mouse epidermal cells, were purchased from American Type Culture Collection (ATCC, Manassas, VA, USA). JB6 P+ were maintained in Eagle's minimum essential medium (EMEM) containing 4% heat-inactivated fetal bovine

serum and 1% penicillin/streptomycin. The HEK-293 cells and MCF-7 cells were obtained from ATCC, cultured in DMEM, supplemented with 10% FBS and 1% penicillin-streptomycin. All cells from cell culture experiments were incubated at 37 °C in 5% CO_2/95% air.

2.7. Anchorage-Independent Growth Assay in Soft Agar

In a 96-well tissue culture plate, 2000 JB6 P+ cells per well were mixed with 0.33% agar suspended on top of a layer of 0.5% agar. Epidermal growth factor (EGF) (10 ng/mL) was used to promote the anchorage-independent growth of JB6 cells. Various concentrations of SWT were added together with EGF into the top and bottom layers of the agar. Plates were incubated at 37 °C for 7–10 days. Colonies with greater than ten cells were counted and images were taken using EVOS Cell Imaging Systems (Thermo Fisher Scientific, Waltham, MA, USA).

2.8. Cell Proliferation Assay

Ninety six-well plates were seeded with 3000–4000 JB6 P+ cells per well and allowed to attach overnight. Cells were treated with test compounds for 72 h and incubated at 37 °C in 5% CO_2/95% air. Cell viability was determined using Sulforhodamine B (SRB) assay (Sigma) according to the manufacturer's protocol.

2.9. Luciferase Reporter Gene Assay

HEK-293 or MCF-7 cells were transfected with pGL4.22-AP1 (gift from Dr. D. Sanchez) or pGL4.22-NF-κB (Promega, Madison, WI, USA), mixed with pRL-TK-luc (Promega) at a 40:1 ratio using FuGENE HD Transfection Reagent (Roche, Indianapolis, IN, USA) according to the manufacturer's instructions. Twenty-four hours after transfection, the cells were exposed to test agents for another 24 h (for AP-1) or 5 h (for NF-κB). Cell lysates were used for determining luciferase activities of both firefly and renilla by the dual luciferase reporter gene assay (Promega). Firefly luciferase activity was normalized to renilla luciferase activity. The experiment was carried out in triplicate and expressed as the mean ± SD.

2.10. Model of Chemically-Induced Murine Skin Hyperplasia

All animal studies were carried out in strict accordance with the recommendations in the Guide for the Care and Use of Laboratory Animals of the National Institutes of Health, and approved by the Western University of Health Sciences Institutional Animal Care and Use Committees. Five-week-old female SENCAR mice (National Cancer Institute, Frederick, MD, USA) were divided into six groups (n = 6 or 8) and the backs of mice shaved. At seven weeks of age, 100 nmol DMBA dissolved in 200 μL acetone was applied topically twice weekly for four weeks. SWT treatment started when mice were five weeks of age, twice weekly, topically in two doses (0.64 and 1.28 mg/mL in 200 μL acetone) 30 min before DMBA exposure, or orally by gavage in two doses (200 and 1000 mg/kg in 1% methyl cellulose in PBS) 2 h before DMBA exposure. Two days after the last treatment mice were sacrificed, and samples of skin were excised and fixed immediately in formalin and embedded in paraffin blocks. The embedded tissues were cut into 3-micron thick sections and stained with H&E to determine the morphology. The images were obtained by EVOS; the epidermal thickness was measured using a Nikon Live-Cell Imaging system (Melville, NY, USA).

2.11. Immunohistochemistry (IHC) Analysis

Paraffin-embedded sections were baked at 60 °C for one hour and deparaffinized in a xylene solution and rehydrated through a graded series of ethanol. The antigen was retrieved using a citrate buffer (pH 6.0) for 20 min at 95 °C. Briefly, sections were blocked by 10% normal goat serum for 2 h followed by overnight incubation at 4 °C with 1:1000 dilution of the proliferation cell nuclear antigen (PCNA; Cell Signaling Technologies, Danvers, MA, USA) primary antibody. Sections were then

incubated for 2 h with 1:5000 dilution of an horseradish peroxidase (HRP) secondary antibody, followed by 5-min incubation with DAB substrate (Vector labs; Burlingame, CA, USA) and counterstained with Mayer's hematoxylin.

2.12. Competitive Allele-Specific TaqMan PCR (castPCR) Assay

Genomic DNA was isolated from frozen skin tissues by DNAzol (MRC, Inc., Charleston, WV, USA) according to the protocol provided by the manufacturer. CastPCR was performed with TaqMan Mutation Detection Assay designed to detect CAA → CTA transversion in codon 61 of the mouse H-*ras* gene (Applied Biosystems by Life Technologies, Foster City, CA, USA) following the manufacturer's instruction. The castPCR was run on a GeneAmp 7300 Sequence Detection system (Applied Biosystems, Foster City, CA, USA) using the universal mutation detection thermal-cycling protocol. The mutational status of a sample was determined by calculating the ΔCt value between the mutant allele assay and wild-type allele assay to obtain the percent mutation according to manufacturer's instruction.

2.13. Statistical Analysis

All in vitro data are expressed as the mean ± standard deviation of three independent experiments under the same experimental conditions, and in vivo data are expressed as the mean ± standard error. The one-way ANOVA test was used to analyze the results and a p value < 0.05 was denoted as significant. Variants of statistical analysis are otherwise stated in figure legends.

3. Results

3.1. Mutagenic and Antimutagenic Activity of SWT

SWT was firstly evaluated for mutagenic and antimutagenic activity using the Ames test, conducted using the *S. typhimurium* TA100 bacterial strain in the presence or absence of the metabolic activator S9 system. Two reference mutagens were used as positive controls: the direct mutagen 2-nitrofluorene (−S9), and the indirect mutagen DMBA (+S9). Both of them (10 μg/plate) caused a strong mutagenic effect (Table 1: 27 and 11-fold increases in the number of revertant colonies in comparison with the negative controls for direct and indirect mutagens, respectively). However, no cytotoxic (i.e., normal bacterial lawn) and no mutagenic (i.e., similarly numbers of revertant colonies as negative controls) activities were observed for all doses tested for SWT up to 5 mg per place in the presence or absence of the S9 system. This result indicates that SWT within the concentration range tested may not be mutagenic nor be metabolized into mutagens. Since mutagenicity is correlated with carcinogenicity [17], this result suggests that it is potentially safe to use SWT (up to 5 mg/plate) as a preventive agent for healthy individuals even at higher doses.

Table 1. Mutagenic activities and antimutagenic activities of SWT with or without S9.

Group	Dose (μg/plate)	−S9		+S9	
		Count	Inhibition (%)	Count	Inhibition (%)
Negative	-	132 ± 6	-	130 ± 25	-
Positive	10	3547 ± 1086	-	1409 ± 595	-
SWT	1250	125 ± 14	-	136 ± 3	-
SWT	2500	138 ± 13	-	123 ± 3	-
SWT	5000	141 ± 6	-	131 ± 6	-
SWT + Positive	1250 + 10	2688 ± 296	24.2	1246 ± 239	11.6
SWT + Positive	2500 + 10	2669 ± 282	23.9	1141 ± 129	19.0
SWT + Positive	5000 + 10	2987 ± 599	15.8	639 ± 147	54.6 **

Negative control: DMSO; Positive control: 2-Nitrofluorene (−S9); DMBA (+S9). **: significance compared to positive control group at $p < 0.01$ ($n = 3$).

When combined with mutagens, SWT at doses <5 mg/plate did not show an effect of inhibition on mutagenicity induced by the direct mutagen 2-nitrofluorene (−S9) (Table 1). However, significant antimutagenic activity ($p < 0.05$) was observed in doses of 5 mg/plate against the mutagenicity induced by DMBA (Table 1). Since antimutagenic agents can possibly also be anticarcinogens, these results indicate that SWT may protect cells against harmful effects resulting from the indirect mutagen DMBA. These results are consistent with the results obtained from the in vivo study described below, which uses DMBA as a carcinogen.

3.2. Effects of SWT on EGF-Induced Neoplastic Transformation of JB6 P+ Cells

We next examined the effects of SWT on EGF-mediated neoplastic transformation of the mouse epidermal JB6 P+ cell line, which is a well-characterized model for studying cellular response to various tumor promoters [18]. Since EGF and its receptor (EGFR) have been reported as an important signaling pathway leading to cancer, EGF was used to promote JB6 transformation. When treated with EGF, the transformation sensitive P+ cells acquired anchorage-independent growth, i.e., colony formation in soft agar. Treatment with SWT resulted in drastic inhibition of EGF-induced transformation and colony formation in a dose-dependent manner compared to the number of colonies induced by EGF alone (Figure 1A). Representative images of colonies in soft agar are shown in Figure 1B.

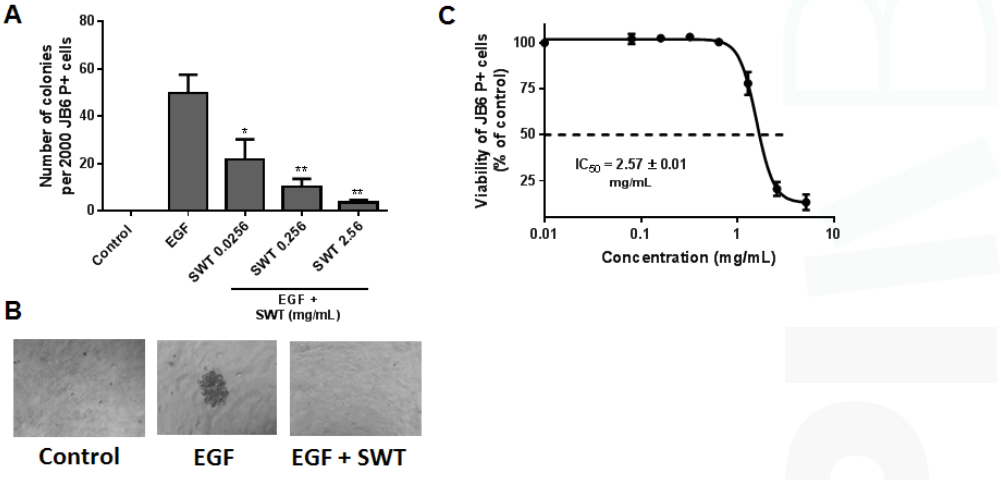

Figure 1. Effects of SWT extract on EGF-mediated neoplastic cell transformation and colony formation in JB6 P+ cells. (**A**) Soft agar assay data for JB6 P+ cells treated with EGF (10 ng/mL) alone or together with SWT at three concentrations. Colonies greater than ten cells were counted manually under a microscope. Data represents a mean ± standard deviation (n = 6-12). *: $p < 0.05$; **: $p < 0.01$, compared to EGF only group; (**B**) representative images of colonies during the soft agar assay after a 10 day incubation period; and (**C**) the cytotoxic effects of SWT on JB6 P+ cells were examined using an SRB assay. Results are expressed as percentage of viability versus control cells with no drug treatment.

As the soft agar assay is dependent on cell viability, we conducted sulforhodamine B (SRB) colorimetric assay for evaluating the effects of SWT on cell growth and cytotoxicity. Treatment of JB6 P+ cells with SWT was non-toxic at concentrations lower than 0.3 mg/mL, while higher concentrations caused growth inhibition (IC_{50} = 2.57 ± 0.01 mg/mL) (Figure 1C). Thus, SWT at the non-toxic concentrations 0.0256 and 0.256 mg/mL inhibited EGF-mediated colony formation due to a direct effect on tumor promotion (Figure 1A), while the colony inhibitory effect of SWT at 2.56 mg/mL may be attributed to a mixed activity of anti-promotion and cytotoxicity. Since the JB6 P+ transformation

assay has a positive predictive value for in vivo efficacy of chemopreventive agents [19], this result indicates that SWT may have chemopreventive activity at non-toxic concentrations and cytotoxic action at higher concentrations.

The soft agar assay experiment was also conducted to examine whether the four herbal components of SWT can also inhibit EGF-induced colony formation in JB6 P+ cells. The results showed that all extracts possess strong and significant chemopreventive activity at higher concentration (2.56 mg/mL) (Figure 2). Among the four herbs, Paeoniae (PR) showed the highest potency because, at 1.28 mg/mL, it completely blocked the colony formation. However, this effect may be due to cytotoxicity. SRB assay showed that the IC_{50} for Paeoniae in JB6 P+ cells was 0.5 mg/mL, while IC_{50} of the other three components was higher than 2.56 mg/mL (data not shown). Therefore, PR may contain the most toxic constituents of SWT. At lower concentrations (0.256 and 1.28 mg/mL), the other three extracts slightly increased EGF-induced colony formation, although such effect is significant only for Chuanxiong (CR). Unlike SWT (Figure 1), none of the four herbs showed significant inhibitory effect at a concentration of 0.256 mg/mL. Thus, SWT showed superior activity against tumor promotion which cannot be simply attributed to an additive effect of mixing four herbs. A synergistic mechanism is possible leading to a unique SWT formula which is not only more effective but also less toxic.

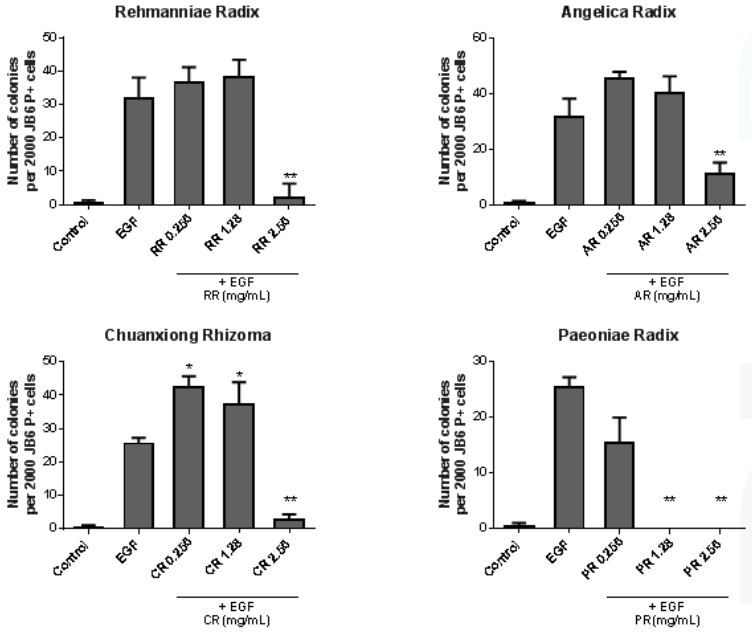

Figure 2. Effects of four single herbal components of SWT on EGF-induced malignant transformation of JB6 P+ cells. Soft agar assay was conducted on JB6 P+ cells treated with EGF (10 ng/mL) and/or SWT herbal components at three concentrations. Colonies greater than ten cells were counted manually under a microscope. Data represents a mean ± standard deviation (n = 6-12). *: $p < 0.05$; **: $p < 0.01$, compared to EGF only group.

3.3. SWT on EGF-Induced AP-1 Activation

AP-1 is a major transcription factor involved in EGF-induced transformation of JB6 P+ cells [20]. To further explore SWT's possible mechanisms of action, its effect on EGF-mediated activation of AP-1 was evaluated. The HEK-293 cells were transfected with AP-1 firefly luciferase reporter and the renilla luciferase control reporter. The transfected cells were treated with vehicle (control), SWT (0.025,

0.256, and 2.56 mg/mL), followed by a 24-h co-incubation with EGF (10 ng/mL). As can been seen in Figure 3A, SWT significantly inhibited EGF-mediated AP-1 activity in a dose-dependent manner ($p < 0.01$). These results indicated that inhibition of AP-1 activation by SWT may partly explain the mechanism underlying the inhibitory activity against EGF-induced cell transformation. Since variety of agents that inhibit AP-1 has been reported as mechanism(s) of chemoprevention [20], and another possible target for SWT is AP-1.

3.4. Effects of SWT on TNF-α-Induced NF-κB Activation

To evaluate the effect of SWT on inducible NF-κB activation, the breast cancer MCF-7 cells were transfected with NF-κB-luc reporter construct and a plasmid encoding renilla luciferase. The transfected cells were treated with vehicle (control), SWT (0.256 and 2.56 mg/mL), followed by a 5-h co-incubation with TNF-α (20 ng/mL). NF-κB activity was measured by a dual luciferase reporter gene assay. TNF-α stimulated NF-κB activity, and this activity was inhibited by SWT (Figure 3B). Since previous findings support a role for NF-κB in promoting carcinogenesis [21], our results suggest that therapeutic targeting of the NF-κB by SWT might be one of the mechanisms of SWT in prevention of cancer.

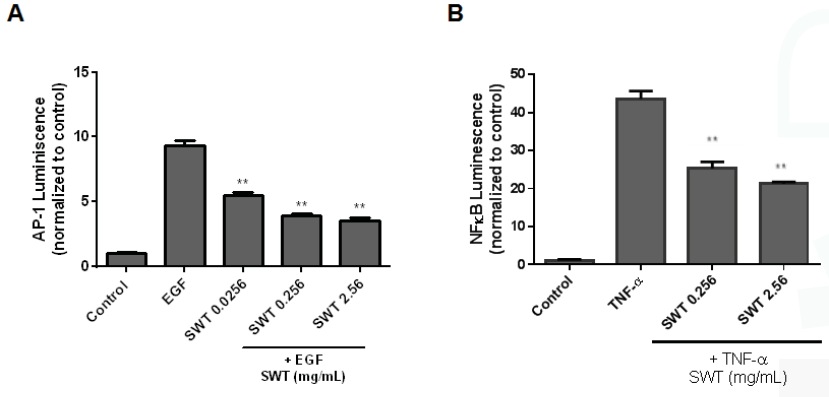

Figure 3. Effects of SWT on AP-1 and NF-κB activation. (**A**) Luciferase assay using HEK-293 cells co-transfected with a plasmid containing an AP-1-luciferase reporter gene (pGL4.22-AP1) and a plasmid encoding renilla luciferase (pGL4.74). The transfected cells were treated with EGF (10 ng/mL) and SWT for 24 h prior to measurement of firefly and renilla luciferase activities using the dual luciferase reporter gene assay; and (**B**) luciferase assay using MCF-7 cells co-transfected with a plasmid containing an NF-κB-luciferase reporter gene (pGL4.22-NF-κB) and a plasmid encoding renilla luciferase (pGL4.74). The transfected cells were treated with TNF-α (20 ng/mL) and SWT for 5 h prior to measurement of firefly and renilla luciferase activities using the dual luciferase reporter gene assay. **: $p < 0.01$.

3.5. Effects of SWT on DMBA-Induced Skin Hyperplasia in SENCAR Mice

To determine the in vivo chemopreventive activity of SWT, a DMBA-induced skin hyperplasia assay in SENCAR mice was utilized [22]. The experimental design is shown in Figure 4A. Epidermal hyperplasia was induced by topical treatments with DMBA for four weeks. The SWT treatments included two topical doses (0.64 and 1.28 mg/mL) and two oral doses (200 and 1000 mg/kg), beginning two weeks before the first dose of DMBA. During this study period, the treatments did not cause animal death; SWT did not cause any visible sign of toxicity or ill health, nor have any significant effect on body weight in mice (data not shown). Representative samples of the epidermis (H&E staining) are shown in Figure 4B. Epidermal thickness was measured 20 times at various locations along the epidermis and averaged to obtain a single sample's value (Figure 4C).

DMBA treatment increased the average epidermal thickness by 4.2-fold from 41.47 ± 14.88 μm in controls to 174.68 ± 47.57 μm in the DMBA group. Both topical and oral treatments resulted in significantly decreased epidermal thickness compared with the DMBA-treated group without obvious dose-dependent effect (Figure 4C). Analogous to the H&E data, immunohistochemical analysis indicated an increased expression of the proliferating cell nuclear antigen (PCNA) in the stratum basale of epidermis after DMBA treatment, while SWT treatment resulted in reducing the number of PCNA positive cells (Figure 4B).

One of the key events in tumor initiation in mouse skin is the mutation of H-*ras* at codon 61 (CAA → CTA) [23]. The Mutation Detection Assays based on Competitive Allele-Specific TaqMan PCR (castPCR) technology was used to assess H-*ras* mutations in mouse skin DNA samples. The castPCR is a highly specific and sensitive method for detecting and quantitating rare mutations in a sample that contains large amounts of normal, wild-type genomic DNA [24]. The results showed that the control mice had no mutations, while the DMBA treatment group harbored an average of 0.1% of the mutations (Figure 4D). The topical treatment by SWT dose-dependently inhibited the mutations induced by DMBA. The high dose topical group resulted in 7.6-fold reduction of the mutation induced by DMBA. For the oral treatment groups, low and high dose treatments resulted in a similar inhibitory effect as the high topical dose group, indicating oral route may also be effective for preventing the oncogenic mutations. These results indicate that SWT effectively blocked skin hyperplasia and tumor-initiating mutations induced by chemical carcinogens in vivo.

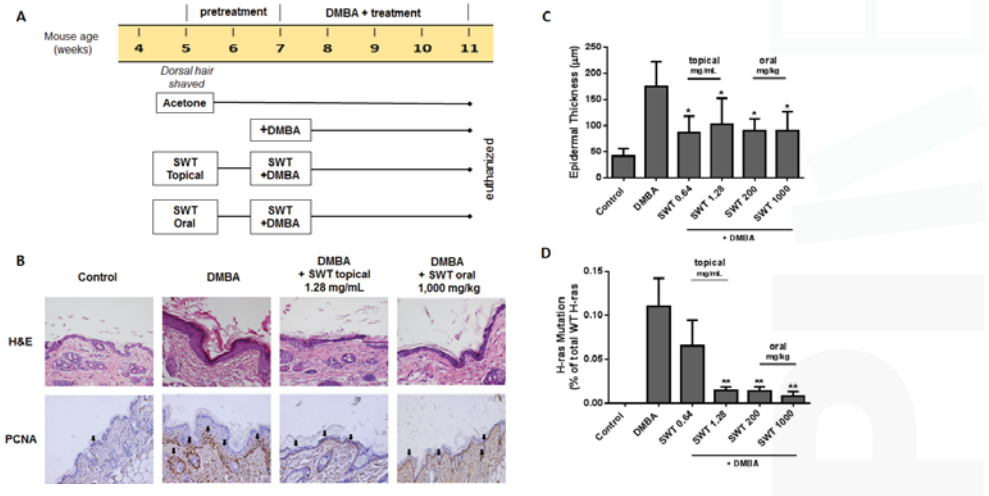

Figure 4. Effects of SWT on DMBA-induced hyperplasia and mutation of H-*ras* in SENCAR mice. (**A**) Experimental design; (**B**) microphotographs of H&E staining, and immunohistochemistry of PCNA to depict DMBA-induced skin hyperplasia and cell proliferation activity. Black arrow: positive PCNA cells in stratum basale of epidermis; (**C**) induction of epidermal thickness with DMBA and the effect of SWT. Data represents the mean ± standard error from repeated measurements of one sample at 20 locations along tissue; and (**D**) the percentage of H-*ras* codon 61 mutations (CAA → CTA) detected using castPCR. Statistical analysis was performed by ANOVA with Dunnett's multiple comparisons post-hoc test. *: $p < 0.05$; **: $p < 0.01$, compared to DMBA only group ($n = 6–8$).

4. Discussion

Many risk factors associated with skin carcinogenesis, including ultraviolet radiation and environmental pollutants, damage epidermal cells through the generation of high levels of reactive oxygen species (ROS) [25]. The formation of ROS can be both an initiator and promoter for skin

cancer. Protecting normal cells from the attack of ROS by increasing the cellular detoxifying and antioxidant machinery is a promising strategy to prevent cancer [26]. We previously reported that SWT activated Nrf2-regulated genes, which play an important role in cellular detoxification [12]. Therefore, in the present study we evaluated the cancer chemopreventive efficacy of SWT in vitro and in vivo. The mouse epidermal JB6 P+ cell line is a well-characterized model for studying neoplastic transformation in response to various tumor promoters and for screening chemopreventive agents [18]. EGF was used to promote transformation, because EGF and its receptor (EGFR) have been found as an important signaling pathway leading to cancer, including skin cancer [27]. Under EGF exposure, the transformation sensitive JB6 P+ cells acquired anchorage-independent growth and tumorigenicity. We found that SWT inhibited anchorage-independent growth of JB6 P+ cells on soft agar induced by EGF (Figure 1), which was further confirmed in vivo using DMBA-induced mouse skin hyperplasia assay (Figure 4). An Ames test was used to test the mutagenic and antimutagenic activities of SWT. Although SWT itself showed an absence of any mutagenic activity, at the dose of 5 mg/plate it exhibited significant inhibition on the reversion of *S. typhimurium* TA100 induced by the indirect mutagen DMBA in the presence of S9. This result indicated that SWT may protect cells against carcinogen-induced DNA damage. The same chemical carcinogen, DMBA, was used to induce skin hyperplasia and oncogenic mutation in mice, and our data confirmed SWT's protective effect in vivo. Although we cannot exclude any direct interaction between SWT components and DMBA, these results demonstrated SWT's anti-carcinogenic effects in vitro and in vivo. One of the possible targets for SWT is the Nrf2 molecule, which is expressed in all cell types of skin and is a key molecule in skin homeostasis [28]. The role of Nrf2 in skin carcinogenesis has been shown using knockout mice or with pharmacological activators of Nrf2 [28]. Other potential targets for SWT identified in our study are AP-1 and NF-κB, which are transcription factors implicated in EGF-induced skin tumor promotion [20]. Inhibition of AP-1 and NF-κB by a variety of agents has been shown as the major mechanism of chemoprevention [20]. It is likely that the multiple components in SWT trigger the signaling in multiple pathways. Alternatively, there may be a common signaling pathway modulating AP-1, NF-κB, and Nrf2 pathways. SWT has been reported by other groups with a suppressive effect on COX-2 [14], which is also involved in promoting skin carcinogenesis [29]. Since carcinogenesis involves multiple abnormal genes/pathways, using herbal medicines, such as SWT, with multiple potential targets may be superior to the agents targeting a single molecule alone. Although there are other natural products known as Nrf2 activators or AP-1/NF-κB inhibitors, SWT provides a good option as a chemopreventive agent due to its safety record. Further work is needed to identify the bioactive components and decipher which chemical components are responsible for these molecular changes. Further mechanistic studies, e.g., using animal models with gene deletion, are also needed to confirm the role of Nrf2, AP-1, and NF-κB in SWT's chemopreventive activity. Additional investigation is needed to identify which component(s) in the AP-1 and NF-κB signal transduction pathways are involved in activity of SWT. Both AP-1 and NF-κB are transcriptional factors playing a crucial role in the regulation of cell proliferation and transformation. The present report only conducted a pilot study using luciferase assay to examine the promoter activity of AP-1 and NF-κB. Among the common downstream effector genes of AP-1 and NF-κB, we used PCNA, which is regulated by both AP-1 and NF-κB. PCNA protein level was high in the DMBA-treated, but was reduced by SWT treatment in mouse skin (Figure 4). This result confirms the role of AP-1 and NF-κB mediating SWT's cancer preventive effect. It also remains to be determined whether SWT is able to prevent other types of cancer that are caused by environmental ROS and cellular oxidative stress.

Taken together, based on these in vitro and in vivo efficacy studies, we demonstrated the scientific evidence for SWT, one of the most popular herbal medicine formulas for women's health, can be used for skin cancer prevention. The preliminary mechanistic studies revealed several potential molecular targets although they may not be the direct targets that the active components bind to. Obviously further studies are needed to decipher the active components for observed effect in vitro

and in vivo. We predict that the chemopreventive activity of SWT should not be limited to skin cancer, but with a broader application for other types of cancer which involve ROS-related carcinogenesis.

Acknowledgments: We thank David Sanchez at Western University of Health Sciences for kindly providing the luciferase reporter construct pGL4.22-AP1. SWT and its herbal components were provided by Zhong Zuo at Chinese University of Hong Kong. The manufacturing of Si-Wu-Tang was supported by the Innovation and Technology Fund (ITS/112/07, PI: Zhong Zuo) from the Innovation and Technology Commission of the Hong Kong Special Administrative Region of the People's Republic of China. This work was partly supported by the Innovation and Technology Grants (ITS/112/07 and ITS/446/09) from the Innovation and Technology Commission of the Hong Kong Special Administrative Region of the People's Republic of China and by Western University of Health Sciences. Suhui Zhang from Shanghai Institute for Food and Drug Control (Shanghai, China) participated in the International Scientist Exchange Program (ISEP) at the National Center for Toxicological Research (NCTR) receiving funding from the Office of International Programs, the U.S., Food and Drug Administration (FDA). Funds for covering the costs to publish in open access are provided by Western University of Health Sciences.

Author Contributions: M.L. and K.M.H carried out most of the experiments and analyzed the data; S.Z. and N.M. conducted the Ames test; A.C. and S.Y. carried out the in vivo studies; S.Y. conducted the H-*ras* mutational assay; C.P. and R.O. contributed to the pathology analysis; Y.H. conceived the studies, coordinated the experiments, and wrote the manuscript. All authors read and approved the final manuscript.

Conflicts of Interest: Provisional patent application No. 62/261, 545. The founding sponsors had no role in the design of the study; in the collection, analyses, or interpretation of data; in the writing of the manuscript, and in the decision to publish the results. The information in this manuscript is not a formal dissemination of information by the U.S. FDA and does not represent agency position or policy.

References

1. Wang, Z.J.; Wo, S.K.; Wang, L.; Lau, C.B.; Lee, V.H.; Chow, M.S.; Zuo, Z. Simultaneous quantification of active components in the herbs and products of si-wu-tang by high performance liquid chromatography-mass spectrometry. *J. Pharm. Biomed. Anal.* **2009**, *50*, 232–244. [CrossRef] [PubMed]
2. Yeh, L.L.; Liu, J.Y.; Lin, K.S.; Liu, Y.S.; Chiou, J.M.; Liang, K.Y.; Tsai, T.F.; Wang, L.H.; Chen, C.T.; Huang, C.Y. A randomised placebo-controlled trial of a traditional chinese herbal formula in the treatment of primary dysmenorrhoea. *PLoS ONE* **2007**, *2*, e719. [CrossRef] [PubMed]
3. Ohta, H.; Ni, J.W.; Matsumoto, K.; Watanabe, H.; Shimizu, M. Peony and its major constituent, paeoniflorin, improve radial maze performance impaired by scopolamine in rats. *Pharmacol. Biochem. Behav.* **1993**, *45*, 719–723. [CrossRef]
4. Watanabe, H. Protective effect of a traditional medicine, shimotsu-to, on brain lesion in rats. *J. Toxicol. Sci.* **1998**, *23*, 234–236. [CrossRef] [PubMed]
5. Zhang, H.; Shen, P.; Cheng, Y. Identification and determination of the major constituents in traditional chinese medicine si-wu-tang by HPLC coupled with dad and esi-ms. *J. Pharm. Biomed. Anal.* **2004**, *34*, 705–713. [CrossRef]
6. Hsu, H.Y.; Ho, Y.H.; Lin, C.C. Protection of mouse bone marrow by si-wu-tang against whole body irradiation. *J. Ethnopharmacol.* **1996**, *52*, 113–117. [CrossRef]
7. Liang, Q.D.; Gao, Y.; Tan, H.L.; Guo, P.; Li, Y.F.; Zhou, Z.; Tan, W.; Ma, Z.C.; Ma, B.P.; Wang, S.Q. Effects of four si-wu-tang's constituents and their combination on irradiated mice. *Biol. Pharm. Bull.* **2006**, *29*, 1378–1382. [CrossRef] [PubMed]
8. Niwa, K.; Hashimoto, M.; Morishita, S.; Lian, Z.; Tagami, K.; Mori, H.; Tamaya, T. Preventive effects of juzen-taiho-to on *N*-methyl-n-nitrosourea and estradiol-17beta-induced endometrial carcinogenesis in mice. *Carcinogenesis* **2001**, *22*, 587–591. [CrossRef] [PubMed]
9. Lian, Z.; Niwa, K.; Onogi, K.; Mori, H.; Harrigan, R.C.; Tamaya, T. Anti-tumor effects of herbal medicines on endometrial carcinomas via estrogen receptor-alpha-related mechanism. *Oncol. Rep.* **2006**, *15*, 1133–1136. [PubMed]
10. McMahon, M.; Itoh, K.; Yamamoto, M.; Chanas, S.A.; Henderson, C.J.; McLellan, L.I.; Wolf, C.R.; Cavin, C.; Hayes, J.D. The cap'n'collar basic leucine zipper transcription factor Nrf2 (nf-e2 p45-related factor 2) controls both constitutive and inducible expression of intestinal detoxification and glutathione biosynthetic enzymes. *Cancer Res.* **2001**, *61*, 3299–3307. [PubMed]

11. Kaulmann, A.; Bohn, T. Carotenoids, inflammation, and oxidative stress—Implications of cellular signaling pathways and relation to chronic disease prevention. *Nutr. Res.* **2014**, *34*, 907–929. [CrossRef] [PubMed]
12. Wen, Z.; Wang, Z.; Wang, S.; Ravula, R.; Yang, L.; Xu, J.; Wang, C.; Zuo, Z.; Chow, M.S.; Shi, L.; et al. Discovery of molecular mechanisms of traditional chinese medicinal formula Si-Wu-Tang using gene expression microarray and connectivity map. *PLoS ONE* **2011**, *6*, e18278. [CrossRef] [PubMed]
13. Liu, M.; Ravula, R.; Wang, Z.; Zuo, Z.; Chow, M.S.; Thakkar, A.; Prabhu, S.; Andresen, B.; Huang, Y. Traditional chinese medicinal formula Si-Wu-Tang prevents oxidative damage by activating nrf2-mediated detoxifying/antioxidant genes. *Cell Biosci.* **2014**, *4*, 8. [CrossRef] [PubMed]
14. Tagami, K.; Niwa, K.; Lian, Z.; Gao, J.; Mori, H.; Tamaya, T. Preventive effect of juzen-taiho-to on endometrial carcinogenesis in mice is based on shimotsu-to constituent. *Biol. Pharm. Bull.* **2004**, *27*, 156–161. [CrossRef] [PubMed]
15. The state pharmacopoeia commission of P.R.China. *Pharmacopoeia of the People's Republic of China*; Chemical Industry Press: Beijing, China, 2005.
16. Maron, D.M.; Ames, B.N. Revised methods for the salmonella mutagenicity test. *Mutat. Res.* **1983**, *113*, 173–215. [CrossRef]
17. Mortelmans, K.; Zeiger, E. The ames salmonella/microsome mutagenicity assay. *Mutat. Res.* **2000**, *455*, 29–60. [CrossRef]
18. Hanausek, M.; Spears, E.; Walaszek, Z.; Kowalczyk, M.C.; Kowalczyk, P.; Wendel, C.; Slaga, T.J. Inhibition of murine skin carcinogenesis by freeze-dried grape powder and other grape-derived major antioxidants. *Nutr. Cancer* **2011**, *63*, 28–38. [CrossRef] [PubMed]
19. Steele, V.E.; Sharma, S.; Mehta, R.; Elmore, E.; Redpath, L.; Rudd, C.; Bagheri, D.; Sigman, C.C.; Kelloff, G.J. Use of in vitro assays to predict the efficacy of chemopreventive agents in whole animals. *J. Cell Biochem. Suppl.* **1996**, *26*, 29–53. [CrossRef] [PubMed]
20. Dhar, A.; Young, M.R.; Colburn, N.H. The role of ap-1, nf-kappab and ros/nos in skin carcinogenesis: The JB6 model is predictive. *Mol. Cell Biochem.* **2002**, *234–235*, 185–193. [CrossRef] [PubMed]
21. Hu, M.; Peluffo, G.; Chen, H.; Gelman, R.; Schnitt, S.; Polyak, K. Role of cox-2 in epithelial-stromal cell interactions and progression of ductal carcinoma in situ of the breast. *Proc. Natl. Acad. Sci. USA* **2009**, *106*, 3372–3377. [CrossRef] [PubMed]
22. Kowalczyk, M.C.; Kowalczyk, P.; Tolstykh, O.; Hanausek, M.; Walaszek, Z.; Slaga, T.J. Synergistic effects of combined phytochemicals and skin cancer prevention in sencar mice. *Cancer Prev. Res. (Phila)* **2010**, *3*, 170–178. [CrossRef] [PubMed]
23. Chakravarti, D.; Mailander, P.; Franzen, J.; Higginbotham, S.; Cavalieri, E.L.; Rogan, E.G. Detection of dibenzo[*a*,*l*]pyrene-induced H-*ras* codon 61 mutant genes in preneoplastic sencar mouse skin using a new pcr-rflp method. *Oncogene* **1998**, *16*, 3203–3210. [CrossRef] [PubMed]
24. Didelot, A.; Le Corre, D.; Luscan, A.; Cazes, A.; Pallier, K.; Emile, J.F.; Laurent-Puig, P.; Blons, H. Competitive allele specific taqman pcr for kras, braf and egfr mutation detection in clinical formalin fixed paraffin embedded samples. *Exp. Mol. Pathol.* **2012**, *92*, 275–280. [CrossRef] [PubMed]
25. Beak, S.M.; Lee, Y.S.; Kim, J.A. Nadph oxidase and cyclooxygenase mediate the ultraviolet b-induced generation of reactive oxygen species and activation of nuclear factor-kappab in hacat human keratinocytes. *Biochimie* **2004**, *86*, 425–429. [CrossRef] [PubMed]
26. Kwak, M.K.; Kensler, T.W. Targeting nrf2 signaling for cancer chemoprevention. *Toxicol. Appl. Pharmacol.* **2009**, *244*, 66–76. [CrossRef] [PubMed]
27. Tas, F.; Oguz, H.; Argon, A.; Duranyildiz, D.; Caica, H.; Yasasever, V.; Topuz, E. The value of serum levels of il-6, tnf-alpha, and erythropoietin in metastatic malignant melanoma: Serum il-6 level is a valuable prognostic factor at least as serum ldh in advanced melanoma. *Med. Oncol.* **2005**, *22*, 241–246. [CrossRef]
28. Schafer, M.; Werner, S. Nrf2-a regulator of keratinocyte redox signaling. *Free Radic. Biol. Med.* **2015**, *88*, 243–252. [CrossRef] [PubMed]
29. Elmets, C.A.; Ledet, J.J.; Athar, M. Cyclooxygenases: Mediators of UV-induced skin cancer and potential targets for prevention. *J. Investig. Dermatol.* **2014**, *134*, 2497–2502. [CrossRef] [PubMed]

nutrients

MDPI

Review

Dietary Sources and Bioactivities of Melatonin

Xiao Meng [1], Ya Li [1], Sha Li [2,*], Yue Zhou [1], Ren-You Gan [3], Dong-Ping Xu [1] and Hua-Bin Li [1,4,*]

1 Guangdong Provincial Key Laboratory of Food, Nutrition and Health, Department of Nutrition, School of Public Health, Sun Yat-sen University, Guangzhou 510080, China; mengx7@mail2.sysu.edu.cn (X.M.); liya28@mail2.sysu.edu.cn (Y.L.); zhouyue3@mail2.sysu.edu.cn (Y.Z.); xudp@mail2.sysu.edu.cn (D.-P.X.)

2 School of Chinese Medicine, Li Ka Shing Faculty of Medicine, The University of Hong Kong, Hong Kong 999077, China

3 School of Biological Sciences, The University of Hong Kong, Hong Kong 999077, China; ganry@connect.hku.hk

4 South China Sea Bioresource Exploitation and Utilization Collaborative Innovation Center, Sun Yat-sen University, Guangzhou 510006, China

* Correspondence: u3003781@connect.hku.hk (S.L.); lihuabin@mail.sysu.edu.cn (H.-B.L.); Tel.: +852-3917-6498 (S.L.); +86-20-873-323-91 (H.-B.L.)

Received: 21 January 2017; Accepted: 31 March 2017; Published: 7 April 2017

Abstract: Insomnia is a serious worldwide health threat, affecting nearly one third of the general population. Melatonin has been reported to improve sleep efficiency and it was found that eating melatonin-rich foods could assist sleep. During the last decades, melatonin has been widely identified and qualified in various foods from fungi to animals and plants. Eggs and fish are higher melatonin-containing food groups in animal foods, whereas in plant foods, nuts are with the highest content of melatonin. Some kinds of mushrooms, cereals and germinated legumes or seeds are also good dietary sources of melatonin. It has been proved that the melatonin concentration in human serum could significantly increase after the consumption of melatonin containing food. Furthermore, studies show that melatonin exhibits many bioactivities, such as antioxidant activity, anti-inflammatory characteristics, boosting immunity, anticancer activity, cardiovascular protection, anti-diabetic, anti-obese, neuroprotective and anti-aging activity. This review summaries the dietary sources and bioactivities of melatonin, with special attention paid to the mechanisms of action.

Keywords: melatonin; food; bioactivity; antioxidant; anticancer; mechanisms of action

1. Introduction

Melatonin, *N*-acetyl-5-methoxy tryptamine, was first isolated from bovine pineal gland [1]. As the biological roles of melatonin were widely studied, the recognized therapeutical effects and the health benefits of melatonin could cover a broad range. Melatonin could regulate human physiological rhythm, alleviate related disorders like jet lag [2] and insomnia [3], scavenge free radical species [4], enhance the immune system [5], show anti-aging [6] and anti-inflammatory effects [7] and perform anticancer activities [8]. Moreover, melatonin could also exhibit neuroprotective effects [9], facilitate the control of chronic diseases, such as cardiovascular diseases [10], diabetes [11] and obesity [12]. In addition, melatonin could even regulate the mood [13], sexual maturation [14] and body temperature [15]. Recent research revealed the promising therapeutical application of melatonin in periodontology [16].

After being long considered as a hormone exclusively produced in the pineal gland of animals (Figure 1), melatonin has been identified in plants [17], insects [18], fungi [19] and bacteria [20]. Given the potent health effects of melatonin, many foods have been tested in the past decades and melatonin was identified and quantified in both animal foods and edible plants [21,22].

Huge differences of melatonin concentrations were reported among various food species and/or organs, ranging from pg/g to mg/g [22,23]. Additionally, it was well documented that the consumption of melatonin-rich foods may induce the potential health impacts by significantly increasing the serum melatonin concentration and antioxidant capacity in human beings [24]. Therefore, those foods containing melatonin are now popular and regarded as promising nutraceuticals [25–27].

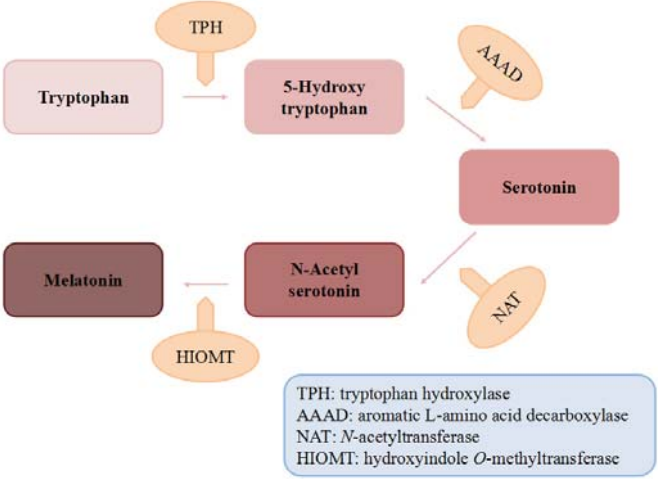

Figure 1. The biosynthesis of melatonin.

This review outlines the dietary sources, summarizes the bioactivities of melatonin, and special attention was paid to the mechanisms of action. A search of PubMed and Web of Science was conducted, and the related peer-reviewed articles published in English within 10 years were included because of the huge number of studies.

2. Dietary Sources of Melatonin

Melatonin exists widely in many kinds of food stuffs (Table 1). However, the content of melatonin in foods exhibits huge differences from species to species. Much higher melatonin was observed in nuts and medical herbs [28,29]. For the same species, it varies in different cultivars [30]. A study qualified the melatonin contents in 58 cultivars of corns, which ranged 10–2034 ng/g dry weight (DW) [31]. Additionally, in both animal foods and plant foods, melatonin could distribute unevenly in one individual animal or plant because of the different biophysical dynamic features in organs [22,32]. In edible plants, fruits generally present the lowest melatonin content, while the seeds and leaves have the highest one [33,34]. Furthermore, the melatonin concentration in the plant food products is also associated with the environment, in which the plants are cultured, including the temperature, sunlight exposing duration, ripening process, agrochemical treatment etc. [35,36]. Therefore, it is challenging and promising to clarify the factors influencing melatonin concentration in foods so as to select the effective approaches, such as germination of seeds, to increase the melatonin content in foods.

2.1. Animal Foods

In animal foods, melatonin concentrations were found higher in eggs and fish than those in meat [22]. Melatonin was detected in breast milk of human beings and also in the milk provided by other animals [22,37]. Similar as the fluctuation in plasma, i.e., relatively low during daytime and relatively high at night, melatonin levels in milk also showed a circadian rhythm, indicating that night milking might increase the benefits from milk as the melatonin concentration was approximately ten

times compared to that in the daytime [38]. Furthermore, melatonin was found in colostrum with the comparable concentration as it in plasma [39], which could benefit the newborns that lack the established rhythmic excretion of melatonin in the first couple of weeks in their lives [40]. Neither the artificial formulas nor the fermented milk drink were tested with detectable melatonin [41,42].

2.2. Plant Foods

2.2.1. Cereals

Cereals are largely consumed all around the world, in which melatonin contents were also investigated. Wang et al. studied melatonin contents in 58 cultivars of corns and 25 of rice, finding huge variety due to genotypes: 0–2034 ng/g (mean: 96.5 ng/g) for corns and 0–264 ng/g (mean: 16 ng/g) for rice [31]. Additionally, they also discovered the pigmented rice contained higher melatonin contents, which was consistent with the findings from Setyaningsih et al. [17]. Moreover, Setyaningsih et al. reported that the level of melatonin in nonglutinous black rice was almost twice as that in the glutinous type and the melatonin concentration was 1/3 less in polished rice compared to that in the whole ones. For other cereals such as wheat, barley and oats, melatonin was found relatively high, e.g., 124.7 ± 14.9 ng/g fresh weight (FW) in wheat, 82.3 ± 6.0 ng/g FW in barley and 90.6 ± 7.7 ng/g FW in oats, respectively [34]. In terms of bread, crumb was found with higher melatonin levels than the crust [20].

2.2.2. Fruits

Generally, melatonin was found in many commonly consumed fruits. Grapes [43], cherries [30] and strawberries [44] were the most popular ones in the investigation of melatonin contents, which also showed the difference between cultivars. The highest melatonin in three kinds of fruits was reported in the range of 8.9–158.9 ng/g DW in the skin of grapes (*Vitis vinifera* L. cv. Malbec) [45], 13.46 ± 1.10 ng/g FW in tart cherries (*Prunus cerasus* L. cv. Balaton) [46], and 11.26 ± 0.13 ng/g FW in strawberry (*Fragaria ananassa* L. cv. Festival) [44]. Other fruits contained melatonin at a relatively low level.

2.2.3. Vegetables

Melatonin exists in lots of common vegetables, although it remains undetectable in potatoes and very low in beetroots [47,48]. Tomatoes and peppers were the most studied vegetables, and they showed relatively high melatonin concentrations in the vegetable group, i.e., 11.9 ng/g FW or 93.4 ng/g DW in pepper (*Capsicum annuum* L. cv. F26) and 14.77 ng/g FW or 249.98 ng/g DW in tomato (*Solanum lycopersicum* L. cv. Optima) [49], and 23.87 ± 2.02 ng/g FW in tomato (*Lycopersicon esculentum* cv. Bonda) [44].

Mushrooms also contain melatonin, e.g., 12,900 ± 770 ng/g DW in Basidiomycota (*Lactarius deliciosus*), 6800 ± 60 ng/g DW in Basidiomycota (*Boletus edulis*) [42], and 4300–6400 ng/g DW in Agaricus bisporus [50].

2.2.4. Legumes and Seeds (Raw and Germinated)

Melatonin occurred in many legumes and seeds, and in some particular seeds, such as white and black mustard seeds, melatonin was as high as 189 ng/g DW and 129 ng/g DW, respectively [51]. Moreover, the germination process of legumes and seeds was proved to be able to increase the melatonin levels significantly [52,53]. For example, in germinated soybean seeds, the melatonin level reached a peak of 1.89 ± 0.11 ng/g DW during germination, which was 400% increase than that in raw soybean seeds [52]. Similarly, melatonin was observed more than 11 folds in the germinated mung bean seeds as it was in the raw ones [53].

2.2.5. Nuts

Melatonin was found in various nuts, and pistachio (*Pistacia vera* L.) was reported with the highest content (233,000 ng/g DW) to date [28].

2.2.6. Juices and Beverages

The popular alcoholic drinks like beer [42,54] and wine [55,56], were tested for melatonin, with 0.09 ± 0.01 ng/mL in beer [42] and up to 129.5 ± 3.5 ng/mL in wine [42,54]. Besides the melatonin originated from the main ingredients, it was also considered to be synthesized during the fermentation process due to the yeast growth [54,57].

As for the other drinks, coffee usually contains high concentration of melatonin because coffee beans contained melatonin at a very high level and even much higher in roasted beans [58]. Melatonin also existed in juices [43], cacao [42] and balsamic vinegars [59]. However, it was not found in concentrates [60] or in tea [42], including green tea and black tea.

2.2.7. Medical Herbs

Many medical herbs were analyzed and some of them contained melatonin at a level of more than 1000 ng/g DW [61,62]. In Huang-qin (*Scutellaria biacalensis*) melatonin was significantly high as 7110 ng/g DW, and in St. John's Wort (*Hypericum perforatum*) melatonin concentration was 4490 ng/g DW in flowers and 1750 ng/g DW in leaves [29]. Besides, 108 Chinese medical herbs were quantified, and melatonin was more than 10 ng/g DW in 64 tested herbs [61].

2.2.8. Edible Oils

Melatonin ranged 0.03–0.29 ng/g in the tested edible oils, among which refined linseed presented 0.29 ng/g and virgin soybean 0.19 ng/g [63,64]. De la Puerta et al. also demonstrated that generally the melatonin levels in the refined olive and sunflower oil were about half of those in the extra virgin olive oil [63].

2.2.9. Yeast

Melatonin was found ranging 2.2 ± 0.14 ng/g in yeast, particularly *Saccharomyces cerevisae*, which is widely used in bread baking and alcohol industry [22].

Collectively, melatonin has been found in lots of foods. In animal foods, eggs and fish are relatively rich in melatonin, whereas in plant foods, nuts contains the highest melatonin contents, and some cereals and germinated legumes or seeds are also with high contents of melatonin. Mushrooms are also high-melatonin foods. However, it should be pointed out that the data on content of melatonin in foods in Table 1 were obtained by different analytical methods. Thus, quality of these data depended on the pretreatment method of sample and the analytical method itself. For example, in terms of radioimmunoassay (RIA) and enzyme-linked immunoabsorbent assay (ELISA), melatonin content could be over-estimated as some other components in the foods might also react with the related antibodies and enzymes, resulting in the lower accuracy. In addition, high-performance liquid chromatograph with ultraviolet detector (HPLC-UV) has low sensitivity and selectivity. Although high-performance liquid chromatograph with fluorescence detector (HPLC-FD) has high sensitivity, its selectivity is also low. Thus, melatonin content could be over-estimated by HPLC-UV or HPLC-FD method. Generally, gas chromatography-mass spectrometry (GC-MS) and high-performance liquid chromatography-mass spectrometry (HPLC-MS) have high resolution and sensitivity. Therefore, the data obtained by GC-MS or HPLC-MS are more accurate than those obtained by other methods [65].

2.3. Other Issues about Melatonin Intake

2.3.1. The Alternation of Endogenous Melatonin along Life Cycle

It has been well-documented that the secretion and/or serum levels of melatonin alter through a human lifetime [66–68]. Specifically, the serum levels of endogenous melatonin during the day and at night were measured in 367 volunteers (210 males and 157 females), aged 3 days to 90 years [67]. The results of this study demonstrated that nighttime serum melatonin concentration was low during the first 6 months of life [27.3 ± 5.4 (±standard error, SE) pg/mL], then reached a peak (329.5 ± 42.0 pg/mL) at 1–3 years of age, followed by a huge drop to 62.5 ± 9.0 pg/mL in the group of aged 15–20 years, probably due to the body size expansion during childhood and puberty without an increase in the rate of secretion. Then an additional decline followed in adulthood until 70–90 year of age (29.2 ± 6.1 pg/mL), attributing to a degenerative pineal gland associated with aging. Overall, the alternations of nocturnal serum melatonin during lifetime showed a fragmentary and inconsistent manner. Meanwhile, daytime serum melatonin levels were low and not age-related.

2.3.2. Bioavailability of Exogenous Melatonin

Melatonin has been known and used to assist sleep disorders [8] or jet lag [69] as a dietary supplement or as a drug, and recently it has also been reported to synergize other drugs as an adjuvant to improve their efficiency or to attenuate their side effects [70]. Herein, the bioavailability of melatonin has been studied by some researchers. In a study in vivo among 12 healthy volunteers, melatonin was administrated intravenously (i.v.) by 2 mg and orally by 2 and 4 mg, and in neither of these two phases the difference in serum half-life was found [71]. This study revealed the poor absolute bioavailability of oral melatonin tablets in both dosages, which was approximately 15%, possibly because of the poor oral absorption, large first-pass metabolism, or combined. Moreover, another study was conducted with 12 young healthy volunteers (6 males, 6 females), with 250 μg oral solution of D_7 melatonin, a molecule in which seven hydrogen atoms are replaced by seven deuterium atoms. It was reported that the absolute bioavailability of melatonin ranged from 1% to 37% and higher in women (16.8% ± 12.7%) than in men (8.6% ± 3.9%). It was also observed that the apparent terminal half-life values were 36 ± 2 and 41 ± 10 min for males and females respectively, indicating the fast-release property of melatonin [72]. Besides, 7 healthy male volunteers (ages 31.1 ± 1.1) were given an ingestion of 3 mg melatonin, and a marked increase in serum melatonin (3561 ± 1201 pg/mL) was found within 20 min, followed by a gradual decrease, but the level still remained higher than the basal level at 240 min after the ingestion [73].

2.3.3. Benefits of Consuming Melatonin-Containing Foods

Since the secretion of endogenous melatonin decreases after childhood, increasing dietary consumption could be a good option. The studies showed that intake of the food rich in melatonin may gain health impacts by increasing circulating melatonin [24,74–77]. For instance, when the rats were fed with walnuts (*Juglans regia* L.) containing melatonin concentrations of 3.5 ± 1.0 ng/g, the increased blood melatonin concentrations and total antioxidant capacity of blood were observed, indicating walnuts could provide beneficial effects as a good food source of melatonin [78]. Additionally, in a study conducted with young, middle-aged and elderly participants (20 ± 10 year-old, 45 ± 10 year-old and 75 ± 10 year-old, respectively), the total antioxidant capacity were reported to significantly increase in the three groups of individuals after the intake of the experimental juice of grape (*Vitis vinifera* cv. Tempranillo), 200 mL twice a day (as the lunch and dinner desserts) for 5 days [76] as well as the urinary 6-sulfatoxymelatonin, a major metabolite of melatonin commonly used as a biomarker indicating its bioavailability [79]. Moreover, it was found in vivo in 12 healthy male volunteers that the consumption of tropical fruit (banana) or fruit juices (orange and pineapple) significantly increased the serum melatonin concentration and the highest value was observed at 120 min after intake, i.e., compared with before consumption, pineapple with 146 pg/mL versus 48 pg/mL ($p = 0.002$),

orange with 151 pg/mL versus 40 pg/mL ($p = 0.005$), and banana with 140 pg/mL versus 32 pg/mL ($p = 0.008$), respectively. Besides, the antioxidant capacity in the serum also markedly increased, suggested by the significant increases in two indicators, i.e., ferric reducing antioxidant power (FRAP) assay and oxygen radical antioxidant capacity (ORAC) [24]. Furthermore, as the germination of legumes significantly increased the melatonin content, it was reported that in Sprague-Dawley rats, the melatonin concentrations in plasma increased by 16% ($p < 0.05$) after the administration of kidney bean sprout extract via gavage, which correspondingly led to the increase of urinary 6-sulfatoxymelatonin content ($p < 0.01$), antioxidant capacities did not show significant variation though [80].

2.3.4. Guidance on Regulating Dietary Supplement of Melatonin

Dietary supplement of melatonin could be another option to recompense the physiologically declined activity of pineal gland. Different authorities have published their guidance on regulating the dietary supplements including melatonin. For instance, European Food Safety Authority published the Scientific Opinion on the substantiation of a health claim related to melatonin and reduction of sleep onset latency (ID 1698, 1780, 4080) pursuant to Article 13(1) of Regulation (EC) No. 1924/20061 in 2010. The Panel on Dietetic Products, Nutrition and Allergies considers that "melatonin is sufficiently characterized" and "reduction of sleep onset latency might be a beneficial physiological effect". In addition, it was also concluded that "a cause and effect relationship has been established between the consumption of melatonin" and "The target population is assumed to be the general population". Moreover, the dose was also suggested as "In order to obtain the claimed effect, 1 mg of melatonin should be consumed close to bedtime" [81]. While according to the latest updated data (on 22 March 2013) from Food Standards Australia New Zealand, melatonin was listed in the original table 3 on their official website [82], which presents the foods or properties of food from food-health relationships derived from 20 EU approved health claims that will not be added to Standard 1.2.7 and the rationale for exclusion "The claim refers to a dietary supplement." Additionally, in each of the databases, named "AUSNUT 2011-13 Australian Health Survey (AHS) Dietary Supplement Details" and "AUSNUT 2011-13 Australian National Nutrition Physical Activity Survey (NNPAS) Dietary Supplement Nutrient Database", only one dietary supplement of melatonin was listed with the same information, i.e., dietary supplement name: Nature's Care Melatonin; ID 122196; 3 mg, Tablet, uncoated; classification code 33505 and classification sub-group, other supplements [82].

Table 1. Concentration of melatonin in food.

Name	Scientific Name/Variety/Origin	MT Value or Range ng/g or pg/mL	No. of Samples	Quantified by	Reference
Animal Foods					
Meat					
Lamb	Not specified	1.6 ± 0.14 ng/g	5	HPLC	[22]
Beef	Not specified	2.1 ± 0.13 ng/g	5	HPLC	[22]
Pork	Not specified	2.5 ± 0.18 ng/g	5	HPLC	[22]
Fish					
Salmon	Not specified	3.7 ± 0.21 ng/g	5	HPLC	[22]
Chicken					
Meat and skin	Not specified	2.3 ± 0.23 ng/g	5	HPLC	[22]
Liver and heart	Not specified	1.1 ± 0.01 ng/g	5	HPLC	[22]
Egg					
Dried solids	Not specified	6.1 ± 0.95 ng/g	5	HPLC	[22]
Raw, whole	Not specified	1.54 ng/g	5	HPLC	[22]
Milk and dairy products					
Human milk					
Indian human milk	Not specified	15.92 ± 1.02 pg/mL	6	LC-MS/MS	[37]
Breast milk	Not specified	0–42 pg/mL	5	ELISA	[41]
Bovine milk					
Fresh colostrum,	Not specified	0.06 ng/g	5	HPLC	[22]
Cow milk	Not specified	14.45 ± 0.12 pg/mL	6	LC-MS/MS	[37]
Cow Milk	Holstein cows	4.03–39.43 pg/mL	3	EIA	[38]
Colostrum powder	Not specified	0.6 ± 0.06 ng/g	5	HPLC	[22]
Toned milk	Not specified	18.41 ± 0.62 pg/mL	6	LC-MS/MS	[37]
Yoghurt	Not specified	0.13 ± 0.01 ng/mL	5	LC-MS/MS	[42]
Artificial formulas	Not specified	nd	15	ELISA	[41]
Fermented milk drink	Kefir	nd	5	LC-MS/MS	[42]

Table 1. *Cont.*

Name	Scientific Name/Variety/Origin	MT Value or Range ng/g or pg/mL	No. of Samples	Quantified by	Reference
Plant foods					
Cereals					
Corn					
Corn (whole, yellow)	Not specified	1.3 ± 0.28 ng/g	5	HPLC	[22]
Corn (germ meal)	Not specified	1.0 ± 0.10 ng/g	5	HPLC	[22]
Corn (YM001-)	58 cultivars	10–2034 ng/g DW	N/A	HPLC	[31]
Corn	Not specified	1.88 ng/g FW	N/A	GC/MS	[47]
Sweet corn	Not specified	1.37 ng/g FW	N/A	HPLC-FD	[83]
Rice					
Rice	*Oryza sativum* L. ssp. japonica	1.50 ng/g FW	N/A	GC/MS	[47]
Rice (SD001-)	25 cultivars	0–264 ng/g DW	N/A	HPLC	[31]
Black glutinous	Long grain, waxy, Thailand (Bran)	73.81 ± 0.07 ng/g DW	9	PLE HPLC-FD	[17]
Black	Not specified	182.04 ± 1.62 ng/g DW	9	PLE HPLC-FD	[17]
Red	Not specified	212.01 ± 1.37 ng/g DW	9	PLE HPLC-FD	[17]
Whole short grain	Not specified	47.83 ± 0.12 ng/g DW	9	PLE HPLC-FD	[17]
Whole semi-long grain	Not specified	42.95 ± 0.64 ng/g DW	9	PLE HPLC-FD	[17]
Polished short grain	Not specified	31.99 ±0.31 ng/g DW	9	PLE HPLC-FD	[17]
Polished long grain	Not specified	27.61 ± 1.16 ng/g DW	9	PLE HPLC-FD	[17]
Basmati	Not specified	38.46 ± 0.07 ng/g DW	9	PLE HPLC-FD	[17]
Parboiled rice	Not specified	28.33 ± 0.61 ng/g DW	9	PLE HPLC-FD	[17]
Rice	*Oryza sativa* cv. Dongjin	0.04 ng/g DW	20	HPLC	[84]
Rice (transgenic)	*Oryza sativa* cv. Dongjin	0.07–1.25 ng/g DW	20	HPLC	[84]
Rice	*Oryza sativum* L. ssp. japonica	1.01 ng/g FW	N/A	HPLC-FD	[83]

Table 1. *Cont.*

Name	Scientific Name/Variety/Origin	MT Value or Range ng/g or pg/mL	No. of Samples	Quantified by	Reference
Wheat					
Wheat	*Triticum aestivum* L.	124.7 ± 14.9 ng/g FW	N/A	HPLC-ECD	[85]
Whole grain	Not specified	2–4 ng/g	N/A	Not specified	[86]
Purple wheat	Not specified	4 ng/g DW	3	HPLC-UV	[87]
Purple (heat stressed)	Not specified	2 ng/g DW	3	HPLC-UV	[87]
Barley					
Barley	*Hordeum vulgare* L.	0.87 ng/g FW	N/A	GC/MS	[47]
Barley	*Hordeum vulgare* L.	82.3 ± 6.0 ng/g FW	N/A	HPLC-ECD	[85]
Barley	*Hordeum vulgare* L.	0.38 ng/g FW	N/A	HPLC-FD	[83]
Oats					
Oats	*Avena sativa* L.	90.6 ± 7.7 ng/g FW	N/A	HPLC-ECD	[85]
Oat	*Avena sativa* L.	1.80 ng/g FW	N/A	HPLC-FD	[83]
Bread					
Crumb	Specific ingredients	0.19–0.63 ng/g DW	3	LC-ESI-MS/MS	[20]
Crumb	Not specified	0.34 ± 0.03 ng/g DW	5	LC-MS/MS	[42]
Crust	Specific ingredients	0.14–0.82 ng/g DW	3	LC-ESI-MS/MS	[20]
Crust	Not specified	0.14 ± 0.02 ng/g DW	5	LC-MS/MS	[42]
Fruits					
Pineapple					
Pineapple	*Ananas comosus* L.	0.28 ng/g FW	N/A	GC/MS	[47]
Pineapple	*Ananas comosus* L.	0.04 ng/g FW	N/A	HPLC-FD	[83]
Kiwi fruit	*Actinidia chinensis* L.	0.02 ng/g FW	N/A	HPLC-FD	[83]

Table 1. *Cont.*

Name	Scientific Name/Variety/Origin	MT Value or Range ng/g or pg/mL	No. of Samples	Quantified by	Reference
Strawberry					
Strawberry	*Fragaria magna* L.	0.14 ng/g FW	N/A	GC/MS	[47]
Strawberry	*Fragaria ananassa* L. cv. Camarosa	5.58 ± 0.01 ng/g FW	3	LC-MS/LC-FD	[44]
Strawberry	*Fragaria ananassa* L. cv. Candonga	5.5 ± 0.6 ng/g FW	3	LC-MS/LC-FD	[44]
Strawberry	*Fragaria ananassa* L. cv. Festival	11.26 ± 0.13 ng/g FW	3	LC-MS/LC-FD	[44]
Strawberry	*Fragaria ananassa* L. cv. Primoris	8.5 ± 0.6 ng/g FW	3	LC-MS/LC-FD	[44]
Strawberry	*Fragaria magna* L.	0.01 ng/g FW	N/A	HPLC-FD	[83]
Banana	*Musa ensete*	0.66 ng/g FW	N/A	GC/MS	[47]
Apple					
Apple	*Malus domestica*	nd	N/A	HPLC-FD	[83]
Apple	*Malus domestica Borkh.* cv. Red Fuji	5 ng/g FW	3	HPLC	[88]
Apple	*Malus domestica*	0.16 ng/g FW	N/A	GC/MS	[47]
Pomegranata	*Punica granatum*	0.17 ng/g FW	N/A	GC/MS	[47]
Mulberry					
Mulberry	*Hongguo2 Morusnigra*, black	1.41 ng/g FW	3	HPLC-ESI-MS/MS	[36]
Mulberry	*Baiyuwang Morus alba*, white	0.58 ng/g FW	3	HPLC-ESI-MS/MS	[36]
Cherry					
Tart cherries (frozen)	*Prunus cerasus* L. cv. Balaton	2.9 ± 0.6 ng/g DW	3	HPLC-EMS	[60]
Tart cherries (dry)	*Prunus cerasus* L. cv. Balaton	nd	3	HPLC-EMS	[60]
Tart cherries	*Prunus cerasus* L. cv. Balaton	13.46 ± 1.10 ng/g FW	3	HPLC-ECD	[46]
Tart cherries (frozen)	*Prunus cerasus* L. cv. Montmorency	12.3 ± 2 ng/g DW	3	HPLC-EMS	[60]
Tart cherries (dry)	*Prunus cerasus* L. cv. Montmorency	nd	3	HPLC-EMS	[60]
Tart cherries	*Prunus cerasus* L. cv. Montmorency	2.06 ± 0.17 ng/g FW	3	HPLC-ECD	[46]

Table 1. *Cont.*

Name	Scientific Name/Variety/Origin	MT Value or Range ng/g or pg/mL	No. of Samples	Quantified by	Reference
Cherry	*Prunus avium* L. cv. Hongdeng	10–20 ng/g FW	3	SPE HPLC	[89]
Cherry	*Prunus avium* L. cv. Rainier	10–20 ng/g FW	3	SPE HPLC	[89]
Cherry	*Prunus avium* L. cv. Burlat	0.22 ng/g FW	3	HPLC-MS	[30]
Cherry	*Prunus avium* L. cv. Navalinda	0.03 ng/g FW	3	HPLC-MS	[30]
Cherry	*Prunus avium* L. cv. Van	0.01 ng/g FW	3	HPLC-MS	[30]
Cherry	*Prunus avium* L. cv. Pico Limón Negro	0.01 ng/g FW	3	HPLC-MS	[30]
Cherry	*Prunus avium* L. cv. Sweetheart	0.06 ng/g FW	3	HPLC-MS	[30]
Cherry	*Prunus avium* L. cv. Pico Negro	0.12 ng/g FW	3	HPLC-MS	[30]
Cherry	*Prunus avium* L. cv. Ambrunés	nd	3	HPLC-MS	[30]
Cherry	*Prunus avium* L. cv. Pico Colorado	0.05 ng/g FW	3	HPLC-MS	[30]
Grape					
Grape	Albana, white	1.2 ng/g	3	HPLC-FD	[43]
Grape (skin)	*Vitis vinifera* L. cv. Merlot	9.3 ± 0.14 ng/g grapes	3	UPLC-MS/MS	[90]
Grape (fresh)	*Vitis vinifera* L. cv. Merlot	3.9 ± 0.06 ng/g grapes	3	UPLC-MS/MS	[90]
Grape (skin)	*Vitis vinifera* L. cv Malbec	8.9–158.9 ng/g DW	3	HPLC-ESI-MS/MS	[45]
Grape (skin)	*Vitis vinifera* L. cv. Nebbiolo	0.97 ng/g	3	HPLC-ELISA	[35]
Grape (skin)	*Vitis vinifera* L. cv. Croatina,	0.87 ng/g	3	HPLC-ELISA	[35]
Grape (skin)	*Vitis vinifera* L. cv. Barbera	0.63 ng/g	3	HPLC-ELISA	[35]
Grape (skin)	*Vitis vinifera* L. cv. Cabernet Sauvignon	0.42 ng/g	3	HPLC-ELISA	[35]
Grape (skin)	*Vitis vinifera* L. cv. Cabernet Franc	0.01 ng/g	3	HPLC-ELISA	[35]
Grape (skin)	*Vitis vinifera* L. cv. Marzemino,	0.03 ng/g	3	HPLC-ELISA	[35]
Grape (skin)	*Vitis vinifera* L. cv. Sangiovese	0.33 ng/g	3	HPLC-ELISA	[35]
Grape (skin)	*Vitis vinifera* L. cv. Merlot,	0.26 ng/g	3	HPLC-ELISA	[35]
Grape (skin)	*Vitis vinifera* L. cv. Malbec,	1.2 ng/g	5	CEC	[56]
Grape (skin)	*Vitis vinifera* L. cv. Cabernet Sauvignon	0.8 ng/g	5	CEC	[56]
Grape (skin)	Chardonnay	0.6 ng/g	5	CEC	[56]

Table 1. *Cont.*

Name	Scientific Name/Variety/Origin	MT Value or Range ng/g or pg/mL	No. of Samples	Quantified by	Reference
Cranberry					
Cranberry	*Vaccinium oxycoccos* L.	40 ± 10 ug/g DW **	5	UPLC-MS	[91]
Cranberry	*Vaccinium vitis-idaea* L.	25 ± 3 ug/g DW **	5	UPLC-MS	[91]
Cranberry	*Vaccinium macrocarpon* Ait.	96 ± 26 ug/g DW **	5	UPLC-MS	[91]
Vegetables					
Onion	*Allium cepa* L.	0.30 ng/g FW	N/A	GC/MS	[47]
Onion	*Allium fistulosum* L., Welsh	0.09 ng/g FW	N/A	HPLC-FD	[83]
Onion	*Allium cepa* L.	0.03 ng/g FW	N/A	HPLC-FD	[83]
Garlic	*Allium sativum* L.	0.59 ng/g FW	N/A	GC/MS	[47]
Cabbage	*Brassica oleraceae* L. var. capitata	0.31 ng/g FW	N/A	GC/MS	[47]
Cauliflower	*Brassica oleraceae* L. var. botrytis	0.82 ng/g FW	N/A	GC/MS	[47]
Turnip	*Brassica rapa* L.	0.50 ng/g FW	N/A	GC/MS	[47]
Cucumber	*Cucumis sativus* L.	0.59 ng/g FW	N/A	GC/MS	[47]
Cucumber	*Cucumis sativus* L.	0.03 ng/g FW	N/A	HPLC-FD	[83]
Cucumber	Not specified	0.01 ng/g	1	GC/MS	[48]
Carrot	*Daucus carota* L.	0.49 ng/g FW	N/A	GC/MS	[47]
Carrot	*Paucus carota* L.	0.06 ng/g FW	N/A	HPLC-FD	[83]
Radish	*Raphnus sativus* L.	0.76 ng/g FW	N/A	GC/MS	[47]
Japanese radish	*Bassica campestris* L.	0.66 ng/g FW	N/A	HPLC-FD	[83]
Potato	*Solanum tuberosum* L.	nd	N/A	GC/MS	[47]
Potato	Not specified	nd	1	GC/MS	[48]
Ginger	*Zingiber officinale* Rosc.	1.42 ng/g FW	N/A	GC/MS	[47]
Black olive	Not specified	0.01 ng/g DW	5	LC-MS/MS	[42]

Table 1. *Cont.*

Name	Scientific Name/Variety/Origin	MT Value or Range ng/g or pg/mL	No. of Samples	Quantified by	Reference
Beetroot	*Beta vulgaris*	0.002 ng/g	1	GC/MS	[48]
Purslane	*Portulaca oleracea* L.	19 ng/g WW	N/A	GC/MS	[92]
Spinach	Not specified	0.04 ng/g WW	N/A	GC/MS	[92]
Indian spinach	*Basella alba* L.	0.04 ng/g FW	N/A	HPLC-FD	[83]
Asparagus	*Asparagus officinalis* L.	0.01 ng/g FW	N/A	HPLC-FD	[83]
Pepper	*Capsicum annuum* L. cv. Barranca	4.48 ng/g FW/31.01 ng/g DW	4	UHPLC-MS/MS	[49]
Pepper	*Capsicum annuum* L. cv. F26	11.9 ng/g FW/93.4 ng/g DW	4	UHPLC-MS/MS	[49]
Tomato	*Solanum lycopersicum* L. cv. Ciliegia	0.64 ng/g FW/7.47 ng/g DW	4	UHPLC-MS/MS	[49]
Tomato	*Solanum lycopersicum* L. cv. Optima	14.77 ng/g FW/249.98 ng/g DW	4	UHPLC-MS/MS	[49]
Tomato	*Solanum lycopersicum* L. cv. Micro-Tom	1.5–66.6 ng/g FW	N/A	EIA	[93]
Tomato	*Lycopersicon pimpinellifolium*	0.11 ng/g	1	GC/MS	[48]
Tomato	*Lycopersicon esculentum Mill.* cv. Sweet 100	0.51 ng/g	1	GC/MS	[48]
Tomato	*Lycopersicon esculentum Mill.* cv. Rutgers California Supreme	0.17 ng/g	1	GC/MS	[48]
Tomatoes	*Lycopersicon pimpinellifolium*	0.30 ng/g FW	N/A	GC/MS	[47]
Tomatoes	*Lycopersicon esculentum* cv. Bonda	23.87 ± 2.02 ng/g FW	3	LC-MS/LC-FD	[44]
Tomatoes	*Lycopersicon esculentum* cv. Borsalinaa	8.2 ± 0.6 ng/g FW	3	LC-MS/LC-FD	[44]
Tomatoes	*Lycopersicon esculentum* cv. Catalinaa	4.1 ± 0.9 ng/g FW	3	LC-MS/LC-FD	[44]
Tomatoes	*Lycopersicon esculentum* cv. Gordala	17.10 ± 1.21 ng/g FW	3	LC-MS/LC-FD	[44]
Tomatoes	*Lycopersicon esculentum* cv. Lucindaa	4.45 ± 0.05 ng/g FW	3	LC-MS/LC-FD	[44]
Tomatoes	*Lycopersicon esculentum* cv. Marbonea	18.13 ± 2.24 ng/g FW	3	LC-MS/LC-FD	[44]
Tomatoes	*Lycopersicon esculentum* cv. Myriadea	8.0 ± 1.3 ng/g FW	3	LC-MS/LC-FD	[44]
Tomatoes	*Lycopersicon esculentum* cv. Pitenzaa	14.0 ± 2.5 ng/g FW	3	LC-MS/LC-FD	[44]
Tomatoes	*Lycopersicon esculentum* cv. Santonioa	7.73 ± 1.22 ng/g FW	3	LC-MS/LC-FD	[44]
Tomatoes (wild type)	*Solanumlycopersicum* L. cv. Micro-Tom	6.58 ng/g FW	3	HPLC	[94]
Tomatoes (transgenic)	*Solanumlycopersicum* L. cv. Micro-Tom	7.39–10.34 ng/g FW	3	HPLC	[94]

Table 1. *Cont.*

Name	Scientific Name/Variety/Origin	MT Value or Range ng/g or pg/mL	No. of Samples	Quantified by	Reference
Tomatoes	Not specified	0.03 ± 0.01 ng/g DW	5	LC-MS/MS	[42]
Tomato	*Lycopersicon esculentum* L.	0.03 ng/g FW	N/A	HPLC-FD	[83]
Japanese butterbur	*Patasites japonicus 50*	nd	N/A	HPLC-FD	[83]
Taro	*Colocasis escutenta*	0.06 ng/g FW	N/A	HPLC-FD	[83]
Cabbage	*Brassica oleracea*	0.11 ng/g FW	N/A	HPLC-FD	[83]
Chinese cabbage	*Raphamus sativas*	0.11 ng/g FW	N/A	HPLC-FD	[83]
Chungitsu	*Chrysanthemum cororarum*	0.42 ng/g FW	N/A	HPLC-FD	[83]
Ginger	*Zinigiber officinale*	0.58 ng/g FW	N/A	HPLC-FD	[83]
Japanese ashitaba	*Angelica* keiskei	0.62 ng/g FW	N/A	HPLC-FD	[83]
Mushrooms					
Mushroom	*Agaricus bisporus**	4300–6400 ng/g DW	3	RP-HPLC	[50]
Basidiomycota	*Armillaria mellea*	<10 ng/g DW	3	HPLC	[19]
Basidiomycota	*Boletus badius*	<10 ng/g DW	3	HPLC	[19]
Basidiomycota	*Boletus edulis*	6800 ± 60 ng/g DW	3	HPLC	[19]
Basidiomycota	*Cantharellus cibarius*	1400 ± 110 ng/g DW	3	HPLC	[19]
Basidiomycota	*Lactarius deliciosus*	12,900 ± 770 ng/g DW	3	HPLC	[19]
Basidiomycota	*Pleurotus ostreatus*	<10 ng/g DW	3	HPLC	[19]
Legumes and seeds (raw)					
Legumes					
Lentils	*Lens culinaris* L.	0.5 ng/g DW	3	HPLC-MS/MS	[53]
Kidney beans	*Phaseolus vulgaris* L	1.0 ng/g DW	3	HPLC-MS/MS	[53]
Soybean	*Glycine max*	0.45 ± 0.03 ng/g DW	N/A	RIA	[52]

Table 1. *Cont.*

Name	Scientific Name/Variety/Origin	MT Value or Range ng/g or pg/mL	No. of Samples	Quantified by	Reference
Seeds					
Lupin (seed-cotyledons)	*Lupinus albus* L.	3.83 ± 0.21 ng/g FW	5	HPLC-FD	[32]
Lupin (seed-coat)	*Lupinus albus* L.	37.50 ± 2.3 ng/g FW	5	HPLC-FD	[32]
Lupin (seed-flour)	*Lupinus albus* L.	0.53 ± 0.04 ng/g DW	5	HPLC-FD	[32]
Grape (seed)	*Vitis vinifera* L. cv. Merlot	10.04 ± 0.49 ng/g grapes	3	UPLC-MS/MS	[90]
Barley (seed)	*Hordeum vulgare* L.	0.58 ± 0.05 ng/g FW	5	HPLC-FD	[32]
Barley(seed-flour)	*Hordeum vulgare* L.	0.09 ± 0.01 ng/g DW	5	HPLC-FD	[32]
Black mustard	*Brassica nigra*	129 ng/g DW	2	HPLC-ECD	[51]
White mustard	*Brassica hirta*	189 ng/g DW	2	HPLC-ECD	[51]
Fenugreek	*Trigonella faena-graecum*	43 ng/g DW	2	HPLC-ECD	[51]
Milk thistle	*Silybum marianum*	2 ng/g DW	2	HPLC-ECD	[51]
Celery	*Apium gravolens*	7 ng/g DW	2	HPLC-ECD	[51]
Alfalfa	*Medicago sativa*	16 ng/g DW	2	HPLC-ECD	[51]
Coriander	*Coriandrum sativum*	7 ng/g DW	2	HPLC-ECD	[51]
Green cardamom	*Elettaria cardamomum*	15 ng/g DW	2	HPLC-ECD	[51]
Fennel	*Foeniculum vulgare*	28 ng/g DW	2	HPLC-ECD	[51]
Poppy	*Popaver somniferum*	6 ng/g DW	2	HPLC-ECD	[51]
Anise	*Pimpinella anisum*	7 ng/g DW	2	HPLC-ECD	[51]
Sunflower	*Helianthus annuus*	29 ng/g DW	2	HPLC-ECD	[51]
Flax	*Linum usitatissimum*	12 ng/g DW	2	HPLC-ECD	[51]
Almond	*Prunus amydalus*	39 ng/g DW	2	HPLC-ECD	[51]
Chinese wolfberry	*Lycium barbarum*	103 ng/g DW	2	HPLC-ECD	[51]
Cucumber	*Cucumissativus* L. cv. Jingyu-1	5.1 ng/g FW	3	UPLC-ESI-MS/MS	[95]
Alfalfa	*Medicago sativa* L.	0.05 ± 0.00 ng/g DW	3	ELISA	[23]
Lentil	*Lens sculenta* L.	0.07 ± 0.01 ng/g DW	3	ELISA	[23]
Mung bean	*Vignaradiata* L.	0.01 ± 0.0 ng/g DW	3	ELISA	[23]

Table 1. *Cont.*

Name	Scientific Name/Variety/Origin	MT Value or Range ng/g or pg/mL	No. of Samples	Quantified by	Reference
Onion	*Allium cepa* L.	0.22 ± 0.01 ng/g DW	3	ELISA	[23]
Broccoli	*Brassica oleraceae* L.	0.41 ± 0.04 ng/g DW	3	ELISA	[23]
Red cabbage	*Brassica oleraceae capitate rubra* L.	0.34 ± 0.04 ng/g DW	3	ELISA	[23]
Radish (mixed)	*Raphanus sativus japonicum* L. *Raphanus sativus rambo* L. *Raphanus sativus sinicum rosae* L.	0.28 ± 0.01 ng/g DW	3	ELISA	[23]
Legumes and seeds (germination)					
Legumes sprouts					
Lentils	*Lens culinaris* L.	1089.8 ng/g DW	3	HPLC-MS/MS	[53]
Lentil	Not specified	0.92 ± 0.06 ng/g DW	N/A	RIA	[52]
Kidney beans	*Phaseolus vulgaris* L.	529.1 ng/g DW	3	HPLC-MS/MS	[53]
Soya bean	*Glycine max* L.	1.89 ± 0.11 ng/g DW	N/A	RIA	[52]
Vetch	*Vicia sativa* L.	1.91 ± 0.11 ng/g DW	N/A	RIA	[52]
Seedling					
Rice	*Oryza sativa* cv. Dongjin	1.9 ng/g DW	3	HPLC	[96]
Rice (transgenic)	*Oryza sativa* cv. Dongjin	2.7–5.2 ng/g DW	3	HPLC	[96]
Cucumber	*Cucumis sativus* L. cv. Jingyu-1	17.3 ng/g FW	3	UHPLC-ESI-MS/MS	[95]
Alfalfa	*Medicago sativa* L.	0.13 ± 0.01 ng/g DW	3	ELISA	[23]
Lentil	*Lens sculenta* L.	0.22 ± 0.0 1 ng/g DW	3	ELISA	[23]
Mung bean	*Vignaradiata* L.	0.17 ± 0.01 ng/g DW	3	ELISA	[23]
Onion	*Allium cepa* L.	0.30 ± 0.02 ng/g DW	3	ELISA	[23]
Broccoli	*Brassica oleraceae* L.	0.44 ± 0.01 ng/g DW	3	ELISA	[23]
Red cabbage	*Brassica oleraceae capitate* rubra L.	0.86 ± 0.05 ng/g DW	3	ELISA	[23]
Radish	*Raphanus sativus japonicum* L. *Raphanus sativus rambo* L. *Raphanus sativus sinicum rosae* L.	0.54 ± 0.04 ng/g DW	3	ELISA	[23]

Table 1. *Cont.*

Name	Scientific Name/Variety/Origin	MT Value or Range ng/g or pg/mL	No. of Samples	Quantified by	Reference
Nuts					
	Pistachio				
Pistachio	*Pistacia vera* L. cv. Ahmad Aghaei	233,000 ng/g DW	N/A	GC/MS	[28]
Pistachio	*Pistacia vera* L. cv. Akbari, Kalle	226,900 ng/g DW	N/A	GC/MS	[28]
Pistachio	*Pistacia vera* L. cv. Qouchi	231,400 ng/g DW	N/A	GC/MS	[28]
Pistachio	*Pistacia vera* L. cv. Fandoghi	228,400 ng/g DW	N/A	GC/MS	[28]
	Walnuts				
Walnuts	*Juglans regia* L. cv. Serr	1.02 ± 0.06 ng/g FW	4	HPLC–MS	[97]
Walnuts	*Juglans regia* L. cv. Hartley	1.77 ± 0.14 ng/g FW	4	HPLC–MS	[97]
Walnuts	*Juglans regia* L. cv. Chandler	1.37 ± 0.37 ng/g FW	4	HPLC–MS	[97]
Walnuts	*Juglans regia* L. cv. Howard	1.9 ± 0.4 ng/g FW	4	HPLC–MS	[97]
Walnuts	Not specified	0.14 ± 0.03 ng/g DW	5	LC–MS/MS	[42]
Walnuts	*Juglans regia* L.	3.5 ± 1.0 ng/g	5	HPLC-ECD	[78]
Juices and beverages					
Beer	Not specified	0.09 ± 0.01 ng/mL	5	LC-MS/MS	[42]
Wine					
Albana must	Albana, Romagna	1.1 ng/mL	3	HPLC-FD	[43]
Albana wine	Albana, Romagna	0.6 ng/mL	3	HPLC-FD	[43]
Albana grappa	Albana, Romagna	0.3 ng/mL	3	HPLC-FD	[43]
Red wine	Not specified	0.26 ± 0.18 ng/mL	3	UHPLCMS/MS	[59]
Dessert ice wine	Not specified	0.17 ± 0.11 ng/mL	3	UHPLCMS/MS	[59]
Groppello wines	*Vitis vinifera* L. cv. Groppello Gentile	5.2 ng/mL	3	UHPLCMS/MS	[59]
Merlot wines	Merlot	8.1 ng/mL	3	UHPLCMS/MS	[59]
Wine	Cabernet Sauvignon	14.2 ± 0.2 ng/mL	3	HPLC-MS/MS	[55]
Wine	Cabernet Sauvignon	0.23 ± 0.01 ng/mL	3	ELISA	[55]
Wine	Jaen Tinto	nd	3	HPLC-MS/MS	[55]
Wine	Jaen Tinto	0.16 ± 0.01 ng/mL	3	ELISA	[55]

Table 1. *Cont.*

Name	Scientific Name/Variety/Origin	MT Value or Range ng/g or pg/mL	No. of Samples	Quantified by	Reference
Wine	*Vitis vinifera* L. cv. Merlot	nd	3	HPLC-MS/MS	[55]
Wine	*Vitis vinifera* L. cv. Merlot	0.21 ± 0.02 ng/mL	3	ELISA	[55]
Wine	Palomino Negro	nd	3	HPLC-MS/MS	[55]
Wine	Palomino Negro	0.28 ± 0.00 ng/mL	3	ELISA	[55]
Wine	Petit Verdot	5.1 ± 0.6 ng/mL	3	HPLC-MS/MS	[55]
Wine	Petit Verdot	0.22 ± 0.01 ng/mL	3	ELISA	[55]
Wine	Prieto Picudo	49.0 ± 4.7 ng/mL	3	HPLC-MS/MS	[55]
Wine	Prieto Picudo	0.19 ± 0.01 ng/mL	3	ELISA	[55]
Wine	Syrah	86.5 ± 2.6 ng/mL	3	HPLC-MS/MS	[55]
Wine	Syrah	0.22 ± 0.02 ng/mL	3	ELISA	[55]
Wine	Tempranillo	129.5 ± 3.5 ng/mL	3	HPLC-MS/MS	[55]
Wine	Tempranillo	0.14 ± 0.01 ng/mL	3	ELISA	[55]
Wine	*Vitis vinifera* L. cv. Malbec	0.24 ng/mL	5	CEC	[56]
Wine	Cabernet Sauvignon	0.32 ng/mL	5	CEC	[56]
Wine	Chardonnay	0.16 ng/mL	5	CEC	[56]
Wine	Sangiovese, red	0.5 ng/mL	3	HPLC-FD	[43]
Wine	Trebbiano, white	0.4 ng/mL	3	HPLC-FD	[43]
Coffee beans					
Green coffee	Not specified	0.040 ± 0.01 ng/g DW	5	LC-MS/MS	[42]
Green beans	*Coffea canephora* L. (robusta)	5800 ± 800 ng/g DW	3	LC-MS-ESI	[58]
Green beans	*Coffea arabica* L. (arabica)	6800 ± 400 ng/g DW	3	LC-MS-ESI	[58]
Roasted beans	*Coffea canephora* L. (robusta)	8000 ±.900 ng/g DW	3	LC-MS-ESI	[58]
Roasted beans	*Coffea arabica* L. (arabica)	9600 ± 800 ng/g DW	3	LC-MS-ESI	[58]
Decoction (Brew)	*Coffea canephora* L. (robusta)	60 ± 12 ng/mL	3	LC-MS-ESI	[58]
Decoction (Brew)	*Coffea arabica* L. (arabica)	78 ± 5 ng/mL	3	LC-MS-ESI	[58]

Table 1. *Cont.*

Name	Scientific Name/Variety/Origin	MT Value or Range ng/g or pg/mL	No. of Samples	Quantified by	Reference
Juices					
Orange juice	*Citrus sinensis* L. var. Navel late (Huelva, Spain)	3.15–21.80 ng/mL	3	UHPLC-QqQ-MS/MS	[98]
Grape juice	Not specified	0.5 ng/mL	3	HPLC-FD	[43]
Cacao powder	Not specified	0.01 ng/g DW	5	LC-MS/MS	[42]
Concentrate					
Tart cherries	*Prunus cerasus* L. cv. Balaton	nd	3	HPLC-EMS	[46]
Tart cherries	*Prunus cerasus* L. cv. Montmorency	nd	3	HPLC-EMS	[46]
Sour cherries	Not specified	nd	5	LC-MS/MS	[42]
Tea					
Green tea	Not specified	nd	5	LC-MS/MS	[42]
Black tea	Not specified	nd	5	LC-MS/MS	[42]
Balsamic vinegars		0.12 ± 0.014 ng/mL	3	UHPLCMS/MS	[59]
Medical Herbs					
Huang-qin	*Scutellaria biacalensis*	7110 ng/g DW	2	Not specified	[29]
St John's Wort (flowers)	*Hypericum perforatum*	4490 ng/g DW	2	Not specified	[29]
Chantui	*Periostracum cicadae*	3771 ng/g DW	3	SPE-HPLC-FD	[61]
Gouteng	*Uncaria rhynchophylla*	2460 ng/g DW	3	SPE-HPLC-FD	[61]
Diding	*Viola philipica Cav.*	2368 ng/g DW	3	SPE-HPLC-FD	[61]
Shiya tea-leaf	*Babreum coscluea*	2120 ng/g DW	3	SPE-HPLC-FD	[61]
Feverfew (fresh leaves)	*Tanacetum parthenium*	1920–2450 ng/g DW	2	Not specified	[29]
St John's Wort (leaves)	*Hypericum perforatum*	1750 ng/g DW	2	Not specified	[29]
Sangye	*Morus alba* L. (Leaf)	1510 ng/g DW	3	SPE-HPLC-FD	[61]
Huangbo	*Phellodendron amurense* Rupr.	1235 ng/g DW	3	SPE-HPLC-FD	[61]
Sangbaipi	*Mori Albae* (Cortex)	1110 ng/g DW	3	SPE-HPLC-FD	[61]
Yinyanghuo	*Epimedium brevicornum Maxim*	1105 ng/g DW	3	SPE-HPLC-FD	[61]
Black pepper	*Piper nigrum* L.	1092.7 ng/g DW	5	SPE HPLC ELISA	[62]
Huanglian	*Coptis chinensis Franch*	1008 ng/g DW	3	SPE-HPLC-FD	[61]

Table 1. *Cont.*

Name	Scientific Name/Variety/Origin	MT Value or Range ng/g or pg/mL	No. of Samples	Quantified by	Reference
Mulberry leaves	*Morus* spp. cv. Buriram 60	279.6 ng/g DW	3	HPLC-FD	[99]
	Morus spp. cv. Sakonnakhon	100.5 ng/g DW	3	HPLC-FD	[99]
	Morus spp. cv. Khunphai	40.7 ng/g DW	3	HPLC-FD	[99]
Edible oil					
Virgin Argan oil	Not specified	0.06 ± 0.05 ng/g	2	HPLC-FD	[64]
Refined sunflower	Not specified	0.03–0.08 ng/g	2	HPLC-FD	[64]
Primrose,	Not specified	0.03–0.08 ng/g	2	HPLC-FD	[64]
Refined grape seed	Not specified	0.03–0.08 ng/g	2	HPLC-FD	[64]
Refined walnut	Not specified	0.03–0.08 ng/g	2	HPLC-FD	[64]
Virgin walnut	Not specified	0.03–0.08 ng/g	2	HPLC-FD	[64]
Virgin linseed	Not specified	0.03–0.08 ng/g	2	HPLC-FD	[64]
Linseed oils	Not specified	0.03–0.08 ng/g	2	HPLC-FD	[64]
Refined linseed	Not specified	0.29 ± 0.00 ng/g	2	HPLC-FD	[64]
Virgin sesame	Not specified	0.03–0.08 ng/g	2	HPLC-FD	[64]
Wheat germ	Not specified	0.03–0.08 ng/g	2	HPLC-FD	[64]
Virgin soybean	Not specified	0.19 ± 0.00 ng/g	2	HPLC-FD	[64]
Olive oil	Extra virgin	0.03 ± 0.00 ng/g	2	HPLC-FD	[64]
D.O. Sierra Ma′gina	Not specified	0.11 ± 0.04 ng/mL	3	ELISA	[63]
D.O. Siurana	Not specified	0.10 ± 0.02 ng/mL	3	ELISA	[63]
D.O. Bajo Arago′n	Not specified	0.07 ± 0.02 ng/mL	3	ELISA	[63]
D.O. Montes de Toledo	Not specified	0.11 ± 0.01 ng/mL	3	ELISA	[63]

Table 1. *Cont.*

Name	Scientific Name/Variety/Origin	MT Value or Range ng/g or pg/mL	No. of Samples	Quantified by	Reference
D.O. Baena	Not specified	0.12 ± 0.00 ng/mL	3	ELISA	[63]
D.O. Sierra de Segura	Not specified	0.09 ± 0.00 ng/mL	3	ELISA	[63]
D.O. Les Garrigues	Not specified	0.10 ± 0.00 ng/mL	3	ELISA	[63]
D.O. Toscano	Not specified	0.11 ± 0.02 ng/mL	3	ELISA	[63]
Refined olive oil sample 1	Not specified	0.05 ± 0.01 ng/mL	3	ELISA	[63]
Refined olive oil sample 2	Not specified	0.08 ± 0.01 ng/mL	3	ELISA	[63]
Refined sunflower oil sample	Not specified	0.05 ± 0.01 ng/mL	3	ELISA	[63]
Microorganisms					
Yeast (dried brewer)	*Saccharomyces cerevisae*	2.2 ± 0.14 ng/g	5	HPLC	[22]

Note: All the values are presented in a pattern of mean ± SD. * in vitro cultures grown on media enriched with zinc salts. ** estimated from the figure. Abbreviation used in the table: CEC: capillary electrochromatography; D.O.: designations of origin; ECD: electron capture detector; EIA: enzyme-linked immunosorbent assay; ELISA: enzyme-linked immunoasorbent assay; EMS: electrospray mass spectrometry; ESI: electronic spray ion; FD: fluorescence detector; GC/MS: gas chromatograph/mass spectrum; HPLC: high-performance liquid chromatography; nd: not detected; PLE: pressurized liquid extraction; RIA: radioimmunoassay; RP-HPLC: reversed-phase high-performance liquid chromatography; SPE: solid phase extraction; UHPLC: ultra-high-performance liquid chromatography; UV: ultraviolet.

3. Bioactivities of Melatonin

Melatonin has been well known as a potent antioxidant, anti-inflammatory factor and immune modulator. It also contributes to regulating the circadian system [100], possesses tumor inhibitory properties [7], and shows its benefits on cardiovascular functions [101], blood pressure [101], and lipid and glucose metabolism [102] (Table 2).

3.1. Antioxidant Activities

Reactive oxygen species (ROS) and reactive nitrogen species (RNS) play an important role in a variety of physiological processes, such as regulating vascular tone, controlling ventilation, producing erythropoietin and transducing signals [103,104]. Importantly, at a desirable level they can promote cell survival, proliferation and differentiation [105]. However, excessive free radicals could result in DNA and RNA damage, protein denaturation, lipid peroxidation, leading to cell apoptosis or necrosis. Consequently, a series of health problems occur, including aging [106], inflammation [107], cancer [108], chronic metabolic disease [109,110], neurodegenerative disorders [9] and sepsis [111]. Many natural products have shown antioxidant activities and free radical scavenging capabilities [112–116], which could be used to prevent and treat the diseases induced by oxidative stress [117–121].

As a powerful endogenous radical scavenger, melatonin can directly remove the excessive free radicals. In addition, melatonin at 10 mg/kg was found to increase the efficiency of electron transport chain in mitochondria in old mice to lower electron leakage and reduce free radical generation [122]. Therefore, melatonin is essential to keep a stable physiological status in human body. Moreover, it could effectively play a role by modulating and acting synergistically with other reducing molecules like reductases [123] and some non-enzyme reductants [124], all of which work together to maintain normal homeostasis.

There are many kinds of reductants in human body like glutathione, NADH and vitamin C or E, compared to which melatonin was documented as a stronger antioxidant in eliminating some free radicals both in vitro and in vivo [123,125]. For instance, it was reported that in vitro the ability of melatonin to scavenge the hydroxyl radical (·OH) was much higher compared with that of vitamin E [123], glutathione and mannitol [126]. Another in vitro study showed that melatonin could significantly inhibit the vasoconstriction induced by H_2O_2 in the human umbilical artery in a dose-dependent manner [127]. Moreover, it was found that in rats, melatonin was several times more powerful than vitamin C and E in protecting tissues from injuries induced by oxidative stress [125,128]. In addition, quite different from the other antioxidants, the metabolites of melatonin are also actively involved in scavenging free radicals, referred as cascade, though they are the intermediates in the process of reactions against radicals [129] (Figure 2). Interestingly, some of the metabolites are even more potent than its precursor. A good example is that the capacity of 3-hydroxymelatonin (C3-OHM) to reduce hypervalent hemoglobin was higher than that of its basic form and another example was N^1-acetyl-5-methoxykynuramine (AMK) showing stronger capability of scavenging ROS and preventing protein oxidation than its precursor [130,131]. Such a profile greatly increases the effectiveness of melatonin as a powerful free radical scavenger. Considering the cascade effects of the metabolites, a melatonin molecule could scavenge up to 10 ROS/RNS molecules [131].

Numerous evidence supports that melatonin is a broad-spectrum free radical scavenger [132–134]. In addition to ROS/RNS, many other molecules could be modulated or scavenged by melatonin and its metabolites, such as hemoglobin-derived oxoferryl radicals [135]. Furthermore, in vitro and/or in vivo, melatonin is able to chelate toxic metals such as cadmium [136], mercury [137], arsenic [138], lead [139], aluminum [140], chromium [141], which are involved in the generation of free radicals. Moreover, melatonin and its metabolites were also documented to exhibit free radical avoidance properties, by downregulating pro-oxidative enzymes like inducible nitric oxide synthase (iNOS) both in vitro (dose-dependent) and in vivo as well as inhibiting the mRNA expression of cyclo-oxygenase 1 (COX-1) and COX-2 in human breast cancer cells (MCF-7) [142,143].

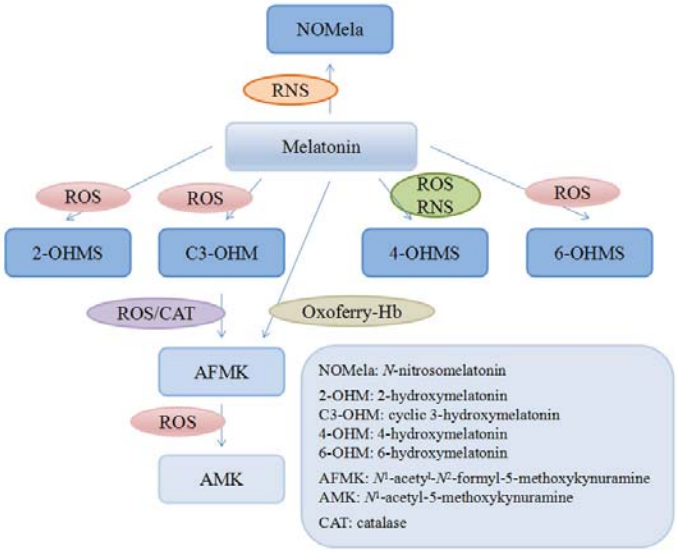

Figure 2. Melatonin and its metabolites.

Melatonin also stimulates the synthesis of other antioxidants. For instance, melatonin was found to induce the expression of gamma-glutamylcysteine synthetase (γ-GCS), the rate-limiting enzyme of GSH synthesis, in human vascular endothelial cells (ECV304) [124]. It was also observed that in 2 neuronal cell lines, melatonin could regulate the expression of antioxidant enzymes (AOEs) at 1 nM under normal conditions, showing the mRNA increase of superoxide dismutase (SOD), glutathione peroxidase (GPx) [144]. Moreover, in vivo and/or in vitro melatonin prevents antioxidant enzymes from oxidative stress, and increases the activities of other redox enzymes, such as catalase (CAT) [145], glutathione reductase (GSH-Rd) [146], and glucose-6-phosphate dehydrogenase (G6PD) [147]. Besides, in vitro melatonin could combine with other antioxidants including vitamin C, vitamin E, glutathione, at the concentration of 2.5–1600 μM, leading to the markedly enhanced protective effects of removing radicals synergistically [148].

3.2. Anti-Inflammatory Activities

Inflammation can commonly occur locally and systematically, caused by many external or intrinsic factors. It has been well documented that the complex interaction of oxidative stress and inflammation results in many diseases. Melatonin could not only reduce the oxidative levels as stated, but also effectively fight against inflammation via different mechanisms such as essential signaling pathways [70,149], the modulation of related genes [150] and the activation membrane receptors [151], as discussed in detail below.

3.2.1. NF-κB Signaling Pathway Involved Mechanisms

Nuclear factor kappa-light-chain-enhancer of activated B cells (NF-κB) is distributed in nearly all the types of animal cells and it is well known to control DNA transcription, cytokine production and cell survival [152,153]. It is an important pro-inflammatory factor that plays a pivotal role in oxidative stress-induced inflammation. In numerous research, melatonin was found to exert anti-inflammatory activity by suppressing NF-κB signaling pathways [70,154–157]. Melatonin and its metabolites such as AFMK and AMK were able to modulate NF-κB and its downstream pro-inflammatory target genes such as iNOS [70], COX-1 [158], COX-2 [156], tumor necrosis factor α (TNF-α) [159], glia and fibrillary

acidic protein (GFAP) [160], which contributed to the pathophysiology of many diseases. In vitro study, melatonin exerted cytoprotective and anti-inflammatory effects on oxidative stress-stimulated human chondrocytes by blocking the activated NF-κB as well as the phosphorylation of phosphatidyl inositol 3-kinase (PI3K)/Akt, p38, extracellular signal-regulated kinase (ERK), Jun *N*-terminal kinase (JNK), and mitogen-activated protein kinase (MAPK) in a dose- and time-dependent manner [161]. Another in vitro study showed melatonin at 1 nM also performed its anti-inflammatory functions by downregulating chemokine expression via the inhibition of NF-κB, signal transducer and activator of transcription (STAT)1/3 phosphorylation, and gamma-activated sequence (GAS)-driven transcriptional activity in lipopolysaccharide (LPS)-stimulated BV2 murine microglial cell line [162]. Additionally, the protective effect of melatonin on cigarette smoke-induced restenosis in rat carotid arteries after balloon injury was also observed as melatonin inhibited the inflammatory reaction via NF-κB signaling pathways [163]. Moreover, in mice with LPS-induced mastitis, besides the suppression of LPS-induced NF-κB activation, activating peroxisome proliferator-activated receptor gamma (PPAR-γ) was regarded as another underlying anti-inflammatory mechanism of melatonin [164]. A recent study indicated that exogenous melatonin could inhibit inhibitor of nuclear factor kappa-B kinase (IKK)/NF-κB signal transduction pathway in stimulated mast cells (RBL-2H3) to prevent inflammation and the effects were directly related with melatonin concentration used at 100 nM and 1 mM, based on which melatonin was implied to be used for the treatment of allergic inflammatory diseases [165].

3.2.2. SIRT1 Pathway Involved Mechanisms

It was suggested that human sirtuins may function as intracellular regulatory proteins with mono-ADP-ribosyl transferase activity, and sirtuin 1 (SIRT1), also known as NAD-dependent deacetylase, was reported to improve insulin sensitivity, as it could affect the activity of both the estrogen-related receptor alpha (ERR-α) and the peroxisome proliferator-activated receptor gamma coactivator-1 alpha (PGC-1α), which are essential metabolic regulatory transcription factors [149]. Specifically, SIRT1 was able to independently enhance ERR-α and modulate the effects of PGC-1α repression of glycolytic genes [166,167]. In a rabbit model with osteoarthritis (OA), intra-articular injection of melatonin at 20 mg/kg significantly reduced cartilage degradation, which was reversed by sirtinol, indicating SIRT1 pathway was involved [161]. Additionally, both in vitro and in vivo studies showed that melatonin reduced LPS-induced oxidative stress damage, acute neuroinflammation, and apoptotic neurodegeneration via SIRT1/Nrf2 (nuclear factor-erythroid 2-related factor 2) signaling pathway activation [168].

In addition to the pathways mentioned above, the anti-inflammatory effects of melatonin were also observed as it regulated the expression of some pro-inflammatory genes [150]. Moreover, it was found that melatonin could inhibit the expression of inflammatory chemokines/cytokines, i.e., chemokine (C-X-C motif) ligand 1 (CXCL1), chemokine (C-C motif) ligand 20 (CCL20), and interleukin 6 (IL-6) that was mediated by IL-17 and enhanced by increased insulin and insulin-like growth factor 1 (IGF-1) in the prostatic tissues of obese mouse through a glycogen synthase kinase 3β (GSK3β)-dependent mechanism [169]. Another study found that melatonin at 10 μM could show its anti-inflammatory impacts time-dependently by inducing temporal up-regulation of gene expression related to ubiquitin/proteasome system (UPS) in the human malaria parasite *Plasmodium falciparum* [170]. Additionally, it was reported that melatonin (10 mg/kg, intraperitoneally, i.p.) attenuated colitis with sleep deprivation in mice by downregulating mRNA of E2F transcription factor (E2F2) and histocompatibility class II antigen A, beta 1 (H2-Aβ1), indicating its clinical potential for patients with inflammatory bowel disease, particularly those suffering from sleep disturbances [171]. Furthermore, melatonin was reported to reduce intestinal ischemia-reperfusion-induced lung injury in rats dose-dependently by activating the expression of *N*-myc downstream-regulated gene 2 (NDRG2), which was involved in cellular differentiation, development, anti-apoptosis, anti-inflammatory cytokine, and antioxidant [172]. However, it should be pointed out that those results were from different animal models. If the same animal model was used, different results might be observed.

Besides, it has been reported that melatonin receptors were involved in its anti-inflammatory mechanism. It was found that melatonin played a role in maintaining the pro- and anti- inflammatory balance during infection by influencing leukocyte migration and apoptosis in carp possibly mediated by melatonin MT1 receptors in/on leukocytes [151].

3.3. Enhancing Immune Activities

Recently, numerous experimental evidence has shown that melatonin is involved in the interaction between the nervous, endocrine, and immune systems on the basis of the research on surgical or functional pinealectomy as well as the association between melatonin production and circadian and seasonal rhythms in the immune system [173–175]. In these three interactive systems, the reciprocal regulation exists. For instance, the immunological parameters such as TNF-α [176], IL-12 [177], interferon gamma (IFN-γ) [178], granulocyte colony-stimulating factor (G-CSF) and granulocyte–macrophage colony-stimulating factor (GM-CSF) [179] can affect the function of pineal gland. In addition, NF-κB could be active during pathogen invasion and melatonin synthesis could be promoted in macrophages while inhibited in pinealocytes. Therefore, immune-pineal axis has been defined as the shift in the melatonin production from pinealocytes to immune competent cells mediated by NF-κB [180,181]. Furthermore, melatonin exerted the neuroimmunomodulatory effect on the immune system via its membrane receptors, which have been identified in immune organs, tissues, bone marrow mononuclear cells (BMMNCs) and leukocytes, and even subcellular compartments [180,182]. With MT1 and MT2 receptors, melatonin was found to inhibit the production of forskolin-stimulated cyclic AMP (cAMP), cyclic GMP (cGMP) and diacylglycerol (DAG), leading to the improved immunity [183,184]. Besides, the specific nuclear melatonin receptors have been identified in Jurkat cells [185], lymphocytes [186], thymus [175] and spleen [187], which belong to the RZR/ROR subfamily of nuclear receptors.

It was observed that melatonin could reverse the weight loss of thymuses [175] and spleens [188] in different pinealectomized animal models and melatonin could increase tonsillar size [189], indicating the protective effects of melatonin on the immune organs. Besides, melatonin and its metabolites like AFMK were found to improve the proliferation, increase the activity and inhibit apoptosis of immune competent cells such as monocyte [190], natural killer (NK) cells [191] and neutrophils [192]. Melatonin could act on the membrane receptors MT1 and MT2 and increase the sensitivity of the immune cells to some cytokines such as TNF-α and IFN-γ in vivo at the dose of 10 mg/kg orally administrated [193]. Furthermore, Ghosh et al. found that melatonin could restored the suppressed immunity of T-cell culture in vitro, indicating melatonin might be valuable in regulating immunity via the functional interactions with gonadal steroid by developing some hormonal microcircuit (gonadal steroid and melatonin) in lymphatic organs [194]. Moreover, melatonin was able to modulate immune mediator production, e.g., increased IL-2, IFN-γ and IL-6 in monocytes [195] in cultured human mononuclear cells, decreased IL-8 and TNF-α in neutrophils [192], decreased IL-1β, IL-6, IL-8, IL-10 and TNF-α in macrophages in RAW264.7 cells [196]. This profile is of great importance as some cytokines have been shown to interact with immune cells and promote their growth, differentiation, activation, and survival. Besides the endocrine actions from the pineal melatonin, the melatonin synthesized in immune system could exhibit direct immunomodulatory effects by means of nonendocrine actions, including intra-, auto-, and/or paracrine actions via its membrane and/or nuclear receptors [197], which were crucial for human lymphocytes to generate an accurate response by modulating the IL-2/IL-2R system [198].

Melatonin was reported to regulate the ROS production in the essential immune cells such as monocytes [199] and neutrophils [200]. Moreover, melatonin was found to augment the general immunity by attenuating oxidative load associated with age in hamsters by 25 μg/100 g body weight for 30 days [201]. It was reported that melatonin could alleviate oxidative damage and suppress the immune status induced by stressful factors via its membrane receptor expression MT1 and MT2 in wild birds [202]. Due to its anti-inflammatory properties, melatonin could suppress systemic innate

immune activation during sepsis in mice both in vivo and in vitro by blocking the NF-κB/NOD-like receptor P3 (NLRP3) connection through a sirtuin1-dependent pathway [154].

Collectively, it has been well documented that melatonin played a fundamental role in resisting harmful invasion and enhancing immunity as a member of the complex neuro–endocrine–immunological system.

3.4. Improving Circadian Rhythm and Sleep

It was estimated that about one-third of the general population is suffering from sleep disorders, mainly insomnia, and there is an increasing trend because of the more stressful working conditions and the progressive aging of society [203]. Circadian rhythms are common in nature and have been widely observed in cyanobacteria, fungi, plants, and animals [204]. Disturbance of circadian rhythms can cause many diseases like cancers [205], metabolic syndromes [206], reproductive diseases [207] etc. Disruption of circadian rhythms and sleep disorders are prevalent, which can do harm to patients' overall health, worsen existing comorbidities and result in impaired quality of life, whereas melatonin could modulate circadian rhythm and improve sleep disorders [100,208–210].

In mammals, most of the physiological processes and behaviors are regulated by a network of circadian clocks. The circadian system consists of a central rhythm generator, the suprachiasmatic nucleus (SCN), and several peripheral oscillators [211]. Besides, the central clock can control the production of melatonin, which could modify the peripheral clocks and inversely alter the expression of circadian clock genes. Johnston et al. [212] found that rising melatonin levels could reset circadian rhythms in the mammalian pars tuberalis. Melatonin has long been known to help prevent and treat jet lag, a typical example of disrupted circadian rhythms often caused by travelling [2].

The animal models of melatonin-proficient (C3H) and melatonin-deficient (C57BL) mice are frequently used to study the role of melatonin on circadian rhythms. In a study, research on three clock gene proteins PER1, BMAL1 and CRY2 in the murine adrenal cortex and medulla was conducted and the results showed that in C3H mice, PER1 and CRY2 maximized in the middle of the light phase, whereas BMAL1 reached its peak in the dark phase and these three clock gene proteins levels displayed day/night variation in both the adrenal cortex and medulla. Similar patterns were revealed in the adrenal medulla of C57BL mice, but in the adrenal cortex of C57BL mice, clock gene protein levels were consistently lower than in C3H mice and did not change with time [211]. In another study, the modulatory effects on clock gene expression of melatonin was investigated in the retina of those two groups of mice, and the results demonstrated that melatonin functioned via post-transcriptional mechanisms and also played a role in rhythmic regulation of phosphorylated cAMP response element-binding protein (pCREB) levels in the mammalian retina [213].

As an external trigger of melatonin production, light, blue-enriched light in particular, was observed to significantly suppress the nocturnal increase in endogenous melatonin levels in human, indicating that a clock gene polymorphism could modulate light sensitivity in humans, especially in the individuals, who are homozygous for the PER3 5/5 allele [214]. Additionally, it was observed that melatonin activated Npas4, which drove the clock gene CRY1 responses to melatonin in vivo [215]. Furthermore, Bracci et al. [216] reported that alterations in peripheral clock gene expression, i.e., a significantly higher expression of BMAL1, CLOCK, NPAS2, PER1, PER2, and REVERBα and a lower expression of PER3, CRY1 and CRY2, were found at the beginning of the morning shift after a day off in rotating shift work nurses as well as significantly higher 17-β-estradiol levels compared to daytime nurses. Another study reported that both Period1 and BMAL1 expression increased in the hippocampus of Siberian hamsters after acute melatonin treatment of 20 μg/day, accompanied by the alterations of dendritic morphology, indicating melatonin could act as a signal to coordinate the circadian rhythm in neuronal remodeling [217]. Additionally, melatonin was found to adjust the expression pattern of clock genes (per1, per2, bmal1 and clock) in the SCN mainly by increasing amplitude in their expressional rhythms without inducing robust phase shifts in them. In addition, melatonin could alter the expression of genes of serotonergic neurotransmission (tph2, sert, vmat2 and

5ht1a) in the dorsal raphe and serotonin contents in the amygdala, and improve the depression-like behavior in C57BL/6J mice with seasonal affective disorder [218].

Melatonin has been known as the 'hormone of darkness' as its synthesis and secretion are controlled by light/dark cycles, i.e., its production decreases during daytime and increases at night. The decreased nocturnal plasma melatonin levels were found in patients with long-lasting insomniac complaints, indicating circadian rhythm dysfunctions [219]. Additionally, it was reported that sleep parameters were positively correlated with melatonin secretion in patients with insomnia in coronary care unit [220]. Furthermore, melatonin was found to regulate sleep by activating receptor MT1, MT2 and enhancing the excitability of medial lateral habenula (MLHb) neurons in rats [221].

Besides, a number of studies have shown that melatonin and melatoninergic agents were effective in the treatment of insomnia, as it could accelerate sleep initiation, increase sleep duration and slightly alter sleep architecture [222,223]. In addition, due to the short half-life of melatonin in circulation, a prolonged-release melatonin medicine (Circadin®) [224], melatonin derivatives (e.g., ramelteon) [203], another melatonin agonists (e.g., agomelatine) [225,226] have been approved by authorities in the EU and USA to treat insomnia and resynchronize circadian rhythms.

3.5. Anticancer Activities

According to the World Cancer Report 2014 from WHO, cancers are among the leading causes of morbidity and mortality all around the world, with approximately 14 million new cases and 8.2 million cancer related deaths in 2012 and the number of new cases is expected to rise by about 70% over the next 2 decades [227]. Many foods were found to contain natural components with strong anticancer activities, indicating the potential for the prevention and treatment of different cancers [7,228–231].

Melatonin has been proved to be highly involved in the etiology, development, metabolism, metastasis, and therapy of different subsets of tumors. The mechanisms include inhibiting tumor cell growth and proliferation [232], modulating the metabolism of tumor cells [233], promoting apoptosis [234], exerting antimetastatic and antiangiogenic effects [235], enhancing the sensitivities to the anticancer drugs, attenuating the side effects of radio- and chemotherapies [157]. In addition, mechanisms of melatonin impacts on cancers comprise the actions of melatonin receptors MT1 and MT2, the regulation of relevant genes expression and the modulation of some signaling pathways [236,237].

3.5.1. Effects on Tumor Cell Cycle, in Terms of Growth, Proliferation, Metabolism and Apoptosis

A study conducted by Wu et al. [232] demonstrated that both in vitro and in vivo, melatonin inhibited gastric tumor growth and peritoneal dissemination through the activation of endoplasmic reticulum (ER) stress and the inhibition of epithelial mesenchymal transition (EMT) via calpain-mediated C/enhancer-binding protein beta (EBPβ) and NF-κB cleavage. Another study demonstrated that melatonin could suppress breast cancer cell proliferation by exhibiting an anti-aromatase effect on hormonal positive breast cancer cells through the selective estrogen enzyme modulators (SEEMs) mechanism [238]. Furthermore, Hevia et al. reported that melatonin (1 mM) reduced glucose uptake and modified the expression of GLUT1 transporter in prostate cancer cells, resulting the attenuated glucose-induced tumor progression and the prolonged lifespan of tumor-bearing mice [233]. Moreover, Sohn et al. reported that the antiangiogenic properties of melatonin (1 mM) in hypoxic PC3 prostate cancer cells were mediated by enhancing the expression of miRNA3195 and miRNA374b [239]. Melatonin at pharmacological concentrations was able to significantly induce apoptosis of colorectal cancer LoVo cells in a dose-dependent manner via histone deacetylase 4 (HDAC4) nuclear import and decreasing H3 acetylation on Bcl-2 promoter, resulting in reduced Bcl-2 expression, which were mediated by inactivating Ca^{2+}/calmodulin-dependent protein kinase II alpha (CaMKIIα) [240]. Besides, melatonin was found to enhance arsenic trioxide-induced apoptotic cell death at the dose of 2 mM by sustainably upregulating Redd1 expression and inhibiting mTORC1 upstream of the activated p38/JNK pathways in human breast cancer cells [234].

3.5.2. Effects on Invasion and Metastasis of Tumor Cells

Melatonin (1 mM) could modulate motility and invasiveness of HepG2 cell in vitro through the upregulation of tissue inhibitor of metalloproteinases 1 (TIMP-1) and the attenuation of matrix metalloproteinase-9 (MMP-9) expression and activity by inhibiting NF-κB signaling pathway [241]. Melatonin was found to suppress the transactivation of MMP-9 and the metastasis of renal cell carcinoma (the most lethal of all urological malignant tumors with the potent metastasis potential) via the inhibition of Akt-MAPKs pathway and NF-κB DNA-binding activity [242]. Additionally, melatonin showed its oncostatic, antimetastatic and antiangiogenic effects in breast cancer both in vitro and in vivo by blocking proliferation of tumor cells and inhibiting the expression of Rho-associated kinase protein (ROCK-1), one of the regulatory and effector molecules in charge of migration/invasion, which could promote tumor growth and metastasis when its expression was increased [235].

3.5.3. Therapy Adjunct in Tumor Treatment

Lu et al. reported that melatonin could enhance the antitumor activity of berberine (B in Figure 3) in lung cancer cells by activating caspase/cytochrome c (cyt c) and inhibiting activator protein 2β (AP-2β)/human telomerase reserve transcriptase (hTERT), NF-κB/COX-2 and Akt/ERK signaling pathways as well as increasing the sensitivities of lung cancer cells to berberine (Figure 3) [157]. Alonso-Gonzalez et al. pointed out that the pretreatment of 1 nM melatonin before radiation could elevate the sensitivity of human breast cancer cells to radiotherapy by reducing the active estrogens levels in cancer cells through the increased p53 expression [243]. It was also found that melatonin-based creams could significantly lower the occurrence of acute radiation dermatitis in a double-blind randomized trial [244]. It was revealed that melatonin, as a powerful antioxidant, played a protective role at 10 mg/kg in rats to alleviate the testicular dysfunction induced by chemotherapy against testicular cancer [245], which is one of the most common cancers in men of reproductive age with a steadily increasing incidence [227]. Another in vivo study reported that melatonin (25 mg/kg) could synergize the chemotherapeutic effect of 5-fluorouracil (one of the most commonly used chemotherapeutic agents to treat colon cancer) in mice with colon cancer, by promoting the activation of the caspase/poly-ADP-ribose polymerase (PARP)-dependent apoptosis pathway, inhibiting PI3K/AKT and NF-κB/iNOS signaling pathways. The results of the same study also demonstrated that melatonin significantly enhanced the 5-fluorouracil-mediated inhibition of cell growth and metastasis of colon cancer cells [70]. Additionally, a meta-analysis of randomized controlled trials reported that melatonin, as an adjuvant, could substantially reduce the side effects caused by radiochemotherapy, presenting the improved tumor remission and the increased 1-year survival [246].

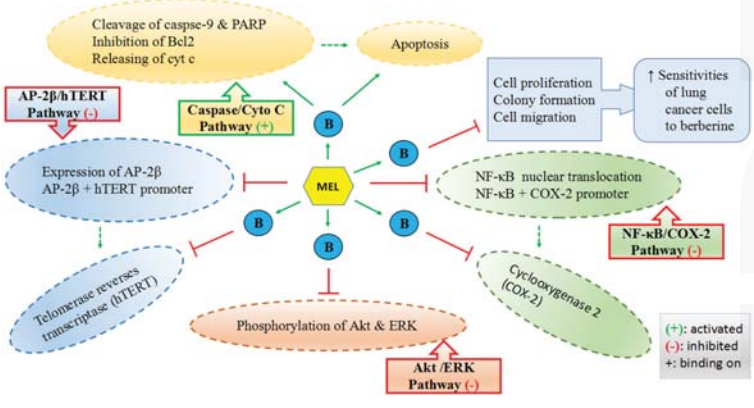

Figure 3. Mechanisms of melatonin enhancing the sensitivities of lung cancer cells to berberine (B).

It was also observed that MT1 and MT2 mRNA expression levels increased markedly in vitro and in samples from cancer patients, indicating that the receptor-mediated mechanisms were involved in the anticancer activities of melatonin [236,237].

3.6. Cardiovascular Protection

Cardiovascular diseases (CVDs) are the No. 1 cause of death worldwide, which accounted for 31% of all global deaths in 2012, i.e., an estimated 17.5 million people died from CVDs [247]. It has been found that melatonin is involved in the pathophysiological process of CVDs, such as plaque formation, atherosclerosis, and infarction. Melatonin was reported to regulate platelet physiology [248], protect the vascular endothelium [249], regulate lipid and glucose metabolism and modulate blood pressure [250], by reducing atherosclerosis, inhibiting thrombosis, which contribute to prevent CVDs or facilitate the restoration of morphology and functions of heart and vessels after injury based on reducing oxidative stress, inhibiting inflammation, decreasing apoptosis and preventing postinfarction remodeling of cardiomyocyte [251].

It was reported that melatonin could reduce heart rate and blood pressure, regulate the cardiac rhythm and the vascular tone via neurohumoral regulation in which the antioxidant capacity was involved [252,253]. Moreover, melatonin has been reported to protect cardiomyocytes and blood vessels against fibrosis necrosis and vasculitis in radiation-induced heart disease in rats when administrated at 50 mg/kg [254]. Furthermore, melatonin was demonstrated to dose-dependently reduce flow shear stress-induced injury in bone marrow mesenchymal stem cells (BM-MSCs) through the activation of melatonin receptors and adenosine monophosphate activated protein kinase (AMPK)/ACC (acetyl-CoA carboxylase) signaling, which could benefit the patients with valvular heart disease [255].

Melatonin was proved to increase the survival of adipose-derived mesenchymal stem cells in infarcted heart in mice at 20 mg/kg by activating SIRT1 signaling [256]. Besides, melatonin was found to significantly reduce the infarct size in myocardial ischemia-reperfusion injury (IRI) and decrease apoptosis through the activation of Janus kinase 2 (JAK2)/STAT3 signaling and PI3K/Akt signaling [257,258]. Additionally, it was reported that melatonin at 5 μM could improve the cardiac regularity in Drosophila melanogaster without affecting heart rate, possibly via a specific G-protein-coupled receptor which is encoded by the CG 4313 gene and considered to be a candidate melatonin receptor, indicating melatonin might play an essential role in cardiac pacemaking [259]. Besides, melatonin was closely related with reverse remodeling after cardiac resynchronization therapy in patients with heart failure and ventricular dyssynchrony [260]. Furthermore, it was observed that melatonin could markedly improve cardiac dysfunction, mitigate cardiac remodeling after myocardial infarction, increase the level of autophagy, attenuate apoptosis, regulate the integrity and restore the function of mitochondria through the inhibition of mammalian Ste20-like kinase 1 (Mst1) and the promotion of SIRT1, indicating the Mst1/SIRT1 signaling was involved [261].

Melatonin has also been found to modulate blood pressure and protect the organs and tissues damaged by hypertension. As reported by WHO, hypertension is one of the leading risk factors for CVDs and it caused 9.4 million deaths in 2010. The worldwide prevalence of hypertension in adults aged 18 years and over was around 22% in 2014 [262]. Melatonin could reduce blood pressure, pulsatility index in the internal carotid artery and catecholamines, indicating melatonin was involved in the renin-angiotensin-aldosterone system, which plays an essential role in blood pressure regulation [250]. In addition, it has been demonstrated that melatonin could regulate blood pressure both experimentally and clinically [263,264]. Hung et al. reported that melatonin was able to improve endothelial dysfunction, suppress vascular inflammation, and ameliorate systemic hypertension in rats on the basis of antioxidant and anti-inflammatory properties [265]. In addition, it was observed that melatonin could mitigate renal injury induced by hypertension by reducing oxidative stress [266,267]. It was demonstrated that melatonin could attenuate intracranial hypertension by reducing cerebral edema via the anti-inflammatory mechanism [268]. Besides, melatonin exerted the regulatory effects on blood pressure due to the interaction with both cardiovascular system and the central nerve system

(CNS), by restoring the balance between the sympathetic and parasympathetic vegetative system in favor with the latter [267]. Furthermore, melatonin could even reduce fetal blood pressure in ovine fetus via the membrane receptors MT1 and MT2, possibly by releasing endothelin [269].

Several studies showed that melatonin could reduce the levels of blood lipid, another risk factor for CVDs. Dyslipidemia is commonly accompanied with other disorders related to metabolic syndromes. Melatonin has been observed to effectively improve dysplipidemia by reducing LDL cholesterol levels, total cholesterol and triglycerides, but increase HDL-C, glucose tolerance and antioxidant potency due to its potent antioxidant effects [270–272].

3.7. Anti-Diabetic Activities

According to the WHO, an estimated 1.5 million deaths were directly caused by diabetes and another 2.2 million deaths were attributable to high blood glucose in 2012. Diabetes prevalence has been rising more rapidly, and there were 422 million diabetic people in 2014. Diabetes can cause severe complications leading to disability and death, and diabetes will be the 7th leading cause of death in 2030, as estimated [273]. It has been investigated that melatonin was able to prevent the complications by attenuating glucotoxicity to the organs and tissues mainly because of its antioxidant, anti-inflammatory and antiapoptotic effects.

Melatonin was found to increase the inhibited activity of catalase in rat liver cells and restore the dysfunctional mitochondria related to diabetes at the dose of 10 mg/kg, indicating melatonin could be a beneficial option to treat diabetes [274]. It was also shown that melatonin could improve dysglycemia in rats through the inhibition of hepatic gluconeogenesis and the activation of hypothalamic Akt via membrane receptors MT1 and MT2 [275]. Another study in rats with 10 mg/kg revealed that chronic melatonin administration at pharmacological doses was able to increases Ca^{2+} levels in lots of organs and tissues, such as liver, pancreas, muscle and white adipose tissues, resulting in the improved insulin sensitivity and secretion, indicating the potential clinical use of melatonin against type 2 diabetes [11]. In addition, melatonin showed its protective capability on myocardial cells in type 2 diabetic rats by reducing oxidative stress and ER stress (induced by the elevated blood glucose) through the activation of SIRT1 signaling pathway and inactivation of protein kinase-like endoplasmic reticulum kinase (PERK)/eukaryotic translation initiation factor 2 (eIF2α)/ATF4 (activating transcription factor 4) signaling pathway [276]. Besides, melatonin could prevent pancreatic islet failure caused by β-cell loss and dysfunction in type 2 diabetes, by attenuating β-cell apoptosis, improving its function, and prolonging its survival through the activation of β-cell melatonin signaling [277]. Recently, melatonin could improve the impaired memory caused by diabetes at 10 mg/kg in rats by improving neurogenesis, synaptogenesis in hippocampi, increasing the receptors of melatonin and insulin, and restoring the downstream signaling pathway for insulin [278]. Additionally, it was found that melatonin (250 μg, i.p.) could accelerate bone healing in rats with diabetes due to its antioxidant properties [279]. Furthermore, melatonin was also observed to restore the endothelial dysfunction and improve vascular responses in diabetic rats with 10 mg/kg administration [271].

3.8. Anti-Obese Activities

Data from WHO shows that more than 39% of adults (1.9 billion) were overweight and over 13% (600 million) were obese in 2014; meanwhile, 41 million children under the age of 5 were overweight or obese [280]. Obesity is also a strong risk factor for other metabolic diseases. Although obesity is a result of imbalance of energy intake and expenditure, many other factors are involved in and contribute to the obese conditions, such as chronic inflammation, oxidative stress, circadian disruption and sleep deprivation [281]. Melatonin has been reported to attenuate the damage caused by obesity.

Melatonin could play an important role in energy metabolism in obese mice based on gene modulatory effects, antioxidant and anti-inflammatory capacity. An in vivo study demonstrated that melatonin at 10 mg/kg could induce white adipose tissue browning in rats with obesity-related type 2 diabetes by increasing the uncoupling protein 1 (UCP1) and PGC-1α, the thermogenic proteins,

which possibly provided the reasons why melatonin was considered as a contributor to control body weight without effects on food intake and physical activity levels [282]. Additionally, melatonin was observed to benefit homeostasis of renal glutathione which was overproduced due to oxidative stress in obese rats [283]. Moreover, melatonin could regulate the cytokines such as IL-8, IL-10, IFN-γ, and inducible protein 10, which were considered as predictors of overweight and obesity [284]. It was also observed that insulin, insulin-like growth factor 1 (IGF1), and IL-17 increased in obesity. In addition, IL-17 alone or combined with insulin could promote CXCL1 and CCL20 expression, which could be suppressed by melatonin at 10 nM through inhibiting Akt activation and increasing GSK3β activity [169]. Since the adipocytes produce adipokines, the increase of TNF-α, resistin, and visfatin was found under obese conditions in mice, which melatonin could suppress to some degree when used at 100 mg/kg, indicating the beneficial impact of melatonin to control obesity [285].

It has been reported that that both clock genes [286] and metabolic genes [287] were identified in adipose tissues, which could regulate lipid generation and metabolism, adipocyte proliferation and differentiation, and adipose endocrine functions. Moreover, a cohort study of women aged 16 and above in the UK revealed that light at night (LAN) was significantly associated with obesity, indicating melatonin was involved in the development of obesity due to its regulatory effects on sleep and circadian rhythms [288]. Furthermore, melatonin could promote circadian rhythm-mediated proliferation in adipose tissue in mice at 20 mg/kg by increasing the expression of adipocyte proliferation genes via a complex of Clock/histone deacetylase 3 (HDAC3)/c-Myc [206].

Melatonin was also reported to prevent the harmful effects induced by obesity on the main functional organs to reduce the complications of obesity. It was found that melatonin at 4 mg/kg could exhibit the cardioprotective effects in rats with diet-induced obesity as shown by the decreased myocardial infarct sizes and insulin resistant, and the increased serum adiponectin, protein kinase B (PKB)/Akt, ERK42/44, GSK-3β and STAT3 without affecting the body weight or visceral adiposity [289]. Melatonin could also prevent renal failure at the dose of 100 mg/kg through improving the morphology and the functions of renal convoluted tubules in obese mice, by increasing mitofusin-2 expression, an apoptosis modulator [290]. In addition, when used at 10 mg/kg, melatonin was proved to markedly improve non-alcoholic liver steatosis in mice with obesity induced by high fat diet, presenting the decreased TNF-α, IL-1β, IL-6, and phosphorylation of p38 and JNK1/2, indicating the MAPK-JNK/p38 signaling pathway was involved [291].

3.9. Neuroprotective Activities

Melatonin was found to exhibit the neuroprotective effects on CNS [292]. In a mouse model of traumatic brain injury (TBI), melatonin was administered by 10 mg/kg i.v. at 0, 1, 2, 3, and 4 h post-TBI, the pathological alternations were significantly ameliorated, such as cortical neuronal degeneration and brain edema, mainly due to its antioxidant property through the Nrf2-ARE (antioxidant responsive element) pathway [293]. It was also reported that melatonin could prevent the adult mice brain from IRI at the dose of 10 mg/kg, administrated intraperitoneally, twice (immediately after induction of ischemia and at reperfusion onset). The suggested underling mechanism was to restore the function of mitochondrial by activating SIRT1 signaling pathway [294]. Another research in rats with early brain injury following a hemorrhagic stroke, in particular subarachnoid hemorrhage (SAH), found that melatonin (150 mg/kg, i.p.) could markedly alleviate brain edema, restore the integrity of blood-brain barrier (BBB) by suppressing cortical expressions of proinflammatory cytokines (e.g., IL-1β, IL-6, and TNF-α) [295]. Besides, it was observed in mice that lower dose of melatonin (5 mg/kg, i.p.) could also reduce the injuries in both gray and white matter and better the neurobehavioral outcomes induced by transient focal cerebral ischemia as a potent radical scavenger [296]. Furthermore, melatonin (10 mg/kg) was found to exhibit the neuroprotective and anti-apoptotic effects on oxidative brain damage induced by hemolytic hyperbilirubinemia in newborn Sprague-Dawley rats by reversing the increased plasma TNF-α, IL-1β levels, as well as the decreased brain derived neurotrophic factor (BDNF), S100 calcium-binding protein B (S100B) and IL-10 values [297].

The benefits that melatonin could provide to the peripheral nerve have also been widely investigated. It was found that the diclofenac sodium (DS) exposure during pregnancy could damage the fetal peripheral nerve system in rats, which could be improved by melatonin at doses of 10 and 50 mg/kg, showing the significant increase in the axon numbers of right sciatic nerve in male newborn rats with both of the doses administrated. Moreover, the significant increase in the diameter of the axons was found only with high dose of melatonin [298]. Additionally, optic neuritis (ON) might induce permanent vision loss, characterized by inflammation, demyelination, and neurodegeneration of the optic nerve. Melatonin showed its preventive effects by subcutaneous pellet of 20 mg in adult male Wistar rats with ON induced by LPS. The mechanism might be preventing the decrease in visual evoked potentials (VEPs) and pupil light reflex (PLR), inhibiting microglial reactivity, astrocytosis, demyelination, and axon and retinal ganglion cell loss and preserving anterograde transport of cholera toxin β-subunit from the retina to the superior colliculus. In the same study, the therapeutical effects of melatonin on ON was also observed as it reversed the decrease in VEPs and PLR completely when the pellet was implanted at 4 days postinjection of LPS [299].

Since reduced melatonin concentrations were identified in chronic neurodegenerative disease, such as Alzheimer's disease (AD) and Parkinson's disease (PD), exogenous melatonin treatment showed excellent neuroprotective effects as melatonin is a member of neuroimmuno-endocrine regulator family, which is involved in circadian rhythm, immune and redox actions and also attributing to its potent capacity of anti-apoptosis, and anti-inflammation [300,301]. It was found that the decreased melatonin concentrations in blood were significantly correlated to the loss of hypothalamic gray matter volume and disease severity in PD patients [302]. In addition, it was reported that the melatonin at 4 mM could improve sleep disorders and synaptic dysfunction in Drosophila caused by human leucine-rich repeat kinase 2 (hLRRK2), the most common genetic factor of PD [303]. For AD, amyloid-beta (Aβ) is one of the key pathological factors, which could initiate of the cognitive symptoms of dementia and its aggregation could result in synaptic loss, inflammation and cell death [304]. It was reported that melatonin administration at 10 mg/kg could significantly restore mRNA and protein levels of β-APP-cleaving enzyme 1 (BACE1) and presenilin 1 (PS1) in aged mice [305]. In addition, melatonin (500 mg/kg in 25% ethanol, i.p.) was found to improve the injured spatial learning and memory induced by Aβ1–42, restore the synaptic plasticity, and attenuate astrogliosis in rat. In addition, the in vitro study in primary hippocampal neuron demonstrated that melatonin (50 μM) exhibited the neuroprotective effects against Aβ1–42 through the Musashi1/Notch1/Hairy and enhancer of split 1(Hes1) signaling pathway [301].

Besides, it is quite common that nerve injuries can also be induced by medications, toxic chemicals, irradiation or other causes. Oxaliplatin (Oxa) can cause neurotoxicity as a third-era platinum-based chemotherapy against colorectal cancers. The outcomes of 10 mg/kg i.p. melatonin pretreament in rats followed by Oxa injections (4 mg/kg, i.p.) showed that the motor activity and muscular strength were improved, presenting that the inactivation of Bcl-2, caspase 3 apoptotic protein and cyt c release were modulated as well as the non-enzymatic, enzymatic antioxidants and complex enzymes of mitochondria [306]. Additionally, melatonin was reported to prevent neurotoxicity induced by cadmium in mouse neuroblastoma cells, via the activation of transcription factor EB-dependent autophagy-lysosome [136]. Moreover, the beneficial effects of melatonin against irradiation was observed after melatonin was administered at 100 mg/kg in male Sprague-Dawley rats, due to the caspase-3 inhibition [307]. In addition, melatonin (50 mg/kg) was found to prevent the neuronal damage in the hippocampus in pregnant rats caused by 900 MHz electromagnetic fields (EMF), which might be associated with the use of mobile phones [308]. Furthermore, it has been suggested that if the *N*-acetyl group of melatonin was removed, its antioxidant and neuroprotective properties would be improved at the expense of toxic methamphetamine-like effects in several cell lines such as HT22 cells [309].

3.10. Other Bioactivities

Melatonin and its receptors are widely distributed in the body, which were identified in numerous organs, tissues, cells and subcellular compartment, such as brain, lung, muscles, bones, renal cells, reproductive cells, mitochondria and nuclei. It has been well documented that melatonin exerts beneficial effects on a large variety of diseases [310]. In terms of bones and muscles, it was suggested that melatonin supplementation of 10 mg/kg could counteract age-related bone loss in rats by improving the microstructure and biomechanical properties of aged bones [311]. Melatonin was also observed to improve muscle function in the animal model of Duchenne muscular dystrophy by causing the dystrophic muscle to contract and relax faster via decreasing plasma creatine kinase activity, providing a better redox status of the muscle [312], and normalizing plasma pro-inflammatory cytokines [150]. In addition, some in vitro study suggested that melatonin could represent a potential therapeutic impact on chronic respiratory diseases, e.g., asthma and chronic obstructive pulmonary diseases, in a dose-dependent manner, by inhibiting mucin 5AC production via the suppression of MAPK signaling in human airway epithelial cells [313]. Besides, a number of studies using rat models showed that melatonin could not only provide protection against acute kidney injury and partially reverse it [314], but also exert its protective effects on chronic kidney disease by scavenging free radicals [315], attenuating the chronic inflammation and limiting apoptosis [316]. Furthermore, an in vitro study found that melatonin pretreatment (100 μM) of human adipose tissue-derived mesenchymal stromal cells could improve their renoprotective and prosurvival effects on human kidney cells [317]. Moreover, it was found that the melatonin levels during pregnancy and labor were elevated and significantly higher than those after birth [318], and studies on pregnant rats indicated that melatonin interacted with other hormones and played a role as a triggering labor contributor [319]. Additionally, melatonin was able to attenuate the inhibitory effects of ROS on fertilization in both men and women [320,321]. It was also demonstrated in vivo that melatonin was closely associated with the health of oral cavity, presenting reducing damage caused by oxidative stress [322], suppressing inflammation, stimulating the proliferation of collagen and osseous tissue, improving wound healing [323] and preventing oral cancer [16]. Furthermore, several researches have shown that melatonin could contribute to a healthy aging and an extended lifespan, and a recent review has summarized the studies regarding the antiaging properties of melatonin [324].

In general, bioactivities of melatonin are commonly investigated with high purity in laboratory. For human beings, as the endogenous melatonin alters all through the life, the dietary intake might partially recompense the declined endogenous melatonin after puberty. While for the aged people, supplements might be more suitable, and even medicine could be applied for patients with sleep disorders.

Table 2. Bioactivities and potential mechanisms of melatonin.

Study Type	Subjects	Dose (mg/kg b.w.)/(Dose Dependent)	Potential Mechanisms (Melatonin (Mel) and/or Its Metabolites)	Reference
Antioxidant Activities				
			Directly scavenging free radical	
In vivo	Mouse	10 mg/kg b.w.	*Increasing the efficiency of electron transport chain:* - lowering electron leakage and reducing free radical generation	[122]
In vitro	Human umbilical artery segment	10^{-6}, 10^{-5}, 10^{-4} M (dose dependent)	Significantly scavenging the hydroxyl radical	[127]
			Cascade effects: removing free radicals efficiently than other reductants:	
In vivo	Rat	43 μmol/kg b.w.	- more efficient than Vitamin C	[128]
	Rat	2 μmol/kg b.w.	- more efficient than Vitamin E	[125]
	Mouse	5 mg/kg b.w.	- more efficient than Vitamin E	[325]
In vitro	Incubation medium	1–1000 mM	- more efficient than Vitamin C & Vitamin E	[123]
			Some metabolites more potent than its precursor in reducing oxidative stress:	
	Fenton reaction-based assay	AFMK: 0.017–0.067 mM AMK: up to 0.2 mM	- the order of efficacy of scavenging ·OH: AMK > AK > AFMK	[130]
N/A	N/A	N/A	- C3-OHM is 2–3 fold more potent than Mel in reducing hypervalent hemoglobin (Tan & Reiter, unpublished observations).	[131]
			Modulating and activating other enzymes	
			Downregulating pro-oxidative enzymes	
In vitro & in vivo	Rat striatum	M & AMK: 10^{-11}–10^{-3} M (dose dependent in vitro)	- Mel & AMK inhibiting nNOS activity - AMK more potent in inhibiting nNOS activity than Mel (in vivo)	[142]
In vitro	MCF-7 cells	1 nM	Inhibiting the mRNA expression of COX 1 and COX-2 in MCF-7 cells	[143]
			Stimulating the synthesis of other antioxidants	
In vitro	ECV304 cells	1 μM	- Inducing γ-GCS expression to promote GSH synthesis	[124]
In vitro	2 neuronal cell lines: PC12 cells & SK-N-SH	1 nM	- Regulating AOEs gene expression - Increasing mRNA of SODs and GPx	[144]
			Preventing antioxidant enzymes from oxidative stress	
In vitro	human BM-MSCs	0 to 1000 μM (dose dependent 10–100 μM)	- significantly restoring SOD ($p < 0.05$) and CAT ($p < 0.01$) - increasing GSH ($p < 0.01$) with pre-treatment of Mel	[145]
In vivo	Sprague-Dawley rats	10 mg/kg b.w.	GSH-Rd activity was completely or partially restored by Mel treatment	[146]

Table 2. *Cont.*

Study Type	Subjects	Dose (mg/kg b.w.)/(Dose Dependent)	Potential Mechanisms (Melatonin (Mel) and/or Its Metabolites)	Reference
In vitro & in vivo	Sprague–Dawley rats	0–0.1 mM (dose dependent in vitro) 10 mg/kg b.w.	G6PG activity dose-dependent in vitro (increased below 0.08 mM Mel concentration and reached a plateau above 0.1 mM) G6PG activity time-dependent (in vivo)	[147]
			Synergistically working with other reductants	
			Combining with other antioxidants to remove radicals synergistically	
In vitro	Rat liver homogenates	2.5–1600 μM	- dramatically enhancing the protective effects after combining	[148]
Anti-inflammatory Activities				
			NF-κB signaling pathway involved mechanisms	
			Modulating NF-κB and its downstream pro-inflammatory target genes	
In vitro	Human colon cancer cell lines SW620 and LOVO	1 mmol/L	- iNOS	[70]
In vitro	RAW 264.7 macrophages	0.5, 1, 2 mM (dose dependent)	- COX-2, PGE_2	[158]
In vitro	Human neuroblastoma dopamine SH-SY5Y cell lines	1, 10, 100 or 1000 nM	- TNF-α	[159]
In vitro	Rat astrocytoma C6 cells	50–200 μM (dose dependent)	- GFAP	[160]
In vitro & in vivo	CHON-001 human chondrocyte cell line Rabbit with osteoarthritis (OA)	0.1, 1, 10, 100 ng (dose- and time-dependent) 20 mg/kg	Protecting cells by blocking the activated NF-κB as well as the phosphorylation of PI3K/Akt, p38, ERK, JNK and MAPK	[161]
In vitro	BV2 murine microglial cell line	1 mM	Downregulating chemokine expression	[162]
In vivo	Rats	5 mg/kg	Inhibiting the inflammatory reaction	[163]
In vivo & in vitro	Female BALB/c mice MMECs	5, 10, 20 mg/kg 25, 50, 100 μM (dose dependent)	Suppressing NF-κB activation and activating PPAR-γ	[164]
In vitro	Mast cells (RBL-2H3)	100 nM and 1 mM (dose dependent)	Inhibiting IKK/NF-κB signal transduction	[165]
			SIRT1 pathway involved mechanisms	
In vitro & in vivo	BV2 cell lysates PND7 rat brain	100 μM 10 mg/kg	Activating SIRT1/Nrf2 signaling pathway to reduce oxidative stress damage	[168]
			Other possible mechanisms	
In vivo	Pediatric patients	10 mg (09:00 h) 60 mg (21:00 h)	Regulating the expression of other pro-inflammatory genes	[150]

Table 2. *Cont.*

Study Type	Subjects	Dose (mg/kg b.w.)/(Dose Dependent)	Potential Mechanisms (Melatonin (Mel) and/or Its Metabolites)	Reference
In vitro	Mouse Gsk3b knockout ($Gsk3b^{-/-}$) and wild-type ($Gsk3b^{+/+}$) MEF cells	10 nM	Inhibiting the expression of inflammatory chemokines/cytokines	[169]
In vivo	Plasmodium	10 μM (time dependent)	Inducing temporal up-regulation of gene expression related to UPS	[170]
In vivo	C57BL mice	10 mg/kg i.p.	Downregulating mRNA of E2F2 and H2-Ab1	[171]
In vivo	Rats	5, 15, and 25 mg/kg (dose-dependent)	Activating the expression of NDRG2, which was involved in cellular differentiation, development, anti-apoptosis, anti-inflammatory cytokine, and antioxidant	[172]
In vivo	Carp	10^{-4}–10^{-12} M	Maintaining the pro- and anti- inflammatory balance during infection by influencing leukocyte migration and apoptosis	[151]
Enhancing Immune Activities				
			Reciprocally regulating the nervous, endocrine, and immune systems	
In vivo & In vitro	Mice Thymus and spleen cells	4–5 mL/day/mouse 1.5 pg/ml to 1.5 pgg/ml	Regulating thymocyte apoptosis	[174]
In vivo	Mice	1.5 pg/mL to 1.5 pg/mL	The concentration of melatonin correspond with the change of seasons	[175]
			Inhibiting the production of cAMP, cGMP and DAG, and improving the immunity	
In vitro	Human blood lymphocyte	N/A (dose-dependent)	Inhibiting adenylyl cyclase and the stimulating phospholipase C	[183]
In vivo	Golden hamsters	25 μg/100 g/hamster/day	Improving immune responses	[184]
			Protecting the immune organs, tissues and cells	
			Reversing the weight loss of thymuses and spleens in pinealectomized animals	
In vivo & In vitro	Mice Thymus and spleen cells	4–5 mL/day/mouse 1.5 pg/mL to 1.5 pg/mL	- thymus	[175]
In vivo	Syrian hamsters	25 μg	- spleen	[188]
In vivo	Pediatric patients	N/A	Increasing tonsillar size	[189]
			Improving proliferation, increasing activity and inhibiting apoptosis of immune cells	
In vitro	cultured monocytes	N/A	- monocyte	[190]
In vivo	ICR mice	10 or 50 mg/kg	- natural killer (NK) cells	[191]
In vitro	Neutrophils & peripheral blood mononuclear cells	10 mM	- neutrophils	[192]
In vivo	Wistar albino rats	10 mg/kg	Increasing the sensitivity of the immune cells to some cytokines	[193]
In vitro & In vitro	Thymocytes of Barbari goats Thymus	500 pg/mL 500 pg/mL	Restoring the suppressed immunity of T-cell cultured by developing some hormonal microcircuit (gonadal steroid and melatonin) in lymphatic organs	[194]

Table 2. *Cont.*

Study Type	Subjects	Dose (mg/kg b.w.)/(Dose Dependent)	Potential Mechanisms (Melatonin (Mel) and/or Its Metabolites)	Reference
			Modulating immune mediator production	
In vitro	Human mononuclear cells	10^{-8} M	Increasing IL-2, IFN-γ and IL-6 in monocytes	[195]
In vitro	Neutrophils & peripheral blood mononuclear cells	10 mM	Mel & AFMK: decreasing IL-8 and TNF-α in neutrophils	[192]
In vitro	RAW264.7 cells	10, 100 or 1000 μM	Decreasing IL-1β, IL-6, IL-8, IL-10 and TNF-α in macrophages	[196]
			Regulating the ROS production in the essential immune cells	
In vitro	Human monocytes	10^{-12} M and above	Activating monocytes (above the activation threshold of 5×10^{-11} M)	[199]
In vitro	Lung neutrophils	0.01, 0.1, 1 mM (dose-dependent)	Activating neutrophils	[200]
In vivo	Hamsters	25 μg/100 g b.w.	Attenuating oxidative load	[201]
In vivo	Wild birds	25 μg/100 g/day	Alleviating oxidative damage and suppressing the immune status induced by stress	[202].
In vitro & in vivo	Heart tissue of C57BL/6 C57BL/6J mice	3 or 4 doses of melatonin 30 mg/kg	Suppressing systemic innate immune activation by blocking the NF-κB/NLRP3 connection through a sirtuin1-dependent pathway	[154].
Improving Circadian Rhythm and Sleep				
In vivo	C3H & C57BL mice	N/A	Being involved in the control of clock gene protein levels in the adrenal cortex of mice	[211]
In vivo	Soay sheep	N/A	Resetting circadian rhythms in the pituitary pars tuberalis	[212]
In vivo	Mice (C3H/HeJCrl and C57BL/6NCrl)	N/A	Influencing PER1 and CRY2 protein levels Playing a role in rhythmic regulation of pCREB levels in the mammalian retina	[213]
In vitro & in vivo	COS7 cells Lambs	N/A	Activating Npas4	[215]
In vivo	Hamster	20 μg/day	Coordinating the diurnal rhythm in neuronal remodeling	[217]
In vivo	Mice	6 μg/day for 2 weeks	Increasing amplitude in expressional rhythms Altering the expression of genes of serotonergic neurotransmission Improve the depression-like behavior	[218]
In vivo	23 patients	N/A	Being positive correlated with sleep parameters	[220]
Anticancer Activities				
			Effects on tumor cell cycle, incl. growth, proliferation, metabolism and apoptosis	
In vitro & In vivo	Human gastric cancer cell lines (AGS and MKN) Male BALB/c nude mice	5 mg/kg/twice/week for 33 days 1 μM to 2 mM (dose-/time- dependent, 15 min to 24 h)	Inhibiting gastric tumor growth and peritoneal metastasis Inhibiting C/EBPβ and NF-κB Inducing ER stress and inhibiting EMT	[232]
In vitro	T47D-BAF co-cultured	20 nM	Suppressing breast cancer cell proliferation and inhibiting aromatase	[238]
In vitro & in vivo	Prostate cancer cells TRAMP male mice	1 mM 200 μg/mL	Reducing glucose uptake and modifying the expression of GLUT1 transporter Attenuating glucose-induced tumor progression and prolonging the lifespan	[233]

Table 2. *Cont.*

Study Type	Subjects	Dose (mg/kg b.w.)/(Dose Dependent)	Potential Mechanisms (Melatonin (Mel) and/or Its Metabolites)	Reference
In vitro	Hypoxic prostate cancer cell line PC-3 cells	1 mM	Anti-angiogenic property Upregulating miRNA3195 and miRNA 374b and downregulating 16 miRNAs	[239]
In vitro	Colorectal cancer LoVo cells	0.1–2.0 mM (dose-dependent)	Suppressing cell proliferation and inducing apoptosis Inducing dephosphorylation and nuclear import of histone deacetylase 4 (HDAC4) Decreasing H3 acetylation by inactivating CaMKIIα and reducing bcl-2 expression	[240]
In vitro	Breast cancer cell line SK-BR-3 & MDA-MB-231	2 mM	Changing the protein levels of Survivin, Bcl-2, and Bax Affecting cyt c release from the mitochondria to the cytosol Enhancing apoptotic cell death via sustained upregulation of Redd1 expression and inhibition of mTORC1 upstream of the activation of the p38/JNK pathways	[234]
			Effects on invasion and metastasis of tumor cells	
In vitro	HepG2 liver cancer cells	1 mM	Exhibiting anti-invasive and antimetastatic activities by suppressing the activity of MMP-9 Reducing IL-1β-induced HepG2 cells MMP-9 gelatinase activity and inhibiting cell invasion and motility through downregulation of MMP-9 gene expression and upregulation of the MMP-9-specific inhibitor tissue inhibitor of TIMP-1 Suppressing IL-1β-induced NF-κB translocation and transcriptional activity	[241]
In vitro	Renal cell carcinoma cells (Caki-1 and Achn)	0.5–2 mM	Reducing the migration and invasion Inhibiting MMP-9 by reducing p65- and p52-DNA-binding activities Regulating MMP-9 transactivation and cell motility refer to the Akt-mediated JNK1/2 and ERK1/2 signaling pathways	[242]
In vivo & in vitro	Female athymic nude mice Metastatic and non-metastatic breast cancer cell lines (MDA-MB-231)	100 mg/kg/day 1 mM	Lowering the numbers of lung metastasis Decreasing ROCK-1 protein expression in metastatic foci Reducing cell viability and invasion/migration Decreasing ROCK-1 gene expression in metastatic cells and protein expression in non-metastatic cell line	[235]
			Therapy adjunct in tumor treatment	
In vitro	Human non-small-cell lung cancer (NSCLC) cells lines H1299 and A549	1 mM	Enhancing the berberine-mediated growth inhibition of lung cancer cells through simultaneous modulation of caspase/cyt C, AP-2β/hTERT, NF-κB/COX-2, and Akt/ERK signaling pathways	[157]
In vitro	Breast cancer cells	1 nM	Mediating the sensitization to the ionizing radiation by decreasing around 50% the activity and expression of proteins involved in the synthesis of estrogens Reducing the amount of active estrogens at cancer cell level Inducing a 2-fold change in p53 expression compared to radiation alone	[243]
In vivo	Female patients	Melatonin-containing cream for twice daily use	Significantly lowering the occurrence of grade 1/2 acute radiation dermatitis in patients with breast-conserving surgery for stage 0–2 breast cancer	[244]
In vivo	Male Wistar rats	10 mg/kg/week	Mitigating PVB-induced testicular dysfunction	[245]

Table 2. *Cont.*

Study Type	Subjects	Dose (mg/kg b.w.)/(Dose Dependent)	Potential Mechanisms (Melatonin (Mel) and/or Its Metabolites)	Reference
In vivo & in vitro	Female athymic nude mice Human colon cancer cell lines SW620	25 mg/kg 1 mmol/L	Exerting synergistic anti-tumor effect by inhibiting the AKT and iNOS pathway Enhancing the 5-FU-mediated inhibition of cell proliferation, colony formation, cell migration and invasion Synergizing with 5-FU to promote the activation of the caspase/PARP-dependent apoptosis pathway and induce cell cycle arrest Synergizing anti-tumor effect of 5-FU by targeting the PI3K/AKT and NF-κB/iNOS signaling	[70]
In vitro	Human colorectal cancer cells	N/A	MT2 mRNA expression levels increased The profile of melatonin receptors gene expression and genes associated with their activity in colorectal cancer	[236]
In vitro	Estrogen receptor-positive endometrial cancer cell line, Ishikawa	1×10^{-9} M	MT1 receptor expressing but not MT2 Attenuating ERα mRNA expression Enhancing anti-tumor effects of paclitaxel among anticancer drugs tested	[237]
Cardiovascular Protection				
In vivo	Patients with confirmed nocturnal hypertension	2 mg 2 h before bedtime for 4 weeks	Reducing nocturnal systolic and diastolic BP significantly ($p = 0.01$)	[249]
In vivo	Spinal cord injury (SCI) mice model	5, 10, 25, 50, 100 mg/kg i.p.	50 mg/kg exhibiting significantly reduced blood spinal cord barrier permeability Restraining microvessel loss and attenuating edema Protecting the tight junction proteins, endothelial cells and pericytes Decreasing cell apoptosis and reducing MP3/AQP4/HIF-1α/VEGF/VEGFR2 expression	[251]
In vivo	Wistar-Kyoto (WKY) and spontaneously hypertensive rats (SHR)	30 mg/kg/day for 4 weeks	Decreasing reflex chronotropic responses to phenylephrine and sodium nitroprusside Reducing mean arterial pressure and heart rate Improving bradycardic and tachycardic baroreflex responses without modifying catecholamine responses Increasing glutathione peroxidase activity in plasma and erythrocytes	[252]
In vivo	Wistar-Kyoto (WKY) and spontaneously hypertensive rats (SHR)	30 mg/kg/day for 4 weeks	Decreasing mean arterial pressure (MAP) and heart rate Restoring the plasma noradrenaline concentrations, the chronotropic response to isoproterenol and the proportions of β1/β2-adrenoceptors in the heart in SHRs to the levels Decreasing the release of [3H] noradrenaline from isolated atria Improving the relaxation in the aorta	[253]
In vivo	Rats	50 mg/kg	Preventing vasculitis Decreasing elementary pathological lesions of radiation-induced heart disease (RIHD) like fibrosis and necrosis	[254]

Table 2. *Cont.*

Study Type	Subjects	Dose (mg/kg b.w.)/(Dose Dependent)	Potential Mechanisms (Melatonin (Mel) and/or Its Metabolites)	Reference
In vitro	BM-MSCs	200, 20, and 2 μM (dose-dependent)	Reducing BM-MSC apoptotic death while increasing the levels of TGF-β, bFGF, VEGF, PDGF and Bcl-2, and decreasing Bax, p53 Upregulating modulator of apoptosis (PUMA) and caspase 3 Upregulating the phosphorylation of AMPK, which promotes ACC phosphorylation	[255]
In vivo & in vitro	Female C57BL/6a mice with MI Adipose-derived MSCs	20 mg/kg/day for 28 days 5 μM	Promoting functional survival of AD-MSCs in infarcted heart and provoking a synergetic effect with AD-MSCs to restore heart function associated with alleviated inflammation, apoptosis, and oxidative stress in infarcted heart Exerting cytoprotective effects against hypoxia/serum deprivation (H/SD) injury Attenuating inflammation, apoptosis, and oxidative stress Enhancing SIRT1 signaling, with the increased expression of anti-apoptotic protein Bcl-2, and decreased the expression of Ac-FoxO1, Ac-p53, Ac-NF-KappaB, and Bax.	[256]
In vitro	Perfused isolated rat hearts and cultured neonatal rat cardiomyocytes	5 μM	Improving postischemic cardiac function, decreasing infarct size, reducing apoptotic index, and diminishing lactate dehydrogenase release Upregulating the anti-apoptotic protein Bcl-2 and downregulating Bax Preserving mitochondrial redox potential and elevating SOD activity Decreasing formation of mitochondrial H_2O_2 and MDA	[257]
In vivo	Rats with sepsis	30 mg/kg	Improving survival rates and cardiac function, attenuating myocardial injury and apoptosis Decreasing the serum LDH, decreasing inflammatory cytokines TNF-α, IL-1β, and HMGB1 Increasing anti-oxidant enzyme activity and p-Akt and Bcl-2 levels	[258]
In vivo	Drosophila melanogaster	5 μM	Increasing the regularity of heartbeat, rescuing rhythmicity in flies bearing mutations, increasing cardiac regularity independent of alteration of heart rate, which is mediated via a specific G-Protein-coupled receptor encoded by the CG 4313 gene	[259]
In vivo	Patients with heart failure	N/A 1-year follow-up	As a predictors of left ventricular reverse remodeling (LVRR) and the adverse clinical events, increasing the area under of curve for the prediction LVRR	[260]
In vivo	Mice with Mst1 transgenic (Mst1 Tg) and Mst1 knockout ($Mst1^{-/-}$)	20 mg/kg/d for 1 week	Alleviating postinfarction cardiac remodeling and dysfunction by upregulating autophagy, decreasing apoptosis, and modulating mitochondrial integrity and biogenesis via Mst1/Sirt1 signaling	[261]
Anti-diabetic Activities				
In vivo	Albino Wistar rats	10 mg/kg b.w.	Increasing the inhibited activity of catalase in liver cells Restoring the dysfunctional mitochondria related to diabetes	[274]
In vivo	Rat	2.8, 14, 28, and 140 nM	Inhibiting hepatic gluconeogenesis Activating hypothalamic Akt via membrane receptors MT1 and MT2	[275]
In vivo	Rat	10 mg/kg/day	Increasing Ca^{2+} levels in lots of organs and tissues	[11]

Table 2. *Cont.*

Study Type	Subjects	Dose (mg/kg b.w.)/(Dose Dependent)	Potential Mechanisms (Melatonin (Mel) and/or Its Metabolites)	Reference
In vitro & in vivo	H9C2 cell line Rat	0.1, 1, 10, 100, 1000 μM 20 mg/kg/day	Activating of SIRT1 signaling pathway (significant at 100 and 1000 μM) Inactivating PERK/eIF2α/ATF4 signaling pathway	[276]
In vitro	INS 832/13 cells	1–100 nM	Attenuating β-cell apoptosis, improving β-cell function, prolonging β-cell survival (particularly evident at 10 nM)	[277]
In vivo	Rat	10 mg/kg/day	Improving neurogenesis, synaptogenesis in hippocampi, increasing the receptors of melatonin and insulin, and restoring the downstream signaling pathway for insulin	[278]
In vivo	Rat	250 μg/animal/day/i.p.	Accelerating bone healing	[279]
In vivo	Rat	10 mg/kg/d, i.p.	Restoring the endothelial dysfunction and improving vascular responses	[271]
Anti-obese Activities				
In vivo	Rat	10 mg/kg/day	Inducing white adipose tissue browning in rats with obesity-related type 2 diabetes	[282]
In vivo	Rat	20 mg/L	Benefiting homeostasis of renal glutathione	[283]
In vitro	Mouse Gsk3b knockout ($Gsk3b^{-/-}$) and wild-type ($Gsk3b^{+/+}$) MEF cells	10 nM	Inhibiting Akt activation Increasing GSK3B activity	[169]
In vivo	Mice	100 mg/kg/day	Ameliorating obesity-induced adipokine alteration	[285]
In vivo	Women	N/A	Melatonin was involved in the development of obesity	[288]
In vitro	Mice	20 mg/kg/day	Promoting circadian rhythm-mediated proliferation in adipose tissue	[206]
In vivo	Rat	4 mg/kg/day	Decreasing myocardial infarct sizes and insulin resistant Increasing serum PKB/Akt, ERK42/44, GSK-3β and STAT3	[289]
In vivo	Mice	100 mg/kg/day	Increasing mitofusin-2 expression	[290]
In vivo	Mice	10 mg/kg/day	Modulating the MAPK-JNK/p38 signaling pathway	[291]
Neuroprotection				
In vivo	Mice	10 mg/kg	Increasing the activity of antioxidant enzymes Mediating the Nrf2-ARE pathway	[293]
In vivo	C57BL/6J mice	10 mg/kg given twice	Reducing IR-induced mitochondrial dysfunction Activating SIRT1 signaling	[294]
In vivo	Rat	150 mg/kg	Suppressing cortical expressions of proinflammatory cytokines	[295]
In vivo	Mice	5 mg/kg	Reducing oxidative damage by scavenging radicals	[296]

Table 2. *Cont.*

Study Type	Subjects	Dose (mg/kg b.w.)/(Dose Dependent)	Potential Mechanisms (Melatonin (Mel) and/or Its Metabolites)	Reference
In vivo	Rat	10 mg/kg	Reversing the increased plasma TNF-α, IL-1β levels Decreasing BDNF, S100B and IL-10 values	[297]
In vivo	Rat	10 mg/kg and 50 mg/kg	Preventing the decrease of the number and the diameter of sciatic nerve axons	[298]
In vivo	Rat	20 mg	Preventing the decrease in VEPs and PLR Inhibiting microglial reactivity, astrocytosis, demyelination, and axon and retinal ganglion cell loss Preserving anterograde transport of cholera toxin β-subunit	[299]
In vivo	Mice	10 mg/kg	Restoring mRNA and protein levels of BACE1 and PS1	[305]
In vitro & in vivo	Rat hippocampal neurons Rat	50 μM 500 mg/kg b.w.	Improving the soluble Abeta1–42-induced impairment of spatial learning and memory, synaptic plasticity and astrogliosis	[301]
In vivo	Rat	10 mg/kg	Improving motor activity and muscular strength	[306]
In vitro	Mouse neuroblastoma cells	1 μM	Activating transcription factor EB-dependent autophagy-lysosome	[136]
In vivo	Rat	100 mg/kg	Inhibiting caspase-3	[307]
In vivo	Rat	50 mg/kg/day	Protecting the cell against neuronal damage in the hippocampus	[308]
Other Bioactivities				
In vivo	Rat	10 mg/kg/day	Improving the microstructure and biomechanical properties of aged bones	[311]
In vivo	Patients	10 mg/day, 60 mg/day	Reducing the hyperoxidative and inflammatory process	[150]
In vivo	Mice	30 mg/kg/day	Decreasing plasma creatine kinase activity, increasing total glutathione content Lowering the oxidized/reduced glutathione ratio	[312]
In vitro	NCI-H292 cells	50, 100, 200, and 400 μM (dose-dependent)	Inhibiting mucin 5AC production	[313]
In vivo	Rat	4 mg/kg, i.p 10 mg/kg, i.p	Exhibits renoprotective effects against ischemia reperfusion induced AKI due to antioxidant properties and the involvement of progesterone receptors	[314]
In vivo	Rat	10 mg/kg/day	Scavenging free radicals	[315]
In vivo	Rat	N/A	Activating SIRT1 signaling	[316]
In vitro	Human ASCs	100 μM for 3 h	Enhancing human ASCs' survival and their therapeutic effectiveness on injured tissue	[317]
In vivo	Rat	10 mg/body	Interacting with other hormones	[319]
In vivo	Rat	10 mg/kg/day	Decreasing the increased myeloperoxidase activities and osteoclast and neutrophil densities	[322]
In vivo	Rat	10 mg/kg/day	Decreasing serum cyclophosphamide levels and increasing ALP levels	[323]

3.11. Adverse Effects

No adverse effects has been observed by the consumption of melatonin in foods or drinks. In addition, 1–10 mg/kg is usually considered as standard dose for assisting sleep and there were no toxicological effects found at a dose of 10 mg melatonin (orally) in a 28-day randomized, double-blind clinical trial [326,327]. Furthermore, no toxic effects were observed with high-dose melatonin in pregnant animal models [328].

Nevertheless, some adverse effects, such as dizziness, headache, nausea and sleepiness, have been reported by administration of high-dose melatonin, which was used as treatment of some diseases [329,330]. In a case of melatonin overdose (oral administration), lethargy and disorientation occurred to a man of 66 years old caused by 24 mg/kg melatonin for relaxation and sleep before operation, though he recovered completely afterwards [331]. In addition, the results of research on intravenous administration of melatonin appeared not consistent. Some studies found no side effects when high-dose melatonin (i.v.) was used repeatedly to treat pain [332], sepsis [333], surgical procedures [334] and lung disease [335]. Other studies reported that minor signs of sedation, impaired psychomotor and disorientation could possibly be associated with melatonin (i.v.) [336,337]. Although melatonin shows its protective and pro-fertilization effects on reproductive organs in both men and women, puberty seems like a sensitive period for melatonin administration regardless of sex. As the exogenous melatonin was given to male rats, reduced testis size and suppressed sperm production were observed, which were reversed by the treatment with exogenous gonadotropins [338]. For female rats, delayed puberty onset were observed with exogenous melatonin as a result of luteinizing hormone and prolactin reduction [14,339]. Those results were because of the inhibitory effects of melatonin on gonadotropin-releasing hormone neurons in hypothalamus [340].

4. Conclusions

Melatonin has been identified and qualified in a large number of foods. The content of melatonin is higher in eggs and fish than that in meat in animal foods, while in plant foods, the highest contents of melatonin was found in nuts, and some cereals and germinated legumes or seeds are also rich in melatonin. Mushrooms are also good dietary sources of melatonin. In addition, the intake of melatonin containing foods could significantly increase the melatonin concentration in human serum, indicating melatonin could provide beneficial effects on health through foods. Studies have shown that melatonin has many bioactivities, such as antioxidant, anti-inflammatory, enhancing immunity, anticancer, improving circadian cycle, cardiovascular protecting, anti-diabetic, anti-obese, anti-aging and neuroprotection. Therefore, the consumption of foods rich in melatonin could not only improve insomnia, which affects one third of the general population worldwide, but also provide other health benefits. In the future, the content of melatonin is worth testing and evaluating in more foods to find new natural sources of melatonin, and the mechanisms of action are needed to be investigated more comprehensively. In addition, more clinical trials are necessary to be conducted to clarify the effects of melatonin on human beings. Meanwhile, some foods with extremely high content of melatonin are of great value to be developed into functional foods, which would contribute to the prevention and treatment of various diseases.

Acknowledgments: This work was supported by the National Natural Science Foundation of China (No. 81372976), Key Project of Guangdong Provincial Science and Technology Program (No. 2014B020205002), and the Hundred-Talents Scheme of Sun Yat-Sen University.

Author Contributions: Xiao Meng, Sha Li and Hua-Bin Li conceived this paper; Xiao Meng, Ya Li, Yue Zhou and Dong-Ping Xu wrote this paper; Sha Li, Ren-You Gan and Hua-Bin Li revised the paper.

Conflicts of Interest: The authors declare no conflict of interest.

Abbreviations

The following abbreviations are used in this manuscript:

2-OHM	2-hydroxymelatonin
4-OHM	4-hydroxymelatonin
6-OHM	6-hydroxymelatonin
AAAD	aromatic L-amino acid decarboxylase
Aβ	amyloid-beta
ACC	acetyl-CoA carboxylase
AD	Alzheimer's disease
AD-MSCs	adipose-derived mesenchymal stem cells
AFMK	N^1-acetyl-N^2-formyl-5-methoxykynuramine
AMK	N^1-acetyl-5-methoxykynuramine
AMPK	adenosine monophosphate-activated protein kinase
AP-2β	activator protein 2β
ARE	antioxidant responsive element
ATF4	activating transcription factor 4
BACE1	β-APP-cleaving enzyme 1
Bax	Bcl-2-associated X protein
BBB	blood-brain barrier
Bcl-2	B-cell lymphoma 2
BDNF	brain derived neurotrophic factor
bFGF	basic fibroblast growth factor
BMMNCs	bone marrow mononuclear cells
BM-MSCs	bone marrow mesenchymal stem cells
C3-OHM	cyclic 3-hydroxymelatonin
CaMKIIα	calmodulin dependent protein kinase II alpha
cAMP	cyclic AMP
CAT	catalase
CCL20	chemokine C-C motif ligand 20
cGMP	cyclic GMP
CNS	central nerve system
COX-2	cyclo-oxygenase 2
CVDs	cardiovascular diseases
CXCL1	chemokine C-X-C motif ligand 1
cyt c	cytochrome c
DAG	diacylglycerol
DS	diclofenac sodium
DW	dry weight
EBPβ	enhancer-binding protein beta
eIF2α	eukaryotic initiation factor 2α
EMF	electromagnetic fields
EMT	epithelial mesenchymal transition
eNOS	endothelial nitric oxide synthase
ER	endoplasmic reticulum
ERK	extracellular signal-regulated kinase
ERR-α	estrogen-related receptor alpha
FRAP	ferric reducing antioxidant power
FSS	flow shear stress
FW	fresh weight
G6PD	glucose-6-phosphate dehydrogenase
GAS	gamma-activated sequence
γ-GCS	gamma-glutamylcysteine synthetase

G-CSF	granulocyte colony-stimulating factor
GFAP	glia and fibrillary acidic protein
GM-CSF	granulocyte–macrophage colony-stimulating factor
GPx	glutathione peroxidase
GSH-Rd	glutathione reductase
GSK3β	glycogen synthase kinase 3β
H2-Ab1	histocompatibility class II antigen A, beta 1
HDAC	histone deacetylase
Hes1	hairy and enhancer of split 1
HIOMT	hydroxyindole *O*-methyltransferase
HOMA-IR index	homeostasis model assessment of insulin resistance index
hTERT	human telomerase reserve transcriptase
i.v.	intravenously
i.p.	intraperitoneally
IFN-γ	interferon gamma
IGF-1	insulin-like growth factor 1
IKK	inhibitor of nuclear factor kappa-B kinase
IL-6	interleukin 6
iNOS	inducible nitric oxide synthase
IRI	ischemia/reperfusion injury
JAK2	Janus kinase 2
JNK	Jun *N*-terminal kinase
LAN	light at night
LPS	lipopolysaccharide
MAPK	mitogen-activated protein kinase
MDH	malondialdehyde
MI	myocardial infarction
MLHb	medial lateral habenula
MMP-9	matrix metalloproteinase-9
Mst1	mammalian Ste20-like kinase 1
MT1, MT2	melatonin receptors
NAD	Nicotinamide adenine dinucleotide
NAT	*N*-acetyltransferase
NDRG2	*N*-myc downstream-regulated gene 2
NF-κB	nuclear factor kappa-light-chain-enhancer of activated B cells
NK	natural killer
NLRP3	NOD-like receptor P3
NO	nitric oxide
NOMela	*N*-nitrosomelatonin
Nrf2	nuclear factor-erythroid 2-related factor 2
OA	osteoarthritis
ON	optic neuritis
ORAC	oxygen radical antioxidant capacity
Oxa	oxaliplatin
p-Akt	phosphorylated protein kinase B
PARP	poly-ADP-ribose polymerase
pCREB	phosphorylated cAMP response element-binding protein
PD	Parkinson's disease
PDGF	platelet-derived growth factor
PGC-1α	peroxisome proliferator-activated receptor gamma coactivator-1 alpha
PI3K	phosphatidyl inositol 3-kinase
PKB	protein kinase B
PLR	pupil light reflex
PPAR-γ	peroxisome proliferator-activated receptor gamma

PRDX1	peroxiredoxin 1
PS1	presenilin 1
PUMA	p53 upregulated modulator of apoptosis
RNS	reactive nitrogen species
ROCK-1	Rho-associated kinase protein
ROS	reactive oxygen species
S100B	S100 calcium-binding protein B
SAH	subarachnoid hemorrhage
SCN	suprachiasmatic nucleus
SE	standard error
SEEMs	selective estrogen enzyme modulators
SIRT1	sirtuin 1
SOD	superoxide dismutase
STAT	signal transducer and activator of transcription
TBI	traumatic brain injury
TGF-β	transforming growth factor β
TIMP-1	tissue inhibitor of metalloproteinases 1
TNF-α	tumor necrosis factor α
TPH	tryptophan hydroxylase
UCP1	uncoupling protein 1
UPS	ubiquitin/proteasome system
VEGF	vascular endothelial growth factor
VEP	visual evoked potentials

References

1. Lerner, A.B.; Case, J.D.; Takahashi, Y.; Lee, T.H.; Mori, W. Isolation of melatonin, a pineal factor that lightens melanocytes. *J. Am. Chem. Soc.* **1958**, *80*, 2587. [CrossRef]
2. Brown, G.M.; Pandi-Perumal, S.R.; Trakht, I.; Cardinali, D.P. Melatonin and its relevance to jet lag. *Travel Med. Infect. Dis.* **2009**, *7*, 69–81. [CrossRef] [PubMed]
3. Pandi-Perumal, S.R.; Srinivasan, V.; Poeggeler, B.; Hardeland, R.; Cardinali, D.P. Drug Insight: The use of melatonergic agonists for the treatment of insomnia-focus on ramelteon. *Nat. Clin. Pract. Neurol.* **2007**, *3*, 221–228. [CrossRef] [PubMed]
4. Li, R.; Luo, X.; Li, L.; Peng, Q.; Yang, Y.; Zhao, L.; Ma, M.; Hou, Z. The protective effects of melatonin against oxidative stress and inflammation induced by acute cadmium exposure in mice testis. *Biol. Trace Elem. Res.* **2016**, *170*, 152–164. [CrossRef] [PubMed]
5. Chen, S.J.; Huang, S.H.; Chen, J.W.; Wang, K.C.; Yang, Y.R.; Liu, P.F.; Lin, G.J.; Sytwu, H.K. Melatonin enhances interleukin-10 expression and suppresses chemotaxis to inhibit inflammation *in situ* and reduce the severity of experimental autoimmune encephalomyelitis. *Int. Immunopharmacol.* **2016**, *31*, 169–177. [CrossRef] [PubMed]
6. Oxenkrug, G.; Requintina, P.; Bachurin, S. Antioxidant and antiaging activity of *N*-acetylserotonin and melatonin in the in vivo models. *Ann. N. Y. Acad. Sci.* **2001**, *939*, 190–199. [CrossRef] [PubMed]
7. Li, F.; Li, S.; Li, H.B.; Deng, G.F.; Ling, W.H.; Wu, S.; Xu, X.R.; Chen, F. Antiproliferative activity of peels, pulps and seeds of 61 fruits. *J. Funct. Foods* **2013**, *5*, 1298–1309. [CrossRef]
8. Anisimov, V.N.; Popovich, I.G.; Zabezhinski, M.A.; Anisimov, S.V.; Vesnushkin, G.M.; Vinogradova, I.A. Melatonin as antioxidant, geroprotector and anticarcinogen. *Biochim. Biophys. Acta* **2006**, *1757*, 573–589. [CrossRef] [PubMed]
9. Pandi-Perumal, S.R.; BaHammam, A.S.; Brown, G.M.; Spence, D.W.; Bharti, V.K.; Kaur, C.; Hardeland, R.; Cardinali, D.P. Melatonin antioxidative defense: Therapeutical implications for aging and neurodegenerative processes. *Neurotox. Res.* **2013**, *23*, 267–300. [CrossRef] [PubMed]
10. Pandi-Perumal, S.R.; Zisapel, N.; Srinivasan, V.; Cardinali, D.P. Melatonin and sleep in aging population. *Exp. Gerontol.* **2005**, *40*, 911–925. [CrossRef] [PubMed]

11. Agil, A.; Elmahallawy, E.K.; Rodriguez-Ferrer, J.M.; Adem, A.; Bastaki, S.M.; Al-Abbadi, I.; Fino Solano, Y.A.; Navarro-Alarcon, M. Melatonin increases intracellular calcium in the liver, muscle, white adipose tissues and pancreas of diabetic obese rats. *Food Funct.* **2015**, *6*, 2671–2678. [CrossRef] [PubMed]
12. Agil, A.; El-Hammadi, M.; Jimenez-Aranda, A.; Tassi, M.; Abdo, W.; Fernandez-Vazquez, G.; Reiter, R.J. Melatonin reduces hepatic mitochondrial dysfunction in diabetic obese rats. *J. Pineal Res.* **2015**, *59*, 70–79. [CrossRef] [PubMed]
13. Chenevard, R.; Suter, Y.; Erne, P. Effects of the heart-lung machine on melatonin metabolism and mood disturbances. *Eur. J. Cardiothorac. Surg.* **2008**, *34*, 338–343. [CrossRef] [PubMed]
14. Esquifino, A.I.; Villanua, M.A.; Agrasal, C. Effect of neonatal melatonin administration on sexual development in the rat. *J. Steroid Biochem.* **1987**, *27*, 1089–1093. [CrossRef]
15. Agilli, M.; Aydin, F.N.; Cayci, T. The effect of body temperature, melatonin and cortisol on obesity in women: A biochemical evaluation? *Clin. Nutr.* **2015**, *34*, 332. [CrossRef] [PubMed]
16. Najeeb, S.; Khurshid, Z.; Zohaib, S.; Zafar, M.S. Therapeutic potential of melatonin in oral medicine and periodontology. *Kaohsiung J. Med. Sci.* **2016**, *32*, 391–396. [CrossRef] [PubMed]
17. Setyaningsih, W.; Saputro, I.E.; Barbero, G.F.; Palma, M.; Garcia Barroso, C. Determination of melatonin in rice (*Oryza sativa*) grains by pressurized liquid extraction. *J. Agric. Food Chem.* **2015**, *63*, 1107–1115. [CrossRef] [PubMed]
18. Escriva, L.; Manyes, L.; Barbera, M.; Martinez-Torres, D.; Meca, G. Determination of melatonin in *Acyrthosiphon pisum aphids* by liquid chromatography-tandem mass spectrometry. *J. Insect Physiol.* **2016**, *86*, 48–53. [CrossRef] [PubMed]
19. Muszynska, B.; Sulkowska-Ziaja, K. Analysis of indole compounds in edible *Basidiomycota* species after thermal processing. *Food Chem.* **2012**, *132*, 455–459. [CrossRef] [PubMed]
20. Yilmaz, C.; Kocadagli, T.; Gokmen, V. Formation of melatonin and its isomer during bread dough fermentation and effect of baking. *J. Agric. Food Chem.* **2014**, *62*, 2900–2905. [CrossRef] [PubMed]
21. Reiter, R.J.; Tan, D.X. Melatonin: An antioxidant in edible plants. *Ann. N. Y. Acad. Sci.* **2002**, *957*, 341–344. [CrossRef] [PubMed]
22. Tan, D.X.; Zanghi, B.M.; Manchester, L.C.; Reiter, R.J. Melatonin identified in meats and other food stuffs: Potentially nutritional impact. *J. Pineal Res.* **2014**, *57*, 213–218. [CrossRef] [PubMed]
23. Aguilera, Y.; Herrera, T.; Benitez, V.; Arribas, S.M.; Lopez De Pablo, A.L.; Esteban, R.M.; Martin-Cabrejas, M.A. Estimation of scavenging capacity of melatonin and other antioxidants: Contribution and evaluation in germinated seeds. *Food Chem.* **2015**, *170*, 203–211. [CrossRef] [PubMed]
24. Sae-Teaw, M.; Johns, J.; Johns, N.P.; Subongkot, S. Serum melatonin levels and antioxidant capacities after consumption of pineapple, orange, or banana by healthy male volunteers. *J. Pineal Res.* **2013**, *55*, 58–64. [CrossRef] [PubMed]
25. Delgado, J.; Terron, M.P.; Garrido, M.; Pariente, J.A.; Barriga, C.; Rodriguez, A.B.; Paredes, S.D. Diets enriched with a Jerte Valley cherry-based nutraceutical product reinforce nocturnal behaviour in young and old animals of nocturnal (*Rattus norvegicus*) and diurnal (*Streptopelia risoria*) chronotypes. *J. Anim. Physiol. Anim. Nutr.* **2013**, *97*, 137–145. [CrossRef] [PubMed]
26. Iriti, M.; Faoro, F. Grape phytochemicals: A bouquet of old and new nutraceuticals for human health. *Med. Hypotheses* **2006**, *67*, 833–838. [CrossRef] [PubMed]
27. Ferrari, C.K. Functional foods, herbs and nutraceuticals: Towards biochemical mechanisms of healthy aging. *Biogerontology* **2004**, *5*, 275–289. [CrossRef] [PubMed]
28. Oladi, E.; Mohamadi, M.; Shamspur, T.; Mostafavi, A. Spectrofluorimetric determination of melatonin in kernels of four different Pistacia varieties after ultrasound-assisted solid-liquid extraction. *Spectrochim. Acta A Mol. Biomol. Spectrosc.* **2014**, *132*, 326–329. [CrossRef] [PubMed]
29. Murch, S.J.; Simmons, C.B.; Saxena, P.K. Melatonin in feverfew and other medicinal plants. *Lancet* **1997**, *350*, 1598–1599. [CrossRef]
30. González-Gómez, D.; Lozano, M.; Fernández-León, M.F.; Ayuso, M.C.; Bernalte, M.J.; Rodríguez, A.B. Detection and quantification of melatonin and serotonin in eight Sweet Cherry cultivars (*Prunus avium* L.). *Eur. Food Res. Technol.* **2009**, *229*, 223–229. [CrossRef]
31. Wang, J.; Liang, C.; Li, S.; Zheng, J. Study on analysis method of melatonin and melatonin content in corn & rice seeds. *Chin. Agric. Sci. Bull.* **2009**, *25*, 20–24.

32. Hernandez-Ruiz, J.; Arnao, M.B. Distribution of melatonin in different zones of lupin and barley plants at different ages in the presence and absence of light. *J. Agric. Food Chem.* **2008**, *56*, 10567–10573. [CrossRef] [PubMed]
33. Reiter, R.J.; Tan, D.X.; Burkhardt, S.; Manchester, L.C. Melatonin in plants. *Nutr. Rev.* **2001**, *59*, 286–290. [CrossRef] [PubMed]
34. Hardeland, R.; Pandi-Perumal, S.R.; Cardinali, D.P. Melatonin. *Int. J. Biochem. Cell Biol.* **2006**, *38*, 313–316. [CrossRef] [PubMed]
35. Iriti, M.; Rossoni, M.; Faoro, F. Melatonin content in grape: Myth or panacea. *J. Sci. Food Agric.* **2006**, *86*, 1432–1438. [CrossRef]
36. Wang, C.; Yin, L.Y.; Shi, X.Y.; Xiao, H.; Kang, K.; Liu, X.Y.; Zhan, J.C.; Huang, W.D. Effect of cultivar, temperature, and environmental conditions on the dynamic change of melatonin in mulberry fruit development and wine fermentation. *J. Food Sci.* **2016**, *81*, M958–M967. [CrossRef] [PubMed]
37. Karunanithi, D.; Radhakrishna, A.; Sivaraman, K.P.; Biju, V.M. Quantitative determination of melatonin in milk by LC-MS/MS. *J. Food Sci. Technol.* **2014**, *51*, 805–812. [CrossRef] [PubMed]
38. Milagres, M.P.; Minim, V.P.; Minim, L.A.; Simiqueli, A.A.; Moraes, L.E.; Martino, H.S. Night milking adds value to cow's milk. *J. Sci. Food Agric.* **2014**, *94*, 1688–1692. [CrossRef] [PubMed]
39. Berthelot, X.; Laurentie, M.; Ravault, J.P.; Ferney, J.; Toutain, P.L. Circadian profile and production rate of melatonin in the cow. *Domest. Anim. Endocrinol.* **1990**, *7*, 315–322. [CrossRef]
40. Kennaway, D.J.; Stamp, G.E.; Goble, F.C. Development of melatonin production in infants and the impact of prematurity. *J. Clin. Endocrinol. Metab.* **1992**, *75*, 367–369. [CrossRef] [PubMed]
41. Cohen Engler, A.; Hadash, A.; Shehadeh, N.; Pillar, G. Breastfeeding may improve nocturnal sleep and reduce infantile colic: Potential role of breast milk melatonin. *Eur. J. Pediatr.* **2012**, *171*, 729–732. [CrossRef] [PubMed]
42. Kocadagli, T.; Yilmaz, C.; Gokmen, V. Determination of melatonin and its isomer in foods by liquid chromatography tandem mass spectrometry. *Food Chem.* **2014**, *153*, 151–156. [CrossRef] [PubMed]
43. Mercolini, L.; Mandrioli, R.; Raggi, M.A. Content of melatonin and other antioxidants in grape-related foodstuffs: Measurement using a MEPS-HPLC-F method. *J. Pineal Res.* **2012**, *53*, 21–28. [CrossRef] [PubMed]
44. Sturtz, M.; Cerezo, A.B.; Cantos-Villar, E.; Garcia-Parrilla, M.C. Determination of the melatonin content of different varieties of tomatoes (*Lycopersicon esculentum*) and strawberries (*Fragariaananassa*). *Food Chem.* **2011**, *127*, 1329–1334. [CrossRef] [PubMed]
45. Boccalandro, H.E.; Gonzalez, C.V.; Wunderlin, D.A.; Silva, M.F. Melatonin levels, determined by LC-ESI-MS/MS, fluctuate during the day/night cycle in *Vitis vinifera* cv. Malbec: Evidence of its antioxidant role in fruits. *J. Pineal Res.* **2011**, *51*, 226–232. [CrossRef] [PubMed]
46. Burkhardt, S.; Tan, D.X.; Manchester, L.C.; Hardeland, R.; Reiter, R.J. Detection and quantification of the antioxidant melatonin in Montmorency and Balaton tart cherries (*Prunus cerasus*). *J. Agric. Food Chem.* **2001**, *49*, 4898–4902. [CrossRef] [PubMed]
47. Badria, F.A. Melatonin, serotonin, and tryptamine in some Egyptian food and medicinal plants. *J. Med. Food* **2002**, *5*, 153–157. [CrossRef] [PubMed]
48. Dubbels, R.; Reiter, R.J.; Klenke, E.; Goebel, A.; Schnakenberg, E.; Ehlers, C.; Schiwara, H.W.; Schloot, W. Melatonin in edible plants identified by radioimmunoassay and by high performance liquid chromatography-mass spectrometry. *J. Pineal Res.* **1995**, *18*, 28–31. [CrossRef] [PubMed]
49. Riga, P.; Medina, S.; Garcia-Flores, L.A.; Gil-Izquierdo, A. Melatonin content of pepper and tomato fruits: Effects of cultivar and solar radiation. *Food Chem.* **2014**, *156*, 347–352. [CrossRef] [PubMed]
50. Muszynska, B.; Kala, K.; Sulkowska-Ziaja, K.; Krakowska, A.; Opoka, W. *Agaricus bisporus* and its in vitro culture as a source of indole compounds released into artificial digestive juices. *Food Chem.* **2016**, *199*, 509–515. [CrossRef] [PubMed]
51. Manchester, L.C.; Tan, D.X.; Reiter, R.J.; Park, W.; Monis, K.; Qi, W. High levels of melatonin in the seeds of edible plants: Possible function in germ tissue protection. *Life Sci.* **2000**, *67*, 3023–3029. [CrossRef]
52. Zielin Ski, H.; Lewczuk, B.; Przybylska-Gornowicz, B.; Kozlowska, H. Melatonin in germinated legume seeds as a potentially significant agent for health. In *Biologically-Active phytochemicals in Food: Analysis, Metabolism, Bioavailability and Function, Norwich, UK, 2001*; Pfannhauser, W., Fenwick, G.R., Khokhar, S.R., Eds.; Royal Society of Chemistry: Cambridge, UK, 2001.

53. Aguilera, Y.; Herrera, T.; Liebana, R.; Rebollo-Hernanz, M.; Sanchez-Puelles, C.; Martin-Cabrejas, M.A. Impact of melatonin enrichment during germination of legumes on bioactive compounds and antioxidant activity. *J. Agric. Food Chem.* **2015**, *63*, 7967–7974. [CrossRef] [PubMed]
54. Garcia-Moreno, H.; Calvo, J.R.; Maldonado, M.D. High levels of melatonin generated during the brewing process. *J. Pineal Res.* **2013**, *55*, 26–30. [CrossRef] [PubMed]
55. Rodriguez-Naranjo, M.I.; Gil-Izquierdo, A.; Troncoso, A.M.; Cantos, E.; Garcia-Parrilla, M.C. Melatonin: A new bioactive compound in wine. *J. Food Compos. Anal.* **2011**, *24*, 603–608. [CrossRef]
56. Stege, P.W.; Sombra, L.L.; Messina, G.; Martinez, L.D.; Silva, M.F. Determination of melatonin in wine and plant extracts by capillary electrochromatography with immobilized carboxylic multi-walled carbon nanotubes as stationary phase. *Electrophoresis* **2010**, *31*, 2242–2248. [CrossRef] [PubMed]
57. Rodriguez-Naranjo, M.I.; Gil-Izquierdo, A.; Troncoso, A.M.; Cantos-Villar, E.; Garcia-Parrilla, M.C. Melatonin is synthesised by yeast during alcoholic fermentation in wines. *Food Chem.* **2011**, *126*, 1608–1613. [CrossRef] [PubMed]
58. Ramakrishna, A.; Giridhar, P.; Sankar, K.U.; Ravishankar, G.A. Melatonin and serotonin profiles in beans of Coffea species. *J. Pineal Res.* **2012**, *52*, 470–476. [CrossRef] [PubMed]
59. Vitalini, S.; Gardana, C.; Simonetti, P.; Fico, G.; Iriti, M. Melatonin, melatonin isomers and stilbenes in Italian traditional grape products and their antiradical capacity. *J. Pineal Res.* **2013**, *54*, 322–333. [CrossRef] [PubMed]
60. Kirakosyan, A.; Seymour, E.M.; Llanes, D.E.U.; Kaufman, P.B.; Bolling, S.F. Chemical profile and antioxidant capacities of tart cherry products. *Food Chem.* **2009**, *115*, 20–25. [CrossRef]
61. Chen, G.; Huo, Y.; Tan, D.X.; Liang, Z.; Zhang, W.; Zhang, Y. Melatonin in Chinese medicinal herbs. *Life Sci.* **2003**, *73*, 19–26. [CrossRef]
62. Padumanonda, T.; Johns, J.; Sangkasat, A.; Tiyaworanant, S. Determination of melatonin content in traditional Thai herbal remedies used as sleeping aids. *Daru* **2014**, *22*, 6. [CrossRef] [PubMed]
63. de la Puerta, C.; Carrascosa-Salmoral, M.P.; García-Luna, P.P.; Lardone, P.J.; Herrera, J.L.; Fernández-Montesinos, R.; Guerrero, J.M.; Pozo, D. Melatonin is a phytochemical in olive oil. *Food Chem.* **2007**, *104*, 609–612. [CrossRef]
64. Venegas, C.; Cabrera-Vique, C.; Garcia-Corzo, L.; Escames, G.; Acuna-Castroviejo, D.; Lopez, L.C. Determination of coenzyme Q10, coenzyme Q9, and melatonin contents in virgin argan oils: Comparison with other edible vegetable oils. *J. Agric. Food Chem.* **2011**, *59*, 12102–12108. [CrossRef] [PubMed]
65. Reinholds, I.; Pugajeva, I.; Radenkovs, V.; Rjabova, J.; Bartkevics, V. Development and validation of new ultra-high-performance liquid chromatography-hybrid quadrupole-orbitrap mass spectrometry method for determination of melatonin in fruits. *J. Chromatogr. Sci.* **2016**, *54*, 977–984. [CrossRef] [PubMed]
66. Vakkuri, O.; Kivela, A.; Leppaluoto, J.; Valtonen, M.; Kauppila, A. Decrease in melatonin precedes follicle-stimulating hormone increase during perimenopause. *Eur. J. Endocrinol.* **1996**, *135*, 188–192. [CrossRef] [PubMed]
67. Waldhauser, F.; Weiszenbacher, G.; Tatzer, E.; Gisinger, B.; Waldhauser, M.; Schemper, M.; Frisch, H. Alterations in nocturnal serum melatonin levels in humans with growth and aging. *J. Clin. Endocrinol. Metab.* **1988**, *66*, 648–652. [CrossRef] [PubMed]
68. Sharma, M.; Palacios-Bois, J.; Schwartz, G.; Iskandar, H.; Thakur, M.; Quirion, R.; Nair, N.P. Circadian rhythms of melatonin and cortisol in aging. *Biol. Psychiatry* **1989**, *25*, 305–319. [CrossRef]
69. Singh, M.; Jadhav, H.R. Melatonin: Functions and ligands. *Drug Discov. Today* **2014**, *19*, 1410–1418. [CrossRef] [PubMed]
70. Gao, Y.; Xiao, X.; Zhang, C.; Yu, W.; Guo, W.; Zhang, Z.; Li, Z.; Feng, X.; Hao, J.; Zhang, K.; et al. Melatonin synergizes the chemotherapeutic effect of 5-fluorouracil in colon cancer by suppressing PI3K/AKT and NF-kappaB/iNOS signaling pathways. *J. Pineal Res.* **2017**, *62*. [CrossRef] [PubMed]
71. DeMuro, R.L.; Nafziger, A.N.; Blask, D.E.; Menhinick, A.M.; Bertino, J.J. The absolute bioavailability of oral melatonin. *J. Clin. Pharmacol.* **2000**, *40*, 781–784. [CrossRef] [PubMed]
72. Fourtillan, J.B.; Brisson, A.M.; Gobin, P.; Ingrand, I.; Decourt, J.P.; Girault, J. Bioavailability of melatonin in humans after day-time administration of D_7 melatonin. *Biopharm. Drug Dispos.* **2000**, *21*, 15–22. [CrossRef]
73. Shirakawa, S.; Tsuchiya, S.; Tsutsumi, Y.; Kotorii, T.; Uchimura, N.; Sakamoto, T.; Yamada, S. Time course of saliva and serum melatonin levels after ingestion of melatonin. *Psychiatry Clin. Neurosci.* **1998**, *52*, 266–267. [CrossRef] [PubMed]

74. Oba, S.; Nakamura, K.; Sahashi, Y.; Hattori, A.; Nagata, C. Consumption of vegetables alters morning urinary 6-sulfatoxymelatonin concentration. *J. Pineal Res.* **2008**, *45*, 17–23. [CrossRef] [PubMed]
75. Maldonado, M.D.; Moreno, H.; Calvo, J.R. Melatonin present in beer contributes to increase the levels of melatonin and antioxidant capacity of the human serum. *Clin. Nutr.* **2009**, *28*, 188–191. [CrossRef] [PubMed]
76. Gonzalez-Flores, D.; Gamero, E.; Garrido, M.; Ramirez, R.; Moreno, D.; Delgado, J.; Valdes, E.; Barriga, C.; Rodriguez, A.B.; Paredes, S.D. Urinary 6-sulfatoxymelatonin and total antioxidant capacity increase after the intake of a grape juice cv. Tempranillo stabilized with HHP. *Food Funct.* **2012**, *3*, 34–39. [CrossRef] [PubMed]
77. González-Flores, D.; Velardo, B.; Garrido, M.; González-Gómez, D.; Lozano, M.; Ayuso, M.C.; Barriga, C.; Paredes, S.D.; Rodríguez, A.B. Ingestion of Japanese plums (*Prunus salicina Lindl.* cv. Crimson Globe) increases the urinary 6-sulfatoxymelatonin and total antioxidant capacity levels in young, middle-aged and elderly humans: nutritional and functional characterization of their content. *J. Food Nutr. Res.* **2011**, *50*, 229.
78. Reiter, R.J.; Manchester, L.C.; Tan, D.X. Melatonin in walnuts: Influence on levels of melatonin and total antioxidant capacity of blood. *Nutrition* **2005**, *21*, 920–924. [CrossRef] [PubMed]
79. Schernhammer, E.S.; Feskanich, D.; Niu, C.; Dopfel, R.; Holmes, M.D.; Hankinson, S.E. Dietary correlates of urinary 6-sulfatoxymelatonin concentrations in the Nurses' Health Study cohorts. *Am. J. Clin. Nutr.* **2009**, *90*, 975–985. [CrossRef] [PubMed]
80. Aguilera, Y.; Rebollo-Hernanz, M.; Herrera, T.; Cayuelas, L.T.; Rodriguez-Rodriguez, P.; de Pablo, A.L.; Arribas, S.M.; Martin-Cabrejas, M.A. Intake of bean sprouts influences melatonin and antioxidant capacity biomarker levels in rats. *Food Funct.* **2016**, *7*, 1438–1445. [CrossRef] [PubMed]
81. Tetens, I. *Scientific Opinion on the Substantiation of Health Claims Related to Melatonin and Alleviation of Subjective Feelings of Jet Lag (ID 1953), and Reduction of Sleep onset Latency, and Improvement of Sleep Quality (ID 1953) Pursuant to Article 13(1) of Regulation (EC) No 1924/2006*; European Food Safety Authority: Parma, Itlay, 2010.
82. Food Standards Australia New Zealand (FSANZ). *Supporting document 9: Consideration of EU Approved Health Claims, P293—Nutrition, Health & Related Claim*; Food Standards Australia New Zealand: Kingston, Australia, Wellington, Newzealand, 2013.
83. Hattori, A.; Migitaka, H.; Iigo, M.; Itoh, M.; Yamamoto, K.; Ohtani-Kaneko, R.; Hara, M.; Suzuki, T.; Reiter, R.J. Identification of melatonin in plants and its effects on plasma melatonin levels and binding to melatonin receptors in vertebrates. *Biochem. Mol. Biol. Int.* **1995**, *35*, 627–634. [PubMed]
84. Byeon, Y.; Back, K. An increase in melatonin in transgenic rice causes pleiotropic phenotypes, including enhanced seedling growth, delayed flowering, and low grain yield. *J. Pineal Res.* **2014**, *56*, 408–414. [CrossRef] [PubMed]
85. Hernandez-Ruiz, J.; Cano, A.; Arnao, M.B. Melatonin acts as a growth-stimulating compound in some monocot species. *J. Pineal Res.* **2005**, *39*, 137–142. [CrossRef] [PubMed]
86. Fardet, A. New hypotheses for the health-protective mechanisms of whole-grain cereals: What is beyond fibre? *Nutr. Res. Rev.* **2010**, *23*, 65–134. [CrossRef] [PubMed]
87. Hosseinian, F.S.; Li, W.; Beta, T. Measurement of anthocyanins and other phytochemicals in purple wheat. *Food Chem.* **2008**, *109*, 916–924. [CrossRef] [PubMed]
88. Lei, Q.; Wang, L.; Tan, D.X.; Zhao, Y.; Zheng, X.D.; Chen, H.; Li, Q.T.; Zuo, B.X.; Kong, J. Identification of genes for melatonin synthetic enzymes in 'Red Fuji' apple (*Malus domestica Borkh.* cv. Red) and their expression and melatonin production during fruit development. *J. Pineal Res.* **2013**, *55*, 443–451. [PubMed]
89. Zhao, Y.; Tan, D.X.; Lei, Q.; Chen, H.; Wang, L.; Li, Q.T.; Gao, Y.; Kong, J. Melatonin and its potential biological functions in the fruits of sweet cherry. *J. Pineal Res.* **2013**, *55*, 79–88. [CrossRef] [PubMed]
90. Vitalini, S.; Gardana, C.; Zanzotto, A.; Simonetti, P.; Faoro, F.; Fico, G.; Iriti, M. The presence of melatonin in grapevine (*Vitis vinifera* L.) berry tissues. *J. Pineal Res.* **2011**, *51*, 331–337. [CrossRef] [PubMed]
91. Brown, P.N.; Turi, C.E.; Shipley, P.R.; Murch, S.J. Comparisons of large (*Vaccinium macrocarpon* Ait.) and small (*Vaccinium oxycoccos* L., *Vaccinium vitis-idaea* L.) cranberry in British Columbia by phytochemical determination, antioxidant potential, and metabolomic profiling with chemometric analysis. *Planta Med.* **2012**, *78*, 630–640. [CrossRef] [PubMed]
92. Simopoulos, A.P.; Tan, D.X.; Manchester, L.C.; Reiter, R.J. Purslane: A plant source of omega-3 fatty acids and melatonin. *J. Pineal Res.* **2005**, *39*, 331–332. [CrossRef] [PubMed]
93. Okazaki, M.; Ezura, H. Profiling of melatonin in the model tomato (*Solanum lycopersicum* L.) cultivar Micro-Tom. *J. Pineal Res.* **2009**, *46*, 338–343. [CrossRef] [PubMed]

94. Wang, L.; Zhao, Y.; Reiter, R.J.; He, C.; Liu, G.; Lei, Q.; Zuo, B.; Zheng, X.D.; Li, Q.; Kong, J. Changes in melatonin levels in transgenic 'Micro-Tom' tomato overexpressing ovine AANAT and ovine HIOMT genes. *J. Pineal Res.* **2014**, *56*, 134–142. [CrossRef] [PubMed]
95. Zhang, H.J.; Zhang, N.; Yang, R.C.; Wang, L.; Sun, Q.Q.; Li, D.B.; Cao, Y.Y.; Weeda, S.; Zhao, B.; Ren, S.; Guo, Y.D. Melatonin promotes seed germination under high salinity by regulating antioxidant systems, ABA and GA(4) interaction in cucumber (*Cucumis sativus* L.). *J. Pineal Res.* **2014**, *57*, 269–279. [CrossRef] [PubMed]
96. Byeon, Y.; Park, S.; Lee, H.Y.; Kim, Y.S.; Back, K. Elevated production of melatonin in transgenic rice seeds expressing rice tryptophan decarboxylase. *J. Pineal Res.* **2014**, *56*, 275–282. [CrossRef] [PubMed]
97. Tapia, M.I.; Sánchez-Morgado, J.R.; García-Parra, J.; Ramírez, R.; Hernández, T.; González-Gómez, D. Comparative study of the nutritional and bioactive compounds content of four walnut (*Juglans regia* L.) cultivars. *J. Food Compos. Anal.* **2013**, *31*, 232–237. [CrossRef]
98. Fernandez-Pachon, M.S.; Medina, S.; Herrero-Martin, G.; Cerrillo, I.; Berna, G.; Escudero-Lopez, B.; Ferreres, F.; Martin, F.; Garcia-Parrilla, M.C.; Gil-Izquierdo, A. Alcoholic fermentation induces melatonin synthesis in orange juice. *J. Pineal Res.* **2014**, *56*, 31–38. [CrossRef] [PubMed]
99. Pothinuch, P.; Tongchitpakdee, S. Melatonin contents in mulberry (*Morus* spp.) leaves: Effects of sample preparation, cultivar, leaf age and tea processing. *Food Chem.* **2011**, *128*, 415–419. [CrossRef] [PubMed]
100. Wehr, T.A.; Duncan, W.C., Jr.; Sher, L.; Aeschbach, D.; Schwartz, P.J.; Turner, E.H.; Postolache, T.T.; Rosenthal, N.E. A circadian signal of change of season in patients with seasonal affective disorder. *Arch. Gen. Psychiatry* **2001**, *58*, 1108–1114. [CrossRef] [PubMed]
101. Rexhaj, E.; Pireva, A.; Paoloni-Giacobino, A.; Allemann, Y.; Cerny, D.; Dessen, P.; Sartori, C.; Scherrer, U.; Rimoldi, S.F. Prevention of vascular dysfunction and arterial hypertension in mice generated by assisted reproductive technologies by addition of melatonin to culture media. *Am. J. Physiol. Heart Circ. Physiol.* **2015**, *309*, H1151–H1156. [CrossRef] [PubMed]
102. Michurina, S.V.; Ishchenko, I.Y.; Arkhipov, S.A.; Klimontov, V.V.; Rachkovskaya, L.N.; Konenkov, V.I.; Zavyalov, E.L. Effects of melatonin, aluminum oxide, and polymethylsiloxane complex on the expression of LYVE-1 in the liver of mice with obesity and type 2 diabetes mellitus. *Bull. Exp. Biol. Med.* **2016**, *162*, 269–272. [CrossRef] [PubMed]
103. Bielli, A.; Scioli, M.G.; Mazzaglia, D.; Doldo, E.; Orlandi, A. Antioxidants and vascular health. *Life Sci.* **2015**, *143*, 209–216. [CrossRef] [PubMed]
104. Barton, S.K.; Tolcos, M.; Miller, S.L.; Christoph-Roehr, C.; Schmolzer, G.M.; Moss, T.J.; Hooper, S.B.; Wallace, E.M.; Polglase, G.R. Ventilation-induced brain injury in preterm neonates: A review of potential therapies. *Neonatology* **2016**, *110*, 155–162. [CrossRef] [PubMed]
105. Droge, W. Free radicals in the physiological control of cell function. *Physiol. Rev.* **2002**, *82*, 47–95. [CrossRef] [PubMed]
106. Singh, A.K.; Haldar, C. Age dependent nitro-oxidative load and melatonin receptor expression in the spleen and immunity of goat *Capra hircus*. *Exp. Gerontol.* **2014**, *60*, 72–78. [CrossRef] [PubMed]
107. Aktoz, T.; Aydogdu, N.; Alagol, B.; Yalcin, O.; Huseyinova, G.; Atakan, I.H. The protective effects of melatonin and vitamin E against renal ischemia-reperfusion injury in rats. *Ren. Fail.* **2007**, *29*, 535–542. [CrossRef] [PubMed]
108. Lissoni, P.; Chilelli, M.; Villa, S.; Cerizza, L.; Tancini, G. Five years survival in metastatic non-small cell lung cancer patients treated with chemotherapy alone or chemotherapy and melatonin: A randomized trial. *J. Pineal Res.* **2003**, *35*, 12–15. [CrossRef] [PubMed]
109. Paredes, S.D.; Forman, K.A.; Garcia, C.; Vara, E.; Escames, G.; Tresguerres, J.A. Protective actions of melatonin and growth hormone on the aged cardiovascular system. *Horm. Mol. Biol. Clin. Investig.* **2014**, *18*, 79–88. [CrossRef] [PubMed]
110. Zephy, D.; Ahmad, J. Type 2 diabetes mellitus: Role of melatonin and oxidative stress. *Diabetes Metab. Syndr.* **2015**, *9*, 127–131. [CrossRef] [PubMed]
111. Chen, H.H.; Lin, K.C.; Wallace, C.G.; Chen, Y.T.; Yang, C.C.; Leu, S.; Chen, Y.C.; Sun, C.K.; Tsai, T.H.; Chen, Y.L.; et al. Additional benefit of combined therapy with melatonin and apoptotic adipose-derived mesenchymal stem cell against sepsis-induced kidney injury. *J. Pineal Res.* **2014**, *57*, 16–32. [CrossRef] [PubMed]
112. Deng, G.F.; Lin, X.; Xu, X.R.; Gao, L.L.; Xie, J.F.; Li, H.B. Antioxidant capacities and total phenolic contents of 56 vegetables. *J. Funct. Foods* **2013**, *5*, 260–266. [CrossRef]

113. Fu, L.; Xu, B.T.; Xu, X.R.; Qin, X.S.; Gan, R.Y.; Li, H.B. Antioxidant capacities and total phenolic contents of 56 wild fruits from South China. *Molecules* **2010**, *15*, 8602–8617. [CrossRef] [PubMed]
114. Guo, Y.J.; Deng, G.F.; Xu, X.R.; Wu, S.; Li, S.; Xia, E.Q.; Li, F.; Chen, F.; Ling, W.H.; Li, H.B. Antioxidant capacities, phenolic compounds and polysaccharide contents of 49 edible macro-fungi. *Food Funct.* **2012**, *3*, 1195–1205. [CrossRef] [PubMed]
115. Li, A.N.; Li, S.; Li, H.B.; Xu, D.P.; Xu, X.R.; Chen, F. Total phenolic contents and antioxidant capacities of 51 edible and wild flowers. *J. Funct. Foods* **2014**, *6*, 319–330. [CrossRef]
116. Li, S.; Li, S.K.; Gan, R.Y.; Song, F.L.; Kuang, L.; Li, H.B. Antioxidant capacities and total phenolic contents of infusions from 223 medicinal plants. *Ind. Crops Prod.* **2013**, *51*, 289–298. [CrossRef]
117. Deng, G.F.; Xu, X.R.; Zhang, Y.; Li, D.; Gan, R.Y.; Li, H.B. Phenolic compounds and bioactivities of pigmented rice. *Crit. Rev. Food Sci.* **2013**, *53*, 296–306. [CrossRef] [PubMed]
118. Li, A.N.; Li, S.; Zhang, Y.J.; Xu, X.R.; Chen, Y.M.; Li, H.B. Resources and biological activities of natural polyphenols. *Nutrients* **2014**, *6*, 6020–6047. [CrossRef] [PubMed]
119. Li, Y.; Zhang, J.J.; Xu, D.P.; Zhou, T.; Zhou, Y.; Li, S.; Li, H.B. Bioactivities and health benefits of wild fruits. *Int. J. Mol. Sci.* **2016**, *17*, 1258. [CrossRef] [PubMed]
120. Zhang, J.J.; Li, Y.; Zhou, T.; Xu, D.P.; Zhang, P.; Li, S.; Li, H.B. Bioactivities and health benefits of mushrooms mainly from China. *Molecules* **2016**, *21*, 938. [CrossRef] [PubMed]
121. Zhang, Y.J.; Gan, R.Y.; Li, S.; Zhou, Y.; Li, A.N.; Xu, D.P.; Li, H.B. Antioxidant phytochemicals for the prevention and treatment of chronic diseases. *Molecules* **2015**, *20*, 21138–21156. [CrossRef] [PubMed]
122. Okatani, Y.; Wakatsuki, A.; Reiter, R.J.; Miyahara, Y. Acutely administered melatonin restores hepatic mitochondrial physiology in old mice. *Int. J. Biochem. Cell Biol.* **2003**, *35*, 367–375. [CrossRef]
123. Khaldy, H.; Escames, G.; Leon, J.; Vives, F.; Luna, J.D.; Acuna-Castroviejo, D. Comparative effects of melatonin, L-deprenyl, Trolox and ascorbate in the suppression of hydroxyl radical formation during dopamine autoxidation in vitro. *J. Pineal Res.* **2000**, *29*, 100–107. [CrossRef] [PubMed]
124. Urata, Y.; Honma, S.; Goto, S.; Todoroki, S.; Iida, T.; Cho, S.; Honma, K.; Kondo, T. Melatonin induces gamma-glutamylcysteine synthetase mediated by activator protein-1 in human vascular endothelial cells. *Free Radic. Biol. Med.* **1999**, *27*, 838–847. [CrossRef]
125. Montilla, P.; Cruz, A.; Padillo, F.J.; Tunez, I.; Gascon, F.; Munoz, M.C.; Gomez, M.; Pera, C. Melatonin versus vitamin E as protective treatment against oxidative stress after extra-hepatic bile duct ligation in rats. *J. Pineal Res.* **2001**, *31*, 138–144. [CrossRef] [PubMed]
126. Poeggeler, B.; Reiter, R.J.; Tan, D.X.; Chen, L.D.; Manchester, L.C. Melatonin: A potent, endogenous hydroxyl radical scavenger. *J. Pineal Res.* **1993**, *14*, 57–60.
127. Okatani, Y.; Watanabe, K.; Hayashi, K.; Wakatsuki, A.; Sagara, Y. Melatonin inhibits vasospastic action of hydrogen peroxide in human umbilical artery. *J. Pineal Res.* **1997**, *22*, 163–168. [CrossRef] [PubMed]
128. Hsu, C.; Han, B.; Liu, M.; Yeh, C.; Casida, J.E. Phosphine-induced oxidative damage in rats: Attenuation by melatonin. *Free Radic. Biol. Med.* **2000**, *28*, 636–642. [CrossRef]
129. Tan, D.X.; Hardeland, R.; Manchester, L.C.; Poeggeler, B.; Lopez-Burillo, S.; Mayo, J.C.; Sainz, R.M.; Reiter, R.J. Mechanistic and comparative studies of melatonin and classic antioxidants in terms of their interactions with the ABTS cation radical. *J. Pineal Res.* **2003**, *34*, 249–259. [CrossRef] [PubMed]
130. Ressmeyer, A.R.; Mayo, J.C.; Zelosko, V.; Sainz, R.M.; Tan, D.X.; Poeggeler, B.; Antolin, I.; Zsizsik, B.K.; Reiter, R.J.; Hardeland, R. Antioxidant properties of the melatonin metabolite N^1-acetyl-5-methoxykynuramine (AMK): Scavenging of free radicals and prevention of protein destruction. *Redox Rep.* **2003**, *8*, 205–213. [CrossRef] [PubMed]
131. Tan, D.X.; Manchester, L.C.; Terron, M.P.; Flores, L.J.; Reiter, R.J. One molecule, many derivatives: A never-ending interaction of melatonin with reactive oxygen and nitrogen species? *J. Pineal Res.* **2007**, *42*, 28–42. [CrossRef] [PubMed]
132. Escames, G.; Lopez, L.C.; Ortiz, F.; Ros, E.; Acuna-Castroviejo, D. Age-dependent lipopolysaccharide-induced iNOS expression and multiorgan failure in rats: Effects of melatonin treatment. *Exp. Gerontol.* **2006**, *41*, 1165–1173. [CrossRef] [PubMed]
133. Sonmez, M.F.; Narin, F.; Akkus, D.; Ozdamar, S. Effect of melatonin and vitamin C on expression of endothelial NOS in heart of chronic alcoholic rats. *Toxicol. Ind. Health* **2009**, *25*, 385–393. [CrossRef] [PubMed]

134. Buldak, R.J.; Pilc-Gumula, K.; Buldak, L.; Witkowska, D.; Kukla, M.; Polaniak, R.; Zwirska-Korczala, K. Effects of ghrelin, leptin and melatonin on the levels of reactive oxygen species, antioxidant enzyme activity and viability of the HCT 116 human colorectal carcinoma cell line. *Mol. Med. Rep.* **2015**, *12*, 2275–2282. [PubMed]
135. Tesoriere, L.; Allegra, M.; D'Arpa, D.; Butera, D.; Livrea, M.A. Reaction of melatonin with hemoglobin-derived oxoferryl radicals and inhibition of the hydroperoxide-induced hemoglobin denaturation in red blood cells. *J. Pineal Res.* **2001**, *31*, 114–119. [CrossRef] [PubMed]
136. Li, M.; Pi, H.; Yang, Z.; Reiter, R.J.; Xu, S.; Chen, X.; Chen, C.; Zhang, L.; Yang, M.; Li, Y.; et al. Melatonin antagonizes cadmium-induced neurotoxicity by activating the transcription factor EB-dependent autophagy-lysosome machinery in mouse neuroblastoma cells. *J. Pineal Res.* **2016**, *61*, 353–369. [CrossRef] [PubMed]
137. Rao, M.V.; Chhunchha, B. Protective role of melatonin against the mercury induced oxidative stress in the rat thyroid. *Food Chem. Toxicol.* **2010**, *48*, 7–10. [CrossRef] [PubMed]
138. Zhang, Y.; Wei, Z.; Liu, W.; Wang, J.; He, X.; Huang, H.; Zhang, J.; Yang, Z. Melatonin protects against arsenic trioxide-induced liver injury by the upregulation of Nrf2 expression through the activation of PI3K/AKT pathway. *Oncotarget* **2017**, *8*, 3773–3780. [CrossRef] [PubMed]
139. Hernandez-Plata, E.; Quiroz-Compean, F.; Ramirez-Garcia, G.; Barrientos, E.Y.; Rodriguez-Morales, N.M.; Flores, A.; Wrobel, K.; Wrobel, K.; Mendez, I.; Diaz-Munoz, M.; et al. Melatonin reduces lead levels in blood, brain and bone and increases lead excretion in rats subjected to subacute lead treatment. *Toxicol. Lett.* **2015**, *233*, 78–83. [CrossRef] [PubMed]
140. Karabulut-Bulan, O.; Bayrak, B.B.; Arda-Pirincci, P.; Sarikaya-Unal, G.; Us, H.; Yanardag, R. Role of exogenous melatonin on cell proliferation and oxidant/antioxidant system in aluminum-induced renal toxicity. *Biol. Trace Elem. Res.* **2015**, *168*, 141–149. [CrossRef] [PubMed]
141. Navarro-Alarcon, M.; Ruiz-Ojeda, F.J.; Blanca-Herrera, R.M.; Kaki, A.; Adem, A.; Agil, A. Melatonin administration in diabetes: Regulation of plasma Cr, V, and Mg in young male Zucker diabetic fatty rats. *Food Funct.* **2014**, *5*, 512–516. [CrossRef] [PubMed]
142. Leon, J.; Escames, G.; Rodriguez, M.I.; Lopez, L.C.; Tapias, V.; Entrena, A.; Camacho, E.; Carrion, M.D.; Gallo, M.A.; Espinosa, A.; et al. Inhibition of neuronal nitric oxide synthase activity by N^1-acetyl-5-methoxykynuramine, a brain metabolite of melatonin. *J. Neurochem.* **2006**, *98*, 2023–2033. [CrossRef] [PubMed]
143. Martinez-Campa, C.; Gonzalez, A.; Mediavilla, M.D.; Alonso-Gonzalez, C.; Alvarez-Garcia, V.; Sanchez-Barcelo, E.J.; Cos, S. Melatonin inhibits aromatase promoter expression by regulating cyclooxygenases expression and activity in breast cancer cells. *Br. J. Cancer* **2009**, *101*, 1613–1619. [CrossRef] [PubMed]
144. Mayo, J.C.; Sainz, R.M.; Antoli, I.; Herrera, F.; Martin, V.; Rodriguez, C. Melatonin regulation of antioxidant enzyme gene expression. *Cell. Mol. Life Sci.* **2002**, *59*, 1706–1713. [CrossRef] [PubMed]
145. Mehrzadi, S.; Safa, M.; Kamrava, S.K.; Darabi, R.; Hayat, P.; Motevalian, M. Protective mechanisms of melatonin against hydrogen peroxide induced toxicity in human bone-marrow derived mesenchymal stem cells. *Can. J. Physiol. Pharmacol.* **2016**. [CrossRef] [PubMed]
146. Bilici, D.; Suleyman, H.; Banoglu, Z.N.; Kiziltunc, A.; Avci, B.; Ciftcioglu, A.; Bilici, S. Melatonin prevents ethanol-induced gastric mucosal damage possibly due to its antioxidant effect. *Dig. Dis. Sci.* **2002**, *47*, 856–861. [CrossRef] [PubMed]
147. Ciftci, M.; Bilici, D.; Kufrevioglu, O.I. Effects of melatonin on enzyme activities of glucose-6-phosphate dehydrogenase from human erythrocytes in vitro and from rat erythrocytes in vivo. *Pharmacol. Res.* **2001**, *44*, 7–11. [CrossRef] [PubMed]
148. Gitto, E.; Tan, D.X.; Reiter, R.J.; Karbownik, M.; Manchester, L.C.; Cuzzocrea, S.; Fulia, F.; Barberi, I. Individual and synergistic antioxidative actions of melatonin: Studies with vitamin E, vitamin C, glutathione and desferrioxamine (desferoxamine) in rat liver homogenates. *J. Pharm. Pharmacol.* **2001**, *53*, 1393–1401. [CrossRef] [PubMed]
149. Sun, C.; Zhang, F.; Ge, X.; Yan, T.; Chen, X.; Shi, X.; Zhai, Q. SIRT1 improves insulin sensitivity under insulin-resistant conditions by repressing PTP1B. *Cell Metab.* **2007**, *6*, 307–319. [CrossRef] [PubMed]

150. Chahbouni, M.; Escames, G.; Venegas, C.; Sevilla, B.; Garcia, J.A.; Lopez, L.C.; Munoz-Hoyos, A.; Molina-Carballo, A.; Acuna-Castroviejo, D. Melatonin treatment normalizes plasma pro-inflammatory cytokines and nitrosative/oxidative stress in patients suffering from Duchenne muscular dystrophy. *J. Pineal Res.* **2010**, *48*, 282–289. [CrossRef] [PubMed]
151. Kepka, M.; Szwejser, E.; Pijanowski, L.; Verburg-van Kemenade, B.M.; Chadzinska, M. A role for melatonin in maintaining the pro- and anti-inflammatory balance by influencing leukocyte migration and apoptosis in carp. *Dev. Comp. Immunol.* **2015**, *53*, 179–190. [CrossRef] [PubMed]
152. Perkins, N.D. Integrating cell-signalling pathways with NF-kappaB and IKK function. *Nat. Rev. Mol. Cell Biol.* **2007**, *8*, 49–62. [CrossRef] [PubMed]
153. Gilmore, T.D. Introduction to NF-kappaB: Players, pathways, perspectives. *Oncogene* **2006**, *25*, 6680–6684. [CrossRef] [PubMed]
154. Garcia, J.A.; Volt, H.; Venegas, C.; Doerrier, C.; Escames, G.; Lopez, L.C.; Acuna-Castroviejo, D. Disruption of the NF-kappaB/NLRP3 connection by melatonin requires retinoid-related orphan receptor-alpha and blocks the septic response in mice. *FASEB J.* **2015**, *29*, 3863–3875. [CrossRef] [PubMed]
155. Hu, Z.P.; Fang, X.L.; Fang, N.; Wang, X.B.; Qian, H.Y.; Cao, Z.; Cheng, Y.; Wang, B.N.; Wang, Y. Melatonin ameliorates vascular endothelial dysfunction, inflammation, and atherosclerosis by suppressing the TLR4/NF-kappaB system in high-fat-fed rabbits. *J. Pineal Res.* **2013**, *55*, 388–398. [PubMed]
156. Yi, C.; Zhang, Y.; Yu, Z.; Xiao, Y.; Wang, J.; Qiu, H.; Yu, W.; Tang, R.; Yuan, Y.; Guo, W.; et al. Melatonin enhances the anti-tumor effect of fisetin by inhibiting COX-2/iNOS and NF-kappaB/p300 signaling pathways. *PLoS ONE* **2014**, *9*, e99943. [CrossRef] [PubMed]
157. Lu, J.J.; Fu, L.; Tang, Z.; Zhang, C.; Qin, L.; Wang, J.; Yu, Z.; Shi, D.; Xiao, X.; Xie, F.; et al. Melatonin inhibits AP-2beta/hTERT, NF-kappaB/COX-2 and Akt/ERK and activates caspase/Cyto C signaling to enhance the antitumor activity of berberine in lung cancer cells. *Oncotarget* **2016**, *7*, 2985–3001. [PubMed]
158. Mayo, J.C.; Sainz, R.M.; Tan, D.X.; Hardeland, R.; Leon, J.; Rodriguez, C.; Reiter, R.J. Anti-inflammatory actions of melatonin and its metabolites, N^1-acetyl-N^2-formyl-5-methoxykynuramine (AFMK) and N^1-acetyl-5-methoxykynuramine (AMK), in macrophages. *J. Neuroimmunol.* **2005**, *165*, 139–149. [CrossRef] [PubMed]
159. Permpoonputtana, K.; Govitrapong, P. The anti-inflammatory effect of melatonin on methamphetamine-induced proinflammatory mediators in human neuroblastoma dopamine SH-SY5Y cell lines. *Neurotox. Res.* **2013**, *23*, 189–199. [CrossRef] [PubMed]
160. Niranjan, R.; Nath, C.; Shukla, R. Melatonin attenuated mediators of neuroinflammation and alpha-7 nicotinic acetylcholine receptor mRNA expression in lipopolysaccharide (LPS) stimulated rat astrocytoma cells, C6. *Free Radic. Res.* **2012**, *46*, 1167–1177. [CrossRef] [PubMed]
161. Lim, H.D.; Kim, Y.S.; Ko, S.H.; Yoon, I.J.; Cho, S.G.; Chun, Y.H.; Choi, B.J.; Kim, E.C. Cytoprotective and anti-inflammatory effects of melatonin in hydrogen peroxide-stimulated CHON-001 human chondrocyte cell line and rabbit model of osteoarthritis via the SIRT1 pathway. *J. Pineal Res.* **2012**, *53*, 225–237. [CrossRef] [PubMed]
162. Min, K.J.; Jang, J.H.; Kwon, T.K. Inhibitory effects of melatonin on the lipopolysaccharide-induced CC chemokine expression in BV2 murine microglial cells are mediated by suppression of Akt-induced NF-kappaB and STAT/GAS activity. *J. Pineal Res.* **2012**, *52*, 296–304. [CrossRef] [PubMed]
163. Yang, G.H.; Li, Y.C.; Wang, Z.Q.; Liu, B.; Ye, W.; Ni, L.; Zeng, R.; Miao, S.Y.; Wang, L.F.; Liu, C.W. Protective effect of melatonin on cigarette smoke-induced restenosis in rat carotid arteries after balloon injury. *J. Pineal Res.* **2014**, *57*, 451–458. [CrossRef] [PubMed]
164. Shao, G.; Tian, Y.; Wang, H.; Liu, F.; Xie, G. Protective effects of melatonin on lipopolysaccharide-induced mastitis in mice. *Int. Immunopharmacol.* **2015**, *29*, 263–268. [CrossRef] [PubMed]
165. Maldonado, M.D.; Garcia-Moreno, H.; Gonzalez-Yanes, C.; Calvo, J.R. Possible involvement of the inhibition of NF-kappaB factor in anti-inflammatory actions that melatonin exerts on mast cells. *J. Cell Biochem.* **2016**, *117*, 1926–1933. [CrossRef] [PubMed]
166. Wilson, B.J.; Tremblay, A.M.; Deblois, G.; Sylvain-Drolet, G.; Giguere, V. An acetylation switch modulates the transcriptional activity of estrogen-related receptor alpha. *Mol. Endocrinol.* **2010**, *24*, 1349–1358. [CrossRef] [PubMed]
167. Rodgers, J.T.; Lerin, C.; Haas, W.; Gygi, S.P.; Spiegelman, B.M.; Puigserver, P. Nutrient control of glucose homeostasis through a complex of PGC-1alpha and SIRT1. *Nature* **2005**, *434*, 113–118. [CrossRef] [PubMed]

168. Shah, S.A.; Khan, M.; Jo, M.H.; Jo, M.G.; Amin, F.U.; Kim, M.O. Melatonin stimulates the SIRT1/Nrf2 signaling pathway counteracting lipopolysaccharide (LPS)-induced oxidative stress to rescue postnatal rat brain. *CNS Neurosci. Ther.* **2016**. [CrossRef] [PubMed]
169. Ge, D.; Dauchy, R.T.; Liu, S.; Zhang, Q.; Mao, L.; Dauchy, E.M.; Blask, D.E.; Hill, S.M.; Rowan, B.G.; Brainard, G.C.; et al. Insulin and IGF1 enhance IL-17-induced chemokine expression through a GSK3B-dependent mechanism: A new target for melatonin's anti-inflammatory action. *J. Pineal Res.* **2013**, *55*, 377–387. [CrossRef] [PubMed]
170. Koyama, F.C.; Azevedo, M.F.; Budu, A.; Chakrabarti, D.; Garcia, C.R. Melatonin-induced temporal up-regulation of gene expression related to ubiquitin/proteasome system (UPS) in the human malaria parasite *Plasmodium falciparum*. *Int. J. Mol. Sci.* **2014**, *15*, 22320–22330. [CrossRef] [PubMed]
171. Chung, S.H.; Park, Y.S.; Kim, O.S.; Kim, J.H.; Baik, H.W.; Hong, Y.O.; Kim, S.S.; Shin, J.H.; Jun, J.H.; Jo, Y.; et al. Melatonin attenuates dextran sodium sulfate induced colitis with sleep deprivation: Possible mechanism by microarray analysis. *Dig. Dis. Sci.* **2014**, *59*, 1134–1141. [CrossRef] [PubMed]
172. Yang, B.; Ni, Y.F.; Wang, W.C.; Du, H.Y.; Zhang, H.; Zhang, L.; Zhang, W.D.; Jiang, T. Melatonin attenuates intestinal ischemia—Reperfusion-induced lung injury in rats by upregulating *N*-myc downstream-regulated gene 2. *J. Surg. Res.* **2015**, *194*, 273–280. [CrossRef] [PubMed]
173. Singh, A.K.; Ghosh, S.; Basu, P.; Haldar, C. Daily variation in melatonin level, antioxidant activity and general immune response of peripheral blood mononuclear cells and lymphoid tissues of Indian goat *Capra hircus* during summer and winter. *Indian J. Exp. Biol.* **2014**, *52*, 467–477. [PubMed]
174. Zhang, M.; Wang, T.; Chen, H.M.; Chen, Y.Q.; Deng, Y.C.; Li, Y.T. Serum levels of interleukin-1 beta, interleukin-6 and melatonin over summer and winter in kidney deficiency syndrome in Bizheng rats. *Chin. Med. Sci. J.* **2014**, *29*, 107–111. [CrossRef]
175. Provinciali, M.; Di Stefano, G.; Bulian, D.; Tibaldi, A.; Fabris, N. Effect of melatonin and pineal grafting on thymocyte apoptosis in aging mice. *Mech. Ageing Dev.* **1996**, *90*, 1–19. [CrossRef]
176. Fernandes, P.A.; Cecon, E.; Markus, R.P.; Ferreira, Z.S. Effect of TNF-alpha on the melatonin synthetic pathway in the rat pineal gland: Basis for a 'feedback' of the immune response on circadian timing. *J. Pineal Res.* **2006**, *41*, 344–350. [CrossRef] [PubMed]
177. Lissoni, P.; Rovelli, F.; Giani, L.; Fumagalli, L.; Mandala, M. Immunomodulatory effects of IL-12 in relation to the pineal endocrine function in metastatic cancer patients. *Nat. Immun.* **1998**, *16*, 178–184. [CrossRef] [PubMed]
178. Withyachumnarnkul, B.; Nonaka, K.O.; Santana, C.; Attia, A.M.; Reiter, R.J. Interferon-gamma modulates melatonin production in rat pineal glands in organ culture. *J. Interferon Res.* **1990**, *10*, 403–411. [CrossRef] [PubMed]
179. Tan, D.X.; Manchester, L.C.; Reiter, R.J. CSF generation by pineal gland results in a robust melatonin circadian rhythm in the third ventricle as an unique light/dark signal. *Med. Hypotheses* **2016**, *86*, 3–9. [CrossRef] [PubMed]
180. Markus, R.P.; Cecon, E.; Pires-Lapa, M.A. Immune-pineal axis: Nuclear factor kappaB (NF-êB) mediates the shift in the melatonin source from pinealocytes to immune competent cells. *Int. J. Mol. Sci.* **2013**, *14*, 10979–10997. [CrossRef] [PubMed]
181. Pontes, G.N.; Cardoso, E.C.; Carneiro-Sampaio, M.M.; Markus, R.P. Injury switches melatonin production source from endocrine (pineal) to paracrine (phagocytes)—Melatonin in human colostrum and colostrum phagocytes. *J. Pineal Res.* **2006**, *41*, 136–141. [CrossRef] [PubMed]
182. Ahmad, R.; Haldar, C. Photoperiodic regulation of MT1 and MT2 melatonin receptor expression in spleen and thymus of a tropical rodent *Funambulus pennanti* during reproductively active and inactive phases. *Chronobiol. Int.* **2010**, *27*, 446–462. [CrossRef] [PubMed]
183. Garcia-Perganeda, A.; Pozo, D.; Guerrero, J.M.; Calvo, J.R. Signal transduction for melatonin in human lymphocytes: Involvement of a pertussis toxin-sensitive G protein. *J. Immunol.* **1997**, *159*, 3774–3781. [PubMed]
184. Vishwas, D.K.; Haldar, C. Photoperiodic induced melatonin regulates immunity and expression pattern of melatonin receptor MT1 in spleen and bone marrow mononuclear cells of male golden hamster. *J. Photochem. Photobiol. B* **2013**, *128*, 107–114. [CrossRef] [PubMed]

185. Lardone, P.J.; Rubio, A.; Cerrillo, I.; Gomez-Corvera, A.; Carrillo-Vico, A.; Sanchez-Hidalgo, M.; Guerrero, J.M.; Fernandez-Riejos, P.; Sanchez-Margalet, V.; Molinero, P. Blocking of melatonin synthesis and MT(1) receptor impairs the activation of Jurkat T cells. *Cell Mol. Life Sci.* **2010**, *67*, 3163–3172. [CrossRef] [PubMed]
186. Mohseni, M.; Mihandoost, E.; Shirazi, A.; Sepehrizadeh, Z.; Bazzaz, J.T.; Ghazi-khansari, M. Melatonin may play a role in modulation of bax and bcl-2 expression levels to protect rat peripheral blood lymphocytes from gamma irradiation-induced apoptosis. *Mutat. Res.* **2012**, *738–739*, 19–27. [CrossRef] [PubMed]
187. Guo, Q.; Dong, Y.; Cao, J.; Wang, Z.; Zhang, Z.; Chen, Y. Developmental changes of melatonin receptor expression in the spleen of the chicken, *Gallus domesticus*. *Acta Histochem.* **2015**, *117*, 559–565. [CrossRef] [PubMed]
188. Vaughan, M.K.; Hubbard, G.B.; Champney, T.H.; Vaughan, G.M.; Little, J.C.; Reiter, R.J. Splenic hypertrophy and extramedullary hematopoiesis induced in male Syrian hamsters by short photoperiod or melatonin injections and reversed by melatonin pellets or pinealectomy. *Am. J. Anat.* **1987**, *179*, 131–136. [CrossRef] [PubMed]
189. Lopez Gonzalez, M.A.; Guerrero, J.M.; Ceballo Pedraja, J.M.; Delgado Moreno, F. Melatonin in palate tonsils with recurrent acute tonsillitis and tonsillar hypertrophy. *Acta Otorrinolaringol. Esp.* **1998**, *49*, 625–628. [PubMed]
190. Barjavel, M.J.; Mamdouh, Z.; Raghbate, N.; Bakouche, O. Differential expression of the melatonin receptor in human monocytes. *J. Immunol.* **1998**, *160*, 1191–1197. [PubMed]
191. Kim, Y.O.; Ahn, Y.K.; Kim, J.H. Influence of melatonin on immunotoxicity of cadmium. *Int. J. Immunopharmacol.* **2000**, *22*, 275–284. [CrossRef]
192. Silva, S.O.; Rodrigues, M.R.; Ximenes, V.F.; Bueno-da-Silva, A.E.; Amarante-Mendes, G.P.; Campa, A. Neutrophils as a specific target for melatonin and kynuramines: Effects on cytokine release. *J. Neuroimmunol.* **2004**, *156*, 146–152. [CrossRef] [PubMed]
193. Suke, S.G.; Pathak, R.; Ahmed, R.S.; Tripathi, A.K.; Banerjee, B.D. Melatonin treatment prevents modulation of cell-mediated immune response induced by propoxur in rats. *Indian J. Biochem. Biophys.* **2008**, *45*, 278–281. [PubMed]
194. Ghosh, S.; Singh, A.K.; Haldar, C. Seasonal modulation of immunity by melatonin and gonadal steroids in a short day breeder goat *Capra hircus*. *Theriogenology* **2014**, *82*, 1121–1130. [CrossRef] [PubMed]
195. Garcia-Maurino, S.; Pozo, D.; Carrillo-Vico, A.; Calvo, J.R.; Guerrero, J.M. Melatonin activates Th1 lymphocytes by increasing IL-12 production. *Life Sci.* **1999**, *65*, 2143–2150. [CrossRef]
196. Xia, M.Z.; Liang, Y.L.; Wang, H.; Chen, X.; Huang, Y.Y.; Zhang, Z.H.; Chen, Y.H.; Zhang, C.; Zhao, M.; Xu, D.X.; et al. Melatonin modulates TLR4-mediated inflammatory genes through MyD88- and TRIF-dependent signaling pathways in lipopolysaccharide-stimulated RAW264.7 cells. *J. Pineal Res.* **2012**, *53*, 325–334. [CrossRef] [PubMed]
197. Carrillo-Vico, A.; Reiter, R.J.; Lardone, P.J.; Herrera, J.L.; Fernandez-Montesinos, R.; Guerrero, J.M.; Pozo, D. The modulatory role of melatonin on immune responsiveness. *Curr. Opin. Investig. Drugs* **2006**, *7*, 423–431. [PubMed]
198. Carrillo-Vico, A.; Lardone, P.J.; Fernandez-Santos, J.M.; Martin-Lacave, I.; Calvo, J.R.; Karasek, M.; Guerrero, J.M. Human lymphocyte-synthesized melatonin is involved in the regulation of the interleukin-2/interleukin-2 receptor system. *J. Clin. Endocrinol. Metab.* **2005**, *90*, 992–1000. [CrossRef] [PubMed]
199. Morrey, K.M.; McLachlan, J.A.; Serkin, C.D.; Bakouche, O. Activation of human monocytes by the pineal hormone melatonin. *J. Immunol.* **1994**, *153*, 2671–2680. [PubMed]
200. Bouhafs, R.K.; Jarstrand, C. Effects of antioxidants on surfactant peroxidation by stimulated human polymorphonuclear leukocytes. *Free Radic. Res.* **2002**, *36*, 727–734. [CrossRef] [PubMed]
201. Vishwas, D.K.; Mukherjee, A.; Haldar, C.; Dash, D.; Nayak, M.K. Improvement of oxidative stress and immunity by melatonin: An age dependent study in golden hamster. *Exp. Gerontol.* **2013**, *48*, 168–182. [CrossRef] [PubMed]
202. Yadav, S.K.; Haldar, C. Experimentally induced stress, oxidative load and changes in immunity in a tropical wild bird, *Perdicula asiatica*: Involvement of melatonin and glucocorticoid receptors. *Zoology* **2014**, *117*, 261–268. [CrossRef] [PubMed]

203. Miyamoto, M. Pharmacology of ramelteon, a selective MT1/MT2 receptor agonist: A novel therapeutic drug for sleep disorders. *CNS Neurosci. Ther.* **2009**, *15*, 32–51. [CrossRef] [PubMed]
204. Edgar, R.S.; Green, E.W.; Zhao, Y.; van Ooijen, G.; Olmedo, M.; Qin, X.; Xu, Y.; Pan, M.; Valekunja, U.K.; Feeney, K.A.; et al. Peroxiredoxins are conserved markers of circadian rhythms. *Nature* **2012**, *485*, 459–464. [CrossRef] [PubMed]
205. Sturgeon, S.R.; Luisi, N.; Balasubramanian, R.; Reeves, K.W. Sleep duration and endometrial cancer risk. *Cancer Causes Control* **2012**, *23*, 547–553. [CrossRef] [PubMed]
206. Liu, Z.; Gan, L.; Luo, D.; Sun, C. Melatonin promotes circadian rhythm-induced proliferation through interaction of Clock/HDAC3/c-Myc in mice adipose tissue. *J. Pineal Res.* **2016**. [CrossRef]
207. Tamura, H.; Takasaki, A.; Taketani, T.; Tanabe, M.; Lee, L.; Tamura, I.; Maekawa, R.; Aasada, H.; Yamagata, Y.; Sugino, N. Melatonin and female reproduction. *J. Obstet. Gynaecol. Res.* **2014**, *40*, 1–11. [CrossRef] [PubMed]
208. Lundmark, P.O.; Pandi-Perumal, S.R.; Srinivasan, V.; Cardinali, D.P.; Rosenstein, R.E. Melatonin in the eye: Implications for glaucoma. *Exp. Eye Res.* **2007**, *84*, 1021–1030. [CrossRef] [PubMed]
209. Espino, J.; Pariente, J.A.; Rodriguez, A.B. Role of melatonin on diabetes-related metabolic disorders. *World J. Diabetes* **2011**, *2*, 82–91. [CrossRef] [PubMed]
210. Hardeland, R. Neurobiology, pathophysiology, and treatment of melatonin deficiency and dysfunction. *Sci. World J.* **2012**, *2012*, 640389. [CrossRef] [PubMed]
211. Torres-Farfan, C.; Seron-Ferre, M.; Dinet, V.; Korf, H.W. Immunocytochemical demonstration of day/night changes of clock gene protein levels in the murine adrenal gland: Differences between melatonin-proficient (C3H) and melatonin-deficient (C57BL) mice. *J. Pineal Res.* **2006**, *40*, 64–70. [CrossRef] [PubMed]
212. Johnston, J.D.; Tournier, B.B.; Andersson, H.; Masson-Pevet, M.; Lincoln, G.A.; Hazlerigg, D.G. Multiple effects of melatonin on rhythmic clock gene expression in the mammalian pars tuberalis. *Endocrinology* **2006**, *147*, 959–965. [CrossRef] [PubMed]
213. Dinet, V.; Ansari, N.; Torres-Farfan, C.; Korf, H.W. Clock gene expression in the retina of melatonin-proficient (C3H) and melatonin-deficient (C57BL) mice. *J. Pineal Res.* **2007**, *42*, 83–91. [CrossRef] [PubMed]
214. Chellappa, S.L.; Viola, A.U.; Schmidt, C.; Bachmann, V.; Gabel, V.; Maire, M.; Reichert, C.F.; Valomon, A.; Gotz, T.; Landolt, H.P.; et al. Human melatonin and alerting response to blue-enriched light depend on a polymorphism in the clock gene PER3. *J. Clin. Endocrinol. Metab.* **2012**, *97*, E433–E437. [CrossRef] [PubMed]
215. West, A.; Dupre, S.M.; Yu, L.; Paton, I.R.; Miedzinska, K.; McNeilly, A.S.; Davis, J.R.; Burt, D.W.; Loudon, A.S. Npas4 is activated by melatonin, and drives the clock gene Cry1 in the ovine pars tuberalis. *Mol. Endocrinol.* **2013**, *27*, 979–989. [CrossRef] [PubMed]
216. Bracci, M.; Manzella, N.; Copertaro, A.; Staffolani, S.; Strafella, E.; Barbaresi, M.; Copertaro, B.; Rapisarda, V.; Valentino, M.; Santarelli, L. Rotating-shift nurses after a day off: Peripheral clock gene expression, urinary melatonin, and serum 17-beta-estradiol levels. Scand. *J. Work Environ. Health* **2014**, *40*, 295–304. [CrossRef] [PubMed]
217. Ikeno, T.; Nelson, R.J. Acute melatonin treatment alters dendritic morphology and circadian clock gene expression in the hippocampus of Siberian hamsters. *Hippocampus* **2015**, *25*, 142–148. [CrossRef] [PubMed]
218. Nagy, A.D.; Iwamoto, A.; Kawai, M.; Goda, R.; Matsuo, H.; Otsuka, T.; Nagasawa, M.; Furuse, M.; Yasuo, S. Melatonin adjusts the expression pattern of clock genes in the suprachiasmatic nucleus and induces antidepressant-like effect in a mouse model of seasonal affective disorder. *Chronobiol. Int.* **2015**, *32*, 447–457. [CrossRef] [PubMed]
219. Rodenbeck, A.; Hajak, G. Neuroendocrine dysregulation in primary insomnia. *Rev. Neurol.* **2001**, *157*, S57–S61. [PubMed]
220. Takaesu, Y.; Futenma, K.; Kobayashi, M.; Komada, Y.; Tanaka, N.; Yamashina, A.; Inoue, Y. A preliminary study on the relationships between diurnal melatonin secretion profile and sleep variables in patients emergently admitted to the coronary care unit. *Chronobiol. Int.* **2015**, *32*, 875–879. [CrossRef] [PubMed]
221. Evely, K.M.; Hudson, R.L.; Dubocovich, M.L.; Haj-Dahmane, S. Melatonin receptor activation increases glutamatergic synaptic transmission in the rat medial lateral habenula. *Synapse* **2016**, *70*, 181–186. [CrossRef] [PubMed]
222. Waldhauser, F.; Kovacs, J.; Reiter, E. Age-related changes in melatonin levels in humans and its potential consequences for sleep disorders. *Exp. Gerontol.* **1998**, *33*, 759–772. [CrossRef]
223. Carpentieri, A.; Diaz De Barboza, G.; Areco, V.; Peralta Lopez, M.; Tolosa De Talamoni, N. New perspectives in melatonin uses. *Pharmacol. Res.* **2012**, *65*, 437–444. [CrossRef] [PubMed]

224. Lemoine, P.; Zisapel, N. Prolonged-release formulation of melatonin (Circadin) for the treatment of insomnia. *Expert Opin. Pharmacother.* **2012**, *13*, 895–905. [CrossRef] [PubMed]
225. Srinivasan, V.; Pandi-Perumal, S.R.; Trahkt, I.; Spence, D.W.; Poeggeler, B.; Hardeland, R.; Cardinali, D.P. Melatonin and melatonergic drugs on sleep: Possible mechanisms of action. *Int. J. Neurosci.* **2009**, *119*, 821–846. [CrossRef] [PubMed]
226. Vimala, P.V.; Bhutada, P.S.; Patel, F.R. Therapeutic potential of agomelatine in epilepsy and epileptic complications. *Med. Hypotheses* **2014**, *82*, 105–110. [CrossRef] [PubMed]
227. WHO (World Health Organization). Cancer Fact Sheet No. 297. Available online: https://www.google.com.hk/url?sa=t&rct=j&q=&esrc=s&source=web&cd=2&ved=0ahUKEwjT_cjhzYfTAhVIqJQKHYFWCRgQFggjMAE&url=http%3A%2F%2Fwww.afro.who.int%2Findex.php%3Foption%3Dcom_docman%26task%3Ddoc_download%26gid%3D6139&usg=AFQjCNE1HISbfHk2ijLPCzy3VxfgMAbK3Q (accessed on 20 November 2016).
228. Li, F.; Li, S.; Li, H.B.; Deng, G.F.; Ling, W.H.; Xu, X.R. Antiproliferative activities of tea and herbal infusions. *Food Funct.* **2013**, *4*, 530–538. [CrossRef] [PubMed]
229. Zheng, J.; Zhou, Y.; Li, Y.; Xu, D.P.; Li, S.; Li, H.B. Spices for prevention and treatment of cancers. *Nutrients* **2016**, *8*, 495. [CrossRef] [PubMed]
230. Zhou, Y.; Li, Y.; Zhou, T.; Zheng, J.; Li, S.; Li, H.B. Dietary natural products for prevention and treatment of liver cancer. *Nutrients* **2016**, *8*, 156. [CrossRef] [PubMed]
231. Zhou, Y.; Zheng, J.; Li, Y.; Xu, D.P.; Li, S.; Chen, Y.M.; Li, H.B. Natural polyphenols for prevention and treatment of cancer. *Nutrients* **2016**, *8*, 515. [CrossRef] [PubMed]
232. Wu, S.M.; Lin, W.Y.; Shen, C.C.; Pan, H.C.; Keh-Bin, W.; Chen, Y.C.; Jan, Y.J.; Lai, D.W.; Tang, S.C.; Tien, H.R.; et al. Melatonin set out to ER stress signaling thwarts epithelial mesenchymal transition and peritoneal dissemination via calpain-mediated C/EBPbeta and NFkappaB cleavage. *J. Pineal Res.* **2016**, *60*, 142–154. [CrossRef] [PubMed]
233. Hevia, D.; Gonzalez-Menendez, P.; Quiros-Gonzalez, I.; Miar, A.; Rodriguez-Garcia, A.; Tan, D.X.; Reiter, R.J.; Mayo, J.C.; Sainz, R.M. Melatonin uptake through glucose transporters: A new target for melatonin inhibition of cancer. *J. Pineal Res.* **2015**, *58*, 234–250. [CrossRef] [PubMed]
234. Yun, S.M.; Woo, S.H.; Oh, S.T.; Hong, S.E.; Choe, T.B.; Ye, S.K.; Kim, E.K.; Seong, M.K.; Kim, H.A.; Noh, W.C.; et al. Melatonin enhances arsenic trioxide-induced cell death via sustained upregulation of Redd1 expression in breast cancer cells. *Mol. Cell Endocrinol.* **2016**, *422*, 64–73. [CrossRef] [PubMed]
235. Borin, T.F.; Arbab, A.S.; Gelaleti, G.B.; Ferreira, L.C.; Moschetta, M.G.; Jardim-Perassi, B.V.; Iskander, A.S.; Varma, N.R.; Shankar, A.; Coimbra, V.B.; et al. Melatonin decreases breast cancer metastasis by modulating Rho-associated kinase protein-1 expression. *J. Pineal Res.* **2016**, *60*, 3–15. [CrossRef] [PubMed]
236. Ziolko, E.; Kokot, T.; Skubis, A.; Sikora, B.; Szota-Czyz, J.; Kruszniewska-Rajs, C.; Wierzgon, J.; Mazurek, U.; Grochowska-Niedworok, E.; Muc-Wierzgon, M. The profile of melatonin receptors gene expression and genes associated with their activity in colorectal cancer: A preliminary report. *J. Biol. Regul. Homeost. Agents* **2015**, *29*, 823–828. [PubMed]
237. Watanabe, M.; Kobayashi, Y.; Takahashi, N.; Kiguchi, K.; Ishizuka, B. Expression of melatonin receptor (MT1) and interaction between melatonin and estrogen in endometrial cancer cell line. *J. Obstet. Gynaecol. Res.* **2008**, *34*, 567–573. [CrossRef] [PubMed]
238. Chottanapund, S.; Van Duursen, M.B.; Navasumrit, P.; Hunsonti, P.; Timtavorn, S.; Ruchirawat, M.; Van den Berg, M. Anti-aromatase effect of resveratrol and melatonin on hormonal positive breast cancer cells co-cultured with breast adipose fibroblasts. *Toxicol. In Vitro* **2014**, *28*, 1215–1221. [CrossRef] [PubMed]
239. Sohn, E.J.; Won, G.; Lee, J.; Lee, S.; Kim, S.H. Upregulation of miRNA3195 and miRNA374b Mediates the anti-angiogenic properties of melatonin in Hypoxic PC-3 prostate cancer cells. *J. Cancer* **2015**, *6*, 19–28. [CrossRef] [PubMed]
240. Wei, J.Y.; Li, W.M.; Zhou, L.L.; Lu, Q.N.; He, W. Melatonin induces apoptosis of colorectal cancer cells through HDAC4 nuclear import mediated by CaMKII inactivation. *Philos. Trans. R. Soc. Lond. B Biol. Sci.* **2015**, *58*, 429–438. [CrossRef] [PubMed]
241. Ordonez, R.; Carbajo-Pescador, S.; Prieto-Dominguez, N.; Garcia-Palomo, A.; Gonzalez-Gallego, J.; Mauriz, J.L. Inhibition of matrix metalloproteinase-9 and nuclear factor kappa B contribute to melatonin prevention of motility and invasiveness in HepG2 liver cancer cells. *J. Pineal Res.* **2014**, *56*, 20–30. [CrossRef] [PubMed]

242. Lin, Y.W.; Lee, L.M.; Lee, W.J.; Chu, C.Y.; Tan, P.; Yang, Y.C.; Chen, W.Y.; Yang, S.F.; Hsiao, M.; Chien, M.H. Melatonin inhibits MMP-9 transactivation and renal cell carcinoma metastasis by suppressing Akt-MAPKs pathway and NF-kappaB DNA-binding activity. *J. Pineal Res.* **2016**, *60*, 277–290. [CrossRef] [PubMed]
243. Alonso-Gonzalez, C.; Gonzalez, A.; Martinez-Campa, C.; Menendez-Menendez, J.; Gomez-Arozamena, J.; Garcia-Vidal, A.; Cos, S. Melatonin enhancement of the radiosensitivity of human breast cancer cells is associated with the modulation of proteins involved in estrogen biosynthesis. *Cancer Lett.* **2016**, *370*, 145–152. [CrossRef] [PubMed]
244. Ben-David, M.A.; Elkayam, R.; Gelernter, I.; Pfeffer, R.M. Melatonin for prevention of breast radiation dermatitis: A phase II, prospective, double-blind rendomized trial. *Isr. Med. Assoc. J.* **2016**, *18*, 188–192. [PubMed]
245. Madhu, P.; Reddy, K.P.; Reddy, P.S. Role of melatonin in mitigating chemotherapy-induced testicular dysfunction in Wistar rats. *Drug Chem. Toxicol.* **2016**, *39*, 137–146. [CrossRef] [PubMed]
246. Wang, Y.M.; Jin, B.Z.; Ai, F.; Duan, C.H.; Lu, Y.Z.; Dong, T.F.; Fu, Q.L. The efficacy and safety of melatonin in concurrent chemotherapy or radiotherapy for solid tumors: A meta-analysis of randomized controlled trials. *Cancer Chemother. Pharmacol.* **2012**, *69*, 1213–1220. [CrossRef] [PubMed]
247. WHO. Cardiovascular Diseases. Available online: http://www.who.int/mediacentre/factsheets/fs317/en/ (accessed on 8 December 2016).
248. Wolf, K.; Braun, A.; Haining, E.J.; Tseng, Y.L.; Kraft, P.; Schuhmann, M.K.; Gotru, S.K.; Chen, W.; Hermanns, H.M.; Stoll, G.; et al. Partially defective store operated calcium entry and Hem(ITAM) signaling in platelets of serotonin transporter deficient Mice. *PLoS ONE* **2016**, *11*, e147664. [CrossRef] [PubMed]
249. Grossman, E.; Laudon, M.; Yalcin, R.; Zengil, H.; Peleg, E.; Sharabi, Y.; Kamari, Y.; Shen-Orr, Z.; Zisapel, N. Melatonin reduces night blood pressure in patients with nocturnal hypertension. *Am. J. Med.* **2006**, *119*, 898–902. [CrossRef] [PubMed]
250. Arangino, S.; Cagnacci, A.; Angiolucci, M.; Vacca, A.M.; Longu, G.; Volpe, A.; Melis, G.B. Effects of melatonin on vascular reactivity, catecholamine levels, and blood pressure in healthy men. *Am. J. Cardiol.* **1999**, *83*, 1417–1419. [CrossRef]
251. Wu, Q.; Jing, Y.; Yuan, X.; Zhang, X.; Li, B.; Liu, M.; Wang, B.; Li, H.; Liu, S.; Xiu, R. Melatonin treatment protects against acute spinal cord injury-induced disruption of blood spinal cord barrier in mice. *J. Mol. Neurosci.* **2014**, *54*, 714–722. [CrossRef] [PubMed]
252. Girouard, H.; Denault, C.; Chulak, C.; de Champlain, J. Treatment by *N*-acetylcysteine and melatonin increases cardiac baroreflex and improves antioxidant reserve. *Am. J. Hypertens.* **2004**, *17*, 947–954. [CrossRef] [PubMed]
253. Girouard, H.; Chulak, C.; LeJossec, M.; Lamontagne, D.; de Champlain, J. Chronic antioxidant treatment improves sympathetic functions and beta-adrenergic pathway in the spontaneously hypertensive rats. *J. Hypertens.* **2003**, *21*, 179–188. [CrossRef] [PubMed]
254. Gurses, I.; Ozeren, M.; Serin, M.; Yucel, N.; Erkal, H.S. Histopathological evaluation of melatonin as a protective agent in heart injury induced by radiation in a rat model. *Pathol. Res. Pract.* **2014**, *210*, 863–871. [CrossRef] [PubMed]
255. Yang, Y.; Fan, C.; Deng, C.; Zhao, L.; Hu, W.; Di, S.; Ma, Z.; Zhang, Y.; Qin, Z.; Jin, Z.; et al. Melatonin reverses flow shear stress-induced injury in bone marrow mesenchymal stem cells via activation of AMP-activated protein kinase signaling. *J. Pineal Res.* **2016**, *60*, 228–241. [CrossRef] [PubMed]
256. Han, D.; Huang, W.; Li, X.; Gao, L.; Su, T.; Li, X.; Ma, S.; Liu, T.; Li, C.; Chen, J.; et al. Melatonin facilitates adipose-derived mesenchymal stem cells to repair the murine infarcted heart via the SIRT1 signaling pathway. *J. Pineal Res.* **2016**, *60*, 178–192. [CrossRef] [PubMed]
257. Yang, Y.; Duan, W.; Jin, Z.; Yi, W.; Yan, J.; Zhang, S.; Wang, N.; Liang, Z.; Li, Y.; Chen, W.; et al. JAK2/STAT3 activation by melatonin attenuates the mitochondrial oxidative damage induced by myocardial ischemia/reperfusion injury. *J. Pineal Res.* **2013**, *55*, 275–286. [CrossRef] [PubMed]
258. An, R.; Zhao, L.; Xi, C.; Li, H.; Shen, G.; Liu, H.; Zhang, S.; Sun, L. Melatonin attenuates sepsis-induced cardiac dysfunction via a PI3K/Akt-dependent mechanism. *Basic Res. Cardiol.* **2016**, *111*, 8. [CrossRef] [PubMed]
259. VanKirk, T.; Powers, E.; Dowse, H.B. Melatonin increases the regularity of cardiac rhythmicity in the Drosophila heart in both wild-type and strains bearing pathogenic mutations. *J. Comp. Physiol. B* **2017**, *187*, 63–78. [CrossRef] [PubMed]

260. Dominguez-Rodriguez, A.; Abreu-Gonzalez, P.; Piccolo, R.; Galasso, G.; Reiter, R.J. Melatonin is associated with reverse remodeling after cardiac resynchronization therapy in patients with heart failure and ventricular dyssynchrony. *Int. J. Cardiol.* **2016**, *221*, 359–363. [CrossRef] [PubMed]
261. Hu, J.; Zhang, L.; Yang, Y.; Guo, Y.; Fan, Y.; Zhang, M.; Man, W.; Gao, E.; Hu, W.; Reiter, R.J.; et al. Melatonin alleviates postinfarction cardiac remodeling and dysfunction by inhibiting Mst1. *J. Pineal Res.* **2017**. [CrossRef] [PubMed]
262. WHO. Global Status Report on Noncommunicable Diseases 2014. Available online: http://www.who.int/nmh/publications/ncd-status-report-2014/en/ (accessed on 9 December 2016).
263. Simko, F.; Paulis, L. Melatonin as a potential antihypertensive treatment. *J. Pineal Res.* **2007**, *42*, 319–322. [CrossRef] [PubMed]
264. Reiter, R.J.; Tan, D.X.; Leon, J.; Kilic, U.; Kilic, E. When melatonin gets on your nerves: Its beneficial actions in experimental models of stroke. *Exp. Biol. Med.* **2005**, *230*, 104–117.
265. Hung, M.W.; Kravtsov, G.M.; Lau, C.F.; Poon, A.M.; Tipoe, G.L.; Fung, M.L. Melatonin ameliorates endothelial dysfunction, vascular inflammation, and systemic hypertension in rats with chronic intermittent hypoxia. *J. Pineal Res.* **2013**, *55*, 247–256. [CrossRef] [PubMed]
266. Qiao, Y.F.; Guo, W.J.; Li, L.; Shao, S.; Qiao, X.; Shao, J.J.; Zhang, Q.; Li, R.S.; Wang, L.H. Melatonin attenuates hypertension-induced renal injury partially through inhibiting oxidative stress in rats. *Mol. Med. Rep.* **2016**, *13*, 21–26. [CrossRef] [PubMed]
267. Pechanova, O.; Paulis, L.; Simko, F. Peripheral and central effects of melatonin on blood pressure regulation. *Int. J. Mol. Sci.* **2014**, *15*, 17920–17937. [CrossRef] [PubMed]
268. Deng, Y.Y.; Shen, F.C.; Xie, D.; Han, Q.P.; Fang, M.; Chen, C.B.; Zeng, H.K. Progress in drug treatment of cerebral edema. *Mini Rev. Med. Chem.* **2016**, *16*, 917–925. [CrossRef] [PubMed]
269. Tao, J.; Lv, J.; Li, W.; Zhang, P.; Mao, C.; Xu, Z. Exogenous melatonin reduced blood pressure in late-term ovine fetus via MT1/MT2 receptor pathways. *Reprod. Biol.* **2016**, *16*, 212–217. [CrossRef] [PubMed]
270. Butun, I.; Ekmekci, H.; Ciftci, O.; Sonmez, H.; Caner, M.; Altug, T.; Kokoglu, E. The effects of different doses of melatonin on lipid peroxidation in diet-induced hypercholesterolemic rats. *Bratisl. Lek. Listy* **2013**, *114*, 129–132. [CrossRef] [PubMed]
271. Salmanoglu, D.S.; Gurpinar, T.; Vural, K.; Ekerbicer, N.; Dariverenli, E.; Var, A. Melatonin and L-carnitin improves endothelial disfunction and oxidative stress in Type 2 diabetic rats. *Redox Biol.* **2016**, *8*, 199–204. [CrossRef] [PubMed]
272. She, M.; Hu, X.; Su, Z.; Zhang, C.; Yang, S.; Ding, L.; Laudon, M.; Yin, W. Piromelatine, a novel melatonin receptor agonist, stabilizes metabolic profiles and ameliorates insulin resistance in chronic sleep restricted rats. *Eur. J. Pharmacol.* **2014**, *727*, 60–65. [CrossRef] [PubMed]
273. World Health Organization (WHO). Global Report on Diabetes. Available online: http://www.who.int/mediacentre/factsheets/fs312/en/ (accessed on 18 December 2016).
274. Zavodnik, I.B.; Lapshina, E.A.; Cheshchevik, V.T.; Dremza, I.K.; Kujawa, J.; Zabrodskaya, S.V.; Reiter, R.J. Melatonin and succinate reduce rat liver mitochondrial dysfunction in diabetes. *J. Physiol. Pharmacol.* **2011**, *62*, 421–427. [PubMed]
275. Faria, J.A.; Kinote, A.; Ignacio-Souza, L.M.; de Araujo, T.M.; Razolli, D.S.; Doneda, D.L.; Paschoal, L.B.; Lellis-Santos, C.; Bertolini, G.L.; Velloso, L.A.; et al. Melatonin acts through MT1/MT2 receptors to activate hypothalamic Akt and suppress hepatic gluconeogenesis in rats. *Am. J. Physiol. Endocrinol. Metab.* **2013**, *305*, E230–E242. [CrossRef] [PubMed]
276. Yu, L.; Liang, H.; Dong, X.; Zhao, G.; Jin, Z.; Zhai, M.; Yang, Y.; Chen, W.; Liu, J.; Yi, W.; et al. Reduced silent information regulator 1 signaling exacerbates myocardial ischemia-reperfusion injury in type 2 diabetic rats and the protective effect of melatonin. *J. Pineal Res.* **2015**, *59*, 376–390. [CrossRef] [PubMed]
277. Costes, S.; Boss, M.; Thomas, A.P.; Matveyenko, A.V. Activation of melatonin signaling promotes beta-cell survival and function. *Mol. Endocrinol.* **2015**, *29*, 682–692. [CrossRef] [PubMed]
278. Wongchitrat, P.; Lansubsakul, N.; Kamsrijai, U.; Sae-Ung, K.; Mukda, S.; Govitrapong, P. Melatonin attenuates the high-fat diet and streptozotocin-induced reduction in rat hippocampal neurogenesis. *Neurochem. Int.* **2016**, *100*, 97–109. [CrossRef] [PubMed]
279. Yildirimturk, S.; Batu, S.; Alatli, C.; Olgac, V.; Firat, D.; Sirin, Y. The effects of supplemental melatonin administration on the healing of bone defects in streptozotocin-induced diabetic rats. *J. Appl. Oral Sci.* **2016**, *24*, 239–249. [CrossRef] [PubMed]

280. WHO. Obesity and Overweight. Available online: http://www.who.int/mediacentre/factsheets/fs311/en/ (accessed on 18 December 2016).
281. Szewczyk-Golec, K.; Wozniak, A.; Reiter, R.J. Inter-relationships of the chronobiotic, melatonin, with leptin and adiponectin: Implications for obesity. *J. Pineal Res.* **2015**, *59*, 277–291. [CrossRef] [PubMed]
282. Jimenez-Aranda, A.; Fernandez-Vazquez, G.; Campos, D.; Tassi, M.; Velasco-Perez, L.; Tan, D.X.; Reiter, R.J.; Agil, A. Melatonin induces browning of inguinal white adipose tissue in Zucker diabetic fatty rats. *J. Pineal Res.* **2013**, *55*, 416–423. [CrossRef] [PubMed]
283. Winiarska, K.; Focht, D.; Sierakowski, B.; Lewandowski, K.; Orlowska, M.; Usarek, M. NADPH oxidase inhibitor, apocynin, improves renal glutathione status in Zucker diabetic fatty rats: A comparison with melatonin. *Chem. Biol. Interact.* **2014**, *218*, 12–19. [CrossRef] [PubMed]
284. Sharabiani, M.T.; Vermeulen, R.; Scoccianti, C.; Hosnijeh, F.S.; Minelli, L.; Sacerdote, C.; Palli, D.; Krogh, V.; Tumino, R.; Chiodini, P.; et al. Immunologic profile of excessive body weight. *Biomarkers* **2011**, *16*, 243–251. [CrossRef] [PubMed]
285. Favero, G.; Stacchiotti, A.; Castrezzati, S.; Bonomini, F.; Albanese, M.; Rezzani, R.; Rodella, L.F. Melatonin reduces obesity and restores adipokine patterns and metabolism in obese (ob/ob) mice. *Nutr. Res.* **2015**, *35*, 891–900. [CrossRef] [PubMed]
286. Guo, B.; Chatterjee, S.; Li, L.; Kim, J.M.; Lee, J.; Yechoor, V.K.; Minze, L.J.; Hsueh, W.; Ma, K. The clock gene, brain and muscle Arnt-like 1, regulates adipogenesis via Wnt signaling pathway. *FASEB J.* **2012**, *26*, 3453–3463. [CrossRef] [PubMed]
287. Otway, D.T.; Mantele, S.; Bretschneider, S.; Wright, J.; Trayhurn, P.; Skene, D.J.; Robertson, M.D.; Johnston, J.D. Rhythmic diurnal gene expression in human adipose tissue from individuals who are lean, overweight, and type 2 diabetic. *Diabetes* **2011**, *60*, 1577–1581. [CrossRef] [PubMed]
288. McFadden, E.; Jones, M.E.; Schoemaker, M.J.; Ashworth, A.; Swerdlow, A.J. The relationship between obesity and exposure to light at night: Cross-sectional analyses of over 100,000 women in the Breakthrough Generations Study. *Am. J. Epidemiol.* **2014**, *180*, 245–250. [CrossRef] [PubMed]
289. Nduhirabandi, F.; Huisamen, B.; Strijdom, H.; Blackhurst, D.; Lochner, A. Short-term melatonin consumption protects the heart of obese rats independent of body weight change and visceral adiposity. *J. Pineal Res.* **2014**, *57*, 317–332. [CrossRef] [PubMed]
290. Stacchiotti, A.; Favero, G.; Giugno, L.; Lavazza, A.; Reiter, R.J.; Rodella, L.F.; Rezzani, R. Mitochondrial and metabolic dysfunction in renal convoluted tubules of obese mice: Protective role of melatonin. *PLoS ONE* **2014**, *9*, e111141. [CrossRef] [PubMed]
291. Sun, H.; Wang, X.; Chen, J.; Song, K.; Gusdon, A.M.; Li, L.; Bu, L.; Qu, S. Melatonin improves non-alcoholic fatty liver disease via MAPK-JNK/P38 signaling in high-fat-diet-induced obese mice. *Lipids Health Dis.* **2016**, *15*, 202. [CrossRef] [PubMed]
292. Sagrillo-Fagundes, L.; Assuncao Salustiano, E.M.; Yen, P.W.; Soliman, A.; Vaillancourt, C. Melatonin in pregnancy: Effects on brain development and CNS programming disorders. *Curr. Pharm. Des.* **2016**, *22*, 978–986. [CrossRef] [PubMed]
293. Ding, K.; Wang, H.; Xu, J.; Li, T.; Zhang, L.; Ding, Y.; Zhu, L.; He, J.; Zhou, M. Melatonin stimulates antioxidant enzymes and reduces oxidative stress in experimental traumatic brain injury: The Nrf2-ARE signaling pathway as a potential mechanism. *Free Radic. Biol. Med.* **2014**, *73*, 1–11. [CrossRef] [PubMed]
294. Yang, Y.; Jiang, S.; Dong, Y.; Fan, C.; Zhao, L.; Yang, X.; Li, J.; Di, S.; Yue, L.; Liang, G.; et al. Melatonin prevents cell death and mitochondrial dysfunction via a SIRT1-dependent mechanism during ischemic-stroke in mice. *J. Pineal Res.* **2015**, *58*, 61–70. [CrossRef] [PubMed]
295. Chen, J.; Chen, G.; Li, J.; Qian, C.; Mo, H.; Gu, C.; Yan, F.; Yan, W.; Wang, L. Melatonin attenuates inflammatory response-induced brain edema in early brain injury following a subarachnoid hemorrhage: A possible role for the regulation of pro-inflammatory cytokines. *J. Pineal Res.* **2014**, *57*, 340–347. [CrossRef] [PubMed]
296. Lee, E.J.; Lee, M.Y.; Chen, H.Y.; Hsu, Y.S.; Wu, T.S.; Chen, S.T.; Chang, G.L. Melatonin attenuates gray and white matter damage in a mouse model of transient focal cerebral ischemia. *J. Pineal Res.* **2005**, *38*, 42–52. [CrossRef] [PubMed]
297. Pazar, A.; Kolgazi, M.; Memisoglu, A.; Bahadir, E.; Sirvanci, S.; Yaman, A.; Yegen, B.C.; Ozek, E. The neuroprotective and anti-apoptotic effects of melatonin on hemolytic hyperbilirubinemia-induced oxidative brain damage. *J. Pineal Res.* **2016**, *60*, 74–83. [CrossRef] [PubMed]

298. Keskin, I.; Kaplan, S.; Kalkan, S.; Sutcu, M.; Ulkay, M.B.; Esener, O.B. Evaluation of neuroprotection by melatonin against adverse effects of prenatal exposure to a nonsteroidal anti-inflammatory drug during peripheral nerve development. *Int. J. Dev. Neurosci.* **2015**, *41*, 1–7. [CrossRef] [PubMed]
299. Aranda, M.L.; Fleitas, M.F.G.; De Laurentiis, A.; Sarmiento, M.I.K.; Chianelli, M.; Sande, P.H.; Dorfman, D.; Rosenstein, R.E. Neuroprotective effect of melatonin in experimental optic neuritis in rats. *J. Pineal Res.* **2016**, *60*, 360–372. [CrossRef] [PubMed]
300. Willis, G.L. Parkinson's disease as a neuroendocrine disorder of circadian function: Dopamine-melatonin imbalance and the visual system in the genesis and progression of the degenerative process. *Rev. Neurosci.* **2008**, *19*, 245–316. [CrossRef] [PubMed]
301. Zhang, S.; Wang, P.; Ren, L.; Hu, C.; Bi, J. Protective effect of melatonin on soluble Abeta1–42-induced memory impairment, astrogliosis, and synaptic dysfunction via the Musashi1/Notch1/Hes1 signaling pathway in the rat hippocampus. *Alzheimers Res. Ther.* **2016**, *8*, 40. [CrossRef] [PubMed]
302. Breen, D.P.; Nombela, C.; Vuono, R.; Jones, P.S.; Fisher, K.; Burn, D.J.; Brooks, D.J.; Reddy, A.B.; Rowe, J.B.; Barker, R.A. Hypothalamic volume loss is associated with reduced melatonin output in Parkinson's disease. *Mov. Disord.* **2016**, *31*, 1062–1066. [CrossRef] [PubMed]
303. Sun, X.; Ran, D.; Zhao, X.; Huang, Y.; Long, S.; Liang, F.; Guo, W.; Nucifora, F.C., Jr.; Gu, H.; Lu, X.; et al. Melatonin attenuates hLRRK2-induced sleep disturbances and synaptic dysfunction in a Drosophila model of Parkinson's disease. *Mol. Med. Rep.* **2016**, *13*, 3936–3944. [CrossRef] [PubMed]
304. Cardinali, D.P.; Vigo, D.E.; Olivar, N.; Vidal, M.F.; Furio, A.M.; Brusco, L.I. Therapeutic application of melatonin in mild cognitive impairment. *Am. J. Neurodegener. Dis.* **2012**, *1*, 280–291. [PubMed]
305. Mukda, S.; Panmanee, J.; Boontem, P.; Govitrapong, P. Melatonin administration reverses the alteration of amyloid precursor protein-cleaving secretases expression in aged mouse hippocampus. *Neurosci. Lett.* **2016**, *621*, 39–46. [CrossRef] [PubMed]
306. Waseem, M.; Tabassum, H.; Parvez, S. Neuroprotective effects of melatonin as evidenced by abrogation of oxaliplatin induced behavioral alterations, mitochondrial dysfunction and neurotoxicity in rat brain. *Mitochondrion* **2016**, *30*, 168–176. [CrossRef] [PubMed]
307. Li, J.G.; Zhang, G.W.; Meng, Z.Z.; Wang, L.Z.; Liu, H.Y.; Liu, Q.; Buren, B. Neuroprotective effect of acute melatonin treatment on hippocampal neurons against irradiation by inhibition of caspase-3. *Exp. Ther. Med.* **2016**, *11*, 2385–2390. [CrossRef] [PubMed]
308. Koc, G.E.; Kaplan, S.; Altun, G.; Gumus, H.; Deniz, O.G.; Aydin, I.; Onger, M.E.; Altunkaynak, Z. Neuroprotective effects of melatonin and omega-3 on hippocampal cells prenatally exposed to 900 MHz electromagnetic fields. *Int. J. Radiat. Biol.* **2016**, *92*, 590–595.
309. Letra-Vilela, R.; Sanchez-Sanchez, A.M.; Rocha, A.M.; Martin, V.; Branco-Santos, J.; Puente-Moncada, N.; Santa-Marta, M.; Outeiro, T.F.; Antolin, I.; Rodriguez, C.; et al. Distinct roles of *N*-acetyl and 5-methoxy groups in the antiproliferative and neuroprotective effects of melatonin. *Mol. Cell Endocrinol.* **2016**, *434*, 238–249. [CrossRef] [PubMed]
310. Acuna-Castroviejo, D.; Escames, G.; Venegas, C.; Diaz-Casado, M.E.; Lima-Cabello, E.; Lopez, L.C.; Rosales-Corral, S.; Tan, D.X.; Reiter, R.J. Extrapineal melatonin: Sources, regulation, and potential functions. *Cell Mol. Life Sci.* **2014**, *71*, 2997–3025. [CrossRef] [PubMed]
311. Tresguerres, I.F.; Tamimi, F.; Eimar, H.; Barralet, J.E.; Prieto, S.; Torres, J.; Calvo-Guirado, J.L.; Tresguerres, J.A. Melatonin dietary supplement as an anti-aging therapy for age-related bone loss. *Rejuvenation Res.* **2014**, *17*, 341–346. [CrossRef] [PubMed]
312. Hibaoui, Y.; Reutenauer-Patte, J.; Patthey-Vuadens, O.; Ruegg, U.T.; Dorchies, O.M. Melatonin improves muscle function of the dystrophic mdx5Cv mouse, a model for Duchenne muscular dystrophy. *J. Pineal Res.* **2011**, *51*, 163–171. [CrossRef] [PubMed]
313. Shin, I.S.; Park, J.W.; Shin, N.R.; Jeon, C.M.; Kwon, O.K.; Lee, M.Y.; Kim, H.S.; Kim, J.C.; Oh, S.R.; Ahn, K.S. Melatonin inhibits MUC5AC production via suppression of MAPK signaling in human airway epithelial cells. *J. Pineal Res.* **2014**, *56*, 398–407. [CrossRef] [PubMed]
314. Sehajpal, J.; Kaur, T.; Bhatti, R.; Singh, A.P. Role of progesterone in melatonin-mediated protection against acute kidney injury. *J. Surg. Res.* **2014**, *191*, 441–447. [CrossRef] [PubMed]
315. Elbe, H.; Vardi, N.; Esrefoglu, M.; Ates, B.; Yologlu, S.; Taskapan, C. Amelioration of streptozotocin-induced diabetic nephropathy by melatonin, quercetin, and resveratrol in rats. *Hum. Exp. Toxicol.* **2015**, *34*, 100–113. [CrossRef] [PubMed]

316. Bai, X.Z.; He, T.; Gao, J.X.; Liu, Y.; Liu, J.Q.; Han, S.C.; Li, Y.; Shi, J.H.; Han, J.T.; Tao, K.; et al. Melatonin prevents acute kidney injury in severely burned rats via the activation of SIRT1. *Sci. Rep.* **2016**, *6*, 32199. [CrossRef] [PubMed]
317. Zhao, J.; Young, Y.K.; Fradette, J.; Eliopoulos, N. Melatonin pretreatment of human adipose tissue-derived mesenchymal stromal cells enhances their prosurvival and protective effects on human kidney cells. *Am. J. Physiol. Ren. Physiol.* **2015**, *308*, F1474–F1483. [CrossRef] [PubMed]
318. Wierrani, F.; Grin, W.; Hlawka, B.; Kroiss, A.; Grunberger, W. Elevated serum melatonin levels during human late pregnancy and labour. *J. Obstet. Gynaecol.* **1997**, *17*, 449–451. [CrossRef] [PubMed]
319. Takayama, H.; Nakamura, Y.; Tamura, H.; Yamagata, Y.; Harada, A.; Nakata, M.; Sugino, N.; Kato, H. Pineal gland (melatonin) affects the parturition time, but not luteal function and fetal growth, in pregnant rats. *Endocr. J.* **2003**, *50*, 37–43. [CrossRef] [PubMed]
320. Tola, E.N.; Mungan, M.T.; Uguz, A.C.; Naziroglu, M. Intracellular Ca^{2+} and antioxidant values induced positive effect on fertilisation ratio and oocyte quality of granulosa cells in patients undergoing in vitro fertilisation. *Reprod. Fertil. Dev.* **2013**, *25*, 746–752. [CrossRef] [PubMed]
321. Bromfield, E.G.; Aitken, R.J.; Anderson, A.L.; McLaughlin, E.A.; Nixon, B. The impact of oxidative stress on chaperone-mediated human sperm-egg interaction. *Hum. Reprod.* **2015**, *30*, 2597–2613. [CrossRef] [PubMed]
322. Kose, O.; Arabaci, T.; Kara, A.; Yemenoglu, H.; Kermen, E.; Kizildag, A.; Gedikli, S.; Ozkanlar, S. Effects of melatonin on oxidative stress index and Alveolar bone loss in diabetic rats with periodontitis. *J. Periodontol.* **2016**, *87*, e82–e90. [CrossRef] [PubMed]
323. Arabaci, T.; Kermen, E.; Ozkanlar, S.; Kose, O.; Kara, A.; Kizildag, A.; Duman, S.B.; Ibisoglu, E. Therapeutic effects of melatonin on alveolar bone resorption after experimental periodontitis in rats: A biochemical and immunohistochemical study. *J. Periodontol.* **2015**, *86*, 874–881. [CrossRef] [PubMed]
324. Hardeland, R. Melatonin and the theories of aging: A critical appraisal of melatonin's role in antiaging mechanisms. *J. Pineal Res.* **2013**, *55*, 325–356. [CrossRef] [PubMed]
325. Wahab, M.H.; Akoul, E.S.; Abdel-Aziz, A.A. Modulatory effects of melatonin and vitamin E on doxorubicin-induced cardiotoxicity in Ehrlich ascites carcinoma-bearing mice. *Tumori* **2000**, *86*, 157–162. [PubMed]
326. Andersen, L.P.; Rosenberg, J.; Gogenur, I. Perioperative melatonin: Not ready for prime time. *Br. J. Anaesth.* **2014**, *112*, 7–8. [CrossRef] [PubMed]
327. Seabra, M.L.; Bignotto, M.; Pinto, L.R., Jr.; Tufik, S. Randomized, double-blind clinical trial, controlled with placebo, of the toxicology of chronic melatonin treatment. *J. Pineal Res.* **2000**, *29*, 193–200. [CrossRef] [PubMed]
328. Jahnke, G.; Marr, M.; Myers, C.; Wilson, R.; Travlos, G.; Price, C. Maternal and developmental toxicity evaluation of melatonin administered orally to pregnant Sprague-Dawley rats. *Toxicol. Sci.* **1999**, *50*, 271–279. [CrossRef] [PubMed]
329. Wright, B.; Sims, D.; Smart, S.; Alwazeer, A.; Alderson-Day, B.; Allgar, V.; Whitton, C.; Tomlinson, H.; Bennett, S.; Jardine, J.; et al. Melatonin versus placebo in children with autism spectrum conditions and severe sleep problems not amenable to behaviour management strategies: A randomised controlled crossover trial. *J. Autism Dev. Disord.* **2011**, *41*, 175–184. [CrossRef] [PubMed]
330. Gringras, P.; Gamble, C.; Jones, A.P.; Wiggs, L.; Williamson, P.R.; Sutcliffe, A.; Montgomery, P.; Whitehouse, W.P.; Choonara, I.; Allport, T.; et al. Melatonin for sleep problems in children with neurodevelopmental disorders: Randomised double masked placebo controlled trial. *BMJ* **2012**, *345*, e6664. [CrossRef] [PubMed]
331. Holliman, B.J.; Chyka, P.A. Problems in assessment of acute melatonin overdose. *South. Med. J.* **1997**, *90*, 451–453. [CrossRef] [PubMed]
332. Gitto, E.; Aversa, S.; Salpietro, C.D.; Barberi, I.; Arrigo, T.; Trimarchi, G.; Reiter, R.J.; Pellegrino, S. Pain in neonatal intensive care: Role of melatonin as an analgesic antioxidant. *J. Pineal Res.* **2012**, *52*, 291–295. [CrossRef] [PubMed]
333. Gitto, E.; Karbownik, M.; Reiter, R.J.; Tan, D.X.; Cuzzocrea, S.; Chiurazzi, P.; Cordaro, S.; Corona, G.; Trimarchi, G.; Barberi, I. Effects of melatonin treatment in septic newborns. *Pediatr. Res.* **2001**, *50*, 756–760. [CrossRef] [PubMed]

334. Gitto, E.; Romeo, C.; Reiter, R.J.; Impellizzeri, P.; Pesce, S.; Basile, M.; Antonuccio, P.; Trimarchi, G.; Gentile, C.; Barberi, I.; et al. Melatonin reduces oxidative stress in surgical neonates. *J. Pediatr. Surg.* **2004**, *39*, 184–189. [CrossRef] [PubMed]
335. Gitto, E.; Reiter, R.J.; Amodio, A.; Romeo, C.; Cuzzocrea, E.; Sabatino, G.; Buonocore, G.; Cordaro, V.; Trimarchi, G.; Barberi, I. Early indicators of chronic lung disease in preterm infants with respiratory distress syndrome and their inhibition by melatonin. *J. Pineal Res.* **2004**, *36*, 250–255. [CrossRef] [PubMed]
336. Acil, M.; Basgul, E.; Celiker, V.; Karagoz, A.H.; Demir, B.; Aypar, U. Perioperative effects of melatonin and midazolam premedication on sedation, orientation, anxiety scores and psychomotor performance. *Eur. J. Anaesthesiol.* **2004**, *21*, 553–557. [CrossRef] [PubMed]
337. Naguib, M.; Samarkandi, A.H. The comparative dose-response effects of melatonin and midazolam for premedication of adult patients: A double-blinded, placebo-controlled study. *Anesth. Analg.* **2000**, *91*, 473–479. [PubMed]
338. Edmonds, K.E.; Stetson, M.H. Pineal gland and melatonin affect testicular status in the adult marsh rice rat (*Oryzomys palustris*). *Gen. Comp. Endocrinol.* **1995**, *99*, 265–274. [CrossRef] [PubMed]
339. Kennaway, D.J.; Rowe, S.A. Controlled-release melatonin implants delay puberty in rats without altering melatonin rhythmicity. *J. Pineal Res.* **1997**, *22*, 107–116. [CrossRef] [PubMed]
340. Kelestimur, H.; Ozcan, M.; Kacar, E.; Alcin, E.; Yilmaz, B.; Ayar, A. Melatonin elicits protein kinase C-mediated calcium response in immortalized GT1–7 GnRH neurons. *Brain Res.* **2012**, *1435*, 24–28. [CrossRef] [PubMed]

nutrients

MDPI

Article

Improvement of Antioxidant Defences and Mood Status by Oral GABA Tea Administration in a Mouse Model of Post-Stroke Depression

Maria Daglia [1,*], Arianna Di Lorenzo [1,2], Seyed Fazel Nabavi [3], Antoni Sureda [4], Sedigheh Khanjani [5], Akbar Hajizadeh Moghaddam [6], Nady Braidy [7,8] and Seyed Mohammad Nabavi [3,*]

1 Department of Drug Sciences, Medicinal Chemistry and Pharmaceutical Technology Section, Pavia University, VialeTaramelli 12, 27100 Pavia, Italy; arianna.dilorenzo01@universitadipavia.it
2 KOLINPHARMA S.p.A., Lainate, Corso Europa 5, 20020 Lainate (MI), Italy
3 Applied Biotechnology Research Center, Baqiyatallah University of Medical Sciences, P.O. Box 19395-5487, Tehran 19395-5487, Iran; Nabavisf@gmail.com
4 Grup de Nutrició Comunitària i Estrès Oxidatiu and CIBEROBN (Physiopathology of Obesity and Nutrition), Universitat de les Illes Balears, Palma de E-07122 Mallorca, Spain; tosugo@hotmail.com
5 Department of Physiology, Faculty of Biological Sciences, Shahid Behshti University, P.O. Box 19615-1178, Tehran 19615-1178, Iran; S.khanjani66@yahoo.com
6 Department of Biology, Faculty of Basic Sciences, University of Mazandaran, 47416-95447 Babolsar, Iran; a.hajizadeh@umz.ac.ir
7 Centre for Healthy Brain Ageing, School of Psychiatry, University of New South Wales, Sydney, NSW 2052, Australia; n.braidy@unsw.edu.au
8 CHeBA NPI, Euroa Centre, Prince of Wales Hospital, Barker Street, Randwick, NSW 2031, Australia
* Correspondence: maria.daglia@unipv.it (M.D.); nabavi208@gmail.com (S.M.N.); Tel.: +39-03-8298-7388 (M.D.)

Received: 26 February 2017; Accepted: 24 April 2017; Published: 29 April 2017

Abstract: Green GABA (GGABA) and Oolong GABA (OGABA) teas are relatively new varieties of tea, whose chemical composition and functional properties are largely under-studied, despite their promising health capacities. Post stroke depression (PSD) is a complication of stroke with high clinical relevance, yielding increasing mortality and morbidity rates, and a lower response to common therapies and rehabilitation. Methods: Two chemically characterized commercial samples of GGABA and OGABA were investigated for effects on mood following oral administration using a mouse model of PSD, through common validated tests including the Despair Swimming Test and Tail Suspension Test. Moreover, the antioxidant activity of GGABA and OGABA was evaluated by determining the levels of lipid peroxidation products and the activity of antioxidant enzymes in the mouse brain in vivo. Results: GGABA and OGABA attenuated depressed mood by influencing behavioral parameters linked to depression. GGABA was more active than OGABA in this study, and this effect may be likely due to a higher content of polyphenolic substances and amino acids in GGABA compared to OGABA. GGABA also exerted a greater antioxidant activity. Conclusions: Our data suggests that GABA tea is a promising candidate that can be used as an adjuvant in the management of PSD.

Keywords: GABA green tea; GABA oolong tea; post-stroke depression; antioxidant activity

1. Introduction

Stroke is a cerebrovascular event affecting one in 400 people each year worldwide. It represents the second leading cause of mortality, and one of the most common causes of long-term disability [1].

According to brain imaging studies, two different types of stroke can be recognized: ischemic stroke, which accounts for more than 80% of all cases and results from vessel occlusion due to thrombosis, embolysism or systemic hypoperfusion, and hemorrhagic stroke, caused by vessel rupture [2]. Known complications of stroke of high clinical relevance, due to their frequency and impact on both cognitive and physical outcomes for patients, include neuropsychiatric disorders in general and depression in particular. Post-stroke depression (PSD) affects one third of patients, manifesting between 4 weeks to 1 year after the cerebrovascular event, influencing mortality and morbidity rates, and reducing the effect of common therapies and rehabilitation [3]. Patients who develop PSD have significantly higher mortality rates than similarly impaired stroke patients who do not experience mood disorders [4–6]. The common therapeutic approach for the treatment of PSD is based on treatment with antidepressants, which appear to be efficient adjuvants towards reaching partial or full recovery and independence. On the other hand, antidepressants may cause various and serious adverse effects, especially in the elderly, which may lead to the suspension of treatment, compromising the healing process.

Oxidative stress, defined as an imbalance between oxidant agents and endogenous and exogenous antioxidant defenses, plays a pivotal role in the development of ischemic damage, since it mainly occurs during the post-ischemic reperfusion stage. Many studies have identified potential peripheral biomarkers of oxidative stress in the biological fluids of stroke patients (i.e., blood, urine and cerebrospinal fluid). These biomarkers are mainly products of oxidative damage, which are not to be confused with reactive oxygen species (ROS). The latter are not suitable biomarkers due to their short half-life and high reactivity. For example, decreases in vitamin C and increases in thiobarbituric-reactive substances (TBARS) have been measured 2 days following the onset of stroke [7]. Another study highlights increased levels of malondialdehyde (MDA) and hydroxynonenal (HNE), two main products of lipid peroxidation, in ischemic stroke patients compared with healthy subjects [8]. Plasma levels of vitamin E, vitamin A, and uric acid were also reported to be lower in patients with ischemic stroke [9,10]. Taken together, this evidence highlights the clinical relevance of oxidative damage in the pathophysiology of ischemic stroke.

A series of environmental, genetic, and medical factors can promote oxidative and nitrosative stress in depressed patient brain, which, in turn, stimulates the production of pro-inflammatory cytokines leading to neuro-inflammation. Both oxidative and nitrosative stress and neuro-inflammation can affect the development of depressive symptoms and promote cellular damages and dysfunctions, which might contribute to depressive symptoms and to the decrease of neurogenesis and neuroplasticity, promoting neuronal apoptosis. Moreover, the cellular damages can stimulate autoimmune and inflammatory pathways, which could lead to an increase of oxidative and nitrosative stress itself, reinforcing depressogenic effects [11].

An imbalance between oxidative stress biomarkers and antioxidants has also been identified in patients with depression. Several enzymes related to the production and cleavage of ROS, such as xanthine oxidase, superoxide dismutase (SOD), catalase and glutathione peroxidase, have been found to be lower in the blood of depressed patients when compared with non-depressed controls [12–14]. Higher serum levels of 8-hydroxy-2′-deoxyguanosine (a marker of oxidative DNA damage) and lower plasma levels of vitamins C and E have been found in depressed patients than in healthy subjects [15,16].

A growing body of evidence suggests that (i) oxidative stress could be recognized as an important pathophysiological agent common to both stroke and depression, and (ii) polyphenols and secondary plant metabolites may exert protective activity against oxidative stress in both stroke and depression. Our research group put forward the hypothesis that polyphenols could have a positive role in the management of post-stroke depression on the basis of their antioxidant properties [17–19].

Green and GABA green tea, are new types of tea with high levels of γ-aminobutyric acid which accumulate in tea leaves due to anaerobic fermentation under a nitrogen atmosphere [20]. The efficacy of both these tea beverages against PSD was subsequently demonstrated by our research group [21]. Furthermore, we have demonstrated that green tea and GABA green tea, administered

intraperitoneally for one week at two different doses (50 mg/kg and 100 mg/kg) to experimental animals with induced PSD, are able to restore parameters linked to behavior, assessed through three common validated tests (i.e., the Despair Swimming Test -DST-, Tail Suspension Test -TST- and Open Field Test -OFT-). Moreover, both teas exerted an in vivo antioxidant effect, and were able to reduce the levels of lipid peroxidation products and to increase endogenous antioxidant defenses (i.e., SOD and catalase activities and GSH levels). Intraperitoneal administration is not a treatment representative of regular tea consumption, but was used to bypass gastroduodenal digestion, which induces significant changes in phytochemical composition [22]. Our data provides the first evidence of the in vivo antioxidant and antidepressive-like activities of green and GABA green tea, as well as their first exhaustive phytochemical profile. Since GABA green tea was found to be more active than common green tea, especially with regards to behavioral parameters, we have focused our attention on this particular type of tea. Thus, the aim of this study was to investigate the effects of orally administered, chemically characterized GABA green tea (GGABA) and GABA oolong tea (OGABA) extracts on the antioxidant and mood status on a mouse model of PSD.

2. Materials and Methods

2.1. Chemicals and Reagents

GABA green tea and GABA oolong tea were purchased from an Italian specialist tea shop (La Teiera Eclettica, Milan, Italy). Gallic acid, epigallocatechin-gallate, epicatechin-gallate, theanine, glutamic acid and glutamine were obtained from PhytolabGmbH and Co., KG (Vestenbergsgreuth, Germany). Bovine serum albumin and a kit for protein determination were purchased from ZiestChem Company (Tehran, Iran). In addition, 5,5-dithiobis(2-nitrobenzoic acid), ethylenediaminetetraacetic acid, nitro blue tetrazolium chloride, potassium dihydrogen phosphate, reduced glutathione, sodium dihydrogen phosphate, trichloroacetic acid, thiobarbituric acid, hydrogen peroxide, sodium carbonate, hydroxylamine chloride, ketamine, lidocaine, xylazine, FolinCiocalteau's reagent, LC/MS-grade methanol and acetonitrile, formic acid solution 1 M, caffeine, epicatechin, catechin, sodium acetate, trimethylamine, tetrahydrofuran, ortho-phthalaldehyde, fluorenylmethylchloroformate were purchased from Sigma-Aldrich Chemical Company (St. Louis, MO, USA). Other chemical reagents and solvents were purchased from Merck Chemical Company, Darmstadt, Germany.

2.2. Preparation of GABA Tea Extracts

GABA tea extracts were prepared as recommended by the supplier, under conditions commonly used for the infusion of tea. The aqueous extract was taken from a suspension containing 25 g of dried leaves in 500 mL of mineral water, whose mineral composition and content are reported in Table 1, at 85 °C for 2 min. After infusion the suspension was cooled at room temperature and filtered through a paper filter under vacuum. The aqueous extracts were submitted to centrifugation at 8000 rpm at room temperature for 10 min and the supernatant was filtered through a cellulose acetate/cellulose nitrate mixed esters membrane (0.45 μm; Millipore Corporation, Billerica, MA, USA). The extracts were subdivided into different aliquots and freeze-dried in order to be submitted to qualitative and quantitative analyses and pharmacological evaluation.

Table 1. Composition of water utilized for tea infusion, expressed as mg of anion or cation dissolved in 1 L of water.

Anions/Cations	mg/L
HCO_3^-	7.5
F^-	<0.1
NO_3^-	1.1
SO_4^{2-}	3.8
Ca^{2+}	2.4
Na^+	1.7
Total dissolved solids	23.8

2.3. Total Polyphenol Content

The total polyphenol content of both tea extracts was evaluated using the Folin-Ciocalteu's method, with gallic acid used as standard [21]. In brief, 0.5 mL of Folin Ciocalteau's reagent was added to 0.1 mL of each tea extract at a concentration of 1 mg/mL in water. After mixing, 2 mL of 15% Na_2CO_3 were added and the volume was brought up to 10 mL with Millipore-grade water. After mixing, the samples were kept in the dark for 2 h. After the reaction period, the absorbance was measured at 750 nm. Each tea sample was analyzed in triplicate and the concentration of total polyphenols was determined in terms of gallic acid equivalents (GAE), according to the following calibration curve: Absorbance (Abs) = 0.0017 concentration (μg/mL) + 0.0598 (R^2 = 0.9984), obtained from analyses of gallic acid solutions ranging from 10 to 500 μg/mL.

2.4. RP-HPLC-PDA-ESI-MS^n Analysis

RP-HPLC-PDA-ESI-MS^n analysis was performed using a Thermo Finnigan Surveyor Plus HPLC, equipped with a quaternary pump, a Surveyor UV-Vis diode array detector, and a LCQ Advantage Max ion trap mass spectrometer (Thermo Fisher Scientific, Waltham, MA, USA), connected through an ESI source. A Zorbax Eclipse XDB-C18 column (150 × 4.6 mm, 5 μm), equipped with a Hypersil Gold C18 precolumn (10 × 2.1 mm, 5 μm), both from Agilent (Waldbronn, Germany), was used. The mobile phase contained water acidified with 0.1% formic acid (eluent A) and methanol (eluent B), and was eluted in a gradient as follows: from 10 to 70% B in 84 min, from 70% to 80% B in 5 min, from 80% to 100% B in 10 min, followed by a 5 min isocratic run of 100% B. Total run time was 105 min, including column reconditioning. The flow rate was maintained at 0.3 mL/min, the autosampler and column temperatures were maintained at 4 and 25 °C, respectively. Tea extracts were analyzed at a concentration of 5 mg/mL in water and 5 μL of the solution was injected into the chromatographic system. Chromatograms were registered at 210, 254, and 280 nm; spectral data were collected in the range of 200–800 nm for all peaks.

HPLC-ESI-MS^n data were acquired under positive and negative ionization modes, using Xcalibur software. To achieve this, the ion trap operated in full scan (100–2000 m/z), data-dependent scan and MS^n modes. To obtain MS^2 data, a 35% collision energy and an isolation width of 2 m/z were applied. A preliminary experiment was performed to optimize MS operating conditions: 5 μg/mL caffeine (0.1% formic acid and methanol, 50:50, % v/v) and 10 μg/mL (±)-catechin (0.1% formic acid and methanol, 50:50, % v/v) solutions were directly infused through the ESI interface at a flow rate of 25 μL/min into the mass spectrometer. The optimum conditions for the assay were the following: sheath gas 60, capillary temperature 220 °C, spray voltage 4.5, auxiliary gas 25 and 20, capillary voltage—47.20 V for the negative and 5 V for the positive ionization modes.

2.5. RP-HPLC-PDA Analysis

The quantification of caffeine and flavan-3-ols in tea samples was performed through a RP-HPLC-PDA method developed and validated on a 1100 Agilent HPLC system (Agilent, Waldbronn, Germany) equipped with a gradient quaternary pump and a diode array detector. Agilent Chemstation

software was used for HPLC system control and data processing. Separation was achieved on a Zorbax Eclipse XDB-C18 column (150 × 4.6 mm, 5 μm), equipped with a Hypersil Gold C18 (10 × 2.1 mm, 5 μm) precolumn, both from Agilent (Waldbronn, Germany). The mobile phase consisted of water acidified with 0.1% formic acid (eluent A) and methanol (eluent B) and was eluted in a gradient as follows: from 10 to 70% B in 84 min, from 70 to 80% B in 5 min, from 80 to 100% B in 10 min, followed by a 5 min isocratic run of 100% B. Total run time was 105 min, including column reconditioning. The flow rate was maintained at 0.5 mL/min, the autosampler and column temperatures were maintained at 4 and 25 °C respectively, and the injection volume was 5 μL. Spectral data were acquired between 190 and 600 nm for all peaks, while chromatograms were registered at 210, 254 and 280 nm. Caffeine, epicatechin (EC), catechin (C), epicatechin-3-gallate (ECG), epigallocatechin-3-gallate (EGCG) and gallic acid (GA) were identified by comparing their retention time and UV-Vis spectrum with that of commercial standards.

2.6. RP-HPLC-PDA Method Validation

Validation of the analytical method was performed following ICH guidelines [23]. Stock solutions of selected analytes (500 μg/mL) were prepared by dissolving 5 mg of each in 10 mL of 0.1% formic acid and methanol (50:50, % *v*/*v*) and stored at 4 °C until assay. A series of working solutions for GA and EC (7, 10, 25, 50, 100, 250, 300, 400 μg/mL) and for EGCG, ECG, caffeine and catechin (10, 25, 50, 100, 250, 300, 400 μg/mL) were prepared by diluting the stock solution with 0.1% formic acid and methanol (50:50, % *v*/*v*).

Linearity was determined through the external standard method: for each compound, eight solutions at different concentrations, ranging from 25 to 500 μg/mL for catechin, from 7 to 500 μg/mL for GA and EC, and from 10 to 500 μg/mL for EGCG, ECG and caffeine, were analyzed in triplicate. The calibration curve for each analyte was obtained by plotting the mean peak areas (y) versus their nominal concentrations (x). Calibration curves (slope and intercept) and correlation coefficient (R^2) were calculated as regression parameters by linear regression.

The accuracy of this method was measured through a recovery assay, where spiked tea samples were analyzed at the same concentration levels as the standard concentrations. The study was performed in triplicate, and accuracy expressed as a percentage of the amount recovered compared to that from standard concentrations. Both intra-day (repeatability) and inter-day (intermediate precision) measurements were taken. Repeatability was investigated analyzing spiked tea samples in triplicate using three levels of concentration, corresponding to 25%, 50% and 100% of analytes. Intermediate precision was established using newly prepared solutions, using the same concentration levels as the repeatability study, over two successive days. Results are expressed as the relative standard deviation percentage of the measurements (RSD %). The sensibility of the method was evaluated as the limit of quantification (LOQ) and limit of detection (LOD). The LOD and LOQ were estimated using calibration curves calculated during the validation procedure, from which the average of the slope (S) and the standard deviation of the intercept (δ) were calculated. LOD and LOQ were obtained as follows: LOD = 3.3 δ/S, LOQ = 10 δ/S.

2.7. Determination of Glutamic Acid, Glutamine, γ-Amino Butyric Acid and Theanine

Amino acid analysis was performed as previously reported by Di Lorenzo et al. [21]. In detail, the analysis was performed using a Jasco X-LC system equipped with a 3159AS autosampler, 3185PU Xtreme high pressure pumps, a 3080DG degasser, a CO2060Plus column oven compartment, and a 3020FP fluorescence detector connected to a HP ProDesk G1 400 MT processor, Intel Core i5. Separation was achieved on Hypersil ODS (250 × 2.1 mm, 5 μm) thermostated at 40 °C. The mobile phase consisted of a solution of sodium acetate (20 mM), triethylamine (TEA, 0.018%–*v*/*v*) and tetrahydrofuran (THF, 0.3%–*v*/*v*), at pH 7.2 (eluent A) and an aqueous solution of sodium acetate (100 mM), methanol (40%) and acetonitrile (40%), at pH 7.2 (eluent B). The elution was performed in 17 min, using a gradient between 1 and 60% B, at a flow rate of 0.45 mL/min with an injection volume of 1 μL. The tea samples

underwent gas-phase hydrolysis with HCL 6M prior to amino acid analysis. Hydrolysis was performed in glass sterilized tubes at 110 °C for 24 h under a nitrogen atmosphere. Free amino acids were then derivatized by ortho-phthalaldehyde (OPA) and fluorenylmethylchloroformate (FMOC) leading to the formation of derivatives from primary amino acids and secondary amino acids respectively. Derivatization was performed according to the Jasco autosampler program, preparing a mixture of sample:OPA:FMOC at a 1:1:1 ratio at room temperature (OPA and FMOC are CPS products). The derivatives were detected with a fluorometric detector (emission λ = 456 nm–excitation λ = 342 nm for OPA derivatives and emission λ = 272 nm–excitation λ = 312 nm for FMOC derivatives). Amino acid identification was performed via elution times of the obtained derivatives and compared to a mixture of standard amino acids submitted to derivation in identical test conditions.

2.8. Animals

Male balb/c mice (5 weeks old, weighing between 20–25 g), were bought from the amol branch of the Pasteur Institute of Iran. All animals were kept in an appropriate room at 24 ± 2 °C under a light/dark 12/12 h cycle and 60% ± 5% humidity. Food and water were supplied ad libitum. The mice were acclimated to the test room for at least 24 h before the behavioral assay. In this study, behavioral examination was performed between 10.00 and 14.00 h. The animal experiments were processed following internationally accepted ethical guidelines for the care of laboratory animals in accordance with Principles of Laboratory Animals Care (NIH Publication No. 85-23, revised 1996). The ethical approval number is "81/021, 10 July 2002".

2.9. Induction of Stroke

Ischemic stroke was induced in the mice after anesthesia with ketamine (60 mg/kg i.p.) and xylazine (5 mg/kg i.p.). Bilateral occlusion of the common carotid artery (BCCAO) was done according to standard experimental animal procedure for ischemic stroke. Briefly, the right and left carotid arteries were located and held over 5 min with vascular clamps (time under ischemia). Subsequently, the vascular clamps were removed for the following 10 min (time of reperfusion), and both carotid arteries were again restrained for 5 min. Finally, the vascular clamps were removed in order to allow the blood circulation to return to both carotid arteries. Lidocaine was used as local anesthesia to suture the surgical incisions and the area was rinsed with an antiseptic solution. All animals were housed in separated cages at room temperature until body temperature was recovered. Rectal temperature was checked daily and animals at 37 ± 1 °C were included in the experiment. Animals reporting abnormal behavior, diarrhea or seizures were discarded [24].

2.10. Tea Extract Administration

Animals were randomly classified into 6 groups of 10 animals each. GABA green tea and GABA oolong tea were gavaged at 10 mg/kg or 20 mg/kg for a week, starting from the first day after induction of stroke. Animal weights were recorded daily to ensure precise dosage and a 20-gauge gavage needle was used for the administration of extracts. Depressive-like behavior was evaluated in all animals 30 min after the last application, measuring despair swimming and tail suspension tests.

2.11. Examination of Stroke-Induced Anhedonia

For the examination of stroke-induced anhedonia, water bottles were removed from animal cages for a period of 6 h. Subsequently, two bottles were introduced to each cage. The first contained a 2% *w*/*v* sucrose solution while the second contained only water. This experiment focuses on evaluating the differences in quantity of sucrose and water consumed. The sucrose solution and water consumption were measured over 6 h [25].

2.12. Despair Swimming Test (DST) and Tail Suspension Test (TST)

The DST is a very common and standardized model for assessing depressive-like behavior in experimental animals. In brief, the mice were individually placed in an open cylinder (25 cm high and 10 cm diameter) filled with a 19 cm depth of fresh water at room temperature. The mice were left to swim for 6 min, analyzing the time of swimming, periods of immobility (the time spent without horizontal movement, simply retaining the head above the water surface), and climbing (the time in which animals try to maintain their forelegs above the water surface through active vertical movement).

The TST is another widespread assay system which is used for examining depressive-like behavior of animals. In brief, the experimental animals were suspended at a height of 58 cm for 5 min, using sticky tape placed 1 cm from the tail tip. Immobility time was calculated as the time without any movement for the 5 min monitoring period [26].

2.13. Anesthesia and Tissue Collection

After the behavioral assay and 12 h starvation, the animals were anesthetized through administration of a ketamine (60 mg/kg, i.p.) and xylazine (5 mg/kg, i.p.) mixture. The entire brain was carefully dissected and held at −60 °C prior to biochemical analysis.

2.14. Preparation of Tissue Homogenate

All brain tissue from each mouse was homogenized in 1 mM EDTA containing 100 mM ice cold phosphate buffered saline (1:10, % *w*/*v*) pH 7.4, and centrifuged for 30 min at 12,000× *g* and 4 °C. The upper layer was recovered and utilized for biochemical assays.

2.15. Measurement of Protein Content

Protein levels were assayed in brain homogenates by employing the Bradford method with bovine serum albumin as standard [27].

2.16. Estimation of Lipid Peroxidation, Reduced Glutathione Level, Superoxide Dismutase and Catalase Activities

Thiobarbituric acid reactive substance (TBARS), a marker of lipid peroxidation, was evaluated following the method developed by Esterbauer and Cheeseman [28]. Superoxide dismutase activity (SOD) was determined as according to the method developed by Misra and Fridovich [29]. Catalase activity was determined by following the method used by Bonaventura et al. [30] with slight modifications [21]. The levels of reduced glutathione (GSH) were evaluated using Ellman's method [31].

2.17. Statistical Analysis

Statistical analysis was performed with a statistical package for the social sciences (IBM SPSS 21.0 for Windows, Chicago, IL, USA). The data were assessed using a Shapiro-Wilk W test to determine the normal distribution. Statistical significance of the data was determined by one-way analysis of variance (ANOVA). When significant differences were found, Bonferroni's post-hoc analysis was used to establish the relationships between groups. Data was reported as a mean ± standard deviation (SD), and $p < 0.05$ was considered statistically significant.

3. Results

GABA green tea (GGABA) and GABA oolong tea (OGABA) extracts were prepared, starting from commercial samples and following the instructions provided by the supplier, to mimic the common conditions used for the preparation of tea beverages. The beverages were freeze-dried and the dry residue was assessed at 11.2 mg/mL and 7.2 mg/mL for GGABA and OGABA, respectively. Both extracts were submitted to RP-HPLC-PDA-ESI-MS^n analysis to determine their metabolite profiling; to

RP-HPLC-PDA and RP-HPLC-FD analysis to quantify some representative components and amino acids, and to in vivo tests, to assess their antioxidant activity and antidepressive-like activity in a mouse model of PSD.

3.1. RP-HPLC-PDA-ESI-MS^n Analysis

To the best of our knowledge, the metabolite profiles of GABA oolong tea were yet to be studied. So, the metabolite profiling of GGABA and OGABA extracts were determined through RP-HPLC-PDA-ESI-MS^n analysis, which allowed for the identification of 53 compounds, listed in Table 2. The identification was performed through comparison of experimental data (chromatographic behavior, UV-Vis, MS and MS^n spectra, Table 2) with that available in the literature. Figure 1 shows, as an example, a OGABA chromatogram, acquired as total scan PDA.

Table 2. Chromatographic behavior (retention time, RT), UV, MS and MS/MS data of the compounds identified in GGABA and OGABA extracts.

Peak	RT (min)	λ_{max} (nm)	*m/z*	HPLC-ESI-MS/MS *m/z* (% of Base Peak)	Proposed Structure
			Xanthines		
8	22.5	222, 273	181 $^+$	137 (100)	theobromine [a,b]
24	38.7	230, 270	195 $^+$	138 (100)	caffeine [a,b]
			Organic and phenolic acids		
1	5.2	211	191	127 (100), 85 (80)	quinic acid [a,b]
4	13.6	219, 274	343	191 (100), 169 (10), 125 (2)	galloylquinic acid [a,b]
11	27.5	219, 270	169	125 (100)	Gallic acid [a]
19	34.1	211, 330	337	163 (100), 191 (10), 119 (10), 173 (5)	3-*p*-coumaroylquinic acid [a,b]
27	43.5	211, 310	337	191 (100), 173 (25), 163 (10)	5-*p*-coumaroylquinic acid [a,b]
29	46.3	211, 309	337	173 (100), 163 (15), 191 (10)	4-*p*-coumaroylquinic acid [a,b]
			Flavones		
30	47.7	210, 270, 333	593	473 (100), 353 (25), 383 (15), 503 (30)	dihexosyl-apigenin [a,b]
32	52.9	210, 275	563	503 (70), 473 (100), 443 (80), 383 (45), 353 (50)	6-*C*-arabinosyl-8-*C*-glucosyl apigenin [a,b]
33	54.2	210, 275	563	503 (30), 473 (100), 443 (100), 383 (40), 353 (40)	6-*C*-glucosyl-8-*C*-arabinosyl apigenin [a,b]
38	58.6	211, 258, 352	577	413 (100), 293 (30), 457 (10), 353 (2)	rhamnosyl-hexosylapigenin [a]
39	59.08	211, 271, 336	593	413 (100), 293 (10), 473 (10)	dihexosyl-apigenin [a,b]
42	60.6	256, 353	533	443 (100), 473 (50), 353 (20)	6,8-*C*-dipentoside apigenin [b]
			Flavan-3-ols		
6	19.5	220, 270	305	261 (40), 221 (85), 219 (75), 179 (100), 165 (35), 125 (20)	gallocatechin [a,b]
15	31.3	240, 270	305	261 (40), 179 (100), 219 (70), 165 (35) 221 (85), 125 (25)	epigallocatechin [a,b]
16	32.4	211, 278	289	245 (100), 205 (40), 179 (15), 203 (40), 109 (5)	catechin [b]
25	39.2	233, 274	457	331 (70), 169 (100), 305 (35)	epigallocatechingallate [a,b]
26	43.1	232, 278	289	245 (100), 205 (40), 109 (5), 137 (10), 125 (2)	epicatechin [a,b]
31	52.8	230, 276	441	289 (100), 331 (20), 169 (25)	epicatechin-gallate [a,b]
35	55.8	219, 270, 352	455	289 (100), 183 (25)	epicatechina-3-*O*-(3-metil)-gallato [a]
37	57.2	209, 270	425	273 (100), 169 (40), 125 (5)	epiafzelechin-gallate [a,b]

Table 2. *Cont.*

Peak	RT (min)	λ_{max} (nm)	*m*/*z*	HPLC-ESI-MS/MS *m*/*z* (% of Base Peak)	Proposed Structure
			Theaflavins		
49	84.8	223, 270, 364, 470	867	715 (65), 697 (100), 679 (15), 527 (45), 545 (25), 559 (20)	theaflavin-digallate [a]
50	84.9	213, 269, 367, 478	715	527 (100), 545 (80), 563 (70), 501 (40), 407 (10)	theaflavin-gallate [a]
51	85.8	215, 270, 364	563	545 (100), 527 (30), 519 (55), 501 (30), 407 (70), 379 (50)	theaflavin [a]
52	86.6	213, 269, 367, 478	715	527 (30), 545 (60), 563 (100), 501 (20), 407 (60)	theaflavin-gallate [a]
			Flavonols		
34	54.5	210, 273	787	316 (100), 769 (30), 359 (20), 625 (15), 725 (20)	myricetinhexosylrutinoside [b]
36	55.9	215, 266, 350	479	316 (100), 317 (30)	myricetinhexoside [a,b]
41	60.4	211, 256, 356	771	301 (100), 609 (10), 463 (2)	quercetinhexosylrutinoside [a,b]
43	62.7	207, 267, 356	463	301 (100)	quercetinhexoside [a,b]
44	63.1	211, 256, 357	609	301 (100), 271 (15)	quercetinrutinoside [a,b]
45	64.5	210, 267, 348	755	285 (100)	kaempferolhexosylrutinoside [a,b]
46	67.3	210, 267, 348	755	285 (100)	kaempferolhexosylrutinoside [a,b]
47	70.7	206, 268	447	285 (40), 284 (100), 327 (20)	kaempferolhexoside [a,b]
48	70.7	207, 266, 345	593	285 (100)	kaempferolrutinoside [a]
53	96.3	220, 270	885	739 (100), 431 (20), 285 (10)	kaempferol-3-*O*-*p*-coumaroyl-dirhamnosyl hexoside [a]
			Tannins		
2	7.71	216, 267	609	471 (100), 591 (80), 565 (20), 525 (30)	theasinensin C [a]
3	9.6	210, 260	331	169 (100), 271 (80), 211 (40), 193 (20), 125 (15)	galloylglucose[a,b]
5	18.1	211	609	483 (30), 441 (100), 423 (70), 305 (20), 591 (29)	prodelphinidin [a,b]
7	22.0	211, 275	761	609 (100), 423 (80), 305 (20), 591 (70)	prodelphinidingallate [b]
9	22.8	217, 270	761	609 (40), 591 (100), 453 (10)	theasinensin B [a]
10	24.4	211, 278	577	425 (100), 407 (40), 289 (10), 451 (25)	procyanidin [a]
12	29.4	210, 254	865	739 (15), 695 (100), 577 (45)	(epi)afzelechingallate-(epi)catechingallate [a]
13	29.5	226, 275	633	301 (100), 463 (15)	strictinin [a,b]
14	29.9	211, 278	577	425 (100), 407 (40), 289 (10), 451 (25)	procyanidin [a,b]
17	32.5	223, 271	913	743 (100), 761 (50), 591 (80), 573 (45)	theasinensin C [a]
18	34.0	221, 275	483	271 (100), 331 (20), 169 (10)	digalloylglucose [b]
20	34.2	211, 276	745	559 (65), 407 (100), 619 (90), 577 (65), 441 (40)	(epi)catechin-(epi)gallocatechingallate [a]
21	35.1	211, 278	577	425 (100), 407 (40), 289 (10), 451 (25)	procyanidin [a,b]
22	35.9	211, 277	729	559 (100), 577 (95), 407 (20), 441 (5) 603 (25), 451 (35), 711 (15), 289 (10)	procyanidingallate [a,b]
23	38.4	211, 277	729	407 (80), 577 (80), 711 (20), 559 (100), 28451 (50), 603 (50), 441 (50), 289 (10)	procyanidingallate [a,b]
28	45.8	220, 280	635	465 (100), 483 (70), 313 (20)	trigalloylglucose [b]

[+] Compounds revealed in positive ionization mode; [a] compounds identified in GABA oolong tea extract; [b] compounds identified in GABA green tea extract.

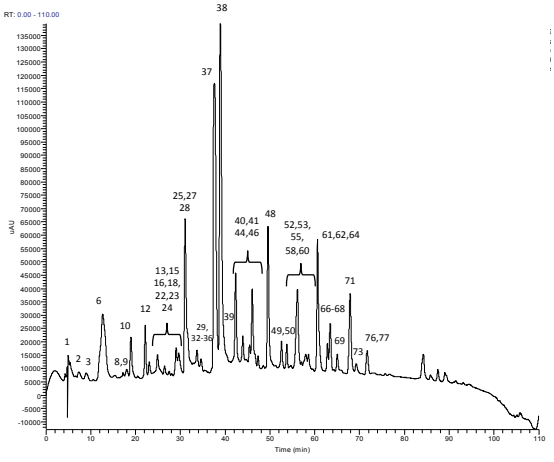

Figure 1. Chromatogram, acquired as total scan Photodiode Array (PDA) Detector, of Oolong GABA (OGABA) extract at 5 mg/mL.

The identified compounds consisted of: (a) two xanthines (caffeine and theobromine); (b) six organic and phenolic acids (gallic acid, quinic acid, galloylquinic acid, 3-*O*-*p*-coumaroylquinic acid, 4-*O*-*p*-coumaroylquinic acid and 5-*O*-*p*-coumaroylquinic acid); (c) six flavones (6-*C*-arabynoil-8-*C*-glucosyl apigenin, 6-*C*-glucosyl-8-*C*-arabynoil apigenin, di-pentosylapigenin, rhamnosyl-hexosylapigenin, and two isoforms of di-hexosylapigenin); (d) eight flavan-3-ols (gallocatechin, epigallocatechin, catechin, epicatechin, epicatechingallate, epigallocatechingallate, (epi)catechin-3-*O*-(3-*O*-methyl)-gallate, and (epi)-afzelechin); (e) four theaflavins (theaflavin, theaflavindigallate, and two isoforms of theaflavingallate); (f) 14 tannins (galloylglucose, digalloylglucose, trigalloylglucose, strictinin, prodelphinidin, prodelphinidingallate, (epi)afzelechingallate-(epi)catechingallate, (epi)catechin-(epi) gallocatechingallate, theasinensin A, theasinensin B, theasinensin C, three isoforms of procyanidin and two isoforms of procyanidingallate); and (g) 10 flavonols (myricetinhexoside, myricetinhexosylrutinoside, quercetinhexoside, quercetinhexosylrutinoside, quercetinrutinoside, kaempferolhexoside, kaempferolrutinoside, two isoforms of kaempferolhexosylrutinoside, and kaempferol 3-*O*-*p*-coumaroyl-dirhamnosyl-hexoside).

3.2. RP-HPLC-PDA Method Validation and Bioactives Quantification

The quantification of GA, caffeine, EGCG, ECG, EC and catechin in GGABA and OGABA extracts was performed by the standard addition method and expressed as μg/mL of tea beverage, taking into account tea dried residue after freeze-drying. Prior to quantification, the developed RP-HPLC-PDA method was validated following the ICH guidelines [23]. For each analyte, the concentration range, the calibration curve and the correlation coefficient (R^2) were calculated and are reported in Table 3. The method was linear within the following ranges: 25 to 500 μg/mL for catechin, from 7 to 500 μg/mL for GA and EC, and from 10 to 500 μg/mL for EGCG, ECG and caffeine, and the correlation coefficients were all higher than 0.999.

To evaluate the accuracy and precision of the method, one spiked tea sample was analyzed at three different concentration levels on three different days. Accuracy, intra-day and inter-day precision values are reported in Table 4. The results obtained indicate that the developed method was accurate, providing recoveries ranging from 86.1% to 106.3%, and precise, since the intra-day and inter-day variation were lower than 1% and 5% for all the analytes, respectively.

Table 3. Concentration ranges, calibration curves, correlation coefficients of the RP-HPLC-PDA method for gallic acid (GA), caffeine, catechin, epigallocatechin-3-gallate (EGCG), epicatechin-3-gallate (ECG) and epicatechin (EC).

Analyte	Concentration Range (μg/mL)	Calibration Curve	R^2
GA	7–500	$y = 18.941x - 41.578$	0.9999
caffeine	10–500	$y = 19.254x - 49.677$	0.9999
catechin	25–500	$y = 5.4294x - 84.198$	0.9998
EGCG	10–500	$y = 9.6778x - 51.975$	0.9999
ECG	10–500	$y = 14.997x - 63.054$	0.9999
EC	7–500	$y = 5.6054x - 13.496$	0.9999

Table 4. Accuracy (recovery %), intraday precision (RSD %), interday precision (RSD %), limit of quantification (LOQ) and limit of detection (LOD) of the analytical method, suitable for the quantification of GA, caffeine, catechin, EGCG, ECG and EC in tea samples. The concentration (μg/mL) of each analyte added to tea samples is reported.

	μg/mL	GA	μg/mL	Caffeine	μg/mL	Catechin	μg/mL	EGCG	μg/mL	ECG	μg/mL	EC
recovery (%)	2.75	105.7	12	100.6	5	87.3	10	90.7	5	91.1	3.75	95.9
	5.5	106.3	24.5	101.4	10	86.1	20	89.2	10	88.7	7.5	93.2
	11	103.1	49	101.0	20	87.5	40	87.8	20	86.4	15	91.3
Intraday precision (RSD %)	2.75	0.5	12	0.5	5	0.7	10	0.1	5	0.3	3.75	0.5
	5.5	0.3	24.5	0.1	10	0.2	20	0.1	10	0.3	7.5	0.3
	11	0.8	49	0.1	20	0.9	40	0.3	20	0.1	15	0.2
Interday precision (RSD %)	2.75	1.2	12	0.3	5	1.8	10	3.4	5	3.6	3.75	0.5
	5.5	2.3	24.5	0.3	10	0.5	20	4.6	10	1.9	7.5	0.4
	11	0.7	49	0.2	20	0.8	40	0.5	20	1.6	15	0.2
LOQ (μg/mL)		2.6		0.4		11.5		7.2		1.2		0.6
LOD (μg/mL)		0.4		0.1		3.8		2.4		0.4		0.2

As far as sensibility is concerned, LOQ and LOD values determined for each analyte are listed in Table 4. The very low concentrations indicate that the RP-HPLC-PDA method was very sensible for both quantification and detection purposes.

The validated RP-HPLC-PDA method was applied to the quantification of catechin, epicatechin, ECG, EGCG, GA and caffeine in GGABA and OGABA extracts. The results, reported in Table 5, showed that GGABA tea is richer in flavan-3-ols and caffeine than OGABA. Moreover, OGABA, as expected showed a higher content of gallic acid deriving from the oxidative reactions, which gallate esters of flavan-3-ols undergo during the fermentation process.

Table 5. Bioactive components concentration (μg/mL of tea beverage) in green GABA (GGABA) and OGABA extracts. Data are expressed as mean of three independent measurements ± standard deviation. N.D. = no detected.

Compound	GGABA	OGABA
	Flavan-3-ols	
catechin	361.93 ± 3.9	N.D.
epicatechin	329.80 ± 2.43	33.70 ± 0.11
epicatechin-gallate	208.64 ± 0.65	46.67 ± 0.14
epigallocatechingallate	906.42 ± 0.7	94.81 ± 0.30
	Amino acids	
GABA	17.81 ± 0.55	22.25 ± 0.65
Glutamic acid	27.10 ± 0.33	15.19 ± 0.45
Glutamine	10.08 ± 0.10	4.39 ± 0.08
Theanine	90.84 ± 0.87	46.15 ± 0.93
gallic acid	N.D.	59.47 ± 0.31
caffeine	1039.85 ± 4.32	525.05 ± 4.28

3.3. RP-HPLC-FD Analysis

The determination of proteic and non-proteic amino acids was performed by means of a RP-HPLC-FD analysis, preceded by pre-column derivatization of amino acids. Their identification was based on the chromatographic behavior of amino acid derivatives using derivatised commercial standards as a reference. Figure 2 reported, as an example, the chromatogram of GGABA extract.

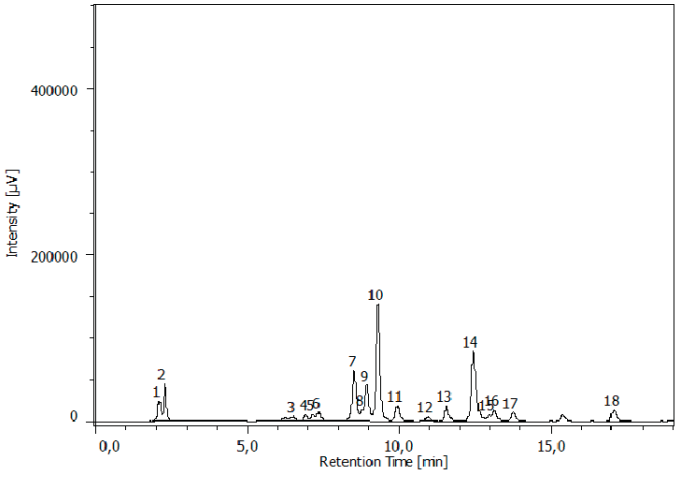

Figure 2. HPLC/FLD chromatograms of GGABA extract at the concentration of 0.5 mg/mL, respectively. The analysis showed the presence of (1) aspartic acid; (2) glutamic acid; (3) serine; (4) glutamine; (5) glycine; (6) threonine; (7) alanine; (8) arginine; (9) GABA 1; (10) theanine; (11) tyrosine; (12) cysteine; (13) valine; (14) GABA 2; (15) phenylalanine; (16) isoleucine; (17) leucine; (18) proline.

The analysis revealed the presence of 18 amino acids, with GABA, glutamine, glutamic acid and theanine quantified among these by the standard addition method. As reported in Table 5, GGABA extract showed a higher amount of all quantified amino acids, with the exception of GABA content which was higher in the OGABA extract.

3.4. Antidepressive-Like Activity and In Vivo Antioxidant Effects of GGABA and OGABA Extracts

In this study, animals were divided into 4 major groups: (a) a control group containing healthy non ischemic mice; (b) a BCCAO group, made up of mice in which ischemic stroke was induced through bilateral common carotid artery occlusion (BCCAO) and which did not receive any treatment; (c) 2 groups treated with GABA green tea (GGABA) extract at two dosages (10 and 20 mg/kg), after the induction of ischemic stroke; and (d) 2 groups treated with GABA oolong tea (OGABA) extract at two dosages (10 and 20 mg/kg) after surgery. Tea extracts were administered through oral gavage, to mimic the conventional way of drinking tea. This administration route makes it possible to evaluate the in vivo activities of tea following gastroduodenal digestion, which is known to cause deep changes in the chemical composition of tea [22], and the hepatic first pass effect. Mouse anhedonia, is defined as a loss of ability to experience satisfaction and is considered a central clinical trait of mental illness, including depression. Anhedonia is assessed in experimental animals by measuring the volume of consumption of both water and sucrose. As shown in Figure 3, the BCCAO group showed a significant decrease ($p < 0.05$) in sucrose consumption and a significant ($p < 0.05$) increase in water consumption compared to the control group, highlighting that our murine model is suitable for the study of PSD. The oral administration of both GGABA and OGABA extracts mitigates mice anhedonia, producing an

increase in sucrose consumption and a decrease in water consumption. In both cases, the highest effect was registered at the highest dose, with GGABA being more active at both doses.

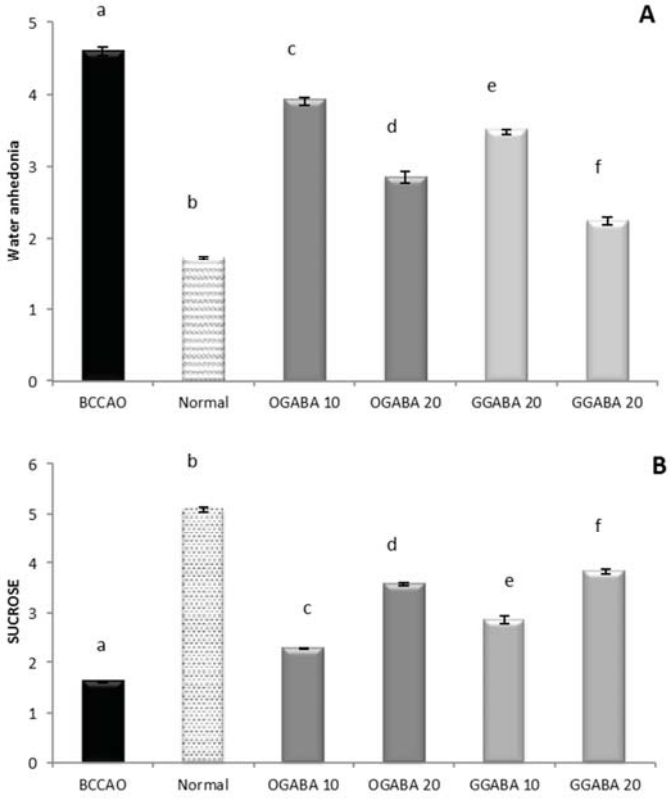

Figure 3. Volume of water (**A**) and sucrose solution (**B**) consumption in stroke-induced anhedonia model. Data are shown as a mean (mL) ± SD ($n = 3$); different letters indicate statistically significant differences ($p < 0.05$) between the two groups.

GGABA and OGABA were tested for antidepressant behavior using two common, validated tests: the despair swimming test (DST) and the tail suspension test (TST). All behavioral assessments were performed 30 min after the final administration. In DST, mice are forced to swim in a cylinder full of water. The test lasts 6 min, during which three parameters are registered: immobility, swimming and climbing times. For all three parameters (Figures 4–6), a significant statistical difference was registered between BCCAO and control groups ($p < 0.05$), confirming that the selected animal model is suitable for the evaluation of PSD.

At both concentrations, tea extracts showed good antidepressive-like activity, since they were able to restore and even improve the normal behavior. In fact, tea administration significantly ($p < 0.05$) increase mobility periods (swimming times, Figure 4, and climbing times, Figure 5) and decrease immobility time (Figure 6). In all cases, GABA green tea was the most effective in reducing behavioral abnormalities, especially at the highest dose (20 mg/kg).

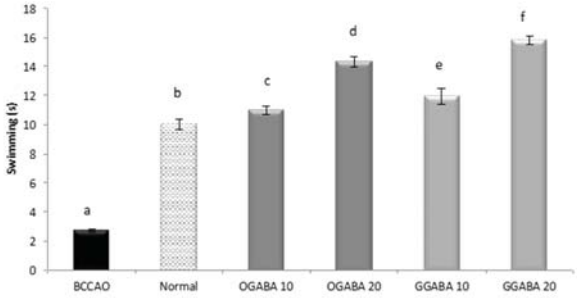

Figure 4. Effects of oral administration of OGABA and GGABA extracts on swimming time in forced swimming model. Data are mean(s) ± SD (n = 7); different letters indicate statistically significant differences ($p < 0.05$) between the two groups.

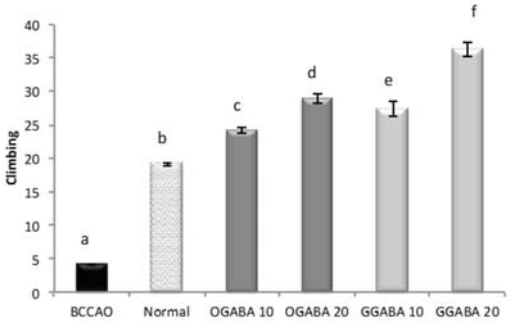

Figure 5. Effects of oral administration of OGABA and GGABA extracts on climbing time in forced swimming model. Data are mean(s) ± SD (n = 7); different letters indicate statistically significant differences ($p < 0.05$) between the two groups.

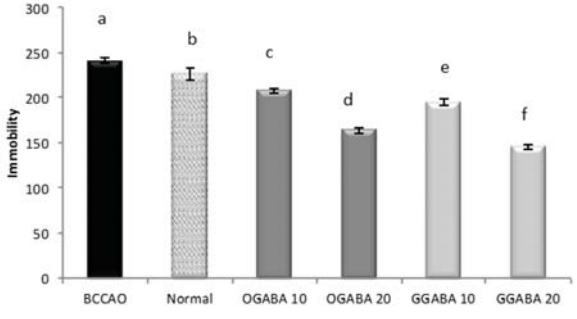

Figure 6. Effects of oral administration of OGABA and GGABA extracts on immobility time in forced swimming model. Data are mean(s) ± SD (n = 7); different letters indicate statistically significant differences ($p < 0.05$) between the two groups.

TST is a common behavioral test used for the evaluation of new potential antidepressant drugs in unavoidable and unescapable stress conditions. During the 6 min of test duration, one parameter (immobility time) is registered, which is reduced effective antidepressant agents. As shown in Figure 7, the oral administration of GGABA and OGABA extracts produced a significant ($p < 0.05$) reduction of the immobility time, with GGABA and OGABA showing the same activity ($p > 0.05$) at the lowest

dosage (10 mg/kg). At the highest concentration (20 mg/kg), GGABA was once more found to be the most active. In our previous review article, we formulated the hypothesis that polyphenols could assume a positive role in the management of PSD, due to their antioxidant activity [19].

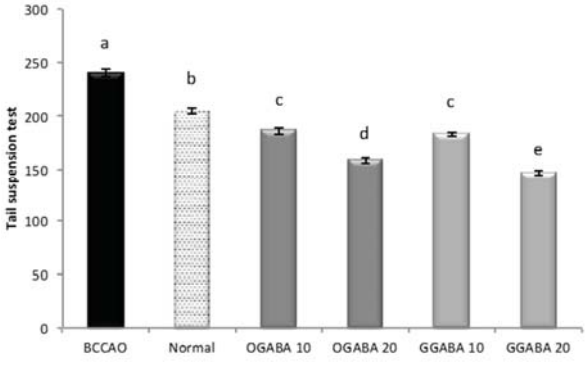

Figure 7. Effects of oral administration of OGABA and GGABA extracts on immobility time in tail suspension model. Data are mean(s) ± SD (n = 7); different letters indicate statistically significant differences ($p < 0.05$) between the two groups.

Our previous research on tea revealed that the intraperitoneal administration of both Chun Mee green tea and GABA green tea produced a mitigation of oxidative stress in mice brain [21]. TBAR levels were lower in brain homogenates of treated mice than in the control group, with GABA green tea successfully restoring normal values at the higher concentration tested (100 mg/kg). SOD activity and GSH levels were found to be higher, though complete restoration to normal, healthy values has not been registered [21]. Therefore, in this study we wanted to establish if this in vivo antioxidant activity of GABA tea is maintained with oral administration.

Lipid peroxidation was estimated from the TBAR levels, and taken for BCCAO, control and treated groups (Figure 8). As expected, stroke induced intense oxidative stress in mouse brain producing a significant ($p < 0.05$) increase in TBAR levels compared to control group. The administration of different dosages of OGABA and GGABA extracts produced a significant reduction in lipid peroxidation products, with GGABA being most active at both doses. The effect exerted by the highest dose was found to be highest. Anyway, the highest dosage was still unable to restore normal levels. A similar data trend can be seen in endogenous antioxidant defenses. BCCAO is characterized by lower levels of SOD and catalase activity and lowered GSH levels compared to healthy mice, indicating the presence of intense cerebral oxidative stress in mice affected by stroke. The administration of OGABA and GGABA extracts increase the antioxidant defenses, with GGABA being the most active. Even so, at the highest concentration tested (20 mg/kg) GGABA was not able to restore normal GSH levels and normal SOD and catalase activities.

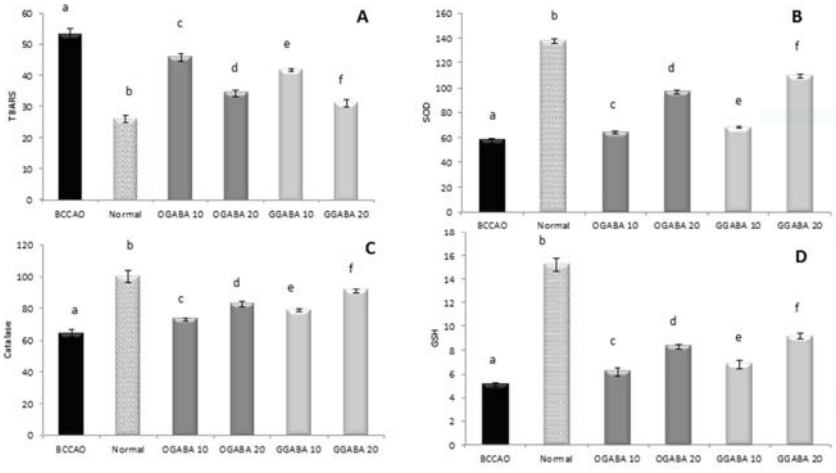

Figure 8. Effects of oral administration of OGABA and GGABA extracts on oxidative stress levels. In detail, thiobarbituric-reactive substances (TBARS) levels, expressed as nmol malondialdehyde (MDA) eq/g tissues (**A**); superoxide dismutase (SOD) activity, expressed as U/mg protein (**B**); Catalase activity, expressed as U/mg protein (**C**); and glutathione (GSH) levels, expressed as μg/mg protein (**D**) in mouse brain tissue are reported. Data are mean ± SD (n = 7); different letters indicate statistically significant differences ($p < 0.05$) between the two groups.

To evaluate a potential correlation between oxidative stress and mouse behavior, we decided to determine Pearson's linear correlation between parameters linked to mood status and oxidative stress biomarkers. As shown in Table 6, the coefficients highlighted that oxidative stress biomarkers and mood parameters are well related. Of all the possible combinations, the TBAR levels and Cat activities were most closely related to mood parameters. TBAR levels showed a moderate negative correlation with swimming and climbing times: the higher the TBARs, the lower the animals' mobility. However, TBAR levels showed a moderate positive correlation with the immobility times registered in both tests. Catalase activity showed the opposite correlation with both mobility and immobility times.

Table 6. Pearson's linear correlation between the data obtained from antioxidant assays and the data obtained from behavioral tests (DST and TST).

	TBARS	SOD	Cat	GSH
Swimming	−0.674 [a] $p < 0.001$	0.448 [a] $p = 0.003$	0.593 [a] $p < 0.001$	0.279 $p = 0.076$
Climbing	−0.595 [a] $p < 0.001$	0.356 [b] $p = 0.021$	0.526 [a] $p < 0.001$	0.188 $p = 0.234$
Immobility (DST)	0.483 [a] $p = 0.001$	−0.271 $p = 0.088$	−0.366 [b] $p = 0.020$	−0.020 $p = 0.901$
Immobility (TST)	0.568 [a] $p < 0.001$	−0.339 [b] $p = 0.029$	−0.468 [a] $p = 0.002$	−0.129 $p = 0.415$

TBARS: thiobarbituric-reactive substances; SOD: superoxide dismutase activity, Cat: catalase activity; GSH: glutathione. Bivariate Correlations: [a] Indicates a correlation at $p < 0.01$.[b] Indicates a correlation at $p < 0.05$.

4. Discussion

This study demonstrates that the oral administration of GGABA and OGABA extracts to experimental animals, in which PSD has been induced by BCCAO, (1) mitigates depressed mood, being able to improve behavioral parameters linked to depression, and (2) exerts in vivo antioxidant activity, being able to decrease lipid peroxidation product levels and increase SOD and catalase activities and GSH levels in mouse brain. GGABA, which was found to be the most active, exhibited higher caffeine, proteic and non proteic amino acid, and polyphenolic content, which could justify the highest capacity

to influence mood status and antioxidant activity of this kind of tea. In particular, GGABA has twice the amount of caffeine and theanine in comparison with OGABA. A number of studies showed that when administered together, theanine and caffeine combination increases alertness, attention, and memory and influence positively mood status [32,33]. GGABA showed higher content of glutamic acid and glutamine, but these compounds probably do not exert any effect at brain level. In fact, as far as glutamic acid is concerned, several investigations have shown that the blood brain barrier (BBB) is impermeable to glutamate, even at high concentrations [34]. In addition, large amounts of glutamate administered to experimental animals and humans resulted to induce very small changes in glutamate plasma concentration in view of the fact that it is almost completely metabolized to produce energy. As regards glutamine, it is mainly deaminated by phosphate-dependent glutaminases to glutamate, which in turn is used as a source of energy [35,36]. As far as GABA is concerned, OGABA showed a slightly higher concentration (about 20%) than that found in GGABA. It is not easy to draw a conclusion about the influence of GABA considering that literature data regarding the GABA ability to cross the BBB are often contradictory, especially because of the different methods of administration (i.e., oral versus injection), and species used for the experiments [37]. In recent years, Boonstra et al. have speculated that GABA of food origin does exert a direct effect on central nervous system, being unable to cross the BBB, but acts on mood with an indirect mechanism of action via the enteric nervous system [37]. Finally, GGABA showed a polyphenolic content about ten times greater than that determined in OGABA, thereby justifying its higher in vivo antioxidant activity. In addition, Pearson's correlation coefficients highlighted a relationship between mouse behavioral parameters and oxidative stress biomarkers, confirming our initial hypothesis, and showing that these biochemical markers could be good predictive parameters of depression in preclinical studies, to be confirmed by clinical trials. The obtained results were in agreement with those reported in our previous paper [21] and provided by Schuch et al. [38], which reported that TBARS serum levels are higher in severely depressed patients and showed that exercise, which reduces depression, also reduces serum TBARS levels after 3 weeks of treatment.

This investigation also represents the first study of metabolite profiling of GABA oolong tea, detecting 48 compounds. The results from chemical analyses have revealed that the composition of GGABA and OGABA extracts is different, with OGABA being more complex than GGABA. The main differences are in the presence of tannins (i.e., flavan-3-ols dimers, theasinensins and procyanidins) and theaflavins. It is interesting to notice that some flavan-3-ols (i.e., epigallocatechin and (epi)catechin-3-*O*-(3-*O*-methyl)-gallate) were only detected in the OGABA extract.

While further efforts must be made to elucidate the molecular mechanisms underlying the antidepressive-like and in vivo antioxidant activities of GABA tea and the pharmacokinetics of GABA tea components, the varying effectiveness of GGABA and OGABA could be attributed to the higher amount of polyphenols, theanine and glutamine found in GGABA.

5. Conclusions

In conclusion, this investigation showed that green and oolong GABA teas were able to exert positive effects on mood following oral administration using the mouse model of PSD, being green GABA tea more active than oolong GABA tea. In addition, these teas showed *in vivo* antioxidant activity, being able to decrease the levels of lipid peroxidation products and increase the activity of antioxidant enzymes in the mouse brain. The chemical composition of these teas, at least in part, explains the higher antidepressive-like and antioxidant activities of green GABA tea, which resulted to be richer in bioactive compounds than oolong GABA tea (i.e polyphenolic substances and amino acids). Taken together, the results obtained here and in our previous investigation suggest that GABA tea is a promising candidate to be used as an adjuvant in the management of PSD.

Acknowledgments: The authors would like to thank Patrizia Arcidiaco for her excellent support in the analysis of aminoacids and La Teiera Eclettica (Milan, Italy), for providing tea samples used in the present work. A. Sureda was supported by Instituto de Salud Carlos III, the Spanish Biomedical Research Centre in Physiopathology of Obesity and Nutrition, CIBEROBN (CB12/03/30038).

Author Contributions: Maria Daglia and Seyed Mohammad Nabavi designed the research, were responsible for the correctness of the chemical and biological analyses, respectively, and contributed to writing the manuscript; Arianna Di Lorenzo performed the sample preparation, chemical analyses and contributed to the writing the manuscript; Seyed Fazel Nabavi, Sedigheh Khanjani, and Akbar Hajizadeh Moghaddam performed the biological tests; Antoni Sureda performed the statistical analysis and revised the final version; Nady Braidy contributed to the critical analysis of data and revised the final version. All authors approved the final manuscript.

Conflicts of Interest: The authors have declared no conflict of interest.

References

1. Allen, C.L.; Bayraktutan, U. Oxidative stress and its role in the pathogenesis of ischaemic stroke. *Int. J. Stroke* **2009**, *4*, 461–470. [CrossRef] [PubMed]
2. Shirley, R.; Ord, E.N.; Work, L.M. Oxidative Stress and the Use of Antioxidants in Stroke. *Antioxidants* **2014**, *3*, 472–501. [CrossRef] [PubMed]
3. Robinson, R.G.; Jorge, R.E. Post-Stroke Depression: A Review. *Am. J. Psychiatry* **2016**, *173*, 221–231. [CrossRef] [PubMed]
4. Morris, P.L.; Robinson, R.G.; Andrzejewski, P.; Samuels, J.; Price, T.R. Association of depression with 10-year poststroke mortality. *Am. J. Psychiatry* **1993**, *150*, 124–129. [PubMed]
5. House, A.; Knapp, P.; Bamford, J.; Vail, A. Mortality at 12 and 24 months after stroke may be associated with depressive symptoms at 1 month. *Stroke* **2001**, *32*, 696–701. [CrossRef] [PubMed]
6. Williams, L.S.; Ghose, S.S.; Swindle, R.W. Depression and other mental health diagnoses increase mortality risk after ischemic stroke. *Am. J. Psychiatry* **2004**, *161*, 1090–1095. [CrossRef] [PubMed]
7. Sharpe, P.C.; Mulholland, C.; Trinick, T. Ascorbate and malondialdehyde in stroke patients. *Ir. J. Med. Sci.* **1994**, *163*, 488–491. [CrossRef] [PubMed]
8. Polidori, M.C.; Cherubini, A.; Stahl, W.; Senin, U.; Sies, H.; Mecocci, P. Plasma carotenoid and malondialdehyde levels in ischemic stroke patients: Relationship to early outcome. *Free Radic. Res.* **2002**, *36*, 265–268. [CrossRef] [PubMed]
9. Chang, C.Y.; Lai, Y.C.; Cheng, T.J.; Lau, M.T.; Hu, M.L. Plasma levels of antioxidant vitamins, selenium, total sulfhydryl groups and oxidative products in ischemic-stroke patients as compared to matched controls in Taiwan. *Free Radic. Res.* **1998**, *28*, 15–24. [CrossRef] [PubMed]
10. Cherubini, A.; Polidori, M.C.; Bregnocchi, M.; Pezzuto, S.; Cecchetti, R.; Ingegni, T.; di Iorio, A.; Senin, U.; Mecocci, P. Antioxidant profile and early outcome in stroke patients. *Stroke* **2000**, *31*, 2295–2300. [CrossRef] [PubMed]
11. Moylan, S.; Berka, M.; Dean, O.M.; Samuni, Y.; Williams, L.J.; O'Neil, A.; Hayley, A.C.; Pasco, J.A.; Anderson, G.; Jacka, F.N.; et al. Oxidative & nitrosative stress in depression: Why so much stress? *Neurosci. Biobehav. Rev.* **2014**, *45*, 46–62. [PubMed]
12. Herken, H.; Akyol, O.; Yilmaz, H.R.; Tutkun, H.; Savas, H.A.; Ozen, M.E.; Kalenderoglu, A.; Gulec, M. Nitric oxide, adenosine deaminase, xanthine oxidase and superoxide dismutase in patients with panic disorder: Alterations by antidepressant treatment. *Hum. Psychopharmacol.* **2006**, *21*, 53–59. [CrossRef] [PubMed]
13. Maes, M.; Mihaylova, I.; Kubera, M.; Uytterhoeven, M.; Vrydags, N.; Bosmans, E. Lower whole blood glutathione peroxidase (GPX) activity in depression, but not in myalgic encephalomyelitis/chronic fatigue syndrome: Another pathway that may be associated with coronary artery disease and neuroprogression in depression. *Neuro Endocrinol. Lett.* **2011**, *32*, 133–140. [PubMed]
14. Behr, G.A.; Moreira, J.C.; Frey, B.N. Preclinical and clinical evidence of antioxidant effects of antidepressant agents: Implications for the pathophysiology of major depressive disorder. *Oxid. Med. Cell. Longev.* **2012**, *2012*, 609421. [CrossRef] [PubMed]
15. Forlenza, M.J.; Miller, G.E. Increased serum levels of 8-hydroxy-2′-deoxyguanosine in clinical depression. *Psychosom. Med.* **2006**, *68*, 1–7. [CrossRef] [PubMed]

16. Yanik, M.; Erel, O.; Kati, M. The relationship between potency of oxidative stress and severity of depression. *Acta Neuropsychiatr.* **2004**, *16*, 200–203. [CrossRef] [PubMed]
17. Behravan, E.; Razavi, B.M.; Hosseinzadeh, H. Review of plants and their constituents in the therapy of cerebral ischemia. *Phytother. Res.* **2014**, *28*, 1265–1274. [CrossRef] [PubMed]
18. Nabavi, S.M.; Daglia, M.; Braidy, N.; Nabavi, S.F. Natural products, micronutrients, and nutraceuticals for the treatment of depression: A short review. *Nutr. Neurosci.* **2017**, *20*, 180–194. [CrossRef] [PubMed]
19. Nabavi, S.F.; Dean, O.M.; Turner, A.; Sureda, A.; Daglia, M.; Nabavi, S.M. Oxidative stress and post-stroke depression: Possible therapeutic role of polyphenols? *Curr. Med. Chem.* **2015**, *22*, 343–351. [CrossRef] [PubMed]
20. Tsushida, T.; Murai, T.; Ohmori, M.; Okamoto, J. Production of a new type of tea containing a high level of γ-aminobutyric acid. *Nippon Nogeikagaku Kaishi* **1987**, *61*, 817–822. [CrossRef]
21. Di Lorenzo, A.; Nabavi, S.F.; Sureda, A.; Moghaddam, A.H.; Khanjani, S.; Arcidiaco, P.; Nabavi, S.M.; Daglia, M. Antidepressive-like effects and antioxidant activity of green tea and GABA green tea in a mouse model of post-stroke depression. *Mol. Nutr. Food Res.* **2016**, *60*, 566–579. [CrossRef] [PubMed]
22. Marchese, A.; Coppo, E.; Sobolev, A.P.; Rossi, D.; Mannina, L.; Daglia, M. Influence of in vitro simulated gastroduodenal digestion on the antibacterial activity, metabolic profiling and polyphenols content of green tea (*Camellia sinensis*). *Food Res. Int.* **2014**, *63*, 182–191. [CrossRef]
23. ICH Harmonised Tripartite guideline. Validation of Analytical Procedures: Text and Methodology Q2(R1). Available online: http://www.ich.org/fileadmin/Public_Web_Site/ICH_Products/Guidelines/Quality/Q2_R1/Step4/Q2_R1__Guideline.pdf (accessed on 10 May 2012).
24. Nabavi, S.F.; Nabavi, S.M.; Habtemariam, S.; Moghaddam, A.H.; Sureda, A.; Mirzaei, M. Neuroprotective effects of methyl-3-*O*-methyl gallate against sodium fluoride-induced oxidative stress in the brain of rats. *Cell. Mol. Neurobiol.* **2013**, *33*, 261–267. [CrossRef] [PubMed]
25. Nabavi, S.F.; Sobarzo-Sánchez, E.; Nabavi, S.M.; Sureda, A.; Moghaddam, A.H. Bi-3-azaoxoisoaporphine derivatives have antidepressive properties in a murine model of post stroke-depressive like behavior. *Curr. Neurovasc. Res.* **2013**, *10*, 164–171. [CrossRef] [PubMed]
26. Nabavi, S.F.; Habtemariam, S.; Di Lorenzo, A.; Sureda, A.; Khanjani, S.; Nabavi, S.M.; Daglia, M. Post-Stroke Depression Modulation and in vivo Antioxidant Activity of Gallic Acid and Its Synthetic Derivatives in a Murine Model System. *Nutrients* **2016**, *8*, 248. [CrossRef] [PubMed]
27. Bradford, M.M. A rapid and sensitive method for the quantitation of microgram quantities of protein utilizing the principle of protein-dye binding. *Anal. Biochem.* **1976**, *72*, 248–254. [CrossRef]
28. Esterbauer, H.; Cheeseman, K.H. Determination of aldehydic lipidperoxidation products: Malonaldehyde and 4-hydroxynonenal. *Methods Enzymol.* **1990**, *186*, 407–421. [PubMed]
29. Misra, H.P.; Fridovich, I. The role of superoxide anion in the autoxidation of epinephrine and a simple assay for superoxide dismutase. *J. Biol. Chem.* **1972**, *247*, 3170–3175. [PubMed]
30. Bonaventura, J.; Schroeder, W.A.; Fang, S. Human erythrocyte catalase: Animproved method of isolation and a reevaluation of reported properties. *Arch. Biochem. Biophys.* **1972**, *150*, 606–617. [CrossRef]
31. Ellman, G.L. Tissue sulfhydryl groups. *Arch. Biochem. Biophys.* **1959**, *82*, 70–77. [CrossRef]
32. Owen, G.N.; Parnell, H.; De Bruin, E.A.; Rycroft, J.A. The combined effects of L-theanine and caffeine on cognitive performance and mood. *Nutr. Neurosci.* **2008**, *11*, 193–198. [CrossRef] [PubMed]
33. Dodd, F.L.; Kennedy, D.O.; Riby, L.M.; Haskell-Ramsay, C.F. A double-blind, placebo-controlled study evaluating the effects of caffeine and L-theanine both alone and in combination on cerebral blood flow, cognition and mood. *Psychopharmacology* **2015**, *232*, 2563–2576. [CrossRef] [PubMed]
34. Hawkins, R.A.; Viña, J.R. How Glutamate Is Managed by the Blood-Brain Barrier. *Biology* **2016**, *5*, E37. [CrossRef] [PubMed]
35. Tsai, P.J.; Huang, P.C. Circadian variations in plasma and erythrocyte glutamate concentrations in adult men consuming a diet with and without added monosodium glutamate. *J. Nutr.* **2000**, *130*, 1002S–1004S. [PubMed]
36. Hanson, P.J.; Parsons, D.S. Transport and metabolism of glutamine and glutamate in the small intestine. In *Glutamine and Glutamate in Mammals*; Kvamme, E., Ed.; CRC Press Inc.: Boca Raton, FL, USA, 1988; pp. 235–253.

37. Boonstra, E.; de Kleijn, R.; Colzato, L.S.; Alkemade, A.; Forstmann, B.U.; Nieuwenhuis, S. Neurotransmitters as food supplements: The effects of GABA on brain and behavior. *Front. Psychol.* **2015**, *6*, 1520. [CrossRef] [PubMed]
38. Schuch, F.B.; Vasconcelos-Moreno, M.P.; Borowsky, C.; Zimmermann, A.B.; Wollenhaupt-Aguiar, B.; Ferrari, P.; de Almeida Fleck, M.P. The effects of exercise on oxidative stress (TBARS) and BDNF in severely depressed inpatients. *Eur. Arch. Psychiatry Clin. Neurosci.* **2014**, *264*, 605–613. [CrossRef] [PubMed]

nutrients

MDPI

Article

Different Intestinal Microbial Profile in Over-Weight and Obese Subjects Consuming a Diet with Low Content of Fiber and Antioxidants

Tania Fernández-Navarro [1,2], Nuria Salazar [2,*], Isabel Gutiérrez-Díaz [1], Clara G. de los Reyes-Gavilán [2], Miguel Gueimonde [2] and Sonia González [1,*]

1 Area of Physiology, Department of Functional Biology, University of Oviedo, 33006 Asturias, Spain; tfnavarro214@gmail.com (T.F.-N.); igutidiaz@gmail.com (I.G.-D.)

2 Department of Microbiology and Biochemistry of Dairy Products, Instituto de Productos Lácteos de Asturias, Consejo Superior de Investigaciones Científicas (IPLA-CSIC), Paseo Río Linares s/n, Villaviciosa, 33300 Asturias, Spain; greyes_gavilan@ipla.csic.es (C.G.d.l.R.-G.); mgueimonde@ipla.csic.es (M.G.)

* Correspondence: nuriasg@ipla.csic.es (N.S.); soniagsolares@uniovi.es (S.G.)

Received: 18 April 2017; Accepted: 23 May 2017; Published: 27 May 2017

Abstract: Obesity has been related to an increased risk of multiple diseases in which oxidative stress and inflammation play a role. Gut microbiota has emerged as a mediator in this interaction, providing new mechanistic insights at the interface between fat metabolism dysregulation and obesity development. Our aim was to analyze the interrelationship among obesity, diet, oxidative stress, inflammation and the intestinal microbiota in 68 healthy adults (29.4% normal-weight). Diet was assessed through a food frequency questionnaire and converted into nutrients and dietary compounds using food composition tables. The intestinal microbiota was assessed by quantitative PCR, fecal short chain fatty acids by gas chromatography and serum biomarkers by standard protocols. Higher levels of malondialdehyde (MDA), C reactive protein (CRP), serum leptin, glucose, fat percentage and the intestinal *Lactobacillus* group were found in the obese people. Cluster analysis of body mass index, fat mass, glucose, LDL/HDL ratio, leptin, MDA and CRP classified the subjects into two groups. The levels of the intestinal *Bacteroides-Prevotella-Porphyromonas* group were lower in the cluster and linked to a higher pro-oxidant and pro-inflammatory status, whose individuals also had lower intake of fruits, dried fruits, and fish. These results could be useful for designing strategies targeted to obesity prevention.

Keywords: oxidative stress; microbiota; obesity; antioxidant; western diet

1. Introduction

The prevalence of obesity is growing worldwide, with nearly half a billion of the world's population considered to be overweight. Obesity, defined by the World Health Organization (WHO) as an "abnormal or excessive fat accumulation", has been associated with an increasing risk of multiple diseases, characterized by changes in the oxidative/antioxidant balance and the presence of subclinical inflammation [1–4], including diabetes, metabolic syndrome, hypertension, dyslipidemia and cardiovascular disease among others [5]. Thanks to the great efforts made in obesity research during the last decades, several genetic, environmental and lifestyle-related factors have been identified as etiological risk elements for this condition. However, there are still factors in this equation, such as the gut microbiota, whose contribution remains to be fully elucidated. It has been proposed that the reduction of carbohydrates accessible to gut microbes from fiber-containing foodstuffs may result in a long-term reduction of microbiota diversity and in the appearance of "unhealthy" microbiomes [6–8]. Although it has not been possible to establish the directionality of this relationship, the gradual increase

in energy intake, together with the dramatic change in the proportion of macronutrients of the Western diet, seems to be linked with the increase of the obesity prevalence [9] mediated by changes in intestinal microbial populations.

In contrast, the content in bioactive compounds of the Mediterranean Diet has been linked with the prevention of obesity and metabolic syndrome, by means of restoring the intestinal microbial balance of these patients [10,11]. An increase of the intestinal *Firmicutes/Bacteroidetes* ratio has been reported in several studies with obese humans [12], in obese leptin deficient ob/ob mice [13] and in wild-type animals receiving Western diets [14]. The benefits of dietary fiber in host health have been reported to be partly mediated by physiological effects linked to the formation in the colon of fecal short chain fatty acids (SCFA) produced by the microbial fermentation of complex carbohydrates. In this regard, it is known that the major SCFA synthesized by the colonic microbiota (acetic, propionic, and butyric) play a key role in regulating host energy balance in extra-intestinal organs, such as the liver and adipose tissue [15,16]. In an apparently contradictory way, high levels of fecal SCFA have been frequently found in obese subjects [17]. The specific mechanisms explaining the higher levels of fecal SCFA in obesity still remain a matter of debate and different hypotheses have been proposed, including: an increase on colonic fermentation due to the higher dietary intake; a higher capacity for energy harvest by the modification of the intestinal microbial metabolic profile linked to obesity [18,19]; and the reduction of the in vivo fluxes of SCFA from the intestinal lumen to other host organs, with accumulation in the colonic lumen [20].

The currently available evidences highlight the complex network of physiological mechanisms underlying obesity [21]. In this scenario, the intestinal microbiota may provide new mechanistic insights at the interface between fat metabolism dysregulation and obesity development. To the best of our knowledge, there are no currently available interdisciplinary studies addressing the interrelationships among obesity, diet, oxidative stress, inflammation and gut microbiota. However, a better understanding of these interactions could be useful for the development of new approaches for preventing and controlling obesity. Therefore, our aim was to determine differences in the serum concentration of malondialdehyde (MDA), glucose, lipid profile, and C reactive protein (CRP), according to the grade of obesity, to describe the gut microbial composition linked with this pathology and to analyze the role of the diet in the possible associations among these parameters.

2. Subjects and Methods

2.1. Participants

This cross-sectional study is part of a research into diet and gut microbiota in different population groups. The study sample comprised 68 adult volunteers 27 men and 41 women, aged from 19 to 67 years (mean $\pm$ SD, 52.4 $\pm$ 11.2). Participants were recruited in Asturias Region (Northern Spain) between the years 2009 and 2015 among subjects attending a program of the University of Oviedo for people older than 50 years, as well as among individuals participating in a study on nutritional habits from the Alimerka Foundation. In a personal interview, volunteers were informed of the objectives of the study and those deciding to participate gave their fully informed written consent. Then, personal appointments were made to collect the dietary information. Subjects were initially classified according to their Body Mass Index (BMI) [22]. From the initial sample four subjects were excluded from cluster analysis because no data were recorded for some of the parameters introduced as variables in our study. Moreover, three subjects had missing values for fecal microbiota and, therefore, were not included for further analyses. The following inclusion criteria were used: not being diagnosed of autoimmune diseases, inflammatory bowel disease or other conditions known to affect the intestinal function, as well as not having undergone medical treatment with oral corticoids, immunosuppressive agents, monoclonal antibodies, antibiotics or immunotherapy or not having consumed any supplement containing probiotics or prebiotics during the previous month. Volunteers diagnosed for diabetes mellitus type II were specifically excluded from the study. Ethical approval for this study was obtained

from the Bioethics Committee of CSIC (Consejo Superior de Investigaciones Científicas) and from the Regional Ethics Committee for Clinical Research ("Servicio de Salud del Principado de Asturias nº13/2010") in compliance with the Declaration of Helsinki of 1964. All experiments were carried out in accordance with approved guidelines and regulations.

2.2. Nutritional Assessment

Dietary intake was assessed in a personal interview by means of an annual semi-quantitative food frequency questionnaire (FFQ) method which details 160 items and has been widely used and validated in previous studies [23,24]. The consumption of foods was converted into energy and macronutrients using the nutrient food composition tables developed by the Centro de Enseñanza Superior de Nutrición y Dietética (CESNID) [25]; the intake of monosaccharides (glucose, galactose, fructose) sucrose, starch and digestible polysaccharides and trans fatty acids was converted using the National Nutrient Database for Standard Reference from the United States Department of Agriculture (USDA) [26]. Information about dietary soluble and insoluble fibers was completed from Marlett et al. [27] and phenolic intake was estimated from the Phenol Explorer database [28]. Data about the Oxygen Radical Absorbance Capacity (ORAC) of foods was obtained from the Database from the ORAC of Selected Foods from USDA [29]. This database reports the hydrophilic ORAC, lipophilic ORAC and total ORAC values for 275 foods as μmol of Trolox equivalents (TE)/100 g. For the estimation of these variables in the study sample we used the information contained in our database regarding the daily intake of each food in g/day for all the evaluated subjects. This information has been crossed with the data contained in the ORAC database in order to calculate the intake of ORAC hydrophilic, lipophilic and total in μmol TE for each food and subject. Once this partial information was available, the summary of all the hydrophilic ORAC, lipophilic ORAC and total ORAC obtained per subject was calculated in order to estimate the total antioxidant capacity of the diet by subject.

2.3. Anthropometric Measures

At the same time of carrying out the blood extraction, between eight and nine o'clock and after over-night fast, anthropometric measures were taken. Height was registered using a stadiometer with an accuracy of $\pm$1 mm (Año-Sayol, Barcelona, Spain). Subjects stood barefoot, in an upright position and with the head positioned in the Frankfort horizontal plane. Weight was measured on a scale with an accuracy of $\pm$100 g (Seca, Hamburg, Germany). BMI was calculated and stratified according to the Sociedad Española para el Estudio De la Obesidad (SEEDO) [22] criteria: lean–normal weight ($\leq$25.0 kg/m^2), over-weight (25.0–30.0 kg/m^2), and obese ($\geq$30.0 kg/m^2). Body fat percentage was measured by bioelectrical impedance (BIA) with $\pm$1% variation, with subjects in light clothes and in fasted state (Tanita Corporation of America, Inc., Arlington Heights, IL, USA). Basal Metabolic Rate (BMR) was calculated by the Harris-Benedict formula [30].

2.4. Blood Biochemical Analyses

Fasting blood samples were drawn by venepuncture after a 12 h fast and collected in separate tubes for serum and plasma. Samples were kept on ice and centrifuged (1000$\times$ *g*, 15 min) within 2–4 h after collection. Plasma and serum aliquots were kept at -20 °C until analyses were performed. Plasma glucose, cholesterol, and triglycerides were determined by standard methods. Serum levels of CRP were determined by using a CRP Human Instant ELISA kit (Ebioscience, San Diego, CA, USA), and those of MDA with a colorimetric assay of lipid peroxidation (Byoxytech LPO-586, Oxis International S.A., Paris, France); the within-run coefficient of variation ranged from 1.2% to 3.4%, depending on the concentration of MDA [31].

Serum leptin was measured by a sensitive ELISA test (Human Leptin ELISA Development Kit, 900-K90 PeproTech Inc., Rocky Hill, NJ, USA) according to the manufacturer's instructions. The detectable concentration range was 63–4000 pg/mL. The intra-assay and interassay coefficients of variation were 5.21% and 5.20%, respectively.

2.5. Fecal Collection and Microbiological Analyses

Participants received detailed instructions to collect fecal samples and were provided with a sterile container. Samples were immediately frozen at −20 °C after deposition. For analyses, fecal samples were melted, weighed, diluted 1/10 in sterile PBS, and homogenized in a LabBlender 400 Stomacher (Seward Medical, London, UK) for 4 min; the DNA was extracted using the QIAamp DNA stool mini kit (Qiagen, Hilden, Germany) as previously described [32]. Quantification of different bacterial populations that covered the major bacterial groups present in the gut microbial ecosystem (Table 1) was performed in feces with a 7500 Fast Real-Time PCR System (Applied Biosystems, Foster City, CA, USA) using SYBR Green PCR Master Mix (Applied Biosystems). One microlitre of template fecal DNA (~5 ng) and 0.2 µM of each primer were added to the 25-µL reaction mixture. PCR cycling consisted of an initial cycle of 95 °C 10 min, followed by 40 cycles of 95 °C 15 s, and 1 min at the appropriate primer-pair temperature (Table 1). The number of cells was determined by comparing the Ct values obtained from a standard curve constructed using the pure cultures of appropriate strains that were grown overnight in GAM (Gifu Anaerobic Medium) medium (Nissui Pharmaceutical Co., Tokyo, Japan) under anaerobic conditions (Table 1). The Ct values were plotted as a linear function of the base-10 logarithm of the number of cells calculated by plate counting. Fecal DNA extracts were analysed and the mean quantity per gram of fecal wet weight was calculated.

Table 1. Bacterial groups, standard cultures, primers, and annealing temperatures (Tm) used for qPCR in this study.

Microbial Target	Strain Used for Standard Curve	Primer Sequence 5′–3′	Tm (°C)	Reference
Akkermansia	*Akkermansia muciniphila* CIP 107961	F: CAGCACGTGAAGGTGGGGAC R: CCTTGCGGTTGGCTTCAGAT	60	[32]
Bacteroides group *Bacteroides-Prevotella-Porphiromonas*	*Bacteroides thetaiotaomicron* DSMZ 2079	F: GAGAGGAAGGTCCCCCAC R: CGCKACTTGGCTGGTTCAG	60	[32]
Bifidobacterium	*Bifidobacterium longum* NCIMB 8809	F:GATTCTGGCTCAGGATGAACGC R: CTGATAGGACGCGACCCCAT	60	[32]
Faecalibacterium	*Faecalibacterium prausnitzi* DSMZ 17677	F:GGAGGAAGAAGGTCTTCGG R: AATTCCGCCTACCTCTGCACT	60	[33]
Clostridia XIVa *Blautia coccoides—Eubacterium rectale group*	*Blautia coccoides* DSMZ 935	F: CGGTACCTGACTAAGAAGC R: AGTTTYATTCTTGCGAACG	55	[32]
Lactobacillus group	*Lactobacillus gasseri* IPLA IF7/5	F: AGCAGTAGGGAATCTTCCA R: CATGGAGTTCCACTGTCCTC	60	[32]

2.6. Short Chain Fatty Acids (SCFA) Analyses

The analysis of SCFA was performed by gas chromatography to determine the concentrations of acetate, propionate and butyrate. Supernatants from 1 mL of the homogenized feces were obtained by centrifugation and filtration as previously indicated [32,33]. A chromatograph 6890N (Agilent Technologies Inc., Palo Alto, CA, USA) connected to a mass spectrometry detector (MS) 5973N (Agilent Technologies) and a flame ionization detector (FID) was used for identification and quantification of SCFA, respectively. Chromatographic conditions and SCFA analyses were carried out essentially as described by Salazar et al. [34].

2.7. Statistical Analysis

Statistical analysis was performed using the IBM SPSS program version 22.0 (IBM SPSS, Inc., Chicago, IL, USA). Goodness of fit to the normal distribution was analyzed by means of the Kolmogorov-Smirnov test. When the distribution of variables was skewed, the natural logarithm of each value was used in the statistical test. Overall, categorical variables were summarized with counts and percentages while continuous variables were summarized using means and standard deviations. The chi-squared test and independent samples *t*-test were used for group comparisons where appropriate. Differences in general characteristics, anthropometric, blood parameters, major

microbial target and SCFA were assessed in accordance to body mass index classification by means of uni- and multivariate analyses controlling by gender or energy, as appropriate. Also, in order to explore the association between the intestinal microbiota and SCFA with BMI, a linear regression was conducted.

Using the program R (version 3.3.1 for Windows), a cluster analysis using the Ward's method was performed in order to classify the participants based on the similarity of the different obesity related factors evaluated (BMI, percentage of fat mass, serum glucose, leptin, MDA, CRP and LDL/HDL ratio). This is a hierarchical cluster technique done on the basis of Euclidean distances; therefore, the centers of clusters are grounded on least squares estimation. Differences in the intake of food groups, macronutrients and some dietary components, including antioxidants, were obtained by means of a multivariate analysis controlling for energy intake. The conventional probability value of 0.05 was used in the interpretation of results to indicate statistical significance.

3. Results

The general characteristics of the sample classified according to BMI are presented in Table 2.

Table 2. General characteristics of the studied population according to BMI.

	Normal Weight BMI $\leq$ 25.0 *n* = 20	**Over Weight BMI 25.0–30.0 *n* = 35**	***p***	**Obesity BMI $\geq$ 30.0 *n* = 13**	***p***
Age (years) [a]	56.4 ± 10.1	51.7 ± 11.7	0.152	47.8 ± 10.2	0.033
Female (%)	80.0	51.4	0.036	53.8	0.110
BMI (kg/m^2) [a]	23.0 ± 1.5	27.5 ± 1.4	<0.001	34.1 ± 2.7	<0.001
Energy intake (Kcal/day) [a]	1958 ± 537	1790 ± 482	0.261	2040 ± 548	0.681
Basal Metabolic rate (Kcal/day) [a]	1280 ± 167	1416 ± 228	<0.001	1548 ± 324	<0.001
Sedentary lifestyle (%)	20.0	17.1	0.792	30.8	0.481
Current smokers (%)	27.8	26.5	0.729	25.0	0.978
Alcohol consumers (%)	70.0	54.3	0.252	61.5	0.614
Body fat (%) [a]	26.2 ± 7.5	35.6 ± 9.3	<0.001	51.7 ± 10.8	<0.001
Blood parameters					
Serum glucose (mg/dL) [a]	97.1 ± 14.2	96.0 ± 9.1	0.711	108 ± 11.1	0.020
Triglycerides (mg/dL) [a]	100 ± 47.8	117 ± 56.9	0.288	147 ± 91.0	0.070
LDL/HDL ratio [a]	2.5 ± 0.8	2.6 ± 0.8	0.869	2.3 ± 0.6	0.347
Leptin (ng/mL) [a]	6.1 ± 4.3	9.2 ± 5.2	0.021	14.7 ± 6.8	<0.001
MDA (μM) [a]	2.1 ± 0.6	2.2 ± 0.9	0.700	3.2 ± 1.6	0.012
CRP (mg/L) [a]	0.9 ± 0.8	3.8 ± 8.4	0.150	5.4 ± 7.4	0.009

[a] Results from univariate analysis were adjusted by gender and presented as mean ± standard deviation. Differences in categorical variables were examined using chi-squared analysis and presented as percentage (%). BMI, body mass index. LDL, low-density lipoprotein. HDL, high-density lipoprotein. MDA, malondialdehyde. CRP, C reactive protein. *p* value was calculated using normal weight volunteers as reference.

As was expected, obese subjects had significantly higher basal metabolic rate, percentage of fat mass, serum glucose, leptin, MDA and CRP than normal weight volunteers. Regarding the fecal microbial composition and the microbial metabolic activity (SCFA), the levels of *Lactobacillus* group and acetate concentrations were directly related with the grade of obesity (Table 3).

To explore whether the fecal microbiota may be related with the pro-oxidant and pro-inflammatory status frequently linked to obesity, subjects were classified into clusters performed by jointly considering values for BMI, fat mass, serum glucose, LDL/HDL ratio, serum leptin, MDA and CRP. This approach established two independent groups of individuals, thereafter referred to as cluster I (n = 38) and cluster II (n = 26) (Figure 1).

Table 3. Differences in fecal short chain fatty acids (SCFA) concentration and major microbial groups according to BMI (kg/m^2) and results of linear regression analyses to estimate their association with BMI.

	Normal Weight **BMI ≤ 25.0** ***n* = 20**	**Over Weight** **BMI 25.0–30.0** ***n* = 31**	**Obesity** **BMI ≥ 30.0** ***n* = 13**	**BMI**		
				R^2	β	*p*
Model 1. Fecal SCFA concentration (mM)						
Acetate	35.7 ± 14.6	38.0 ± 16.8	46.6 ± 17.0	0.081	0.282	0.025
Propionate	14.4 ± 6.5	13.7 ± 6.7	17.1 ± 8.2	0.022	0.136	0.288
Butyrate	11.6 ± 8.7	10.3 ± 6.4	12.3 ± 9.0	0.047	0.040	0.748
Model 2. Microbial target(log n° cells/gram of faeces)						
Akkermansia	6.3 ± 2.2	5.6 ± 1.6	5.6 ± 2.1	0.026	−0.143	0.264
Bacteroides-Prevotella-Porphyromonas	8.8 ± 1.3	8.9 ± 1.1	8.2 ± 1.2	0.067	−0.245	0.052
Bifidobacterium	7.7 ± 2.0	8.2 ± 0.8	8.2 ± 0.7	0.090	0.126	0.305
Clostridia cluster XIVa group	7.7 ± 1.7	8.2 ± 1.3	8.4 ± 1.1	0.048	0.150	0.236
Lactobacillus group	5.7 ± 1.3	6.0 ± 1.1	6.7 ± 0.9 *	0.194	0.256	0.029
Faecalibacterium prausnitzii	7.3 ± 1.0	7.5 ± 1.0	7.7 ± 0.9	0.024	0.152	0.233

Results derived from multivariate analysis are presented as mean ± standard deviation. Variables included in model 1: acetate, propionate, butyrate and energy; model 2: *Akkermansia*, *Bacteroides-Prevotella-Porphyromonas*, *Bifidobacterium*, *Clostridia* cluster XIVa, *Lactobacillus* group, *Faecalibacterium prausnitzii* and energy. Linear regression analyses are adjusted by energy; R^2, coefficient of multiple determination; β, standardized regression coefficient. * $p \leq 0.05$.

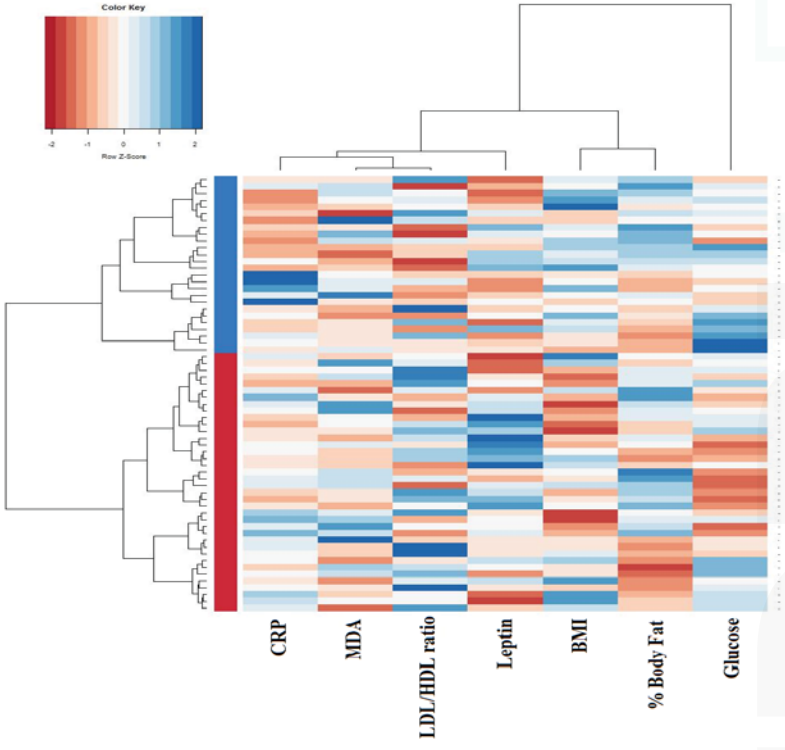

Figure 1. Dendogram clustering based on individual body composition, serum glucose, lipid profile, and oxidative stress biomarkers. The heatmap shows the dendrogram classification for clusters, based on C reactive protein (CRP), malondialdehyde (MDA), LDL/HDL ratio, serum leptin, Body Mass Index (BMI), body fat percentage and serum glucose (columns). Colors in the vertical bar at the left of the heatmap identify Cluster I (red) and Cluster II (blue).

Cluster II was characterized by higher BMI and body fat together with higher concentration of serum glucose, MDA and CRP. The LDL/HDL ratio and serum leptin, however, did not show significant differences between both clusters (Table 4).

Table 4. Differences in the parameters used for cluster analyses.

	Cluster I ***n* = 38**	**Cluster II** ***n* = 26**	***p***
BMI (kg/m^2)	25.2 ± 2.7	30.3 ± 4.3	<0.001
Body fat (%)	30.5 ± 8.0	42.3 ± 13.3	<0.001
Blood parameters			
Serum glucose (mg/dL)	92.7 ± 8.2	108.2 ± 10.9	<0.001
LDL/HDL ratio	2.6 ± 0.8	2.5 ± 0.8	0.921
Leptin (ng/mL)	8.2 ± 5.1	10.8 ± 6.4	0.074
MDA (μM)	2.0 ± 0.6	2.8 ± 1.3	0.001
CRP (mg/L)	0.9 ± 0.9	6.7 ± 10.4	0.001

Univariate analysis was adjusted by gender and presented as mean ± standard deviation. LDL, low-density lipoprotein. HDL, high-density lipoprotein. MDA, malondialdehyde. CRP, C reactive protein.

When we compared the microbiota variables between both groups no significant differences were found for most of the microbial groups and SCFA studied, except for acetate, which displayed higher fecal concentration in cluster II, and the *Bacteroides* group whose levels resulted higher in cluster I (Table 5).

Table 5. Differences in fecal SCFA and major microbial groups between clusters.

	Cluster I ***n* = 37**	**Cluster II** ***n* = 24**
Model 1. Fecal SCFA concentration (mM)		
Acetate	35.8 ± 14.8	44.8 ± 17.7 *
Propionate	14.0 ± 6.7	16.2 ± 7.3
Butyrate	11.1 ± 8.0	11.8 ± 7.7
Model 2. Microbial target (log nº cells/gram of feces)		
Akkermansia	6.0 ± 1.8	5.6 ± 2.2
Bacteroides-Prevotella-Porphyromonas	9.0 ± 1.0	8.3 ± 1.3 *
Bifidobacterium	8.1 ± 0.9	7.9 ± 1.8
Clostridia cluster XIVa group	7.9 ± 1.4	8.2 ± 1.4
Lactobacillus group	6.0 ± 1.1	6.1 ± 1.3
Faecalibacterium prausnitzii	7.4 ± 0.9	7.5 ± 0.9

Results derived from multivariate analysis are presented as mean ± standard deviation. Variables included in model 1: acetate, propionate, butyrate and energy; model 2: *Akkermansia, Bacteroides-Prevotella-Porphyromonas, Bifidobacterium, Clostridia* cluster XIVa, *Lactobacillus* group, *Faecalibacterium prausnitzii* and energy. * $p \leq 0.05$.

With the above information, and in order to evaluate whether differential daily consumption of foods may be related with the pro-oxidant and pro-inflammatory status linked to obesity, food groups and nutrient intake profiles were compared between clusters I and II (Figure 2). Cluster II was characterized by a profile with a higher intake of oils and fats, sweetened foods and sauces and lower intake of fruits, dried fruits, and fish, representative of a Western pattern (Figure 2A). Among nutrients, higher intake of sucrose and lower intake of fiber and total animal protein was observed in individuals from cluster II (Figure 2B,C).

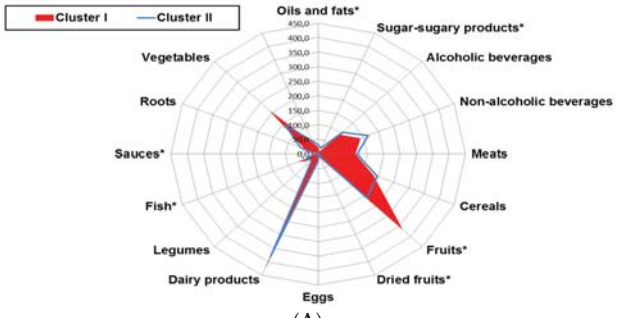

(**A**)

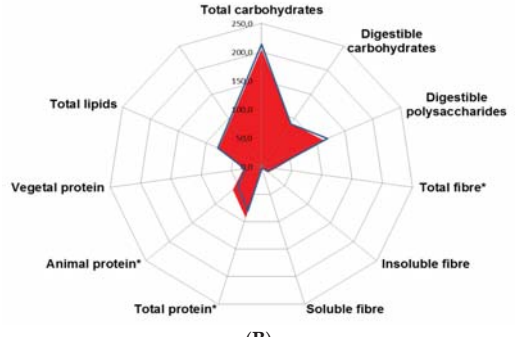

(**B**)

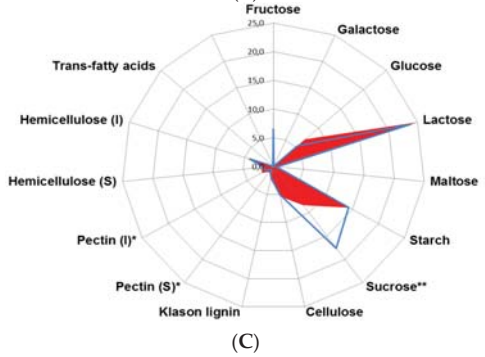

(**C**)

Figure 2. Radar plot representing differences in the daily intake of (**A**) major food groups (g/day); (**B**) macronutrient and fiber (g/day) and (**C**) detailed carbohydrate and fibers (g/day) among clusters. Cluster I (n = 38), Cluster II (n = 26). Multivariate regression analyses were adjusted by energy intake (Kcal/day). * $p \leq 0.05$.

The intake of major antioxidants among clusters was also investigated (Table 6). Subjects from cluster II obtained lower total antioxidant capacity from diet, both for water soluble and fat soluble antioxidant compounds (hydrophilic and lipophilic ORAC, respectively). This group also had lower intake of total carotenoids, vitamin C, total polyphenols and flavonoids than cluster I.

In order to elucidate the role of the fecal microbiota in the observed associations, differences in some biomarkers related to obesity according to the tertiles formed with the fecal levels of *Bacteroides-Prevotella-Porphyromonas* (log nº cells/gram of feces) were assessed (Figure 3). Higher serum concentrations of MDA were found across the tertiles of *Bacteroides-Prevotella-Porphyromonas* in relation with the decrease in abundance of this microbial group.

Table 6. Differences in the intake of the major dietary antioxidants between clusters.

	Cluster I $n = 38$	**Cluster II** $n = 26$	p
ORAC, hydrophilic (μmol TE/day)	10367 ± 6641	6089 ± 4179	0.004
ORAC, lipophilic (μmol TE/day)	244 ± 193	138 ± 103	0.011
ORAC, Total (μmol TE/day)	10609 ± 6790	6229 ± 4224	0.004
Selenium (μg/day)	123 ± 40.3	115 ± 43.6	0.250
Total carotenoids (μg/day)	2391 ± 1538	1660 ± 1001	0.034
γ-Tocopherol (mg/day)	2.6 ± 1.1	2.1 ± 2.2	0.249
Vitamin C (mg/day)	222 ± 196	131 ± 102	0.021
Vitamin E (mg/day)	10.1 ± 4.1	12.7 ± 8.2	0.063
Total polyphenols (mg/day)	2057 ± 1076	1553 ± 975	0.043
Total flavonoids (mg/day)	435 ± 291	303 ± 232	0.049
Total phenolics (mg/day)	198 ± 192	224 ± 236	0.626
Flavanols (mg/day)	222 ± 187	189 ± 194	0.505

Results adjusted by energy derived from multivariate analysis are presented as mean ± standard deviation. ORAC, Oxygen radical absorbance capacity. TE, Trolox equivalents.

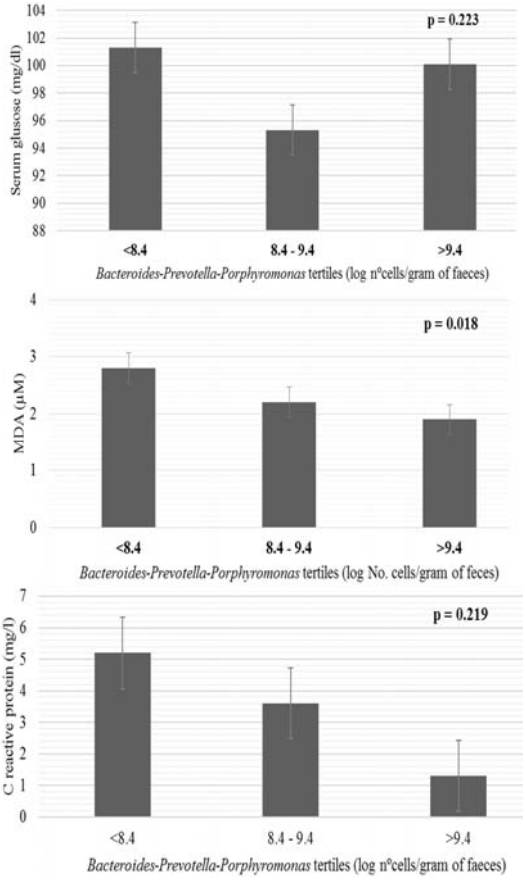

Figure 3. Differences in blood parameters related to obesity according to the levels of *Bacteroides-Prevotella-Porphyromonas* tertiles (log nº cells/gram of feces). Bars represent mean and whiskers standard error derived from univariate analysis adjusted by energy. MDA, malondialdehyde.

4. Discussion

In line with previous evidence from other authors, an association between obesity and higher serum concentrations of leptin [35], MDA [3,36], CRP [3] and glucose was corroborated in our study. However, our work also provides novel insight into the differences found in some intestinal bacterial groups related to BMI and obesity-associated oxidative stress and inflammation in the general population. Furthermore, the identification of different dietary patterns in overweight and obese people, who have a more pro-oxidant and inflammatory status than the normal-weight group, points to the potential interest of designing strategies based on the consideration of the impact of a balanced diet (with high content of antioxidants in comparison with fats and refined sugars) on the microbiota, in order to improve or prevent obesity-associated disorders.

In recent years, hyperleptinemia has also been identified as an independent risk factor for cardiovascular disease and myocardial infarction [37,38] directly linked to inflammation [39] and oxidative stress [3,35]. In the present study, we have found that leptin level increased proportionally with the degree of obesity (Table 2) and is positively correlated with adiposity (Pearson correlation with the percentage of fat mass $r = 0.590$, $p < 0.001$, data not shown), its serum concentration being similar to that previously reported by other authors [40,41]. Higher serum levels of MDA and CRP have been previously reported in obesity and metabolic syndrome [42] and have also linked obesity to alterations in the lipoprotein particles profile as well as to increased lipid peroxidation, during which the MDA is one of the most abundant products formed [43–47]. In this way, our results regarding levels of MDA are in-line with previous findings and the levels of CRP corroborate studies relating to the presence of obesity with chronic low-grade inflammation [48]. In our sample the mean concentrations of MDA and CRP were higher in obese than in overweight and normal-weight groups, however the range observed for MDA was far from the cutoff points associated with increased risk of mortality by different causes [49]. It should be noted in the interpretation of these results that we have excluded people with cancer, autoimmune, or digestive diseases, as these are linked to oxidative stress. Despite the fact that the mechanisms linking oxidative damage to adipose tissue dysfunction remain largely unknown, we suggest that the MDA values determined in this study could reflect the degree of adipose oxidative stress [50]. Moreover, in agreement with our results, an increasing body of evidence supports the notion that diets high in glucose and fats, as occurs in obesity, may activate inflammatory signalling pathways in cells, potentially by increasing oxidative stress [51–54].

In recent years, it has been repeatedly reported that the gut microbiota in obese humans is different to that of lean people, both in terms of diversity and in the relative abundance of the dominant phyla *Bacteroidetes* and *Firmicutes* [55–60]. The different bacterial populations assessed in this study (*Akkermansia, Bacteroides-Prevotella-Porphyromonas, Bifidobacterium, Clostridia* cluster XIVa group (*Lactobacillus* group and *Faecalibacterium prausnitzzi*) represent more than 95% of the overall phylogenetic types of the human intestinal microbiota [8]. Our data identify the microorganisms related to *Lactobacillus* as a potential risk factor related with obesity. This result, that would have been surprising a few years ago, is in good agreement with some recent studies reporting higher levels of *Lactobacillus* in obese children [56] and adults [61]. Despite not reaching statistical significance, our results show a trend towards reduced levels of the *Bacteroides*-group in obese subjects. These observations are in good agreement with the increased Firmicutes/Bacteroidetes ratio [12] and the reduced *Bacteroides* levels repeatedly reported in obese subjects [57,60]. In addition, we found the majority of intestinal SCFA (acetate) to be another risk factor, with its levels increasing with BMI, which is in agreement with the higher levels of SCFA observed in obese subjects by other authors [15]. At this point, and based on the ability of the intestinal microbiota to act as an endocrine organ [50,56] we wonder to what extent this microbial ecosystem could be acting as a link between diet, systemic inflammation, metabolic dysfunction and obesity [62,63].

In this scenario, the traditional statistical analysis which considers the variables independently may be unrealistic when applied to complex biological systems; such is the case with obesity, in which there is a wide range of interrelated variables and mutually supporting disturbances. Therefore,

we have gone one step further by evaluating the differences in the microbiota and dietary levels in those individuals in which different obesity-related factors occur together. The analyses of these obesity-related factors separated the individuals into two clusters. One of them (Cluster II) comprised the obese/over-weight participants showing higher serum concentrations of glucose, MDA and CRP. Interestingly, the negative association between *Bacteroides* and obesity reported previously by other authors [57,60,64] was also identified in our study when individuals were classified in clusters, while the association of *Lactobacillus* with obesity (BMI $\geq$ 30) did not raise statistical significance when also considering oxidative stress and inflammation related parameters.

Both obesity and dietary patterns have been shown to be related to changes in gut microbiota composition [65,66]. Therefore, when analyzing the differences in diets between clusters I and II, it was not surprising that the higher intake of fat and oils and sweetened foods, suggestive of consuming a highly palatable diet, was associated with the presence of a chronic pro-inflammatory and pro-oxidant status linked to overweight and obese subjects from cluster II [67–73]. The mechanisms by which dietary components may produce changes at the microbiota level remain largely unknown. However, considering both our results and the evidence from experimental studies with germ free animals receiving a diet high in fats and sucrose, it is likely that the impact of these foods in obesity and related pathologies is mediated through microbiota modulation [74]. This is supported by the fact that we found an inverse association between the levels of MDA and those of the *Bacteroides* group.

In addition, the reduced intake of fruits, which have a known anti-obesogenic effect, could be also linked to changes in the microbiota composition. Vegetables and fruits were the major dietary sources of pectin in our cohort [23] which can be metabolized in the colon by bacteria such as *Bacteroides* resulting in the production of SCFA [75] that may exert different beneficial effects on the host [76]. Moreover, in our studied population, vegetables and fruits were also the main sources of vitamin C and carotenoids, compounds that have a known anti-inflammatory activity and also provide other bioactive compounds, such as polyphenols, that are involved in the regulation of some metabolic conditions linked to obesity [77,78] and inflammation [78]. Considering these preliminary results, we hypothesize that the *Bacteroides* group could act as a mediator in antioxidant metabolism, playing a key role in some of the health effects attributed to these compounds.

The limited sample size of this study may have somewhat hampered our ability to detect other significant associations. Moreover, although FFQ is the most suitable tool to describe long-term habits, its ability to accurately quantify the dietary intake is limited. In addition, fecal SCFA measurements comprise only the 5% to 10% that is not absorbed in the colon [75]. These facts underline the difficulty of drawing firm conclusions from the studies conducted in this area of research.

Acknowledgments: This work was funded through the Grant GRUPIN14-043 "Microbiota Humana, Alimentación y Salud" funded by "Plan Regional de Investigación del Principado de Asturias", Spain, by grants AGL2010-14952 from Spanish "Plan Nacional I + D + I", by Biopolis group S.L., Valencia, within the framework of the e-CENIT Project SENIFOOD from the Spanish Ministry of Science and Innovation, and by the Alimerka Foundation. NS was the recipient of a postdoctoral contract supported by a Clarin regional grant (ACB 14-08) cofinanced by the Marie Curie CoFund European Program and IG-D benefits for a grant supported by Fundación Universia. Regional and national grants received cofounding from European Union FEDER funds. We show our greatest gratitude to all the volunteers participating in the study.

Author Contributions: S.G. performed most of the experimental procedures. T.F.-N., I.G.-D. and S.G. were involved in the nutritional assessments, anthropometrical measurements and collection of samples. N.S., M.G., C.G.d.l.R.-G. and S.G. provided biological samples, performed microbiological analyses and financial support. T.F.-N., I.G.-D. and S.G. drafted the manuscript. All authors participated in the study design and data interpretation, reviewed the manuscript and approved the final version.

Conflicts of Interest: The authors declared no potential competing financial interests concerning this study. Funders had no role in study conception, design, analysis of the results or decision to publish.

References

1. Becer, E.; Cirakoglu, A. Association of the Ala16Val MnSOD gene polymorphism with plasma leptin levels and oxidative stress biomarkers in obese patients. *Gene* **2015**, *568*, 35–39. [CrossRef] [PubMed]

2. Furukawa, S.; Fujita, T.; Shimabukuro, M.; Iwaki, M.; Yamada, Y.; Nakajima, Y.; Nakayama, O.; Makishima, M.; Matsuda, M.; Shimomura, I. Increased oxidative stress in obesity and its impact on metabolic syndrome. *J. Clin. Investig.* **2004**, *114*, 1752–1761. [CrossRef] [PubMed]
3. Hopps, E.; Noto, D.; Caimi, G.; Averna, M.R. A novel component of the metabolic syndrome: The oxidative stress. *Nutr. Metab. Cardiovasc. Dis.* **2010**, *20*, 72–77. [CrossRef] [PubMed]
4. Vincent, H.K.; Taylor, A.G. Biomarkers and potential mechanisms of obesity-induced oxidant stress in humans. *Int. J. Obes.* **2006**, *30*, 400–418. [CrossRef] [PubMed]
5. Pego-Fernandes, P.M.; Bibas, B.J.; Deboni, M. Obesity: The greatest epidemic of the 21st century? *Sao Paulo Med. J.* **2011**, *129*, 283–284. [CrossRef] [PubMed]
6. Sonnenburg, E.D.; Smits, S.A.; Tikhonov, M.; Higginbottom, S.K.; Wingreen, N.S.; Sonnenburg, J.L. Diet-induced extinctions in the gut microbiota compound over generations. *Nature* **2016**, *529*, 212–215. [CrossRef] [PubMed]
7. Sonnenburg, J.L.; Xu, J.; Leip, D.D.; Chen, C.H.; Westover, B.P.; Weatherford, J.; Buhler, J.D.; Gordon, J.I. Glycan foraging in vivo by an intestine-adapted bacterial symbiont. *Science* **2005**, *307*, 1955–1959. [CrossRef] [PubMed]
8. Yatsunenko, T.; Rey, F.E.; Manary, M.J.; Trehan, I.; Dominguez-Bello, M.G.; Contreras, M.; Magris, M.; Hidalgo, G.; Baldassano, R.N.; Anokhin, A.P.; et al. Human gut microbiome viewed across age and geography. *Nature* **2012**, *486*, 222–227. [CrossRef] [PubMed]
9. Broussard, J.L.; Devkota, S. The changing microbial landscape of Western society: Diet, dwellings and discordance. *Mol. Metab.* **2016**, *5*, 737–742. [CrossRef] [PubMed]
10. De Filippis, F.; Pellegrini, N.; Vannini, L.; Jeffery, I.B.; La Storia, A.; Laghi, L.; Serrazanetti, D.I.; Di Cagno, R.; Ferrocino, I.; Lazzi, C.; et al. High-level adherence to a Mediterranean diet beneficially impacts the gut microbiota and associated metabolome. *Gut* **2015**. [CrossRef] [PubMed]
11. Haro, C.; Montes-Borrego, S.M.; Rangel-Zúñiga, O.A.; Alcalá-Díaz, J.F.; Gómez-Delgado, F.; Pérez-Martínez, P.; Delgado-Lista, J.; Quintana-Navarro, G.M.; Tinahones, F.J.; Landa, B.B.; et al. Two healthy diets modulate gut microbial community improving insulin sensitivity in a human obese population. *J. Clin. Endocrinol. Metab.* **2016**, *101*, 233–242. [CrossRef] [PubMed]
12. De los Reyes-Gavilán, C.G.; Delzenne, N.M.; González, S.; Gueimonde, M.; Salazar, N. Development of functional foods to fight against obesity: Opportunities for probiotics and prebiotics. *Agro FOOD Ind. Hi Tech.* **2014**, *25*, 35–39.
13. Ley, R.E.; Backhed, F.; Turnbaugh, P.; Lozupone, C.A.; Knight, R.D.; Gordon, J.I. Obesity alters gut microbial ecology. *Proc. Natl. Acad. Sci. USA* **2005**, *102*, 11070–11075. [CrossRef] [PubMed]
14. Turnbaugh, P.J.; Backhed, F.; Fulton, L.; Gordon, J.I. Diet-induced obesity is linked to marked but reversible alterations in the mouse distal gut microbiome. *Cell Host Microbe* **2008**, *3*, 213–223. [CrossRef] [PubMed]
15. Samuel, B.S.; Shaito, A.; Motoike, T.; Rey, F.E.; Backhed, F.; Manchester, J.K.; Hammer, R.E.; Williams, S.C.; Crowley, J.; Yanagisawa, M.; et al. Effects of the gut microbiota on host adiposity are modulated by the short-chain fatty-acid binding G protein-coupled receptor, Gpr41. *Proc. Natl. Acad. Sci. USA* **2008**, *105*, 16767–16772. [CrossRef] [PubMed]
16. Den Besten, G.; van Eunen, K.; Groen, A.K.; Venema, K.; Reijngoud, D.J.; Bakker, B.M. The role of short-chain fatty acids in the interplay between diet, gut microbiota, and host energy metabolism. *J. Lipid Res.* **2013**, *54*, 2325–2340. [CrossRef] [PubMed]
17. Schwiertz, A.; Taras, D.; Schafer, K.; Beijer, S.; Bos, N.A.; Donus, C.; Hardt, P.D. Microbiota and SCFA in lean and overweight healthy subjects. *Obesity* **2010**, *18*, 190–195. [CrossRef] [PubMed]
18. Clarke, G.; Stilling, R.M.; Kennedy, P.J.; Stanton, C.; Cryan, J.F.; Dinan, T.G. Minireview: Gut microbiota: The neglected endocrine organ. *Mol. Endocrinol.* **2014**, *28*, 1221–1238. [CrossRef] [PubMed]
19. Turnbaugh, P.J.; Ley, R.E.; Mahowald, M.A.; Magrini, V.; Mardis, E.R.; Gordon, J.I. An obesity-associated gut microbiome with increased capacity for energy harvest. *Nature* **2006**, *444*, 1027–1031. [CrossRef] [PubMed]
20. Den Besten, G.; Havinga, R.; Bleeker, A.; Rao, S.; Gerding, A.; van Eunen, K.; Groen, A.K.; Reijngoud, D.; Bakker, B.M. The short-chain fatty acid uptake fluxes by mice on a guar gum supplemented diet associate with amelioration of major biomarkers of the metabolic syndrome. *PLoS ONE* **2014**, *9*, e107392. [CrossRef] [PubMed]
21. Lean, M.E.; Malkova, D. Altered gut and adipose tissue hormones in overweight and obese individuals: Cause or consequence? *Int. J. Obes.* **2016**, *40*, 622–632. [CrossRef] [PubMed]

22. Salas-Salvadó, J.; Rubio, M.A.; Barbany, M.; Moreno, B. SEEDO 2007 Consensus for the evaluation of overweight and obesity and the establishment of therapeutic intervention criteria. *Med. Clin.* **2007**, *128*, 184–196. [CrossRef]
23. Cuervo, A.; Valdés, L.; Salazar, N.; de los Reyes-Gavilán, C.G.; Ruas-Madiedo, P.; Gueimonde, M.; González, S. Pilot study of diet and microbiota: Interactive associations of fibers and polyphenols with human intestinal bacteria. *J. Agric. Food Chem.* **2014**, *62*, 5330–5336. [CrossRef] [PubMed]
24. Cuervo, A.; Hevia, A.; López, P.; Suárez, A.; Sánchez, B.; Margolles, A.; González, S. Association of polyphenols from oranges and apples with specific intestinal microorganisms in systemic lupus erythematosus patients. *Nutrients* **2015**, *7*, 1301–1317. [CrossRef] [PubMed]
25. Centro de Enseñanza Superior de Nutrición Humana y Dietética (CESNID). *Tablas de Composición de Alimentos por Medidas Caseras de Consumo Habitual en España*; McGraw-Hill, Plublicaciones y Ediciones de la Universidad de Barcelona: Barcelona, Spain, 2008.
26. United States Department of Agriculture (USDA). Agriculture Research Service, 2016 USDA National Nutrient Database for Standard References. Available online: http://www.ars.usda.gov/services/docs.htm?docid=8964 (accessed on 15 March 2017).
27. Marlett, J.A.; Cheung, T.F. Database and quick methods of assessing typical dietary fiber intakes using data for 228 commonly consumed foods. *J. Am. Diet. Assoc.* **1997**, *97*, 1139–1151. [CrossRef]
28. Neveu, V.; Perez-Jiménez, J.; Vos, F.; Crespy, V.; Chaffaut, L.D.; Mennen, L.; Knox, C.; Eisner, R.; Cruz, J.; Wishart, D.; et al. Phenol-Explorer: An online comprehensive database on polyphenol contents in foods. *Database Oxf.* **2010**, bap024. [CrossRef] [PubMed]
29. United States Department of Agriculture (USDA). Database for the Oxigen Radical Absorbance Capacity (ORAC) of Selected Foods. U.S. Dep. Agric, 2017. Available online: http://www.ars.usda.gov/ba/bhnrc/ndl (accessed on 14 March 2017).
30. Harris, J.A.; Benedict, F.G. A biometric study of human basal metabolism. *Proc. Natl. Acad. Sci. USA* **1918**, *4*, 370–373. [CrossRef] [PubMed]
31. Gerard-Monnier, D.; Erdelmeier, I.; Regnard, K.; Moze-Henry, N.; Yadan, J.C.; Chaudiere, J. Reactions of 1-methyl-2-phenylindole with malondialdehyde and 4-hydroxyalkenals. Analytical applications to a colorimetric assay of lipid peroxidation. *Chem. Res. Toxicol.* **1998**, *11*, 1176–1183. [CrossRef] [PubMed]
32. Arboleya, S.; Binetti, A.; Salazar, N.; Fernández, N.; Solis, G.; Hernández-Barranco, A.; Margolles, A.; de los Reyes-Gavilán, C.G.; Gueimonde, M. Establishment and development of intestinal microbiota in preterm neonates. *FEMS Microbiol. Ecol.* **2012**, *79*, 763–772. [CrossRef] [PubMed]
33. Ramirez-Farias, C.; Slezak, K.; Fuller, Z.; Duncan, A.; Holtrop, G.; Louis, P. Effect of inulin on the human gut microbiota: Stimulation of Bifidobacterium adolescentis and Faecalibacterium prausnitzii. *Br. J. Nutr.* **2009**, *101*, 541–550. [CrossRef] [PubMed]
34. Salazar, N.; Gueimonde, M.; Hernández-Barranco, A.M.; Ruas-Madiedo, P.; de los Reyes-Gavilán, C.G. Exopolysaccharides produced by intestinal Bifidobacterium strains act as fermentable substrates for human intestinal bacteria. *Appl. Environ. Microbiol.* **2008**, *74*, 4737–4745. [CrossRef] [PubMed]
35. Pandey, G.; Shihabudeen, M.S.; David, H.P.; Thirumurugan, E.; Thirumurugan, K. Association between hyperleptinemia and oxidative stress in obese diabetic subjects. *J. Diabetes Metab. Disord.* **2015**, *14*, 24. [CrossRef] [PubMed]
36. Lee, S.M.; Cho, Y.H.; Lee, S.Y.; Jeong, D.W.; Cho, A.R.; Jeon, J.S.; Park, E.J.; Kim, Y.J.; Lee, J.G.; Yi, Y.H.; et al. Urinary malondialdehyde is associated with visceral abdominal obesity in middle-aged men. *Mediat. Inflamm.* **2015**, *2015*, 524291. [CrossRef] [PubMed]
37. Gundala, R.; Chava, V.K.; Ramalingam, K. Association of leptin in periodontitis and acute myocardial infarction. *J. Periodontol.* **2014**, *85*, 917–924. [CrossRef] [PubMed]
38. Karbowska, J.; Kochan, Z. Leptin as a mediator between obesity and cardiac dysfunction. *Postepy Hig. Med. Dosw.* **2012**, *66*, 267–274. [CrossRef]
39. Paepegaey, A.C.; Genser, L.; Bouillot, J.C.; Oppert, J.M.; Clément, K.; Poitou, C. High levels of CRP in morbid obesity: The central role of adipose tissue and lessons for clinical practice before and after bariatric surgery. *Surg. Obes. Relat. Dis.* **2015**, *11*, 148–154. [CrossRef] [PubMed]
40. Havel, P.J.; Kasim-Karakas, S.; Dubuc, G.R.; Mueller, W.; Phinney, S.D. Gender differences in plasma leptin concentrations. *Nat. Med.* **1996**, *2*, 949–950. [CrossRef] [PubMed]

41. Saad, M.F.; Riad-Gabriel, M.G.; Khan, A.; Sharma, A.; Michael, R.; Jinagouda, S.D.; Boyadjian, R.; Steil, G.M. Diurnal and ultradian rhythmicity of plasma leptin: Effects of gender and adiposity. *J. Clin. Endocrinol. Metab.* **1998**, *83*, 453–459. [CrossRef] [PubMed]
42. Piccoli de Melo, L.G.; Vargas Nunes, S.O.; Anderson, G.; Vargas, H.O.; Barbosa, D.S.; Galecki, P.; Carvalho, A.F.; Maes, M. Shared metabolic and immune-inflammatory, oxidative and nitrosative stress pathways in the metabolic syndrome and mood disorders. *Prog Neuro-Psychopharmacol. Biol. Psychiatry* **2017**, *17*. [CrossRef]
43. Solomon, C.G.; Manson, J.E. Obesity and mortality: A review of the epidemiologic data. *Am. J. Clin. Nutr.* **1997**, *66*, 1044–1050.
44. World Health Organisation. *Obesity: Preventing and Managing the Global Epidemic*; Report of a WHO Consultation. WHO Technical Report Series 894, World Health Organization Technical Report Series; World Health Organisation: Geneva, Switzerland, 2000; Volume 894.
45. He, Q.R.; Yu, T.; Fau-Li, P.; Li, P. Association of oxidative stress and serum adiponectine in patients with metabolic syndrome. *Sichuan Da Xue Xue Bao Yi Xue Ban* **2009**, *40*, 623–627. [PubMed]
46. Maes, M.; Ruckoanich, P.; Fau-Chang, Y.S.; Chang, Y.S.; Fau-Mahanonda, N.; Mahanonda, N.; Fau-Berk, M.; Berk, M. Multiple aberrations in shared inflammatory and oxidative & nitrosative stress (IO&NS) pathways explain the co-association of depression and cardiovascular disorder (CVD), and the increased risk for CVD and due mortality in depressed patients. *Prog. Neuro-Psychopharmacol. Biol. Psychiatry* **2011**, *35*, 769–783.
47. Sankhla, M.; Sharma, T.K.; Fau-Mathur, K.; Mathur, K.; Fau-Rathor, J.S.; Rathor, J.S.; Fau-Butolia, V.; Butolia, V.; Fau-Gadhok, A.K.; Gadhok, A.K.; et al. Relationship of oxidative stress with obesity and its role in obesity induced metabolic syndrome. *Clin. Lab.* **2012**, *58*, 385–392. [PubMed]
48. Illán-Gómez, F.; Gonzálvez-Ortega, M.; Aragón-Alonso, A.; Orea-Soler, I.; Alcatraz-Tafalla, M.S.; Pérez-Paredes, M.; Lozano-Almeda, M.L. Obesity, endothelial function and inflammation: The effects of weight loss after bariatric surgery. *Nutr. Hosp.* **2016**, *33*, 1340–1346. [CrossRef] [PubMed]
49. Proctor, P.H.; Reynolds, E.S. Free radicals and disease in man. *Physiol. Chem. Phys. Med. NMR* **1984**, *16*, 175–195. [PubMed]
50. Murdolo, G.; Piroddi, M.; Luchetti, F.; Tortoioli, C.; Canonico, B.; Zerbinati, C.; Galli, F.; Iuliano, L. Oxidative stress and lipid peroxidation by-products at the crossroad between adipose organ dysregulation and obesity-linked insulin resistance. *Biochimie* **2013**, *95*, 585–594. [CrossRef] [PubMed]
51. Gregor, M.F.; Hotamisligil, G.S. Inflammatory mechanisms in obesity. *Annu. Rev. Immunol.* **2011**, *29*, 415–445. [CrossRef] [PubMed]
52. Belza, A.; Toubro, S.; Stender, S.; Astrup, A. Effect of diet-induced energy deficit and body fat reduction on high-sensitive CRP and other inflammatory markers in obese subjects. *Int. J. Obes.* **2009**, *33*, 456–464. [CrossRef] [PubMed]
53. Aljada, A.; Mohanty, P.; Ghanim, H.; Abdo, T.; Tripathy, D.; Chaudhuri, A.; Dandona, P. Increase in intranuclear nuclear factor κB and decrease in inhibitor κB inmononuclear cells after a mixed meal: Evidence for a proinflammatory effect. *Am. J. Clin. Nutr.* **2004**, *79*, 682–690. [PubMed]
54. Dalmas, E.; Rouault, C.; Abdennour, M.; Rovere, C.; Rizkalla, S.; Bar-Hen, A.; Nahon, J.L.; Bouillot, J.L.; Guerre-Millo, M.; Clément, K.; et al. Variations in circulating inflammatory factors are related to changes in calorie and carbohydrate intakes early in the course of surgery-induced weight reduction. *Am. J. Clin. Nutr.* **2011**, *94*, 450–458. [CrossRef] [PubMed]
55. Abdallah, I.N.; Ragab, S.H.; Abd, E.A.; Shoeib, A.R.; Alhosary, Y.; Fekry, D. Frequency of *Firmicutes* and *Bacteroidetes* in gut microbiota in obese and normal weight Egyptian children and adults. *Arch. Med. Sci.* **2011**, *7*, 501–507.
56. Bervoets, L.; Van, H.K.; Kortleven, I.; Van, N.C.; Hens, N.; Vael, C.; Goossens, H.; Desager, K.N.; Vankerckhoven, V. Differences in gut microbiota composition between obese and lean children: A cross-sectional study. *Gut Pathog.* **2013**, *5*, 10. [CrossRef] [PubMed]
57. Duca, F.A.; Sakar, Y.; Lepage, P.; Devime, F.; Langelier, B.; Dore, J.; Covasa, M. Replication of obesity and associated signaling pathways through transfer of microbiota from obese-prone rats. *Diabetes* **2014**, *63*, 1624–1636. [CrossRef] [PubMed]
58. Harris, K.; Kassis, A.; Major, G.; Chou, C.J. Is the gut microbiota a new factor contributing to obesity and its metabolic disorders? *J. Obes.* **2012**, *2012*, 879151. [PubMed]

59. Hartstra, A.V.; Bouter, K.E.; Backhed, F.; Nieuwdorp, M. Insights into the role of the microbiome in obesity and type 2 diabetes. *Diabetes Care* **2015**, *38*, 159–165. [CrossRef] [PubMed]
60. Park, J.S.; Seo, J.H.; Youn, H.S. Gut microbiota and clinical disease: Obesity and nonalcoholic fatty liver disease. *Pediatr. Gastroenterol. Hepatol. Nutr.* **2013**, *16*, 22–27. [CrossRef] [PubMed]
61. Million, M.; Maraninchi, M.; Henry, M.; Armougom, F.; Richet, H.; Carrieri, P.; Valero, R.; Raccah, D.; Vialettes, B.; Raoult, D. Obesity-associated gut microbiota is enriched in *Lactobacillus* reuteri and depleted in *Bifidobacterium animalis* and *Methanobrevibacter smithii*. *Int. J. Obes.* **2012**, *36*, 817–825. [CrossRef] [PubMed]
62. Escobedo, G.; López-Ortíz, E.; Torres-Castro, I. Gut microbiota as a key player in triggering obesity, systemic inflammation and insulin resistance. *Rev. Investig. Clin.* **2014**, *66*, 450–459.
63. Sanz, Y.; Santacruz, A.; Gauffin, P. Gut microbiota in obesity and metabolic disorders. *Proc. Nutr. Soc.* **2010**, *69*, 434–441. [CrossRef] [PubMed]
64. Chakraborti, C.K. New-found link between microbiota and obesity. *World J. Gastrointest. Pathophysiol.* **2015**, *6*, 110–119. [CrossRef] [PubMed]
65. David, L.A.; Maurice, C.F.; Carmody, R.N.; Gootenberg, D.B.; Button, J.E.; Wolfe, B.E.; Ling, A.V.; Devlin, A.S.; Varma, Y.; Fischbach, M.A.; et al. Diet rapidly and reproducibly alters the human gut microbiome. *Nature* **2014**, *505*, 559–563. [CrossRef] [PubMed]
66. Turnbaugh, P.J.; Ridaura, V.K.; Faith, J.J.; Rey, F.E.; Knight, R.; Gordon, J.I. The effect of diet on the human gut microbiome: A metagenomic analysis in humanized gnotobiotic mice. *Sci. Transl. Med.* **2009**, *1*, 6ra14. [CrossRef] [PubMed]
67. Da, R.R.; Assaloni, R.; Ceriello, A. Postprandial hyperglycemia and diabetic complications. *Recenti Prog. Med.* **2005**, *96*, 436–444.
68. Hennig, B.; Toborek, M.; McClain, C.J. High-energy diets, fatty acids and endothelial cell function: Implications for atherosclerosis. *J. Am. Coll. Nutr.* **2001**, *20*, 97–105. [CrossRef] [PubMed]
69. Klop, B.; Proctor, S.D.; Mamo, J.C.; Botham, K.M.; Castro, C.M. Understanding postprandial inflammation and its relationship to lifestyle behaviour and metabolic diseases. *Int. J. Vasc. Med.* **2012**, *2012*, 947417. [CrossRef] [PubMed]
70. Nappo, F.; Esposito, K.; Cioffi, M.; Giugliano, G.; Molinari, A.M.; Paolisso, G.; Marfella, R.; Giugliano, D. Postprandial endothelial activation in healthy subjects and in type 2 diabetic patients: Role of fat and carbohydrate meals. *J. Am. Coll. Cardiol.* **2002**, *39*, 1145–1150. [CrossRef]
71. Ong, P.J.; Dean, T.S.; Hayward, C.S.; Della Monica, P.L.; Sanders, T.A.; Collins, P. Effect of fat and carbohydrate consumption on endothelial function. *Lancet* **1999**, *354*, 2134. [CrossRef]
72. Roberts, C.K.; Barnard, R.J.; Sindhu, R.K.; Jurczak, M.; Ehdaie, A.; Vaziri, N.D. Oxidative stress and dysregulation of NAD(P)H oxidase and antioxidant enzymes in diet-induced metabolic syndrome. *Metabolism* **2006**, *55*, 928–934. [CrossRef] [PubMed]
73. Wallace, J.P.; Johnson, B.; Padilla, J.; Mather, K. Postprandial lipaemia, oxidative stress and endothelial function: A review. *Int. J. Clin. Pract.* **2010**, *64*, 389–403. [CrossRef] [PubMed]
74. Sonnenburg, J.L.; Backhed, F. Diet-microbiota interactions as moderators of human metabolism. *Nature* **2016**, *535*, 56–64. [CrossRef] [PubMed]
75. Topping, D.L.; Clifton, P.M. Short-chain fatty acids and human colonic function: Roles of resistant starch and nonstarch polysaccharides. *Physiol. Rev.* **2001**, *81*, 1031–1064. [PubMed]
76. Ríos-Covián, D.; Ruas-Madiedo, P.; Margolles, A.; Gueimonde, M.; de los Reyes-Gavilán, C.G.; Salazar, N. Intestinal short chain fatty acids and their link with diet and human health. *Front. Microbiol.* **2016**, *7*, 185. [CrossRef] [PubMed]
77. Boque, N.; Campion, J.; de la Iglesia, R.; de la Garza, A.L.; Milagro, F.I.; San, R.B.; Banuelos, O.; Martínez, J.A. Screening of polyphenolic plant extracts for anti-obesity properties in Wistar rats. *J. Sci. Food Agric.* **2013**, *93*, 1226–1232. [CrossRef] [PubMed]
78. Shen, C.L.; Cao, J.J.; Dagda, R.Y.; Chanjaplammootil, S.; Lu, C.; Chyu, M.C.; Gao, W.; Wang, J.S.; Yeh, J.K. Green tea polyphenols benefits body composition and improves bone quality in long-term high-fat diet-induced obese rats. *Nutr. Res.* **2012**, *32*, 448–457. [CrossRef] [PubMed]

nutrients

MDPI

Article

Curcumin Anti-Apoptotic Action in a Model of Intestinal Epithelial Inflammatory Damage

Claudia Loganes [1], Sara Lega [2], Matteo Bramuzzo [1], Liza Vecchi Brumatti [1], Elisa Piscianz [2], Erica Valencic [1], Alberto Tommasini [1] and Annalisa Marcuzzi [2,*]

[1] Department of Paediatrics, Institute for Maternal and Child Health, IRCCS Burlo Garofolo, Via dell'Istria 65/1, Trieste 34137, Italy; claudia.loganes@gmail.com (C.L.); matteo.bramuzzo@burlo.trieste.it (M.B.); liza.vecchibrumatti@burlo.trieste.it (L.V.B.); erica.valencic@burlo.trieste.it (E.V.); alberto.tommasini@burlo.trieste.it (A.T.)

[2] Department of Medicine, Surgery, and Health Sciences, University of Trieste, Strada di Fiume, 447, Trieste 34100, Italy; saralega83@gmail.com (S.L.); elisa.piscianz@burlo.trieste.it (E.P.)

* Correspondence: annalisa.marcuzzi@burlo.trieste.it; Tel.: +39-040-3785422

Received: 24 April 2017; Accepted: 1 June 2017; Published: 6 June 2017

Abstract: The purpose of this study is to determine if a preventive treatment with curcumin can protect intestinal epithelial cells from inflammatory damage induced by IFNγ. To achieve this goal we have used a human intestinal epithelial cell line (HT29) treated with IFNγ to undergo apoptotic changes that can reproduce the damage of intestinal epithelia exposed to inflammatory cytokines. In this model, we measured the effect of curcumin (curcuminoid from *Curcuma Longa*) added as a pre-treatment at different time intervals before stimulation with IFNγ. Curcumin administration to HT29 culture before the inflammatory stimulus IFNγ reduced the cell apoptosis rate. This effect gradually declined with the reduction of the curcumin pre-incubation time. This anti-apoptotic action by curcumin pre-treatment was paralleled by a reduction of secreted IL7 in the HT29 culture media, while there was no relevant change in the other cytokine levels. Even though curcumin pre-administration did not impact the activation of the NF-κB pathway, a slight effect on the phosphorylation of proteins in this inflammatory signaling pathway was observed. In conclusion, curcumin pre-treatment can protect intestinal cells from inflammatory damage. These results can be the basis for studying the preventive role of curcumin in inflammatory bowel diseases.

Keywords: curcumin; epithelial cell line; intestinal inflammation; apoptosis; cytokines

1. Introduction

Chronic inflammation in inflammatory bowel disease (IBD) results from an inappropriate response to intestinal microbes in a genetically-susceptible host [1].

The incidence of IBD is increasing worldwide, and this increase seems to be more rapid in areas of the world that are experiencing a rapid socioeconomic transformation, particularly from low-income, rural to high-income, urbanized countries [2]. This epidemiological data, together with the observation that children of immigrants moving from countries with a low incidence of IBD to countries with high incidence have the same risk of developing IBD as the population of the country of immigration, indicate that environmental factors may play a major role in determining the risk of the disease [3].

Among the environmental factors, the role of diet gained a large amount of attention, and various substances in food have been found to influence the composition of gut microbiota, as well as the mucosal permeability and immune function within the gut [4]. Restrictive diets have a therapeutic role in pediatric Crohn's disease (CD). Exclusive enteral nutrition (EEN) with elemental and semi-elemental formulas are the most widely studied restrictive diet which, in clinical trials in children with CD, proved to reduce clinical disease activity and improve mucosal inflammation [5].

The role of dietary supplements known for their anti-inflammatory properties such as vitamin D, soluble fibers, and long chain fatty acid have also been investigated both in animal models and clinical studies, and some evidence exists to suggest a potential protective role against the development or progression of gut inflammation [6].

Preventive dietary intervention may be critical, particularly in children, considered that there is a trend toward an earlier onset of IBD in Western countries.

Curcuma Longa, also known as turmeric, is a perennial plant of the ginger family widely cultivated in Southern Asia. The root powder of *Curcuma Longa* is widely used for culinary purposes and in traditional medicine, mostly in Asia. The best-studied component of this plant is curcumin, which usually represents about 3% of turmeric powder. Curcumin has several pharmacological properties, including anti-inflammatory, anti-microbial, and anti-tumorigenic activities which seem all to be related to the ability of curcumin to modulate the expression of molecules involved in the inflammatory cascade and programmed cell death [7,8]. The role of curcumin in IBD has been investigated in two small, randomized, placebo-controlled trials where curcumin was given in association with a 5-aminosalicylic acid (5-ASA) compound to induce and maintain remission in patients with mild to moderate ulcerative colitis (UC). In both studies, the association of curcumin to 5-ASA was superior to the 5-ASA alone in inducing and maintaining clinical and endoscopic remission [9,10].

The effects of curcumin in gut inflammation has been studied both in mouse and human models providing a rationale for the possible beneficial role of curcumin use in IBD.

Preclinical studies in cellular and animal models showed that curcumin can modulate the inflammatory cytokine cascade and the vascular adhesion molecule expression and inhibit the nuclear factor-kappa B (NF-κB) [11]. Recently Midura-Kiela et al. found that, in human and mouse colonocytes, curcumin reduces the expression of IFNγ, one of the most prominent proinflammatory cytokines which drives a cascade of events that are thought to contribute to the pathogenesis of IBD [12].

In mouse models of colitis induced by chemicals, curcumin administration before the chemical insult exerted a protective effect limiting the histopathological damage and the activation of the inflammatory cascade [13–15].

In this study, we investigated the effect of curcumin pre-administration on human intestinal cells exposed to IFNγ as a proinflammatory insult.

We used the human colorectal adenocarcinoma cell line HT29. HT29 is a model of intestinal epithelium susceptible to the damage induced by inflammatory cytokines, such as IFNγ and TNFα which represent a suitable in vitro model to study the effect of inflammation on intestinal epithelia [16,17].

Increased apoptosis of epithelial cells is a well-known pathological feature in IBD. In particular, colonic biopsies of subjects with UC typically show increased apoptosis in crypt epithelial cells [18,19]; an increased enterocyte apoptosis is a common finding also in CD [20]. Of note, anti-inflammatory treatments also downregulate epithelial apoptosis [21]. This is particularly important if we consider that epithelial cell apoptosis can lead to barrier dysfunction and amplification of disease. Taken together, these data highlight the role of epithelial cells apoptosis in IBD.

It is commonly assumed that curcumin exerts its action through antioxidant and anti-apoptotic effects [22–24]. However, other authors recently claimed that chemical properties of curcumin could have interfered with in vitro experiments in most studies, raising doubts on the beneficial effect of this substance [25]. To obtain more robust data, we analyzed the anti-apoptotic properties of curcumin by exploiting different methods including label-free measures.

The primary aim of this study was to investigate whether pre-treatment with curcumin can prevent the development of apoptosis in HT29 cells treated with IFNγ. Apoptosis and cell death were measured by classical methods, such as flow cytometry, MTT assay, but also by more innovative label-free instrumentation measuring the change in impedance due to the adherent cells on the surface of the plate well.

In addition, we assessed if the action of curcumin on IFNγ-induced apoptosis is associated with a modulation of NF-κB signaling and inflammatory cytokine production [8,26,27].

We showed that pretreatment with curcumin 24 h before the administration of IFNγ can downregulate apoptosis in intestinal epithelial cells. Further studies will address whether curcumin anti-apoptotic properties may have a possible role in IBD prevention and treatment.

2. Materials and Methods

2.1. Cell Culture and Experimental Design

HT29 cells (human colorectal adenocarcinoma cell line), obtained from Sigma Aldrich (Sigma Aldrich, St. Louis, MO, USA) were cultured in Roswell Park Memorial Institute medium (RPMI) supplemented with 10% fetal bovine serum (FBS), 2 mM L-glutamine, 100 U/mL penicillin, and 0.1 mg/mL streptomycin (all from EuroClone, Milano, Italy). HT29 cells were seeded in different well plates, depending on the experimental needs, at a density of about 80,000–90,000/cm^2.

Forty-eight hours after seeding, cells were stimulated with 100 U/mL IFNγ (Interferon Gamma 1b, Imukin, Boehringer Ingelheim, Milano, Italy) as inflammatory stimulus. To investigate the protective effect of curcumin, HT29 cells were pre-incubated with 1 μM curcumin (derived from *Curcuma Longa*, Sigma Aldrich) at different time intervals: 24, 12, 6, 4, 2, or 0 h before the IFNγ treatment. Curcumin alone, without any inflammatory stimulus, was also added to the cells to evaluate the effect on cell status. At 96 h of culture, after 48 h from the addition of IFNγ, cells were harvested for analysis. The experimental design is reproduced graphically in Figure 1. Curcumin was dissolved and solubilized in 100% ethanol (Sigma Aldrich). The final concentration of the vehicle in the cultured media did not exceed 0.01% (*v*/*v*).

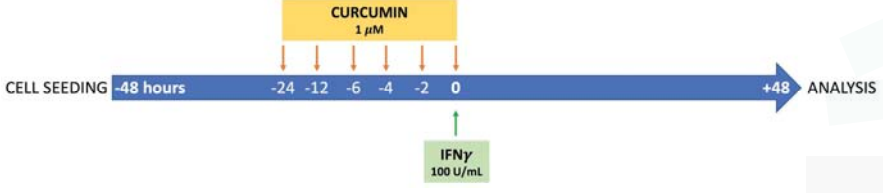

Figure 1. Representative illustration of the experimental design. Forty-eight hours after seeding, HT29 cells were stimulated with 100 U/mL IFNγ as inflammatory stimulus. To investigate the protective effect of curcumin, cells were pre-incubated with 1 μM curcumin (derived from *Curcuma Longa*) at different time points: 24, 12, 6, 4, 2, or 0 h before the IFNγ treatment. At 96 h of culture (48 h after the addition of IFNγ) cells were harvested for analysis.

2.2. Programmed Cell Death Assay

The apoptosis rate of HT29 was analyzed by flow cytometry using FITC-conjugated Annexin V (An) and propidium iodide staining (Annexin V-FITC Apoptosis Detection Kit, Immunostep, Salamanca, Spain), according to the producer's instructions. HT29 cells were seeded in a 24-well plate at an initial concentration of 1.8×10^5 per well. Forty-eight hours after IFNγ treatment, cells were harvested from the culture plate using 0.05% Trypsin-EDTA solution (EuroClone), washed with phosphate-buffered saline, and resuspended in the provided staining buffer for the incubation with Annexin V and propidium iodide. Flow cytometry analysis was performed on a BD FACSCalibur cytometer (Becton Dickinson, NJ, USA), and data were then analyzed with FlowJo software (version 7.6, Treestar, Inc., Ashland, OR, USA). The apoptotic cells (Annexin V positive, An+) were characterized based on the fluorescence emitted. Results were obtained by three independent experiments, performed in duplicate, and expressed as the fold increase after normalization on untreated controls.

2.3. Cell Viability Assay

Cytotoxicity was evaluated with MTT (3-(4,5-dimethylthiazol-2-yl)-2,5-diphenyltetrazolium bromide; Sigma Aldrich) colorimetric assay. Briefly, 2.5×10^4 HT29 cells per well were seeded in a 96-well plate, pre-treated or not with curcumin for 24 h and stimulated with IFNγ at 48 h of culture. Ninety-six hours after seeding the MTT solution (5 mg/mL) was added to cell culture. The tetrazolium dye was reduced by metabolically-viable cells in purple formazan. After four hours of incubation at 37 °C, dimethyl sulfoxide was used to dissolve the insoluble formazan in a colored solution, quantified by a spectrophotometer at 595 nm (GloMax®-Multi+ Microplate Multimode Reader, Promega Corporation, Madison, WI, USA). The absorbance values are directly proportional to the number of viable cells and normalized to the untreated condition.

2.4. Analysis of Impedance with xCELLigence System

The xCELLigence RTCA DP Instrument (Roche, Penzberg, Germany) was used to assess number, viability, and morphology of the cultured cells. The xCELLigence RTCA system is a label-free approach that uses the electrical impedance of the adherent cells, expressed as a cell index (CI) value, to monitor the biological status of cells. With this instrument, any change in cellular morphology or growth rate that leads to detachment or death of cultured cells (for example the addition of toxic compounds) determines a reduction of the CI.

For this analysis, 2.5×10^4 HT29 cells per well were seeded in a 16-well plate (E-plate; Roche) in 200 μL of complete medium, and cultured at 37 °C in 5% CO_2. The cells were stimulated with IFNγ, with a curcumin 24-h pre-incubation. The impedance values were automatically measured every 15 min for 96 h. This assay was repeated twice in triplicate. The CI curves were normalized at the addition of IFNγ to compare more precisely the effect of the tested treatment. Ninety-six hours after seeding, CI was also normalized to the untreated control.

2.5. NF-kB Signaling Assay

The MILLIPLEX® MAP 6-plex magnetic bead signaling kit (EMD Millipore Corporation, Billerica, MA, USA), was used to detect changes in phosphorylated NF-κB (Ser536), FADD (Ser194), IKKα/β (Ser177/Ser181), IκBα (Ser32) and in total protein levels of TNFR1 and c-Myc, in HT29 cell lysates. Briefly, cells were seeded in a 12-well plate at a cell density of 3.3×10^5 per well, pre-incubated or not with curcumin, and then stimulated with IFNγ. Forty-eight hours after stimulation cell were harvested, washed with phosphate-buffered saline and lysed in the provided lysis buffer supplemented with protease inhibitors. To remove particulate matter, lysates were centrifuged at $14{,}000 \times g$ for 20 min at 4 °C. Cell lysates were analyzed following manufacturer's instructions using the Luminex technology. Samples were acquired with the Bio-Plex® 200 reader (BioRad, Hemel Hempstead, UK) and data were analyzed by Bio-Plex Manager® software, which returned data as median fluorescence intensities (MFI). Results were represented as means and standard deviations of four replicate wells.

2.6. Cytokine Quantifications

Cytokines and chemokines released in the culture medium were quantified using the Bio-Plex Pro® Human Cytokine 17-plex Assay, according to the manufacturer's instructions (BioRad). Briefly, for the cytokine analysis, cells were seeded in a 12-well plate at a cell density of 3.3×10^5 per well. Forty-eight hours after seeding, cells were pre-incubated or not with curcumin and then stimulated with 100 U/mL IFNγ. The cell supernatants were collected forty-eight hours after IFNγ treatment. Analytes examined by this method were Interleukin (IL)1β, IL2, IL4, IL5, IL6, IL7, IL8, IL10, IL12 (p70), IL13, IL17, granulocyte-colony stimulating factor (G-CSF), granulocyte/macrophage-colony stimulating factor (GM-CSF), interferon (IFN)γ, monocyte chemotactic and activating factor (MCP1; MCAF), macrophage inflammatory protein (MIP)1β, and Tumor necrosis factor (TNF)α. Data were

acquired with a Bio-Plex® 200 reader (BioRad), using Bio-Plex Manager® software, which returned data as median fluorescence intensities (MFI) and concentrations (pg/mL).

2.7. Data Analysis

All results are expressed as means ± standard deviation (SD). Statistical significance was calculated using one-way analysis of variance (ANOVA) and Bonferroni post-test. Statistical significance was set at $p < 0.05$ (a), $p < 0.01$ (b), and $p < 0.001$ (c). Analyses were carried out using GraphPad Prism software (version 5.0, GraphPad Software Inc., La Jolla, CA, USA).

3. Results

3.1. Time-Dependent Modulation of Apoptosis by Curcumin Pre-Treatment

Apoptosis rate of HT29 was assessed by the Annexin V-FITC (An) Apoptosis Detection Kit. As expected, treatment with IFNγ alone led to a significantly increased cell apoptosis (1.749-fold more An-positive cells compared with the unstimulated control, $p < 0.001$; Figure 2). Cultures pre-incubated with curcumin had a lower fraction of apoptotic cells compared to non-pre-treated cell cultures, with a trend of higher preventive effect at longer pre-incubation times. Indeed, the preventive effect was particularly evident, albeit not complete, when curcumin pretreatment was started 24 h before the addition of IFNγ (IFNγ: 1.749 vs. Cur_{-24h} + IFNγ: 1.348; $p < 0.05$). This beneficial effect gradually declined with the reduction of the pre-incubation period. Curcumin, alone (administered 24 h before the inflammatory stimulus), did not perturb the cell viability (Figures 2 and 3).

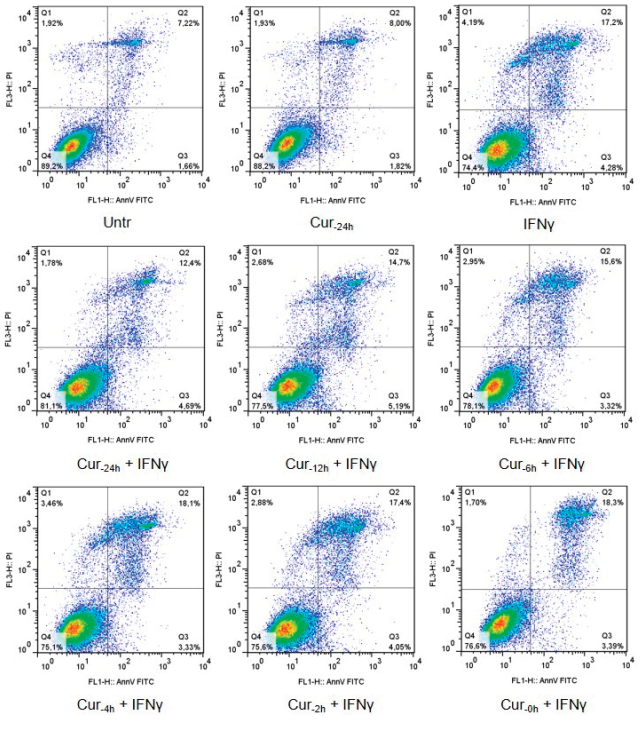

Figure 2. Representative flow cytograms of Annexin V-propidium iodide staining, for each experimental condition.

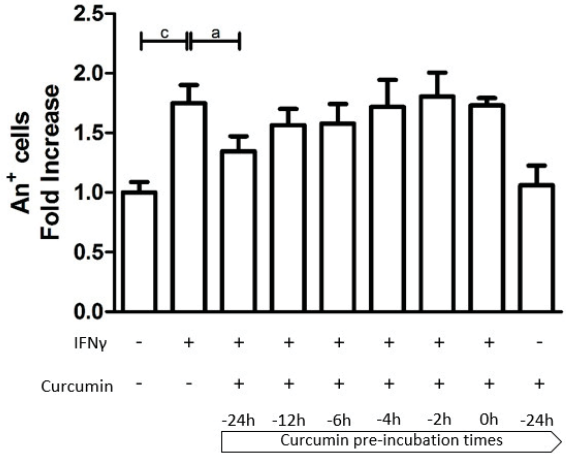

Figure 3. The effect of curcumin pre-treatment on HT29 apoptosis. The HT29 cell line was pre-incubated with curcumin at different time intervals and then stimulated with IFNγ for an additional 48 h. Programmed cell death is represented by Annexin V-positive cells (An+) expressed as a fold increase compared to untreated cells. Results are expressed as means ± SD of three independent experiments performed in duplicate. Data were analyzed with one-way ANOVA using the Bonferroni post-test (a: $p < 0.05$; c: $p < 0.001$).

3.2. Curcumin Effect on Cell Viability

The HT29 viability was evaluated with the MTT reagent, which allows quantifying the colorimetric reaction of the tetrazolium reduction to formazan in live cells. As expected, in the presence of IFNγ, the HT29 were metabolically less vital when compared to the untreated condition (Untreated: 100 ± 7.21; IFNγ: 44 ± 5.29; $p < 0.01$; Figure 4). Curcumin pre-incubation led to a significant, albeit partial, restoration of the metabolic activity, coherently with results from An V staining (Cur_{-24h} + IFNγ: 73.67 ± 9.81; $p < 0.05$).

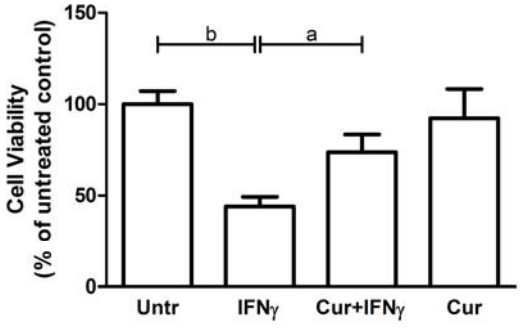

Figure 4. Viability analysis on HT29 pre-stimulated with curcumin. HT29 cell line was pre-incubated with curcumin (Cur) and after 24 h stimulated with IFNγ for an additional 48 h, to evaluate cell viability through MTT assay. Results are expressed as means ± SD, in percentage (%), normalized to the control condition (Untr). Data were analyzed with one-way ANOVA using the Bonferroni post-test (a: $p < 0.05$; b: $p < 0.01$).

3.3. Curcumin Effect on the Impedance Profile

The impedance measurement has confirmed the toxic effect of the IFNγ on cell status and the protective action of the curcumin administered 24 h before the addition of IFNγ. The representative xCELLigence graph (Figure 5) showed that the IFNγ addition led to a slight decrease in CI values (blue line), and the pre-treatment with curcumin stabilized the course of the line (pink line) up to the untreated condition (red line). Curcumin, alone, induced an increase of the impedance profile, possibly due to a change in cell morphology or adhesion strength (green line). Reporting the average of the normalized CI values obtained by different experiments after about 96 h of cell culture, it was possible to highlight that these differences are significant (Untr: 99.67 ± 26.84 vs. IFNγ 54.50 ± 14.39, $p < 0.05$; Cur_{-24h} + IFNγ: 101.0 ± 18.40, $p < 0.05$; Figure 6).

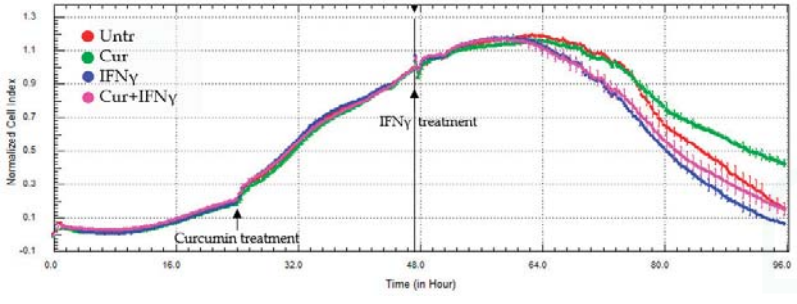

Figure 5. Representative impedance profile after curcumin pre-treatment. HT29 cells, cultured in a 16-well E-plate, were pre-treated with curcumin (Cur, 24 h after seeding), and stimulated with IFNγ (48 h after seeding) for a further 48 h. The graph shows the cell index values, normalized at the time of the IFNγ stimulation. The experiment was performed in triplicate.

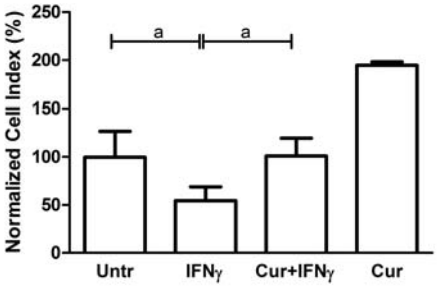

Figure 6. Impedance analysis of HT29 pre-treated with curcumin. The HT29 cells were pre-treated with curcumin (Cur, 24 h after seeding), and stimulated with IFNγ (48 h after seeding). The histograms represent, as a percentage (%), the mean of the normalized cell index values, reached after about 48 h IFNγ stimulation, compared to the untreated condition (Untr). Data are expressed as the mean ± SD. Data analyses were performed with one-way ANOVA and the Bonferroni post-test (a: $p < 0.05$).

3.4. Absence of NF-κB Modulation by Curcumin Pre-Treatment

IFNγ, as an inflammatory stimulus, was capable of activating the NF-κB (nuclear factor kappa B) pathway, as evidenced by the increased level of phosphoprotein of this signaling cascade, such as the transcription factor NF-κB and the upstream factors, IκBα and IKKα/β (NF-κB: 136.4 ± 23.39 vs. 314.5 ± 52.14 $p < 0.001$; IKKα/β: 43.20 ± 15.79 vs. 105.0 ± 29.60 $p < 0.01$; IκBα: 274.8 ± 45.38 vs. 453.7 ± 116 $p < 0.01$). The pre-treatment with curcumin lowered the levels of these phosphorylated

analytes slightly, but these trends were not significant (Figure 7). The other proteins analyzed (FADD, TNFR1, and c-Myc) did not show any significant differences after the inflammatory and curcumin treatment (data not shown).

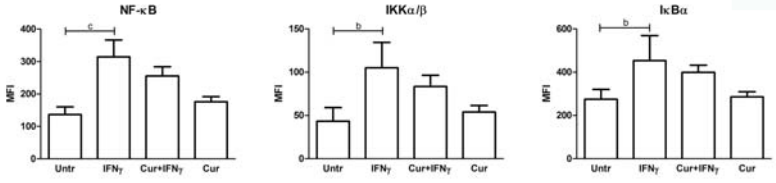

Figure 7. Multiplex analysis of phosphorylated proteins of NF-κB pathway in curcumin pre-treated HT29 cells. HT29 cells were pre-treated with curcumin (Cur) and then, after 24 h, stimulated with IFNγ for a further 48 h to detect changes in phosphorylated proteins belonging to the NF-κB pathway (NF-κB, IKKα/β, and IκBα), using a magnetic bead signaling kit and a Bio-Plex multiplex reader. Data, expressed as the median fluorescence intensity (MFI), represent the mean ± SD of four replicates and were analyzed with one-way ANOVA using the Bonferroni post-test (b: $p < 0.01$; c: $p < 0.001$).

3.5. Downregulation of the IL7 Secretion by Curcumin

The IFNγ treatment induced an increase of IL7 release in the HT29 culture media (Untr: 21.51 ± 2.40 vs. IFNγ: 88.76 ± 15.01, $p < 0.001$, Figure 8). When administered 24 h before the inflammatory stimulus, curcumin led to a significant downregulation of the levels of cytokines secreted, compared with the values obtained after the administration of IFNγ alone (IFNγ: 88.76 ± 15.01 vs. Cur_{-24h} + IFNγ: 54.54 ± 5.25, $p < 0.01$, Figure 8). With respect to the other analytes, no significant and biological differences were found between the four analyzed conditions (data not shown).

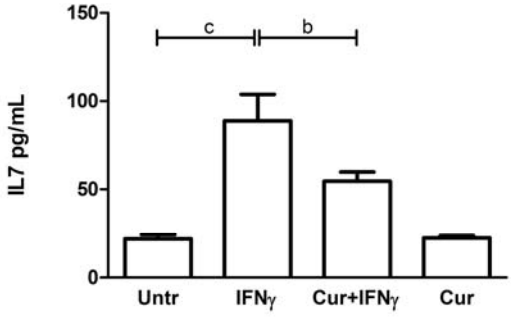

Figure 8. IL7 quantification after curcumin pre-treatment. The HT29 cell line was pre-incubated with curcumin (Cur) and, after 24 h, stimulated with IFNγ for an additional 48 h to evaluate the cytokine secretion. The histograms represent the concentration (pg/mL) of IL7 expressed as the mean ± SD of four replicates. Data were analyzed with one-way ANOVA using the Bonferroni post-test; (b: $p < 0.01$; c: $p < 0.001$).

4. Discussion

Curcumin, the active substance of *Curcuma longa* which is attributed most of the beneficial properties of turmeric, is chemically classified among the polyphenols.

The many beneficial properties attributed to curcumin, as antioxidant, anti-inflammatory, anti-infective, anti-tumor, and preventive agent, are closely correlated with each other and could be associated with the ability to modulate the molecules involved in inflammation, programmed cell death, and morphology.

In the present work, we demonstrated that pre-treatment with curcumin is able to reduce the levels of apoptosis in intestinal epithelial cells exposed to IFNγ. The fact that concordant data were obtained with different methods strengthens the interpretation of the results. In particular, there was a recent warning about the possibility that much of the research data on curcumin may be weakened, or even invalidated, when natural properties of fluorescence and protein binding of the compound are taken into account [25]. The inclusion in our research plan of a label-free assay based on cell impedance analysis allows ruling out such interferences.

When we further investigated the protective mechanisms of action of curcumin on HT29 cells, we observed that pre-treatment with this compound led to a significant reduction in the amount of IL7 secreted in response to IFNγ. IL7 is a crucial cytokine, usually secreted by intestinal epithelial cells in response to bacterial infections, which contributes to the organization of secondary lymphoid structures [28,29]. While basal secretion of this cytokine in response to the intestinal microbiota may be required for an optimal homeostasis of the mucosal immunity [30,31], higher levels may play a role in the pathogenesis of IBD and inhibition of IL7 has been proposed as a complementary approach to target inflammation in these disorders [32–35]. Since mucosal production of IL7 in vivo has been implicated in the activation of pathogenic CD4 T lymphocytes, the action of curcumin on this cytokine may be independently useful to contrast intestinal inflammation [36,37].

Although a cell line cultured in the laboratory can hardly reflect the complex physiology of intestinal mucosa, HT29 cells are considered a good model to study cytokine-induced apoptosis in epithelial cells. The model is coherent with in vivo data showing that epithelial apoptosis is increased in intestinal mucosa in subjects with the active disease while it is reversed by anti-inflammatory treatment with anti-TNFα antibodies. Increased apoptosis in epithelial cells is thought to contribute to increased permeability and amplification of inflammation. Thus, inhibiting inflammation-induced epithelial cell apoptosis may be relevant to the prevention or the treatment of IBD, as suggested by recent data [10].

It is not clear how curcumin acts on IFNγ-induced apoptosis and cytokine secretion. One of the known actions of curcumin regards iron chelation and reduction [38–41], but it is not clear if the anti-inflammatory and anti-apoptotic effects of the drug may depend on this property. We evaluated NF-κB activation since this pathway is a known target of IFNγ. Even if there was a trend toward reduction of the levels of phosphorylated components of NF-κB, this did not reach statistical significance. Thus, we could not conclude that the downregulation of the NF-κB pathway is the main mechanism of action of curcumin. A possible alternative explanation is that curcumin exerts its anti-inflammatory property by a direct modulation of mitochondrial function, as suggested by other authors [42].

Although we must put much caution in translating data obtained in vitro on a cell line, we can hypothesize that our results may be relevant to the understanding of the action of curcumin in vivo. In particular, a protective effect of curcumin was described in a mouse model of UC [43]. Moreover, small clinical trials in UC seem to suggest that curcumin may be a promising and safe complementary medication for maintaining remission in patients with quiescent disease [44].

An issue that should be addressed to assess the real potential of curcumin into the clinic concerns its poor aqueous solubility and low bioavailability, which may hinder in vivo efficacy [45]; low plasma levels and limited tissue distribution of curcumin appear to be due to poor absorption, high-rate metabolism, and rapid systemic clearance. A possible solution to these issues would be the development of different types of curcumin formulations, such as nanoparticles, liposomes, or phospholipid complexes, which increase and improve not only its stability, but also its biodistribution and absorption [46]. With these new strategies, an enhanced bioavailability and efficacy have been documented in different experimental models. Therefore, further exploration to increase the medical value for human applications are needed.

Our study was carried out on a single cell-type model. Even if preliminary studies in animals and patients are promising and coherent with our data, we should consider the possibility that similar

results cannot be obtained in vivo. Moreover, since we used ultra-pure curcumin, we should warn about the risk of translating our results to commercially-available preparations of curcuma, which may contain several other compounds with contrasting effects on mucosal immunity [47].

5. Conclusions

Despite being encouraging, our results need further and deeper investigations aimed at establishing whether curcumin could be a potential therapeutic molecule for IBD and, in particular, for UC.

In conclusion, even though our results are preliminary and need to be verified in order to be translated into the model of IBD patients, they should be considered as a first step to better characterize turmeric anti-inflammatory properties.

Acknowledgments: This work was supported by a grant from the Institute for Maternal and Child Health IRCCS "Burlo Garofolo" (RC 03/2009).

Author Contributions: A.M., A.T., M.B. and S.L. designed the research; C.L. carried out the experiments and performed the statistical analysis; E.P., L.V.B. and E.V. analyzed and interpreted the data; A.M., C.L., S.L. and A.T. wrote the paper; and E.P., L.V.B., E.V. and S.L. revised the manuscript critically for important intellectual content. All authors read and approved the final version of this manuscript.

Conflicts of Interest: The authors declare no conflict of interest.

References

1. Abraham, C.; Cho, J.H. Inflammatory bowel disease. *N. Engl. J. Med.* **2009**, *361*, 2066–2078. [CrossRef] [PubMed]
2. Yang, Y.; Owyang, C.; Wu, G.D. East Meets West: The Increasing Incidence of Inflammatory Bowel Disease in Asia as a Paradigm for Environmental Effects on the Pathogenesis of Immune-Mediated Disease. *Gastroenterology* **2016**, *151*, e1–e5. [CrossRef] [PubMed]
3. Benchimol, E.I.; Mack, D.R.; Guttmann, A.; Nguyen, G.C.; To, T.; Mojaverian, N.; Quach, P.; Manuel, D.G. Inflammatory bowel disease in immigrants to Canada and their children: A population-based cohort study. *Am. J. Gastroenterol.* **2015**, *110*, 553–563. [CrossRef] [PubMed]
4. Kim, H. Natural products to improve quality of life targeting for colon drug delivery. *Curr. Drug Deliv.* **2012**, *9*, 132–147. [CrossRef] [PubMed]
5. Zachos, M.; Tondeur, M.; Griffiths, A.M. Enteral nutritional therapy for induction of remission in Crohn's disease. *Cochrane Database Syst. Rev.* **2007**, *1*, CD000542. [CrossRef]
6. Lewis, J.D.; Abreu, M.T. Diet as a Trigger or Therapy for Inflammatory Bowel Diseases. *Gastroenterology* **2016**, *152*, 398–414. [CrossRef] [PubMed]
7. Vecchi Brumatti, L.; Marcuzzi, A.; Tricarico, P.M.; Zanin, V.; Girardelli, M.; Bianco, A.M. Curcumin and inflammatory bowel disease: Potential and limits of innovative treatments. *Molecules* **2014**, *19*, 21127–21153. [CrossRef] [PubMed]
8. Shishodia, S. Molecular mechanisms of curcumin action: Gene expression. *Biofactors* **2013**, *39*, 37–55. [CrossRef] [PubMed]
9. Taylor, R.A.; Leonard, M.C. Curcumin for inflammatory bowel disease: A review of human studies. *Altern. Med. Rev.* **2011**, *16*, 152–156. [PubMed]
10. Lang, A.; Salomon, N.; Wu, J.C.; Kopylov, U.; Lahat, A.; Har-Noy, O.; Ching, J.Y.; Cheong, P.K.; Avidan, B.; Gamus, D.; et al. Curcumin in Combination With Mesalamine Induces Remission in Patients With Mild-to-Moderate Ulcerative Colitis in a Randomized Controlled Trial. *Clin. Gastroenterol. Hepatol.* **2015**, *13*, 1444–1449.e1. [CrossRef] [PubMed]
11. Panahi, Y.; Darvishi, B.; Ghanei, M.; Jowzi, N.; Beiraghdar, F.; Varnamkhasti, B.S. Molecular mechanisms of curcumins suppressing effects on tumorigenesis, angiogenesis and metastasis, focusing on NF-κB pathway. *Cytokine Growth Factor Rev.* **2016**, *28*, 21–29. [CrossRef] [PubMed]
12. Midura-Kiela, M.T.; Radhakrishnan, V.M.; Larmonier, C.B.; Laubitz, D.; Ghishan, F.K.; Kiela, P.R. Curcumin inhibits interferon-γ signaling in colonic epithelial cells. *Am. J. Physiol. Gastrointest. Liver Physiol.* **2012**, *302*, G85–G96. [CrossRef] [PubMed]

13. Jian, Y.T.; Mai, G.F.; Wang, J.D.; Zhang, Y.L.; Luo, R.C.; Fang, Y.X. Preventive and therapeutic effects of NF-kappaB inhibitor curcumin in rats colitis induced by trinitrobenzene sulfonic acid. *World J. Gastroenterol.* **2005**, *11*, 1747–1752. [CrossRef] [PubMed]
14. Deguchi, Y.; Andoh, A.; Inatomi, O.; Yagi, Y.; Bamba, S.; Araki, Y.; Hata, K.; Tsujikawa, T.; Fujiyama, Y. Curcumin prevents the development of dextran sulfate Sodium (DSS)-induced experimental colitis. *Dig. Dis. Sci.* **2007**, *52*, 2993–2998. [CrossRef] [PubMed]
15. Arafa, H.M.; Hemeida, R.A.; El-Bahrawy, A.I.; Hamada, F.M. Prophylactic role of curcumin in dextran sulfate sodium (DSS)-induced ulcerative colitis murine model. *Food Chem. Toxicol.* **2009**, *47*, 1311–1317. [CrossRef] [PubMed]
16. Mastropietro, G.; Tiscornia, I.; Perelmuter, K.; Astrada, S.; Bollati-Fogolín, M. HT-29 and Caco-2 reporter cell lines for functional studies of nuclear factor kappa B activation. *Mediat. Inflamm.* **2015**, *2015*. [CrossRef] [PubMed]
17. Guo, Y.; Shu, L.; Zhang, C.; Su, Z.Y.; Kong, A.N. Curcumin inhibits anchorage-independent growth of HT29 human colon cancer cells by targeting epigenetic restoration of the tumor suppressor gene DLEC1. *Biochem. Pharmacol.* **2015**, *94*, 69–78. [CrossRef] [PubMed]
18. Iwamoto, M.; Koji, T.; Makiyama, K.; Kobayashi, N.; Nakane, P.K. Apoptosis of crypt epithelial cells in ulcerative colitis. *J. Pathol.* **1996**, *180*, 152–159. [CrossRef]
19. Hagiwara, C.; Tanaka, M.; Kudo, H. Increase in colorectal epithelial apoptotic cells in patients with ulcerative colitis ultimately requiring surgery. *J. Gastroenterol. Hepatol.* **2002**, *17*, 758–764. [CrossRef] [PubMed]
20. Di Sabatino, A.; Ciccocioppo, R.; Luinetti, O.; Ricevuti, L.; Morera, R.; Cifone, M.G.; Solcia, E.; Corazza, G.R. Increased enterocyte apoptosis in inflamed areas of Crohn's disease. *Dis. Colon. Rectum.* **2003**, *46*, 1498–1507. [CrossRef] [PubMed]
21. Zeissig, S.; Bojarski, C.; Buergel, N.; Mankertz, J.; Zeitz, M.; Fromm, M.; Schulzke, J.D. Downregulation of epithelial apoptosis and barrier repair in active Crohn' s disease by tumour necrosis factor alpha antibody treatment. *Gut* **2004**, *53*, 1295–1302. [CrossRef] [PubMed]
22. Banerjee, S.; Singh, S.K.; Chowdhury, I.; Lillard, J.W., Jr.; Singh, R. Combinatorial effect of curcumin with docetaxel modulates apoptotic and cell survival molecules in prostate cancer. *Front. Biosci. (Elite Ed.)* **2017**, *1*, 235–245.
23. Park, S.I.; Lee, E.H.; Kim, S.R.; Jang, Y.P. Anti-apoptotic effects of *Curcuma longa* L. extract and its curcuminoids against blue light-induced cytotoxicity in A2E-laden human retinal pigment epithelial cells. *J. Pharm. Pharmacol.* **2017**, *69*, 334–340. [CrossRef] [PubMed]
24. Zheng, L.; Li, Y.; Li, X.; Kou, J.; Zhong, Z.; Jiang, Y.; Liu, Z.; Tian, Y.; Yang, L. Combination of Hydroxyl Acetylated Curcumin and Ultrasound Induces Macrophage Autophagy with Anti-Apoptotic and Anti-Lipid Aggregation Effects. *Cell Physiol. Biochem.* **2016**, *39*, 1746–1760. [CrossRef] [PubMed]
25. Baker, M. Deceptive curcumin offers cautionary tale for chemists. *Nature* **2017**, *541*, 144–145. [CrossRef] [PubMed]
26. Hackler, L., Jr.; Ózsvári, B.; Gyuris, M.; Sipos, P.; Fábián, G.; Molnár, E.; Marton, A.; Faragó, N.; Mihály, J.; Nagy, L.I.; et al. The Curcumin Analog C-150, Influencing NF-κB, UPR and Akt/Notch Pathways Has Potent Anticancer Activity in Vitro and in Vivo. *PLoS ONE* **2016**, *11*, e0149832. [CrossRef] [PubMed]
27. Li, W.; Wang, H.; Kuang, C.Y.; Zhu, J.K.; Yu, Y.; Qin, Z.X.; Liu, J.; Huang, L. An essential role for the Id1/PI3K/Akt/NFkB/survivin signalling pathway in promoting the proliferation of endothelial progenitor cells in vitro. *Mol. Cell Biochem.* **2012**, *363*, 135–145. [CrossRef] [PubMed]
28. Cimbro, R.; Vassena, L.; Arthos, J.; Cicala, C.; Kehrl, J.H.; Park, C.; Sereti, I.; Lederman, M.M.; Fauci, A.S.; Lusso, P. IL-7 induces expression and activation of integrin α4β7 promoting naive T-cell homing to the intestinal mucosa. *Blood* **2012**, *120*, 2610–2619. [CrossRef] [PubMed]
29. Zhang, W.; Du, J.Y.; Yu, Q.; Jin, J.O. Interleukin-7 produced by intestinal epithelial cells in response to Citrobacter rodentium infection plays a major role in innate immunity against this pathogen. *Infect. Immun.* **2015**, *83*, 3213–3223. [CrossRef] [PubMed]
30. Shalapour, S.; Deiser, K.; Sercan, O.; Tuckermann, J.; Minnich, K.; Willimsky, G.; Blankenstein, T.; Hämmerling, G.J.; Arnold, B.; Schüler, T. Commensal microflora and interferon-gamma promote steady-state interleukin-7 production in vivo. *Eur. J. Immunol.* **2010**, *40*, 2391–2400. [CrossRef] [PubMed]

31. Shalapour, S.; Deiser, K.; Kühl, A.A.; Glauben, R.; Krug, S.M.; Fischer, A.; Sercan, O.; Chappaz, S.; Bereswill, S.; Heimesaat, M.M.; et al. Interleukin-7 links T lymphocyte and intestinal epithelial cell homeostasis. *PLoS ONE* **2012**, *7*, e31939. [CrossRef] [PubMed]
32. Kanai, T.; Nemoto, Y.; Kamada, N.; Totsuka, T.; Hisamatsu, T.; Watanabe, M.; Hibi, T. Homeostatic (IL-7) and effector (IL-17) cytokines as distinct but complementary target for an optimal therapeutic strategy in inflammatory bowel disease. *Curr. Opin. Gastroenterol.* **2009**, *25*, 306–313. [CrossRef] [PubMed]
33. Watanabe, M.; Ueno, Y.; Yajima, T.; Iwao, Y.; Tsuchiya, M.; Ishikawa, H.; Aiso, S.; Hibi, T.; Ishii, H. Interleukin 7 is produced by human intestinal epithelial cells and regulates the proliferation of intestinal mucosal lymphocytes. *J. Clin. Investig.* **1995**, *95*, 2945–2953. [CrossRef] [PubMed]
34. Andreu-Ballester, J.C.; Pérez-Griera, J.; Garcia-Ballesteros, C.; Amigo, V.; Catalán-Serra, I.; Monforte-Albalat, A.; Bixquert-Jiménez, M.; Ballester, F. Deficit of interleukin-7 in serum of patients with Crohn's disease. *Inflamm. Bowel Dis.* **2013**, *19*, E30-1. [CrossRef] [PubMed]
35. Totsuka, T.; Kanai, T.; Nemoto, Y.; Makita, S.; Okamoto, R.; Tsuchiya, K.; Watanabe, M. IL-7 is essential for the development and the persistence of chronic colitis. *J. Immunol.* **2007**, *178*, 4737–4748. [CrossRef] [PubMed]
36. Nemoto, Y.; Kanai, T.; Takahara, M.; Oshima, S.; Nakamura, T.; Okamoto, R.; Tsuchiya, K.; Watanabe, M. Bone marrow-mesenchymal stem cells are a major source of interleukin-7 and sustain colitis by forming the niche for colitogenic CD4 memory T cells. *Gut* **2013**, *62*, 1142–1152. [CrossRef] [PubMed]
37. Willis, C.R.; Seamons, A.; Maxwell, J.; Treuting, P.M.; Nelson, L.; Chen, G.; Phelps, S.; Smith, C.L.; Brabb, T.; Iritani, B.M.; et al. Interleukin-7 receptor blockade suppresses adaptive and innate inflammatory responses in experimental colitis. *J. Inflamm. (Lond.)* **2012**, *9*, 39. [CrossRef] [PubMed]
38. Yang, C.; Ma, X.; Wang, Z.; Zeng, X.; Hu, Z.; Ye, Z.; Shen, G. Curcumin induces apoptosis and protective autophagy in castration-resistant prostate cancer cells through iron chelation. *Drug Des. Dev. Ther.* **2017**, *11*, 431–439. [CrossRef] [PubMed]
39. Du, X.X.; Xu, H.M.; Jiang, H.; Song, N.; Wang, J.; Xie, J.X. Curcumin protects nigral dopaminergic neurons by iron-chelation in the 6-hydroxydopamine rat model of Parkinson' s disease. *Neurosci. Bull.* **2012**, *28*, 253–258. [CrossRef] [PubMed]
40. Dairam, A.; Fogel, R.; Daya, S.; Limson, J.L. Antioxidant and iron-binding properties of curcumin, capsaicin, and S-allylcysteine reduce oxidative stress in rat brain homogenate. *J. Agric. Food Chem.* **2008**, *56*, 3350–3356. [CrossRef] [PubMed]
41. Galleggiante, V.; De Santis, S.; Cavalcanti, E.; Scarano, A.; De Benedictis, M.; Serino, G.; Caruso, M.L.; Mastronardi, M.; Pinto, A.; Campiglia, P.; et al. Dendritic Cells Modulate Iron Homeostasis and Inflammatory Abilities Following Quercetin Exposure. *Curr. Pharm. Des.* **2017**. [CrossRef]
42. Jiang, A.J.; Jiang, G.; Li, L.T.; Zheng, J.N. Curcumin induces apoptosis through mitochondrial pathway and caspases activation in human melanoma cells. *Mol. Biol. Rep.* **2015**, *42*, 267–275. [CrossRef] [PubMed]
43. Sugimoto, K.; Hanai, H.; Tozawa, K.; Aoshi, T.; Uchijima, M.; Nagata, T.; Koide, Y. Curcumin prevents and ameliorates trinitrobenzene sulfonic acid-induced colitis in mice. *Gastroenterology* **2002**, *123*, 1912–1922. [CrossRef] [PubMed]
44. Hanai, H.; Iida, T.; Takeuchi, K.; Watanabe, F.; Maruyama, Y.; Andoh, A.; Tsujikawa, T.; Fujiyama, Y.; Mitsuyama, K.; Sata, M.; et al. Curcumin maintenance therapy for ulcerative colitis: Randomized, multicenter, double-blind, placebo-controlled trial. *Clin. Gastroenterol. Hepatol.* **2006**, *4*, 1502–1506. [CrossRef] [PubMed]
45. Anand, P.; Kunnumakkara, A.B.; Newman, R.A.; Aggarwal, B.B. Bioavailability of curcumin: Problems and promises. *Mol. Pharm.* **2007**, *4*, 807–818. [CrossRef] [PubMed]
46. Prasad, S.; Tyagi, A.K.; Aggarwal, B.B. Recent developments in delivery, bioavailability, absorption and metabolism of curcumin: The golden pigment from golden spice. *Cancer Res. Treat.* **2014**, *46*, 2–18. [CrossRef] [PubMed]
47. Holt, P.R. Curcumin for Inflammatory Bowel Disease: A Caution. *Clin. Gastroenterol. Hepatol.* **2016**, *14*, 168. [CrossRef] [PubMed]

nutrients

MDPI

Article

Melatonin Modulates Neuronal Cell Death Induced by Endoplasmic Reticulum Stress under Insulin Resistance Condition

Juhyun Song [1] and Oh Yoen Kim [2,*]

[1] Department of Biomedical Sciences, Center for Creative Biomedical Scientists at Chonnam National University, Gwangju 61469, Korea; alj1008@nate.com

[2] Department of Food Sciences and Nutrition, Dong-A University, 37 550beon-gil Nakdongdaero, Saha-gu, Busan 49315, Korea

* Correspondence: oykim@dau.ac.kr; Tel.: +82-51-200-7326; Fax: +82-51-200-7353

Received: 30 April 2017; Accepted: 8 June 2017; Published: 10 June 2017

Abstract: Insulin resistance (IR) is an important stress factor in the central nervous system, thereby aggravating neuropathogenesis and triggering cognitive decline. Melatonin, which is an antioxidant phytochemical and synthesized by the pineal gland, has multiple functions in cellular responses such as apoptosis and survival against stress. This study investigated whether melatonin modulates the signaling of neuronal cell death induced by endoplasmic reticulum (ER) stress under IR condition using SH-SY5Y neuroblastoma cells. Apoptosis cell death signaling markers (cleaved Poly [ADP-ribose] polymerase 1 (PARP), p53, and Bax) and ER stress markers (phosphorylated eIF2α (p-eIF2α), ATF4, CHOP, *p-IRE1*, and spliced XBP1 (sXBP1)) were measured using reverse transcription-PCR, quantitative PCR, and western blottings. Immunofluorescence staining was also performed for *p-ASK1* and *p-IRE1*. The mRNA or protein expressions of cell death signaling markers and ER stress markers were increased under IR condition, but significantly attenuated by melatonin treatment. Insulin-induced activation of *ASK1* (*p-ASK1*) was also dose dependently attenuated by melatonin treatment. The regulatory effect of melatonin on neuronal cells under IR condition was associated with *ASK1* signaling. In conclusion, the result suggested that melatonin may alleviate ER stress under IR condition, thereby regulating neuronal cell death signaling.

Keywords: melatonin; neuroblastoma cells; insulin resistance; endoplasmic reticulum stress; cell death

1. Introduction

Insulin resistance (IR) is a pathological condition observed in people with type 2 diabetes mellitus (T2DM) [1], obesity, or older age [2]. Recent epidemiological and human studies have reported that IR leads to cognitive decline and dementia in the central nervous system [3–6]. Animal studies have also demonstrated that IR impaired behavioral function in high fat-fed mice [7,8]. IR is directly involved in the dysregulation of cellular homeostasis [9], and endoplasmic reticulum (ER) stress, which triggers cell death signaling [10,11]. Under stressful conditions, three ER stress receptors on the ER membrane are activated sequentially, with pancreatic ER kinase (PKR)-like ER kinase (PERK) being the first, followed by the activation of transcription factor 6 (ATF6), and with IRE1 being the last [12]. Activated PERK blocks protein synthesis by phosphorylating eIF2α [13], and the phosphorylation makes ATF4, a transcription factor, to translocate into the nucleus, and induce the transcription of genes needed to restore ER homeostasis (i.e., amino acid synthesis and transport, stress response, redox reaction, and CHOP, etc.) [14]. CHOP is a protein regulating ER stress mediated apoptosis through the modulation of pro-apoptotic and anti-apoptotic proteins [14,15], and also a cardinal mediator in

IR [16], mitochondrial apoptosis [17], and inflammation [18]. Activated ATF6, a transcription factor, also regulates the expressions of ER chaperones, CHOP, and XBP1 [19]. Spliced XBP1 (sXBP1), which is an active form of XBP1 spliced by IRE1, translocates into the nucleus and controls the transcription of chaperones, $P58^{IPK}$, and genes for protein degradation [20,21]. In fact, increased sXBP1 levels were observed in patients with metabolic diseases [22,23]. Additionally, phosphorylated IRE1 (*p-IRE1*) was reported to recruit the adaptor molecule tumor necrosis factor-receptor-associated factor 2 (TRAF2) [24]. The IRE1–TRAF2 complex formed under the ER stress can recruit an apoptosis signal-regulating kinase 1 (*ASK1*), a member of a large MAPK kinase family known to aggravate cell death [24–28]. That is, under persistent stress, IRE1 triggers apoptosis by recruiting ASK1. These above factors may strongly suggest that ER stress is an important therapeutic target for IR and T2DM [29,30]. Collectively, ER stress should be highlighted for the investigation on the mechanisms of neuropathogenesis caused by IR.

Recently, melatonin (5-methoxy-*N*-acetyltryptamine) was reported to alleviate ER stress by stimulating cell survival signaling such as the Akt pathway in oxidative stress [31]. Melatonin is a pleiotropic hormone synthesized by the pineal gland, secreted into the blood stream, and involved in the entrainment of the circadian rhythm such as sleep and wake timing, blood pressure controlling, energy balance favoring and inhibiting brown adipose tissue formation, and seasonal reproduction, etc. [32,33]. It is also a phytochemical compound present in various foods from fungi to animals and plants [34]. Melatonin (and its metabolites) also plays multiple roles as a potent antioxidant and a free radical scavenger in cellular homeostasis (i.e., cell survival, apoptosis, thermogenesis, inflammation, etc.) by binding specific melatonin receptors (i.e., MT1, MT2) [35–44], and also improves the nuclear or mitochondria dysfunction in diabetic and obese animal model through its antioxidant capacity [45–48]. However, few studies have reported the regulatory effect of melatonin on ER stress-induced neuronal cell death signaling under IR condition. Therefore, this present study investigated whether melatonin modulates the ER stress under IR condition, thereby regulating neuronal cell death signaling. The results would provide a specific mechanism for how melatonin affects cell survival against IR-induced stress.

2. Methods and Materials

2.1. Cell Culture

SH-SY5Y neuroblastoma cells (ATCC, Manassas, VA, USA) are capable of differentiating into neuron-like cells in the presence of retinoic acid (RA). Undifferentiated SH-SY5Y cells were cultured at 37 °C with 5% CO_2 in Dulbecco's modified Eagle's medium (DMEM) supplemented with 10% fetal bovine serum (FBS; Gibco, Grand Island, NY, USA) and 100 μg/mL of penicillin-streptomycin (Gibco). SH-SY5Y cells were passaged at least twice, and differentiated with a replacement of fresh media supplemented with 1% FBS and 5 μM of RA, and cultured in DMEM media with 100 nM of insulin (Wako Chemicals, Richmond, VA, USA) for 3 days, with a replacement of fresh medium every 24 h [17]. Afterwards, medium was replaced with serum-free DMEM media. After 30 min, cells were exposed to 1 μM of insulin for 15 min [18,19]. NQDI-1, an apoptosis signal-regulating kinase 1 (ASK1) inhibitor, was purchased from Tocris Bioscience (Bristol, UK). Cells were pretreated with *ASK1* inhibitor (600 nM) for 2 h to inhibit *ASK1* activation before IR stress.

2.2. Cell Viability Assay

SH-SY5Y cells (2×10^5 cells/mL) were seeded in 96-well plates for monitoring all experimental conditions including melatonin pretreatment (100 μM) and insulin stimulation (1 μM), separately. Next, culture medium was replaced with serum-free medium, and 100 μL of 3-(4,5-dimethylthiazol-2-yl)-2, 5-diphenyltetrazolium bromide (MTT) (Sigma-Aldrich, St.Louis, MO, USA) solution (5 mg/mL in PBS) was added to each well. After incubation for 1 h, medium was removed and dimethyl sulfoxide was added to each well to solubilize the purple formazan product of MTT reaction. The supernatant

from each well was analyzed using a microplate reader at 570 nm (Labsystems Multiskan MCC/340; Fisher Scientific, Pittsburgh, PA, USA). All experiments were repeated three times. Cell viability in medium of non-treated cells was considered 100%.

2.3. Reverse Transcription-PCR

To examine the mRNA expressions of cleaved Poly [ADP-ribose] polymerase 1 (cleaved PARP), p53, Bax, phosphorylated eukaryotic initiation factor 2 alpha (p-eIF2α), activating transcription factor 4 (ATF4), C/EBP homologous protein (CHOP), and phosphorylated inositol requiring kinase 1 alpha (*p-IRE1*), reverse transcription-PCR (RT-PCR) was performed using each primer. Briefly, samples were lysed with Trizol reagent (Invitrogen), and total RNA was extracted according to the manufacturer's protocol. PCR was performed using the following primers (5′ to 3′): cleaved PARP (F): AGG CCC TAA AGG CTC AGA AT, (R): CTA GGT TTC TGT GTC TTG AC, p53 (F): CTG CCC TCA ACA AGA TGT TTT G , (R): CTA TCT GAG CAG CGC TCA TGG , Bax (F): AAG AAG CTG AGC GAG TGT, (R): GGA GGA AGT CCA ATG TC, p-eIF2α (F): ACG CTT TGG GGC TAA TTC TT, (R): TCT GGG CTT TTC TTC CAC AC, ATF4 (F): GTC CTA TCT GGG GTC TCC TC, (R): TAC CTA GTG GCT GCT GTC TT, CHOP: (F): AGA ACC AGG AAA CGG AAA CAG A (R): TCT CCT TCA TGC GCT GCT TT, *p-IRE1* (F): GCT GTG GAG ACC CTA CGC TAT , (R): TCG ATG TTT GGG AAG ATT GTT AG, and glyceraldehyde-3-phosphate dehydrogenase (GAPDH) (F): ACA GTC CAT GCC ATC ACT GCC, (R): GCC TGC TTC ACC ACC TTC TTG. PCR products were electrophoresed in 1.5% agarose gels and stained with ethidium bromide. All experiments were repeated three times.

2.4. Quantitative Real Time-PCR

To examine the mRNA expression of sliced X-box binding protein 1 (XBP1) in cells under IR conditions, quantitative real time-PCR (qPCR) was performed. Total cellular RNA was extracted from the cells using Trizol reagent (Invitrogen, Carlsbad, CA, USA) according to the manufacturer instructions. Poly (A) was added using poly (A) polymerase (Ambion, Austin, TX, USA). One Step SYBR® Prime Script TM RT-PCR Kit II (Takara, Japan) was used to conduct qPCR. PCR was performed using the following primers (5′ to 3′); sliced XBP1 (F): CTG AGT CCG AAT CAG GTG CAG, (R): ATC CAT GGG GAG ATG TTC TGG, β-actin (F): TCT GGC ACC ACA CCT TCT A, (R): AGG CAT ACA GGG ACA GCA C. The expression of each of the factors was assessed using an ABI prism 7500 Real-Time PCR System (Life Technologies Corporation, Carlsbad, CA, USA) and analyzed with comparative Ct quantification. β-actin was amplified as an internal control. The values were presented by relative quantity (RQ). All experiments were repeated three times.

2.5. Western Blot Analysis

SH-SY5Y cells were washed with PBS and harvested together. Cell pellets were lysed with cold radioimmunoprecipitation assay buffer (Sigma-Aldrich, St. Louis, MO, USA). The lysates were centrifuged at 13,000 rpm for 20 min at 4 °C to produce whole-cell extracts. Cellular proteins (30 μg) were separated on a 10% sodium dodecyl sulfate-polyacrylamide gel (SDS-PAGE) and transferred onto a polyvinylidene difluoride membrane. Blocking with skimmed milk prepared in Tris-buffered saline with Tween™ 20 detergent (TBST) (20 nM Tris (pH 7.2) and 150 mM NaCl, 0.1 % Tween™ 20) was performed for 1 h at room temperature. Immunoblots were then incubated for 15 h at 4 °C with primary antibodies that detect cleaved PARP (1:1000, Abcam, Cambridge, MA, USA), p-eIF2α (1:1000, Cell Signaling, Danvers, MA, USA), and β-actin (1:1000; Millipore, Billerica, MA, USA). Blots were then incubated with each secondary antibody (Abcam, Cambridge, MA, USA) for 1 h 30 min at room temperature. Blots were visualized using ECL solution (Millipore, Billerica, MA, USA).

2.6. Immunofluorescence for p-ASK-1 and p-IRE1

SH-SY5Y cells were incubated with the primary antibody overnight at 4 °C. The following primary antibodies were used: anti-goat phosphor apoptosis signal regulating kinase 1 (*p-ASK1*) (1:200, Santa

Cruz Biotechnology, Santa Cruz, CA, USA) and anti-goat phosphor-IRE1 (*p-IRE1*) (1:200, Cell Signaling, Danvers, MA, USA). The primary antibody was then removed, and the cells were washed three times for 3 min with PBS. The cells were incubated with second antibody for 1 h 30 min at room temperature. The cells were then washed again three times for 3 min with PBS, followed by counterstaining with 1 μg/mL of 4′,6-diamidino-2-phenylindole (DAPI, 1:200, Invitrogen) for 15 min at room temperature. The cells were imaged using a Zeiss LSM 700 confocal microscope (Carl Zeiss, Thornwood, NY, USA).

2.7. Statistical Analysis

Statistical analyses were performed using SPSS ver.22.0 software (IBM Corp., Armonk, NY, USA). Results were expressed as mean ± standard deviation (S.D.). Differences among the groups were determined by one-way analysis of variance (ANOVA) followed by Bonferroni post hoc multiple comparison tests. A p-value less than 0.05 was considered statistically significant.

3. Results

3.1. Melatonin Increases SH-SY5Y Cell Viability under IR Conditions

The SH-SY5Y cell viabilities were measured using MTT assay (Figure 1A). The cell viability was markedly reduced by insulin stimulation compared with non-stimulated control. On the other hand, the decreased cell viability by insulin stimulation was recovered when treated with melatonin.

3.2. Melatonin Treatment Alleviates IR-Induced Neuronal Cell Death Signaling

To investigate if neuronal cell death signaling under insulin stimulation is regulated by melatonin treatment, we measured mRNA expressions of cleaved PARP, p53, and Bax using RT-PCR (Figure 1B–D). mRNA expressions of cleaved PARP, p53, and Bax were significantly increased under IR condition. Melatonin treatment dramatically attenuated mRNA expressions of cleaved PARP and p53 in the cells stimulated by insulin or not. Furthermore, the attenuated levels by melatonin treatment were much lower than those in non-stimulated controls. In addition, the increased mRNA levels of Bax under IR condition were significantly attenuated by melatonin treatment. In addition, western blot assay shows that melatonin treatment significantly attenuated the insulin-induced expression of cleaved PARP (Figure 2A).

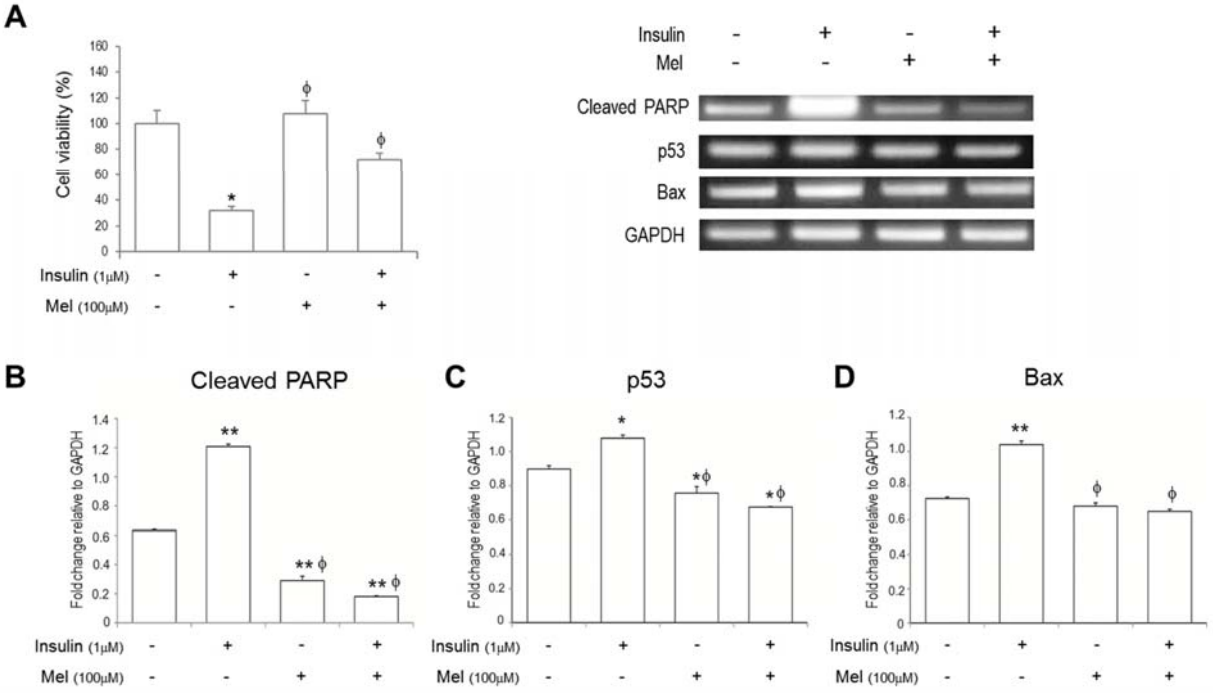

Figure 1. Melatonin alleviates insulin resistance (IR)-induced SH-SY5Y neuronal cell death signaling. (**A**) Cell viability was assessed by 3-(4,5-dimethylthiazol-2-yl)-2, 5-diphenyltetrazolium bromide (MTT) assay. The mRNA levels of (**B**) cleaved PARP; (**C**) p53; and (**D**) Bax were measured by reverse transcription PCR. Data are expressed as mean ± standard error and each experiment included three repeats per conditions. * $p < 0.05$, ** $p < 0.01$ compared with non-stimulated control; $^{\phi}$ $p < 0.05$ compared with insulin stimulated cells. Mel: melatonin pretreatment for 24 h before insulin stimulation.

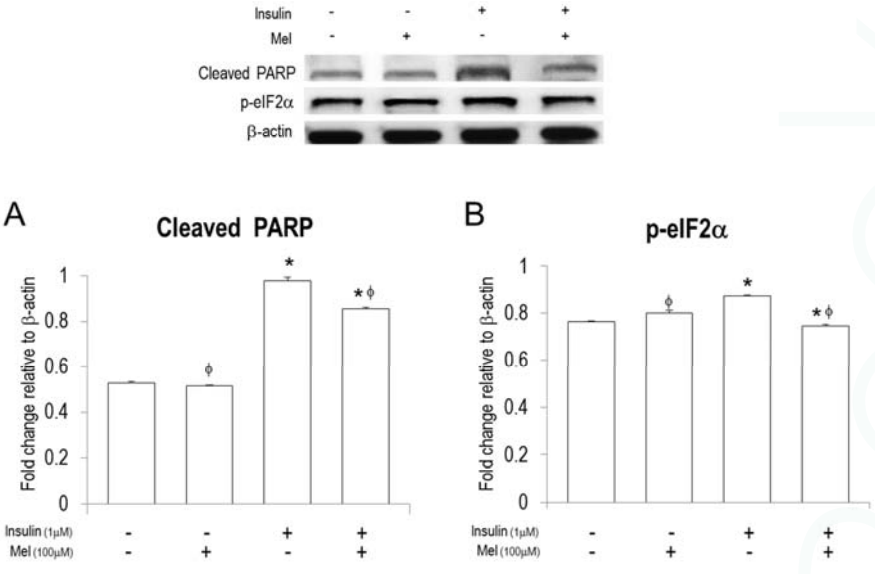

Figure 2. Melatonin regulates protein levels of cleaved PARP and p- p-eIF2α in the insulin stimulated SH-SY5Y neuronal cells. Protein levels of (**A**) cleaved PARP and (**B**) activation of eIF2α, (p-eIF2α) were measured by western blot analysis. Data are expressed as mean ± standard error and each experiment included three repeats per conditions. * $p < 0.05$ compared with non-stimulated control; $^{\phi}$ $p < 0.05$ compared with insulin stimulated cells. Mel: melatonin pretreatment for 24 h before insulin stimulation.

3.3. Melatonin Treatment Regulates IR-Induced ER Stress Signaling in Neuronal Cells

To investigate if melatonin treatment regulates ER stress in neuronal cells under insulin stimulation, we performed RT-PCR, qPCR, and Immunofluorescence analysis (Figures 3 and 4). As shown in Figure 3A–C, mRNA expressions of p-eIF2α, ATF4, and CHOP were significantly increased by insulin stimulation, but the increased expressions were significantly attenuated by melatonin treatment. Similar patterns were observed when *ASK1* signaling was inhibited. Western blot assay also showed that melatonin treatment significantly attenuated the insulin-induced expression of p-eIF2α (Figure 2B).

It can be observed in Figure 4 that significantly increased mRNA expressions of sXBP1 under IR condition were dramatically attenuated when melatonin was treated together with or without *ASK1* inhibitor. As shown in Figure 3A, mRNA expressions of sXBP1 were dramatically increased by insulin stimulation, but the increased expressions were significantly attenuated by melatonin treatment together with or without *ASK1* inhibitor. mRNA expression of *p-IRE1* was also significantly increased by insulin stimulation, and attenuated by melatonin treatment (Figure 4B). Interestingly, when *ASK1* signaling was inhibited, mRNA expressions of *p-IRE1* stimulated by insulin treated with melatonin or not were dramatically attenuated. In addition, immunofluorescence analysis confirmed that *p-IRE1* induced by insulin stimulation was significantly suppressed by melatonin treatment (Figure 4C).

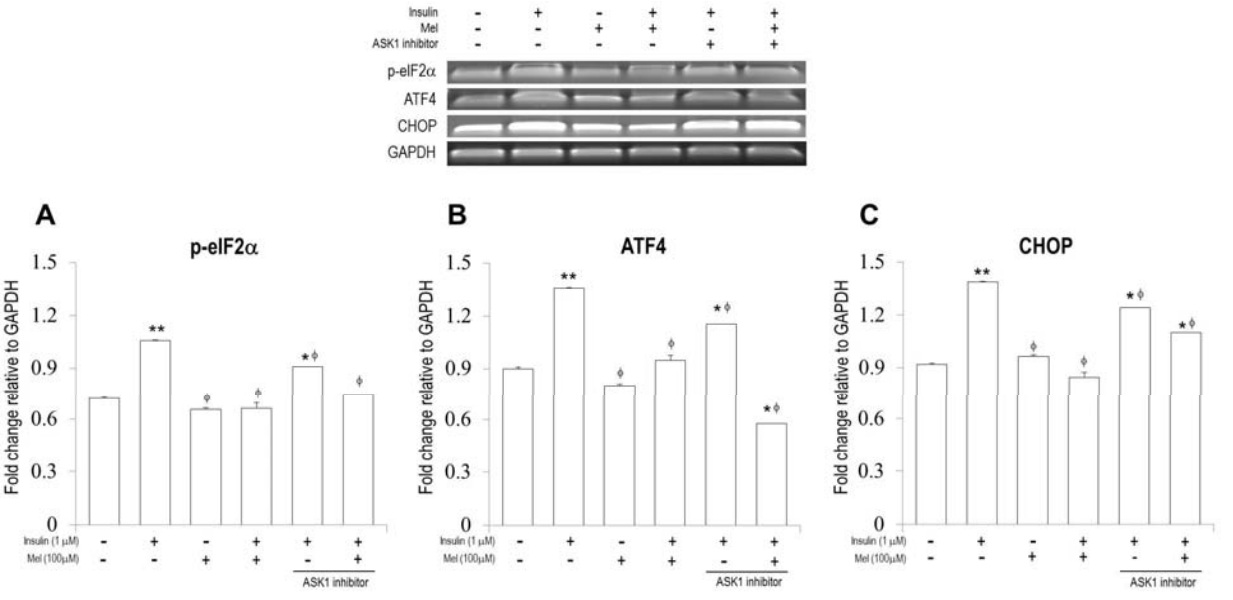

Figure 3. Melatonin regulates IR-induced endoplasmic reticulum (ER) stress signaling (p-eIF2α, ATF4, and CHOP) in the SH-SY5Y neuronal cells. The mRNA levels of (**A**) activation of eIF2α, (p-eIF2α); (**B**) ATF4, and (**C**) CHOP were measured by reverse transcription PCR. Data are expressed as mean ± standard error and each experiment included three repeats per conditions. * $p < 0.05$, ** $p < 0.01$ compared with non-stimulated control; $^{\phi}$ $p < 0.05$ compared with insulin stimulated cells. Mel: melatonin pretreatment for 24 h before insulin stimulation; *ASK1* inhibitor: NQDI-1 600 nM treatment for 2 h before sampling.

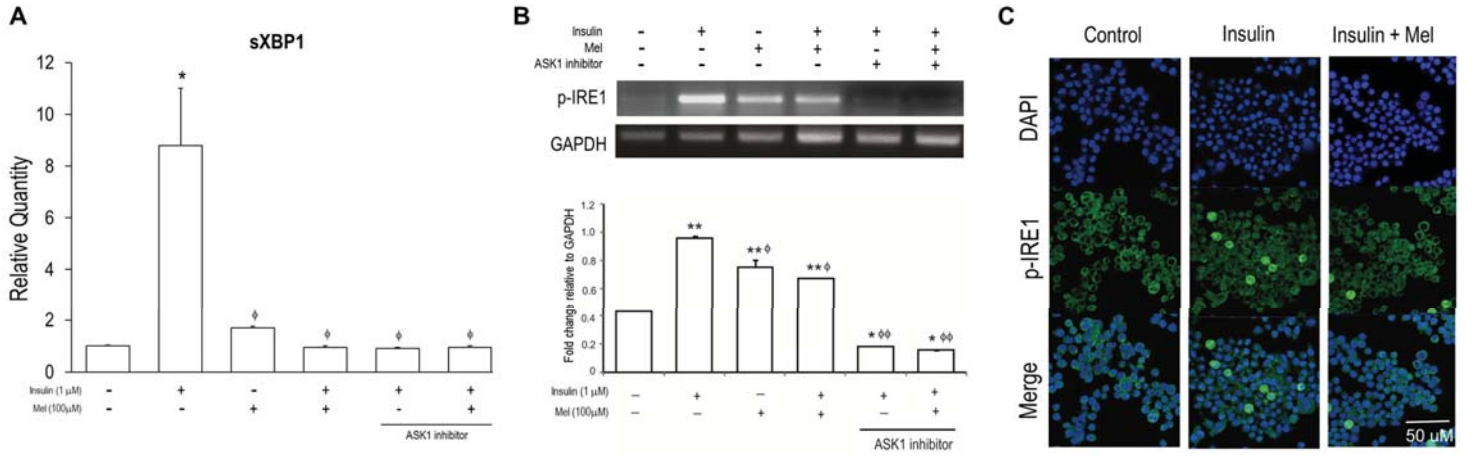

Figure 4. Melatonin alleviates IR-induced ER stress signaling (sXBP1 and *p-IRE1*) in the SH-SY5Y neuronal cells. (**A**) The mRNA levels of sXBP1 were measured by quantitative real time PCR; (**B**) The mRNA levels of activation of IRE1 (*p-IRE1*) were measured by reverse transcription PCR. Data are expressed as mean ± standard error and each experiment included three repeats per conditions. * $p < 0.05$, ** $p < 0.01$ compared with non-stimulated control; $^{\phi}$ $p < 0.05$, $^{\phi\phi}$ $p < 0.001$ compared with insulin stimulated cells; (**C**) *p-IRE1* was visualized by immunofluorescence staining using confocal microscopy analysis. *p-IRE1* is represented by green staining, nuclear DNA is indicated by 4′,6-diamidino-2-phenylindole (DAPI) staining (blue color), and the combined images are presented. Mel: melatonin pretreatment for 24 h before insulin stimulation; *ASK1* inhibitor: NQDI-1 600 nM treatment for 2 h before sampling.

3.4. Melatonin Attenuates the Activation of ASK1 under IR Condition

Immunofluorescence analysis was conducted to check if melatonin regulates the activation of *ASK1* under IR condition (Figure 5). *ASK1* was markedly phosphorylated by insulin stimulation, but the activation was dose-dependently attenuated by melatonin treatment (10 μM and 100 μM).

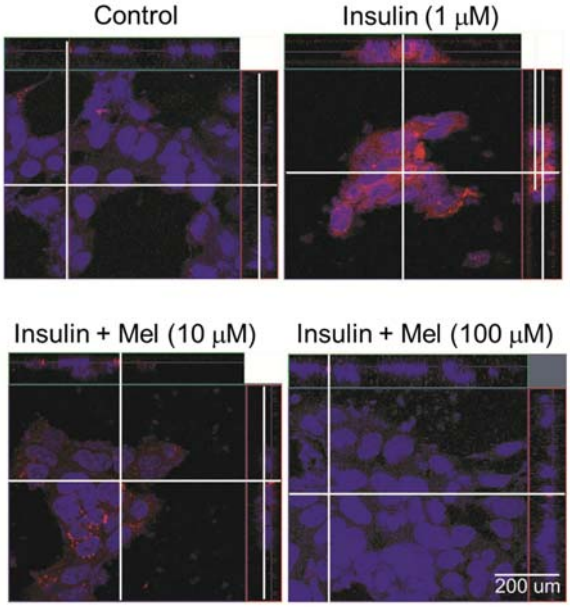

Figure 5. Melatonin attenuates the activation of *ASK1* in insulin stimulated SH-SY5Y cells. Immunofluorescence staining was performed to check the activation of *ASK1* (*p-ASK1*). Confocal microscopy analysis was performed to visualize *p-ASK1*. SH-SY5Y cells were pretreated with melatonin for 24 h before insulin stimulation. *p-ASK1* is represented by red staining, nuclear DNA is indicated by DAPI staining (blue color), and the combined images are presented; Control: non-treated cells, Mel: melatonin.

4. Discussion

The present study shows that melatonin modulates neuronal cell death induced by ER stress under IR condition. Insulin-induced mRNA or protein expressions of cell death signaling markers such as cleaved PARP, p53, and Bax, as well as the ER stress markers such as p-eIF2α, ATF4, CHOP, sXBP1, and *p-IRE1* were significantly attenuated by melatonin treatment. In addition, the regulatory effect of melatonin on insulin-induced ER stress in neuronal cells was associated with *ASK1* signaling. These results suggested that melatonin may ameliorate IR-induced neuropathogenesis via the regulation of ER stress.

Recent studies reported that IR is closely linked to hippocampus cognitive dysfunction [3–6,49], and is a crucial factor for determining the processing of neuropathogenesis [50,51]. It may be associated with the dysregulation of cellular homeostasis [9] and ER stress, which triggers cell death signaling [10,11]. The ER is highly sensitive to stresses, which reduce the protein folding capacity of the ER, thereby resulting in the accumulation and aggregation of unfolded proteins [12]. The aggregation of proteins is toxic to cells and consequently, associated with various pathophysiological conditions such as DM, ischemia, and neurodegenerative disease [52–59]. In our study, we found that mRNA and protein expressions of ER stress markers (p-eIF2α, ATF4, CHOP, *p-IRE1*, and sXBP1) [13–15] in

the SH-SY5Y neuronal cells were significantly increased by insulin stimulation. mRNA expressions of apoptotic cell death markers (cleaved PARP, Bax, and p53) [60–62] were also significantly increased by insulin stimulation. In addition, the imaging analysis demonstrated that IR condition dramatically activated ASK. As mentioned above, under stressful conditions, IR might sequentially activate the ER stress receptors, thereby triggering ER stress-induced cell death signaling: for example, PERK, one of the ER stress receptors, might phosphorylate eIF2α, which translocated ATF4 into nucleus, and then increased the gene transcription such as CHOP to restore ER homeostasis, thereby regulating ER stress mediated apoptosis [12–15]. In addition, IRE, another ER stress receptor might be activated by IR stress, and spliced XBP1, one of the ER chaperones, which was translocated into the nucleus, and then modulates the gene transcription involved in protein degradation [20,21]. Under the ER stress, the activated IRE makes complex with TRAF2, and then recruits ASK1, thereby triggering cell death [24–28].

As mentioned above, melatonin and its metabolites were reported to modulate inflammation, cell survival, and apoptosis in various pathophysiological conditions [51–55] through their capacity as potent antioxidants and free radical scavengers [56,57]. According to previous reports [48,63–65], melatonin supplementation significantly improves antioxidant status by increasing the activity of antioxidant enzymes (i.e., superoxide dismutase, glutathione peroxidase, catalase, etc.) in T2DM and obesity [48,63–65]. These enzymes also contain antioxidant minerals such as Zn, Mn, Fe, Se, Cu, etc. [48,63–65]. In the present study, we found that insulin-induced mRNA or protein expressions of the ER stress markers and cell death signaling markers in the neuronal cells were significantly attenuated by melatonin treatment, and the activation of *ASK1* induced by insulin stimulation was also dose dependently attenuated by melatonin treatment. Our results might be supported by previous reports [66–69]. Melatonin can significantly inhibit ER stress by reducing XBP1 splicing, the target of the IRE1 pathway [67,68], JNK phosphorylation [68], and insulin receptor substrate-1 (IRS-1) phosphorylation [69], thereby ameliorating insulin sensitivity. Melatonin was also reported to attenuate tunicamycin-induced ER stress by restoring insulin stimulated Akt phosphorylation and IRS-1 tyrosine phosphorylation, and reducing the IRE-1/JNK phosphorylation and IRS-1 serine phosphorylation [66]. Tunicamycin was known to induce IR through the inhibition of insulin-stimulated Akt phosphorylation, IRE-1/JNK phosphorylation, and IRS-1 serine phosphorylation [66]. In regard to this point, our results demonstrated that melatonin, through its antioxidant properties, modulates the ER stress-induced neuronal cell death under IR condition. Interestingly, our study also shows that when *ASK1* signaling was inhibited, mRNA expressions of *p-IRE1* that were stimulated by insulin treated with melatonin or not were dramatically attenuated. ASK1, which triggers apoptotic cell death, is activated by the IRE1–TRAF2 complex formed under the ER stress [24–28]. According to previous reports [28,70], *ASK1* overexpression induces apoptosis in various cell types, whereas neurons from the *ASK1* knock-out mice exhibited resistance to lethal ER stress. Based on our results and the previous reports, we assumed that *ASK1* signaling is important in ER stress-induced cell death. Further study is needed to identify the precise mechanism on the role of melatonin in *ASK1* signaling in neuronal cells

In addition, ER stress was reported to induce autophagy [71]. Autophagy is a dynamic process which promotes self-digestion of misfolded proteins and damaged organelles in the cells [35]. Activation of autophagy signaling was observed in obese people [72], and is critical to regulate IR-induced ER stress in diabetic patients [73]. For example, autophagy captures and ubiquitinates inflammasome, thereby recruiting *LC3* as well as *beclin 1*, marker proteins for autophagy detection [74–76]. In our study, we did not directly measure the expressions of autophagic cell death related factors such as *belcin1* and *LC3*, but we observed that mRNA expressions of sXBP1 and CHOP, which are involved in autophagic response, were significantly increased by insulin stimulation, and dramatically attenuated by melatonin treatment. sXBP1 was reported to directly bind to the promoter of *beclin 1* in the nucleus, and promotes an autophagic response [77]. CHOP is also known to promote autophagy gene expression (i.e., *LC3*, *NIX*, *NBR1*), and its capacity to dephosphorylate eIF2α is implicated in the initiation of autophagy.

5. Conclusions

Taken together, this study demonstrated that melatonin modulates neuronal cell death signaling induced by ER stress under IR condition, and it may be related to the suppression of *ASK1* activation. Furthermore, melatonin may be a potential solution in ameliorating IR associated neuropathogenesis and cognitive decline. Further studies are needed to elucidate the mechanism though which melatonin affects IR-induced ER stress autophagic signaling in order to better understand the neuronal cell damage caused by IR.

Acknowledgments: This study was supported by the National Research Foundation of Korea Grant funded by the Korean Government (2016R1A2B4013627).

Author Contributions: J.S. and O.Y.K. designed the experiments and wrote the manuscript. J.S. conducted the experiments. J.S. and O.Y.K. analyzed the data. O.Y.K. revised the manuscript and provided the research funding. All authors reviewed and agreed on final version of the manuscript.

Conflicts of Interest: The author declares that there are no conflicts of interest.

References

1. Kahn, S.E.; Cooper, M.E.; Del Prato, S. Pathophysiology and treatment of type 2 diabetes: Perspectives on the past, present, and future. *Lancet* **2014**, *383*, 1068–1083. [CrossRef]
2. Koekkoek, P.S.; Kappelle, L.J.; van den Berg, E.; Rutten, G.E.; Biessels, G.J. Cognitive function in patients with diabetes mellitus: Guidance for daily care. *Lancet Neurol.* **2015**, *14*, 329–340. [CrossRef]
3. Gudala, K.; Bansal, D.; Schifano, F.; Bhansali, A. Diabetes mellitus and risk of dementia: A meta-analysis of prospective observational studies. *J. Diabetes Investig.* **2013**, *4*, 640–650. [CrossRef] [PubMed]
4. Biessels, G.J.; Strachan, M.W.; Visseren, F.L.; Kappelle, L.J.; Whitmer, R.A. Dementia and cognitive decline in type 2 diabetes and prediabetic stages: Towards targeted interventions. *Lancet Diabetes Edocrinol.* **2014**, *2*, 246–255. [CrossRef]
5. Convit, A.; Wolf, O.T.; Tarshish, C.; de Leon, M.J. Reduced glucose tolerance is associated with poor memory performance and hippocampal atrophy among normal elderly. *Proc. Natl. Acad. Sci. USA* **2003**, *100*, 2019–2022. [CrossRef] [PubMed]
6. Bruehl, H.; Sweat, V.; Hassenstab, J.; Polyakov, V.; Convit, A. Cognitive impairment in nondiabetic middle-aged and older adults is associated with insulin resistance. *J. Clin. Exp. Neuropsychol.* **2010**, *32*, 487–493. [CrossRef] [PubMed]
7. Greenwood, C.E.; Winocur, G. Cognitive impairment in rats fed high-fat diets: A specific effect of saturated fatty-acid intake. *Behav. Neurosci.* **1996**, *110*, 451–459. [CrossRef] [PubMed]
8. Takeda, S.; Sato, N.; Uchio-Yamada, K.; Sawada, K.; Kunieda, T.; Takeuchi, D.; Kurinami, H.; Shinohara, M.; Rakugi, H.; Morishita, R. Diabetes-accelerated memory dysfunction via cerebrovascular inflammation and Abeta deposition in an Alzheimer mouse model with diabetes. *Proc. Natl. Acad. Sci. USA* **2010**, *107*, 7036–7041. [CrossRef] [PubMed]
9. Lee, J.; Ozcan, U. Unfolded protein response signaling and metabolic diseases. *J. Biol. Chem.* **2014**, *289*, 1203–1211. [CrossRef] [PubMed]
10. Guerrero-Hernandez, A.; Leon-Aparicio, D.; Chavez-Reyes, J.; Olivares-Reyes, J.A.; DeJesus, S. Endoplasmic reticulum stress in insulin resistance and diabetes. *Cell Calcium* **2014**, *56*, 311–322. [CrossRef] [PubMed]
11. Oyadomari, S.; Mori, M. Roles of CHOP/GADD153 in endoplasmic reticulum stress. *Cell Death Differ.* **2004**, *11*, 381–389. [CrossRef] [PubMed]
12. Szegezdi, E.; Logue, S.E.; Gorman, A.M.; Samali, A. Mediators of endoplasmic reticulum stress-induced Apoptosis. *EMBO Rep.* **2006**, *7*, 880–885. [CrossRef] [PubMed]
13. Boyce, M.; Bryant, K.F.; Jousse, C.; Long, K.; Harding, H.P.; Scheuner, D.; Kaufman, R.J.; Ma, D.; Coen, D.M.; Ron, D.; et al. A selective inhibitor of eIF2α dephosphorylation protects cells from ER stress. *Science* **2005**, *307*, 935–939. [CrossRef] [PubMed]
14. Ohoka, N.; Yoshii, S.; Hattori, T.; Onozaki, K.; Hayashi, H. TRB3, a novel ER stress-ind, ucible gene, is induced via ATF4–CHOP pathway and is involved in cell death. *EMBO J.* **2005**, *24*, 1243–1255. [CrossRef] [PubMed]

15. Marciniak, S.J.; Yun, C.Y.; Oyadomari, S.; Novoa, I.; Zhang, Y.; Jungreis, R.; Nagata, K.; Harding, H.P.; Ron, D. CHOP induces death by promoting protein synthesis and oxidation in the stressed endoplasmic reticulum. *Gene Dev.* **2004**, *18*, 3066–3077. [CrossRef] [PubMed]
16. Maris, M.; Overbergh, L.; Gysemans, C.; Waget, A.; Cardozo, A.K.; Verdrengh, E.; Cunha, J.P.; Gotoh, T.; Cnop, M.; Eizirik, D.L.; et al. Deletion of C/EBP homologous protein (Chop) in C57Bl/6 mice dissociates obesity from insulin resistance. *Diabetologia* **2012**, *55*, 1167–1178. [CrossRef] [PubMed]
17. Zhong, J.T.; Xu, Y.; Yi, H.W.; Su, J.; Yu, H.M.; Xiang, X.Y.; Li, X.N.; Zhang, Z.C.; Sun, L.K. The BH3 mimetic S1 induces autophagy through ER stress and disruption of Bcl-2/*Beclin 1* interaction in human glioma U251 cells. *Cancer Lett.* **2012**, *323*, 180–187. [CrossRef] [PubMed]
18. Namba, T.; Tanaka, K.; Ito, Y.; Ishihara, T.; Hoshino, T.; Gotoh, T.; Endo, M.; Sato, K.; Mizushima, T. Positive role of CCAAT/enhancer-binding protein homologous protein, a transcription factor involved in the endoplasmic reticulum stress response in the development of colitis. *Am. J. Pathol.* **2009**, *174*, 1786–1798. [CrossRef] [PubMed]
19. Yoshida, H.; Matsui, T.; Yamamoto, A.; Okada, T.; Mori, K. XBP1 mRNA is induced by ATF6 and spliced by IRE1 in response to ER stress to produce a highly active transcription factor. *Cell* **2001**, *107*, 881–891. [CrossRef]
20. Wang, X.Z.; Harding, H.P.; Zhang, Y.; Jolicoeur, E.M.; Kuroda, M.; Ron, D. Cloning of mammalian Ire1 reveals diversity in the ER stress responses. *EMBO J.* **1998**, *17*, 5708–5717. [CrossRef] [PubMed]
21. Lee, A.H.; Iwakoshi, N.N.; Glimcher, L.H. XBP-1 regulates a subset of endoplasmic reticulum resident chaperone genes in the unfolded protein response. *Mol. Cell. Biol.* **2003**, *23*, 7448–7459. [CrossRef] [PubMed]
22. Boden, G.; Duan, X.; Homko, C.; Molina, E.J.; Song, W.; Perez, O.; Cheung, P.; Merali, S. Increase in endoplasmic reticulum stress-related proteins and genes in adipose tissue of obese, insulin-resistant individuals. *Diabetes* **2008**, *57*, 2438–2444. [CrossRef] [PubMed]
23. Yoshiuchi, K.; Kaneto, H.; Matsuoka, T.A.; Kohno, K.; Iwawaki, T.; Nakatani, Y.; Yamasaki, Y.; Hori, M.; Matsuhisa, M. Direct monitoring of in vivo ER stress during the development of insulin resistance with ER stress-activated indicator transgenic mice. *Biochem. Biophys. Res. Commun.* **2008**, *366*, 545–550. [CrossRef] [PubMed]
24. Nishitoh, H.; Saitoh, M.; Mochida, Y.; Takeda, K.; Nakano, H.; Rothe, M.; Miyazono, K.; Ichijo, H. *ASK1* is essential for JNK/SAPK activation by TRAF2. *Mol. Cell* **1998**, *2*, 389–395. [CrossRef]
25. Ichijo, H.; Nishida, E.; Irie, K.; ten Dijke, P.; Saitoh, M.; Moriguchi, T.; Takagi, M.; Matsumoto, K.; Miyazono, K.; Gotoh, Y. Induction of apoptosis by ASK1, a mammalian MAPKKK that activates SAPK/JNK and p38 signaling pathways. *Science* **1997**, *275*, 90–94. [CrossRef] [PubMed]
26. Takeda, K.; Noguchi, T.; Naguro, I.; Ichijo, H. Apoptosis signal-regulating kinase 1 in stress and immune response. *Annu. Rev. Pharmacol.* **2008**, *48*, 199–225. [CrossRef] [PubMed]
27. Kanamoto, T.; Mota, M.; Takeda, K.; Rubin, L.L.; Miyazono, K.; Ichijo, H.; Bazenet, C.E. Role of apoptosis signal-regulating kinase in regulation of the c-Jun *N*-terminal kinase pathway and apoptosis in sympathetic neurons. *Mol. Cell. Biol.* **2000**, *20*, 196–204. [CrossRef] [PubMed]
28. Hatai, T.; Matsuzawa, A.; Inoshita, S.; Mochida, Y.; Kuroda, T.; Sakamaki, K.; Kuida, K.; Yonehara, S.; Ichijo, H.; Takeda, K. Execution of apoptosis signal-regulating kinase 1 (ASK1)-induced apoptosis by the mitochondria-dependent caspase activation. *J. Biol. Chem.* **2000**, *275*, 26576–26581. [CrossRef] [PubMed]
29. Cao, S.S.; Kaufman, R.J. Targeting endoplasmic reticulum stress in metabolic disease. *Expert Opin. Ther. Targets* **2013**, *17*, 437–448. [CrossRef] [PubMed]
30. Oz-Levi, D.; Gelman, A.; Elazar, Z.; Lancet, D. TECPR2: A new autophagy link for neurodegeneration. *Autophagy* **2013**, *9*, 801–802. [CrossRef] [PubMed]
31. Hadj Ayed Tka, K.; Mahfoudh Boussaid, A.; Zaouali, M.A.; Kammoun, R.; Bejaoui, M.; Ghoul Mazgar, S.; Rosello Catafau, J.; Ben Abdennebi, H. Melatonin modulates endoplasmic reticulum stress and Akt/GSK3-beta signaling pathway in a rat model of renal warm ischemia reperfusion. *Anal. Cell. Pathol. (Amst.)* **2015**, *2015*, 635172. [CrossRef] [PubMed]
32. Meng, X.; Li, Y.; Li, S.; Zhou, Y.; Gan, R.Y.; Xu, D.P.; Li, H.B. Dietary Sources and Bioactivities of Melatonin. *Nutrients* **2017**, *9*, 367. [CrossRef] [PubMed]
33. Altun, A.; Ugur-Altun, B. Melatonin: Therapeutic and clinical utilization. *Int. J. Clin. Pract.* **2007**, *61*, 835–845. [CrossRef] [PubMed]

34. De la Puerta, C.; Carrascosa-Salmoral, M.P.; García-Luna, P.P.; Lardone, P.J.; Herrera, J.L.; Fernández-Montesinos, R.; Guerrero, J.M.; Pozo, D. Melatonin is a phytochemical in olive oil. *Food Chem.* **2007**, *104*, 609–612. [CrossRef]
35. Fernandez, A.; Ordonez, R.; Reiter, R.J.; Gonzalez-Gallego, J.; Mauriz, J.L. Melatonin and endoplasmic reticulum stress: Relation to autophagy and apoptosis. *J. Pineal Res.* **2015**, *59*, 292–307. [CrossRef] [PubMed]
36. Mauriz, J.L.; Collado, P.S.; Verneroso, C.; Reiter, R.J.; González-Gallego, J. A review ofthe molecular aspects of melatonin's anti-inflammatory actions: Recent insights and new perspectives. *J. Pineal Res.* **2013**, *54*, 1–14. [CrossRef] [PubMed]
37. Tunon, M.J.; San Miguel, B.; Crespo, I.; Jorquera, F.; Santamaría, E.; Alvarez, M.; Prieto, J.; González-Gallego, J. Melatonin attenuates apoptotic liver damage in fulminant hepatic failure induced by the rabbit hemorrhagic disease virus. *J. Pineal Res.* **2011**, *50*, 38–45. [CrossRef] [PubMed]
38. Kim, S.H.; Lee, S.M. Cytoprotective effects of melatonin against necrosis and apoptosis induced by ischemia/reperfusion injury in rat liver. *J. Pineal Res.* **2008**, *44*, 165–171. [CrossRef] [PubMed]
39. Wang, H.; Xu, D.X.; Lv, J.W.; Nin, H.; Wei, W. Melatonin attenuates lipopolysaccharide (LPS)-induced apoptotic liver damage in D-galactosamine-sensitized mice. *Toxicology* **2007**, *237*, 49–57. [CrossRef] [PubMed]
40. Galano, A.; Tan, D.X.; Reiter, R.J. Melatonin as a natural ally against oxidative stress: A physicochemical examination. *J. Pineal Res.* **2011**, *51*, 1–16. [CrossRef] [PubMed]
41. Galano, A.; Tan, D.X.; Reiter, R.J. On the free radical scavenging activities of melatonin's metabolites, AFMK and AMK. *J. Pineal Res.* **2013**, *54*, 245–257. [CrossRef] [PubMed]
42. Pechanova, O.; Paulis, L.; Simko, F. Peripheral and central effects of melatonin on blood pressure regulation. *Int. J. Mol. Sci.* **2014**, *15*, 17920–17937. [CrossRef] [PubMed]
43. Galano, A. On the direct scavenging activity of melatonin towards hydroxyl and a series of peroxyl radicalsfree radical scavenging activities of melatonin's metabolites, AFMK and AMK. *Phys. Chem. Chem. Phys.* **2011**, *13*, 7178–7188. [CrossRef] [PubMed]
44. Witt-Enderby, P.A.; Bennett, J.; Jarzynka, M.J.; Firestine, S.; Melan, M.A. Melatonin receptors and their regulation: Biochemical and structural mechanisms. *Life Sci.* **2003**, *72*, 2183–2198. [CrossRef]
45. Agil, A.; El-Hammadi, M.; Jiménez-Aranda, A.; Tassi, M.; Abdo, W.; Fernández-Vázquez, G.; Reiter, R.J. Melatonin reduces hepatic mitochondrial dysfunction in diabetic obese rats. *J. Pineal Res.* **2015**, *59*, 70–79. [CrossRef] [PubMed]
46. Elmahallawy, E.K.; Jiménez-Aranda, A.; Martínez, A.S.; Rodriguez-Granger, J.; Navarro-Alarcón, M.; Gutiérrez-Fernández, J.; Agil, A. Activity of melatonin against *Leishmania infantum* promastigotes by mitochondrial dependent pathway. *Chem. Biol. Interact.* **2014**, *220*, 84–93. [CrossRef] [PubMed]
47. Jimenéz-Aranda, A.; Fernández-Vázquez, G.; Mohammad A-Serrano, M.; Reiter, R.J.; Agil, A. Melatonin improves mitochondrial function in inguinal white adipose tissue of Zücker diabetic fatty rats. *J. Pineal Res.* **2014**, *57*, 103–109. [CrossRef] [PubMed]
48. Navarro-Alarcon, M.; Ruiz-Ojeda, F.J.; Blanca-Herrera, R.M.; Agil, A. Antioxidant activity of melatonin in diabetes in relation to the regulation and levels of plasma Cu, Zn, Fe, Mn, and Se in Zucker diabetic fatty rats. *Nutrition* **2013**, *29*, 785–789. [CrossRef] [PubMed]
49. Biessels, G.J.; Reagan, L.P. Hippoocampal insulin resistance and cognitive dysfunction. *Nat. Rev. Neurosci.* **2015**, *16*, 660–671. [CrossRef] [PubMed]
50. Novak, V.; Milberg, W.; Hao, Y.; Munshi, M.; Novak, P.; Galica, A.; Manor, B.; Roberson, P.; Craft, S.; Abduljalil, A. Enhancement of vasoreactivity and cognition by intranasal insulin in type 2 diabetes. *Diabetes Care* **2014**, *37*, 751–759. [CrossRef] [PubMed]
51. Yarchoan, M.; Arnold, S.E. Repurposing diabetes drugs for brain insulin resistance in Alzheimer disease. *Diabetes* **2014**, *63*, 2253–2261. [CrossRef] [PubMed]
52. Kaufman, R.J. Orchestrating the unfolded protein response in health and disease. *J. Clin. Investig.* **2002**, *110*, 1389–1398. [CrossRef] [PubMed]
53. Hummasti, S.; Hotamisligil, G.S. Endoplasmic reticulum stress and inflammation in obesity and diabetes. *Circ. Res.* **2010**, *107*, 579–591. [CrossRef] [PubMed]
54. Guo, J.Y.; Chen, H.Y.; Mathew, R.; Fan, J.; Strohecker, A.M.; Karsli-Uzunbas, G.; Kamphorst, J.J.; Chen, G.; Lemons, J.M.; Karantza, V.; et al. Activated Ras requires autophagy to maintain oxidative metabolism and tumorigenesis. *Gene Dev.* **2011**, *25*, 460–470. [CrossRef] [PubMed]

55. Walter, P.; Ron, D. The unfolded protein response: From stress pathway to homeostatic regulation. *Science* **2011**, *334*, 1081–1086. [CrossRef] [PubMed]
56. Wang, S.; Kaufman, R.J. The impact of the unfolded protein response on human disease. *J. Cell Biol.* **2012**, *197*, 857–867. [CrossRef] [PubMed]
57. Fonseca, S.G.; Gromada, J.; Urano, F. Endoplasmic reticulum stress and pancreatic beta-cell death. *Trends Endocrinol. Metab.* **2011**, *22*, 266–274. [PubMed]
58. Kolattukudy, P.E.; Niu, J. Inflammation, endoplasmic reticulum stress, autophagy, and the monocyte chemoattractant protein-1/CCR2 pathway. *Circ. Res.* **2012**, *110*, 174–189. [CrossRef] [PubMed]
59. Oslowski, C.M.; Hara, T.; O'Sullivan-Murphy, B.; Kanekura, K.; Lu, S.; Hara, M.; Ishigaki, S.; Zhu, L.J.; Hayashi, E.; Hui, S.T.; et al. Thioredoxin-interacting protein mediates ER stress-induced beta cell death through initiation of the inflammasome. *Cell Metab.* **2012**, *16*, 265–273. [CrossRef] [PubMed]
60. Zeng, H.; Zhang, S.; Yang, K.Y.; Wang, T.; Hu, J.L.; Huang, L.L.; Wu, G. Knockdown of second mitochondria-derived activator of caspase expression by RNAi enhances growth and cisplatin resistance of human lung cancer cells. *Cancer Biother. Radiopharm.* **2010**, *25*, 705–712. [CrossRef] [PubMed]
61. Wei, Q.; Dong, G.; Franklin, J.; Dong, Z. The pathological role of Bax in cisplatin nephrotoxicity. *Kidney Int.* **2007**, *72*, 53–62. [CrossRef] [PubMed]
62. Akpinar, B.; Bracht, E.V.; Reijnders, D.; Safarikova, B.; Jelinkova, I.; Grandien, A.; Vaculova, A.H.; Zhivotovsky, B.; Olsson, M. 5-Fluorouracil-induced RNA stress engages a TRAIL-DISC-dependent apoptosis axis facilitated by p53. *Oncotarget* **2015**, *6*, 43679–43697. [PubMed]
63. Othman, A.I.; El-Missiry, A.; Amer, M.A.; Arafa, M. Melatonin controls oxidative stress and modulates iron, ferritin, and transferrin levels in Adriamycin treated rats. *Life Sci.* **2008**, *83*, 563–568. [CrossRef] [PubMed]
64. Kedziora-Kornatowska, K.; Szewcyk-Golec, K.; Kozakiewicz, M.; Pawluk, H.; Czuczejko, J.; Kornatowski, T.; Bartosz, G.; Kedziora, J. Melatonin improves oxidative stress parameters measured in the blood of elderly type 2 diabetic patients. *J. Pineal Res.* **2009**, *46*, 333–337. [CrossRef] [PubMed]
65. Kozirog, M.; Poliwczak, A.R.; Duchnowicz, P.; Koter-Michalak, M.; Sikora, J.; Broncel, M. Melatonin improves blood pressure, lipid profile, and parameters of oxidative stress in patients with metabolic syndrome. *J. Pineal Res.* **2011**, *50*, 261–266. [CrossRef] [PubMed]
66. Quan, X.; Wang, J.; Liang, C.; Zheng, H.; Zhang, L. Melatonin inhibits tunicamycin-induced endoplasmic reticulum stress and insulin resistance in skeletal muscle cells. *Biochem. Biophys. Res. Commun.* **2015**, *463*, 1102–1107. [CrossRef] [PubMed]
67. Carloni, S.; Albertini, M.C.; Galluzzi, L.; Buonocore, G.; Proietti, F.; Balduini, W. Melatonin reduces endoplasmic reticulum stress and preserves sirtuin 1 expression in neuronal cells of newborn rats after hypoxia-ischemia. *J. Pineal Res.* **2014**, *57*, 192–199. [CrossRef] [PubMed]
68. Ji, Y.L.; Wang, H.; Meng, C.; Zhao, X.F.; Zhang, C.; Zhang, Y.; Zhao, M.; Chen, Y.H.; Meng, X.H.; Xu, D.X. Melatonin alleviates cadmium-induced cellular stress and germ cell apoptosis in testes. *J. Pineal Res.* **2012**, *52*, 71–79. [CrossRef] [PubMed]
69. She, M.; Hou, H.; Wang, Z.; Zhang, C.; Laudon, M.; Yin, W. Melatonin rescues 3T3-L1 adipocytes from FFA-induced insulin resistance by inhibiting phosphorylation of IRS-1 on Ser307. *Biochimie* **2014**, *103*, 126–130. [CrossRef] [PubMed]
70. Nishitoh, H.; Matsuzawa, A.; Tobiume, K.; Saegusa, K.; Takeda, K.; Inoue, K.; Hori, S.; Kakizuka, A.; Ichijo, H. *ASK1* is essential for endoplasmic reticulum stress-induced neuronal cell death triggered by expanded polyglutamine repeats. *Genes Dev.* **2002**, *16*, 1345–1355. [CrossRef] [PubMed]
71. Yorimitsu, T.; Nair, U.; Yang, Z.; Klionsky, D.J. Endoplasmic reticulum stress triggers autophagy. *J. Biol. Chem.* **2006**, *281*, 30299–30304. [CrossRef] [PubMed]
72. Kovsan, J.; Bluher, M.; Tarnovscki, T.; Kloting, N.; Kirshtein, B.; Madar, L.; Shai, I.; Golan, R.; Harman-Boehm, I.; Schon, M.R.; et al. Altered autophagy in human adipose tissues in obesity. *J. Clin. Endocrinol. Metab.* **2011**, *96*, E268–E277. [CrossRef] [PubMed]
73. Zhang, N.; Cao, M.M.; Liu, H.; Xie, G.Y.; Li, Y.B. Autophagy regulates insulin resistance following endoplasmic reticulum stress in diabetes. *J. Physiol. Biochem.* **2015**, *71*, 319–327. [CrossRef] [PubMed]
74. Levine, B.; Mizushima, N.; Virgin, H.W. Autophagy in immunity and inflammation. *Nature* **2011**, *469*, 323–335. [CrossRef] [PubMed]

75. BLi, D.D.; Wang, L.L.; Deng, R.; Tang, J.; Shen, Y.; Guo, J.F.; Wang, Y.; Xia, L.P.; Feng, G.K.; Liu, Q.Q.; et al. The pivotal role of c-Jun NH2-terminal kinase-mediated *Beclin 1* expression during anticancer agents-induced autophagy in cancer cells. *Oncogene* **2009**, *28*, 886–898.
76. Mizushima, N. The role of the Atg1/ULK1 complex in autophagy regulation. *Curr. Opin. Cell Biol.* **2010**, *22*, 132–139. [CrossRef] [PubMed]
77. Margariti, A.; Li, H.; Chen, T.; Martin, D.; Vizcay-Barrena, G.; Alam, S.; Karamariti, E.; Xiao, Q.; Zampetaki, A.; Zhang, Z.; et al. XBP1 mRNA splicing triggers an autophagic response in endothelial cells through BECLIN-1 transcriptional activation. *J. Biol. Chem.* **2013**, *288*, 859–872. [CrossRef] [PubMed]

nutrients

MDPI

Article

Alpha- and Gamma-Tocopherol and Telomere Length in 5768 US Men and Women: A NHANES Study

Larry A. Tucker

Department of Exercise Sciences, Brigham Young University, Provo, UT 84602, USA; tucker@byu.edu

Received: 7 June 2017; Accepted: 8 June 2017; Published: 13 June 2017

Abstract: Antioxidants have a number of potential health benefits. The present investigation was designed to determine the relationship between serum alpha- and gamma-tocopherol levels (powerful antioxidants), and leukocyte telomere length (a biomarker of biological aging). A cross-sectional design was employed to study 5768 adults from the National Health and Nutrition Examination Survey (NHANES). DNA was obtained via blood samples. Telomere length was assessed using the quantitative polymerase chain reaction method. Serum concentrations of alpha- and gamma-tocopherol were measured using high performance liquid chromatography (HPLC). Results showed that for each one-year increase in age, telomeres were 15.6 base pairs shorter ($F = 410.4$, $p < 0.0001$). After adjusting for differences in the demographic covariates, for each μg/dL higher level of gamma-tocopherol, telomeres were 0.33 base pairs shorter ($F = 7.1$, $p = 0.0126$). Telomeres were approximately 1 year shorter (15.6 base pairs) for each increment of 47.3 to 55.7 μg/dL of gamma-tocopherol in the blood, depending on the variables controlled. Adults at the 75th percentile of gamma-tocopherol had 2.8–3.4 years greater cellular aging than those at the 25th percentile, depending on the covariates in the model. However, alpha-tocopherol was not related to telomere length. Evidently, gamma-tocopherol levels, but not alpha-tocopherol, account for meaningful increases in biological aging.

Keywords: cell aging; antioxidant; vitamin E; DNA

1. Introduction

Vitamin E is an essential nutrient and a powerful antioxidant. It is a fat-soluble vitamin that occurs naturally in eight forms. Vitamin E can be divided into two principal classes: tocopherols and tocotrienols. These can be further categorized into slightly different compounds, known as alpha, beta, delta, and gamma [1].

Many claims have been made about the potential of vitamin E to improve health and prevent disease because it is a chain-breaking antioxidant that prevents free radical reactions and lipid peroxidation. The most abundant and biologically active form of vitamin E is alpha-tocopherol [2]. Although alpha- and gamma-tocopherol differ by only one methyl group, alpha- is the only form of vitamin E considered necessary to satisfy human nutrition needs [3]. However, unlike alpha-tocopherol, gamma- also counters reactive nitrogen species [4]. Moreover, some scientists indicate that the antioxidant characteristics of gamma-tocopherol may actually exceed those of alpha-tocopherol [5]. In the US, blood levels of alpha-tocopherol are about five times higher than gamma-levels [6].

Although alpha- and gamma-tocopherol differ only slightly in molecular structure, some studies indicate that they have different consequences on the body [2,7–10]. Marchese et al. [2] suggest that alpha- and gamma-tocopherol oppose each other under certain conditions. For example, some experiments show that alpha-tocopherol protects, whereas gamma-tocopherol promotes lung inflammation and airway hyper-responsiveness [10,11]. According to data from the CARDIA (coronary artery risk development in young adults) study, serum concentrations of alpha-tocopherol are favorably

associated with lung function, whereas gamma-tocopherol levels are negatively related to spirometry results [2].

Other investigations focusing on the health effects of alpha- and gamma-tocopherol have also yielded conflicting findings. A meta-analysis involving approximately 370,000 participants showed that blood alpha-tocopherol levels were inversely associated with risk of prostate cancer, whereas gamma-tocopherol levels were not [12]. Further, in a NHANES (national health and nutrition examination survey) study of 1289 US adults, blood levels of alpha-tocopherol were predictive of lower fasting blood glucose concentrations, suggesting better glucose regulation, but gamma-tocopherol levels were associated with higher fasting glucose levels and also higher glycosylated haemoglobin (A1c) concentrations [13]. Additionally, in women, blood alpha-tocopherol levels were favorably associated with hemorrhagic stroke mortality, but gamma-tocopherol concentrations were directly linked to death from hemorrhagic stroke [14].

The literature includes far more investigations about alpha-tocopherol than gamma-, even though gamma-tocopherol is the primary form of vitamin E in the American diet [15]. Consequently, some researchers recommend that more research focus on gamma-tocopherol [15,16]. In a review article, Jiang et al. [16] indicate plainly that gamma-tocopherol "deserves more attention" (p. 714). Given the inconsistent findings in the literature, it is of public health interest that the biological effects of both alpha- and gamma-tocopherol be investigated and their contributions to human health be compared.

A good gauge of cell aging and biological health is the length of leukocyte telomeres. Telomeres are protective caps found on the ends of chromosomes. When cells divide, some of the telomeric DNA does not replicate. Therefore, with mitosis, telomeres become consistently shorter. Hence, it follows that scientists refer to telomeres as the molecular clock of cells [17,18].

A number of investigations show that oxidative stress shortens telomeres [19–23]. Furthermore, many studies indicate that shorter telomeres are predictive of premature disease, independent of age, including cancer [24–26], cardiovascular disease [27–30], diabetes [31–33], and cognitive dysfunction [34,35]. Given that oxidative stress shortens telomeres, and given the antioxidant characteristics of vitamin E and its capacity to prevent free radical reactions, it follows that vitamin E could preserve telomeres and reduce cell aging. However, little research is available indicating if vitamin E—particularly blood levels of alpha- and gamma-tocopherol—account for differences in telomere length in US men and women. Hence, the present study was conducted. A random sample of 5768 men and women collected by NHANES was used, representing non-institutionalized civilian adults in the United States. A secondary purpose was to determine the influence of several covariates, including age, gender, race, smoking, BMI (body mass index), physical activity, alcohol use, total serum cholesterol, dietary vitamin E intake, and supplement use, on the associations between alpha- and gamma-tocopherol and telomere length.

2. Materials and Methods

2.1. Sample

In order to provide national estimates of the nutrition, health, and lifestyles of individuals living in the United States, the Centers for Disease Control and Prevention administers an ongoing study called NHANES. The investigation uses a multistage probability sampling design, so the results can be generalized broadly across the United States.

Only two 2-year data cycles of NHANES contain values for telomere length, 1999–2000 and 2001–2002. All of the data are cross-sectional. The telomere data became available to the public in November, 2014, and all of the NHANES data sets are available to the public online [36].

All participants ages 20 years and older were asked to give a blood sample containing their DNA during the 1999–2000 and 2001–2002 data cycles. A total of 10,291 adults were eligible and 7827 donated a valid sample (76%). Because NHANES records the age of all participants age 85 or older as 85 to maximize confidentiality, subjects $\geq$85 were excluded from the sample.

To be included in the present investigation, participants were required to have data for each variable of the study. A total of 5768 adults—3043 women and 2725 men—were included. Written informed consent was obtained from each participant and the National Center for Health Statistics Ethics Review Board approved collection of the NHANES data and posting of the files online for public use [37].

2.2. Measures

A total of 13 variables were studied in this investigation. The exposure variables were blood levels of alpha- and gamma-tocopherol. The outcome variable was leukocyte telomere length. Covariates included: age, gender, race, BMI, smoking, physical activity, alcohol use, total serum cholesterol, supplement use, and dietary vitamin E intake.

2.2.1. Alpha- and Gamma-Tocopherol

To provide objective measures of alpha- and gamma-tocopherol levels, blood specimens were collected at the NHANES mobile examination centers (MECs). Serum concentrations of alpha- and gamma-tocopherol were measured using high performance liquid chromatography (HPLC) with photodiode array detection [38]. Exclusion criteria included hemophiliacs, individuals who had received chemotherapy during the previous 4 weeks, and participants with rashes, gauze dressings, casts, edema, open sores or wounds, etc. The laboratory staff included certified medical technologists and phlebotomists. Members of the laboratory staff each completed comprehensive training before working in the MEC. The NHANES quality control and quality assurance protocols met the Clinical Laboratory Improvement Act standards [38].

2.2.2. Telomere Length

NHANES [39] has described in detail the procedures employed to measure telomere length. According to NHANES, DNA was extracted from blood samples and stored at −80 °C at the Centers for Disease Control and Prevention. Specimens were then shipped to the University of California, San Francisco for analysis in the Blackburn laboratory. Leucocyte telomere length was measured using the quantitative polymerase chain reaction method and compared to standard reference DNA (T/S ratio). Five 96-well quality control plates, representing 5% of the complete set, were used. The investigators were blinded regarding the duplicate samples [39].

According to NHANES [39], "Each sample was assayed 3 times on 3 different days. The samples were assayed on duplicate wells, resulting in 6 data points. Sample plates were assayed in groups of 3 plates, and no 2 plates were grouped together more than once. Each assay plate contained 96 control wells with 8 control DNA samples. Assay runs with 8 or more invalid control wells were excluded from further analysis (<1% of runs). Control DNA values were used to normalize between-run variability. Runs with more than 4 control DNA values falling outside 2.5 standard deviations from the mean for all assay runs were excluded from further analysis (<6% of runs). For each sample, any potential outliers were identified and excluded from the calculations (<2% of samples). The mean and standard deviation of the T/S ratio were then calculated normally. The interassay coefficient of variation was 6.5%" [39]. Mean T/S ratio values were converted to base pairs using the formula: $3274 + 2413 \times (T/S)$.

2.2.3. Covariates

Age, gender, and race were used as demographic covariates. NHANES used five categories to differentiate among races and ethnicities: Non-Hispanic White, Non-Hispanic Black, Mexican American, Other race or multi-racial, and Other Hispanic. Additional covariates were employed to index lifestyle variables, including BMI, smoking, physical activity, alcohol use, dietary intake of vitamin E, supplement use, and total serum cholesterol.

2.2.4. Body Mass Index (BMI)

BMI was used to compare the body weight of participants, independent of height. The standard BMI formula was used (kg/m^2): weight in kilograms divided by height in meters, squared. BMI categories were used to differentiate among participants who were underweight (<18.5), normal weight (≥18.5 and <25.0), overweight (≥25.0 and <30.0), obese (≥30.0), or missing.

2.2.5. Smoking

Pack-years, representing cumulative exposure to tobacco smoke, were used to index cigarette smoking. Pack years were calculated as the number of years smoked times the average number of cigarettes smoked per day, divided by 20.

2.2.6. Physical Activity

Daily physical activity was assessed using four descriptive statements. Participants were asked to identify the statement that best described their physical activity level. Subjects were categorized according to the level of activity reported. The statements were: (1) You sit during the day and do not walk about very much; (2) You stand or walk about much of the day, but do not have to carry or lift things very often; (3) You lift light loads or have to climb stairs or hills often; (4) You do heavy work or carry heavy loads.

2.2.7. Alcohol Use

A total of three categories were used to differentiate among participants relative to alcohol use: abstainers, moderate drinkers, and heavy drinkers. Heavy drinkers were women who reported drinking two or more alcoholic beverages per day over the past 12 months or men reporting three or more alcoholic drinks per day over the past 12 months. Moderate drinkers were women who reported drinking more than zero but less than two drinks per day over the past 12 months, or men who reported drinking more than zero and less than three alcoholic beverages per day during the past 12 months. Abstainers were those reporting no alcohol use in the past 12 months.

2.2.8. Dietary Vitamin E Intake and Supplement Use

Using a computer-assisted interview system, a 24-h dietary recall was administered by NHANES [40]. Dietary supplement use was also assessed. Each interviewer was a college graduate in Food and Nutrition or Home Economics, with at least 10 credits in food and nutrition. Interviewers were trained and bilingual, and interviews were administered in a private setting in a NHANES MEC. The dietary assessment was used to collect detailed information about all foods and beverages consumed. Interviewers followed scripts provided in the system, and the computer-assisted program provided a standardized interview format. The diet recall included food probes that have been used in previous NHANES and USDA surveys. A multi-pass format was used during the interview. Nutrients and non-nutrient food components, including vitamin E intake, were calculated from foods and beverages that were eaten during a 24-h period prior to the interview (midnight to midnight).

2.2.9. Total Serum Cholesterol

Cholesterol was measured enzymatically in a series of coupled reactions that hydrolyzed cholesteryl esters and oxidized the 3-OH group of cholesterol. One of the reaction byproducts, H_2O_2, was measured quantitatively in a peroxidase-catalyzed reaction that produced a color. Absorbance was measured at 500 nm. The color intensity was proportional to the cholesterol concentration [41].

2.3. Statistical Analysis

Strata, clusters, and individual-level sample weights were used to produce results generalizable to the non-institutionalized, civilian, adult population of the United States. By using unequal selection

probability, the weights resulted in unbiased national estimates. For categorical variables, SAS SurveyFreq was used to calculate weighted frequencies to describe the data. For continuous variables, weighted means (±SE) were generated using SAS SurveyMeans. For the present study, sample weights were based on 4 years of MEC data, which included the blood alpha- and gamma-tocopherol levels and telomere lengths.

For this investigation, blood levels of alpha- and gamma-tocopherol served as the exposure variables, reported in μg/dL. The outcome variable was leukocyte telomere length. Regression analysis using the SAS SurveyReg procedure was employed to evaluate the extent of the linear associations between alpha- and gamma-tocopherol and telomere length. Regression estimates for each model were based on the complex, multistage, probability sampling process of NHANES. The effect of three demographic variables (age, gender and race) on the tocopherol and telomere relationships was tested using partial correlation and the SAS SurveyReg procedure. Additional potential mediating variables, including BMI, smoking, physical activity, alcohol use, total serum cholesterol, dietary vitamin E intake, and supplement use, were also evaluated. To study the associations between the covariates and telomere length, mean differences in telomere length were compared across each level of the covariates.

Because individuals with short telomeres are at greater risk of several diseases, the extent to which adults divided into sex-specific blood alpha- and gamma-tocopherol quartiles differed in odds of possessing short telomeres was calculated using SAS SurveyLogistic. Short telomeres were operationalized as participants in the lowest sex-specific quartile of the sample.

Statistical significance was accepted when alpha was <0.05 and all *p*-values were two-sided. SAS version 9.4 was used to conduct the statistical analyses (SAS Institute, Inc., Cary, NC, USA).

3. Results

In the present investigation, sample weights were employed to produce results that are generalizable to the non-institutionalized civilian adult population of the United States. Mean (±SE) age was 46.5 ± 0.5 years, and average telomere length was 5839 ± 41 base pairs. Mean blood concentrations of alpha- and gamma-tocopherol were 1328.3 ± 15.5 μg/dL and 241.5 ± 4.7 μg/dL, respectively—a 5.5-fold differential. Average dietary vitamin E intake, excluding supplements, was 7.5 ± 0.1 mg per day. Table 1 displays the weighted percentiles (±SE) for blood alpha- and gamma-tocopherol levels (μg/dL) and telomere length (base pairs), which represent those of the US adult population.

Table 1. Percentiles for blood levels of alpha-tocopherol and gamma-tocopherol and telomere length (base pairs) among US women and men (*n* = 5768).

Variable	Percentile (±SE)				
	5th	25th	50th	75th	95th
Alpha Tocopherol (μg/dL)					
Women (*n* = 3043)	689 ± 10	920 ± 13	1168 ± 17	1556 ± 22	2704 ± 116
Men (*n* = 2725)	678 ± 14	903 ± 9	1139 ± 23	1490 ± 31	2414 ± 59
Combined (*n* = 5768)	683 ± 10	912 ± 9	1156 ± 17	1523 ± 23	2594 ± 56
Gamma Tocopherol (μg/dL)					
Women (*n* = 3043)	65 ± 3	139 ± 5	217 ± 5	299 ± 8	486 ± 17
Men (*n* = 2725)	63 ± 4	146 ± 3	226 ± 5	311 ± 5	489 ± 15
Combined (*n* = 5768)	64 ± 3	143 ± 3	221 ± 4	306 ± 6	486 ± 14
Telomere Length (base pairs)					
Women (*n* = 3043)	4938 ± 46	5403 ± 40	5753 ± 40	6190 ± 53	7061 ± 131
Men (*n* = 2725)	4961 ± 32	5364 ± 30	5735 ± 37	6155 ± 51	7010 ± 98
Combined (*n* = 5768)	4957 ± 36	5387 ± 34	5745 ± 35	6179 ± 47	7034 ± 99

SE: standard error. Table values include person-level weighted adjustments based on the sampling design of NHANES so that values reflect those of the US adult population.

3.1. Age and Telomeres

In the present sample, chronological age was linearly and inversely associated with telomere length, as expected. For each one-year increase in age, telomeres were 15.6 base pairs shorter, on average ($F = 410.4$, $p < 0.0001$). Age-squared (age^2) was not predictive of telomere length beyond the linear term ($F = 0.3$, $p = 0.5785$). Table 2 shows mean differences in the length of telomeres across sequential categories based on chronological age.

Table 2. Mean differences in telomere length (base pairs) across age categories in US men and women.

Variable	Age Category (Years)						*F*	*p*
	20–29	30–39	40–49	50–59	60–69	70–84		
	Mean ± SE	Mean ± SE	Mean ± SE	Mean ± SE	Mean ± SE	Mean ± SE		
Telomere Length								
Men ($n = 2725$)	6201 ± 64	5970 ± 50	5868 ± 56	5690 ± 59	5507 ± 55	5312 ± 35	136.5	0.0001
Women ($n = 3043$)	6229 ± 74	6032 ± 60	5887 ± 50	5727 ± 51	5614 ± 56	5430 ± 47	83.0	0.0001
All ($n = 5768$)	6216 ± 59	6002 ± 50	5877 ± 45	5710 ± 49	5568 ± 49	5382 ± 39	184.2	0.0001

SE: standard error. Each mean differed significantly ($p < 0.05$) from each other mean on the same row. With age and telomere length both treated as continuous variables, telomere length was 15.6 base pairs longer for each year of age ($F = 410.4$, $p < 0.0001$). Table values above include person-level weighted adjustments based on the sampling design of NHANES so that values reflect those of the US population.

3.2. Gamma-Tocopherol and Telomere Length

Blood levels of gamma-tocopherol and telomere length were inversely related, as shown in Table 3. After adjusting for differences in the demographic covariates, for each μg/dL higher level of gamma-tocopherol, telomeres were 0.33 base pairs shorter, on average ($F = 7.1$, $p = 0.0126$). Telomeres were 0.27 base pairs shorter for each μg/dL increment in gamma-tocopherol with all of the covariates controlled, including age, gender, race, BMI, physical activity, smoking, alcohol use, total serum cholesterol, supplement use, and dietary vitamin E intake.

Table 3. Relationship between gamma- and alpha-tocopherol blood levels and telomere length (base pairs) in 5768 US adults, independent of covariates.

	Telomere Length (Base Pairs)			
Exposure				
Variable controlled	Regression Coefficient	SE	*F*	*p*
Blood Gamma-Tocopherol (per μg/dL)				
demographic covariates	−0.33	0.12	7.1	0.0126
demographic and lifestyle covariates	−0.27	0.13	4.4	0.0439
Blood Alpha-Tocopherol (per 10 μg/dL)				
demographic covariates	0.28	0.24	1.4	0.2506
demographic and lifestyle covariates	0.36	0.34	1.1	0.3099

Demographic covariates included: age, gender, and race. The lifestyle covariates were: BMI, physical activity, pack years of smoking, alcohol use, total serum cholesterol, dietary vitamin E intake, and supplement use. Interpretation of the regression coefficients would be as follows for the first row: After adjusting for differences in the demographic covariates, for each 1 μg/dL higher level of gamma-tocopherol, telomeres were 0.33 base pairs shorter, on average. Hence, a hypothetical difference of 191 μg/dL in gamma-tocopherol would result in an estimated difference of 4 years of biological aging ($191 \times 0.33 = 63$; $63 \div 15.6 = 4$).

With chronologic age and telomere length both treated as continuous variables, the relationship between age and telomere length was 15.6 base pairs per year of age. Hence, telomeres were approximately 1 year shorter (15.6 base pairs) for each increment of 47.3 to 55.7 μg/dL of gamma-tocopherol in the blood, depending on the variables controlled. Given adults at the 75th percentile (quartile 3) had 163 μg/dL higher levels of blood gamma-tocopherol than those at the 25th percentile (quartile 1), as shown in Table 1, adults of the same age, gender, race, etc. at the 75th

percentile had 2.8–3.4 years greater cellular aging than those at the 25th percentile, depending on the covariates controlled (163 × 0.27 = 44.0 ÷ 15.6 = 2.8 years; 163 × 0.33 = 53.8 ÷ 15.6 = 3.4 years).

3.3. Alpha-Tocopherol and Telomere Length

Blood levels of alpha-tocopherol were not associated with telomere length, as shown in Table 3. In general, telomeres were longer as blood alpha-tocopherol levels increased, but none of the relationships were statistically significant.

3.4. Alpha- and Gamma-Tocopherol

Blood levels of alpha- and gamma-tocopherol were inversely associated ($F = 39.9$, $p < 0.0001$). After adjusting for differences in the demographic and lifestyle covariates, for each μg/dL increase of gamma-tocopherol in the blood, alpha-tocopherol levels decreased by 1.2 μg/dL.

3.5. Dietary Vitamin E

Dietary vitamin E consumption was not related to telomere length after controlling for the demographic ($F = 0.5$, $p = 0.4696$) or the demographic and lifestyle covariates together ($F = 0.3$, $p = 0.5977$). However, vitamin E intake was inversely related to gamma-tocopherol blood levels, with the demographic covariates ($F = 8.3$, $p = 0.0074$) and the demographic plus lifestyle covariates controlled ($F = 8.9$, $p = 0.0059$). Specifically, for each mg of dietary vitamin E consumed in the diet, blood gamma- levels decreased by 1.5 and 1.2 μg/dL, respectively. Additionally, dietary vitamin E intake was directly associated with alpha-tocopherol blood levels, with the demographic covariates controlled ($F = 12.3$, $p = 0.0015$) and also with the demographic and lifestyle covariates held constant ($F = 12.2$, $p = 0.0016$). Specifically, for each mg of dietary vitamin E consumed, alpha-tocopherol blood levels were 9.2 and 9.1 μg/dL higher, respectively.

3.6. Dietary Supplement Use

A total of 51 ± 1% of the sample reported using dietary supplements. Use of dietary supplements was strongly related to blood levels of gamma-tocopherol. Specifically, after controlling for differences in age, gender, and race, participants who used dietary supplements (192.4 ± 6.8 μg/dL) had significantly lower gamma-tocopherol levels than those reporting they did not take supplements (279.3 ± 6.2 μg/dL)—a difference of 86.9 ± 6.1 μg/dL ($F = 203.8$, $p < 0.0001$). The relationship remained virtually identical after adjusting for differences in the demographic and lifestyle covariates combined ($F = 204.0$, $p < 0.0001$). Conversely, dietary supplement users (1569.8 ± 24.0 μg/dL) had significantly higher levels of blood alpha-tocopherol than non-supplement users (1157.7 ± 18.1 μg/dL)—a difference of 412 ± 23.4 μg/dL ($F = 309.8$, $p < 0.0001$), after adjusting for the demographic covariates. Controlling for the demographic and lifestyle covariates together produced a blood alpha-tocopherol difference of 394.9 ± 20.5 μg/dL ($F = 371.5$, $p < 0.0001$).

Dietary supplement users (7.3 ± 0.1 mg) also had higher intakes of dietary vitamin E from foods compared to non-users (6.6 ± 0.2 mg)—a difference of 0.7 ± 0.2 mg ($F = 11.7$, $p = 0.0019$), with the demographic variables controlled statistically. Comparable results were revealed after adjusting for the demographic and lifestyle covariates together ($F = 8.3$, $p = 0.0074$).

The relationship between dietary supplement use and telomere length was not significant after adjusting for the demographic covariates ($F = 2.6$, $p = 0.1151$) or after controlling for the demographic and lifestyle covariates combined ($F = 1.3$, $p = 0.2573$).

3.7. Odds of Possessing Short Telomeres

Participants with short telomeres (i.e., lowest sex-specific quartile) were compared to all other adults regarding their blood gamma-tocopherol levels. Specifically, participants with high levels of gamma- (i.e., highest sex-specific quartile) were compared to those in the other three quartiles.

Findings showed that adults with high gamma-tocopherol levels were 53% (95% Confident Interval (CI): 1.1–2.1) more likely to possess short telomeres than their counterparts. After adjusting for the demographic covariates, the odds of having short telomeres was 46% (95% CI: 1.1–2.0) greater in those with high blood gamma- levels compared to all others. After controlling for all of the covariates, demographic, and lifestyle, the odds of possessing short telomeres was 42% (95% CI: 1.0–2.0) greater in those with high gamma- levels compared to adults with other gamma-tocopherol blood levels.

4. Discussion

The chief objective of the present study was to evaluate the association between blood levels of alpha- and gamma-tocopherol and the length of leukocyte telomeres—a biological marker of cellular aging—in a large nationally-representative sample of US adults aged 20–84. Results showed that blood levels of alpha-tocopherol were not related to telomere length. However, telomeres were progressively shorter as the gamma-tocopherol concentrations in the blood increased (Table 3). Moreover, adults with high levels of gamma-tocopherol (highest sex-specific quartile) were 42% to 53% more likely to possess short telomeres (lowest sex-specific quartile) compared to other adults, indicating increased risk of advanced cellular aging.

In the present investigation, telomere shortening occurred at the rate of 15.6 base pairs per year of chronologic age. In other words, 42-year-olds tended to have telomeres that were 31.2 base pairs shorter than 40-year-olds, and 75-year-olds had telomeres that were approximately 46.8 base pairs shorter than 72-year-olds. Given there was a gamma-tocopherol difference of 163 μg/dL between those at the 75th percentile compared to those at the 25th percentile, regression results revealed an estimated difference in biological age of about 3 years, based on telomere length. Similarly, by comparing those with gamma-tocopherol levels at the 10th percentile (86.7 μg/dL) to those at the 90th percentile (408.1 μg/dL), there was a cellular aging difference of approximately 6 years, depending on the variables controlled. Hence, the inverse relationship between blood gamma-tocopherol levels and telomere length appears significant and meaningful.

Insight can be gained by comparing the associations between blood gamma-tocopherol levels and telomere length to telomere length and other factors. For instance, in the present investigation, after adjusting for differences in the demographic covariates, U.S. men and women with a history of 20 pack-years of smoking had telomeres that were approximately 70.5 base pairs shorter than non-smokers ($F = 17.8$, $p = 0.0002$), indicating $4\frac{1}{2}$ years of increased biological aging. Moreover, in the present sample, telomeres differed significantly in length across the various BMI categories ($F = 3.3$, $p = 0.0246$), with obese adults exhibiting telomeres that were 114.9 base pairs shorter than normal weight adults, suggesting more than 7 years of additional cellular aging. Conversely, the NHANES data showed no relationship between total serum cholesterol and telomere length ($F = 2.4$, $p = 0.1321$). Overall, it appears that blood levels of gamma-tocopherol account for differences in telomere length in US adults, consistent with common risk factors, including smoking and obesity.

According to the results, about one-half of American adults report using dietary supplements, but supplement use was not related to telomere length in this national sample. However, blood alpha- and gamma-tocopherol levels were highly related to supplement use, in opposite directions. Supplement users had 36% higher levels of blood alpha-tocopherol and 31% lower levels of gamma-tocopherol, on average, compared to their counterparts. Dietary vitamin E intake, alpha-tocopherol based, was directly related to higher levels of blood alpha-tocopherol levels and inversely related to gamma-tocopherol concentrations. Although differences in supplement use and dietary vitamin E intake were highly related to tocopherol blood levels, when statistical adjustments were made for differences in these covariates, the inverse relationship between gamma-tocopherol and telomere length remained statistically significant and the direct association between alpha-tocopherol and telomere length remained non-significant.

An extensive review by Wolf explains how the consumption of alpha-tocopherol can influence gamma-tocopherol levels [42]. The review states that excess alpha-tocopherol taken in

supplements causes a reduction of gamma-tocopherol concentrations. Furthermore, reductions in gamma-tocopherol concentrations during increased consumption of alpha-tocopherol occurs because of accelerated metabolism of gamma-tocopherol. Recent research with rodents suggests that competition for an intestinal transporter protein could play a role in the reduction of gamma- concentrations associated with high doses of alpha-tocopherol [43]. The unfavorable association between gamma-tocopherol and telomere length could be partly a function of the interaction and competition between alpha- and gamma-tocopherol.

The literature includes a number of studies designed to determine the effect of supplemental vitamin E intake on disease. For example, in a classic randomized controlled trial [44], male smokers supplemented with alpha-tocopherol had no improvements in lung cancer rates, but deaths from ischemic heart disease and stroke were reduced. On the other hand, deaths from cancers other than lung cancer were higher among vitamin E users, as were deaths from hemorrhagic stroke. The authors concluded that vitamin E "may actually have harmful as well as beneficial effects" (p. 1029).

The Heart Outcomes Prevention Evaluation (HOPE) Study, which investigated nearly 10,000 adults at high risk of heart attack or stroke for 4.5 years, determined that 400 IU of natural vitamin E supplementation had no protective effect [45]. However, 2.5 years of additional treatment with vitamin E in the HOPE–TOO trial concluded with an unexpected increase in heart failure, indicating that vitamin E supplementation was unhealthy [46].

In another randomized placebo-controlled trial, no cardiovascular benefits in women with established heart disease were seen in those supplemented with vitamins E and C, but all-cause mortality was increased significantly [47]. Further, two meta-analyses of randomized controlled trials have shown that vitamin E supplementation results in increased all-cause mortality [48,49]. Consequently, none of the major health organizations in the US recommend that supplements be used to increase serum tocopherol levels.

In the present investigation, alpha- and gamma-tocopherol levels were linked to different telomere outcomes. A number of studies have shown similar conflicting results. Based on spirometric parameters, Marchese et al. [2] reported that there are opposing associations for alpha- and gamma-tocopherol. Specifically, using data from the CARDIA investigation, alpha- levels were positively related to spirometry findings and gamma-tocopherol levels were negatively related to lung-function [2]. Research by Ford et al. showed that blood glucose levels decreased as alpha-tocopherol levels increased (a desirable association), whereas fasting glucose and glycosylated haemoglobin (A1c) both increased as gamma-tocopherol concentrations increased, unfavorable outcomes [13].

Nagao et al. [14] also uncovered conflicting results in a study of more than 39,000 Japanese adults followed for more than a decade. In women, alpha-tocopherol levels were inversely related to total stroke and hemorrhagic stroke mortality. Gamma- concentrations were indirectly associated with ischemic stroke mortality in men, but directly and unfavorably related to hemorrhagic stroke in women.

Hak et al. [50] also found unhealthy results for gamma-tocopherol. Low-risk male physicians from the Physician's Health Study were followed for up to 13 years. Those who had a heart attack were paired with controls, and a number of risk factors were adjusted statistically. After controlling for all of the potential confounders, men with high levels of gamma-tocopherol had more than twice the risk of a heart attack compared to those with low gamma- concentrations, and the overall P for trend was significant.

Overall, a number of epidemiologic investigations have produced conflicting outcomes for alpha- and gamma-tocopherol. Although both are antioxidants, their effects on health and disease are inconsistent and sometimes opposing. Findings from the present study were no exception to this pattern.

The present investigation had multiple limitations. First, because the study had a cross-sectional design, cause-and-effect conclusions are not defendable. Second, although 10 demographic and

lifestyle covariates were controlled statistically, there are always other factors that could account for the undesirable relationship between gamma-tocopherol and telomere length. Similarly, residual confounding is a possibility. Elevated concentrations of gamma-tocopherol could be a marker for a generally unhealthy lifestyle, which could explain the shorter telomeres found in these adults.

There were also many strengths associated with this study. A total of 5768 adults were included in the sample, which was multi-racial and representative of the non-institutionalized population of the United States, 20–84 years of age. Second, statistical adjustments were made for several potential confounders, including age, gender, race, smoking, BMI, physical activity, alcohol use, total cholesterol, dietary vitamin E intake, and supplement use. Third, NHANES used a highly respected independent lab to measure telomere length. Fourth, chronological age was strongly associated with telomere length, consistent with the literature.

5. Conclusions

In conclusion, the effect of alpha- and gamma-tocopherol on morbidity and mortality appears to be erratic. In the present study, blood levels of alpha-tocopherol were not related to telomere length. However, gamma- concentrations were unfavorably and inversely linked to telomere length in a randomly selected sample of almost 6000 adults. Men and women with gamma- levels at the 75th percentile had much shorter telomeres than those at the 25th percentile, accounting for about 3 years of additional biological aging. Moreover, adults in the top quartile of gamma-tocopherol were approximately 45% more likely to possess short telomeres than other adults. Evidently, as gamma-tocopherol levels increase in the blood, cell aging increases as well. Given the many studies in the literature showing opposing findings between alpha- and gamma-tocopherol (including the present investigation), more research is clearly warranted.

Acknowledgments: A special thanks to all of the women and men who gave freely of their time to participate in the NHANES data collection. Without their involvement, this study could not have been completed.

Author Contributions: L.A.T. conceived the study, organized the data, analyzed the data, and wrote the paper.

Conflicts of Interest: The author declares no conflict of interest.

References

1. NIH US National Library of Medicine. TOXNET: Vitamin E. Available online: https://toxnet.nlm.nih.gov/cgi-bin/sis/search2/r?dbs+hsdb:@term+@rn+59-02-9 (accessed on 12 June 2017).
2. Marchese, M.E.; Kumar, R.; Colangelo, L.A.; Avila, P.C.; Jacobs, D.R., Jr.; Gross, M.; Sood, A.; Liu, K.; Cook-Mills, J.M. The vitamin E isoforms alpha-tocopherol and gamma-tocopherol have opposite associations with spirometric parameters: The CARDIA study. *Respir. Res.* **2014**, *15*, 31. [CrossRef] [PubMed]
3. Dutta, A.; Dutta, S.K. Vitamin E and its role in the prevention of atherosclerosis and carcinogenesis: A review. *J. Am. Col. Nutr.* **2003**, *22*, 258–268. [CrossRef]
4. Patel, A.; Liebner, F.; Netscher, T.; Mereiter, K.; Rosenau, T. Vitamin E chemistry. Nitration of non-alpha-tocopherols: Products and mechanistic considerations. *J. Org. Chem.* **2007**, *72*, 6504–6512. [CrossRef] [PubMed]
5. Singh, U.; Jialal, I. Anti-inflammatory effects of alpha-tocopherol. *Ann. N. Y. Acad. Sci.* **2004**, *1031*, 195–203. [CrossRef] [PubMed]
6. Ford, E.S.; Schleicher, R.L.; Mokdad, A.H.; Ajani, U.A.; Liu, S. Distribution of serum concentrations of alpha-tocopherol and gamma-tocopherol in the US population. *Am. J. Clin. Nutr.* **2006**, *84*, 375–383. [PubMed]
7. Cook-Mills, J.M.; Abdala-Valencia, H.; Hartert, T. Two faces of vitamin E in the lung. *Am. J. Respir. Crit. Care Med.* **2013**, *188*, 279–284. [CrossRef] [PubMed]
8. Cook-Mills, J.M. Isoforms of Vitamin E Differentially Regulate PKC alpha and Inflammation: A Review. *J. Clin. Cell. Immunol.* **2013**. [CrossRef] [PubMed]
9. Cook-Mills, J.M.; McCary, C.A. Isoforms of vitamin E differentially regulate inflammation. *Endocr. Metab. Immune Disord. Drug Targets* **2010**, *10*, 348–366. [CrossRef] [PubMed]

10. Berdnikovs, S.; Abdala-Valencia, H.; McCary, C.; Somand, M.; Cole, R.; Garcia, A.; Bryce, P.; Cook-Mills, J.M. Isoforms of vitamin E have opposing immunoregulatory functions during inflammation by regulating leukocyte recruitment. *J. Immunol.* **2009**, *182*, 4395–4405. [CrossRef] [PubMed]
11. McCary, C.A.; Abdala-Valencia, H.; Berdnikovs, S.; Cook-Mills, J.M. Supplemental and highly elevated tocopherol doses differentially regulate allergic inflammation: Reversibility of alpha-tocopherol and gamma-tocopherol's effects. *J. Immunol.* **2011**, *186*, 3674–3685. [CrossRef] [PubMed]
12. Cui, R.; Liu, Z.Q.; Xu, Q. Blood alpha-tocopherol, gamma-tocopherol levels and risk of prostate cancer: A meta-analysis of prospective studies. *PLoS ONE* **2014**, *9*, e93044. [CrossRef]
13. Ford, E.S.; Mokdad, A.H.; Ajani, U.A.; Liu, S. Associations between concentrations of alpha- and gamma-tocopherol and concentrations of glucose, glycosylated haemoglobin, insulin and C-peptide among US adults. *Br. J. Nutr.* **2005**, *93*, 249–255. [CrossRef] [PubMed]
14. Nagao, M.; Moriyama, Y.; Yamagishi, K.; Iso, H.; Tamakoshi, A.; Group, J.S. Relation of serum alpha-and gamma-tocopherol levels to cardiovascular disease-related mortality among Japanese men and women. *J. Epidemiol.* **2012**, *22*, 402–410. [CrossRef] [PubMed]
15. Dietrich, M.; Traber, M.G.; Jacques, P.F.; Cross, C.E.; Hu, Y.; Block, G. Does gamma-tocopherol play a role in the primary prevention of heart disease and cancer? A review. *J. Am. Coll. Nutr.* **2006**, *25*, 292–299. [CrossRef] [PubMed]
16. Jiang, Q.; Christen, S.; Shigenaga, M.K.; Ames, B.N. gamma-tocopherol, the major form of vitamin E in the US diet, deserves more attention. *Am. J. Clin. Nutr.* **2001**, *74*, 714–722. [PubMed]
17. Rubin, H. The disparity between human cell senescence in vitro and lifelong replication in vivo. *Nat. Biotechnol.* **2002**, *20*, 675–681. [CrossRef] [PubMed]
18. Kong, C.M.; Lee, X.W.; Wang, X. Telomere shortening in human diseases. *FEBS J.* **2013**, *280*, 3180–3193. [CrossRef] [PubMed]
19. Kepinska, M.; Szyller, J.; Milnerowicz, H. The influence of oxidative stress induced by iron on telomere length. *Environ. Toxicol. Pharmacol.* **2015**, *40*, 931–935. [CrossRef] [PubMed]
20. Guan, J.Z.; Guan, W.P.; Maeda, T.; Guoqing, X.; GuangZhi, W.; Makino, N. Patients with multiple sclerosis show increased oxidative stress markers and somatic telomere length shortening. *Mol. Cell. Biochem.* **2015**, *400*, 183–187. [CrossRef] [PubMed]
21. Li, H.; Hedmer, M.; Wojdacz, T.; Hossain, M.B.; Lindh, C.H.; Tinnerberg, H.; Albin, M.; Broberg, K. Oxidative stress, telomere shortening, and DNA methylation in relation to low-to-moderate occupational exposure to welding fumes. *Environ. Mol. Mutagen.* **2015**, *56*, 684–693. [CrossRef] [PubMed]
22. Kim, K.S.; Kwak, J.W.; Lim, S.J.; Park, Y.K.; Yang, H.S.; Kim, H.J. Oxidative Stress-induced Telomere Length Shortening of Circulating Leukocyte in Patients with Obstructive Sleep Apnea. *Aging Dis.* **2016**, *7*, 604–613. [CrossRef] [PubMed]
23. Palmieri, D.; Cafueri, G.; Mongelli, F.; Pezzolo, A.; Pistoia, V.; Palombo, D. Telomere shortening and increased oxidative stress are restricted to venous tissue in patients with varicose veins: A merely local disease? *Vasc. Med.* **2014**, *19*, 125–130. [CrossRef] [PubMed]
24. Willeit, P.; Willeit, J.; Mayr, A.; Weger, S.; Oberhollenzer, F.; Brandstatter, A.; Kronenberg, F.; Kiechl, S. Telomere length and risk of incident cancer and cancer mortality. *JAMA* **2010**, *304*, 69–75. [CrossRef] [PubMed]
25. Prescott, J.; Wentzensen, I.M.; Savage, S.A.; De Vivo, I. Epidemiologic evidence for a role of telomere dysfunction in cancer etiology. *Mutat. Res.* **2012**, *730*, 75–84. [CrossRef] [PubMed]
26. Wentzensen, I.M.; Mirabello, L.; Pfeiffer, R.M.; Savage, S.A. The association of telomere length and cancer: A meta-analysis. *Cancer Epidemiol. Biomarkers Prev.* **2011**, *20*, 1238–1250. [CrossRef] [PubMed]
27. Samani, N.J.; Boultby, R.; Butler, R.; Thompson, J.R.; Goodall, A.H. Telomere shortening in atherosclerosis. *Lancet* **2001**, *358*, 472–473. [CrossRef]
28. Willeit, P.; Willeit, J.; Brandstatter, A.; Ehrlenbach, S.; Mayr, A.; Gasperi, A.; Weger, S.; Oberhollenzer, F.; Reindl, M.; Kronenberg, F.; et al. Cellular aging reflected by leukocyte telomere length predicts advanced atherosclerosis and cardiovascular disease risk. *Arterioscler. Thromb. Vasc. Biol.* **2010**, *30*, 1649–1656. [CrossRef] [PubMed]

29. Brouilette, S.W.; Moore, J.S.; McMahon, A.D.; Thompson, J.R.; Ford, I.; Shepherd, J.; Packard, C.J.; Samani, N.J.; West of Scotland Coronary Prevention Study Group. Telomere length, risk of coronary heart disease, and statin treatment in the West of Scotland Primary Prevention Study: A nested case-control study. *Lancet* **2007**, *369*, 107–114. [CrossRef]
30. Fitzpatrick, A.L.; Kronmal, R.A.; Gardner, J.P.; Psaty, B.M.; Jenny, N.S.; Tracy, R.P.; Walston, J.; Kimura, M.; Aviv, A. Leukocyte telomere length and cardiovascular disease in the cardiovascular health study. *Am. J. Epidemiol.* **2007**, *165*, 14–21. [CrossRef] [PubMed]
31. Zee, R.Y.; Castonguay, A.J.; Barton, N.S.; Germer, S.; Martin, M. Mean leukocyte telomere length shortening and type 2 diabetes mellitus: A case-control study. *Transl. Res.* **2010**, *155*, 166–169. [CrossRef] [PubMed]
32. Salpea, K.D.; Talmud, P.J.; Cooper, J.A.; Maubaret, C.G.; Stephens, J.W.; Abelak, K.; Humphries, S.E. Association of telomere length with type 2 diabetes, oxidative stress and UCP2 gene variation. *Atherosclerosis* **2010**, *209*, 42–50. [CrossRef] [PubMed]
33. Tamura, Y.; Takubo, K.; Aida, J.; Araki, A.; Ito, H. Telomere attrition and diabetes mellitus. *Geriatr. Gerontol. Int.* **2016**, *16*, 66–74. [CrossRef] [PubMed]
34. Von Zglinicki, T.; Serra, V.; Lorenz, M.; Saretzki, G.; Lenzen-Grossimlighaus, R.; Gessner, R.; Risch, A.; Steinhagen-Thiessen, E. Short telomeres in patients with vascular dementia: An indicator of low antioxidative capacity and a possible risk factor? *Lab. Investig.* **2000**, *80*, 1739–1747. [CrossRef] [PubMed]
35. Panossian, L.A.; Porter, V.R.; Valenzuela, H.F.; Zhu, X.; Reback, E.; Masterman, D.; Cummings, J.L.; Effros, R.B. Telomere shortening in T cells correlates with Alzheimer's disease status. *Neurobiol. Aging* **2003**, *24*, 77–84. [CrossRef]
36. NHANES. Data Files: Questionnaires, Datasets, and Related Documentation. Available online: http://www.cdc.gov/nchs/nhanes/nhanes_questionnaires.htm (accessed on 12 June 2017).
37. NHANES. National Center of Health Statistics Research Ethics Review Board (ERB) Approval. Available online: http://www.cdc.gov/nchs/nhanes/irba98.htm (accessed on 12 June 2017).
38. NHANES. Vitamin A, Vitamin E, and Carotenoids (L06VIT_B): Data Documentation, Codebook, and Frequencies. Available online: https://wwwn.cdc.gov/Nchs/Nhanes/2001-2002/L06VIT_B.htm (accessed on 12 June 2017).
39. NHANES. 2001–2002 Data Documentation, Codebook, and Frequencies. Telomere Mean and Standard Deviation. Available online: https://wwwn.cdc.gov/Nchs/Nhanes/2001-2002/TELO_B.htm (accessed on 12 June 2017).
40. NHANES. Dietary Interview, Individual Foods: Data Documentation, Codebook, and Frequencies. Available online: https://wwwn.cdc.gov/Nchs/Nhanes/2001-2002/DRXIFF_B.htm (accessed on 12 June 2017).
41. NHANES. Cholesterol—Total and HDL (Lab13): Data Documentation, Codebook, and Frequencies. Available online: https://wwwn.cdc.gov/Nchs/Nhanes/1999-2000/LAB13.htm (accessed on 12 June 2017).
42. Wolf, G. How an increased intake of alpha-tocopherol can suppress the bioavailability of gamma-tocopherol. *Nutr. Rev.* **2006**, *64*, 295–299. [CrossRef] [PubMed]
43. Reboul, E.; Klein, A.; Bietrix, F.; Gleize, B.; Malezet-Desmoulins, C.; Schneider, M.; Margotat, A.; Lagrost, L.; Collet, X.; Borel, P. Scavenger receptor class B type I (SR-BI) is involved in vitamin E transport across the enterocyte. *J. Biol. Chem.* **2006**, *281*, 4739–4745. [CrossRef] [PubMed]
44. Alpha-Tocopherol, Beta Carotene Cancer Prevention Study Group. The effect of vitamin E and beta carotene on the incidence of lung cancer and other cancers in male smokers. *N. Engl. J. Med.* **1994**, *330*, 1029–1035. [CrossRef]
45. Jialal, I.; Devaraj, S. Vitamin E supplementation and cardiovascular events in high-risk patients. *N. Engl. J. Med.* **2000**, *342*, 1917–1918. [CrossRef] [PubMed]
46. Lonn, E.; Bosch, J.; Yusuf, S.; Sheridan, P.; Pogue, J.; Arnold, J.M.; Ross, C.; Arnold, A.; Sleight, P.; Probstfield, J.; et al. Effects of long-term vitamin E supplementation on cardiovascular events and cancer: A randomized controlled trial. *JAMA* **2005**, *293*, 1338–1347. [CrossRef] [PubMed]
47. Waters, D.D.; Alderman, E.L.; Hsia, J.; Howard, B.V.; Cobb, F.R.; Rogers, W.J.; Ouyang, P.; Thompson, P.; Tardif, J.C.; Higginson, L.; et al. Effects of hormone replacement therapy and antioxidant vitamin supplements on coronary atherosclerosis in postmenopausal women: A randomized controlled trial. *JAMA* **2002**, *288*, 2432–2440. [CrossRef] [PubMed]

48. Miller, E.R., III; Pastor-Barriuso, R.; Dalal, D.; Riemersma, R.A; Appel, L.J.; Guallar, E. Meta-analysis: High-dosage vitamin E supplementation may increase all-cause mortality. *Ann. Intern. Med.* **2005**, *142*, 37–46. [CrossRef] [PubMed]
49. Bjelakovic, G.; Nikolova, D.; Gluud, L.L.; Simonetti, R.G.; Gluud, C. Mortality in randomized trials of antioxidant supplements for primary and secondary prevention: Systematic review and meta-analysis. *JAMA* **2007**, *297*, 842–857. [CrossRef] [PubMed]
50. Hak, A.E.; Stampfer, M.J.; Campos, H.; Sesso, H.D.; Gaziano, J.M.; Willett, W.; Ma, J. Plasma carotenoids and tocopherols and risk of myocardial infarction in a low-risk population of US male physicians. *Circulation* **2003**, *108*, 802–807. [CrossRef] [PubMed]

nutrients

MDPI

Article

Strawberry-Based Cosmetic Formulations Protect Human Dermal Fibroblasts against UVA-Induced Damage

Massimiliano Gasparrini [1,†], Tamara Y. Forbes-Hernandez [1,2,†], Sadia Afrin [1], Patricia Reboredo-Rodriguez [1,3], Danila Cianciosi [1], Bruno Mezzetti [4], Josè L. Quiles [5], Stefano Bompadre [6], Maurizio Battino [1,7,*] and Francesca Giampieri [1,*]

1 Dipartimento di Scienze Cliniche Specialistiche ed Odontostomatologiche (DISCO)-Sez. Biochimica, Facoltà di Medicina, Università Politecnica delle Marche, 60131 Ancona, Italy; m.gasparrini@univpm.it (M.G.); tamara.forbe@gmail.com (T.Y.F.-H.); dolla.bihs@gmail.com (S.A.); preboredo@uvigo.es (P.R.-R.); danila.cianciosi@gmail.com (D.C.)

2 Area de Nutrición y Salud, Universidad Internacional Iberoamericana (UNINI), 24040 Campeche, Mexico

3 Departamento de Quimica Analıtica y Alimentaria, Grupo de Nutricion y Bromatologıa, Universidade de Vigo, 32004 Ourense, Spain

4 Dipartimento di Scienze Agrarie, Alimentari e Ambientali, Università Politecnica delle Marche, 60131 Ancona, Italy; b.mezzetti@univpm.it

5 Department of Physiology, Institute of Nutrition and Food Technology "José Mataix", Biomedical Research Centre, University of Granada, 18000 Granada, Spain; jlquiles@ugr.es

6 Dipartimento di Scienze Biomediche e Sanità Pubblica, Facoltà di Medicina, Università Politecnica delle Marche Via Ranieri 65, 60131 Ancona, Italy; s.bompadre@univpm.it

7 Centre for Nutrition & Health, Universidad Europea del Atlantico (UEA), 39011 Santander, Spain

* Correspondence: m.a.battino@univpm.it (M.B.); f.giampieri@univpm.it (F.G.); Tel.: +39-071-220-4646 (M.B.); +39-071-220-4136 (F.G.); Fax: +39-071-220-4123 (M.B.); +39-071-220-4123 (F.G.)

† These authors contributed equally to this work.

Received: 15 May 2017; Accepted: 8 June 2017; Published: 14 June 2017

Abstract: Extreme exposure of skin to Ultraviolet A (UVA)-radiation may induce a dysregulated production of reactive oxygen species (ROS) which can interact with cellular biomolecules leading to oxidative stress, inflammation, DNA damage, and alteration of cellular molecular pathways, responsible for skin photoaging, hyperplasia, erythema, and cancer. For these reasons, the use of dietary natural bioactive compounds with remarkable antioxidant activity could be a strategic tool to counteract these UVA-radiation-caused deleterious effects. Thus, the purpose of the present work was to test the efficacy of strawberry (50 μg/mL)-based formulations supplemented with Coenzyme Q_{10} (100 μg/mL) and sun protection factor 10 in human dermal fibroblasts irradiated with UVA-radiation. The apoptosis rate, the amount of intracellular reactive oxygen species (ROS) production, the expression of proteins involved in antioxidant and inflammatory response, and mitochondrial functionality were evaluated. The results showed that the synergic topical use of strawberry and Coenzyme Q_{10} provided a significant ($p < 0.05$) photoprotective effect, reducing cell death and ROS, increasing antioxidant defense, lowering inflammatory markers, and improving mitochondrial functionality. The obtained results suggest the use of strawberry-based formulations as an innovative, natural, and useful tool for the prevention of UVA exposure-induced skin diseases in order to decrease or substitute the amount of synthetic sunscreen agents.

Keywords: skin damage; UVA-radiation; ROS; apoptosis; mitochondria functionality; antioxidant defense; inflammatory status; strawberry polyphenols; cosmetic formulation

1. Introduction

Even if ultraviolet (UV) radiation possesses some health benefits, such as the stimulation of cholecalciferol production, and is often used to cure some skin pathologies, such as vitiligo and psoriasis, it remains the principal cause of different skin disorders [1,2]. The main pathological effects of UV radiation range from erythema and premature aging to cancer; at the same time, it is able to induce cellular modifications such as alterations in elastic fibers and collagen, loss of subcutaneous adipose tissue, and photo-carcinogenic changes [1]. UVA makes up 95% of incident light and is more penetrating than UVB, reaching the subcutaneous tissue, and affecting both dermal and epidermal skin structures [3]. Exposure to UVA radiation can, in fact, lead to several biological phenomena, including inflammation, oxidative stress, damage to DNA, and signaling pathway dysregulation, mainly through the production of ROS [4]. The harmful effects of UV radiation on the skin are generally counteracted through the use of topical sunscreen products [5,6]. Sunscreens protect the skin against cancer and they also prevent the onset of other skin diseases caused by solar radiation, such as wrinkle formation, collagen loss, undesired pigmentation, and aging. Indeed, the topical application of sunscreens represents an effective precautionary measure against these problems mainly in regions with high solar radiation levels [1]. Recently, compounds derived from natural sources have attracted remarkable attention for their implementation in sunscreen products and have encouraged the market trend towards natural cosmetics. This aspect underlines the importance of identifying an extensive selection of natural active molecules in sunscreen formulations, in order to reduce the quantity of synthetic sunscreen agents present in cosmetic formulations [5]. For these reasons, in the last few years, protective properties have been studied for diverse natural polyphenols, including luteolin, silymarin, grape seed proanthocyanidins, green tea polyphenols, genistein, and strawberry anthocyanins [7,8]. Strawberries (*Fragaria X ananassa*, Duch.) are a considerable source of minerals, vitamins, sugars, and polyphenols such as anthocyanins, phenolic acids, and flavonoids [9,10]. Altogether, these bioactive molecules have synergistic activities on the promotion of health and the prevention of different diseases, such as aging, cardiovascular diseases, inflammatory-related pathologies, and cancer [11–13]. In particular, we recently evidenced that polyphenols and vitamins present in strawberries exert an effective protection against skin damage induced by oxidative- and UVA-stressors, reducing DNA damage, lipid peroxidation, free radical levels, and improving mitochondrial functionality when added in the culture medium, and increasing cell-viability when combined in a sunscreen formulation [6,8,14]. Here, we used a specific combination of a strawberry extract enriched with coenzyme Q_{10} (CoQ_{10}) in a cosmetic formulation to counteract UVA's damaging effects on human dermal fibroblasts (HDF), assessing apoptosis rate, ROS intracellular production, the level of antioxidant and inflammatory marker proteins, and mitochondria functionality.

2. Materials and Methods

2.1. Standard and Reagents

UV-filters samples were kindly supplied by BASF (Cesano Maderno, Italy): bis-ethylhexyloxyphenol methoxyphenyl triazine (Tinosorb S Aqua, active), diethylamino hydroxybenzoyl hexyl benzoate (Uvinul A Plus) and Octocrylene (Uvinul N539T). Liquid CoQred (Quinomit®) was kindly provided by MSE Pharmazeutika GmbH (Bad Homburg, Germany). All chemicals and solvent were of analytical grade. Cyanidin (Cy)-3-glucoside, Pelargonidin (Pg)-3-glucoside, ferrous sulphate ($FeSO_4$), 2,20-azino-bis-(3-ethylbenzothiazoline-6-sulfonic acid) diammonium salt (ABTS), 2,2-diphenyl-1-picrylhydrazyl (DPPH), 6-hydroxy-2,5,7,8-tetramethyl-chroman-2-carboxylic acid (Trolox), oligomycin, 2,4-dinitrophenol (2,4-DNP), antimycin A, rotenone and all other reagents and solvents were purchased from Sigma-Aldrich chemicals, Milan, Italy. CellROX® Orange reagent was purchased from Invitrogen™, Life Technologies, Milan, Italy. Dulbecco's Modified Eagle Medium (DMEM), were obtained from Carlo Erba Reagents, Milan, Italy, as well as all other products for cell cultivation. Primary and secondary antibodies were purchased

from Santa Cruz Biotechnology, Dallas, TX, USA and Bioss Inc., Woburn, MA, USA and all the other products for western blot analysis from Bio-Rad Laboratories, Inc., Hercules, CA, USA.

2.2. Strawberry Samples

Strawberry fruits (*Fragaria* × *ananassa*, Alba variety) were collected in the experimental fields of the Agricultural Faculty of Università Politecnica Marche; within 2 h after harvest, whole fruits were stored at -20°C before analyses and subjected to methanolic extraction as previously described [14]. The total phenolic content (TPC) of strawberry extract was determined by the Folin–Ciocalteu method [15], total flavonoid content (TFC) by the aluminium chloride spectrophotometric method [16], while vitamin C (vit C) and folate content were analyzed by a HPLC system [17,18]. Anthocyanins (ACYs) solid-phase extraction and HPLC-MS/MS analysis were performed as previously described [19]. Finally, total antioxidant capacity (TAC) was determined using Trolox Equivalent Antioxidant Capacity (TEAC) [20], Ferric Reducing Antioxidant Power (FRAP) assays [21] and the 2,2-DiPhenyl-1-PicrylHydrazyl free radical method (DPPH) [22]. For filter preparation, strawberry extract was concentrated under vacuum at 40 °C to eliminate total methanol and suspended in the final formulation. Results were reported as mean value of three replicates ± standard deviation (SD).

2.3. Filter and Formulation Preparation

A UV filter combination often used in sun protection factor 10 (SPF10) sunscreen products was chosen for this study and prepared as follows: 2% bis-ethylhexyloxyphenol methoxyphenyl triazine, 2% diethylamino hydroxybenzoyl hexyl benzoate and 2% Octocrylene. According to our preliminary viability data [6], this formulation (SPF10 group) was enriched with (i) Alba strawberry extract at 50 μg/mL (Strw group); (ii) reduced CoQ_{10} (CoQ_{10red} group) at 100 μg/mL and (iii) a combination of strawberry extract + CoQ_{10red} (Strw+CoQ_{10red} group).

2.4. Cell Culture

HDF were Human Dermal Fibroblasts isolated from adult skin obtained from the American Type Culture Collection (Manassas, VA, USA). HDF were plated into a T-75 flasks and cultured as previously described [6]. Cells were maintained in a HeraCell CO_2 incubator at 37 °C with 5% CO_2 and the medium was changed every 2–3 days. All the tests were conducted on cells between the 4th and the 6th passage.

2.5. UVA Treatment

As previously described [6], a Saalmann Palma Plant Box Universal (Biosonic, Bologna, Italy) equipped with a 320 W ozone-free lamp, UV type 3, was used as UVA irradiating source. The source delivered 15 mW/cm^2 between 300 and 400 nm at a distance of 20 cm from the cell cultures; it was always pre-run for 10 min to allow the output to stabilize. The incident dose of UVA received by the samples was 275 kJ/m^2 (60 min of exposure), i.e., a dose approximately equivalent to about 90 min of sunshine at the French Riviera (Nice, France) in summer at noon [23]. Cells grown on different plates, depending on the analysis to be performed, were washed twice with phosphate buffered saline (PBS) and covered with a thin layer of PBS prior to exposure. Each formulation (2 mg/cm^2) was spread onto quartz-bottom petri dishes (Hubei Yunsheng Quarts Products Co., Ltd., Xiaogan Hanchuan, China) of exactly the same dimensions as the cell culture plates and the dishes were placed on top of the wells prior to irradiation. The cells were placed on a brass block embedded in ice in order to reduce the temperature and hence the evaporation during exposure, which could eventually dry out the medium. The cells were then either not exposed (UV−), or exposed to the UVA source (UV+) as previously described for 60 min (Figure 1), because longer exposure times showed a significant loss of vitality.

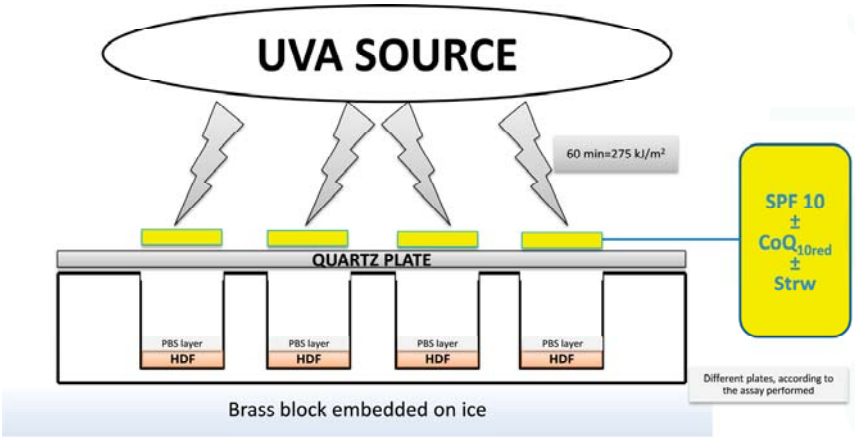

Figure 1. Schematic representation of the experimental setup used to apply the different formulations to the cell cultures. UVA, Ultraviolet A; PBS, phosphate buffered saline; HDF, Human Dermal Fibroblast; SPF 10, sun protection factor 10; CoQ_{10red}, reduced coenzyme Q_{10} and Strw, strawberry.

2.6. Apoptosis Detection

Apoptosis was measured using the Tali™ apoptosis assay kit and propidium iodide (Invitrogen™, Life Technologies, Milan, Italy) as previously reported [24]. Concisely, on the first day of the assay 1.5×10^5 cells were seeded in a 6-well plate and left to adhere for 16–18 h. The day after seeding, the cells were subjected to UV radiation, with different SPF10-enriched filter combinations, as previously described. At the end of the treatment cells were centrifuged (1500 rpm for 5 min), and resuspended in 100 µL of annexin binding buffer (ABB). After that, 5 µL of Annexin V Alexa Fluor® 488 was added, mixed well, and the solution was incubated in the dark at room temperature for 20 min. Then cells were centrifuged at 1500 rpm, resuspended in 100 µL of ABB, and 1 µL of propidium iodide was added, mixed well, and incubated in the dark at room temperature for 5 min. Samples were analyzed using the Tali® Image-Based cytometer and the percentage of apoptotic nuclei, dead cells, and live cells was determined on the basis of the corresponding fluorescence histogram compared with an untreated control. The results were expressed as fold increase compared with the control.

2.7. Intracellular ROS Concentration

Intracellular ROS generation was determined by CellROX® Orange Reagent (Invitrogen™, Life Technologies, Milan, Italy) as previously described [25]. On the first day of the assay, 1.5×10^5 cells were seeded in a 6-well plate, and left to adhere for 16–18 h. The day after seeding, the cells were subjected to UV radiation, with different SPF10-enriched filter combinations, as previously described. At the end of the treatment, the medium was removed and collected, then CellROX® Orange Reagent, a fluorogenic probe for measuring oxidative stress in live cells, was added (1:500 dilution) to 1 mL of DMEM. This cell-permeant dye is non-fluorescent while in a reduced state and exhibits bright fluorescence upon oxidation by ROS. Samples were incubated at 37 °C for 30 min, centrifuged at $320\times$ *g*, and then resuspended in PBS. Cells were analyzed with the Tali® Image-Based cytometer and unexposed cells were used to determine baseline levels of intracellular ROS and to set the fluorescence threshold for the Tali® instrument. The results were expressed as fold increase compared with the control.

2.8. Evaluation of Mitochondria Functionality

Oxygen consumption rate (OCR) was measured in real-time using a XF-24 Extracellular Flux Analyzer (Seahorse Bioscience, Billerica, MA, USA), as previously reported [26]. Briefly, cells were seeded for 16 h in the XF-24 plate before the UVA treatment with different SPF10-enriched filter combinations, as previously described. At the end of the treatment, the medium was replaced with 450 μL/well of XF-24 running media (supplemented with 25 mM glucose, 2 mM glutamine, 1 mM sodium Pyruvate, without serum) and pre-incubated at 37 °C for 20 min in the XF Prep Station incubator (Seahorse Bioscience, Billerica, MA, USA) in the absence of CO_2. The plate was then transferred to the XF-24 Extracellular Flux Analyzer and after an OCR baseline measurement, a profiling of mitochondrial function was performed by sequential injection of four compounds that affect bioenergetics, as follows: 55 μL of oligomycin (2.5 μg/mL) at injection in port A, 61 μL of 2,4-dinitrophenol (2,4-DNP) (1 mM) at injection in port B, and 68 μL of antimycin A/rotenone (10 μM/1 μM) at injection in port C. The best concentration of each inhibitor and uncoupler was obtained on the basis of a proper titolation curve. The final results were expressed as pmol of O_2 consumed per 10^5 cells per min (pmol $O_2/10^5$ cells/min). Moreover, the Maximal Respiratory Capacity value of each treatment was calculated with the following equation [27]:

$$\text{Maximal Respiratory Capacity} = (\text{2,4-dinitrophenol OCR value} - \text{antimycin A/rotenone OCR value}) \quad (1)$$

Also in this case, the final results were expressed as pmol $O_2/10^5$ cells/min.

2.9. Immunoblotting Assay

After UVA exposure with different filter-enriched combinations, cells were collected, washed with PBS, lysed in 100 μL lysis buffer (120 mmol/L NaCl, 40 mmol/L Tris [pH 8], 0.1% NP40), and centrifuged at 13,000× *g* for 15 min. An immunoblotting assay was performed as previously described [26]. Proteins from cell supernatants were separated on a 10–15% acrylamide SDS/PAGE (Bio-Rad, Hercules, CA, USA). Proteins were transferred onto a nitrocellulose 0.2 μm membrane (Bio-Rad, Hercules, CA, USA) using the trans-blot SD semidry electrophoretic transfer cell (Bio-Rad, Hercules, CA, USA) and then membranes were blocked with TBS-T containing 5% non-fat milk for 1 h at room temperature. Membranes were incubated at 4 °C overnight with the primary antibody solution, diluted at 1:500 (*v*/*v*), specific for the detection of: nuclear factor kappa-light-chain-enhancer of activated B cells (NF-kB), phosphorylated nuclear factor of kappa light polypeptide gene enhancer in B-cell inhibitor, alpha (pIκBα), interleukin (IL)-6, IL-1β, tumor necrosis factor alpha (TNF-α), nuclear factor E2-related factor 2 (Nrf2), catalase, superoxide dismutase (SOD), and heme oxygenase 1 (HO-1). The GAPDH protein was used for the measurement of the amount of protein analyzed. Then, membranes were probed for 1 h at room temperature with their specific alkaline phosphatase-conjugated secondary antibodies (1:80,000 dilution *v*/*v*). Immunolabeled proteins were detected by using a chemiluminescence method (CDiGit Blot Scanner, LI-COR, Bad Homburg, Germany). Quantification of gene expression was carried out using the software provided by the manufacturer of the Blot Scanner (Image Studio 3.1). The protein concentration was determined by the Bradford method [28]. Data were expressed as fold increase compared to control.

2.10. Statistical Analysis

Each analysis was carried out in triplicate and the results were given as mean ± standard deviation (SD). Data between different groups were analyzed statistically using the one-way ANOVA and Turkey's post hoc test. Statistical analyses were performed using STATISTICA software (Statsoft Inc., Tulsa, OK, USA). $p < 0.05$ was considered as significant.

3. Results and Discussion

3.1. Analysis of Strawberry Fruits

As already reported in our previous studies [6,25,26], the Alba cultivar contained a good amount of polyphenols (TPC), flavonoids (TFC) and vitamin C (vit C), with values of 2.52 mg Gallic Acid Equivalent/g fresh weight (FW), 0.66 mg Catechin Equivalent/g FW, and 0.58 mg vit C/g FW, respectively (Table 1). HPLC-DAD/ESI-MS analysis allowed us to detect five anthocyanin pigments, with Pelargonidin (Pg) 3-glucoside (39.74 mg/100g FW) and Pg 3-malonylglucoside (6.69 mg/100g FW) representing the most relevant components (Table 1). Alba extract showed total antioxidant capacity (TAC) values of 22.64, 7.71, and 22.85 μmol Trolox Equivalent/g FW for Trolox Equivalent Antioxidant Capacity (TEAC), 2,2-DiPhenyl-1-PicrylHydrazyl (DPPH) and for Ferric Reducing Antioxidant Power (FRAP), respectively, confirming the results obtained with other strawberry varieties (Table 1) [8,14,29]. Finally, the Alba cultivar possessed 0.99 μg of folinic acid calcium salt hydrate/g FW and 0.06 μg of 5-methyltetrahydrofolic acid/g FW (Table 1): these folate compounds are responsible, synergistically with other strawberry bioactives, for several health effects, as previously highlighted by different authors [30,31].

Table 1. Phenolic content and antioxidant capacity of Alba strawberry extract. Data are presented as mean value ± SD. TPC, total polyphenols content; TFC, total flavonoids content; vit C, vitamin C; ACYs, anthocyanins; Cy-3-glucoside, cyanidin-3-glucoside; Pg 3-glucoside, pelargonidin 3-glucoside; Pg 3-rutinoside, pelargonidin 3-rutinoside; Pg 3-malonylglucoside, pelargonidin 3-malonylglucoside; Pg 3-acetylglucoside, pelargonidin 3-acetylglucoside; TAC, total antioxidant capacity; TEAC, Trolox Equivalent Antioxidant Capacity; DPPH, 2,2-DiPhenyl-1-PicrylHydrazyl and FRAP, Ferric Reducing Antioxidant Power.

Parameter	Mean Value
TPC (mg GAEq/g FW)	2.52 ± 0.01
TFC (mg CEq/g FW)	0.66 ± 0.01
vit C (mg vit C/g FW)	0.58 ± 0.02
ACYs (mg/100g FW)	
Cy-3-glucoside	3.11 ± 0.03
Pg 3-glucoside	39.74 ± 0.13
Pg 3-rutinoside	3.87 ± 0.16
Pg 3-malonylglucoside	6.69 ± 0.04
Pg 3-acetylglucoside	0.39 ± 0.01
TAC (μmol Teq/g FW)	
TEAC	22.64 ± 0.49
DPPH	7.71 ± 0.32
FRAP	22.85 ± 0.39
Folate (μg folate/g FW)	
folinic acid calcium salt hydrate	0.99 ± 0.09
5-methyltetrahydrofolic acid	0.06 ± 0.01

3.2. Apoptosis Rate Regulation by Different Formulation

UV irradiation can promote different harmful effects including DNA damage, sunburn, and apoptosis [32]. Apoptosis is widely considered as a major mechanism of regulated cell death which is defined by distinct morphological and biochemical features and exerts a key role in embryogenesis, aging and tissue homeostasis. The ability of different bioactive compounds to modulate the life or death of a cell is recognized as a tool of therapeutic potential [5,32]. Consequently, many existing treatments have been developed which may act through the regulation of apoptosis [24,33]. In our work, we first confirmed the results previously obtained (Figure 2) [6]: the combined action of strawberry and

CoQ_{10red} significantly reduced the level of dead cells compared to UV exposed cells ($p < 0.05$), restoring the level of live cells to values similar to the control group (UV−) ($p < 0.05$). Taking into account the apoptosis rate, no significant differences were detected between the tested groups, even if the apoptotic cell level increased with Strw, CoQ_{10red} and Strw + CoQ_{10red} treatments. These results, with the concomitant reduction of dead cells, could be interpreted as a possible protective mechanism exerted by Strw and CoQ_{10}, which delay cellular death in UV-exposed cells. As far as we know, this is the first study which explores the apoptotic effects of strawberries on UV-exposed HDF, however further studies will be necessary to confirm these results.

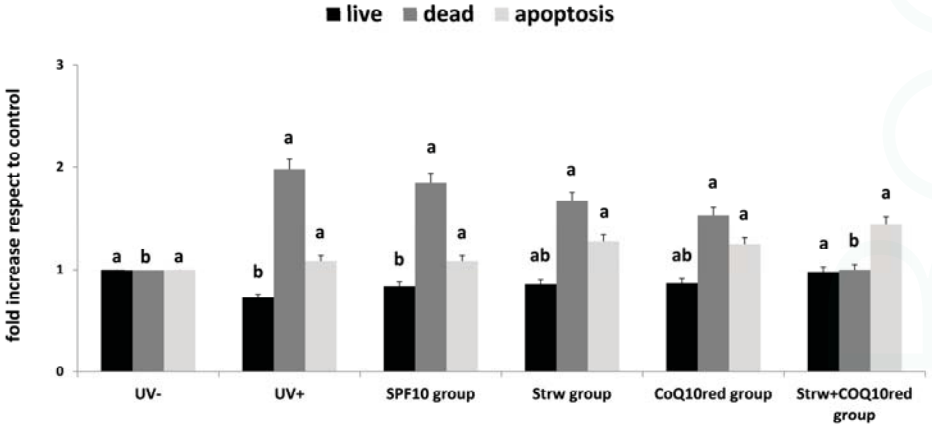

Figure 2. Live, dead, and apoptosis levels in human dermal fibroblast (HDF) cells irradiated with ultraviolet A (UVA, 275 kJ/m^2) radiation (UV+) or not irradiated (UV−), after 1 h of exposure. HDF were screened with different formulations as explained in the text. Data are expressed mean values ± standard deviation (SD). Columns with different superscript letters are significantly different ($p < 0.05$).

3.3. Protection of Different Formulations Against ROS Accumulation

Inflammation, immunosuppression and DNA damage are the main consequences of UV radiation exposure. These effects are directly and indirectly caused by high levels of ROS which destabilize biomolecules and induce chain reactions leading to membrane degradation, mitochondrial damage, telomere shortening and deterioration, and oxidation of enzymatic and structural proteins [4]. Oxidative stress induced by ROS is also the primary cause of photoaging and also promotes cell death and cancer [2]. For this reason, the measurement of ROS production could be a valuable tool to estimate UVA-induced oxidative damage. In our work, the protective effect of the different cosmetic formulations was demonstrated (Figure 3). In HDF cells subjected to UV radiation (UV+), a significant increase in the amount of ROS was detected, compared to untreated cells (UV−) ($p < 0.05$). This effect was efficiently counteracted through the different formulations applied: a significant difference ($p < 0.05$) compared to UV-exposed cells was detected in the Strw group and the CoQ_{10red} group. Interestingly, the maximal protective effect was found in the Strw + CoQ_{10red} group ($p < 0.05$), suggesting an important synergic action. These data obtained with this berry were in line with previous results found using a topical pretreatment of green tea polyphenolic extract in a human model [34], and with other berry and natural bioactive compounds applied in different cellular [35–39] and animal models [40,41] exposed to UV radiation.

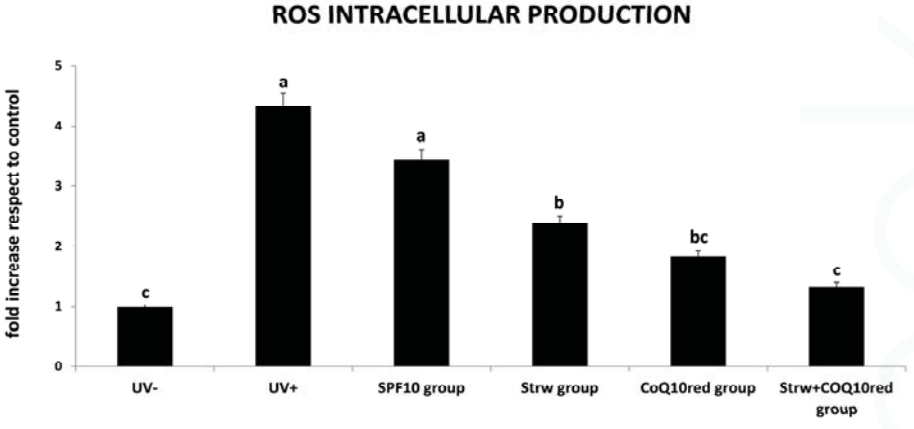

Figure 3. Reactive oxygen species (ROS) level in human dermal fibroblast (HDF) cells irradiated with ultraviolet A (UVA, 275 kJ/m^2) radiation (UV+) or not irradiated (UV−), after 1 h of exposure. HDF were screened with different formulations as explained in the text. Data are expressed mean values ± standard deviation (SD). Columns with different superscript letters are significantly different ($p < 0.05$).

3.4. Effect of Different Fomulations on Mitochondrial Respiration Rate

The most important site of ROS production is the mitochondrial electron transport chain (ETC) [33]. In this process, in fact, a small percentage of electrons directly reacts with oxygen, causing the formation of ROS as secondary ETC products [33]. As previously reported, UV irradiation causes mutations to mitochondrial DNA, altering its function by reducing the consumption of O_2 and the production of ATP, which affects cell migration and division [4,42]. UV exposure promotes mitochondrial dysfunction and toxicity mainly through the activation of caspases, the release of cytochrome C, and the depolarization of the membrane. Additionally, mitochondrial dysfunction augments the oxidative stress levels at mitochondrial complexes [4]. In this context, we investigated the implication of mitochondrial dysfunction in HDF cells after UVA radiation in association with the different protective formulations, through OCR measurement. Basal respiration is mainly driven by the concomitant re-entry pathways through the proton leak and ATP synthases. After that, cells were exposed consecutively to four modulators of oxidative phosphorylation, such as oligomycin, 2,4-DNP, and antimycin/rotenone. Oligomycin stops the ATP synthase so that residual respiration is due solely to the proton leak. The addition of the protonophore 2,4 DNP causes an artificial proton conductance into the membrane. This maximal respiration is now regulated by the activity of the ETC and/or the delivery of substrate. The maximal respiratory capacity is defined as the increased respiratory capacity above basal respiration. At the end, ETC inhibitors were added: antimycin A/rotenone that block complex III and I, respectively. In this way, any residual respiration is nonmitochondrial and needs to be subtracted from the other rates. In Figure 4, the trend of the different treatments was shown as a function of the different inhibitors applied. Basal OCR was noticeably damaged in cells subjected to UV radiation (UV+). On the contrary, the different formulations applied to screen the cells improved mitochondrial functionality, increasing the OCR value and restoring values to levels similar to those of unexposed cells (UV−) in Strw + CoQ_{10red} group (Figure 3).

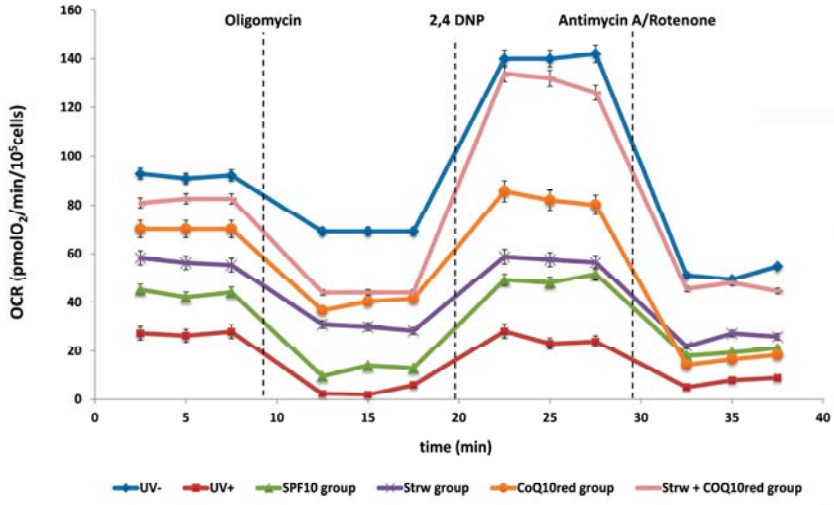

Figure 4. Oxygen consumption rate (OCR) value of human dermal fibroblast (HDF) cells irradiated with ultraviolet A (UVA, 275 kJ/m^2) radiation (UV+) or not irradiated (UV−), after 1 h of exposure. HDF were screened with different formulations as explained in the text. Data are expressed as mean values ± standard deviation (SD).

Taking into account the maximal respiratory capacity (Figure 5), UV-irradiated cells showed the lowest values, while the different protective formulations applied raised this rate, in particular in the Strw + CoQ_{10red} group, which presented a value similar to unexposed cells ($p < 0.05$).

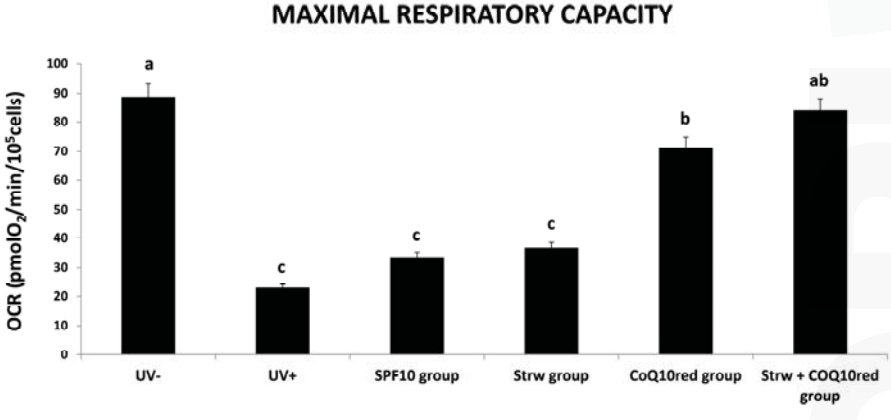

Figure 5. Maximal respiratory capacity value of human dermal fibroblast (HDF) cells irradiated with ultraviolet A (UVA, 275 kJ/m^2) radiation (UV+) or not irradiated (UV−), after 1 h of exposure HDF were screened with different formulations as explained in the text. Data are expressed as mean values ± standard deviation (SD). Columns with different superscript letters are significantly different ($p < 0.05$).

As far as we know, there are no published studies that underline the effect of different sunscreen formulations against UV irradiation in HDF cells, especially regarding OCR results. For this reason, further investigations are needed to clarify and investigate the possible protection mechanisms exerted on mitochondrial functionality.

3.5. Different Formulations Positively Regulated Antioxidant and Inflammatory-Related Pathways

Estimation of the antioxidant and anti-inflammatory effects of the different enriched formulations on different molecular pathways involved in cellular response was performed by protein expression analysis. UV radiation activates pro-inflammatory genes which represent significant mediators of photocarcinogenesis and the photoaging processes, such as IL-6 and TNF-α [4]. The transcriptional factor that controls the inflammatory response is NF-κB which plays a crucial role in the carcinogenesis and inflammation induced by UV exposure [43]. In the cytoplasm, NF-kB is in an inactive form due to complexation with IkBα. In response to inflammatory stimuli, after IkBα phosphorylation (to form pIkBα), NF-kB is activated and migrates to the nucleus, up-regulating inflammation-related genes such as pro-inflammatory cytokines [26]. In our work, the different formulations applied reduced the levels of the tested inflammatory markers (NF-kB, pIkBα, TNF-α, IL-6, and IL-1β), whose expression was considerably increased after UV-exposure ($p < 0.05$) (Figures 6 and 7). In the case of NF-kB and pIkBα, a significant reduction in protein expression was registered with CoQ_{10red} and Strw + CoQ_{10red} enriched formulations, respectively ($p < 0.05$) (Figure 6). Similar results were obtained for IL-6 and IL-1β: also in this case the efficient reduction provided by the Strw-enriched formulation ($p < 0.05$) was enhanced by the combination with CoQ_{10red}. Finally, in the case of TNF-α, a value similar to the control group (UV−) was obtained with theCoQ_{10red}-enriched formulation ($p < 0.05$) (Figure 7). Interestingly, in all the proteins investigated, the combination of Strw and CoQ_{10red} provided the best results in terms of inflammatory marker reduction (Figures 6 and 7). These data are in line with the results obtained in previous studies, in which the expression of NF-kB and pro-inflammatory cytokines induced by UV radiation was improved through treatment with different bioactive compounds in dermal keratinocytes and fibroblast cells [37,44–46]

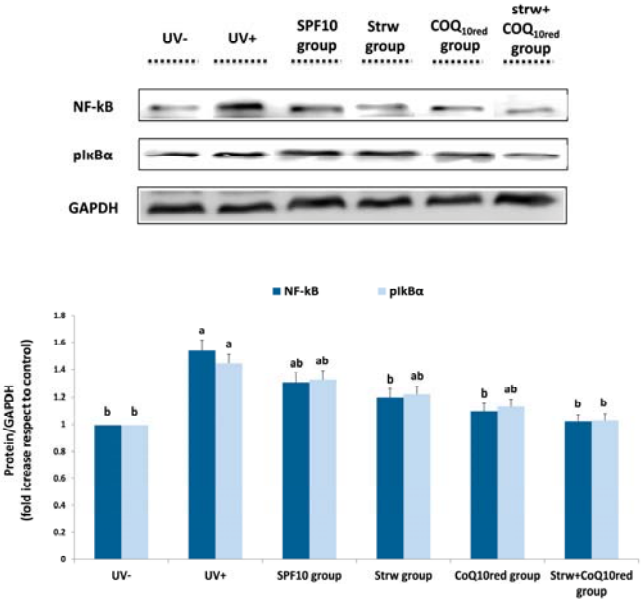

Figure 6. Levels of inflammatory markers (NF-kB, pIkBα) in human dermal fibroblast (HDF) cells irradiated with ultraviolet A (UVA, 275 kJ/m^2) radiation (UV+) or not irradiated (UV−), after 1 h of exposure. HDF were screened with different formulations as explained in the text. Data are expressed as mean values ± standard deviation (SD). Columns belonging to the same set of data with different superscript letters are significantly different ($p < 0.05$).

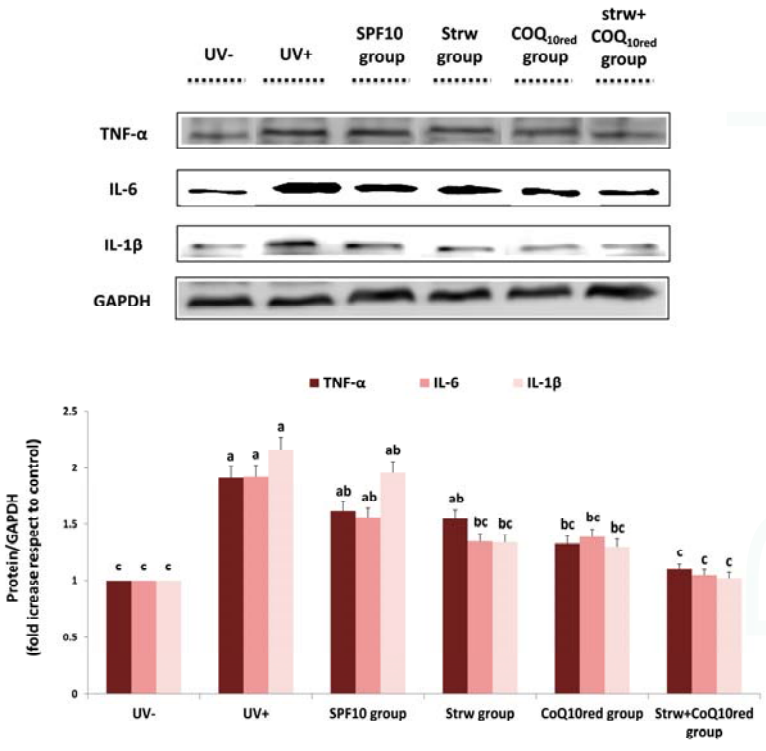

Figure 7. Levels of inflammatory markers (TNF-α, IL-1β, IL-6) in human dermal fibroblast (HDF) cells irradiated with ultraviolet A (UVA, 275 kJ/m^2) radiation (UV+) or not irradiated (UV−), after 1 h of exposure. HDF were screened with different formulations as explained in the text. Data are expressed as mean values ± standard deviation (SD). Columns belonging to the same set of data with different superscript letters are significantly different ($p < 0.05$).

Nrf2 is also targeted by UV radiation. This protein is the main regulator of cellular antioxidant defense, since it regulates the expression of many "antioxidant responsive elements" (ARE), which positively regulate a wide array of antioxidant and detoxification enzymes involved in cellular defense against oxidative stress, such as catalase, SOD, and HO-1 [26]. Nrf2 also regulates the bioavailability of mitochondrial respiration, highlighting the role of bioenergetics in antioxidant protection and in cell structure stabilization [4]. In our work, the different enriched formulations applied increased Nrf2 levels, restoring values similar to control (UV−) levels, especially in the Strw + CoQ_{10red} group ($p < 0.05$) (Figure 8). An analogous trend was detected with the other genes investigated (Figure 8). In the case of SOD, an efficient improvement with respect to UV-exposed cells was obtained with the Strw group ($p < 0.05$), restoring values similar to unexposed cells in the Strw + CoQ_{10red} group ($p < 0.05$) (Figure 8). Similar results were obtained for catalase and HO-1 (Figure 8), even if the protein expression level of the unexposed cells was never reached. These results confirm previous data, which highlights the protective mechanism of plant phenolic compounds against UV-induced damage through Nrf2 activation [47], and the improvement of antioxidant reserves [48,49]. All the collected evidence underlines the idea that strawberry-enriched sun-protective formulations were able to counteract the UV-mediated inflammatory response by acting on the different pathways. The different formulations efficiently reduced the inflammatory conditions created by UV radiation through

the augmentation of antioxidant defense expression, the modulation of the NF-kB pathway, and the reduction of inflammatory cytokine production.

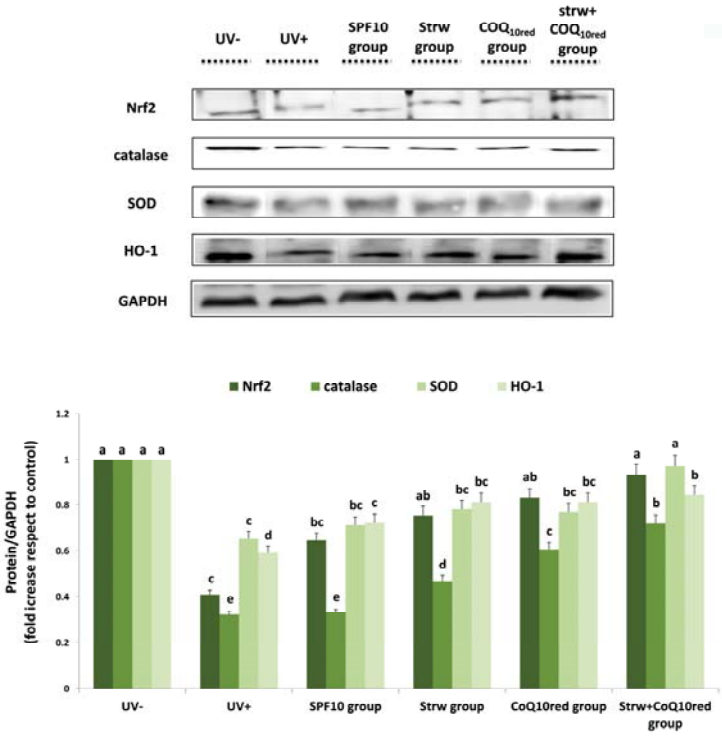

Figure 8. Levels of proteins related to antioxidant response (Nrf2, catalase, SOD, HO-1) in human dermal fibroblast (HDF) cells irradiated with ultraviolet A (UVA, 275 kJ/m^2) radiation (UV+) or not irradiated (UV−), after 1 h of exposure. HDF were screened with different formulations as explained in the text. Data are expressed as mean values ± standard deviation (SD). Columns belonging to the same set of data with different superscript letters are significantly different ($p < 0.05$).

4. Conclusions

There is a global tendency towards the use of natural cosmetics and to create high UV-protection formulations with little amounts of chemical substances. The combination of synthetic agents and natural compounds may offer an effective tool for preventing the damaging effects of UV exposure. In our work, the use of strawberry/reduced CoQ_{10}-based formulations has been proposed as an innovative instrument for the prevention of UVA exposure-induced inflammation. The obtained results suggest the possible applications of this natural screen against dermal damage caused by UV radiation, as highlighted by the reduction of ROS and pro-inflammatory markers, and the improvement of mitochondrial functionality and antioxidant enzyme expressions. Further research is strongly encouraged to deeply investigate the molecular mechanisms involved, and to find the main classes of bioactive compounds responsible for this anti-inflammatory effect.

Acknowledgments: The authors wish to thank Monica Glebocki for extensively editing the manuscript.

Author Contributions: Massimiliano Gasparrini, Francesca Giampieri and Tamara Y. Forbes-Hernandez conceived and designed the experiments under the supervision of Maurizio Battino, Jose L. Quiles and Stefano Bompadre. Massimiliano Gasparrini, Francesca Giampieri, Tamara Y. Forbes-Hernandez, Sadia Afrin, Patricia

Reboredo-Rodriguez and Danila Cianciosi performed the experiments and analyzed the data together with Maurizio Battino, Jose L. Quiles and Stefano Bompadre. Maurizio Battino contributed reagents/materials/analysis tools. Massimiliano Gasparrini and Tamara Y. Forbes-Hernandez wrote the paper.

Conflicts of Interest: The authors declare no conflict of interest.

References

1. Cefali, L.C.; Ataide, J.A.; Moriel, P.; Foglio, M.A.; Mazzola, P.G. Plant-based active photoprotectants for sunscreens. *Int. J. Cosmet. Sci.* **2016**, *38*, 346–353. [CrossRef] [PubMed]
2. Działo, M.; Mierziak, J.; Korzun, U.; Preisner, M.; Szopa, J.; Kulma, A. The Potential of Plant Phenolics in Prevention and Therapy of Skin Disorders. *Int. J. Mol. Sci.* **2016**, *17*, 160. [CrossRef] [PubMed]
3. Bachelor, M.A.; Bowden, G.T. UVA-mediated activation of signaling pathways involved in skin tumor promotion and progression. *Semin. Cancer Biol.* **2004**, *14*, 131–138. [CrossRef] [PubMed]
4. Bosch, R.; Philips, N.; Suárez-Pérez, J.A.; Juarranz, A.; Devmurari, A.; Chalensouk-Khaosaat, J.; González, S. Mechanisms of Photoaging and Cutaneous Photocarcinogenesis, and Photoprotective Strategies with Phytochemicals. *Antioxidants* **2015**, *4*, 248–268. [CrossRef] [PubMed]
5. Saewan, N.; Jimtaisong, A. Natural products as photoprotection. *J. Cosmet. Dermatol.* **2015**, *14*, 47–63. [CrossRef] [PubMed]
6. Gasparrini, M.; Forbes-Hernandez, T.Y.; Afrin, S.; Alvarez-Suarez, J.M.; Gonzàlez-Paramàs, A.M.; Santos-Buelga, C.; Bompadre, S.; Quiles, J.L.; Mezzetti, B.; Giampieri, F. A Pilot Study of the Photoprotective Effects of Strawberry-Based Cosmetic Formulations on Human Dermal Fibroblasts. *Int. J. Mol. Sci.* **2015**, *16*, 17870–17884. [CrossRef] [PubMed]
7. Nichols, J.A.; Katiyar, S.K. Skin photoprotection by natural polyphenols: anti-inflammatory, antioxidant and DNA repair mechanisms. *Arch. Dermatol. Res.* **2010**, *302*, 71–83. [CrossRef] [PubMed]
8. Giampieri, F.; Alvarez-Suarez, J.M.; Tulipani, S.; Gonzàles-Paramàs, A.M.; Santos-Buelga, C.; Bompadre, S.; Quiles, J.L.; Mezzetti, B.; Battino, M. Photoprotective potential of strawberry (Fragaria × ananassa) extract against UV-A irradiation damage on human fibroblasts. *J. Agric. Food Chem.* **2012**, *60*, 2322–2327. [CrossRef] [PubMed]
9. Giampieri, F.; Forbes-Hernandez, T.Y.; Gasparrini, M.; Alvarez-Suarez, J.M.; Afrin, S.; Bompadre, S.; Quiles, J.L.; Mezzetti, B.; Battino, M. Strawberry as a health promoter: an evidence based review. *Food Funct.* **2015**, *6*, 1386–1398. [CrossRef] [PubMed]
10. Mazzoni, L.; Perez-Lopez, P.; Giampieri, F.; Alvarez-Suarez, J.M.; Gasparrini, M.; Forbes-Hernandez, T.Y.; Quiles, J.L.; Mezzetti, B.; Battino, M. The genetic aspects of berries: from field to health. *J. Sci. Food Agric.* **2016**, *96*, 365–371. [CrossRef] [PubMed]
11. Giampieri, F.; Alvarez-Suarez, J.M.; Cordero, M.D.; Gasparrini, M.; Forbes-Hernandez, T.Y.; Afrin, S.; Santos-Buelga, C.; González-Paramás, A.M.; Astolfi, P.; Rubini, C.; et al. Strawberry consumption improves aging-associated impairments, mitochondrial biogenesis and functionality through the AMP-Activated Protein Kinase signaling cascade. *Food Chem.* **2017**. [CrossRef] [PubMed]
12. Afrin, S.; Gasparrini, M.; Forbes-Hernandez, T.Y.; Reboredo-Rodriguez, P.; Mezzetti, B.; Varela-López, A.; Giampieri, F.; Battino, M. Promising Health Benefits of the Strawberry: A Focus on Clinical Studies. *J Agric. Food Chem.* **2016**, *64*, 4435–4449. [CrossRef] [PubMed]
13. Forbes-Hernandez, T.Y.; Gasparrini, M.; Afrin, S.; Bompadre, S.; Mezzetti, B.; Quiles, J.L.; Giampieri, F.; Battino, M. The Healthy Effects of Strawberry Polyphenols: Which Strategy behind Antioxidant Capacity? *Crit. Rev. Food Sci. Nutr.* **2016**, *56*, S46–S59. [CrossRef] [PubMed]
14. Giampieri, F.; Alvarez-Suarez, J.M.; Mazzoni, L.; Forbes-Hernandez, T.Y.; Gasparrini, M.; Gonzàlez-Paramàs, A.M.; Santos-Buelga, C.; Quiles, J.L.; Bompadre, S.; Mezzetti, B.; et al. An anthocyanin-rich strawberry extract protects against oxidative stress damage and improves mitochondrial functionality in human dermal fibroblasts exposed to an oxidizing agent. *Food Funct.* **2014**, *5*, 1939–1948. [CrossRef] [PubMed]
15. Slinkard, K.; Singleton, V.L. Total Phenol analysis: Automation and comparison with manual methods. *Am. J. Enol. Viticult.* **1977**, *28*, 49–55.
16. Dewanto, V.; Wu, X.; Adom, K.K.; Liu, R.H. Thermal processing enhances the nutritional values of tomatoes by increasing the total antioxidant activity. *J. Agric. Food Chem.* **2002**, *50*, 3010–3014. [CrossRef] [PubMed]

17. Patring, J.D.; Jastrebova, J.A.; Hjortmo, S.B.; Andlid, T.A.; Jägerstad, I.M. Development of a simplified method for the determination of folates in baker's yeast by HPLC with ultraviolet and fluorescence detection. *J. Agric. Food Chem.* **2005**, *53*, 2406–2411. [CrossRef] [PubMed]
18. Jastrebova, J.; Witthoft, C.; Grahn, A.; Svensson, U.; Jagerstad, M. HPLC determination of folates in raw and processed beetroots. *Food Chem.* **2003**, *80*, 579–588. [CrossRef]
19. Giusti, M.; Wrolstad, R.E. Characterization and Measurement of Anthocyanins by UV-Visible Spectroscopy. *Curr. Prot. Food Analyt. Chem.* **2001**, F1.2.1–F1.2.13. [CrossRef]
20. Re, R.; Pellegrini, N.; Proteggente, A.; Pannala, A.; Yang, M.; Rice-Evans, C. Antioxidant activity applying an improved ABTS radical cation decolorization assay. *Free Radic. Biol. Med.* **1999**, *26*, 1231–1237. [CrossRef]
21. Benzie, I.F.F.; Strain, J.J. Ferric reducing ability of plasma (FRAP) as a measure of antioxidant power: The FRAP assay. *Anal. Biochem.* **1996**, *239*, 70–76. [CrossRef] [PubMed]
22. Prymont-Przyminska, A.; Zwolinska, A.; Sarniak, A.; Wlodarczyk, A.; Krol, M.; Nowak, M.; de Graft-Johnson, J.; Padula, G.; Bialasiewicz, P.; Markowski, J.; et al. Consumption of strawberries on a daily basis increases the non-urate 2,2-diphenyl-1-picryl-hydrazyl (DPPH) radical scavenging activity of fasting plasma in healthy subjects. *J. Clin. Biochem. Nutr.* **2014**, *55*, 48–55. [CrossRef] [PubMed]
23. Seite, S.; Moyal, D.; Richard, S.; de Rigal, J.; Leveque, J.L.; Hourseau, C.; Fourtanier, A. Mexoryl SX: A broad absorption UVA filter protects human skin from the effects of repeated suberythemal doses of UVA. *J. Photochem. Photobiol. B* **1998**, *44*, 69–76. [CrossRef]
24. Islam, M.S.; Giampieri, F.; Janjusevic, M.; Gasparrini, M.; Forbes-Hernandez, T.Y.; Mazzoni, L.; Greco, S.; Giannubilo, S.R.; Ciavattini, A.; Mezzetti, B.; et al. An anthocyanin rich strawberry extract induces apoptosis and ROS while decreases glycolysis and fibrosis in human uterine leiomyoma cells. *Oncotarget* **2017**, *8*, 23575–23587. [CrossRef] [PubMed]
25. Gasparrini, M.; Forbes-Hernandez, T.Y.; Giampieri, F.; Afrin, S.; Mezzetti, B.; Quiles, J.L.; Bompadre, S.; Battino, M. Protective Effect of Strawberry Extract against Inflammatory Stress Induced in Human Dermal Fibroblasts. *Molecules* **2017**, *22*, 164. [CrossRef] [PubMed]
26. Gasparrini, M.; Forbes-Hernandez, T.Y.; Giampieri, F.; Afrin, S.; Alvarez-Suarez, J.M.; Mazzoni, L.; Mezzetti, B.; Quiles, J.L.; Battino, M. Anti-inflammatory effect of strawberry extract against LPS-induced stress in RAW 264.7 macrophages. *Food Chem. Toxicol.* **2017**, *102*, 1–10. [CrossRef] [PubMed]
27. Brand, M.D.; Nicholls, D.G. Assessing mitochondrial dysfunction in cells. *Biochem. J.* **2011**, *435*, 297–312. [CrossRef] [PubMed]
28. Bradford, M.M. A rapid and sensitive method for the quantitation of microgram quantities of protein utilizing the principle of protein-dye binding. *Anal. Biochem.* **1976**, *72*, 248–254. [CrossRef]
29. Ariza, M.T.; Martínez-Ferri, E.; Domínguez, P.; Medina, J.J.; Miranda, L.; Soria, C. Effects of harvest time on functional compounds and fruit antioxidant capacity in ten strawberry cultivars. *J. Berry Res.* **2015**, *5*, 71–80. [CrossRef]
30. Buendía, B.; Gil, M.I.; Tudela, J.A.; Gady, A.L.; Medina, J.J.; Soria, C.; López, J.M.; Tomás-Barberán, F.A. HPLC-MS analysis of proanthocyanidin oligomers and other phenolics in 15 strawberry cultivars. *J. Agric. Food Chem.* **2010**, *58*, 3916–3926. [CrossRef] [PubMed]
31. Tulipani, S.; Mezzetti, B.; Capocasa, F.; Bompadre, S.; Beekwilder, J.; de Vos, C.H.; Capanoglu, E.; Bovy, A.; Battino, M. Antioxidants, phenolic compounds, and nutritional quality of different strawberry genotypes. *J. Agric. Food Chem.* **2008**, *56*, 696–704. [CrossRef] [PubMed]
32. Shin, S.; Kum, H.; Ryu, D.; Kim, M.; Jung, E.; Park, D. Protective effects of a new phloretin derivative against UVB-induced damage in skin cell model and human volunteers. *Int. J. Mol. Sci.* **2014**, *15*, 18919–18940. [CrossRef] [PubMed]
33. Forbes-Hernandez, T.Y.; Giampieri, F.; Gasparrini, M.; Mazzoni, L.; Quiles, J.L.; Alvarez-Suarez, J.M.; Battino, M. The effects of bioactive compounds from plant foods on mitochondrial function: a focus on apoptotic mechanisms. *Food Chem. Toxicol.* **2014**, *68*, 154–182. [CrossRef] [PubMed]
34. Camouse, M.M.; Domingo, D.S.; Swain, F.R.; Conrad, E.P.; Matsui, M.S.; Maes, D.; Declercq, L.; Cooper, K.D.; Stevens, S.R.; Baron, E.D. Topical application of green and white tea extracts provides protection from solar-simulated ultraviolet light in human skin. *Exp. Dermatol.* **2009**, *18*, 522–526. [CrossRef] [PubMed]
35. Psotova, J.; Svobodova, A.; Kolarova, H.; Walterova, D. Photoprotective properties of prunella vulgaris and rosmarinic acid on human keratinocytes. *J. Photochem. Photobiol. B* **2006**, *84*, 167–174. [CrossRef] [PubMed]

36. Svobodová, A.; Rambousková, J.; Walterová, D.; Vostalová, J. Bilberry extract reduces UVA-induced oxidative stress in HaCaT keratinocytes: A pilot study. *Biofactors* **2008**, *33*, 249–266. [CrossRef] [PubMed]
37. Bae, J.Y.; Lim, S.S.; Kim, S.J.; Choi, J.S.; Park, J.; Ju, S.M.; Han, S.J.; Kang, I.J.; Kang, Y.H. Bog blueberry anthocyanins alleviate photoaging in ultraviolet-B irradiation-induced human dermal fibroblasts. *Mol. Nutr. Food Res.* **2009**, *53*, 726–738. [CrossRef] [PubMed]
38. Cha, J.W.; Piao, M.J.; Kim, K.C.; Yao, C.W.; Zheng, J.; Kim, S.M.; Hyun, C.L.; Ahn, Y.S.; Hyun, J.W. The Polyphenol Chlorogenic Acid Attenuates UVB-mediated Oxidative Stress in Human HaCaT Keratinocytes. *Biomol. Ther. (Seoul)* **2014**, *22*, 136–142. [CrossRef] [PubMed]
39. Pérez-Sánchez, A.; Barrajón-Catalán, E.; Caturla, N.; Castillo, J.; Benavente-García, O.; Alcaraz, M.; Micol, V. Protective effects of citrus and rosemary extracts on UV-induced damage in skin cell model and human volunteers. *J. Photochem. Photobiol. B* **2014**, *136*, 12–18. [CrossRef] [PubMed]
40. F'Guyer, S.; Afaq, F.; Mukhtar, H. Photochemoprevention of skin cancer by botanical agents. *Photodermatol. Photoimmunol. Photomed.* **2003**, *19*, 56–72. [CrossRef] [PubMed]
41. Katiyar, S.K.; Meleth, S.; Sharma, S.D. Silymarin, a flavonoid from milk thistle (*Silybum marianum* L.), inhibits UV-induced oxidative stress through targeting infiltrating CD11b+ cells in mouse skin. *Photochem. Photobiol.* **2008**, *84*, 266–271. [CrossRef] [PubMed]
42. Villa, A.; Viera, M.H.; Amini, S.; Huo, R.; Perez, O.; Ruiz, P.; Amador, A.; Elgart, G.; Berman, B. Decrease of ultraviolet A light-induced "common deletion" in healthy volunteers after oral Polypodium leucotomos extract supplement in a randomized clinical trial. *J. Am. Acad. Dermatol.* **2010**, *62*, 511–513. [CrossRef] [PubMed]
43. Parrado, C.; Mascaraque, M.; Gilaberte, Y.; Juarranz, A.; Gonzalez, S. Fernblock (Polypodium leucotomos Extract): Molecular Mechanisms and Pleiotropic Effects in Light-Related Skin Conditions, Photoaging and Skin Cancers, a Review. *Int. J. Mol. Sci.* **2016**, *17*, 1026. [CrossRef] [PubMed]
44. Jańczyk, A.; Garcia-Lopez, M.A.; Fernandez-Peñas, P.; Alonso-Lebrero, J.L.; Benedicto, I.; López-Cabrera, M.; Gonzalez, S. A Polypodium leucotomos extract inhibits solar-simulated radiation-induced TNF-alpha and iNOS expression, transcriptional activation and apoptosis. *Exp. Dermatol.* **2007**, *16*, 823–829. [CrossRef] [PubMed]
45. Shin, S.W.; Jung, E.; Kim, S.; Lee, K.E.; Youm, J.K.; Park, D. Antagonist effects of veratric acid against UVB-induced cell damages. *Molecules* **2013**, *18*, 5405–5419. [CrossRef] [PubMed]
46. Potapovich, A.; Kostyuk, V.A.; Kostyuk, T.V.; de Luca, C.; Korkina, L.G. Effects of pre- and post-treatment with plant polyphenols on human keratinocyte responses to solar UV. *Inflamm. Res.* **2013**, *62*, 773–780. [CrossRef] [PubMed]
47. Almeida, I.F.; Pinto, A.S.; Monteiro, C.; Monteiro, H.; Belo, L.; Fernandes, J.; Bento, A.R.; Duarte, T.L.; Garrido, J.; Bahia, M.F.; et al. Protective effect of C. sativa leaf extract against UV mediated-DNA damage in a human keratinocyte cell line. *J. Photochem. Photobiol. B* **2015**, *144*, 28–34. [CrossRef] [PubMed]
48. González, S.; Pathak, M.A. Inhibition of ultraviolet-induced formation of reactive oxygen species, lipid peroxidation, erythema and skin photosensitization by polypodium leucotomos. *Photodermatol. Photoimmunol. Photomed.* **1996**, *12*, 45–56. [CrossRef] [PubMed]
49. Lyons, N.M.; O'Brien, N.M. Modulatory effects of an algal extract containing astaxanthin on irradiated cells in culture. *J. Dermatol. Sci.* **2002**, *30*, 73–84. [CrossRef]

nutrients

MDPI

Article

Lipid Accumulation in HepG2 Cells Is Attenuated by Strawberry Extract through AMPK Activation

Tamara Y. Forbes-Hernández [1,2], Francesca Giampieri [1], Massimiliano Gasparrini [1], Sadia Afrin [1], Luca Mazzoni [3], Mario D. Cordero [4], Bruno Mezzetti [3], José L. Quiles [5] and Maurizio Battino [1,6,*]

1 Dipartimento di Scienze Cliniche Specialistiche ed Odontostomatologiche (DISCO)-Sez. Biochimica, Facoltà di Medicina, Università Politecnica delle Marche, 60131 Ancona, Italy; tamara.forbe@gmail.com (T.Y.F.-H.); f.giampieri@univpm.it (F.G.); m.gasparrini@univpm.it (M.G.); dolla.bihs@gmail.com (S.A.)

2 Área de Nutrición y Salud, Universidad Internacional Iberoamericana (UNINI), Campeche 24040, Mexico

3 Dipartimento di Scienze Agrarie, Alimentari e Ambientali, Università Politecnica delle Marche, 60131 Ancona, Italy; l.mazzoni@univpm.it (L.M.); b.mezzetti@univpm.it (B.M.)

4 Research Laboratory, Dental School, University of Sevilla, 41009 Sevilla, Spain; mdcormor@us.es

5 Department of Physiology, Institute of Nutrition and Food Technology "José Mataix", Biomedical Research Centre, University of Granada, 18000 Granada, Spain; jlquiles@ugr.es

6 Centre for Nutrition & Health, Universidad Europea del Atlantico (UEA), 39011 Santander, Spain

* Correspondence: m.a.battino@univpm.it; Tel.: +39-071-220-4646; Fax: +39-071-220-4123

Received: 9 May 2017; Accepted: 13 June 2017; Published: 16 June 2017

Abstract: Regulation of lipid metabolism is essential for treatment and prevention of several chronic diseases such as obesity, diabetes, and cardiovascular diseases, which are responsible for most deaths worldwide. It has been demonstrated that the AMP-activated protein kinase (AMPK) has a direct impact on lipid metabolism by modulating several downstream-signaling components. The main objective of the present work was to evaluate the in vitro effect of a methanolic strawberry extract on AMPK and its possible repercussion on lipid metabolism in human hepatocellular carcinoma cells (HepG2). For such purpose, the lipid profile and the expression of proteins metabolically related to AMPK were determined on cells lysates. The results demonstrated that strawberry methanolic extract decreased total cholesterol, low-density lipoprotein (LDL)-cholesterol, and triglycerides levels (up to 0.50-, 0.30-, and 0.40-fold, respectively) while it stimulated the p-AMPK/AMPK expression (up to 3.06-fold), compared to the control. AMPK stimulation led to the phosphorylation and consequent inactivation of acetyl coenzyme A carboxylase (ACC) and inhibition of 3-hydroxy-3-methylglutaryl-CoA reductase (HMGCR), the major regulators of fatty acids and cholesterol synthesis, respectively. Strawberry treatment also entailed a 4.34-, 2.37-, and 2.47-fold overexpression of LDL receptor, sirtuin 1 (Sirt1), and the peroxisome proliferator activated receptor gamma coactivator 1-alpha (PGC-1α), respectively, compared to control. The observed results were counteracted by treatment with compound C, an AMPK pharmacological inhibitor, confirming that multiple effects of strawberries on lipid metabolism are mediated by the activation of this protein.

Keywords: strawberry; cholesterol synthesis; fatty acids synthesis; hypolipidemic agent

1. Introduction

Dyslipidemia—a major disorder of lipoprotein metabolism—is one of the main risk factors for cardiovascular diseases (CVDs) including coronary heart disease, heart attacks, strokes, and peripheral vascular disease [1–3], which are responsible for most deaths worldwide [4,5]. Elevated total cholesterol, low-density lipoprotein (LDL)-cholesterol, and triglycerides levels are also correlated with type 2 diabetes, insulin resistance [1], and chronic renal disease [6]. Hence, understanding lipid metabolism is essential for the treatment and prevention of all these pathologies.

Recently, the AMP-activated protein kinase (AMPK) has been proposed as a potential therapeutic target for the treatment of several chronic diseases including obesity, type 2 diabetes, and CVDs [7,8]. AMPK is a serine/threonine protein kinase that plays a central role in regulating cellular metabolism and energy balance in mammalian cells [9]. When cellular energy stores are depleted by stimuli such as muscle contraction, hypoxia, or myocardial ischaemia, AMPK is activated. Once activated, AMPK induces ATP generation pathways such as glycolysis, fatty acid oxidation, and lipolysis. On the contrary, anabolic pathways like gluconeogenesis, and cholesterol and protein synthesis are inhibited. The overall effects of this protein—when activated—on the lipid metabolism are to stimulate fatty acid oxidation and to block cholesterol and triglycerides synthesis [9,10].

Of current interest are the effects of naturally occurring compounds in the treatment and/or prevention of particular diseases by activating AMPK. Many of these natural compounds, including epigallocatechin gallate, resveratrol, quercetin, theaflavin, curcumin, berberine, ginsenoside, and caffeic acid phenethyl ester, belong to the polyphenols family [10]. Therefore, it is suggested that polyphenolic compounds from natural sources may be used to activate AMPK.

In this context, strawberries (*Fragaria* × *ananassa*) are one of the richest dietary sources of phytochemicals, mainly represented by flavonoids, hydrolysable tannins, and phenolic acids [11,12].

Scientific evidence indicates the role of this berry in the diminution of oxidative damage and inflammation, which play a critical role in the development of chronic diseases [13]. In different models of obesity/diabetes, it has been demonstrated that whole strawberries or purified anthocyanin supplementation normalize blood glucose levels and limit glucose transport and uptake [14]. In addition, data from in vitro experiments suggest that the bioactive compounds from strawberries can modify the cell membrane composition, functionality, and fluidity, protecting lipid bilayers against oxidative damage [15,16].

In obese and lean C57BL/6 mice models, strawberry supplementation decreases plasma c-reactive protein (CRP) and overall blood glucose concentrations independently of the dietary fat content, demonstrating a protective effect against cardiovascular risk [17]. In addition, some clinical studies observed that strawberry intake ameliorates some atherosclerotic risk factors by reducing circulating levels of vascular cell adhesion molecule 1 [13], and CRP [18,19], decreasing lipid peroxidation [19], and improving lipid profile [13,19,20].

The reduction of lipid levels in plasma can be explained through the ability of strawberry polyphenols to activate the molecular signaling pathways involved in lipid metabolism, but this hypothesis must still be confirmed. The main objective of the present work was to evaluate the in vitro effect of strawberry (cv. Romina) methanolic extract on AMP-activated protein kinase (AMPK) cascade and its possible repercussion on lipid metabolism in human hepatocellular carcinoma cells (HepG2).

2. Materials and Methods

2.1. Preparation of Strawberry Extract

Strawberry fruits, *Fragaria* × *ananassa* (cv. Romina) were collected in the experimental fields of Azienda Agraria Didattico Sperimentale (Università Politecnica delle Marche, Ancona, Italy). Within 2 h after harvest, whole fruits were stored at −80 °C until time of analyses. For the strawberry extract preparation, 10 g of fruits were added to 100 mL of the extraction solution, consisting of methanol/MilliQ water/concentrated formic acid (80:20:0.1 v/v), and homogenized using an Ultraturrax T25 homogenizer (Janke & Kunkel, IKA Labortechnik). Extraction was maximized by stirring the suspension for 2 h in the dark at room temperature. The mixture was then centrifuged at 2400× g for 15 min in two sequential times, to sediment solids. Supernatants were filtered through a 0.45 µm Minisart filter (PBI International), transferred to 5.0 mL amber glass vials, and stored at −80 °C until analysis. For cellular treatment, the methanolic extract was further concentrated and dried through a rotary evaporator and stored in aliquots at −80 °C.

2.2. Strawberry Extract Characterization

2.2.1. Total Phenolic Compounds (TPC) and Flavonoids Content Determination

TPC of the strawberry extract was determined using the Folin-Ciocalteu method, as modified by Slinkard and Singleton [21], while the total flavonoid content was determined through a colorimetric method previously described by Jia et al. [22] and Dewanto et al. [23].

2.2.2. Vitamin C Content Determination

For vitamin C quantification, the extracting solution consisted of MilliQ water containing 5% meta-phosphoric acid and 1 mM ethylenediaminetetraacetic acid. Vitamin C was extracted by sonication of 1 g of frozen strawberries in 4 mL of extracting solution, for the duration of 5 min, after a previous homogenization using an Ultraturrax T25 homogenizer (Janke & Kunkel, IKA Labortechnik, Staufen im Breisgau, Germany) at medium-high speed for 2 min. After the ultrasound assisted extraction, solids were precipitated by centrifugation at 1720× *g* for 10 min at 4 °C, and the supernatant was filtered through a 0.45 μm filter into 1.8 mL high-performance liquid chromatography (HPLC) vials and immediately analyzed as described by Helsper et al. [24] in an HPLC system (Jasco, PU-2089 plus).

2.2.3. Identification and Quantification of Strawberries Anthocyanins

Analysis of anthocyanins was carried out following the method described by Terefe et al. [25]. Anthocyanins were separated from the methanolic extract on an Aqua Luna C18 (2) (250 × 4.6 mm) reverse phase column with a particle size of 5 μm (Phenomenex) protected by a Phenomenex 4.0 × 3.0 mm C18 ODS guard column. The samples were diluted appropriately and filtered using a 0.45 μm filter prior to injection into the HPLC system (Jasco, PU-2089 plus). Anthocyanins were quantified using external Cyanidin-3-*O*-glucoside, Pelargonidin-3-*O*-glucoside, and Pelargonidin-3-*O*-rutinoside calibration curves.

2.2.4. Total Antioxidant Capacity (TAC) Determination

For TAC determination, three different methods were employed: the Ferric Reducing Antioxidant Power (FRAP) method described by Deighton et al. [26]; the 2,2-diphenyl-1-picrylhydrazyl (DPPH) free radical method described by Kumaran and Karunakaran [27]; and the Trolox Equivalent Antioxidant Capacity (TEAC) method described by Re et al. [28].

2.3. Cells Culture and Cells' Lysates Preparation

HepG2 cells were kindly provided by the Biological Research Laboratory of Seville University (Spain), and were grown in Dulbecco's modified Eagle's medium (DMEM), supplemented with 10% fetal bovine serum (FBS), 100 IU/mL penicillin, and 100 μg/mL streptomycin at 37 °C with 5% CO_2.

After treatments with the strawberry dried methanolic extract, compound C, or lovastatin for the indicated times (as detailed below), cells were lysed in a buffer containing 20 mM Tris–HCl (pH 7.5), 0.9% NaCl, 0.2% Triton X-100, and 1% of the protease inhibitor cocktail (Sigma-Aldrich, Milan, Italy) and then stored at −80 °C for further western blot analysis or were lysed in radioimmunoprecipitation assay (RIPA) buffer (Sigma-Aldrich, Milan, Italy) for lipid profile determination. All the analyses were conducted on cells between the third and the sixth passage.

2.4. Cytotoxicity Assay

Cells were seeded at a density of 5×10^3 cells/well into 96-well plates and treated with different concentrations of the dried methanolic extract (from 0 to 1 mg/mL) for 24, 48, and 72 h. Therefore, 30 μL of RPMI medium containing 2 mg/mL of 3-(4,5-dimethylthiazol-2-yl)-2,5-diphenyltetrazolium bromide (MTT) were added and cells were incubated for other 2 h. MTT solution was then discarded and 100 μL of dimethyl sulfoxide were added to dissolve the formazan crystals. The level of colored formazan

derivative was analyzed on a microplate reader (Thermo Scientific Multiskan EX, Monza, Italy) at a wavelength of 590 nm [29,30]. The viable cells were directly proportional to the formazan production.

2.5. Western Blotting Analysis

Equal amounts of protein (75 μg) of each sample were loaded and separated in a 10% acrylamide sodium dodecyl sulfate polyacrylamide gel electrophoresis (SDS/PAGE) and transferred to nitrocellulose membranes (Bio-Rad) by using a Trans-Blot Turbo Transfer System (Bio-Rad Laboratories, Inc., Hercules, CA, USA). Membranes were washed three times with PBS, blocked with 5% non-fat dry blocker (Bio-Rad), and incubated with the primary antibody at 4 °C overnight. All the polyclonal antibodies for the protein of interest were purchased from Santa Cruz Biotechnology, Inc., Dallas, TX, USA. Next, membranes were washed with 5% Tween 20 in Tris HCl buffered saline and incubated with the secondary anti-rabbit immunoglobulin G-Peroxidase antibody (Sigma-Aldrich, Milan, Italy). Protein bands were visualized using Immobilon Western Chemiluminescent Substrate (Millipore Corporation, Billerica, MA, USA), and the protein signals were detected by a Lycor C-Digit Blot Scanner. Quantification of protein expression was made using the software (Image Studio 3.1) provided by the manufacturer of the Blot Scanner (LI-COR Biotechnology, Bad Homburg, Germany).

2.6. Mitochondrial Functionality

Oxygen consumption rate (OCR) was measured in real-time using an XF24 Extracellular Flux Analyzer (Seahorse Bioscience, Billerica, MA, USA) according to the manufacturer's protocol. Cells were seeded at a density of 3×10^4 cells/well in 24-well plates and treated with the strawberry dried methanolic extract for 24 h. Before the running started, the medium was replaced with DMEM (containing 25 mM glucose, 2 mM glutamine, 1 mM sodium pyruvate, and without serum, pH 7.4) and plates were pre-incubated in the absence of CO2 in a XF Prep Station (Seahorse Bioscience, Billerica, MA, USA) at 37 °C. After finishing calibration, the plate containing cells was placed into the XF24 Extracellular Flux Analyzer (Seahorse Bioscience, Billerica, MA, USA) and mitochondrial functionality was evaluated by sequential injection of four compounds that affect bioenergetics, as follows: 55 μL of oligomycin into port A (final concentration 2.5 μg/mL); 61 μL of carbonyl cyanide-4-(trifluoromethoxy) phenylhydrazone (FCCP) into port B (final concentration 2.5 μM); and 68 μL of rotenone/antimycin A into port C (final concentration 1 μM/10 μM). The best concentration of each inhibitor and uncoupler, as well as the optimal cells seeding density were determined in preliminary analyses. A minimum of five wells per treatment were utilized in any given experiment.

2.7. Determination of Total Cholesterol, LDL-Cholesterol, and Triglycerides Levels

Total cholesterol, LDL-cholesterol, and triglycerides levels were determined by enzymatic colorimetric kits (Spinreact, St. Esteve d'en Bas, Girona, Spain) with the employment of a microplate reader (Thermo Scientific Microplate Reader, Multiskan®, Monza, Italy) coupled to an Ascent software program (Thermo LabSystems Oy, Version 2.6, Navi Mumbai, India).

2.8. Determination of Total Lipid Accumulation by Oil Red O Staining

Total lipid accumulation was evaluated according to the method previously described by Liu et al. [31]. Cells were seeded at a density of 1.5×10^5 cells/well in 6-well plates and treated for 24 h with the strawberry dried methanolic extract, compound C, or lovastatin. Subsequently, cells were rinsed twice with PBS and fixed in 4% paraformaldehyde in PBS for 30 min. Then, cells were stained with Oil Red O working solution for 1 h at room temperature and subsequently rinsed with water. The Oil Red O stock solution was prepared by dissolving 0.35 g of Oil Red O (Sigma Aldrich, Milan, Italy) in 100 mL of isopropanol by gentle heating and then cooled and filtered through a 0.45 μm filter. The working solution was prepared by diluting three parts of the stock solution in two parts of MilliQ water (stock solution:MilliQ water; 3:2 v/v). The cell images were captured with a Leitz Fluovert FU (Leica Microsystems, Wetzlar, Germany) microscope. Lipids appeared red.

For quantitative analysis of cellular lipids, 1 mL isopropanol was added to each well of the stained culture plate. The extracted dye was immediately removed by gentle pipetting and its absorbance was measured at 510 nm.

2.9. Statistical Analysis

Statistical analyses were performed using STATISTICA software (Statsoft Inc., Tulsa, OK, USA). Data were subjected to one-way analysis of variance for mean comparison, and significant differences among different treatments were calculated according to Tukey's HSD (honest significant difference) multiple range test. Data are reported as mean ± standard deviation (SD). Differences at $p < 0.05$ were considered statistically significant. All the analyses were performed in triplicate.

3. Results

3.1. Characterization of Romina Strawberry Extract

The phytochemical composition of the strawberry extract demonstrated that the Romina strawberry cultivar is a significant source of polyphenols (2.64 ± 2.63 mg gallic acid equivalent (GAeq)/g fresh weight (FW)), in particular of flavonoids (1.02 ± 0.87 mg catechin equivalent (CATeq)/g FW) (Table 1). TPC was similar to the values reported by Capocasa et al. [32] and Tulipani et al. [16] for other commercial varieties like Sveva (2.7 mg GAeq/g FW) and Camarosa (2.6 mg GAeq/g FW) and even higher than the values reported for Adria and Alba (1.8 and 2 mg GAeq/g FW, respectively).

Table 1. Phytochemical composition and antioxidant capacity of strawberry fruit and methanolic extract.

Parameters	Fresh Fruit	Dried Methanolic Extract
Total Polyphenols (mg GAeq/g)	2.64 ± 2.63	23.44 ± 0.22
Total Flavonoids (mg CATeq/g)	1.02 ± 0.87	5.21 ± 0.29
Vitamin C (mg/g)	0.39 ± 0.23	9.09 ± 4.45
Cyanidin-3-*O*-glucoside (mg/g)	0.03 ± 0.02	0.69 ± 0.41
Pelargonidin-3-*O*-glucoside (mg/g)	0.70 ± 0.25	16.32 ± 5.71
Pelargonidin-3-*O*-rutinoside (mg/g)	0.04 ± 0.08	0.93 ± 1.39
TAC (μmol Txeq/g)		
FRAP	22.70 ± 2.03	168.25 ± 3.95
DPPH	8.11 ± 0.25	30.29 ± 0.18
TEAC	10.71 ± 0.58	35.51 ± 0.06

mg GAeq/g: mg of gallic acid equivalent/g of fresh fruit or dried strawberry methanolic extract; mg CATeq/g: mg of catechin equivalent/g of fresh fruit or dried strawberry methanolic extract; μmol Txeq/g: μmol of Trolox equivalent/g of fresh fruit or dried strawberry methanolic extract; TAC: total antioxidant capacity; FRAP: Ferric Reducing Antioxidant Power; DPPH: 2,2-diphenyl-1-picrylhydrazyl; TEAC: Trolox Equivalent Antioxidant Capacity.

Also, the total flavonoids content (TFC) was higher than the values reported for Adria (0.4 mg CATeq/g FW) and Sveva (0.6 mg CATeq/g FW) [16] while the vitamin C content (0.39 ± 0.23 mg/g FW) was within the values reported by Tulipani et al. [33], who indicated that the average vitamin C content in five selected cultivars (Alba, Irma, Patty, Adria, and Sveva) and three advanced selections (AN94.414.52, AN03.338.51, AN00.239.55) of strawberries ranged from 0.23 to 0.47 mg/g FW.

Regarding the anthocyanins reported in Table 1, they were identified through their spectral and chromatographic characteristics and were in correspondence with the main anthocyanins reported for strawberries. The individual quantified value of Pelargonidin-3-*O*-glucoside (the most representative compound of this group) was significantly higher (0.70 ± 0.25 mg/g FW) than the values reported for Sveva, Alba, and Adria [16,33], although lower than the value reported for this cultivar by Diamanti et al. [34]. These results confirmed that the quality of this cultivar is quite good.

Once the strawberry methanolic extract was concentrated and dried, its TPC, TFC, and Pelargonidin-3-*O*-glucoside concentration were 23.44 ± 0.22 mg GAeq/g dried weight (DW), 5.21 ± 0.29 mg CATeq/g DW, and 16.32 ± 5.71 mg/g DW, respectively. In general, the presence of phenolic compounds and vitamin C is often correlated to the antioxidant power of fruits, since these compounds are efficient oxygen radical scavengers. TAC of Romina fruits was determined by three different methods (Table 1). Results confirmed that the Romina strawberry variety not only presents a good nutritional quality but also a high antioxidant capacity.

3.2. Effects of Strawberry Extract on HepG2 Cell Viability

Viability of HepG2 cells treated with different concentrations of strawberry dried methanolic extract was first determined using the MTT assay. The results showed that after 24 h of treatment the strawberry dried methanolic extract at concentrations up to 100 μg/mL did not significantly ($p < 0.05$) cause cell death with respect to control (Figure 1).

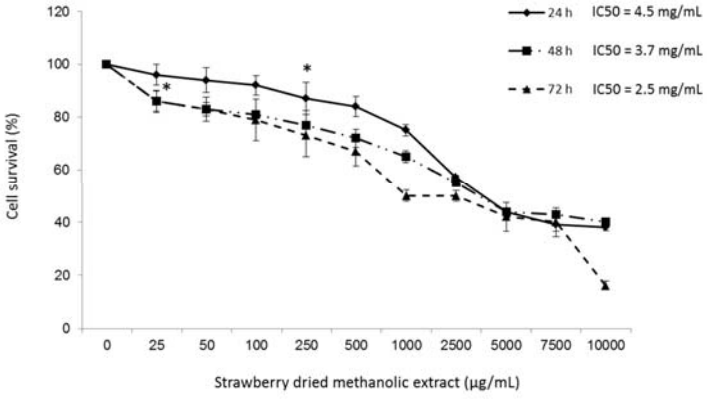

Figure 1. Viability of human hepatocellular carcinoma cells (HepG2) cells after treatment with strawberry dried methanolic extract. Cells were incubated with the indicated concentrations for 24, 48, and 72 h. IC50 indicates the concentration of strawberry dried methanolic extract which reduces the cells viability about 50%. Values are expressed as mean ± SD of three independent experiments ($n = 3$). Asterisk marks indicate the concentrations from which significant differences ($p < 0.05$) were observed compared to the control.

Significant cytotoxicity ($p < 0.05$) was observed at higher concentrations or longer treatment times, although in all cases the IC50 was higher than 2.5 mg/mL. Hence, the concentrations 10, 50, and 100 μg/mL of dried methanolic extract were used in subsequent experiments.

3.3. Effects of Strawberry Extract on AMPK Activation

To investigate whether strawberry extract regulates metabolism in HepG2 cells via AMPK pathway, the protein levels of phosphorylated AMPK (p-AMPK), total AMPK, sirtuin1 (Sirt1), and liver kinase B1 (LKB1) were examined. As demonstrated in Figure 2, treatment with strawberry dried methanolic extract significantly ($p < 0.05$) increased the expression of all these proteins in a dose dependent manner.

Twenty-four hours of treatment with the highest concentration (100 μg/mL) of strawberry dried methanolic extract, led to a 3.06-, 2.37-, and 3.16-fold overexpression of p-AMPK/AMPK, Sirt1, and LKB1, respectively, compared to control.

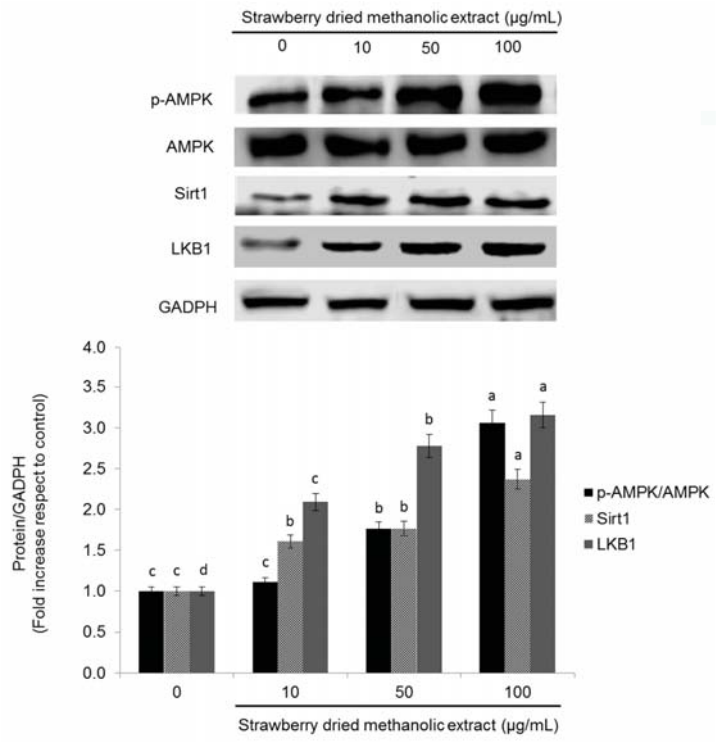

Figure 2. Effects of strawberry dried methanolic extract on p-AMPK, AMPK, Sirt1, and LKB1 expression. HepG2 cells were treated with the indicated concentrations for 24 h. The protein signals were detected by a Lycor C-Digit Blot Scanner and quantification was made using the software Image Studio 3. Values are expressed as mean ± SD of three independent experiments (n = 3) and normalized to the GADPH signal. Different superscript letters between different strawberry dried methanolic extract concentrations for each assayed protein indicate statistical significance ($p < 0.05$). p-AMPK: phosphorylated AMP-activated protein kinase; AMPK: AMP-activated protein kinase; Sirt1: sirtuin 1; LKB1: liver kinase B1; GADPH: glyceraldehyde 3-phosphate dehydrogenase.

Activation of AMPK by strawberry dried methanolic extract was accompanied by an overexpression of the inactive form of the ACC (phosphorylated ACC) and upregulation of the peroxisome proliferator activated receptor gamma coactivator 1-alpha (PGC-1α)—another downstream target of AMPK—in a dose dependent manner (Figure 3). p-ACC/ACC expression was 1.58-, 1.82-, and 2.48-fold, and PGC-1α expression 1.47-, 2.22-, and 2.47-fold higher compared to the control when cells were treated with 10, 50, and 100 μg/mL of the strawberry dried methanolic extract, respectively.

In addition, the expression of HMG-CoA reductase (HMGCR), which catalyzes a rate limiting step in cholesterol synthesis, was suppressed by the strawberry treatment (Figure 3). HMGCR expression was significantly ($p < 0.05$) lower (from 0.62 to 0.52 times compared to the control) when strawberry extract was applied at 10 μg/mL or 50–100 μg/mL, respectively. Inhibition of HMGCR and ACC confirms the hypothesis that strawberry extracts should have positive effects in lipid metabolism in HepG2 cells.

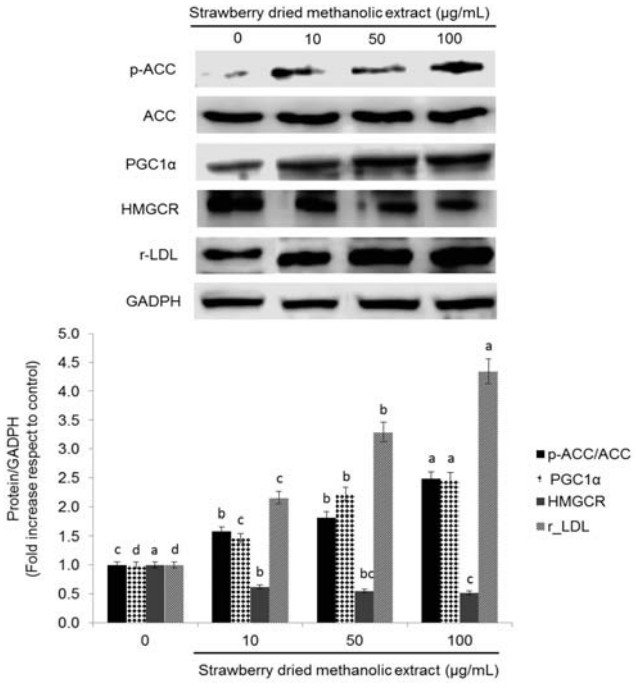

Figure 3. Effects of strawberry dried methanolic extract on p-ACC, ACC, r-LDL, PGC-1α, and HMGCR expression. HepG2 cells were treated with the indicated concentrations for 24 h. The protein signals were detected by a Lycor C-Digit Blot Scanner and quantification was made using the software Image Studio 3. Values are expressed as mean ± SD of three independent experiments (n = 3) and normalized to the GADPH signal. Different superscripts letters between different strawberry dried methanolic extract concentrations for each assayed protein indicate statistical significance ($p < 0.05$). p-ACC: phosphorylated acetyl coenzyme A carboxylase; ACC: acetyl coenzyme A carboxylase; PGC-1α: peroxisome proliferator activated receptor gamma coactivator 1-alpha; HMGCR: 3-hydroxy-3-methylglutaryl-CoA reductase; r-LDL: low density lipoprotein receptor; GADPH: glyceraldehyde 3-phosphate dehydrogenase.

In order to address whether strawberry extracts can influence lipid metabolism through transcriptional regulation, the expression of LDL receptor (r-LDL) was investigated. Dried methanolic extract at 10, 50, and 100 µg/mL led to significantly ($p < 0.05$) higher r-LDL expression compared to the control by up to 2.15-, 3.29-, and 4.34-fold, respectively.

The effects of strawberry extract in the expression of all the proteins tested was also time-dependent (Figure 4A,B). In most cases (p-AMPK, Sirt1, LKB1, p-ACC, PGC-1α), the highest protein expression was observed after 24 h of treatment, although, the first significant effects ($p < 0.05$) were observed just after 30 min. Only in the case of r-LDL and HMCGR, the maximal activation/inhibition was obtained after 48 h, respectively.

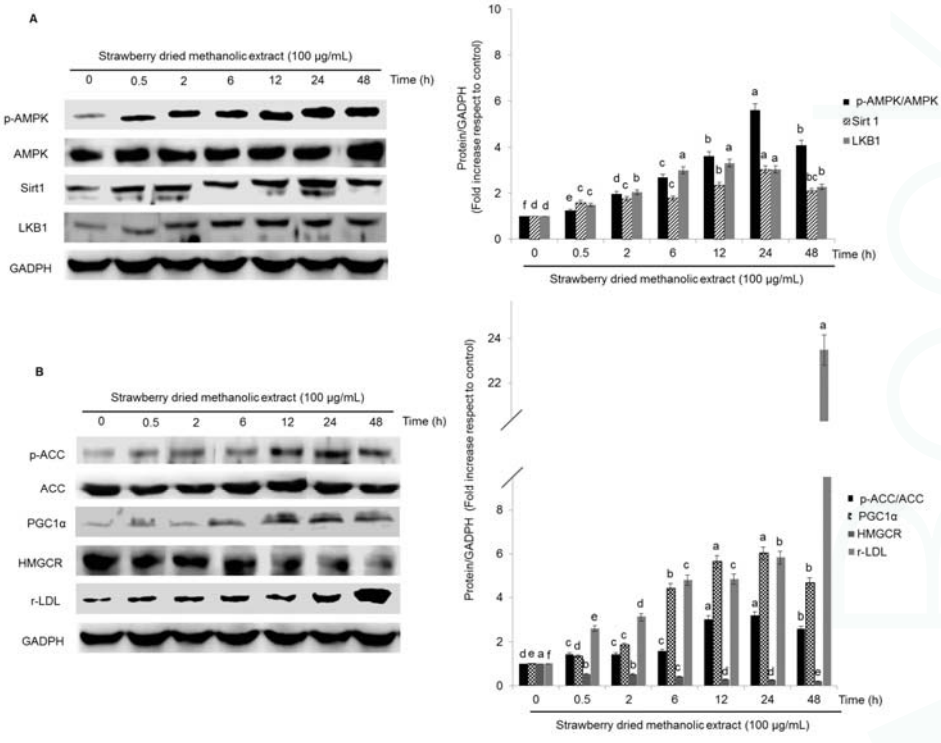

Figure 4. Protein ((**A**): p-AMPK, AMPK, Sirt1, LKB1 and (**B**): p-ACC, ACC, PGC-1α, HMGCR, r-LDL) expression in HepG2 cells after treatment with strawberry dried methanolic extract for different times. Cells were treated with 100 μg/mL of the extract. The protein signals were detected by a Lycor C-Digit Blot Scanner. p-AMPK: phosphorylated AMP-activated protein kinase; AMPK: AMP-activated protein kinase; Sirt1: sirtuin 1, LKB1: liver kinase B1; p-ACC: phosphorylated acetyl coenzyme A carboxylase; ACC: acetyl coenzyme A carboxylase; PGC-1α: peroxisome proliferator activated receptor gamma coactivator 1-alpha; HMGCR: 3-hydroxy-3-methylglutaryl-CoA reductase; r-LDL: low density lipoprotein receptor; GADPH: glyceraldehyde 3-phosphate dehydrogenase.

Since AMPK is activated not only through its upstream kinases but also by an increase in the AMP/ATP ratio or in response to other stimuli such as hypoxia or oxidative stress [9,35,36], mitochondrial functionality in treated HepG2 cells was also determined. For that purpose, the OCR was examined (Figure 5A).

Increasing concentrations of strawberry dried methanolic extract had no significant ($p < 0.05$) effect on basal respiration, while they caused a diminution in the spare and the maximal respiration compared to the control (Figure 5B).

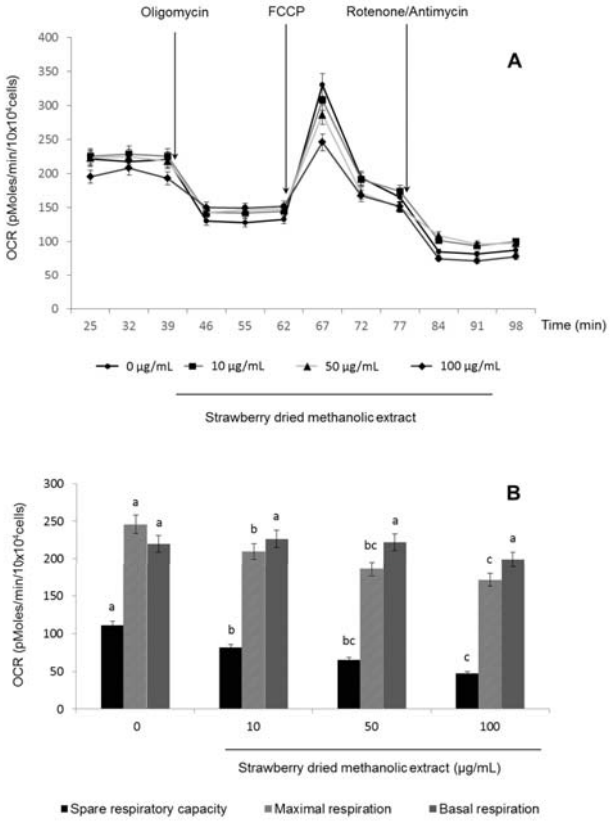

Figure 5. Effects of strawberry dried methanolic extract on mitochondrial respiration in HepG2 cells: XF cell Mito stress test profile (**A**) and spare respiratory capacity, maximal respiration and basal respiration (**B**). Cells were treated with the indicated concentration for 24 h. Values are expressed as mean ± SD of three independent experiments (n = 3). Different superscript letters between different strawberry dried methanolic extract concentrations for each parameter in the chart bar indicate statistical significance ($p < 0.05$). OCR: oxygen consumption rate; FCCP: carbonyl cyanide-4-(trifluoromethoxy)phenylhydrazone.

To further confirm the effect of strawberry extracts on lipid metabolism through AMPK pathway activation, HepG2 cells were incubated with 100 μg/mL strawberry dried methanolic extract in the presence of an AMPK inhibitor (compound C, 10 mM) or a positive control (lovastatin, 10 mM). Then, the expression of AMPK pathway related proteins was determined.

As shown in Figure 6A,B, phosphorylation of AMPK by strawberry dried methanolic extract was significantly ($p < 0.05$) reversed in the presence of compound C, reaching values comparable to the untreated control.

Also, the expression of p-ACC, r-LDL, and PGC-1α was lower in the presence of the inhibitor, supporting the role of AMPK in the activation of these proteins by strawberry extracts, at least in part. Inhibition of HMGCR induced by strawberry extracts was also significantly ($p < 0.05$) reversed by compound C treatment.

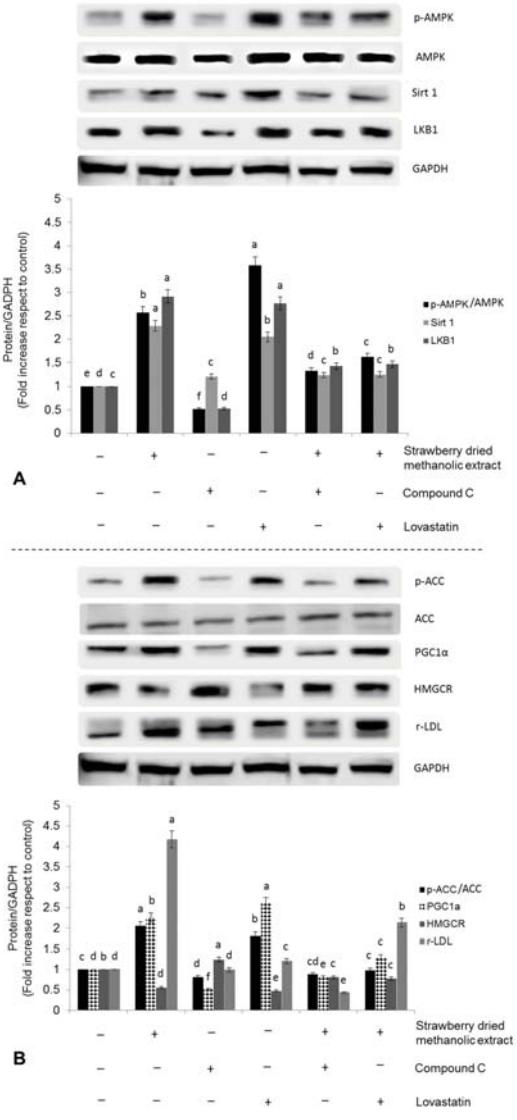

Figure 6. Effects of strawberry dried methanolic extract (100 μg/mL) in the expression of AMPK pathway related proteins ((**A**): p-AMPK, AMPK, Sirt1, LKB1 and (**B**): p-ACC, ACC, PGC1α, HMGCR, r-LDL) in the presence of 10 μM Compound C (negative control) or 10 μM Lovastatin (positive control) in HepG2 cells. Cells were treated for 24 h. Values are expressed as mean ± SD of three independent experiments (n = 3). Different superscript letters between different assayed conditions for each assayed protein indicate statistical significance ($p < 0.05$). p-AMPK: phosphorylated AMP-activated protein kinase: AMPK: AMP-activated protein kinase; Sirt1: sirtuin 1; LKB1: liver kinase B1; p-ACC: phosphorylated acetyl coenzyme A carboxylase; ACC: acetyl coenzyme A carboxylase; PGC-1α: peroxisome proliferator activated receptor gamma coactivator 1-alpha; HMGCR: 3-hydroxy-3-methylglutaryl-CoA reductase; r-LDL: low density lipoprotein receptor; GADPH: glyceraldehyde 3-phosphate dehydrogenase.

On the contrary, and as expected, treatment with 10 μM lovastatin for 24 h led to a higher expression of p-AMPK, with the corresponding implications for its downstream targets. It has been demonstrated that lovastatin treatment (1–25 μM, 24 h) impairs mitochondrial function, decreases cellular ADP/ATP ratios, and consequently activates LKB1/AMPK pathway [37]. Statins can rapidly activate AMPK via increased Thr-172 phosphorylation in vitro and in vivo [38–40].

It was interesting that no synergistic effects were observed when the cells were simultaneously treated with lovastatin and strawberry dried methanolic extract.

3.4. Effects of Strawberry Extract on Lipid Profile

The effects of the strawberry extract in lipid metabolism in HepG2 cells were confirmed by determining total cholesterol, LDL-cholesterol, and triglycerides content after treatment for 24 h. As shown in Figure 7A, strawberry dried methanolic extract significantly ($p < 0.05$) improved the lipid profile in a dose dependent manner.

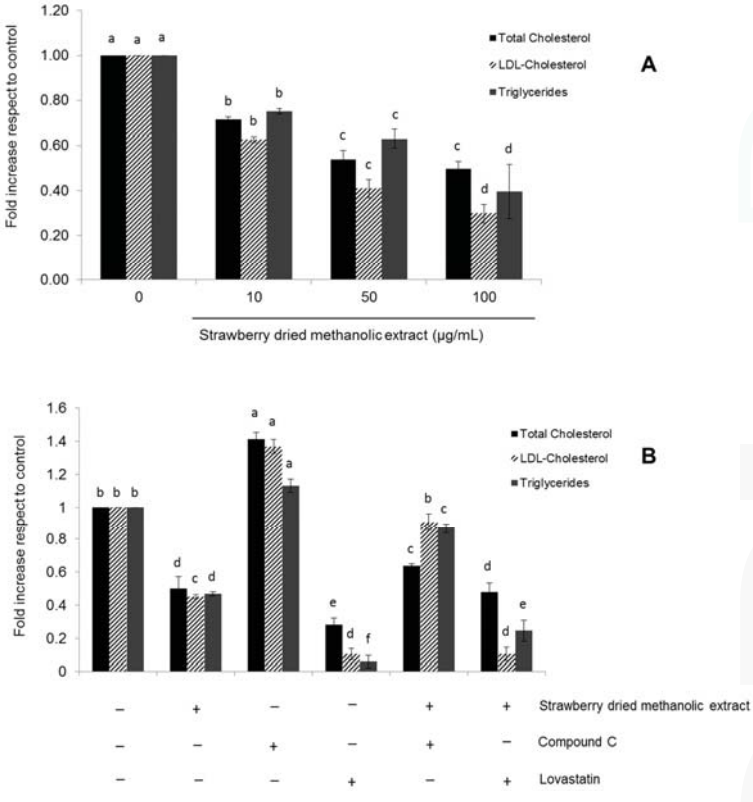

Figure 7. Effects of strawberry dried methanolic extract on lipid profile (total cholesterol and LDL-cholesterol and triglycerides) in HepG2 cells. (**A**) Cells were treated with the indicated concentration of the extract for 24 h. (**B**) Cells were treated with 100 μg/mL of the extract in the presence of 10 μM Compound C (negative control) or 10 μM Lovastatin (positive control) for 24 h. Values are expressed as mean ± SD ($n = 3$) of three independent experiments. Different superscript letters between different assayed conditions for each marker (total cholesterol, LDL-cholesterol, or triglycerides) indicate statistical significance ($p < 0.05$).

Total cholesterol, LDL-cholesterol, and triglycerides levels were lower (up to 0.50-, 0.30-, and 0.40-fold) compared to control when cells were treated with the higher concentration of the extract (100 μg/mL).

The same determinations were performed in the presence of compound C or lovastatin (Figure 7B). In cells treated simultaneously with compound C and strawberry dried methanolic extract, the total cholesterol, LDL-cholesterol, and triglycerides levels were, respectively, 1.27, 2.01, and 1.86 times higher compared to cells treated exclusively with the strawberry extract (100 μg/mL). The highest lipids content was observed in cells treated exclusively with the AMPK inhibitor, while the best results were observed after treatment with lovastatin.

Also, the total lipid accumulation determined by O red oil staining was significantly higher ($p < 0.05$) in cells treated with the inhibitor of AMPK activation and almost similar in control cells compared to the cells treated simultaneously with compound C and strawberry extract (Figure 8).

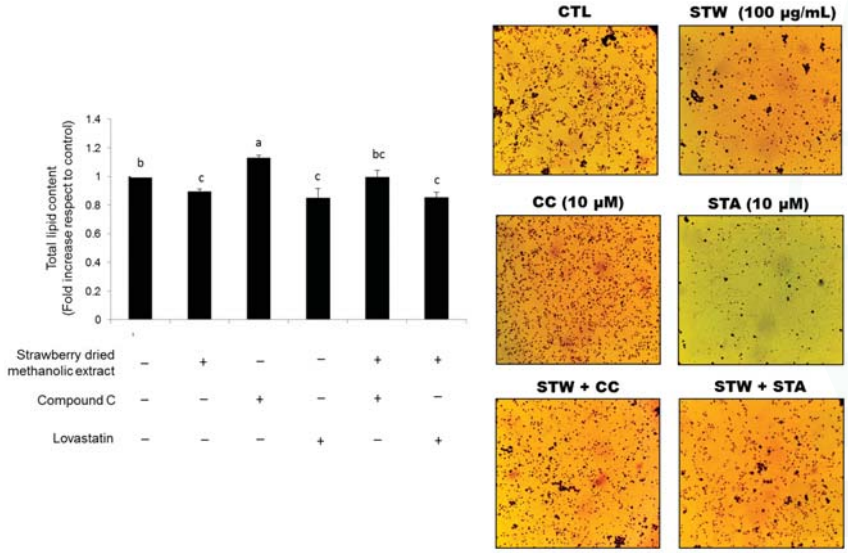

Figure 8. Effects of strawberry dried methanolic extract (100 μg/mL) on total lipid accumulation in HepG2 cells in the presence of 10 μM Compound C (negative control) or 10 μM Lovastatin (positive control). Cells were treated for 24 h. Stained intercellular oil droplets were eluted with isopropanol and quantified by spectrophotometrical analysis at 510 nm. Values are expressed as mean ± SD of three independent experiments ($n = 3$). Columns with different superscript letters are significantly different ($p < 0.05$). CTL: untreated cells; STW: cells treated with strawberry dried methanolic extract; CC: compound C; STA: lovastatin.

4. Discussion

Beneficial effects of strawberry consumption comprise a wide range of biological activities, from antioxidant capacity to anti-inflammatory, anti-hypertensive, and anti-proliferative actions [11,12,19,41–43]. Epidemiological and clinical studies indicate that acute consumption of strawberry improves postprandial glycemic response, circulating inflammatory markers, and increases plasma antioxidant capacity. Likewise, a sustained strawberry consumption ameliorates plasma lipid profile and decreases chronic inflammation, mainly in subjects with high risk for metabolic syndrome. These beneficial effects have been frequently attributed to the antioxidant capacity of strawberry bioactive compounds. However, it has been recently suggested that strawberry's biological properties are also related to the modulation of several molecular pathways implicated in cell proliferation,

survival, and metabolism [43]. In this report, we showed for the first time that the effects of strawberry extract in lipid metabolism are related to the AMPK pathway.

AMPK complex has a direct impact on glucose and lipid metabolism improving glucose uptake and inhibiting fat accumulation through the modulation of several downstream-signaling components like the ACC [9,10]. Thus, pharmacological activation of AMPK in the liver would be expected to improve lipid profile and to decrease the incidence of dyslipidemia related diseases.

Our data illustrate that strawberry dried methanolic extract led not only to higher AMPK phosphorylation but also to a higher expression of LKB1 and Sirt1 as well. LKB1 was the first upstream kinase of AMPK phosphorylation to be described, while Sirt1 is a histone/protein deacetylase that cross-regulates AMPK [36]. Evidence indicates that both Sirt1 and AMPK mutually affect lipid metabolism, but their relationship in the signaling cascade appears to be uncertain [44,45].

The AMPK activation through LKB1 stimulation in HepG2 cells has been previously reported for other natural compounds but not for strawberries. For example, Kim et al. [46] reported that thymoquinone relieves the inflammatory response and hepatic fibrosis through the activation of the LKB1/AMPK signaling pathway, and honokiol, a bioactive compound obtained from the stem bark of *Magnolia officinalis*, protects against liver injury caused by hypoxia/reoxygenation and hepatotoxicants via an LKB1-dependent pathway [47].

Induction of Sirt1 is also related to the expression of PGC-1α that turned out to be stimulated by strawberry extract treatment in a dose-dependent manner. Sirt1 can directly interact and deacetylate PGC-1α, which is closely related with enhanced PGC-1α transcriptional activation. Sirt1-mediated regulation of PGC-1α activity may play a major role in the metabolic adaptations to energy metabolism in different tissues [48]. In liver, Sirt1 regulates gluconeogenic activity by modulating cAMP responsive element binding protein regulated transcription coactivator 2 and PGC-1α, which is also an important mediator of AMPK-induced gene expression. In that sense, AMPK activation increases PGC-1α expression at the same time as it requires PGC-1α activity to regulate the expression of several key players in glucose and mitochondrial metabolism [49–51]. Therefore, the relation between AMPK and PGC-1α connects the sensing of the cellular energetic status and the stimulation of transcriptional programs that control energy expenditure [51].

Furthermore, in the present study, strawberry extract led to a higher phosphorylation of the AMPK substrate ACC. Phosphorylation of ACC leads to its inactivation and consequently to the acute interruption of fatty acid synthesis by blocking the conversion of acetyl CoA to malonyl CoA. In addition, the ACC inhibition could also increase β-oxidation by promoting the activity of carnitine palmitoyltransferase (CPT1), which is essential for the entry of long-chain fatty acids into mitochondria.

Strawberry extract also inhibited HMGCR and stimulated r-LDL, which is subjected to sensitive feedback control that regulates intracellular and extracellular cholesterol levels. When cholesterol levels rise within the cell, r-LDL production decrease contemporarily with the HMGCR diminution, leading to a reduction of cholesterol input from both plasma and endogenous synthesis. On the contrary, in cholesterol depleted cells the production of r-LDL and HMGCR are increased. The mechanism for this dual regulation is controlled by the sterol regulatory element-binding protein (SREBP). In cholesterol depleted cells, SREBP activates HMGCR, r-LDL, and all the other enzymes implicated in cholesterol biosynthesis, at a transcriptional level. When LDL-derived cholesterol enters the cells, it blocks the proteolytic release of the active fragment of SREBP from membranes, leading to a failure in the transcription of the target genes, which in turn decreases cells cholesterol biosynthesis and prevents cholesterol overload [52].

SREBP-mediated regulation of LDL receptors is essential for the action of statins, a class of plasma cholesterol lowering drugs which have been found to reduce CVDs and mortality in individuals at high risk. In the liver, statins are capable of inhibiting HMGCR and subsequently reducing the cholesterol production. This cholesterol diminution activates SREBP-mediated regulation resulting in an increased number of r-LDL on cell membranes and an increased amount of HMGCR. Nevertheless, cholesterol biosynthesis is not stimulated due to the inhibitory effect of statin on the enzyme. The newly produced

r-LDL translocate LDL from the blood into the cell, where its transformation releases cholesterol that becomes available for metabolic purposes. The overall effect is that the amount of cholesterol in the liver remains at a normal level while the level of LDL-cholesterol in the blood is maintained low [52]. Similar effects to those described for statins could explain the effects reported for strawberries in the present work concerning cell cholesterol levels. In fact, our results showed that both strawberry extract and lovastatin presented similar effects on lipid profile, cell lipid accumulation, and on the expression of the proteins related to the AMPK pathway. Interestingly, no synergistic effects on the expression levels of such proteins were observed when cells were treated with strawberry extract and lovastatin simultaneously. We hypothesized that strawberry extract may interfere with the cellular uptake of the drug and/or its metabolism. For example, it is well known that some Cytochrome P450 3A4 inducers may reduce the efficacy of lovastatin. On the contrary, the positive effects of the strawberry extract were remarkably inhibited in the presence of the AMPK-pharmacological inhibitor compound C, demonstrating that activation of the AMPK pathway is needed, at least in part, for the strawberry effects on cell lipid metabolism.

Finally, strawberry extract also caused a diminution on the spare and the maximal respiratory capacity. The spare, or reserve respiratory capacity, describes the amount of extra ATP that can be produced by oxidative phosphorylation in case of a rapid increase in energy demand. The energy requirement of different tissues fluctuates constantly and the ATP metabolism is correspondingly regulated to avoid futile energy expenditure and to provide their specific needs. Concomitantly, the mitochondrial respiration rate augments when more ATP is synthetized by mitochondria, underlying the link between cellular ATP demand and oxidative phosphorylation regulation [53]. Therefore, a decrease in the spare respiratory capacity and consequently a disturbance in the cellular energy state, as described after the strawberry extract treatment in the present study, could lead to AMPK activation. However further analyses should be performed to confirm that the AMP/ATP ratio certainly increases.

Usually, reduced mitochondrial function has been linked to the pathogenesis of numerous diseases and their complications. However, some authors [53] have recently suggest that overstimulation of mitochondria is a probable risk factor for insulin resistance, while moderate mitochondrial dysfunction may actually be protective under certain conditions, suggesting the mitochondrial modulation as a prospective therapy for metabolic diseases. In fact, it has been demonstrated that several mitochondrial modulators ameliorate insulin sensitivity and metabolic complications [54–56]. For example, it has been reported that metformin—which is widely used for the treatment of type 2 diabetes—directly inhibits complex I of the electron transport chain (ETC) and thus reduces mitochondrial respiration [53,57–59]. Therefore, it can be hypothesized that strawberry extract activates AMPK not only via LKB1 but also through alterations on the electron transport chain functionality, subsequently affecting cell energy state. Similar results have been reported for berberine [60] and licochalcone A [61].

Activation of AMPK by strawberry methanolic extract could also be related to its antioxidant capacity, since the AMPK pathway is implicated in the endogenous antioxidant response of the organism through the activation of the nuclear related factor 2 and consequently of some antioxidant responsive elements [62–64].

5. Conclusions

In summary, our results provide new insights into the molecular mechanism of the hypocholesterolemic effects of strawberry extract. Strawberry treatment activated the energy sensing molecule AMPK, which in turn inhibited the proteins involved in fatty acids and cholesterol synthesis. These findings support the further employment of strawberry fruits as functional foods and a potential hypolipidemic agent.

Acknowledgments: The authors wish to thank Monica Glebocki for extensively editing the manuscript. The research work was carried out thanks to the GoodBerry, from the European Union's Horizon 2020 research and innovation programme under grant agreement No. 679303.

Author Contributions: Tamara Yuliett Forbes-Hernández performed the cell cultures experiments and wrote the paper; Mario D. Cordero, Maurizio Battino, and Tamara Yuliett Forbes-Hernández conceived and designed the experiments; Luca Mazzoni performed the HPLC determinations while Sadia Afrin and Massimiliano Gasparrini made the spectrophotometric determinations; Mario Cordero, Francesca Giampieri, Sadia Afrin, Massimiliano Gasparrini, Bruno Mezzetti, José L. Quiles and Maurizio Battino made essential contributions to the data analysis and manuscript revision. Bruno Mezzetti provided strawberry fruits and contributed reagents/materials/analysis tools together with Maurizio Battino.All the authors approved the final version of the text.

Conflicts of Interest: The authors declare no conflicts of interest.

References

1. Goldberg, I.J. Clinical review 124: Diabetic dyslipidemia: Causes and consequences. *J. Clin. Endocrinol. Metab.* **2001**, *86*, 965–971. [CrossRef] [PubMed]
2. Jellinger, P.S.; Mace, M.D.; Smith, D.A.; Mehta, A.E.; Ganda, O.; Handelsman, Y.; Rodbard, H.W.; Shepherd, M.D.; Seibel, J.A. American association of clinical endocrinologists' guidelines for management of dyslipidemia and prevention of atherosclerosis. *Endocr. Pract.* **2012**, *18* (Suppl. 1), 1–78. [CrossRef] [PubMed]
3. Houston, M.C. New concepts in cardiovascular disease. *J. Restor. Med.* **2013**, *2*, 30–44. [CrossRef]
4. Wagner, K.H.; Brath, H. A global view on the development of non-communicable diseases. *Prev. Med.* **2012**, *54*, 38–41. [CrossRef] [PubMed]
5. World Health Organization. *Global Status Report on Non-Communicable Diseases 2014*; WHO Press: Geneva, Switzerland, 2015.
6. Wanner, C.; Quaschning, T. Dyslipidemia and renal disease: Pathogenesis and clinical consequences. *Curr. Opin. Nephrol. Hypertens.* **2001**, *10*, 195–201. [CrossRef] [PubMed]
7. Zhang, B.B.; Zhou, G.; Li, C. AMPK: An Emerging Drug Target for Diabetes and the Metabolic Syndrome. *Cell Metab.* **2009**, *9*, 407–416. [CrossRef] [PubMed]
8. Hardie, D.G. AMPK: A target for drugs and natural products with effects on both diabetes and cancer. *Diabetes* **2013**, *62*, 2164–2172. [CrossRef] [PubMed]
9. Hwang, J.T.; Kwon, D.Y.; Yoon, S.H. AMP-activated protein kinase: A potential target for the diseases prevention by natural occurring polyphenols. *New Biotechnol.* **2009**, *26*, 17–22. [CrossRef] [PubMed]
10. Gasparrini, M.; Giampieri, F.; Alvarez Suarez, J.M.; Mazzoni, L.; Forbes-Hernandez, T.Y.; Quiles, J.L.; Bullon, P.; Battino, M. AMPK as a New Attractive Therapeutic Target for Disease Prevention: The Role of Dietary Compounds. *Curr. Drug Targets* **2016**, *17*, 865–889. [CrossRef] [PubMed]
11. Mazzoni, L.; Perez-Lopez, P.; Giampieri, F.; Alvarez-Suarez, J.M.; Gasparrini, M.; Forbes-Hernandez, T.Y.; Quiles, J.L.; Mezzetti, B.; Battino, M. The genetic aspects of berries: From field to Health. *J. Sci. Food Agric.* **2015**, *96*, 365–371. [CrossRef] [PubMed]
12. Giampieri, F.; Forbes-Hernandez, T.Y.; Gasparrini, M.; Alvarez-Suarez, J.M.; Afrin, S.; Bompadre, S.; Quiles, J.L.; Mezzetti, B.; Battino, M. Strawberry as a health promoter: An evidence based review. *Food Funct.* **2015**, *6*, 1386–1398. [CrossRef] [PubMed]
13. Basu, A.; Xu, F.D.; Wilkinson, M.; Simmons, B.; Wu, M.; Betts, N.M.; Du, M.; Lyons, T.J. Strawberries decrease atherosclerotic markers in subjects with metabolic syndrome. *Nutr. Res.* **2010**, *30*, 462–469. [CrossRef] [PubMed]
14. Torronen, R.; Sarkkinen, E.; Niskanen, E.; Tapola, N.; Kilpi, K.; Niskanen, L. Postprandial glucose, insulin and glucagon-like peptide 1 responses to sucrose ingested with berries in healthy subjects. *Br. J. Nutr.* **2012**, *107*, 1445–1451. [CrossRef] [PubMed]
15. Chaudhuri, S.; Banerjee, A.; Basu, K.; Sengupta, B.; Sengupta, P.K. Interaction of flavonoids with red blood cell membrane lipids and proteins: Antioxidant and antihemolytic effects. *Int. J. Biol. Macromol.* **2007**, *41*, 42–48. [CrossRef] [PubMed]
16. Tulipani, S.; Alvarez-Suarez, J.M.; Busco, F.; Bompadre, S.; Quiles, J.L.; Mezzetti, B.; Battino, M. Strawberry consumption improves plasma antioxidant status and erythrocyte resistance to oxidative haemolysis in humans. *Food Chem.* **2011**, *128*, 180–186. [CrossRef] [PubMed]
17. Parelman, M.A.; Storms, D.H.; Kirschke, C.P.; Huang, L.; Zunino, S.J. Dietary strawberry powder reduces blood glucose concentrations in obese and lean C57BL/6 mice, and selectively lowers plasma C-reactive protein in lean mice. *Br. J. Nutr.* **2012**, *108*, 1789–1799. [CrossRef] [PubMed]

18. Edirisinghe, I.; Banaszewski, K.; Cappozzo, J.; Sandhya, K.; Ellis, C.L.; Tadapaneni, R.; Kappagoda, C.T.; Burton-Freeman, B.M. Strawberry anthocyanin and its association with postprandial inflammation and insulin. *Br. J. Nutr.* **2011**, *106*, 913–922. [CrossRef] [PubMed]
19. Afrin, S.; Gasparrini, M.; Forbes-Hernandez, T.Y.; Reboredo-Rodriguez, P.; Mezzetti, B.; Varela-López, A.; Giampieri, F.; Battino, B. Promising Health Benefits of the Strawberry: A Focus on Clinical Studies. *J. Agric. Food Chem.* **2016**, *64*, 4435–4449. [CrossRef] [PubMed]
20. Alvarez-Suarez, J.M.; Giampieri, F.; Tulipani, S.; Casoli, T.; Di Stefano, G.; González-Paramás, A.M.; Santos-Buelga, C.; Busco, F.; Quiles, J.L.; Cordero, M.D.; et al. One-month strawberry-rich anthocyanin supplementation ameliorates cardiovascular risk, oxidative stress markers and platelet activation in humans. *J. Nutr. Biochem.* **2014**, *25*, 289–294. [CrossRef] [PubMed]
21. Slinkard, K.; Singleton, V.L. Total Phenol analysis: Automation and comparison with manual methods. *Am. J. Enol. Vitic.* **1977**, *28*, 49–55.
22. Jia, Z.; Tang, M.; Wu, J. The determination of flavonoid contents in mulberry and their scavenging effects on superoxides radicals. *Food Chem.* **1998**, *64*, 555–559. [CrossRef]
23. Dewanto, V.; Wu, X.; Adom, K.K.; Liu, R.H. Thermal processing enhances the nutritional values of tomatoes by increasing the total antioxidant activity. *J. Agric. Food Chem.* **2002**, *50*, 3010–3014. [CrossRef] [PubMed]
24. Helsper, J.P.; de Vos, C.H.; Maas, F.M.; Jonker, H.H.; van den Broeck, H.C.; Jordi, W.; Pot, C.S.; Keizer, L.C.; Schapendonk, A.H. Response of selected antioxidants and pigments in tissues of Rosa hybrida and Fuchsia hybrida to supplemental UV-A exposure. *Physiol. Plant.* **2003**, *117*, 171–187. [CrossRef]
25. Terefe, N.S.; Kleintschek, T.; Gamage, T.; Fanning, K.J.; Netzel, G.; Versteeg, C.; Netzel, M. Comparative effects of thermal and high pressure processing on phenolic phytochemicals in different strawberry cultivars. *Innov. Food Sci. Emerg. Technol.* **2013**, *19*, 57–65. [CrossRef]
26. Deighton, N.; Brennan, R.; Finn, C.; Davies, H.V. Antioxidant properties of domesticated and wild Rubus species. *J. Sci. Food Agric.* **2000**, *80*, 1307–1313. [CrossRef]
27. Kumaran, A.; Karunakaran, R.J. Activity-guided isolation and identification of free radical scavenging components from an aqueous extract of Coleus aromaticus. *Food Chem.* **2007**, *100*, 356–361. [CrossRef]
28. Re, R.; Pellegrini, N.; Proteggente, A.; Pannala, A.; Yang, M.; Rice-Evans, C.A. Antioxidant activity applying an improved ABTS radical cation decolorization assay. *Free Radic. Biol. Med.* **1999**, *26*, 1231–1237. [CrossRef]
29. Moongkarndi, P.; Srivattana, A.; Bunyapraphatsara, N.; Puthong, S.; Laohathai, K. Cytotoxicity assay of hispidulin and quercetin using colorimetric technique. *Mahidol Univ. J. Pharm. Sci.* **1991**, *18*, 25–31.
30. Studzinski, G.P. (Ed.) *Cell Growth and Apoptosis a Practical Approach*; Oxford University Press: Oxford, UK, 1995; ISBN 9780199635696.
31. Liu, J.F.; Ma, Y.; Wang, Y.; Du, Z.Y.; Shen, J.K.; Peng, H.L. Reduction of lipid accumulation in HepG2 Cells by luteolin is associated with activation of AMPK and Mitigation of oxidative stress. *Phytother. Res.* **2010**, *25*, 588–596. [CrossRef] [PubMed]
32. Capocasa, F.; Scalzo, J.; Mezzetti, B.; Battino, M. Combining quality and antioxidant attributes in the strawberry: The role of genotype. *Food Chem.* **2008**, *111*, 872–878. [CrossRef]
33. Tulipani, S.; Mezzetti, B.; Capocasa, F.; Bompadre, S.; Beekwilder, J.; de Vos, C.H.; Capanoglu, E.; Bovy, A.; Battino, M. Antioxidants, phenolic compounds, and nutritional quality of different strawberry genotypes. *J. Agric. Food Chem.* **2008**, *56*, 696–704. [CrossRef] [PubMed]
34. Diamanti, J.; Mezzetti, B.; Giampieri, F.; Alvarez-Suarez, J.M.; Quiles, J.L.; Gonzalez-Alonso, A.; Ramirez-Tortosa, M.C.; Granados-Principal, S.; Gonzalez Paramas, A.M.; Santos-Buelga, C.; et al. Doxorubicin-Induced Oxidative Stress in Rats Is Efficiently Counteracted by Dietary Anthocyanin Differently Enriched Strawberry (*Fragaria* × *ananassa* Duch.). *J. Agric. Food Chem.* **2014**, *62*, 3935–3943. [CrossRef] [PubMed]
35. Schimmack, G.; De Fronzo, R.; Musi, N. AMP-activated protein kinase: Role in metabolism and therapeutic implications. *Diabetes. Obes. Metab.* **2006**, *8*, 591–602. [CrossRef] [PubMed]
36. Jiang, S.; Wang, W.; Miner, J.; Fromm, M. Cross regulation of Sirtuin 1, AMPK and PPARγ in conjugated linoleic acid treated adipocytes. *PLoS ONE* **2012**, *7*, e48874. [CrossRef] [PubMed]
37. Ma, L.; Niknejad, I.; Gorn-Hondermann, I.; Dayekh, K.; Dimitroulakos, J. Lovastatin Induces Multiple Stress Pathways Including LKB1/AMPK Activation That Regulate Its Cytotoxic Effects in Squamous Cell Carcinoma Cells. *PLoS ONE* **2012**, *7*, e46055. [CrossRef] [PubMed]

38. Sun, W.; Lee, T.S.; Zhu, M.; Gu, C.; Wang, Y.; Zhu, Y.; Shyy, J.Y. Statins Activate AMP-Activated Protein Kinase In Vitro and In Vivo. *Circulation* **2006**, *114*, 2655–2662. [CrossRef] [PubMed]
39. Sun, W.; Wang, L.; Shyy, J.Y.; Sun, W. Atorvastatin Activates CaMKK-beta as an Upstream Kinase of AMPK in Endothelium. *Circulation* **2008**, *118*, S_404.
40. Choi, H.C.; Song, P.; Xie, Z.; Wu, Y.; Xu, J.; Zhang, M.; Dong, Y.; Wangs, L.K.; Zou, M.H. Reactive Nitrogen Species Is Required for the Activation of the AMP-activated Protein Kinase by Statin In Vivo. *J. Biol. Chem.* **2008**, *283*, 20186–20197. [CrossRef] [PubMed]
41. Hakkinen, S.H.; Torronen, A.R. Content of flavonols and selected phenolic acids in strawberries and Vaccinium species: Influence of cultivar, cultivation site and technique. *Food Res. Int.* **2000**, *33*, 517–524. [CrossRef]
42. Hannun, S.M. Potential impact of strawberries on human health: A review of the science. *Crit. Rev. Food Sci. Nutr.* **2004**, *44*, 1–17. [CrossRef] [PubMed]
43. Forbes-Hernandez, T.Y.; Gasparrini, M.; Afrin, S.; Bompadre, S.; Mezzetti, B.; Quiles, J.L.; Giampieri, F.; Battino, M. The Healthy Effects of Strawberry Polyphenols: Which Strategy behind Antioxidant Capacity? *Crit. Rev. Food Sci. Nutr.* **2016**, *56* (Suppl. 1), S46–S59. [CrossRef] [PubMed]
44. Schug, T.T.; Li, X. Sirtuin 1 in lipid metabolism and obesity. *Ann. Med.* **2011**, *43*, 198–211. [CrossRef] [PubMed]
45. Wang, Y.; Liang, Y.; Vanhoutte, P.M. SIRT1 and AMPK in regulating mammalian senescence: A critical review and a working model. *FEBS Lett.* **2011**, *585*, 986–994. [CrossRef] [PubMed]
46. Kim, Y.W.; Lee, S.M.; Shin, S.M.; Hwang, S.J.; Brooks, J.S.; Kang, H.E.; Lee, M.G.; Kim, S.C.; Kim, S.G. Efficacy of sauchinone as a novel AMPK-activating lignan for preventing iron-induced oxidative stress and liver injury. *Free Radic. Biol. Med.* **2009**, *47*, 1082–1092. [CrossRef] [PubMed]
47. Seo, M.S.; Kim, J.H.; Kim, H.J.; Chang, K.C.; Park, S.W. Honokiol activates the LKB1–AMPK signaling pathway and attenuates the lipid accumulation in hepatocytes. *Toxicol. Appl. Pharmacol.* **2015**, *284*, 113–124. [CrossRef] [PubMed]
48. Lagouge, M.; Argmann, C.; Gerhart-Hines, Z.; Meziane, H.; Lerin, C.; Daussin, F.; Messadeq, N.; Milne, J.; Lambert, P.; Elliott, P.; et al. Resveratrol Improves Mitochondrial Function and Protects against Metabolic Disease by Activating SIRT1 and PGC-1α. *Cell* **2006**, *127*, 1109–1122. [CrossRef] [PubMed]
49. Jager, S.; Handschin, C.; St Pierre, J.; Spiegelman, B.M. AMP-activated protein kinase (AMPK) action in skeletal muscle via direct phosphorylation of PGC-1alpha. *Proc. Natl. Acad. Sci. USA* **2007**, *104*, 12017–12022. [CrossRef] [PubMed]
50. Cantó, C.; Gerhart-Hines, Z.; Feige, J.N.; Lagouge, M.; Noriega, L.; Milne, J.C.; Elliott, P.G.; Puigserver, P.; Auwerx, J. AMPK regulates energy expenditure by modulating NAD + metabolism and SIRT1 activity. *Nature* **2009**, *458*, 1056–1060. [CrossRef] [PubMed]
51. Cantó, C.; Auwerx, J. PGC-1alpha, SIRT1 and AMPK, an energy sensing network that controls energy expenditure. *Curr. Opin. Lipidol.* **2009**, *20*, 98–105. [CrossRef] [PubMed]
52. Goldstein, J.L.; Brown, M.S. The LDL Receptor. *Arterioscler. Thromb. Vasc. Biol.* **2009**, *29*, 431–438. [CrossRef] [PubMed]
53. Desler, C.; Hansen, T.L.; Frederiksen, J.B.; Marcker, M.L.; Singh, K.K.; Rasmussen, L.J. Is There a Link between Mitochondrial Reserve Respiratory Capacity and Aging? *J. Aging. Res.* **2012**, *2012*, 192503:1–192503:9. [CrossRef] [PubMed]
54. Jenkins, Y.; Sun, T.Q.; Markovtsov, V.; Foretz, M.; Li, W.; Nguyen, H.; Li, Y.; Pan, A.; Uy, G.; Gross, L.; et al. AMPK activation through mitochondrial regulation results in increaed substrated oxidation and improved metabolic parmeter in models of diabetes. *PLoS ONE* **2013**, *8*, e81870. [CrossRef] [PubMed]
55. Zhang, Y.; Ye, J. Mitochondrial inhibitor as a new class of insulin sensitizer. *Acta Pharm. Sin. B* **2012**, *2*, 341–349. [CrossRef] [PubMed]
56. Colca, J.R.; Vander Lugt, J.T.; Adams, W.J.; Shashlo, A.; McDonald, W.G. Clinical proof-of-concept study with MSDC-0160, a prototype mTOT-modulating insulin sensitizer. *Clin. Pharmacol. Ther.* **2013**, *93*, 352–359. [CrossRef] [PubMed]
57. Owen, M.R.; Doran, E.; Halestrap, A.P. Evidence that metformin exerts its anti-diabetic effects through inhibition of complex 1 of the mitochondrial respiratory chain. *Biochem. J.* **2000**, *348*, 607–614. [CrossRef] [PubMed]

58. Hawley, S.A.; Gadalla, A.E.; Olsen, G.S.; Hardie, D.G. The Antidiabetic Drug Metformin Activates the AMP-Activated Protein Kinase Cascade via an Adenine Nucleotide-Independent Mechanism. *Diabetes* **2002**, *51*, 2420–2425. [CrossRef] [PubMed]
59. Brunmair, B.; Staniek, K.; Gras, F.; Scharf, N.; Althaym, A.; Clara, R.; Roden, M.; Gnaiger, E.; Nohl, H.; Waldhausl, W.; et al. Thiazolidinediones, like metformin, inhibit respiratory complex I. A common mechanism contributing to their antidiabetic action? *Diabetes* **2004**, *53*, 1052–1059. [CrossRef] [PubMed]
60. Turner, N.; Li, J.Y.; Gosby, A.; To, S.; Cheng, Z.; Miyoshi, H.; Taketo, M.M.; Cooney, G.J.; Kraegen, E.W.; James, D.E.; et al. Berberine and its more biologically available derivative, Dihydroberberine, inhibit mitochondrial respiratory complex I. A mechanism for the action of berberine to activate AMP-Activated protein kinase and improve insulin action. *Diabetes* **2008**, *57*, 1414–1418. [CrossRef] [PubMed]
61. Quan, H.Y.; Kim, D.Y.; Chung, S.H. Caffeine attenuates lipid accumulation via activation of AMP-activated protein kinase signaling pathway in HepG2 cells. *BMB Rep.* **2013**, *46*, 207–212. [CrossRef] [PubMed]
62. Jeong, H.W.; Hsu, K.C.; Lee, J.W.; Ham, M.; Huh, J.Y.; Shin, H.J.; Kim, W.S.; Kim, J.B. Berberine suppresses proinflammatory responses through AMPK activation in macrophages. *Am. J. Physiol. Endocrinol. Metab.* **2009**, *296*, E955–E964. [CrossRef] [PubMed]
63. Hwang, Y.P.; Choi, J.H.; Yun, H.J.; Han, E.H.; Kim, H.G.; Kim, J.Y.; Park, B.H.; Khanal, T.; Choi, J.M.; Chung, Y.C.; et al. Anthocyanins from purple sweet potato attenuate dimethylnitrosamine-induced liver injury in rats by inducing Nrf2-mediated antioxidant enzymes and reducing COX-2 and iNOS expression. *Food Chem. Toxicol.* **2011**, *49*, 93–99. [CrossRef] [PubMed]
64. Yun, H.; Park, S.; Kim, M.J.; Yang, W.K.; UkIm, D.; Yang, K.R.; Hong, J.; Choe, W.; Kang, I.; Kim, S.S.; et al. AMP-activated protein kinase mediates the antioxidant effects of resveratrol through regulation of the transcription factor FoxO1. *FEBS J.* **2014**, *281*, 4421–4438. [CrossRef] [PubMed]

nutrients

MDPI

Review

Antioxidants Mediate Both Iron Homeostasis and Oxidative Stress

Mustapha Umar Imam [1,†], Shenshen Zhang [1,†], Jifei Ma [1], Hao Wang [1,2] and Fudi Wang [1,2,*]

1 Department of Nutrition, Precision Nutrition Innovation Center, School of Public Health, Zhengzhou University, Zhengzhou 450001, China; mustyimam@gmail.com (M.U.I.); zsslb2005@163.com (S.Z.); mjf15188351024@163.com (J.M.); 0016896@zju.edu.cn (H.W.)

2 Department of Nutrition, Nutrition Discovery Innovation Center, School of Public Health, Collaborative Innovation Center for Diagnosis and Treatment of Infectious Diseases, School of Medicine, Zhejiang University, Hangzhou 310058, China

* Correspondence: fudiwang.lab@gmail.com or fwang@zju.edu.cn

† These authors contributed equally to this work.

Received: 4 June 2017; Accepted: 22 June 2017; Published: 28 June 2017

Abstract: Oxidative stress is a common denominator in the pathogenesis of many chronic diseases. Therefore, antioxidants are often used to protect cells and tissues and reverse oxidative damage. It is well known that iron metabolism underlies the dynamic interplay between oxidative stress and antioxidants in many pathophysiological processes. Both iron deficiency and iron overload can affect redox state, and these conditions can be restored to physiological conditions using iron supplementation and iron chelation, respectively. Similarly, the addition of antioxidants to these treatment regimens has been suggested as a viable therapeutic approach for attenuating tissue damage induced by oxidative stress. Notably, many bioactive plant-derived compounds have been shown to regulate both iron metabolism and redox state, possibly through interactive mechanisms. This review summarizes our current understanding of these mechanisms and discusses compelling preclinical evidence that bioactive plant-derived compounds can be both safe and effective for managing both iron deficiency and iron overload conditions.

Keywords: iron homeostasis; iron overload; antioxidants; plant extracts; oxidative stress; ferroptosis

1. Overview of Iron Metabolism

1.1. Dietary Requirements for Iron and Iron Absorption, Transport, Storage, and Utilization

The processes underlying iron metabolism are as complex as they are perplexing. Given that iron is an essential trace element required for maintaining physiological homeostasis, it is both surprising and somewhat alarming that iron overload and iron deficiency are common conditions in the general population. Upon closer inspection, however, the underlying causes of these conditions are not difficult to understand. Dietary iron is the principal source of iron in the body; in addition, iron can be recycled from body stores, particularly the liver and senescent red blood cells (RBCs). Interestingly, despite its important role in maintaining plasma iron levels, iron excretion is less regulated than iron absorption [1,2]. Moreover, excessive iron levels can lead to toxicity and cell death via free radical formation and lipid peroxidation; therefore, iron homeostasis is tightly regulated [3–5]. Blood loss through menstruation and other routes, sloughed intestinal mucosal cells, and sweating help the body maintain normal plasma iron levels. Iron is used primarily as a component of heme in RBCs for oxygen transport, while relatively smaller amounts are present in muscle as heme myoglobin and in the liver as ferritin [1,2]. In most other tissues in the body, iron serves as a component of protein cofactors in the form of iron-sulfur (Fe-S) clusters and heme, which are involved in the electron transport chain to

produce ATP [6,7]. In this process, ferrous iron (Fe^{2+}) and ferric iron (Fe^{3+}) serve as an electron donor and acceptor, respectively. In effect, iron plays an essential role in maintaining adequate stores of ATP during oxidative phosphorylation in the mitochondrial inner membrane [8].

In industrialized countries, the majority of the population has adequate iron stores, usually totaling approximately 4–5 g (representing approximately 38 and 50 mg iron/kg body weight for adult women and men, respectively). Approximately 2.5 g of this iron is present in hemoglobin for oxygen transport, and another 2 g is stored in the form of ferritin, largely in the bone marrow, liver, and spleen [9]. In the bone marrow, iron is used for hemoglobin formation. In the liver, iron serves as the principal iron reserve, and the reticuloendothelial cells in the spleen recycle iron form senescent RBCs. Finally, a relatively small amount of iron (approximately 400 mg) is present in cellular proteins such as myoglobin and cytochromes, and even less (approximately 3–4 mg) is in the circulation bound to transferrin [1,2].

Before iron can fulfill its crucial biological roles, it must be absorbed across intestinal enterocytes into the blood. Dietary iron from animal sources (blood and heme-containing proteins) is absorbed better than iron from plant sources (mitochondrial heme) [10,11]. Both heme-bound iron and ionic iron are absorbed at the apical surface of duodenal enterocytes (Figure 1). Ionic iron (Fe^{3+}) is not bioavailable and must be reduced to Fe^{2+} by the duodenal enzyme cytochrome b reductase (Dcytb), a membrane-bound ferroxidase expressed at the duodenal brush border; Fe^{2+} can then be absorbed via divalent metal transporter 1 (DMT1), an enzyme that also transports other metals, including manganese, zinc, copper, and cobalt [1,2].

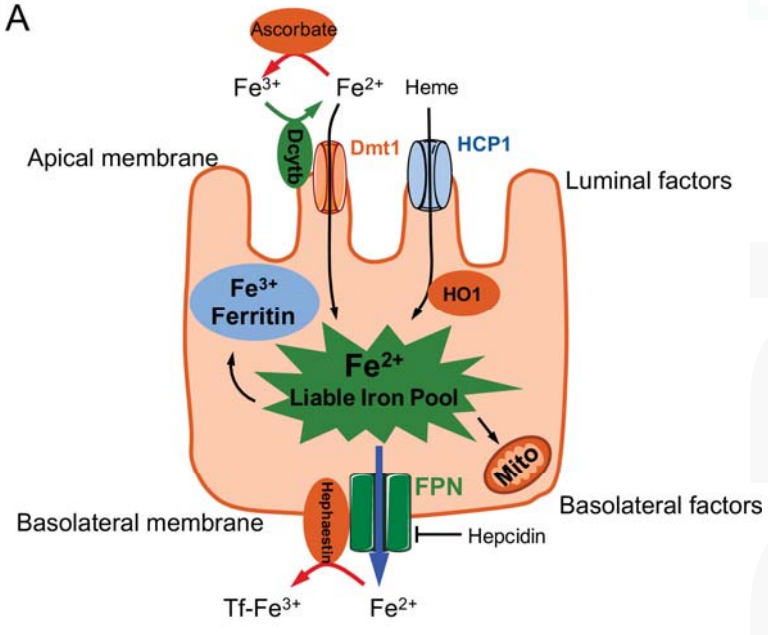

Figure 1. *Cont.*

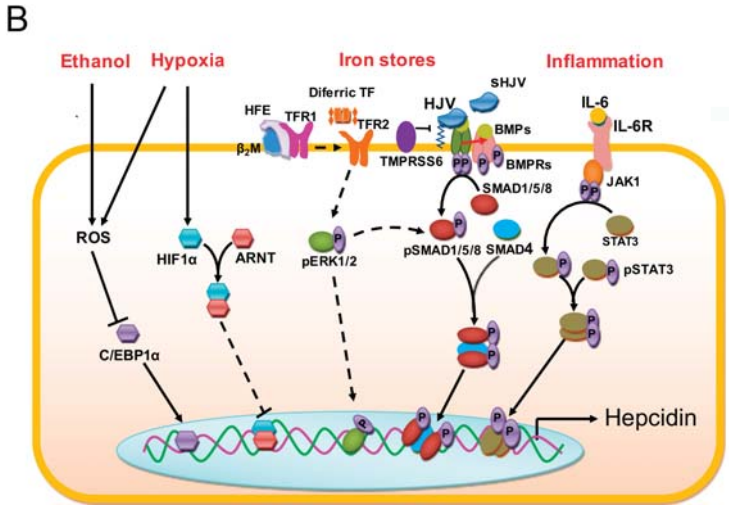

Figure 1. Schematic overview of iron transport into and across duodenal enterocytes (**A**) and the pathways involved in regulating transcription of the hepcidin antimicrobial peptide (*HAMP*) gene to drive hepcidin expression (**B**). Iron is imported as heme via the heme carrier protein 1 (HCP1) or as Fe^{2+} (after reduction by duodenal cytochrome b (Dcytb) via the divalent metal transporter (DMT) 1. The labile iron pool within the enterocyte can be stored as ferritin, utilized for mitochondrial oxidative phosphorylation, or exported via ferroportin (Fpn). Hephaestin or ceruloplasmin then converts Fe^{2+} to Fe^{3+}, which then binds to transferrin (Tf). Hepcidin negatively regulates Fpn. ARNT: aryl hydrocarbon nuclear receptor translocator; β_2m:beta-2-microglobulin; BMP: bone morphogenetic protein; BMPR: BMP receptor; C/EBP1α: CCAAT/enhancer-binding protein 1α; ERK1/2: extracellular signal-regulated kinase; HIF1α: hypoxia-inducible factor 1α; HFE: human hemochromatosis protein; HJV: hemojuvelin; HO1: heme oxygenase 1; IL-6: interleukin 6; IL-6R: IL-6 receptor; JAK: Janus kinase; Mito: mitochondria; p: phosphate group; ROS: reactive oxygen species; sHJV: serum HJV; SMAD1/5/8: mothers against decapentaplegic homolog1/5/8; SMAD4: mothers against decapentaplegic homolog 4; STAT3: signal transducer and activator of transcription 3; TfR: Tf receptor; TMPRSS6: transmembrane protease, serine 6.

Once inside the enterocyte, iron is then stored in the cell as ferritin, where it is often lost as sloughed duodenal cells or is released into the body via ferroportin, after which it is oxidized back to Fe^{3+} in the basolateral side of the duodenum by the ferroxidase hephaestin (HEPH). Iron is then transported in the plasma as a complex with transferrin (Tf), which is detected by transferrin receptor 1 (TfR1) or 2 (TfR2) and endocytosed as the Fe-Tf complex [12] (Figure 2); TfR1-mediated endocytosis is approximately 30 times more efficient than TfR2-mediated endocytosis [13]. Alternatively, iron can be taken up via the Glyceraldehyde 3-phosphate dehydrogenase (GAPDH) pathway [14,15]. A decrease in pH within the resulting endosomes (due to of the active transport of protons into the endosomes) causes the complex to dissociate, after which transferrin and the TfR are recycled back to the cell membrane; transferrin is then available to bind iron again, and the TfR is again available for sensing new Fe-Tf complexes. The labile iron within the endosomes is transported to the cytoplasm via DMT1 after conversion to Fe^{2+} by a member of the Six transmembrane epithelial antigen of the prostate (STEAP) family of reductase proteins [16]. Conversely, extracellular iron that has been converted to Fe^{2+} state by a STEAP family reductase can enter the cell directly via an alternate surface transporter such as Zrt-Irt-like protein 14 (ZIP14, also known as SLC39A14), thereby contributing to the labile pool of iron [17]. This labile pool of iron is then stored as ferritin-bound or hemosiderin-bound iron [2,18].

Under steady-state conditions, the serum ferritin level is directly proportional to total body iron stores; therefore, serum ferritin is commonly used as a convenient laboratory test for estimating iron stores [19]. However, other pathological conditions unrelated to iron status—for example, chronic inflammation—have been shown to increase serum ferritin [16].

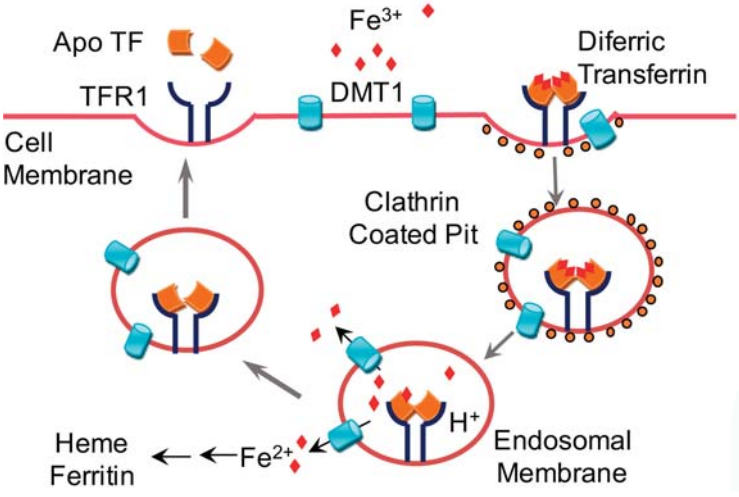

Figure 2. Schematic depiction of iron trafficking across the plasma membrane into the cell. Transferrin-(Tf-) bound iron is transported into the cell via transferrin receptor 1 (TfR1) or 2 (TfR2). The complex is endocytosed, and a decrease in luminal pH causes the release of iron from the complex. Tf that is completely free of iron (apotransferrin, ApoTf) and the TfR are then recycled back to the cell membrane. The labile pool of iron within the cell exits the endosome via divalent metal transporter 1 (DMT1) and is stored as ferritin. ApoTf: apotransferrin.

Ferritin is a globular protein complex consisting of 24 protein subunits; the primary function of ferritin is to store iron intracellularly in order to prevent iron toxicity [20,21]. Moreover, ferritin releases iron via a controlled mechanism in response to appropriate stimuli [22], thereby protecting against both iron deficiency and iron overload [1,2]. Extremely high amounts of ferritin—particularly within reticuloendothelial cells—are converted to hemosiderin, which is more difficult to access. When iron is released from cells such as neurons, erythrocytes, and macrophages, it is exported via ferroportin in the same manner described above, although ceruloplasmin and hephaestin can also oxidize iron to form Fe^{3+} in other cells outside of the duodenum [16,23].

1.2. Regulation of Iron Stores

In humans, iron homeostasis is coordinated by a series of complex, tightly regulated processes. At the systemic level, iron levels are regulated through the controlled absorption of dietary iron via enterocytes, duodenal cell sloughing, sweating, blood loss, and recycling of systemic iron [1,2]. At the cellular level, however, regulatory molecules such as ferroportin and hepcidin contribute to iron regulation [23,24]. Hepcidin (encoded by the hepcidin antimicrobial peptide, or *HAMP*, gene) is a peptide hormone produced primarily in the liver, and its expression is tightly controlled at the transcriptional level by iron levels, erythroferrone (erythropoiesis), inflammation, and hypoxia via the bone morphogenetic protein/suppressor of mothers against decapentaplegic (BMP/SMAD) and Janus kinase/signal transducer and activator of transcription (JAK/STAT) signaling pathways (Figure 1) [16,25]. Hepcidin can post-translationally repress ferroportin, whereas erythroferrone produced by erythroblasts inhibits ferroportin synthesis, leading to increased availability of iron

for use in hemoglobin [26]. Hepcidin represses ferroportin by causing its internalization, thereby decreasing iron export. In addition, hepcidin can downregulate both TfR1 and DMT1, also reducing iron export [27]. Conversely, in response to iron deficiency, the body can synthesize additional Dcytb, DMT1, and ferroportin [16,24,25].

In addition to transcriptional regulation, iron homeostasis can also be regulated at the translational level, representing an even more significant form of regulation. Accordingly, the iron-responsive element (IRE)-binding proteins IRP1 and IRP2 bind to IREs in the untranslated regions (UTRs) of mRNAs of genes that encode a variety of iron-regulating molecules, including ferroportin, DMT1, and TfR1 [28] (Figure 3). For example, in an iron-deficient state, IRP2 binds to IREs in order to maximize cellular iron levels. Specifically, binding of IRP2 to IREs in the 5′-UTR of mRNAs encoding ferritin and ferroportin repress translation, while binding of IRP2 to IREs in the 3′-UTR of mRNAs encoding TfR1 and DMT1 stabilize the mRNA resulting in efficient translation.

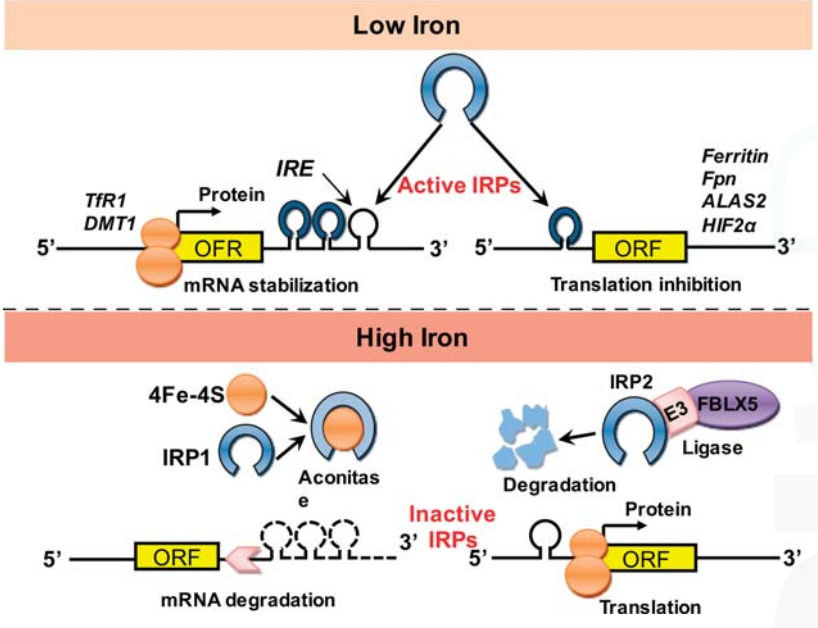

Figure 3. Post-transcriptional control of iron homeostasis. Iron-responsive element-binding proteins (IRP1 and IRP2) bind to the iron-responsive element (IRE) in the untranslated region (UTR) of mRNAs encoding various iron-regulating molecules, thereby regulating their translation. ALAS2: aminolevulinic acid synthase 2; DMT1: divalent metal transporter 1; E3: ubiquitin ligase subunit; FBLX5: F-box and leucine-rich repeat protein 5; Fpn: ferroportin; HIF2α: hypoxia-inducible factor 2α; mRNA: messenger ribonucleic acid; ORF: open reading frame; TfR1: transferrin receptor 1.

2. Iron Toxicity, Oxidative Stress, and Antioxidants

2.1. Iron Toxicity

Iron is a potentially toxic molecule, as it can both donate and accept electrons. Iron can catalyze the formation of free radicals from reactive oxygen species (ROS) via the Fenton reaction, which is the reduction of H_2O_2 by a single electron to produce a hydroxyl radical [3–5]; this ultimately leads to damage to a wide variety of cellular structures. Therefore, the majority of iron is bound to other molecules for storage and/or transport, and only minute amounts of iron are available in the labile pool [16]. Even in this labile pool, however, iron is not completely unbound, as the majority is believed

to form a complex with peptides, carboxylates, and/or phosphates [29–32]. Despite the abundance of complexes to which iron can bind in the body, iron levels in the body can occasionally exceed the pool of available transferrin molecules. For example, iron toxicity is common during iron overload states associated with genetic factors or acquired factors such as repeated blood transfusions.

2.2. Oxidative Stress

Reactive species are formed as the result of normal metabolic processes. However, the human body is equipped with detoxifying mechanisms that regulate the generation of reactive species and can even repair damage caused by reactive species [33,34]. If radical species are not neutralized, they can damage proteins, lipids, nucleic acids, and other cellular components, serving as the underlying basis of many chronic diseases. Furthermore, oxidized cellular components can contribute to oxidative damage of other components and/or cause additional adverse oxidative changes [35]. Labile iron is the most important contributor of this oxidative damage to cellular components [3–5]. Superoxide radical (O_2^-) is the initial reactive species produced during these reactions, serving as the precursor for additional reactive radicals, including H_2O_2 and the hydroxyl radical (OH^-), one of the most potent free radical species that can react with a wide range of cellular constituents [36].

2.2.1. Oxidative Stress and Iron Deficiency Anemia

Iron deficiency can result from a variety of causes, including blood loss, nutritional deficiency due to inadequate intake of iron, and inhibition of iron absorption by certain foods and/or compounds such as calcium, phytates, tannins, and proton pump inhibitors. Diseases that affect the intestinal lining (for example, Crohn's disease) can also affect iron absorption, leading to iron deficiency [37]. Iron deficiency first affects stored iron in the body; depletion of these stores is believed to produce non-specific symptoms such as dizziness, weakness and fatigue. Moreover, iron deficiency can have severe obstetric consequences for both the mother and fetus. In fact, iron deficiency anemia in infants and growing children has been associated with delayed psychomotor development and cognitive deficits due to abnormal neurodevelopment [38,39]. Oxidative stress does not necessarily result from iron deficiency, but it often appears as a co-morbidity, as the conditions that give rise to iron deficiency also promote oxidative stress. For example, during infection and/or inflammation, the body tends to absorb less iron in order to deprive the invading bacteria of the iron that they need to thrive [40]. Moreover, oxidative stress is a common feature in many chronic diseases with long-term iron deficiency; in this case, the negative regulation of ferroportin by hepcidin is believed to be responsible for the iron deficiency [26,27]. Additionally, the hypoxic condition induced by anemia may worsen oxidative stress via pro-oxidant changes, including altered cellular metabolism, increased catecholamine metabolism, and leukocyte activation, thereby leading to increased free radical production and oxidative stress [41]. In managing iron deficiency, iron supplementation can be given in order to build up iron stores for hemoglobin production; however, it is also important to manage any underlying conditions that could negate the benefits of iron supplementation therapy; in this respect, antioxidant therapy can ameliorate anemia-related oxidative damage [42].

2.2.2. Oxidative Stress and Iron Overload

As discussed above, iron is potentially toxic due to the generation of free radicals via the Fenton reaction. Thus, the human body has developed processes to regulate the amount of iron absorbed in accordance with the body's needs in order to prevent the adverse effects of iron overload. Despite these processes, however, iron overload can still occur. For example, ingesting large amounts of supplemental iron can damage the intestinal lining, causing increased absorption of iron into the body. Repeated blood transfusions and some genetic mutations are also associated with iron overload. For example, hereditary hemochromatosis (HH), which is caused by mutations in the genes that encode hemojuvelin (*HJV*, or *HFE2*) and hepcidin (*HAMP*) are associated with excessive iron absorption and iron-related toxicity, particularly in juvenile HH [43]. In general, the detrimental effects of iron overload begin to

manifest when the complexes to which iron can bind become saturated. In particular, excess iron in the blood begins to deposit in tissues when available transferrin proteins are saturated. Large amounts of labile iron in the circulation can eventually damage the liver, heart, and other metabolically active organs [44]. Therefore, iron chelation is important for managing patients with iron overload, and returning iron levels to normal levels can help ameliorate the associated side effects.

2.2.3. Iron Overload and Cell Death

Iron and ROS are important mediators of cell death in many organisms and in many pathological processes that involve altered iron homeostasis. Studies have shown that iron overload is associated with increased apoptosis, necrosis, and autophagy, albeit via different mechanisms [45–48]. Mitochondrial ROS are an important trigger of iron-induced apoptosis, which results in the peroxidation of cardiolipins and the release of cytochrome c to activate caspase-3/7 [48]. On the other hand, heme induces necrosis in macrophages via two synergistic mechanisms: (1) heme induces Toll-like receptor 4/Myeloid differentiation primary response gene 88- (TLR4/Myd88-) dependent tumor necrosis factor (TNF) expression; and (2) TNF activates the receptor-interacting protein (RIP) kinases 1 and 3, thereby initiating necrosis [47]. Finally, *Hamp* knockout mice fed a high-iron diet develop lysosomal iron overload in hepatocytes, leading to autophagy [46].

In addition to these "classic" mechanisms of cell death, an iron-dependent, oxidative form of cell death called ferroptosis has recently been identified. First described in Ras-mutated cancer cells treated with oncogenic Ras-selective lethal small molecules, ferroptosis is morphologically, biochemically, and genetically distinct from other forms of cell death, including apoptosis and necrosis [49,50]. The features of ferroptosis include an increased intracellular pool of liable iron, increased lipid peroxidation at the plasma membrane, and depletion of reduced nicotinamide adenine dinucleotide phosphate (NADPH); ferroptosis can be prevented by iron chelation or by the use of a lipophilic antioxidant, but not by inhibitors of other forms of cell death [49–52]. Furthermore, ferroptosis occurs in mouse models of hemochromatosis following iron overload [53]. Moreover, genetic and pharmacological inhibition of iron-related genes (e.g., *HO-1*, *TfR1*, and *FTH1*, which encode heme oxygenase-1, transferrin receptor 1, and ferritin, respectively) can inhibit ferroptosis in tumor cells [54–56]. Thus, although the relationship between ferroptosis and systemic iron metabolism is complex, it represents a promising target for managing iron-induced oxidative cell death, particularly in iron overload conditions [53].

2.3. Antioxidants

The damage induced by oxidized cellular components is associated with the depletion of endogenous cellular antioxidant systems [33,34]. Numerous endogenous antioxidants maintain the cell's redox state and prevent the harmful effects of oxidative stress; these antioxidants include superoxide dismutase (SOD), catalase, glutathione (GSH), thioredoxin (Trx), and ferritin (Figure 4). As discussed above, superoxide (O_2^-) is the first reactive radical produced, and this radical can be neutralized by SOD. There are three distinct SODs [57], each of which performs a specific function in human cells. SOD1 (Cu/Zn-SOD) is present in the cytoplasm, whereas SOD2 (Mn-SOD) is present in the mitochondria; SOD3, on the other hand, is almost exclusively extracellular [36].

When O_2^- is neutralized, H_2O_2 is produced, which can be metabolized into non-toxic products by a catalase ($H_2O_2 + H_2O_2 \rightarrow 2H_2O + O_2$) and glutathione peroxidase (GPx) in conjunction with glutathione ($2GSH + H_2O_2 \rightarrow GS–SG + 2H_2O$). Catalase is present in peroxisomes, whereas the location of the GPx depends on the subtype. For example, GPx1, GPx2, and GPx4 are cytoplasmic, whereas GPx3 is extracellular; GPx4 can also be found in the nucleus and endoplasmic reticulum [36]. Glutathione (GSH) is present in nearly all cells in the body and is present in high levels in organs with high oxygen consumption and energy production (e.g., the brain) [36,58]. In conjunction with its oxidized form (GSSG), GSH plays a major role in controlling cellular redox state. Similarly, the ubiquitous thioredoxin system also plays an important role in maintaining the cell's redox state. Thioredoxins are small proteins with two adjacent cysteine residues that can undergo reversible

oxidation to form a disulfide bond; when oxidized by H_2O_2 in a reaction catalyzed by Trx peroxidase in the presence of NADPH, this results in the generation of reduced Trx. The thioredoxin system protects the cell against oxidative stress—provided that sufficient NADPH is available. Thus, the production of Trx proteins and GSH increases under conditions of oxidative stress [36,59]. Finally, ferritin is considered an endogenous antioxidant, as it performs the important function of sequestering potentially toxic labile iron.

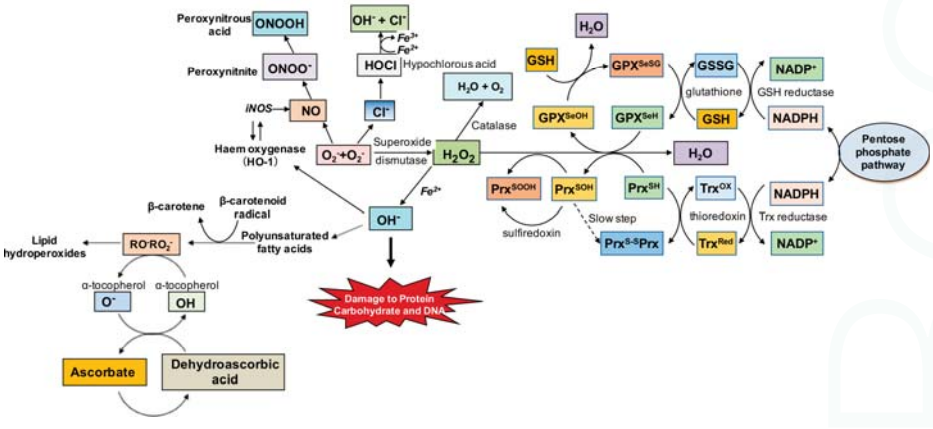

Figure 4. Summary of the oxidative stress cascade, including endogenous antioxidant defenses. Superoxide free radicals (O_2^-) generated during metabolic processes are endogenously neutralized by superoxide dismutase to hydrogen peroxide (H_2O_2), and subsequently to water (H_2O) and oxygen (O_2), although the glutathione (GSH) system can also neutralize H_2O_2 to H_2O. Conversely, when O_2^- is not neutralized, it can form more reactive species in the presence of nitric oxide (NO) and chloride (Cl^-) thereby leading to further oxidative damage. Similarly, H_2O_2 in the presence of Fe^{2+} can produce hydroxyl free radicals (OH^-), which are highly toxic to proteins and DNA, and can even lead to the generation of lipid peroxides that are also prooxidant. DNA: deoxyribonucleic acid; GSSG: glutathione disulfide; NADP: nicotinamide adenine dinucleotide phosphate; NADPH: reduced NADP; RO^-: alkoxyl radical; RO_2^-: peroxyl radical.

Under certain conditions, endogenous antioxidants are unable to neutralize oxidative stress; in this case, exogenous antioxidants can be used to augment the body's antioxidant systems. Thus, in addition to reducing the levels of oxidative stress common in many chronic diseases, antioxidants can also serve as an adjuvant to standard therapies in order to provide a synergistic clinical effect [60,61]. Vitamin A (beta-carotene), vitamin C, vitamin E (alpha-tocopherol), polyphenols, and other bioactive plant-derived compounds are effective exogenous antioxidants. Because several of these antioxidants can also regulate iron metabolism, they are ideal candidates for helping manage oxidative stress, particularly in the case of iron overload and/or iron deficiency (Table 1, Figure 5). Moreover, the addition of antioxidants to their respective therapies has been shown to provide superior effects against oxidative damage in iron overload [62,63] and iron deficiency anemia [42]. At the transcriptional level, antioxidant enzymes are regulated by the transcription factor Nrf2, which binds to the antioxidant response element (ARE) in the target gene's promoter region. Nuclear factor erythroid 2-related factor 2 (Nrf2) is believed to be phosphorylated by protein kinase C (PKC), which causes the transcription factor to translocate to the nucleus, where it activates ARE-containing genes [36,64], ultimately leading to the neutralization of free radicals and the attenuation of oxidative damage.

Table 1. Select antioxidants and their mechanisms of iron regulation.

Antioxidant	Mechanism of Fe Regulation	Reference(s)
Citrus flavonoid-rich extracts of orange and bergamot juice	Chelation of iron in iron-overloaded human lung epithelial cells (A549), induction of catalase enzyme, and attenuation of reactive oxygen species (ROS) and membrane lipid peroxidation.	[65]
Epigallocatechin-3-gallate	Chelation of iron, reduced basolateral iron export in Caco-2 cells, and activation of nuclear factor erythroid 2-related factor 2 (Nrf2), a master transcriptional regulator of antioxidant genes in human mesenchymal stem cells (hMSCs).	[66,67]
Grape seed extract and anthocyanins	Grape seed extract induced chelation of iron and reduced basolateral iron export in Caco-2 cells. Anthocyanins induced attenuation of sodium fluoride-induced oxidative damage to human embryo hepatic cells via decreased iron content and increased antioxidants including glutathione peroxidase (GPx), superoxide dismutase (SOD), and total antioxidant capacity, mediated via decreased hepcidin and increased ferroportin expression.	[66,68]
Curcumin	Decreased iron levels in the bone marrow, spleen and liver, attenuated lipopolysaccharide (LPS)-induced oxidative stress-related inflammation, activated hepatic iron-responsive element-binding protein (IRP) and transferrin receptor 1 (TfR1), and repressed hepatic ferritin and hepcidin synthesis.	[69]
Quercetin	Attenuation of hepatic iron deposition in mice exposed to ethanol or excess iron, induction of bone morphogentic protein 6 (BMP6), intranuclear suppressor of mother of mothers against decapentaplegic homolog 4 (SMAD4), SMAD4 binding to hepcidin antimicrobial peptide (HAMP) promoter and hepcidin expression.	[70]
Black soybean seed coat anthocyanins	Reduced hepatic hepcidin expression, decreased splenic iron and increased serum iron, mediated via reduced SMAD1/5/8 phosphorylation.	[71]
Myrecitin	Reduced hepatic hepcidin expression, reduced hepcidin promoter activity, and reduced SMAD1/5/8 phosphorylation in HepG2 cells. Reduced hepatic hepcidin expression, decreased splenic iron levels, and increased serum iron levels in mice.	[72]
Genistein	Increased hepcidin expression and promoter activity in zebrafish and human hepatocytes in a signal transducer and activator of transcription 3- (STAT3-) dependent and SMAD4-dependent manner.	[73]
Silymarin	Iron chelation.	[74]
Ferulic acid	Attenuates iron-induced oxidative stress by reducing liver injury, apoptotic changes and ROS production; increases hepatic antioxidants and mitochondrial membrane potential; and reverses mitochondrial swelling.	[75]
Resveratrol	Attenuation of iron-induced cardiac iron overload, oxidative stress, altered Ca^{2+} homeostasis and myocardial fibrosis; increased cardiac nuclear and acetylated Forkhead box protein O1 (FOXO1) levels; Decreased sirtuin 1 (SIRT1) and sarco/endoplasmic reticulum Ca^{2+}-ATPase 2a (SERCA2a) levels.	[76]
Chokeberries	Reduced inflammatory markers; increased total antioxidant status and serum iron levels.	[77]
Vitamin A and beta-carotene	Increased expression of TfR and hepcidin; increased intestinal iron absorption; reduced ferroportin expression; reduced inflammatory signaling; increased intracellular ferritin levels; release of intracellular trapped iron.	[78–80]
Vitamin C	Reduction of Fe^{3+} to Fe^{2+}; inhibition of hepcidin expression.	[81]
Tucum-Do-Cerrado (Bactris setosaMart.)	Attenuation of iron-induced increases in serum and tissue iron levels, transferrin (Tf) saturation, and lipid oxidation via increasing expression of hepatic HAMP, ferritin, heme oxygenase 1 (Hmox1), NADPH dehydrogenase quinone 1 (Nqo1), and Nrf2 and BMP6, and intestinal Nrf2; increased antioxidant enzymes including catalase, glutathione reductase, and GPx.	[82]
Baicalein (Scutellaria baicalensis)	Iron chelation; inhibition of iron-mediated Fenton reaction under physiological conditions in vitro.	[83]
Caulis spatholobi	Inhibition of hepcidin, BMP6, and SMAD1/5/8 expression in Huh7 cells; reduced hepatic iron levels; increased serum iron levels in mice.	[84]
Astragalus polysaccharide	Attenuation of ROS and Nrf1 accumulation in human cardiac myocytes (HCMs); increased hepcidin expression via the activation of p38 mitogen-activated protein kinase (MAPK) and release of interleukin 6 (IL-6).	[85,86]
Angelica sinensis polysaccharide (ASP)	Increased chondrocyte cell viability, and increased SOD and catalase levels; reduced malondialdehyde production, apoptosis, and inflammatory cytokines; reduced levels of serum hepcidin, IL-6, ferritin, Tf, TfR1, and TfR2 in H22-bearing mice.	[87,88]
Mexidol	Reversal of oxidative hemolysis and increased serum hepcidin levels in hemochromatosis patients.	[89]

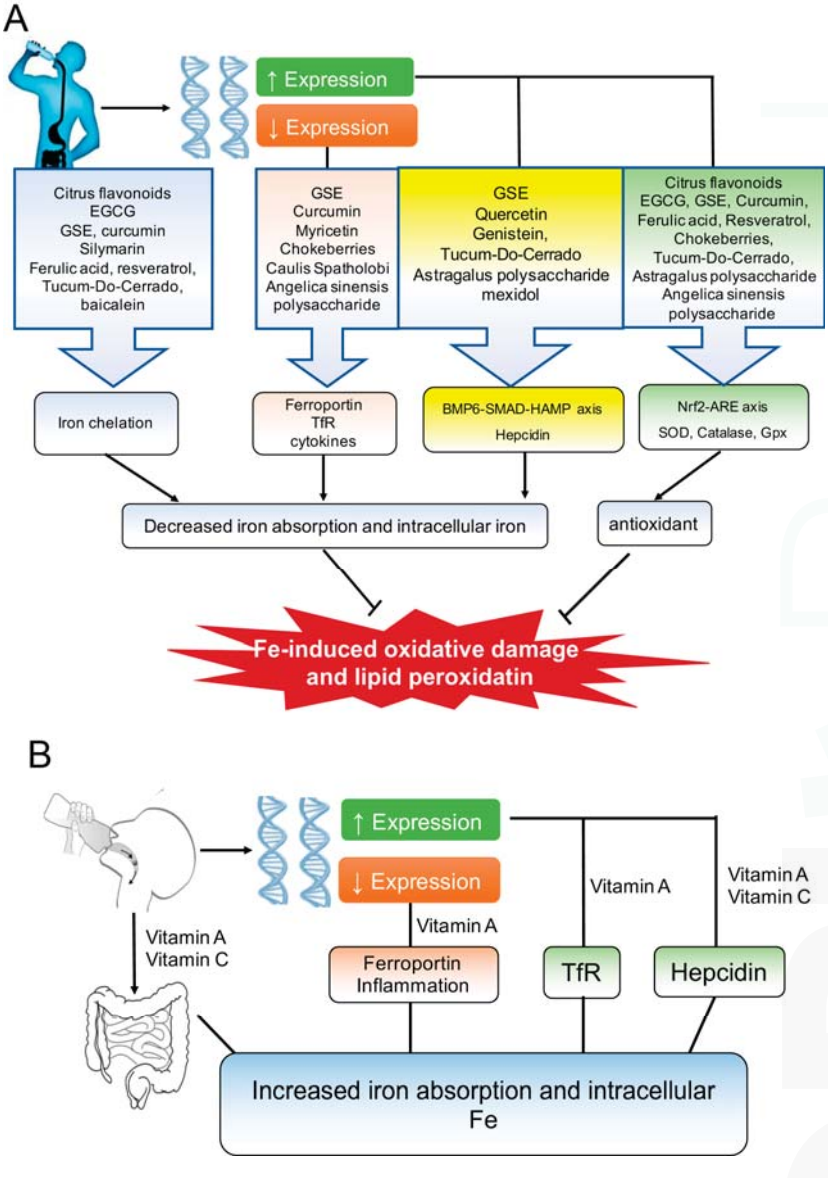

Figure 5. Overview of the mechanisms by which antioxidants regulate iron and oxidative stress. (**A**) A variety of antioxidants regulate iron absorption by chelating iron and/or by modulating the expression of antioxidant and iron metabolism-regulating genes, ultimately reducing oxidative damage due to excess iron during iron overload; (**B**) Vitamins A and C can increase iron absorption and modulate the expression of several proteins (e.g., transferrin receptor (TfR), hepcidin, and ferroportin) and inflammatory signals, providing clinical benefits under iron deficient conditions. BMP6-SMAD-HAMP: bone morphogenetic factor-mothers against decapentaplegic homolog-hepcidin antimicrobial peptide; EGCG: epigallocatechin gallate; GPx: glutathione peroxidase; GSE: grape seed extract; Nrf2-ARE: nuclear factor erythroid 2-related factor 2-antixodant response element; SOD: superoxide dismutase.

3. Bioactive Compounds That Regulate Oxidative Stress and Iron Metabolism

3.1. Polyphenols

Polyphenols are organic chemicals containing several phenol groups, which determine the chemical's properties. Most polyphenols occur naturally as secondary metabolites in plants, where their primary role is to protect the plant from ultraviolet radiation and pathogens [90]. Interestingly, polyphenols can functionally counteract the effects of oxidative stress, making them suitable for therapeutic purposes. Moreover, polyphenols are reported to confer protection against the development of certain types of cancer, cardiovascular disease, diabetes, osteoporosis, and neurodegenerative disease [91]. Four main classes of polyphenols have been identified: flavonoids, phenolic acids, lignans, and stilbenes.

3.1.1. The Flavonoids: Tea Catechins, Black Soy Bean Seed Anthocyanins and Myricetin, Citrus Flavonoids, Grape Seed Extract, Curcumin, Quercetin, Genistein, and Silymarin

Flavonoids are the most common class of polyphenols and are present in a wide variety of plants, imparting many of these plants with their specific colors. Their primarily functions are to protect the plant and to act as chemical messengers, physiological regulators, and cell cycle inhibitors. However, because flavonoids are relatively non-toxic to animal cells, humans and other animals can safely ingest them, thereby benefiting from their positive properties [92]. Examples of flavonoids include quercetin, catechins, curcumin, and kaempferol, which are abundant in fruits, vegetables, legumes, red wine, and green tea.

Table 1 summarizes the flavonoids and other antioxidants that regulate both iron homeostasis and redox state, in some cases via independent mechanisms. A flavonoid-rich extract of orange and bergamot juice has been shown to chelate iron in iron-overloaded A549 cells (a human lung epithelial cell line); in addition, this extract was shown to activate the antioxidant enzyme catalase, leading to a decrease in ROS production and membrane lipid peroxidation [65]. Based on these effects, the authors suggested that this flavonoid-rich extract is a promising candidate for regulating both iron homeostasis and oxidative stress [65]. Similarly, the tea-derived catechin epigallocatechin-3-gallate (EGCG) and grape seed extract (GSE)—both of which have potent antioxidant properties—are good candidates for chelating iron, given their ability to reduce basolateral iron export in Caco-2 cells [66]. Moreover, because EGCG can activate Nrf2—a master transcriptional regulator of antioxidant genes [67]—it may also help restore a balanced redox state in patients with iron overload. GSE is rich in anthocyanins, which are believed to be the bioactive compounds responsible for GSE's ability to modulate iron homeostasis and oxidative stress [68]. Specifically, GSE-derived anthocyanins prevent sodium fluoride-induced oxidative damage in human embryo-derived hepatic cells by decreasing iron content and increasing antioxidants, including GPx, SOD, and total antioxidant capacity, by decreasing hepcidin expression and increasing ferroportin expression [68].

Another potent flavonoid antioxidant, curcumin, can also chelate iron in addition to modulating redox state [93]. Curcumin decreases iron levels in the bone marrow, spleen, and liver, and it can induce signs of iron deficiency anemia in mice by activating hepatic IRP and TfR1, as well as by repressing hepatic ferritin and hepcidin expression. Interestingly, curcumin can also reduce oxidative stress-related inflammation induced by lipopolysaccharides (LPS) [69]. As discussed above, inflammation can activate hepcidin expression, which can reduce iron absorption, ultimately leading to iron deficiency. However, the fact that curcumin can reduce inflammation and hepcidin expression while inducing signs of iron deficiency suggests that this compound has iron chelation properties that are independent of hepcidin.

Recently, Tang et al. [70] reported that quercetin can reduce hepatic iron deposition in mice that were exposed to either ethanol or excess iron. They found that quercetin increased BMP6, intranuclear SMAD4, SMAD4 binding to the *HAMP* promoter, and hepcidin expression, which led to decreased hepatic iron levels and reduced iron-related damage. Conversely, we reported that an anthocyanin-rich

extract of black soybean seed coat extract can decrease hepatic hepcidin expression, resulting in decreased splenic iron and increased serum iron via reduced SMAD1/5/8 phosphorylation [71]. In a follow-up study, we found that myricetin is the principal bioactive compound in black soybean seed coat extract responsible for suppressing hepcidin expression [72]. Although myricetin is structurally similar to quercetin [94], unlike quercetin it inhibits hepcidin expression by modulating the BMP/SMAD signaling pathway in both in vitro and in vivo systems [72]. Specifically, myricetin decreases hepcidin expression by inhibiting the *HAMP* promoter; in addition, myricetin reduces SMAD1/5/8 phosphorylation in HepG2 cells, even in the presence of potent stimulators of hepcidin such as BMP6 and interleukin (IL)-6. In mice, myricetin also suppresses hepatic hepcidin expression, decreases splenic iron levels, and increases serum iron levels [72].

Genistein, another flavonoid that has potent antioxidant and anti-inflammatory properties, reduces ethanol-induced inflammation and oxidative stress in mice [95]. However, similar to quercetin, genistein increases *HAMP* promoter activity in both zebrafish and human hepatocytes via a Stat3- and Smad4-dependent process [73]. This suggests that genistein's ability to induce hepcidin expression may be independent of its inflammation-reducing properties. Silymarin, another flavonoid, is present in milk thistle plant extract and may have iron-chelating properties [74]. Silymarin is actually a mixture of flavonolignans, including silibinin, isosilibinin, silicristin, and silidianin; silibinin has both antioxidant and hepatoprotective properties. Silymarin is a safe, well-tolerated, cost-effective alternative to currently available iron-chelation therapies for treating patients with β-thalassemia [74].

Flavonoids have already been shown to have both anti-inflammatory and antioxidant effects [96]. Recently, Bayele et al. reported that the transcription factor Nrf2 regulates hepcidin expression as part of an antioxidant regulatory network, whereas several flavonoids modulate iron homeostasis by blocking Keap1-mediated transcriptional repression, providing further evidence that Nrf2 modulates the activity of the *HAMP* promoter when activated as part of an antioxidant response [97]. However, the physicochemical properties of flavonoids can influence their pharmacokinetics, which can affect their bioavailability in vivo, thereby determining their ability to exert biological activities relevant to human health [98]. Thus, on one hand, flavonoids such as EGCG and curcumin can chelate iron, prevent the basolateral export of iron across Caco-2 cells, and induce signs of iron deficiency by increasing hepcidin expression and depleting iron stores, thereby providing clinical value during iron overload conditions and eventually restoring redox state; on the other hand, their iron-chelating property can also be detrimental and may even lead to iron deficiency.

3.1.2. Ferulic Acid

Ferulic acid is a phenolic compound present in a wide variety of plants. Ferulic acid can exist in the free form, or it can be bound to polysaccharides, flavonoids, fatty acids, and/or other phytochemicals, where it has antioxidant, anti-inflammatory, and other functional properties. The antioxidant effects of ferulic acid are believed to be mediated via the neutralization of free radicals [99]. Treating iron-overloaded mice with sodium ferulate reduces iron-induced oxidative stress, thereby reducing liver injury and apoptotic changes, increasing hepatic antioxidants, improving mitochondrial membrane potential, reversing mitochondrial swelling, and decreasing the production of ROS [75]. In contrast, unlike many flavonoids, ferulic acid does not affect iron uptake, suggesting that it does not have a direct iron-chelating property and that its effects are mediated by reducing the adverse effects induced by iron overload.

3.1.3. Resveratrol

Consuming moderate amounts of red wine has long been suggested to improve cardiovascular health, and this beneficial effect has been linked to resveratrol present in red wine [100]. The antioxidant effects of resveratrol may prevent adverse changes that lead to cardiovascular disease by modulating vascular cell function, low density lipoprotein (LDL) oxidation, and platelet aggregation, thereby reducing myocardial damage [100]. However, these ideas were recently called into question [101].

For example, resveratrol was recently reported to reduce iron-induced myocardial oxidative stress and myocardial fibrosis, ultimately reducing the risk of cardiomyopathy [76]. These effects appear to be mediated by attenuating iron-induced cardiac iron overload and oxidative stress, altering Ca^{2+} homeostasis, and reducing myocardial fibrosis. At the molecular level, resveratrol reverses iron-induced increases in cardiac nuclear and acetylated forkhead box protein O1 (FOXO1) levels, and it decreases the expression of both sirtuin 1 (SIRT1) and sarco/endoplasmic reticulum Ca^{2+}-ATPase 2a (SERCA2a).

3.1.4. Chokeberries

Chokeberries can be eaten raw or in other food products, including wine, juice, and gummy chews. Chokeberries are rich in polyphenols, including anthocyanins, quercetin, and epicatechin [102,103], and the anti-inflammatory effects of chokeberry extract have been well-documented. For example, in an 8-week trial, athletes who consumed chokeberry juice had lower levels of inflammatory markers, as well as higher levels of total antioxidants and higher serum iron levels [77].

3.2. Vitamin A and Vitamin C

Both vitamin A and vitamin C have well-established antioxidant properties that are mediated via the attenuation of oxidative damage [104]. Vitamin A is a fat-soluble molecule that can interfere with the oxidation of polyunsaturated fatty acids in membrane phospholipids, thereby preventing lipid peroxidation [105]. Vitamin A metabolism also has implications with respect to iron homeostasis; indeed, vitamin A deficiency and iron deficiency are reported to co-occur in some populations [106]. Moreover, the serum levels of retinol (vitamin A1) are positively correlated with iron-related RBC indices, including serum iron, hemoglobin, and transferrin saturation levels [107,108]. In addition, vitamin A has been shown to affect the expression of transferrin receptors [109] and intestinal iron absorption [78]. Specifically, vitamin A modulates the expression of hepatic hepcidin and ferritin in mice, and it modulates ferroportin-1 (Fpn1) expression in Caco-2 cells via a hepcidin-independent mechanism, suggesting that several mechanisms may be involved in the vitamin A-induced regulation of iron homeostasis, including changes in hepcidin-independent iron absorption and hepcidin-dependent iron mobilization [79]. In another study, beta-carotene—the precursor of vitamin A—was found to modulate iron absorption across Caco-2 cells even in the presence of the potent pro-inflammatory ligand IL-1β [80]. Specifically, beta-carotene: (1) attenuated iron-induced IL-8 release; (2) increased intracellular ferritin levels; and (3) reduced ferroportin levels. These changes resulted in normalized ferritin and ferroportin levels, reduced inflammatory signaling, and the release of intracellular trapped iron [80].

Vitamin C is a water-soluble molecule that can regenerate the radical form of alpha-tocopherol, thereby playing a major role in regulating redox state. In addition, vitamin C can influence intestinal iron absorption by affecting the reduction of Fe^{3+} to Fe^{2+} [1,2]. As discussed above, Fe^{2+} is imported into duodenal enterocytes via DMT1, and it exits the enterocytes through the basolateral membrane via Fpn1, which can be negatively regulated by hepcidin. Thereafter, transferrin transports the iron as Fe^{3+} to the bone marrow (for hematopoiesis), liver, and other organs (for storage). Aside from its role in iron reduction prior to intestinal absorption, vitamin C also regulates iron homeostasis by inhibiting hepcidin expression (for example, in HepG2 cells), potentially helping attenuate iron deficiency [81].

3.3. Other Plant Extracts

The desire to maximize the benefits of plant phytochemicals while avoiding the adverse effects often associated with synthetic pharmaceutical agents is fueling the search for new therapies based on plant-derived compounds [110]. In this regard, several plant extracts have been studied for their putative effects on iron homeostasis and oxidative stress, and plant phytochemicals present in the extracts of tucum-do-cerrado, astragalus, *Angelica sinensis*, *Caulis Spatholobi*, *Scutellaria baicalensis*, and others have shown promise.

Cerrado plant species are edible antioxidant-rich plants commonly found in Brazil. Among these species, the extract of the fruit of the tucum-do-cerrado plant (a fruit with a purple skin, whitish pulp, and a large seed) was shown to attenuate iron-induced increases in serum and tissue iron levels, transferrin saturation, and lipid oxidation (by increasing the expression of intestinal Nrf2 and hepatic hepcidin, ferritin, heme oxygenase 1 [Hmox1], NADPH dehydrogenase quinone 1 [Nqo1], Nrf2, and Bmp6), ultimately increasing the activity of antioxidant enzymes, including catalase, glutathione reductase, and GPx [82]. The authors found a general correlation between reduced oxidative damage and iron availability. Similarly, baicalein and baicalin are two major bioactive compounds with antioxidative properties found in the Chinese herb *Scutellaria baicalensis*. For example, in an in vitro assay, baicalein scavenged iron and inhibited the iron-mediated Fenton reaction under physiological conditions, thereby preventing oxidative damage [83]. Another Chinese herb, *Caulis Spatholobi*, is traditionally used to manage anemia. In Huh7 cells, this compound inhibits the expression of hepcidin, BMP6, and SMAD1/5/8; in mice, it reduces hepatic iron levels and increases serum iron levels by inhibiting hepcidin expression [84].

The polysaccharides contained in astragalus and *Angelica sinensis* have also been shown to modulate iron homeostasis and oxidative stress. These traditional Chinese herbs have been used for thousands of years for their anti-cancer and immunomodulatory properties. Recently, astragalus-derived polysaccharides were reported to suppress the accumulation of ROS and Nrf1 in human cardiac myocytes [85] and to increase hepcidin expression by activating the p38 mitogen-activated protein kinase (MAPK) signaling pathway and the release of IL-6 [86]. *Angelica sinensis* can protect chondrocytes from H_2O_2-induced oxidative stress by inducing changes in cell viability, SOD activity, catalase activity, malondialdehyde production, apoptosis, and inflammatory cytokines [87]. In addition, in mice transplanted with hepatoma-22 cells, *Angelica sinensis* reduces the serum levels of hepcidin, IL-6, ferritin, transferrin, TfR1, and TfR2 [88]. Emoxypine (trade name Mexidol), an antioxidant structurally similar to pyridoxine, was synthesized in Russia but is currently not used outside of Russia. Emoxypine is reported to have antioxidant and anti-inflammatory properties, and it has been shown to both reverse oxidative hemolysis and increase serum hepcidin levels in patients with hemochromatosis [89].

4. Conclusions

Many diseases and conditions related to a perturbation in iron homeostasis are associated with inflammation and oxidative stress, and a growing list of bioactive antioxidants and other plant-derived phytochemicals can simultaneously regulate iron homeostasis, oxidative stress, and inflammation (Figure 5). Some of these compounds are clinically beneficial with respect to lowering serum and/or tissue iron levels, whereas others may be beneficial to patients with iron deficiency. For example, with the exception of myricetin, most flavonoids reduce inflammation, chelate iron, and reduce iron absorption (and the resulting oxidative damage) predominantly via hepcidin-independent pathways; therefore, these compounds are beneficial in iron overload conditions. On the other hand, certain vitamins reduce inflammation and increase iron uptake and iron mobilization via both hepcidin-dependent and hepcidin-independent mechanisms, thereby providing clinical benefits in iron deficiency. Nevertheless, the majority of data collected to date are derived from in vitro and animal experiments. Therefore, further studies in humans are needed in order to evaluate the efficacy of these phytochemicals and their feasibility as a natural substitute for pharmaceutical agents, many of which are associated with adverse side effects.

Acknowledgments: The authors were supported by grants from the National Natural Science Foundation of China (31530034, 31330036, and 31225013 to FW). The authors thank the members of the Min and Wang laboratories for their contributions to this review.

Author Contributions: M.U.I., S.Z. and F.W. conceived of the idea of the manuscript. M.U.I., S.Z., J.M., H.W. and F.W. wrote the manuscript.

Conflicts of Interest: The authors declare no conflicts of interest.

References

1. Kohgo, Y.; Ikuta, K.; Ohtake, T.; Torimoto, Y.; Kato, J. Body iron metabolism and pathophysiology of iron overload. *Int. J. Hematol.* **2008**, *88*, 7–15. [CrossRef] [PubMed]
2. Beard, J.L.; Dawson, H.; Piñero, D.J. Iron metabolism: A comprehensive review. *Nutr. Rev.* **1998**, *54*, 295–317. [CrossRef]
3. Papanikolaou, G.; Pantopoulos, K. Iron metabolism and toxicity. *Toxicol. Appl. Pharm.* **2005**, *202*, 199–211. [CrossRef] [PubMed]
4. Bresgen, N.; Eckl, P.M. Oxidative stress and the homeodynamics of iron metabolism. *Biomolecules* **2015**, *5*, 808–847. [CrossRef] [PubMed]
5. Emerit, J.; Beaumont, C.; Trivin, F. Iron metabolism, free radicals, and oxidative injury. *Biomed. Pharmacother.* **2001**, *55*, 333–339. [CrossRef]
6. Rouault, T.A.; Tong, W.H. Iron–sulfur cluster biogenesis and human disease. *Trends Genet.* **2008**, *24*, 398–407. [CrossRef] [PubMed]
7. Beinert, H.; Holm, R.H.; Münck, E. Iron-sulfur clusters: Nature's modular, multipurpose structures. *Science* **1997**, *277*, 653–659. [CrossRef] [PubMed]
8. Oexle, H.; Gnaiger, E.; Weiss, G. Iron-dependent changes in cellular energy metabolism: Influence on citric acid cycle and oxidative phosphorylation. *Biochim. Biophys. Acta* **1999**, *1413*, 99–107. [CrossRef]
9. Gropper, S.S.; Smith, J.L. *Advanced Nutrition and Human Metabolism*, 6th ed.; Wadsworth: Belmont, CA, USA, 2013; p. 481.
10. Hambræus, L. Animal-and plant-food-based diets and iron status: Benefits and costs. *Proc. Nutr. Soc.* **1999**, *58*, 235–242. [CrossRef] [PubMed]
11. Martınez-Navarrete, N.; Camacho, M.M.; Martınez-Lahuerta, J.; Martınez-Monzó, J.; Fito, P. Iron deficiency and iron fortified foods—A review. *Food Res. Int.* **2002**, *35*, 225–231. [CrossRef]
12. Wang, J.; Pantopoulos, K. Regulation of cellular iron metabolism. *Biochem. J.* **2011**, *434*, 365–381. [CrossRef] [PubMed]
13. West, A.P.; Bennett, M.J.; Sellers, V.M.; Andrews, N.C.; Enns, C.A.; Bjorkman, P.J. Comparison of the interactions of transferrin receptor and transferrin receptor 2 with transferrin and the hereditary hemochromatosis protein HFE. *J. Biol. Chem.* **2000**, *275*, 38135–38138. [CrossRef] [PubMed]
14. Kumar, S.; Sheokand, N.; Mhadeshwar, M.A.; Raje, C.I.; Raje, M. Characterization of glyceraldehyde-3-phosphate dehydrogenase as a novel transferrin receptor. *Int. J. Biochem. Cell Biol.* **2012**, *44*, 189–199. [CrossRef] [PubMed]
15. Sheokand, N.; Kumar, S.; Malhotra, H.; Tillu, V.; Raje, C.I.; Raje, M. Secreted glyceraldehye-3-phosphate dehydrogenase is a multifunctional autocrine transferrin receptor for cellular iron acquisition. *Biochim. Biophys. Acta* **2013**, *1830*, 3816–3827. [CrossRef] [PubMed]
16. Hentze, M.W.; Muckenthaler, M.U.; Galy, B.; Camaschella, C. Two to tango: Regulation of Mammalian iron metabolism. *Cell* **2010**, *142*, 24–38. [CrossRef] [PubMed]
17. Lane, D.J.R.; Merlot, A.M.; Huang, M.L.-H.; Bae, D.-H.; Jansson, P.J.; Sahni, S.; Kalinowski, D.S.; Richardson, D.R. Cellular iron uptake, trafficking and metabolism: Key molecules and mechanisms and their roles in disease. *Biochim. Biophys. Acta* **2015**, *1853*, 1130–1144. [CrossRef] [PubMed]
18. Ganz, T. Cellular iron: Ferroportin is the only way out. *Cell Metab.* **2005**, *1*, 155–157. [CrossRef] [PubMed]
19. Cook, J.D.; Lipschitz, D.A.; Miles, L.E.; Finch, C.A. Serum ferritin as a measure of iron stores in normal subjects. *Am. J. Clin. Nutr.* **1974**, *27*, 681–687. [PubMed]
20. Theil, E.C.; Elizabeth, C. Ferritin protein nanocages—The story. *Nanotechnol. Percept.* **2012**, *8*, 7–16. [CrossRef] [PubMed]
21. Theil, E.C. Ferritin: structure, gene regulation, and cellular function in animals, plants, and microorganisms. *Annu. Rev. Biochem.* **1987**, *56*, 289–315. [CrossRef] [PubMed]
22. Zhang, Y.; Mikhael, M.; Xu, D.; Li, Y.; Soe-Lin, S.; Ning, B.; Ponka, P. Lysosomal proteolysis is the primary degradation pathway for cytosolic ferritin and cytosolic ferritin degradation is necessary for iron exit. *Antioxid. Redox Signal.* **2010**, *13*, 999–1009. [CrossRef] [PubMed]
23. Roeser, H.P.; Lee, G.R.; Nacht, S.; Cartwright, G.E. The role of ceruloplasmin in iron metabolism. *J. Clin. Investig.* **1970**, *49*, 2408. [CrossRef] [PubMed]

24. Nemeth, E.; Ganz, T. Regulation of iron metabolism by hepcidin. *Annu. Rev. Nutr.* **2006**, *26*, 323–342. [CrossRef] [PubMed]
25. Ganz, T.; Nemeth, E. Hepcidin and iron homeostasis. *Biochim. Biophys. Acta* **2012**, *1823*, 1434–1443. [CrossRef] [PubMed]
26. Schmidt, P.J. Regulation of iron metabolism by hepcidin under conditions of inflammation. *J. Biol. Chem.* **2015**, *290*, 18975–18983. [CrossRef] [PubMed]
27. Ganz, T. Hepcidin, a key regulator of iron metabolism and mediator of anemia of inflammation. *Blood* **2003**, *102*, 783–788. [CrossRef] [PubMed]
28. Pantopoulos, K. Iron metabolism and the IRE/IRP regulatory system: An update. *Ann. N. Y. Acad. Sci.* **2004**, *1012*, 1–13. [CrossRef] [PubMed]
29. Laurent, S.; Saei, A.A.; Behzadi, S.; Panahifar, A.; Mahmoudi, M. Superparamagnetic iron oxide nanoparticles for delivery of therapeutic agents: Opportunities and challenges. *Expert Opin. Drug Deliv.* **2014**, *11*, 1449–1470. [CrossRef] [PubMed]
30. Cabantchik, Z.I.; Kakhlon, O.; Epsztejn, S.; Zanninelli, G.; Breuer, W. Intracellular and extracellular labile iron pools. *Adv. Exp. Med. Biol.* **2002**, *509*, 55–75. [PubMed]
31. Finney, L.A.; O'Halloran, T.V. Transition metal speciation in the cell: Insights from the chemistry of metal ion receptors. *Science* **2003**, *300*, 931–936. [CrossRef] [PubMed]
32. Philpott, C.C.; Ryu, M.S. Special delivery: Distributing iron in the cytosol of mammalian cells. *Front. Pharmacol.* **2014**, *5*, 173. [CrossRef] [PubMed]
33. Halliwell, B. Free radicals, antioxidants, and human disease curiosity, cause, or consequence? *Lancet* **1994**, *344*, 721–724. [CrossRef]
34. Valko, M.; Leibfritz, D.; Moncol, J.; Cronin, M.T.D.; Mazur, M.; Telser, J. Free radicals and antioxidants in normal physiological functions and human disease. *Int. J. Biochem. Cell Biol.* **2007**, *39*, 44–84. [CrossRef] [PubMed]
35. Mylonas, C.; Kouretas, D. Lipid peroxidation and tissue damage. *In Vivo (Athens, Greece)* **1999**, *13*, 295–309.
36. Crichton, R.R.; Wilmet, S.; Legssyer, R.; Ward, R.J. Molecular and cellular mechanisms of iron homeostasis and toxicity in mammalian cells. *J. Inorg. Biochem.* **2002**, *91*, 9–18. [CrossRef]
37. Camaschella, C. Iron deficiency anemia. *N. Engl. J. Med.* **2015**, *372*, 1832–1843. [CrossRef] [PubMed]
38. Leung, A.K.; Chan, K.W. Iron deficiency anemia. *Adv. Pediatr.* **2000**, *48*, 385–408.
39. Tsai, S.F.; Chen, S.J.; Yen, H.J.; Hung, G.Y.; Tsao, P.C.; Jeng, M.J.; Lee, Y.S.; Soong, W.J.; Tang, R.B. Iron deficiency anemia in predominantly breastfed young children. *Pediatr. Neonatol.* **2014**, *55*, 466–469. [CrossRef] [PubMed]
40. Allen, L.H. Anemia and iron deficiency: Effects on pregnancy outcome. *Am. J. Clin. Nutr.* **2000**, *71*, 1280s–1284s. [PubMed]
41. Cassat, J.E.; Skaar, E.P. Iron in infection and immunity. *Cell Host Microbe* **2013**, *13*, 509–519. [CrossRef] [PubMed]
42. Grune, T.; Sommerburg, O.; Siems, W.G. Oxidative stress in anemia. *Clin. Nephrol.* **2000**, *53*, S18–S22. [PubMed]
43. Fibach, E.; Rachmilewitz, E. The role of oxidative stress in hemolytic anemia. *Curr. Mol. Med.* **2008**, *8*, 609–619. [CrossRef] [PubMed]
44. Merryweather-Clarke, A.T.; Cadet, E.; Bomford, A.; Capron, D.; Viprakasit, V.; Miller, A.; Livesey, K.J. Digenic inheritance of mutations in HAMP and HFE results in different types of haemochromatosis. *Hum. Mol. Genet.* **2003**, *12*, 2241–2247. [CrossRef] [PubMed]
45. Kruszewski, M. Labile iron pool: The main determinant of cellular response to oxidative stress. *Mutat. Res.* **2003**, *531*, 81–92. [CrossRef] [PubMed]
46. Dixon, S.J.; Stockwell, B.R. The role of iron and reactive oxygen species in cell death. *Nat. Chem. Biol.* **2014**, *10*, 9–17. [CrossRef] [PubMed]
47. Lunova, M.; Goehring, C.; Kuscuoglu, D.; Mueller, K.; Chen, Y.; Walther, P.; Deschemin, J.C.; Vaulont, S.; Haybaeck, J.; Lackner, C.; et al. Hepcidin knockout mice fed with iron-rich diet develop chronic liver injury and liver fibrosis due to lysosomal iron overload. *J. Hepatol.* **2014**, *61*, 633–641. [CrossRef] [PubMed]
48. Fortes, G.B.; Alves, L.S.; de Oliveira, R.; Dutra, F.F.; Rodrigues, D.; Fernandez, P.L.; Souto-Padron, T.; De Rosa, M.J.; Kelliher, M.; Golenbock, D.; et al. Heme induces programmed necrosis on macrophages through autocrine TNF and ROS production. *Blood* **2012**, *119*, 2368–2375. [CrossRef] [PubMed]

49. Garcia-Perez, C.; Roy, S.S.; Naghdi, S.; Lin, X.; Davies, E.; Hajnoczky, G. Bid-induced mitochondrial membrane permeabilization waves propagated by local reactive oxygen species (ROS) signaling. *Proc. Natl. Acad. Sci. USA* **2012**, *109*, 4497–4502. [CrossRef] [PubMed]
50. Dixon, S.J.; Lemberg, K.M.; Lamprecht, M.R.; Skouta, R.; Zaitsev, E.M.; Gleason, C.E.; Patel, D.N.; Bauer, A.J.; Cantley, A.M.; Yang, W.S.; et al. Ferroptosis: An iron-dependent form of nonapoptotic cell death. *Cell* **2012**, *149*, 1060–1072. [CrossRef] [PubMed]
51. Yang, W.S.; SriRamaratnam, R.; Welsch, M.E.; Shimada, K.; Skouta, R.; Viswanathan, V.S.; Cheah, J.H.; Clemons, P.A.; Shamji, A.F.; Clish, C.B.; et al. Regulation of ferroptotic cancer cell death by GPX4. *Cell* **2014**, *156*, 317–331. [CrossRef] [PubMed]
52. Shimada, K.; Hayano, M.; Pagano, N.C.; Stockwell, B.R. Cell-line selectivity improves the predictive power of pharmacogenomicanalyses and helps identify NADPH as biomarker for ferroptosissensitivity. *Cell Chem. Biol.* **2016**, *23*, 225–235. [CrossRef] [PubMed]
53. Jiang, L.; Kon, N.; Li, T.; Wang, S.J.; Su, T.; Hibshoosh, H.; Baer, R.; Gu, W. Ferroptosis as a p53-mediated activity during tumour suppression. *Nature* **2015**, *520*, 57–62. [CrossRef] [PubMed]
54. Wang, H.; An, P.; Xie, E.; Wu, Q.; Fang, X.; Gao, H.; Zhang, Z.; Li, Y.; Wang, X.; Zhang, J.; et al. Characterization of ferroptosis in murine models of hemochromatosis. *Hepatology* **2017**. [CrossRef] [PubMed]
55. Kwon, M.Y.; Park, E.; Lee, S.J.; Chung, S.W. Heme oxygenase-1 accelerates erastin-induced ferroptotic cell death. *Oncotarget* **2015**, *6*, 24393–24403. [CrossRef] [PubMed]
56. Gao, M.; Monian, P.; Quadri, N.; Ramasamy, R.; Jiang, X. Glutaminolysis and transferrin regulate ferroptosis. *Mol. Cell* **2015**, *59*, 298–308. [CrossRef] [PubMed]
57. Hou, W.; Xie, Y.; Song, X.; Sun, X.; Lotze, M.T.; Zeh, H.J.; Kang, R.; Tang, D. Autophagy promotes ferroptosis by degradation of ferritin. *Autophagy* **2016**, *12*, 1425–1428. [CrossRef] [PubMed]
58. Zelko, I.N.; Mariani, T.J.; Folz, R.J. Superoxide dismutase multigene family: a comparison of the CuZn-SOD (SOD1), Mn-SOD (SOD2), and EC-SOD (SOD3) gene structures, evolution, and expression. *Free Radic. Biol. Med.* **2002**, *33*, 337–349. [CrossRef]
59. Wu, G.; Fang, Y.Z.; Yang, S.; Lupton, J.R.; Turner, N.D. Glutathione metabolism and its implications for health. *J. Nutr.* **2004**, *134*, 489–492. [PubMed]
60. Chae, H.Z.; Kim, H.J.; Kang, S.W.; Rhee, S.G. Characterization of three isoforms of mammalian peroxiredoxin that reduce peroxides in the presence of thioredoxin. *Diabetes Res. Clin. Pract.* **1999**, *45*, 101–112. [CrossRef]
61. Willcox, J.K.; Ash, S.L.; Catignani, G.L. Antioxidants and Prevention of Chronic Disease. *Crit. Rev. Food Sci. Nutr.* **2010**, *4*, 275–295. [CrossRef] [PubMed]
62. Temple, N.J. Antioxidants and disease: More questions than answers. *Nutr. Res.* **2000**, *20*, 449–459. [CrossRef]
63. Sripetchwandee, J.; Pipatpiboon, N.; Chattipakorn, N.; Chattipakorn, S. Combined therapy of iron chelator and antioxidant completely restores brain dysfunction induced by iron toxicity. *PLoS ONE* **2014**, *9*, e85115. [CrossRef] [PubMed]
64. Wongjaikam, S.; Kumfu, S.; Khamseekaew, J.; Sripetchwandee, J.; Srichairatanakool, S.; Fucharoen, S.; Chattipakorn, N. Combined iron chelator and antioxidant exerted greater efficacy on cardioprotection than monotherapy in iron-overloaded rats. *PLoS ONE* **2016**, *11*, e0159414. [CrossRef] [PubMed]
65. Galati, G.; O'brien, P.J. Potential toxicity of flavonoids and other dietary phenolics: Significance for their chemopreventive and anticancer properties. *Free Radic. Biol. Med.* **2004**, *37*, 287–303. [CrossRef] [PubMed]
66. Ferlazzo, N.; Visalli, G.; Cirmi, S.; Lombardo, G.E.; Laganà, P.; Di Pietro, A.; Navarra, M. Natural iron chelators: Protective role in A549 cells of flavonoids-rich extracts of Citrus juices in Fe^{3+}—Induced oxidative stress. *Environ. Toxicol. Pharmacol.* **2016**, *43*, 248–256. [CrossRef] [PubMed]
67. Ma, Q.; Kim, E.Y.; Lindsay, E.A.; Han, O. Bioactive dietary polyphenols inhibit heme iron absorption in a dose-dependent manner in human intestinal Caco-2 Cells. *J. Food Sci.* **2011**, *76*, H143–H150. [CrossRef] [PubMed]
68. Shin, J.H.; Jeon, H.J.; Park, J.; Chang, M.S. Epigallocatechin-3-gallate prevents oxidative stress-induced cellular senescence in human mesenchymal stem cells via Nrf2. *Int. J. Mol. Med.* **2016**, *38*, 1075–1082. [CrossRef] [PubMed]
69. Jiao, Y.; Wilkinson, J.; Di, X.; Wang, W.; Hatcher, H.; Kock, N.D.; Torti, S.V. Curcumin, a cancer chemopreventive and chemotherapeutic agent, is a biologically active iron chelator. *Blood* **2009**, *113*, 462–469. [CrossRef] [PubMed]

70. Zhong, W.; Qian, K.; Xiong, J.; Ma, K.; Wang, A.; Zou, Y. Curcumin alleviates lipopolysaccharide induced sepsis and liver failure by suppression of oxidative stress-related inflammation via PI3K/AKT and NF-κB related signaling. *Biomed. Pharmacother.* **2016**, *83*, 302–313. [CrossRef] [PubMed]
71. Tang, Y.; Li, Y.; Yu, H.; Gao, C.; Liu, L.; Chen, S.; Yao, P. Quercetin prevents ethanol-induced iron overload by regulating hepcidin through the BMP6/SMAD4 signaling pathway. *J. Nutr. Biochem.* **2014**, *25*, 675–682. [CrossRef] [PubMed]
72. Mu, M.; An, P.; Wu, Q.; Shen, X.; Shao, D.; Wang, H.; Wang, F. The dietary flavonoid myricetin regulates iron homeostasis by suppressing hepcidin expression. *J. Nutr. Biochem.* **2016**, *30*, 53–61. [CrossRef] [PubMed]
73. Zhen, A.W.; Nguyen, N.H.; Gibert, Y.; Motola, S.; Buckett, P.; Wessling-Resnick, M.; Fraenkel, P.G. The small molecule, genistein, increases hepcidin expression in human hepatocytes. *Hepatology* **2013**, *58*, 1315–1325. [CrossRef] [PubMed]
74. Moayedi Esfahani, B.A.; Reisi, N.; Mirmoghtadaei, M. Evaluating the safety and efficacy of silymarin in β-thalassemia patients: A review. *Hemoglobin* **2015**, *39*, 75–80. [CrossRef] [PubMed]
75. Qiao, Y.; He, H.; Zhang, Z.; Liao, Z.; Yin, D.; Liu, D.; He, M. Long-term sodium ferulate supplementation scavenges oxygen radicals and reverses liver damage induced by iron overloading. *Molecules* **2016**, *21*, 1219. [CrossRef] [PubMed]
76. Das, S.K.; Wang, W.; Zhabyeyev, P.; Basu, R.; McLean, B.; Fan, D.; Dyck, J.R. Iron-overload injury and cardiomyopathy in acquired and genetic models is attenuated by resveratrol therapy. *Sci. Rep.* **2014**, *5*, 18132. [CrossRef] [PubMed]
77. Skarpańska-Stejnborn, A.; Basta, P.; Sadowska, J.; Pilaczyńska-Szczeńniak, Ł. Effect of supplementation with chokeberry juice on the inflammatory status and markers of iron metabolism in rowers. *J. Int. Soc. Sports Nutr.* **2014**, *11*, 48. [CrossRef] [PubMed]
78. García-Casal, M.N.; Layrisse, M.; Solano, L.; Barón, M.A.; Arguello, F.; Llovera, D.; Ramírez, J.; Leets, I.; Tropper, E. Vitamin A and β-carotene can improve nonheme iron absorption from rice, wheat and corn by humans. *J. Nutr.* **1997**, *128*, 646–650.
79. Citelli, M.; Bittencourt, L.L.; Da Silva, S.V.; Pierucci, A.P.; Pedrosa, C. Vitamin A modulates the expression of genes involved in iron bioavailability. *Biol. Trace Elem. Res.* **2012**, *149*, 64–70. [CrossRef] [PubMed]
80. Katz, O.; Reifen, R.; Lerner, A. β-Carotene can reverse dysregulation of iron protein in an in vitro model of inflammation. *Immunol. Res.* **2015**, *61*, 70–78. [CrossRef] [PubMed]
81. Chiu, P.F.; Ko, S.Y.; Chang, C.C. Vitamin C affects the expression of hepcidin and erythropoietin receptor in HepG2 cells. *J. Ren. Nutr.* **2012**, *22*, 373–376. [CrossRef] [PubMed]
82. Fustinoni-Reis, A.M.; Arruda, S.F.; Dourado, L.P.; da Cunha, M.S.; Siqueira, E. Tucum-Do-Cerrado (Bactrissetosa Mart.) consumption modulates iron homeostasis and prevents iron-induced oxidative stress in the rat liver. *Nutrients* **2016**, *8*, 38. [CrossRef] [PubMed]
83. Perez, C.A.; Wei, Y.; Guo, M. Iron-binding and anti-Fenton properties of baicalein and baicalin. *J. Inorg. Biochem.* **2009**, *103*, 326–332. [CrossRef] [PubMed]
84. Guan, Y.; An, P.; Zhang, Z.; Zhang, F.; Yu, Y.; Wu, Q.; Wang, F. Screening identifies the Chinese medicinal plant Caulis Spatholobi as an effective HAMP expression inhibitor. *J. Nutr.* **2013**, *143*, 1061–1066. [CrossRef] [PubMed]
85. Zhang, J.; Gu, J.Y.; Chen, Z.S.; Xing, K.C.; Sun, B. Astragalus polysaccharide suppresses palmitate-induced apoptosis in human cardiac myocytes: The role of Nrf1 and antioxidant response. *Int. J. Clin. Exp. Pathol.* **2015**, *8*, 2515. [PubMed]
86. Ren, F.; Qian, X.H.; Qian, X.L. Astragalus polysaccharide upregulateshepcidin and reduces iron overload in mice via activation of p38 mitogen-activated protein kinase. *Biochem. Biophys. Res. Commun.* **2016**, *472*, 163–168. [CrossRef] [PubMed]
87. Zhuang, C.; Xu, N.W.; Gao, G.M.; Ni, S.; Miao, K.S.; Li, C.K.; Xie, H.G. Polysaccharide from Angelica sinensis protects chondrocytes from H_2O_2-induced apoptosis through its antioxidant effects in vitro. *Int. J. Biol. Macromol.* **2016**, *87*, 322–328. [CrossRef] [PubMed]
88. Cheng, Y.; Zhou, J.; Li, Q.; Liu, Y.; Wang, K.; Zhang, Y. The effects of polysaccharides from the root of Angelica sinensis on tumor growth and iron metabolism in H22-bearing mice. *Food Funct.* **2016**, *7*, 1033–1039. [CrossRef] [PubMed]
89. Scherbinina, S.P.; Levina, A.A.; Lisovskaya, I.L.; Ataullakhanov, F.I. Effect of exogenous antioxidants on erythrocyte redox status and hepcidin content in disorders of iron metabolism regulation. *Biochemistry* **2012**, *6*, 338–342. [CrossRef]

90. Nguyen, T.; Nioi, P.; Pickett, C.B. The Nrf2-antioxidant response element signaling pathway and its activation by oxidative stress. *J. Biol. Chem.* **2009**, *284*, 13291–13295. [CrossRef]
91. Vauzour, D.; Rodriguez-Mateos, A.; Corona, G.; Oruna-Concha, M.J.; Spencer, J.P. Polyphenols and human health: prevention of disease and mechanisms of action. *Nutrients* **2010**, *2*, 1106–1131. [CrossRef] [PubMed]
92. Pandey, K.B.; Rizvi, S.I. Plant polyphenols as dietary antioxidants in human health and disease. *Oxid. Med. Cell. Longev.* **2009**, *2*, 270–278. [CrossRef] [PubMed]
93. Niu, Q.; Mu, L.; Li, S.; Xu, S.; Ma, R.; Guo, S. Proanthocyanidin protects human embryo hepatocytes from fluoride-induced oxidative stress by regulating iron metabolism. *Biol. Trace Elem. Res.* **2016**, *169*, 174–179. [CrossRef] [PubMed]
94. Cao, G.; Sofic, E.; Prior, R.L. Antioxidant and prooxidant behavior of flavonoids: Structure-activity relationships. *Free Radic. Biol. Med.* **1997**, *22*, 749–760. [CrossRef]
95. Zhao, L.; Wang, Y.; Liu, J.; Wang, K.; Guo, X.; Ji, B.; Zhou, F. Protective Effects of genistein and puerarin against chronic alcohol-induced liver injury in mice via antioxidant, anti-inflammatory, and anti-apoptotic mechanisms. *J. Agric. Food Chem.* **2016**, *64*, 7291–7297. [CrossRef] [PubMed]
96. Rathee, P.; Chaudhary, H.; Rathee, S.; Rathee, D.; Kumar, V.; Kohli, K. Mechanism of action of flavonoids as anti-inflammatory agents: A review. *Inflamm. Allergy Drug Targets* **2009**, *8*, 229–235. [CrossRef] [PubMed]
97. Bayele, H.K.; Balesaria, S.; Srai, S.K. Phytoestrogens modulate hepcidin expression by Nrf2: Implications for dietary control of iron absorption. *Free Radic. Biol. Med.* **2015**, *89*, 1192–1202. [CrossRef] [PubMed]
98. Oboh, G.; Ademosun, A.O.; Opeyemi, O.B. Quercetin and its role in chronic diseases. *Adv. Exp. Med. Biol.* **2016**, *929*, 377–387. [PubMed]
99. Kumar, N.; Pruthi, V. Potential applications of ferulic acid from natural sources. *Biotechnol. Rep.* **2014**, *4*, 86–93. [CrossRef] [PubMed]
100. Bradamante, S.; Barenghi, L.; Villa, A. Cardiovascular protective effects of resveratrol. *Cardiovasc. Drug Rev.* **2004**, *22*, 169–188. [CrossRef] [PubMed]
101. Tang, P.C.T.; Ng, Y.F.; Ho, S.; Gyda, M.; Chan, S.W. Resveratrol and cardiovascular health—Promising therapeutic or hopeless illusion? *Pharmacol. Res.* **2014**, *90*, 88–115. [CrossRef] [PubMed]
102. Wu, X.; Gu, L.; Prior, R.L.; McKay, S. Characterization of anthocyanins and proanthocyanidins in some cultivars of Ribes, Aronia and Sambucus and their antioxidant capacity. *J. Agric. Food Chem.* **2004**, *52*, 7846–7856. [CrossRef] [PubMed]
103. Taheri, R.; Connolly, B.A.; Brand, M.H.; Bolling, B.W. Underutilized chokeberry (Aroniamelanocarpa, Aroniaarbutifolia, Aroniaprunifolia) accessions are rich sources of anthocyanins, flavonoids, hydroxycinnamic acids, and proanthocyanidins. *J. Agric. Food Chem.* **2013**, *61*, 8581–8588. [CrossRef] [PubMed]
104. McDowell, L.R.; Wilkinson, N.; Madison, R.; Felix, T.L. Vitamins and minerals functioning as antioxidants with supplementation considerations. In *Florida Ruminant Nutrition Symposium*; Best Western Gateway Grand: Gainesville, FL, USA, 2007; pp. 30–31.
105. Kennedy, T.A.; Liebler, D.C. Peroxyl radical scavenging by beta-carotene in lipid bilayers. Effect of oxygen partial pressure. *J. Biol. Chem.* **1992**, *267*, 4658–4663. [PubMed]
106. Ramalho, A.; Padilha, P.; Saunders, C. Critical analysis of Brazilian studies about vitamin A deficiency in maternal child group. *Rev. Paul. Pediatr.* **2008**, *26*, 392–399. [CrossRef]
107. Mejía, L.A.; Chew, F. Hematological effect of supplementing anemic children with vitamin A alone and in combinations with iron. *Am. J. Clin. Nutr.* **1998**, *48*, 595–600.
108. Bloem, M.W.; Wedel, M.; van Agtamal, E.J.; Speek, A.J.; Saowakontha, S.; Schreurs, W.H. Vitamin A intervention: Short-term effects of a single, oral, massive dose on iron metabolism. *Am. J. Clin. Nutr.* **1990**, *51*, 76–79. [PubMed]
109. Kelleher, S.L.; Lönnerdal, B. Low vitamin A intake affects milk iron and iron transporters in rat mammary gland and liver. *J. Nutr.* **2005**, *135*, 27–32. [PubMed]
110. Imam, M.U.; Ismail, M.; Ooi, D.J.; Azmi, N.H.; Sarega, N.; Chan, K.W.; Bhanger, M.I. Are bioactive-rich fractions functionally richer? *Crit. Rev. Biotechnol.* **2016**, *36*, 585–593. [PubMed]

nutrients

MDPI

Article

Ferulic Acid on Glucose Dysregulation, Dyslipidemia, and Inflammation in Diet-Induced Obese Rats: An Integrated Study

Norma Julieta Salazar-López [1] , Humberto Astiazarán-García [2] , Gustavo A. González-Aguilar [2], Guadalupe Loarca-Piña [3], Josafat-Marina Ezquerra-Brauer [1], J. Abraham Domínguez Avila [2] and Maribel Robles-Sánchez [1,*]

1 Departamento de Investigación y Posgrado en Alimentos, Universidad de Sonora, Blvd. Luis Encinas y Rosales S/N, Colonia Centro, Hermosillo, Sonora, C.P. 83000 Sonora, Mexico; njulietasl@yahoo.es (N.J.S.-L.); ezquerra@guayacan.mx (J.-M.E.-B.)

2 Centro de Investigación en Alimentación y Desarrollo, A.C., Carretera a La Victoria km 0.6, Hermosillo, Sonora, C.P. 83304 Sonora, Mexico; hastiazaran@ciad.mx (H.A.-G.); gustavo@ciad.mx (G.A.G.-A.); abrahamdominguez9@yahoo.com (J.A.D.A.)

3 Departamento de Investigación y Posgrado en Alimentos, Facultad de Química, Universidad Autónoma de Querétaro, Cerro de Las Campanas, S/N, Colonia Las Campanas, Santiago de Querétaro, Querétaro, C.P. 76010 Querétaro, Mexico; loarca@uaq.mx

* Correspondence: rsanchez@guayacan.uson.mx; Tel.: +52-662-259-2207

Received: 26 May 2017; Accepted: 21 June 2017; Published: 29 June 2017

Abstract: Obesity is considered to be a low-grade chronic inflammatory process, which is associated with cardiovascular and metabolic diseases. An integral evaluation of the effects of ferulic acid on biomarkers of glucose dysregulation, dyslipidemia, inflammation, and antioxidant potential induced by a high-fat diet (HFD) in rats was carried out. Three groups of male Wistar rats (six per group) consumed a basal diet (BD), which was supplemented with either lard at 310 g/kg (HFD) or lard and ferulic acid at 2 g/kg (HFD + FA), ad libitum for eight weeks. Body weight gain, hyperplasia, and hypertrophy in abdominal fat tissues were higher in the HFD group than in the HFD+FA group. The rats fed a HFD + FA significantly inhibited the increase in plasma lipids and glucose, compared with the HFD group. Biomarkers associated with inflammation were found at higher concentrations in the serum of rats fed a HFD than the HFD + FA group. Plasma antioxidant levels were lower in HFD rats compared to rats fed the HFD + FA. These results suggest that ferulic acid improves the obesogenic status induced by HFD, and we elucidated the integral effects of ferulic acid on a biological system.

Keywords: ferulic acid; dyslipidemia; inflammation; glucose dysregulation; high fat diet

1. Introduction

The World Health Organization defines overweight and obesity as abnormal or excessive fat accumulation that may impair health [1]. In overweight and obese individuals, the increase in body weight promotes adipose tissue hyperplasia and hypertrophy, which increases secretion of various pro-inflammatory chemokines, cytokines, and hormones, such as C-reactive protein (CRP), resistin, inducible nitric oxide synthase (iNOS), monocyte chemotactic protein (MCP)-1, tumor necrosis factor (TNF)-α, and interleukin (IL)-1, IL-6, and IL-8. This results in a state of low-grade chronic inflammation associated with obesity-related metabolic diseases [2,3]. This condition increases the risk of developing comorbidities, such as coronary artery disease, hypertension, dyslipidemia, insulin resistance, type 2 diabetes mellitus, nonalcoholic fatty liver disease, and respiratory disorders [2,4].

Phytochemicals may have a positive impact on obesity through the control of the lipid metabolism, inflammation, and carbohydrate metabolism [5,6]. Ferulic acid is a hydroxycinnamic acid with potential health benefits due to its antioxidant and anti-inflammatory capacity, among others, and is widely distributed in foods of plant origin [6,7]. In a recent investigation, ferulic acid inhibited the expression of TNF-α and IL-1β in lipopolysaccharide LPS-activated monocyte-derived THP-1 macrophages by inhibiting the activation of nuclear factor-kappa B (NF-κB), which could contribute to preventing chronic inflammatory diseases [7]. In another study, ferulic acid alleviated metabolic syndrome in rats administered high-fat and high-fructose diets [8]. The above results are consistent with Senaphan et al. [9], who showed that ferulic acid alleviates changes in metabolic syndrome in rats through suppression of oxidative stress by down-regulation of p47phox, increased nitric oxide (NO) bioavailability with upregulation of endothelial nitric oxide synthase (eNOS) and suppression of TNF-α [9]. Ferulic acid also prevents acute liver injury by inhibiting intrahepatic inflammation and liver apoptosis in mice via the reduction of hepatocellular degeneration, lymphocyte infiltration, the number of apoptotic hepatocytes, serum levels of tumor necrosis factor alpha (TNF-α) and interferon-γ (IFN-γ), and liver myeloperoxidase (MPO) activity [10].

In the present study, an integral evaluation of the effect of ferulic acid on biomarkers of glucose dysregulation, dyslipidemia, inflammation, and antioxidant potential in rats fed high-fat diets (HFD) was carried out.

2. Materials and Methods

2.1. Animals and Treatments

Eighteen male Wistar rats (eight weeks old) were obtained from the Department of Research and Postgraduate Studies, Universidad de Sonora (Mexico). They were housed individually in suspended wire mesh-bottomed cages. Lighting in the animal room was on a 12-h light:dark cycle. The temperature was maintained at 22 °C and relative humidity at 40–70%. After a one week acclimation period, rats were randomly assigned to one of the three experimental groups (six per group).

All diets were formulated from the AIN-93G diet [11], with slight modifications. Briefly, to obtain the basal diet (BD), AIN-93G was modified to contain lard and soybean oil at 19 and 24 g/kg of diet, respectively. For induction of obesity, the rats were given a high-fat diet (HFD) (formulated to contain lard and soybean oil at 316 and 32 g/kg of diet, respectively). Ferulic acid (FA) was added to the HFD at 2 g/kg of diet and was referred to as HFD + FA. The composition of the diets is given in Table 1. The level of FA used in the test diet in this study represent moderate, subtoxic and subpharmacologic levels in the diet and were based on levels used in previous studies [12,13]. All diets were stored at 4 °C until fed to the rats. Rats consumed their respective diets and water ad libitum. Body weight and food intake were monitored weekly throughout the experiment. At the end of the eight-week feeding period, rats were anaesthetized using sodium phenobarbital (60 mg/kg). Blood from these rats was drawn from the left atrium of the heart after previous overnight fasting (12 h) and placed into centrifuge tubes coated with and without sodium EDTA. Serum and plasma from each rat were separated by centrifugation (2000 g/15 min), aliquoted in 0.5 mL fractions and stored at −80 °C for later analyses. Abdominal fat was obtained as follows: after opening the peritoneum and removing the viscera, abdominal fat was carefully dissected, weighed and kept in 4% formaldehyde for histological analysis. All animal procedures were conducted in strict conformation with the NIH guidelines [14] for animal care and the study submitted for the approval of the Bioethics Committee of the Research Center in Food and Development (CIAD, A.C.), Hermosillo, Sonora, Mexico (animal permit number: CE/004/2017).

Table 1. Composition of the experimental diets (g/kg).

	BD [1]	HFD [2]	HFD + FA [3]
Casein	200.0	200.0	200.0
Lard	19	316	316
Oil	24	32	32
Corn starch	501	0.0	0.0
Maltodextrin	118	185	183
Sucrose	0.0	129	129
Methionine	18	18	18
Choline bitartrate	25	25	25
Cellulose	50	50	50
Vitamin mix	10	10	10
Mineral mix	35	35	35
trans-Ferulic acid	0.0	0.0	2
Energy (kcal/g)	4.00	6.00	5.98

[1] BD: basal diet; [2] HFD: high-fat diet; [3] HFD + FA: high-fat diet supplemented with 0.2% ferulic acid.

2.2. Biochemical Analysis

Plasma glucose, triglycerides (TG), total cholesterol (TC), high-density lipoprotein-cholesterol (HDL-C), and low-density lipoprotein-cholesterol (LDL-C) concentrations were measured with commercial kits, following the supplier's instructions (Randox, Crumlin, Antrim, UK). Apolipoprotein B (ApoB) and Apolipoprotein A1 (ApoA1) concentrations were quantified with commercial ELISA kits from LifeSpan BioSciences, Inc. (Seattle, WA, USA). Very-low-density lipoprotein-cholesterol (VLDL-C) concentration was calculated by dividing triglycerides by five [15]. The atherogenic index was calculated as (total cholesterol – HDL-C)/HDL-C [16]. Interleukin-1β (IL-1β), interleukin-4 (IL-4), interleukin-6 (IL-6), interleukin-10 (IL-10), interleukin-12 (IL-12), and granulocyte macrophage colony-stimulating factor (GMC-SF) concentrations were measured by commercial ELISA kits from QIAGEN (Germantown, MD, USA). Serum insulin concentration was determined with an ELISA kit (Industrial MexLab SA de CV, Zapopan, Jalisco, México). The homeostatic model assessment index of insulin resistance (HOMA-IR) for each group assayed was calculated by multiplying insulin plasma (μUI/mL) by glucose plasma (mmol/L) and dividing by 22.5 [17].

2.3. Antioxidant Capacity

2.3.1. Oxygen Radical Absorbance Capacity Assay (ORAC)

The ORAC assay was carried out on a microplate fluorescence reader FLUOstar® Omega (Ortenberg, Germany). The procedure was based on a previous report by Huang et al. [18]. The experiment was conducted at 37 °C at pH 7.4 with a blank sample in parallel. The analyzer was programmed to record the fluorescence of fluorescein (10 nM) every five minutes after addition of 240 mM AAPH (2,2′-azobis (2-methylpropionamidine) dihydrochloride), for 90 min, at an excitation wavelength of 485 and an emission wavelength of 530 nm. The final results were calculated using the differences between areas under the curve of fluorescein decay of the blank and the sample, and were expressed as micromoles of Trolox equivalents ((±)-6-hydroxy-2,5,7,8-tetramethylchromane-2-carboxylic acid) per mL (μmol TE/mL).

2.3.2. Trolox Equivalent Antioxidant Capacity (TEAC) Assay

Trolox equivalent antioxidant capacity (TEAC) assay is based on the ability of antioxidant molecules to scavenge the ABTS●+ cation radical (2,2′-azino-bis(3-ethylbenzothiazoline-6-sulfonic acid) diammonium salt), which produces a change in color that can be spectrophotometrically quantified [19]. A stable stock solution of ABTS●+ was prepared by mixing 5 mL of an aqueous solution of ABTS (7 mM)

with 0.088 mL of sodium persulfate (148 mM), and incubating it in the dark at room temperature for 16–18 h. The ABTS●+ working solution was prepared immediately before use by diluting the stock solution in ethanol (∼1:88, *v*/*v*), and its absorbance was adjusted to 0.700 ± 0.02 at 734 nm. Then, 280 µL of the ABTS●+ working solution was combined with 10 µL of the sample in a microplate well. The changes in absorbance (734 nm) were recorded as ABTS●+ radical-scavenging activity. A standard curve was prepared using Trolox as a standard, which was used to convert the changes in absorbance of the samples to µmol of Trolox equivalents (TE)/mL of plasma.

2.4. Histological Analysis

Abdominal fat tissue was extracted, fixed in 10% formalin and paraffin embedded. The tissue of was cut into 3–5 µm sections, which were stained with hematoxylin and eosin (H and E). Adipocyte size (superficial area) and number of adipocytes per area on abdominal fat tissue were evaluated. The adipocyte superficial area was measured with the software ZEN 2 (Carl Zeiss Microscopy GmbH, Göttingen, Germany).

2.5. Statistical Analysis

Results are expressed as the mean ± standard error mean (SEM) ($n = 6$). Samples were analyzed in duplicate. To contrast dietary groups, one way analysis of variance (ANOVA) followed by Tukey's comparison tests was used. The level of significance was $p < 0.05$. Correlations between response variables were calculated using standard Pearson correlation. The statistical software JMP 5.0.1 (SAS Institute, Inc., Cary, NC, USA) was used.

3. Results

3.1. Effect of FA on Body Weight Gain, Diet Intake, Food Efficiency, and Adipose Tissue Weight

The induction of obesity in rats was achieved by administration of a high-fat diet for 60 days. This was due to the diet composition, as the rats fed the HFD had 50% more caloric content compared to rats fed the BD. The rats fed a HFD showed an increased body weight gain (BWG), energy intake, caloric efficiency, and weight of abdominal fat tissue (WAFT) compared to rats fed the BD (Table 2).

Table 2. Effect of ferulic acid on food intake, body weight gain, and weight of abdominal fat tissue in rats fed a high-fat diet.

Parameters	BD [1]	HFD [2]	HFD + FA [3]
Food intake (g/day)	12.80 ± 0.44 [a]	10.85 ± 0.56 [b]	11.02 ± 0.69 [b]
Energy Intake (kcal/day)	51.07 ± 1.75 [b]	65.11 ± 3.38 [a]	65.91 ± 4.15 [a]
Food efficiency (g/kcal)	0.022 ± 0.0013 [b]	0.035 ± 0.0039 [a]	0.027 ± 0.0029 [b]
BWG [4] (g)	96.50 ± 4.57 [c]	132 ± 12.59 [a]	112.15 ± 1.20 [b]
WAFT [5] (g)	5.21 ± 0.97 [b]	7.77 ± 0.99 [a]	5.58 ± 0.85 [b]
Abdominal fat index	1.49 ± 0.27 [b]	2.07 ± 0.28 [a]	1.59 ± 0.22 [b]

[1] BD: basal diet; [2] HFD: high-fat diet; [3] HFD + FA: high-fat diet supplemented with 0.2% ferulic acid; [4] BWG: body weight gain; [5] WAFT: weight of abdominal fat tissue. Values represent the mean ± SEM ($n = 6$). Significant differences between dietary treatments are marked in rows with different letters ($p < 0.05$). The food efficiency (g/kcal) was obtained by body weight gain (g/day)/energy intake (kcal/day) [20].

As shown in Table 2, intake of HFD+FA decreased body weight gain (15%, $p < 0.05$) and WAFT values (28%, $p < 0.05$) compared to the HFD group, and similar results were observed with the fat index (23%, $p < 0.05$).

3.2. Effect of Ferulic Acid on the Serum Lipid Profile (Biochemical Analysis)

The serum lipid profile of rats is presented in Figure 1. TC was significantly increased (28%) in the HFD group, as compared to the BD group ($p < 0.05$). An increase of LDL-C (34%) was also observed

in the HFD group versus the BD group. An increase of TG in HFD fed rats versus the BD group was 12% ($p < 0.05$). The HFD + FA diet prevented the increase of the lipids versus HFD by 16% (TC), 20% (LDL-C), and 12% (TG). The HFD + FA diet improved the atherogenic index (AI) by approximately 22%, although significant differences were not observed ($p > 0.05$). No significant changes in HDL-C concentration were registered.

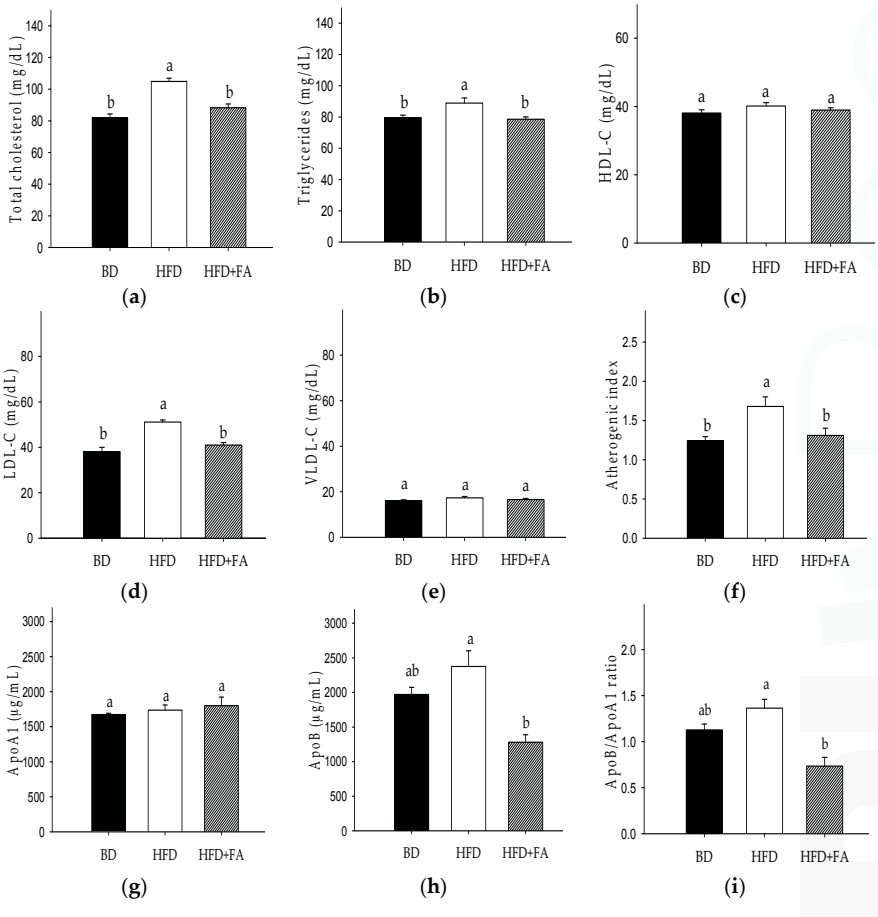

Figure 1. Effect of ferulic acid on the lipid profile in Wistar rats fed a high fat diet (HFD). (**a**) Total cholesterol (TC); (**b**) triglycerides (TG); (**c**) high-density lipoprotein-cholesterol (HDL-C); (**d**) low-density lipoprotein-cholesterol (LDL-C); (**e**) very-low-density lipoprotein-cholesterol (VLDL-C); (**f**) atherogenic index; (**g**) apolipoprotein A1 (ApoA1); (**h**) apolipoprotein B (ApoB); (**i**) ApoB/Apo A1 ratio. Each bar represents the mean ± SEM. Different letters in the bars represent significant differences ($p < 0.05$) between dietary treatments.

HFD–fed rats showed 1.2-fold more ApoB compared with BD-fed rats, whereas that HFD + FA-fed rats showed twofold decreases in the serum ApoB level with respect to HFD-fed rats (Figure 1).

Positive Pearson's correlations were observed between weight abdominal fat tissue and atherogenic index ($r = 0.8168$, $p = 0.0012$), total cholesterol ($r = 0.5949$, $p = 0.0248$), LDL-C ($r = 0.6082$, $p = 0.021$), and VLDL-C ($r = 0.6822$, $p = 0.0072$) (Table 3).

Table 3. Pearson's correlation for biomarkers of glucose dysregulation, dyslipidemia, inflammation, and antioxidant status in diet-induced obese rats.

	TC	TG	LDL-C	VLDL-C	WAFT	Insulin	IL-1β	IL-4	IL-6	AI	HOMA IR	TEAC	ORAC	ApoB
G	0.5765 (0.0002)	0.49 (0.0028)	0.6418 (<0.0001)	-	0.7159 (0.0027)	0.7695 (<0.0001)	0.7668 (<0.0001)	0.6881 (0.0003)	0.6131 (0.0019)	0.4945 (0.004)	0.8672 (<0.0001)	−0.4959 (0.0053)	-	-
TC			0.7947 (<0.0001)	-	0.5949 (0.0248)	-	0.7012 (0.0004)	0.5668 (0.0074)	0.5304 (0.0134)	0.7727 (<0.0001)	0.5933 (0.0253)	-	-	-
TG				0.9126 (<0.0001)	0.765 (0.0014)	0.7739 (<0.0001)	-	-	-	-	0.8083 (0.0005)	-	-	-
LDL-C					0.6082 (0.021)	-	0.7475 (0.0001)	0.6515 (0.001)	0.5855 (0.0042)	0.6154 (0.0001)	0.7853 (0.0009)	-	-	-
VLDL-C					0.6822 (0.0072)	0.5003 (0.0049)	-	-	-	-	-	-	-	-
WAFT						-	0.7952 (0.0004)	0.7106 (0.003)	0.6953 (0.004)	0.8168 (0.0012)	0.85 (0.032)	-	-	-
Insulin							0.6399 (0.0185)	-	0.6214 (0.0234)	-	0.994 (<0.0001)	−0.599 (0.0086)	−0.662 (0.0099)	-
IL-1β								0.9618 (<0.0001)	0.9201 (<0.0001)	-	0.9864 (<0.0001)	−0.6236 (0.0043)	−0.6371 (0.0079)	-
IL-4									0.9611 (<0.0001)	-	0.9623 (<0.0001)	−0.7269 (0.0004)	−0.7278 (0.0014)	0.5767 (0.0308)
IL-6										-	0.9399 (0.0002)	−0.7184 (0.0005)	−0.7344 (0.0012)	0.5793 (0.0299)
HOMA IR												−0.7755 (0.0018)	−0.778 (0.0081)	-

p-values are in parenthesis.

3.3. Effect of Ferulic Acid on Biomarkers of Insulin Sensitivity

Figure 2 shows the effect of BD, HFD, and HFD + FA on rat blood glucose and insulin levels and HOMA-IR. Blood glucose and insulin levels in the HFD group were significantly higher than those in the BD group ($p < 0.05$). The addition of FA to the high-fat diet significantly reduced blood glucose and insulin levels (Figure 2a,b). As shown in Figure 2c, the HOMA-IR value was eight-fold higher in the HFD compared with BD–fed rats, but this increase was reversed by 0.2% FA supplementation in the HFD. The glucose levels showed a positive correlation with insulin levels ($r = 0.7695$, $p < 0.0001$) and the HOMA-IR ($r = 0.8672$, $p < 0.0001$). Furthermore, positive correlations between weight, abdominal fat tissue, and glucose ($r = 0.7159$, $p = 0.0027$) and HOMA-IR ($r = 0.85$, $p = 0.0320$) were observed (Table 3).

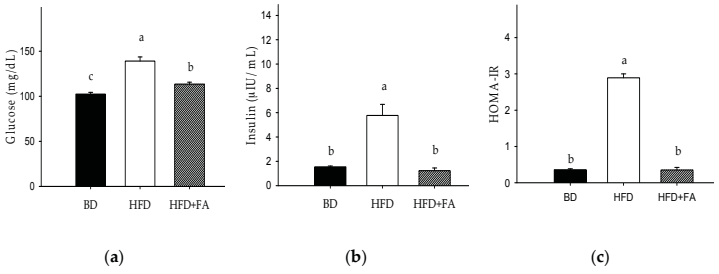

Figure 2. Effect of ferulic acid on biomarkers of glucose metabolism in Wistar rats fed a basal diet (BD), high-fat diet (HFD), and high-fat diet with ferulic acid (HFD + FA) for 60 days. (**a**) Glucose; (**b**) Insulin; (**c**) Homeostatic model assessment index of insulin resistance (HOMA-IR). Each bar represents the mean ± SEM. Different letters in the bars represent significant differences ($p < 0.05$) between dietary treatments.

3.4. Effect of Ferulic Acid on Inflammatory Biomarkers

An assessment of the major cytokines produced after eight weeks of the HFD diet (Figure 3) revealed a significant elevation in the production of IL-1β, IL-4, and IL-6 compared with serum levels of animals in the BD group. The cytokines IL-10 in HFD-fed animals was slightly decreased with respect to BD, whereas IL-12 showed no significant changes among the dietary groups ($p > 0.05$). The production of GM-CSF did not show significant changes between the HFD and BD, but a significant reduction was observed in the HFD + FA group.

Positive Pearson correlations of IL-6 with glucose ($r = 0.6131$, $p = 0.0019$), HOMA index ($r = 0.9399$, $p = 0.0002$), abdominal fat weight ($r = 0.6953$, $p = 0.0040$), TC ($r = 0.5304$, $p = 0.0134$), LDL-C ($r = 0.5855$, $p = 0.0042$), ApoB ($r = 0.5793$, $p = 0.0299$), IL-1β ($r = 0.9201$, $p < 0.0001$), and IL-4 ($r = 0.9611$, $p < 0.0001$) were observed. Positive correlations of IL-1β with IL-4 ($r = 0.9618$, $p < 0.0001$) and abdominal fat weight ($r = 0.7952$, $p = 0.0004$) were observed (Table 3).

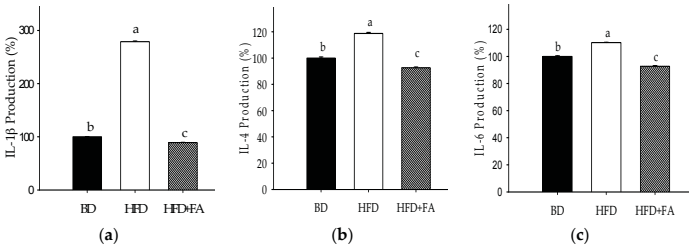

Figure 3. *Cont.*

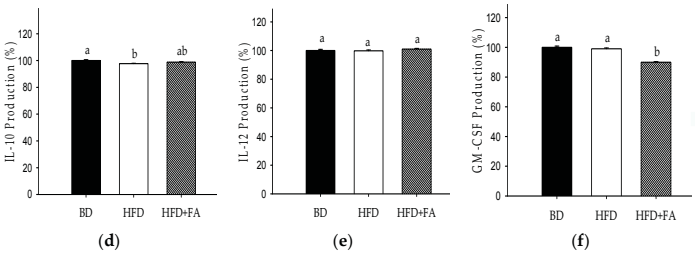

Figure 3. Production (%) of cytokines in plasma of rats fed a HFD and HFD + FA after 60 days of treatment compared to BD poduction (100%). (**a**) Interleukin-1β (IL-1β); (**b**) interleukin-4 (IL-4); (**c**) interleukin-6 (IL-6); (**d**) interleukin-10 (IL-10); (**e**) interleukin-12 (IL-12); (**f**) granulocyte macrophage colony stimulating factor (GM-CSF). Each bar represents the mean ± SEM. Different letters in the bars represent significant differences ($p < 0.05$) between dietary treatments.

3.5. Antioxidant Capacity of Plasma

The antioxidant status during obesity and overweight is a key factor that contribute to the initiation and progression of noncommunicable diseases. The plasma antioxidant capacity (ORAC and TEAC assays) in the HFD group was decreased (Figure 4) compared with the BD group rats; however, this decrease was not significant ($p > 0.05$). A significant increase in the plasma antioxidant capacity of the rats in the HFD + FA group compared to the HFD group was found ($p < 0.05$). TEAC and ORAC showed negative Pearson correlations with IL-6 (Table 3).

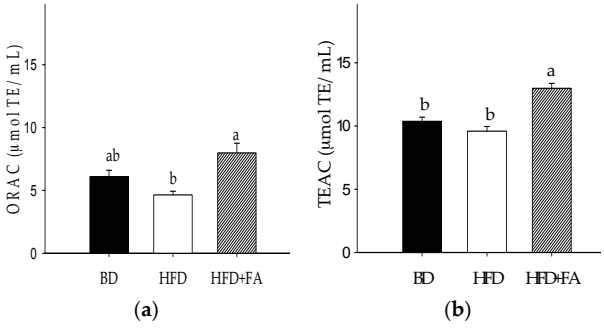

Figure 4. Antioxidant capacity of plasma from rats fed a basal diet (BD), high-fat diet (HFD), and high-fat diet with ferulic acid (HFD + FA) for 60 days. (**a**) Oxygen radical absorbance capacity (ORAC); (**b**) Trolox equivalent antioxidant capacity (TEAC). Each bar represents the mean ± SEM. Different letters in the bars represent significant differences ($p < 0.05$) between dietary treatments.

3.6. Histological Study

Regarding histological appearance, adipocyte size distribution (superficial area) was larger in the HFD group (500–10,500 μm^2; mean 4506.10 ± 166.71 μm^2) than in the BD group (500–5500 μm^2; mean 3240.4 ± 100.53 μm^2). However, those in the HFD + FA group were smaller than those in the BD group and the HFD group (Figure 5).

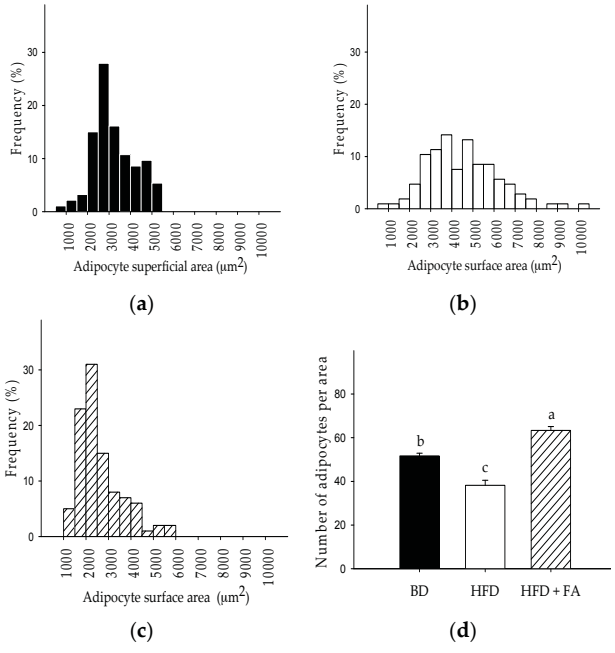

Figure 5. Distribution frequencies of adipocyte size in abdominal adipose tissue of rats were obtained by counting at least 100 cells per subject fed with (**a**) basal diet (BD); (**b**) high-fat diet (HFD); and (**c**) high-fat diet with ferulic acid (HFD + FA) during 60 days; (**d**) Number of adipocytes per area (150,000 μm^2). The number of adipocytes per area is expressed as the mean ± SEM of five replicates. Different letters on bars represent significant differences ($p < 0.05$) between dietary treatments.

The addition of ferulic acid to HFD significantly affected the development of adipocytes. The HFD + FA group had decreased the average size of the adipocytes by 43%, and reduced the size range (1000–6000 μm^2) compared to rats fed a HFD. The size of the adipocytes was consistent with the results obtained for the number of adipocytes counted per constant area (Figure 5d). In addition to changes in adipocyte size due to intake of the HFD, changes in the hexagonal structure of the normal adipocytes were observed, as shown in Figure 6. The adipocytes of abdominal fat tissue showed a clear hyperplasia (cell number increase) and hypertrophy (cell size increase), which are characteristic of increased fat storage in the adipose tissue.

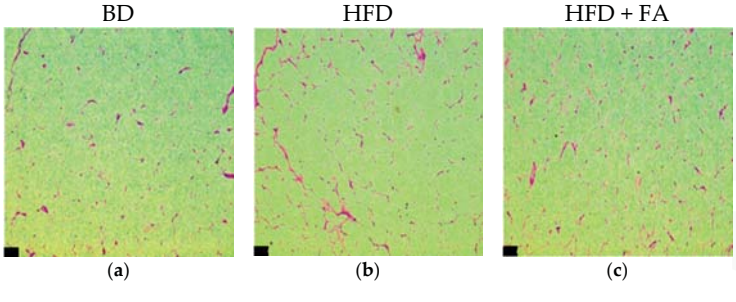

Figure 6. *Cont.*

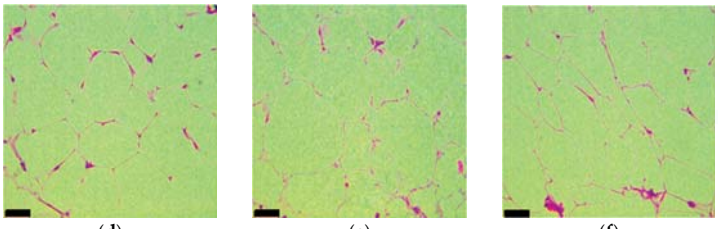

(**d**) (**e**) (**f**)

Figure 6. Representative images of adipocytes of abdominal fat tissue of rats fed with a BD, HFD, and HFD + FA during 60 days. The adipocytes were stained with H and E, and the pictures were taken at 10× (**a**–**c**) and 40× (**d**–**f**). Bars on figures represent 34 μm.

4. Discussion

Obesity and overweight are global health problems, which create an environment conducive to the development of chronic noncommunicable diseases. The study of diseases associated with obesity and overweight, and the search for treatments and strategies for disease control have been the subject of multiple investigations [2,20–23]. In the present study, the effect of ferulic acid on the abdominal adipose tissue, lipid and glucose homeostasis, inflammation biomarkers, and antioxidant capacity in rats fed with a HFD was investigated.

Ferulic acid showed anti-adipogenic properties because it decreases the weight of abdominal fat tissue, fat index, hyperplasia, and hypertrophy compared to rats fed with a HFD (Table 2). Such results could be due to ferulic acid inhibiting adipocyte differentiation or suppressing lipid accumulation in cells [24] whereby the ferulic acid intake could contribute to the prevention of atherosclerotic cardiovascular disease and its risk factors, which has been associated with abdominal obesity indices [23].

The intake of HFD causes the appearance of typical dyslipidemia characterized by increased content of free fatty acid and triglycerides and, often, increased LDL-C and ApoB with decreased HDL-C [4]. In that aspect, it was observed that ferulic acid supplementation in the HFD reduced the TC and triglycerides levels by 16% and 12%, respectively, compared to the HFD group (Figure 1). In addition, ferulic acid intake decreased ApoB, the ApoB/ApoA1 ratio, and LDL-C, but did not affect HDL-C levels. Therefore, the ferulic acid intake could decrease the coronary heart disease risk associated with overweight and obesity via the reduction of the ApoB/ApoA1 ratio and LDL-C [25]. These results are consistent with previous studies, which showed that ferulic acid has anti-atherogenic properties [26].

Additionally, a positive correlation between inflammatory biomarkers (IL-1β, IL-4, and IL-6) and lipids biomarkers and WAFT ($p < 0.05$) was observed. Previous reports have shown the intake of HFD modified adipocyte normal function with the consequent production of free fatty acids, free radicals and adipokines (TNF-α, IL-6), and monocyte chemoattractant protein-1 (MCP-1). This is a key factor for the development of low-grade inflammation [2,27], which is a determinant factor in lipids and glucose homeostasis [2,28].

In our study, ferulic acid modulated the glucose dyshomeostasis induced by HFD by reducing the glucose, insulin levels, and HOMA-IR (Figure 2), which contribute to the prevention of insulin resistance and type 2 diabetes. In a previous study, ferulic acid was shown to improve lipid and glucose homeostasis by modulating the expression of lipogenic genes (SREBP1c, FAS, ACC), stimulating β-oxidation genes (CPT1a, PPARα), and gluconeogenic enzymes (PEPCK and G6Pase) [29]. Additionally, ferulic acid regulates hepatic GLUT2 gene expression through the modulation of transcription factors, which has been observed in high-fat and fructose-induced type-2 diabetic on adult male rats [30].

On the other hand, HFD + FA hindered inflammatory biomarker production (IL-1β, IL-4, and IL-6). Biomarker IL-6 showed positive correlations with HOMA-IR ($r = 0.9399$) and it was higher than that observed with glucose and insulin ($r > 0.6$). Based on the foregoing, IL-6 production directly affected the glucose metabolism and the HOMA-IR was a major predictor of glucose homeostasis

affectation that the individual glucose and insulin measures. Additionally, IL-1β showed to be a key biomarker in the glucose dyshomeostasis, because it showed a positive correlation with glucose, insulin, and HOMA-IR ($r = 0.9864$, $p < 0.0001$). The HOMA-IR index was considered the major predictor of glucose metabolism affectation instead of the individual glucose and insulin measures. Previous research showed IL-1β to be a key factor in the development of insulin resistance and suppression of insulin-induced glucose transport. This can be via the inhibition of insulin-induced phosphorylation of the insulin receptor beta subunit, insulin receptor substrate 1, Akt/protein kinase B, and extracellular regulated kinase [31].

These results indicated that ferulic acid regulated the inflammatory biomarkers induced by HFD, which are determinant factors in lipid and glucose homeostasis. Our results are consistent with previous reports, which showed that ferulic acid has anti-inflammatory properties because of the decrease in the expression of the transcription factor inhibitor of kappa B (IκB), and the increase of the nuclear translocation of the p65 subunit of nuclear factor kappa B (NFκBp65) [10]. Furthermore, ferulic acid may contribute to the modulation of inflammatory processes through suppression of NO production by downregulating the expression of NF-κB-mediated iNOS gene [32].

On the other hand, results showed that HFD + FA increased the antioxidant serum capacity compared to rats fed with a HFD, measured by TEAC and ORAC assays. Additionally, a negative correlation between antioxidant capacity and glucose, insulin, and HOMA-IR was observed showing that the reduction of antioxidant status negatively affected the glucose homeostasis. Similarly, a negative correlation between antioxidant capacity and inflammatory biomarkers (IL-1β, IL-4, and IL-6) was observed. The ferulic acid intake may be beneficial when dyslipidemia and proinflammatory conditions are present since, together, they create an enabling environment for the development of cardiovascular diseases, such as atherosclerosis [4].

Figure 7 represents a summary of our results, and possible implications are represented. Finally, the results are integrated to show that ferulic acid could be an alternative for prevention of diseases related to dyslipidemia and glucose homeostasis such as diabetes, cardiovascular diseases, and hypertension, which are triggered when the inflammatory processes and oxidative stress are present.

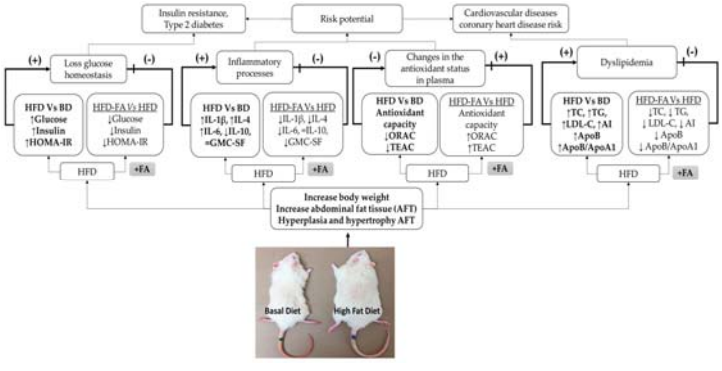

Figure 7. Ferulic acid may contribute to the prevention of the development of chronic noncommunicable diseases induced by the intake of a high-fat diet (HFD). The intake of HFD increased fat storage in adipocytes, consequently increasing the body weight and abdominal fat tissue (AFT), hyperplasia, and hypertrophy in AFT. The factors mentioned above promote dyslipidemia and loss of glucose homeostasis. The modification of adipocytes function causes the release of proinflammatory cytokines which contribute to the generation of chronic low-grade inflammation, which, together with the antioxidant status reduction, are key factors in the development of insulin resistance, type 2 diabetes, cardiovascular diseases, and coronary heart disease risks. The intake of ferulic acid increased the antioxidant status and reduced the proinflammatory cytokines production and storage fat, therefore, ferulic acid may hinder the development of diseases associated with overweight and obesity.

5. Conclusions

The results of our study supported our hypothesis since ferulic acid exhibited an integral anti-obesity, anti-inflammatory, and anti-oxidant effects in rats fed a high-fat diet. These results suggest that ferulic acid could be used as a functional and nutraceutical treatment for obesity-related diseases.

Acknowledgments: This work was performed with the support of the PROINNOVA grant (project No. 218169). Norma Julieta Salazar Lopez received a scholarship from CONACyT (National Research and Technology Council), Mexico.

Author Contributions: N.J.S.-L., M.R.-S. and H.A.-G. designed the experiments and analyzed the data; N.J.S.-L. performed the experiments and wrote the article; J.A.D.A. assisted with the apolipoprotein test; H.A.-G., G.L.-P., J.-M.E.-B., G.A.G.-A. and M.R.-S. critically read the manuscript and contributed to the manuscript discussion; and M.R.-S. secured the funding and has the primary responsibility for the final content. All authors read and approved the final manuscript.

Conflicts of Interest: The authors declare no conflict of interest.

References

1. World Health Organization. *Obesity and Overweight*; WHO: Genewe, Switzerland, 2016; Available online: http://www.who.int/mediacentre/factsheets/fs311/en/ (accessed on 5 January 2017).
2. Jung, U.J.; Choi, M. Obesity and its metabolic complications: The role of adipokines and the relationship between obesity, inflammation, insulin resistance, dyslipidemia and nonalcoholic fatty liver disease. *Int. J. Mol. Sci.* **2014**, *15*, 6184–6223. [CrossRef] [PubMed]
3. Hassan, H.A.; El-Gharib, N.E. Obesity and clinical riskiness relationship: Therapeutic management by dietary antioxidant supplementation—A Review. *Appl. Biochem. Biotechnol.* **2015**, *173*, 647–669. [CrossRef] [PubMed]
4. Klop, B.; Elte, J.W.F.; Cabezas, M.C. Dyslipidemia in obesity: Mechanisms and potential targets. *Nutrients* **2013**, *5*, 1218–1240. [CrossRef] [PubMed]
5. Leiherer, A.; Mündlein, A.; Drexel, H. Phytochemicals and their impact on adipose tissue inflammation and diabetes. *Vascul. Pharmacol.* **2013**, *58*, 3–20. [CrossRef] [PubMed]
6. Alam, A.; Subhan, N.; Hossain, H.; Hossain, M.; Reza, H.M. Hydroxycinnamic acid derivatives: A potential class of natural compounds for the management of lipid metabolism and obesity. *Nutr. Metab. Lond.* **2016**, *13*, 1–13. [CrossRef] [PubMed]
7. Navarrete, S.; Alarcón, M.; Palomo, I. Aqueous extract of tomato (*Solanum lycopersicum* L.) and ferulic acid reduce the expression of TNF-α and IL-1β in LPS-Activated macrophages. *Molecules* **2015**, *20*, 15319–15329. [CrossRef] [PubMed]
8. Wang, O.; Liu, J.; Cheng, Q.; Guo, X.; Wang, Y.; Zhao, L.; Zhou, F.; Ji, B. Effects of ferulic acid and γ-Oryzanol on metabolic syndrome in rats. *PLoS ONE* **2015**, *10*, e0118135. [CrossRef]
9. Senaphan, K.; Kukongviriyapan, U.; Sangartit, W.; Pakdeechote, P.; Pannangpetch, P.; Prachaney, P.; Greenwald, S.E.; Kukongviriyapan, V. Ferulic acid alleviates changes in a rat model of metabolic syndrome induced by high-carbohydrate, high-fat diet. *Nutrients* **2015**, *7*, 6446–6464. [CrossRef] [PubMed]
10. Niu, C.; Sheng, Y.; Zhu, E.; Ji, L.; Wang, Z. Ferulic acid prevents liver injury induced by Diosbulbin B and its mechanism. *Biosci. Trends* **2016**, *10*, 386–391. [CrossRef] [PubMed]
11. Reeves, P.G.; Nielsen, F.H.; Fahey, G.C.J. AIN-93 purified diets for laboratory rodents: Final report of the American Institute of Nutrition ad hoc writing committee on the reformulation of the AIN-76A rodent diet. *J. Nutr.* **1993**, *123*, 1939–1951. [PubMed]
12. Mancuso, C.; Santangelo, R. Ferulic acid: Pharmacological and toxicological aspects. *Food Chem. Toxicol.* **2014**, *65*, 185–195. [CrossRef] [PubMed]
13. Yeh, Y.-H.; Lee, Y.-T.; Hsieh, H.-S.; Hwang, D.-F. Dietary caffeic acid, ferulic acid and coumaric acid supplements on cholesterol metabolism and antioxidant activity in rats. *J. Food Drug Anal.* **2009**, *17*, 123–132.
14. National Research Council (US) Committee for the Update of the Guide for the Care and Use of Laboratory Animals. *Guide for the Care and Use of Laboratory Animals*, 8th ed.; National Academies Press: Washington, DC, USA, 2011.

15. Robles-Sánchez, M.; Astiazarán-García, H.; Martín-Belloso, O.; Gorinstein, S.; Alvarez-Parrilla, E.; de la Rosa, L.A.; Yepiz-Plascencia, G.; González-Aguilar, G.A. Influence of whole and fresh-cut mango intake on plasma lipids and antioxidant capacity of healthy adults. *Food Res. Int.* **2011**, *44*, 1386–1391. [CrossRef]
16. Muruganandan, S.; Srinivasan, K.; Gupta, S.; Gupta, P.K.; Lal, J. Effect of mangiferin on hyperglycemia and atherogenicity in streptozotocin diabetic rats. *J. Ethnopharmacol.* **2005**, *97*, 497–501. [CrossRef] [PubMed]
17. Xia, S.; Le, G.; Wang, P.; Qiu, Y.; Jiang, Y.; Tang, X. Regressive effect of myricetin on hepatic steatosis in mice fed a high-fat diet. *Nutrients* **2016**, *8*, 799. [CrossRef] [PubMed]
18. Huang, D.; Ou, B.; Hampsch-Woodill, M.; Flanagan, J.; Prior, R.L. High-Throughput assay of oxygen radical absorbance capacity (ORAC) using a multichannel liquid handling system coupled with a microplate fluorescence reader in 96-well format. *J. Agric. Food Chem.* **2002**, *50*, 4437–4444. [CrossRef] [PubMed]
19. Blancas-Benitez, F.J.; Mercado-Mercado, G.; Quirós-Sauceda, A.E.; Montalvo-González, E.; González-Aguilar, G.A.; Sáyago-Ayerdi, S.G. Bioaccessibility of polyphenols associated with dietary fiber and in vitro kinetics release of polyphenols in Mexican "Ataulfo" mango (*Mangifera indica* L.) by-products. *Food Funct.* **2015**, *6*, 859–868. [CrossRef] [PubMed]
20. Hsu, C.L.; Wu, C.H.; Huang, S.L.; Yen, G.C. Phenolic compounds rutin and o-coumaric acid ameliorate obesity induced by high-fat diet in rats. *J. Agric. Food Chem.* **2009**, *57*, 425–431. [CrossRef] [PubMed]
21. Tan, H.Y.; Mei, I.; Tse, Y.; Tsze, E.; Li, S.; Wang, M. Oxyresveratrol supplementation to C57bl/6 mice fed with a high-fat diet ameliorates obesity-associated symptoms. *Nutrients* **2017**, *9*, 147. [CrossRef] [PubMed]
22. Xu, Y.; Zhang, M.; Wu, T.; Dai, S.; Xu, J.; Zhou, Z. The anti-obesity effect of green tea polysaccharides, polyphenols and caffeine in rats fed with a high-fat diet. *Food Funct.* **2015**, *6*, 297–304. [CrossRef] [PubMed]
23. Fan, H.; Li, X.; Zheng, L.; Chen, X.; Wu, H.; Ding, X.; Qian, D.; Shen, Y.; Yu, Z.; Fan, L.; et al. Abdominal obesity is strongly associated with cardiovascular disease and its risk factors in elderly and very elderly community-dwelling Chinese. *Sci. Rep.* **2016**, *6*, 21521. [CrossRef] [PubMed]
24. Seo, C.-R.; Yi, B.; Oh, S.; Kwon, S.-M.; Kim, S.; Song, N.-J.; Cho, J.Y.; Park, K.-M.; Ahn, J-Y.; Hong, J.-W.; et al. Aqueous extracts of hulled barley containing coumaric acid and ferulic acid inhibit adipogenesis in vitro and obesity in vivo. *J. Funct. Foods* **2015**, *12*, 208–218. [CrossRef]
25. Lu, M.; Lu, Q.; Zhang, Y.; Tian, G. ApoB/apoA1 is an effective predictor of coronary heart disease risk in overweight and obesity. *J. Biomed. Res.* **2011**, *25*, 266–273. [CrossRef]
26. Kwon, E.Y.; Do, G.M.; Cho, Y.Y.; Park, Y.B.; Jeon, S.M.; Choi, M.S. Anti-atherogenic property of ferulic acid in apolipoprotein E-deficient mice fed Western diet: Comparison with clofibrate. *Food Chem. Toxicol.* **2010**, *48*, 2298–2303. [CrossRef] [PubMed]
27. Gregor, M.F.; Hotamisligil, G.S. Inflammatory Mechanisms in Obesity. *Annu. Rev. Immunol.* **2011**, *29*, 415–445. [CrossRef] [PubMed]
28. Kahn, S.E.; Hull, R.L.; Utzschneider, K.M. Mechanisms linking obesity to insulin resistance and type 2 diabetes. *Nature* **2006**, *444*, 840–846. [CrossRef] [PubMed]
29. Naowaboot, J.; Piyabhan, P.; Munkong, N.; Parklak, W.; Pannangpetch, P. Ferulic acid improves lipid and glucose homeostasis in high-fat diet-induced obese mice. *Clin. Exp. Pharmacol. Physiol.* **2016**, *43*, 242–250. [CrossRef] [PubMed]
30. Narasimhan, A.; Chinnaiyan, M.; Karundevi, B. Ferulic acid regulates hepatic GLUT2 gene expression in high fat and fructose-induced type-2 diabetic adult male rat. *Eur. J. Pharmacol.* **2015**, *761*, 391–397. [CrossRef] [PubMed]
31. Lagathu, C.; Yvan-Charvet, L.; Bastard, J.P.; Maachi, M.; Quignard-Boulangé, A.; Capeau, J.; Caron, M. Long-term treatment with interleukin-1beta induces insulin resistance in murine and human adipocytes. *Diabetologia* **2006**, *49*, 2162–2173. [CrossRef] [PubMed]
32. Kim, E.O.; Min, K.J.; Kwon, T.K.; Um, B.H.; Moreau, R.A.; Choi, S.W. Anti-inflammatory activity of hydroxycinnamic acid derivatives isolated from corn bran in lipopolysaccharide-stimulated RAW 264.7 macrophages. *Food Chem. Toxicol.* **2012**, *50*, 1309–1316. [CrossRef] [PubMed]

MDPI
St. Alban-Anlage 66
4052 Basel, Switzerland
Tel. +41 61 683 77 34
Fax +41 61 302 89 18
http://www.mdpi.com

Nutrients Editorial Office
E-mail: nutrients@mdpi.com
http://www.mdpi.com/journal/nutrients

MDPI
St. Alban-Anlage 66
4052 Basel
Switzerland

Tel: +41 61 683 77 34
Fax: +41 61 302 89 18

www.mdpi.com

ISBN 978-3-03842-886-2